VISIT…

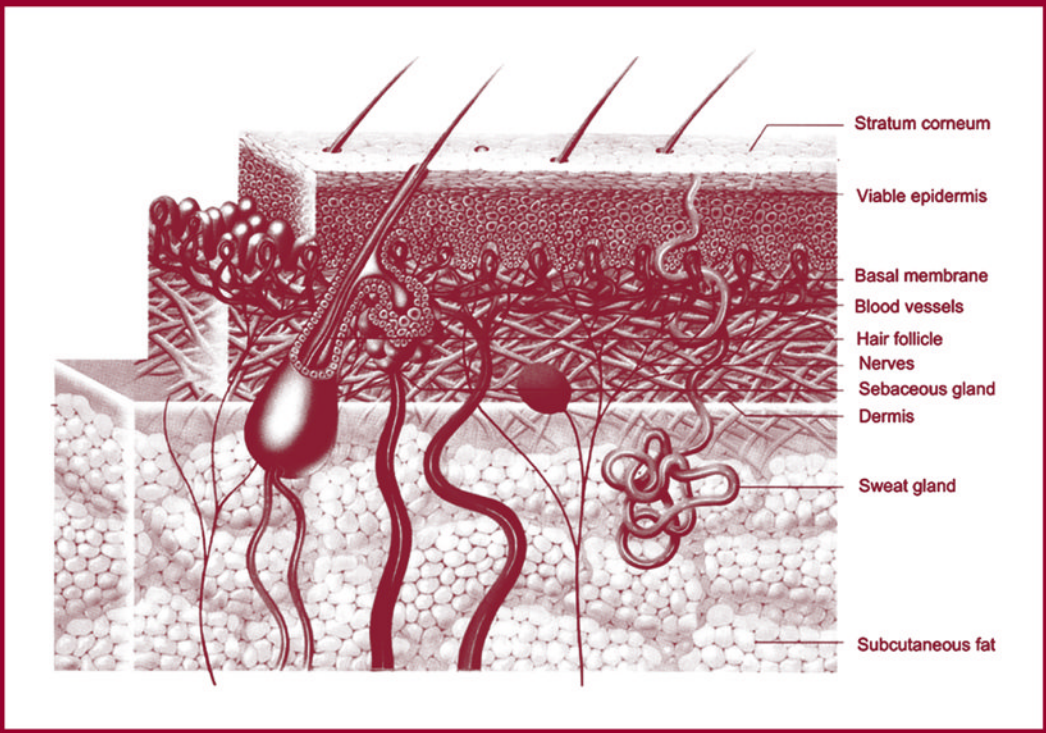


DRUGS AND THE PHARMACEUTICAL SCIENCES VOLUME 155

Percutaneous Absorption

Drugs—Cosmetics—Mechanisms—Methodology

Fourth Edition



edited by
Robert L. Bronaugh
Howard I. Maibach

Percutaneous Absorption

DRUGS AND THE PHARMACEUTICAL SCIENCES

Executive Editor
James Swarbrick
PharmaceuTech, Inc.
Pinehurst, North Carolina

Advisory Board

Larry L. Augsburger
University of Maryland
Baltimore, Maryland

Harry G. Brittain
Center for Pharmaceutical Physics
Milford, New Jersey

Jennifer B. Dressman
Johann Wolfgang Goethe University
Frankfurt, Germany

Anthony J. Hickey
University of North Carolina School of Pharmacy
Chapel Hill, North Carolina

Jeffrey A. Hughes
University of Florida College of Pharmacy
Gainesville, Florida

Ajaz Hussain
U.S. Food and Drug Administration
Frederick, Maryland

Trevor M. Jones
The Association of the British Pharmaceutical Industry
London, United Kingdom

Hans E. Junginger
Leiden/Amsterdam Center for Drug Research
Leiden, The Netherlands

Vincent H. L. Lee
University of Southern California
Los Angeles, California

Stephen G. Schulman
University of Florida
Gainesville, Florida

Jerome P. Skelly
Alexandria, Virginia

Elizabeth M. Topp
University of Kansas School of Pharmacy
Lawrence, Kansas

Geoffrey T. Tucker
University of Sheffield
Royal Hallamshire Hospital
Sheffield, United Kingdom

Peter York
University of Bradford School of Pharmacy
Bradford, United Kingdom

DRUGS AND THE PHARMACEUTICAL SCIENCES

A Series of Textbooks and Monographs

1. Pharmacokinetics, *Milo Gibaldi and Donald Perrier*
2. Good Manufacturing Practices for Pharmaceuticals: A Plan for Total Quality Control, *Sidney H. Willig, Murray M. Tuckerman, and William S. Hitchings IV*
3. Microencapsulation, *edited by J. R. Nixon*
4. Drug Metabolism: Chemical and Biochemical Aspects, *Bernard Testa and Peter Jenner*
5. New Drugs: Discovery and Development, *edited by Alan A. Rubin*
6. Sustained and Controlled Release Drug Delivery Systems, *edited by Joseph R. Robinson*
7. Modern Pharmaceutics, *edited by Gilbert S. Banker and Christopher T. Rhodes*
8. Prescription Drugs in Short Supply: Case Histories, *Michael A. Schwartz*
9. Activated Charcoal: Antidotal and Other Medical Uses, *David O. Cooney*
10. Concepts in Drug Metabolism (in two parts), *edited by Peter Jenner and Bernard Testa*
11. Pharmaceutical Analysis: Modern Methods (in two parts), *edited by James W. Munson*
12. Techniques of Solubilization of Drugs, *edited by Samuel H. Yalkowsky*
13. Orphan Drugs, *edited by Fred E. Karch*
14. Novel Drug Delivery Systems: Fundamentals, Developmental Concepts, Biomedical Assessments, *Yie W. Chien*
15. Pharmacokinetics: Second Edition, Revised and Expanded, *Milo Gibaldi and Donald Perrier*
16. Good Manufacturing Practices for Pharmaceuticals: A Plan for Total Quality Control, Second Edition, Revised and Expanded, *Sidney H. Willig, Murray M. Tuckerman, and William S. Hitchings IV*
17. Formulation of Veterinary Dosage Forms, *edited by Jack Blodinger*
18. Dermatological Formulations: Percutaneous Absorption, *Brian W. Barry*
19. The Clinical Research Process in the Pharmaceutical Industry, *edited by Gary M. Matoren*
20. Microencapsulation and Related Drug Processes, *Patrick B. Deasy*
21. Drugs and Nutrients: The Interactive Effects, *edited by Daphne A. Roe and T. Colin Campbell*
22. Biotechnology of Industrial Antibiotics, *Erick J. Vandamme*
23. Pharmaceutical Process Validation, *edited by Bernard T. Loftus and Robert A. Nash*

24. Anticancer and Interferon Agents: Synthesis and Properties, *edited by Raphael M. Ottenbrite and George B. Butler*
25. Pharmaceutical Statistics: Practical and Clinical Applications, *Sanford Bolton*
26. Drug Dynamics for Analytical, Clinical, and Biological Chemists, *Benjamin J. Gudzinowicz, Burrows T. Younkin, Jr., and Michael J. Gudzinowicz*
27. Modern Analysis of Antibiotics, *edited by Adjoran Aszalos*
28. Solubility and Related Properties, *Kenneth C. James*
29. Controlled Drug Delivery: Fundamentals and Applications, Second Edition, Revised and Expanded, *edited by Joseph R. Robinson and Vincent H. Lee*
30. New Drug Approval Process: Clinical and Regulatory Management, *edited by Richard A. Guarino*
31. Transdermal Controlled Systemic Medications, *edited by Yie W. Chien*
32. Drug Delivery Devices: Fundamentals and Applications, *edited by Praveen Tyle*
33. Pharmacokinetics: Regulatory • Industrial • Academic Perspectives, *edited by Peter G. Welling and Francis L. S. Tse*
34. Clinical Drug Trials and Tribulations, *edited by Allen E. Cato*
35. Transdermal Drug Delivery: Developmental Issues and Research Initiatives, *edited by Jonathan Hadgraft and Richard H. Guy*
36. Aqueous Polymeric Coatings for Pharmaceutical Dosage Forms, *edited by James W. McGinity*
37. Pharmaceutical Pelletization Technology, *edited by Isaac Ghebre-Sellassie*
38. Good Laboratory Practice Regulations, *edited by Allen F. Hirsch*
39. Nasal Systemic Drug Delivery, *Yie W. Chien, Kenneth S. E. Su, and Shyi-Feu Chang*
40. Modern Pharmaceutics: Second Edition, Revised and Expanded, *edited by Gilbert S. Banker and Christopher T. Rhodes*
41. Specialized Drug Delivery Systems: Manufacturing and Production Technology, *edited by Praveen Tyle*
42. Topical Drug Delivery Formulations, *edited by David W. Osborne and Anton H. Amann*
43. Drug Stability: Principles and Practices, *Jens T. Carstensen*
44. Pharmaceutical Statistics: Practical and Clinical Applications, Second Edition, Revised and Expanded, *Sanford Bolton*
45. Biodegradable Polymers as Drug Delivery Systems, *edited by Mark Chasin and Robert Langer*
46. Preclinical Drug Disposition: A Laboratory Handbook, *Francis L. S. Tse and James J. Jaffe*

47. HPLC in the Pharmaceutical Industry, *edited by Godwin W. Fong and Stanley K. Lam*
48. Pharmaceutical Bioequivalence, *edited by Peter G. Welling, Francis L. S. Tse, and Shrikant V. Dinghe*
49. Pharmaceutical Dissolution Testing, *Umesh V. Banakar*
50. Novel Drug Delivery Systems: Second Edition, Revised and Expanded, *Yie W. Chien*
51. Managing the Clinical Drug Development Process, *David M. Cocchetto and Ronald V. Nardi*
52. Good Manufacturing Practices for Pharmaceuticals: A Plan for Total Quality Control, Third Edition, *edited by Sidney H. Willig and James R. Stoker*
53. Prodrugs: Topical and Ocular Drug Delivery, *edited by Kenneth B. Sloan*
54. Pharmaceutical Inhalation Aerosol Technology, *edited by Anthony J. Hickey*
55. Radiopharmaceuticals: Chemistry and Pharmacology, *edited by Adrian D. Nunn*
56. New Drug Approval Process: Second Edition, Revised and Expanded, *edited by Richard A. Guarino*
57. Pharmaceutical Process Validation: Second Edition, Revised and Expanded, *edited by Ira R. Berry and Robert A. Nash*
58. Ophthalmic Drug Delivery Systems, *edited by Ashim K. Mitra*
59. Pharmaceutical Skin Penetration Enhancement, *edited by Kenneth A. Walters and Jonathan Hadgraft*
60. Colonic Drug Absorption and Metabolism, *edited by Peter R. Bieck*
61. Pharmaceutical Particulate Carriers: Therapeutic Applications, *edited by Alain Rolland*
62. Drug Permeation Enhancement: Theory and Applications, *edited by Dean S. Hsieh*
63. Glycopeptide Antibiotics, *edited by Ramakrishnan Nagarajan*
64. Achieving Sterility in Medical and Pharmaceutical Products, *Nigel A. Halls*
65. Multiparticulate Oral Drug Delivery, *edited by Isaac Ghebre-Sellassie*
66. Colloidal Drug Delivery Systems, *edited by Jörg Kreuter*
67. Pharmacokinetics: Regulatory • Industrial • Academic Perspectives, Second Edition, *edited by Peter G. Welling and Francis L. S. Tse*
68. Drug Stability: Principles and Practices, Second Edition, Revised and Expanded, *Jens T. Carstensen*
69. Good Laboratory Practice Regulations: Second Edition, Revised and Expanded, *edited by Sandy Weinberg*
70. Physical Characterization of Pharmaceutical Solids, *edited by Harry G. Brittain*

71. Pharmaceutical Powder Compaction Technology, *edited by Göran Alderborn and Christer Nyström*
72. Modern Pharmaceutics: Third Edition, Revised and Expanded, *edited by Gilbert S. Banker and Christopher T. Rhodes*
73. Microencapsulation: Methods and Industrial Applications, *edited by Simon Benita*
74. Oral Mucosal Drug Delivery, *edited by Michael J. Rathbone*
75. Clinical Research in Pharmaceutical Development, *edited by Barry Bleidt and Michael Montagne*
76. The Drug Development Process: Increasing Efficiency and Cost Effectiveness, *edited by Peter G. Welling, Louis Lasagna, and Umesh V. Banakar*
77. Microparticulate Systems for the Delivery of Proteins and Vaccines, *edited by Smadar Cohen and Howard Bernstein*
78. Good Manufacturing Practices for Pharmaceuticals: A Plan for Total Quality Control, Fourth Edition, Revised and Expanded, *Sidney H. Willig and James R. Stoker*
79. Aqueous Polymeric Coatings for Pharmaceutical Dosage Forms: Second Edition, Revised and Expanded, *edited by James W. McGinity*
80. Pharmaceutical Statistics: Practical and Clinical Applications, Third Edition, *Sanford Bolton*
81. Handbook of Pharmaceutical Granulation Technology, *edited by Dilip M. Parikh*
82. Biotechnology of Antibiotics: Second Edition, Revised and Expanded, *edited by William R. Strohl*
83. Mechanisms of Transdermal Drug Delivery, *edited by Russell O. Potts and Richard H. Guy*
84. Pharmaceutical Enzymes, *edited by Albert Lauwers and Simon Scharpé*
85. Development of Biopharmaceutical Parenteral Dosage Forms, *edited by John A. Bontempo*
86. Pharmaceutical Project Management, *edited by Tony Kennedy*
87. Drug Products for Clinical Trials: An International Guide to Formulation • Production • Quality Control, *edited by Donald C. Monkhouse and Christopher T. Rhodes*
88. Development and Formulation of Veterinary Dosage Forms: Second Edition, Revised and Expanded, *edited by Gregory E. Hardee and J. Desmond Baggot*
89. Receptor-Based Drug Design, *edited by Paul Leff*
90. Automation and Validation of Information in Pharmaceutical Processing, *edited by Joseph F. deSpautz*
91. Dermal Absorption and Toxicity Assessment, *edited by Michael S. Roberts and Kenneth A. Walters*

92. Pharmaceutical Experimental Design, *Gareth A. Lewis, Didier Mathieu, and Roger Phan-Tan-Luu*
93. Preparing for FDA Pre-Approval Inspections, *edited by Martin D. Hynes III*
94. Pharmaceutical Excipients: Characterization by IR, Raman, and NMR Spectroscopy, *David E. Bugay and W. Paul Findlay*
95. Polymorphism in Pharmaceutical Solids, *edited by Harry G. Brittain*
96. Freeze-Drying/Lyophilization of Pharmaceutical and Biological Products, *edited by Louis Rey and Joan C. May*
97. Percutaneous Absorption: Drugs–Cosmetics–Mechanisms–Methodology, Third Edition, Revised and Expanded, *edited by Robert L. Bronaugh and Howard I. Maibach*
98. Bioadhesive Drug Delivery Systems: Fundamentals, Novel Approaches, and Development, *edited by Edith Mathiowitz, Donald E. Chickering III, and Claus-Michael Lehr*
99. Protein Formulation and Delivery, *edited by Eugene J. McNally*
100. New Drug Approval Process: Third Edition, The Global Challenge, *edited by Richard A. Guarino*
101. Peptide and Protein Drug Analysis, *edited by Ronald E. Reid*
102. Transport Processes in Pharmaceutical Systems, *edited by Gordon L. Amidon, Ping I. Lee, and Elizabeth M. Topp*
103. Excipient Toxicity and Safety, *edited by Myra L. Weiner and Lois A. Kotkoskie*
104. The Clinical Audit in Pharmaceutical Development, *edited by Michael R. Hamrell*
105. Pharmaceutical Emulsions and Suspensions, *edited by Francoise Nielloud and Gilberte Marti-Mestres*
106. Oral Drug Absorption: Prediction and Assessment, *edited by Jennifer B. Dressman and Hans Lennernäs*
107. Drug Stability: Principles and Practices, Third Edition, Revised and Expanded, *edited by Jens T. Carstensen and C. T. Rhodes*
108. Containment in the Pharmaceutical Industry, *edited by James P. Wood*
109. Good Manufacturing Practices for Pharmaceuticals: A Plan for Total Quality Control from Manufacturer to Consumer, Fifth Edition, Revised and Expanded, *Sidney H. Willig*
110. Advanced Pharmaceutical Solids, *Jens T. Carstensen*
111. Endotoxins: Pyrogens, LAL Testing, and Depyrogenation, Second Edition, Revised and Expanded, *Kevin L. Williams*
112. Pharmaceutical Process Engineering, *Anthony J. Hickey and David Ganderton*
113. Pharmacogenomics, *edited by Werner Kalow, Urs A. Meyer, and Rachel F. Tyndale*
114. Handbook of Drug Screening, *edited by Ramakrishna Seethala and Prabhavathi B. Fernandes*

115. Drug Targeting Technology: Physical • Chemical • Biological Methods, *edited by Hans Schreier*

116. Drug–Drug Interactions, *edited by A. David Rodrigues*

117. Handbook of Pharmaceutical Analysis, *edited by Lena Ohannesian and Anthony J. Streeter*

118. Pharmaceutical Process Scale-Up, *edited by Michael Levin*

119. Dermatological and Transdermal Formulations, *edited by Kenneth A. Walters*

120. Clinical Drug Trials and Tribulations: Second Edition, Revised and Expanded, *edited by Allen Cato, Lynda Sutton, and Allen Cato III*

121. Modern Pharmaceutics: Fourth Edition, Revised and Expanded, *edited by Gilbert S. Banker and Christopher T. Rhodes*

122. Surfactants and Polymers in Drug Delivery, *Martin Malmsten*

123. Transdermal Drug Delivery: Second Edition, Revised and Expanded, *edited by Richard H. Guy and Jonathan Hadgraft*

124. Good Laboratory Practice Regulations: Second Edition, Revised and Expanded, *edited by Sandy Weinberg*

125. Parenteral Quality Control: Sterility, Pyrogen, Particulate, and Package Integrity Testing: Third Edition, Revised and Expanded, *Michael J. Akers, Daniel S. Larrimore, and Dana Morton Guazzo*

126. Modified-Release Drug Delivery Technology, *edited by Michael J. Rathbone, Jonathan Hadgraft, and Michael S. Roberts*

127. Simulation for Designing Clinical Trials: A Pharmacokinetic-Pharmacodynamic Modeling Perspective, *edited by Hui C. Kimko and Stephen B. Duffull*

128. Affinity Capillary Electrophoresis in Pharmaceutics and Biopharmaceutics, *edited by Reinhard H. H. Neubert and Hans-Hermann Rüttinger*

129. Pharmaceutical Process Validation: An International Third Edition, Revised and Expanded, *edited by Robert A. Nash and Alfred H. Wachter*

130. Ophthalmic Drug Delivery Systems: Second Edition, Revised and Expanded, *edited by Ashim K. Mitra*

131. Pharmaceutical Gene Delivery Systems, *edited by Alain Rolland and Sean M. Sullivan*

132. Biomarkers in Clinical Drug Development, *edited by John C. Bloom and Robert A. Dean*

133. Pharmaceutical Extrusion Technology, *edited by Isaac Ghebre-Sellassie and Charles Martin*

134. Pharmaceutical Inhalation Aerosol Technology: Second Edition, Revised and Expanded, *edited by Anthony J. Hickey*

135. Pharmaceutical Statistics: Practical and Clinical Applications, Fourth Edition, *Sanford Bolton and Charles Bon*

136. Compliance Handbook for Pharmaceuticals, Medical Devices, and Biologics, *edited by Carmen Medina*

137. Freeze-Drying/Lyophilization of Pharmaceutical and Biological Products: Second Edition, Revised and Expanded, *edited by Louis Rey and Joan C. May*
138. Supercritical Fluid Technology for Drug Product Development, *edited by Peter York, Uday B. Kompella, and Boris Y. Shekunov*
139. New Drug Approval Process: Fourth Edition, Accelerating Global Registrations, *edited by Richard A. Guarino*
140. Microbial Contamination Control in Parenteral Manufacturing, *edited by Kevin L. Williams*
141. New Drug Development: Regulatory Paradigms for Clinical Pharmacology and Biopharmaceutics, *edited by Chandrahas G. Sahajwalla*
142. Microbial Contamination Control in the Pharmaceutical Industry, *edited by Luis Jimenez*
143. Generic Drug Product Development: Solid Oral Dosage Forms, *edited by Leon Shargel and Izzy Kanfer*
144. Introduction to the Pharmaceutical Regulatory Process, *edited by Ira R. Berry*
145. Drug Delivery to the Oral Cavity: Molecules to Market, *edited by Tapash K. Ghosh and William R. Pfister*
146. Good Design Practices for GMP Pharmaceutical Facilities, *edited by Andrew Signore and Terry Jacobs*
147. Drug Products for Clinical Trials, Second Edition, *edited by Donald Monkhouse, Charles Carney, and Jim Clark*
148. Polymeric Drug Delivery Systems, *edited by Glen S. Kwon*
149. Injectable Dispersed Systems: Formulation, Processing, and Performance, *edited by Diane J. Burgess*
150. Laboratory Auditing For Quality and Regulatory Compliance, *edited by Donald Singer, Raluca-Ioana Stefan, and Jacobus van Staden*
151. Active Pharmaceutical Ingredients: Development, Manufacturing, and Regulation, *edited by Stanley Nusim*
152. Preclinical Drug Development, *edited by Mark C. Rogge and David R. Taft*
153. Pharmaceutical Stress Testing: Predicting Drug Degradation, *edited by Steven W. Baertschi*
154. Handbook of Pharmaceutical Granulation Technology: Second Edition, *edited by Dilip M. Parikh*
155. Percutaneous Absorption: Drugs–Cosmetics–Mechanisms–Methodology, Fourth Edition, *edited by Robert L. Bronaugh and Howard I. Maibach*

Percutaneous Absorption

Drugs—Cosmetics—Mechanisms—Methodology

Fourth Edition

edited by

Robert L. Bronaugh
Food and Drug Administration
Laurel, Maryland, U.S.A.

Howard I. Maibach
University of California
San Francisco, California, U.S.A.



Taylor & Francis
Taylor & Francis Group

Boca Raton London New York Singapore

Published in 2005 by
Taylor & Francis Group
6000 Broken Sound Parkway NW, Suite 300
Boca Raton, FL 33487-2742

© 2005 by Taylor & Francis Group, LLC

No claim to original U.S. Government works
Printed in the United States of America on acid-free paper
10 9 8 7 6 5 4 3 2 1

International Standard Book Number-10: 1-57444-869-2 (Hardcover)
International Standard Book Number-13: 978-1-57444-869-6 (Hardcover)

This book contains information obtained from authentic and highly regarded sources. Reprinted material is quoted with permission, and sources are indicated. A wide variety of references are listed. Reasonable efforts have been made to publish reliable data and information, but the author and the publisher cannot assume responsibility for the validity of all materials or for the consequences of their use.

No part of this book may be reprinted, reproduced, transmitted, or utilized in any form by any electronic, mechanical, or other means, now known or hereafter invented, including photocopying, microfilming, and recording, or in any information storage or retrieval system, without written permission from the publishers.

For permission to photocopy or use material electronically from this work, please access www.copyright.com (http://www.copyright.com/) or contact the Copyright Clearance Center, Inc. (CCC) 222 Rosewood Drive, Danvers, MA 01923, 978-750-8400. CCC is a not-for-profit organization that provides licenses and registration for a variety of users. For organizations that have been granted a photocopy license by the CCC, a separate system of payment has been arranged.

Trademark Notice: Product or corporate names may be trademarks or registered trademarks, and are used only for identification and explanation without intent to infringe.

Library of Congress Cataloging-in-Publication Data

Catalog record is available from the Library of Congress

T&F informa
Taylor & Francis Group
is the Academic Division of T&F Informa plc.

Visit the Taylor & Francis Web site at
http://www.taylorandfrancis.com

Preface

The study of the percutaneous absorption of chemicals encompasses many scientific disciplines from toxicology and pharmacology to medicine, cosmetic science, physical chemistry, and many others. But in spite of the reason for evaluating skin absorption, the principles and techniques that are discovered can be beneficial to a wide range of investigators in this area. This multi-authored text from experts in the field of percutaneous absorption reflects this difference in scientific background that helps to enrich our understanding of the subject.

It has been six years since the publication of the *Third Edition* and many advances have taken place in this field. There have been major advances in our ability to enhance the penetration of chemicals through the skin; therefore, special emphasis has been placed on adding chapters on new drug delivery techniques such as the use of nanotechnology, microneedles, liposomes, microemulsions, and phonophoresis. Important strides have been made in the last few years in our understanding of the penetration of macromolecular compounds. This subject area is addressed with new chapters concerning skin absorption of protein allergens, transcutaneous immunization methodology, and chemical and physical methods to enhance the penetration of oligonucleotide drugs. Our knowledge concerning mechanisms of skin absorption has greatly increased as reflected in new chapters on the effect of skin desquamation on absorption, the effects of skin occlusion, the importance of hair follicle penetration, and how mixtures of chemicals can alter penetration of individual chemicals. We have also added new chapters on hair dye absorption, the penetration of cosmetics, in vivo–in vitro absorption correlations, and many other subjects. The *Fourth Edition* has been significantly expanded in size and range of topics covered since the *First Edition* published 19 years ago. These changes reflect the large increase in numbers of scientists working in the field and the many discoveries that have been made during this period.

We would like to thank the authors for preparing outstanding chapters and Sandra Beberman and Joseph Stubenrauch of Taylor & Francis for their expert editorial guidance.

Robert L. Bronaugh
Howard I. Maibach

Contents

Preface . . . . . *iii*
Contributors . . . . . *xxi*

1. Mathematical Models in Percutaneous Absorption ***1***
Michael S. Roberts and Yuri G. Anissimov
I. In Vitro Skin Diffusion Models in Percutaneous Absorption 3
II. Release Profiles from Topical Products 21
III. Compartmental Models as an Alternative to Diffusion Models in Percutaneous Absorption 22
IV. Other Processes Affecting In Vitro Percutaneous Absorption 23
V. Simple In Vivo Models in Percutaneous Absorption 27
VI. Modeling with Facilitated Transdermal Delivery 35
VII. Practical Issues in Applying Mathematical Models to Percutaneous Absorption Data 36
VIII. Conclusion 37
References 38

2. Skin Metabolism During In Vitro Percutaneous Absorption ***45***
Robert L. Bronaugh, Margaret E. K. Kraeling, and Jeffrey J. Yourick
I. Introduction 45
II. Skin Viability 45
III. Skin Metabolism 46
References 48

3. Cutaneous Metabolism of Xenobiotics ***51***
Saqib J. Bashir and Howard I. Maibach
I. Introduction 51
II. Xenobiotic-Metabolizing Enzymes 51
III. Phase I Metabolism: Cytochrome P-450 Monooxygenases 52
IV. Phase II Metabolism 54
V. Examples of Xenobiotic Metabolism 56
VI. Metabolism of Environmental Xenobiotics 57

VII. Factors Affecting Cutaneous Metabolism 59
VIII. Consequences of Cutaneous Xenobiotic Metabolism 61
References 62

4. Occlusion Does Not Uniformly Enhance Penetration In Vivo *65*
Daniel Bucks and Howard I. Maibach
I. Introduction 65
II. Percutaneous Absorption of *p*-Phenylenediamine (PPDA) in Guinea Pigs 66
III. Percutaneous Absorption of Volatile Compounds 66
IV. Percutaneous Absorption of Steroids in Humans 68
V. Percutaneous Absorption of Phenols in Humans 72
VI. Discussion 74
References 82

5. Regional Variation in Percutaneous Absorption: Principles and Applications to Human Risk Assessment *85*
Ronald C. Wester and Howard I. Maibach
I. Introduction 85
II. Regional Variation in Humans 85
III. Regional Variation in Animals 89
IV. Applications to Human Risk Assessment 91
V. Conclusion 92
References 92

6. In Vivo Relationship Between Percutaneous Absorption and Transepidermal Water Loss *95*
André Rougier, Claire Lotte, and Howard I. Maibach
I. Percutaneous Absorption Measurements 95
II. Transepidermal Water Loss Measurements 96
References 104

7. Skin Contamination and Absorption of Chemicals from Water and Soil *107*
Ronald C. Wester and Howard I. Maibach
I. Introduction 107
II. Discussion 116
References 120

8. In Vivo Percutaneous Absorption: A Key Role for Stratum Corneum/Vehicle Partitioning *123*
André Rougier
I. Introduction 123
II. Materials and Methods 123
III. Results 128
IV. Discussion 128
References 136

9. Protein Allergens: Skin as a Route of Exposure *139*
Camilla K. Pease, David A. Basketter, and Ian R. White
I. Summary 139
II. Introduction 139
III. Disease States Involving Protein Absorption in Skin 140
IV. In Vivo Studies Suggesting Proteins Can Be Absorbed Through the Skin 143
V. In Vitro Skin Penetration of Macromolecules 146
VI. Stratum Corneum Structure and Barrier Disruption 148
VII. Conclusions 149
References 150

10. Percutaneous Absorption of Chemical Mixtures *155*
Jim E. Riviere
I. Introduction 155
II. Risk Assessment 156
III. Mechanisms of Interactions 157
IV. Impact of Multiple Interactions 160
V. Conclusions 161
References 162

11. Does Desquamation Reduce Permeation? *165*
Micaela B. Reddy and Annette L. Bunge
I. Introduction 165
II. Modeling Dermal Absorption and Desquamation 166
III. Results and Discussion 167
IV. Conclusions 174
References 175

12. Penetration and Distribution in Human Skin Focusing on the Hair Follicle *177*
Ylva Grams and Joke Bouwstra
I. Abstract 177
II. Skin 178
III. Transdermal and Dermal Delivery 182
IV. Follicular Delivery 183
References 188

13. Evaluation of Stratum Corneum Heterogeneity *193*
Gerald B. Kasting, Matthew A. Miller, and Priya S. Talreja
I. What Is Meant by Skin Heterogeneity 194
II. The Role of Appendages and the Skin's Polar Pathway 194
III. The Role of Corneocytes in the Stratum Corneum Barrier 195
IV. The Influence of Asymmetry on SC Transport 197
V. Discussion 207
VI. Conclusions 208
References 209

14. The Skin Reservoir for Topically Applied Solutes *213*
Michael S. Roberts, Sheree E. Cross, and Yuri G. Anissimov
I. Introduction 213
II. What Is the Skin Reservoir and Why Is Its Understanding in Nature Important? 213
III. Historical Perspective on the Stratum Corneum Reservoir for Drugs 214
IV. Modeling the Formation and Duration of the Stratum Corneum Corticosteroid Reservoir 215
V. Stratum Corneum Reservoir and Epidermal Flux 218
VI. Stratum Corneum Reservoir and Substantivity 218
VII. Modeling the Vasoconstrictor Effect Associated with the Corticosteroid Reservoir 220
VIII. Changes in Plasma Steroid Levels Associated with the Corticosteroid Reservoir 223
IX. Role of Desquamation on Stratum Corneum Reservoir Effect 224
X. Stratum Corneum Reservoir for Other Solutes 226
XI. Viable Epidermis and Dermal Reservoir 228
XII. In Vitro–In Vivo Correlations 230
XIII. Conclusion 231
References 232

15. Effects of Occlusion: Percutaneous Absorption *235*
Hongbo Zhai and Howard I. Maibach
I. Introduction 235
II. Percutaneous Absorption In Vitro 235
III. Percutaneous Absorption In Vivo 237
IV. Discussion 240
References 243

16. Variations of Hair Follicle Size and Distribution in Different Body Sites *247*
Nina Otberg, Heike Richter, Hans Schaefer, Ulrike Blume-Peytavi, Wolfram Sterry, and Jürgen Lademann
I. Introduction 247
II. Materials and Methods 248
III. Results 250
IV. Discussion 253
V. Summary 255
References 255

17. Methodology: In Vivo Methods for Percutaneous Absorption Measurements *257*
Ronald C. Wester and Howard I. Maibach
I. Introduction 257
II. Method Analyses: Atrazine 257

III. Method Analyses: Borates 258
IV. Solvents 260
V. Limitations 261
VI. Discussion 262
References 262

18. Determination of Percutaneous Absorption by In Vitro Techniques *265*
Robert L. Bronaugh, Margaret E. K. Kraeling, and Jeffrey J. Yourick
I. Introduction 265
II. Preliminary Steps 265
III. Diffusion Cell 265
IV. Source of Skin 266
V. Viability of Skin 266
VI. Preparation of Skin 266
VII. Receptor Fluid 266
VIII. Recovery 267
IX. Determination of Absorption 267
X. Expression of Results 268
XI. Conclusions 268
References 268

19. The Fate of Cutaneous Levels of Absorbed Compounds *271*
Robert L. Bronaugh, Margaret E. K. Kraeling, and Jeffrey J. Yourick
I. Introduction 271
II. Modification of Receptor Fluid 271
III. Systemic Absorption 272
IV. Skin Reservoir Formation 272
V. Fate of Absorbed Material in Skin 272
References 275

20. Dermal Decontamination and Percutaneous Absorption *277*
Ronald C. Wester and Howard I. Maibach
I. In Vivo Decontamination Model 277
II. In Vitro Decontamination Model 281
III. Effects of Occlusion and Early Washing 282
IV. Traditional Soap and Water Wash and Emergency Shower 285
V. Conclusion: Substantivity 287
References 288

21. Chemical Partitioning into Powdered Human Stratum Corneum: A Useful In Vitro Model for Studying Interaction of Chemicals and Human Skin *291*
Xiao-Ying Hui, Ronald C. Wester, Hongbo Zhai, and Howard I. Maibach
I. Introduction 291
II. PHSC and Physical–Chemical Properties of Stratum Corneum 292

III. PHSC and Chemical Partitioning 293
IV. PHSC and Percutaneous Absorption 295
V. PHSC and the Skin Barrier Function 295
VI. PHSC and Diseased Skin 296
VII. PHSC and Environmentally Hazardous Chemicals 296
VIII. PHSC and Chemical Decontamination 297
IX. PHSC and Enhanced Topical Formulation 298
X. PHSC and QSAR Predictive Modeling 298
XI. Discussion 300
References 301

22. Percutaneous Absorption of Hazardous Chemicals from Fabric into and Through Human Skin *303*
Ronald C. Wester, Danyi Quan, Rebecca M. Wester, and Howard I. Maibach
I. Introduction 303
II. Glyphosate (Water-Soluble Herbicide) 303
III. Malathion (Lipid-Soluble Pesticide) 305
IV. Parathion (Lipid-Soluble Pesticide) 306
V. Ethylene Oxide (Colorless Gas at Ordinary Room Temperature and Pressure) 307
VI. 2-Butoxyethanol (Vapor) 308
VII. Discussion 309
References 310

23. Human Cadaver Skin Viability for In Vitro Percutaneous Absorption: Storage and Detrimental Effects of Heat-Separation and Freezing *311*
Ronald C. Wester, Julie Christoffel, Tracy Hartway, Nicholas Poblete, Howard I. Maibach, and James Forsell
I. Abstract 311
II. Introduction 312
III. Materials and Methods 312
IV. Results 312
V. Discussion 315
References 316

24. Interrelationships in the Dose–Response of Percutaneous Absorption *317*
Ronald C. Wester and Howard I. Maibach
I. Dose–Response in Real Time 317
II. Pharmacodynamic Dose–Response 319
III. Dose–Response Interrelationships 319
IV. Accountability (Mass Balance) 320
V. Effects of Concentration on Percutaneous Absorption 321
VI. Concentration and Newborns 324

VII. Concentration and Water Temperature 324
VIII. Concentration and Duration of Contact 325
IX. Concentration, Duration of Contact, and Multiple-Dose Application 325
X. Concentration and Surface Area 326
XI. Effect of Application Frequency 326
XII. Application Frequency and Toxicity 327
XIII. Discussion 327
References 328

25. Blood Flow as a Technology in Percutaneous Absorption: The Assessment of the Cutaneous Microcirculation by Laser Doppler and Photoplethysmographic Techniques *331*
Ethel Tur
I. Introduction 331
II. The Method of Laser Doppler 332
III. Concepts and Design of Experimental Studies Using LDF 333
IV. Applications 335
V. Conclusion and Future Prospects 349
References 350

26. Drug Concentration in the Skin *361*
Christian Surber, Fabian P. Schwarb, Eric W. Smith, and Howard I. Maibach
I. Introduction 361
II. Sampling Techniques 362
III. Analytical Techniques 371
IV. C^* Concept: Relationship of Skin Target Site Free Drug Concentration (C^*) to the In Vivo Efficacy 375
V. Conclusion 376
References 376

27. Stripping Method for Measuring Percutaneous Absorption In Vivo *383*
André Rougier, Didier Dupuis, Claire Lotte, and Howard I. Maibach
I. In Vivo Relationship Between Stratum Corneum Concentration and Percutaneous Absorption 384
II. Influence of Application Conditions on the Relationship Between Stratum Corneum Concentration and Percutaneous Absorption 387
References 396

28. Tape-Stripping Technique *399*
Christian Surber, Fabian P. Schwarb, and Eric W. Smith
I. Introduction 399

II. Application of the Tape-Stripping Technique in Dermatopharmacology 399
III. The Potential of the Tape-Stripping Methods 403
IV. Protocol Outline for a Tape-Stripping Experiment 403
V. Unanswered Questions and Concerns 404
VI. Related Techniques 406
VII. Conclusions 407
References 407

29. Percutaneous Drug Delivery to the Hair Follicle *411*
Andrea C. Lauer
I. Introduction 411
II. Considerations for Experimental Design 412
III. Hair Follicle and Sebaceous Gland Anatomy 412
IV. Animal Models 413
V. Methodologies to Assess Follicular Permeation 418
VI. Formulation Effects on Follicular Deposition 422
VII. Summary 426
References 426

30. In Vivo Percutaneous Absorption in Human Volunteers: Exhaled Breath Analysis *429*
Karla D. Thrall and Angela D. Woodstock
I. Introduction 429
II. Materials and Methods 429
III. Results 433
IV. Discussion 435
References 436

31. Relative Contributions of Human Skin Layers to Partitioning of Chemicals with Varying Lipophilicity *439*
Tatiana E. Gogoleva, John I. Ademola, Ronald C. Wester, Philip S. Magee, and Howard I. Maibach
I. Introduction 439
II. Materials and Methods 439
III. Results 441
IV. Conclusion 446
References 446

32. Effect of Single vs. Multiple Dosing in Percutaneous Absorption *449*
Ronald C. Wester and Howard I. Maibach
I. Introduction 449
II. Discussion 456
References 456

33. Electrical Enhancement of Transdermal Delivery of Ultradeformable Liposomes *459*
Ebtessam A. Essa, Michael C. Bonner, and Brian W. Barry
I. Introduction 459
II. Liposomes Under Electrical Potential 461
III. Concluding Remarks 467
References 469

34. In Vitro Release from Semisolid Dosage Forms—What Is Its Value? *473*
Vinod P. Shah
I. Introduction 473
II. In Vitro Release Testing 474
III. Discussion 475
IV. In Vitro Release-Corticosteroids 476
V. Applications 478
VI. Conclusion 479
References 479

35. Chemical Warfare Agent VX Penetration Through Military Uniform and Human Skin: Risk Assessment and Decontamination *481*
Rebecca M. Wester, Howard I. Maibach, and Ronald C. Wester
I. Introduction 481
II. Methodology 482
III. Results 483
IV. Discussion 483
References 487

36. Transepidermal Water Loss Measurements for Assessing Skin Barrier Functions During In Vitro Percutaneous Absorption Studies *489*
Avinash Nangia, Bret Berner, and Howard I. Maibach
I. Introduction 489
II. Methods 490
III. Results and Discussion 491
References 494

37. Assessment of Microneedles for Transdermal Drug Delivery *497*
Mark R. Prausnitz
I. Introduction 497
II. Microneedles for Transdermal Delivery 498
III. Pain, Safety, and Convenience of Microneedles 501
IV. Conclusions 505
References 506

38. Human Percutaneous Absorption and Transepidermal Water Loss (TEWL) Correlation *509*
Ronald C. Wester and Howard I. Maibach
I. Introduction 509
II. Transepidermal Water Loss 514
III. Discussion 519
References 519

39. Natural Nano-Injectors as a Vehicle for Novel Topical Drug Delivery *521*
Tamar Lotan
I. Introduction 521
II. Principal of Operation 522
III Topical Formulation and Application 524
IV. Human Safety 524
V. Immediate Delivery 525
VI. Induction of Local Anesthesia 525
VII. Discussion 526
References 526

40. Human Risk Assessment of Chemical Warfare Agents from Skin Exposure *529*
Ronald C. Wester, Hanafi Tanojo, Xiao-Ying Hui, Hongbo Zhai, Howard I. Maibach, Eugene Olajos, and Harry Salem
I. Abstract 529
II. Introduction 530
III. Discussion 552
References 556

41. The Relationship Between In Vivo Dermal Penetration Studies in Humans and In Vitro Predictions Using Human Skin *561*
Simon C. Wilkinson and Faith M. Williams
I. Introduction 561
II. Studies Comparing In Vitro Absorption in Excised Skin with Human Volunteers or Primates In Vivo 562
III. Microdialysis Studies in Volunteers and In Vitro 570
IV. Conclusions 570
References 572

42. Permethrin Bioavailability and Body Burden for a Uniformed Soldier *575*
Ronald C. Wester, Rebecca M. Wester, and Howard I. Maibach
I. Abstract 575
II. Introduction 576
III. Permethrin 576
IV. Permethrin Pharmacokinetics 576

V. Source for Bioavailability and Body Burden Calculations 577
VI. Discussion 579
References 580

43. The Correlation Between Transepidermal Water Loss and Percutaneous Absorption: An Overview *583*
Jackie Levin and Howard Maibach
I. Abstract 583
II. Introduction 583
III. Discussion 587
IV. Conclusion 591
References 591

44. Percutaneous Penetration as It Relates to the Safety Evaluation of Cosmetic Ingredients *595*
Jeffrey J. Yourick and Robert L. Bronaugh
I. Introduction 595
II. Hazard Identification 596
III. Exposure Estimate 596
IV. Safety Assessments 597
V. Case Study—Exposure Estimate for the Dermally Applied Fragrance Musk XYLOL 599
References 604

45. Percutaneous Absorption of Hair Dyes *605*
Jeffrey J. Yourick and Robert L. Bronaugh
I. Introduction 605
II. Skin Absorption and Metabolism of 2-Nitro-*p*-Phenylenediamine 606
III. Discussion 610
IV. Skin Absorption of Disperse Blue 1 615
V. Hair Dye Absorption: Correlation with Partition Coefficients 619
VI. Conclusion 620
References 621

46. Hair Dye Penetration in Monkey and Man *623*
Leszek J. Wolfram and Howard I. Maibach
I. Experimental 623
II. Results 626
References 633

47. In Vitro Percutaneous Absorption of Triethanolamine in Human Skin *635*
Margaret E. K. Kraeling and Robert L. Bronaugh
I. Introduction 635
II. Materials and Methods 635

III. Analysis 638
IV. Data 638
V. Results 638
VI. Discussion 641
References 642

48. Nail Penetration—Enhance Topical Delivery of Antifungal Drugs by Chemical Modification of the Human Nail *643*
Xiao-Ying Hui, Ronald C. Wester, Sherry Barbadillo, and Howard I. Maibach
I. Introduction 643
II. Review of Nail Physical and Chemical Properties that Affect Topical Penetration 644
III. Methodology 645
IV. Results 648
V. Discussion 650
References 652

49. Topical Dermatological Vehicles: A Holistic Approach *655*
Eric W. Smith, Christian Surber, and Howard I. Maibach
I. Introduction 655
II. Classification of Topical Vehicles 656
III. The Ideal Vehicle 657
IV. The Choice of Vehicle 659
V. Conclusion 660
References 660

50. Measurements of Drug Penetration Using Non-invasive Methods: Fourier Transform Infrared Spectroscopy *663*
S. Wartewig and Reinhard H. H. Neubert
I. Introduction 663
II. Instrumentation 664
III. Penetration of Drugs into Membranes Studied by FT-IR–ATR 669
IV. Penetration of Drugs into Membranes Studied FT-IR–PAS 673
V. Lateral Drug Diffusion Studied by IR Microspectroscopy 676
VI. Conclusion 678
References 678

51. Percutaneous Absorption of Sunscreens *681*
Kenneth A. Walters and Michael S. Roberts
I. Introduction 681
II. Skin Permeation of Sunscreens 682
III. Prediction of the Skin Penetration of Sunscreens 694

IV. Risks and Benefits Associated with Topical Sunscreen Use 695
V. Conclusions 696
References 697

52. Use of Microemulsions for Topical Drug Delivery *701*
Sandra Heuschkel, Anuj Shukla, and Reinhard H. H. Neubert
I. Introduction 701
II. Characterization 702
III. Dermal and Transdermal Drug Delivery Using Microemulsions 708
IV. Conclusion 714
References 715

53. Solid Lipid Nanoparticles (SLN) and Nanostructured Lipid Carriers (NLC) for Dermal Delivery *719*
R. H. Müller, W. Mehnert, and E. B. Souto
I. Introduction 719
II. Definitions 720
III. Production of LIPID Nanoparticles 721
IV. Production of Final Topical Formulations 723
V. Properties of LIPID Particles and Effects on Skin 726
VI. Conclusions and Perspectives 734
References 734

54. Transdermal Transport by Phonophoresis *739*
Laurent Machet and Alain Boucaud
I. Abstract 739
II. Introduction 739
III. Physical Characteristics of Ultrasound 740
IV. Ultrasound-Enhanced Percutaneous Absorption: Pharmacokinetic Data 741
V. Mechanism of Action of Ultrasound on Transdermal Transport 747
VI. Biological Consequences of Ultrasound Application on Skin 751
VII. Stability of Drugs Exposed to Ultrasound 753
VIII. Prospects: Is Painless Needle-Free Injection a Realistic Goal? 754
References 755

55. Percutaneous Penetration of Oligonucleotide Drugs *759*
Myeong Jun Choi, Hongbo Zhai, and Howard I. Maibach
I. Introduction 759
II. Skin Barrier and Functions 760

III. Skin Interaction of Oligonucleotides 760
IV. Oligonucleotides Modification 761
V. Tape Stripping 761
VI. Electroporation and Iontophoresis 762
VII. Antisense Oligonucleotides Semisolid Formulations 763
VIII. Liposomal Formulations 764
IX. First Oligonucleotide Drug: ISIS 2922 765
X. Conclusions 766
References 766

56. Transcutaneous Immunization: Antigen and Adjuvant Delivery to the Skin *769*
Gregory M. Glenn, Sarah A. Frech, Richard T. Kenney, and Larry R. Ellingsworth
I. Introduction 769
II. Background 770
III. Adjuvants and the Skin 771
IV. Optimization of Delivery 771
V. Immune Responses to TCI—Adjuvant and Antigen in a Patch 775
VI. Human Studies 777
VII. Summary 784
References 785

57. Topical Vaccination of DNA Antigens: Topical Delivery of DNA Antigens *789*
Myeong Jun Choi and Howard I. Maibach
I. Introduction 789
II. Skin Barrier and Plasmid DNA Penetration 790
III Stripping vs. Immune Response 790
IV. Electroporation 791
V. Micromechanical Disruption Method 792
VI. Liposome and Liposomal Cream Formulation 793
VII. Microemulsion Delivery System 794
VIII. Th1 and Th2 Response of Topical DNA Vaccine 795
IX. Mechanism of Topical DNA Vaccines 796
X. Topical DNA Vaccines Efficacy 797
XI. Conclusions 797
References 798

58. Topical Dermatological Vehicles: Engineering the Delivery System *801*
C. G. Azzi, J. Zhang, C. H. Purdon, Eric W. Smith, Christian Surber, and Howard I. Maibach
I. Introduction 801
II. Vehicle Effects on Permeation of Drugs Through the Skin 803

III. Novel Transdermal Delivery Vehicles 806
IV. Conclusions 808
References 809

59. Effect of Tape Stripping on Percutaneous Penetration and Topical Vaccination *811*
Myeong Jun Choi, Hongbo Zhai, Harald Löffler, Frank Dreher, and Howard I. Maibach
I. Introduction 811
II. Skin Barrier Function 812
III. Stripping Factors 812
IV. Tape Stripping Vs. Percutaneous Absorption and Penetration 814
V. Tape Stripping and Topical Vaccination 815
VI. Unanswered Questions 817
VII. Conclusion 818
References 818

60. Percutaneous Absorption of Arsenic from Environmental Media *823*
Yvette W. Lowney, Michael V. Ruby, Ronald C. Wester, Rosalind A. Schoof, Stewart E. Holm, Xiao-Ying Hui, Sherry Barbadillo, and Howard I. Maibach
I. Introduction 823
II. Toxicity of Arsenic from Percutaneous Absorption 824
III. Study Design 830
IV. Conclusions 839
References 841

61. Clinical Testing of Microneedles for Transdermal Drug Delivery *843*
Raja K. Sivamani, Gabriel C. Wu, Boris Stoeber, Dorian Liepmann, Hongbo Zhai, and Howard I. Maibach
I. Introduction 843
II. Clinical Studies 845
References 848

62. Skin Impedance–Guided High Throughput Screening of Penetration Enhancers: Methods and Applications *851*
Amit Jain, Pankaj Karande, and Samir Mitragotri
I. Introduction 851
II. Overview of INSIGHT Screening 853
III. Skin Impedance–Skin Permeability Correlation 855
IV. Validation of INSIGHT with FDCs 857
V. Applications of INSIGHT Screening 858
References 860

Index *865*

Contributors

John I. Ademola Department of Dermatology, School of Medicine, University of California, San Francisco, California, U.S.A.

Yuri G. Anissimov Department of Medicine, University of Queensland, Princess Alexandra Hospital, Woolloongabba, Queensland, Australia

C. G. Azzi College of Pharmacy, University of South Carolina, Columbia, South Carolina, U.S.A.

Sherry Barbadillo Department of Dermatology, School of Medicine, University of California, San Francisco, California, U.S.A.

Brian W. Barry University of Bradford, Bradford, U.K.

Saqib J. Bashir Department of Dermatology, School of Medicine, University of California, San Francisco, California, U.S.A.

David A. Basketter SEAC, Unilever Colworth Laboratory, Sharnbrook Bedford, U.K.

Bret Berner Cygnus, Redwood City, California, U.S.A.

Ulrike Blume-Peytavi Humboldt University Berlin, Berlin, Germany

Michael C. Bonner University of Bradford, Bradford, U.K.

Alain Boucaud Université François-Rabelais, Laboratoire Ultrasons Signaux Instrumentation (CNRS FRE 2448), University Hospital of Tours, Tours, France

Joke Bouwstra Department of Drug Delivery Technology, Leiden Amsterdam Center for Drug Research, Leiden University, Leiden, The Netherlands

Robert L. Bronaugh Office of Cosmetics and Colors, Food and Drug Administration, Laurel, Maryland, U.S.A.

Daniel Bucks School of Medicine, University of California, San Francisco and Dow Pharmaceutical Sciences, Petaluma, California, U.S.A.

Annette L. Bunge Chemical Engineering Department, Colorado School of Mines, Golden, Colorado, U.S.A.

Myeong Jun Choi Charmzone Research and Development Center, 1702-1 Taejang 2-dong, Wonju, Kangwon-do, Korea

Julie Christoffel Department of Dermatology, School of Medicine, University of California, San Francisco, California, U.S.A.

Sheree E. Cross Department of Medicine, University of Queensland, Princess Alexandra Hospital, Woolloongabba, Queensland, Australia

Frank Dreher Department of Dermatology, School of Medicine, University of California, San Francisco, California, U.S.A.

Didier Dupuis Laboratoires de Recherche Fondamentale, L'Oréal, Aulnay sous Bois, France

Larry R. Ellingsworth IOMAI Corporation, Gaithersburg, Maryland, U.S.A.

Ebtessam A. Essa University of Bradford, Bradford, U.K.

James Forsell Northern California Transplant Bank, San Rafael, California, U.S.A.

Sarah A. Frech IOMAI Corporation, Gaithersburg, Maryland, U.S.A.

Gregory M. Glenn IOMAI Corporation, Gaithersburg, Maryland, U.S.A.

Tatiana E. Gogoleva Department of Dermatology, School of Medicine, University of California, San Francisco, California, U.S.A.

Ylva Grams Department of Drug Delivery Technology, Leiden Amsterdam Center for Drug Research, Leiden University, Leiden, The Netherlands

Tracy Hartway Department of Dermatology, University of California, San Francisco, California, U.S.A.

Sandra Heuschkel Department of Pharmacy, Institute of Pharmaceutics and Biopharmaceutics, Martin-Luther-University Halle-Wittenberg, Halle (Saale), Germany

Stewart E. Holm Georgia-Pacific Corporation, Atlanta, Georgia, U.S.A.

Xiao-Ying Hui Department of Dermatology, School of Medicine, University of California, San Francisco, California, U.S.A.

Amit Jain University of California, Santa Barbara, California, U.S.A.

Pankaj Karande University of California, Santa Barbara, California, U.S.A.

Gerald B. Kasting College of Pharmacy, University of Cincinnati, Cincinnati, Ohio, U.S.A.

Richard T. Kenney IOMAI Corporation, Gaithersburg, Maryland, U.S.A.

Margaret E. K. Kraeling Office of Cosmetics and Colors, Food and Drug Administration, Laurel, Maryland, U.S.A.

Jürgen Lademann Humboldt University Berlin, Berlin, Germany

Andrea C. Lauer Senior Clinical Scientist/Global Medical Marketing, South San Francisco, California, U.S.A.

Jackie Levin Department of Dermatology, School of Medicine, University of California, San Francisco, California, U.S.A.

Dorian Liepmann University of California, Berkeley, California, U.S.A.

Harald Löffler Philipp University of Marburg, Marburg, Germany

Tamar Lotan NanoCyte Inc., Research Center, Jordan Valley, Israel

Claire Lotte Laboratoires de Recherche Fondamentale, L'Oréal, Aulnay sous Bois, France

Yvette W. Lowney Exponent, Boulder, Colorado, U.S.A.

Laurent Machet Department of Dermatology, Université François-Rabelais, University Hospital of Tours, Tours, France

Philip S. Magee Department of Dermatology, School of Medicine, University of California, San Francisco, California, U.S.A.

Howard I. Maibach Department of Dermatology, School of Medicine, University of California, San Francisco, California, U.S.A.

W. Mehnert Department of Pharmacy, Free University of Berlin, Berlin, Germany

Matthew A. Miller College of Pharmacy, University of Cincinnati, Cincinnati, Ohio, U.S.A.

Samir Mitragotri University of California, Santa Barbara, California, U.S.A.

R. H. Müller Department of Pharmacy, Free University of Berlin, Berlin, Germany

Avinash Nangia ALZA Corporation, Palo Alto, California, U.S.A.

Reinhard H. H. Neubert Department of Pharmacy, Institute of Pharmaceutics and Biopharmaceutics, Martin-Luther-University Halle-Wittenberg, Halle (Saale), Germany

Eugene Olajos Aberdeen Proving Grounds, Aberdeen, Maryland, U.S.A.

Nina Otberg Humboldt University Berlin, Berlin, Germany

Camilla K. Pease SEAC, Unilever Colworth Laboratory, Sharnbrook, Bedford, U.K.

Nicholas Poblete Department of Dermatology, School of Medicine, University of California, San Francisco, California, U.S.A.

Mark R. Prausnitz Schools of Chemical and Biomedical Engineering, Georgia Institute of Technology, Atlanta, Georgia, U.S.A.

C. H. Purdon College of Pharmacy, University of South Carolina, Columbia, South Carolina, U.S.A.

Danyi Quan School of Medicine, University of California, San Francisco, California, U.S.A.

Micaela B. Reddy Quantitative and Computational Toxicology Group, Center for Environmental Toxicology and Technology, Colorado State University, Fort Collins, Colorado, U.S.A.

Heike Richter Humboldt University Berlin, Berlin, Germany

Jim E. Riviere Center for Chemical Toxicology, Research, and Pharmacokinetics, College of Veterinary Medicine, North Carolina State University, Raleigh, North Carolina, U.S.A.

Michael S. Roberts Department of Medicine, University of Queensland, Princess Alexandra Hospital, Woolloongabba, Queensland, Australia

André Rougier Laboratoire Pharmaceutique, La Roche-Posay, Courbevoie, France

Michael V. Ruby Exponent, Boulder, Colorado, U.S.A.

Harry Salem Aberdeen Proving Grounds, Aberdeen, Maryland, U.S.A.

Hans Schaefer Humboldt University Berlin, Berlin, Germany

Rosalind A. Schoof Integral Consulting, Mercer Island, Washington, U.S.A.

Fabian P. Schwarb Institut für Spital-Pharmazie, Universitätskliniken, Kantonsspital, Basel, Switzerland

Vinod P. Shah Food and Drug Administration, Rockville, Maryland, U.S.A.

Anuj Shukla Department of Pharmacy, Institute of Pharmaceutics and Biopharmaceutics, Martin-Luther-University Halle-Wittenberg, Halle (Saale), Germany

Raja K. Sivamani UCSF/UC Berkeley Joint Department of Bioengineering, University of California, San Francisco, California, U.S.A.

Eric W. Smith College of Pharmacy, University of South Carolina, Columbia, South Carolina, U.S.A.

E. B. Souto Department of Pharmacy, Free University of Berlin, Berlin, Germany

Wolfram Sterry Humboldt University Berlin, Berlin, Germany

Boris Stoeber University of California, Berkeley, California, U.S.A.

Christian Surber Institut für Spital-Pharmazie, Universitätskliniken, Kantonsspital, Basel, Switzerland

Priya S. Talreja College of Pharmacy, University of Cincinnati, Cincinnati, Ohio, U.S.A.

Hanafi Tanojo Department of Dermatology, School of Medicine, University of California, San Francisco, California, U.S.A.

Karla D. Thrall Battelle, Pacific Northwest Laboratory, Richland, Washington, U.S.A.

Ethel Tur Department of Dermatology, Sourasky Medical Center, Tel Aviv University, Tel Aviv, Israel

Kenneth A. Walters Control Delivery Systems Inc., Watertown, Massachusetts, U.S.A.

S. Wartewig Institute of Applied Dermatopharmacy, Martin-Luther-University Halle-Wittenberg, Halle (Saale), Germany

Ronald C. Wester Department of Dermatology, School of Medicine, University of California, San Francisco, California, U.S.A.

Rebecca M. Wester Methodist Health System, Dallas, Texas, U.S.A.

Ian R. White St. John's Institute of Dermatology, St. Thomas' Hospital, London, U.K.

Simon C. Wilkinson Health Protection Agency, Newcastle upon Tyne, U.K.

Faith M. Williams University of Newcastle, Newcastle upon Tyne, U.K.

Leszek J. Wolfram Clairol Inc., Stamford, Connecticut, U.S.A.

Angela D. Woodstock Battelle, Pacific Northwest Laboratory, Richland, Washington, U.S.A.

Gabriel C. Wu UCSF/UC Berkeley Joint Department of Bioengineering, University of California, San Francisco, California, U.S.A.

Jeffrey J. Yourick Office of Cosmetics and Colors, Food and Drug Administration, Laurel, Maryland, U.S.A.

Hongbo Zhai Department of Dermatology, School of Medicine, University of California, San Francisco, California, U.S.A.

J. Zhang College of Pharmacy, University of South Carolina, Columbia, South Carolina, U.S.A.

1

Mathematical Models in Percutaneous Absorption

Michael S. Roberts and Yuri G. Anissimov
Department of Medicine, University of Queensland, Princess Alexandra Hospital, Woolloongabba, Queensland, Australia

A number of mathematical models have been used to describe percutaneous absorption kinetics. In general, most of these models have used either diffusion or compartmental-based equations. The object of any mathematical model is to (a) be able to represent the processes associated with absorption accurately, (b) be able to describe/summarize experimental data with parametric equations or moments, and (c) predict kinetics under varying conditions. However, in describing the processes involved, some developed models often suffer from being too complex to be practically useful. In this chapter, we have attempted to approach the issue of mathematical modeling in percutaneous absorption from four perspectives. These are to (a) describe simple practical models, (b) provide an overview of the more complex models, (c) summarize some of the more important/useful models used to date, and (d) examine some practical applications of the models. This chapter revises an earlier one (1) incorporating some of the more recent findings.

The range of processes involved in percutaneous absorption and considered in developing the mathematical models in this chapter are shown in Figure 1. We initially address in vitro skin diffusion models and consider (a) constant donor concentration and receptor conditions, (b) the corresponding flux, donor, skin, and receptor amount–time profiles for solutions, and (c) amount and flux–time profiles when the donor phase is removed. More complex issues such as finite volume donor phase, finite volume receptor phase, the presence of an efflux rate constant at the membrane–receptor interface, and two-layer diffusion are then considered. We then look at specific models and issues concerned with (a) release from topical products, (b) use of compartmental models as alternatives to diffusion models, (c) concentration-dependent absorption, (d) modeling of skin metabolism, (e) role of solute–skin–vehicle interactions, (f) effects of vehicle loss, (g) shunt transport, and (h) in vivo diffusion, compartmental, physiological, and deconvolution models. We conclude by examining topics such as (a) deep tissue penetration, (b) pharmacodynamics, (c) iontophoresis, (d) sonophoresis, and (e) pitfalls in modeling.

Each model is described in diagrammatic and equation form. Given that the analytical solution to most models is in the form of infinite series, often involving

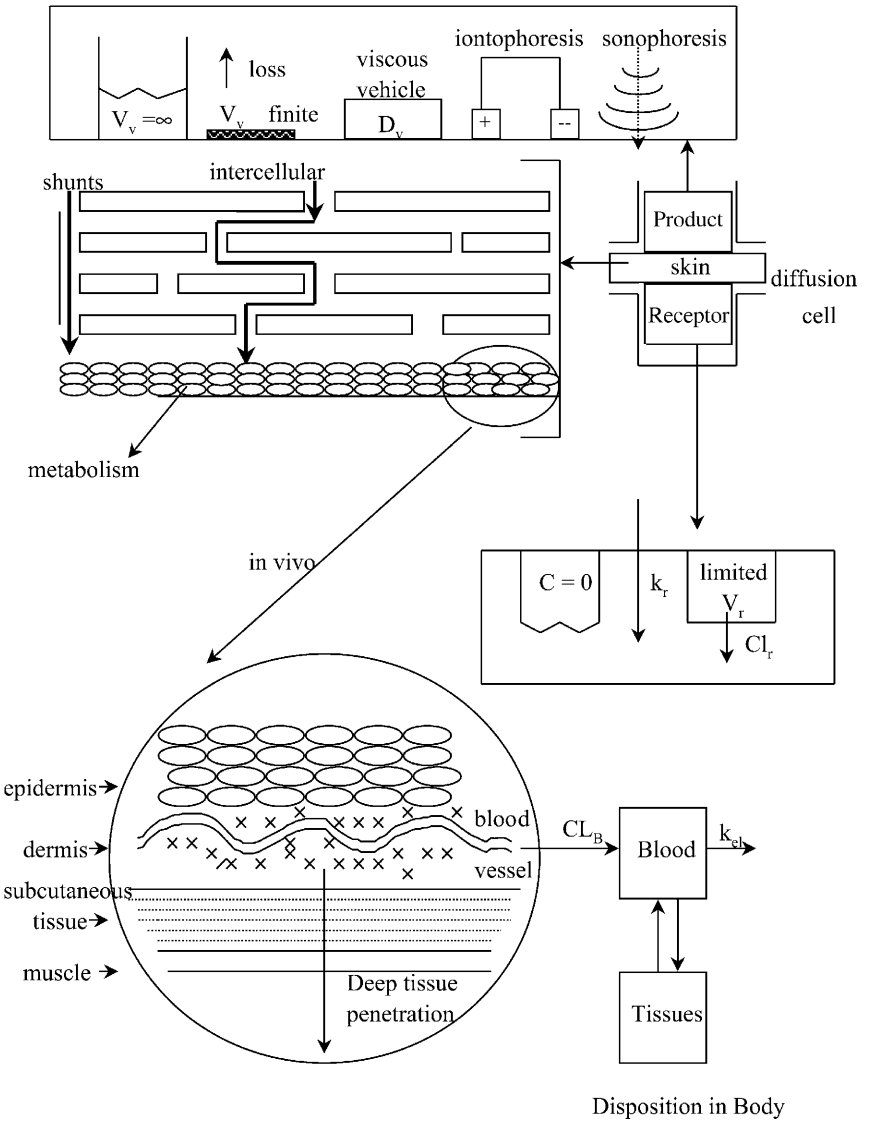


Figure 1 Diagrammatic overview of percutaneous processes associated with mathematical models.

solutions to transcendental equations, we have emphasized the Laplace domain and steady state solutions. Most nonlinear regression programs such as MULTI FILT, MINIM, and SCIENTIST enable analysis of concentration–time data using numerical inversion of Laplace domain solutions and avoid some of the computational difficulties associated with series solutions especially those involving solving transcendental equations. The steady state solutions describing the linear portion of a cumulative amount versus time profile for a constant donor concentration are of great practical use, being described by a linear equation with lag time and steady state flux as the intercept and the slope, respectively. In order to make equations in this chapter as useable as possible each equation has been presented in non-dimensionless form (all variables have their normal dimensions). Simulations and

nonlinear regressions presented in this review were undertaken using either SCIENTIST 2.01 or MINIM 3.09.

I. IN VITRO SKIN DIFFUSION MODELS IN PERCUTANEOUS ABSORPTION

We consider first mathematical models associated with solute penetration through excised skin. The simplest of these models is when a well-stirred vehicle of infinite volume is applied to the stratum corneum (SC) and the solute passes into a receptor sink (Fig. 2A). Increasing complexity of the models arise when the vehicle volume is finite (Fig. 2B), when the receptor is no longer a sink (Fig. 2C), and when the vehicle cannot be considered well-stirred (Fig. 2D). We examine each of these models in terms of expressions for amount penetrating, flux, and, where possible, summary parameters such as mean absorption time, normalized variance, peak time for flux, and maximum flux.

A. In Vitro Skin Permeability Studies with a Constant Donor Concentration and Sink Receptor Conditions

Most in vitro skin permeability studies are carried out assuming that both (a) the concentration of solute in a vehicle applied to the skin and (b) the sink conditions provided by the receptor remain constant over the period of the study. Significant depletion of solute in the donor vehicle or an inadequate receptor sink requires more complex modeling as discussed later. If transport through the SC is rate limiting, the steady-state approximation of amount of solute absorbed (Q) when concentration C_v is applied to an area of application (A) for an exposure time (T) is given in Equation (1) (see Ref. 2):

$$Q = k_p A C_v (T - lag) \tag{1}$$

where k_p is the permeability coefficient (unit: cm/h) of the SC. In reality, absorption does not cease after removal of the vehicle so that the overall absorption is slightly over $k_p A C_v T$. The permeability coefficient in Equation (1) is normally defined in terms of the dimensionless partition coefficient between the SC and vehicle (K_m) and D_m, the diffusivity of a solute in SC over a diffusion path length h_m:

$$k_p = \frac{K_m D_m}{h_m} \tag{2}$$

K_m is defined as the ratio of solute concentrations in the SC (C_m) and vehicle (C_v) under equilibrium i.e., $K_m = C_m/C_v$.

In practice, the permeability coefficient k_p is a composite parameter. When solute transport occurs via both a lipid pathway of permeability coefficient $k_{p.lipid}$ and a polar pathway of permeability coefficient $k_{p.polar}$, an aqueous boundary layer of the epidermis provides a rate limiting permeability coefficient $k_{p.aqueous}$, k_p is more properly expressed as:

$$k_p = \left(\frac{1}{k_{p.lipid} + k_{p.polar}} + \frac{1}{k_{p.aqueous}} \right)^{-1} \tag{3}$$

As discussed by Roberts and Walters (2), for most solutes, $k_p \approx k_{p.lipid}$.

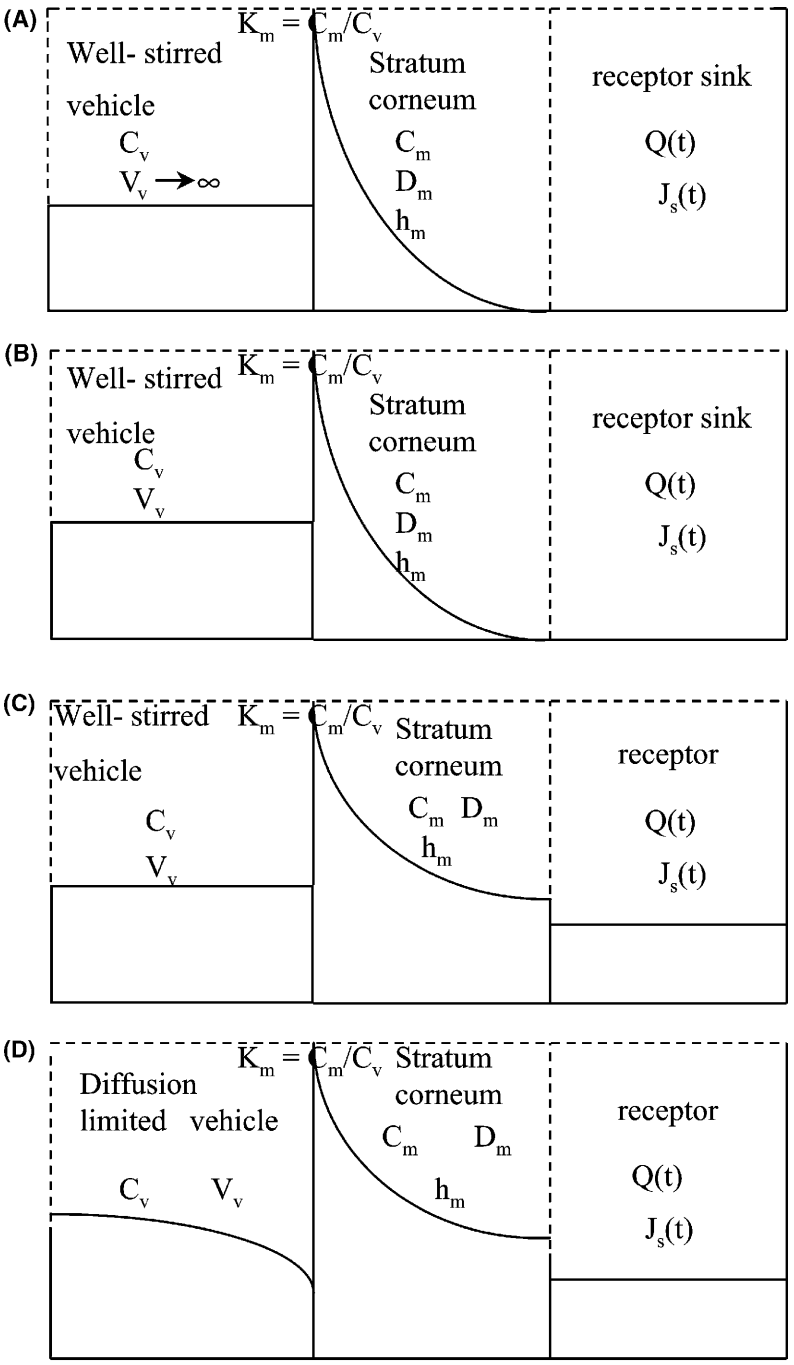


Figure 2 In vitro skin models of transport. (**A**)Well-stirred vehicle containing solute concentration C_v in volume V_v (where $V_v = \infty$) adjacent to assumed homogenous SC with solute concentration C_m at distance x from applied vehicle. Solute moves with a diffusion coefficient D_m over an effective pathlength h_m and penetrates into a receptor sink to give an amount penetrated $Q(t)$ in time t or flux $J(t)$. (**B**) as for (**A**), but with V_v finite. (**C**) as for (B) but the receptor is not a sink. (**D**) as for (**B**) but the vehicle is not well-stirred.

Absorption is more commonly expressed in terms of the steady state flux J_{ss} or the absorption rate per unit area:

$$J_{ss} = \frac{Q}{A(T - lag)} = k_p C_v \tag{4}$$

Equations (1) and (4) are the simplified forms of a more complex expression based on the solution of the diffusion equation for transport of solute in the skin:

$$\frac{\partial C_m}{\partial t} = D_m \frac{\partial^2 C_m}{\partial x^2} \tag{5}$$

the initial condition:

$$C_m(x, 0) = 0 \tag{6}$$

and boundary conditions:

$$C_m(0, t) = K_m C_v \tag{7}$$

$$C_m(h_m, t) = 0 \tag{8}$$

Traditionally Equation (5) is solved in terms of the amount of solute $Q(t)$ exiting from the membrane in time t and expressed as a series solution (3):

$$Q(t) = -D_m A \int_0^t \left.\frac{\partial C_m}{\partial x}\right|_{x=h_m} dt = K_m A C_v h_m \left(\frac{t}{t_d} - \frac{1}{6} - \frac{2}{\pi^2}\sum_{n=1}^{\infty}\frac{(-1)^n}{n^2}\exp\left(-\frac{t}{t_d}\pi^2 n^2\right)\right) \tag{9}$$

where the diffusion time is given by:

$$t_d = \frac{h_m^2}{D_m} \tag{10}$$

It should be noted that as the exponent of a very large negative number approaches zero, the summation term in Equation (9) can be ignored at long times so that Equation (9) reduces to the form of Equation (1):

$$Q(t) = K_m A C_v h_m \left(\frac{D_m t}{h_m^2} - \frac{1}{6}\right) = k_p A C_v \left(t - \frac{h_m^2}{6D_m}\right) = k_p A C_v (t - \text{lag}) \tag{11}$$

where lag is given by:

$$\text{lag} = \frac{h_m^2}{6D_m} = \frac{t_d}{6} \tag{12}$$

Given the advent of numerical Fast Inverse Laplace Transforms (FILT) (4–6) with nonlinear regression modeling, we would normally analyze cumulative amount vs. time data numerically inverting from the Laplace domain using Equation (13), where s is the Laplace variable:

$$\widehat{Q}(s) = -D_m A \frac{1}{s}\left.\frac{\partial \widehat{C}_m}{\partial x}\right|_{x=h_m} = \frac{k_p A C_v}{s^2}\frac{\sqrt{s t_d}}{\sinh\sqrt{s t_d}} \tag{13}$$

Figure 3 shows a plot of the cumulative amount penetrated for the diffusion [Eq. (13), curve 2] and steady state [Eq. (11), curve 1] models versus time. Equation (9) or (13) can be used to analyze in vitro experimental data by nonlinear regression as shown in Figure 4.

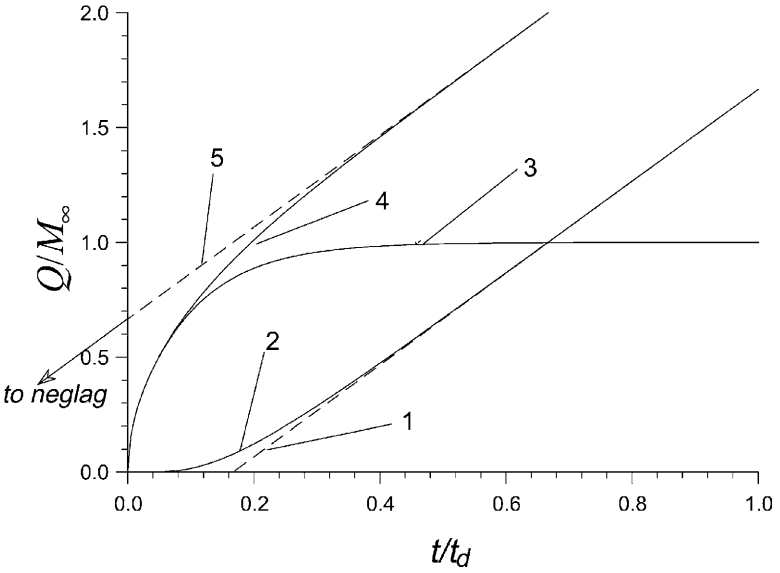


Figure 3 Normalized cumulative amount of solute penetrating Q/M_∞ [curve 2, Eq. (13)]; taken up by the SC [curve 3, Eq. (15)]; and leaving vehicle [curve 4, Eq. (18)] with normalized time. Curves 1 and 5 represent steady-state approximations of the cumulative amount penetrating the SC [Eq. (11)] and leaving the vehicle [Eq. (17)] with normalized time.

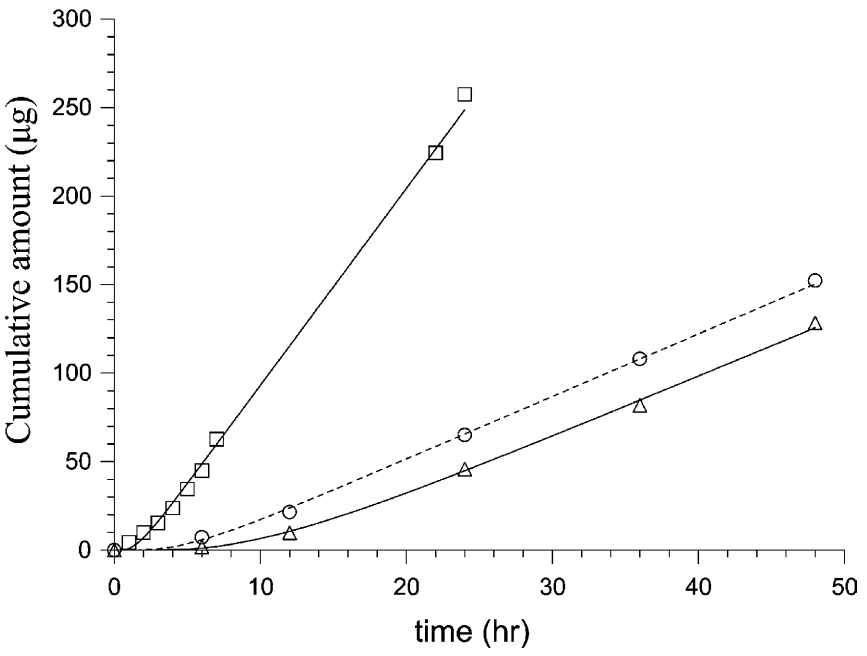


Figure 4 Nonlinear regressions of cumulative amount penetrating human epidermis with time using Equation (13) and a weighting of $1/y_{obs}$. Data corresponds to triethanolamine salicylate [□, $t_d = 9.8$ hr, $J_{ss} = 11.1$ μg/hr, diclofenac skin 1 (○, $t_d = 32.7$ hr, $J_{ss} = 3.5$ μg/hr) and diclofenac skin 2 (Δ, $t_d = 68.0$ hr, $J_{ss} = 3.8$ μg/hr)].

Figure 3 (curve 3) also shows the amount of solute taken up by the SC with time. These profiles are of interest for those solutes that may be targeted for retention in this tissue, e.g., sunscreens, or that may be sequestered in this tissue, e.g., steroids. The time domain and Laplace domain solutions for the amount of solute $M(t)$ taken up into an assumed homogeneous SC with time are:

$$M(t) = M_\infty \left\{ 1 - \frac{8}{\pi^2} \sum_{n=0}^{\infty} \frac{1}{(2n+1)^2} \exp\left[-\frac{t}{t_\mathrm{d}} \pi^2 (2n+1)^2 \right] \right\} \tag{14}$$

$$\widehat{M}(s) = M_\infty \frac{2}{s} \frac{\cosh \sqrt{st_\mathrm{d}} - 1}{\sqrt{st_\mathrm{d}} \sinh \sqrt{st_\mathrm{d}}} \tag{15}$$

where M_∞ is the amount of solute in the skin at steady state and is given when a linear concentration gradient is assumed.

The summation of $Q(t)$ and $M(t)$ yields the expression for the amount, which leaves the vehicle $Q_\mathrm{in}(t)$ (the profile shown in Fig. 3, curve 4):

$$Q_\mathrm{in}(t) = K_\mathrm{m} A C_\mathrm{v} h_\mathrm{m} \left[\frac{t}{t_\mathrm{d}} + \frac{1}{3} - \frac{2}{\pi^2} \sum_{n=1}^{\infty} \frac{1}{n^2} \exp\left(-\frac{t}{t_\mathrm{d}} \pi^2 n^2 \right) \right] \tag{16}$$

When $t \to \infty$, Equation (16) reduces to:

$$Q_\mathrm{in}(t) = K_\mathrm{m} A C_\mathrm{v} h_\mathrm{m} \left(\frac{t}{t_\mathrm{d}} + \frac{1}{3} \right) = k_\mathrm{p} A C_\mathrm{v} \left(t + \frac{t_\mathrm{d}}{3} \right) = k_\mathrm{p} A C_\mathrm{v} (t + \mathrm{neglag}) \tag{17}$$

Hence, the linear portion of $Q_\mathrm{in}(t)$ vs. t has a slope of $k_\mathrm{p} A C_\mathrm{v}$ and intercepts on the negative side of the time axis at a point of neglag $= = t_\mathrm{d}/3 = {h_m}^2/3D_\mathrm{m}$ (Fig. 3, curve 5).

The corresponding Laplace domain expression for $Q_\mathrm{in}(t)$ is:

$$\widehat{Q}_\mathrm{in}(s) = \frac{k_\mathrm{p} A C_\mathrm{v}}{s^2} \sqrt{st_\mathrm{d}} \operatorname{cotanh} \sqrt{st_\mathrm{d}} \tag{18}$$

The absorption rate or flux of solutes in the period before steady state is important for many agents applied topically for local effects and in the toxicology of agents applied to the skin. The flux of solutes exiting membrane per unit area of membrane, $J_\mathrm{s}(t)$, is defined by $J_\mathrm{s}(t) = (1/A)\, \partial Q/\partial t$ or $\widehat{J}_s(s) = s\widehat{Q}(s)/A$ in the Laplace domain. Using Equations (9) and (13) we find therefore:

$$J_\mathrm{s}(t) = -D_\mathrm{m} \frac{\partial C_\mathrm{m}}{\partial x}_{|x=h_\mathrm{m}} = k_\mathrm{p} C_\mathrm{v} \left[1 + 2 \sum_{n=1}^{\infty} (-1)^n \exp\left(-\frac{t}{t_d} \pi^2 n^2 \right) \right] \tag{19}$$

$$\widehat{J}_\mathrm{s}(s) = \frac{k_\mathrm{p} C_\mathrm{v}}{s} \frac{\sqrt{st_\mathrm{d}}}{\sinh(\sqrt{st_\mathrm{d}})} \tag{20}$$

The corresponding equation for the flux of solute from the vehicle into the membrane, $J_{in}(t)$, is:

$$J_\mathrm{in}(t) = k_\mathrm{p} C_\mathrm{v} \left[1 + 2 \sum_{\mathrm{n}=1}^{\infty} \exp\left(-\frac{t}{t_\mathrm{d}} \pi^2 n^2 \right) \right] \tag{21}$$

$$\widehat{J}_\mathrm{in}(s) = \frac{k_\mathrm{p} C_\mathrm{v}}{s} \sqrt{st_\mathrm{d}} \operatorname{cotanh} \sqrt{st_\mathrm{d}} \tag{22}$$

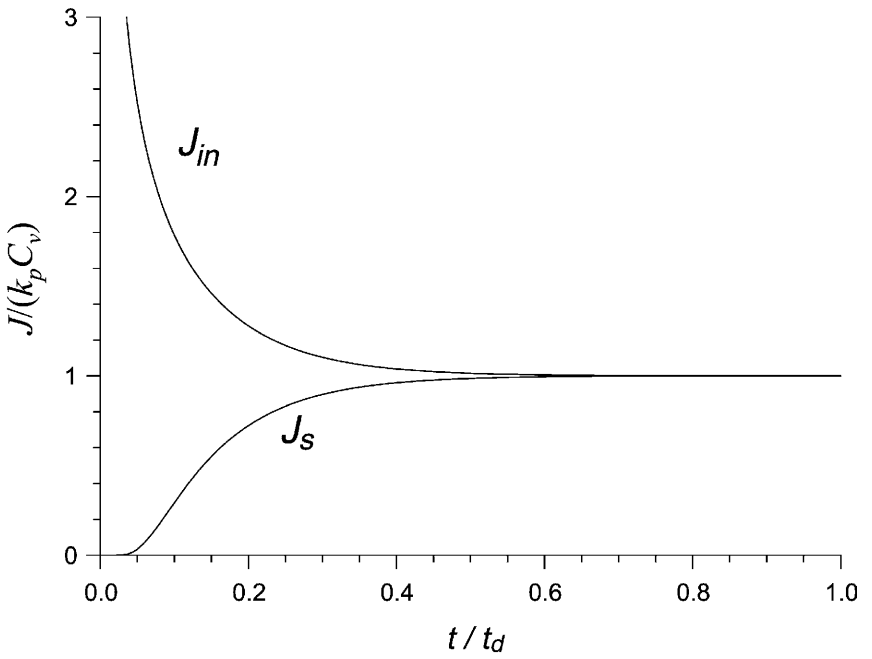


Figure 5 Normalized flux (J/k_pC_v) against normalized time (t/t_d) for flux of solutes penetrating the SC [J_s, Eq. (20)] and entering the SC [J_{in}, Eq. (22)].

Figure 5 shows the flux profiles for solutes leaving the membrane and vehicle, respectively.

B. Amount and Flux–Time Profiles on Removing the Donor Phase After Reaching the Steady State for Conditions Described in sec. I.A

We now consider the amount and flux–time profiles for the specific case in which the donor phase has been removed after a steady state has been reached. This equates to a number of practical cases of interest such as patch removal, sunscreen, and other products and toxins being washed and removed from the skin, when the assumption can be made that there has not been a significant ($>10\%$) depletion in the concentration of solute at the surface. The amount absorbed into a systemic circulation across the skin from the time the dosage form is removed is given by:

$$Q(t) = M_\infty \left\{ 1 - \frac{4}{\pi^3} \sum_{n=0}^{\infty} \frac{(-1)^n}{[n + (1/2)]^3} \exp\left[-\frac{t}{t_d} \pi^2 \left(n + \frac{1}{2} \right)^2 \right] \right\} \tag{23}$$

where $M_\infty = K_m C_v A h_m / 2 = k_p A C_v t_d / 2$ is amount of solute present in the skin before removed of the vehicle. The Laplace domain equivalent of this expression is:

$$\widehat{Q}(s) = \frac{M_\infty}{s^2} \frac{2}{t_d} \left(1 - \frac{1}{\cosh \sqrt{s t_d}} \right) \tag{24}$$

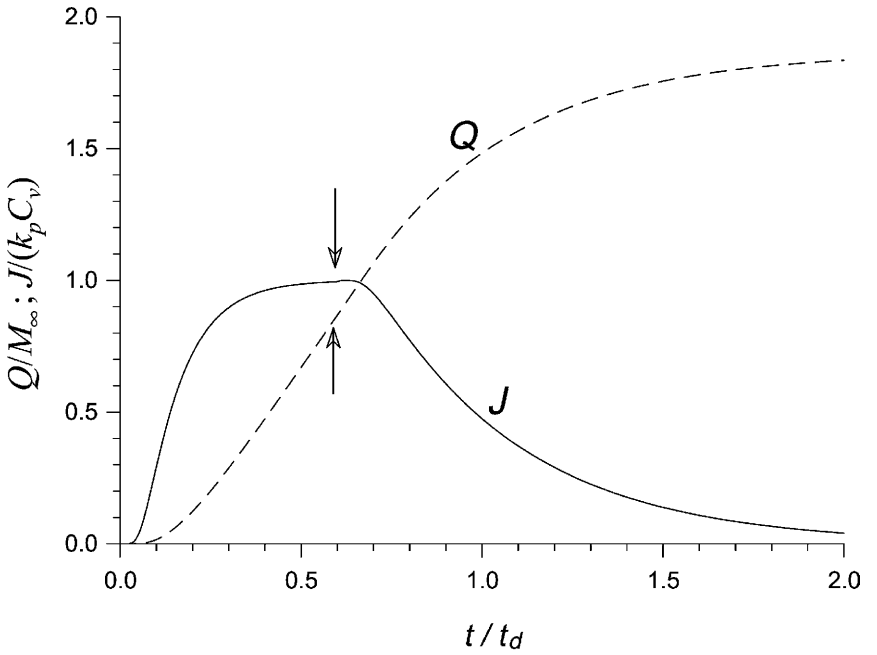


Figure 6 Changes in normalized cumulative amounts penetrating (Q/M_∞) and flux (J/k_pC_v) when the vehicle is removed (as indicated by *arrows*) at a specific normalized time (t/t_d) after application.

The corresponding equations for flux are:

$$J_s(t) = k_p C_v \frac{2}{\pi} \sum_{n=0}^{\infty} \frac{(-1)^n}{n + (1/2)} \exp\left[-\frac{t}{t_d} \pi^2 \left(n + \frac{1}{2} \right)^2 \right] \tag{25}$$

$$\widehat{J}_s(s) = \frac{k_p C_v}{s} \left(1 - \frac{1}{\cosh \sqrt{s t_d}} \right) \tag{26}$$

Figure 6 shows the amount and flux–time profiles associated with donor phase removal.

The mean time for absorption of solute from the skin in this case is given by:

$$\text{MAT} = \frac{\int_0^\infty J_s(t) t \mathrm{d}t}{\int_0^\infty J_s(t) \mathrm{d}t} = -\lim_{s \to 0} \frac{\mathrm{d}}{\mathrm{d}s} \ln(\widehat{J}_s) = \frac{5 h_m^2}{12 D_m} = \frac{5}{12} t_d \tag{27}$$

and the amount absorbed after infinite time is the amount in the skin before the vehicle is removed, which is equal to M_∞.

Given the complexity of solute–distance–time profiles in membranes, the expressions for these profiles are not reproduced here. However, it should be emphasized that these may be important as illustrated in the use of in vivo ATR–FTIR to examine the kinetics of solute uptake into human SC in vivo (7).

C. In Vitro Permeability Studies with a Constant Donor Concentration and Finite Receptor Volume

In most in vitro studies, it is assumed that sink conditions apply in the receptor phase. However, the receptor phase is a finite volume and solute accumulation

may be possible if there is an inadequate removal rate of the solute penetrating through. Siddiqui et al. (8) related the steady state flux of steroids through human epidermis to the differences in concentrations between donor C_v and receptor C_{ss} concentrations. In the present notation, this equation is:

$$J_{ss} = k_p\left(C_v - \frac{C_{ss}}{K_r}\right) \tag{28}$$

where K_r is the partition coefficient between the membrane and vehicle $K_r = C_r/C_v$ and K_m is the partition coefficient between the membrane and vehicle $K_m = C_m/C_v$. Siddiqui et al. (8) assumed that $K_r = 1$.

Implicit in the underlying boundary conditions for the receptor phase is a constant clearance of solute Cl_r, due to repeated sampling or use of a flow through cell. If such a clearance was absent, C_{ss} would continually increase and approach C_vK_r. The value of C_{ss} is defined by the relative magnitudes of the clearance Cl_r and k_pA/K_r:

$$C_{ss} = \frac{k_pAC_v}{Cl_r + (k_pA/K_r)} \tag{29}$$

Siddiqui et al. (8) also applied this equation and the dermal clearance of solutes Cl_r to predict the steady state epidermal concentrations of solutes C_{ss}. Roberts (9) considered the limits of large k_pA as exists for phenols absorption and low k_pA as exists for steroid absorption. He suggested that, when $k_pA \gg K_rCl_r$ C_{ss} would eventually approach the donor concentrations used (C_vK_r). In contrast, when $k_pA \ll K_rCl_r$ C_{ss} approaches k_pAC_v/Cl_r.

The derivation of the full equation, from which steady state Equations (28) and (29) arise, needs to take into account a finite receptor or epidermis volume. The boundary condition at $x = h_m$ in this case is $C_m(h_m, t)/K_m = C_r(t)/K_r$, together with (10):

$$V_r\frac{dC_r}{dt} = -AD_m\frac{\partial C_m}{\partial x}_{|x=h_m} - Cl_rC_r \tag{30}$$

where Cl_r is the clearance (mL/min) of solution containing solute from the receptor phase, V_r is the volume of the receptor, and C_r is the concentration in the receptor.

Using this boundary condition together with boundary condition (7) yields for the amount of solute, which penetrated the skin into the receptor (= amount in receptor + amount cleared from receptor), and for the flux of solute into the receptor (9):

$$\widehat{Q}(s) = \frac{k_pAC_v}{s^2}\frac{\sqrt{st_d}}{\sinh\sqrt{st_d} + \{[\sqrt{st_d}/(st_dV_{rN} + Cl_{rN})]\cosh\sqrt{st_d}\}} \tag{31}$$

$$\widehat{J}_s(s) = \frac{k_pC_v}{s}\frac{\sqrt{st_d}}{\sinh\sqrt{st_d} + \{[\sqrt{st_d}/(st_dV_{rN} + Cl_{rN})]\cosh\sqrt{st_d}\}} \tag{32}$$

where dimensionless parameter $Cl_{rN} = Cl_rK_r/(k_pA)$is a measure of the magnitude of the removal rate from the receptor phase (Cl_r) relative to transport through the membrane (k_pA) and $V_{rN} = V_rK_r/V_mK_m$ is the dimensionless receptor volume defined as the ratio of the amount of drug in the receptor phase and membrane (C_rV_r/C_mV_m) assuming equilibrium exists between phases.

Figure 7 shows the effect of receptor volume (as defined by V_{rN}) and clearance of solution from the receptor phase (as defined by Cl_{rN}) on $J_s(t)$–time profile.

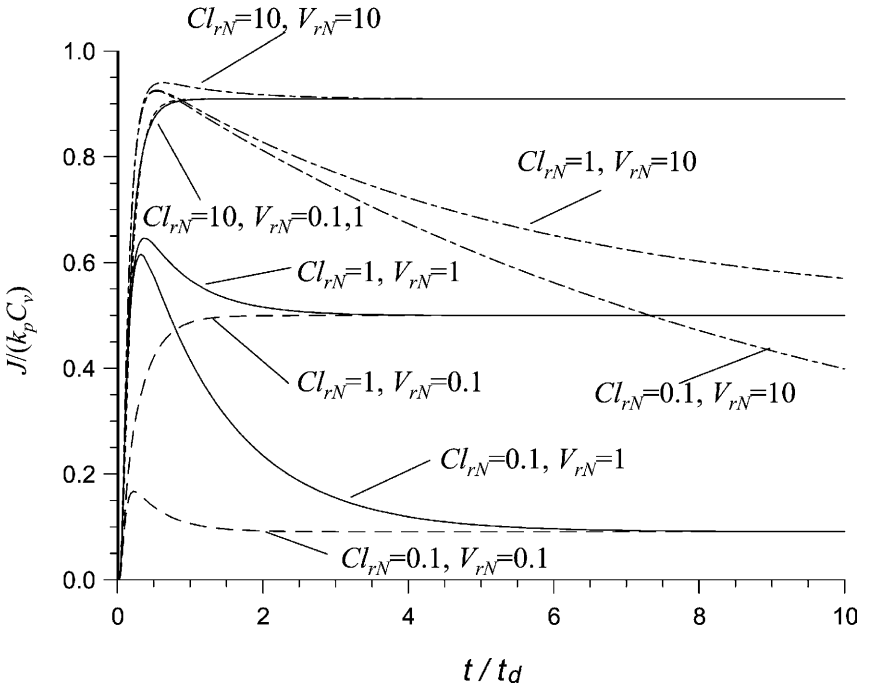


Figure 7 Normalized flux (J/k_pC_v) versus normalized time (t/t_d) for a finite receptor volume and limited clearance [Eq. (32)], $Cl_{rN} = Cl_rK_r/k_pA$, $V_{rN} = V_rK_R/V_mK_m$.

The steady state approximation of Equation (31) is:

$$Q(t) \approx AJ_{ss}(t - \text{lag}) \tag{33}$$

where:

$$J_{ss} = k_pC_v \frac{Cl_r}{Cl_r + (k_pA/K_r)} = \frac{k_pC_v}{1 + (1/Cl_{rN})} \tag{34}$$

and:

$$\text{lag} = \frac{t_d}{6}\left[1 + \frac{2Cl_{rN} - 6V_{rN}}{Cl_{rN}(Cl_{rN} + 1)}\right] \tag{35}$$

We note that if Equation (29) is substituted into Equation (28), the expression for J_{ss} is identical to Equation (34). We also note that when $Cl_r \rightarrow \infty$ (infinite sink), J_{ss} and lag reduce to Equations (4) and (12), respectively.

The corresponding solution for the receptor/epidermal concentration with the above boundary conditions is:

$$\hat{C}_r(s) = \frac{k_pAC_v}{s} \frac{\sqrt{st_d}}{(V_rs + Cl_r)\{\sinh\sqrt{st_d} + [\sqrt{st_d}/(st_dV_{rN} + Cl_{rN})]\cosh\sqrt{st_d}\}} \tag{36}$$

At long times $t \rightarrow \infty$, C_r is defined by Equation (29).

Parry et al. (11) has described a percutaneous absorption model in which both the donor and receptor compartments for an in vitro membrane study were well-stirred and finite. Boundary conditions similar in form to that defined by Equations (42)

and (30), but with $Cl_r = 0$, were used to describe the disappearance of solute from the donor chamber into the membrane and efflux of solute from the membrane into the receptor chamber. The resultant expression included a complex function requiring the solution of transcendental equations. It should be emphasized that this model differs from others described in this section in that it does not have a clearance term to account for sampling.

D. In Vitro Permeability Studies with a Constant Donor Concentration or Defined Input Flux and Finite Clearance of Solute from the Epidermis

The importance of receptor conditions on epidermal transport has been the subject of various studies over the last 30 years. Two models are widely used. In the first model, it is assumed that the viable epidermis or aqueous diffusion layer below the SC can exert a significant influence on skin penetration (12,13). The second model is one where there is an effectively desorption rate limited step in partitioning from the membrane to the next phase (e.g., epidermis → receptor solution, SC → epidermis, epidermis → dermis). This rate constant, which we will define as k_c, and the interfacial barrier rate constant are identical if the lag time for the interfacial barrier can be assumed to be negligible. In the specific case of an aqueous diffusion layer being a barrier, $k_c = D_{aq}/l_{aq}^2$ where l_{aq} is the thickness of the layer and D_{aq} is the diffusion coefficient in the layer (13).

Guy and Hadgraft (14,15) developed a pharmacokinetic model for skin absorption based on the diffusion model with the boundary conditions defined by (a) the influx into the membrane being related to an assumed exponential decline in vehicle donor concentration and (b) the efflux from the membrane being related to first order removal at a rate constant k_c. These authors went on to examine short and long-time approximations. Kubota and Ishizaki (16) presented a more generalized diffusion model for drug absorption through excised skin by using the boundary conditions of the fluxes (a) into the skin being defined by an arbitrary function $f(t)$ and (b) out of the skin being defined by $ClC(x = h_m)$ where Cl is the clearance from the skin and $C(x = h_m)$ is the concentration of solute at the skin–system interface. They considered a boundary condition at the membrane–vehicle interface defined by an input rate into the membrane $f(t)$ together with a first order rate constant k_c determined efflux from the membrane. Accordingly, the amount of solute absorbed across the skin $Q(t)$ at various times t is defined in the Laplace domain as:

$$\widehat{Q}(s) = \frac{A}{s} \frac{k_c t_d \hat{f}(s)}{\sqrt{st_d}\,\sinh(\sqrt{st_d}) + k_c t_d\,\cosh(\sqrt{st_d})} \tag{37}$$

Of particular interest in this overview is the case of a constant donor concentration (infinite donor) and sink receptor. $\widehat{Q}(s)$ is then defined by:

$$\widehat{Q}(s) = \frac{k_p C_v A}{s^2} \frac{k_c t_d \sqrt{st_d}}{\sqrt{st_d}\,\cosh\sqrt{st_d} + k_c t_d\,\sinh\sqrt{st_d}} \tag{38}$$

Figure 8A shows the effect of k_c (as defined by $\alpha = k_c t_d$) on $Q(t)$ versus time profile.

It is to be noted that, at long times, the linear portion of $Q(t)$ [defined by Eq. (38)] versus t profile describes a steady state flux J_{ss} and lag time (lag):

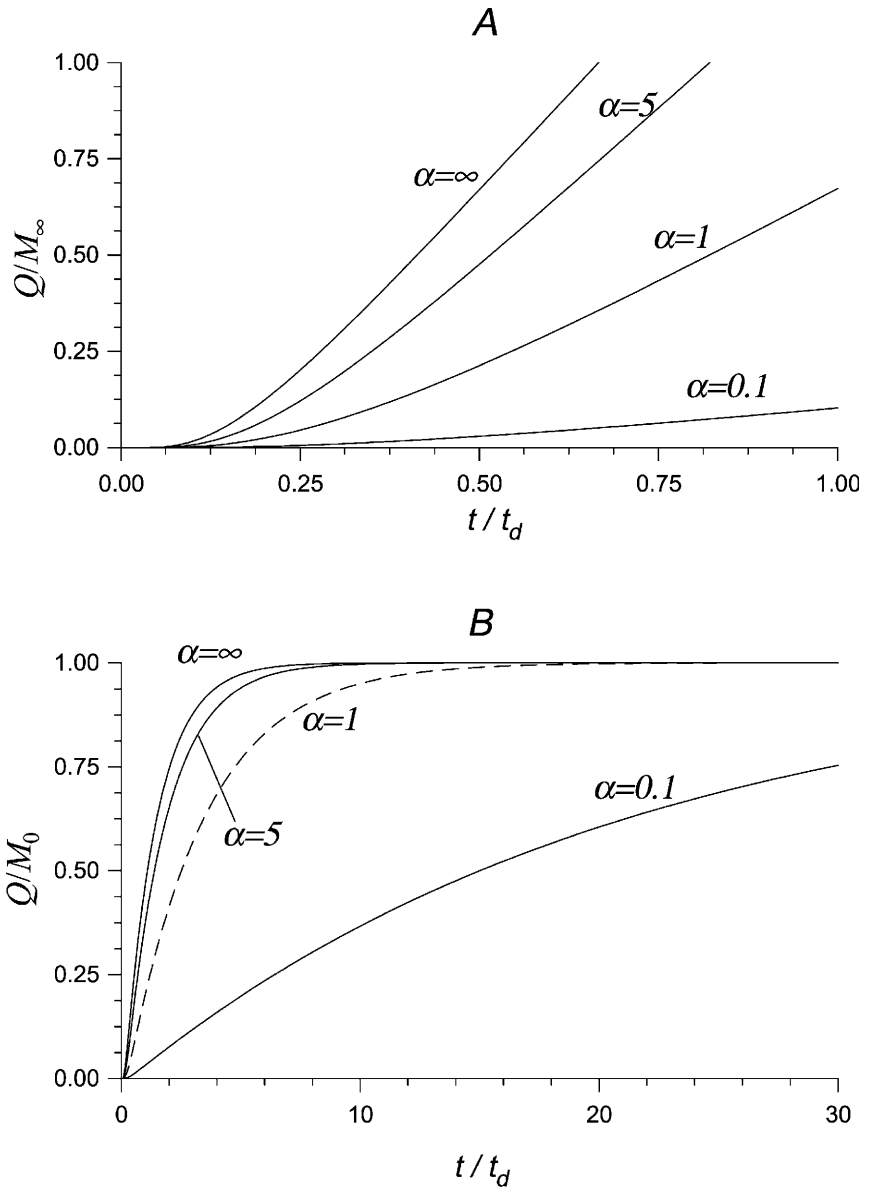


Figure 8 Effect of interfacial barrier rate constant (expressed as $\alpha = k_c t_d$) on exit from SC on normalized amount penetrating the epidermis with normalized time (t/t_d). (**A**) constant donor concentration and (**B**) a finite dose in well-stirred vehicle, where $V_{rN}(= V_r K_R / V_m K_m) = 1$ for time normalized to diffusion time.

$$Q(t) = J_{ss} A(t - \text{lag}) = C_v k_p A \frac{k_c t_d}{1 + k_c t_d}(t - \text{lag}) \tag{39}$$

$$\text{lag} = \frac{t_d}{6}\left(1 + \frac{2}{1 + k_c t_d}\right) \tag{40}$$

Thus, both the slope and lag of the steady state portion of a $Q(t)$ versus t plot depend on k_c.

J_{ss} in Equation (39) can be re-expressed as:

$$J_{ss} = C_v k_p \frac{1}{1 + (1/k_c t_d)} \tag{41}$$

which is identical to Equation (34) if $k_c t_d$ is replaced with Cl_{rN}.

Elsewhere we have analyzed a more general case with simultaneous rate limitations due to clearance from receptor (Cl_r) finite receptor volume (V_r), finite permeability through viable epidermis k_p^{ve}, and finite permeability through unstirred donor layer k_d^p (10). Equations (31) and (38) for $\hat{Q}(s)$ are limiting cases of this more general solution.

E. In Vitro Skin Permeability Studies with Finite Donor Volume and Receptor Sink Conditions

In practice, the solute concentration applied to the skin does not remain constant but declines owing to the finite volumes of vehicles or pure substances applied to the skin. We therefore need to examine solutions for Equation (5) in which the boundary condition allows for depletion in solute concentration. We assume, initially, the simplest boundary conditions applying to the sorption of solutes into a membrane from the well-stirred vehicle at $x = 0$ and from membrane into a systemic circulation [Eqs. (7) and (8)] together with a condition of depletion of concentration in the vehicle at $x = h_m$ (3):

$$V_v \frac{dC_v}{dt} = AD_m \frac{\partial C_m}{\partial x} \Big|_{x=0} \tag{42}$$

where $V_v = Ah_v$ is the volume of the vehicle applied to the skin. Solution of Equation (5) with Equations (7), (8), and (42) as boundary conditions gives (17):

$$Q(t) = M_0 \left\{ 1 - \sum_{n=1}^{\infty} \frac{2\exp\left[-(t/t_d)\gamma_n^2\right]}{\cos\gamma_n [1 + V_{vN}\gamma_n^2 + (1/V_{vN})]} \right\} \tag{43}$$

where $M_0 = C_{v0} V_v = C_{v0} A h_v$ is the initial amount of solute in the vehicle, C_{v0} is the initial concentration in the vehicle, h_v is the effective thickness of the vehicle, V_{vN} is a dimensionless parameter defined by:

$$V_{vN} = \frac{V_v}{K_m V_m}$$

and γ_n are positive roots of transcendental equation:

$$\gamma \tan\gamma = \frac{1}{V_{vN}}$$

The Laplace transform of $Q(t)$ is given by (18):

$$\hat{Q}(s) = \frac{M_0}{s} \frac{1}{V_{vN}\sqrt{st_d}\,\sinh(\sqrt{st_d}) + \cosh(\sqrt{st_d})} \tag{44}$$

The corresponding expressions for flux are given by Equations (45) and (46):

$$J_s(t) = V_{vN} C_{v0} k_p \sum_{n=0}^{\infty} \frac{2\gamma_n^2 \exp\left[-(t/t_d)\gamma_n^2\right]}{\cos\gamma_n \left[1 + V_{vN}\gamma_n^2 + (1/V_{vN})\right]} \tag{45}$$

$$\widehat{J}_s(s) = V_{vN} C_{v0} k_p \frac{t_d}{V_{vN}\sqrt{st_d}\,\sinh\sqrt{st_d} + \cosh\sqrt{st_d}} \tag{46}$$

Equation identical to Equation (45) was used by Kasting (19) for analysis of the in vitro absorption rates of varying finite doses of vanillylnonamide applied to excised human skin from propylene glycol.

Figure 9 shows the predicted profiles for the flux of solute [Eq. (46)] with varying $V_{vN} = V_v/(K_m V_m)$. It is apparent that both the peak time and area under the curve decrease with the decreasing V_{vN}. The longer peak time with increasing V_v reflects the movement from a finite to an infinite donor source. The larger area under the curve reflects the higher dose associated with an increase in V_v.

Two summary parameters can be derived from Equation (46).

1. Mean absorption time measuring from systemic side of the skin is:

$$\mathrm{MAT_s} = -\frac{d\,[\ln\widehat{J}_v(s)]}{ds}_{|s=0} = \frac{1}{2}t_d + V_{vN}t_d \tag{47}$$

It needs to be emphasized that $\mathrm{MAT_S}$ differs from MTT, which is mean transit time through SC. MTT can be calculated as:

$$\mathrm{MTT} = \mathrm{MAT_s} - \mathrm{MAT_v}$$

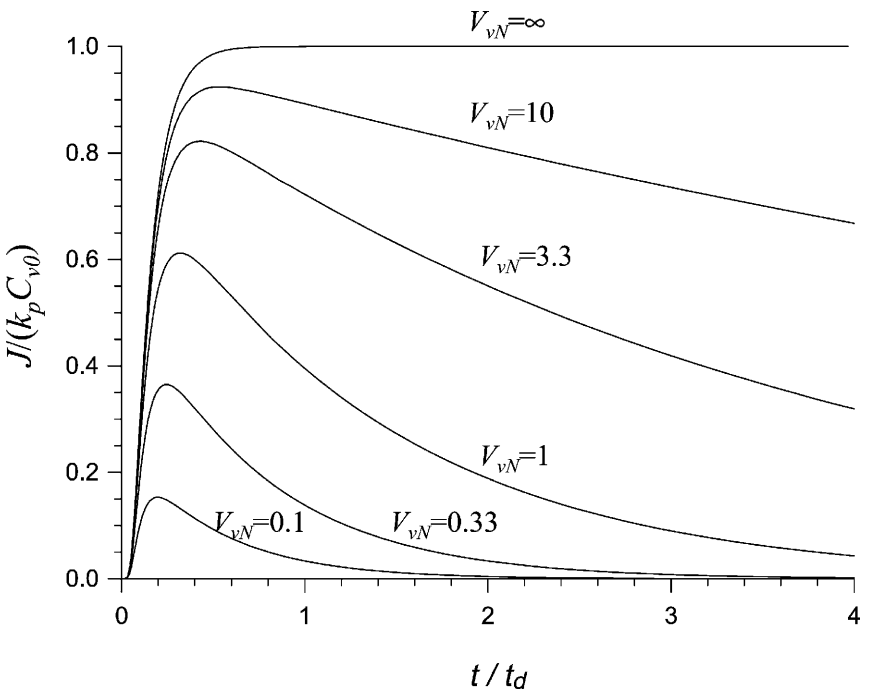


Figure 9 Normalized flux for penetration of a solute from a finite dose in a well-stirred vehicle J/k_pC_{vo} against normalized time (t/t_d) for diffusion time with varying $V_{rN}(= V_rK_R/V_mK_m)$.

where MAT_v is the mean absorption time from the vehicle:

$$MAT_v = -\frac{d\ \ln\hat{J}_v(s)}{ds}_{|s=0}$$

where $\hat{J}_v(s)$ is the Laplace transform of the flux from the vehicle into the skin. It can be found that:

$$\hat{J}_v(s) = V_{vN} C_{v0} k_p \frac{t_d}{V_{vN}\sqrt{st_d}\ \tanh\sqrt{st_d} + 1}$$

and $MAT_v = V_{vN} t_d$. We therefore have $MTT = t_d/2$.

2. CV^2 for absorption:

$$CV^2 = \frac{d^2/ds^2\left[\ln\hat{J}_s(s)\right]}{d/ds[\ln\hat{J}_s(s)]}\bigg|_{s=0} = \frac{2}{3} + \frac{4}{3[2 + (1/V_{vN})]^2} \tag{48}$$

Another two summary parameters can be derived from Equation (46) when $V_{vN} = 1$ ($V_v = V_m K_m$). This applies in a specific case of solvent deposited solids. Scheuplein and Ross (20) described the application of drugs when 25 μL of acetone is applied to 2.54 cm^2 and allowed to evaporate, leaving a very thin layer of solid material. When $V_{vN} = 1$ Equation (46) reduces to:

$$\hat{J}_s(s) = V_{vN} C_{v0} k_p \frac{t_d}{\cosh\sqrt{st_d}}$$

and therefore $J(t)$ can be written as:

$$J(t) = V_{vN} C_{v0} k_p f\left(\frac{t}{t_d}\right) = V_{vN} C_{v0} k_p f(\tau)$$

where $\tau = t/t_d$, $f(\tau)$ is a function independent of V_{vN} and whose Laplace transform is $\hat{f}(s) = 1/\cosh\sqrt{s}$. It can be shown by the numerical inversion of $\hat{f}(s)$ that the maximum of the function $f(\tau)$ occurs at $\tau = 1/6$ with the value $f(\tau_{max}) = 1.850$. The maximum flux, J_{max}, and for the time of maximum flux, t_{max}, for finite dose absorption solvent deposited solutes are therefore described by the simple equations:

$$J_{max} = 1.85 V_{vN} C_{v0} k_p = \frac{1.85 C_{v0} D_m h_v}{h_m^2},\ t_{max} = \frac{t_d}{6} = \frac{h_m^2}{6D_m} \tag{49}$$

Hence the peak time corresponds to the lag time observed after application of a constant donor solution [Eq. 12]. Scheuplein and Ross (20) provided experimental data to show: (a) J_{max} is proportional to C_{v0} for benzoic acid, (b) t_{max} for different solutes is inversely related to their D_m values, and (c) penetration was facilitated by hydrating the SC.

F. In Vitro Permeability Studies with a Finite Donor Volume and a Finite Clearance from the Epidermis into the Receptor

Another case of particular practical interest is when the donor phase is assumed to be well-stirred and finite in volume and there is limiting clearance from the epidermis to

the receptor phase. Applying the boundary condition defined by Equation (42), together with boundary condition for $x = h_m$:

$$D_m \frac{\partial C_m}{\partial x}\bigg|_{x=h_m} = h_m k_c C_m(h_m, t) \tag{50}$$

yields for $\widehat{Q}(s)$:

$$\widehat{Q}(s) = \frac{M_0}{s} \frac{1}{\sqrt{st_d}\sinh\sqrt{st_d}[V_{vN} + (1/t_d k_c)] + \cosh\sqrt{st_d}[1 + V_{vN}(s/k_c)]} \tag{51}$$

The profiles for $Q(t)$ versus t defined by Equation (51) for different values of k_c ($\alpha = k_c t_d$) and $V_{vN} = 1$ are shown in Figure 8B.

A case of finite volume of the vehicle with simultaneous rate limitations due to clearance from receptor (Cl_r), finite receptor volume (V_r), finite permeability through viable epidermis (k_p^{ve}), and finite permeability through unstirred donor layer (k_p^{d}) were analyzed by Anissimov and Roberts (18). Equations (44) and (51) presented here for $\widehat{Q}(s)$ are limiting cases of their more general solution.

G. In Vitro Skin Permeability Studies with Diffusion Limited Finite Donor and Sink Receptor Conditions

One of the first attempts at modeling percutaneous absorption with diffusion limiting uptake from both the vehicle and the skin was made by Kakemi et al. (21). Their one-dimensional model is shown in Figure 2D. Guy and Hadgraft (22) used a similar model with sink receptor conditions as shown in Figure 10.

In the latter model, the solute has a diffusivity D_v in a finite vehicle of volume V_v, which is in contact with SC in which a solute has a diffusivity D_m down a pathlength h_m. The Laplace transform for the amount penetrating the epidermis $\widehat{Q}(s)$ into an absorbing "sink" is:

$$\widehat{Q}(s) = \frac{M_0}{s} \frac{\sinh\sqrt{st_{dv}}}{\sqrt{st_{dv}}\left(V_{vN}\sqrt{t_d/t_{dv}}\sinh\sqrt{st_{dv}}\sinh\sqrt{st_d} + \cosh\sqrt{st_{dv}}\cosh\sqrt{st_d}\right)} \tag{52}$$

where as usual $M_0 = C_{v0}V_v$ and t_{dv} is the diffusion time in the vehicle, $t_{dv} = h_v^2/D_v$.

When the transport across the epidermis is also dependent on a first order rate constant k_c for removal from the epidermis, the Laplace transform becomes:

$$\widehat{Q}(s) = \frac{M_0}{s}\frac{\sinh\sqrt{st_{dv}}}{\sqrt{st_{dv}}}\left[V_{vN}\sqrt{\frac{t_d}{t_{dv}}}\sinh\sqrt{st_{dv}}\sinh\sqrt{st_d} + \cosh\sqrt{st_{dv}}\cosh\sqrt{st_d} + \frac{\sqrt{st_d}}{t_d k_c}\left(V_{vN}\sqrt{\frac{t_d}{t_{dv}}}\cosh\sqrt{st_d}\sinh\sqrt{st_{dv}} + \cosh\sqrt{st_{dv}}\sinh\sqrt{st_d}\right)\right]^{-1} \tag{53}$$

Figure 11 shows profiles of $Q(t)$ versus t as defined be Equation (53) for different vehicle diffusivities ($\gamma = t_{dv}/t_d$) and k_c ($\alpha = k_c t_d$) for $V_{vN} = 1$.

In the particular cases when $t_{dv} \gg t_d$ and $t_d \gg t_{dv}$ Equation (52) reduces to Equations (65) and (44), respectively.

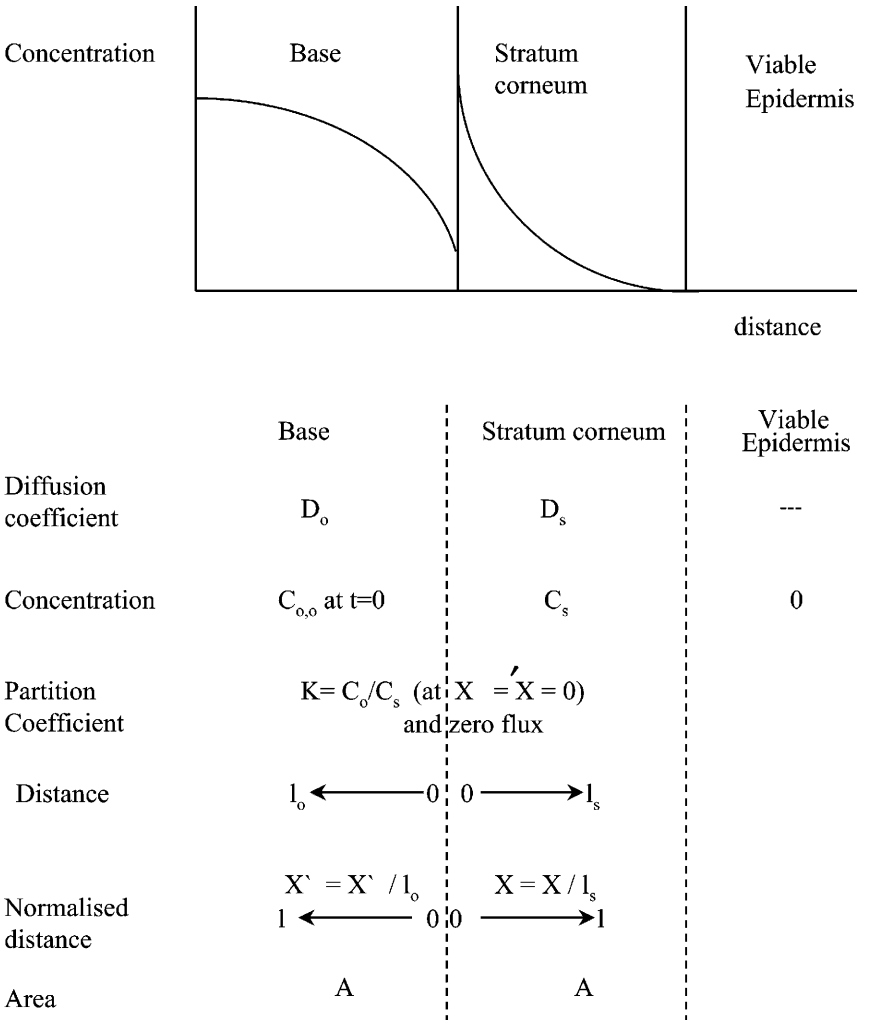


Figure 10 Two-layer diffusion model for in vitro percutaneous absorption kinetics as defined by Guy and Hadgraft (22).

H. In Vitro Permeability Studies with Two-Layer Diffusion Limitations in Transport

The complex cases of diffusion being a limitation in the transport through both the SC and epidermis have been considered by Hadgraft (23,24). He considered the case when solute exists as a reservoir in the SC. In his approach, the solute initially present in the SC diffuses from it into and through the epidermis. The case of rate limiting removal from the epidermis (k_c) was considered.

Cleek and Bunge (25) considered similar two phases in series model for the amount of solute entering this two phase in series model [$Q_{in}(t)$] and determined it both as an analytical solution and simulations. This model was then extended to include solute properties as a determinant of uptake (26). They suggested that steady state permeability would be under estimated if not corrected for the relative permeabilities of the SC and epidermis. The result of these considerations is a steady state

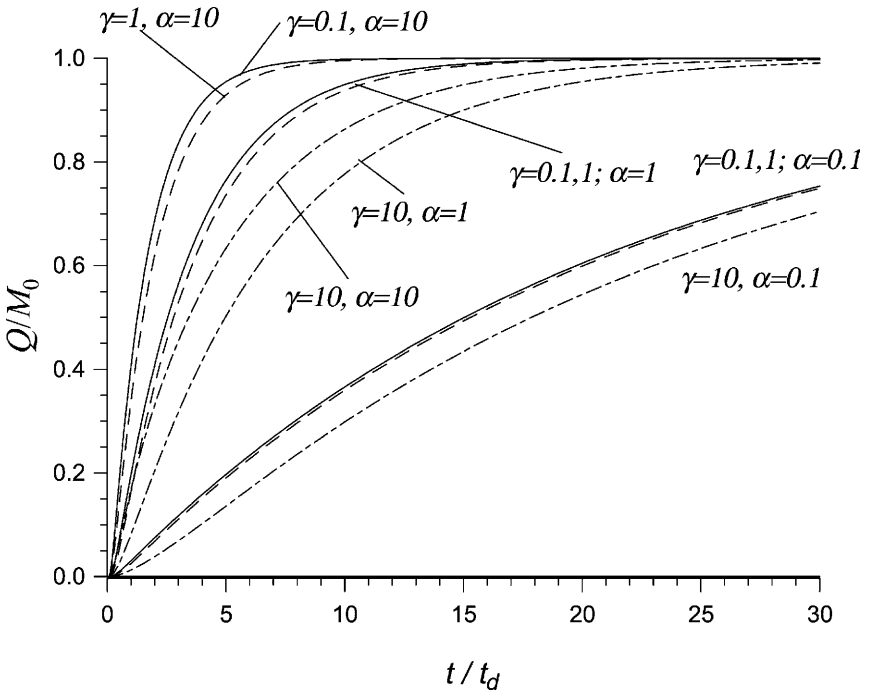


Figure 11 Cumulative amount penetrated Q normalized for amount applied M versus time normalized for diffusion time t_d for the case of both vehicle and SC limited diffusion. The two parameters varied define the relative diffusion time in vehicle relative to that in SC $\gamma(= t_{dv}/t_d)$ and the interfacial barrier rate constant effect on the exit of solutes from the stratum $\alpha = k_e t_d$ [Eq. (55)].

Equation (54) similar to Equations (39) and (40):

$$Q_{in}(t) = C_{v0} k_p A \frac{1}{1+B}\left[t + t_{ds}\frac{G(1+3B)+B(1+3BG)}{3G(1+B)}\right] \tag{54}$$

where and $k_p = K_{sv}\ D_{sc}/h_{sc}$, $G = t_{ds}/t_{de}$, $B = D_{sc}h_e K_e/D_e h_{sc}$ and K_{sv} is the partition coefficient between SC and the vehicle $K_{sv} = C_{sc}/C_v$.

Seko et al. (27) considered similar model with the solute metabolism in the second phase (viable epidermis). The resulting equations for the amount exiting the epidermis for drug Q_d and metabolite Q_m are:

$$\widehat{Q}_d(s) = \frac{AK_{sd}C_v h_s\sqrt{st_{sd}}}{s^2 t_{sd}\left[\cosh\sqrt{st_{sd}}\sinh\sqrt{(s+k_m)t_{ed}} + (K_{sd}h_s\sqrt{st_{ed}}/K_{ed}h_e\sqrt{st_{ed}})\sinh\sqrt{st_{sd}}\cosh\sqrt{(s+k_m)t_{ed}}\right]} \tag{55}$$

$$\widehat{Q}_m(s) = \frac{k_m t_{ed}}{(\sqrt{(s+k_m)t_{ed}} - \sqrt{st_{em}})}\left(\frac{\cosh\sqrt{(s+k_m)t_{ed}}}{\cosh\sqrt{st_{em}}} - 1\right)\widehat{Q}_d(s) \tag{56}$$

where k_m is the rate of metabolism in the viable epidermis, $t_{ed} = h_e^2/D_{ed}$, $t_{ed} = h_s^2/D_{sd}$;$t_{em} = h_e^2/D_{em}$ and first subscripts (s and e) denote the SC and the viable epidermis, and second subscripts (d and m) denote the drug and its metabolite,

respectively. We note that boundary conditions used in this work excluded the metabolite from diffusing back into SC and the donor. This simplifies the solution for the metabolite, but could in some cases slightly overestimate its amount penetrating into the receptor.

I. Desorption

Although penetration (absorption) experiments are most common in studying percutaneous kinetics, desorption experiments have been used to study SC solute transport (28,29). In these desorption experiments, the membrane is initially saturated with the solute so that it is at equilibrium with the donor phase with concentration C_d. The membrane is then immersed into the receptor phase with no solute present at time $t = 0$. Assuming sink conditions in the receptor, the initial and boundary conditions for this case are:

$$C_m(x, 0) = K_m C_d \tag{57}$$

$$C_m(0, t) = 0 \tag{58}$$

$$C_m(h_m, t) = 0 \tag{59}$$

Solving Equation (5) with initial and boundary conditions [Eqs. (57–59)] in the Laplace domain yields for the amount of solute desorbed into receptor phase:

$$\widehat{Q}(s) = \frac{1}{s} \frac{A K_m C_d h_m}{\sqrt{s t_d}} 2 \tan\left(\frac{\sqrt{s t_d}}{2}\right) \tag{60}$$

Equation (60) could be inverted to time domain to yield infinite series solution:

$$Q(t) = M_\infty \left\{ 1 - \frac{8}{\pi^2} \sum_{n=0}^{\infty} \frac{\exp\left[-(t/t_d)\pi^2(2n+1)^2\right]}{(2n+1)^2} \right\} \tag{61}$$

where M_∞ ($= C_d K_m A h_m$) is the total amount of solute absorbed by the membrane. Equation (61) was used by Roberts et al. (29) to fit experimental desorption profiles for some solutes to yield t_d and K_m. These parameters could then be used to calculate permeability coefficient:

$$k_p = \frac{K_m h_m}{t_d} \tag{62}$$

J. SC Heterogeneity

A homogeneous membrane model is assumed for the majority of the mathematical analysis of solute transport in SC in this chapter and in most of the literature. In reality the SC consists of at least two phases the stratum disjunctum and stratum compactum and may be seen to be heterogeneous in structure. The applicability of the homogeneity assumption to SC has therefore been questioned (30) and solutions for variable diffusion and partition coefficients in the SC have been presented (31). In general, penetration flux experiments are relatively insensitive even to extreme values of diffusion and partition coefficient heterogeneity, whereas for desorption experiments using Equation (62) may lead to a misinterpretation when the SC is heterogeneous. Concentration–distance profiles are the most sensitive to

SC heterogeneity. Ignoring partition coefficient heterogeneity in using tape-stripping data to predict penetration flux–time profiles may result in a significant miscalculation of the steady state flux and lag time values (31).

II. RELEASE PROFILES FROM TOPICAL PRODUCTS

A number of transdermal systems are now available for clinical use. Hadgraft (23,24) considered the solutions for release from patches for a range of boundary conditions. When a drug is contained in both the contact adhesive (priming dose) and patch, the release rate R_s approximates to (32):

$$R_s = R_0 + H\ \exp(-at) \tag{63}$$

where R_0 is the zeroth order flux from the patch assuming no depletion, and H and a are constants defining the release kinetics of the priming dose. Iordanski et al. (33) simulated factors such as matrix diffusion, partition coefficient, and polymer membrane thickness in the modeling of drug delivery kinetics from the adhesive of transdermal delivery device into skin imitating membranes.

A. Diffusion-Controlled Release

Of practical interest is a homogenous phase in which the drug is released by diffusion. The expression for the drug release from slabs is well-known to be that of the "burst" effect (3):

$$Q(t) = M_0\left\{1 - \frac{8}{\pi^2}\sum_{n=1}^{\infty}\frac{1}{(2n+1)^2}\exp\left[-\frac{t}{4t_{dv}}\pi^2(2n+1)^2\right]\right\} \tag{64}$$

where again $M_0 = C_{v0}V_v$ and $t_{dv} = h_v^2/D_v$. The Laplace expression for Equation (64) is:

$$\widehat{Q}(s) = \frac{M_0}{s}\frac{\tanh\sqrt{st_{dv}}}{\sqrt{st_{dv}}} \tag{65}$$

At short times when the amount released is less than 30%, Equation (64) can be approximated to:

$$Q(t) = 2M_0\left(\frac{t}{\pi t_{dv}}\right)^{1/2} \tag{66}$$

B. Release of a Suspended Drug by Diffusion

Another special case is that for a vehicle or patch containing a suspended drug. In this case, the amount of solute released into a perfect sink is given by (34):

$$Q(t) = A\sqrt{tD_v(2C_{v0} - C_s)C_s} \tag{67}$$

where C_{v0} in this context have the meaning of the total amount of drug (soluble and suspended) in the vehicle per unit volume, and C_s is the saturation concentration of the drug in the vehicle.

III. COMPARTMENTAL MODELS AS AN ALTERNATIVE TO DIFFUSION MODELS IN PERCUTANEOUS ABSORPTION

Riegelman (35) analyzed a range of in vivo skin absorption data using a unidirectional absorption and simple compartment based pharmacokinetic models (Fig. 12A). A more complex series of models (Fig. 12B–D) were used by Wallace and Barnett (36) to describe the in vitro methotrexate absorption across the skin. A discussion of the various models and their approximations is given in our earlier version of this chapter (1). More recently, a comprehensive review of compartmental models has been presented (37).

The key models developed (38) match (a) steady state SC concentration and penetration rate with an assumption of equilibrium at the two boundaries of the membrane (equilibrium model), (b) steady state SC concentration, penetration rate and lag time for all blood and vehicle concentration ratios, and for large blood concentrations (general time lag model), (c) as in (b) but for low blood concentrations

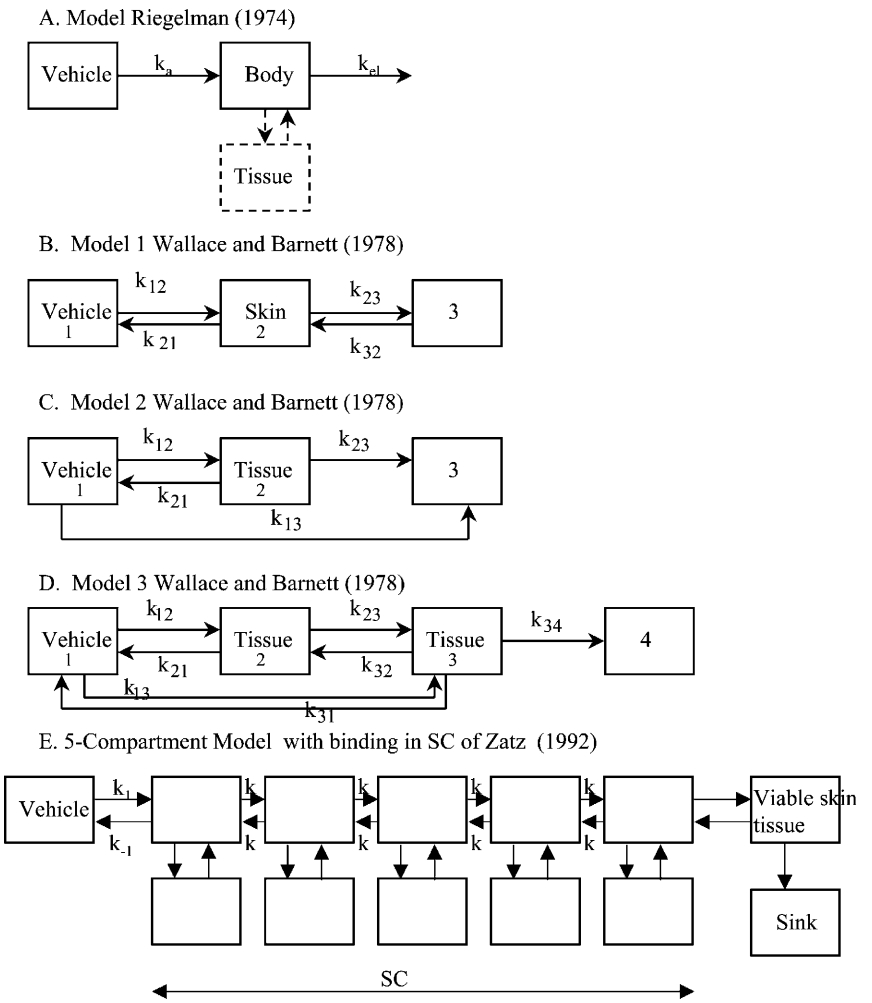


Figure 12 Examples of compartmental models of skin penetration.

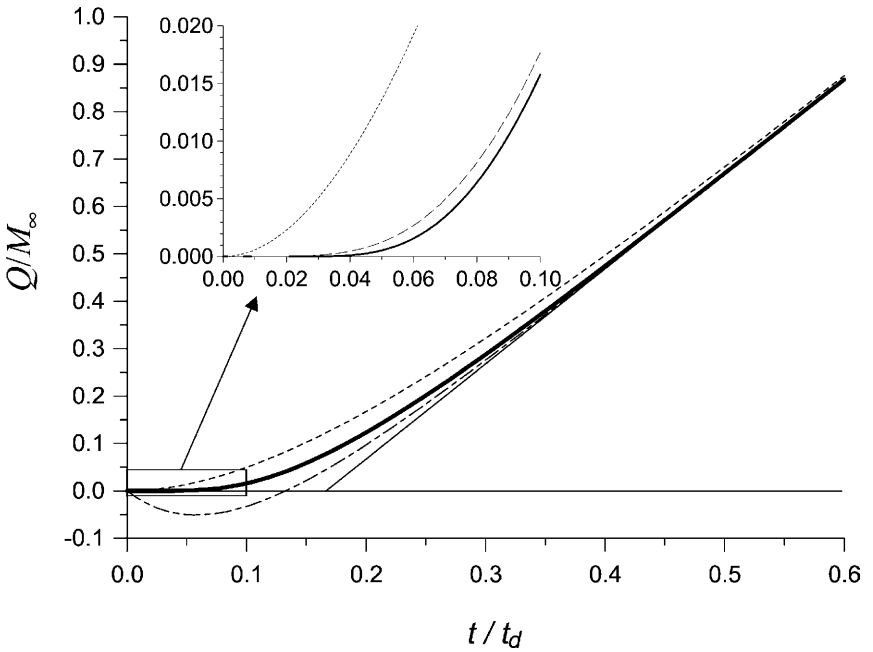


Figure 13 Normalized cumulative amount penetrated (Q/M_∞) versus normalized time (t/t_d) for diffusion model [*thick solid line*, Eq. (13)], steady state approximation of diffusion model [*solid line*, Eq. (11)], two-compartmental approximations (*short dashed* and *dash dotted lines*, discussed in our earlier version of this chapter; see Ref. 1), and 5-compartmental approximation of Zatz (39) assuming no binding in SC (*long dashed*, inset).

(simplified time lag model), and (d) the traditional model. The real contribution of this work has been a systematic derivation of equations for coefficients of compartmental models, expressed in terms of physicochemical parameters, which are documented in the paper in a readily accessible form.

It could be argued that the model representing SC as five compartments (Fig. 12E) (39) corresponds best to the diffusion model (Fig. 13). This model was developed to account for potential binding of solute to SC proteins for finite vehicle volume.

IV. OTHER PROCESSES AFFECTING IN VITRO PERCUTANEOUS ABSORPTION

A. Concentration-Dependent Diffusive Transport Processes

It is well-known that the permeability of solutes through the skin may be affected by their concentration-dependent interaction with the skin as shown for the alcohols (12) and phenols (40). At this time, relatively little work has been published on mathematical models for diffusion in a swelling or denaturing skin environment. Wu (41) has attempted to relate water diffusivity $D(C)$ as a function of its water concentration (C) in a keratinous membrane. The expression $D(C) = D_o + AC^B$, where D_o, A, and B are constants, best described the results. Giengler et al. (42) have described the numerical solution of solute concentrations in a system consisting

of a polymer film, microporous membrane, adhesive, skin layer, and capillary sink and in which the diffusion coefficients were time dependent.

Higuchi and Higuchi (43) summarized the theory associated with diffusion through heterogeneous membranes and vehicles. They suggested that transport through a two-phase system was a function of the volume fraction and permeability of each phase. They also derived an expression for lag time across a membrane when simultaneous diffusion and Langmuir adsorption has occurred. The lag time across the membrane is increased by binding of solute to membrane's binding sites:

$$\text{lag} = \frac{h_{\text{m}}^2}{4D_{\text{m}}} + \frac{h_{\text{m}}^2 A}{2D_{\text{m}} K_1 V_1 C_{\text{v}}} \tag{68}$$

where D_{m} is effective diffusion constant in heterogeneous membrane, A is amount of solute taken up by filler per unit volume of membrane material, K_1 is the partition coefficient of the solute in vehicle and phase 1 in the membrane, V_1 is volume fraction of phase 1, and C_{v} is concentration of solute in the vehicle.

When the solute concentration in the vehicle increases, the second term in Equation (68) decreases and the overall lag time is shorter.

Chandrasekaran et al. (32,44) assumed that uptake of solutes by skin was described by a dual-sorption model:

$$Z\frac{\mathrm{d}C}{\mathrm{d}t} = D\frac{\mathrm{d}^2 C}{\mathrm{d}x^2} \tag{69}$$

where:

$$Z = B\left\{1 + \frac{C_{\text{i}}\text{b}/\text{k}_{\text{D}}}{[1 + (C_{\text{D}} b/kD)]^2}\right\}$$

However, these authors then assumed that Z was a constant. This model reduces to the conventional diffusion model in which the effective diffusivity is the diffusion coefficient of free solute modified by the instantaneous partitioning of solute into immobile sites in the diffusion path (45). Expressions were presented for plasma concentrations and urinary excretion rate profiles after single and multiple patch applications of scopolamine to humans. Kubota et al. (46,47) applied the dual sorption model to account for the nonlinear percutaneous absorption of timolol. The model accounted for the prolongation in timolol lag time associated with the decrease in applied concentration.

B. Bioconversion/Metabolism of Solutes in the Skin

Roberts and Walters (2) related the in vitro (metabolically inactive) skin flux $J_{\text{s,in vitro}}$ to that in vivo $J_{\text{s,in vivo}}$ by a first pass bioavailability F_{s} and a fraction released from the product into the skin F_{R}:

$$J_{\text{s,in vivo}} = F_{\text{s}} F_{\text{R}} J_{\text{s,in vitro}} \tag{70}$$

The importance of recognizing F_{s} is illustrated by methylsalicylate where $F_{\text{s}} < 0.05$ (2). Caution must therefore be applied in extrapolating in vitro data into likely in vivo absorption.

The modeling of percutaneous absorption kinetics in the epidermis when diffusion and metabolic processes occur simultaneously leads to relatively complex

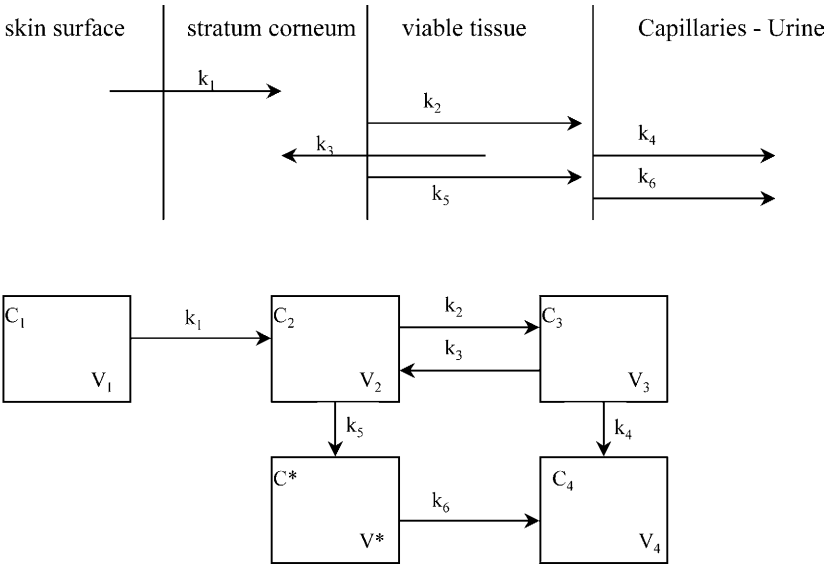


Figure 14 The compartmental model for skin penetration modified to include epidermal metabolism. *Source:* Adapted from Ref. (Guy and Hadgraft, 1984b).

solutions. Ando et al. (48) examined the diffusive transport of a solute through a metabolically inactive SC and hence through the epidermis, where it was assumed that there was homogeneous distribution of metabolizing enzymes. Subsequent work developed this model to examine the bioconversion prodrug → drug → metabolite (49,50). The work applied the diffusion equation and derived expressions for the steady state fluxes and cutaneous concentration–distance relationships for each of the species. Yu et al. (51) then solved this model for non-uniform enzyme distribution in the skin. Fox et al. (52) considered Michaelis–Menten kinetics in their examination of prodrug, drug, and metabolite concentrations in the epidermis and dermis. Most recently Seko et al. (27) used a two-layer skin diffusion/metabolism model to describe parabens cutaneous metabolism after topical application [see also Eqs. (55) and (56)]. Analysis involved nonlinear regression of numerical inversion of Laplace transform solutions. Approximations to diffusion-based models were applied by Hadgraft (53), Guy and Hadgraft (54), and Kubota et al. (55) to describe the effect of linear and saturable (Michaelis–Menten) epidermal metabolism on percutaneous absorption.

Guy and Hadgraft (56–59) adapted their pharmacokinetic model defined by k_1, k_1, k_2, k_3, and k_4 (Fig. 14) to include a metabolic step k_5 and removal of metabolite k_6. Linear kinetics was assumed to enable solution in the Laplace domain and inversion to give analytical solutions. A number of theoretical plasma concentration profiles were then constructed. In reality, Michaelis–Menten kinetics may be operative for a number of solutes.

C. Solute–Vehicle, Vehicle–Skin, and Solute–Skin Interactions

The practical application of mathematical models in percutaneous absorption to therapeutics or risk assessment is dependent on an understanding of solute–skin, solute–vehicle, and vehicle–skin interactions. Some aspects of each of these areas

have been discussed by Roberts and Walters (2), Hadgraft and Wolff (60), Robinson (61), and Roberts et al. (45).

The present analysis has generally been limited to percutaneous absorption kinetics in which the underlying physicochemical parameters are time-independent. In practice, the application of a vehicle to the skin will lead to a time-dependent change in permeability due to either a solute–skin interaction or a vehicle–skin interaction. The solutions of the resultant concentration—dependent diffusion processes also lead to a time- and space-dependent change in solute diffusivity—are relatively complex and felt to be beyond the scope of this overview.

Of critical importance in both therapeutics and toxicology is the maximum flux of a solute J_{max}. This flux is normally attained at the solubility of the solute in the given vehicle S_v, consistent with the solubility of the solute in the SC transport pathway S_m:

$$J_{max} = \frac{D_m K_m S_v}{h_m} = k_p S_v = \frac{D_m S_m}{h_m} \tag{71}$$

The importance of J_{max} as a parameter describing penetration through the skin is in its invariance for a given solute transport from different vehicles, unlike k_p, which is vehicle-dependant. This invariance holds unless the vehicle affects either D_m or S_m (45). J_{max} (in mol/cm^2 hr) may be expressed in terms of their molecular weight (MW), melting point (Mpt), and hydrogen bonding acceptor ability (Ha) (62):

$$\log J_{max} = -4.35 - 0.0154\text{MW} - 0.293\text{Mp}^* + 0.371\text{Ha}, \quad n = 87, \ r^2 = 0.937 \tag{72}$$

where J_{max} is in mol/cm^2 hr and the dependence on Mpt being described using the Mpt term: $\text{Mp}^* = \Delta S_f$ (Mpt $-$ T) u(Mpt $-$ T)/T, from Yalkowsky's solubility equation (63), where T is the temperature, ΔS_f is the entropy of fusion of a solute, and $u(x)$ is the unit step function [i.e., $u(x) = 1$ for $x > 0$ and $u(x) = 0$ for $x < 0$)]. Most of the regression variance for J_{max} is defined by MW, showing the dominance of size as a determinant of maximum flux (62):

$$\log J_{max} = -3.90 - 0.0190\text{MW}, \qquad n = 87, \quad r^2 = 0.847 \tag{73}$$

D. Effect of Surface Loss Through Processes Such as Evaporation and Adsorption to Skin Surface

There is a potential change in solute concentration as a consequence of surface loss during percutaneous absorption. The loss may result in (a) an effective reduction in the volume of the vehicle alone due to evaporation and an increase in solute concentration as a consequence, (b) a reduction in both solute and vehicle due to a removal process, and (c) a loss of solute only due to volatilization or adsorption to skin surface. For instance, Reifenrath and Robinson (64) have shown that mosquito repellents may be lost due to evaporation at a rate comparable to their percutaneous absorption. The loss of vehicle at a defined rate creates a moving boundary problem and does not appear to have been considered to any great extent in the literature. Guy and Hadgraft (56,57) examined the first and zero order loss of solute from the vehicle surface using diffusion and compartment models, respectively. Recently Saiyasombati and Kasting (65) examined disposition of benzyl alcohol after topical application to human skin in vitro and shown that evaporation plays a significant

role. They found that two-compartment models were adequate to describe first order loss of benzyl alcohol from the vehicle surface.

E. Shunt Transport

The importance of shunt transport by appendages has been well-recognized. Scheuplein (66) and Wallace and Barnett (36) assumed a parallel pathway with a minimal lag time relative to transepidermal transport for diffusion and compartmental models, respectively. In our attempted modeling of epidermal and shunt diffusion, we assumed that the overall amount penetrating was the sum of the amounts penetrating through independent epidermal and shunt pathways (8). The amount penetrating through each pathway was assumed to be defined by Equation (9) in which K_m and D_m were defined in terms of the corresponding constants for the two pathways.

More recently, the presence of polar and non-polar pathways through the intercellular region of the SC has been recognized as described in Equation (3). Mathematical models described include those for steady state conditions (67,68), and an infinite dosing condition (69). Yamashita et al. (70) have presented the Laplace solution for a well-stirred finite donor phase in contact with SC in which solutes can diffuse through both polar and non-polar routes. The solute can then diffuse through the epidermis into a sink. Numerical inversion of the Laplace transform with FILT was then undertaken to generate real time profiles. Edwards and Langer (71) have derived expressions for a range of conditions and suggested their theory confirmed the importance of shunt and intercellular transport for small ions and uncharged solutes, respectively.

F. Reservoir Effect

It is well recognized that significant amounts of solute can accumulate in the SC and be released into lower tissues on rapid skin hydration, the so-called "reservoir" effect (72,73). Modeling of this process including the effects of desquamation has been undertaken using both diffusion (74) and compartmental models (75). In the latter model, the kinetics of reservoir depletion was shown to be dependant on solute diffusivity in the SC solute clearance from the underlying tissue and the rate of epidermal turnover.

V. SIMPLE IN VIVO MODELS IN PERCUTANEOUS ABSORPTION

A. Compartmental Pharmacokinetic Models

One of the first evaluations of the pharmacokinetics of skin penetration was reported by Riegelman (35). Absorption of solutes through the skin was generally assumed to follow first order kinetics with a rate constant k_a (unit: sec^{-1}). Much of the data analyzed appeared to be characterized by "flip–flop" kinetics where the absorption half-time is much longer than the elimination half-time, as illustrated later in Figure 15. This modeling approach has been used by a number of authors including the recent work of Rohatagi et al. (76). This work described an integrated pharmacokinetic–metabolic model for selegiline after application of a transdermal system for 24 hours. A series of differential equations and nonlinear regressions were then used to solve drug and metabolite concentrations.

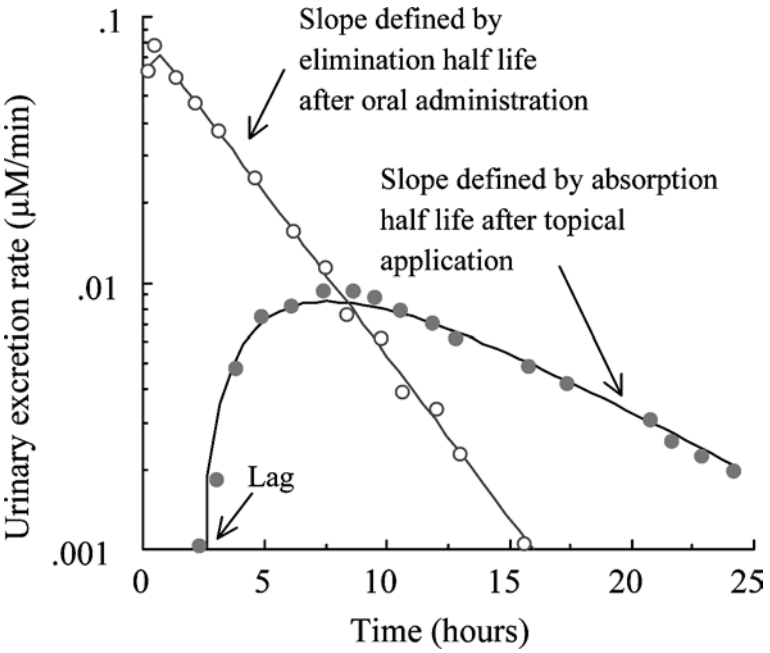


Figure 15 Simultaneous nonlinear regression of urinary excretion rate–time data for norephedrine hydrochloride administered orally (○) and free base applied topically (●) using a weighting of $1/y_{obs}$ and a common elimination half-life for norephedrine. The regression yielded an absorption half-life of 0.09 hour for oral administration. A lag of 2.2 hours and an absorption half-life of 6.0 hours for topical application and an elimination half-life of 2.5 hours ($r^2 = 0.999$). *Source:* Data from Ref. 120.

Roberts and Walters (2) have suggested that four processes are commonly used to describe plasma concentrations C_{plasma} with time after topical application when the body is assumed to be a single compartment, with an elimination rate constant k_{el} and apparent distribution volume V_B.

1. Depletion of the applied dose at a first order rate constant k_a:

$$C_{plasma} = k_a F \quad \text{Dose}\{\exp[-k_a(t - \text{lag})] - \exp[-k_{el}(t - \text{lag})]\}, \quad t > lag \qquad (74)$$

where lag is the lag time for absorption through the skin and F is the fraction that would be absorbed if the product were applied for an infinite time.

Figure 15 shows the nonlinear regression of norephedrine urinary excretion rate after topical application using Equation (74). Also shown in Figure 15 is the profile for an equimolar dose given orally. It is apparent that the topical application is associated with a lag of two hours and an absorption half-life (the terminal phase) of eight hours ($0.693/k_a$). A common elimination half-life ($0.693/k_{el}$) of 3.3 hours is found for both routes of administration.

Cross et al. (77,78) related the cumulative amount-eluted $Q(t)$–time t profiles, after dermal absorption of solutes into a perfused limb preparation, to Equation (75):

$$Q(t) = M_0\left[1 + \frac{k_a}{k_{el} - k_a}\exp(-k_{el}t) - \frac{k_{el}}{k_{el} - k_a}\exp(-k_a t)\right] \qquad (75)$$

where M_0 is the initial amount applied to the dermis, k_a is the absorption rate constant for solute absorption from the dermis, defined by fraction remaining in dermis with time [$F_{dermins} = \exp(-K_a t)$], and k_{el} is the elimination rate constant from the preparation. It can be shown, that after some rearrangement, Equation (16) in Williams et al. (79) for the perfused porcine skin flap model (Fig. 12G) simplifies to Equation (75).

Recently, Reddy et al. (80) have described a one-compartment skin pharmacokinetic model to describe in vivo absorption. The model is identical to Model III in Wallace and Barnett (36) when the shunt transport in the latter is assumed to be negligible. They found that the general time lag model derived by McCarley and Bunge (38), and discussed earlier in section 3, predicted best diffusion in a membrane for most situations.

Each of the above models may lead to erroneous estimates for the absorption rate constant if significant tissue distribution occurs in the body (as represented by the dotted lines in Fig. 12A). We have recently reported that estimates for k_a based on a single exponential (one compartmental) disposition are often twice those for the more correct bi-exponential (two compartmental) disposition model (81). Surprisingly, to date, most analyses of in vivo percutaneous absorption kinetics have assumed monoexponential disposition kinetics and have not considered this potential error.

2. Delivery at a constant rate J_s, for a time period T:

$$C_b = \begin{cases} \dfrac{J_{s,invitro} F}{Cl_{body}} [1 - \exp(-k_{el}[t - lag])], t < lag + T \\ \dfrac{J_{s,invitro} F}{Cl_{body}} [1 - \exp(-k_{el}[t - lag])] \exp[-k_{el}(t - T - lag)], t \geq lag + T \end{cases} \tag{76}$$

Singh et al. (82) used Equation (76) to describe the in vivo absorption kinetics of a number of solutes iontophoresed transdermally in vivo at a presumed constant flux for a time T. Good fits were obtained in the nonlinear regression of each of the data sets.

Imanidis et al. (83) used a similar approach to describe a constant total flux of acyclovir from a patch $J_T = [C_s/(1/k_{pm} + 1/k_{pp})]$ into the blood stream when acyclovir disposition is described by a bi-exponential elimination after IV administration [$C_b = A \exp(-\alpha t) + B \exp(-\beta t)$]. The resulting blood concentration (C_b)–time (t) profile is:

$$C_b = \frac{J_T}{V_c k_{el}} \left[1 + \frac{\beta - k_{el}}{\alpha - \beta} \exp(-\alpha t) + \frac{k_{el} - \alpha}{\alpha - \beta} \exp(-\beta t) \right] \tag{77}$$

where C_s is the acyclovir concentration in the patch, k_{pm} is the permeability coefficient of acyclovir in the skin, k_{pp} is the permeability coefficient of acyclovir in the rate controlling patch of the membrane, V_c is the apparent volume of distribution of the central compartment and A, B, α, and β are constants describing the disposition process. Tegeder et al. (84) described muscle microdialysate after topical application by a first order absorption process after a lag time (t_{lag}) with a two-

compartment-disposition model and a fraction of drug unbound to tissue (*fu*):

$$C_{\mathrm{t,free}}(t) = \frac{fuk_{21}\mathrm{Dose}k_{\mathrm{a}}}{V_c(\alpha-\beta)} \left\{\frac{1}{\beta-k_{\mathrm{a}}}\left[e^{-k_{\mathrm{a}}(t-t_{\mathrm{lag}})} - e^{-\beta(t-t_{\mathrm{lag}})}\right] - \frac{1}{\alpha-k_{\mathrm{a}}}\left[e^{-k_{\mathrm{a}}(t-t_{\mathrm{lag}})} - e^{-\alpha(t-t_{\mathrm{lag}})}\right]\right\} \tag{78}$$

Hadgraft and Wolff (60) have recently examined the prediction of in vivo plasma data after topical application. Their modeling appeared to adequately describe the in vivo percutaneous absorption kinetics for a range of drugs.

3. Steady-state conditions:

$$C_{\mathrm{bss}} = \frac{FJ_{\mathrm{s,in\ vitro}}}{\mathrm{Cl}_{\mathrm{body}}} = \frac{Fk_{\mathrm{p}}C_{\mathrm{v}}A}{\mathrm{Cl}_{\mathrm{body}}} \tag{79}$$

This equation is a reduced form of Equation (76) for $t \to \infty$ and $t < \mathrm{lag} + T$ Equation (79) has been used by Roberts and Walters (2) to define desired patch release rate for a number of drugs in vivo from a knowledge of the drug's clearance and desired plasma concentration.

4. A time-dependent transdermal flux best analyzed assuming a model deduced from in vitro absorption kinetics (sec. I.H) or deconvolution analysis (sec. V.D).

B. Diffusion Pharmacokinetic Models

In vivo absorption models usually represent the body as one or more compartments with input into the body via percutaneous absorption. Cooper (85) derived an expression for the total amount of solute excreted into the urine after topical absorption. Other models of Guy, Hadgraft, Kubota, and Chandrasekaran (described earlier) have adopted a similar approach in describing either plasma concentrations or urinary excretion rates from one- or two- compartment models. Cooper assumed diffusion through the skin according to Equation (19) into the body, represented as a single compartment. When his model is modified to include a SC–vehicle partition coefficient K_{m}, the plasma concentration, $C_{\mathrm{p}}(t)$, and the amount excreted into urine, $M(t)$, are defined by the equations:

$$C_{\mathrm{p}}(t)\frac{Ak_{\mathrm{p}}C}{V_{\mathrm{c}}}\left\{\frac{1-\exp(-k_{\mathrm{el}}t)}{k_{\mathrm{a}}} + 2\sum_{n=1}^{\infty}\frac{(-1)^n}{k_{\mathrm{el}}-n^2\pi^2/t_d}\left[\exp\left(-\frac{t}{t_{\mathrm{d}}}n^2\pi^2\right) - \exp(-k_{\mathrm{el}}t)\right]\right\} \tag{80}$$

$$M(t) = Ak_{\mathrm{p}}C_{\mathrm{v}}k_{\mathrm{u}}\left\{\frac{tk_{\mathrm{el}}-1+\exp(-k_{\mathrm{a}}t)}{k_{\mathrm{el}}^2} + 2\sum_{n=1}^{\infty}\frac{(-1)^n}{k_{\mathrm{el}}-(n^2\pi^2/t_d)}\left(\frac{t_d}{n^2\pi^2}\left[1-\exp\left(-\frac{t}{t_{\mathrm{d}}}n^2\pi^2\right)\right] - \frac{1}{k_{el}}[1-\exp(-k_{el}t)]\right]\right\} \tag{81}$$

where k_{el} is the total effective elimination rate constant, k_{u} is the rate constant for excretion in the urine, and V_{c} is the total effective volume of the compartment.

The steady-state portion of the $M(t)$ versus t plot from Equation (81) yields a slope of $k_{\mathrm{u}}k_{\mathrm{p}}A/k_{\mathrm{el}} = f_{\mathrm{e}}k_{\mathrm{p}}A$ where k_{p} is the permeability coefficient $= K_{\mathrm{m}}D_{\mathrm{m}}/h_{\mathrm{m}}$, A is

the area of application, k_{el} is the elimination rate constant of the solute from the body, and f_e is the fraction of the solute excreted in the urine. This plot is associated with a lag time t_L of:

$$t_L = \frac{1}{k_{el}} + \frac{t_d}{6} \tag{82}$$

where again $t_d = h^2_m/D$, D is the diffusivity of the solute in a SC and h_m is the distance of the pathway of diffusion. Even for multi-compartmental disposition kinetics, the total lag time for elimination of a solute is uncoupled, and is the sum of epidermal diffusion and pharmacokinetic lag times (86). When only a finite dose of solute is applied to the skin, the urinary excretion rate is also a function of the vehicle thickness (17).

In practice, the direct application of Equation (19) to in vivo absorption may be limited. Equation (32), which takes into account the effectiveness of blood flow in removal of solute from the epidermis and the accumulation of solute in the epidermis in vivo, may be more appropriate. Accordingly, the actual steady-state flux is less than $k_p A C_v$ due to this limitation in blood flow clearance as defined by Equation (34).

C. Physiologically Based Pharmacokinetic and Pharmacodynamic (PBPK/PD) Models

A number of authors have advocated the use of physiological rather than compartmental representations of the body. McDougal (87) has summarized the modeling in this area. These models utilize the numerical integration of a series of differential equations representing each compartment, to solve for blood concentration–time profiles after topical application. Individual organs or types of tissues are represented as the compartments with blood flow into and out of the organs defining the transport in the body system. Input into the skin, as a perfused organ, is assumed to follow Fick's first law and may allow for evaporation. Jepson and McDougal (88) have used this model to estimate the permeability constants for halogenated methanes from an aqueous solution after topical application in a whole animal study. Timchalk et al. (89) described an integrated PBPK/PD model for the organophosphate insecticide chlorpyrifos using the McDougal model (Fig. 16). The percutaneous absorption of perchlorethylene from a soil matrix has been recently described using modification of this model in which solute could evaporate from soil, reversibly partition into SC, and subsequently reversibly partition into dermis (90). Poet et al. (91,92) and Thrall et al. (93) used exhaled breath data with the McDougal model to assess the percutaneous absorption of methyl chloroform, trichloroethylene, and toluene. The dermal absorption, evaporation, distribution, metabolism, and excretion of a range of potential toxic solutes has been described using a multi-compartment "dermatatoxicokinetic" model based on skin surface, SC dosing device, plasma, tissue, and urine pharmacokinetics after topical and intravenous administration (94) (Fig. 17). This modeling has been used to suggest that urinary *p*-nitrophenol may be used as a marker for organophosphate insecticide exposure. The perfuse skin flap enables a simpler model description as illustrated by its application in the study of jet fuel topical absorption (95).

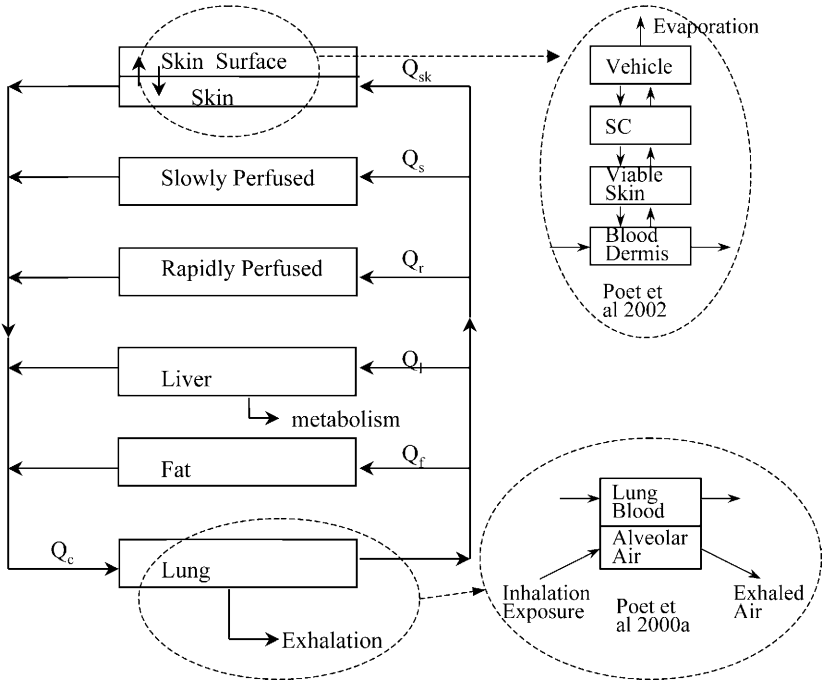


Figure 16 Physiological pharmacokinetic model for percutaneous absorption. *Source:* Adapted from Refs. 87 and 88.

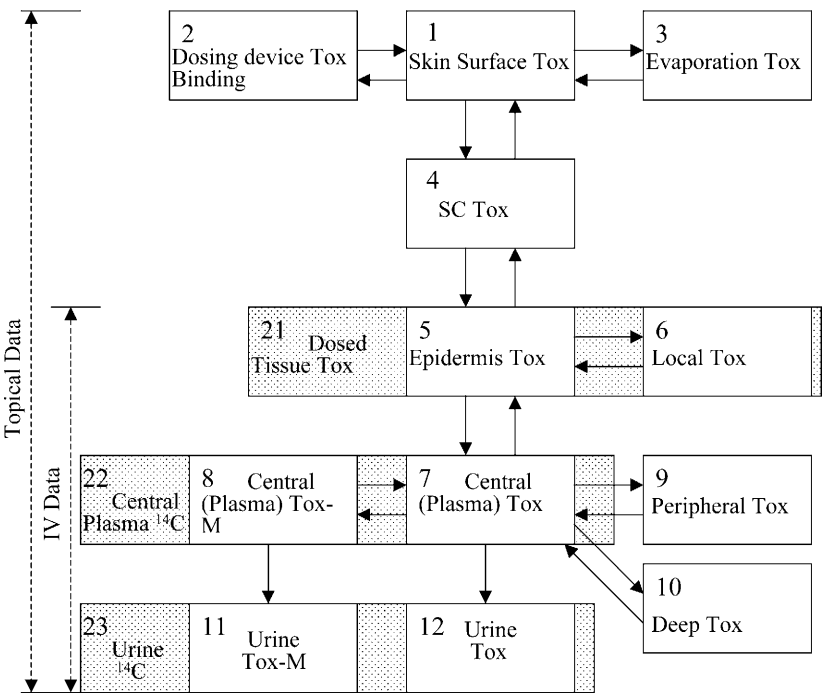


Figure 17 Dermatotoxicokinetic model for a toxic compound (Tox) and its metabolite (Tox-M). *Source:* Adapted from Ref. 94.

D. Deconvolution Analysis in Pharmacokinetic Modeling

Deconvolution analysis is based on the principle that the observed plasma or blood concentration–time profiles, $C_b(t)$, are defined by the percutaneous absorption flux, $J_s(t)$, and the disposition kinetics in the body after a unit intravenous bolus (impulse) injection, $C_{iv}(t)$:

$$\widehat{C}_b(s) = \widehat{J}_s(s)\widehat{C}_{iv}(s) \tag{83}$$

Hence from the observed $C_b(t)$ and $C_{iv}(t)$ and inversion of the resulting Laplace domain expression for $\hat{j}_s$ (s) enables $J_s(t)$ to be defined. This technique is especially useful when the mathematical model for the percutaneous absorption process is not known. A comparison of the observed profile with theoretical profiles may define the underlying model for percutaneous absorption kinetics.

Examples of deconvolution analysis applied in this area include the evaluation of the absorption function from nicotine patches (96), the modeling of subcutaneous absorption kinetics (81), and modeling of a topically applied local anesthetic agent (97).

E. Penetration into Tissues Underlying Topical Application Site

Epidermal concentrations in vivo after topical application, assuming D_e is sufficiently large to approximate well-stirred (i.e., compartmental representation), is defined by Equation (36) and at long times ($t \rightarrow \infty$) by Equation (29) via:

$$C_{ss} = \frac{k_p A C_v}{Cl_r + (k_p A / K_r)} \tag{84}$$

where Cl_r is the in vivo epidermal clearance.

A similar expression can be defined for subsequent deeper tissues using a compartment in-series model in parallel with removal to the systemic circulation and recirculation (Fig. 18) to define deeper tissue concentrations after topical application (98). Transport into deeper tissues could occur by either "convective" blood flow (99) or by diffusion. Nonlinear regressions of experimentally treated and contralateral tissue data with the model used simultaneous numerical integration of a series of differential equations (98,100,101). The analysis showed that, whereas direct deep tissue penetration was apparent at early times, recirculation of drug from the systemic circulation accounted for tissue levels at longer times to define deep tissue penetration of dermally applied solutes (Fig. 18A). Roberts and Cross (102) have suggested that the half-life for elimination of a solute in such tissues is dependent not only on tissue blood flow (Q_p), but also on the fraction unbound of solute in the tissue (fu_T) and blood (fu_B) as well as the apparent unbound volume of distribution (V_T):

$$t_{1/2} \approx \frac{0.693 fu_B V_T}{fu_T Q_p} \tag{85}$$

A further set of studies has been reported using stripped skin and an integrated application site—contralateral site model (Fig. 18B) (103,104). This work extended earlier work (101,105–107), which showed significant direct penetration to deeper tissues underlining the topical application site in both rats and in humans. As discussed earlier, Tegeder et al. (84) have described muscle microdialysate pharmacokinetics [Eq. (78)] after topical application.

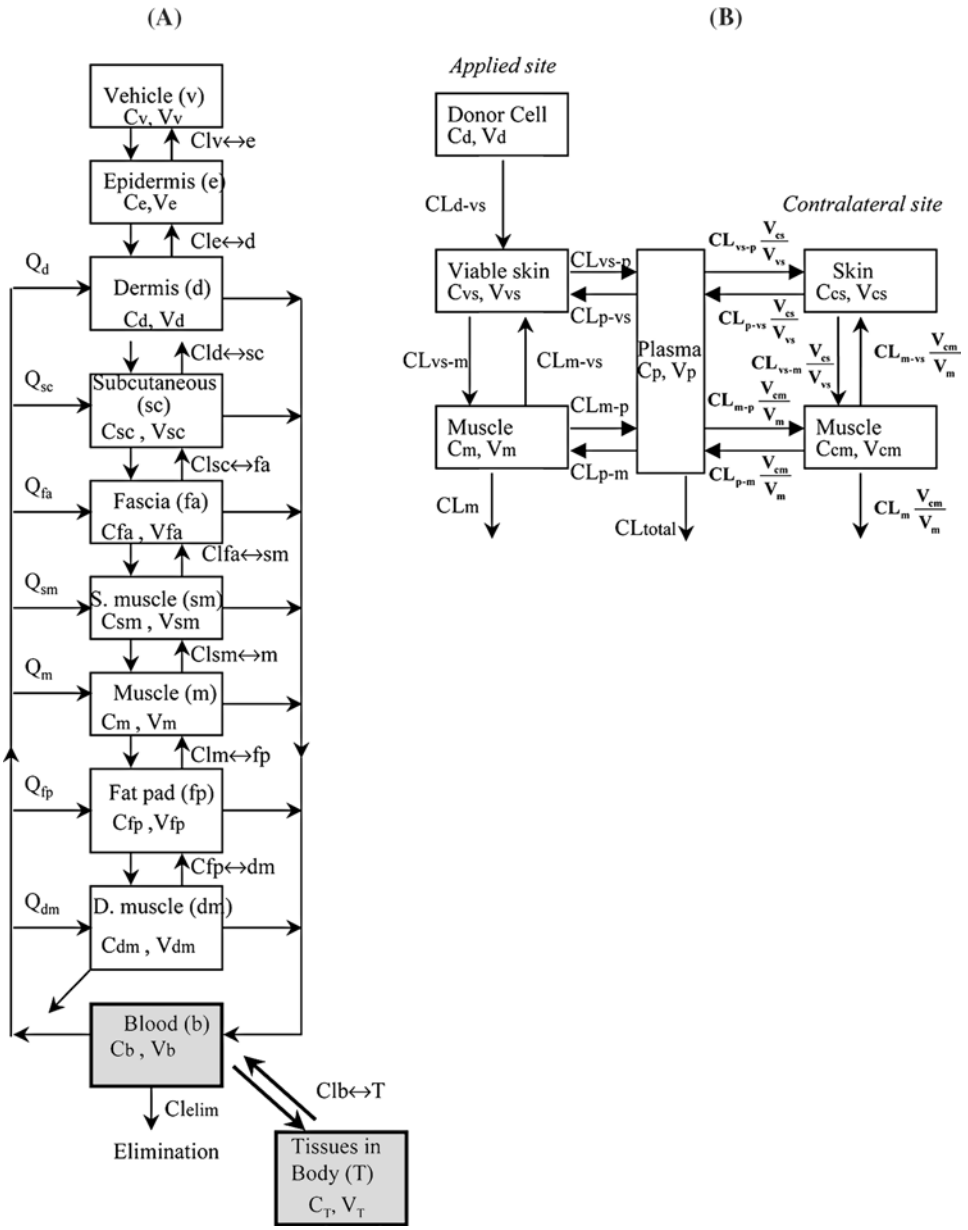


Figure 18 A pharmacokinetic model for local deep tissue penetration after topical application. The main symbols are: Q, blood flow; C, concentration; V, volume; and CL, clearance as they relate to the various tissues and the rest of the body. *Source:* Adapted from (**A**) Ref. 98 and (**B**) Ref.105.

F. Pharmacodynamic Modeling

In principle, established pharmacodynamic models used in whole body pharmacokinetic modeling can be directly used when solutes are delivered by skin. Complexities can exist when the site of drug targeting is the skin itself. Imanidis et al. (83) showed that the antiviral efficacy to HSV-1 skin infections of acyclovir was directly related to the

logarithm of the flux from transdermal patches—consistent with classical log dose–response relationships. However, an equivalent systemic dose was relatively ineffective.

Beastall et al. (108) examined the onset of erythema (t_E) as a function of solute concentration (C_o). Applying Fick's law of diffusion they obtained the expression:

$$\log\frac{n_E}{h_m} = \log\left(C_v t_E^{3/2}\right) + \log\left[\frac{K_m}{1 + K_m/p^{1/2}}\right] + \log\left[\frac{8D_{sc}^{3/2}}{\pi^{1/2}h_m^3}\right] - \frac{h_m^2}{9.2D_{sc}t_E} \tag{86}$$

where D_{sc} is the diffusion coefficient of nicotinate in the SC, K_m is its partition coefficient between vehicle and skin, h_m is diffusion path length, p is the ratio of the diffusion coefficients of the nicotinate in the vehicle and the skin, and n_E is the concentration of nicotinate required to trigger erythema. This expression showed a linear relationship should and did exist between $\log C_v t^{2/3}{}_E$ and $1/t_E$. The gradient of the relationship $D_{sc}/h^2{}_m$ was greatly affected by the co-administration of the enhancer urea.

The human skin-blanching assay for evaluating the bioequivalence of topical corticosteroid products should follow standardized guidelines as developed by the U.S. Food and Drug Administration (FDA) in 1995. Demana et al. (109) evaluated the area under the effect curve (AUEC), also called the effect (E), for both visual and chromameter-derived data. The visual data were best described by a sigmoidal E_{max} model [Eq. (87)] whilst the chromameter data were described by a simple E_{max} model [Eq. (88)]:

$$E = E_0 \pm \frac{E_{max}D}{D + ED_{50}} \tag{87}$$

$$E = E_0 \pm \frac{E_{max}D^{\gamma}}{D^{\gamma} + ED_{50}^{\gamma}} \tag{88}$$

where E_{max} is the maximal AUEC, D is the dose duration, ED_{50} is the dose duration for half maximal E, and γ is a sigmoidicity factor related to the shape of the curve. The parameter E_0, not explicitly stated in the modeling by Demana et al. (109), should be included in the model fitting to correct for baseline readings (110). Smith et al. (111) have pointed out that they had corrected for E_0 using unmedicated site values in their earlier work (109). A key aspect in this mathematical modeling is varying the dose administered by varying the duration of application. Varying dose duration is then used to relate the vasoconstrictor response to a range of corticosteroid amounts. Demana et al. (109) used a weighting of $1/\text{AUEC}$ and a number of goodness of fit criteria in their analyses.

More recently, Cordero et al. (112) developed an index to predict topical efficiency of a series of non-steroidal anti-inflammatory drugs. This index took into account both, the biopharmaceutic aspect, based on the maximal flux, and the pharmacodynamic aspect, based on the ability to inhibit cyclooxygenase-2 in vitro.

VI. MODELING WITH FACILITATED TRANSDERMAL DELIVERY

A. Iontophoresis

There are a number of mathematical models used in iontophoresis. As described by Kasting (113), these are generally defined by the Nernst Planck and Poisson equations. Of particular practical usefulness is the iontophoretic flux of a solute through the epidermis. This flux can be incorporated into various pharmacokinetic models for the body to enable the description of plasma concentration and urinary excretion-time data. Singh et al. (82) examined in vivo plasma data after

iontophoretic transport with simple pharmacokinetic models. In vivo blood concentrations for most solutes delivered by iontophoresis appear to be able to be described by zero order input into a one-compartment model [Eqs. (76) and (79)] (82).

The iontophoretic flux depends on a number of factors, including: solute ionization, interaction of solutes with pore walls, solute size, solute shape, solute charge, Debye layer thickness, solute concentration, and presence of extraneous ions is accounted for. We have recently proposed an integrating expression for the flux of the *j*-th solute (114):

$$J_{j\text{iont}} = C_j \left[\frac{2\mu_j f i_j F z_j I_T \Omega \text{PRT}_j}{(k_{s,a} + k_{s,c})[1 + f u_i \theta_{ju} + f i_j \theta_{ji})} \pm (1 - \sigma_j)\nu_m \right] \tag{89}$$

where C_j is concentration of the *j*-th solute, μ_j is its mobility, fi_j, and fu_i are ionized and unionized fractions of the solute, z_j is its charge, PRT_j is partial restriction term, σ_j is the reflection coefficient term, v_m is the velocity of water flow across the membrane, I_T is the total current across the membrane, Ω is the permselectivity for cations, $k_{s,a}$ and $k_{s,c}$ are conductivities of the anode and cathode solutions, θ_{ju} and θ_{ji} are parameters describing interaction of unionized and ionized fractions of the solute with the pore, and F is Faraday's constant.

Dermal and subcutaneous concentrations of solutes after in vivo iontophoretic application can also be determined in terms of clearance by blood supply to the tissue, clearance to deeper tissues, and influx by iontophoresis (115).

B. Sonophoresis

The sonophoretic iontophoretic flux can also be included in pharmacokinetic models in a manner analogous to that described under "Iontophoresis". Mitragotri et al. (116) have suggested that sonophoresis induces cavitation. They have suggested that the sonophoretic permeability $k_{p\ \text{sono}}$ can be defined in terms of the passive permeability coefficient k_p (unit: cm/hr) and solute octanol–water partition coefficient K_{ow} as:

$$k_{p\ \text{sono}} = k_p + 2.5 \times 10^{-5} K_{ow}^{3/4} \tag{90}$$

Later work examined the threshold frequency dependency (117) and transport at low frequency (118).

VII. PRACTICAL ISSUES IN APPLYING MATHEMATICAL MODELS TO PERCUTANEOUS ABSORPTION DATA

A major limitation in a number of reported percutaneous absorption studies, including those from our laboratories, has been the assumption of a given mathematical model. Whether that model is strictly the most appropriate one is often difficult to confirm. Most studies appear to have used the simplest model, as defined by Equation (1), in which the steady-state flux and lag time is defined by the steady-state portion of the curve. There are a number of limitations in using such a model as discussed by Robinson (61) and other authors.

Robinson (61) points out that errors can be made if (a) the burst influx and lag containing through flux are represented by a steady state approximation at early times, (b) an infinite vehicle is assumed when the concentration is actually declining due to the finite volume used, (c) penetration of a solute by passive diffusion also

involves modification of the skin barrier properties (solute–skin interactions), (d) vehicle effects on solute concentration, e.g., evaporation or skin permeability (vehicle–skin interactions) exist, (e) skin reservoir effects exist, as illustrated by the extensive uptake of sunscreens into, but not necessarily through, the skin (119), (f) discrepancies exist between in vitro and in vivo absorption due to the role of capillaries in absorption in vivo, and (g) the resistance barrier of the skin is compromised.

The expressions for a number of the more complex models contain the necessary correction factors to overcome some of the inherent limitations in the simplest model (sec. I.A) representation of data. For instance, the steady-state flux may be affected by the sampling rate from the receptor compartment as defined by Equation (34). The lag time will be dependent on both this clearance and the volume ratios of the membrane and receptor phases, corrected for partitioning effects, as defined by Equation (35). A different set of correction factors apply if an interfacial barrier or desorption rate constant exists [Eqs. (39) and (40)]. As Kubota et al. (46,47) point out, although a simple compartmental model may describe percutaneous penetration kinetics, the parameters obtained may not necessarily represent the membrane diffusion and partition coefficient.

Relating data to a specific model using nonlinear regression techniques also requires an appropriate weighting of the data in accordance with the underlying errors associated with the data. In the absence of known error structures, a weighting of $1/y_{obs}$ may be appropriate. This weighting assumes that the coefficient of variation (standard deviation/mean) of the data is relatively constant.

Some of the dilemmas in the mathematical modeling of percutaneous absorption are enunciated in the letters to pharmaceutical research written by Singh et al. (110) and Smith et al. (111), especially in relation to pharmacodynamic modeling of skin blanching after topical application. Issues raised include: (a) reliability of visual and chromameter methods, (b) analysis of "naive" pool data by nonlinear regression versus mixed effect modeling, (c) baseline correction, (d) consistency of parameter values, e.g., sigmoidicity with independent literature estimates, (e) precision of critical small and long dose duration data, and (f) subject (skin) selection. Smith et al. (111) suggest that the current methodology prepared by the FDA requires further evaluation.

Finally, there is probably a greater need for deconvolution techniques to be used with in vivo data. Such techniques do not make any assumption as to the underlying mathematical model of the absorption kinetics. Indeed, such an approach is a powerful way of determining whether assumed models are indeed applicable (81).

VIII. CONCLUSION

This chapter has attempted to overview some of the more important mathematical models used in percutaneous absorption. Given the substantive number of reported models and the complexity in many of the models, the overview is limited in its ability to give each of the models the credit they may deserve. However, it is hoped that the emphasis on the more practical models has enabled this fairly complex area to be presented in a manner useful for ready reference.

Our analysis has considered a number of boundary conditions associated with solute transport across a membrane, including clearance from the receptor solution, clearance from the membrane, and diffusion in an underlying layer (e.g., epidermis below SC). Each situation is defined by a steady-state flux J_{ss} and lag time of the forms:

$$J_{ss} = \frac{k_p C_v}{1 + M} \tag{91}$$

$$\text{lag} = \frac{t_d}{6} N \tag{92}$$

where M and N are functions of the transport processes below the membrane. When the clearance of the solute is very high ($C1 \gg k_p$), J_{ss} approaches the usual $k_p C_v$. Approximations for the lag time are less well defined so that the use of lag time as an estimate for t_d is much less justified. Consequently, there are dangers of parameter mis-specification with obvious consequences when extensions such as structure–transport relationships are based on the uncorrected parameters. Ultimately, therefore, mathematical modeling in this area is a balance between simplicity and an accurate representation of the underlying processes.

ACKNOWLEDGMENTS

We thank the NH&MRC of Australia PAH Research Foundation and the NSW and Qld Lions Medical Research Foundation for the support of this work.

REFERENCES

1. Roberts MS, Anissimov YG, Gonsalvez RA. Mathematical models in percutaneous absorption. In: Bronaugh RL, Maibach HI, eds. Percutaneous Absorption Drugs–Cosmetics–Mechanisms–Methodology. New York: Marcel Dekker, 1999:3–55.
2. Roberts MS, Walters KA. The relationship between structure and barrier function of skin. In: Roberts MS, Walters KA, eds. Dermal Absorption and Toxicity Assessment. New York: Marcel Dekker, 1998.
3. Crank J. The Mathematics of Diffusion. 2nd ed. Oxford: Clarendon Press, 1975.
4. Yano Y, Yamaoka K, Aoyama Y, Tanaka H. Two-compartment dispersion model for analysis of organ perfusion system of drugs by fast inverse Laplace transform (FILT). J Pharmacokinet Biopharm 1989a; 17:179–202.
5. Yano Y, Yamaoka K, Tanaka H. A non-linear least squares program, MULTI(FILT), based on fast inverse Laplace transform (FILT) for microcomputers. Chem Pharm Bull 1989b; 37:1535–1538.
6. Purves RD. Accuracy of numerical inversions of Laplace transforms for pharmacokinetic parameter estimation. J Pharm Sci 1995; 84:71–74.
7. Pirot F, Kalia YN, Stinchcomb AL, Keating G, Bunge A, Guy RH. Characterization of the permeability barrier of human skin in vivo. Proc Natl Acad Sci USA 1997; 94(4):1562–1567.
8. Siddiqui O, Roberts MS, Polack AE. Percutaneous absorption of steroids relative contributions of epidermal penetration and dermal clearance. J Pharmacokinet Biopharm 1989; 17(Aug):405–424.
9. Robert MS. Structure-permeability considerations in percutaneous absorption. Prediction of Percutaneous Penetration. Scott RC, Guy RH, Hadgraft J, Bodde HE. Vol.2. London: IBC Technical Services:210–228.
10. Anissimov YG, Roberts MS. Diffusion modeling of percutaneous absorption kinetics: 1. Effects of flow rate, receptor sampling rate and viable epidermal resistance for a constant donor concentration. J Pharm Sci 1999; 88(11):1201–1209.

11. Parry GE, Bunge AL, Silcox GD, Pershing LK, Pershing DW. "Percutaneous-absorption of benzonic-acid across human skin .1. invitro experiments and mathematical-modeling". Pharmaceutical Research 1990; 7(3):230–236.
12. Scheuplein RJ, Blank IH. Mechanism of percutaneous absorption IV. Penetration of non-electrolytes (alcohols) from aqueous solutions and from pure liquids. J Invest Dermatol 1973; 60:286–296.
13. Roberts MS, Anderson RA, Swarbrick J, Moore DE. The percutaneous absorption of phenolic compounds: the mechanism of diffusion across the stratum corneum. J Pharm Pharmacol 1978; 30(8):486–490.
14. Guy RH, Hadgraft J. Physicochemical interpretation of the pharmacokinetics of percutaneous absorption. J Pharmacokinet Biopharm 1983; 11(2):189–203.
15. Guy RH, Hadgraft J, Maibach HI. Percutaneous absorption: multidose pharmacokinetics. Int J Pharm 1983; 17:23–28.
16. Kubota K, Ishizaki T. A theoretical consideration of percutaneous drug absorption. J Pharmacokinet Biopharm 1985; 13(1):55–72.
17. Cooper ER, Berner B. Finite dose pharmacokinetics of skin penetration. J Pharm Sci 1985; 74(10):1100–1102.
18. Anissimov YG, Roberts MS. Diffusion modeling of percutaneous absorption kinetics: 2. Finite vehicle volume and solvent deposited solids. J Pharm Sci 2001; 90(4):504–520.
19. Kasting GB. Kinetics of finite dose absorption through skin 1. Vanillylnonanamide. J Pharm Sci 2001; 90(2):202–212.
20. Scheuplein RJ, Ross LW. Mechanism of percutaneous absorption. V. Percutaneous absorption of solvent deposited solids. J Invest Dermatol 1974; 62:353–360.
21. Kakemi K, Kameda H, Kakemi M, Veda M, Koizumi T. Model studies on percutaneous absorption and transport in the ointment. I. Theoretical aspects. Chem Pharm Bull 1975; 23(9):2109–2113.
22. Guy RH, Hadgraft J. Theoretical description relating skin penetration to the thickness of the applied medicament. Int J Pharm 1980; 6:321–332.
23. Hadgraft J. Calculations of drug release rates from controlled release devices. The slab. Int J Pharm 1979; 2:177–194.
24. Hadgraft J. The epidermal reservoir: a theoretical approach. Int J Pharm 1979; 2: 265–274.
25. Cleek RL, Bunge AL. A new method for estimating dermal absorption from chemical exposure. 1. General approach. Pharm Res 1993; 10(4):497–506.
26. Bunge AL, Cleek RL. A new method for estimating dermal absorption from chemical exposure: 2. Effect of molecular weight and octanol–water partitioning. Pharm Res 1995; 12(1):88–95.
27. Seko N, Bando H, Lim CW, Yamashita F, Hashida M. Theoretical analysis of the effect of cutaneous metabolism on skin permeation of parabens based on a two-layer skin diffusion/metabolism model. Biol Pharm Bull 1999; 22(3):281–287.
28. Scheuplein RJ, Morgan LJ. "Bound water" in keratin membranes measured by a microbalance technique. Nature 1967; 214(87):456–458.
29. Roberts MS, Triggs EJ, Anderson RA. Permeability of solutes through biological membranes measured by a desorption technique. Nature 1975; 275:225–227.
30. Watkinson AC, Bunge AL, Hadgraft J, Naik A. Computer simulation of penetrant concentration-depth profiles in the stratum corneum. Int J Pharm 1992; 87:175–182.
31. Anissimov YG, Roberts MS. Diffusion modeling of percutaneous absorption kinetics: 3. Variable diffusion and partition coefficients, consequences for stratum corneum depth profiles and desorption kinetics. J Pharm Sci 2004; 93(2):470–487.
32. Chandrasekaran SK, Bayne W, Shaw JE. Pharmacokinetics of drug permeation through human skin. J Pharm Sci 1978; 67(10):1370–1374.
33. Iordanskii AL, Feldstein MM, Markin VS, Hadgraft J, Plate NA. Modeling of the drug delivery from a hydrophilic transdermal therapeutic system across polymer membrane. Eur J Pharm Biopharm 2000; 49(3):287–293.

34. Higuchi WI. Diffusional models useful in biopharmaceutics. Drug release rate process. J Pharm Sci 1967; 56(3):315–324.
35. Riegelman S. Pharmacokinetics. Pharmacokinetic factors affecting epidermal penetration and percutaneous adsorption. Clin Pharmacol Ther 1974; 16(5 Part 2):873–883.
36. Wallace SM, Barnett G. Pharmacokinetic analysis of percutaneous absorption: evidence of parallel penetration pathways for methotrexate. J Pharmacokinet Biopharm 1978; 6(4):315–325.
37. McCarley KD, Bunge AL. Physiologically relevant two-compartment pharmacokinetic models for skin. J Pharm Sci 2000; 89(9):1212–1235.
38. McCarley KD, Bunge AL. Physiologically relevant one-compartment pharmacokinetic models for skin. 1. Development of models. J Pharm Sci 1998; 87(4):470–481.
39. Zatz J. Simulation studies of skin permeation. J Soc Cosmet Chem 1992; 43:37–48.
40. Roberts MS, Anderson RA, Swarbrick J. Permeability of human epidermis to phenolic compounds. J Pharm Pharmacol 1977; 29(11):677–683.
41. Wu MS. Determination of concentration-dependent water diffusivity in a keratinous membrane. J Pharm Sci 1983; 72(12):1421–1423.
42. Giengler G, Knoch A, Merkle HP. Modeling and numerical computation of drug transport in laminates: model case evaluation of transdermal delivery system. J Pharm Sci 1986; 75(1):9–15.
43. Higuchi WI, Higuchi T. Theoretical analysis of diffusional movements through heterogeneous barriers. J Am Pharm Assoc Sci Ed 1960; 49(9):598–606.
44. Chandrasekaran SK, Michaels AS, Campbell PS, Shaw JE. Scopolamine permeation through human skin in vitro. AIChE J 1976; 22(5):828–832.
45. Roberts MS, Cross SE, Pellett MA. Skin Transport. In: Walters KA, ed. Dermatological and transdermal formulations. New York: Marcel Dekker, 2002:89–195.
46. Kubota K, Sznitowska M, Maibach HI. Percutaneous absorption: a single layer model. J Pharm Sci 1993; 82(5):450–456.
47. Kubota K, Koyama E, Twizell EH. Dual sorption model for the nonlinear percutaneous permeation kinetics of timolol. J Pharm Sci 1993; 82(12):1205–1208.
48. Ando HY, Ho NFH, Higuchi WI. Skin as an active metabolising barrier. 1. Theoretical analysis of topical bioavailability. J Pharm Sci 1977; 66(11):1525–1528.
49. Yu CD, Fox JL, Ho NFH, Higuchi WI. Physical model evaluation of topical prodrug delivery-simultaneous transport and bioconversion of vidarabine 5′-valerate. Part 1. Physical model development. J Pharm Sci 1979; 68(11):1341–1346.
50. Yu CD, Fox JL, Ho NFH, Higuchi WI. Physical model evaluation of topical prodrug delivery-simultaneous transport and bioconversion of vidarabine 5′-valerate. Part 2. Parameter determinations. J Pharm Sci 1979; 68(11):1347–1357.
51. Yu CD, Gordon NA, Fox JL, Higuchi WI, Ho NFH. Physical model evaluation of topical prodrug delivery-simultaneous transport and bioconversion of vidarabine 5′ -valerate. Part 5. Mechanistic analysis of influence of non-homogeneous enzyme distributions in hairless mouse skin. J Pharm Sci 1980; 69(7):775–780.
52. Fox JL, Yu CD, Higuchi WI, Ho NFH. General physical model for simultaneous diffusion and metabolism in biological membranes. Computational approach for the steady state case. Int J Pharm 1979; 2:41–57.
53. Hadgraft J. Theoretical aspects of metabolism in the epidermis. Int J Pharm 1980; 4:229–239.
54. Guy RH, Hadgraft J. Percutaneous metabolism with saturable enzyme kinetics. Int J Pharm 1982; 11:187–197.
55. Kubota K, Ademola J, Maibach HI. Simultaneous diffusion and metabolism of betamethasone 17-valerate in the living skin equivalent. J Pharm Sci 1995; 84(12):1478–1481.
56. Guy RH, Hadgraft J. A theoretical description of the effects of volatility and substantivity on percutaneous absorption. Int J Pharm 1984; 18:139–147.
57. Guy RH, Hadgraft J. Pharmacokinetics of percutaneous absorption with concurrent metabolism. Int J Pharm 1984; 20:43–51.

58. Guy RH, Hadgraft J. Percutaneous absorption kinetics of topically applied agents liable to surface loss. J Soc Cosmet Chem 1984; 35:103–113.
59. Guy RH, Hadgraft J. Prediction of drug disposition kinetics in skin and plasma following topical administration. J Pharm Sci 1984; 73(7):883–887.
60. Hadgraft J, Wolff HM. In vitro/in vivo correlations in transdermal drug delivery. In: Roberts MS, Walters KA, eds. Dermal Absorption and Toxicity Assessment. New York: Marcel Dekker, 1998.
61. Robinson PJ. Prediction: simple risk Models and overview of dermal risk assessment. In: Roberts MS, Walters KA, eds. Dermal Absorption and Toxicity Assessment. New York: Marcel Dekker, 1998.
62. Magnusson BM, Anissimov YG, Cross SE, Roberts MS. Molecular size as the main determinant of solute maximum flux across the skin. J Invest Dermatol 2004;122: 993–999.
63. Yalkowsky SH, Valvani SC. Solubility and partitioning I: solubility of nonelectrolytes in water. J Pharm Sci 1980; 69(8):912–922.
64. Reifenrath WG, Robinson PB. In vitro skin evaporation and penetration characteristics of mosquito repellents. J Pharm Sci 1982; 71(9):1014–1018.
65. Saiyasombati P, Kasting GB. Disposition of benzyl alcohol after topical application to human skin in vitro. J Pharm Sci 2003; 92(10):2128–2139.
66. Scheuplein RJ. Mechanism of percutaneous absorption. II. Transient diffusion and the relative importance of various routes of skin penetration. J Invest Dermatol 1967; 48(1):79–88.
67. Ghanem AH, Mahmoud H, Higuchi WI, Rohr DD, Borsadia S, Liu P, Fox JL, Good WR. The effects of ethanol on the transport of bestradiol and other permeants in the hairless mouse skin. II. A new quantitative approach. J Control Release 1987; 6:75–83.
68. Hatanaka T, Inuma M, Sugibayashi K, Morimoto Y. Prediction of skin permeability of drugs. II. Development of composite membrane as a skin alternative. Int J Pharm 1992; 79:21–28.
69. Tojo K, Chiang CC, Chien YW. Drug permeation across the skin: effect of penetrant hydrophilicity. J Pharm Sci 1987; 76(2):123–126.
70. Yamashita F, Yoshioka T, Koyama Y, Okamoto H, Sezaki H, Hashida M. Analysis of skin penetration enhancement based on a two layer skin diffusion model with polar and non-polar routes in the stratum corneum: dose-dependent effect of 1-geranylazacycloheptan-2-one on drugs with different lipophilicities. Biol Pharm Bull 1993; 16(7): 690–697.
71. Edwards DA, Langer R. A linear theory of transdermal transport phenomena. J Pharm Sci 1994; 83(9):1315–1334.
72. Malkinson FD, Ferguson EH. Percutaneous absorption of hydrocortisone-4-C14 in two human subjects. J Invest Dermatol 1955; 25(5):281–283.
73. Vickers CF. Stratum corneum reservoir for drugs. Adv Biol Skin 1972; 12:177–189.
74. Reddy MB, Guy RH, Bunge AL. Does epidermal turnover reduce percutaneous penetration? Pharm Res 2000; 17(11):1414–1419.
75. Roberts MS, Cross SE, Anissimov YG. Factors affecting the formation of a skin reservoir for topically applied solutes. Skin Pharmacol Appl Skin Physiol 2004; 17:3–16.
76. Rohatagi S, Barrett JS, Dewitt KE, Morales RJ. Integrated pharmacokinetics and metabolic modeling of selegiline and metabolites after transdermal administration. Biopharm Drug Dispos 1997; 18(7):567–584.
77. Cross SE, Wu ZY, Roberts MS. Effect of perfusion flow rate on the tissue uptake of solutes after dermal application using the rat isolated perfused hindlimb preparation. J Pharm Pharmacol 1994; 46:844–850.
78. Cross SE, Wu ZY, Roberts MS. The effect of protein binding on the deep tissue penetration and elution of transdermally applied water, salicylic acid, lignocaine and diazepam in the perfused rat. J Pharmacol Exp Ther 1996; 277:366–374.

79. Williams PL, Carver MP, Riviere JE. A physiologically relevant pharmacokinetic model of xenobiotic percutaneous absorption using the isolated perfused porcine skin flap. J Pharm Sci 1990; 79(4):305–311.
80. Reddy MB, McCarley KD, Bunge AL. Physiologically relevant one- compartment pharmacokinetic model for skin. 2. Comparison of models when combined with a systemic pharmacokinetic model. J Pharm Sci 1998; 87(4):482–490.
81. Roberts MS, Lipschitz S, Campbell AJ, Wanwimolruk S, Mcqueen EG, Mcqueen M. Modeling of subcutaneous absorption kinetics of infusion solutions in the elderly using technetium. J Pharmacokinet Biopharm 1997; 25(1):1–19.
82. Singh P, Roberts MS, Maibach HI. Modeling of plasma levels of drugs following transdermal iontophoresis. J Control Release 1995; 33:293–298.
83. Imanidis G, Song W, Lee PH, Su MH, Kern ER, Higuchi WI. Estimation of skin target site acyclovir concentrations following controlled transdermal drug delivery in topical and systemic treatment of cutaneous HSV -1 infections in hairless mice. Pharm Res 1994; 11(7):1035–1041.
84. Tegeder I, Muth-Selbach U, Lotsch J, Rusing G, Oelkers R, Brune K, Meller S, Kelm GR, Sorgel F, Geisslinger G. Application of microdialysis for the determination of muscle and subcutaneous tissue concentrations after oral and topical ibuprofen administration. Clin Pharmacol Ther 1999; 65(4):357–368.
85. Cooper ER. Pharmacokinetics of skin penetration. J Pharm Sci 1976; 65(9):1396–1397.
86. Cooper ER. Effect of diffusional lag time on multicompartmental pharmacokinetics for transepidermal infusion. J Pharm Sci 1979; 68(11):1469–1470.
87. McDougal JN. Prediction-physiological models. In: Roberts MS, Walters KA, eds. Dermal Absorption and Toxicity Assessment. New York: Marcel Dekker, 1998.
88. Jepson GW, McDougal JN. Physiologically based modeling of nonsteady state dermal absorption of halogenated methanes from an aquous solution. Toxicol Appl Pharmacol 1997; 144:315–324.
89. Timchalk C, Nolan RJ, Mendrala AL, Dittenber DA, Brzak KA, Mattsson JL. A physiologically based pharmacokinetic and pharmacodynamic (PBPK/PD) model for the organophosphate insecticide chlorpyrifos in rats and humans. Toxicol Sci 2002; 66(1):34–53.
90. Poet TS, Weitz KK, Gies RA, Edwards JA, Thrall KD, Corley RA, Tanojo H, Hui X, Maibach HI, Wester RC. PBPK modeling of the percutaneous absorption of perchloroethylene from a soil matrix in rats and humans. Toxicol Sci 2002; 67(1):17–31.
91. Poet TS, Thrall KD, Corley RA, Hui X, Edwards JA, Weitz KK, Maibach HI, Wester RC. Utility of real time breath analysis and physiologically based pharmacokinetic modeling to determine the percutaneous absorption of methyl chloroform in rats and humans. Toxicol Sci 2000a; 54(1):42–51.
92. Poet TS, Corley RA, Thrall KD, Edwards JA, Tanojo H, Weitz KK, Hui X, Maibach HI, Wester RC. Assessment of the percutaneous absorption of trichloroethylene in rats and humans using MS/MS real-time breath analysis and physiologically based pharmacokinetic modeling. Toxicol Sci 2000b; 56(1):61–72.
93. Thrall KD, Weitz KK, Woodstock AD. Use of real-time breath analysis and physiologically based pharmacokinetic modeling to evaluate dermal absorption of aqueous toluene in human volunteers. Toxicol Sci 2002; 68(2):280–287.
94. Qiao GL, Chang SK, Brooks JD, Riviere JE. Dermatoxicokinetic modeling of *p*-nitrophenol and its conjugation metabolite in swine following topical and intravenous administration. Toxicol Sci 2000; 54(2):284–294.
95. Riviere JE, Brooks JD, Monteiro-Riviere NA, Budsaba K, Smith CE. Dermal absorption and distribution of topically dosed jet fuels jet-A, JP-8, and JP-8(100). Toxicol Appl Pharmacol 1999; 160(1):60–75.
96. Benowitz NL, Chan K, Denaro CP, Jacob P. Stable isotope method for studying transdermal drug absorption: nicotine patch. Clin Pharmacol Ther 1991; 50(Sep):286–293.

97. Welin-Berger K, Neelissen JA, Emanuelsson BM, Bjornsson MA, Gjellan K. In vitro–in vivo correlation in man of a topically applied local anesthetic agent using numerical convolution and deconvolution. J Pharm Sci 2003; 92(2):398–406.
98. Singh P, Maibach HI, Roberts MS. Site of effects. In: Roberts MS, Walters KA, eds. Dermal Absorption and Toxicity Assessment. New York: Marcel Dekker, 1998b.
99. McNeill SC, Potts RO, Francoeur ML. Local enhanced topical delivery (LETD) of drugs: does it truly exist? Pharm Res 1992; 9:1422–1427.
100. Singh P, Roberts MS. Blood flow measurements in skin and underlying tissues by microsphere method: application to dermal pharmacokinetics of polar non-electrolytes. J Pharm Sci 1993a; 82(9):873–879.
101. Singh P, Roberts MS. Dermal and underlying tissue pharmacokinetics of salicylic acid after topical application. J Pharmacokinet Biopharm 1993b; 21(4):337–373.
102. Roberts MS, Cross SE. A physiological pharmacokinetic model for solute disposition in tissues below a topical application site. Pharm Res 1999; 16(9):1392–1398.
103. Nakayama K, Matsuura H, Asai M, Ogawara K, Higaki K, Kimura T. Estimation of intradermal disposition kinetics of drugs: I. Analysis by compartment model with contralateral tissues. Pharm Res 1999; 16(2):302–308.
104. Higaki K, Asai M, Suyama T, Nakayama K, Ogawara K, Kimura T. Estimation of intradermal disposition kinetics of drugs: II. Factors determining penetration of drugs from viable skin to muscular layer. Int J Pharm 2002; 239(1–2):129–141.
105. Singh P, Roberts MS. Effects of vasoconstriction on dermal pharmacokinetics and local tissue distribution of compounds. J Pharm Sci 1994; 83(6):783–791.
106. Cross SE, Anderson C, Thompson MJ, Roberts MS. Is there tissue penetration after application of topical salicylate formulations?. Lancet 1997; 350(Aug 30):636.
107. Muller M, Mascher H, Kikuta C, Schafer S, Brunner M, Dorner G, Eichler HG. Diclofenac concentrations in defined tissue layers after topical administration. Clin Pharmacol Ther 1997; 62(3):293–299.
108. Beastall J, Guy RH, Hadgraft J, Wilding I. The influence of urea on percutaneous absorption. Pharm Res 1986; 3(5):294–297.
109. Demana PH, Smith EW, Walker RB, Haigh JM, Kanfer I. Evaluation of the proposed FDA pilot dose-response methodology for topical corticosteroid bioequivalence testing. Pharm Res 1997; 14(3):303–308.
110. Singh GJ, Fleischer N, Lesko L, Williams R. Evaluation of the proposed FDA pilot dose–response methodology for topical corticosteroid bioequivalence testing. Pharm Res 1998a; 15(1):4–7.
111. Smith EW, Walker RB, Haigh JM, Kanfer I. Evaluation of the proposed FDA pilot dose–response methodology for topical corticosteroid bioequivalence testing. The authors reply. Pharm Res 1998; 15(1):5–7.
112. Cordero JA, Camacho M, Obach R, Domenech J, Vila L. In vitro based index of topical anti-inflammatory activity to compare a series of NSAIDs. Eur J Pharm Biopharm 2001; 51(2):135–142.
113. Kasting GB. Theoretical models for iontophoretic delivery. Adv Drug Del Rev 1992; 9:177–199.
114. Roberts MS, Lai PM, Anissimov YG. Epidermal iontophoresis: I. Development of the ionic mobility-pore model. Pharm Res 1998; 15(10):1569–1578.
115. Cross SE, Roberts MS. The importance of dermal blood supply and the epidermis on the transdermal iontophoretic delivery of monovalent cations. J Pharm Sci 1995; 84:584–592.
116. Mitragotri S, Blankschtein D, Langer R. An explanation for the variation of the sonophoretic transdermal transport enhancement from drug to drug. J Pharm Sci 1997; 86(10):1190–1192.
117. Tezel A, Sens A, Tuchscherer J, Mitragotri S. Frequency dependence of sonophoresis. Pharm Res 2001; 18(12):1694–1700.

118. Tezel A, Sens A, Mitragotri S. Description of transdermal transport of hydrophilic solutes during low-frequency sonophoresis based on a modified porous pathway model. J Pharm Sci 2003; 92(2):381–393.
119. Jiang R, Roberts MS, Collins DM, Benson HA. Absorption of sunscreens across human skin: an evaluation of commercial products for children and adults. Br J Clin Pharmacol 1999; 48(4):635–637.
120. Beckett AH, Gorrod JW, Taylor DC. Comparison of oral and percutaneous routes in man for systemic administration of ephedrine. J Pharm Pharmacol 1972; 24(suppl):65–70.

2
Skin Metabolism During In Vitro Percutaneous Absorption

Robert L. Bronaugh, Margaret E. K. Kraeling, and Jeffrey J. Yourick
Office of Cosmetics and Colors, Food and Drug Administration, Laurel, Maryland, U.S.A.

I. INTRODUCTION

The skin is a portal of entry and the largest organ of the body. It has been shown to contain the major enzymes found in other tissues of the body (1). Topically applied compounds may be metabolized in skin resulting in altered pharmacologic or toxicologic activity.

The metabolism of benzo[a]pyrene applied to mouse skin floating in an organ culture demonstrated the potential importance of metabolism of compounds during percutaneous absorption (2). A flow-through diffusion cell was subsequently developed to aid in quantitating skin absorption and metabolism (3). Viability of skin in the diffusion cell, which was assessed by light microscopy, was found to be maintained for at least 17 hours (3).

Other early work on skin absorption and metabolism was conducted in pig skin, with viability of skin maintained in flow-through cells by using a tissue culture medium (4). The degradation of diethyl malonate during percutaneous absorption was determined to be partially due to a heat labile enzymatic process. The suitability of conditions used to maintain pig skin viability in diffusion cells was assessed in initial studies by the ability to graft the skin to nude mice (5).

II. SKIN VIABILITY

The use of viable skin in percutaneous absorption studies is essential for investigating skin metabolism of absorbed compounds. The viability of skin in flow-through diffusion cells was systematically examined (6). Viability could be conveniently determined from glucose utilization by skin by measuring lactate appearing in the receptor fluid. Viability could be assessed this way throughout the course of the experiment. It was observed that a HEPES-buffered Hanks' balanced salt solution (HHBSS) was equivalent to minimal essential media in maintaining skin viability for at least 24 hours. The viability of skin was also confirmed by electron microscopy and by the maintenance of estradiol and testosterone metabolism.

More recent studies have demonstrated the usefulness of the 3-[4,5-dimethylthiazol-2yl]-2,5-diphenyltetrazolium bromide (MTT) assay for determining skin viability. We have observed that the addition of 4% BSA to HHBSS results in a lowering of lactate levels measured in the skin viability assay (7). Therefore, the MTT assay was adapted to assess skin viability when BSA was required in the receptor fluid. The MTT assay of skin viability was not affected by addition of BSA to the receptor fluid. The viability of human, fuzzy rat, and hairless guinea pig skin was found to be maintained for 24 hours. However, the assay can only be conducted at the end of a study when skin can be removed from the diffusion cell. As previously noted, the lactate measurement of glucose utilization can be conducted throughout the course of an experiment.

III. SKIN METABOLISM

The following summary of skin absorption/metabolism studies illustrate the types of compounds that are metabolized in skin. In many cases, the metabolites formed from the parent compounds have been determined and important metabolic reactions in skin have been thereby identified.

In early studies from our laboratory, the penetration and metabolism of estradiol and testosterone (6), acetylethyl tetramethyl tetralin (AETT) and butylated hydroxytoluene (BHT) (8), benzo[a]pyrene and 7-ethoxycoumarin (9), and azo colors (10) were examined by using viable dermatome skin sections from mice, rats, hairless guinea pigs, and humans. These early studies will not be discussed here, but may be examined separately by the interested reader.

The percutaneous absorption and metabolism of three structurally related compounds, benzoic acid, *p*-aminobenzoic acid (PABA), and ethyl aminobenzoate (benzocaine), were determined in vitro with hairless guinea pig and human skin (11). Approximately 7% of the absorbed benzoic acid was conjugated with glycine to form hippuric acid.

Acetylation of primary amines was found to be an important metabolic step in skin. For benzocaine, a molecule susceptible to both *N*-acetylation and ester hydrolysis, 80% of the absorbed material was acetylated, while less than 10% of the absorbed ester was hydrolyzed. PABA was much more slowly absorbed than benzocaine and was also less extensively *N*-acetylated. Acetyl-PABA was found primarily in the receptor fluid at the end of the experiments but the receptor fluid contained only 20% of the absorbed dose. Much of the absorbed PABA remained unmetabolized and in the skin, as might be expected for an effective sunscreen agent. The PABA in the skin would probably not have been exposed to *N*-acetylating enzymes if it was localized primarily in the stratum corneum. A similar pattern of benzocaine metabolism was observed in human and hairless guinea pig skin; however, there appeared to be less enzyme activity in human skin.

The extent of metabolism of radiotracer doses of benzocaine in the above studies was compared to metabolism of much larger doses of benzocaine in formulations simulating exposure from use of topical benzocaine anesthetic products (12). When a therapeutic dose (200 $\mu g/cm^2$) was applied, the metabolism of benzocaine was reduced presumably because of the saturation of enzyme activity in skin. However, 34% of the absorbed dose was still converted to acetylbenzocaine. Although the percent applied dose absorbed decreased with increasing dose of benzocaine, total absorption of benzocaine and metabolites increased as the applied

dose increased. Benzocaine and acetylbenzocaine were found to have similar potencies in blocking nerve conduction in the isolated squid giant axon.

Esterase activity and alcohol dehydrogenase activity were characterized in hairless guinea pig skin with the model compounds methyl salicylate and benzyl alcohol (13). Subsequently, the absorption and metabolism of the cosmetic ingredient retinyl palmitate were determined in human and hairless guinea pig skin. Skin absorption for this lipophilic material was considered to be the sum of the absorbed compound in skin and in the receptor fluid at the end of the 24-hour study. Most of the absorbed radiolabel remained in the skin. A substantial amount of the absorbed compound was hydrolyzed to retinol but no oxidation of the alcohol to retinoic acid was observed. Any effects of retinyl palmitate on the structure of skin may be due to the formation of retinol during percutaneous absorption.

Absorption values from in vitro studies with viable hairless guinea pig skin have been found to compare closely with in vivo results for phenanthrene (14) and for pyrene, benzo[a]pyrene, and di(2-ethylhexyl) phthalate (14). Also, significant metabolism was observed in vitro during the absorption of all four compounds. Phenanthrene was metabolized in vitro to 9,10-dihydrodiol, 3,4-dihydrodiol, 1,2-dihydrodiol and traces of hydroxy phenanthrenes (14). After topical administration of phenanthrene, approximately 7% of the percutaneously absorbed material was metabolized to the dihydrodiol metabolites.

Numerous metabolites of benzo[a]pyrene were formed during percutaneous absorption through hairless guinea pig skin (15). Of particular interest was the identification of benzo[a]pyrene 7,8,9,10-tetrahydrotetrol in the diffusion cell receptor fluid. This metabolite is the hydrolysis product of the ultimate carcinogen, 7,8-dihydroxy, 9,10-epoxy-7,8,9,10-tetrahydro-benzo[a]pyrene. This study demonstrates that skin metabolism is likely responsible for skin tumors formed following topical benzo[a]pyrene administration. In the earlier phenanthrene study (14), no known carcinogenic metabolites were formed during skin permeation. This finding is consistent with the lack of tumorigenicity of phenanthrene in rodents.

The percutaneous absorption and metabolism of trinitrobenzene was examined in human, rat, and hairless guinea pig skin (16). Rapid absorption of trinitrobenzene was observed through human and animal skin. The two major metabolites found were 1,3,5 -benzene triacetamide and 3,5-dinitroaniline. It appears that nitro groups on trinitrobenzene can be reduced in skin to amino groups, which are sometimes further metabolized by acetylation to an acetamide derivative.

The metabolism of 2-nitro-*p*-phenylenediamine (2NPPD) absorbed by rat skin and rat intestine was determined in receptor fluid fractions using an HPLC method (17). More than 50% of the 2NPPD applied to rat skin remained unmetabolized, while only 40% of 2NPPD was unmetabolized by rat intestine (Fig. 1). Substantially more acetylation of 2NPPD to N4-acetyl-2NPPD occurred during absorption through skin. However, triaminobenzene was formed to a greater extent in intestine. The amount of sulfated 2NPPD and/or metabolites (actual compound or compounds not determined) was also greater in effluent from intestinal tissue. The extent of metabolism of 2NPPD in human skin (in a semipermanent hair dye vehicle) was also determined. Approximately 60% of the absorbed radiolabeled dose was metabolized to equal amounts of triaminobenzene and N4-acetyl-2NPPD. No sulfated compounds were found in effluents from human skin. These studies showed significant differences in metabolism during penetration through human and rat skin as well as differences in metabolism through rat skin and intestinal tissue.

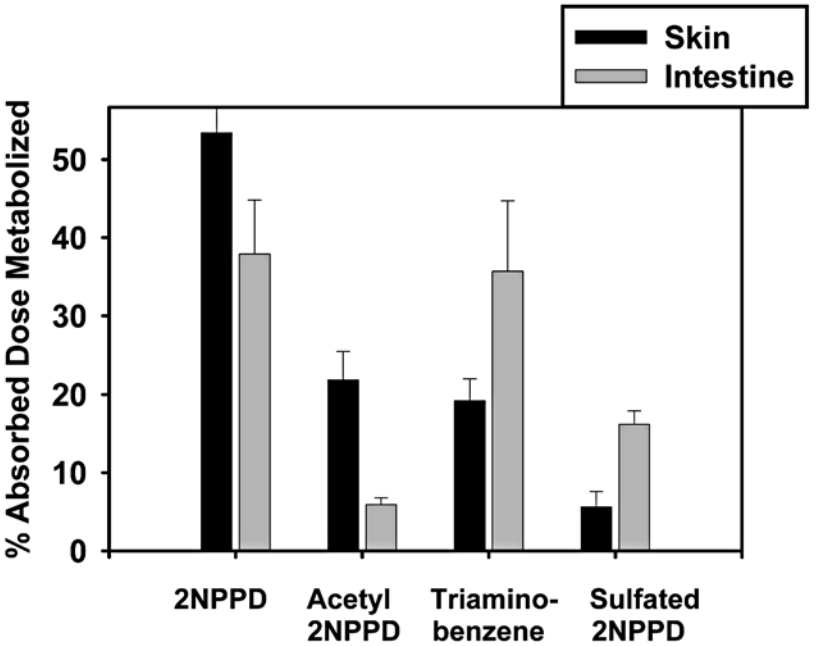


Figure 1 Percent of the absorbed dose of 2NPPD metabolized in rat skin and intestinal tissue. Values are the mean ± SE from three studies. *Abbreviation*: 2NPPD, 2-nitro-**p**-phenylenediamine

The effect of skin metabolism on the biological response to topically applied compounds is only beginning to be investigated. The task is complicated since skin metabolism is difficult to measure in vivo without interference from systemic enzymes. In addition, certain metabolic systems in skin, such as cytochrome P450, have relatively low activity when compared with liver. An in vitro system permits isolation of the skin so that metabolism in the organ can be distinguished from systemic metabolism. In vitro studies indicate that significant metabolism can occur during the percutaneous absorption process.

REFERENCES

1. Pannatier A, Jenner P, Testa B, Etter JC. The skin as a drug metabolizing organ. Drug Metab Rev 1978; 8:319–343.
2. Smith LH, Holland JM. Interaction between benzo[a]pyrene and mouse skin in organ culture. Toxicology 1981; 21:47–57.
3. Holland JM, Kao JY, Whitaker MJ. A multisample apparatus for kinetic evaluation of skin penetration in vitro: the influence of viability and metabolic status of skin. Toxicol Appl Pharmacol 1984; 72:272–280.
4. Chellquist EM, Reifenrath WG. Distribution and fate of diethyl malonate and diisopropyl fluorophosphate on pig skin in vitro. J Pharm Sci 1988; 77:850–854.
5. Hawkins GS, Reifenrath WG. Influence of skin source, penetration cell fluid, and partition coefficient on in vitro skin penetration. J Pharm Sci 1986; 75:378–381.
6. Collier SW, Sheikh NM, Sakr A, Lichtin JL, Stewart RF, Bronaugh RL. Maintenance of skin viability during in vitro percutaneous absorption /metabolism studies. Toxicol Appl Pharmacol 1989; 99:522–533.

7. Hood HL, Bronaugh RL. A comparison of skin viability assays for in vitro skin absorption and metabolism studies. In Vitro Mol Toxicol 1999; 12:3–9.
8. Bronaugh RL, Stewart RF, Storm JE. Extent of cutaneous metabolism during percutaneous absorption of xenobiotics. Toxicol Appl Pharmacol 1989; 99:534–543.
9. Storm JE, Collier SW, Stewart RF, Bronaugh RL. Metabolism of xenobiotics during percutaneous penetration: role of absorption rate and cutaneous enzyme activity. Fund Appl Toxicol 1990; 15:132–141.
10. Collier SW, Storm JE, Bronaugh RL. Reduction of azo dyes during in vitro percutaneous absorption. Toxicol Appl Pharmacol 1993; 118:73–79.
11. Nathan D, Sakr A, Lichtin JL, Bronaugh RL. In vitro skin absorption and metabolism of benzoic acid, *p*-aminobenzoic acid, and benzocaine in the hairless guinea pig. Pharm Res 1990; 7:1147–1151.
12. Kraeling MEK, Lipicky RJ, Bronaugh RL. Metabolism of benzocaine during percutaneous absorption in the hairless guinea pig: acetylbenzocaine formation and activity. Skin Pharmacol 1996; 9:221–230.
13. Boehnlein J, Sakr A, Lichtin JL, Bronaugh RL. Characterization of esterase and alcohol dehydrogenase activity in skin. Metabolism of retinyl palmitate to retinol (vitamin A) during percutaneous absorption. Pharm Res 1994; 11:1155–1159.
14. Ng KME, Chu I, Bronaugh RL, Franklin CA, Somers DA. Percutaneous absorption/metabolism of phenanthrene in the hairless guinea pig: comparison of in vitro and in vivo results. Fund Appl Toxicol 1991; 16:517–524.
15. Ng KME, Chu I, Bronaugh RL, Franklin CA, Somers DA. Percutaneous absorption and metabolism of pyrene, benzo[a]pyrene, and di(2-ethylhexyl) phthalate: comparison of in vitro and in vivo results in the hairless guinea pig. Toxicol Appl Pharmacol 1992; 115:216–223.
16. Kraeling MEK, Reddy G, Bronaugh RL. Percutaneous absorption of trinitrobenzene. Animal models for human skin. J Appl Toxicol 1998; 18:387–392.
17. Yourick JJ, Bronaugh RL. Percutaneous penetration and metabolism of 2-nitro-*p*-phenylenediamine in human and fuzzy rat skin. Toxicol Appl Pharmacol 2000; 166:13–23.

3
Cutaneous Metabolism of Xenobiotics

Saqib J. Bashir and Howard I. Maibach
Department of Dermatology, School of Medicine, University of California, San Francisco, California, U.S.A.

I. INTRODUCTION

The human skin is exposed to many topical agents, either intentionally or by accident. The variety of these foreign agents (xenobiotics) reflects the variety of their intended uses: cosmetics are intended, in theory, to decorate the skin rather than penetrate it, while dermatological drugs such as corticosteroids are intended to act locally within the skin, with little or minimal systemic action. Some drugs, such as nitroglycerin, are not intended to act at the skin, but at distant target organs, in this case the coronary arteries.

Therefore, it is clear that the application of substances to human skin is widespread. One must pause to consider the consequences of this behavior with respect to the skin, and the body as a whole. Although many preparations are placed on the skin on the assumption that the skin is biologically inert, this chapter demonstrates that many exogenous compounds are metabolized in skin (xenobiotic metabolism). We review the existence of enzymes that are capable of metabolizing cutaneous xenobiotics, and some of the factors regulating their activity. Recent work documenting the metabolism of commonly prescribed drugs and environmental agents on the skin is also reviewed.

The role of cutaneous xenobiotic metabolism in the production of toxic metabolites, irritants, and allergens is discussed, in addition to the implication of cutaneous metabolism on transdermal drug delivery in healthy and damaged skin (Fig. 1).

II. XENOBIOTIC-METABOLIZING ENZYMES

These are enzymes participating in the metabolism of foreign compounds. They metabolize substrates that are predominantly lipophilic (and thus penetrate the skin well) into substances that are hydrophilic and less active and can then be excreted in the urine via the kidney.

There are two distinct metabolic steps in their process. The first step is known as phase I reaction and introduces a polar reactive group into a molecule, which renders the molecule suitable for further metabolism as part of phase II reaction.

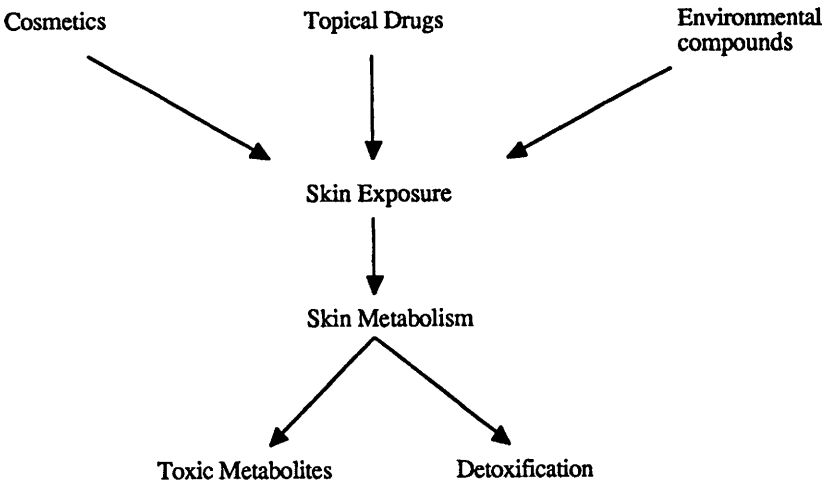


Figure 1 Metabolism of xenobiotics.

Phase I reactions include metabolism by cytochrome P-450–dependent monooxygeases, which have been demonstrated in skin (1). These enzymes add a single oxygen atom from a molecule of O_2 to a carbon atom, resulting in the formation of an OH group on the substrate (hydroxylation) and one molecule of water, H_2O.

Subsequently, these metabolites formed by the phase I reaction by undergo further metabolism, known as phase II reactions. These are conjugation reactions, which render the substrate more hydrophilic, allowing renal excretion. Metabolites can be conjugated with substances such as glucuronic acid, sulfur, or glutathione, resulting in the production of easily excretable products.

III. PHASE I METABOLISM: CYTOCHROME P-450 MONOOXYGENASES

The cytochrome P-450 monooxygenase enzymes are microsomal enzymes demonstrated in the liver and other organs, including skin (2). They play an important role in the phase I metabolism of both exogenous and endogenous compounds such as fatty acids, prostaglandins, leukotrienes, and steroid hormones, and it has been suggested that many dermatological topical drugs are suitable substrates for their enzymes (3).

Cytochrome P-450 enzymes are cofactor-dependent enzymes: They require energy from an external source such as NADPH to catalyze the reaction. This is in contrast to cofactor-independent reactions, which require only the enzyme to catalyze the reaction.

Cytochrome P-450 exists in both prokaryotes and eukaryotes. In eukaryotes, the enzyme is mainly located in the membranes of the endoplasmic reticulum and the mitochondria. The structure of cytochrome P-450 is a protoporphyrin ring that contains a centrally placed Fe^{3+} and a polypeptide chain of approximately 45,000–55,000 kDa (4).

The substrate to be metabolized binds to the protein moiety of the cytochrome P-450, inducing a conformational change. This triggers the necessary cofactor

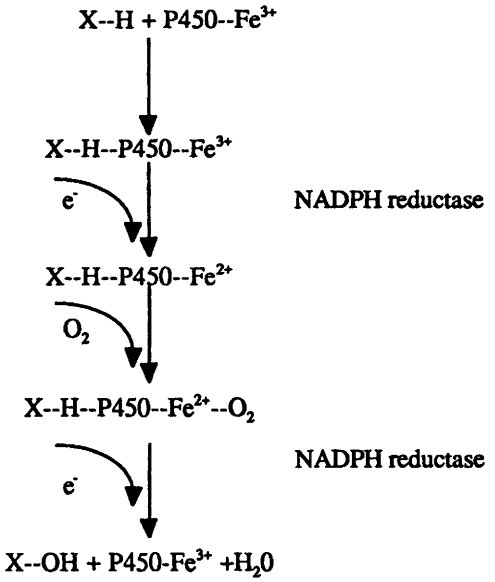


Figure 2 Mechanism of action of cytochrome P-450. *Abbreviations*: X, Substrate; P450, cytochrome P-450 enzyme.

NADPH–P-450 reductase, which donates an electron to the cytochrome P-450; the Fe^{3+} is reduced to Fe^{2+}.

This reduced cytochrome P-450–substrate complex may now bind to a molecule of oxygen. Another electron is donated from NADPH–P-450 reductase; the oxygen molecule is split into two oxygen atoms, with one binding to the substrate, which is then released from the enzyme as a hydroxylated product. The second oxygen atom is released as water (Fig. 2) (4).

Evidence for the existence of cutaneous cytochrome P-450 was initially obtained from the study of the carcinogenic effects of polycyclic aromatic hydrocarbons on the skin. The carcinogenic consequences of cutaneous metabolism are discussed later. Other more recent studies have demonstrated that cytochrome P-450 metabolizes topically applied medications in a fashion similar to the metabolism of systemic medications by the liver.

For example, recent work has demonstrated the relevance of cytochrome P-450 in the context of therapeutic agents. Ademola et al. (5) studied the diffusion and metabolism of theophylline using a flow-through in vitro system. Theophylline is metabolized in the liver by monooxygenases to the metabolites 1,3-dimethyluric acid, 3-methylxanthine, and 1-methyluric acid. In this study of in vitro human skin metabolism of theophylline, these metabolites were also found, suggesting that the cytochrome P-450–dependent enzymes in the skin metabolized the xenobiotic.

A. Isoenzymes of Cytochrome P-450

Many isoenzymes of cytochrome P-450 exist (Table 1), and there are many genes that encode for them. No particular isoenzyme has unique substrate specificity; rather, there is an overlap of substrates. The isoenzymes are categorized by their

Table 1 Cytochrome P-450 Isomers Determined in Mammals and Their Functions

Isomer	Function
CYP 1	Metabolism of xenobiotics
CYP 2	Metabolism of xenobiotics and steroids
CYP 3	Metabolism of xenobiotics and steroids
CYP 4	Fatty acid ω and ω-1 hydroxylation
CYP 5	Thromboxane synthase
CYP 7	Cholesterol 7α-hydroxylase
CYP 11	Steroid 11β-hydroxylase
CYP 17	Steroid 17β-hydroxylase
CYP 19	Aromatase
CYP 21	Steroid 21-hydroxylase
CYP 24	Vitamin D-25 hydroxylase
CYP 27	Cholesterol 27-hydroxylase

amino acid similarities into families, named with the root CYP followed by the family number, a capital letter denoting the subfamily, and a number identifying the particular form.

The family CYP1 has been implicated in xenobiotic metabolism and the families CYP2 and CYP3 in the metabolism of both xenobiotics and steroids. The CYP1A1 is a well-studied member of the cytochrome P-450 family and is expressed in the skin (6). The CYPs, including CYP1A1, are normally expressed at a low level in the skin; however, their activity can be induced by a variety of agents, discussed later in this chapter.

IV. PHASE II METABOLISM

Much of the literature on cutaneous metabolism of xenobiotics focuses on phase I reactions, especially on the role of cytochrome P-450 enzymes. However, phase I reactions are only part of the metabolic process. Following the phase I reaction, the metabolite must be conjugated to facilitate its elimination.

A. Transferases

Transferase activities in the skin can be as high as 10% of that of liver. In comparison, the relative activity of cytochrome P-450 in skin may be only 1% to 5% of the liver's (7). Raza et al. (8) have demonstrated the presence of glutathione S-transferase in skin. Higo et al. (9) have shown that the cutaneous metabolism of nitroglycerin (GTN) to 1,2-GDN (glyceryl di-nitrate) and 1,3-GDN is heavily dependent on the presence of glutathione, which is a cofactor for the transferase enzyme. They exposed GTN to skin homogenates with and without the glutathione cofactor to determine its role in cutaneous metabolism. In the tissue with the cofactor, 30% of the GTN was metabolized within two hours, whereas only 5% of the GTN was metabolized in the tissue without glutathione.

Glycine conjugation is another mechanism of metabolism in the skin. Nasseri-Sina et al. (10) described glycine conjugation in both human and rat keratinocytes.

The metabolic pathway involves the activation of the carboxylic acid group with coenzyme A (CoA) in an ATP-dependent reaction. This is followed by the reaction of the S-CoA derivative with the glycine molecule, catalyzed by a mitochondrial acyltransferase. The resulting glycine conjugation renders the metabolite more polar than the parent compound, and it can then be excreted renally (Fig. 3).

Nasseri-Sina et al. (10) investigated the metabolism of benzoic acid, used topically for the treatment of tinea infestations. Benzoic acid, when administered systemically, is excreted as hippuric acid in urine. This group found that cultured keratinocytes in both humans and rats also metabolized benzoic acid to hippuric acid, but to a much smaller extent than hepatocytes.

Both of the studies just described demonstrated that transferase activity may play a significant role in the metabolism of topically applied compounds.

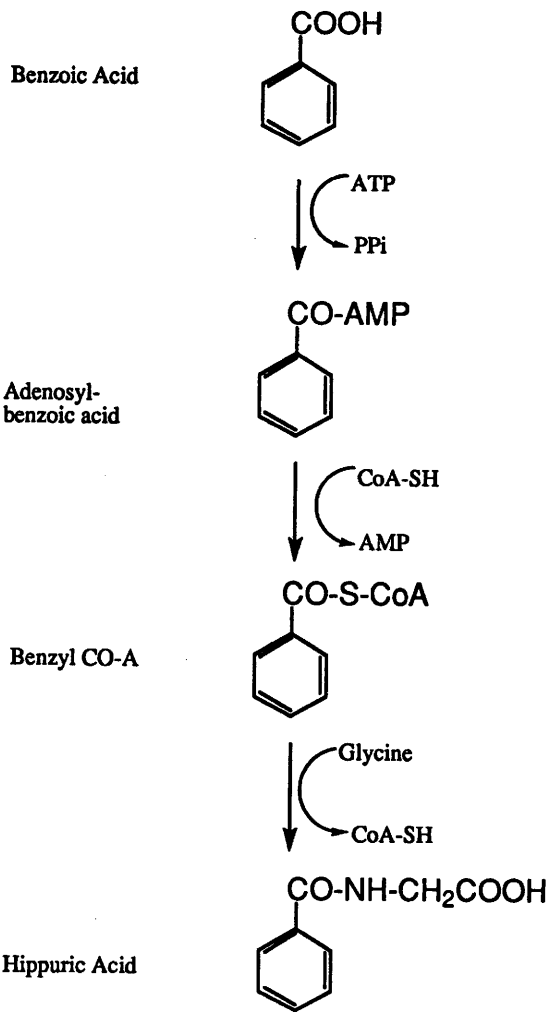


Figure 3 Metabolism of benzoic acid: An example of a conjugation reaction.

V. EXAMPLES OF XENOBIOTIC METABOLISM

A. Corticosteroids

Topical corticosteroids are extensively prescribed for dermatological conditions. Kubota et al. (11) studied the metabolism of betamethasone 17-valerate (B-17) in the living skin equivalent (LSE) model. The betamethasone 17-valerate was initially isomerized to betamethasone 21-valerate (B-21), before it was hydrolyzed to the more polar betamethasone. The rate of conversion of B-17 to B-21 was the same with or without skin homogenate, suggesting that the initial isomerization step was not enzyme dependent but possibly a passive chemical degradation.

Taking this study further, Kubota et al. (12) compared the rates of metabolism of the two isomers B-17 and B-21. When the B-17 isomer was applied to the LSE, half of the drug was left unchanged. In contrast, when B-21 was applied to the LSE, almost all of the drug was metabolized. Thus, the esterases that are responsible for this second, enzyme-dependent step demonstrate preference for the B-21 isomer.

Applying this knowledge in the human setting, Ademola and Maibach (13) demonstrated that B-17 isomer is metabolized to form the B-21 isomer and betamethasone in both human skin in vivo and in the LSE model. This work showed that the B-17 isomer accumulated in the human skin. This was possibly because the B-21 isomer was metabolized faster than the B-17 isomer, which would be consistent with isomeric preference shown in vitro.

These studies have therefore shown that corticosteroids are metabolized in human skin. Further, this metabolism may involve a passive step of chemical degradation as well as active enzyme-dependent metabolism. Importantly, the isomeric structure of the topical agent may influence the rate of metabolism within the skin. Therefore, different isomers of the same compound may be more or less suitable than one another for topical application. This must be considered in the study of any agent to which the skin is exposed.

B. Beta-Adrenoceptor Antagonists

Propanolol is a widely prescribed, highly lipophilic beta-adrenoceptor antagonist. As it is lipophilic, having a partition coefficient of 5.39 at pH 7.0, the topical route of administration may theoretically achieve a steady drug release and plasma concentration. Oral propanolol is subject to first-pass metabolism, leading to variable adsorption and low systemic bioavailability.

Ademola et al. (14), studying percutaneous absorption and metabolism of propanolol in vitro using intact human skin and microsomal preparations, found that between 10.4% and 36.6% of the drug was absorbed, but only 4.1% to 16.1% of the drug penetrated the skin. Some propanolol was retained in the skin, and metabolites of propanolol were found. Naphthoxyacetic acid, 4-hydroxypropanolol, and *N*-desisopropyl propanolol were formed by intact human skin. The concentration of these metabolites was lower compared with hepatic metabolism, suggesting less enzymatic activity in the skin compared to the liver. These metabolites were also formed by the skin microsomes, in a greater concentration than in intact skin. This may be the result of the greater surface area that the microsomes (everted endoplasmic reticulum) had to react with the drug. Additionally, the microsomes biotransformed propanolol to norpropanolol, which the intact skin did not form.

Ademola and Maibach (13) took this study further, using human, LSE, and keratinocyte models. Propanolol does indeed accumulate in human skin, which

may be responsible for irritant or toxic effects. They suggest that the differences between the metabolism of propanolol in skin and liver may explain the accumulation of the drug in the skin. This difference could not be attributed to the degree of enzyme activity, as the enzyme saturation points in the metabolism of propanolol in liver and skin were similarly high.

Ademola and Maibach postulated that the difference in metabolism may lie in the stereoisomeric structure. Using racemic propanolol, they demonstrated that the S-enantiomer was eliminated more efficiently by the skin than the R-enantiomer. This is in contrast to hepatocytes, which are more efficient at removing the R-enantiomer (15). Therefore, the irritation caused by the topical application of propanolol may be the result of accumulation of the R-enantiomer (16).

These studies therefore suggest that propanolol is metabolized by human skin, and that its metabolism may be stereoselective. This metabolism and the retention of propanolol in the skin may explain both the low plasma concentration and irritant dermatitis after topical application.

C. Topical Nitrates

Higo et al. (9) used intact skin and homogenates from hairless mice to study the metabolism of nitroglycerin. In the homogenate study, GTN was incubated with homogenized tissue. After two hours of incubation, 30% of the GTN had been metabolized to the breakdown products 1,2- and 1,3-GDN. This metabolism was shown to be heavily dependent on the presence of glutathione (see earlier). Using the intact skin model, the investigators compared the extent of metabolism using different formulations of the GTN: a 1-mg/mL aqueous solution, a 2% ointment, and a transdermal delivery system. The percentage of metabolites formed was greatest with the aqueous solution (61%), followed by the patch (49%), and least of all with the ointment (35%). This difference is thought to be explained by the greater transdermal flux with the patch and ointment compared to the solution: The smaller the flux, the greater the relative level of skin metabolism.

D. Theophylline

Theophylline is a xanthine derivative that is used as a bronchodilator. Ademola et al. (5) studied the effect of cutaneous metabolism on its topical administration. This drug has a narrow therapeutic index at which optimal bronchodilation is maintained with minimal adverse effects occurring. Considering this, topical administration may give theoretical advantage over the oral route, as the latter results in variable plasma concentrations and is subject to altered absorption with the presence or absence of food in the gastro-intestinal tract. Using both human skin samples and its microsomes, Ademola et al. determined that theophylline was metabolized with the production of 1,3-dimethyl uric acid, 3-methyl uric acid, and 3-methylxanthine from the skin samples. These metabolites of theophylline are produced via cytochrome P-450–dependent metabolism in the liver, and the authors proposed that a similar mechanism may occur in skin (Fig. 4).

VI. METABOLISM OF ENVIRONMENTAL XENOBIOTICS

An important consideration in this subject is the metabolism by the skin of compounds it is exposed to in the environment. The skin forms a barrier against

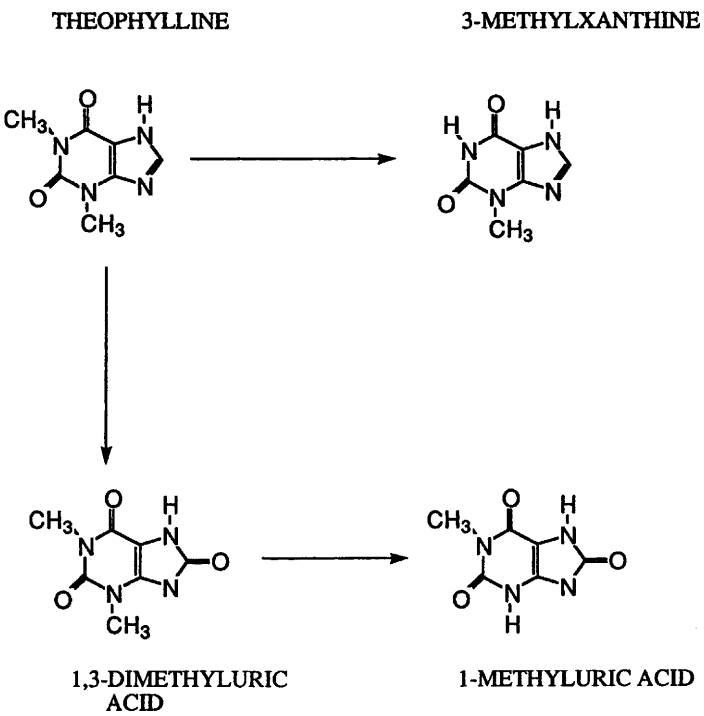


Figure 4 Pathways of theophylline metabolism.

our environment and is constantly exposed to compounds both natural and man-made. In this section, we address the effects of their metabolism.

A. Polycyclic Aromatic Hydrocarbons

Polycyclic aromatic hydrocarbons (PAHs) are produced by the incomplete combustion of fossil fuels and other organic matter. Their potential role in human carcinogenesis is suggested by their presence in the environment and the carcinogenicity of their metabolites.

Cutaneous metabolism of PAH is capable of forming carcinogenic metabolites (see Ref. 17 for review). Studies with model compounds such as benzo[a]pyrene have demonstrated that cutaneous metabolism of PAHs can lead to the formation of phenols, quinones, dihydrodiols, and reactive diol epoxides. The diol epoxides are thought responsible for the carcinogenic effect, binding covalently to macromolecules. Covalent binding with DNA correlates well with the tumorigenicity of the metabolites of benzo[a]pyrone (18).

The PAHs are present in crude coal tar, which is extensively used in dermatological practice. Merk et al. (19) demonstrated that exposure of crude coal tar to the human hair follicle results in the induction of aromatic hydrocarbon hydroxylase (AHH), which is a cytochrome P-450–dependent enzyme. This resulted in the production of benzo[a]pyrene derivatives that were shown to bind to DNA.

These studies of PAHs therefore exemplify the potentially hazardous nature of the cutaneous metabolism of environmental xenobiotics. We discuss the metabolism of other environmental agents and their potential for toxicity next.

B. Pesticides

Ademola et al. (20) studied the cutaneous metabolism of an environmental pesticide, 2-chloro-2,6-diethyl-*N*-(butoxymethyl) acetanilide (butachlor), on human skin in vitro. This study is significant in our discussion of the role of cutaneous metabolism in our everyday lives and its potential consequences. Skin is the most important route of exposure to such agents; topical exposure could result in systemic absorption, which may be toxic, and also could result in cutaneous or systemic metabolism, either of which could toxify or detoxify the compound. In this study, the butachlor was metabolized to 4-hydroxybutachlor and was NADPH dependent, implying that the metabolism may be dependent on monooxygenases in the skin. The 4-hydroxybutachlor metabolite was noted to accumulate in skin.

Cysteine- and glutathione-conjugated metabolites were also found. The formation of glutathione conjugates is consistent with the known presence of glutathione in human skin (8). Although the significance of these metabolites is not yet known, their formation and accumulation in the skin may be potentially hazardous.

Ademola et al. (21) also investigated the metabolism of a widely used herbicide, atrazine, within the skin. The metabolites 2-chloro-4-ethyl-amino-6-amino-*s*-triazine (desisopropylatrazine) and 2-chloro-4,6-diamino-s-triazine were found in the receptor fluid and the skin supernates. An additional metabolite (2-chloro-4-amino-6-isopropylamino-s-triazine) was found in the skin supernates. This study again showed that metabolites of an environmental agent can be produced in the skin, further reinforcing the need for the detailed study of skin metabolism as a possible source of pathology (Table 2).

VII. FACTORS AFFECTING CUTANEOUS METABOLISM

The factors that influence the metabolism of cutaneous xenobiotics can be dynamic or static. Dynamic metabolism may vary according to the physiological and pathological condition of the skin. In contrast, static factors may be related to the structure of the skin at a particular site.

A. Dynamic Factors

The dynamic response of enzymes to inductive and inhibitory stimuli could be an important factor in determining the extent of metabolism within the skin. Also, in the case of isoenzymes, such as the cytochrome P-450 family, which particular isoenzymes are induced and in what proportions must also be considered.

1. Enzyme Induction

The induction of enzymes that metabolize xenobiotics may increase the rate and/or amount of metabolites produced. Some xenobiotics may induce enzymes for which they themselves are substrates, or may induce enzymes that act on other exogenous or endogenous substrates.

Schlede and Connely (22) demonstrated a 10-fold increase in aryl hydrocarbon hydroxylase (AHH) activity in skin homogenates from rats pretreated with 3-methychloranthene. The AHH is a cytochrome P-450–dependent enzyme associated with the expression of CYP1A1 (3). Further studies have shown that topically applied

Table 2 Examples of Some Xenobiotics and Their Metabolites

Compound	Major metabolites	Comment
Betamethasone 17-valerate	Betamethasone 21-valerate	Chemical degradation
Propanolol	Betamethasone	Active metabolism
	Naphthoxyacetic acid	Produced by intact skin
	4-Hydroxypropanolol	Produced by intact skin
	N-Desisopropyl propanolol	Produced by intact skin
	Norpropanolol	Only produced by microsomes
Nitrogylcerin	1,2-GDN	
	1,3-GDN	
Theophylline	1,3-Dimethyl uric acid	
	3-Methyl uric acid	
	3-Methyl xanthene	
Polycyclic aromatic hydrocarbons	Phenols	
	Quinones	
	Dihydrodiols	
	Diol epoxides	Carcinogenic
Butachlor	4-Hydroxybutachlor	
	Cysteine conjugates	
	Glutathione conjugates	
Atrazine	Desisopropylatrazine	
	2-Chloro-4,6-diamino-*s*-triazine	

polycyclic hydrocarbons, coal tar, and petroleum derivatives are also effective in the induction of AHH in human skin (17).

Jugert et al. (23) studied the effect of topically applied dexamethasone on the induction of cutaneous cytochrome P-450 isoenzymes in murine skin. The induction of cytochromes 1A1, 2B1, 2E, and 3A was seen, in addition to induction of the monoxygenase enzymes catalyzed by these CYPs. The group further employed immunohistochemistry to localize the expression of the CYP2B1 isoenzyme within the epidermis. This particular isoenzyme was investigated as it was involved in the greatest enzyme induction. The isoenzyme was localized to the suprabasal layer of the epidermis and the cells of the hair follicle.

That dexamethasone can induce several isoenzymes of cytochrome P-450 is a significant finding because the cytochrome P-450 monooxygenases are not substrate specific. Therefore, if one substrate induces a series of enzymes, other xenobiotics that are applied to the skin, either intentionally or unintentionally, may be metabolized at an increased rate. For example, if one comes in contact with benzo[a]pyrone while using topical corticosteroids for atopic dermatitis, the metabolism of carcinogenic metabolites could be increased.

2. *Enzyme Activity Inhibition*

In contrast to induction, the inhibition of enzymes must also be considered. Inhibition of the cutaneous metabolism of xenobiotics has several theoretical advantages. For example, selectively inhibiting an enzyme may increase the overall percutaneous

absorption of a particular medication. Kao and Carver (17) reviewed work in this field. The imidazole antifungal agents, widely prescribed in dermatological practice, are potent inhibitors of the microsomal P-450–dependent monooxygenases. In skin, they inhinit the activity of AHH and epoxide hydrolase activity (EPOH). Also, imidazoles induce glutathione-s-transferase activity and inhibit the cutaneous metabolism, marcromolecular binding, and carcinogenicity of topically applied benzopyrene in cultured mouse keratinocytes (24). Plant phenols also inhibit the monooxygenase metabolism of benzo[a]pyrene in vitro (25). The studies suggest that inhibitors of xenometabolizing enzymes may be useful in the prevention of polycyclic hydrocarbon skin malignancies.

B. Barrier Disruptions and Cutaneous Xenometabolism

Several studies have attempted to study the metabolism of xenobiotics following disruption of the skin barrier. Higo et al. (26) studied the effect of skin condition in vitro on the cutaneous metabolism of nitroglycerin. Full thickness excised skin from hairless mice was placed in a plastic bag prior to immersion in boiling water for 10 minutes. Heating the skin disrupted its barrier function, a fact that can be inferred from the increased total nitrate flux across the heated skin compared to controls. The skin did continue to metabolize the GTN; however, compared to control skin, the heated skin showed a preference for the formation of 1,3-GDN rather than 1,2-GTN. The heated tissue continued to metabolize the nitroglycerin at a steady rate during the 10 hours experiment, whereas the control specimen's metabolism decreased with time. This suggests that the altered metabolism may be the result of nonenzymatic metabolism of the drug. In the same study, the authors also damaged the skin barrier using tape stripping. The greater the number of strippings, the more damaged was the skin, with greater flux of nitrates and less metabolic activity.

However, Shaikh et al. (27) demonstrated that freezing human skin did not alter its metabolic capacity. Investigating the metabolism of 8-methoxypsoralen (8-MOP) on human skin in vitro, it was demonstrated that the skin barrier had been perturbed as there was a greater flux of 8-MOP in the frozen specimen compared to the control. However, the metabolic capacity of the skin remained constant.

Different insults to the human skin barrier may alter the metabolism of xenobiotics in different ways. These studies demonstrate that further investigation of skin barrier function in cutaneous metabolism is necessary. As products for topical use become increasingly popular, their use on damaged skin must be investigated.

VIII. CONSEQUENCES OF CUTANEOUS XENOBIOTIC METABOLISM

For any drug metabolized in the skin, the potentially toxic nature of any metabolite must be considered. For example, a metabolite may be irritant, allergenic, or even carcinogenic, either locally or systemically. The precarcinogen benzo[a]pyrene was described earlier as an example of this, as was the metabolism of propanolol.

The ability of the enzymes responsible for xenometabolism to be induced or inhibited may affect the rate and extent of metabolism of any compound on the skin. This may affect the efficacy of drugs applied topically either for local or systemic administration. Indeed, there is potential for topical formulations to include inhibitors of enzymes to enhance drug delivery.

Metabolism of the drug at the cutaneous level constitutes "first-pass metabolism," which may result in subtherapeutic doses reaching the systemic circulation. Indeed, the metabolic activity of the enzymes may be dynamic rather than static; this implies that under different physiological and pathological conditions, variable doses of the drug may be delivered through the skin, perhaps resulting in toxicity or decreased effectiveness. Particular regard must therefore be paid to drugs of narrow therapeutic index.

In conclusion, this chapter has demonstrated that cutaneous metabolism is relevant in the application of any topical agent to the skin, whether for superficial use or end-organ effect.

REFERENCES

1. Goerz G. Animal models for cutaneous drug metabolising enzymes. In: Maibach HI, Lowe NJ, eds. Models in Dermatology. Vol. III. Basel: Karger, 1989:93–105.
2. Gonzalez FJ. The molecular biology of cytochrome P-450s. Pharmacol Rev 1989; 40:243–388.
3. Ahmad N, Agarwal R, Mukhtar H. Cytochrome P-450-dependent drug metabolism in skin. Clin Dermatol 1996; 14:407–415.
4. Goeptar AR, Scheerens H, Vermeulen NP. Oxygen and xenobiotic reductase activities of cytochrome P450. Crit Rev Toxicol 1995; 25(1):25–65.
5. Ademola JI, Wester RC, Maibach HH. Cutaneous metabolism of theophylline by human skin. J Invest Dermatol 1992; 98(3):310–314.
6. Bickers DR, Dutta-Chaudhury T, Mukhtar H. Epidermis: A site of drug metabolism in rat skin. Studies on cytochrome P-450 content and mixed function oxidase and epoxide hydrolase activity. Mol Pharmacol 1982; 21:239–247.
7. Merk HF, Jergert FK, Frankenberg S. Biotransformations in the skin. In: Marzulli FN, Maibach HI, eds. Dermatoxicology. 5th ed. Ch. 6. Washington, DC: Taylor & Francis, 1996:61–76.
8. Raza H, Awasthi YC, Zaim MT, Eckert RL, Mukhtar H. Glutathione-*S* transferase in human and rodent skin; Multiple forms and species specific expression. J Invest Dermatol 1991; 96:463–467.
9. Higo N, Hinz RS, Lau DTW, Benet LZ, Guy RH. Cutaneous metabolism of nitroglycerin in vitro. Pharm Res 1992a; 9(2):187–191.
10. Nasseri-Sina P, Hotchkiss SA, Caldwell J. Cutaneous xenobiotic metabolism glycine conjugation in human and rat keratinocytes. Food and Chemical Toxicology 1997; 35(3–4):409–416.
11. Kubota K, Ademola JI, Maibach HI. Metabolism of topical drugs within the skin, in particular glucocorticoids. In: Korting HC, Maibach HI, eds. Topical Glucocorticoids with Increased Benefit/Risk Ratio. Current Problems in Dermatology. Vol. 21. Basel: Karger, 1993:61–66.
12. Kubota K, Ademola JI, Maibach HI. Simultaneous diffusion and metabolism of betamethasone 17-valerate in the living skin equivalent. J Pharm Sci 1995; 84(12):1478–1481.
13. Ademola JI, Maibach HI. Cutaneous metabolism and penetration of methoxypsoralen, betamethasone 17-valerate, retinoic acid, nitroglycerin and theophylline. Curr Problems Dermatol 1995; 22:201–213.
14. Ademola JI, Chow CA, Wester RC, Maibach HI. Metabolism of propanolol during percutaneous absorption in human skin. J Pharm Sci 1991; 82(8):767–770.
15. Ward S, Walle T, Walle K, Wilkinson GR, Branch RA. Propanolol's metabolism is determined by both mephenytoin and debrisoquin hydroxylase. Clin Pharm Ther 1989; 45:72–78.

16. Melendres JL, Nangia A, Sedik L, Mitsuhiko H, Maibach HI. Nonane enhances propanolol hydrochloride penetration in human skin. Int J Pharm 1992; 92:243–248.
17. Kao J, Carver MP. Skin metabolism. In: Marzulli N, Maibach HI, eds. Dermatotoxicology. 4th ed. Washington, DC: Hemisphere, 1991:143–200.
18. Mukhtar H, Agarwal R, Bickers DR. Cutaneous metabolism of xenobiotics and steroid hormones. In: Mukhtar H, ed. Pharmacology of the Skin. Boca Raton, FL: CRC Press, 1992:89–110.
19. Merk HF, Mukhtar H, Kaufmann I, Das M, Bickers DR. Human hair follicle benzo(a)-pyrene and benzo(a)pyrene 7,8-diol metabolism; Effect of exposure to a crude coal tar containing shampoo. J Invest Dermatol 1987; 88:71–76.
20. Ademola JI, Wester RC, Maibach HI. Absorption and metabolism of 2-chloro-2,6-diethyl-*N*-(butoxymethyl)acetanilide (butachlor) in human skin in vitro. Toxicol Appl Pharmacol 1993a; 121(1):78–86.
21. Ademola JI, Sedik LE, Wester RC, Maibach HI. In vitro percutaneous absorption and metabolism in man of 2-chloro-4-ethyl amino-6-isopropylamine-s-triazine (atrazine). Arch Toxicol 1993b; 67(2):85–91.
22. Schlede E, Connely AH. Induction of benzo(a)pyrene hydroxylase activity in rat skin. Life Sci 1970; 9(II):1295–1303.
23. Jugert FK, Agarwal R, Kuhn A, Bickers DR, Merk HF, Mukhtar H. Multiple cytochrome P450 isozymes in murine skin: induction of P450 1A, 2B, 2E, and 3A by dexamethasone. J Invest Dermatol 1994; 102(6):970–975.
24. Das M, Mukhtar H, Del Tito BJ Jr, Marcelo CL, Bickers DR. Clotrimaozole, an inhibitor of benzo(a)pyrene metabolism and its subsequent glucuronidation, Sulfation, and macromolecular binding in BALB/c mouse culured keratinocytes. J Invest Dermatol 1986; 87:4–10.
25. Das M, Mukhtar H, Bik DP, Bickers DR. Inhibition of epidermal xenobiotic metabolism in SENCAR mice by naturally occurring phenols. Cancer Res 1987; 47:760–766.
26. Higo N, Hinz RS, Lau DTW, Benet LZ, Guy RH. Cutaneous metabolism of nitroglycerin in vitro. II. Effects of skin condition and penetration enhancement. Pharm Res 1992a; 9(3):303–306.
27. Shaikh NA, Ademola JI, Maibach HI. Effects of freezing and azide treatment of in vitro human skin on the flux and metabolism of 8-methoxypsoralen. Skin Pharmacol 1996; 9:274–280.

4

Occlusion Does Not Uniformly Enhance Penetration In Vivo

Daniel Bucks
School of Medicine, University of California, San Francisco and Dow Pharmaceutical Sciences, Petaluma, California, U.S.A.

Howard I. Maibach
Department of Dermatology, School of Medicine, University of California, San Francisco, California, U.S.A.

I. INTRODUCTION

Mammalian skin provides a relatively efficient barrier to the ingress of exogenous materials and the egress of endogenous compounds, particulary water. Loss of this vital function results in death from dehydration. Compromised function is associated with complications seen in several dermatological disorders. Stratum corneum intercellular lipid domains form a major transport pathway for penetration (1–4). Perturbation of these lamellar lipids causes skin permeation resistance to fall and has implicated their crucial role in barrier function. Indeed, epidermal sterologenesis appears to be modulated by the skin's barrier requirements (5). Despite the fact that the skin is perhaps the most impermeable mammalian membrane, it is permeable to a degree, that is, it is semipermeable; as such, the topical application of pharmaceutical agents has been shown to be a viable route of entry into the systemic circulation as well as an obvious choice in the treatment of dermatological ailments. Of the various approaches employed to enhance the percutaneous absorption of drugs, occlusion (defined as the complete impairment of passive transepidermal water loss at the application site) is the simplest and perhaps one of the most common methods in use. In this chapter we have summarized the literature to evaluate the effect of occlusion on the percutaneous absorption of topically applied compounds and to look at how certain compound physicochemical properties (such as volatility, partition coefficient, and aqueous solubility) may predict what effect occlusion may have.

The increased clinical efficacy of topical drugs caused by covering the site of application was first documented by Garb (6). Subsequently, Scholtz (7), using fluocinolone acetonide, and Sulzberger and Witten (8), using hydrocortisone, reported enhanced corticoid activity with occlusion in the treatment of psoriasis. The enhanced pharmacological effect of topical corticosteroids under occlusion

was further demonstrated by the vasoconstriction studies of McKenzie (9) and McKenzie and Stoughton (10). Occlusion has also been reported to increase the percutaneous absorption of various other topically applied compounds (11–17). However, as shown later, short-term occlusion does not necessarily increase the percutaneous absorption of all chemicals.

II. PERCUTANEOUS ABSORPTION OF *P*-PHENYLENEDIAMINE (PPDA) IN GUINEA PIGS

The in vivo percutaneous absorption of *p*-phenylenediamine (PPDA) from six occlusive patch test systems was investigated by Kim et al. (18). The extent of absorption was determined using ^{14}C radiotracer methodology. The ^{14}C-PPDA was formulated as 1% PPDA in petrolatum (USP) and applied from each test system at a skin surface dose of $2\,mg/cm^2$. Thus, the amount of PPDA was normalized with respect to the surface area of each patch test system (and, hence, to the surface area of treated skin). A sixfold difference in the level of skin absorption ($p < 0.02$) was found between the patches (Table 1). It should be noted that a non-occlusive control was not included in this study.

The rate of ^{14}C excretion following topical application of the radiolabeled PPDA in the various patch test systems is shown in Figure 1. Clearly, the rate and extent of PPDA absorption were dependent upon the patch test system employed. The mechanism responsible for differences in PPDA percutaneous absorption from these patch test systems is not known. However, magnitude of occlusiveness of each dressing is hypothesized to correspond to enhanced absorption.

III. PERCUTANEOUS ABSORPTION OF VOLATILE COMPOUNDS

The effect of occlusion on the in vivo percutaneous absorption of two fragrances (safrole and cinnamyl anthranilate) and two chemical analogs (cinnamic alcohol and cinnamic acid) in rhesus monkeys was evaluated by Bronaugh et al. (19). Each compound was applied at a topical dose of $4\,\mu g/cm^2$ from a small volume of acetone.

Table 1 Percutaneous Absorption of PPDA from Patch Test Systems

Patch test system	Mean % dose absorbed (SD)
Hill Top chamber	53 (21)
Teflon (control)	49 (9)
Small Finn chamber	30 (9)
Large Finn chamber	23 (7)
AL-Test chamber	8 (1)
Small Finn chamber with paper disc insert	34 (20)

Note: The rate of ^{14}C excretion following topical application of the radiolabeled PPDA in the various patch test systems is shown in Figure 1. The extent of PPDA absorption was dependent upon the occlusive patch test system employed. It should be noted that a non-occlusive control study was not conducted. The test system used $2\,mg/mm^2$ PPDA for 48 hours on the dorsal mid-lumbar region of the guinea pig. *Source*: Data from Ref. 18.

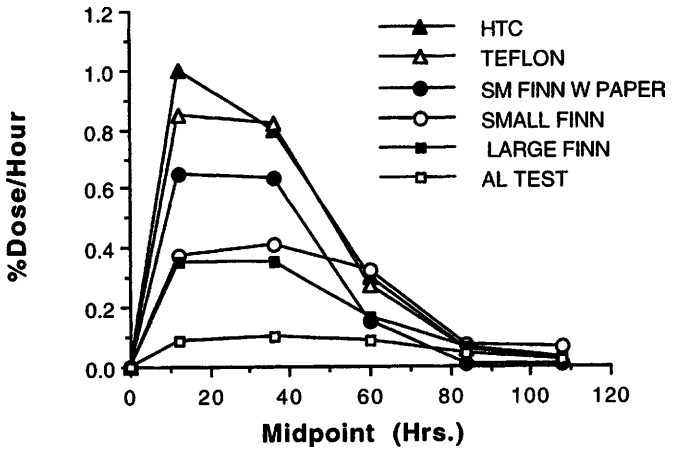


Figure 1 In vivo percutaneous absorption of PPDA (2 mg/mm^2) following a 48-hour exposure on the dorsal lumbar region of guinea pigs. *Abbreviations*: HTC, Hill Top chamber; Teflon, sheet of Teflon; sm Finn w paper, small Finn chamber with paper insert included; small Finn, small Finn chamber with paper insert removed; large Finn, large Finn chamber with paper insert removed. *Source*: Redrawn from Ref. 18.

Occlusion was achieved by covering of the site of application with plastic wrap (Saran Wrap, a chlorinated hydrocarbon polymer) after the acetone had evaporated from the skin surface. The extent of absorption following single-dose administration was determined using ^{14}C radiotracer methodology. The fragrance materials were well absorbed through monkey skin. Plastic-wrap occlusion of the application site resulted in large increases in absorption (Table 2). The authors also presented in vitro data documenting the significant increase in percutaneous absorption of these chemicals under occluded compared to non-protected conditions, that is, left open to the air.

Investigation of the effect of occlusion on the percutaneous absorption of six additional volatile compounds (benzyl acetate, benzamide, benzoin, benzophenone, benzyl benzoate, and benzyl alcohol) was conducted using the same in vivo methodology. These studies included occlusion of the site of application with a glass cylinder secured to the skin by silicone glue and capped with Parafilm, occlusion with plastic wrap, and non-protected conditions (20). As shown in Table 3, occlusion, in general, enhances the percutaneous absorption of these compounds. However,

Table 2 In Vivo Percutaneous Absorption of Fragrances in Monkeys

	Percent dose absorbed[a]	
	Non-protected	Plastic-wrap occlusion
Cinnamyl anthranilate	26.1 (4.6)	39.0 (5.6)
Safrole	4.1 (1.6)	13.3 (4.6)
Cinnamic alcohol	25.4 (4.4)	74.6 (14.4)
Cinnamic acid	38.6 (16.6)	83.9 (5.4)

Note: Values were corrected for incomplete renal elimination. Mean ± SD ($N = 4$).
[a]Single 4-μg/cm^2 dose with a 24-hours exposure prior to soap and water washing.
Source: Data from Ref. 19.

Table 3 In Vivo Percutaneous Absorption of Benzyl Derivatives in Monkeys

	% dose absorbed[a]			
	Non-protected	Plastic wrap occlusion	Glass chamber occlusion	log $K_{o/w}$
Benzamide	47 (14)	85 (8)	73 (20)	0.64
Benzyl alcohol	32 (9)	56 (29)	80 (15)	0.87
Benzoin	49 (6)	43 (12)	77 (4)	1.35
Benzyl acetate	35 (19)	17 (5)	79 (15)	1.96
Benzophenone	44 (15)	69 (12)	69 (10)	3.18
Benzyl benzoate	57 (21)	71 (9)	65 (20)	3.97

Note: Values corrected for incomplete renal elimination. Mean ± SD ($N = 4$).
[a]Single 4-μg/cm^2 dose with a 24-hours exposure prior to soap and water washing.
Source: Data from Ref. 20.

differences in percutaneous absorption were observed between plastic wrap and ''glass chamber'' occlusive conditions. The absorption of benzoin and that of benzyl acetate were lower under plastic wrap compared to the non-protected condition. This discrepancy might be due to compound sequestration by the plastic wrap. Glass-chamber occlusion resulted in greater bioavailability than non-protected or plastic-wrap occlusion except for benzyl benzoate, where plastic-wrap conditions resulted in greater absorption, and for benzophenone, where glass-chamber and plastic-wrap conditions resulted in the same magnitude increase over non-protected test conditions.

An attempt was made to correlate occlusion-enhanced bioavailability with each compound's octanol/water partition coefficient. Unexpectedly, no apparent trends were noted for these volatile fragrance compounds. Absence of a trend is in contradiction to results obtained with steroids and phenol derivatives discussed later, given the range of log $K_{O/W}$ evaluated with these fragrances.

Gummer and Maibach (16) studied the penetration of methanol and ethanol through excised, full-thickness guinea-pig skin. Occlusion significantly enhanced the cumulative amount penetrating as well as the profiles of the amount penetrating per hour for both methanol and ethanol. Consistent with results from other investigators reported already, occlusion-induced penetration enhancement was dependent upon the nature of the occlusive material, with the greatest enhancement observed with a plastic Hill Top chamber (21). Intuitively, occlusion-induced enhancement in the penetration of volatile compounds should be one of the items related to the degree to which the occlusive device inhibits evaporative loss of compound from the skin surface.

IV. PERCUTANEOUS ABSORPTION OF STEROIDS IN HUMANS

The earliest attempt to correlate the increased pharmacological effect of hydrocortisone under occlusive conditions with the pharmacokinetics of absorption was reported by Feldmann and Maibach (12). In this study, the rate and extent of ^{14}C-label excretion into the urine following topical application of [^{14}C]hydrocortisone to the ventral forearm of normal human volunteers were measured. Radiolabeled hydrocortisone (75 μg) was applied in acetone solution (1000 μL) as a surface deposit

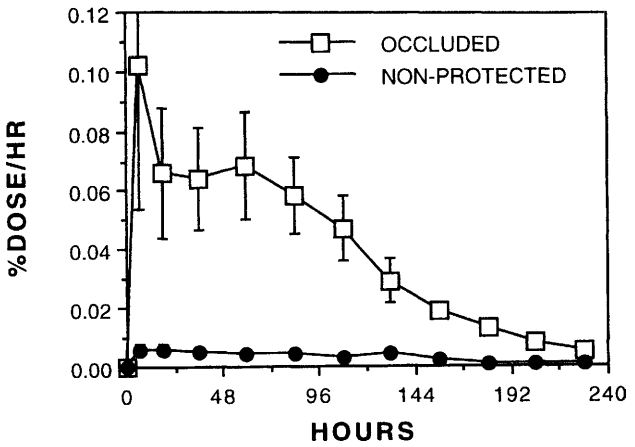


Figure 2 Percutaneous absorption of hydrocortisone in humans. Human 96-hour occluded versus. 24-hours non-protected exposure of hydrocortisone at $4\,\mu g/cm^2$ prior to soap and water washing. Occlusion was with plastic wrap. *Source*: Data from Ref. 12.

over $13\,cm^2$ of skin. The authors estimated that this was equivalent to a sparing application of a 0.5% hydrocortisone topical preparation ($5.8\,\mu g/cm^2$). The site of application was either non-protected or occluded with plastic wrap (Saran Wrap). When the skin was non-protected, the dosing site was washed 24 hours post-application. On the other hand, when the skin was occluded, the plastic wrap remained in place for 96 hours (4 days) post-application before the application site was washed. The percent of the applied dose excreted into the urine, corrected for incomplete renal elimination, was (mean $\pm$ SD) 0.46 ± 0.20 and 5.9 ± 3.5 under non-protected and occluded conditions, respectively (Fig. 2). A paired *t*-test of the results indicates a significant difference ($p = 0.01$) in cumulative absorption of hydrocortisone between the two exposure conditions. Quantitatively, the occlusive conditions employed increased the cumulative absorption of hydrocortisone (HC) by about an order of magnitude. However, note that the occlusive system retained the drug in contact with the skin for 96 hours, compared to the 24-hours exposure period under non-protected conditions, and this could affect absorption as measured by the cumulative measurement of drug excreted into the urine, but the dramatic difference in percent dose absorbed per hour between occluded and non-protected at 12 and 24 hours is not expected to be dependent upon differences in times of washing. This enhancement in HC absorption afforded by occlusion is not consistent with the additional studies reported next.

Guy et al. (13) investigated the effect of occlusion on the percutaneous absorption of steroids in vivo following single and multiple application. The extent of absorption of four steroids (progesterone, testosterone, estradiol, and hydrocortisone), using radiotracer elimination into the urine following topical application to the ventral forearm of male volunteers, was reported. The chemical dose was $4\,\mu g/cm^2$ over an application area of $2.5\,cm^2$. The ^{14}C-labeled chemicals were applied in $20\,\mu L$ acetone. In the occlusive studies, after evaporation of the vehicle, the site of application was covered with a plastic (polyethylene–vinyl acetate copolymer, Hill Top) chamber. In all cases, after 24 hours, the site of application was washed with soap and water using a standardized procedure (22). In the occlusive studies, the

Table 4 Percutaneous Absorption of Steroids in Humans

	Mean % applied dose absorbed (± SD)	
	Non-protected	Occluded
Hydrocortisone		
Single application	2 ± 2[a]	4 ± 2
Multiple application		
First dose	3 ± 1	4 ± 1
Eighth dose	3 ± 1	3 ± 1
Estradiol		
Single application	11 ± 5[a]	27 ± 6
Multiple application		
First dose	10 ± 2	38 ± 8
Eighth dose	11 ± 5	22 ± 7
Testosterone		
Single application	13 ± 3[a]	46 ± 15
Multiple application		
First dose	21 ± 6	51 ± 10
Eighth dose	20 ± 7	50 ± 9
Progesterone		
Single application	11 ± 6[a]	33 ± 9

[a]*Source*: Data from Refs. 11,23 and 42.

administration site was then covered again with a new chamber. An essentially identical protocol was also performed following a multiple dosing regime (23). Daily topical doses of three of the steroids (testosterone, estradiol, and hydrocortisone) were administered over a 14-day period. The first and eighth doses were ^{14}C-labeled and urinary excretion of radiolabel was followed. As described earlier, the 24-hours washing procedure was performed daily and a new chamber was applied. Occlusive

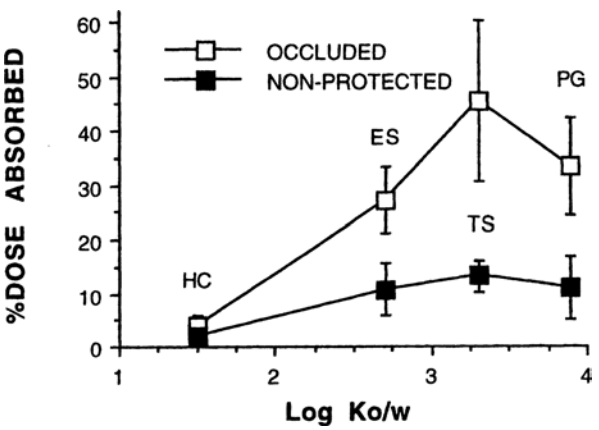


Figure 3 Percutaneous absorption of four steroids in humans as a function of penetrant octanol/water partition coefficient. Exposure period 24 hours at 4 μg/cm^2 prior to soap and water washing. *Abbreviations*: HC, hydrocortisone; ES, estradiol; TS, testosterone; PG, progesterone. *Source*: From Ref. 13.

Table 5 Accountability of Applied Dose[a] in Occluded Studies

	Absorbed (%)	Removed from skin (%)	Total % dose
Hydrocortisone			
Single dose[b]	4 ± 2	64 ± 5	68 ± 4
First MD[c]	4 ± 1	82 ± 5	85 ± 4
Eighth MD[d]	3 ± 1	78 ± 2	81 ± 3
Estradiol			
Single dose[b]	27 ± 6	60 ± 12	87 ± 13
First MD[c]	38 ± 8	62 ± 6	100 ± 4
Eighth MD[d]	22 ± 7	59 ± 8	81 ± 6
Testosterone			
Single dose[b]	46 ± 15	44 ± 7	90 ± 8
First MD[b]	51 ± 10	48 ± 9	99 ± 4
Eighth MD[d]	50 ± 9	42 ± 9	92 ± 17
Progesterone			
Single dose[b]	33 ± 9	47 ± 10	80 ± 6

Note: Values corrected for incomplete renal elimination, mean $\pm$ SD. Occluded with a plastic (Hill Top) chamber.
[a]Single 4-$\mu g/cm^2$ dose with a 24-hours exposure prior to soap and water washing.
[b]Single dose study.
[c]First dose of a 14-day multiple-dose study.
[d]Eighth dose of a 14-day multiple-dose study.
Source: Adapted from Ref. 43.

chambers and washes were collected and assayed for residual surface chemical. The results of this study are summarized in Table 4. Steroid percutaneous absorption as a function of penetrant octanol/water partition coefficient ($K_{O/W}$) is shown in Figure 3. The studies indicate that:

1. The single-dose measurements of the percutaneous absorption of hydrocortisone, estradiol, and testosterone are predictive of percutaneous absorption following a comparable multiple dose regimen (see chapter 27 on the effect of repetitive application), under both occluded and nonoccluded conditions.
2. Occlusion significantly ($p < 0.05$) increased the percutaneous absorption of estradiol, testosterone, and progesterone, but not that of hydrocortisone (the compound with the lowest $K_{o/W}$ value in this series of steroids).
3. Percutaneous absorption increases with increasing $K_{o/W}$ up to testosterone but declines for progesterone, under occluded and non-occluded conditions.
4. The occlusive procedure generally permits excellent dose accountability (Table 5).

The percutaneous absorption of these same four steroids under ''protected'' (i.e., covered, but non-occlusive) conditions has also been measured in vivo (11,24) using the same methodology. The data obtained from these later experiments permitted the effect of occlusion to be rigorously assessed (since complete mass balance of the applied dose was possible). With the exception of hydrocortisone (Table 6), occlusion significantly increased the percutaneous absorption ($p < 0.01$) of the steroids. These results were in excellent agreement with the comparable non-protected

Table 6 Percutaneous Absorption of Steroids in Humans: Single Dose Application for 24 hours at 4 μg/cm^2

	Mean % dose absorbed (± SD; $N \geq 5$)	
	Protected[a]	Occluded[b]
Hydrocortisone	4 ± 2	4 ± 2
Estradiol	3 ± 1	27 ± 6
Testosterone	18 ± 9	46 ± 15
Progesterone	13 ± 6	33 ± 9

[a]Dose site covered with a ventilated plastic chamber.
[b]Dose site covered with an occlusive plastic chamber.
Source: Data from Refs. 11, 13, and 43.

studies described earlier. As stated before, excellent dose accountability was reported (Table 7).

To investigate the apparent discrepancy between the effect of plastic wrap occlusion (12) and that of the plastic chamber on hydrocortisone absorption (13), we repeated the measurements of penetration using plastic wrap (Saran Wrap) with the experimental protocol of Guy et al. (13). Under these circumstances, we found no difference between plastic-wrap and plastic-chamber occlusion on the percutaneous absorption of hydrocortisone (Table 8).

V. PERCUTANEOUS ABSORPTION OF PHENOLS IN HUMANS

We subsequently investigated the effect of occlusion on the in vivo percutaneous absorption of phenols following single-dose application. The occlusive and protective chamber methodology described by Bucks et al. (24,25) was utilized. Nine ^{14}C-ring-labeled *para*-substituted phenols (4-aminophenol, 4-acetamidophenol, 4-propionylamidophenol, phenol, 4-cyanophenol, 4-nitrophenol, 4-iodophenol, 4-heptyloxyphenol, and 4-pentyloxyphenol) were used. As in the earlier steroid studies, the site of application was the ventral forearm of male volunteers and the area of application 2.5 cm^2. Penetrants were applied in 20 μL ethanol (95%). The chemical dose was 2–4 μg/cm^2. After vehicle evaporation, the application site was covered with either an occlusive or protective device. After 24 hours, the patch was removed and the site washed with a standardized procedure (22). The application site was

Table 7 Accountability of Applied Dose[a] in Protected Studies Using Ventilated Plastic Chambers

	Absorbed	Removed from skin (%)	Total % accounted for
Hydrocortisone	4 ± 2	85 ± 6	89 ± 6
Estradiol	3 ± 1	96 ± 1	100 ± 1
Testosterone	18 ± 9	77 ± 8	96 ± 2
Progesterone	13 ± 6	82 ± 7	96 ± 3

[a]Single 4-μg/cm^2 dose with a 24-hour exposure prior to soap and water washing; penetration corrected for incomplete renal elimination.
Source: Data from Refs. 11 and 24.

Table 8 Percutaneous Absorption of Hydrocortisone in Humans

	Plastic dose absorbed[a]
Plastic-wrap occlusion	4.7 ± 2.1
Plastic-chamber occlusion	4.0 ± 2.4
"Protected" condition	4.4 ± 1.7

[a]Single 4-μg/cm^2 dose with a 24-hours exposure prior to soap and water washing; penetration corrected for incomplete renal elimination.
Source: Adapted from Ref. 43.

then re-covered with a new chamber of the same type. Urine was collected for seven days. On the seventh day: (a) the second chamber was removed, (b) the dosing site was washed with the same procedure, and (c) the upper layers of stratum corneum from the application site were removed by cellophane tape stripping. Urine, chambers, washes, and skin-tape strips were collected and assayed for radiolabel. Percutaneous absorption of each compound under protected and occluded conditions is presented in Figures 4–12. Phenol-percutaneous absorption as a function of the penetrant $K_{O/W}$ is shown in Figure 13. Phenol percutaneous absorption is summarized in Table 9. The methodology permitted excellent dose accountability (Tables 10 and 11). The studies indicate that:

1. Occlusion significantly increased (unpaired t-test, $p < 0.05$) the absorption of phenol, heptyloxyphenol, and pentyloxyphenol.
2. Occlusion did not statistically enhance the absorption of aminophenol, acetaminophen, propionylamidophenol, cyanophefiol, nitrophenol, and iodophenol.
3. The methodology employed again permitted excellent dose accountability.
4. In general, the two compounds with the lowest $K_{o/W}$ values of this series of compounds showed the least enhancement in absorption afforded by occlusion.

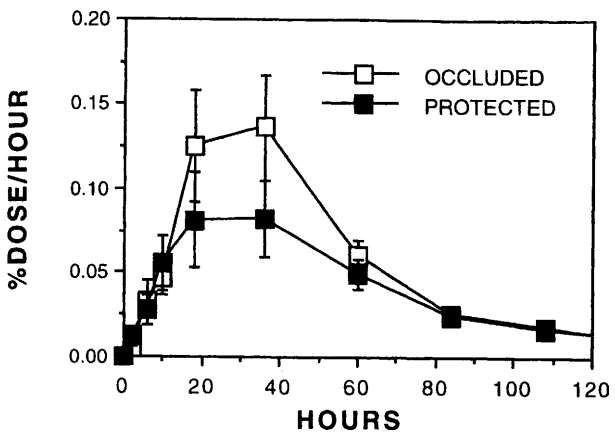


Figure 4 Percutaneous absorption of aminophenol in humans under occluded and protected conditions (mean ± SEM, $N = 6$). Exposure 24-hours prior to soap and water washing. *Source*: Redrawn from Refs. 34 and 35.

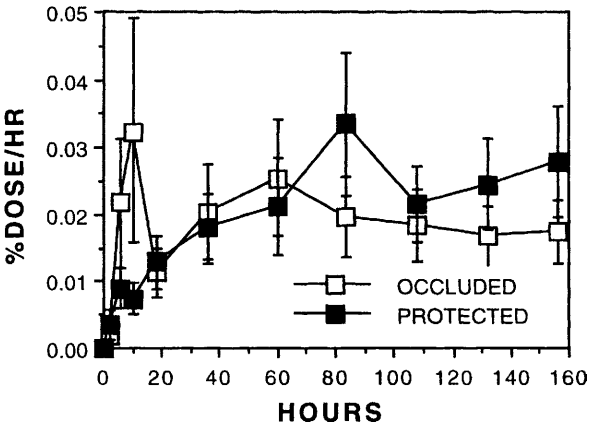


Figure 5 Percutaneous absorption of acetaminophen in man under occluded and protected conditions (mean ± SEM, $N = 6$). Exposure 24-hours prior to soap and water washing. *Source*: Redrawn from Refs. 34 and 35.

VI. DISCUSSION

A predominant effect of occlusion is to increase hydration of the stratum corneum, thereby swelling the corneocytes, and promoting the uptake of water into intercellular lipid domains. The magnitude of increased stratum corneum hydration is related to the degree of occlusion exerted and is dependent upon the physicochemical nature of the dressing (26). The normal water content of stratum corneum is 5% to 15%, a value that can be increased up to 50% by occlusion (27,28). Upon removal of a plastic occlusive dressing after 24 hours of contact, transepidermal water loss values are increased by an order of magnitude (24); the elevated rate then returns rapidly (~15 min) to normal with extraneous water dissipation from the stratum corneum. With occlusion, skin temperature generally increases from 32°C to as much as 37°C (29). Faergemann et al. (30) showed that occlusion: (a) increases the transepidermal

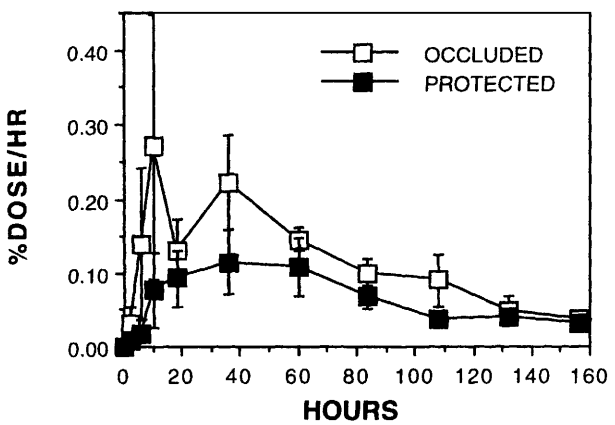


Figure 6 Percutaneous absorption of propionylamidophenol in humans under occluded and protected conditions (mean ± SEM, $N = 6$). Exposure 24-hours prior to soap and water washing. *Source*: Redrawn from Refs. 34 and 35.

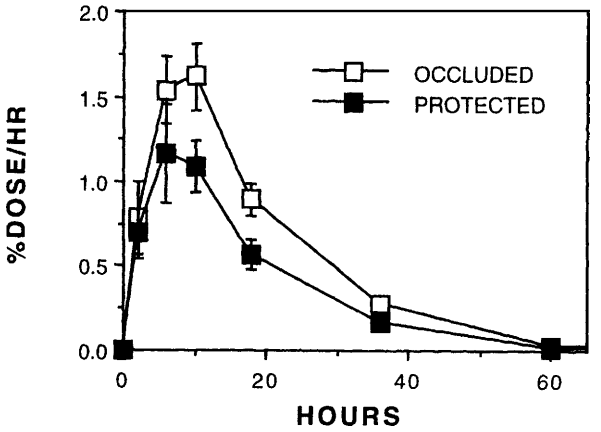


Figure 7 Percutaneous absorption of phenol in humans under occluded and protected conditions (mean ± SEM, $N = 6$). Exposure 24-hours prior to soap and water washing. *Source*: Redrawn from Refs. 34 and 35.

flux of chloride and carbon dioxide, (b) increases microbial counts on skin, and (c) increases the surface pH of skin from a preoccluded value of 5.6–6.7. Anhidrosis results from occlusion (31,32). Plastic-chamber occlusion can also cause skin irritation (personal observation). Occlusion-induced increases in mitotic rate of skin and epidermal thickening have been documented by Fisher and Maibach (33).

With respect to percutaneous absorption, occlusion or a protective cover may prevent loss of the surface-deposited chemical by evaporation, friction, and/or exfoliation; bioavailability may, thereby, be increased. However, comparison of the data in Tables 6 and 8 for the percutaneous absorption of steroids under non-protected and protected conditions shows clearly that the potential increase in bioavailability from protection of the site of application does not explain the increase in steroid absorption under occluded conditions.

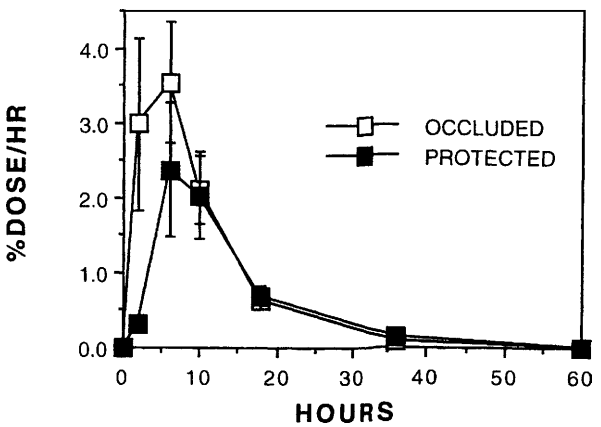


Figure 8 Percutaneous absorption of cyanophenol in humans under occluded and protected conditions (mean ± SEM, $N = 6$). Exposure 24-hours prior to soap and water washing. *Source*: Redrawn from Refs. 34 and 35.

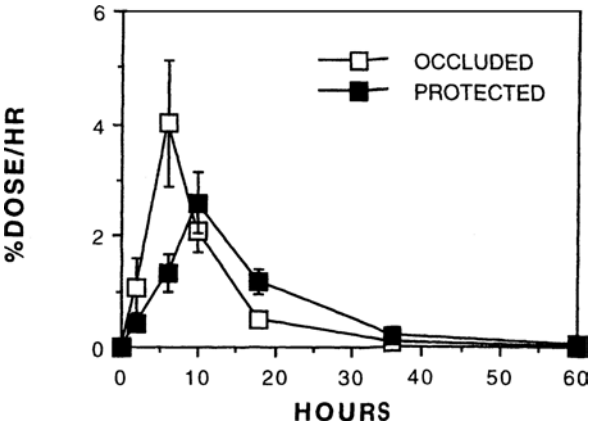


Figure 9 Percutaneous absorption of nitrophenol in humans under occluded and protected conditions (mean ± SEM, $N = 6$). Exposure 24-hours prior to soap and water washing. *Source*: Redrawn from Refs. 34 and 35.

Occlusion does not necessarily increase percutaneous absorption. Hydrocortisone absorption under occluded conditions was not enhanced in single-dose or multiple-dose application studies (Table 12). This lack of penetration enhancement under occluded conditions has also been observed with certain para-substituted phenols (34,35) as well as with ddI (2′,3′-dideoxyinosine, aqueous solubility of 27.3 mg/mL at pH ~6) (36). However, a trend of occlusion-induced absorption enhancement with increasing penetrant lipophilicity is apparent. This trend is also supported by the results of Treffel et al. (37), who have shown that the in vitro permeation of citropten (a lipophilic compound) increased 1.6 times under occlusion whereas that of caffeine (an amphiphilic compound) remained unchanged. However, the degree of lipophilicity (such as measured by $K_{O/W}$) exhibited by a penetrant in order for occlusion-induced enhanced skin permeation to be manifested is not clear and may be chemical-class dependent.

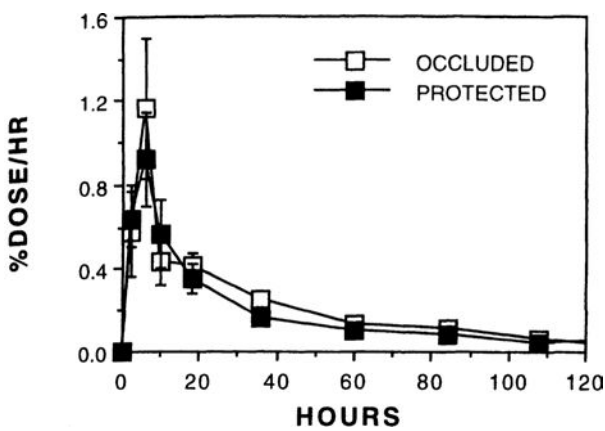


Figure 10 Percutaneous absorption of iodophenol in humans under occluded and protected conditions (mean ± SEM, $N = 6$). Exposure 24-hours prior to soap and water washing. *Source*: Redrawn from Refs. 34 and 35.

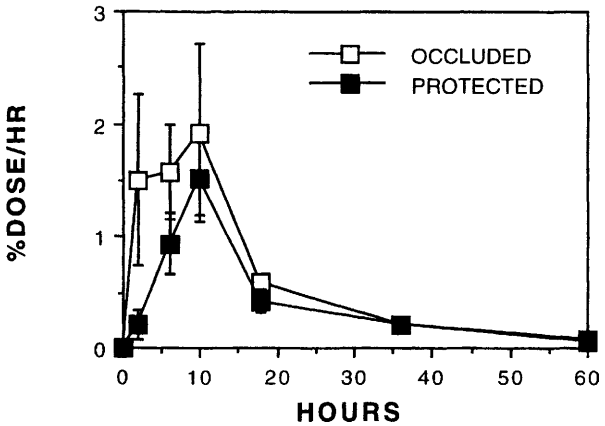


Figure 11 Percutaneous absorption of heptyloxyphenol in humans under occluded and protected conditions (mean ± SEM, $N = 6$). Exposure 24-hours prior to soap and water washing. *Source*: Redrawn from Refs. 34 and 35.

The increase in percutaneous absorption of hydrocortisone under occlusive conditions observed by Feldmann and Maibach (12) may be due to an acetone solvent effect. In this early work, the chemical was applied in 1.0 mL acetone over an area of 13 cm. Might the pretreatment of the skin with a large volume of acetone compromise stratum corneum barrier function? It has been reported that acetone can damage the stratum corneum (38,39). It is conceivable that the large volume of acetone used (76.9 $\mu L/cm^2$) may be responsible for the observed increase in hydrocortisone penetration under plastic wrap occlusion. In addition, it is reasonable to suggest that the increased duration of exposure (96 hours compared to 24 hours) may also contribute to the increase in observed hydrocortisone percutaneous absorption. This enhancement in absorption was not observed in the experiments with hydrocortisone under occlusion (24) when the acetone surface concentration was only 8.0 $\mu L/cm^2$ (20 μL over $2.5/cm^{-2}$) and skin surface exposure was limited to 24 hours.

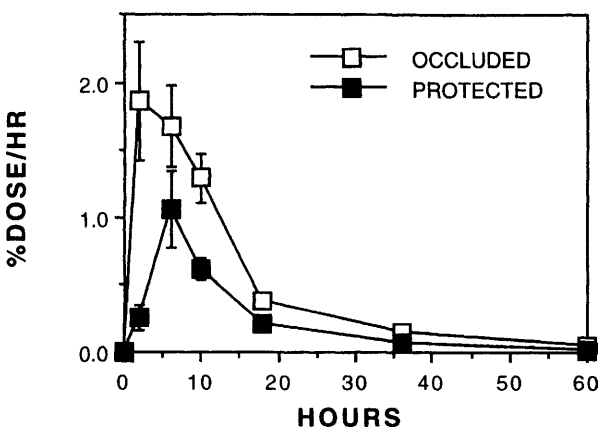


Figure 12 Percutaneous absorption of pentyloxyphenol in humans under occluded and protected conditions (mean ± SEM, $N = 6$). Exposure 24-hours prior to soap and water washing. *Source*: Redrawn from Refs. 34 and 35.

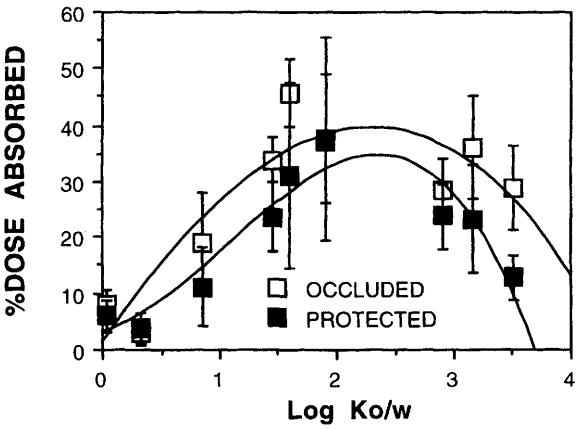


Figure 13 Percutaneous absorption of phenols in humans under occluded and protected conditions as a function of penetrant octanol/water partition coefficient ($K_{o/w}$).
Source: Redrawn from Refs. 34 and 35.

The occlusion-induced enhancement of lipophilic compounds may be understood by considering the steps involved in the percutaneous absorption process. Minimally, after application in a volatile solvent, the penetrant must (a) dissolve/partition into the surface lipids of the stratum corneum, (b) diffuse through the lamellar lipid domains of the stratum corneum, (c) partition from the stratum corneum into the more hydrophilic viable epidermis, (d) diffuse through the epidermis and upper dermis, and (e) encounter a capillary of the cutaneous microvasculature and gain access to the systemic circulation (Fig. 14).

Table 9 Percutaneous Absorption of Phenols[a] in Humans

		Mean % dose absorbed (SD)	
Compound	Log $K_{o/w}$	Occluded	Protected
Aminophenol	0.04	8 (3)	6 (3)
Acetaminophen	0.32	3 (2)	4 (3)
Propionylamido-phenol	0.86	19 (9)	11 (7)
Phenol[b]	1.46	34 (4)	24 (6)[c]
Cyanophenol	1.60	46 (6)	31 (16)
Nitrophenol	1.91	37 (18)	38 (11)
Iodophenol	2.91	28 (6)	24 (6)
Heptyloxyphenol	3.16	36 (9)	23 (10)[d]
Pentyloxyphenol	3.51	29 (8)	13 (4)[c]

[a]Single dose application from 95% ETOH ($N = 6$) at 2–4 $\mu g/cm^2$ to the ventral forearm; 24-hours exposure prior to soap and water washing.
[b]Data analysis accounts for 27.2% of applied dose evaporating off skin surface during application.
[c]Significant difference at $p < 0.01$.
[d]Significant difference at $p < 0.05$.
Source: Data from Refs. 34 and 35.

Table 10 Accountability of Applied Dose[a] in Occluded Studies: Mean Percent Dose Absorbed (SD)

Compound	Absorbed (%)	Removed from skin (%)	Total % dose
Aminophenol	8 (3)	55 (18)	63 (17)
Acetaminophen	3 (2)	61 (24)	64 (24)
Propionylamido-phenol	19 (9)	77 (9)	96 (2)
Phenol[b]	34 (4)	61 (13)	95 (10)
Cyanophenol	46 (6)	41 (9)	87 (7)
Nitrophenol	37 (18)	50 (11)	87 (13)
Iodophenol	28 (6)	63 (4)	91 (3)
Heptyloxyphenol	36 (9)	59 (7)	95 (3)
Pentyloxyphenol	29 (8)	71 (8)	100 (2)

[a]Single dose application from 95% ETOH ($N = 6$) at 2–4 $\mu g/cm^2$ to the ventral forearm; 24-hours exposure prior to soap and water washing.
[b]Data analysis accounts for 27.2% of applied dose evaporating off skin surface during application.
Source: Data from Refs. 34 and 35.

As stated earlier, occlusion hydrates the stratum corneum, and if the effect of hydration were simply to decrease the viscosity of the stratum corneum intercellular domain, then the penetration of all chemicals should be equally enhanced by occlusion. In other words, the relative increase in the effective diffusion coefficient of the penetrant across the stratum corneum would be independent of the nature of the penetrant. But this is not the situation observed; the degree of enhancement is compound specific. To account for this effect, we postulate that stratum corneum hydration alters the stratum corneum-viable epidermis partitioning step. Occlusion hydrates the keratin in corneocytes and increases the water content between adjacent intercellular lipid lamellae. A penetrant diffusing through the intercellular lipid

Table 11 Accountability of Applied Dose[a] in Protected Studies: Mean Percent Dose Absorbed (SD)

Compound	Absorbed (%)	Removed from skin (%)	Total % dose
Aminophenol	6 (3)	85 (4)	91 (2)
Acetaminophen	4 (3)	93 (5)	97 (4)
Propionylamido-phenol	11 (7)	84 (7)	95 (2)
Phenol[b]	24 (6)	68 (15)	92 (18)
Cyanophenol	31 (16)	70 (12)	101 (5)
Nitrophenol	38 (11)	65 (12)	103 (4)
Iodophenol	24 (6)	73 (7)	97 (2)
Heptyloxyphenol	23 (10)	71 (10)	95 (4)
Pentyloxyphenol	13 (4)	85 (3)	98 (2)

[a]Single dose application from 95% ETOH ($N = 6$) at 2–4 $\mu g/cm^2$ to the ventral forearm; 24-hours exposure prior to soap and water washing.
[b]Data analysis accounts for 27.2% of applied dose evaporating off skin surface during application.
Source: Data from Refs. 34 and 35.

Table 12 Percutaneous Absorption of Hydrocortisone in Humans Following Application from Acetone Solution

	Percent dose absorbed[a]	Applied dose ($\mu g/cm^2$)
Plastic-wrap occlusion; single dose[b]	9 (6)	5.8
Plastic-wrap occlusion; single dose[c]	5 (2)	4.0
Plastic-chamber occlusion[d]	4 (2)	4.0
Plastic-chamber occlusions[e]	4 (1)	4.0
Plastic-chamber occlusion[f]	3 (1)	4.0
"Protected" condition; single dose[g]	4 (2)	4.0
Nonprotected; single dose[h]	1 (0.3)	5.8
Nonprotected; single dose[i]	2 (2)	4.0
Nonprotected; multiple dose[j]	3 (1)	4.0
Nonprotected; multiple dose[k]	3 (1)	4.0

[a]Absorption values, mean (SD), corrected for incomplete renal elimination.
[b]Occluded for four days, washed 96 hours post-application with soap and water (12).
[c]Occluded for one day, washed 24 hours post-application with soap and water (35).
[d]Single dose occluded for seven days, washed 24 hours post-application with soap and water (13).
[e]Percent of first dose absorbed following daily doses. Occluded for 14 days, washed 24 hours post-application with soap and water (13).
[f]Percent of eighth dose absorbed following daily doses. Occluded for 14 days, washed 24 hours post-application with soap and water (13).
[g]Site covered for seven days with a ventilated plastic chamber, washed 24 hours post-application with soap and water (11,24).
[h]Site washed 24 hours post-application with soap and water (12).
[i]Site washed 24 hours post-application with soap and water (42).
[j]Percent of first dose absorbed following daily doses or 14-day site washed 24 hours post-application with soap and water (23).
[k]Percent of eighth dose following daily doses or 14-day site washed 24 hours post-application with soap and water (23).

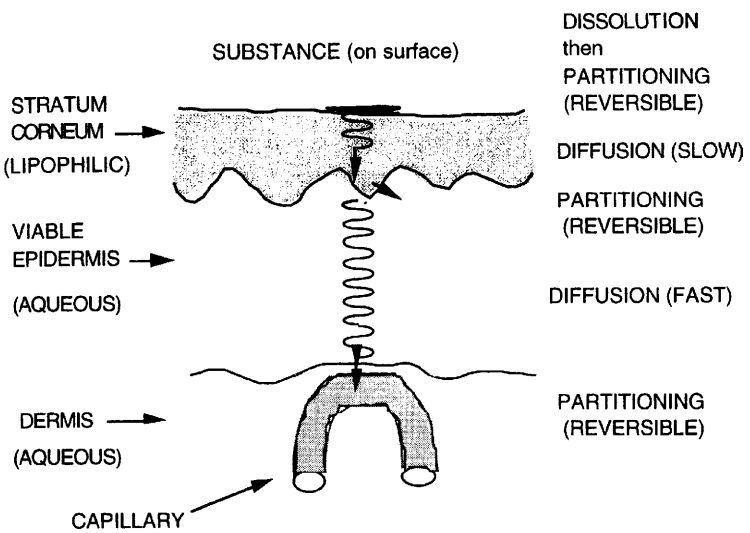


Figure 14 Schematic depiction of percutaneous absorption.

domains will distribute between the hydrophobic bilayer interiors and the aqueous regions separating the head groups of adjacent bilayers. Stratum corneum hydration magnifies the latter environment and increases the "hydrophilic" character of the stratum corneum somewhat. It follows that this leads, in turn, to a reduction in the stratum corneum-viable epidermis partition coefficient of the penetrant (because the two tissue phases now appear more similar). The decrease should facilitate the kinetics of transfer of penetrant through the stratum corneum and from the stratum corneum to the viable epidermis, and the relative effect on this rate should become greater as the lipophilicity of the absorbing molecule increases (40). The limit of this mechanism of enhancement would occur when penetrant is either (a) completely insoluble in the aqueous phases of the stratum corneum or (b) sterically hindered from penetrating the skin at a measurable rate due to, for example, large molecular size.

The importance of the partitioning step is implied by the dependence of percutaneous absorption with compound lipophilicity, as would be predicted if the skin behaved as a simple lipid membrane. Attenuation in absorption may be explained by a shift in the rate-limiting step from diffusion through the stratum corneum to the transfer across the stratum corneum-viable epidermis interface with increasing compound lipophilicity. The effect should be most apparent when the penetrant's aqueous solubility is extremely low; thus, it follows that this transfer process, or partitioning into the viable epidermis, should become slower as penetrant lipophilicity increases. This suggested mechanism is further supported by results obtained with the para-substituted phenols described earlier (25,41) (Fig. 13).

Restricting evaporative loss of volatile compounds using plastic-wrap occlusion enhances percutaneous absorption (38). Clearly, this effect may increase the extent of absorption of these lipophilic, volatile compounds, in addition to the possible enhancement afforded by occlusion-induced hydration of the stratum corneum.

As noted earlier, occlusion does not always increase the percutaneous absorption of topically applied agents. Furthermore, the extent of penetration may depend upon the method of occlusion. This finding has important implications in the design of a transdermal drug delivery system (TDS) for which the duration of application exceeds 24 hours. We have found that about a third of normal, healthy, male volunteers experience plastic-chamber occlusion-induced irritation following contact periods greater than 24 hours; however, we have not observed any irritation of the skin using the nonocclusive patch system (made from these occlusive chambers) on the same volunteers following identical contact periods with the same penetrant. In those situations for which occlusion does not significantly increase the percutaneous absorption of a topically applied drug, or an occlusion-induced enhancement in percutaneous absorption is not required, a nonocclusive TDS is an approach worthy of consideration.

Conclusions drawn from the preceding discussion are as follows:

1. Studies from multiple investigators indicate that the extent of percutaneous absorption may depend upon the occlusive system used (16,18–20).
2. Occlusion does not necessarily increase percutaneous absorption. Penetration of hydrophilic compounds (e.g., compounds with low $K_{o/w}$ values), in particular, may not be enhanced by occlusion.
3. Mass balance (dose accountability) has been demonstrated using occlusive and nonocclusive patch systems in vivo in humans. Dose accountability

rigorously quantifies percutaneous absorption measured using radiotracer methodology and allows objective comparison between different treatment modalities.

4. Occlusion, per se, can cause local skin irritation, and the implication of this observation in the design of TDS should be considered.

REFERENCES

1. Elias PM, Brown BE. The mammalian cutaneous permeability barrier. Lab Invest 1978; 39:574–583.
2. Elias PM, Cooper ER, Korc A, Brown B. Percutaneous transport in relation to stratum corneum structure and lipid composition. J Invest Dermatol 1981; 76:297–301.
3. Elias P. Epidermal lipids, barrier function, and desquamation. J Invest Dermatol 1983; 80:44s–49s.
4. Golden GM, Guzek DB, McKie JE, Potts RO. Role of stratum corneum lipid fluidity in transdermal drug flux. J Pharm Sci 1987; 76:25–31.
5. Menon GK, Feingold KR, Moser AH, Brown BE, Elias PM. De novo sterologenesis in the skin. II. Regulation by cutaneous barrier requirements. J Lipid Res 1985; 26:418–427.
6. Garb J. Nevus verrucosus unilateralis cured with podophyllin ointment. Arch Dermatol 1960; 81:606–609.
7. Scholtz JR. Topical therapy of psoriasis with fluocinolone acetonide. Arch Dermatol 1961; 84:1029–1030.
8. Sulzberger MB, Witten VH. Thin pliable plastic films in topical dermatological therapy. Arch Dermatol 1961; 84:1027–1028.
9. McKenzie AW. Percutaneous absorption of steroids. Arch Dermatol 1962; 86:91–94.
10. McKenzie AW, Stoughton RB. Method for comparing percutaneous absorption of steroids. Arch Dermatol 1962; 86:88–90.
11. Bucks DAW, McMaster JR, Maibach HI, Guy RH. Bioavailability of topically administered steroids: a "mass balance" technique. J Invest Dermatol 1988; 90:29–33.
12. Feldmann RJ, Maibach HI. Penetration of ^{14}C hydrocortisone through normal skin. Arch Dermatol 1965; 91:661–666.
13. Guy RH, Bucks DAW, McMaster JR, Villaflor DA, Roskos KV, Hinz RS, Maibach HI. Kinetics of drug absorption across human skin in vivo. In: Shroot B, Schaefer H, eds. Skin Pharmacokinetics. Basel: Karger, 1987:70–76.
14. Wiechers JW. The barrier functions of the skin in relation to percutaneous absorption of drugs. Pharm Weekbl [Sci] 1989; 11:185–198.
15. Qiao GL, Riviere. Significant effects of application site and occlusion on the pharmacokinetics of cutaneous penetration and biotransformation of parathion in vivo in swine. J Pharm Sci 1995; 84:425–432.
16. Gummer CL, Maibach HI. The penetration of [^{14}C]ethanol and [^{14}C]methanol through excised guinea-pig skin in vitro. Food Chem Toxicol 1986; 24:305–306.
17. Riley RT, Kemppainen BW, Norred WP. Penetration of aflatoxins through isolated human epidermis. J Toxicol Environ Health 1985; 15:769–777.
18. Kim HO, Wester RC, McMaster JR, Bucks DAW, Maibach HI. Skin absorption from patch test systems. Contact Dermatitis 1987; 17:178–180.
19. Bronaugh RL, Stewart RF, Wester RC, Bucks DAW, Maibach HI. Comparison of percutaneous absorption of fragrances by humans and monkeys. Food Chem Toxicol 1985; 23: 111–114.
20. Bronaugh RL, Wester RC, Bucks DAW, Maibach HI, Sarason R. In vivo percutaneous absorption of fragrance ingredients in rhesus monkeys and humans. Food Chem Toxicol 1990; 28:369–373.

21. Quisno RA, Doyle RL. A new occlusive patch test system with a plastic chamber. J Soc Cosmet Chem 1983; 34:13–19.
22. Bucks DAW, Marty J-PL, Maibach HI. Percutaneous absorption of malathion in the guinea pig: effect of repeated skin application. Food Chem Toxicol 1985; 23:919–922.
23. Bucks DAW, Maibach HI, Guy RH. Percutaneous absorption of steroids: effect of repeated application. J Pharm Sci 1985; 74:1337–1339.
24. Bucks DAW, Maibach HI, Guy RH. Mass balance and dose accountability in percutaneous absorption studies: development of non-occlusive application system. Pharm Res 1988; 5:313–315.
25. Bucks DAW, McMaster JR, Maibach HI, Guy RH. Percutaneous absorption of phenols in vivo [abstr]. Clin Res 1987; 35:672A.
26. Berardesca E, Vignoli GP, Fideli D, Maibach H. Effect of occlusive dressings on the stratum corneum water holding capacity. Am J Med Sci 1992; 304:25–28.
27. Blank IH, Scheuplein RJ. The epidermal barrier. In: Rook AJ, Champion RH, eds. Progress in the Biological Sciences in Relation to Dermatology. Vol 2. Cambridge: Cambridge University Press, 1964:245–261.
28. Potts RO. Stratum corneum hydration: experimental techniques and interpretation of results. J Soc Cosmet Chem 1986; 37:9–33.
29. Kligman AM. A biological brief on percutaneous absorption. Drug Dev Ind Pharm 1983; 9:521–560.
30. Faergemann J, Aly R, Wilson DR, Maibach HI. Skin occlusion: effect on Pityrosporum orbiculate, skin permeability of carbon dioxide, pH, transepidermal water loss, and water content. Arch Dermatol Res 1983; 275:383–387.
31. Gordon B, Maibach HI. Studies on the mechanism of aluminum anhirdrosis. J Invest Dermatol 1968; 50:411–413.
32. Orentreich N, Berger RA, Auerbach R. Anhidrotic effects of adhesive tapes and occlusive film. Arch Dermatol Res 1966; 94:709–711.
33. Fisher LB, Maibach HI. The effect of occlusive and semipermeable dressings on the mitotic activity of normal and wounded human epidermis. Br J Dermatol 1972; 86:593–600.
34. Bucks DAW. Prediction of Percutaneous Absorption. Ph.D. dissertation, University of California, San Francisco, 1989.
35. Bucks D, Guy R, Maibach H. Effect of occlusion. In: Bronaugh RL, Maibach HI, eds. In Vitro Percutaneous Absorption: Principles, Fundamentals, and Applications. Boston: CRC Press, 1991:85–114.
36. Mukherji E, Millenbaugh HJ, Au JL. Percutaneous absorption of 2′,3′-dideoxyinosine in rats. Pharm Res 1994; 11:809–815.
37. Treffel P, Muret P, Muret-D'Aniello P, Coumes-Marquet S, Agache P. Effect of occlusion on in vitro percutaneous absorption of two compounds with different physicochemical properties. Skin Pharmacol 1992; 5:108–113.
38. Bond JR, Barry BW. Damaging effect of acetone on the permeability barrier of hairless mouse skin compared with that of human skin. Int J Pharmaceut 1988; 41:91–93.
39. Schaefer H, Zesch A, Stuttgen G. Skin Permeability. Berlin: Springer–Verlag, 1982: 541–896.
40. Guy RH, Hadgraft J, Bucks DAW. Transdermal drug delivery and cutaneous metabolism. Xenobiotica 1987; 17:325–343.
41. Bucks DAW, McMaster JR, Maibach HI, Guy RH. Prolonged residence of topically applied chemicals in the stratum corneum: effect of lipophilicity [abstr]. Clin Res 1987; 35:672A.
42. Feldmann R, Maibach HI. Percutaneous absorption of steroids in man. J Invest Dermatol 1969; 52:89–94.
43. Bucks DAW, Maibach HI, Guy RH. Occlusion does not uniformly enhance penetration in vivo. In: Bronaugh R, Maibach H, eds. Percutaneous Absorption. Vol. 2. New York: Marcel Dekker, 1989:77–94.

5

Regional Variation in Percutaneous Absorption: Principles and Applications to Human Risk Assessment

Ronald C. Wester and Howard I. Maibach
School of Medicine, University of California, San Francisco, California, U.S.A.

I. INTRODUCTION

The first occupational disease in recorded history was scrotal cancer in chimney sweepers (1). The historical picture of a male worker holding a sweeper and covered from head to toe with black soot is vivid. But why the scrotum?

Percutaneous absorption in man and animals varies depending on the area of the body on which the chemical resides. This is called regional variation. When a certain skin area is exposed, any effect of the chemical will be determined by how much is absorbed through the skin. Where systemic drug delivery is desired, such as transdermal delivery, a high-absorbing area may be desirable to deliver sufficient drug. Scopolamine transdermal systems are supposedly placed in the postauricular area (behind the ear) because at this skin site the percutaneous absorption of scopolamine is sufficiently enhanced to deliver effective quantities of the drug. A third example is with estimating human health hazard effects of environmental contaminants. This could be pesticide residue on exposed parts of the skin (head, face, neck, and hands) and trying to determine the amount of pesticide that might be absorbed into the body. The estimate for skin absorption is an integral part of the estimate for potential hazard, thus, accuracy of estimate is very relevant.

Therefore, when considering skin absorption in humans, the site of application is important. Principles are reviewed and examples of applications to human risk assessment are given. Human risk assessment assigns a number to skin absorption and multiplies by skin area involved. This should include human anatomy and clothing worn.

II. REGIONAL VARIATION IN HUMANS

Feldmann and Maibach (2) were the first to systematically explore the potential for regional variation in percutaneous absorption. The first absorption studies were

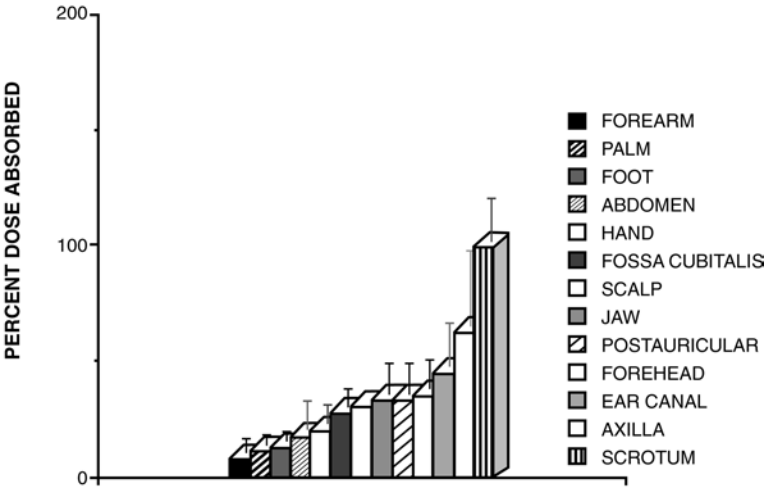


Figure 1 Anatomic regional variation with parathion percutaneous absorption in humans.

done with the ventral forearm, because this site is convenient to use. However, skin exposure to chemicals exists over the entire body. They first showed regional variation with the absorption of hydrocortisone (Fig. 1). The scrotum was the highest-absorbing skin site (scrotal cancer in chimney sweeps is the key). Skin absorption was lowest for the foot area and highest around the head and face.

Table 1 gives the percutaneous absorption of pesticides in humans by anatomical region (3). There are two major points in this study. First, regional variation was confirmed with two different chemicals, parathion and malathion. Second, those skin areas that would be exposed to the pesticides, the head and face, were among the higher-absorbing sites. The body areas most exposed to environmental contaminants are the areas with the higher skin absorption.

Table 1 Effect of Anatomical Region on In Vivo Percutaneous Absorption of Pesticides in Humans

	Dose absorbed (%)		
Anatomical region	Hydrocortisone	Parathion	Malathion
Forearm	1.0	8.6	6.8
Palm	0.8	11.8	5.8
Foot, ball	0.2	13.5	6.8
Abdomen	1.3	18.5	9.4
Hand, dorsum	—	21.0	12.5
Forehead	7.6	36.3	23.2
Axilla	3.1	64.0	28.7
Jaw angle	12.2	33.9	69.9
Fossal cubitalis	—	28.4	—
Scalp	4.4	32.1	—
Ear canal	—	46.6	—
Scrotum	36.2	101.6	—

Table 2 Site Variation and Decontamination Time for Parathion

Skin residence time before soap and water wash	Parathion dose absorbed[a] (%)		
	Arm	Forehead	Palm
1 min	2.8	8.4	—
5 min	—	—	6.2
15 min	6.7	7.1	13.6
30 min	—	12.2	13.3
1 hr	8.4	10.5	11.7
4 hr	8.0	27.7	7.7
24 hr	8.6	36.3	11.8

[a]Each value is a mean for four volunteers. The fact that there were different volunteers at each time point accounts for some of the variability with time for each skin site.

Table 2 gives site variability for parathion skin absorption with time. Soap and water wash in the first few minutes after exposure is not a perfect decontaminant. Site variation is apparent early in skin exposure (4).

Guy and Maibach (5) took the hydrocortisone and pesticide data and constructed penetration indices for five anatomical sites (Table 3). These indices should be used with their total surface areas (Table 4) when estimating systemic availability relative to body exposure sites.

Van Rooy et al. (6) applied coal–tar ointment to various skin areas of volunteers and determined absorption of polycyclic aromatic hydrocarbons (PAH) by surface disappearance of PAH and the excretion of urinary I–OH–pyrene. Using PAH disappearance, skin ranking (highest to lowest) was shoulder > forearm > forehead > groin > hand (palmar) > ankle. Using I–OH–pyrene excretion, skin ranking (highest to lowest) was neck > calf > forearm > trunk hand. Table 5 compares their results with Guy and Maibach (5).

In another study, Wester et al. (7) determined the percutaneous absorption of paraquat in humans. Absorption was the same for the leg ($0.29 \pm 0.02\%$), hand ($0.23 \pm 0.1\%$), and forearm ($0.29 \pm 0.1\%$). Here, the chemical nature of the low-absorbing paraquat overcame any regional variation.

Rougier et al. (8) examined the influence of anatomical site on the relationship between total penetration of benzoic acid in humans and the quantity present in the stratum corneum 30 minutes after application. Total penetration of benzoic acid

Table 3 Penetration Indices for Five Anatomical Sites Assessed Using Hydrocortisone Skin Penetration Data and Pesticide (Malathion and Parathion) Absorption Results

Site	Penetration index based on	
	Hydrocortisone data	Pesticide data
Genitals	40	12
Arms	1	1
Legs	0.5	1
Trunk	2.5	3
Head	5	4

Table 4 Body Surface Areas Distributed over Five Anatomical Regions for Adult and Neonate

	Adult		Neonate	
Anatomical region	Body area (%)	Area (cm^2)	Body area (%)	Area (cm^2)
Genitals	1	190	1	19
Arms	18	3,420	19	365
Legs	36	6,840	30	576
Trunk	36	6,840	31	595
Head	9	1,710	19	365
Totals		**19,000**		**1,920**

varied according to anatomical site. There was correlation between the level of penetration of benzoic acid within four days and its level in the stratum corneum after a 30-minute application relative to anatomical site.

Wertz et al. (9) determined regional variation in permeability through human and pig skin and oral mucosa (Table 6). In the oral mucosa of both species permeability ranked floor of mouth > buccal mucosa > palate. Skin remains a greater barrier, absorption of which been some 10-fold less than oral mucosa.

The barrier properties of skin relative to oral mucosa have been a benefit for longer-term transdermal delivery. Nityroglycerine buccal tablets are effective for about 20 minutes, due to rapid buccal absorption. In contrast, transdermal nitroglycerin is prescribed for 24 hours of continuous dose delivery. The transdermal nitroglycerin patch is placed on the chest more for psychological reasons than that related to scientific regional variation skin absorption. Some transdermal systems take advantage of regional variation skin absorption and some do not (Table 7).

Shriner and Maibach (10) studied skin contact irritation and showed that areas of significant response were neck > perioral > forehead. The volar forearm was the least sensitive of eight areas tested. This is in contrast to the commonly-

Table 5 Absorption Indices of Hydrocortisone and Pesticides (Parathion/Malathion) Calculated by Guy and Maibach (5) Compared with Absorption Indices of Pyrene and PAH for Different Anatomical Sites by Van Rooy et al. (6)

	Absorption index			
Anatomical site	Hydrocortisone[a]	Pesticides[b]	Pyrene[c]	PAH[d]
Genitals	40	12	—	—
Arm	1	1	1	1
Hand	1	1	0.8	0.5
Leg/ankle	0.5	1	1.2	0.8/0.5
Trunk/shoulder	2.5	3	1.1	/2.0
Head/neck	5	4	/1.3	1.0

[a]Based on hydrocortisone penetration data (2).
[b]Based on parathion and malathion absorption data (3).
[c]Based on excreted amount of I–OH–pyrene in urine after coal–tar ointment application (6).
[d]Based on the PAH absorption rate constant (K_a) after coal–tar ointment application (6).
Abbreviation: PAH, polycylic aromatic hydrocarbons.

Table 6 Permeability Constants for the Diffusion of ^3H_2O Through Human and Porcine Skin and Oral Mucosa

	K_p (10^{-7} cm/min) (mean ± standard error)	
Site	Human	Pig
Skin	44 ± 4	62 ± 5
Palate	450 ± 27	364 ± 18
Buccal	579 ± 16	634 ± 19
Floor of mouth	973 ± 3	808 ± 23

Table 7 Site Variation in Transdermal Delivery

Transdermal drug	Body site	Reason
Nitroglycerin	Chest	Psychological: the patch is placed over the heart
Scopolamine	Postauricular	Scientific: behind the ear was found to be the best absorbing area
Estradiol	Trunk	Convenience: easy to place, and out of view
Testosterone	Scrotum	Scientific: highest skin absorbing area
Testosterone	Trunk	Scientific/convenience: removal from trunk skin is easier than scrotal skin

held belief that the forearm is one of the best locations to test for immediate contact irritation.

III. REGIONAL VARIATION IN ANIMALS

Percutaneous absorption data obtained in man are most relevant for human exposure. However, many estimates for humans are made from animal models. Therefore, regional variation in animals may affect prediction for humans. Also, if regional variation exists in an animal, that variation should be relative to humans.

Bronaugh (11) reported the effect of body site (back vs. abdomen) on male rat skin permeability. Abdominal rat skin was more permeable to water, urea, and cortisone. Skin thickness (stratum corneum, whole epidermis, and whole skin) is less in the abdomen than in the back. With the hairless mouse, Behl et al. (12) showed dorsal skin to be more permeable than abdominal skin (reverse that of the male rat) (Table 8). Hairless mouse abdominal skin is thicker than dorsal skin (also reverse that of the male rat) (Table 8).

Skin absorption in the rhesus monkey is considered to be relevant to that of humans. Table 9 shows the percutaneous absorption of testosterone (13), fenitrothion, aminocarb, and diethyltoluamide (DEET) (14) (Moody et al., personal communication, 1988) in the rhesus monkey compared with the rat. What is interesting is that for the rhesus monkey there is regional variation between forehead (scalp) and forearm. If one determines the ratio of forehead (scalp/forearm for the rhesus monkey) and compares the results with humans, the similarities are the same, (Table 10). Therefore, the rhesus monkey probably is a relevant animal model for human skin regional variation.

Table 8 Effect of Body Site on Rat Skin Permeability

Compound	Permeability constant (cm/hr $\times 10^4$)
Water	
Back	4.9 ± 0.4
Abdomen	13.1 ± 2.1
Urea	
Back	1.6 ± 0.5
Abdomen	18.8 ± 5.5
Cortisone	
Back	1.7 ± 0.4
Abdomen	12.2 ± 0.6

Table 9 Percutaneous Absorption of Fenitrothion, Aminocarb, DEET, and Testosterone in Rhesus Monkey and Rat

		Applied dose absorbed (%) skin site		
Chemical	Species	Forehead	Forearm	Back
Fenitrothion	Rhesus	49	21	
	Rat			84
Aminocarb	Rhesus	74	37	
	Rat			88
Testosterone	Rhesus	20.4[a]	8.8	
	Rat			47.4
DEET	Rhesus	33	14	
	Rat			36

[a]Scalp

Table 10 Percutaneous Absorption Ratio for Scalp and Forehead to Forearm in Humans and Rhesus Monkey

		Percutaneous absorption ratio	
Chemical	Species	Scalp/forearm	Forehead/forearm
Hydrocortisone	Human	3.5	6.0
Benzoic acid	Human		2.9
Parathion	Human	3.7	4.2
Malathion	Human		3.4
Testosterone	Rhesus	2.3	
Fenitrothion	Rhesus		2.3
Aminocarb	Rhesus		2.0
DEET	Rhesus		2.4

IV. APPLICATIONS TO HUMAN RISK ASSESSMENT

Chemical warfare agents (CWAs) are easily and inexpensively produced and are a significant threat to military forces and to the public. Most well known CWAs are organophosphorus compounds, a number of which are used as pesticides, including parathion. This study determined the in vitro percutaneous absorption of parathion as a CWA stimulant through naked human skin and uniformed skin (dry and sweated). Parathion percentage dose absorbed through naked skin (1.78 ± 0.41) was greater than dry uniformed skin (0.29 ± 0.17; $p = 0.000$) and sweated uniformed skin (0.65 ± 0.16; $p = 0.000$). Sweated and dry uniformed skin absorption was also different ($p = 0.007$) (Table 11). These relative dry and sweated uniformed skin absorption were then applied to VX skin permeability for naked skin (head, neck, arms, and hands) and the remaining uniformed skin over the various regions of the human body. Risk assessment shows VX 50% lethality within the first hour for a soldier wearing a sweated uniform. By eight-hour postexposure to naked skin plus trunk area lethality was predicted for both dry and sweated uniform, and at 96 hour postexposure, all body regions individually exposed would produce lethality (15).

A second example of human regional variation application is that of pemethrin bioavailability and body burden for the uniformed soldier. Pemethrin is imbedded in military uniform material and is available to the soldier in spray cans for unprotected skin. Pemethrin repels insects that could be carrying disease. Pemethrin, by design as

Table 11 VX Systemic Absorption and Toxicity to Uniformed Military Personnel

		Calculated VX systemic dose[a]	
Exposure time	Body exposure	Compromised[b] (mg)	Protected[c] (mg)
1 hr	Head/neck[d]	4.16	4.16
	Arms and hands[d]	0.52	0.52
	Trunk	4.07	1.35
	Genital-s	0.45	0.15
	Legs	0.68	0.22
	Total	9.87*	6.40
8 hr	Head/neck[d]	33.26*	33.26*
	Arms and hands[d]	4.16	4.16
	Trunk	32.52*	10.77*
	Genital-s	3.61	1.2
	Legs	5.42	1.8
	Total	78.98*	51.18*
96 hr	Head/neck[d]	399.16*	399.16*
	Arms and hands[d]	49.90*	49.90*
	Trunk	390.29*	129.25*
	Genital-s	43.37*	14.36*
	Legs	65.05*	21.54*
	Total	947.76*	614.21*

*Estimated systemic LD50 of VX is 6.5 mg (human, 70 kg). Systemic concentration is more than 50% lethality dose.

[a]Dose: 4 μg/cm^2 on whole body area (1.8 m^2).

[b]Compromised: uniform with perspiration.

[c]Protected: dry uniform.

[d]Head/neck and arms and hands are unprotected.

Table 12 Pemethrin Bioavailability and Body Burden for Uniformed Soldier

Human part	Body surface srea (cm^2)	Pemethrin dose[a] ($\mu g/cm^2$)	Percutaneous absorption[b]	Body region index[c]	Uniform effect[d]	Total (μg)
Head	1,180	4	0.087	×4	1	1,642.56
Neck	420	4	0.087	×4	1	584.64
Trunk	5,690	125	0.087	×3	0.29	53,834.51
Arms	2,280	125	0.087	×1	0.29	7,190.55
Hands	840	4	0.087	×1	1	292.32
Genitals	180	125	0.087	×12	0.29	6,812.10
Legs	5,050	125	0.087	×1	0.29	15,926.44
Feet	1,120	4	0.087	×1	1	389.76
Total (μg)						86,672.88
Total (mg)						86.67
Total body burden (mg/70 kg soldier)						1.24 mg/kg

[a]Uniform = 125 $\mu g/cm^2$ (NRC 1994)/spray open skin 4 $\mu g/cm^2$.
[b]8.7% (0.087) pemethrin dose absorbed.
[c]Region body absorption index.
[d]The 0.29 is 29% absorption from cloth relative to open skin (index).

a pesticide, is also toxic. Table 12 summarizes predicted pemethrin human bioavailability from uniformed and exposed skin at 1.24 mg/kg body burden. The NOEL estimates from animal studies were? at 5 mg/kg, giving a fivefold safety margin.

V. CONCLUSION

This chapter outlines 30 years of progress. Careful review of the data shows some general trends; however, most parts of various animal skins have not been explored, and many possible special areas in humans remain unstudied, i.e., finger and toe nails, eyelids, perirectal skin, upper versus. lower arm, thigh versus. leg, and so on. It is hoped that as more complete maps are available that cover a range of chemical moieties, we should be in a position to further refine those aspects of dermatopharmacology and dermatotoxicology that require knowledge of skin penetration. However the data are sufficient to make reasonable estimates from regional variation percutaneous absorption applied to human risk assessment. Proper risk assessment should also include absorption from clothing because that is what exists.

REFERENCES

1. Wester RC. Twenty absorbing years. In: Surber C, Elsner P, Bircher AJ, eds. Exogenous Dermatology. Basel: Karger, 1995:112–123.
2. Feldmann RJ, Maibach HI. Regional variation in percutaneous penetration of (^{14}C) cortisol in man. J Invest Dermatol 1967; 48:181–183.
3. Maibach HI, Feldmann RJ, Milby TH, Sert WF. Regional variation in percutaneous penetration in man. Arch Environ Health 1971; 23:208–211.
4. Wester RC, Maibach HI. In vivo percutaneous absorption and decontamination of pesticides in humans. J Toxicol Environ Health 1985; 16:25–37.

5. Guy RH, Maibach HI. Calculations of body exposure from percutaneous absorption data. In: Bronaugh RL, Maibach HI, eds. Percutaneous Absorption. New York: Marcel Dekker, 1985:461–466.
6. Van Rooy TGM, De Roos JHC, Bodelier-Bode MM, Jongeneelen FJ. Absorption of polycyclic aromatic hydrocarbons through human skin: differences between anatomic sites and individuals. J Toxicol Environ Health 1993; 38:355–368.
7. Wester RC, Maibach HI, Bucks DAW, Aufrere MB. In vivo percutaneous absorption of paraquat from hand, leg and forearm of humans. J Toxicol Environ Health 1984; 14:759–762.
8. Rougier A, Dupuis D, Lotte C, Roquet R, Wester RC, Maibach HI. Regional variation in percutaneous absorption in man: measurement by the stripping method. Arch Dermatol Res 1986; 278:465–469.
9. Wertz PW, Swartzendruber DC, Squier CA. Regional variation in the structure and permeability of oral mucosa and skin. Adv Drug Deliv Rev 1993; 12:1–12.
10. Shriner DL, Maibach HI. Regional variation of nonimmunological contact urticaria. Skin Pharmacol 1996; 348:1–11.
11. Bronaugh RL. Determination of percutaneous absorption by in vitro techniques. In: Bronaugh RL, Maibach HI, eds. Percutaneous Absorption. New York: Marcel Dekker, 1985:267–279.
12. Behl CR, Bellantone NH, Flynn GL. Influence of age on percutaneous absorption of drug substances. In: Bronaugh RL, Maibach HI, eds. Percutaneous Absorption. New York: Marcel Dekker, 1985:183–212.
13. Wester RC, KNoonan P, Maibach HI. Variation on percutaneous absorption of testosterone in the Rhesus monkey due to anatomic site of application and frequency of application. Arch Dermatol Res 1980; 267:229–235.
14. Moody RP, Franklin CA. Percutaneous absorption of the insecticides fenitrothion and aminocarb. J Toxicol Environ Health 1987; 20:209–219.
15. Wester RM, Tanjo H, Maibach HI, Wester RC. Predicted chemical warfare agent VX toxicity to uniformed soldier using parathion in vitro human exposure and absorption. Toxicol Appl Pharmacol 2000; 168:149–152.

6

In Vivo Relationship Between Percutaneous Absorption and Transepidermal Water Loss

André Rougier
Laboratoire Pharmaceutique, La Roche-Posay, Courbevoie, France

Claire Lotte
Laboratoires de Recherche Fondamentale, L'Oréal, Aulnay sous Bois, France

Howard I. Maibach
Department of Dermatology, School of Medicine, University of California, San Francisco, California, U.S.A.

In its role as a barrier the skin participates in homeostasis by limiting (a) water loss (1,2) and (b) percutaneous absorption of environmental agents (3,4).

The stratum corneum's role as a double barrier is intimately linked by its degree of hydration (5,6), transport mechanisms being diffusional (3,7). In humans (8,9) and in animals (10), an increase in water permeability of the skin corresponds to an increase in permeability to topically applied compounds. However, most of the studies dealing with this topic are only quantitative observations, and the relationship linking these two factors is unknown.

At present, transepidermal water loss (TEWL) can be considered a determinant indicative of the functional state of the cutaneous barrier (11–13). Apart from pathological considerations, the functional state of the cutaneous barrier may vary considerably under physiological conditions (13). Thus, in humans, cutaneous permeability to applied compounds varies from one site to another (14–16). This chapter investigates the influence of anatomical site, age, and sex in humans on both TEWL and percutaneous absorption to establish the precise relationship between these two indicators of the functional state of the cutaneous barrier.

I. PERCUTANEOUS ABSORPTION MEASUREMENTS

The penetration of benzoic acid was measured at 10 anatomical sites, the locations of which are shown in Figure 1. A group of six to eight informed male volunteers, aged 20 to 30 years, was used for each anatomical site. The influence of aging on skin absorption of benzoic acid was studied on groups of seven to eight male volunteers,

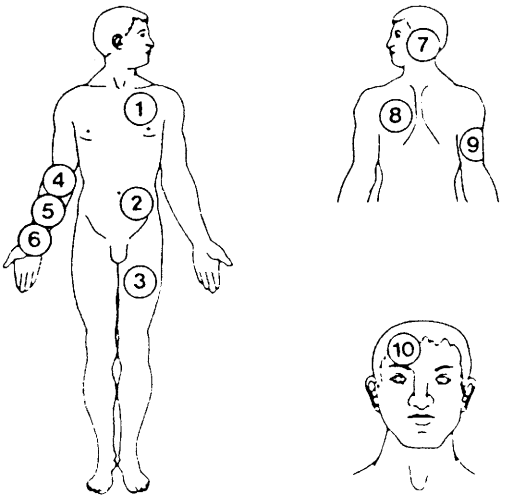


Figure 1 Anatomical sites tested: 1, chest; 2, abdomen; 3, thigh; 4, forearm (ventral elbow); 5, forearm (ventral mid); 6, forearm (ventral wrist); 7, postauricular; 8, back; 9, arm (upper outer); 10, forehead.

aged 45 to 55 years and 65 to 80 years. The anatomical site involved was the upper outer arm. The influence of gender on skin absorption was assessed on the upper outer arms and on the foreheads of groups of seven to eight female volunteers, aged 20 to 30 years.

One thousand nanomoles of benzoic acid (ring-^{14}C) (New England Nuclear) with a specific activity of 10^{-3} μCi/nmol were applied to an area of 1 cm^2 in 20 μL of a vehicle consisting of ethylene glycol to which 10% Triton X-100 had been added as surfactant. The treated area was demarcated by an open circular cell fixed by silicone glue to prevent chemical loss. After 30 minutes, excess chemical was quickly removed by two successive washes (2×300 μL) with a 95:5 ethanol/water mixture, followed by two rinses (2×300 μL) with distilled water and light drying with a cotton swab.

Benzoic acid was selected because of the rapidity and high level of its urinary excretion. Thus, from literature data on the kinetics of urinary excretion of this compound when administered intravenously and orally (17,18) or percutaneously (19–21) in different species, the proportion of the total amount of benzoic acid absorbed that would be excreted in the urine within the first 24 hours was 75%. The total quantities absorbed during the four days after application could therefore be calculated, after scintillation counting, from the quantities found in the urines during the first 24 hours.

II. TRANSEPIDERMAL WATER LOSS MEASUREMENTS

After completion of the benzoic acid treatment, TEWL was measured with an Evaporimeter EPIC (Servo Med, Sweden) from a contralateral site (same anatomical region) in each subject. The handheld probe was fitted with a 1-cm tail chimney, to reduce air turbulence around the hydrosensors, and a metallic shield (supplied by Servo Med), minimizing the possibility of sensor contamination. Measurements (g/m^2 hr) stabilized within 30 to 45 seconds. As the room environment was comfortable (room temperature 20°C, relative humidity 70%) and the subjects were

physically inactive, the TEWL should closely reflect stratum corneum water flux without significant sweating interference.

Table 1 gives the figures for permeability to water (TEWL) and to benzoic acid (percutaneous absorption) according to anatomical site, age, and sex. In male subjects aged from 20 to 30, cutaneous permeability to both water and benzoic acid was: forearm (ventral elbow) $<$ forearm (ventral mid) $<$ back $<$ arm (upper outer) $\leq$ chest $\leq$ thigh $=$ abdomen $<$ forearm (ventral wrist) $<$ postauricular $<$ forehead. In the sites studied (upper outer arm, forehead) no differences between sexes were observed.

In relation to age, no alterations in skin permeability appeared to occur before the age of 55. In subjects aged from 65 to 80 (upper outer arm), although there was no change in TEWL, percutaneous absorption of benzoic acid decreased appreciably (factor of 4; $p < 0.001$). Irrespective of anatomical site and sex, there exists a linear relationship (Fig. 2; $r = 0.92$, $p < 0.001$) between total penetration of benzoic acid and TEWL. (Point number 3, corresponding to subjects aged 65 to 80 measured on the upper outer arm, is a special case that will be discussed later and that was not taken into account in the calculation of the correlation coefficient.)

Among factors that might modify skin permeability, both in vitro (22) and in vivo (14–16,23,24), the anatomical location is of great importance, even if the connection between the differences observed, the structure of the skin, and the physicochemical nature of the penetrant remain obscure. As a matter of fact, general reviews often give contradictory explanations of the differences observed from one site to another (22,25).

The laws describing diffusion through a membrane accord a major role to membrane thickness. These general laws have been applied to several biophysical phenomena, including TEWL and percutaneous absorption. However, examination of the literature shows that it is not unusual that these laws, predicated on pure mathematical logic, are found wanting when applied to a discontinuous membrane of great physicochemical complexity such as the stratum corneum. Thus, the skin permeability of the forehead to water and benzoic acid is, respectively, four and eight times higher than on the forearm (ventral elbow), despite the fact that the stratum corneum thicknesses of these two sites are comparable (on average 12 μm and 18 cell layers; see Refs. 26, 27). This example, therefore, seems to run counter to the inverse relationship that should exist between permeability and membrane thickness. Hence, simple consideration of the thickness of the stratum corneum cannot, of itself, explain the differences in TEWL and penetration observed between anatomical sites. Other criteria must be considered.

A possible explanation of the higher permeability of the forehead to both benzoic acid and water could partly be because of the great number of sebaceous and sweat glands found in this area. However, even if it is relatively easy to imagine a molecule's penetration by simultaneously adopting the follicular, sweat, and transcorneal routes, it is, unfortunately, difficult to evaluate the relative extent of each route. Because of the density of active sebaceous glands, the forehead is the richest of all the sites tested in terms of sebum. It forms a discontinuous film on the surface of the skin, between 0.4-μm and 4-μm thick (28). It is reasonable to question to what extent the physicochemical nature of benzoic acid interacts with this film and to what extent this initial contact influences its absorption. However, previous studies have shown that the same ratio exists between the permeability levels of areas such as the forehead, which is rich in sebum, and the arm, which has very little sebum, for molecules with totally different lipid/water solubilities

Table 1 Influence of Anatomical Site, Age, and Sex on Transepidermal Water Loss (TEWL) and Percutaneous Absorption of Benzoic Acid

Group number	Volunteers per group	Anatomical site	Age (years)	Sex	TEWL[a] (g/m^2 hr)	Total penetration of benzoic acid within 4 days[a] ($nmol/cm^2$)
1	8	Arm (upper outer)	20–30	M	4.24 (0.35)	9.15 (1.01)
2	8	Arm (upper outer)	45–55	M	5.07 (0.23)	10.02 (1.02)
3	7	Arm (upper outer)	65–80	M	4.73 (0.45)	2.53 (0.82)
4	7	Arm (upper outer)	20–30	F	5.12 (0.35)	11.20 (1.20)
5	7	Abdomen	20–30	M	4.40 (0.51)	12.50 (1.64)
6	8	Postauricular	20–30	M	8.35 (0.41)	22.49 (5.14)
7	7	Forehead	20–30	M	10.34 (0.70)	26.80 (3.19)
8	8	Forehead	20–30	F	9.39 (0.73)	28.99 (1.81)
9	7	Forearm (ventral elbow)	20–30	M	2.50 (0.30)	3.48 (0.33)
10	8	Forearm (ventral mid)	20–30	M	4.00 (0.32)	5.51 (1.70)
11	7	Forearm (ventral wrist)	20–30	M	7.19 (0.39)	12.18 (1.62)
12	8	Back	20–30	M	4.51 (0.57)	8.55 (1.32)
13	8	Chest	20–30	M	4.73 (0.26)	11.70 (1.30)
14	7	Thigh	20–30	M	4.39 (0.32)	12.50 (1.43)

[a]Values are means, with SD in parentheses.

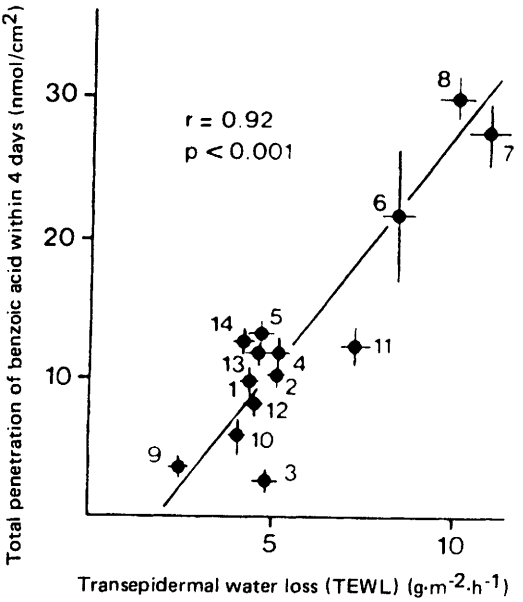


Figure 2 In vivo relationship between transepidermal water loss (TEWL) and percutaneous absorption of benzoic acid according to the anatomical site, age, and sex in humans (cf. Table 1).

(23). Moreover, it has been demonstrated that removing the lipidic film from the skin surface or artificially increasing its thickness has no effect on TEWL (29), which is another indicator of skin permeability.

Regional variations in cell size of the desquaming part of the human stratum corneum have been demonstrated by Plewig and Marples (30) and Marks et al. (31). When taking into account that in all the sites tested the individual thickness of the corneocytes does not change (32), the relationship between the flat area of corneocytes and barrier function of the horny layer must be addressed.

In permeability phenomena, the current trend is to assign priority to intercellular, rather than transcellular, penetration. Thus, if we consider two anatomical sites with an equal volume of stratum corneum but that contain corneocytes of unequal volume, such as the abdomen and the forehead, it is obvious that the intercorneal space will be greater in the stratum corneum that has smaller corneocytes. In adults (30,31), the flat surface of the forehead stratum corneum cells is approximately 30% less in area than that of cells from the arm, abdomen, or thigh. Moreover, as a function of the anatomical site, it has been demonstrated that an inverse relationship exists between the area of the horny layer cells and the value of the TEWL (31). What influence the intercorneal volume has on percutaneous absorption presents a question we have undertaken to answer.

As our results show (Table 1), there is no difference in benzoic acid absorption and TEWL between the 20 to 30 and 45 to 55 age groups. In subjects aged 65 to 80, on the other hand, absorption of this molecule is greatly reduced (factor of four). These findings agree with those of Malkinson and Fergusson (33), who failed to show any difference in percutaneous absorption of hydrocortisone in adults aged from 41 to 58. The reduced absorption of benzoic acid observed in the elderly (65 to 80) was similar to that obtained with testosterone by others (34,35). It is a

reasonable presumption that this change could be partly a consequence of alterations in keratinization and epidermal cell production, and itself results in altered structure and function of the stratum corneum. It has been established that corneocyte surface area increases with age (36–38). Moreover, recent studies have shown that, at the same time, a linear decrease occurred in the size of epidermal cells (39).

Although there is no change in total thickness of the stratum corneum with age (40), the question of whether or not there is an increase in surface area of corneocytes concomitant with a decrease in corneocyte thickness has not been finally decided. However, preliminary studies do not suggest that this value alters in aging stratum corneum (31,41). So, if we assume that this latter factor does not change with advancing age, then the volume of intercellular spaces must decrease as the surface area of the corneocytes increases. The spaces between the corneocytes probably act as the molecular ''reservoir'' of the stratum corneum (19). For a given molecule, the smaller the capacity of this reservoir, the less it is absorbed (16,19,23,42,43). As the general morphological organization of the stratum corneum does not appear to be affected by aging (40,44), it is tempting to conclude that the great differences observed in percutaneous absorption of benzoic acid, according to age, are solely due to the change in corneocyte size. However, this would be too simplistic an approach, and we should take into account other factors that affect the physical and physicochemical properties of the barrier, such as changes in the lipid composition of the intercellular cements, cohesion between corneocytes, which decreases with age (45,46), or the hydration level of the horny layer (1,47). Moreover, morphological and functional changes in adjacent structures, in particular the dermis, should also be taken into consideration. Thus, in advancing age, the underside of the epidermis becomes flattened, with this flattening being accompanied by diminution of superficial blood vessels (48,49). These alterations in the vascular bed and extracellular matrix may lead to decreased clearance of transdermally absorbed materials from the dermis (39,50).

Although the barrier function of the stratum corneum to the penetration of environmental agents appears to increase with age, we agree with others that TEWL does not statistically vary (45,46,51). This is a strange situation because a particular feature of aged skin is the roughness and apparent dryness of its surface. If it is true that the stratum corneum is the differentiated cellular end of the viable epidermis and, as such, must share the general effect of aging that takes place in all cells, the absolute need to maintain homeostasis suggests that to maintain its functional integrity, functional alterations of the horny structure will be subtle and difficult to detect.

In the areas studied (upper outer arm and forehead), no differences have been found between male and female subjects, either in percutaneous absorption of benzoic acid or in water loss. There has been no systematic study showing the effects of sex on cutaneous permeability in humans. We cannot, therefore, compare our results with the literature.

Although most authors recognize the importance of the anatomical site either on the degree of absorption of molecules or on TEWL, the literature does not include any quantitative data on the relationship that may exist in humans between these two functions. Our results show (Fig. 2) that for the anatomical sites studied, and within the range of TEWL and penetration values determined, a highly significant linear relationship exists ($r = 0.92$, $p < 0.001$) between the permeability of skin to water and the percutaneous absorption of a non-water-soluble compound such as

benzoic acid. Only those values obtained for aged subjects (65 to 80 years, upper outer arm, point number 3) do not fit on this correlation curve.

Although it is generally agreed that either of these factors can be considered as a reflection of the functional state and integrity of the cutaneous barrier, our results have demonstrated that they are directly linked. However, before over generalizing, we have examined the relationship existing between TEWL and percutaneous absorption of different molecules of varying physicochemical properties. The percutaneous absorption of three radiolabeled compounds (New England Nuclear)—acetylsalicylic acid (carboxyl-^{14}C), caffeine (1-methyl-^{14}C), and benzoic acid sodium salt (ring-^{14}C)—was determined for four anatomical sites, the exact locations of which are shown in Figure 3. For each molecule and for each site, six to eight male caucasion volunteers aged 28 $\pm$ two years were studied.

One thousand nanomoles of each compound, with a specific activity adjusted to 10^{-3} μCi/nmol, were applied to an area of 1 cm^2, in 20 μL of the appropriate vehicle. The composition of these vehicles, shown in Table 2, was selected according to the solubility of each compound. Triton X-100 was added as a surfactant to obtain smooth spreading of the vehicle over the treated area, the boundaries of which were circumscribed by an open circular cell fixed by silicone glue to prevent any chemical loss. After 30 minutes, excess substance was rapidly removed by washing, rinsing, and drying the treated area as previously described.

The molecules tested were selected on the basis of the rapidity and high level of their urinary excretion. In view of the literature concerning urinary excretion kinetics for these substances after administration by various routes in different species (18–21,43), the total amounts that had penetrated during the four days following application could be calculated, after scintillation counting, from the quantities found in the urine during the first 24 hours. The proportion of the total amounts

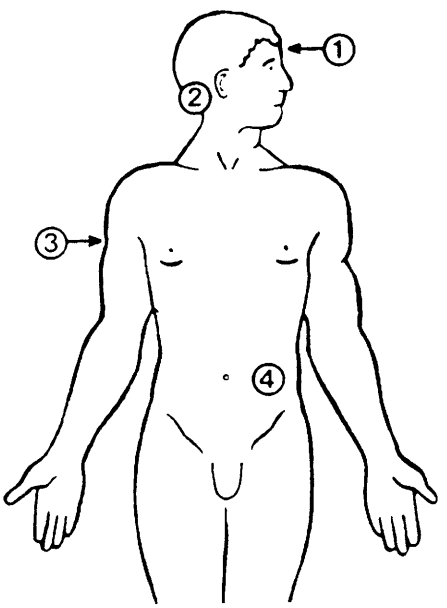


Figure 3 Anatomical sites tested: 1, forehead; 2, postauricular; 3, arm (upper outer); 4, abdomen.

Table 2 Percutaneous Absorption and Transepidermal Water Loss (TEWL) Values According to Anatomical Site

n and anatomical site	Amount in urines after 24 hr	Total amount penetrated within 4 days[a]	TEWL	Relative permeability to arm	
				Penetration	TEWL
Compound: benzoic acid sodium salt, vehicle A					
6, Arm (upper outer)	3.02 (0.34)	4.02 (0.45)	6.06 (0.36)	1	1
6, Abdomen	5.73 (0.54)	7.65 (0.72)	5.37 (0.46)	1.9	0.9
6, Postauricular	7.54 (0.62)	10.06 (0.82)	7.72 (0.64)	2.5	1.3
8, Forehead	9.31 (1.76)	12.32 (2.30)	12.29 (0.96)	3.1	2
Compound: caffeine, vehicle B					
7, Arm (upper outer)	6.04 (0.92)	12.09 (1.84)	7.04 (0.95)	1	1
6, Abdomen	3.76 (0.67)	7.53 (1.34)	6.05 (0.43)	0.6	0.9
7, Postauricular	5.87 (0.52)	11.72 (1.05)	8.74 (0.62)	1	1.2
6, Forehead	11.17 (1.20)	22.35 (2.39)	12.77 (1.05)	1.9	1.8
Compound: acetylsalicylic acid, vehicle A					
7, Arm	5.27 (0.18)	17.00 (0.37)	5.08 (0.79)	1	1
6, Abdomen	5.34 (1.03)	17.20 (3.35)	5.16 (0.43)	1	1
7, Postauricular	11.04 (2.50)	29.17 (5.37)	9.04 (0.84)	2.1	1.8
6, Forehead	10.89 (1.02)	35.14 (3.29)	11.22 (0.96)	2.1	2.2

Note: Values are expressed in nmol/cm^2 with SD in parentheses. Vehicle A, (ethylene glycol/Triton X-100), 90:10; Vehicle B, (ethylene glycol/Triton X-100), 90:10/H2O;50:50.
[a]Calculated from urinary excretion for benzoic acid sodium salt (amount in urines)/0.75; for caffeine (amount in urines)/0.5; for acetylsalicylic acid (amount in urines)/0.31.
[b]Measured just before the application in g/m^{-2}hr.

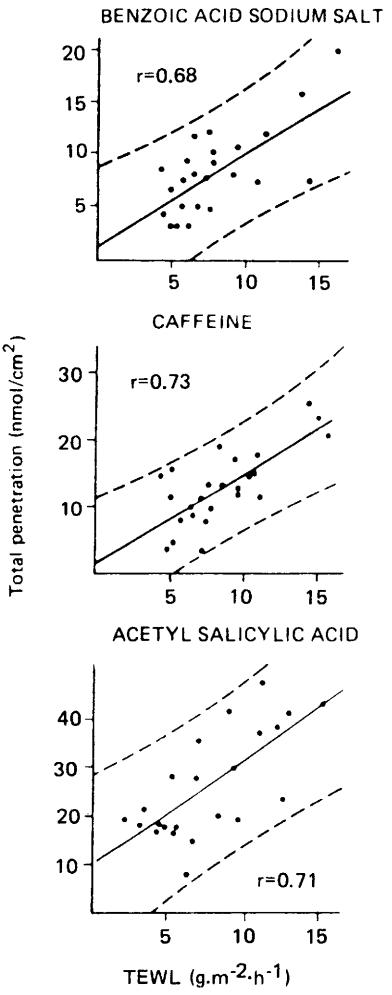


Figure 4 In vivo relationship between transepidermal water loss (TEWL) and percutaneous absorption of some organic compounds according to the anatomical site in humans.

of benzoic acid sodium salt, caffeine, and acetylsalicylic acid absorbed that were excreted within 24 hours were 75%, 50%, and 31%, respectively.

After topical administration of the tested compound, TEWL was measured from a contralateral site (same anatomical region) in each subject as described earlier. The results (Table 2) show that the percutaneous penetration of the test molecules varied with the anatomical location. The area behind the ear and that on the forehead were the most permeable, regardless of the physicochemical properties of the compound tested. In general, the order of cutaneous permeability was as follows: arm $\leq$ abdomen $<$ postauricular $<$ forehead. Although the literature provides few details about the influence of anatomical site on the absorption of molecules, the rank order obtained here agrees with studies performed with other chemicals (14,15,20,52).

Cutaneous permeability is generally considered a mirror of the integrity of the horny layer. Even in normal skin, the efficacy of this barrier is not constant. Thus, as

shown in Table 2, for a given anatomical site the permeability varies widely in relation to the nature of the molecule administered because this is related to the physicochemical interactions that may occur between the molecule, the vehicle, and the stratum corneum. For the anatomical sites investigated and for the range of TEWL and penetration observed, there exists a linear relationship between the permeability of the skin to the outward movement of water and the inward uptake of molecules. Table 2 shows that this relationship fits with all the compounds tested, with caffeine being an apparent exception (decreased penetration on abdomen and postauricular regions as compared with the arm, whereas TEWL showed a slight decrease on the abdomen and an increase in the postauricular region). It is, however, worth noting that the same relationship, when expressed with individual values (Fig. 4), shows correlation coefficients between 0.68 and 0.73 ($p < 0.05$), the latter (and better one) corresponding to caffeine (the confidence limits represent a risk of 5%).

Thus, it appears that the linear relationship linking TEWL and percutaneous absorption is independent of the physicochemical properties of the compound applied. Moreover, with the three molecules investigated, a mean increase of 2.7 in percutaneous absorption corresponded to an increase of three in the TEWL value. This fact supports the hypothesis that the efficiency of the barrier is dependent on the physicochemical properties of the molecule administered, but its functional state is independent of these. Consequently, as with determinations of TEWL, percutaneous absorption measurement provides a good marker of the cutaneous barrier integrity.

REFERENCES

1. Blank IH, Moloney J, Emslie AG, Simon I, Apt CH. The diffusion of water across the stratum corneum as a function of its water content. J Invest Dermatol 1984; 82:188–194.
2. Scheuplein RJ, Blank IH. Permeability of the skin. Physiol Rev 1971; 51:702–747.
3. Marzulli FN. Barriers to skin penetration. J Invest Dermatol 1962; 39:387–393.
4. Malkinson FD. Studies on percutaneous absorption of ^{14}C-labelled steroids by use of the Gaz low cell. J Invest Dermatol 1958; 31:19–28.
5. Fritsch WF, Stoughton RB. The effect of temperature and humidity on the penetration of ^{14}C acetylsalicylic acid in excised human skin. J Invest Dermatol 1963; 41:307–311.
6. Wurter DE, Kramer SF. Investigation of some factors influencing percutaneous absorption. J Pharm Sci 1961; 50:288–293.
7. Scheuplein RJ. The skin as a barrier. In: Jarrett A, ed. The Physiology and Pathophysiology of the Skin. Vol. 5. New York: Academic Press, 1978:1669–1692.
8. Guillaume JC, de Rigal J, Leveque JL, Galle P, Touraine R, Dubertret L. Etude comparée de la perée insensible d'eau et de la pénétration cutanïé des corticoides. Dermatologïca 1981; 162:380—390.
9. Smith JG, Fischer RW, Blank IH. The epidermal barrier: a comparison between scrotal and abdominal skin. J Invest Dermatol 1961; 36:337–343.
10. Lamaud E, Lambrey B, Schalla W, Schaefer H. Correlation between transepidermal water loss and penetration of drugs. J Invest Dermatol 1984; 82:556.
11. Maibach HI, Bronaugh R, Guy R, Turr E, Wilson D, Jacques S, Chaing D. Noninvasive techniques for determining skin function. In: Drill VA, Lazar P, eds. Cutaneous Toxicity. New York: Raven Press, 1984:63–97.
12. Surinchak JS, Malinowski JA, Wilson DR, Maibach HI. Skin wound healing determined by water loss. J Surg Res 1985; 38:258–262.
13. Wilson DR, Maibach HI. A review of transepidermal water loss: physical aspects and measurements as related to infants and adults. In: Maibach HI, Boisits EK, eds. Neonatal Skin. New York: Marcel Dekker, 1982:83.

14. Feldman RJ, Maibach HI. Regional variations in percutaneous penetration of ^{14}C cortisol in man. J Invest Dermatol 1967; 48:181–183.
15. Maibach HI, Feldmann RJ, Milby T, Serat W. Regional variation in percutaneous penetration in man. Arch Environ Health 1971; 23:208–211.
16. Rougier A, Dupuis D, Lotte C, Roguet R, Wester R, Maibach HI. Regional variation in percutaneous absorption in man: measurement by the stripping method. Arch Dermatol Res 1986; 278:465–469.
17. Bridges JW, French MR, Smith RL, Williams RT. The fate of benzoic acid in various species. Biochem J 1970; 188:47–51.
18. Bronaugh RL, Stewart RF, Congdon ER, Giles AL. Methods for in vitro percutaneous absorption studies. I. Comparison with in vivo results. Toxicol Appl Pharmacol 1982; 62:474–480.
19. Dupuis D, Rougier A, Roguet R, Lotte C, Kalopissis G. In vivo relationship between horny layer reservoir effect and percutaneous absorption in human and rat. J Invest Dermatol 1984; 82:353–356.
20. Feldmann RJ, Maibach HI. Absorption of some organic compounds through the skin in man. J Invest Dermatol 1970; 54:399–404.
21. Rougier A, Dupuis D, Lotte C, Roguet R, Schaefer H. In vivo correlation between stratum corneum reservoir function and percutaneous absorption. J Invest Dermatol 1983; 81:275–278.
22. Scheuplein RJ. Site variations in diffusion and permeability. In: Jarrett A, ed. The Physiology and Pathology of the Skin. Vol. 5. New York: Academic Press, 1979:1731–1752.
23. Rougier A, Lotte C, Maibach HI. In vivo percutaneous penetration of some organic compounds related to anatomic site in man: Predictive assessment by the stripping method. J Pharm Sci 1987;.
24. Wester RC, Maibach HI, Bucks DA, Aufrere MB. In vivo percutaneous absorption of paraquat from hand, leg and forearm of humans. J Toxicol Environ Health 1984; 84:759–761.
25. Idson B. Percutaneous absorption. J Pharm Sci 1975; 64:901–924.
26. Holbrook KA, Odland GF. Regional differences in the thickness (cell layers) of the human stratum corneum: an ultrastructural analysis. J Invest Dermatol 1974; 62: 415–422.
27. Pathiak MA, Fitzpatrick TB. The role of natural photoprotective agents in human skin. In: Fitzpatrick TB, ed. Sunlight and Man. Tokyo: University Tokyo Press, 1974:725–750.
28. Kligman AM. The use of sebum. Br J Dermatol 1983a; 75:307–319.
29. Kligman AM. A biological brief on percutaneous absorption. Drug Dev Ind Pharm 1983b; 9:521–560.
30. Plewig G, Marples RR. Regional differences of cell sizes in human stratum corneum. Part I. J Invest Dermatol 1970; 54:13–18.
31. Marks R, Nicholls S, King CS. Studies on isolated corneocytes. Int J Cosmet Sci 1981; 3:251–258.
32. Plewig G, Scheuber E, Reuter B, Waidelich W. Thickness of corneocytes. In: Marks R, Plewig G, eds. Stratum Corneum. Berlin-Heidelberg, New York: Springer-Verlag, 1983:171–174.
33. Malkinson FD, Ferguson EH. Percutaneous absorption of hydrocortisone-4-^{14}C in two human subjects. J Invest Dermatol 1955; 25:281–283.
34. Christophers E, Kligman AM. Percutaneous absorption in aged skin. In: Montagna W, ed. Advances in Biology of the Skin. New York: Pergamon Press, 1964:163–175.
35. Roskos K, Guy R, Maibach HI. Percutaneous penetration in the aged. Dermatol Clin 1986; 4:455–465.
36. Grove GL. Exfoliative cytological procedures as a nonintrusive method for dermatogerontological studies. J Invest Dermatol 1979; 79:67–69.
37. Plewig G. Regional differences of cell sizes in the human stratum corneum. Part II: Effect of sex and age. J Invest Dermatol 1970; 54:19–23.

38. Grove GL, Lavker RM, Holzle E, Kligman AM. The use of nonintrusive tests to monitor age associated changes in human skin. J Soc Cosmet Chem 1981; 32:15–26.
39. Marks R. Measurement of biological aging in human epidermis. Br J Dermatol 1981; 104:627–633.
40. Lavker RM. Structural alterations in exposed and unexposed aged skin. J Invest Dermatol 1979; 73:59–66.
41. Marks R, Barton SP. The significance of size and shape of corneocytes. In: Marks R, Plewig G, eds. Stratum Corneum. Berlin-Heidelberg, New York: Springer-Verlag, 1983:161–170.
42. Dupuis D, Rougier A, Roguet R, Lotte C. The measurement of the stratum corneum reservoir: a simple method to predict the influence of vehicles on in vivo percutaneous absorption. Br J Dermatol 1986; 115:233–238.
43. Rougier A, Dupuis D, Lotte C, Roguet R. The measurement of the stratum corneum reservoir. A predictive method for in vivo percutaneous absorption studies: influence of application time. J Invest Dermatol 1985; 84:66–68.
44. McKenzye IC, Zimmerman K, Peterson L. The pattern of cellular organization of human epidermis. J Invest Dermatol 1981; 76:459–461.
45. Leveque JL, Corcuff P, de Rigal J, Agache P. In vivo studies of the evolution of physical properties of the human skin with age. Int J Dermatol 1984; 23:322–329.
46. Marks R, Lawson A, Nicholls S. Age-related changes in stratum corneum structure and function. In: Marks R, Plewig G, eds. Stratum Corneum. Berlin-Heidelberg, New York: Springer-Verlag, 1983:175–180.
47. Blank IH. Factors which influence the water content of the stratum corneum. J Invest Dermatol 1952; 18:433–437.
48. Ellis RA. Aging of the human male scalp. In: Montagna W, Ellis RA, eds. The Biology of Hair Growth. New York: Academic Press, 1958:469–485.
49. Montagna W, Carlisle K. Structural changes in aging human skin. J Invest Dermatol 1979; 73:47–53.
50. Küstala G. Dermal epidermal separation: influence of age, sex and body region on suction blister formation in human skin. Ann Clin Res 1972; 4:10–22.
51. Kligman AM. Perspectives and problems in cutaneous gerontology. J Invest Dermatol 1979; 73:39–46.
52. Taskovitch L, Shaw JE. Regional differences in the morphology of human skin: correlation with variations in drug permeability. J Invest Dermatol 1978; 70:217.

7

Skin Contamination and Absorption of Chemicals from Water and Soil

Ronald C. Wester and Howard I. Maibach
Department of Dermatology, School of Medicine, University of California, San Francisco, California, U.S.A.

I. INTRODUCTION

Contamination of soil and water (ground and surface water) and the transfer of hazardous chemicals is a major concern. When the large surface area of skin is exposed to contaminated soil and water (work, play, swim, and daily bath), skin absorption may be significant. Brown et al. (1) suggested that skin absorption of contaminants in water has been underestimated and that ingestion may not constitute the sole, or even the primary, route of exposure. Soil has become an environmental depository for potentially hazardous chemicals. Exposure through work in pesticide-sprayed areas on chemical dump sites seems obvious. However, there may be hidden dangers in weekend gardening or in the child's play area where the soil has become laden with lead or other hazardous chemicals.

A. Water

Tables 1 and 2 give concentrations of chemical contaminants in drinking water. These lists are extensive, but not inclusive. And, because the problem of drinking water contamination is just becoming appreciated, we must assume that the lists and concentrations of chemicals are also just a beginning.

Methodology to calculate an acceptable level of a chemical in drinking water has been developed (3), but the underlying assumption of this methodology is that ingestion constitutes the chief route of exposure to the contaminant. Such an assumption disregards other routes of exposure, such as skin absorption during daily bathing or swimming. Indeed, this assumption is so overlooked that it is not uncommon to see bottled water being used in a home were the well water has been shown to be contaminated. Certainly, this bottled water will not be connected to the shower or swimming pool.

Brown et al. (1) showed that the skin absorption rates for solvents are high. They concluded that skin absorption of contaminants in drinking water has been underestimated, and that ingestion may not constitute the sole, or even the primary,

Table 1 Drinking Water Contamination Levels

Compound	Ranges detected in ground water (μg/L)	Ranges detected in surface water (μg/L)
Trichloroethylene	Trace–35,000	Trace–3.2
Tetrachloroethylene	Trace–3,000	Trace–21
Carbon tetrachloride	Trace–379	Trace–30
1,1,1-Trichloroethane	Trace–401,300	Trace–3.3
1,2-Dichloroethane	Trace–400	Trace–4.8
Vinyl chloride	Trace–380	Trace–9.8
Methylene chloride	Trace–3,600	Trace–13
1,1-Dichloroethylene	Trace–860	Trace–2.2
cis-1,2-Dichloroethylene		
trans-l,2-Dichlorethylene	Trace–2,000	
Ethylbenzene		
Xylene	Trace–300	
Toluene	Trace–6,400	

Table 2 Concentration of Drinking Water Contaminants

Compound	NAS[a] 10^{-6} (μg/L)	CAG[b] 10^{-6} (μg/L)
Acrylonitrile	0.77	0.034
Arsenic		0.004
Benzene		3.0
Benzo[a]pyrene		
Beryllium		0.02
Bis (2-chloroethyl) ether	0.83	
Carbon tetrachloride	9.09	0.086
Chlordane	0.056	0.012
Chloroform	0.59	0.48
DDT	0.083	
1,2-Dichlorethane	1.4	1.46
1,1-Dichlorethylene		.28
Dieldrin	0.004	
Ethylenedibromide	0.11	0.0022
ETU	0.46	
Heptachlor	0.024	2.4
Hexachlorobutadiene		1.4
Hexachlorobenzene	0.034	
N-Nitrosodimethylamine		0.0052
Kepone	0.023	
Lindane	0.108	
PCB	0.32	
PCNB	7.14	
TCDD		5.0×10^{-6}
Tetrachloroethylene	0.71	0.82
Trichloroethylene	9.09	5.8
Vinyl chloride	2.13	106.0

[a]NAS, National Academy of Science.
[b]CAG, Cancer Assessment Group.
Source: From Ref. 2.

Table 3 Estimated Dose and Contribution Per Exposure for Skin Absorption Vs. Ingestion

Compound	Concentration (mg/L)	Dose (mg/kg)					
		Case 1[a]		Case 2[b]		Case 3[c]	
		Dermal	Oral	Dermal	Oral	Dermal	Oral
Toluene	0.005	67	33	44	56	91	9
	0.10	63	37	46	54	89	11
	0.5	59	41	45	55	89	11
Ethylbenzene	0.005	75	25	44	56	91	9
	0.10	63	37	46	54	89	11
	0.5	68	31	45	55	89	11
Styrene	0.005	67	33	29	71	83	17
	0.10	50	50	35	65	84	16
	0.5	59	41	29	71	83	17

[a]A 7-kg adult bathing 15 minutes, 80% immersed (skin absorption). Two liters of water consumed per day (ingestion).
[b]A 10.5-kg infant bathed 15 minutes, 75% immersed (skin absorption). One liter of water consumed per day (ingestion).
[c]A 21.9-kg child swimming one hour, 90% immersed (skin absorption). One liter of water consumed per day (ingestion).
Source: From Ref. 2.

route of exposure. Table 3 gives their estimates of the relative contribution for skin absorption versus ingestion. The dermal route usually equals or exceeds the oral.

Wester and Maibach (4) estimated the body burden of environmental contaminants from short-term exposure to skin absorption while bathing or swimming. They concluded that, for chemicals for which there was published data, the body burden was low for short-term exposure at water concentrations detected in surface water. However, for higher contaminant concentrations, such as those detected in ground water, skin exposure has a potential for being hazardous to human health.

Wester et al. (5) further investigated the interactions of chemical contaminants in water and their skin absorption and potential systemic availability. Table 4 shows that when chemicals in water solution come in contact with skin (powdered human stratum corneum), the chemicals partition/bind to human skin, depending upon their physiochemical interactions with skin. This partitioning was also shown to be linear for a 10-fold concentration range of nitroaniline.

Table 5 shows that each of these chemicals is able to distribute into the inner layers of skin after binding and that a significant portion of the chemical is absorbed. Other experiments showed that the absorption of nitroaniline was linear over a 10-fold concentration range. Also, multiple doses of benzene were at least additive

Table 4 Partition of Contaminants from Water Solution to Powdered Human Stratum Corneum Following 30-minute Exposure

Chemical contaminant	Dose partitioned to skin (%)
Benzene (21.7 μg/mL)	16.6 ± 1.4
54% PCB (1.6 μ/mL)	95.7 ± 0.6
Nitroanaline (4.9 μ/mL)	2.5 ± 1.1

Abbreviations: PCB, polychlorinated biphenyl

Table 5 In Vitro Percutaneous Absorption and Skin Distribution of Contaminants in Water Solution for 30-minute Exposure

	Chemical contaminant (% dose)[a]		
Parameter	Benzene	54% PCB	Nitroaniline
Percutaneous absorption (systemic)	0.045 ± 0.037	0.03 ± 0.00	5.2 ± 1.6
Surface bound/stratum corneum	0.036 ± 0.005	6.8 ± 1.0	0.2 ± 0.17
Epidermis and dermis	0.065 ± 0.057	5.5 ± 0.7	0.61 ± 0.25
Total (skin/systemic)	0.15	12.3	6.1
Skin wash/residual	2.51 ± 0.94	71.2 ± 0.2	0.47 ± 0.03
Apparatus wash	0.006 ± 0.005	0.25 ± 0.2	0.47 ± 0.03
Total (accountability)	2.67	83.3	99.0

[a]Percentage of applied dose (n=4 for each parameter): Benzene, 21.7 μg/mL; 54% PCB, 1.6 μg/mL; Nitroaniline, 4.9 μg/mL.
Abbreviation: PCB, polychlorinated biphenyl.

and, perhaps, exceeded single-dose predictions. This is due to benzene evaporation into the air during the absorption period. There is a partition of benzene between the air and skin. This is illustrated in Table 6, which gives the human skin absorption of 0.1% benzene in water and in toluene. From water vehicle a total of 5.7% dose benzene was absorbed, while only 0.16% dose was absorbed from toluene vehicle. This is because the benzene and toluene rapidly evaporate off the skin, leaving little benzene absorbed. Contrary, water is less volatile than toluene so there is more time for benzene absorption.

The in vivo percutaneous absorption of nitroaniline in the rhesus monkey, an animal model relevant for skin absorption in humans (6) was $4.1 \pm 2.3\%$ of applied dose. This compared well with the $2.5 \pm 1.6\%$ binding to powdered human stratum corneum and the $5.2 \pm 1.6\%$ in vitro absorption (Table 5).

Table 7 gives a hypothetical percutaneous absorption of a chemical contamination from water while bathing or swimming for a single 30-minute period. Thus, it is possible for milligram amounts to be absorbed for single exposure and, thus, would be at least cumulative in daily life.

A more detailed overview of the complexities of percutaneous flux and, more specifically, implications of penetration from bathing and swimming, are outlined in Reference 7. The estimates provided are tentative; few chemical moieties have

Table 6 In Vitro Percutaneous Absorption of Benzene in Human Skin

	Percent dose absorbed	
Parameter	Water vehicle	Toluene vehicle
Receptor fluid	5.0 ± 1.9	0.11 ± 0.08
Skin		
Epidermis	0.4 ± 0.3	0.04 ± 0.02
Dermis	0.3 ± 0.2	0.01 ± 0.01
RF + skin (absorbed)	5.7	0.16
Skin surface wash	1.8 ± 0.9	0.04 ± 0.02
Total	7.5 ± 1.0	0.19 ± 0.07

0.1% benzene in water or toluene dosed at 5 μL/cm^2 skin area.
Abbreviation: RF, Receptor fluid

Table 7 Hypothetical Percutaneous Absorption of Chemical Contaminant from Water While Bathing or Swimming for 30 Minutes

Parameters	
Concentration of chemical in water	1.0 μh/mL
Volume of water on skin surface in study	1.5 mL
Skin surface area in study	5.7 cm^2
Total skin surface area of human adult	17,000 cm^2
Percentage dose absorbed, 30-min exposure	5%
Calculation of body burden per single bath or swim	$\frac{1.0\,\mu g}{mL} \times \frac{1.5\,mL}{5.7\,cm^2} \times \frac{17,000\,cm^2}{1} \times 0.05 = 223.7\,\mu g$

The amount will obviously vary owing to concentration of chemical contaminant in water, percutaneous absorption of contaminant, and frequency of bathing and swimming.

been examined. Specialized skin sites (ear canal, genitalia, face, etc.) offer substantial opportunity for penetration enhancement. Workers, e.g., housewives, cooks, mechanics, and the like, may wash their hands and arms many times daily. Damaged skin and occluded skin (from diapers), as well as skin in the infant and aged, offer other possibilities for enhanced flux.

B. Water: Finite and Infinite Doses

Table 8 compares the in vitro and in vivo absorption from water for boric acid, borax, and disodium octaborate tetrahydrate (DOT). The K_p values from the infinite dose are a 1000-fold higher than from the in vivo study, while the finite dose K_p of boric acid was only 10-fold higher. Clearly, use of a similar dose volume was critical to the comparison. The in vitro system used a phosphate-buffered saline perfusion as well as a water solution dose. The in vivo dose was applied and allowed to dry, and absorption took place in whatever water content the skin of each volunteer contained. The preponderance of water in the infinite dose may have influenced

Table 8 In Vivo and In Vitro Percutaneous Absorption of Boron Administered as Boric Acid, Borax, and Disodium Octaborate Tetrahydrate (DOT) in Human Skin

	In vitro		In vitro	
Dose	Flux (μg/cm^2/hr)	K_p (cm/hr)	Flux (μg/cm^2/hr)	K_p (cm/hr)
Boric acid				
5% at 2 μL/cm^2	0.07	1.4×10^{-6}	0.009	1.9×10^{-7}
5% at 1 mL/cm^2	14.6	2.9×10^{-4}		
Borax				
5% at 2 μL/cm^2			0.009	1.8×10^{-7}
5% at 1 mL/cm^2	8.5	1.7×10^{-4}		
DOT				
5% at 2 μL/cm^2			0.010	1.0×10^{-7}
5% at 1 mL/cm^2	7.9	0.8×10^{-4}		

Note: 2 μL/cm^2 is a finite water dose on in vivo skin. More will just run off the body. 1 mL/cm^2 is an infinite dose only capable of being used with an in vitro system.

the skin membrane during 24 hour continual exposure, and this may have increased the permeability of the borate chemicals. This would make the in vivo data and the in vitro finite dose data more relevant for the usual exposure conditions. The only exception might be where a subject bathed in a boric acid, borax, or DOT solution for an extended period of time. The in vitro infinite dosing conditions may better predict the bathing situation. Note that there was a 1000-fold difference between in vivo absorption and in vitro absorption where the in vitro dose was infinite. General risk assessment from in vitro infinite dosing may be greatly over estimated.

C. Soil

The study design should be such that percutaneous absorption from soil is relative to actual exposure conditions. The gardener or the child playing in dirt will have some stationary contact with the soil (sitting on it; dust that settles on the skin). There also will be dirt manipulated with the hands where skin contacts an ever-changing layer of dirt. The exposed worker will certainly have airborne dust settle on skin; manipulated dirt will depend on the job. In all cases, the dirt covering skin is exposed to air (dirt in clothing is noted as an exception). Laboratory studies, to be relevant, should have the soil on skin open to air exchange. This is simple with in vitro studies where the soil is contained. With in vivo studies the soil needs to be contained and the best method is to use a nonocclusive cover that allows free passage of air and moisture. A Gore-Tex film accomplishes this (8). Use of an occlusive cover such as glass (9) will cause changes in the microenvironment under the cover, which will enhance skin absorption. The in vitro diffusion cell is a truly stationary system where chemical passage from soil to skin is physically undisturbed and will function according to the chemical kinetics of the components. An in vivo study may have some animal or human movement, which could shift/rotate soil confined under the nonocclusive patch if space under the patch permits this (the patch can be sufficiently concave to allow soil movement in the open space).

It is important to know the relevant characteristics of the test soil. This should include percent sand, clay, silt, and organic content. Soil can be passed through mesh sieves to be uniform in size. Mixing of the test chemical added in solvent to the soil should be done open to air to allow dissipation of the solvent. The "dust" fraction of soil can be avoided by the sieving method. This is for safety purposes so that airborne particles containing radioactivity do not contaminate laboratory personnel. An uncontrolled airborne fraction may also affect study results.

Table 9 gives the in vitro (human skin) and in vivo (rhesus monkey) percutaneous absorption of organic chemicals from soil and a comparative vehicle (water or solvent, depending upon vehicle). The soil is the same source for all chemicals. For each chemical the concentration of mass (μg) per unit skin area (cm^2) is the same for each vehicle. Receptor fluid (human plasma) accumulation of DDT was negligible in the in vitro study due to solubility restriction. Chemicals with higher log *P*s are lipophilic and therefore are not soluble in biological fluid receptor fluid (plasma and buffered saline) (8,10). Human skin content was 18.1% dose from acetone vehicle. In vivo absorption in the rhesus monkey was 18.9% dose from acetone vehicle. These values are comparable to the published 10% dose absorbed in vivo in man from acetone vehicle. Percutaneous absorption from soil was predicted to be 1.0% dose in human skin in vitro and a comparative 3.3% dose in vivo in rhesus monkey.

Table 9 In Vitro and In Vivo Percutaneous Absorption of Organic Chemicals

		Percent dose		
		In vitro		
Compound	Vehicle	Skin	Receptor fluid	In vivo
DDT	Acetone	18.1 ± 13.4	0.08 ± 0.02	18.9 ± 9.4
	Soil	1.0 ± 0.7	0.04 ± 0.01	3.3 ± 0.5
Benzo[a]pyrene	Acetone	23.7 ± 9.7	0.09 ± 0.06	51.0 ± 22.0
	Soil	1.4 ± 0.9	0.01 ± 0.06	13.2 ± 3.4
Chlordane	Acetone	10.8 ± 8.2	0.07 ± 0.06	6.0 ± 2.8
	Soil	0.3 ± 0.3	0.04 ± 0.05	4.2 ± 1.8
Pentachlorophenol	Acetone	3.7 ± 1.17	0.6 ± 0.09	29.2 ± 5.8
	Soil	0.11 ± 0.04	0.01 ± 0.00	24.4 ± 6.4

In vivo percutaneous absorption of benzo[a]pyrene is high, 51.0% reported here for rhesus monkey and 48.3% (12) and 35.3% (13) for the rat. Benzo[a]pyrene absorption from soil was approximately one-fourth that of solvent vehicle (8,14).

For chlordane, pentachlorophenol, and 2,4-D, the in vivo percutaneous absorption in rhesus monkey from soil was equal to or slightly less than that obtained from solvent vehicle (Table 9). Validation to man in vivo is available for 2,4-D, where the percutaneous absorption is the same for rhesus monkey and man (Wester and Maibach, 1985). In vitro percutaneous absorption is variable, probably due to solubility problems relative to high lipophilicity.

In vivo studies have an advantage over in vitro studies in that in vivo pharmacokinetic data can be obtained and these data applied to better understand the potential toxicokinetics of a chemical (Table 10). The percutaneous absorption of phencyclidine hydrochloride (PCP) from acetone vehicle was 29.2 ± 5.8% of total dose applied for a 24-hour exposure period. Compared to other compounds the absorption of PCP would be considered high. In vivo absorption from soil was 3.3% for DDT, 13.2% for benzo[a]pyrene, and 4.2% for chlordane. Additionally, the ^{14}C excretion for PCP in urine was slow, a half-life of 4.5 days for both intravenous and topical application. If biological exposure is considered in terms of dose X time, then PCP biological exposure can be considered high. The percutaneous absorption of PCP from soil vehicle was also high (24.4 ± 6.4%) and not statistically different. The study of Reigner et al. (15) and this study show PCP to have high

Table 10 In Vivo Percutaneous Absorption of Pentachlorophenol in Rhesus Monkey

	Percent Dose[a]		
	Topical		
	Soil	Acetone	Intravenous
Percent dose absorbed	24.4 ± 6.4	29.2 ± 5.8	—
Surface recovery[b]	38.0 ± 13.4	59.6 ± 4.1	—
Half-life (days)	4.5	4.5	4.5

[a]Means ± SD four animals
[b]Includes chamber, residue, and surface washes.

Table 11 In Vitro and In Vivo Percutaneous Absorption of PCBs

		Percent dose		
		In vitro		
Compound	Vehicle	Skin	Receptor fluid	In vivo
PCBs (1242)	Acetone	—	—	21.4 ± 8.5
	TCB	—	—	18.0 ± 8.3
	Mineral oil	64 ± 6.3	0.3 ± 0.6	20.8 ± 8.3
	Soil	1.6 ± 1.1	00.4 ± 0.05	14.1 ± 1.0
PCBs (1254)	Acetone	—	—	14.6 ± 3.6
	TCB	—	—	20.8 ± 8.3
	Mineral oil	10.0 ± 16.5	0.1 ± 0.07	20.4 ± 8.5
	Soil	2.8 ± 2.8	0.04 ± 0.05	13.8 ± 2.7

Abbreviations: PCBs, polychlorinated biphenyls; TCB, trichlorinated biphenyls.

bioavailability, both topical and oral, and PCP also exhibits an extensive half-life. This suggests that PCP has the potential for extensive biological interactions.

Table 11 gives the in vitro and in vivo percutaneous absorption of polychlorinated biphenyls (PCBs) (16). As with the other organic chemicals with high log *P*, receptor fluid accumulation in vitro was essentially nil. Skin accumulation in vitro did exhibit some PCB accumulation. In vivo, PCB percutaneous absorption for both Aroclor 1242 and 1254 was (a) high, ranging from 14% to 21%, and (b) generally independent of formulation vehicle. The PCBs thus have a strong affinity for skin and are relatively easily absorbed into and through skin.

Selected salts of arsenic, cadmium, and mercury are soluble in water and thus are amenable to in vitro percutaneous absorption with human skin (Table 12) (17,18). Arsenic absorption in vitro was 2.0% (1.0% plus 0.9% receptor fluid) and the same in vivo in rhesus monkey. Absorption from soil was equal to (in vivo) or approximately one-third (in vitro). Cadmium and mercury both accumulate in human skin and are slowly absorbed into the body (note that in vivo studies with cadmium and mercury are difficult to perform; cadmium accumulates in the body and mercury is not excreted via urine). Note the high skin content with cadmium and mercury.

Table 12 In Vitro and In Vivo Percutaneous Absorption of Metals

		Percent dose		
		In vitro		
Compound	Vehicle	Skin	Receptor fluid	In vivo
Arsenic	Water	10 ± 1.0	0.9 ± 1.1	2.0 ± 1.2
	Soil	0.3 ± 0.2	0.4 ± 0.5	3.2 ± 1.9
Cadmium	Water	6.7 ± 4.8	0.4 ± 0.2	—
	Soil	0.09 ± 0.03	00.3 ± 0.02	—
Mercury	Water	28.5 ± 6.3	00.7 ± 0.01	—
	Soil	7.9 ± 2.2	0.07 ± 0.01	—

Table 13 Effect of Soil Load on 2,4-D Percutaneous Absorption

Compound	Soil load[a]	Percent dose absorbed[b]
In vivo, rhesus monkey[c]	1	9.8 ± 4.0
	40	15.9 ± 4.7
In vitro, human skin[c]	5	1.8±1.7
	10	1.7±1.3
	40	1.4±1.2

[a]Concentration of 2,4-D chemical per cm^2 skin area was kept constant, while soil load per cm^2 skin area was varied.
[b]In vivo percutaneous absorption measured by urinary ^{14}C accumulation; in vitro absorption determined by ^{14}skin content.
[c]Mean± SD (n=4)

D. Soil Load

Percutaneous absorption of 2,4-D for 24-hour exposure was 8.6 ± 2.1% dose for a (dose load of 4.2 μ/cm^2 in acetone vehicle. The same 2,4-D dose was then loaded into 1 mg soil or 40 mg soil per cm^2 skin surface area. Percutaneous absorption for 24 hours from the 1 mg soil load was 9.8 ± 4.0% dose (Table 13) (19).

Percutaneous absorption from the 40 mg soil load for 24 hours was 15.9 ± 4.7% (dose $p = 0.178$ non-significant for paired t-test). Thus, the in vivo percutaneous absorption of 2,4-D was not affected by soil load (1 mg vs. 40 mg soil; chemical dose constant). Additionally, the percutaneous absorption from the two soil loads was the same as from acetone vehicle.

The 2,4-D at a constant chemical dose 2 μ/cm^2 was applied to human skin in vitro in soil loads of 5, 10, and 40 mg. Dose accumulation in buffered saline receptor fluid was low (0.02 ± 0.02%), presumably due to relative low solubility of 2,4-D in water. The 2,4-D human skin content was analyzed after the 24-hour exposure period and the results show no difference relative to the three soil loads. The in vitro skin content would predict a 2,4-D percent-dose absorption from soil of approximately 2%, which is approximately one-fifth of that in monkey in vivo.

E. Skin Contact Time

Table 14 provides the effect of skin deposition time on 2,4-D percutaneous absorption. In acetone vehicles the percutaneous absorption of 2,4-D over eight hour was

Table 14 Effect of Skin Contact Time on In Vivo Percutaneous Absorption of 2, 4-D

		Percent dose absorbed[a]	
		Soil vehicle	
Skin contact time	Acetone vehicle	1 mg/cm^2	40 mg/cm^2
8 hr	3.2 ± 1.0 etc.	0.05 ± 0.04	0.03 ± 0.02
16 hr	—	2.2 ± 1.2	—
24 hr	8.6–2.1	15.9	±4.7

[a]Mean ± SD (n = 4).

$3.2 \pm 1.0\%$ dose. This is approximately one-third of the absorption seen for 24 hours ($8.6 \pm 2.1\%$). Thus, with acetone vehicle (where the dose is in immediate contact with the skin) the percutaneous absorption was linear over time. With soil as the vehicle, the absorption was only $0.05 \pm 0.04\%$ for 1 mg soil/cm^2 and $0.03 \pm 0.02\%$ for 40 mg/cm^2 at eight hours. The 16-hour absorption for 1 mg/cm^2 soil was $2.2 \pm 1.2\%$. This suggests that percutaneous absorption of 2,4-D from soil was not linear over time. There may be a "lag" time where chemical must partition from soil into skin.

F. Soil and Risk Assessment Assumptions

In the study with 2,4-D and the other compounds mentioned previously, an experimental soil load of 40 mg/cm^2 skin surface area was used. Studies on dermal soil adherence show that less than 1 mg to perhaps 5 mg of soil will adhere to skin (20). It then becomes the practice in estimating potential health hazard to assume linearity and divide the results of 40 mg by a soil adhesion factor, thus reducing estimated body burden by 1/40 or 5/40, etc. (20). the data generated here for 2,4-D, where soil load (range 1–40 mg) had no effect on percutaneous absorption, suggest that this mathematical practice can severely underestimate absorption.

A second assumption, and that transferred to the laboratory, is that chemical and soil are "static." The gardener planting summer flowers will certainly have multiple contacts with soil. Chemicals are also mobile within soil. On the short-term, as seen in the data, chemicals move from soil to skin. Calderbank (21) reports that with time adsorbed residues in soil will become more stable. Therefore, some dynamics in the system need to be understood.

A third assumption of linearity is also placed on time. That 2,4-D absorption in acetone vehicle was $3.2 \pm 1.0\%$ for eight hours and $8.6 \pm 2.1\%$ for 24 hour suggests that absorption is linear over time and that the compound can be removed with washing (Fig. 1). With acetone vehicle the total dose is deposited on the skin surface and percutaneous absorption is dependent on skin barrier diffusion. With soil vehicle a lag time is needed for the 2,4-D to "mobilize" within soil and become available for absorption. Sufficient time is needed for 2,4-D to become available, then skin barrier function becomes the rate-limiting step in absorption. Should it turn out that a substantial lag time does exist for transfer from soil to skin, this would favor risk assessment for the worker. However, the data to date show that substantial amounts of hazardous chemicals can be absorbed from soil (Fig. 2).

II. DISCUSSION

The evolution of skin resulted in a tissue that protects precious body fluids and constituents from excessive uptake of water and contaminants in the external environment. The outermost surface of the skin that emerged for humans is the stratum corneum, which restricts but does not prevent penetration of water and other molecules. This is a complex lipid–protein structure that is exposed to contaminants during bathing, swimming, and exposure to the environment. Industrial growth has resulted in the production of organic chemical and toxic metals whose disposal results in contamination of water supplies. As one settles into a tub or pool, the skin (with a surface area of approximately 18,000 cm^2) acts as a lipid sink (stratum corneum) for the lipid-soluble contaminants. Skin also serves as transfer membrane for water and whatever contaminants may be dissolved in it. Note that (a) water

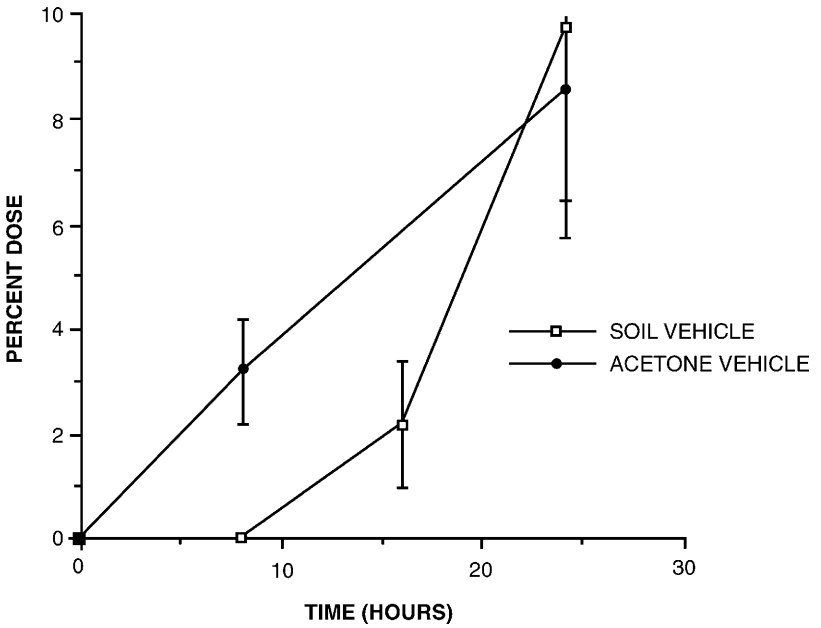


Figure 1 In vivo percutaneous absorption of 2,4-D is linear over time, except where there is an initial time from soil vehicle.

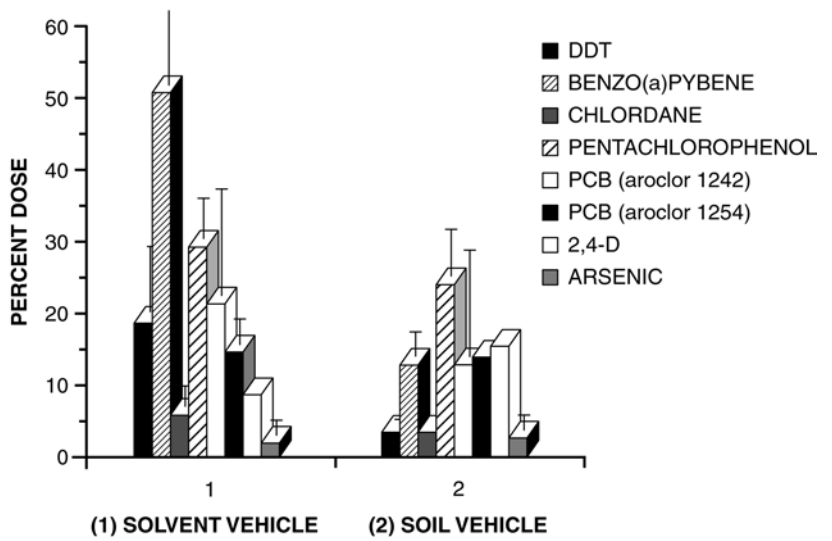


Figure 2 The in vivo percutaneous absorption of several hazardous substaces from soil and solvent (either acetone or water). Overall, soil reduced absorption to about 60%, compared to solvent. There is caution, however, because the absorption of some compounds is the same for soil and solvent.

transfers through skin and can carry chemicals and (b) the outer layer of skin is lipid in nature. Thus, highly lipophilic chemicals such as DDT, PCBs, and chlordane residing in soil will quickly transfer to skin. Percutaneous absorption can be linear, orderly and predictive (a measured flux from water). However, evidence exists that chemicals may transfer to skin with short-term exposure.

The objective of guidelines should be a process whereby results are achieved with a minimum of error. Estimates of dermal absorption for human risk assessment can produce two types of errors, one that overestimates absorption (false positive) and one that underestimates absorption (false negative). The overestimate has a built-in safety margin. The other error, to underestimate, is the more serious because it states that a margin of safety has been achieved when in fact it has not been achieved. This more serious type of error can be manifested in guidelines with dependence on in vitro percutaneous absorption and the backup of computer models based on in vitro data, all without in vivo (especially human) validation.

The series of studies in this chapter were done in part for California EPA and U.S. EPA to determine percutaneous absorption from soil for some chemicals of environmental concern. Both in vitro human skin and rhesus monkey in vivo (rhesus is a validated model for man) percutaneous absorption were determined and in vivo results are shown in Table 15. Based up in vitro receptor fluid accumulations, none of the compounds are absorbed from soil into and through human skin. The in vitro data are false negative data, the worse error that a risk assessment can produce. The error is verified with the in vivo data. The limitations are due to lack of chemical solubility (high log *P*) in the water-based receptor fluid. To overcome this limitation, some investigators are adding solvents miscible with water (example ethanol) to the receptor fluid. This then questions where the "absorption process" is diffusion or extraction.

Human skin is recommended for in vitro studies. What is lacking is quality assurance, which can affect the in vitro diffusion rate. Examples are:

Table 15 In Vitro and In Vivo Percutaneous Absorption

		Percent dose absorbed (24 hr)	
Compound (log *P*)	Vehicle	In vitro[a] receptor fluid accumulation	In vivo[b]
DDT (6.91)	Acetone	0.08 ± 0.02	18.9 ± 9.4
	Soil	0.04 ± 0.01	3.3 ± 0.5
Benzo(a) pyrene (5.97)	Acetone	0.09 ± 0.06	51.0 ± 22.0
	Soil	0.01 ± 0.06	13.2 ± 3.4
Pentachlorophenol (5.12)	Acetone	0.6 ± 0.09	29.2 ± 5.08
	Soil	0.01 ± 0.00	2.44 ± 6.4
PCB 1242 (mixture)	Mineral oil	0.3 ± 0.6	20.4 ± 8.3
(high log *P*)	Soil	0.04 ± 0.05	13.8 ± 2.7
PCB 1254 (mixture)	Mineral oil	0.1 ± 0.007	20.8 ± 8.3
(high log *P*)	Soil	0.04 ± 0.05	14.1 ± 1.0
2,4-D (2.81)	Acetone	—	8.6 ± 2.1
	Soil	0.02 ±0.01	15.9 ± 4.7

[a]Human skin (mean ± SD).
[b]rhesus monkey (mean ± SD).

a. *Human skin*: fresh, frozen, viable, whole segmented, derma toned, age, and source
b. *Diffusion cell*: static, flow-through, and composition (glass, metal, and composite)
c. *Receptor fluid*: composition and flow-rate

The fallback to the in vitro diffusion-produced permeability coefficient is the computer generated coefficient. This originated as the Flynn database. Guy and Potts and other have manipulated, expanded, and contracted it in many computer systems. The lack of acceptance has revolved around data sets being inappropriate with respect to the distribution of major molecular descriptors. Lack of in vivo human validation has been sited. Limited in vivo validation regarding soil (Table 15) suggests a need. With proper validation to a database and with sufficient molecular descriptors, this could be a valuable tool for risk assessment.

Guidelines contain a soil fraction based upon extensive studies of soil adhesion to skin. Only a limited amount of soil can adhere to skin, and only the smaller particles. The correlation between this limited soil adhesion to skin and hazardous

Table 16 Human and In Vivo Percutaneous Absorption Effect of Washing (Soap and Water) Percent Penetration

	Min				Hr				
$\mu m/cm^2$	1	5	15	30	1	2	4	8	24
Azodrin, 4 arm			2.3				8.6		14.7
Ethion, 4 arm			1.6				2.9		3.3
Guthion, 4 arm									
Malathion, 4 arm	1.3		4.3	4.5	6.1	8.3	12.1		6.8
Malathion, 40 arm			4.7				6.8		
Malathion, 400 arm			1.4		2.0		4.7		
Parathion, 4 arm	2.8		6.7		8.4		8.0	15.8	8.6
Parathion, 40 arm			3.1				6.9		9.5
Parathion, 400 arm			2.2		2.3		4.2		4.8
Parathion 4 forehead	8.4		7.1	12.2	10.5	20.1	27.7		36.3
Parathion 4 palm		6.2	13.6	13.3	11.7	9.4	7.7		11.8
Lindane, 4 arm		1.7	1.8	4.2	3.9	6.7	15.5		9.3
Baygon, 4 arm	1.2		4.7	4.5	4.7	11.8	15.5	11.3	19.6
2,4-D, 4 arm	0.5		0.7	1.8	1.2	3.7	3.7		5.8
2,4-D, 40 arm			0.7				2.8		

chemical exposure in soil has not been established. If the child makes one mud pie, the soil adhering to the hand will be x. If the child goes on to make 50 mud pies, the soil on the hand will still be x due to the adhesion limits. The focus should be on the chemical within soil. There will be soil turnover during an exposure below. The key is the chemical adherence to skin during this soil turnover.

Guidelines state that only the exposed skin surface areas of head, hands, forearms, and lower leg, some 5700 cm^2 skin surface area, should be considered. There is clinical evidence of chemical transfer from clothing to skin (rash from a favorite blouse, skin disease from a work uniform). There are published reports on hazardous chemical transfer from clothing into and through skin.

Another oversight is the question of decontamination, especially the potential ineffectiveness of soap and water washing. Exposure may end when the in vitro system is shut. Visible dirt washed away may seem effective. But what about the hazardous chemical on a living person? Table 16 is part of an in vivo human study (22) representative of the real world. There is no lag time. There are no solubility limits and false negative results. Soap and water washing is not the perfect decontaminant.

In vitro and computer generated permeability coefficient are easily obtained, easy to use, and can be cost effective. This is a nice comfort level. However, real world risk assessment involves people's lives and jobs, and errors can be tragic and costly. In vivo studies have proved safe and effective for regulatory agencies in the past; it seems risky to eliminate them for convenience.

REFERENCES

1. Brown HS, Bishop DR, Rowan CA. The role of skin absorption as a route of exposure for volatile organic compounds (VOCs) in drinking water. Am J Public Health 1984; 74:479–484.
2. Office of Technological Assessment. Factors associated with cancer. In: Assessment of Technologies for Determining Cancer Risks from the Environment. Chapter 3. Washington: Office of Technological Assessment, 1981.
3. National Academy of Sciences. Drinking Water and Health. Washington: NAS/NRC, 1977.
4. Wester RC, Maibach HI. Body burden of environmental contaminants from acute exposure to percutaneous absorption while bathing or swimming. Toxicologist 1985; 5:177.
5. Wester RC, Mobayen M, Maibach HI. In vivo and in vitro absorption and binding to powdered stratum corneum as methods to evaluate skin absorption of environmental chemical contaminants from ground and surface water. J Toxicol Environ Health 1987; 22:367–374.
6. Wester RC, Maibach HI. Cutaneous pharmacokinetics: 10 steps to percutaneous absorption. Drug Metab Rev 1983; 14:169–205.
7. Wester RC, Maibach HI. Assessment of dermal absorption of contaminants in drinking water. EPA contract No. 68002–3168.
8. Wester RC, Maibach HI, Bucks DAW, Sedik L, Melendres J, Liao C, Di Zio S. Percutaneous absorption of [^{14}C] DDT and [^{14}C] benzo[a]pyrene from soil. Fundam Appl Toxicol 1990a; 15:510–516.
9. Turkall RM, Skowronski GA, Kadry AM, Abdel–Rahman MS. A comparative study of the kinetics and bioavailability of pure and soil-absorbed naphthalene in dermally exposed male rates. Arch Environ Contam Toxicol 1994; 26:504–509.
10. Wester RC, Maibach HI, Sedik L, Melendres J, Wade M, DiZio S. In vitro percutaneous absorption of pentachlorophenol from soil. Fundam Appl Toxicol 1990b; 19:68–71.

11. Wester RC, Maibach HI, Sedik L, Melendres J, Liao C, DiZio S. Percutaneous absorption of [^{14}C] chlordane from soil. J Toxicol Environ Health 1992a; 35:269–277.
12. Bronaugh RL, Stewart RF. Methods for in vitro percutaneous absorption studies. VI. Preparation of the barrier layer. J Pharm Sci 1986; 75:487–491.
13. Yang JJ, Roy TA, Kruger AJ, Neil W, Mackerer CR. In vitro and in vivo percutaneous absorption of benzo[a]pyrene from petroleum crude-fortified soil in the rat. Bull Environ Contam Toxicol 1989; 43:207–214.
14. Shu H, Teitelbaum P, Webb AS, Marple L, Brunck B, Del Rossi D, Murray FJ, Paustenbach D. Bioavailability of soil-bound TCDD. Dermal bioavailability in the rat. Fundam Appl Toxicol 1988; 10:335–343.
15. Reigner BG, Gungon RA, Hoag MK, Tozer TN. Pentachlorophenol toxicokinetics after intravenous and oral administration to rat. Zenobiotica 1991; 21:1547–1558.
16. Wester RC, Maibach HI, Sedik L, Melendres J, Wade M. Percutaneous absorption of PCBs from soil: in vivo rhesus monkey, in vitro human skin, and binding to powdered human stratum corneum. J Toxicol Environ Health 1993a; 39:375–382.
17. Wester RC, Maibach HI, Sedik L, Melendres J, DiZio S, Wade M. In vitro percutaneous absorption of cadmium from water and soil into human skin. Fundam Appl Toxicol 1992b; 19:1–5.
18. Wester RC, Maibach HI, Sedik L, Melendres J, Wade M. In vivo and in vitro percutaneous absorption and skin decontamination of arsenic from water and soil. Fundam Appl Toxicol 1993b; 20:336–340.
19. Wester RC, Melendres J, Logan F, Hui X, Maibach HI. Percutaneous absorption of 2,,4-dichlorophenoxyacetic acid from soil with respect to soil load and skin contact time: in vivo absorption in rhesus monkey and in vitro absorption in human skin. J Toxicol Environ Health 1996; 47:335–344.
20. EPA. Dermal Exposure Assessment: Principles and Applications, EPA/600/8-91/011B, Office of Research and Development, Washington, DC, Section 5:48–49.
21. Calderbank A. The occurrence and significance of bound pesticide residues in soil. Rev Environ Contam Toxicol 1989; 108:71–103.
22. Maibach HI, Feldmann RJ. Systemic absorption of pesticides through the skin of man. Occupational Exposure to Pesticides; Federal Working Group on Pest Management; Washington DC, 1974; 2:120–127.

8

In Vivo Percutaneous Absorption: A Key Role for Stratum Corneum/ Vehicle Partitioning

André Rougier
Laboratoire Pharmaceutique, La Roche-Posay, Courbevoie, France

I. INTRODUCTION

Over the past two decades considerable attention has been paid to understanding the mechanisms and routes by which chemical compounds penetrate the skin. Irrespective of the different theories on mechanisms relating to percutaneous absorption, it is well established that the stratum corneum (SC) constitutes the main barrier (1–4). Thus, it is to be expected that the overall kinetic process will depend mainly on the pharmacokinetic parameters governing the penetration of compounds through this membrane.

The interaction between the drug, the vehicle, and the SC as a consequence of their physicochemical properties is likely to be an important pharmacokinetic parameter in an early step of the absorption process. In studies in rats (5) and humans (6), we have demonstrated a correlation between the amount of the test substance found in the SC at the end of a 30-minute application and the total amount absorbed over four days. The predictive aspect of the so-called "stripping method" was found to take into account the main factors influencing percutaneous absorption (7–10).

It has been suggested that the amount of chemical absorbed within the SC after 30 minutes of application could reflect its SC vehicle partitioning, and also its rate of entry into the skin (7). Previous studies in hairless rats (8) showed clearly that the amount of various compounds that penetrated in vivo was strictly proportional to the time of application, thus providing indirect evidence that a constant flux of penetration really does exist in vivo.

In the light of these results, the present study was carried out to determine whether the stripping method could also be used to predict the in vivo steady-state flux of a test compound.

II. MATERIALS AND METHODS

Five radiolabeled compounds (Radiochemical Centre, Amersham, U.K.) with very different physicochemical properties and belonging to different chemical classes

were compared: benzoic acid, caffeine, thiourea, hydrocortisone, and inulin (Table 1).

A group of six 12-week-old hairless Sprague-Dawley female rats (IFFA-CREDO, Lyon, France) weighing 200 ± 20 g was used for each compound and each application time.

A. Percutaneous Absorption Measurements

Each compound (1000 nmol) was applied to a 1-cm^2 area of the back of anesthetized animals [intraperitoneal (IP) injection of gammabutyrolactone, 0.5 ml/kg in 20 μL ethylene glycol/Triton W100 mixtures] (Table 1). The treated area was delimited by an open circular cell attached with silicone glue in order to prevent spreading. The application times were from one to five hours.

At the end of the application time, the treated area was washed twice (2×300 μL) with ethanol/water (95/5), rinsed twice with water, and dried with cotton in order to remove excess product. We considered that the compounds had effectively penetrated when they had crossed the SC and reached the viable epidermis. The SC was then stripped 10 times (using adhesive tape 810, 3M U.S.A.) in order to exclude any compound that had not penetrated during the time of application (previous histological studies in hairless rat have shown that this procedure almost totally removes the SC). The remaining skin (epidermis plus dermis) was sampled and counted by liquid scintillation (Packard 360, Packard Instruments, Downers Grove, Illinois, U.S.A.) after digestion in Soluene 350 (United Technology, Packard).

The carcasses were then lyophilized and homogenized, and samples were counted by liquid scintillation after combustion (Oxidizer 306, Packard Instruments). In the case of tritiated molecules (caffeine, hydrocortisone, inulin), the water resulting from the lyophilization of the carcasses was sampled and assayed for radioactivity. The radioactivity found was added to that detected in the carcasses, thus obtaining the overall percutaneous absorption values. The urine excreted during the time of application was collected to take into account any product contained therein in the overall absorption. The total amount of each compound penetrating at each application time was determined by summation of the amount found in the epidermis, dermis, and the carcass.

B. Stratum Corneum/Vehicle Partitioning Measurement

Six strippings (using 3M adhesive tape 810) were performed on the treated area of each group of six animals for each compound after a fixed application time of 30 minutes (the reasons for this choice of time are discussed later). The amount of product within the SC was assessed after complete digestion of the keratin material in Soluene 350 by liquid scintillation counting.

C. Measurement of the Thickness of the Stratum Corneum

The thickness of the SC was measured in biopsies from the backs of six rats according to the technique described by McKenzie (11). Each biopsy was placed on a strip of acetyl cellulose coated with Tekt issue (Miles Scientific, Naperville, Illinois, U.S.A.), then frozen in dry ice. Transverse sections (8 μm) were then cut with the acid of a cryomicrotome (HRLM Slee, London, U.K.). The sections obtained were fixed for 10 minutes in a 70% alcohol bath, then stained for 30 seconds with a 0.5%

Table 1 Application Conditions

Compound	Specific activity	Purity (%)	Molecular weight (Da)	Vehicle
Benzoic acid [7– ^{14}C]	21.3 mCi/mmol	> 98	122	Ethylene glycol/Triton X100 (90/10)
Caffeine [8– ^{3}H]	24 Ci/mmol	> 98	194	Ethylene glycol/Triton X100/water (45/5/50)
Thiourea [^{14}C]	58 mCi/mmol	> 98	76	Ethylene glycol/Triton X100 (90/10)
Hydrocortisone (1.2.6.7)[^{3}H]	98.5 Ci/mmol	> 99	362	Ethylene glycol/Triton X100/isopropanol (72/8/20)
Inulin [^{3}H]	3.2 Ci/mmol	> 98	5,200	Ethylene glycol/Triton X100 (90/10)

Note: Dose applied for all compounds: 1000 nmol/cm^2 in 20 μL vehicle.

aqueous solution of methylene blue. After rinsing with distilled water the sections were mounted between a slide and a coverslip with the aid of aquamount (hydrophilic mounting medium). The thickness of the horny layer was measured at 20 different points on each section by means of a semiautomatic image analyzer (Digipet, Reichert, Wien, Austria) connected to a microscope (Polyvar, Reichert, Austria) and hence a mean thickness could be calculated.

D. Effect of Vehicles Used on the Stratum Corneum Integrity

After anesthesia, 20 μL of each of the vehicles used was applied to a 1-cm^2 area on the backs of groups of five rats. The area was delimited by an open circular cell as described previously. After five hours of contact, the treated area was washed twice (2×300 μL) with water and dried with cotton in order to remove excess vehicle. One hour after completion of the vehicle treatment, transepidermal water loss (TEWL) was measured with an Evaporimeter EP1 (ServoMed, Stockholm, Sweden). The hand-held probe was fitted with a 1-cm tail chimney, to reduce air turbulence around the hydrosensors, and a metallic shield (supplied by ServoMed) to minimize the possibility of sensor contamination. Measurements ($G/m^2/hr$) stabilized within one minute. The effects of total destruction of the SC have also been studied by measuring TEWL from the backs of a group of five animals, five hours after a series of 10 strippings (using 3M adhesive tape 810).

E. Theory and Data Treatment

The mass transfer of compounds from the surface of the skin to the interior of the body through the SC is generally considered to be due to passive diffusion. A classical but oversimplified description of the transport process is represented in Figure 1. The SC is assumed to be a homogeneous membrane (thickness h); D is the diffusion coefficient of the solute through the membrane. The concentration of solute (C) within the outermost layer of the membrane ($x = 0$) depends on the concentration

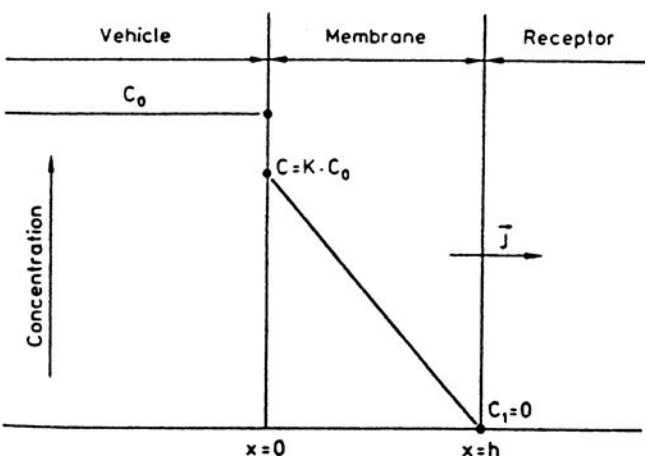


Figure 1 Concentration profile across homogeneous membrane at steady state (zero-order flux case).

within the vehicle (c_o) and the partition coefficient (K) between the membrane and the vehicle:

$$C = CK_o \tag{1}$$

For all values of time (t) the concentration of solute within the innermost layer of the membrane ($x = h$) is assumed to be negligible (sink condition). The validity of such an assumption is discussed in the "Results" section. The change in the cumulative amount of solute (Q) that passes through the membrane per unit area as a function of time is represented in Figure 2. When a steady state is reached, the curve $Q(t)$ is linear and can be described by the equation:

$$Q = J_s(t - L) \tag{2}$$

where J_s corresponds to the steady-state flux (the slope of the straight line):

$$J_s = Kc_o d/h \tag{3}$$

and L is the lag time (the intercept of the straight line on the time axis):

$$L = \frac{h^2}{6D} \tag{4}$$

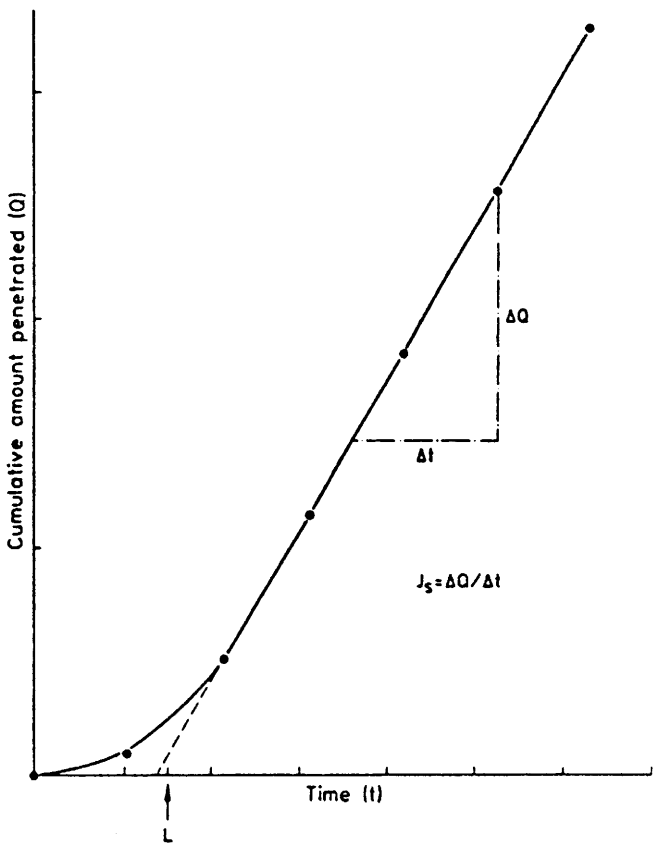


Figure 2 Typical profile of concentration versus. time for diffusion through the stratum corneum.

In practice, J_S and L were calculated for each compound using a linear regression obtained with the aid of a computer (Vax 11/750, Digital Corporation, Bedford, Massachusetts, U.S.A.) and standard software (RS/Explore BBN Software Product Corporation, Bedford, Massachusetts, U.S.A.).

III. RESULTS

Figure 3 shows that, irrespective of the nature of the compound tested, the plot of the cumulative amount of solute that passes through a unit surface area of the SC as a function of the application time appears to be linear ($r = 0.99$, $p < 0.001$). As shown in Figure 3 and Table 2, the steady-state values (J_S) are strongly molecule dependent. Thus, the values for inulin and benzoic acid differ by a factor of 40. The rank order of the J_S values is: inulin < hydrocortisone < thiourea < caffeine < benzoic acid.

In the present case, a constant flux of penetration ought to be attained within a contact time of about 30 minutes (11 × 2.7). According to Zatz (12), the attainment of a constant flux would be expected to coincide with the delivery of a constant amount at the SC. In order to test this hypothesis, we measured the amount present in the horny layer after an application time of 30 minutes (it should be recalled that the time of 30 minutes corresponds to that used in the stripping method). The results obtained for the five molecules are shown in Table 3. The total amounts of solute accumulated in the first six stoppings rank as follows: inulin < hydrocortisone < thiourea < caffeine < benzoic acid.

IV. DISCUSSION

Our results in vivo, like those in vitro, show that the phenomenon of transport across the SC can be considered as a process obeying the general laws governing passive membrane diffusion. Thus, after a time to attain equilibrium, a constant flux of penetration is established. From a theoretical point of view, this can occur only if the

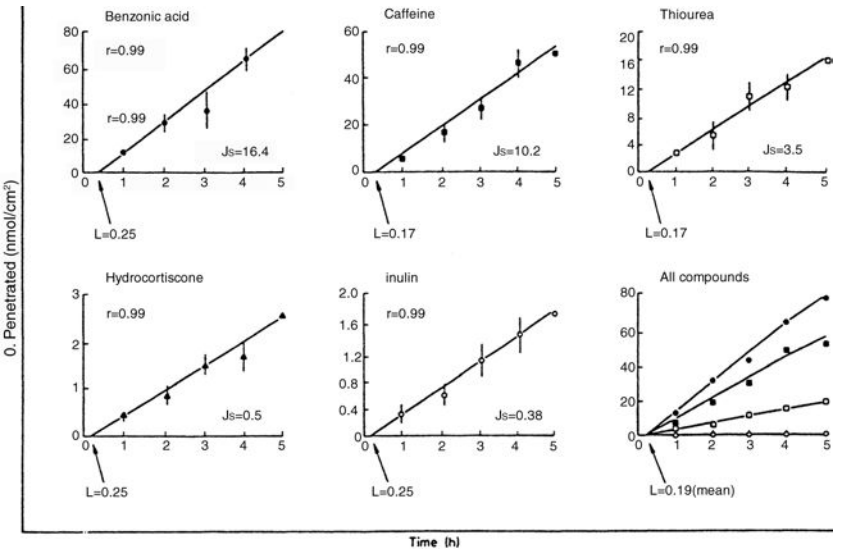


Figure 3 Cumulative amount of solute penetrating through the stratum corneum as a function of application time. *Abbreviations*: J_s, steady-state flux (nmol/cm^2/hr); L, lag time (hr).

Table 2 Amount of Chemical Penetrating Through the Stratum Corneum (nmol/cm^2), Measured at the End of the Application Time, and the Steady-state Parameters

	Application time (hr)						
Compound	1	2	3	4	5	Steady-state flux (J)(nmol/cm^2/hr)	Lag time (hr)
Benzoic acid	12.5 (SE 3)	30 (SE 2)	39 (SE 10)	64 (SE 6)	78 (SE 7)	16.4 (SE 0.8)	0.25
Caffeine	7.4 (SE 0.8)	18.6 (SE 2.9)	29.5 (SE 2)	45 (SE 5)	52 (SE 8.5)	10.2 (SE 0.6)	0.17
Thiourea	3 (SE 0.7)	6 (SE 2)	10.7 (SE 2)	13.4 (SE 1.8)	17 (SE 2.2)	3.5 (SE 0.2)	0.17
Hydrocortisone	0.49 (SE 0.05)	0.9 (SE 0.1)	1.5 (SE 0.1)	1.8 (SE 0.3)	2.6 (SE 0.4)	0.5 (SE 0.04)	0.16
Inulin	0.32 (SE 0.04)	0.63 (SE 0.04)	1.1 (SE 0.2)	1.5 (SE 0.2)	1.8 (SE 0.3)	0.38 (SE 0.02)	0.20
						Mean	0.19

Abbreviations: SE, standard error.

Table 3 Percutaneous Absorption Parameters of the Tested Compounds

Compound	Log *p* octanol/water[a]	K[b]	Q_{sc}[c] calculated (nmol/cm^2)	Q_{sc} measured (nmol/cm^2)	Steady-state flux (J_s) (nmol/cm^2/hr)	
					Predicted from Eq. (8)	Measured
Benzoic acid	1.87	0.30	8.77	9.07 (SE 0.66)	15.87 (SE 1.15)	16.4 (SE 0.80)
Caffeine	−0.07	0.14	6.46	5.92 (SE 0.46)	10.36 (SE 0.80)	10.2 (SE 0.60)
Thiourea	−1.02	0.066	3.86	3.34 (SE 0.2)	5.85 (SE 0.35)	3.5 (SE 0.20)
Hydrocortisone	1.61	0.077	0.52	2.36 (SE 0.09)	4.1 (SE 0.16)	0.5 (SE 0.04)
Inulin	−3.58	0.078	0.46	0.85 (SE 0.12)	1.49 (SE 0.20)	0.38 (SE 0.02)

Note: C_0 = solute concentration within the vehicles, taking into account vehicle evaporation (Fig. 4): benzoic acid, thiourea, inulin = 4.5×10^4 nmol/cm^3; hydrocortisone = 5.2×10^4 nmol/cm^3; caffeine = 7.1×10^4 nmol/cm^3.

[a]From Ref. 12.

[b]Partition coefficient calculated from Equation (5) [h = 13 μm; L = 11 minutes; C_0 (see Note)].

[c]Q_{sc} calculated from Equation (6) [h = 13 μm, K = calculated from Eq. (5), (C_0 (see Note)].

Abbreviations: SE, standard error.

solute distribution within the membrane remains constant. This implies that the solute concentration in the outermost layer of the membrane has to remain constant throughout the entire experiment (infinite dose condition), and that the solute concentration in the innermost layer of the membrane has to remain constant and be negligible (sink condition).

As shown in Figure 4, the amount of the vehicle applied (20 $\mu L/cm^2$) changes only during the first hour of administration. Then it remains constant throughout the time of percutaneous absorption measurements one to five hours. In the case of the most penetrating compound (benzoic acid), the amount that penetrated after five hours of application (78 nmol) was far below the amount applied (1000 nmol). It can therefore be assumed that the solute concentration in the vehicle remained relatively constant between one and five hours. Experimentally, we can consider that the first condition is met.

It can be assumed that the epidermis and the uppermost part of the papillary layer of the dermis constitute a negligible barrier in comparison with the SC (13), and the microvascularization of the dermal papillae prevents solute accumulation in the region of the capillaries. Thus, the solute concentration in the innermost layer of the SC can be considered to be negligible in comparison with the concentration in the outermost layer. Hence, the sink condition is apparently fulfilled.

Although the existence of a steady-state flux of penetration in vivo was predicted about 20 years ago by Tregear (14) and subsequently by others (8,15,16), the problem is still the subject of debate (17,18). Our results clearly demonstrate

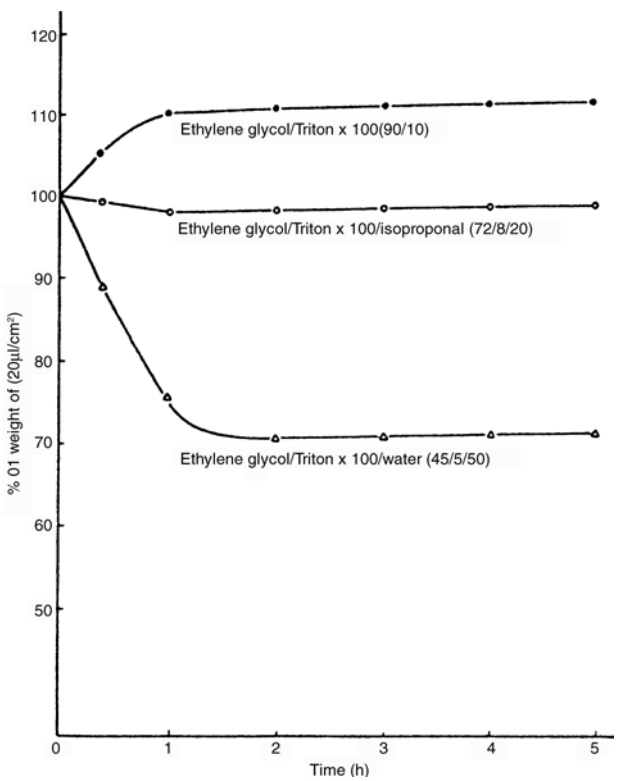


Figure 4 Modification of the vehicles during their administration (20 $\mu L/cm^2$, room temperature 27°C).

(Fig. 3) that a constant flux can be achieved in vivo just as in vitro experiments. Although this seems to be quite logical in our view, this is the first time that it has been demonstrated experimentally. Our results thus fill a gap in the understanding of the mechanisms governing in vivo percutaneous absorption. It should, however, be emphasized that the existence of such a gap is in no way due to negligence on the part of investigators in the field, but rather to the technical difficulties of measuring a steady-state flux of penetration in vivo.

Our results show (Fig. 3 and Table 2) that lag times for the different molecules tested are very close and extremely short. One explanation is that the vehicles used alter the SC and therefore modify the barrier to penetration. However, Table 4 clearly shows that TEWL is not affected by vehicle treatment, whereas removing the SC by 10 successive strippings increases TEWL by a factor of 18.

It is therefore possible to consider that, until the contrary is demonstrated experimentally, such a situation may exist in vivo, even if it upsets some theories that have been built upon in vitro studies. It is important to emphasize that such observations have rarely been made in vitro, perhaps because sink conditions are not necessarily met in vitro. In a dynamic in vitro system, a concentration close to zero in the medium bathing the tissue does not necessarily imply that the concentration in the innermost layer of the membrane is constant with time (13). It is not unusual to observe an increase in the concentration of solute with time in the innermost layers of the epidermis or dermis, depending on the in vitro model adopter (13–20). This increase may be linked either to incomplete resorption by the bathing fluid (21–24) or to a possible affinity of the molecule for these structures (25).

On the basis of knowledge concerning the thickness of the SC ($h = 13 + 2\,\mu m$) and the value for the mean lag time ($L = 11$ minutes), it is possible to deduce a mean value for the apparent diffusion coefficient (D_m) by using Equation (4): $D_m = 4.3 \times 10^{-10}$ cm^2/sec. This does not mean that the values of the diffusion coefficients for molecules having physicochemical properties as different as those used in this study are identical. It means that it is impossible to control, with the required degree of precision, all the physical, physicochemical, and biological parameters likely to affect diffusion through a membrane as complex as the SC. From a purely practical point of view, it is thus possible, as a first approximation, to consider different molecules as having the same apparent diffusion coefficient in the case of percutaneous absorption in vivo. On the other hand, it is reasonable to ask whether this coefficient may vary as a function of parameters such as animal species, anatomical site, age, etc.

Table 4 Effect of the Applied Vehicles on the Barrier Function of the Stratum Corneum (Transepidermal Water Loss)

Ethylene glycol/ Triton XI00 (90/10) (g/m^2/hr)	Ethylene glycol/ Triton XI00/water (45/5/50) (g/m^2/hr)	Ethylene glycol/ Triton XI00/ isopropanol (72/8/20) (g/m^2/hr)	Stratum corneum removed (10 strippings) (g/m^2/hr)
5.8 (SE 0.3)	5.7 (0.4)	5.6 (0.3)	91 (3.0)
Controls:			
5.1 (SE 0.3)	5.3 (0.4)	5.1 (0.3)	5.1 (0.3)

Abbreviations: SE, standard error.

It follows from Equations (3) and (4) that the flux at equilibrium can be written in the form:

$$J_s = \frac{1}{6} K c_o \frac{h}{L} \tag{5}$$

As we have shown earlier, the values of the lag times for the five molecules are similar. This results in the apparent "velocity of diffusion," defined by the ratio h/L, being independent of the nature of the diffusion substance for a given thickness of the horny layer and a given anatomical site. Only the number of molecules in transit (Kc_o) would be characteristic for a given substance and would determine the value of its flux at equilibrium. Since, for a given compound, the value of c_o may be considered to be constant within the time of percutaneous absorption measurements one to five hours, the value of this flux would depend only on the SC/vehicle partition coefficient (K).

Using Equation (5) and the values of flux (J_S) determined experimentally (Table 3) we have calculated the values of K for each of the five molecules (Table 3) taking into account in the C_o values the evaporation of the vehicles (Fig. 4). The values for the octanol/water partition coefficients (log P) reported in the literature for these five molecules (26) are also shown in Table 3. It appears that no relationship exists between these values and the values for flux at equilibrium. Although many examples appear to support the use of log P for predicting the degree of penetration of a molecule (27,28), there are many others that show the limitations of such a procedure (29–32). The partition coefficient of a given compound between two solvents can be considered as a constant physical property of that compound. It is now generally accepted that the percutaneous absorption of a compound can vary considerably as a function of the conditions of administration (vehicle, dose, anatomical site, animal species, etc.). This raises the question: How is it possible to predict the value of a variable parameter only from a constant? Thus, in agreement with Scheuplein (33), we consider that, at present, no solvent system is capable of simulating the extreme complexity of the SC. Only the measurement of the partition coefficient between the SC and the vehicle can be representative of reality.

The amount of substance present in the SC at equilibrium (Q_{sc}) can be measured. According to the model adopted, this quantity is related to the partition coefficient by the equation:

$$Q_{sc} = \frac{1}{2} K c_o \tag{6}$$

As shown in Table 3 and Figure 5, there exists a very good agreement between the values of Q_{sc} measured by stripping the treated area after 30 minutes and the values of Q_{sc} calculated from Equation (6) (c_o values take into account vehicle evaporation).

In light of Equations (5) and (6), the flux at equilibrium can be written:

$$J_s = \frac{Q_{sc}}{3L} \tag{7}$$

Since the lag times of the molecules under study are similar, the fluxes at equilibrium would be expected to depend only on the amount present in the SC.

According to the theoretical model adopted, using Equation (7) and a mean lag time of 0.19 hour, the theoretical relationship between J_S and Q_{sc} should be:

$$J_s = 1.75 Q_{sc} \tag{8}$$

(J_s being expressed in nmol/cm^2/hr). As shown in Figure 6, the curve derived from Equation (8) is contained within the 5% confidence limits of the experimental values.

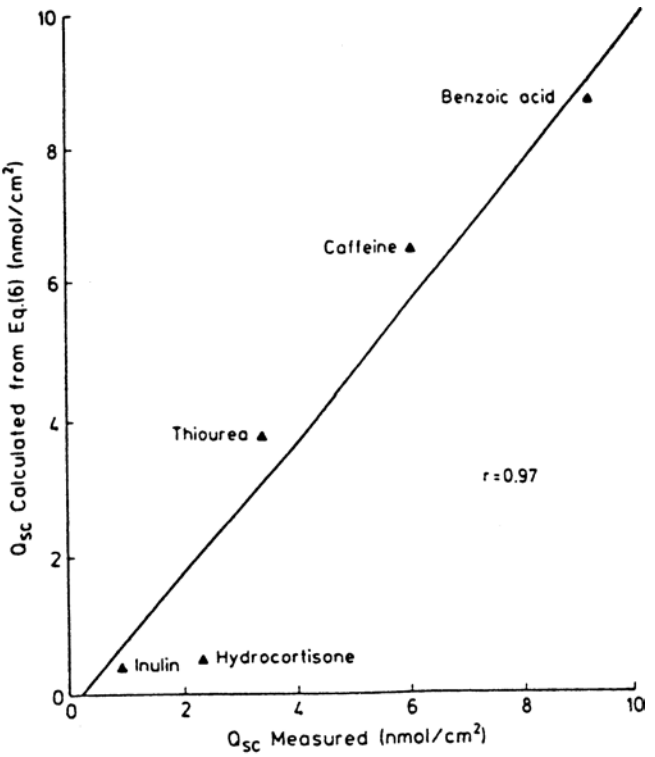


Figure 5 Relationship between the quantity of chemical within the stratum corneum measured after 30 minutes of contact and predicted using Equation (6).

In view of the approximations made in the theoretical model and the inevitable errors arising from the inaccuracies of the measurements and biological variation, we can consider that there exists a very satisfactory agreement between experimental values and theory as in Equation (8). Only hydrocortisone does not appear to fit well with the theoretical linear relationship linking steady-state flux of penetration (J_s) and amount in the SC (Q_{sc}). This is not really surprising, since steroids are known to form a depot or reservoir within the SC (34,35). A fraction of the available molecules may bind to the keratin or other tissue components, while the remainder diffuses slowly downward.

Six years after the development of the stripping method (5–10), the results obtained provide a better understanding of why it is possible to predict the total penetration during four days of a substance administered for 30 minutes with satisfactory precision. As shown in Table 3, from a purely practical point of view, the flux of penetration at equilibrium of a substance administered in vivo in a given vehicle can be predicted using Equation (8) from the simple measurement of the amount present in the SC (Q_{sc}) after a contact time of 30 minutes. Since the validity of the stripping method has been verified for many molecules administered under different conditions in different species, it is reasonable to think that it would also hold for the predictive assessment of the in vivo steady-state flux of penetration.

Using an original experimental approach we have obtained data leading to a better understanding of the mechanisms implicated in molecular transport across

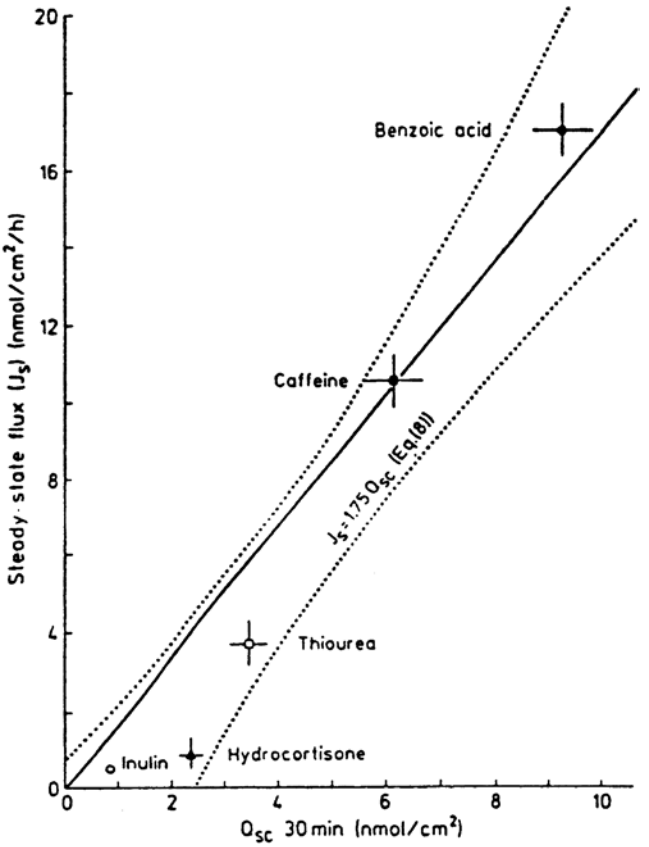


Figure 6 In vivo relationship between steady-state flux of penetration (J_s) and quantity of solute within the stratum corneum after 30 minutes of contact.

the SC in vivo. Thus, it appears that the SC/vehicle partitioning plays a determining role in the percutaneous absorption of chemicals in vivo.

We can easily conceive that our results, especially those related to lag times and diffusion coefficients, may not be readily accepted. The strength of the data presented lies in the fact that they are experimental. To reason only in terms of in vitro data would be to admit from the outset that there are no differences between the in vitro and in vivo processes of percutaneous absorption. However, considering the theoretical importance of these results, it would be important to see them verified using other chemicals of widely different physicochemical properties. It would also be interesting to ascertain that the theory we have developed concerning the in vivo mechanism of percutaneous absorption is verified when the same chemical is dissolved in different vehicles.

ACKNOWLEDGMENTS

The author thanks Dr. C. Berrebi for her expertise in the histometric measurements, and A. M. Cabaillot, C. Patouillet, and M. Zanini for their excellent technical assistance.

REFERENCES

1. Malkinson FD. Studies on percutaneous absorption of ^{14}C labeled steroids by use of the gas-flow cell. J Invest Dermatol 1958; 31:19–28.
2. Marzulli FN. Barrier to skin penetration. J Invest Dermatol 1962; 39:387–393.
3. Stoughton RB. Penetration absorption. Toxicol Appl Pharmacol 1965; 7(suppl 2):1–6.
4. Vinson LJ, Singer EJ, Koehler WR, Lehmann MD, Masurat T. The nature of the epidermal barrier and some factors influencing skin permeability. Toxicol Appl Pharmacol 1965; 7:7–19.
5. Rougier A, Dupuis D, Lotte C, Roguet R, Schaefer H. Correlation between stratum corneum reservoir function and percutaneous absorption. J Invest Dermatol 1983; 81: 275–278.
6. Dupuis D, Rougier A, Roguet R, Lotte C, Kalopissis G. In vivo relationship between horny layer reservoir effect and percutaneous absorption in human and rat. J Invest Dermatol 1984; 82:353–356.
7. Dupuis D, Rougier A, Roguet R, Lotte C. The measurement of the stratum corneum reservoir: a simple method to predict the influence of vehicles on in vivo percutaneous absorption. Br J Dermatol 1986; 115:233–238.
8. Rougier A, Dupuis D, Lotte C. The measurement of the stratum corneum reservoir. A predictive method for in vivo percutaneous absorption studies: influence of the application time. J Invest Dermatol 1985; 84:66–68.
9. Rougier A, Dupuis D, Lotte C, Roguet R, Wester RE, Maibach HI. Regional variation in percutaneous absorption in man: measurement by the stripping method. Arch Dermatol Res 1986; 278:465–469.
10. Rougier A, Lotte C, Maibach HI. In vivo percutaneous absorption of some organic compounds related to anatomic site in man. J Pharmacol Sci 1987; 76:451–454.
11. McKenzie IC. A simple method of orientation and storage of specimens for cryomicrotomy. J Periodont Res 1975; 10:49–50.
12. Zatz JL. Influence of depletion on percutaneous absorption characteristics. J Soc Cosmet Chem 1985; 36:237–249.
13. Schaefer H, Zesch A, Stuttgen G. Skin Permeability. New York: Springer, 1982:607–616.
14. Tregear RT. The permeability of mammalian skin to ions. J Invest Dermatol 1966; 46:16–22.
15. Arita T, Hori R, Anmo T, Washitake M, Akatsu M, Yasima T. Studies on percutaneous absorption of drugs. Chem Pharm Bull 1970; 18:1045–1049.
16. Wepierre J, Corroler M, Didry JR. Distribution and dissociation of benzoyl peroxide in cutaneous tissues after application on skin in the hairless rat. Int J Cosmet Sci 1986; 8: 97–104.
17. Guy R, Hadgraft J. Mathematical models of percutaneous absorption. In: Bronaugh RL, Maibach HI, eds. Percutaneous Absorption. New York: Marcel Dekker, 1985:3–15.
18. Tojo K, Lee AE-RI. A method for predicting steady-state rate of skin penetration in vivo. J Invest Dermatol 1989; 92:105–108.
19. Loden M. The in vivo permeability of human skin to benzene, ethylene glycol, formaldehyde and *n*-hexane. Acta Pharmacol Toxicol 1986; 58:382–389.
20. Zesch A, Schaefer H. Penetration of radioactive hydrocortisone in human skin for various ointment bases. II. In vivo experiments. Arch Dermatol Forsch 1975; 252:245–256.
21. Bronaugh RL. Determination of percutaneous absorption by in vivo techniques. In: Bronaugh RL, Maibach HI, eds. Percutaneous Absorption. New York: Marcel Dekker, 1985:267–279.
22. Bronaugh RL, Stewart RF. Methods for in vitro percutaneous absorption studies. III. Hydrophobic compounds. J Pharm Sci 1984; 73:1255–1258.
23. Bronaugh RL, Stewart RF. Methods for in vitro percutaneous absorption studies. VI. Preparation the barrier layer. J Pharm Sci 1986; 75:487–491.

24. Scott RC. Percutaneous absorption in vivo-in vitro comparisons. In: Shroot B, Schaefer H, eds. Pharmacology of the Skin. Basel: Karger, 1987:103–110.
25. Miselnicky SR, Lichtin JL, Sakr A, Bronaugh RL. The influence of solubility, protein binding and percutaneous absorption on reservoir formation in skin. J Soc Cosmet Chem 1988; 39:169–177.
26. Hansch C, Leo AJ. Log *P* Data Base., Pomona, CA: Pomona College Medical Chemistry Project, 1984.
27. Blank HI, Scheuplein RJ. Transport into within the skin. Br J Dermatol 1969; 81(suppl 4): 4–10.
28. Scheuplein RJ, Blank HI. Mechanism of percutaneous absorption. IV. Penetration of non-electrolytes (alcohols) from aqueous solution and from pure liquids. J Invest Dermatol 1973; 60:286–296.
29. Bronaugh RL. (1985) Determination of percutaneous absorption by in vivo techniques. In: Bronaugh RL, Ackerman C, Flynn GL, eds. Ether-Water Partitioning and Permeability through nude Mouse Skin In Vitro. I. Urea, thiourea, glycerol and glucose. Int J Pharmacol 1987; 36:61–66.
30. Blank HI, Scheuplein RJ, McFarlane DJ. Mechanism of percutaneous absorption. II. The effect of temperature on the transport of non-electrolytes across the skin. J Invest Dermatol 1967; 49:582–589.
31. Poulsen BJ, Flynn GL. In vitro methods used to study dermal delivery and percutaneous absorption. In: Bronaugh RL, Maibach HI, eds. Percutaneous Absorption. New York: Marcel Dekker, 1985:431–459.
32. Scheuplein RJ, Blank HI, Branner GJ, McFarlane DJ. Percutaneous absorption of steroids. J Invest Dermatol 1969; 52:63–70.
33. Scheuplein RJ. Mechanism of percutaneous absorption. I Routes of penetration and the influence of solubility. J Invest Dermatol 1965; 45:334–346.
34. Barry BW. Dermatological formulations percutaneous absorption. In: Swarbrick J, ed. Drug and Pharmaceutical Sciences. Vol 18. New York: Marcel Dekker, 1983:49–54.
35. Malkinson FD, Ferguson EH. Preliminary and short report. Percutaneous absorption of hydrocortisone 4 C in two human subjects. J Invest Dermatol 1955; 25:281–283.

9

Protein Allergens: Skin as a Route of Exposure

Camilla K. Pease and David A. Basketter
SEAC, Unilever Colworth Laboratory, Sharnbrook, Bedford, U.K.

Ian R. White
St. John's Institute of Dermatology, St. Thomas' Hospital, London, U.K.

I. SUMMARY

Clinical conditions, such as protein contact dermatitis and immunologic contact urticaria, occur following protein contact with the skin. Yet it has long been assumed that macromolecular compounds cannot penetrate the skin barrier. In this chapter, we review the clinical, in vivo, and in vitro evidence that proteinaceous materials can penetrate skin. However, it is concluded that while penetration of intact proteins through normal skin is extremely low and normally without consequence, it is when the skin is damaged or compromised in some way that penetration of macromolecules may occur. As a result, risk assessment for contact of protein with skin must take into account potential barrier impairment and thus the possibility of both the induction and the elicitation of allergic skin reactions.

II. INTRODUCTION

Our skin, or more precisely the compact layer of keratin-rich corneocytes that comprises the outer horny layer (stratum corneum), acts as an important primary barrier to exogenous compounds. However, a normal healthy stratum corneum barrier is not totally impenetrable and many topically applied, low molecular weight, moderately lipophilic compounds have been demonstrated to readily penetrate the skin in vivo and in vitro (1). In contrast, ionized compounds do not penetrate the predominantly lipophilic stratum corneum particularly easily. In addition, it is generally considered that there is a molecular weight cutoff involved in the permeability of healthy skin and it has been suggested that a compound must be less than about 500 Da to penetrate the stratum corneum (2). This viewpoint can be challenged, however, as cases of cutaneous reactions arise in humans following skin contact with proteinaceous substances. Although it remains unclear whether human skin

contact with proteins can induce sensitization, predictive rodent sensitization and allergenicity tests with proteinaceous test materials yield positive results. In order to induce these forms of skin toxicity, either the protein or a smaller toxic moiety derived from the substance must penetrate or bypass the stratum corneum and enter the viable epidermis. Here we discuss the evidence for skin penetration of macromolecules > 500 Da and the potential for proteases, present within the stratum corneum or skin microflora, to break down proteins that come into contact with the skin into smaller, possibly more easily penetrating, but still potentially antigenic moieties. An improved understanding of this area is of importance to risk assessment for proteinaceous materials that may come into repeated contact with the skin.

III. DISEASE STATES INVOLVING PROTEIN ABSORPTION IN SKIN

The discussion that follows is intended to exemplify potential evidence for protein absorption through human skin rather than provide an exhaustive review of the literature. A detailed discussion of atopic dermatitis has been deliberately avoided, not because it is unimportant, but rather to aid clarity; it is our view that the somewhat contentious role of skin contact with proteins in atopic dermatitis would only complicate discussion without adding significantly to the scientific considerations herein.

A. Protein Contact Dermatitis and Contact Urticaria

The term "protein contact dermatitis" was introduced by Hjorth and Roed-Petersen (3) to describe a distinct type of chronic recurrent occupational dermatitis (not urticaria) observed in Danish food handlers. The condition resulted from either simultaneous type I (IgE-mediated) immediate and type IV (T-cell-mediated) delayed sensitivities or type I sensitivity alone, following contact with certain foods (Table 1). Contact urticaria is an immediate wheal-and-flare reaction that can result from either IgE-mediated immunologic contact urticaria (reviewed in Section IV) or nonimmunologic mechanisms (4). Foods that can produce either protein contact dermatitis or contact urticaria include raw fish (and other seafoods), meats, egg, peanut, flour, milk, cheese, fruits, and vegetables (5). Contact with other substances [e.g., birch pollen allergen, natural rubber latex proteins, and industrial enzymes, such as those used in the detergent (subtilisins and cellulases) and baking (amylases) industries (6)] is also known to cause protein contact dermatitis or urticaria (Table 1). In order to cause these conditions, the allergen must be able to penetrate or bypass the stratum corneum and enter the epidermis/dermis. Once the allergen has been absorbed into the skin, it is considered that IgE bound to the skin's unique antigen presenting cell, the Langerhans' cell, possibly mediates the development of protein contact dermatitis (7,8).

In the clinic, prick or scratch tests (which allow antigen to bypass the stratum corneum) yield strong wheal-and-flare reactions immediately (within 20 minutes) following exposure to a causative agent in a sensitized individual. Specific IgE antibodies to the allergen can usually (but not always) be detected in the blood of affected individuals [e.g., using the radioallergosorbent test (9)]. Standard patch tests (requiring penetration of the allergen through the stratum corneum) to the proteinaceous materials are frequently negative. This suggests that larger molecules cannot penetrate the stratum corneum of normal, healthy skin. However, positive reactions

Table 1 Examples of Proteinaceous Substances that Can Cause Dermatitis and Urticaria Following Human Skin Contact

Substance	Mol wt (kDa)
Foods	
Egg (albumin)	~45
Raw fish	—
Milk (casein)	~25
Cheese	—
Peanut (lectin)	~29
Meat	—
Wheat/flour (α-amylase)	~45
Plant proteins	
Birch pollen allergen	18
Ragweed pollen	—
Natural rubber latex proteins	
Heveins	
Hev b1 (insoluble)	14.6
Hev b2 (soluble)	34–41.3
Hev b3 (insoluble)	23–27
Hev b4 (soluble)	50–75
Hev b5 (soluble)	16
Hev b6.01 (soluble)	20
Hev b6.02 (soluble)	4.7
Hev b7 (soluble)	46
Hev b8 (soluble)	14
Hev b9 (soluble)	51
Other classes/enzymes	
Cellulases	
Glucoamylases	
Papains	
Subtilisins (proteases)	
Xylanases	

can be generated in specially developed types of patch testing in atopic individuals, such as the infant (age < 4 years) skin application food test (SAFT) (10) or "rub tests" where the allergen is applied with friction (11), in whom skin barrier function may be disrupted or compromised. With many of the proteinaceous substances, careful differential diagnosis is required to eliminate the possibility of the dermatitis arising from contact with a low molecular weight compound.

Interestingly, in recent years the "atopy patch test" has been proposed (12,13). In this method, extracts of materials containing suspect protein allergens of interest are applied to the normal back skin of individuals with atopic dermatitis. The patches are left in place for 48 hours in order to determine whether delayed reactions to the proteins are present. While the procedure is still largely experimental and the results sometimes are of questionable relevance, the very fact that positive reactions do occur suggests that protein antigens of some sort do penetrate into the skin, at least under occlusive conditions.

However, a vital question is by what route individuals diagnosed with protein contact dermatitis have absorbed proteinaceous material so as to cause the production of specific IgE antibodies. They may come into frequent or prolonged skin contact

with a proteinaceous substance, and it seems likely that a defective skin barrier function, present, for example, as a result of atopy, an inflammatory skin condition, skin abrasion and/or irritative mechanisms, etc., may favor the development of protein contact dermatitis or contact urticaria. Certainly, evidence for this comes from studies on protein hydrolysates (derived from collagens, keratins, wheat, milk, silk, etc.) in hair conditioners. Patch tests to 22 different types of protein hydrolysates (5% dose) were negative in 11 hairdressers who were suffering from hand dermatitis (14). Only one of these hairdressers, already suffering from hand dermatitis, had a positive prick test to Crotein Q (hydroxypropyl trimonium hydrolyzed collagen) and suffered from contact urticaria. Of 2160 patients with respiratory symptoms (from an undefined cause), only 10 individuals exhibited a positive prick/scratch test to Crotein Q and none of these suffered from any clinical skin symptoms. However, two adults, already suffering from chronic atopic dermatitis and hence probable reduced skin barrier function, also had contact urticaria resulting from hydrolysate contact. This suggests that preexisting skin damage plays a role in protein contact dermatitis and contact urticaria in humans. Nevertheless, there is evidence that allergy to protein hydrolysates is very low, despite extensive exposure (15).

B. Latex Allergy

Natural rubber latex proteins are present in latex gloves and other devices and are now an important cause of type I allergy and contact urticaria "syndrome" in humans (9). The cornstarch powder on medical gloves adsorbs latex proteins and transfers them to the skin (16) and airways (when aerosolized) of the user (17). Contact of natural rubber latex-catheters and gloves directly with internal organs during surgery has led to anaphylactic shock (18,19).

Issues surrounding latex allergy have been extensively reviewed (17,20,21). The routes of exposure to natural rubber latex proteins through which individuals become sensitized are unknown, although it is known that certain groups are at greater risk of developing latex protein allergy through increased exposure. In health care workers, the use of powdered gloves, which generate aerosolized allergens, has been linked with increased latex allergic responses (22), and many afflicted individuals have had preexisting skin lesions or dermatitis (23). Increased hydration and irritation of the occluded skin with excessive glove use and hand washing may also exacerbate skin conditions. Provocation tests, where dermatitis sufferers applied skin protection cream to one hand and none to the other, suggest that the use of skin protection creams may favor the uptake of allergens from gloves into the skin, thus increasing allergic reactions and not decreasing them as intended by their use (24).

C. Skin Conditions and Enzymes

Enzymes have a low order of general toxicity, the main safety concern is the generation of IgE-mediated respiratory allergy. Historically, there is ample evidence of the capacity of enzymes to give rise to allergic asthma (25,26). Although these cases of asthma arose through excessive occupational exposure, the protease enzymes involved only gave rise to skin irritation, not skin allergy, even though, via diagnosis of the asthma, there was clear evidence of enzyme-specific IgE (26). Incidences of allergic skin reactions to enzymes have been reported in certain susceptible individuals in an occupational setting (26–31). However, the vast majority of

enzyme-related dermatoses are a result of irritancy. Exposure to toxicologically relevant quantities of enzymes is mainly occupational; in final products, such as laundry products, the levels of enzymes are low, ranging from 0.1% to 2% (29–31). Indeed, one very detailed investigation of possible adverse skin reactions to laundry detergents in a large cohort of individuals failed to find any evidence of enzyme allergy (31). Thus, the evidence from this sector suggests that the ability of enzyme proteins to penetrate skin and either induce or elicit allergy is very low.

The safe history of use of enzymes in laundry products has prompted the consideration of use of enzymes in other consumer product applications such as moisturizing skin creams and soaps (to combat dry skin caused by desquamation) and cosmetics (32). Some notable examples of allergic reactions to proteases are from the use of papain in contact lens cleaning solution (33,34). Given the potential for enzymes to cause allergy from cosmetic applications, careful risk assessment for any new topical use scenario of enzymes is vital. For example, one often-overlooked consideration is the potential for the deposition of enzyme on the skin from the use of a leave-on product and its subsequent aerosolization after showering. Inhalation, not penetration through the skin, is the route of exposure in this scenario that could lead to the induction of a specific IgE antibody response (32).

IV. IN VIVO STUDIES SUGGESTING PROTEINS CAN BE ABSORBED THROUGH THE SKIN

In this section, we have documented examples of the evidence from animal studies that shed light on the subject of the skin penetration of proteins. It appears that allergens derived from proteinaceous materials can be absorbed into the skin; standard predictive skin sensitization studies, such as the guinea-pig maximization test (GPMT) (35) often give positive results with proteins. Although the initial sensitization is most often effected by intradermal (ID) injection in the GPMT, thus bypassing the stratum corneum, subsequent induction and challenge by topical application of protein allergens elicits varying strengths of responses with different test materials. Some examples of GPMT data are presented in Table 2. To clarify what these data really mean, we have documented in detail the information available for a common antigenic protein, ovalbumin, and for latex, a protein allergen in recent years recognized as an important cause of immunologic contact urticaria.

A. Ovalbumin

Ovalbumin is a 45 kDa glycoprotein that comprises 60% to 65% of the total protein in egg white (36). It has been shown that in mice, sensitization (i.e., the generation of allergen-specific proliferative responses) to ovalbumin (and ragweed or birch extracts) may be effected through skin contact (37). The study was designed to model primary sensitization in atopic skin disease. Hence, Balb/c mice (high IgE responders and considered "atopics" among mice) were used in their study. Test substances were painted on the shaved abdomen skin of the mouse every two days over a two week period. Allergen-specific proliferative responses were only seen in the skin-draining lymph node cells and not in the gut-draining lymph nodes, suggesting that none of the material had been ingested and the skin was the target immunoresponsive organ. Significant IgE responses in the serum of the treated mice were observed indicating that immediate-type allergy had been induced. The authors propose that

Table 2 Guinea-Pig Maximization Test Results for a Range of Proteins/Enzymes Following Topical Induction and Challenge

	Dose				
GPMT data test substance	Induction (inj) (%)	Induction (patch) (%)	Induction (patch) (%)	Challenge (patch) (%)	Outcome
Egg ovalbumin	1	20		5	Strong
	—	50	0.1	25	Weak
Milk glycoproteins	5	50		10	Strong
Cellulase	0.01	5		0.1	Strong
Collagen hydrolysate	5	65		25	Strong
Elastin hydrolysate	10	20		20	Weak

Note: Standard GPMT methods and interpretation as outlined by Magnusson and Kligman (35) were used. These data indicate that for proteins, topical induction requires high doses to achieve a positive response.

allergen-specific primary sensitization has been effected in mice. However, careful analysis of this study is required to correlate the findings to human sensitization in atopic disease, particularly with respect to protein allergen absorption. In mice, the skin is much thinner and may have been abraded upon shaving, hair follicle density is much greater and the mechanisms responsible for IgE production may be very different, than in man. Also, prior to test compound application, an alcoholic solution was applied to the skin, which may have disturbed and dehydrated the normal stratum corneum structure.

Ovalbumin yields different responses in the GPMT depending upon whether the initial induction was effected by ID injection or topical application: With ID induction ovalbumin was a strong sensitizer and with topical induction it was a weak sensitizer (Table 2). This reveals that sensitization is more effective when direct exposure to ovalbumin, bypassing the stratum corneum and epidermis, occurs. However, it also reveals that topical exposure to this allergen can elicit a response, presumably via skin penetration of the immunogenic species. In the murine local lymph node assay (LLNA), topical application of a 25% dose of ovalbumin in saline yielded a positive sensitization response [defined as test/control lymph node cellular proliferation (T/C) ratio >3] on one occasion. This dose was comparable to topical doses in the GPMT. Lower doses in the LLNA were negative. However, when the ovalbumin was intradermally administered, the outcome was a strongly positive reaction (T/C ratios >11) (Table 3).

The ability of ovalbumin to effect histamine release, an indication of type I immunostimulation, has been used to show that ovalbumin can penetrate guinea-pig skin in vitro (39). Guinea pigs were sensitized by subcutaneous injection of a 0.2% solution of ovalbumin. Abdominal/dorsal skin was excised after two weeks and circular samples were placed in diffusion cells incubated at 37°C. Samples were treated with either receptor solution or 10 μg/mL ovalbumin. In seven out of 11 experiments, histamine release in the ovalbumin-treated samples was three fold more than in the receptor solution-treated samples. The authors conclude that ovalbumin must have penetrated the skin for histamine levels to be increased.

Table 3 In Vivo Murine Local Lymph Node Assay (LLNA) Data (Previously Unpublished) for Ovalbumin (Using Standard Methods as Described Previously[a])

	Dose			
	A	B	C	D
Ovalbumin (μL)	25	25	10	25
Vehicle	Topical saline	Topical saline	Intradermal saline	Topical 6% acetone and saline
Concentration (%)	T/C	T/C	T/C	T/C
5	1.6	1.1	11.9	1.3
10	2.1	1.5	12.1	1.9
25	3.6	1.4	16.2	2.2

Note: In studies A–C, ovalbumin was tested aqt concentrations of 5% to 25% in saline. In D, the same concentrations were tested using 6% acetone and saline as the vehicle. Mice in studies A, B, and D were dosed topically, and in study C mice were dosed intradermally. A value for T/C of >3 indicates that the test material is a sensitizer.
[a]From Ref. 38.
Abbreviations: T/C, test/control lymph node cellular proliferation.

B. Latex Proteins

Differences in IgE responsiveness to latex allergens have been observed in BALB/c mice ($n = 5$) depending upon sensitization route (40). Mice were exposed to nonammoniated latex proteins (NAL) either by subcutaneous, topical, intranasal, or intratracheal routes. The skin of the mice treated topically for five days/week with 50 μg NAL was either abraded by tape stripping or nonabraded. After 23 days, levels of IgE in mice with abraded skin became significantly higher than in vehicle control animals. In mice with nonabraded skin, IgE levels did not rise higher than levels in vehicle control animals. These data suggest that skin barrier disruption is necessary to effect type I immunostimulation topically. Indeed, hand dermatitis has been proposed to be a risk factor in latex allergy (41).

In addition to this difference in the level of IgE production, the allergen specificity profiles were different. Immunoblots of IgE from subcutaneously sensitized mice showed recognition of latex proteins of molecular weights ~14 and ~27 kDa (similar to Hev b1/Hev b8 and Hev b3). A high percentage of spina bifida patients exposed to latex gloves and cathethers during surgery develop IgE to Hev b1 and Hev b3 allergens. In contrast, immunoblots of IgE following topical (abraded skin) sensitization showed recognition of latex proteins ~14, 35, and 92 kDa (similar to Hev b1/Hev b8, Hev b2, and Hev b4, commonly recognized in health care workers). These differences in IgE profiles suggest that the exposure route leading to type I immunostimulation can determine the primary allergens generated and play a role in the clinical manifestations observed.

In a recent study, where natural rubber latex was repeatedly applied to mouse skin, evidence of the manifestation of protein contact dermatitis as well as immediate type I allergy was observed (42). The mice were shaved with an electric razor and their skin was tape stripped four times to remove the stratum corneum barrier. Epicutaneous sensitization was effected in BALB/c mice by applying 100 μg of natural rubber latex on occlusive patches. Each mouse had a total of three one week

exposures separated by intervals of two weeks. In comparison to control skin (treated with phosphate-buffered saline vehicle), epicutaneous natural rubber latex-sensitized skin was characterized by skin thickening (3.5-fold epidermal thickening and 1.5-fold dermal thickening), mast cell degranulation, and infiltration of inflammatory cells (fourfold increase in eosinophils). It must be noted that concomitant irritant properties of the natural rubber latex in an occlusive setting may also have contributed to the overall inflammation observed. Epicutaneous sensitization but not IP immunization led to significant elevation (20-fold over PBS control) of total serum IgE and latex-specific IgE. In contrast, IP immunization led to the increase in IgG2a levels.

Also, in this study, proinflammatory (IL-1β), Th2 (IL-4), and Th1 (IFN-γ) cytokines and several chemokines were investigated to characterize the inflammatory response within the skin at the mRNA level. Significant increases in IL-1β and IL-4 but not IFN-γ mRNA expression were observed within the skin following epicutaneous sensitization. Significant mRNA induction of the chemokines CCL3, CCL4, CCL2, and CCL11 was also observed. These profiles are indicative of a Th2-type allergic response within the skin, thus indicating that skin exposure to natural rubber latex in gloves (which provide an occlusive environment that could exacerbate damage to the skin) may play a direct role in the development of IgE antibodies and in the development of hand dermatitis. Similar observations and conclusions have also been reported for the epicutaneous application of ovalbumin in BALB/c mouse (43). It should be emphasized that the experimental design in this epicutaneous mouse model requires that the stratum corneum be removed by tape stripping, so these effects would only be true in the context of human exposure if the material could penetrate through damaged skin. Some recent work has also suggested that physical damage to the skin in this model, by scratching with a wire brush, can switch the immune response from a Th2 response to a Th1 response (44).

V. IN VITRO SKIN PENETRATION OF MACROMOLECULES

Given that it has been considered for some time that macromolecules cannot penetrate human skin, there have been few in vitro studies, as described below, to investigate this phenomenon.

A. Lectins

Lectins are plant and animal glycoproteins that reversibly bind saccharides with some degree of specificity. An in vitro study in human skin has shown the association of fluorescein-labeled peanut lectin (a galactose-specific lectin) with the epidermal granular layer (45). The skin in this study was excised and sectioned prior to incubation with a solution of peanut lectin. This study does not provide evidence that peanut lectin can penetrate intact skin. However, it is of interest in terms of peanut allergy and the skin, in that it indicates that once penetrated, peanut lectin can localize in precise areas of the skin. Such information may provide clues as to why peanut lectin is such a potent allergen, even when an individual comes into skin contact with very low levels (46,47).

B. Latex Protein Penetration

In order to discuss the penetration of latex proteins, it is necessary to understand the nature of the allergenic proteins. During collection of natural rubber latex from the

rubber tree (*Hevea brasiliensis*), the elastomeric material is normally preserved with ammonia. This ammonia treatment decreases the homogeneity of latex proteins and generates new antigenic determinants, with respect to NALs. It has been suggested that during ammoniation, protein modification occurs and newly generated polypeptides, which remain in the liquid suspension of rubber used to manufacture products, may be responsible for the observed allergy (48). Of the approximately 240 polypeptides in natural rubber latex, approximately 60 have been reported to be antigenic (49,50). Nine protein antigens (heveins, named Hev b1–b9) have been registered by the World Health Organization—International Union of Immunological Societies' Allergen Nomenclature Subcommittee (Table 1). Of these proteins, the 43 amino acid (4.7 kDa) chitin-binding protein hevein (Hev b6.02) is the predominant soluble protein in natural rubber latex (~70% of the total glove allergen) (51). Hevein derives from the posttranslational modification of its preproprotein (prohevein, Hev b6.01), a 20 kDa cysteine-rich protein. Protein processing results in hevein, an N-terminal fragment, and other cleavage peptides (52). Some latex proteins have homology to plant enzymes (e.g., endo-1,3-β-glucosidase, triose-phosphate isomerase, and superoxide dismutase) and some act as lysozyme/chitinases. Cow's milk casein, added to latex as a stabilizer, has also been suspected as a hidden allergen in rubber gloves (51). Hence, natural rubber latex is a mixture of potentially allergenic proteins, ranging in molecular weight from 4.7 to 75 kDa.

A recent 24-hour in vitro study (53) using excised dermatomed human and hairless guinea-pig skin has shown that ammoniated and NALs can penetrate non-abraded skin of both species albeit at low levels (between 0.45% and 0.88% of the applied dose). Levels of proteins remaining within the skin ranged from 0.73% to 1.32% of the applied dose. In comparison, penetration levels of latex proteins through abraded human skin were increased up to 50-fold to a maximum of 23% of the applied dose in receptor fluid. The molecular weights of proteins present in receptor fluid samples, following abraded skin penetration, ranged from 3 to 36 kDa suggesting that there may be a threshold of barrier disruption for the larger latex proteins.

C. Penetration of Other Macromolecules

Much of the information we have to date on protein skin penetration comes from studies aimed at delivering peptides and proteins to the skin as active therapeutics. These studies are evidence in themselves that intact skin acts as a good barrier to proteins as penetration is low, often preventing the delivery of therapeutic doses to the target site. A 1.8 kDa melanotropin analogue only penetrated rat and mouse skin in vitro between 0.05% and 0.08% of the applied dose (54). In both flow-through and static in vitro skin penetration studies, low or undetectable levels of growth hormone releasing factor analogues (3 and 3.9 kDa) were seen to penetrate (55,56). Ogiso et al. (57) observed extremely low penetration levels of the small proteins elcatonin (3.3 kDa) and insulin (5.8 kDa) in in vitro intact rat skin absorption experiments. However, they also observed rapid degradation of these proteins on the dermal side of the viable skin in vitro, and penetration levels were only detectable when protease inhibitors were present in receptor fluid bathing the dermis. From selective inhibition studies, aminopeptidases, endopeptidases, and serine proteases were suspected to be the enzymes in viable skin responsible for the observed degradation.

Studies have been performed using liposome vehicles aiming to increase the skin penetration levels of proteins. Liposomes (ranging from 30 to1000 nm) carrying protein G-gold conjugates predominantly penetrated the skin of guinea pigs by the follicular route (particularly along the hair sheaths) (58). Specially developed ultraflexible "transfersomes," derived from liposomes in the presence of the detergent sodium cholate, have been used to increase the penetration (or "carry") insulin through mouse (with manually trimmed hair) and human skin (59). Transfersomes were also seen to carry the cyclic peptide cyclosporin A into and through mouse skin in vitro (60). The amounts of cyclosporin A found in serum four hours post epicutaneous application in transfersomes, was more than three times greater in mice with shaved skin (~364 ng/mL) than in nonshaved mice (~120 ng/mL).

Such in vitro studies suggest that penetration of proteins through intact skin is too low under normal circumstances to allow therapeutic or toxic levels into the skin. However, an intact stratum corneum barrier can be damaged or compromised (by chemical and physical means) to allow penetration of proteins.

VI. STRATUM CORNEUM STRUCTURE AND BARRIER DISRUPTION

Flynn (61) commented in 1990 that for small molecule penetration, "The intracellular protein (*of the stratum corneum*) is dense and presents such a thermodynamically and kinetically impossible passageway that, for all practical purposes, it is impenetrable. Current dogma says that diffusion is around the platelets by way of the interstitial lipid." It remains likely that intercellular pathways are also the most favorable but still tortuous routes for the penetration of macromolecules through healthy human skin; hence, penetration is normally low. Evidence for this comes from studies on the absorption of dextrans (4–10 kDa peptides) in the presence of the penetration enhancer *n*-octyl-b-d-thioglucoside (OTG) (62). In intact skin, dextran penetration was negligible (flux $J_s = 0.096\,\mu g/cm^2/hr$). In OTG-treated skin, penetration was greatly enhanced (flux $J_s = 27.67\,\mu g/cm^2/hr$). The levels of dextran penetration in OTG-treated skin were similar to those in tape-stripped skin (flux $J_s = 33.88\,\mu g/cm^2/hr$). Electron microscopy revealed that OTG exfoliated the cell membranes and dissociated adherent cornefied cells in the stratum corneum, suggesting that the intercellular cohesive laminae and the barrier functions were destroyed. OTG also solubilized the stratum corneum proteins and extracellular ceramides.

Ceramides are the major lamellar phase-forming lipids of the stratum corneum and are an end product of keratinocyte differentiation. Ceramides are secreted in the extracellular space and act as a mantle around the cornified cells of the stratum corneum (63). Atopic dermatitis patients show reduced levels of ceramides in their nonlesional and lesional skin, in comparison to healthy individuals (64,65). As a result, their skin barrier is impaired and it is feasible that macromolecules may be absorbed into their skin. The levels of production of skin ceramides have been attributable to the balance of enzyme activity involved in sphingolipid synthesis in the outer layers of the skin. One such cutaneous enzyme that is expressed highly in atopic dermatitis patients is sphingomyelin deacylase (66). Ceramidase, which breaks down ceramides and is expressed by *Staphylococcal* bacteria on the skin surface, has also been implicated in reduced ceramide levels in atopic individuals (67).

The stratum corneum (granular cells and intercellular space) also possesses other active enzymes, including serine proteases, trypsin, and chymotrypsin, which can cleave peptides and have been implicated in the desquamation process (68–70).

Table 4 Causes of Reduced Stratum Corneum Barrier Integrity in Normal Skin

Preexisting dermatitis—e.g., irritant, allergic
Physical damage—e.g., burned, shaved, wounded
Chemical damage—e.g., detergents and other penetration enhancers
Increased hydration—e.g., excessive hand washing
Occluded skin—e.g., wearing of gloves

Reduced trypsin activity has been seen in the skin of atopics in comparison to normal healthy skin (69). It is interesting to note that ovalbumin is known to be a member of the serine protease inhibitor family (as a noninhibitory homologue) and is a substrate for serine protease (71,72). A 30 kDa trypsin-like protease in the plantar stratum corneum has also been shown to digest casein (68). It is possible that interactions with stratum corneum enzymes may play a role in ovalbumin- and casein-derived skin allergy.

An endogenous lectin, concanavalin A, has also been isolated from human stratum corneum and is exclusively localized to the membranes of the stratum corneum by immunohistochemistry of intact skin (73). These authors suggest that this endogenous lectin may act as a major carbohydrate-binding protein that cross-links adjacent corneocytes together in the stratum corneum. This begs the question as to whether peanut lectin, upon contacting the skin, can disturb normal endogenous lectin functions during the manifestation of peanut-related allergy?

The potential roles of hair follicles, sebaceous glands, and sweat glands in protein penetration have not been investigated extensively. It is expected that the follicular route may be particularly relevant to the rodent studies described above. In humans, the superficial film of sebum/sweat may act as a vehicle for proteins that land on the skin from aerosols. However, the most likely event that allows penetration of levels of proteins significant enough to cause toxicity is the presence of an already damaged/compromised stratum corneum. Damage to normal, healthy skin can be caused in a number of ways (Table 4).

VII. CONCLUSIONS

The available evidence leads us to conclude that penetration of proteins through the intact stratum corneum of "normal" individuals is very low and normally does not produce clinical effects. However, their penetration through chemically/physically compromised skin (including where such damage is not visible to the naked eye) or possible ceramide-deficient skin in atopic individuals, is significant enough to cause toxic manifestations such as contact urticaria and allergic contact dermatitis. Since such compromised skin is common in individuals, an evaluation of potentially increased skin penetration of proteins in this sensitive subpopulation should be included in risk assessments for protein allergy. It is our view that whilst protein contact with absolutely normal skin is essentially without consequence, both the induction and the elicitation of allergic responses may arise via contact of proteinaceous materials with compromised skin.

REFERENCES

1. Smith CK, Hotchkiss SAM. Allergic Contact Dermatitis: Chemical and Metabolic Mechanisms. London: Taylor & Francis Ltd, 2000.
2. Bos JD, Meinardi MM. The 500 Dalton rule for the skin penetration of chemical compounds and drugs. Exp Dermatol 2000; 9:165–169.
3. Hjorth N, Roed-Petersen J. Occupational protein contact dermatitis in food handlers. Contact Dermatitis 1976; 2:28–42.
4. Lahti A, Basketter DA. Immediate contact reactions. In: Rycroft RJG, Menné T, Frosch PJ, Lepoittevin J-P, eds. Textbook of Contact Dermatitis. Heidelberg: Springer Verlag, 2001:111–132.
5. Janssens V, Morren M, Dooms Goossens A, DeGreef H. Protein contact-dermatitis—myth or reality. Br J Dermatol 1995; 132:1–6.
6. Kanerva L, Vanhanen M. Occupational protein contact dermatitis from glucoamylase. Contact Dermatitis 1999; 41:171–173.
7. Bruynzeelkoomen C, Vanwichen DF, Toonstra J, Berrens L, Bruynzeel PLB. The presence of IgE molecules on epidermal Langerhans' cells in patients with atopic dermatitis. Arch Dermatol Res 1986; 278:199–205.
8. Turjanmaa K. Allergy to natural rubber latex—a growing problem. Ann Med 1994; 26:297–300.
9. Johanssen SG, Bennich H, Berg T. In vitro diagnosis of atopic allergy. 3. Quantitative estimation of circulating IgE antibodies by the radioallergosorbent test. Int Arch Allergy Appl Immunol 1971; 41:443–451.
10. Oranje AP, Vangysel D, Mulder PGH, Dieges PH. Food-induced contact urticaria syndrome (CUS) in atopic dermatitis—reproducibility of repeated and duplicate testing with a skin provocation test, the skin application food test (SAFT). Contact Dermatitis 1994; 31:314–318.
11. Oranje AP. Skin provocation test (SAFT) based on contact urticaria: a marker of dermal food allergy. Curr Prob Dermatol 1991; 20:228–231.
12. Ring J, Darsow U, Behrendt H. Role of aeroallergens in atopic eczema: proof of concept with the atopy patch test. J Am Acad Dermatol 2001; 45(suppl):S49–S52.
13. Darsow U, Ring J. Airborne and dietary allergens in atopic eczema: a comprehensive review of diagnostic tests. Clin Exp Dermatol 2000; 25:544–551.
14. Niinimaki A, Niinimaki M, Makinen-Kiljunen S, Hannuksela M. Contact urticaria from protein hydrolysates in hair conditioners. Allergy 1998; 53:1078–1082.
15. Mc Fadden JP, Rycroft RJG, White IR, Wakelin SH, Basketter DA. Hydrolyzed protein shampoo additives are not a common contact allergen. Contact Dermatitis 2000; 43:243.
16. Beezhold D, Beck WC. Surgical glove powders bind latex antigens. Arch Surg 1992; 127:1354–1357.
17. Petsonk EL. Couriers of asthma: antigenic proteins in natural rubber latex. Occup Med State Art Rev 2000; 15:421–429.
18. Ebo DG, Stevens WJ, Declerck LS. Latex anaphylaxis. Acta Clin Belg 1995; 50:87–93.
19. Hepner DL. Sudden bronchospasm on intubation: latex anaphylaxis? J Clin Anesth 2000; 12:162–166.
20. Liss GM, Sussman GL. Latex sensitization: occupational versus general population prevalence rates. Am J Ind Med 1999; 35:196–200.
21. Turjanmaa K. Incidence of immediate allergy to latex gloves in hospital personnel. Contact Dermatitis 1987; 17:270–275.
22. Brehler R, Kolling R, Webb M, Wastell C. Glove powder—a risk factor for the development of latex allergy? Eur J Surg 1997; 163:23–25.
23. Boxer M. Hand dermatitis: a risk factor for latex hypersensitivity. J Allergy Clin Immunol 1996; 98:855–856.

24. Baur X, Chen Z, Allmers H, Raulf-Heimsoth M. Results of wearing test with two different latex gloves with and without the use of skin-protection cream. Allergy 1998; 53: 441–444.
25. Flindt MLH. Pulmonary disease due to inhalation of derivatives of *Bacillus subtilis* containing proteolytic enzymes. Lancet 1969; 7:1177–1181.
26. Pepys J, Wells ID, D'Souza MF, Greenberg M. Clinical and immunological responses to enzymes of *Bacillus subtilis* in factory workers and consumers. Clin Allergy 1973; 3: 143–160.
27. Zachariae H, Thomsen K, Rasmussen OG. Occupational enzyme dermatitis. Acta Dermatovener 1973; 53:145–148.
28. Tarvainen K, Kanerva L, Tupasela O, Grenquistnorden B, Jolanki R, Estlander T, Keskinen H. Allergy from cellulase and xylanase enzymes. Clin Exp Allergy 1991; 21: 609–615.
29. Weill H, Waggensp C, Derouen T, Ziskind M. Follow-up observations of workers exposure to enzyme detergents. Ann New York Acad Sci 1974; 221:76–85.
30. Vanhanen M, Tuomi T, Tiikkainen U, Tupasela O, Voutilainen R, Nordman H. Risk of enzyme allergy in the detergent industry. Occup Environ Med 2000; 57:121–125.
31. White IR, Lewis J, Alamni AE. Possible adverse reactions to an enzyme containing washing powder. Contact Dermatitis 1985; 13:175–179.
32. Pocalyko DJ, Chandar P, Harding CR, Blaikie L, Watkinson A, Rawlings AV. The efficacy, stability and safety of topically applied protease in treating xerotic skin. In: Leyden JJ, Rawlings AV, eds. Skin Moisturization. Texas: Culinary & Hospitality Industry Publications Service, 2002:365–384.
33. Berbstein DI, Gallagher JS, Grad M, Bernstein IL. Local ocular anaphylaxis to papain enzyme contained in a contact lens cleaning solution. J Allergy Clin Immunol 1984; 74:258–260.
34. Fisher AA. Allergic reactions to contact lens solutions. Cutis 1985; 36:209–211.
35. Magnusson B, Kligman AM. The identification of contact allergens by animal assay. The guinea-pig maximisation test. J Invest Dermatol 1969; 52:268–276.
36. Warner RC. Egg proteins. In: Neurath H, Bailey K, eds. The Proteins. New York: Academic Press, 1954:435–485.
37. Saloga J, Knop J. Does sensitization through the skin occur?. Allergy 2000; 55:905–909.
38. Kimber I, Mitchell JA, Griffin AC. Development of a murine local lymph node assay for the determination of sensitising potential. Food Chem Toxicol 1986; 24:585–586.
39. Yamamoto S, Kimura I, Numata T, Yamura T. Antigen-induced histamine-release by penetration of egg-albumin antigen through excised guinea-pig skin. Arch Dermatol Res 1981; 271:357–360.
40. Woolhiser MR, Munson AE, Meade BJ. Immunological responses of mice following administration of natural rubber latex proteins by different routes of exposure. Toxicol Sci 2000; 55:343–351.
41. Nettis E, Assennato G, Ferrannini A, Tursi A. Type I allergy to natural rubber latex and type IV allergy to rubber chemicals in health care workers with glove-related skin symptoms. Clin Exp Allergy 2002; 32:441–447.
42. Lehto M, Koivuluhta M, Wang G, Amghaiab I, Majuri M-L, Savolainen K, Turjanmaa K, Wolff H, Reunala T, Lauerma A, Palosuo T, Alenius H. Epicutaneous natural rubber latex sensitisation induces T helper 2-Type dermatitis and strong prohevein-specific IgE response. J Invest Dermatol 2003; 120:633–640.
43. Hsieh K-Y, Tsai C-C, Herbert Wu CH, Lin R-H. Epicutaneous exposure to protein antigen and good allergy. Clin Exp Allergy 2003; 33:1067–1075.
44. Matsushima H, Hayashi S, Shimada S. Skin scratching switches immune responses from Th2 to Th1 type in epicutaneously immunized mice. J Dermatol Sci 2003; 32(3):223–230.
45. Holt PJA, Anglin JH, Nordquist RE. Localization of specific carbohydrate configurations in human skin using fluorescein-labelled lectins. Br J Dermatol 1979; 100:237–245.

46. Cantani A. Allergic reaction to inadvertent peanut contact in a child. Allergy Asthma Proc 1997; 18:323–326.
47. Hourihane JO, Kilburn SA, Nordlee JA, Hefle SL, Taylor SL, Warner JO. An evaluation of the sensitivity of subjects with peanut allergy to very low doses of peanut protein: a randomized, double-blind, placebo-controlled food challenge study. J Allergy Clin Immunol 1997; 100:596–600.
48. Akasawa A, Hsieh LS, Lin Y. Comparison of latex-specific IgE binding among nonammoniated latex, ammoniated latex, and latex glove allergenic extracts by ELISA and immunoblot inhibition. J Allergy Clin Immunol 1996; 97:1116–1120.
49. Kurup VP, Alenius H, Kelly KJ, Castillo L, Fink JN. A two-dimensional electrophoretic analysis of latex peptides reacting with IgE and IgG antibodies from patients with latex allergy. Int Arch Allergy Immunol 1996; 109:58–67.
50. Posch A, Chen ZP, Wheeler C, Dunn MJ, RaulfHeimsoth M, Baur X. Characterization and identification of latex allergens by two-dimensional electrophoresis and protein microsequencing. J Allergy Clin Immunol 1997; 99:385–395.
51. Alenius H, Kalkkinen N, Reunala T, Turjanmaa K, Palosuo T. The main IgE-binding epitope of a major latex allergen, prohevein, is present in its N-terminal 43-amino acid fragment, hevein. J Immunol 1996; 156:1618–1625.
52. Ylitalo L, Makinen-Kiljunen S, Turjanmaa K, Palosuo T, Reunala T. Cow's milk casein, a hidden allergen in natural rubber latex gloves. J Allergy Clin Immunol 1999; 104: 177–180.
53. Hayes BB, Afshari A, Millecchia L, Willard PA, Povoski SP, Meade BJ. Evaluation of percutaneous penetration of natural rubber latex proteins. Toxicol Sci 2000; 56:262–270.
54. Dawson BV, Hadley ME, Kreutzfeld K, Dorr RT, Hruby VJ, Alobeidi F, Don S. Transdermal delivery of a melanotropic peptide-hormone analog. Life Sci 1988; 43:1111–1117.
55. Loden M, Faijerson Y. The synthetic peptide GRF (1-29)-NH2 with growth-hormone releasing activity penetrates human epidermis in vitro. Acta Pharmaceutica Suecica 1988; 25:27–30.
56. Kumar S, Hing C, Patel S, Piemontese D, Iqbal K, Malick AW, Neugroschel LE, Behl CR. Effect of iontophoresis on in vitro skin permeation of an analog of growth-hormone releasing-factor in the hairless guinea-pig model. J Pharm Sci 1992; 81:635–639.
57. Ogiso T, Iwaki M, Tanino T, Nishioka S, Higashi K, Kamo M. In vitro skin penetration and degradation of enkephalin, elcatonin and insulin. Biol Pharm Bull 1997; 20:54–60.
58. Schramlova J, Blazek K, Bartackova M, Otova B, Mardesicova L, Zizkovsky V, Hulinska D. Electron microscopic demonstration of the penetration of liposomes through skin. Folia Biol 1997; 43:165–169.
59. Cevc G, Gebauer D, Stieber J, Schatzlein A, Blume G. Ultraflexible vesicles, transfersomes, have an extremely low pore penetration resistance and transport therapeutic amounts of insulin across the intact mammalian skin. Biochim Biophys Acta Biomembranes 1998; 1368:201–215.
60. Guo J, Ping Q, Sun G, Jiao C. Lecithin vesicular carriers for transdermal delivery of cyclosporin A. Int J Pharm 2000; 194:201–207.
61. Flynn GL. In: Gerrity TR, Henry CJ, eds. Principles of Route-to-Route Extrapolation for Risk Assessment. Amsterdam: Elsevier Science Publishing Co Inc., 1990.
62. Ogiso T, Paku T, Iwaki M, Tanino T. Mechanism of the enhancement effect of *N*-octyl-beta-D-thioglucoside on the transdermal penetration of fluorescein isothiocyanate-labelled dextrans and the molecular weight dependence of water soluble penetrants through stripped skin. J Pharm Sci 1994; 83:1676–1681.
63. Wertz PW, Swartzendruber DC, Abraham W, Madison KC, Downing DT. Essential fatty-acids and epidermal integrity. Arch Dermatol 1987; 123:1381.
64. Imokawa G, Abe A, Jin K, Higaki Y, Kawashima M, Hidano A. Decreased level of ceramides level of ceramides in stratum corneum of atopic dermatitis—an etiologic factor in atopic dry skin. J Invest Dermatol 1991; 96:523–526.

65. Yamamoto A, Serizawa S, Ito M, Sato Y. Startum corneum lipid abnormalities in atopic dermatitis. Arch Dermatol Res 1991; 283:219–223.
66. Hara J, Higuchi K, Okamoto R, Kawashima M, Imokawa G. High-expression of sphingomyelin deacylase is an important determinant of ceramide deficiency leading to barrier disruption in atopic dermatitis. J Invest Dermatol 2000; 115:406–413.
67. Ohnishi Y, Okino N, Ito M, Imayama S. Ceramidase activity in bacterial skin flora as a possible cause of ceramide deficiency in atopic dermatitis. Clin Diag Lab Immunol 1999; 6:101–104.
68. Cui CY, Takahashi M, Tezuka T. 30-kDa trypsin-like proteases in the plantar stratum corneum. J Dermatol 1997; 24:504–509.
69. Redoules D, Tarroux R, Assalit MF, Perie JJ. Characterisation and assay of five enzymatic activities in the stratum corneum using tape-strippings. Skin Pharmacol Appl Skin Physiol 1999; 12:182–192.
70. Ekholm IE, Brattsand M, Egelrud T. Stratum corneum tryptic enzyme in normal epidermis: a missing link in the desquamation process? J Invest Dermatol 2000; 114:56–63.
71. Wright HT. Ovalbumin is an elastase substrate. J Biol Chem 1984; 259:4335–4336.
72. Stein PE, Leslie AGW, Finch JT, Carrell RW. Crystal-structure of uncleaved ovalbumin at 1.95 Å resolution. J Mol Biol 1991; 221:941–959.
73. Brysk MM, Rajaraman S, Penn P, Chen SJ. Endogenous lectin from terminally differentiated epidermal cells. Differentiation 1986; 32:230–237.

10

Percutaneous Absorption of Chemical Mixtures

Jim E. Riviere
Center for Chemical Toxicology, Research, and Pharmacokinetics, College of Veterinary Medicine, North Carolina State University, Raleigh, North Carolina, U.S.A.

I. INTRODUCTION

A primary route of occupational and environmental exposure to toxic chemicals is often through the skin. Although exposure to complex chemical mixtures is the norm, only mechanisms of absorption for single chemicals have been studied and most risk-assessment profiles are based on the behavior of single chemicals. Effects of co-administered chemicals on the rate and extent of absorption of a topically applied systemic toxicant may determine whether toxicity is ever realized.

The application of risk assessment to dermal absorption by U.S. regulatory agencies (Environmental Protection Agency, Occupational Safety and Health Administration, Agency for Toxic Substance and Disease Registry) is varied and highly dependent upon available data (1–3). A similar concern over lack of data exists for overall risk assessment of chemical mixtures (4–7). A congressional Commission of Risk Assessment and Risk Management (8) recommended moving beyond individual chemical assessments and focusing on the broader issues of toxicity of chemical mixtures. Current approaches are based on assigning toxicological equivalent units to similar chemical congeners (e.g., dioxins) or assessing toxicity after exposure to the complete mixture. It is recognized (4) that the dose–response curves of individual mixture components should be characterized, and then a ''no-interaction'' hypothesis for these components in a mixture tested. With complex mixtures of hundreds of components, these approaches become exceedingly complex. Finally, mixture component interactions that involve modulation of a known toxicant's absorption, and thus systemic bioavailability, have not been defined.

This problem is conceptually similar to that of dermatological formulations in the pharmaceutical arena. The primary difference is that most pharmaceutical formulation components are added for a specific purpose relative to the delivery, stability, or activity of the active ingredient. In the environmental and occupational scenarios, additives are a function on either their natural occurrence or presence in a

mixture for a purpose related to uses of that mixture (e.g., a fuel performance additive) and not for their effects on absorption or toxicity of the potential toxicant.

The appreciation of the importance of chemical mixture interactions to effect chemical and drug disposition, pharmacokinetics, and activity has been well recognized for many years and is extensively reviewed elsewhere (4,5,9–13). Despite the widespread knowledge base of the importance of drug–drug interactions and the importance of chemical interactions in systemic pharmacology and toxicology, very little attention outside of the dermatological and transdermal formulation arenas have been paid to interactions that may occur after topical exposure to complex mixtures. The focus of this chapter is to overview the potential mechanisms operative in topical chemical mixtures as well as to illustrate these interactions with data from our laboratory.

II. RISK ASSESSMENT

Dermal risk assessment of individual chemicals is based on knowledge of the permeability characteristics of specific chemicals through skin, with extrapolations being made to potential absorption in humans (14). Numerous contributions in the present text discuss this field. A great deal of emphasis is appropriately placed on calculating potential exposure, with less attention focused on the actual permeability of the exposed compound through skin, which is required to estimate systemic exposure. Collection of this latter data is preferably done in a controlled and validated laboratory animal model, although one could argue that even quality data in a laboratory rodent might not be optimal for predicting human skin absorption due to well-known species differences. Unfortunately, very little human data exist to support these estimates and it is unethical to expose humans to hazardous materials to generate these parameters. When data are not present, extrapolations of potential absorption are made based on physical chemical parameters (e.g., molecular volume and water solubility) or surrogates such as partition coefficient (PC) (concentration ratio between vehicle and membrane) that correlates to permeability of individual chemicals primarily through in vitro skin models. A great deal of effort has been spent on developing these permeability estimates. However, it is evident from a close review of these approaches that the combination of dermal absorption and mixture guidelines has not yet occurred, despite broad acceptance that the skin is a primary route of exposure for many chemicals, and that most chemical exposure occurs in mixtures.

It is impossible to assess all potential combinations of chemicals in order to determine which have the greatest potential to modulate absorption of a known toxic entity topically exposed in a chemical mixture. The present state of knowledge in this area is particularly weak since the significance of specific interactions has not been quantified, let alone in many cases even identified. In many ways, this same concern continues to define the very nature of chemical mixture toxicology (5,9,10,12,13). In cases where the potential toxicity of a specific mixture is of concern (e.g., at a specific toxic waste site), the complete mixture is often tested (15). However, how does one quantitate the absorption of a mixture consisting of 50 chemicals? How are markers selected? How are these data expressed? Unfortunately, even after a complete toxicological profile of a specific mixture (e.g., ''standard'' mixture of 50 environmentally relevant compounds, surrogate jet fuels, etc.) is defined using all the techniques modern toxicology and toxicogenomics has to offer, one cannot define the links between absorption and the effects seen. Could the

observed toxicity be exerted because a specific toxicant was in the mixture, because two synergistic toxicants were absorbed, *or* was it exerted simply by the presence of a mixture component (e.g., alcohol, surfactant, and fatty acid) that enhanced the absorption of a normally minimally absorbed toxicant? In this latter scenario, if the enhancer were not present, absorption would have fallen below the toxicological threshold. We have demonstrated such an interaction with the putative toxins involved in the Gulf War Syndrome, where systemic pyridostigmine bromide or co-exposure to jet fuel was shown to greatly enhance the dermal absorption of topical permethrin (16,17). Would other pesticides be similarly affected? How does one take into account such critical interactions so that a proper risk assessment may be conducted?

One recently reported approach to address this problem assesses potential interactions in dermal absorption by fractionating the effects of a vehicle on drug penetration onto the two primary parameters describing permeation according to Fick's law: partitioning (PC) and diffusivity (D) [see below; permeability (K_p) = D × PC/membrane thickness] (18). Although this study only reported on four compounds, one (diazepam) was not predictable using this approach as its physiochemical properties were already optimal for absorption, and only absorption enhancers were investigated. This study illustrates the difficulty of making broad generalizations across compounds solely on physical chemical properties.

A more inclusive approach to this problem is to define chemicals on the basis of how they would interact with other components of a mixture as well as with the barrier components of the skin. What are the physical–chemical properties that would significantly modify absorption and potentiate systemic exposure to a toxicant? What are the properties of molecules susceptible to such modulation? Unlike pharmaceutical formulation additives in a dermal medication, chemical components of a mixture are not classified by how they could modulate percutaneous absorption of simultaneously exposed topical chemicals. They are either present *functionally* for specific purposes (e.g., performance additives, lubricants, and modulators of some biological activity), *sequentially* because they were applied to the skin independently at different times for unrelated purposes (cosmetic followed by topical insect repellent), *accidentally* because they were disposed of simultaneously as waste, or they are *coincidentally* associated as part of a complex occupational or environmental exposure.

III. MECHANISMS OF INTERACTIONS

Chemical interactions that may modulate dermal absorption can be conveniently classified according to physical location where an interaction may occur. The advantage of this approach is that potential interactions may be defined on the basis of specific mechanisms of action involved as well as by the biological complexity of the experimental model required to detect it.

Surface of skin:

- Chemical–chemical (binding, ion-pair formation, etc.)
- Altered physical–chemical properties (e.g., solubility, volatility, and critical micelle concentration)
- Altered rates of surface evaporation
- Occlusive behavior
- Binding or interaction with adnexial structures or their products (e.g., hair, sweat, and sebum)

Stratum corneum:

- Altered permeability through lipid pathway (e.g., enhancer)
- Altered partitioning into stratum corneum
- Extraction of intercellular lipids

Epidermis:

- Altered biotransformation
- Induction of and/or modulation of inflammatory mediators

Dermis:

- Altered vascular function (direct or secondary to mediator release)

The first and most widely studied area of chemical–chemical interactions is on the surface of the skin. The types of phenomena that could occur are governed by the laws of solution chemistry and include factors such as altered solubility, precipitation, super-saturation, solvation, or volatility, as well as physical–chemical effects such as altered surface tension from the presence of surfactants, changed solution viscosity, and micelle formation (19–22). For some of these effects, chemicals act independent of one another. However, for many the presence of other component chemicals may modulate the effect seen.

Figure 1 illustrates the effects of the surfactant sodium lauryl sulfate (SLS) on the absorption of methyl and ethyl parathion in perfused porcine skin. Despite differences in the overall absorptive flux of both compounds administered in these aqueous vehicles, SLS decreased the absorption of both.

Chemical interactions may further be modulated by interaction with adnexial structures or their products such as hair, sebum, or sweat secretions. The result is

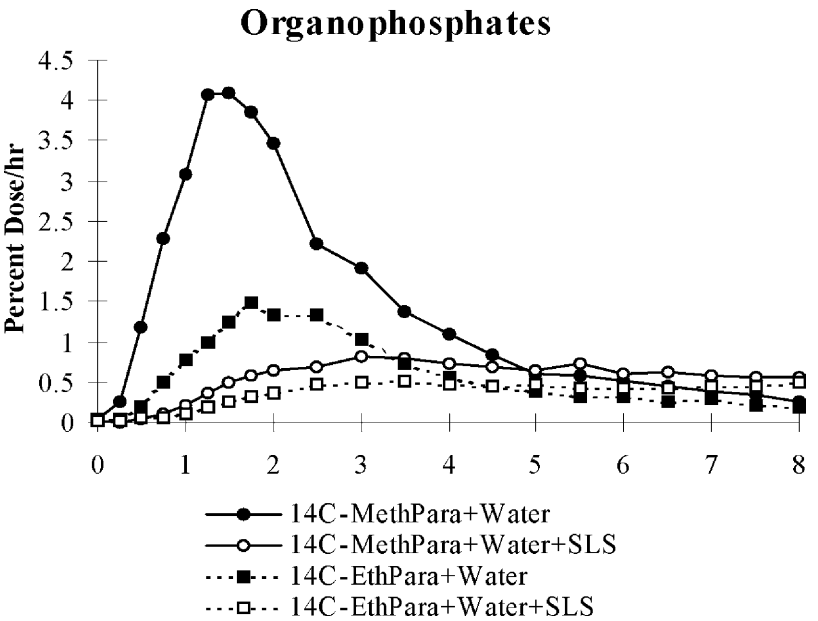


Figure 1 Effect of sodium lauryl sulfate (SLS) on mean absorption profiles of ethyl- and methyl-parathion in isolated perfused porcine skin.

that when a marker chemical is dosed on the skin as a component of a chemical mixture, the amount freely available for subsequent absorption may be significantly affected. The primary driving force for chemical absorption in skin is passive diffusion that requires a concentration gradient of thermodynamically active (free) chemical.

Second levels of potential interaction are those involving the marker and/or component chemicals with the constituents of the stratum corneum. These include the classic enhancers such as oleic acid, Azone or ethanol, widely reviewed elsewhere (22). These chemicals alter a compound's permeability within the intercellular lipids of the stratum corneum. Organic vehicles persisting on the surface of the skin may extract stratum corneum lipids that would alter permeability to the marker chemical (23,24). Compounds may also bind to stratum corneum constituents forming a depot.

The PC between the drug in the surface dosing vehicle and stratum corneum lipids may be altered if chemical components of the mixture also partition and diffuse into the lipids and thus alter their composition. This provides a potential mechanism to assess the effects of a mixture interaction on subsequent absorption. Figure 2 illustrates the PC of pentachlorophenol (PCP) into porcine stratum corneum administered in a series of six mixtures (water, water + ethanol + methyl nicotinate, water + ethanol, water + SLS, ethanol + methyl nicotinate, ethanol). Figure 3 compares PCP absorption in perfused porcine skin dosed in these same mixtures against PC, illustrating that PC determined from the mixture of concern does correlate to absorption across viable skin.

Another level of interaction would be with the viable epidermis. The most obvious point of potential interaction would be with a compound that undergoes biotransformation (25,26). A penetrating chemical and mixture component could interact in a number of ways, including competitive or noncompetitive inhibition for occupancy at the enzyme's active site, or induction or inhibition of drug metabolizing enzymes. Other structural and functional enzymes could also be affected

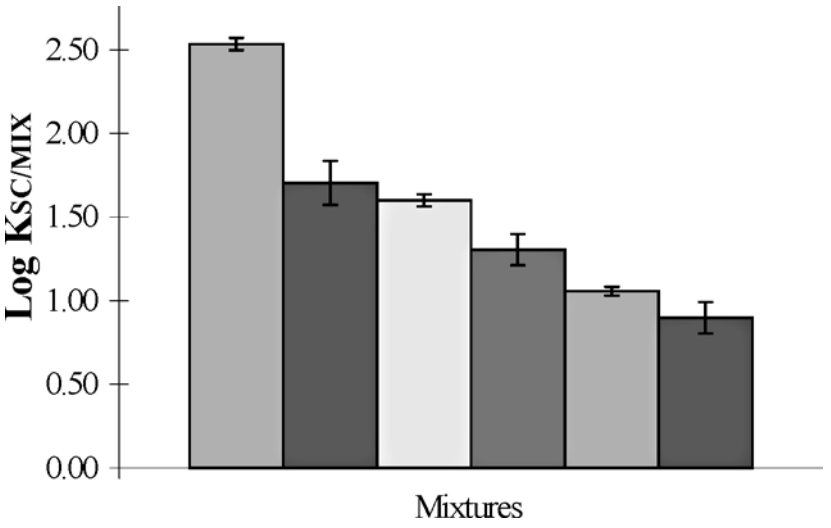


Figure 2 Isolated porcine stratum corneum/vehicle partiton coefficients (log $K_{SC/MIX}$) for pentachlorophenol (PCP) across six different chemical mixtures.

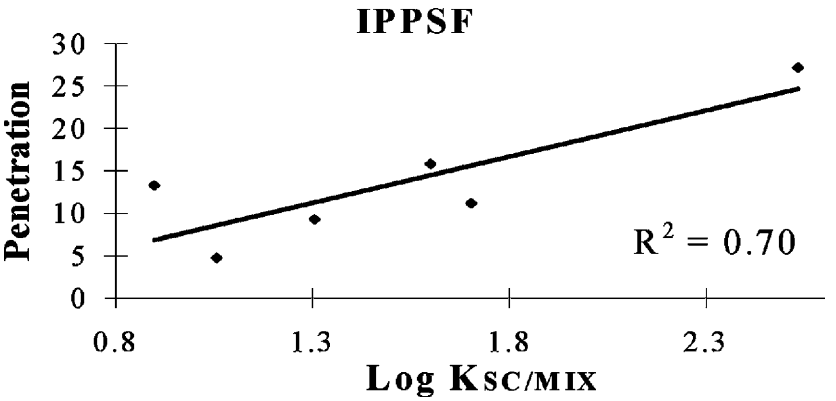


Figure 3 Correlation of pentachlorophenol (PCP) log $K_{SC/MIX}$ and absorption in isolated perfused procine skin.

(e.g., lipid synthesis enzymes) which would modify barrier function (27). A chemical could also induce keratinocytes to release cytokines or other inflammatory mediators (28–30), which could ultimately alter barrier function in the stratum corneum or vascular function in the dermis. Alternatively, cytokines may modulate biotransformation enzyme activities (31).

The last level of potential interaction is in the dermis where a component chemical may directly or indirectly (e.g., via cytokine release in the epidermis) modulate vascular uptake of the penetrated toxicant (32,33). In addition to modulating transdermal flux of chemical, such vascular modulation could also affect the depth and extent of toxicant penetration into underlying tissues.

IV. IMPACT OF MULTIPLE INTERACTIONS

The complexity occurs when one considers that the above interactions are all independent, making the observed effect in vivo a vectorial sum of all interactions. This allows the so-called "emergent properties" of complex systems (34) to be observed when the individual interactions are finally summed in the intact system, in our case in vivo skin. For example, assume that mixture component A decreases absorption of a chemical across skin due to increase binding to skin components. In contrast, mixture component B increases its absorption due to an enhancer effect on stratum corneum lipids. When the mixture components A and B are administered in combination, the transdermal flux of the chemical being studied may not differ from control. This is illustrated by the effect of two different jet-fuel performance additives metal deactivator additive (MDA) and butylated hydroxytoluene (BHT) on dermal absorption of naphthalene administered from the base fuel JP-8 not containing these additives or in combination (Fig. 4). In this case we hypothesize that MDA increases surface retention of naphthalene, thereby decreasing its absorption, while BHT functions more like a penetration enhancer. When both are present, flux returns to base levels. We have previously seen similar effects with other combinations of additives on absorption of jet fuel hydrocarbons (35,36).

It may be a mistake to assume that these opposite effects simply cancel one another out and that the flux of chemical is now equivalent to it being applied alone. The mechanisms behind the similarity in fluxes are different. Fick's first law of

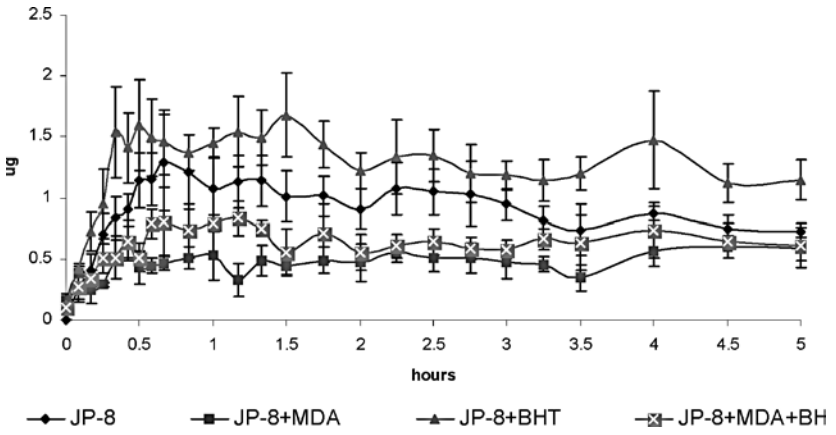


Figure 4 Effects of fuel performance additives butylated hydroxytoluene (BHT) and metal deactivator additive (MDA) on dermal absorption of naphthalene in isolated perfused porcine skin.

diffusion can be used to illustrate this. In the base situation (ø), compound flux would equal:

$$\text{Flux}_{\oslash} = K_{\text{p}}\ \Delta C$$

where K_{p} is the permeability coefficient and ΔC is the concentration gradient driving the absorption process. We will consider ΔC the effective dermal dose since increasing concentration on the surface of skin effectively increases ΔC. In the presence of additives, we had two scenarios where additive A decreased absorption by retaining chemical on the surface, effectively reducing ΔC:

$$\downarrow \text{Flux}_{\text{A}} = K_{\text{p}}\ (\downarrow \Delta C)$$

and scenario B where flux increased due to an increased K_{p}:

$$\uparrow \text{Flux}_{\text{B}} = (\uparrow K_{\text{p}})\ \Delta C$$

When both A and B are present, the flux is now back to base levels, but is governed by a fundamentally different set of diffusion parameters:

$$\text{Flux}_{\text{A+B}} \cong \text{Flux}_{\oslash} = (\uparrow K_{\text{p}})\ (\downarrow \Delta C)$$

One can appreciate how different factors that would interact with these altered parameters could drastically change dermal flux compared to the baseline scenario.

V. CONCLUSIONS

This brief overview of mixture absorption illustrates the complexity involved when trying to extrapolate single interactions seen with binary mixtures onto absorption from more complex mixtures. However, strategies aimed at quantitating potential interactions in the framework of mechanisms of absorption would seem to be the most promising approach to put order into this complex problem. The data that indicate that measured stratum corneum PC correlates to subsequent absorption through intact skin is encouraging as it provides an approach to experimentally assessing the effects of complex mixtures of K_{p}.

ACKNOWLEDGMENTS

The author would like to thank Dr. F. Muhammed for his help in analysis of the naphthalene data depicted in Figure 4 and NIOSH Grant R01-OH-07555 for supporting these mixture studies.

REFERENCES

1. Poet TS, McDougal JN. Skin absorption and human risk assessment. Chem Biol Interact 2002; 140:19–34.
2. EPA. Dermal Exposure Assessment: Principles and Applications. EPA/600/8-91/011B, 1995.
3. EPA. Risk Assessment Guidance for Superfund. Vol. 1: Human Health Evaluation Manual (Part E. Supplemental Guidance for Dermal Risk Assessment) Interim Guidance. Office of Emergency and Remedial Response, Washington, DC, 1999.
4. Borgert CJ, Price B, Wells CS, Simon GS. Evaluating chemical interaction studies for mixture risk assessment. Hum Ecol Risk Assess 2001; 7:259–306.
5. Pohl HR, Hansen H, Selene J, Chou CH. Public health guidance values for chemical mixtures: current practice and future directions. Regul Toxicol Pharmacol 1997; 26:322–329.
6. EPA. Guidelines for the health risk assessment of chemical mixtures. Federal Register 1986; 5:34014–34025.
7. EPA. Technical Support Document on Risk Assessment of Chemical Mixtures. EPA/600/8-90/064, 1988.
8. CRARM (Commission on Risk Assessment and Risk Management). U.S. Congress, Washington, DC, 1997.
9. Bliss CI. The toxicity of poisons applied jointly. Ann Appl Biol 1939; 26:585–615.
10. Yang RSH. Toxicology of Chemical Mixtures. San Diego: Academic Press, 1994.
11. Haddad S, Charest-Tardif G, Tardif R, Krishnan K. Validation of a physiological modeling framework for simulating the toxicokinetics of chemicals in mixtures. Toxicol Appl Pharmacol 2000; 167:199–209.
12. Haddad S, Béliveau M, Tardif R, Krishnan K. A PBPK modeling-based approach to account for interactions in the health risk assessment of chemical mixtures. Toxicol Sci 2001; 63:125–131.
13. Groten JP, Feron VJ, Sühnel J. Toxicology of simple and complex mixtures. Trends Pharmacol Sci 2001; 22:316–322.
14. Robinson PJ. Prediction: simple risk models and overview of dermal risk assessment. In: Roberts MS, Walters KA, eds. Dermal Absorption and Toxicity Assessment. New York: Marcel Dekker, 1998:203–229.
15. McDougal JN, Robinson PJ. Assessment of dermal absorption and penetration of components of a fuel mixture (JP-8). Sci Total Environ 2002; 288:23–30.
16. Baynes RE, Monteiro-Riviere NA, Riviere JE. Pyridostigmine bromide modulates the dermal disposition of C-14 permethrin. Toxicol Appl Pharmacol 2002; 181:164–173.
17. Riviere JE, Monteiro-Riviere NA, Baynes RE. Gulf War Illness-related exposure factors influencing topical absorption of ^{14}C-permethrin. Toxicol Lett 2002; 135:61–71.
18. Rosada C, Cross SE, Pugh WJ, Roberts MS, Hadgraft J. Effect of vehicle pretreatment on the flux, retention, and diffusion of topically applied penetrants in vitro. Pharm Res 2003; 20:1502–1507.
19. Idson B. Vehicle effects in percutaneous absorption. Drug Metab Rev 1983; 14:207–222.
20. Barry BW. Novel mechanisms and devices to enable successful transdermal drug delivery. Eur J Pharm Sci 2001; 14:101–114.
21. Moser K, Kriwet K, Kalia YN, Guy RH. Enhanced skin permeation of a lipophilic drug using supersaturated formulations. J Control Release 2001; 73:245–253.

22. Williams AC, Barry BW. Chemical penetration enhancement: possibilities and problems. In: Roberts MS, Walters KA, eds. Dermal Absorption and Toxicity Assessment. New York: Marcel Dekker, 1998:297–312.
23. Monteiro-Riviere NA, Inman AO, Mak V, Wertz P, Riviere JE. Effects of selective lipid extraction from different body regions on epidermal barrier function. Pharm Res 2001; 18:992–998.
24. Rastogi SK, Singh J. Lipid extraction and transport of hydrophilic solutes through porcine epidermis. Int J Pharm 2001; 225:75–82.
25. Bronaugh RL, Stewart RF, Strom JE. Extent of cutaneous metabolism during percutaneous absorption of xenobiotics. Toxicol Appl Pharmacol 1989; 99:534–543.
26. Mukhtar H. Pharmacology of the Skin. Boca Raton: CRC Press, 1992.
27. Elias PM, Feingold KR. Lipids and the epidermal water barrier: metabolism, regulation, and pathophysiology. Semin Dermatol 1992; 11:176–182.
28. Allen DG, Riviere JE, Monteiro-Riviere NA. Induction of early biomarkers of inflammation produced by keratinocytes exposed to jet fuels Jet-A, JP-8, and JP-8(100). J Biochem Mol Toxicol 2000; 14:231–237.
29. Luger TA, Schwarz T. Evidence for an epidermal cytokine network. J Invest Dermatol 1990; 95:104S–110S.
30. Monteiro-Riviere NA, Baynes RE, Riviere JE. Pyridostigmine bromide modulates topical irritant-induced cytokine release from human epidermal keratinocytes and isolated perfused porcine skin. Toxicology 2003; 183:15–28.
31. Morgan ET. Regulation of cytochrome P450 by inflammatory mediators: why and how? Drug Metab Dispos 2001; 29:207–212.
32. Riviere JE, Williams PL. Pharmacokinetic implications of changing blood flow to the skin. J Pharm Sci 1992; 81:601–602.
33. Williams PL, Riviere JE. Model describing transdermal iontophoretic delivery of lidocaine incorporating consideration of cutaneous microvascular state. J Pharm Sci 1993; 82:1080–1084.
34. Bar-Yum Y. Dynamic of Complex Systems. Reading: Addison-Wesley, 1997.
35. Baynes RE, Brooks JD, Budsaba K, Smith CE, Riviere JE. Mixture effects of JP-8 additives on the dermal disposition of jet fuel components. Toxicol Appl Pharmacol 2001; 175:269–281.
36. Riviere JE, Monteiro-Riviere NA, Brooks JD, Budsaba K, Smith CE. Dermal absorption and distribution of topically dosed jet fuels Jet A, JP-8, and JP-8(100). Toxicol Appl Pharmacol 1999; 160:60–75.

11
Does Desquamation Reduce Permeation?

Micaela B. Reddy
Quantitative and Computational Toxicology Group, Center for Environmental Toxicology and Technology, Colorado State University, Fort Collins, Colorado, U.S.A.

Annette L. Bunge
Chemical Engineering Department, Colorado School of Mines, Golden, Colorado, U.S.A.

I. INTRODUCTION

The skin can be an important exposure route to chemicals from a variety of pharmaceutical, cosmetic, household, agricultural, or industrial products. For organic chemicals of moderate size, penetration through the skin membrane is a solution–diffusion process (1–4). Once chemical is removed from the skin's surface, chemical within the skin can continue to diffuse through the skin and enter the bloodstream. As a result, for brief chemical exposures much of the systemic chemical absorption can occur after the chemical has been removed from the skin surface.

For many chemicals, the outermost skin layer, the stratum corneum (sc), is the rate-limiting barrier for mass transfer into and through skin. For highly lipophilic chemicals, the underlying viable epidermis (ve) also contributes a significant resistance to mass transfer across the skin. Together, the sc and ve comprise the epidermis (epi). The dermis, located beneath the epi, is a highly vascularized tissue that usually has sufficient blood flow to efficiently clear away all chemical passing through the epi (5).

Skin is continuously replaced through epidermal turnover, the process by which new cells are generated at the base of the epidermis while the outermost surface flakes off (i.e., desquamates) at the same rate. Chemical in desquamated skin cannot be absorbed systemically. Some investigators have suggested that desquamation will significantly reduce systemic exposure to dermally absorbed chemicals (6,7). The typical time required to completely replace the sc (i.e., the turnover time for the sc, $t_{t,sc}$) is approximately 14 days but varies with physiological location (8,9) and age (10,11). The turnover time for the ve, $t_{t,ve}$, has been reported as 38 to 61 days (12), 31 days (13), 33 to 34 days (14), and 25 days (15). The variations in reported values of $t_{t,ve}$ arise because in each of the references cited, $t_{t,ve}$ was calculated using different methods, models, and assumptions. Turnover times can be shorter for diseased skin (15). While the rate of desquamation can be changed by

chemically or mechanically forcing desquamation or by protecting a site, the rate of cell proliferation does not change (9,16).

Although the potential contribution of desquamation to chemical elimination from the skin has been mentioned in many papers, quantitative mathematical modeling of the process has been limited. The model developed by Auton et al. (7) to describe dermal absorption of the herbicide fluazifop-butyl did include desquamation and sc turnover. However, their model did not include ve turnover and did not clearly relate sc turnover and chemical loss from the surface layer. Here, a mathematical model describing chemical absorption into the epidermis allowing for epidermal turnover is used to address these issues quantitatively.

II. MODELING DERMAL ABSORPTION AND DESQUAMATION

Typically, mathematical models of dermal absorption account for chemical transport through the skin by passive diffusion alone (17–19). However, cell proliferation at the basal layer of the ve along with desquamation of the outer surface of the sc cause the epi to move slowly outward, carrying chemical dissolved in the sc along with it. Most dermal absorption models neglect this convective transport of absorbed chemical because cell growth is usually much slower than diffusion. By including the epi turnover velocity in the model presented here, we are able to examine theoretically the effect of desquamation on dermal absorption.

In the ve, cells are released from the basal layer and move upward in a random manner (12). However, many cells in the differentiating layers of the ve move in tandem as a front (15). Once the cells reach the sc, they are tightly attached to each other and travel in unison (12). Consequently, we assumed that the sc and ve move outward at constant velocities. For example, the velocity of the sc, u_{sc}, can be estimated as the constant apparent thickness of the sc, L_{sc}, divided by the turnover time for the sc (i.e., $u_{sc} = L_{sc}/t_{t,sc}$).

The mathematical model used to quantify the effect of desquamation on dermal absorption following an exposure has been described in detail elsewhere (20). Briefly, in this model dermal absorption was described as mass transfer by passive diffusion through two pseudohomogenous membranes of constant thickness in series representing the sc and ve. Epidermal turnover was incorporated into the model by including mass transfer by convection due to the outward velocity of the sc and ve. In the model development, it was assumed that the skin was exposed to a constant concentration vehicle for an exposure time t_{exp} and was then cleaned off. The model was developed for nonvolatile chemicals, and so after the exposure ended there was no flux of chemical by diffusion from the skin surface. In addition, it was assumed that local equilibrium existed and that flux was conserved at the sc/ve interface, and that there was an infinite sink at the ve/dermis interface.

This mathematical model was used to quantitatively examine the effect of exposure time, chemical lipophilicity, and epidermal turnover rate on dermal absorption after an exposure ends. In all the calculated results presented here, we assumed that $t_{t,sc}/t_{t,ve} = 0.5$, that the ve is about 10 times thicker than the sc, and that the lag time of the chemical through the sc, $t_{lag,sc}$, is at least 10 times longer than the lag time through the ve. These assumptions are based on physiological properties of normal human skin (20). For example, $L_{sc} \sim 10$ to 40 μm while the apparent thickness of the ve is about 100 to 200 μm (21).

Two additional groups of parameters that vary depending on the properties of the absorbing chemical also had to be specified. First, the ratio $t_{t,sc}/t_{lag,sc}$ representing the rate of desquamation relative to the rate at which a chemical moves through the sc. Second, the B parameter, defined as:

$$B = P_{sc,v}/P_{ve,v} \quad (1)$$

which is the ratio of permeability coefficients of the absorbing chemical in the sc, $P_{sc,v}$, to the ve, $P_{ve,v}$, from the same vehicle. The parameter $P_{sc,v}$ is defined as:

$$P_{sc,v} = K_{sc/v}D_{sc}/L_{sc} \quad (2)$$

where $K_{sc/v}$ is the partition coefficient of the chemical between the sc and the vehicle and D_{sc} is the effective diffusion coefficient of the absorbing chemical through the sc. The B parameter is a measure of the relative contributions of the sc and the ve as mass transfer resistances to dermal absorption.

The mathematical model, which consisted of two coupled partial differential equations (one each for the sc and the ve), was solved numerically using finite differencing (20). The amount absorbed systemically following an exposure was calculated and then used to calculate FA, the fraction of chemical in the skin at the end of an exposure that systemically absorbs. The fraction of chemical eliminated from the skin by desquamation following an exposure is $1 - FA$. Additionally, the model was used to calculate the flux of chemical through the skin at steady state, J_{ss}.

III. RESULTS AND DISCUSSION

Using the mathematical model, two sets of calculations were performed. In the first set of calculations, we examined the effect of t_{exp} on FA. To simplify these computations, we assumed that the sc limits the rate of mass transport through the skin (i.e., B is small). Under these circumstances, the ve is an infinite sink (i.e., $C_{ve} = 0$) and calculated values of FA do not depend on the lipophilicity of the absorbing chemical. The value of FA was calculated as a function of the ratios $t_{exp}/t_{lag,sc}$ and $t_{t,sc}/t_{lag,sc}$.

Figure 1 shows FA as a function of the sc turnover time for short and large values of $t_{exp}/t_{lag,sc}$ (i.e., the length of the exposure relative to the lag time for diffusing across the sc) assuming the sc alone limits dermal absorption (i.e., $B <$ about 0.1). The upper axis of Figure 1 specifies values of $t_{lag,sc}$ for $t_{t,sc} = 14$ days, a typical value for healthy human skin. As $t_{lag,sc}$ increases relative to $t_{t,sc}$, desquamation reduces the amount of dermal absorption (i.e., FA approaches 0). If $t_{lag,sc} < 0.05t_{t,sc}$, FA > 0.8. This corresponds to $t_{lag,sc} <$ about 17 hours for $t_{t,sc} = 14$ days. Many chemicals penetrate the sc with lag times less than 17 hours. For example, $t_{lag,sc}$ for benzoic acid and 4-cyanophenol (with MWs of 122.1 and 119.4, respectively) are less than one hour (22,23). Lag times are affected by molecular size and larger molecules will have longer $t_{lag,sc}$ values. One would expect that for nonvolatile chemicals that are not highly lipophilic or large (i.e., MW $<$ about 350), almost all of the chemical in the sc at the end of an exposure would eventually be absorbed systemically.

Although FA increased with increasing $t_{exp}/t_{lag,sc}$, the effect is relatively minor (Fig. 1). This is because at short exposure times chemical has penetrated only a short distance into the sc. Consequently, the concentration gradient (i.e., the driving force for mass transfer) is larger than at longer exposure times. As a result, the concentration of the absorbing chemical in the outer layers of the sc is reduced more

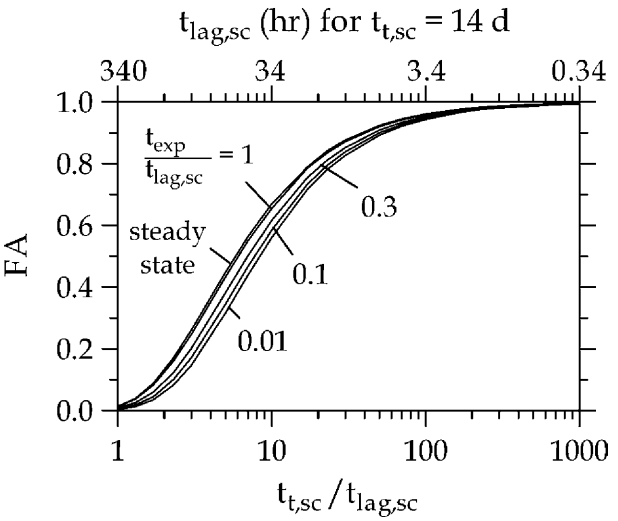


Figure 1 FA as a function of $t_{t,sc}/t_{lag,sc}$ for varying exposure times calculated assuming the viable epidermis adds no significant resistance to dermal absorption.

quickly by diffusion into the sc following a short exposure compared to a longer exposure.

For the calculations shown in Figure 1, the sc was the only significant resistance to mass transfer across skin. However, the conclusion that the duration of the exposure affects FA minimally should apply even when the ve contributes significantly to the skin's barrier (i.e., when B is not small). At exposure times less than the time required to reach steady state, the absorbing chemical has not penetrated far enough into the sc to be affected by the resistance from the ve (i.e., the amount of chemical in the epi is not affected by B when $t_{exp} < t_{lag,sc}$). Furthermore, the amount of chemical absorbed systemically is less sensitive to t_{exp} when B is not small because, compared to chemicals with small B, the variation of C_{sc} with position in the sc is less.

A second set of calculations was performed to examine the effect of chemical lipophilicity (i.e., the impact of the B parameter) on FA and J_{ss}. Since the ve can present a significant barrier to highly lipophilic chemicals, both the sc and ve were included in the general form of the model for these calculations. Based on the results shown in Figure 1, we knew that the steady-state calculations would reasonably represent unsteady-state conditions. Consequently, the computational complexity was partially reduced by assuming the chemical penetration rate had reached steady state before the exposure ended. Values of FA and J_{ss} were calculated as functions of B and $t_{t,sc}/t_{lag,sc}$.

Figure 2 shows the effect of epidermal turnover on J_{ss} for B values varying from 0.01 (i.e., the sc entirely controls the rate of dermal penetration) to 10 (i.e., the ve entirely controls the rate of dermal penetration). In Figure 2, J_{ss} is normalized by the steady-state flux that would occur if there were no epidermal turnover, $J_{ss}(u_{sc} = 0)$, which is the flux calculated using the model for $u_{sc} = 0$ (i.e., for $t_{t,sc}/t_{lag,sc} \rightarrow \infty$). It is clear from Figure 2 that epi turnover does reduce steady-state flux. However, the B parameter does not significantly affect the role of epi turnover in

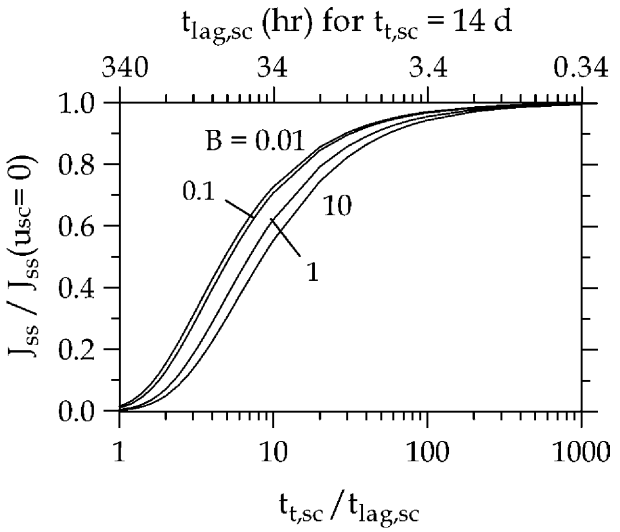


Figure 2 Normalized steady-state flux through the epidermis as a function of $t_{t,sc}/t_{lag,sc}$ for varying values of B.

reducing J_{ss} compared to J_{ss} for $u_{sc} = 0$, as indicated by the narrow spread between curves for $B = 0.01$ to 10.

Once the exposure ends, the B parameter plays a larger role as illustrated in Figure 3, which shows FA plotted as a function of $t_{t,sc}/t_{lag,sc}$ for varying values of B. As B increases, the ve becomes a more significant mass transfer barrier, preventing chemical entrance to systemic circulation from the sc. Thus, the effect of epi turnover on percutaneous penetration is greater when the ve is a significant barrier (i.e., when B is large). For example, if the barrier contributions of the sc and the ve are the same

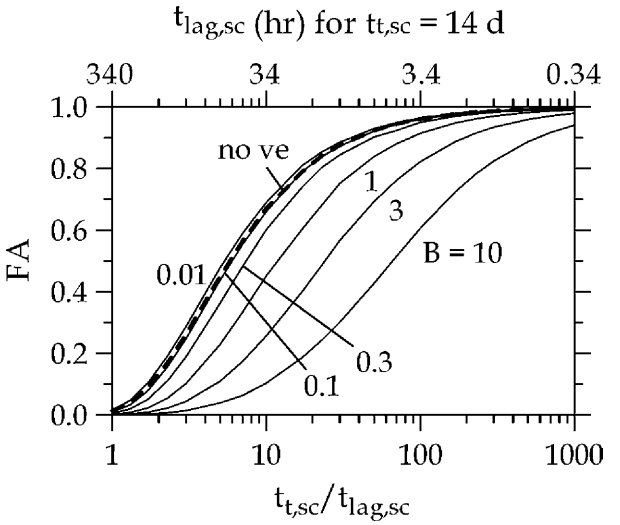


Figure 3 FA as a function of $t_{t,sc}/t_{lag,sc}$ for varying values of B calculated assuming that the exposure ended after steady state was achieved.

(i.e., $B = 1$), 70% of the chemical in the skin systemically absorbs when $t_{lag,sc}$ is less than about 5% of $t_{t,sc}$. For the same situation, only about 20% systemically absorbs if $P_{ve,v}$ is one-tenth of $P_{sc,v}$ (i.e., $B = 10$). The heavy dashed curve in Figure 3 is the steady-state curve from Figure 1, which was calculated assuming that the sc was the only barrier to dermal absorption (i.e., $C_{ve} \sim 0$). As expected, this curve coincides with curves calculated assuming $B < 0.1$.

It is evident from both Figures 1 and 3 that significant amounts of chemical can be removed from the skin by desquamation if $t_{t,sc}$ is short relative to $t_{lag,sc}$. This suggests that chemical removal by desquamation could be more significant in diseased skin involving hyperproliferation (e.g., psoriasis). However, this might not be the case if the barrier function of the sc is reduced as this would simultaneously decrease $t_{lag,sc}$.

Figure 4, which shows combinations of B and $t_{lag,sc}$ that produce various values of FA, can be used to identify those situations in which desquamation may be an important mechanism for eliminating chemical from the skin after an exposure ends. However, to apply the results in Figures 1 through 4 to a specific chemical requires an estimate for B and $t_{lag,sc}$. Methods for estimating B and $t_{lag,sc}$ are presented next.

Permeability coefficients in both the sc and ve have been measured for only a few chemicals, and there are only a few experimental values for B (2). Based on differences in the physical characteristics of the sc and the ve, B should vary with a chemical's lipophilic character, which can be represented approximately by the octanol–water partition coefficient ($K_{o/w}$). In addition, the effect of molecular size is likely to be different in the sc and ve, causing B to depend on molecular weight (MW) as well. Bunge and Cleek (24) proposed that B could be estimated as follows:

$$B = 0.00061\sqrt{\mathrm{MW}}10^{-0.006\mathrm{MW}}K_{o/w}^{0.74} \tag{3}$$

This equation was developed by estimating $P_{sc,v}$ using the correlation proposed by Potts and Guy (3) as reported by Bunge et al. (25) and by estimating $P_{ve,v}$ using these assumptions: (1) the apparent thickness of the ve is 100 μm, (2) the effective diffusion coefficient of the absorbing chemical in the ve is 10^{-6} cm^2/sec for a

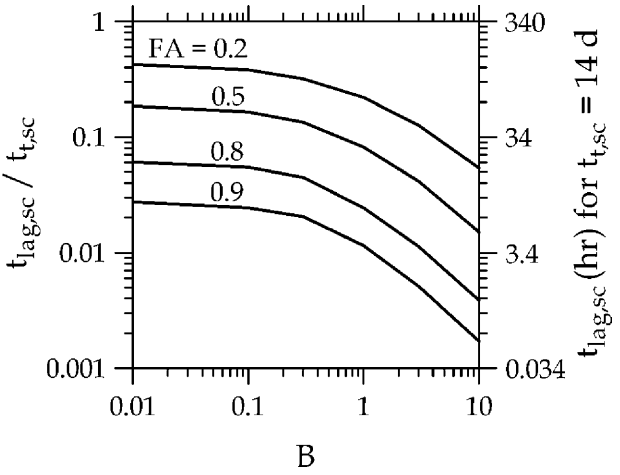


Figure 4 Values of FA corresponding to specific combinations of $t_{lag,sc}/t_{t,sc}$ and B.

chemical with MW = 50 and decreases as $1/\sqrt{\text{MW}}$, and (3) the chemical's solubility in the ve is the same as in water. Although Equation (3) was derived for a water vehicle, the B parameter should be independent of the vehicle if it does not alter skin properties.

While experimental values for lag times are reported for many chemicals, these must be used cautiously for assessing the effect of epidermal turnover. Experimentally determined values of lag times, usually derived from in vitro diffusion cell measurements, are notoriously variable. In addition, skin samples used in diffusion cell experiments often include the ve and part or all of the dermis. The difference between the experimental lag time measured in vitro and $t_{\text{lag,sc}}$ could be relatively small if there was no dermis in the experiment, but could be larger than $t_{\text{lag,sc}}$, the quantity required to use Figures 1 through 4, if the entire dermis was present. Lacking experimental data, the following equation:

$$t_{\text{lag,sc}}[\text{hr}] = 0.17(10^{0.006\text{MW}}) \tag{4}$$

can be used to provide a preliminary estimate for $t_{\text{lag,sc}}$ (20).

In Figure 5, we present $t_{\text{lag,sc}}$ as a function of MW estimated using Equation (4) and B as a function of MW and log $K_{\text{o/w}}$ estimated using Equation (3). The log $K_{\text{o/w}}$ for absorbing chemicals must be larger than ~3.5 (and larger than ~4 for chemicals with MW>200) to produce B values of one or larger. Because $t_{\text{lag,sc}}$ varies exponentially with MW, it increases dramatically when MW is greater than ~350. By combining the information in Figures 4 and 5, we estimate that desquamation might significantly affect FA when log $K_{\text{o/w}}$ > about four or MW>about 350 Da. Chemicals meeting these criteria include several steroids and retinoids as well as highly lipophilic environmental contaminants like benzo[a]pyrene. There is some evidence that in vivo values of $t_{\text{lag,sc}}$ are shorter than reported in vitro values (26). Consequently, MW may need to be 400 or more for desquamation to reduce FA. However, because the models derived here neglect diffusion through appendages (e.g., sweat ducts and hair follicles), the computed results should not be applied to

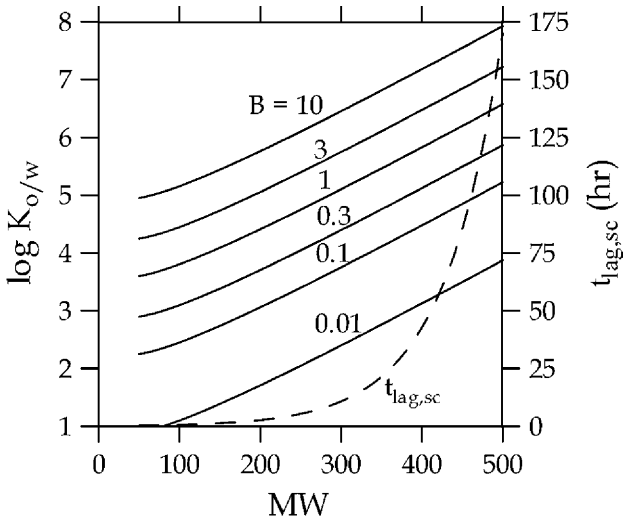


Figure 5 B parameter as function of MW and log $K_{\text{o/w}}$ (solid curves) and $t_{\text{lag,sc}}$ as a function of MW (dashed curve).

extremely large compounds (MW>approximately 500), for which absorption through the sc is likely to be small relative to absorption through the appendages.

The calculations described here are pertinent to the situation where a significant amount of chemical remains in the skin following an exposure relative to the amount of chemical that absorbed systemically during that exposure. An example situation where this arises is with dermal exposures to pesticides (27). Table 1 presents example calculations for B, $t_{lag,sc}$, and FA for five pesticides representing a range of properties.

Recently, Zendzian (29) presented in vivo, rat, dermal absorption data from studies of 19 pesticides that had been submitted to the Office of Pesticide Programs of the U.S. Environmental Protection Agency. The goal of these studies was to determine the fate of radiolabeled pesticide remaining in the skin after the exposure had ended. Dermal penetration was measured in collected urine, feces, and cage wash (which included residues of urine and feces), and in the animal carcass. Some animals were sacrificed immediately at the end of the exposure time, while others were sacrificed after varying times following the end of the exposure.

For all but two volatile pesticides 5-ethyl dipropylthio-carbamate (EPTC) and molinate, systemic absorption continued following the exposure. Volatile chemicals have an additional mechanism of elimination from the skin besides desquamation (i.e., evaporation) that could be responsible for the lack of systemic absorption following the exposure. For 15 out of the 19 pesticides, systemic absorption from the pesticide in the skin over the exposed site continued at all dose levels following washing.

In Figure 6, we present example data from Zendzian (29) for the smallest applied dose of atrazine (a herbicide) and of azinphos-methyl (an insecticide and acaricide). Each data point represents the mean of four animals. For both pesticides, the amount of chemical in the skin (i.e., the chemical found in the skin over the exposed site) decreased with time after the exposures ended (i.e., after the chemical was washed from the skin surface). The amount of chemical that had penetrated through the skin (i.e., the amount systemically absorbed calculated as the amount in the carcass, urine, feces, and cage wash) increased with time following the exposures. For both atrazine and azinphos-methyl, the skin acted as a storage depot slowly releasing chemical into the bloodstream after the exposures ended.

Based on model calculations shown above, FA is expected to be greater than 0.9 for atrazine, and about 0.85 for azinphos-methyl (Table 1). As shown in Figure 6, 70

Table 1 Summary of Chemical Properties and Example Calculations for Five Pesticides

	Pesticide properties[a]		Example calculations		
Pesticide	MW	log $K_{o/w}$	B[b]	$t_{lag,sc}$[c]	FA[d]
Atrazine	215.7	2.5	0.033	3.3	>0.9
Azinphos-methyl	317.3	3.0	0.021	14	0.85
Chlorpyrifos	350.6	4.7	0.27	22	0.75
Cypermethrin	416.3	6.6	3.0	53	<0.2
Endosulfan	406.9	3.6	0.021	47	0.6

[a]From Ref. 28.
[b]Calculated with Equation (3).
[c]Calculated with Equation (4).
[d]Estimated using Figure 4.

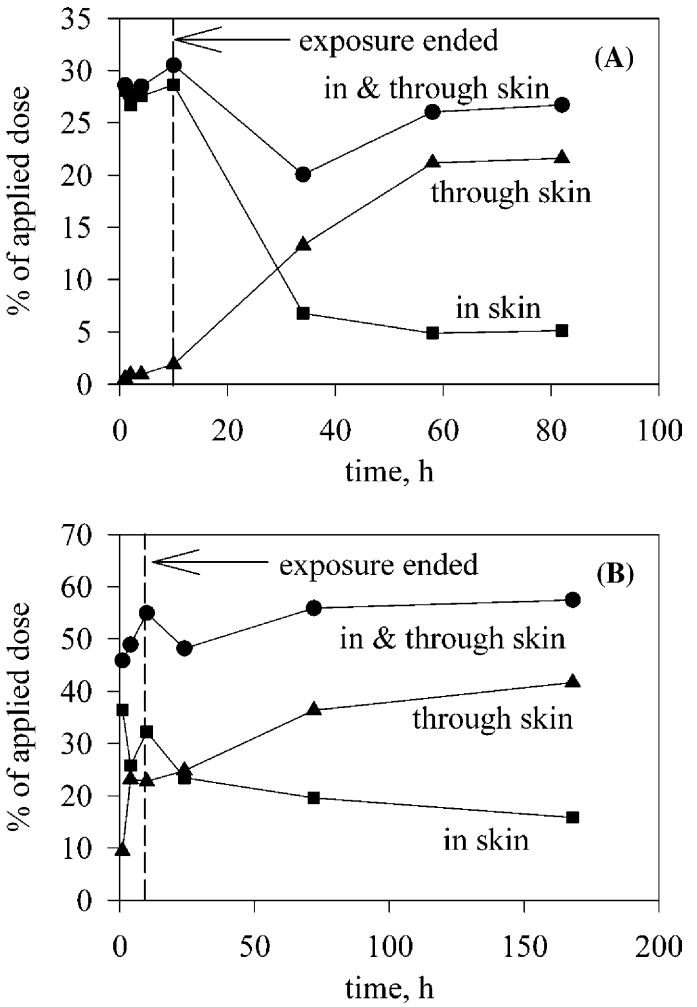


Figure 6 The percent of applied dose in skin (■), through skin (▲), and in and through skin (●) as a function of time in rats following an in vivo dermal exposure to radiolabeled (**A**) atrazine [applied dose, 42 nmol/cm^2] and (**B**) azinphos-methyl [applied dose, 3 nmol/cm^2]. The skin was washed 10 hours after the exposure ended. *Source:* From Ref. 29.

hours after a 10-hour exposure to atrazine, 69% of the amount in the skin at the end of the 10-hour exposure had penetrated through the skin and 18% still remained in the skin. By 158 hours after a 10-hour exposure to azinphos-methyl, 58% of the amount in skin at the end of exposure has penetrated through the skin and 48% remained in the skin. Unfortunately, for comparing with FA predictions, these experiments were not conducted long enough for all of the chemicals to be eliminated from the skin. However, these experiments do illustrate that, consistent with the FA predictions, a significant fraction of the chemical in the skin eventually did reach the systemic circulation.

Of the pesticides reported by Zendzian (29) for which we could find values of log $K_{o/w}$, desquamation would not significantly reduce systemic absorption for

most. Of the 19 pesticides, triphenyltin hydroxide had the highest MW at 367 and only three of the 19 pesticides had MWs larger than 320 Da. Example calculations for other pesticides with a wider variety of properties are presented in Table 1. FA was estimated to be 0.6 for endosulfan and 0.75 for chlorpyrifos. For cypermethrin, which is highly lipophilic, FA was estimated to be less than 0.2.

IV. CONCLUSIONS

Except for highly lipophilic or large MW chemicals, nearly all of the chemical in the epi at the end of an exposure will systemically absorb (i.e., FA ~ 1), regardless of the length of time the skin was exposed to the chemical. Only for chemicals with large values of MW (> about 350) or log $K_{o/w}$ (> approximately four for most chemicals) will epidermal turnover reduce FA significantly.

ACKNOWLEDGMENTS

This work was supported in part by the U.S. Environmental Protection Agency (CR824053 and PR-DC-99–01933/2W9F09) and the U.S. Air Force Office of Scientific Research (F49620–98–1-0060). We thank D. Macalady, K. D. McCarley, M. M. Reddy, and L. Sun for their valuable suggestions.

ABBREVIATIONS

B	ratio of the sc and ve permeability coefficient of the absorbing chemical from the same vehicle, $P_{sc,v}/P_{ve,v}$
D_{sc}	effective diffusion coefficient of the absorbing chemical in the sc
epi	epidermis
FA	fraction of chemical in the epi at t_{exp} that systemically absorbs after the exposure has ended
J_{ss}	steady-state flux of the absorbing chemical
$J_{ss}(u_{sc} = 0)$	steady-state flux of the absorbing chemical with no epidermal turnover
$K_{sc/v}$	equilibrium partition coefficient between the sc and the vehicle for the absorbing chemical
$K_{o/w}$	octanol–water partition coefficient
L_{sc}	apparent thickness of the sc
MW	molecular weight
$P_{sc,v}$	steady-state permeability coefficient of the absorbing chemical through the sc from the vehicle, $K_{sc/v}D_{sc}/L_{sc}$
$P_{ve,v}$	steady-state permeability coefficient of the absorbing chemical through the ve from the vehicle
sc	stratum corneum
t_{exp}	duration of the exposure
$t_{lag,sc}$	lag time for chemical penetrating through the sc, $L_{sc}^2/(6D_{sc})$
$t_{t,sc}$	turnover time of the sc
$t_{t,ve}$	turnover time of the ve
u_{sc}	velocity at which the sc moves, $L_{sc}/t_{t,sc}$
ve	viable epidermis

REFERENCES

1. Scheuplein RJ. Permeability of the skin: a review of major concepts. Curr Probl Dermatol 1978; 7:172–186.
2. Vecchia B. Estimating the Dermally Absorbed Dose from Chemical Exposure: Data Analysis, Parameter Estimation, and Sensitivity to Parameter Uncertainties. MS thesis, Colorado School of Mines, Golden, CO, 1997.
3. Potts RO, Guy RH. Predicting skin permeability. Pharm Res 1992; 9:663–669.
4. US EPA. Dermal Exposure Assessment: Principles and Applications. Washington: EPA/600/8-91/011B, Exposure Assessment Group, Office of Health and Environmental Assessment, 1992.
5. Scheuplein RJ, Bronaugh RL. Percutaneous absorption. In: Goldsmith LA, ed. Biochemistry and Physiology of the Skin. Vol. 2. New York: Oxford University Press, 1983:1255–1295.
6. Schaefer H, Zesch A, Stuttgen G. Skin Permeability. Berlin: Springer-Verlag, 1982.
7. Auton TR, Westhead DR, Woolen BH, Scott RC, Wilks MF. A physiologically based mathematical model of dermal absorption in man. Hum Exp Toxicol 1994; 13:51–60.
8. Finlay AY, Marshall RJ, Marks R. A fluorescence photographic photometric technique to assess stratum corneum turnover rate and barrier function in vivo. Br J Dermatol 1982; 107:35–42.
9. Roberts D, Marks R. The determination of regional and age variations in the rate of desquamation: a comparison of four techniques. J Invest Dermatol 1980; 74:13–16.
10. Grove GL. Physiologic changes in older skin. Dermatol Clin 1986; 4:425–432.
11. Takahashi M, Machida Y, Marks R. Measurement of turnover time of stratum corneum using dansyl chloride fluorescence. J Soc Cosmet Chem 1987; 38:321–331.
12. Halprin KM. Epidermal ''turnover time''—a re-examination. Br J Dermatol 1972; 86: 14–19.
13. Bergstresser PR, Taylor JR. Epidermal 'turnover time'—a new examination. Br J Dermatol 1977; 96:503–509.
14. Iizuka H. Epidermal turnover time. J Dermatol Sci 1994; 8:215–217.
15. Weinstein GD, McCullough JL, Ross P. Cell proliferation in normal epidermis. J Invest Dermatol 1984; 82:623–628.
16. Kligman AM. The biology of the stratum corneum. In: Montagna W, Lobitz WC, eds. The Epidermis. New York and London: Academic Press, 1964:387–433.
17. Silcox GD, Parry GE, Bunge AL, Pershing LK, Pershing DW. Percutaneous absorption of benzoic acid across human skin. II. Prediction of an in vivo, skin-flap system using in vitro parameters. Pharm Res 1990; 7:352–358.
18. Reddy MB, McCarley KD, Bunge AL. Physiologically relevant one-compartment pharmacokinetic models for skin. 2. Comparison of models when combined with a systemic pharmacokinetic model. J Pharm Sci 1998; 87:482–490.
19. Cleek RL, Bunge AL. A new method for estimating dermal absorption from chemical exposure. 1. General approach. Pharm Res 1993; 10:497–506.
20. Reddy MB, Guy RH, Bunge AL. Does epidermal turnover reduce percutaneous penetration?. Pharm Res 2000; 17:1414–1419.
21. Scheuplein RJ. Properties of the skin as a membrane. Adv Biol Skin 1972; 12:125–152.
22. Parry GE, Bunge AL, Silcox GD, Pershing LK, Pershing DW. Percutaneous absorption across human skin. I. In vitro experiments and mathematical modeling. Pharm Res 1990; 7:230–236.
23. Pirot F, Kalia YN, Stinchcomb AL, Keating G, Bunge AL, Guy RH. Characterization of the permeability barrier of human *skin in vivo*. Proc Nat Acad Sci USA 1997; 94: 1562–1567.
24. Bunge AL, Cleek RL. A new method for estimating dermal absorption from chemical exposure. 2. Effect of molecular weight and octanol–water partitioning. Pharm Res 1995; 12:88–95.

25. Bunge AL, Flynn GL, Guy RH. Predictive model for dermal exposure assessment. In: Wang R, ed. Water Contamination and Health: Integration of Exposure Assessment, Toxicology, and Risk Assessment. New York: Marcel Dekker, 1994:347–373.
26. Poet TS, Thrall KD, Corley RA, Hui X, Edwards JA, Weitz KK, Maibach HI, Wester RC. Utility of real time breath analysis and physiologically based pharmacokinetic modeling to determine the percutaneous absorption of methyl chloroform in rats and humans. Toxicol Sci 2000; 54:42–51.
27. Reddy MB, Bunge AL. Dermal absorption from pesticide residues: data analysis. In: Kruse J, Verhaar HJM, de Raat WK, eds. The Practical Applicability of Toxicokinetic Models in the Risk Assessment of Chemicals. The Netherlands: Kluwer Academic Press, 2002:55–79.
28. Tomlin CDS, ed. A World Compendium. The Pesticide Manual. 11th ed. Surrey, United Kingdom: British Crop Protection Council, 1997.
29. Zendzian RP. Pesticide residue on/in the washed skin and its potential contribution to dermal toxicity. J Appl Toxicol 2003; 23:121–136.

12

Penetration and Distribution in Human Skin Focusing on the Hair Follicle

Ylva Grams and Joke Bouwstra
Department of Drug Delivery Technology, Leiden Amsterdam Center for Drug Research, Leiden University, Leiden, The Netherlands

I. ABSTRACT

When focusing on drug delivery to regions in the skin such as the hair follicle, sweat and sebaceous glands, application of the drug on the skin surface has the potential to increase the drug concentration at the site of action and to limit the amount of drug in the systemic circulation. The rational of topical delivery may be of particular interest for skin diseases such as acne, cancer, and alopecia, which originate in the pilosebaeous unit (1–4), and also for cosmetic products to improve, e.g., the hair condition. This can be achieved by targeting active ingredients to the pilosebaceous unit. Local delivery can be improved by two approaches. The first approach is the selection of an appropriate formulation, which might contain particulate carriers and medium additives such as ethanol, surfactants, and propylene glycol. A second approach is the selection of a possible drug candidate. The physicochemical parameters of the drug, e.g., size, charge, and lipophilicity, can affect the degree of delivery and targeting. In those particular cases where formulation variation is not feasible, delivery and targeting can only be improved by the physicochemical parameters of the penetrant itself.

In order to study local drug delivery to the hair follicle, information on changes in drug accumulation in time in the various skin regions is required. Since the hair follicle can reach depth of more than 2 mm in the skin (5), techniques are required that are able not only to measure changes in drug accumulation in time in epidermis but in addition also drug accumulation in great depth beyond the dermis in unfixed skin. Preferably we should be able to measure this on line as that provides information on the drug transport routes. At the end of this chapter, we will summarize studies focusing on on-line visualization of the diffusion process using confocal scanning laser microscopy.

II. SKIN

A. Function

The skin is the largest organ of the body weighing more than 10% of the total body mass (6). Forming the outermost layer of the human body, it has two important functions namely communication and protection (7). The communicative function is based on neuroreceptors, biochemical transmitted signals, and pigmentation. The protective function prevents loss and penetration of a substance from and into the body (8). On the one hand, the skin protects the body from the environment such as physical (radiation, abrasion), biological (microorganisms), or chemical factors (toxic substances). On the other hand, water and ion loss from the body is prevented as well (9). Additionally, the skin with its sweat and sebaceous glands (10), hair follicles, and systemic circulation enables thermoregulation to ensure correct functioning of the biochemical apparatus.

Despite of this general function, regional variations in skin morphology occur. Not only the thickness (11) and composition of the stratum corneum varies (12,13) but also the presence of appendages and the number of hair follicles is not constant over the whole body surface (14). These variations are of functional origin giving, e.g., the soles higher protection against abrasion.

B. Structure

The skin is basically composed of two layers (epidermis and dermis) with an adjacent subcutaneous fat tissue (Fig. 1). The epidermis forms the outer layer of the body comprised of nonviable (stratum corneum) and viable cell layers. The epidermis is generated in the undulating basal cell layer at the epidermal–dermal junction (15). On their way to the skin surface, the keratinocytes start to differentiate and during migration through the stratum spinosum and stratum granulosum undergo a number of changes in both structure and composition. The final differentiation occurs in

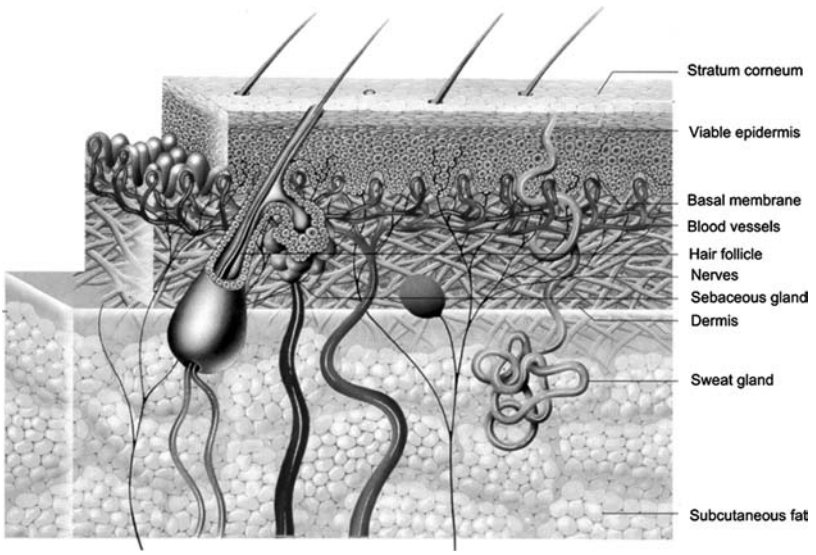


Figure 1 Skin structure of human skin with the main layers being the stratum corneum, viable epidermis including the basal membrane, dermis, and the subcutaneous fat. Local skin structures are blood vessels, hair follicles, nerves, sebaceous glands, and the sweat glands.

the stratum corneum (16). The stratum corneum forms the major hurdle for substances to permeate across the epidermis. The stratum corneum consists of dead corneocytes coated with an impermeable proteinous cornified envelope. The corneocytes are surrounded by lipid matrix (16). This lipid matrix is arranged in multiple layers forming lipid lamellae (17). Due to the impermeable cornified envelope, the intercellular lipid matrix forms the major tortuous pathway for permeation of substances across the stratum corneum.

The dermis is located beneath the epidermis. The thin upper dermis, which is in direct contact with the undulating epidermis, is the papillary dermis while the thicker main part of the dermis is called reticular dermis. It is a fibrous, filamentous, and amorphous connective tissue consisting of collagen, elastin, ground substance, and fibroblasts (18–21). Its main function is to provide support for the epidermis and embedded structures (blood vessels, nerves, hair follicles, sweat, and sebaceous glands) as well as elasticity of the skin (6). In contrast to the epidermis, this tissue is highly vascularized.

The subcutaneous fat tissue is underlying the dermis. It is an assembly of fat cells linked by collagen fibers, thereby creating a thermal barrier, energy storage, and mechanical cushion for the body (6,7).

C. Appendages

Appendages are skin structures penetrating the skin. Appendages originate either from the dermis or the subcutaneous fat. Their presence varies in different skin regions of the body. Since they emerge from the skin, the appendages form discontinuities in the stratum corneum and can therefore act as potential sites of formulation accumulation and routes of penetration.

1. Sweat Gland

Apocrine and eccrine glands are present in large numbers and distributed over the entire body. Apocrine glands emerge into the follicular duct and are located in adults in the axilla and perianal region. Therefore, it has been proposed that the apocrine glands do not contribute to the thermoregulatory function of the sweat glands but are remnants of the secondary sexual organs (7). Eccrine sweat glands are smaller than the apocrine glands and are spread over the whole body surface except from mucosal tissue. They excrete sweat (hypotonic water) via the sweat duct to the skin surface. These sweat ducts perturb the stratum corneum in a spiral form and straighten in deeper skin layers. The secretory gland itself is coiled and situated in the lower dermis. Their main function is the thermal regulation of the body (6).

2. Pilosebaceous Unit

The pilosebaceous unit consists of the hair follicle and the sebaceous gland. The hair follicle can be divided into two classes. The smaller vellus hair is rather thin and reaches down into the dermis. The large terminal hair extends down into the subcutaneous fat (22). The terminal hair occurs mainly on the scalp skin, the region with the highest density of hair follicles.

Sebaceous glands occur over the whole body surface; however, variation in density and activity dependent on age and sex (23–25). A high density of sebaceous glands is present in scalp and forehead skins, while in palm and sole the sebaceous glands are absent (26). Sebum, mainly consisting of trigycerides, free fatty acids, squalene, and waxes, is

secreted by the sebaceous gland into the hair duct at a depth of about 500 μm (27–30). This sebum protects the body from microbial infection and prevents water loss from the body (30). Additionally, it has the potential to interact with topically applied substances on the skin surface and in the upper part of the follicular duct, thereby acting as an additional barrier for permeation of substances across the skin.

3. *The Hair Follicle*

Structure. The basic structure of the hair follicle is displayed in Figure 2 (31). The hair follicle can be divided into several sections starting from the skin surface. The upper part of the hair follicle up to the sebaceous duct is the infundibulum. In this area, there is no tight connection between the hair shaft and the skin so that the hair shaft can move freely within the skin. This gap is filled with sebum from the sebaceous gland. The thickness of the stratum corneum decreases deeper in the

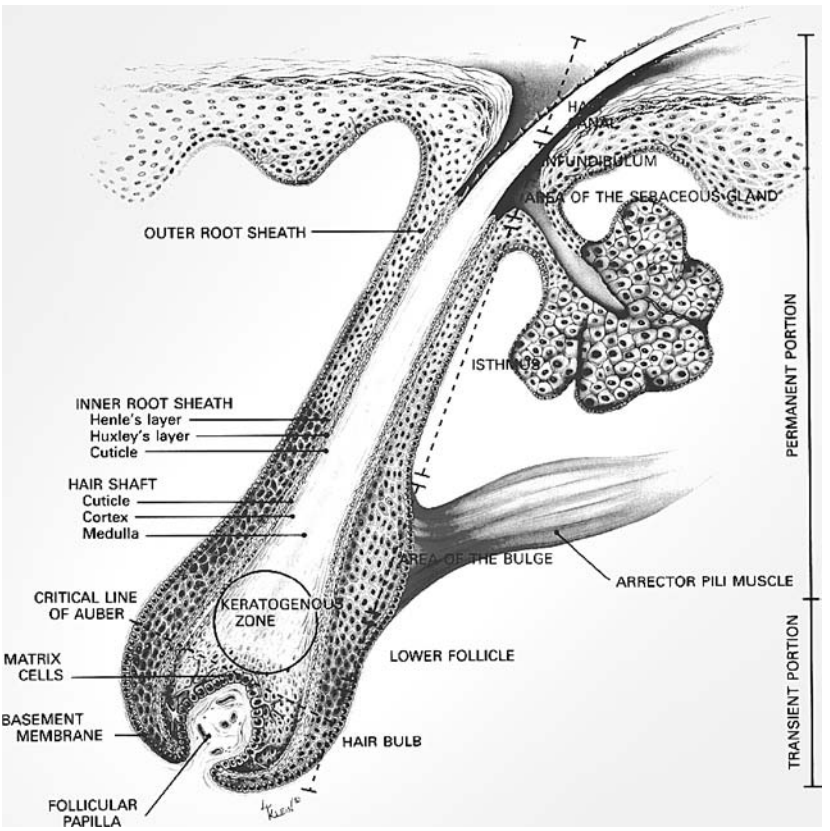


Figure 2 Hair follicle structure (31). The various layers of the hair follicle described in this thesis are from the dermis to the center of the hair: outer root sheath, inner root sheath (Henle's layer, Huxley's layer), cuticle of the inner root sheath, cuticle of the hair shaft, and the remaining hair shaft. Furthermore, it is depicted that the epidermis is continuous with the outer root sheath and the stratum corneum decreases in thickness in the opening of the follicular duct. The sebaceous gland secretes the sebum into the opening of the follicular duct. The bulge area is located below the duct of the sebaceous gland. *Source*: From Ref. 31.

infundibulum. This thinned stratum corneum provides a weaker barrier for penetration as the stratum corneum at the skin surface (32). Just below the sebaceous duct and up to the area where the arector pili muscle is attached to the hair follicle, the isthmus is situated. From the isthmus upward the hair follicle is permanent and does not disintegrate during the growth of the hair follicle. In this region, the inner root sheet is disintegrating and disappears between the outer root sheet and the cuticle further to the surface. The area where the arector pili muscle is in contact with the hair follicle is the bulge area, which is important for regulatory processes during hair growth (33). Below the bulge area is the lower follicle with the keratogeneous zone. The lowest part of the hair follicle is the hair bulb, where the matrix cells, the basement membrane, and the follicular papilla are located. These structures are key features in the regulation of the hair growth In a cross section of the hair follicle situated below the bulge, several almost concentric layers can be identified (Fig. 2) (31,34). Basically from the outside of the hair follicle to the center of the follicle the following layers are encountered: the outer root sheath, the inner root sheath including its Henle's layer, its Huxley's layer, and its cuticle. The inner root sheath is in direct contact with the hair shaft. The hair shaft itself is composed of a cuticle (outermost layer), a cortex, and a medulla (central part). The cuticle of the inner root sheath and of the hair shaft form the connection along which the hair shaft is moving outward during hair growth.

Keratinization is important for hair growth and might be crucial for the transport processes. The outer root sheath is in direct contact with the epidermis. Below the duct of the sebaceous gland, the cells of the outer root sheath are only little keratinized or lack keratinization completely. This allows the molding of the hair shaft and at the same time provides sufficient protection for the shaft. From the sebaceous duct upwards, the outer root sheath cells are keratinized and resemble more closely the epidermal cells (34). The inner root sheath keratinizes deeper in the hair follicle as compared to the outer root sheath with the Henle's layer being the first, followed by the cuticle and the Huxley's layer (34). The cuticle of the inner root sheath keratinizes closer to the hair bulb than the cuticle of the hair shaft, thereby providing guidance during the emerging of the hair shaft and additionally loosens the tight connections between the two cuticles (34).

Growth Cycle of the Hair. Hair growth varies between different body regions with an average growth rate varying between 0.21 mm per 24 hours on the female thigh and 0.38 mm per 24 hours on the male chin (7). The hair growth undergoes a repetitive cycle where the anagen phase is followed by the catagen and telogen phase (35) (Fig. 3). In the anagen phase, the hair is actively growing while the catagen is characterized by degeneration and resorption of the lower region of the hair follicle. The resting period, where the hair is inactive, is the telogen phase. After resting, growth of the hair follicle starts again (36).

Currently, it is not clear how the hair growth is initiated. This is reflected by the various discussions and hypotheses regarding the activation and differentiation of stem cells (37,38). However, the bulge area and the dermal papilla seem to play a crucial role in the growth process.

Local Target Areas. In the pilosebaceous unit, various target areas for topically applied drugs are of interest. One of the potential target areas is the sebaceous gland due to the direct connection of the duct of the sebaceous gland with the hair duct. In case of dysfunction of the sebaceous gland, the topical application has the potential to deliver drugs directly to the target area with limited systemic delivery (39,40). In case of toxic actives efficient targeting is essential to limit the toxic side

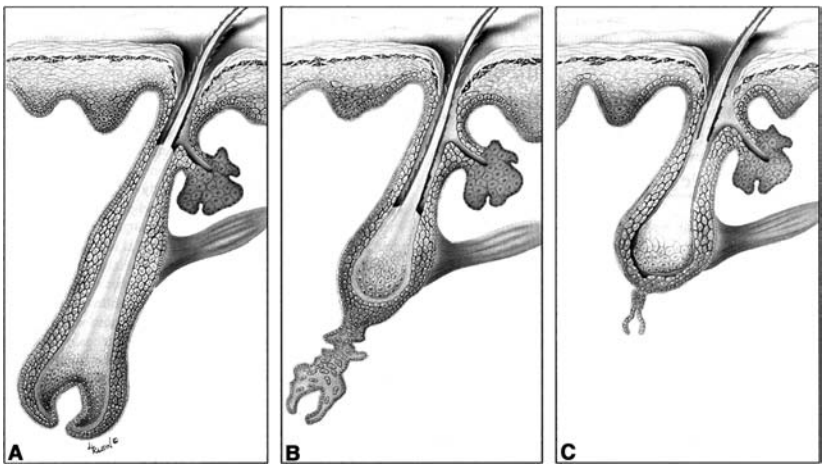


Figure 3 Growth cycle (31). (**A**) Anagen (growth phase), (**B**) catagen (transition phase), (**C**) telogen (resting phase). *Source*: From Ref. 31.

effects such as for isotretinoin in the treatment of acne (41). Regulatory receptors for various molecules (e.g., epidermal growth factor) have also been identified in the hair follicle (42). Target areas can be the bulge area, the bulb, and the various concentric layers in the follicle (39). Several research groups propose that the bulge area initiate the hair growth, although the exact mechanism is yet unknown. Another reason for targeting to the bulge region is that various forms of skin cancer have been thought to originate from this region (43). In the bulb melanocytes are present, which are responsible for the hair color and therefore also for graying of the hair. Treatment of the melanocytes in albino mice has demonstrated that it is possible to grow pigmented hair (44). Furthermore, the bulb contains a proliferating population of cells in the germinal matrix, which is responsible for new cell formation and therefore for hair growth. Sufficient nutrients for the growth process in the bulb area are provided by extensive vascularization (45). Also various attempts for the treatment of hair loss are also of great interest and discussed (46).

III. TRANSDERMAL AND DERMAL DELIVERY

During penetration through the stratum corneum, two possible routes can be distinguished: (i) penetration alternating through the corneocytes and the lipid lamellae (transcellular route) and (ii) penetration along the tortuous pathway along the lipid lamellae (intercellular route). Generally, it is accepted that the dominant route of penetration through the stratum corneum is the intercellular route. This is mainly caused by the densely cross-linked cornified envelope coating the keratinocytes. However, transcellular transport for small hydrophilic molecules such as water cannot completely be excluded (6).

The appendageal route or shunt route occurs via either the duct of the eccrine sweat glands or the follicular duct. The content of the eccrine sweat glands is mainly hydrophilic. In contrast, in the follicular duct the content is lipophilic, mainly due to the sebum excreted into the opening of the follicular duct.

It is generally accepted that due to its large surface area, passive skin permeation mainly occurs through intact stratum corneum. Since the appendages cover approximately 0.1% of the total skin surface, it is discussed that they contribute to a low amount to the overall passive transdermal penetration (48,49). However, Scheuplein (49) has calculated that in the initial phase of diffusion, the influence of the shunt route is very important. Investigations of several other groups provided additional data indicating that the contribution of the follicular pathway might be underestimated. They discovered an accumulation of the selected penetrant in the follicular region (50–53). These results are of great interest for drugs used in the treatment of follicle-related skin diseases.

IV. FOLLICULAR DELIVERY

A. General Aspects of Follicular Delivery

The follicular duct forms an intrusion in the stratum corneum. This interruption of the stratum corneum barrier can serve as a route for drug delivery. Additionally, the orifice of the hair follicle is a site where dermatological formulations may accumulate and deposit, thereby forming a depot for long-term delivery. In the past, the transappendageal route has long been considered of minor importance, since the orifices account for only 0.1% of the total skin surface. However, the density of hair follicles on scalp and face can reach as much as 10% of the total skin surface, creating a higher local surface area (54) and allow greater absorption by this route (55). The hair follicle openings are continuous with the epidermis but possess a much thinner layer of stratum corneum (39), which terminates at a depth of about 200 μm into the duct. The pilosebaceous unit is also closely surrounded by a high density of blood vessels, having the potential of high absorption of permeating substances in the systemic circulation. Nevertheless, parameters governing the follicular delivery are not clear yet.

Lieb et al. (54) demonstrated that permeation into hair follicles depends on size and charge of the permeant and the formulation in which the permeant is applied. Other chemical properties, like lipophilicity might also play a significant role in follicular penetration. Additionally, a certain degree of lipophilicity for compounds entering the hair follicle might be necessary due to the presence of sebum in the follicular duct from the sebaceous gland (39).

Based on theoretical considerations, it has already been proposed by Scheuplein (49) that the follicular route plays an important role in the initial period of the transport process, but that at a later stage penetration occurs predominantly via the stratum corneum. In fact, only little information is available on the contribution of the hair follicles to the total transport across the skin and even less is known about the effect of formulations and the chemical properties of the penetrant itself on this contribution.

B. Analysis Methods for Follicular Delivery

1. Quantification

Quantitative access to deposition of substances in the follicular region is a challenging task, since the hair follicle of human skin extends down into the subcutaneous fat. Most studies have been carried out either using fluorophores or radioactive agents

as model penetrants. The distribution profiles of these labels were mostly determined by quantification of model penetrants in stratum corneum tape strips in combination with quantification in biopsies (56,57), immunohistochemical analysis (54,58), isolation, and dissolution of the various skin regions including hair follicles (58,59), hair plugging, and follicle dissection (54). However, when isolating hair follicles, cell structures can be destroyed, thereby bearing the danger of delocalization of the dye and creating artifacts. Recently, techniques used for relative quantification of substance distribution within the skin have been reviewed elsewhere (57). Turner and Guy (60) have published relative quantification data of cryo-fixed hairless mouse skin samples focusing on the fluorophore distribution after iontophoresis. This was carried out ex vivo. Very recently, Grams and Bouwstra (61) reported a new quantification method, also using confocal laser scanning microscopy. This method included the relative accumulation of the fluorophore in the dermis, epidermis, and the various regions of the hair follicles, such as in the outer root sheet, the inner route sheet, the cuticle, and the hair. The relative accumulation was calculated from the images using a model "skin block" with a certain density and size of hair follicles based on literature data. All studies were performed using human scalp skin. Furthermore, the effect of formulation and the effect of penetrant lipophilicity were assessed (62,63). As far as in vivo quantification is involved, particularly noninvasive methods of quantification, such as in depth-resolved near-IR spectroscopy, have still an insufficient resolution (31 μm) for visualization of the various regions in the hair follicle (64). Furthermore, absolute quantification in unfixed tissue has not yet been reported.

2. *Visualization*

Visualization in Fixed Skin. Visualization methods in skin research have been summarized elsewhere (65). That review provides an excellent overview of advantages and disadvantages of the various methods available (65) to depict penetrated substances. While in conventional light microscopy a penetrant with a strong contrast has to be used, autoradiography requires radioactive labelling of the permeant. Electron microscopy has the advantage of providing images with a very high resolution. However, in most cases, the choice of the permeation agent is limited to substances with high electron density or substances linked to an electron dense marker, such as gold. All of these techniques require fixation, which can be obtained by chemical embedding or cryo-fixation of the skin. This fixation procedure in combination with subsequent slicing of the object can introduce artifacts, such as delocalization of the label. Therefore, fixation by chemicals or by cryo-fixation should be avoided.

Visualization in Non-fixed Skin. Visualization techniques that do not require embedding and freezing of the object are magnetic resonance imaging (66–68), video microscopy (69–72), ultrasound backscatter microscopy (73), and confocal laser scanning microscopy (74–80). The combination of the latter technique with confocal Raman spectroscopy (81) even enables to obtain a molecular composition of selected spot in the skin with high spatial resolution (82). For these techniques, model drugs with adequate characteristics such as Raman-active substances, dipole structures, or fluorescent dyes have to be selected. Confocal Raman spectroscopy has already been used in vivo in humans. Magnetic resonance imaging has the advantage that it can be used in vivo very deep in the skin and subcutaneous tissue; however, the resolution is limited compared to confocal Raman or confocal laser scanning microscopy. The

resolution of video and ultrasound microscopy is even worse and can therefore not be used for visualization of substances in hair follicles.

In hair follicle research, high resolution of the visualized area is necessary, paired with reaching deep layers of the skin for the visualization of the hair bulb. Since the current in vivo visualization techniques described above are either limited in resolution or depth penetration, it was decided to primarily focus on a promising in vitro technique fulfilling the above mentioned requirements. Therefore, confocal laser scanning microscopy is the method of choice, if fixation of the skin is circumvented by alternative methods and if the skin is sliced perpendicular to the skin surface. This immediately limits the confocal method for visualization in deeper follicular regions to the ex vivo situation. Subsequently, the in vitro results might be investigated in vivo using either confocal Raman spectroscopy in combination with confocal laser scanning microscopy or magnetic resonance imaging accepting limited resolution or limited depth visualization. Although these drawbacks have to be accepted, first in vitro/in vivo correlation of penetration into the human hair follicle might be accessible.

Real-Time Diffusion. Recently, a technique has been established that enables one to examine *on-line* the penetration of a fluorophore from the skin surface, across the viable epidermis into the dermis. Importantly, with this method it is also possible to visualize the permeation along the hair follicles in the various depths of the skin even as far as the hair bulb, which is located in the subcutaneous fat.

In order visualize on-line diffusion of fluorphores in one image in the epidermis, dermis, and the pilosebaceous unit, the skin has to be sliced perpendicular to the skin surface along the hair follicle. This was achieved with a specially designed cutting device previously used to create the manual cross sections (61–63,83). This cutting device was modified such that immediately after cutting and placing of an additional subpart of this device, a donor compartment is created at the stratum corneum side and an acceptor compartment at the dermis side of the cross section (Fig. 4). The acceptor and donor compartments were sealed with dental clay and a cover slip. The same cover slip was also covering the skin cross section. This enables to visualize the skin cross section with the confocal scanning laser microscope. Immediately after putting together the on-line diffusion cell, the donor and acceptor phases were injected through the dental clay. The donor phase consisted of the medium lipophilic dye (Bodipy® FL C_5) in citric acid buffer pH 5.0. Directly after application of the dye, images were obtained every 10 minutes for 8.5 hours using a high magnification and focusing on the stratum corneum, the epidermis, and the dermis. After image acquisition, the change in fluorescence was quantified and evaluated as function of time and location in the skin (Fig. 5). Focusing on the epidermis and the dermis, detailed information regarding the change in fluorescence intensity in time and depth (pixel resolution) was obtained. In stratum corneum, the fluorescence gradient was steep in the superficial layers and became gradually less steep in the deeper layers, demonstrating that the stratum corneum is not a homogeneous layer for diffusion. The fluorescent gradient was less steep in viable epidermis and dermis. At the junction of stratum corneum/viable epidermis, a sharp increase in fluorescence is observed while at the epidermal/dermal junction, a sudden drop in fluorescence was detected. This indicated that the dye was more easily dissolved in the epidermis than in the stratum corneum and dermis. From this study, it can be concluded that with the newly developed technique depth- and time-resolved visualization of dye penetration into unfixed skin is possible.

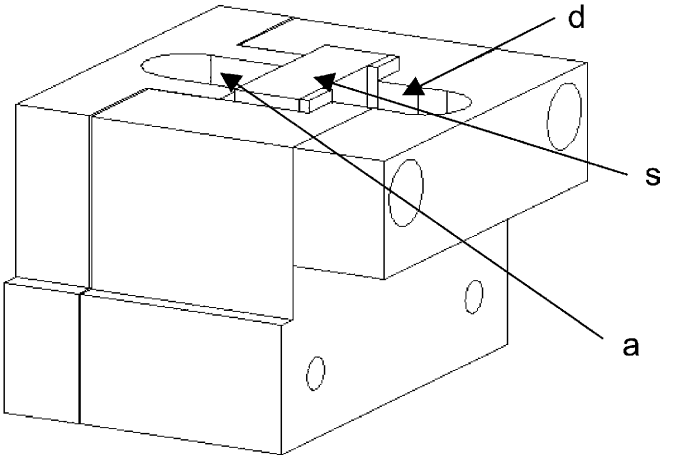


Figure 4 On-line visualization device containing cross-sectioned skin (**s**), donor compartment (**d**), and acceptor compartment (**a**). The stratum corneum of the cross section is facing the donor compartment. The cutting plane of the cross section is sealed with a cover slip and dental clay (not depicted) enabling on-line visualization of the diffusion process by confocal laser scanning microscopy.

Using this on-line visualization technique, the penetration of fluorophores into the hair follicle was also visualized. Images were obtained at a 30-minute interval for 16 hours (83). During image evaluation, the relative quantification method developed for the static visualization (61) was adapted to include additional regions like the gap of the hair follicle and to calculate accumulation at different depths of the same skin cross section. In the initial period, the penetration of the medium lipophilic dye, Bodipy FL C_5, occurred mainly via the gap and cuticle. After this period, penetration via the epidermis became more important. Label in the cuticle originated mainly from the gap and permeated in the cuticular region deeper into the skin. Dye in the outer root sheath originated either from the gap or from the epidermis. This observations are in agreement with the findings of Scheuplein (49).

In order to answer the question, how the diffusion from the hair follicle close to the surface proceeded into deeper skin regions and whether label would reach the hair bulb, a third study was conducted with on-line measurements at increasing depth, at the surface, and typically at 800, 2100, and 4000 μm in depth (84). Due to the dilemma that a high magnification in CLSM cannot be combined with a field of view including the stratum corneum at 0 μm and the hair bulb at >2000 μm depth, different donors had to be used for each selected depth in the skin (800, 2100, and 4000 μm). Close to the skin surface, the gap and the cuticle of the hair follicle was stained at a very early stage of the permeation process. Label, which reached deeper layers in the cuticle region, was permeating from the cuticle into the surrounding areas, namely the inner and outer root sheath. At depth of up to 1000 μm, diffusion via the follicular route (cuticle, outer root sheath) was dominating in the initial time period, while the surrounding dermis was stained afterwards. At greater depths, the diffusion via the dermis gained more importance indicated by the earlier staining of the subcutaneous fat as compared to any part of the hair follicle. Although the hair bulb was visualized, no label diffusion into the bulb was detected.

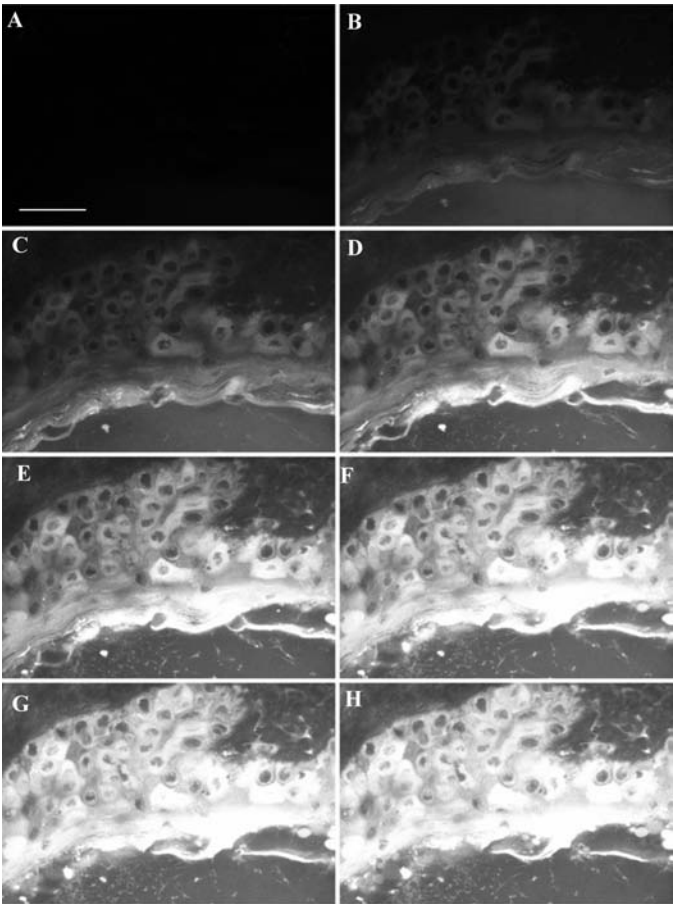


Figure 5 A typical example of on-line visualization of the distribution of 0.1 mg/mL Bodipy FL C_5 in citric acid buffer applied at time point zero in the donor compartment. Images were obtained every 10 minutes from which time points 10 minutes (**A**), 50 minutes (**B**), 1 hour 30 minutes (**C**), 2 hours 10 minutes (**D**), 2 hours 50 minutes (**E**), 3 hours 30 minutes (**F**), 4 hours 10 minutes (**G**), and 4 hours 50 minutes (**H**) are displayed. The box depicted in (**B**) resembles the quantified area at all time points that are provided in Figure 5. The scale bar is equivalent to 25 μm.

The results of these studies demonstrate that the on-line visualization technique is a very powerful tool to visualize diffusion processes into deeper regions of the nonfixed fresh skin. It has also the potential to study in vitro transport processes on cellular level including gene transport studies. In the upper regions of scalp skin, the follicular route is of great importance in the initial diffusion period. Deeper in the skin, diffusion via the dermis gains importance as well. Results indicate that targeting a drug substance with similar lipophilicity as the model penetrant to the hair follicle (especially the cuticle and outer root sheath) in the upper regions of the dermis appears possible. Depths where the bulge region (highly proliferative cells) is present might be reached. However, penetration of the drug substance (especially when lipophilic) via the stratum corneum into the dermis and subsequently the systemic circulation cannot be excluded. Therefore, care has to be taken when using toxic substances. Targeting the hair bulb solely via topical application appears to be difficult and only feasible if highly potent molecules are used.

REFERENCES

1. Cotsarelis G, Sun T, Lavker RM. Label-retaining cells reside in the bulge area of pilosebaceous unit: implications for follicular stem cells, hair cycle, and skin carcinogenesis. Cell 1990; 61:1329–1337.
2. Ebling FJG, Hale PA, Randall VA. Hormones and hair growth. In: Goldsmith LA, ed. Physiology, Biochemistry and Molecular Biology of the Skin. Oxford: Oxford Press, 1991:660–696.
3. Plewig G. Models to study follicular diseases. In: Plewig G, ed. Skin Models to Study Function of and Disease of Skin. Berlin: Springer-Verlag, 1986:13–23.
4. Price VH. Alopecia areata: clinical aspects. J Invest Dermatol 1991; 101:68S.
5. Price ML, Griffiths WAD. Normal body hair—a review. Clin Exp Dermatol 1985; 10:87–97.
6. Schaefer H, Redelmeier TE. Skin Barrier: Principles of Percutaneous Absorption. Basel: Karger, 1996.
7. Barry BW. Dermatological Formulations: Percutaneous Absorption. New York: Marcel Dekker, 1983.
8. Hadgraft J. Skin, the final frontier. Int J Pharm 2001; 224:1–18.
9. Winsor T, Burch GE. Differential roles of layers of human epigastric skin on diffusion of water. Arch Intern Med 1944; 74:428–444.
10. Odland GF. Structure of the skin. In: Goldsmith LA, ed. Physiology, Biochemistry and Molecular Biology of the Skin. New York: Marcel Dekker, 1991:3–62.
11. Marks R, Barton SP. The significance of size and shape of corneocytes. In: Marks R, Plewig G, eds. Stratum Corneum. Berlin: Springer, 1983:175–180.
12. Greene RS, Downing DT, Pochi PESJS. Anatomical variation in the amount and composition of human skin surface. J Invest Dermatol 1970; 54:240–247.
13. Lampe MA, Burlingame AL, Whitney J, Williams ML, Brown BE, Roitman E, Elias PM. Human stratum corneum lipids: characterization and regional differences. J Lipid Res 1983; 24:120–130.
14. Szabo G. The regional frequency and distribution of hair follicles in human skin. In: Montagna W, ed. Biology of Hair Growth. New York: Academic Press, 1958:33–38.
15. Briggaman RA, Wheeler CE. The epidermal–dermal junction. J Invest Dermatol 1975; 65:71–84.
16. Wertz PW, Downing DT. Stratum corneum: biological and biochemical considerations. In: Hadgraft J, Guy RH, eds. Transdermal Drug Delivery. New York: Marcel Dekker, 1989:1–22.
17. Breathnach AS, Goodman T, Stolinski C, Gross M. Freeze fracture replication of cells of stratum corneum of human epidermis. J Anat 1973; 114:65–81.
18. Bachinger HP, Morris NP, Cunstrum GP, Keene DR, Rosenbaum LM, Compton LA, Burgeson RE. The relationship of the biophysical and biochemical characteristics of type VII collagen to the function of anchoring fibrils. J Biol Chem 1990; 265:10095–10101.
19. Holbrook KA, Wolff K. The structure and development of skin. In: Fitzpatrick TB, Eisen AZ, Wolff K, Freedberg IM, Austen KF, eds. Dermatology in General Medicine. New York: McGraw-Hill, 1993:97–154.
20. Sandberg LB, Soske NT, Wolt LTB. Structure of elastic fibre: an overview. J Invest Dermatol 1982; 79:128S–132S.
21. Uitto J. Biology of dermatological cells and extracellular matrix. In: Fitzpatrick TB, Eisen AZ, Wolff K, Freedberg IM, Austen KF, eds. Dermatology in General Medicine. New York: McGraw-Hill, 1993:221–240.
22. Sperling LC. Hair anatomy for the clinician. J Am Acad Dermatol 1991; 25:1–17.
23. Blume U, Ferracin J, Vershoore M, Czernielewski JM, Schaefer H. Physiology of the vellus hair follicle: hair growth and sebum excretion. Br J Dermatol 1991; 124: 21–28.
24. Saint-Leger D. Physiology of the pilosebaceous follicle. Rev Prat 1994; 43:2315–2319.

25. Wester RC, Maibach HI. Animal models for percutaneous absorption. In: Shaw VP, Maibach HI, eds. Topical Drug Bioavailability, Bioequivalence and Penetration. New York: Plenum Press, 1993:333–350.
26. Elias PM. Epidermal lipids, barrier function and desquamation. J Invest Dermatol 1983; 80:44S–49S.
27. Cullander C, Guy RH. Routes of delivery: case studies; transdermal delivery of peptides and proteins. Adv Drug Deliv Rev 1992; 8:291–329.
28. Hashimoto K, Kanzaki T. Surface ultrastructure of human skin. Acta Derm Venerol 1975; 55:413–430.
29. Odland GF. A submicroscopic granular component in human epidermis. J Invest Dermatol 1960; 34:11–15.
30. Stewart ME, Downing DT. Chemistry and function of mammalian sebaceous lipids. Adv Lipid Res 1991; 24:263–301.
31. Bertolino AP, Klein LM, Freedberg IM. Biology of hair follicles. In: Fitzpatrick TB, Eisen AZ, Wolff K, Freedberg IM, Austen KF, eds. Dermatology in General Medicine. New York: McGraw-Hill, 1993:289–293.
32. Schaefer H, Lademann J. The role of follicular penetration—a differential view. Skin Pharmacol Appl Skin Physiol 2001; 14(suppl 1):23–27.
33. Viragh PA, Meuli M. Human scalp hair follicle development from birth to adulthood: statistical study with special regard to putative stem cells in the bulge and proliferating cells in the matrix. Arch Dermatol Res 1995; 287:279–284.
34. Hashimoto K, Shibazaki S. Ultrastructural study on differentiation and function of hair. In: Kobori T, Montagna W, Toda K, Ishibashi Y, Hori Y, Morikawa F, eds. Biology and Disease of the Hair. Tokyo: University of Tokyo Press, 1976:23–57.
35. Chase HB. Growth of the hair. Phys Rev 1954; 34:113–126.
36. Stenn KS, Paus R. Controls of hair follicle cycling. Physiol Rev 2001; 81:449–494.
37. Fuchs E, Merrill BJ, Jamora C, DasGupta R. At the roots of a never-ending cycle. Dev Cell 2001; 1:13–25.
38. Panteleyev AA, Jahoda CAB, Christiano AM. Hair follicle predetermination. J Cell Sci 2001; 114:3419–3431.
39. Agarwal R, Katare OP, Vyas SP. The pilosebaceous unit: a pivotal route for topical drug delivery. Methods find. Exp Clin Pharmacol 2000; 22:129–133.
40. Kitson N, van-Lennep EW. Intercellular junctions and the permeability barrier in human sebaceous glands. Br J Dermatol 1984; 110:601–606.
41. Lowenstein EJ. Isotretinoin made S.M.A.R.T. and simple. Cutis 2002; 70:115–120.
42. Hardy MH. The secret life of hair follicle. Trends Genet 1992; 8:55–61.
43. Ryan TJ. Cutaneous circulation. In: Goldsmith LA, ed. Physiology, Biochemistry and Molecular Biology of the Skin. Oxford: Oxford Press, 1991:1019–1084.
44. Alexeev V, Igoucheva O, Domashenko A, Cotsarelis G, Yoon K. Localized in vivo genotypic and phenotypic correction of the albino mutation in skin by RNA–DNA oligonucleotide. Nat Biotechnol 2000; 18:43–47.
45. Hashimoto K, Ito M, Suzuki Y. In: Orfanos CE, Happle R, eds. Hair and Hair Diseases. Chapter 6. Berlin: Springer, 1990:117–147.
46. Cotsarelis G, Millar S. Towards a molecular understanding of hair loss and its treatment. Trends Mol Med 2001; 7:293–301.
47. Moser K, Kriwet K, Naik A, Kalia YN, Guy RH. Passive skin penetration enhancement and its quantification in vitro. Eur J Pharm Biopharm 2001; 52:103–112.
48. Keister JC, Kasting GB. The use of transient diffusion to investigate transport pathways through skin. J Control Rel 1986; 4:111–117.
49. Scheuplein RJ. Mechanism of percutaneous absorption. II. Transient diffusion and the relative importance of various routes of skin penetration. J Invest Dermatol 1967; 48:79–88.
50. Feldman RJ, Maibach H. Regional variations in percutaneous penetration of ^{14}C-cortisol in man. J Invest Dermatol 1967; 48:181–183.

51. Kao J, Hall J, Helman G. In vitro percutaneous absorption in mouse skin: influence of skin appendages. Toxicol Appl Pharmacol 1988; 94:93–103.
52. Schaefer H, Watts F, Brod J, Illel B. Follicular penetration. In: Scott RC, Guy RH, Hadgraft J, eds. Prediction of Percutaneous Penetration; Methods, Measurements, Modelling. London: IBC Technical Services, 1990:163–173.
53. Wepierre J, Doucet O, Marty JP. Percutaneous absorption of drugs in vitro: role of transepidermal and transfollicular routes. In: Scott RC, Guy RH, Hadgraft J, eds. Prediction of Percutaneous Penetration; Methods Measurements Modeling. Proceedings of the Conference held in April, 1989. London: IBC Technical Services, 1990:129–134.
54. Lieb LM, Liimatta AP, Bryan RN, Brown BD, Krueger GG. Description of the intrafollicular delivery of large molecular weight molecules to follicles of human scalp skin in vitro. J Pharm Sci 1997; 86:1022–1029.
55. Lauer AC, Lieb LM, Ramachandran C, Flynn GL, Weiner ND. Transfollicular drug delivery. Pharm Res 1995; 12:179–186.
56. Kammerau B, Zesch A, Schaefer H. Absolute concentrations of dithranol and triacetyldithranol in the skin layers after local treatment: in vivo investigations with four different types of pharmaceutical vehicles. J Invest Dermatol 1975; 64:145–149.
57. Touitou E, Meidan VM, Horwitz E. Methods for quantitative determination of drug localized in the skin. J Control Rel 1998; 56:7–21.
58. Reifenrath WG, Hawkins GS, Kurtz MS. Percutaneous penetration and skin retention of topically applied compounds: an in vitro–in vivo study. Pharm Sci 1991; 80:526–532.
59. Tsai JC, Flynn GL, Weiner N, Ferry JJ. Influence of application time and formulation reapplication on the delivery of minoxidil through hairless mouse skin as measured in Franz diffusion cells. Skin Pharmacol 1994; 7:270–277.
60. Turner NG, Guy RH. Visualization and quantitation of iontophoretic pathways using confocal microscopy. J Invest Dermatol Symp Proc 1998; 3:136–142.
61. Grams YY, Bouwstra JA. A new method to determine the distribution of a fluorophore in scalp skin with focus on hair follicles. Pharm Res 2002; 19:350–354.
62. Grams YY, Bouwstra JA. Penetration and distribution of three lipophilic probes in vitro in human skin focusing on the hair follicle. J Control Rel 2002; 83:253–262.
63. Grams YY, Alaruikka S, Lashley L, Caussin J, Whitehead L, Bouwstra JA. Permeant lipophilicity and vehicle composition influence accumulation of dyes in hair follicles of human skin. Eur J Pharm Sci 2002; 18:329–336.
64. Nerella NG, Drennen JK. Depth-resolved near-infrared spectroscopy. Appl Spectrosc 1996; 50:285–291.
65. Corcuff P, Pierard GE. Skin imaging: state of the art at the dawn of the year 2000. Skin Bioeng 1998; 26:1–11.
66. Richard S, Querleux B, Bittoun J, Idy-Peretti I, Jolivet O, Cermakova E, Leveque JL. In vivo proton relaxation times analysis of the skin layers by magnetic resonance imaging. J Invest Dermatol 1999; 97:120–125.
67. Song HK, Wehrli FW, Ma JF. In vivo MR microscopy of the human skin. Magn Reson Med 1997; 37:185–191.
68. Szayna M, Kuhn W. In vivo and in vitro investigations of hydration effects of beauty care products by high-field MRI and NMR microscopy. J Eur Acad Dermatol Venerol 1998; 11:122–128.
69. Bull RH, Bates DO, Mortimer PS. Intravital video-capillaroscopy for the study of the microcirculation in psoriasis. Br J Dermatol 1992; 126:436–445.
70. Morris JL. Cotransmission from sympathetic vasoconstrictor neurons to small cutaneous arteries in vivo. Am J Physiol Heart Circ Physiol 1999; 46:H58–H64.
71. Salmon T, Walker RA, Pryer NK. Advances in microscopy—part III; video-enhanced differential interference contrast light microscopy. Biotechniques 1989; 7:624–633.
72. Stanton AWB, Patel HS, Levick JR, Mortimer PS. Increased dermal lymphatic density in the human leg compared with the forearm. Microvasc Res 1999; 57:320–328.

73. Turnbull DH, Starkoski BG, Harasiewicz KA, Semple JL, From L, Gupta AK, Sauder DN, Foster FS. 40–100 MHz B-SCAN ultrasound backscatter microscope for skin imaging. Ultrasound Med Biol 1995; 21:79–88.
74. Aghassi D, Anderson RR, Gonzalez S. Time-sequence histologic imaging of laser-treated cherry angiomas with in vivo confocal microscopy. J Am Acad Dermatol 2000; 43:37–41.
75. Bertrand C, Corcuff P. In vivo spatio-temporal visualization of the human skin by real-time confocal microscopy. Scanning 1994; 16:150–154.
76. Corcuff P, Bertrand C, Leveque JL. Morphometry of human epidermis in vivo by real-time confocal microscopy. Arch Dermatol Res 1993; 285:475–481.
77. Cullander C. Light microscopy of living tissue: the state and future of the art. J Investig Dermatol Symp Proc 1998; 3:166–171.
78. Grewal BS, Naik A, Irwin WJ, Gooris G, de-Grauw GJ, Gerritsen HG, Bouwstra JA. Transdermal macromolecular delivery: real-time visualization of iontophoretic and chemically enhanced transport using two-photon excitation microscopy. Pharm Res 2000; 17:788–795.
79. Hoogstraate AJ, Cullander C, Nagelkerke JF, Spies F, Verhoef J, Schrijvers AHGJ, Junginger HE, Boddé HE. A novel in-situ model for continuous observation of transient drug concentration gradients across buccal epithelium at the microscopical level. J Control Rel 1996; 39:71–78.
80. Rajadhyaksha M, Gonzalez S, Zavislan JM, Anderson RR, Webb RH. In vivo confocal scanning laser microscopy of human skin II: advances in instrumentation and comparison with histology. J Invest Dermatol 1999; 113:293–303.
81. Caspers PJ, Lucassen GW, Wolthuis R, Bruining HA, Puppels GJ. In vitro and in vivo Raman spectroscopy of human skin. Biospectroscopy 1998; 4:S31–S39.
82. Caspers PJ, Lucassen GW, Carter EA, Bruining HA, Puppels GJ. In vivo confocal Raman microspectroscopy of the skin: noninvasive determination of molecular concentration profiles. J Invest Dermatol 2001; 116:434–442.
83. Grams YY, Whitehead L, Cornwell P, Bouwstra JA. Time and depth resolved visualization of the diffusion of a lipophilic dye into the hair follicle of fresh unfixed human scalp skin. J Control Rel 2004; 98:367–378.
84. Grams YY, Whitehead L, Lamers G, Stuurman N, Bouwstra JA. On-line diffusion profile of a lipophilic model dye in different depth of a hair follicle in human scalp skinscalp skin. J Invest Dermatol 2004. In press.

13
Evaluation of Stratum Corneum Heterogeneity

Gerald B. Kasting, Matthew A. Miller, and Priya S. Talreja
College of Pharmacy, University of Cincinnati, Cincinnati, Ohio, U.S.A.

When confronted with an organ as complex as skin, a biologist tends to want to relate structure to function at the most fundamental level, and indeed an enormous amount of complexity may be found. A physical scientist, on the other hand, looks for simplifying assumptions that allow him to describe the system within a mathematical framework and to make quantifiable predictions about its behavior. There is often a credibility gap between the two approaches, and the appropriate balance point moves as different problems are addressed. There is little doubt that the elegant work of Elias (1,2), Steinert (3,4), Wertz (5,6) and many others in the chemistry and structural biology of the stratum corneum (SC) has enormously increased our understanding of skin barrier function; however, the simplifying framework introduced by Scheuplein and Blank (7) and advanced by others, including Flynn (8), Roberts (9,10), Cooper (11), and Potts and Guy (12), has had a comparable impact on quantifying its properties. The Potts–Guy model for steady-state skin permeability (12) and extensions thereof (13) are arguably the most widely used predictive tools in transdermal drug delivery and dermal risk assessment (14).

Potts and Guy treated skin as a homogeneous lipid membrane, arguing against the need for additional features to explain the steady-state absorption of many organic compounds from aqueous solution (12). The molecular properties determining absorption were molecular weight and octanol-water partition coefficient. Elaborations on this scheme have included an aqueous barrier in series with the SC (14,15), a polar pathway in parallel with the lipid pathway (16–18) or both (13,19), providing reasonable limits to skin permeability for extremely hydrophilic and lipophilic compounds. Other descriptors, notably hydrogen bond donor and acceptor strength (20,21), have been proposed, as well as quantitative structure – property relationships (22,23) and neural network approaches (24), yet it is not clear that significant improvements to the basic model have been achieved. Some investigators have considered the tortuosity of the lipid pathway in deriving SC barrier properties (16,25–27), under the assumption that corneocytes are impermeable. Due to the longer path length, these models yield higher effective diffusivities for permeants in the SC than do homogeneous membrane models. However, Frasch and Barbero's notable analysis (27) shows that diffusion via a tortuous pathway and that through a homogeneous slab cannot be

distinguished on the basis of macroscopic observations, unless the underlying transport properties are known. Thus, the tortuous pathway formulation of SC permeability leads to predicted permeation profiles similar to those of Potts and Guy (12). More complex behavior is possible if the corneocytes are considered to be permeable (28,29); however, the full implications of this approach with regard to the time course of permeation have yet to be explored.

I. WHAT IS MEANT BY SKIN HETEROGENEITY?

For the purposes of discussion, three levels of heterogeneity in skin may be distinguished: (1) multiple pathways and barriers for transport through full thickness skin, (2) biphasic "brick-and-mortar" structure of the SC, and (3) variation of SC properties with depth. Much has been learned about the first two levels, as summarized in the preceding paragraph, although complete descriptions of neither are available. Both are considered central to a discussion of barrier function. The impact of the third level, asymmetry of the SC, is less certain. This is an area where effective approximations to the complex structure and composition gradients are essential for predictive transport models, because the microscopic transport properties of individual SC layers are not experimentally accessible. Thus, despite the eloquent arguments of Elias (30) and others regarding the biological complexity of the SC barrier, there is still merit to simpler models. This chapter presents a physical chemistry perspective on the factors that must be included in order to make a generally useful description of transport across the SC. The impact of lower skin layers and the cutaneous circulation, although important to a general picture of skin absorption, is not considered here.

II. THE ROLE OF APPENDAGES AND THE SKIN'S POLAR PATHWAY

The importance of skin appendages—hair follicles and sweat ducts—to the transport of ions and highly polar molecules across skin is easily established. Examples include the perifollicular wheal and flare response induced by topical application of histamine ($K_{oct} = 0.20$) (31), punctuate patterns of dyes administered to skin via iontophoresis (32,33), and localized electric fields observed indirectly at the skin surface during passage of mild electric currents (34–36). Peck and co-workers distinguished permeants penetrating via this "polar pathway," which most likely includes microscopic defects in the SC lipid lamellar structure, by their low permeabilities and low activation energies for diffusion relative to lipophilic permeants (17,18). Appendageal contributions to the transport of lipophilic compounds across the SC are less obvious, but still demonstrable on the basis of transient diffusion analyses (37). Figure 1 shows data obtained recently in our laboratory supporting the need for a two-pathway diffusion model to explain transient diffusion profiles for permeants spanning a wide range of lipophilicity. The data were obtained using small doses of radiolabeled compounds applied to split-thickness (250–300 μm), cadaveric human skin mounted in Franz diffusion cells and tested according to previously described methods (37,38). In each case a homogeneous membrane model (37) failed to describe the early stage of the absorption process, which was much more rapid than can be accounted for by diffusion through a slab. In most cases (but not for the flavonoid, kaempferol), permeation after several hours was well described by the single pathway model. The second pathway having the shorter lag time, but

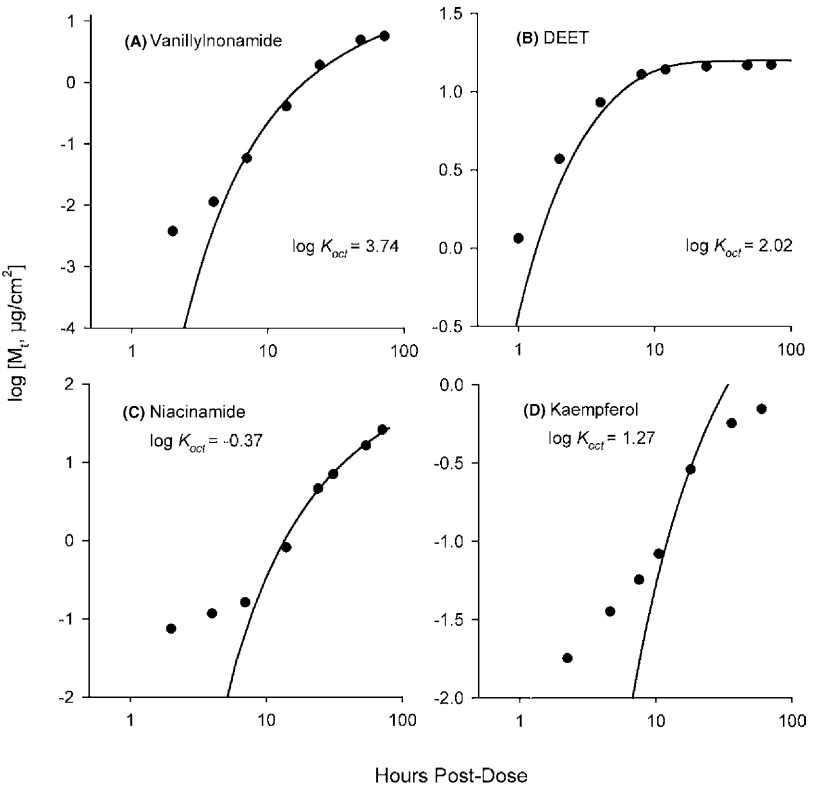


Figure 1 Permeation time course of four radiolabeled compounds through split-thickness human skin in vitro. The compounds were applied in simple solvent systems (5 µL/0.79 cm^2 cell) at doses of 10–100 µg/cm^2. (**A**) ^{14}C-vanillylnonanamide in propylene glycol (37); (**B**) ^{14}C-DEET in ethanol; (**C**) ^{14}C-niacinamide in 1:1 v/v ethanol/water; (**D**) ^{3}H-kaempferol in propylene glycol. The solid lines are theoretical curves for finite dose permeation through a homogeneous membrane (37) that have been fit to the data. The theory for DEET includes a first-order evaporative loss from the skin surface (89). The positive departures of the data from the theory suggest a second (shunt) pathway through the stratum corneum having a very short time lag.

clearly a limited capacity, is most likely related to either skin appendages or to microscopic defects in the SC lipid lamellae. These observations are consistent with the predictions of Scheuplein more than three decades earlier (39) and also with earlier results obtained by one of the authors using aqueous ibuprofen solutions applied to split-thickness skin (40). They may be important for understanding how nicotinate esters cause flushing within minutes of application to skin in vivo (41). It may be concluded that shunt pathways are important for most compounds during the initial transient phase of absorption and at all times for very hydrophilic compounds or for high molecular weight species (17) that cannot otherwise penetrate the skin.

III. THE ROLE OF CORNEOCYTES IN THE STRATUM CORNEUM BARRIER

Perhaps the most unfortunate consequence of the "brick-and-mortar" analogy for SC structure is the tendency to think of corneocytes as impermeable obstacles.

The body of evidence to the contrary is compelling. First and foremost, immersion in water leads to swelling of the SC to several times its normal thickness in about an hour (42–45). Although a small amount of water may hydrate lipid head groups in the lipid lamellae (46), the bulk of the water must enter the corneocytes, as the lamellar spacings do not change significantly with hydration (47). Nuclear magnetic resonance (NMR) studies have shown the diffusivity of mobile protons in partially hydrated SC (guinea pig footpad hydrated to ~43% w/w) to be 2.8×10^{-6} cm^2/s, only 10-fold less than the self-diffusivity of water (48,49). This signal presumably derives largely from water within the corneocytes (49). Water diffusivity in fully hydrated corneocytes is likely to be higher; an estimate from hindered diffusion theory including keratin–water binding interaction is 1.07×10^{-5} cm^2/s (50).

There is a school of thought that it is the cornified cell envelopes (CEs), rather than the keratinized interiors, that leads to corneocyte impermeability. This thinking appears to derive from a consideration of the chemical resistance of the CE, which is indeed formidable. Boiling in alkali is required to degrade these structures. It is supported by microscopic studies of heavy metal distribution in SC that show a higher fraction of metal ions or metal ion precipitates within apical corneocytes following topical administration than in the lower layers (51,52). The published studies of Hg^{2+} distribution (51,52) are supported by additional, unpublished work with Zn^{2+} and Cu^{2+} (Warner, personal communication). Investigators have hypothesized that desmosomal degradation in the outer SC leads to breaches in the CEs, allowing ion entry (52). Although there is merit to this idea, an alternative explanation is possible to which we will return momentarily. First, we note that the impermeable CE concept is inconsistent both with spectroscopic studies of water diffusion in SC (48,49) and with organic solute partitioning and permeability relationships in SC (53,54), as follows.

Packer and Sellwood studied samples of partially hydrated guinea pig footpad SC by ^{1}H NMR, using both relaxation (48) and pulsed field-gradient spin-echo (49) techniques. The latter measurements, which were conducted in oriented SC samples, provided estimates of the diffusivity and the characteristic diffusion length of ''mobile protons'' within the sample. According to their analysis, the characteristic diffusion length of these protons in the direction perpendicular to the plane of the tissue was three to four μm, consistent with diffusion within the interior of a partially hydrated corneocyte. Extraction of lipids with 2:1 chloroform:methanol ''produced fairly large 'holes' in the cell walls which considerably reduced the degree of restriction in the diffusion of the mobile molecules'' (49). If one takes the reasonable position (49,50) that this signal represents largely water within corneocytes, then it is evident that removal of the non-covalently bound lipid from the SC allowed water to diffuse rapidly between corneocytes. Since the cornified cell envelopes are not disrupted by this extraction, it follows that the primary diffusion barrier for water is the intercellular lipids rather than the CEs.

Evidence for corneocyte permeability to other solutes is provided by Anderson and Raykar's thoughtful analysis of SC/water partition coefficients and their relationship to SC permeability (53,54). These workers showed that permeability was directly proportional to partition coefficient for the more lipophilic solutes, but not for moderately lipophilic or hydrophilic solutes. These and related data (16,55) may be understood on the basis of a biphasic SC transport model with transfer of solutes by both lipid-continuous and lipid-corneocyte pathways (28,29). This is a subject of ongoing research in our laboratory.

We return now to the question of metal ion distribution in skin. The best known examples are two studies in which Hg^{2+} was driven into skin (as the chloride) via iontophoresis, then precipitated as the sulfide by exposure to ammonium sulfide vapors and analyzed by transmission electron microscope (TEM) (51,52). In both cases the investigators found precipitated HgS within the corneocytes in the outer layers of the SC, but only within the lipid lamellae in the lower SC. It was hypothesized (52) that the corneocytes in the lower SC are impermeable, whereas those in the upper SC are not due to the degradation of the desmosomal linkages between the corneocytes, allowing access to the corneocyte through the degraded areas. These observations led both groups to the conclusion that mercuric chloride penetrates the SC via an intercellular pathway.

We offer the following alternative interpretation. Mercuric chloride is a salt with considerable covalent character and moderate lipophilicity ($K_{oct} = 0.6$) (56). Mercury is furthermore quite reactive with organic materials, and readily forms organometallic compounds that bioaccumulate in the food chain due to their high lipophilicity (K_{oct} for dimethyl mercury, for example, is about 390) (56). Monteiro-Riviere et al. (52) noted that Hg-containing precipitates found in basal keratinocytes were localized to the mitochondrial membrane; hence, even in a predominately aqueous cellular environment, Hg partitioned into (or absorbed onto) lipid membranes. These observations suggest that the reason that Hg was found in the intercellular lipids of the lower SC is simply equilibrium partitioning rather than corneocyte impermeability. In the upper SC the intercellular lipid content may have been lower due to the desquamation process, leading to more Hg within the corneocytes. According to this reasoning, the pathway for penetration of Hg^{2+} through the tissue cannot be inferred from the distribution of Hg-containing precipitates.

To summarize this section, the partition ratio must always be considered when drawing inferences about transport pathways from steady-state (or pseudo-steady-state) tissue distributions. The key property to consider is permeability, P, defined as the product of diffusivity D and partition coefficient K:

$$P = DK \tag{1}$$

As Heisig (28) and others (25) have pointed out, in a structure such as SC with a high "internal" phase volume of corneocytes surrounded by a continuous lipid matrix, the ratio $\sigma = P_{lip}/P_{cor}$ must exceed about 10^4 before the corneocytes may be considered to be effectively impermeable. A detailed analysis allowing for anisotropic transport properties in the lipid phase and in which corneocyte permeability was carefully estimated from partition data (53–55) and hindered diffusion theory (29) suggests that the contribution of corneocytes to transport across the SC is significant for many permeants, although it cannot be estimated from a single parameter ratio as in Heisig's analysis.

IV. THE INFLUENCE OF ASYMMETRY ON SC TRANSPORT

The location of the transport barrier in skin was debated until the early 1960s, due to the propensity of the tissue to be disrupted (thereby resulting in a "basket-weave" appearance) in routine histological preparations (30). Development of the alkaline swelling technique in Kligman's laboratory (57) was a key step that allowed visualization of the highly organized, compact structure of intact SC. This was complemented by outstanding transport work, much of which was conducted by Scheuplein and Blank (7,39,58–62) that established beyond a doubt that the SC was the primary

diffusion barrier to water and most other permeants. It was also clear by the mid-1960s that the SC barrier extended across the tissue rather than residing in a thin layer at the base of the SC, as had originally been thought (59). Scheuplein and Blank provide a fascinating summary of these developments in their 1971 review (7).

Scheuplein had several lines of evidence available to support the uniformity of the SC transport barrier. Electron microscopy showed a dense, compact structure (63,64), although the staining techniques to bring out the intercellular lipids had not yet been developed. Light microscopy using the alkaline swelling technique (57,65) showed the SC to have a remarkably uniform appearance from top to bottom. An example micrograph from our laboratory is shown in Figure 2. Studies in which water transport was measured across sequentially tape-stripped skin suggested a uniform barrier (66). Osmotic shock experiments in which the SC was split into two sections of approximately equal thickness showed both sections to have excellent barrier properties (33). The latter experiments were evidently more qualitative than quantitative in nature, as details of tissue thickness and permeability were not provided. More recently, careful in vivo studies of transepidermal water loss (TEWL) from skin following sequential tape stripping have tended to confirm the picture of a uniform transport barrier, at least for water (67–69).

Detailed examination of SC structure, biochemistry and transport properties, however, has continued to reveal asymmetric features. The most obvious of these are in the first two categories. It has long been evident that the outer few layers of SC have degraded desmosomes and reduced lamellar lipid content (51,52,70). It is likely these layers offer reduced diffusional resistance due to the disruption of the ordered lipid structure. A closely related concept is that of a stratum "conjunctum" and stratum "disjunctum," the former being the compact lower SC, the latter the upper desquamating layers. This distinction was noted in the 1950s and nicely elaborated by Bowser and White (71). Recent examinations of cryopreserved SC obtained

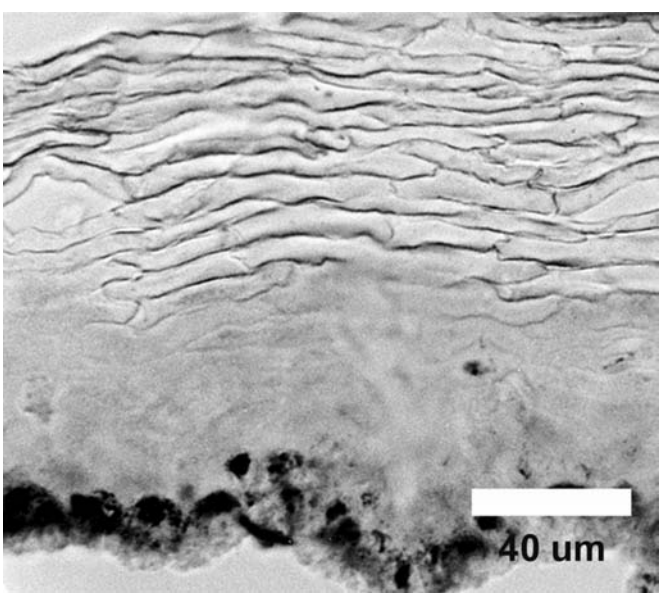


Figure 2 Brightfield image of alkaline-swollen human stratum corneum stained with methylene blue, illustrating partially ordered stacking of corneocytes. *Source*: From Ref. 26.

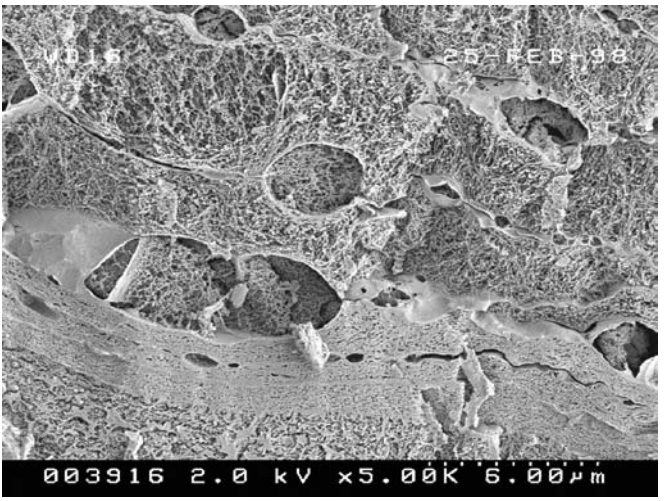


Figure 3 Cryo-SEM image of human stratum corneum (SC) following 24-hour exposure to urine in vivo. The open spaces are cisternae in the intercellular regions of the innermost SC layers, which are seen to be much less swollen than the overlying layers. There are three unswollen corneocyte layers in this micrograph *Source*: From Ref. 70.

from water-exposed skin in vivo have shown that hydration-induced swelling of the SC is also asymmetric (70,72,73). According to both reports, the lower three to four layers of the SC do not swell to the same degree as the middle layers. This phenomenon is clearly demonstrated in Figure 3. Warner argued that the incomplete breakdown of the filaggrin binding the keratin bundles in the lower SC limits the ability of the keratin to swell; moreover, the osmotic gradient contributing to swelling is not fully established because much of it comes from filaggrin breakdown products, i.e., amino acids derived from proteolytic degradation of filaggrin (70). This observation, combined with the established relationship between SC water content and permeability (43,50,74–77) suggests that the lower SC layers may be less permeable than the middle ones, at least for the case of fully hydrated skin. Offsetting this is the fact that the cornified cell envelopes in the lower SC are not fully mature, leading to a distinction between "fragile" (CEf) and "resilient" (CEr) cell envelopes as identified by mechanical properties and light microscopy (78). The CEr are more prevalent in the apical layers of the SC and the CEf more prevalent in the lower layers (78). If the CEf are, in fact, more permeable than the CEr, then the gradient of SC permeability could be opposite to that suggested by the swelling behavior. The uncertainty as to which of these features is the more important led us to conduct the studies described below.

Sorption/desorption studies on isolated SC offer a useful complement to permeation studies because different combinations of membrane properties are emphasized. A desorption study readily yields a time constant h^2/D and a partition coefficient K (79–81), whereas permeation studies give direct information on the permeability coefficient DK/h (33). In making these assignments for a heterogeneous membrane, one must recognize that the values of h, D, and K represent, respectively, *effective* thickness, diffusivity, and partition coefficient and are not in most cases equal to the microscopic transport constants (27). Nevertheless, they do characterize the macroscopic transport properties. In principle, permeation studies also yield the

time constant from the time lag $h^2/6D$; however, the latter measurement is confounded for a membrane such as SC by the contribution of polar or appendageal pathways to the early time data (Fig. 1). Sorption or desorption data are less affected by shunt pathways so long as the total shunt surface area is small compared to that of the bulk membrane. This may be seen by considering the effect of a large pinhole on permeation across and desorption from an otherwise homogeneous membrane (Fig. 4).

Sorption/desorption studies offer the possibility of studying depth-dependent transport properties of SC, because any such dependence destroys the plane of symmetry in the center of the membrane. Anissimov and Roberts (82) have provided an excellent discussion of these effects. They show that permeation and desorption studies are relatively insensitive to variation in D across the membrane, but that desorption studies are highly sensitive to variations in K. The latter is of particular significance because experimental work from the same laboratory has shown a profound variation with depth in the SC for the partition coefficient of a lipophilic permeant, clobetasol propionate (83). This result is reproduced in Figure 5. Anissimov and Roberts (82) concluded that "partition coefficient heterogeneity can be the reason for higher fluxes predicted using desorption as compared with penetration techniques," citing an earlier experimental study by one of the authors (9) in which this behavior was systematically observed.

We show below, without details, the results of several experiments from our laboratory supporting the concepts of multiple pathways and moderate asymmetry for the SC barrier. The studies involved a hydrophilic permeant, niacinamide (MW 122, log $K_{oct} = -0.37$) (84) and a lipophilic permeant, testosterone (MW 288; log $K_{oct} = 3.32$) (56). They were conducted using radiolabeled tracers,^{14}C-niacinamide

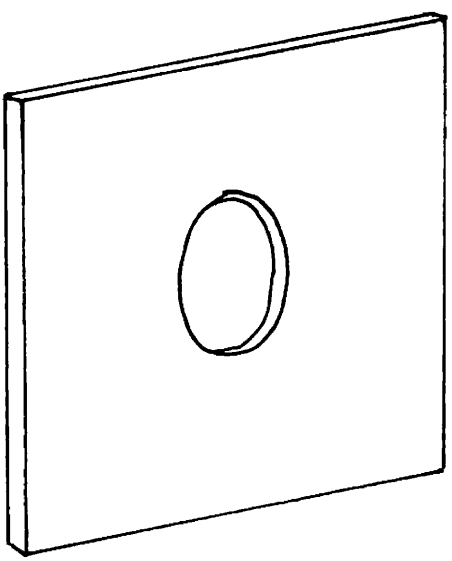


Figure 4 Illustration depicting a membrane with a large pinhole. The impact of the hole on permeation through the membrane (e.g., left to right) is enormous; however, the impact on desorption of a solute from the membrane is much smaller. For a homogeneous membrane the contribution of the hole to the initial desorption rate is proportional to the surface area of its perimeter divided by the full surface area of the membrane.

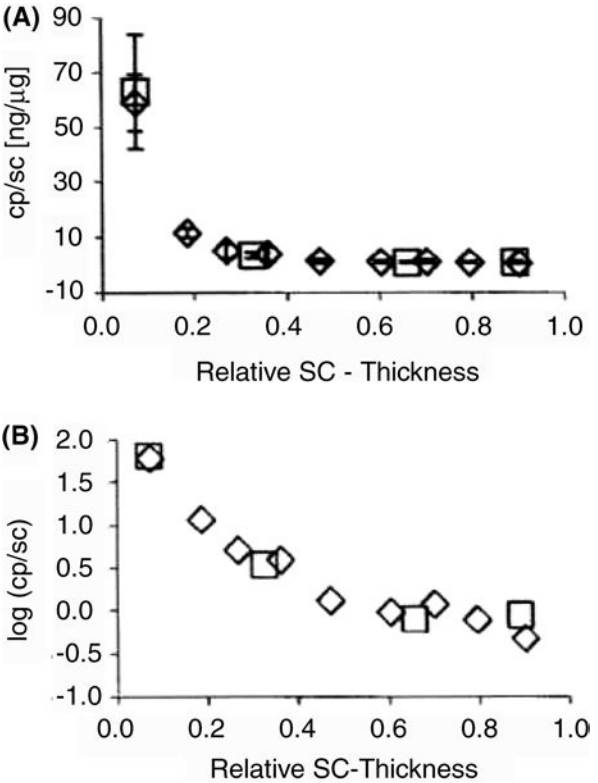


Figure 5 Variation of clobetasol propionate (CP) concentration with depth in human stratum corneum (SC) after 48 hours equilibration in a saturated solution of CP in propylene glycol. Since both sides of the membrane were exposed to the donor solution, this is an equilibrium distribution rather than a steady-state transport distribution. The apical (*upper*) side of the SC corresponds to a relative SC thickness of zero. (**A**) linear scale. (**B**) logarithmic scale *Source*: From Ref. 83.

and ^{3}H-testosterone, dissolved in pH 7.4 aqueous buffers in the presence of 5–10 µg/mL concentrations of unlabeled permeant. All studies were conducted at a skin temperature of 30°C. The first study consisted of permeation measurements across human epidermal membranes (HEM) mounted in Franz diffusion cells and desorption studies conducted with isolated SC obtained by trypsinization of epidermal membrane samples from the same skin donors (85). The skin samples were prepared by heat separation of freshly excised tissue from breast reduction surgery and were shown to have excellent barrier properties to tritiated water (38). Representative results are shown in Figures 6 and 7. The average steady-state permeability coefficients of HEM to niacinamide and testosterone, calculated as:

$$k_p = J_{ss}/\Delta C_v \tag{2}$$

where J_{ss} is steady-state flux in µg/cm^2 hr and ΔC_v is the concentration difference between the donor and receptor solutions were 4.9×10^{-5} and 9.2×10^{-3} cm/hr, respectively (Table 1). These values are in accord with expectations for high quality human skin (16). However, for both permeants, skin samples having comparable values of J_{ss} (and, consequently, of k_p) had widely varying time lags to permeation (Fig. 6). For niacinamide, some samples even showed evidence of a convective burst

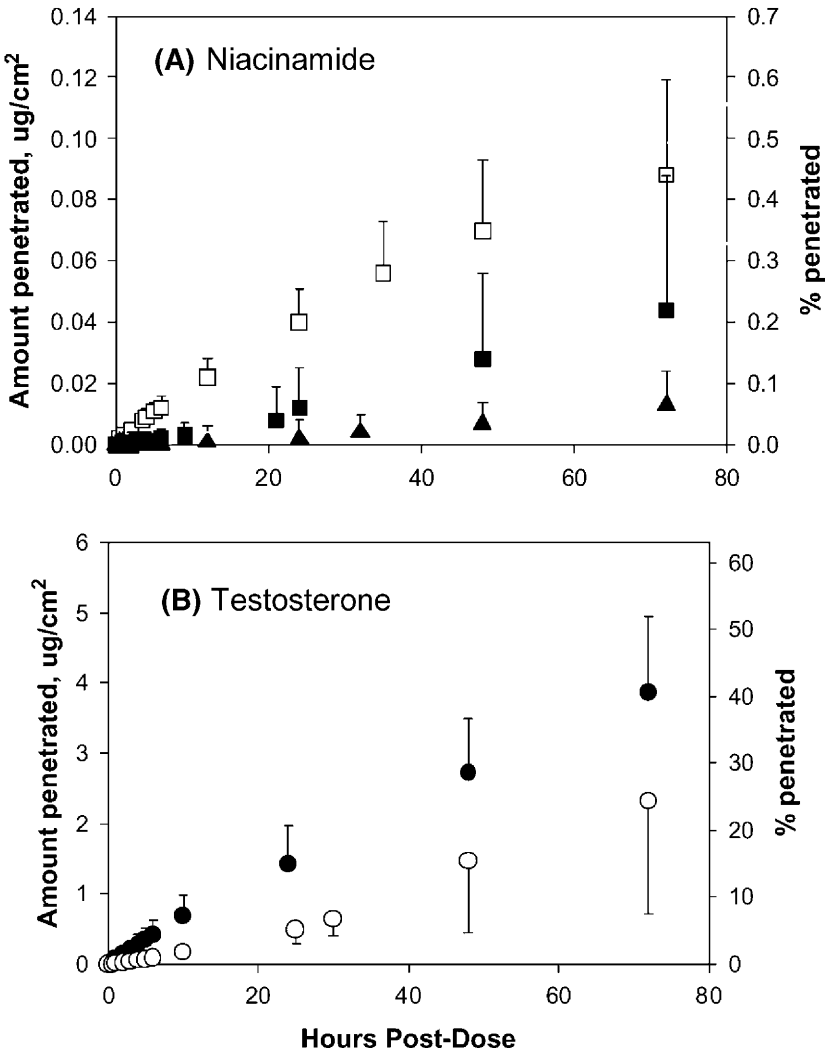


Figure 6 Permeation of (**A**) niacinamide and (**B**) testosterone across freshly excised human epidermal membrane. Each symbol represents the mean ± SE for one donor, $n = 5$–8 samples/donor. The average permeability coefficients calculated from the straight line regions are reported in Table 1.

prior to establishing a steady-state flux (data not shown). Since it is improbable that SC thickness or permeant diffusivities in these skin samples could vary enough to cause large changes in h^2/D while maintaining constant k_p, the variable time lags are most likely due to shunt diffusion. Thus, these data support the conclusion stated in a preceding section that shunt pathways contribute significantly to transient diffusion for many compounds.

Desorption of testosterone from isolated SC (Fig. 7B) was relatively rapid and followed closely the profile expected for a homogeneous membrane (79,80). The process was essentially complete within three hours. A gradual loss of radiolabel at longer times was traced to glass adsorption (85). According to diffusion theory, the initial slope of the plot of amount desorbed from a homogeneous membrane versus

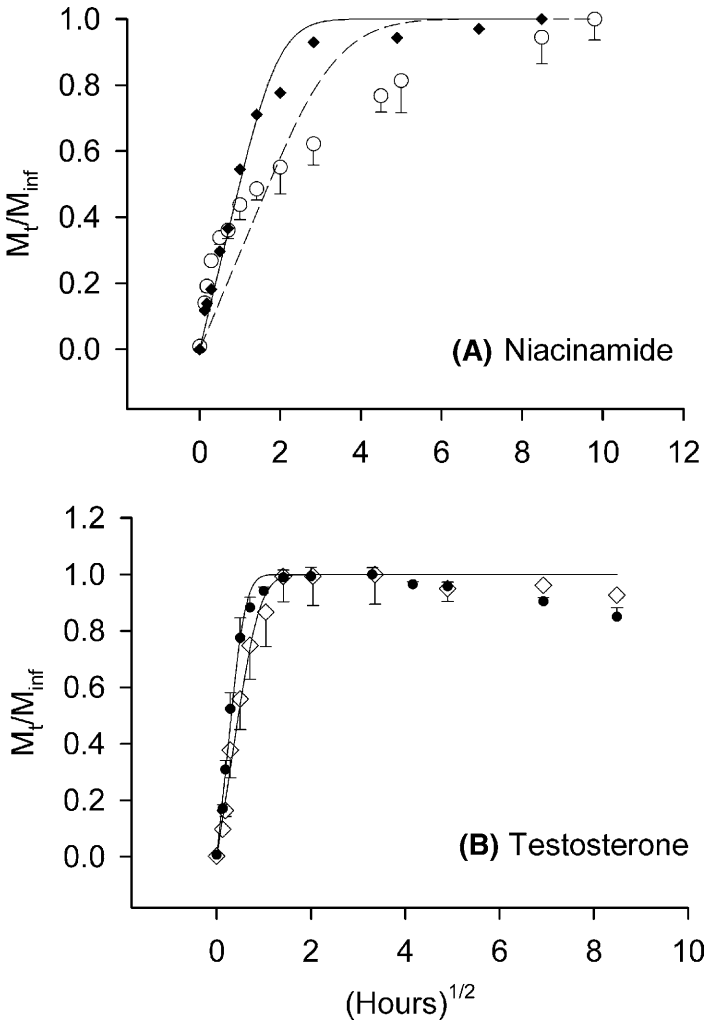


Figure 7 Desorption of (**A**) niacinamide and (**B**) testosterone from isolated human stratum corneum in vitro. Each symbol represents the mean ± SE for one donor, $n = 3$ samples/donor. *Source*: Data from Ref. 85 with revised partition coefficient calculation.

the square root of time yields the time constant h^2/D, i.e. (79,80):

$$M_t/M = 4\sqrt{\frac{Dt}{\pi h^2}} \tag{3}$$

The average time constant so calculated for testosterone was 3.2 ± 1.5 hours (Table 1). Desorption of niacinamide was much slower, although many samples had a rapid initial phase in which about 20% of the dose was desorbed (Fig. 7A). Some samples were still releasing permeant after 100 hours, although others were discharged by 24 hours. Although this behavior was clearly more complex than the homogenous membrane theory, we estimated time constants for the initial phase and the slower phase of desorption according to Equation (3). The results varied widely between samples, but averaged about 10 hours for the initial phase and 230 hours for the slow phase (Table 1).

Table 1 Transport Parameters for Niacinamide and Testosterone in Human Stratum Corneum (SC) Obtained from Analysis of Permeation and Desorption Studies According to Homogeneous Membrane Theory

Compound	No. of donors	$k_p \times 10^5$ (cm/hr)	h^2/D (hr)	$D \times 10^{10}$ (cm^2/s)	K	$P \times 10^{10}$ (cm^2/s)
Niacinamide						
Permeation	5 (31)	4.9 ± 4.7	50 ± 35[a]	4.4 ± 4.0[a]	0.29 ± 0.13	0.8[b]
Desorption (slow)	5 (14)	—	230 ± 230	0.5 ± 0.5	1.2 ± 0.3	0.6[c]
Desorption (initial)	5 (14)	—	10 ± 5	11 ± 5	1.2 ± 0.3	13[c]
Testosterone						
Permeation	3 (24)	920 ± 470	55 ± 4[a]	3.3 ± 0.1[a]	91 ± 43	160[b]
Desorption	4 (13)	—	3.0 ± 1.4	35 ± 17	7 ± 2	250[c]

Note: The thickness of hydrated SC was taken to be $h = 62.1$ μm as described in Ref. 86. Each value represents the mean ± SD of 3 to 5 donors with 3 to 10 Replicates per donor. The total number of samples is given in parentheses.

[a]Estimated from time lag of selected samples as described in Ref. 85.

[b]Calculated as $P = h \times k_p$.

[c]Calculated as $P = D \times K$.

Source: Data from Ref. 85.

Based on the concentrations of radiolabeled permeants in the uptake solutions and the total amounts desorbed, we were able to calculate bulk SC/water partition coefficients from the desorption studies using the relationship:

$$K = \frac{\text{DPM}/g \text{ wet tissue}}{\text{DPM}/g \text{ solution}} \tag{4}$$

Note that Equation (4) defines K on a wet tissue basis rather than the dry tissue basis used elsewhere (53–55). The results were $K = 1.2 \pm 0.3$ for niacinamide and $K = 7 \pm 2$ for testosterone (Table 1). The value of K for niacinamide, combined with its polarity and the fact that the lipid content of hydrated SC is only 3% to 4%, strongly suggests that it partitions into the corneocyte phase. Testosterone, being a highly lipophilic compound, could well achieve its bulk SC/water partition coefficient of seven by residing primarily in the intercellular lipids. For example, for a 3% lipid content, an SC lipid/water partition coefficient of $7/0.03 = 230$ would be required.

We tested the consistency between permeation and desorption results by further analyzing the data according to homogeneous membrane theory (79). This procedure involved estimating h^2/D for permeation from the permeation time lag $h^2/6D$, followed by calculation of D for both methods using the estimate $h = 62.1\ \mu\text{m}$ for the thickness of hydrated SC (86). K for permeation was then calculated from the relationship:

$$k_{\text{p}} = DK/h \tag{5}$$

The details of this analysis are presented elsewhere (85). It can only be viewed as an approximation due to the wide variation in permeation time lags for both compounds and the non-ideal shape of the niacinamide desorption curves. The analysis yielded two sets of transport properties, D and K, for testosterone—one from the permeation study, the other from the desorption study—and three for niacinamide. Permeability P was also calculated using $P = h \times k_p$ for permeation and Equation (5) for desorption. Considering first the slow phase of niacinamide desorption, it can be seen from Table 1 that permeation and desorption studies yielded comparable values for P, but different values for its components, D and K. The testosterone results ($D_{\text{desorption}} > D_{\text{permeation}}$) are similar to previous results obtained by Roberts and co-workers for other lipophilic compounds (9) and recently interpreted by the same group on the basis of membrane asymmetry (82,83). In light of this, we conducted the following experiment to test the symmetry of permeant release from SC.

The test was designed as a desorption study employing the same radiolabeled permeants, ^{14}C-niacinamide and ^{3}H-testosterone, and isolated human SC. In this case, however, the tissue was mounted in side-by-side diffusion cells with attention paid to the orientation of the sample. The study also employed cadaver skin rather than surgical discard skin, which may lead to somewhat higher permeability. Aside from these features, the conditions were the same as those for the experiments in Figure 7. The SC was equilibrated with solutions of each compound (2.5–5.0 μCi/mL and 5–10 μg/mL) in phosphate-buffered saline, pH 7.4, containing 0.02% sodium azide (PBS) for two to three days. The SC was then mounted in side-by-side diffusion cells maintained at 32°C, with the apical (upper) side to the left and the proximal (lower) side to the right. Desorption was initiated by simultaneously filling both the left hand and right hand compartments with PBS. Sequential samples were then withdrawn from each compartment and replaced with an equal volume of PBS.

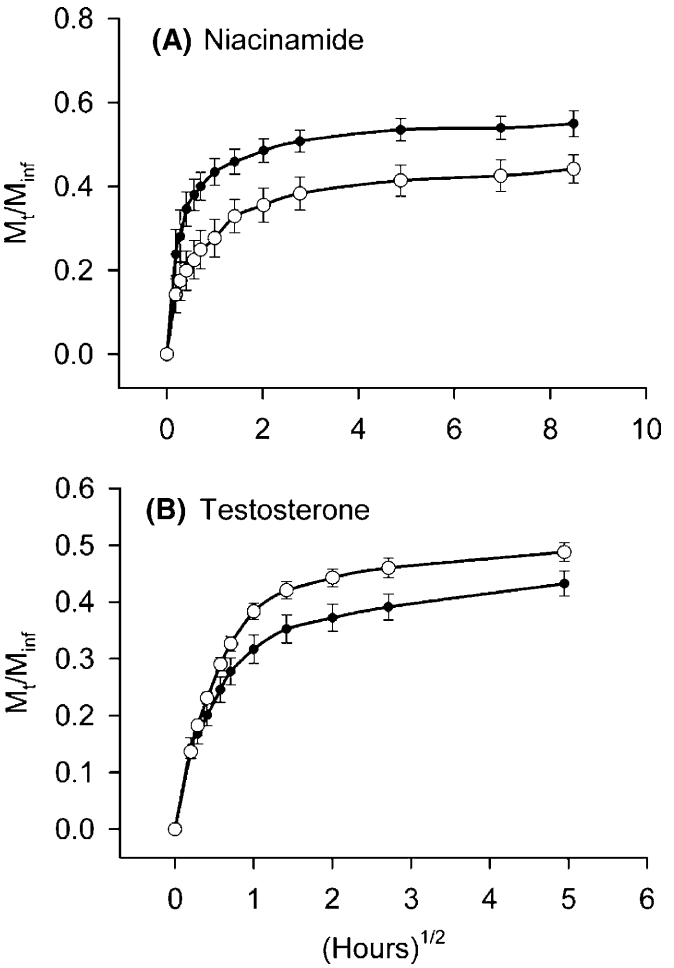


Figure 8 Desorption of (**A**) niacinamide and (**B**) testosterone from isolated human Stratum Corneum mounted in side-by-side diffusion cells. Each point represents the mean ± SE of two donors, n = four to five samples/donor. The open circles were obtained from the compartment exposed to the apical (*upper*) surface, the closed circles from the compartment exposed to the proximal (*lower*) surface.

The results of this study are shown in Figure 8. Significant differences (paired t-test, $p < 0.05$) between apical and proximal surfaces were obtained in both the initial desorption rate and the plateau desorption value for both compounds. Similarly to the studies in Figures 6 and 7, the differences for the hydrophilic and lipophilic permeants were in opposite directions. Niacinamide desorbed more rapidly and extensively from the proximal surface, whereas testosterone did so from the apical surface. Microscopic examination of cross-sectioned, alkaline-expanded sections showed no evidence for residual viable epidermis on the proximal side of the tissue. Thus the SC samples were clearly asymmetric in a rather interesting manner; however, the magnitude of the asymmetry as measured by this technique was modest. (The reader will note that this method somewhat underestimates differences between apical and proximal surfaces because of the simultaneous transport of permeant through the tissue due to the developing concentration gradient.)

V. DISCUSSION

The experiments described in this chapter provide several lines of evidence supporting the premise that SC behaves as a heterogeneous and somewhat asymmetric membrane with respect to transport. The former is not unexpected, based on its brick-and-mortar architecture (Fig. 2) and numerous transport models based on this structure (16,25–29). It should be noted that shunt diffusion is a heterogeneous feature of the SC not anticipated by brick-and-mortar models, yet evidently important in the early stages of absorption of many compounds. The results shown in Figures 1 and 6 establish that shunt diffusion contributes significantly to the transient diffusion of both hydrophilic and lipophilic substances across the SC. Other work has established its importance to the steady-state transport of ions and very polar neutral molecules across the SC, especially under the influence of an electric field (17,18,32,34–36). We consider the shunts of importance in human skin to be hair follicles, sweat ducts, and microscopic defects in the SC lipid lamellae. These penetration routes may also constitute the skin's "polar pathway"; however, their net contributions to transport appear to extend beyond polar compounds (Figs. 1A,B and 6B). Evidence for a fourth potential contributor to the polar pathway—the proteinaceous route consisting of corneocytes and their interconnecting desmosomes—is either weak or nonexistent. Such a pathway would be hard to find experimentally because of the relatively long time lag associated with the filling of the corneocytes.

The symmetry of the SC barrier has been debated for many years as previously discussed. Recent evidence supporting an asymmetric barrier is presented in this report. The SC swells non-uniformly when exposed to water or urine (Fig. 3), sorbs and desorbs compounds unevenly with respect to depth or membrane surface (Figs. 5 and 8), and yields different effective transport properties when studied by permeation and sorption methods (Figs. 6 and 7, Table 1). These phenomena inject a note of caution into inference of transport rates from membrane concentration profiles as in proposed tape-strip bioequivalence methods (87) or inference of transmembrane transport from initial desorption rates (81). The biphasic desorption of niacinamide from SC (Fig. 7A) and associated high and low diffusivities (Table 1) shows that considerable error would be incurred by basing transport calculations for this compound on initial desorption rate. A practical take-home from these studies is that traditional permeation studies (rather than desorption studies or tissue concentration profiles) should always be conducted in order to predict flux, as they integrate over asymmetries present in the membrane. From a modeling perspective, some errors will be incurred by considering the membrane to be vertically isotropic. However, if the spatial variations are of the order suggested in Figure 8, the error is likely to be acceptable. If they are more often like those shown in Figure 5 (83), then let the modeler beware! We note that the hydration gradient present in human skin in vivo (88) is a natural factor that is likely to contribute to a permeability gradient across the SC (50). The balance of this feature (which leads to lower permeability of the drier, apical layers) with the desquamation-related loss of lipids from these layers (which leads to higher permeability) may be the reason that the SC presents a remarkably uniform barrier to transepidermal water loss (67–69).

For lipophilic permeants, there is a consistency between several sets of observations that should be noted. Desorption studies yielded higher values of diffusivity D than did permeation studies for both testosterone (Table 1) and a variety of other compounds (9). This phenomenon is predicted for a membrane with an asymmetric partition coefficient (82). Tissue distribution measurements for another lipophilic

solute, clobetasol proprionate, in SC (Fig. 5) support the premise of an asymmetric partition coefficient, with the higher concentration achieved at the apical (upper) surface. Bidirectional desorption of testosterone from SC (Fig. 8B) supports that higher equilibrium concentrations of this compound are also attained at the apical surface. A possible reason for the enhanced partitioning of lipophilic compounds into the upper SC layers is the presence of sebaceous lipids in this region. Otherwise, one might expect a lower partition coefficient due to the partial loss of lamellar lipids from the upper SC.

The hydrophilic permeant, niacinamide, showed the behavior qualitatively different from testosterone. It desorbed from SC in a complex manner involving a fast and a slow time constant (Fig. 7A, Table 1). The diffusivity calculated from the slow phase of desorption was smaller than that from permeation, not larger. Niacinamide desorbed more rapidly from the proximal (lower) side of the SC rather than the apical side (Fig. 8A). These phenomena, combined with the bulk SC/water partition coefficient of 1.2 (Table 1), suggest that niacinamide partitions into both protein and lipid regions of the SC and that its diffusion rate between the two regions is restricted. It seems possible that the CEs may play a role in this restriction. If the fragile CEf in the lower SC were more permeable to niacinamide than the rigid CEr in the upper SC, then the desorption pattern in Figure 8A is understandable. Thus, detailed comparison of the transport behavior of hydrophilic and lipophilic permeants can provide insights into the permeation mechanism for both.

VI. CONCLUSIONS

Careful examination of mass transport processes in the stratum corneum, focusing especially on transient diffusion rates determined from permeation and desorption methodologies, reveals the heterogeneous and somewhat asymmetric nature of the SC barrier. Although these features are of interest in elucidating transport mechanisms, the most practical way to deal with them is to conduct experiments (e.g., permeation studies) and develop models that integrate over the entire barrier. The concept of SC as a vertically isotropic diffusion barrier has a solid place in current thinking.

ACKNOWLEDGMENTS

This work was supported by Grant R01 OH007529 from the National Institute for Occupational Safety and Health, a branch of the U.S. Centers for Disease Control and Prevention. We thank Shreekripa Balasubramanian and Arjun Santhanum for data and analysis associated with Figure 1 and Fred Frasch for a helpful discussion of membrane tortuosity. Ron Warner and Randall Wickett contributed significantly to the interpretation of the results.

ABBREVIATIONS

CE, cornified cell envelope; CEf, fragile CE; CEr, resilient or rigid CE; HEM, human epidermal membrane; K_{oct}, octanol/water partition coefficient; SC, stratum corneum; VN, vanillylnonanamide.

REFERENCES

1. Lampe MA, Williams ML, Elias PM. Human epidermal lipids: characterization and modulations during differentiation. J Lipid Res 1983; 24:131–140.
2. Elias PM. Structure and function of the stratum corneum permeability barrier. Drug Devel Res 1988; 13:97–105.
3. Steven AC, Bisher ME, Roop DR, Steinert PM. Biosynthetic pathways of filaggrin and loricrin–two major proteins expressed by terminally differentiated epidermal keratinocytes. J Struc Biol 1990; 104:150–162.
4. Nemes Z, Steinert PM. Bricks and mortar of the epidermal barrier. Exp Mol Med 1999; 31:5–19.
5. Wertz PW. Epidermal lipids. Sem Dermatol 1992; 11:106–113.
6. Hill JR, Wertz PW. Molecular models of the intercellular lipid lamellae from epidermal stratum corneum. Biochem Biophys Act 2003; 1616:121–126.
7. Scheuplein RJ, Blank IH. Permeability of the skin. Physiol Rev 1971; 51:702–747.
8. Flynn GL. Mechanism of percutaneous absorption from physicochemical evidence. In: Bronaugh RL, Maibach HI, eds. Percutaneous Absorption. New York: Marcel Dekker, 1985:27–51.
9. Roberts MS, Triggs EJ, Anderson RA. Permeability of solutes through biological membranes measured by a desorption technique. Nature 1975; 257:225–227.
10. Roberts MS, Anissimov YG, Gonsalvez RA. Mathematical models in percutaneous absorption. In: Bronaugh RL, Maibach HI, eds. Percutaneous Absorption Drugs-Cosmetics-Mechanisms-Methodology. New York: Marcel Dekker, 1999:3–56.
11. Kasting GB, Smith RL, Cooper ER. Effect of lipid solubility and molecular size on percutaneous absorption. Skin Pharmacol 1987; 1:138–153.
12. Potts RO, Guy RH. Predicting skin permeability. Pharm Res 1992; 9:663–669.
13. Wilschut A, ten Berge WF, Robinson PJ, McKone TE. Estimating skin permeation. The validation of five mathematical skin penetration models. Chemosphere 1995; 30: 1275–1296.
14. USEPA. ed. Guidelines for Exposure Assessment. Washington, DC: Risk Assessment Forum, U.S. Environmental Protection Agency, 1992.
15. Cleek RL, Bunge AL. A new method for estimating dermal absorption from chemical exposure. 1. General approach. Pharm Res 1993; 10:497–506.
16. Johnson ME, Blankschtein D, Langer R. Evaluation of solute permeation through the stratum corneum: lateral bilayer diffusion as the primary transport mechanism. J Pharm Sci 1997; 86:1162–1172.
17. Peck KD, Ghanem A-H, Higuchi WI. Hindered diffusion of polar molecules through and effective pore radii estimates of intact and ethanol treated human epidermal membranes. Pharm Res 1994; 11:1306–1314.
18. Peck KD, Ghanem A-H, Higuchi WI. The effect of temperature upon the permeation of polar and ionic solutes through human epidermal membrane. J Pharm Sci 1995; 84: 975–982.
19. Kasting GB, Smith RL, Anderson BD. Prodrugs for dermal delivery: solubility, molecular size, and functional group effects. In: Sloan KB, ed. Prodrugs: Topical and Ocular Drug Delivery. New York: Marcel Dekker, 1992:117–161.
20. Potts RO, Guy RH. A predictive algorithm for skin permeability: the effects of molecular size and hydrogen bond activity. Pharm Res 1995; 12:1628–1633.
21. Abraham MH, Martins F, Mitchell RC. Algorithms for skin permeability using hydrogen bond descriptors: the problem of steroids. J Pharm Pharmacol 1997; 49:858–865.
22. Moss GP, Dearden JC, Patel H, Cronin MTD. Quantitative structure-permeability relationships (QSPRs) for percutaneous absorption. Toxicol in Vitro 2002; 16:299–317.
23. Geinoz S, Guy RH, Testa B, Carrupt P-A. Quantitative structure-permeation relationships (QSPeRs) to predict skin permeation: a critical evaluation. Pharm Res 2004; 21:83–92.

24. Degim T, Hadgraft J, Ilbasmis S, Ozkan Y. Prediction of skin penetration using artificial neural networks (ANN) modeling. J Pharm Sci 2003; 92:656–664.
25. Michaels AS, Chandrasekaran SK, Shaw JE. Drug permeation through human skin: theory and in vitro experimental measurement. Am Inst Chem Eng J 1975; 21:985–996.
26. Talreja PS, Kleene NK, Pickens W, Wang T-F, Kasting GB. Visualization of lipid barrier and measurement of lipid path length in human stratum corneum. AAPS Pharm Sci 2001; 3:Article 13.
27. Frasch HF, Barbaro AM. Steady-state flux and lag time in the stratum corneum lipid pathway: results from finite element models. J Pharm Sci 2003; 92:2196–2207.
28. Heisig M, Lieckfeldt R, Wittum G, Mazurkevich G, Lee G. Non steady-state descriptions of drug permeation through stratum corneum. I. The biphasic brick and mortar model. Pharm Res 1996; 13:421–426.
29. Wang T-F. Microscopic Models for the Structure and Permeability of the Stratum Corneum Barrier Layer of Skin. Ph.D. dissertation, Department of Chemical Engineering, State University of New York at Buffalo, 2003.
30. Elias PM. The epidermal permeability barrier: from the early days at Harvard to emerging concepts. J Invest Dermatol 2004; 122:xxxvi–xxxix.
31. Shelley WB, Melton FM. Factors accelerating the penetration of histamine through normal intact human skin. J Invest Dermatol 1949:61–71.
32. Abramson HA, Gorin MH. Skin reactions IX. The electrophoretic demonstration of the patent pores of the living human skin; its relation to the charge of the skin. J Phys Chem 1940; 44:1094–1102.
33. Scheuplein RJ. Skin permeation. In: Jarrett A, ed. The Physiology and Pathophysiology of the Skin. New York: Academic Press, 1978:1669–1752.
34. Grimnes S. Pathways of ionic flow through human skin in vivo. Acta Derm Venereol (Stockh) 1984; 64:93–98.
35. Cullander C, Guy RH. Sites of iontophoretic current flow into the skin: identification and characterization with the vibrating probe electrode. J Invest Dermatol 1991; 97:55–64.
36. Burnette RR, Ongpipattanakul B. Characterization of the pore transport properties and tissue alteration of excised human skin during iontophoresis. J Pharm Sci 1988; 77: 132–137.
37. Kasting GB. Kinetics of finite dose absorption 1. Vanillylnonanamide. J Pharm Sci 2001; 90:202–212.
38. Kasting GB, Filloon TG, Francis WR, Meredith MP. Improving the sensitivity of in vitro skin penetration experiments. Pharm Res 1994; 11:1747–1754.
39. Scheuplein RJ. Mechanism of percutaneous absorption II. Transient diffusion and the relative importance of various routes of skin penetration. J Invest Dermatol 1967; 48:79–88.
40. Keister JC, Kasting GB. The use of transient diffusion to investigate transport pathways through skin. J Control Rel 1986; 4:111–117.
41. Tur E, Maibach HI, Guy RH. Percutaneous penetration of methyl nicotinate at three anatomic sites: evidence for appendageal transport? Skin Pharmacol 1991; 4:230–234.
42. Anderson RL, Cassidy JM, Hansen JR, Yellin W. Hydration of stratum corneum. Biopolymers 1973; 12:2789–2802.
43. Blank IH, Moloney J, Emslie AG, Simon I, Apt C. The diffusion of water across the stratum corneum as a function of its water content. J Invest Dermatol 1984; 82:183–194.
44. El-Shimi AF, Princen HM, Risi DR. Water vapor sorption, desorption, and diffusion in excised skin: Part I. Technique. In: Baier RE, ed. Applied Chemistry at Protein Interfaces. Washington: American Chemical Society, 1975.
45. Anderson RL, Cassidy JM, Hansen JR, Yellin W. The effect of in vivo occlusion on human stratum corneum hydration-dehydration in vitro. J Invest Dermatol 1973; 61:375–379.
46. Potts RO, Francoeur M. The influence of stratum corneum morphology on water permeability. J Invest Dermatol 1991; 96:495–499.

47. Bouwstra JA, Gooris GS, van der Spek JA, Bras W. Structural investigations of human stratum corneum by small angle X-ray scattering. J Invest Dermatol 1991; 97:1005–1012.
48. Packer KJ, Sellwood TC. Proton magnetic resonance studies of hydrated stratum corneum. Part 1. Spin-lattice and transverse relaxation. Chem Soc J (Faraday Trans 2) 1978; 74:1579–1591.
49. Packer KJ, Sellwood TC. Proton magnetic resonance studies of hydrated stratum corneum. Part 2. Self-diffusion. Chem Soc J (Faraday Trans 2) 1978; 74:1592–1606.
50. Kasting GB, Barai ND, Wang T-F, Nitsche JM. Mobility of water in human stratum corneum. J Pharm Sci 2003; 92:2326–2340.
51. Bodde HE, van den Brink I, Koerten HK, de Haan FHN. Visualization of in vitro percutaneous penetration of mercuric chloride transport through intercellular space versus cellular uptake through desmosomes. J Control Rel 1991; 15:227–236.
52. Monteiro-Riviere NA, Inman AO, Riviere JE. Identification of the pathway of iontophoretic drug delivery: light and ultrastructural studies using mercuric chloride in pigs. Pharm Res 1994; 11:251–256.
53. Raykar PV, Fung M-C, Anderson BD. The role of protein and lipid domains in the uptake of solutes by human stratum corneum. Pharm Res 1988; 5:140–150.
54. Anderson BD, Higuchi WI, Raykar PV. Heterogeneity effects on permeability–partition coefficient relationships in human stratum corneum. Pharm Res 1988; 5:566–573.
55. Roberts MS, Pugh WJ, Hadgraft J, Watkinson AC. Epidermal permeability-penetrant structure relationships: 1. An analysis of methods of predicting penetration of monofunctional solutes from aqueous solutions. Int J Pharm 1995; 126:219–233.
56. Hansch C, Leo A. MEDCHEM database and CLOGP 2.0. BioByte Inc., 1999.
57. Christophers E, Kligman AM. Visualization of the cell layers of the stratum corneum. J Invest Dermatol 1964; 42:407–409.
58. Blank IH. Factors which influence the water content of the stratum corneum. J Invest Dermatol 1952; 18:433–440.
59. Scheuplein RJ. Mechanism of percutaneous absorption I. Routes of penetration and the influence of solubility. J Invest Dermatol 1965; 45:334–346.
60. Blank IH, Scheuplein RJ, MacFarlane DJ. Mechanism of percutaneous absorption III. The effect of temperature on the transport of non-electrolytes across the skin. J Invest Dermatol 1967; 49:582–589.
61. Scheuplein RJ. Molecular structure and diffusional processes across intact epidermis. U.S. Army: Edgewood Arsenal, 1967.
62. Scheuplein RJ, Morgan LJ. "Bound water" in keratin membranes measured by a microbalance technique. Nature 1967; 214:456–458.
63. Brody I. The ultrastructure of the horny layer in normal and psoriatic epidermis as revealed by electron microscopy. J Invest Dermatol 1963; 39:519.
64. Odland GF. The fine structure of the inter-relationship of cells in the human epidermis. J Biophys Biochem Cytol 1958; 4:529.
65. Blair C. Morphology and thickness of the human stratum corneum. Brit J Dermatol 1968; 80:430–436.
66. Monash S, Blank IH. Location and reformation of the epithelial barrier to water transport. Arch Dermatol (Chicago) 1958; 78:710.
67. Kalia YN, Pirot F, Guy RH. Homogeneous transport in a heterogeneous membrane: water diffusion across human stratum corneum in vivo. Biophys J 1996; 71:2692–2700.
68. Pirot F, Kalia YN, Stinchcomb AL, Keating G, Bunge A, Guy RH. Characterization of the permeability barrier of human skin in vivo. Proc Nat Acad Sci USA 1997; 94: 1562–1567.
69. Pirot F, Berardesca E, Kalia YN, Singh M, Maibach HI, Guy RH. Stratum corneum thickness and apparent water diffusivity: facile and noninvasive quantitation in vivo. Pharm Res 1998; 15:492–494.
70. Warner RR, Stone KJ, Boissy YL. Hydration disrupts human stratum corneum ultrastructure. J Invest Dermatol 2003; 120:275–284.

71. Bowser PA, White RJ. Isolation, barrier properties and lipid analysis of stratum compactum, a discrete region of the stratum corneum. Brit J Dermatol 1985; 112:1–14.
72. Warner RR, Stone KJ, Boissy YL. Hydration disrupts human stratum corneum ultrastructure. J Invest Dermatol 1998; 110:675.
73. Bouwstra JA, de Graaff A, Gooris GS, Nijsse J, Wiechers JW, van Aelst AC. Water distribution and related morphology in human stratum corneum at different hydration levels. J Invest Dermatol 2003; 120:750–758.
74. Stockdale M. Water diffusion coefficients versus water activity in stratum corneum: a correlation and its implications. J Soc Cosmet Chem 1978; 29:625–639.
75. El-Shimi AF, Princen HM. Water vapor sorption and desorption behavior of some keratins. Colloid Polym Sci 1978; 256:105–114.
76. El-Shimi AF, Princen HM. Diffusion characteristics of water vapor in some keratins. Colloid Polym Sci 1978; 256:209–217.
77. Kasting GB, Barai ND. Equilibrium water sorption in human stratum corneum. J Pharm Sci 2003; 92:1624–1631.
78. Harding CR, Long S, Richardson J, Rogers J, Zhang Z, Bush A, Rawlings AV. The cornified cell envelope: an important marker of stratum corneum maturation in healthy and dry skin. Int J Cosmet Sci 2003; 25:157–167.
79. Crank J. The Mathematics of Diffusion. Oxford: Clarendon Press, 1975.
80. Cooper ER, Berner B. Skin permeability. In: Skerrow D, Skerrow CJ, eds. Methods in Skin Research. New York: John Wiley and Sons, 1985:407–432.
81. Mitragotri S. In situ determination of partition and diffusion coefficients in the lipid bilayers of stratum corneum. Pharm Res 2000; 17:1026–1029.
82. Anissimov YG, Roberts MS. Diffusion modeling of percutaneous absorption kinetics: 3. Variable diffusion and partition coefficients, consequences for stratum corneum depth profiles and desorption kinetics. J Pharm Sci 2004; 93:470–487.
83. Mueller B, Anissimov YG, Roberts MS. Unexpected clobetasol propionate profile in human stratum corneum after topical application in vitro. Pharm Res 2003; 20: 1835–1837.
84. Charman WN, Lai CSC, Finnin BC, Reed BL. Self-association of nicotinamide in aqueous solution: mass transport, freezing-point depression, and partition coefficient studies. Pharm Res 1991; 8:1144–1150.
85. Talreja PS. Determination of transport pathways in human stratum corneum: micro and macro measurements. MS thesis, College of Pharmacy, University of Cincinnati: Cincinnati, OH, 2000.
86. Barai ND. Effect of hydration on skin permeability. MS thesis, College of Pharmacy, University of Cincinnati: Cincinnati, OH, 2002.
87. Rougier A, Lotte C, Maibach HI. In vivo percutaneous penetration of some organic compounds related to anatomic site in humans: predictive assessment by the stripping method. J Pharm Sci 1987; 76:451–454.
88. Warner RR, Myers MC, Taylor DA. Electron probe analysis of human skin: determination of water concentration profile. J Invest Dermatol 1988; 90:218–224.
89. Bhatt V, Kasting GB. A Model for Estimating the Absorption and Evaporation Rates of DEET from Human Skin. AAPS National Meeting, Salt Lake City, UT, 2003.

14

The Skin Reservoir for Topically Applied Solutes

Michael S. Roberts, Sheree E. Cross, and Yuri G. Anissimov
Department of Medicine, University of Queensland, Princess Alexandra Hospital, Woolloongabba, Queensland, Australia

I. INTRODUCTION

The reservoir function of the skin is an important determinant of the duration of action of a topical solute. The reservoir can exist in the stratum corneum, in the viable avascular tissue (viable epidermis and supra-capillary dermis), and in the dermis. There are a number of means by which this reservoir can be formed. A steroid reservoir in the stratum corneum has been demonstrated by the reactivation of a vasoconstrictor effect by occlusion or application of a placebo cream to the skin some time after the original topical application of steroid. Other solutes have also been reported to show a reservoir effect in the skin after topical application. In this work, we develop a simple compartmental model to understand why re-activation of vasoconstriction at some time after a topical steroid application shows dependency on time, topical solute concentration, and product used to cause reactivation. The model is also used to show which solutes are likely to show a reservoir effect and could be potentially affected by desquamation, especially when the turnover of the skin is abnormally rapid. A similar form of the model can be used to understand the promotion of reservoir function in the viable tissue and in the dermis in terms of effective removal by blood perfusing the tissues.

In this overview, we consider published examples consistent with a reservoir effect. In order to understand the effect, we present a simple pharmacokinetic model that we use to explain the reported phenomena. It is recognized that the model used lacks the mathematical rigor and accuracy that would be achieved with the more spatially correct representation of concentration gradients in tissues as would be defined by diffusion models-in-series and a convective loss of squamae from the stratum corneum as a result of desquamation. However, the model does provide a simplistic interpretation of events that aids in understanding observed phenomena and in a generalized predicting of likely formation and evidence of a reservoir effect.

II. WHAT IS THE SKIN RESERVOIR AND WHY IS ITS UNDERSTANDING IN NATURE IMPORTANT?

Topical applications of medications account for about 5% of all products used for therapeutic purposes and may account for more if their cosmetic and cosmeceutic uses are recognized. Most studies on topical products are concerned with the effective penetration of the agents to cause a local or systemic effect or, from an environmental toxicology perspective, their undesirable penetration. What is less well understood is the sequestration of solutes into components of the skin and their rapid release on appropriate provocation of the skin some time later. In some cases, the amount of solute released is sufficient to yield a pharmacological action that replicates that observed when the solute was first applied. This phenomenon is most widely known as the reservoir effect as a consequence of it being used to show the reactivated steroid vasoconstrictor effect when an occlusive dressing was applied to the original steroid application site several weeks after the original application. The reservoir effect is not, however, limited to steroids nor to the stratum corneum.

III. HISTORICAL PERSPECTIVE ON THE STRATUM CORNEUM RESERVOIR FOR DRUGS

The existence of a stratum corneum reservoir for drugs has been expressed in two forms. Vickers (1) has suggested a stratum corneum reservoir because a topical agent such as salicylic acid is excreted in the urine more slowly when applied topically than when injected intradermally (2). One could interpret a reservoir in this context as a function of the time lag associated with a drug diffusing through the skin, the time to reach steady state in the presence of a constant application and the time to desorb after removal of the application. Hence, in this form, the reservoir is most evident for the more slowly diffusing drugs, i.e., those with long lag times. Schaefer et al. (3) also recognized the importance of the stratum corneum barrier as a determinant of reservoir function. They suggested that the reservoir function was the reciprocal function of the multi-layer stratum corneum barrier.

The second form of the reservoir is the recognition that the skin may be a depot for drugs. Malkinson and Ferguson (4) first suggested this concept but as Vickers (1) points out their data could be explained by a slow diffusion process through the stratum corneum. Potential sites for this depot were suggested to be keratin spaces, follicular openings, and surface folds (5). The first definitive evidence of a stratum corneum depot for topical corticosteroids was presented by Vickers in 1963 (6). He conducted the experiments shown in Figure 1. He showed that the initial vasoconstrictor effects of a topical corticosteroid (fluocinolone acetonide or triamcinolone acetonide) occurring after application and occlusion with Saran film firstly disappeared within 10 to 16 hr as expected on removal of the film. The vasoconstrictive effect could be reactivated for up to two weeks after topical application by repeated occlusion of the site. If the stratum corneum was stripped prior to the repeated occlusion, no repeat vasoconstriction is evident providing evidence that the stratum corneum is the main site for the depot (Fig. 1). Vickers (1) confirmed this site by showing tape strips of stratum corneum and biopsies from non-stripped epidermal sites had high counts after application of radiolabeled steroids, whereas the biopsy form stripped sites had a low count. Interestingly, the number of counts decreased with successive strips (1) as would be anticipated with concentration

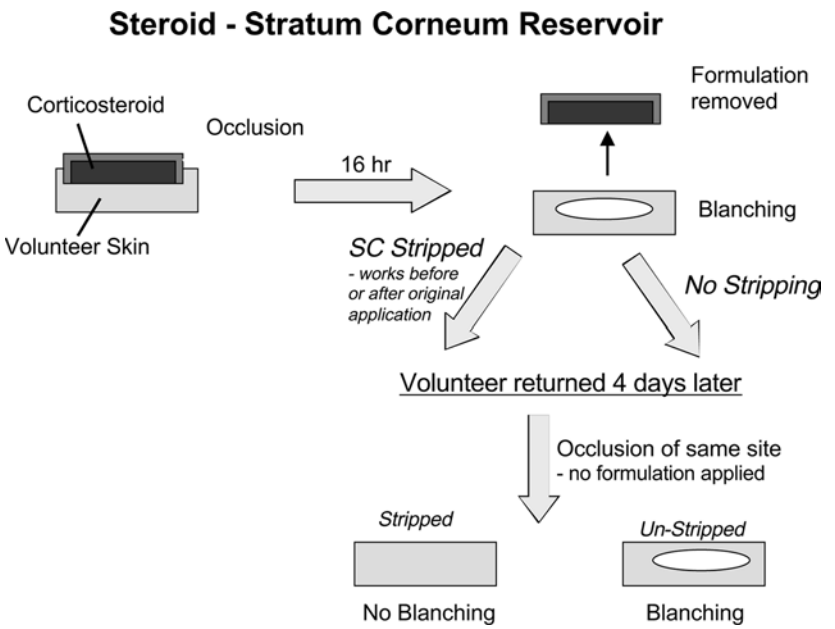


Figure 1 The reservoir effect as demonstrated by Vickers (6) in 1963.

distance profiles when a diffusion model is used to characterize the penetration process (7). The presence of a corticosteroid depot has been confirmed in a number of later papers (8,9). Vickers (1) further observed that the duration of the reservoir depended on the nature of the drug, the vehicle used, the temperature of the skin and the relative humidity to which the skin is exposed.

IV. MODELING THE FORMATION AND DURATION OF THE STRATUM CORNEUM CORTICOSTEROID RESERVOIR

We propose that in a simplistic representation, the stratum corneum reservoir is defined by three independent variables: (a) the diffusivity of the drug in the stratum corneum, (b) the amount of drug in the stratum corneum, and (c) clearance of drug from the epidermis.

A. Diffusivity

The diffusivity of solutes in the stratum corneum determines the time to reach steady state or to desorb from the stratum corneum. When diffusivity is very slow, sufficient drug will not taken up into the stratum corneum to be recognized as establishing a reservoir. Vickers (1) recognized that occlusion (via an increased humidity and temperature) was necessary to promote a reservoir effect. Occlusion leads to an increased hydration of the skin and a promotion of diffusivity (10). Further, as shown in Figure 2, if the duration of the application is too short relative to the diffusion time of the drug, a reservoir may not be evident. Vickers (1) suggested that, for steroids, ''an occlusion of 8 hr resulted in (if any) a short-lived reservoir that was often not reproducible.'' The increase in the stratum corneum reservoir for sodium

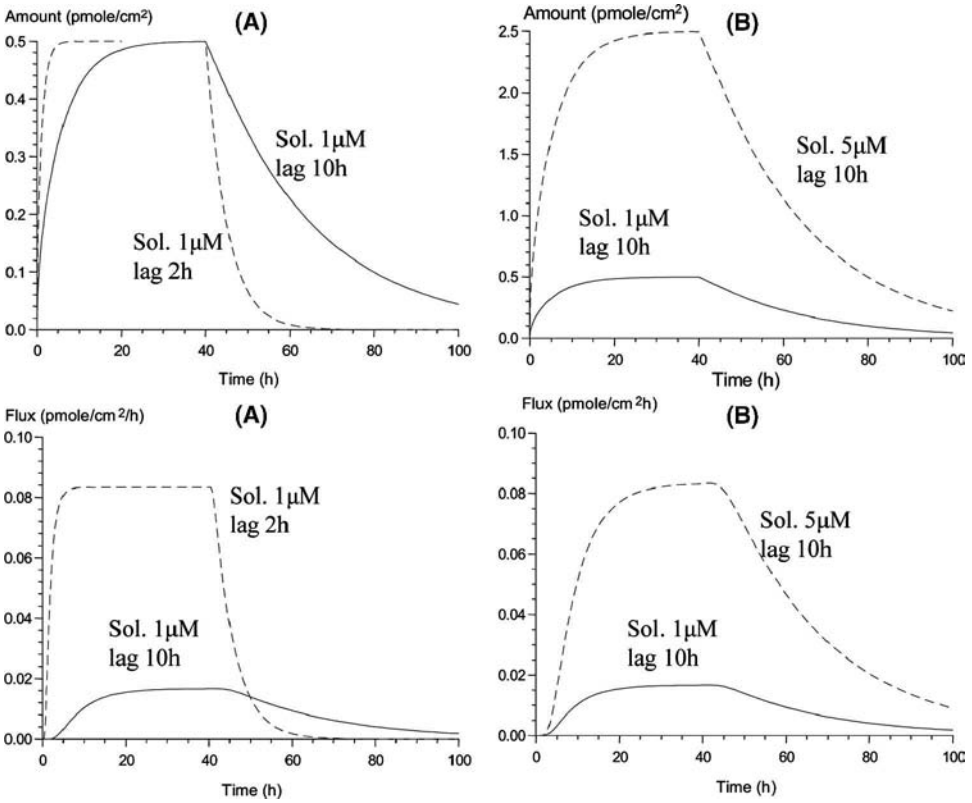


Figure 2 Amount in the stratum corneum (*top*) and flux through epidermis (*bottom*) based on a diffusion model for: (**A**) two drugs with lag times of 2 and 10 hours, and (**B**) two drugs with stratum corneum solubilities of 1 and 5 μM.

fusidate with increases with both temperature and increase in relative humidity is consistent with these variables also increasing the percentage of sodium fusidate that had penetrated through epidermis over 24 hours (1). The duration of the reservoir is also related to the nature of the drug as shown in Figure 3. The duration of the reservoir for aspirin $<$ fusidic acid $<$ fluocinolone acetonide (1). Barry and Woodford (11) have suggested that a corticosteroid reservoir in the skin lasts for 8 to 14 days.

One could, in principle, estimate the duration of the reservoir for a given drug from the time required to reach maximal reservoir concentration (Fig. 2) or from the epidermal lag times obtained in epidermal penetration studies. Using Equation (49) for lag time and the slowest term in Equation (23) from Roberts et al. (7), the duration time for 10% of the reservoir to remain (i.e., 90% has diffused out) is approximately 5.7 times that of the lag time. The corresponding duration time for 5% to be left remaining in the reservoir is 7.4 times the lag time. Accordingly, using a lag time for aspirin in a hydrated epidermal penetration study of about 0.6 hour (unpublished data) would suggest that 90% of the stratum corneum reservoir would be lost after about three to four hours. The actual time reported by Vickers (1) is about 240 hour suggesting that the diffusivity in vivo is about 1/60th that for the hydrated stratum corneum in vitro. An important implication of this difference is that hydration of the stratum corneum by occlusion or other means may substantially increase diffusivity

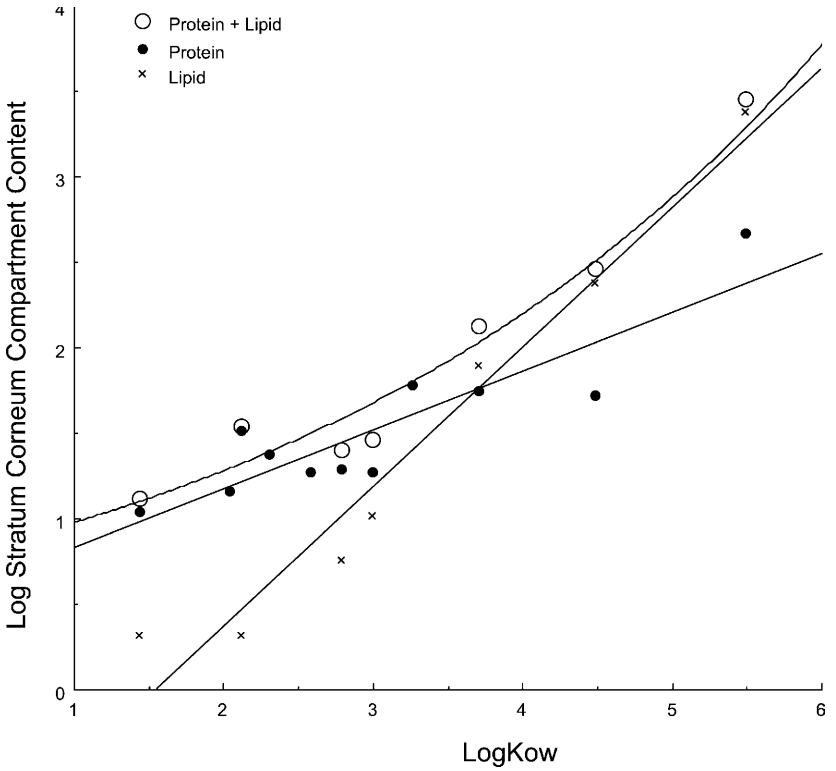


Figure 3 Plot of log apparent stratum corneum (protein and lipid)–water partition coefficient versus log octanol–water partition coefficient (ratio of 0.85 protein: 0.15 lipid). Also shown in the contribution of the stratum corneum protein domain (0.85 protein) and stratum corneum lipid domain (0.15 lipid) to the partition coefficient. *Source:* Data abstracted from Ref. 12.

in the stratum corneum. Hydration and various penetration enhancers such as dimethylsulphfoxide have been reported to induce the steroid stratum corneum reservoir effect (1), probably as a result of their increasing drug diffusivity in the stratum corneum.

B. Stratum Corneum Partitioning or Capacity

The second determinant of the reservoir effect, the amount of drug in the stratum corneum is defined by the affinity of the drug for the stratum corneum. In general, "like-dissolves-like" so that a lipophilic drug dissolved in a polar vehicle such as water will have a high affinity for the stratum corneum whereas a lipophilic drug dissolved in a non-polar vehicle such as oil will have a lower affinity. Figure 2B shows that increasing the affinity of drug for the stratum corneum results in a greater amount taken up into the stratum corneum but does not affect the time to be taken up or the fractional rate of reservoir depletion. Vickers (1) further suggested that the vehicle in which the steroid was applied was important. He suggested that the average duration of reservoir for 95% alcohol > hydrophilic cream > greasy ointment. If the 95% alcohol effectively left a solvent deposited solid, the results may arise in part from the partitioning being in the same rank order. However, these vehicles are also likely to affect skin hydration and stratum corneum diffusivity may be expected to be

in the reverse order. Either or a combination of the two effects may explain the reservoir duration results obtained.

The nature of the drug may also affect the amount present in the reservoir. In general, following the principle of "like-dissolves-like" solutes having the greatest affinity for stratum corneum components would be expected to show the greatest stratum corneum reservoir effect. Figure 3 shows that the partitioning of various hydrocortisone-21-esters from water into the stratum corneum increases with lipophilicity as defined by the octanol–water partition coefficient. These data suggest that partitioning occurs into both the lipid and protein domains of the stratum corneum showing a higher dependency into the protein domain for the more polar steroids and higher dependency into the lipid domain for the more lipophilic steroids. Other autoradiographic data is are consistent with steroids being preferentially located in or close to the intercellular lipids of the stratum corneum, suggesting that the steroid stratum corneum reservoir and lipid transport is in this lipid domain of the stratum corneum (13).

C. Clearance

In general, removal of solutes from the stratum corneum depends on clearance into the viable epidermis and thence into the dermis. Most of the clearance for steroids from the dermis is due to dermal blood flow (14). Whilst clearance is normally assumed not to be rate limiting, a sufficiently low clearance may lead to a reduced flux through the stratum corneum and an increased amount retained in the stratum corneum (15). A reduced clearance may arise for instance due to vasoconstriction being present or a poor solubility in the viable epidermis or dermis. Figure 4 shows that reducing clearance or reducing the partition coefficient between the viable epidermis and stratum corneum increases the duration of the reservoir.

V. STRATUM CORNEUM RESERVOIR AND EPIDERMAL FLUX

Epidermal flux (J_{sc}) is defined by the product of the concentration of available drug in the stratum corneum and the diffusivity of a drug in stratum corneum. Accordingly, percutaneous absorption may be related to the extent of reservoir function. At any given time, the amount of drug in the stratum corneum will be defined by the diffusivity into and affinity for the stratum corneum as discussed earlier. Dupuis and co-workers (16) in 1984 first showed that the amount of different drugs absorbed in the body of a hairless rat could be correlated with the amounts found in the skin after topical application. This work was then confirmed in man (17) and extended to show that the relationship existed irrespective of anatomical site (18) or type of vehicle used (19).

VI. STRATUM CORNEUM RESERVOIR AND SUBSTANTIVITY

Substantivity is a measure of the binding of solutes to sites in the stratum corneum as evident by a resistance to be washed off or removed. Sunscreen substantivity has been defined as resistance to removal by water. The European Cosmetic, Toiletry, and Perfumery Association (COLIPA) has defined a water resistance retention for sunscreens (%WRR) in terms of the sun protection factors prior to (SPF_{dry}) and

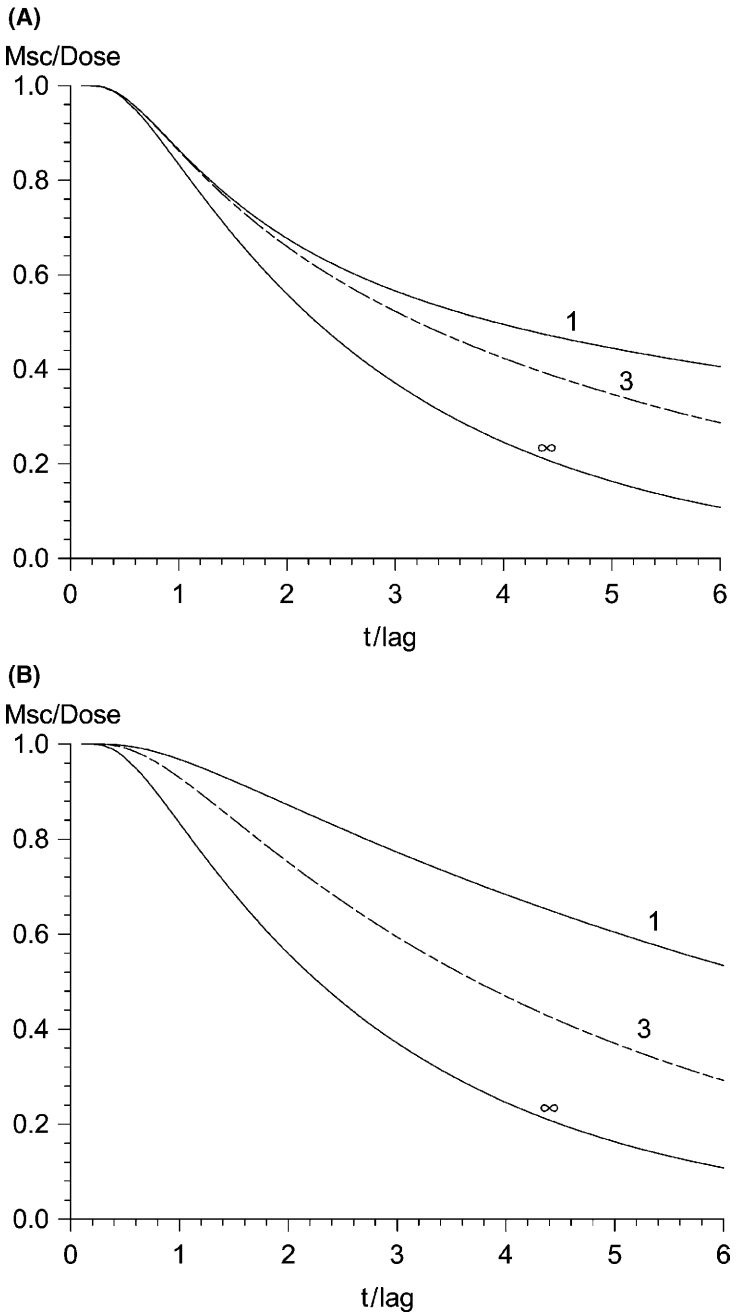


Figure 4 Effect of (**A**) blood clearance and (**B**) viable epidermal resistance relative to that of stratum corneum on the normalized amount remaining in the stratum corneum reservoir (M_{sc}/Dose) with time (t) normalized to lag time (lag time) following application of a solvent deposited solid and using a diffusion model.

after water immersion (SPF_{wet}) (20):

$$WRR(\%) = \frac{SPF_{wet} - 1}{SPF_{dry} - 1} \times 100 \quad (1)$$

Stokes and Diffey (20) showed that moisturizsing products and sunscreens making no claims about water resistance were readily washed off. Waterproof lotions the greatest retention of sunscreen ($>80\%$ after two applications) followed by water resistant sunscreens ($>60\%$ after two applications). Wester et al. (21) showed that the retention of DDT and benzo[a]pyrene in skin after application in vitro for 25 minutes followed by a soap and water wash was 16.7% and 5.1%, respectively, after acetone application and 0.25% and 0.14% after application in soil. Billhimer et al. (22) showed that the amount of 3,4,4′-trichlorocarbanilide remaining on the skin 24 hours after a final soap wash was sufficient to effectively inhibit the growth of *Staphylococcus aureus* added to the skin for 5 hours. A remnant antibacterial effect has been shown for a number of antiseptic products. The substantivity of hair dyes has recently been reviewed (23). Bucks (24) examined the long term substantivity of hydrocortisone, oestradiol, and five phenolic solutes following a one day and a one week wash using 10 stratum corneum tape strips after application of radiolabeled solutes to the ventral forearms of healthy male volunteers. He reported retention levels of 0% to 5% of the applied solutes after a week and suggested that the least lipohilic and most poorly penetrating chemicals had the higher substantivity.

VII. MODELING THE VASOCONSTRICTOR EFFECT ASSOCIATED WITH THE CORTICOSTEROID RESERVOIR

Recently, Clarys et al. (25) carried out a study, which elaborates on the initial work of Vickers. They showed that blanching on re-occlusion depended on the time of the re-occlusion after the original application, the concentration of steroid, and whether an enhancer was used (Fig. 5). The extent to which a reservoir is evident after such an application will be dependent on a number of factors (Fig. 4). Firstly, the reservoir of steroid in the skin achieved after topical application will be being depleted (emptied) at a given rate. As Clarys et al. (25) point out, the amount of steroid remaining in the skin after low concentrations of halocinonide (0.005% and 0.05%) is not sufficient to exert a dermal vasoconstrictive effect when the site was re-occluded between 34 and 106 hours after the initial application. However, with 0.2%, a reservoir effect was demonstrated on re-occlusion for at least 106 hours. Second, if the enhancement increased more than provided by re-occlusion alone, it is possible that a reservoir effect will be evident with a lower steroid concentration but only for a short time. Clarys et al. (25) showed that when the enhancer urea was included in re-occlusion after halcinonide 0.005%, a significant vasoconstriction was achieved when re-occlusion was conducted at 34 hours but not at other later times.

Understanding changes in vasoconstriction associated with a stratum corneum reservoir effect through re-occlusion or application of an enhancer at a time after the origination application is most easily achieved using an appropriate mathematical model. While a diffusion model may be the most appropriate to describe transport events in the skin and relatively easy to use when expressed in the Laplace domain (7), such a model is difficult to use when model parameters change during the time

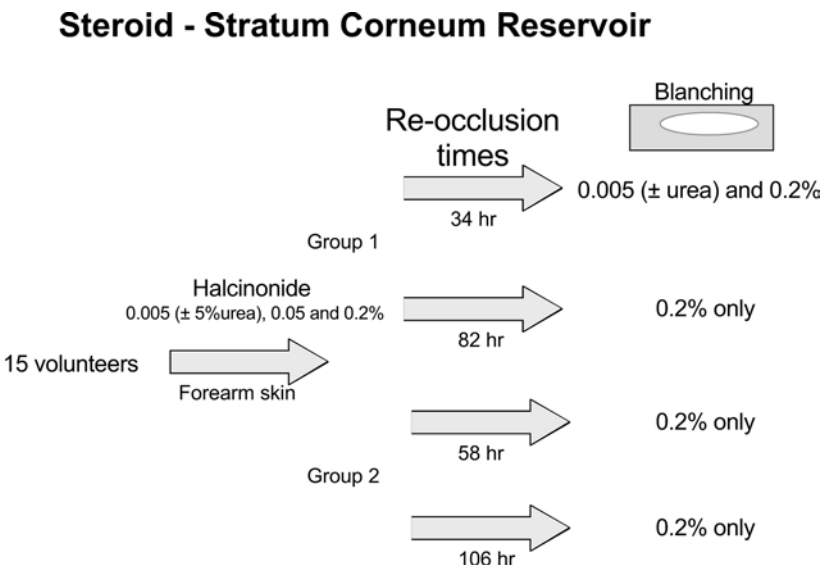


Figure 5 Time, concentration, and enhancer dependency of the reservoir effect as illustrated for halcinonide. *Source:* From Ref. 25.

course of an experiment. Further, precise modeling is further complicated by the known steroid vasoconstrictor nonlinear topical dose–effect relationships (7). Accordingly, for this purpose, we have represented the stratum corneum and viable epidermis as simple well-stirred compartments (Fig. 6). We have further limited the model to situations where the reservoir has already been established so as to recognize that this model poorly predicts lag times associated with steady-state epidermal penetration (7,26). As stated in the introduction, the model has an obvious limitation

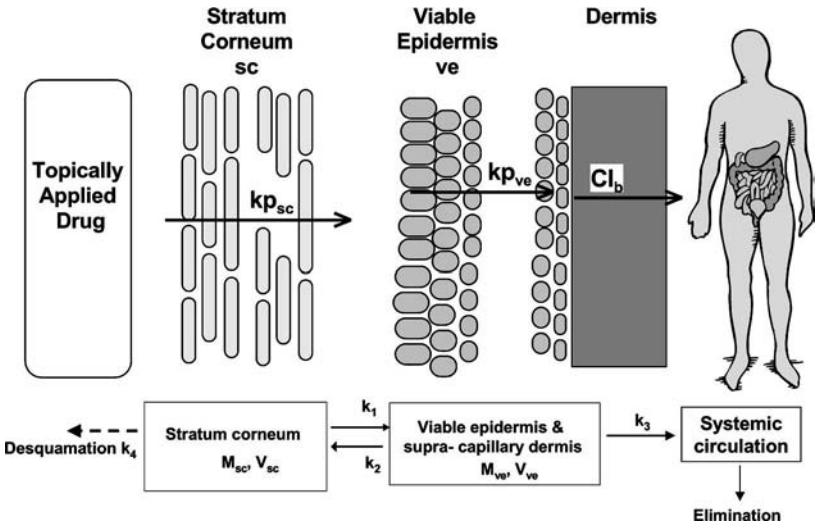


Figure 6 One-compartmental model representations of stratum corneum and viable avascular tissues used to examine the stratum corneum reservoir effect.

in that it assumes all of the tissues are well stirred when a diffusional process would better describe the solute transport therein.

The rate constant k_1 is related to the diffusion time i.e., $k_1 = \pi^2 D_{sc}/4h_{sc}^2$, where D_{sc} is the diffusivity and h_{sc} is the thickness of the stratum corneum. This definition is also equivalent to $\pi^2 k_p A_s/4V_{apsc}$ as $k_p = K_{sc-ve} D_s/h_{sc}$, and $V_{apsc} = K_{sc-ve} V_{sc} = K_{sc-ve} A_s h_{sc}$, where V_{apsc} is the apparent distribution volume of the solute in the stratum corneum and A_s is the area of application. This constant k_1 could be further complicated by also being a function of micro-constants defining other transport events in the stratum corneum. The rate constant k_2 is a function of both the diffusion time and stratum corneum–viable epidermis partition coefficient K_{sc-ve}, i.e., k_2 is equivalent to $K_{sc-ve}\ k_1 V_{sc}/V_{ve}$, where V_{ve} is the volume of distribution of the solute in the viable tissue. It is apparent that when k_2 or K_{sc-ve} is large a reservoir effect in the stratum corneum is promoted. The rate constant k_3 defines the removal of the solute from the viable tissue and can be derived from the clearance of solute from the tissue as $k_3 = CL_{ve}/V_{ve}$.

The model differential equations are as follows:

$$\frac{dM_{sc}}{dt} = k_2 M_{ve} - k_1 M_{sc}, \quad \frac{dM_{ve}}{dt} = k_1 M_{sc} - (k_2 + k_3) M_{ve} \tag{2}$$

where M_{ve} is the amount in the viable tissue and M_{sc} is the amount of solute in the stratum corneum. Sink conditions are defined by $k_3 \gg k_2$, k_1, for this special case M_{ve} is relatively small and we apply an approximation of M_{ve} 0 and dM_{ve}/dt 0 in Equation (2), to give:

$$M_{ve} \approx M_{sc} \frac{k_1}{k_2 + k_3} \tag{3}$$

Equation (2) defines the amount of solute in the viable tissue as well as the concentration C_{ve}, since $C_{ve} = M_{ve}/V_{ve}$. It is evident from Equation (3) that an increase in stratum corneum permeability as evident by an increase in k_1 from, for instance, re-occlusion, will increase M_{ve} and therefore, in the case of steroids, extent of vasoconstriction. The more k_1 is increased, the greater is M_{ve}. It should also be noted that the amount remaining in the stratum corneum is expressed in this case as:

$$M_{sc} \approx M_r \exp(-k_1 t) \tag{4}$$

where M_r is the amount of drug in the stratum corneum reservoir after loading. Hence, an increase in stratum corneum permeability rate constant k_1 will deplete the amount in the reservoir M_{sc} more rapidly. Also, Equation (4) states that the amount in the reservoir M_{sc} is depleting at a rate defined by a rate constant k_1 so that at a sufficient time and in the absence of no further application, the reservoir will be sufficiently depleted so that it no longer exists. Figure 7 shows an illustration of these concepts for corticosterone. It is evident that a 20-fold increase in diffusivity as a consequence of occlusion greatly accelerates steroid loss from the stratum corneum reservoir and increases the viable epidermal concentration with the consequential effect of likely vasoconstriction.

In general, the reservoir effect will be observed when a stratum corneum permeability enhancer is applied and causes an increase in the release of the solute from the stratum corneum. In the case of corticosteroids, the most commonly applied enhancer used to demonstrate the reservoir effect is water (10). Application of an occlusive dressing leads to a reduction of transepidermal water loss and retention of water in the stratum corneum, leading to an increased hydration of various

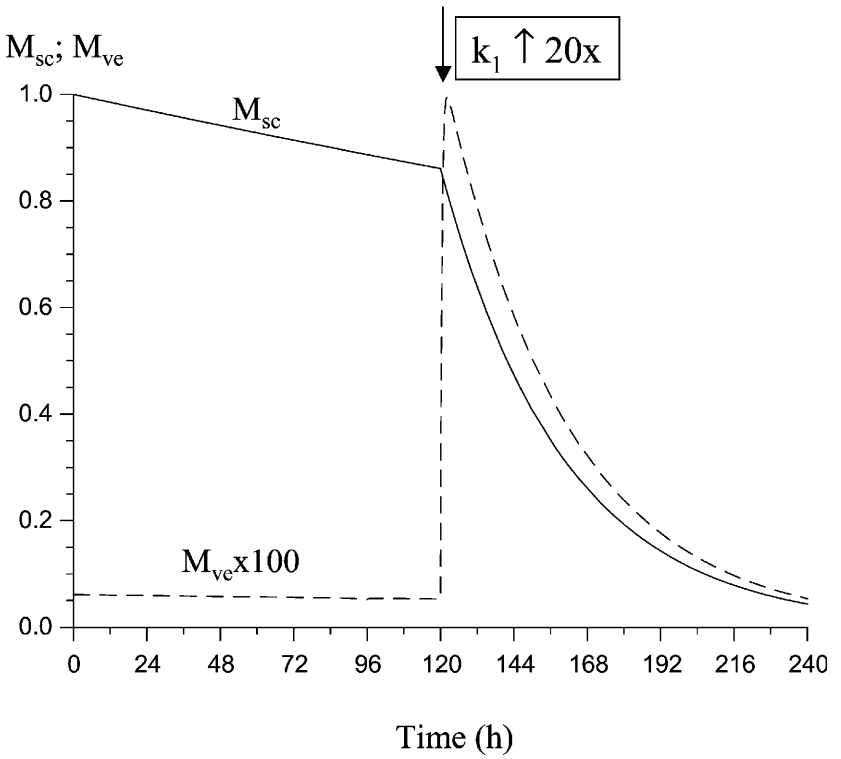


Figure 7 Amount of corticosterone remaining in stratum corneum reservoir M_{sc} (—) and in the viable epidermis M_{ve} ($\times 100$) (– –) as a function of time based on a simple compartmental model. At 120 hours, it is assumed occlusion has increased stratum corneum diffusivity (k_1 in the compartment model shown in Fig. 6) 20×. A lag time of 16.5 hours for hydrated epidermis (14), a stratum corneum–viable epidermis partition coefficient of about 0.5 (unpublished data) and k_3 0.3 hr^{-1} [using dermal clearance (14) and assuming a viable epidermis to stratum corneum thickness ratio of 20].

stratum corneum components and an increase in the diffusivity of corticosteroids from the stratum corneum into the viable epidermis and dermis. However, other enhancers such as urea (25) and propylene glycol (27) have also been shown to promote release of steroids from stratum corneum.

VIII. CHANGES IN PLASMA STEROID LEVELS ASSOCIATED WITH THE CORTICOSTEROID RESERVOIR

Figure 8 shows that after topical application of hydrocortisone a rebound effect in its plasma levels can be achieved when a placebo cream is applied 12 hours after the original product (27). The profiles are consistent with those predicted in Figure 7. One possible explanation for the data is a loss of occlusion and decrease in the stratum corneum diffusivity (k_1) between 4 and 12 hours as a result of the cream dryingout or subject activity. Application of the placebo cream containing an enhancer leads to an increase in stratum corneum diffusivity and an increase in hydrocortisone

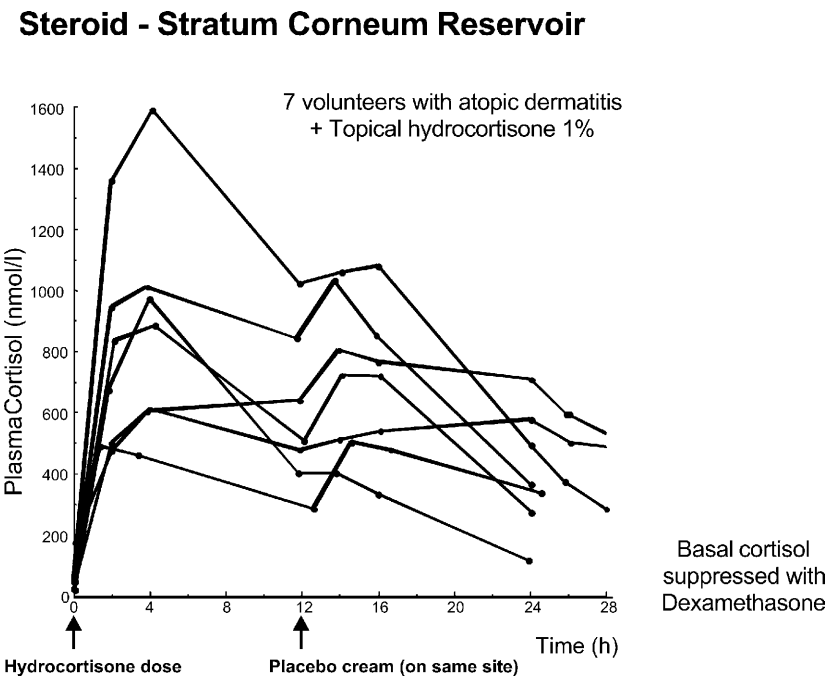


Figure 8 Evidence of a reservoir effect for hydrocortisone demonstrated by application of a placebo cream 12 hours after the original application of topical hydrocortisone 1%. *Source:* Data from Ref. 22.

release to lower tissues (Fig. 6) and then into the blood giving the profile observed in Figure 8.

IX. ROLE OF DESQUAMATION ON STRATUM CORNEUM RESERVOIR EFFECT

In general, it has been asserted that the stratum corneum reservoir is "continuously emptied" by desquamation (28) and that desquamation may have a greater effect on the percutaneous penetration of more lipophilic solutes than would be indicated by the initial partitioning (29). Reddy et al. (30) have recently examined the effects of desquamation on permeation, using a theoretical analysis based on a number of assumptions including an epidermal turnover time of 14 days, that the viable epidermis turns over at twice the rate of the stratum corneum and that the viable epidermis is 10-fold the thickness of the stratum corneum. They concluded that significant amounts of drug could be removed if the epidermal turnover was fast relative to the rate of diffusion through the stratum corneum. However, this event was only likely for highly lipophilic or very large solutes.

Desquamation is likely to have a greater effect on the reservoir effect for diseased skin to which corticosteroids are applied. The effect of desquamation can be examined using the simple compartmental model in Figure 6 by adding a rate constant k_4 for desquamation. When clearance from the skin is high so that $k_3 \gg k_2$, it is evident that desquamation will only affect the amount of solute remaining in the

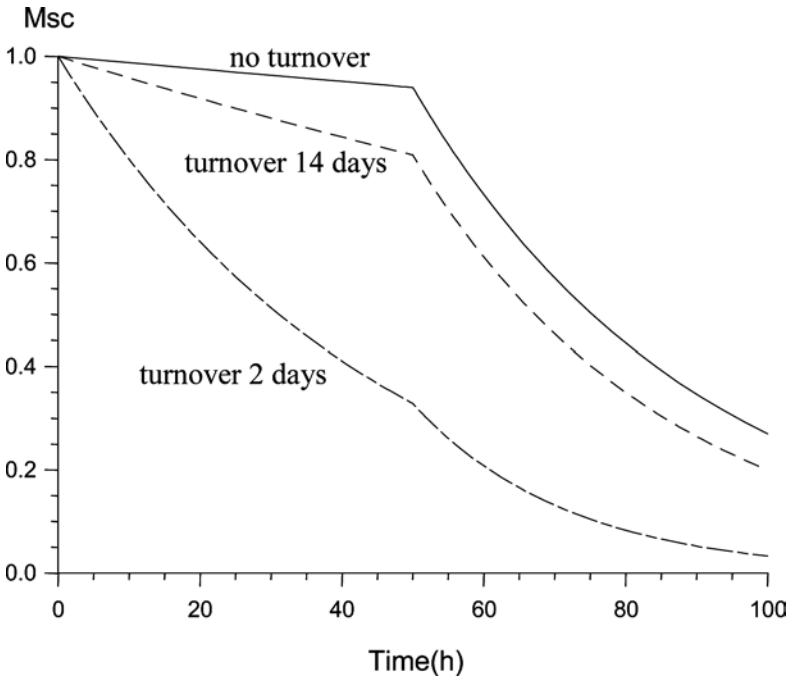


Figure 9 Amount remaining in stratum corneum reservoir of corticosterone (using hydrated epidermal lag time 16.5 hours and other parameters from Fig. 7) with no desquamation (—), a normal epidermal turnover of 14 days (– –), and a psoriatic epidermal turnover of 2 days (— –), and the compartmental model described in Figure 6.

stratum corneum M_{sc} when the desquamation rate constant k_4 it is of a similar order or higher than the diffusion rate constant k_1 through the stratum corneum Equation (5):

$$M_{sc} = M_r[-\{k_1 + k_4\}t] \tag{5}$$

It is evident that for the corticosteroid corticosterone, desquamation may increase the rate of depletion of solute from the stratum corneum and that this contribution is likely to be most significant when the epidermis is diseased and has a faster than normal turnover rate as in psoriasis. A flow-on from this analysis is that slowing down the epidermal turnover rate by steroid application is also likely to be associated with an increase in the steroid stratum corneum reservoir at later times (Fig. 9).

It is to be reemphasized that the model used here is limited by its assumption of a well-mixed compartment for the stratum corneum when the desquamation process is a convective process occurring in the opposite direction to the diffusion defined chemical concentration–distance gradient in the stratum corneum (Fig. 10). As Reddy et al. (30) points out, the permeability of the viable epidermis may also be a determinant of stratum corneum concentrations leading to a decrease in the loss from the stratum corneum for the more lipophilic solutes. Mimicking an increased resistance from the viable epidermis by reducing in k_3 in the present simple model leads to the amount in stratum corneum being lost at a slower rate [Eqs. (2) and (3)]. The use of convection diffusion equations by Reddy et al. (30) provides a more realistic representation of events. Figure 10, developed using such a model, shows

	description	Pesticide	MW	log $K_{o/w}$	B	$t_{lag,sc}$, h
1	small, hydrophilic	carbaryl	201	1.6	0.01	2.7
2	medium, lipophilic	chlorpyrifos	351	4.7	0.3	22
3	large, highly lipophilic	cypermethrin	416	6.6	3	53

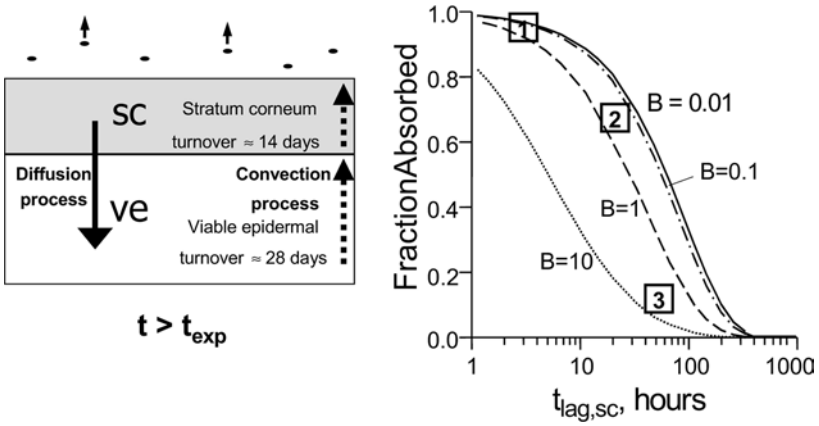


Figure 10 Effect of ratio of stratum corneum to viable epidermis permeabilities (B) and diffusional lag time on the fraction absorbed from human stratum corneum with a normal turnover highlighting differences in absorption for the pesticides carbaryl, chloropyrifos, and cypermethrin. (Based on two convection–diffusion models and a continuity of flux across the stratum corneum–viable epidermal interface. *Source*: Adapted from material provided by A. Bunge, personal communication.

that when chemical diffuse slowly (i.e., long lag times—often associated with large molecules) the fraction absorbed from the stratum corneum is likely to be reduced as a result of desquamation. Increasing solute lipophilicity (i.e., increased B) will result in a greater viable epidermal resistance to transport and also a reduced fraction of solute likely to be absorbed from the stratum corneum. Figure 10 also shows that two of the lipophilic pesticides should have a lower fraction absorbed into the body from the stratum corneum as a consequence of desquamation.

X. STRATUM CORNEUM RESERVOIR FOR OTHER SOLUTES

It is to be emphasized that a reservoir effect is not restricted to steroids. Benowitz et al. (31) showed that continued absorption of nicotine from the skin after decontamination and is therefore evidence of the stratum corneum acting as a reservoir for nicotine (Fig. 11).

Caffeine has also been shown to have a reservoir in the stratum corneum and this reservoir is greater for an emulsion than for acetone (32) (Fig. 12).

Yagi et al. (33) have suggested that cationic beta blocking drugs may accumulate in stratum corneum intercellular lipids as a consequence of binding to endogenous anionic lipids such as cholesterol-3-sulfate, palmitic acid, stearic acid, and oleic acid. As shown in Figure 13, caffeine and a number of sunscreen agents were retained in the stratum corneum and had not penetrated into the epidermis, dermis, or receptor fluid after 16 hours. Other solutes have a high affinity for the stratum

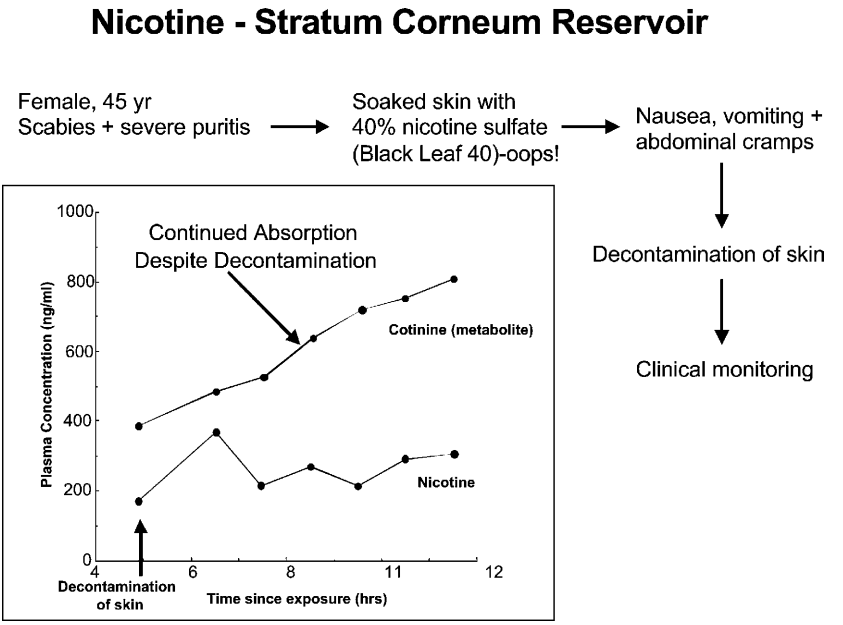


Figure 11 Evidence of a nicotine reservoir in the skin as shown by the appearance of nicotine and its metabolite cotinine in plasma after topical decontamination. *Source:* From Ref. 31.

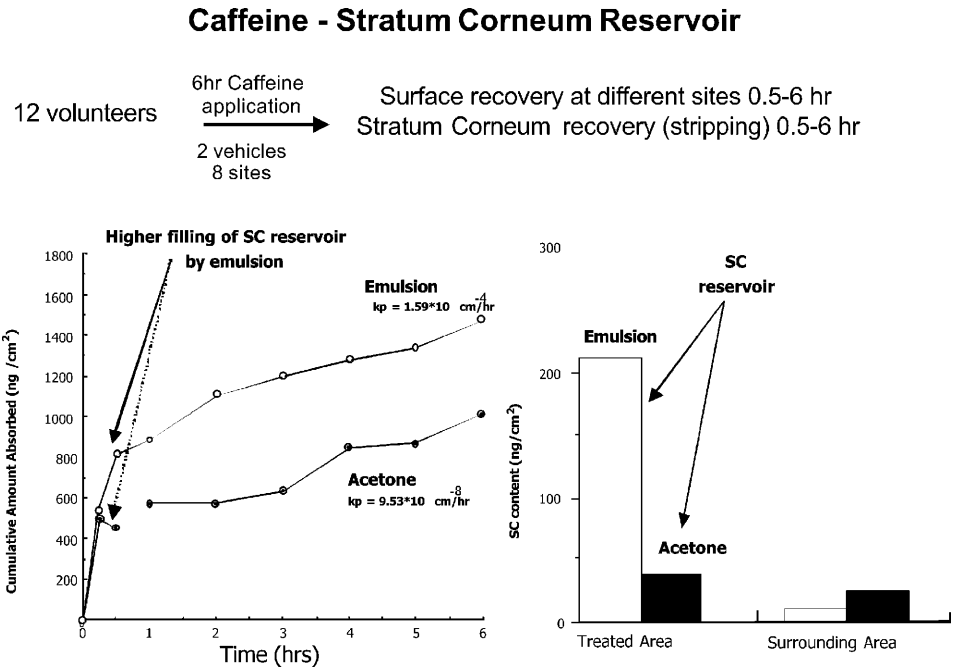


Figure 12 Effect of formulation on the extent to which a reservoir is formed in the stratum corneum for caffeine. *Source*: From Ref. 32.

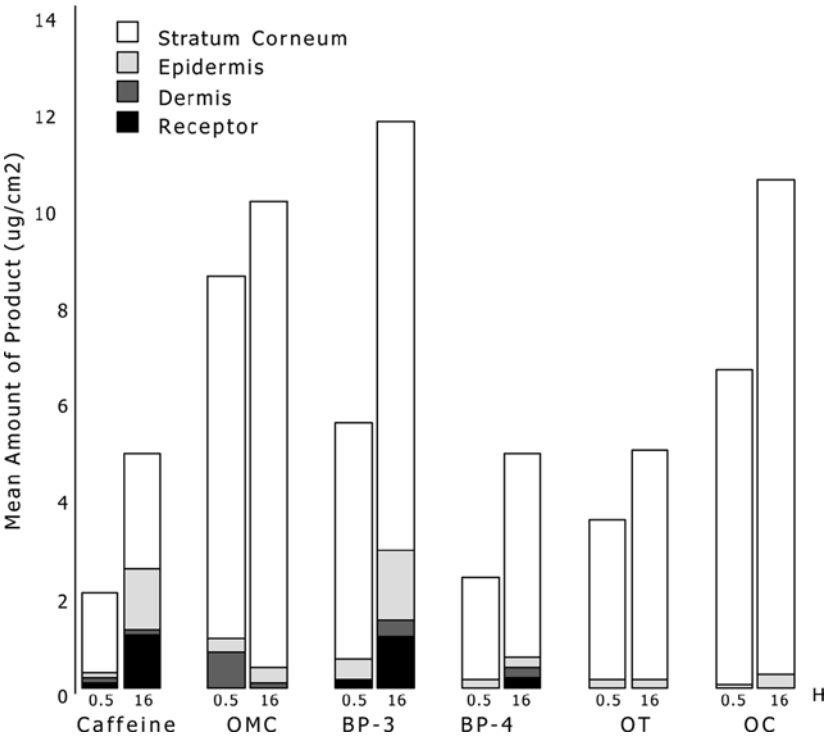


Figure 13 Differential distributions of caffeine and a number of sunscreens between the stratum corneum, epidermis, dermis, and receptor after in vitro penetration studies. *Source*: From Ref. 34.

corneum including surfactants testosterone (35). The magnitude of epidermal binding of testosterone exceeds by several fold that of the dermis, but because of the many-fold thickness of the dermis, far larger amounts are associatively bound from which it is eluted in body fluids. It is plasma protein bound and therefore its absorption is enhanced. Malathione (36), hair dyes (37), and vitamin E (38) are examples of the many compounds shown to be bound to stratum corneum components.

XI. VIABLE EPIDERMIS AND DERMAL RESERVOIR

Most studies have emphasized the stratum corneum as a reservoir. However, the viable epidermis, dermis, and underlying tissues may themselves also act as reservoirs. Baker et al. (39) have reported binding of topical steroids to epidermal tissue. The effect of viable epidermal and dermal tissues as reservoirs may be limited by the often-extensive metabolism, which can occur in viable tissue and its location. For beta-estradiol, metabolic activity mainly resided in the basal layer of the viable epidermis (40). Accumulation and the concentration in the basal cell layer of the epidermis is important for many solutes and it has been suggested that it is the free drug concentration that exerts a pharmacological effect (41). Accumulation in the viable epidermis can be deduced using the model described in Figure 6 and this has been used to examine epidermal concentrations of steroids (14). Walter and Kurz (42) have reported that the binding of 10 drugs to both epidermis and dermis was

related to the lipophilicity of the drugs. Yagi et al. (33) have commented that binding of beta-blockers to viable epidermis components is an important determinant of the residence time in viable skin. In addition to binding, the rate of removal by the perfusing blood should also be a determinant of the extent of reservoir formation in these tissues as is evident by prolonged anaesthesia when a vasoconstrictor is included with a local anaesthetic in intradermal injections. Dermal and lower tissue level concentrations when a drug is applied together with a vasoconstrictor (43).

As an illustration of this principle, the dermal clearance and retention of diclofenac can be shown to depend on both binding to dermal tissues and to blood flow and this effect is most evident when binding protein is not present in the blood (44).

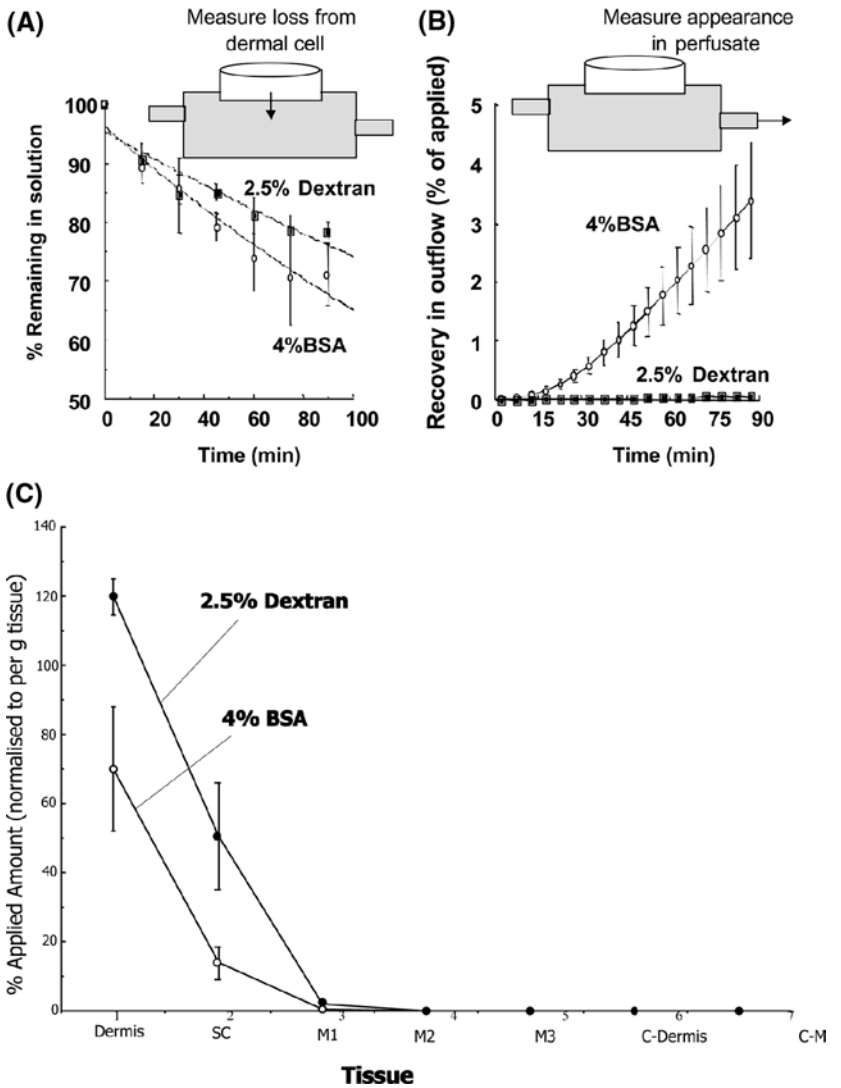


Figure 14 Amount remaining in (**A**) dermal absorption cell, (**B**) eluting in the perfusate, and (**C**) present in dermis, subcutaneous tissue (SC), muscle (M), and contralateral tissue after dermal application of diclofenac using perfusate, which binds (4% albumin) and does not bind (2.5% dextran) to diclofenac. *Source*: From Ref. 44.

When dextran rather than albumin is used as the perfusate, diclofenac is retained in the skin after dermal application and the retention sites are the dermis and subcutaneous tissue (Fig. 14).

The expression for the retention half-life ($t_{0.5}$) for solutes in the dermis and other tissues can be related to three key parameters, binding to plasma components (fraction unbound (fu_p), binding to the dermis (fu_T), and the blood flow to the topical site (Q_p) as well as the relative volumes for solute distribution in the plasma (V_p) and in extravascular tissue space (V_{TE}) (44). Drugs such as diclofenac show much greater binding to dermis (and plasma) than some other solutes and therefore are preferentially retained.

XII. IN VITRO–IN VIVO CORRELATIONS

Recently considerable recent interest has concerned the skin reservoir associated with in vitro skin penetration studies (45). Conflict presently exists as to whether or not skin levels remaining in the stratum corneum and epidermis/dermis at the end of an in vitro study should be included in the overall estimation of absorbed material. As Yourick et al. (45) point out, guidelines issued by COLIPA and the Scientific Committee on Cosmetic Product and Non-food Products suggest that material remaining in the stratum corneum at the end of a study should not be considered as systemically available, whereas that in the viable epidermis and dermis should. In contrast, European Centre for Ecotoxicology and Toxicology of Chemicals suggests that percutaneous absorption should be based on receptor fluid concentrations only. The draft Organization for Economic Co-operation and Development guidelines take an intermediate position, namely that the amount of material should include both the skin and receptor fluid unless additional studies can demonstrate that the material in the skin is effectively not available.

As a consequence, any exposure assessment should include an assessment of the likely skin reservoir that exists in terms of whether the chemical in the skin is available for systemic absorption. In principle, the likely extent of the stratum corneum reservoir should be defined at the end of the application together with an estimate of the extent of binding/partitioning to lipid and protein components (Fig. 3). Prediction of the stratum corneum reservoir is complicated by effects such as binding of solutes to keratin in the stratum corneum and viable epidermis, lipophilicity, and ionization (23,46,47), the dependence of the skin reservoir on the nature of formulation used (45,48), and the use of soaps (49). Further, the stratum corneum and the viable epidermis are not homogenous membranes but ones in which partitioning may vary with depth from the surface (50,51) and/or being more evident in specific regions, e.g., around hair (45).

However, a cautious adoption of the present guidelines would suggest that it is the reservoir effect in the viable epidermis and dermis that is of most interest in dermal exposure risk assessment. Of note, it may be that all of the skin will eventually be seen to be important. At this stage there is insufficient data available to be definitive. Yourich et al. (45) point out that, when the sun tanning color additive dihydroxyacetone and a fluorescent brightening agent 7-(2H-naphthol[1,2-d]triazole-2-yl)-3-phenylcoumarin is applied to human skin in vitro for 24 hours, the amount remaining in the viable epidermis and dermis constituted 50% or more of the dose calculated to have penetrated. Neither dihydroxyacetone nor 7-(2H-naphthol[1,2-d]triazole-2-yl)-3-phenylcoumarin was metabolized and only 5% of dihydroxyace-

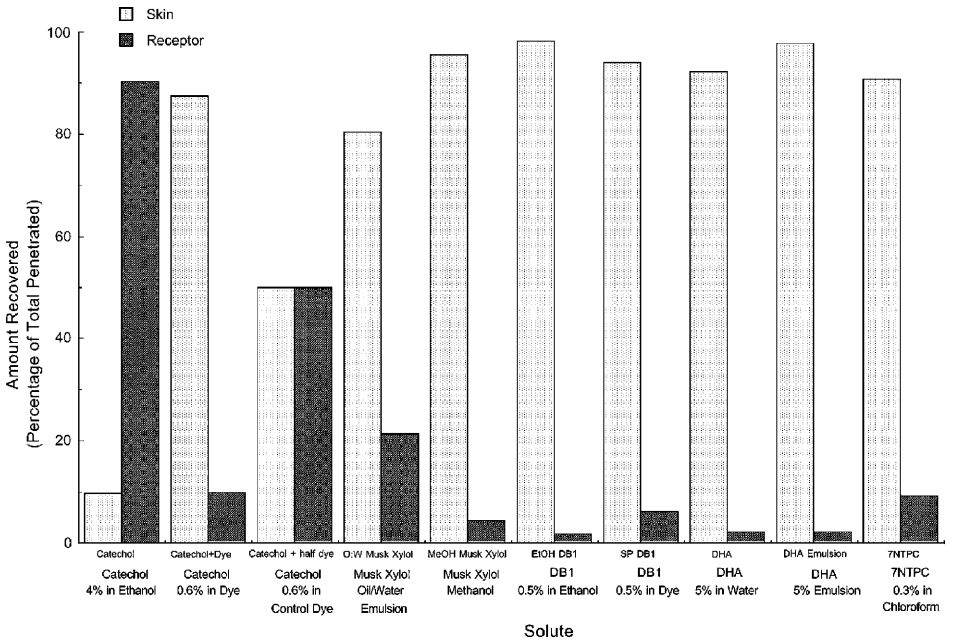


Figure 15 Comparison of the amount of solute retained in human skin to that penetrating into receptor fluid as a percentage of the total amount penetrated. *Source*: Data from Refs. 45, 52, and 53.

tone was covalently bound to protein. In contrast, the comparable fractions of the amount in the viable epidermis and dermis relative to dose penetrated for the dye agents disperse blue 1 and catechol were small (45,52). Further, Jung et al. (52) showed that, whereas 7% of a catechol dose is absorbed from an ethanol vehicle, less than 0.5% of catechol is absorbed in a consumer permanent hair dye product, the lower absorption reflecting oxidation of catechol in the latter product. Yurich et al. (45) suggest that it is appropriate to add skin levels to receptor fluids to gain a more realistic measure of dermal absorption when movement of the chemical from the skin to the receptor fluid is known to occur. They further suggest that significant retention in the skin occurs for both polar and nonpolar solutes. Figure 15 shows some examples of the relative percentages of solutes penetrating the skin that were recovered in the skin itself and in the receptor fluid. Accordingly, they suggest that further characterization and quantification of the skin reservoir is needed in dermal exposure assessment.

XIII. CONCLUSION

The skin or transdermal reservoir effect is a well established phenomena that is both dependent on the amount accumulating in the skin and is evident as some time after the original application by application of some type of skin enhancement such as re-occlusion or a chemical enhancer. The time of the follow-up application and the extent of the enhancement will govern the presence of a reservoir effect. Desquamation will only affect the reservoir effect when the penetration rate of the solute is very slow. The reservoir effect is also important in dermal exposure risk assessments.

ACKNOWLEDGMENTS

This work was supported by the Australian National Health and Medical Research Council and the Lions Medical Research Foundation. We are grateful to Professor Annette Bunge and Dr. Micaela Reddy for providing us with the material for Figure 10. This chapter is an update of our recently published review (54).

REFERENCES

1. Vickers CF. Stratum corneum reservoir for drugs. Adv Biol Skin 1972; 12:177–189.
2. Guillot M. Physiochemical conditions of cutaneous absorption. J Physiol 1954; 46:31–49.
3. Schaefer H, Stuttgen G, Zesch A, Schalla W, Gazith J. Quantitative determination of percutaneous absorption of radiolabeled drugs in vitro and in vivo by human skin. Curr Probl Dermatol 1978; 7:80–94.
4. Malkinson FD, Ferguson EH. Percutaneous absorption of hydrocortisone-4-C14 in two human subjects. J Invest Dermatol 1955; 25:281–283.
5. Sulzberger MB, Hermann F. On some characteristics and biological functions of the skin surface. Dermatologica (Basel) 1961; 123:1–23.
6. Vickers CFH. Existence of reservoir in the stratum corneum—experimental proof. Arch Dermatol 1963; 88:20–33.
7. Roberts MS, Anissimov Y, Gonsalvez R. Mathematical models in percutaneous absorption. In: Bronaugh RL, Maibach HI, eds. Percutaneous Absorption: Drugs Cosmetics Mechanisms Methodology. 3d ed. New York: Marcel Dekker, 1999:3–55.
8. Carr RD, Wieland RG. Corticosteroid reservoir in the stratum corneum. Arch Dermatol 1966; 94:81–84.
9. Zesch A, Schaefer H, Hoffmann W. Barrier and reservoir function of individual areas of the horny layers of human skin for locally administered drugs. Arch Derm Forsch 1973; 246:103–107.
10. Roberts MS, Walker M. Water—the most natural penetration enhancer. In: Walters KA, Hadgraft J, eds. Skin Penetration Enhancement. New York: Marcel Dekker, 1993: 1–30.
11. Barry BW, Woodford R. Comparatove bio-availability and activity of proprietary topical corticosteroid preparations: vasoconstrictor assays on thirty-one ointments. Br J Dermatol 1975; 93:563–571.
12. Anderson BD, Higuchi WI, Raykar PV. Heterogeneity effects on permeability—partition coefficients in human stratum corneum. Pharm Res 1988; 5:566–573.
13. Neelissen JA, Arth C, Wolff M, Schrijvers AH, Junginger HE, Bodde HE. Visualization of percutaneous 3H-estradiol and 3H-norethindrone acetate transport across human epidermis as a function of time. Acta Derm Venereol Suppl (Stockh) 2000; 208:36–43.
14. Siddiqui O, Roberts MS, Polack AE. Percutaneous absorption of steroids: relative contributions of epidermal penetration and dermal clearance. J Pharmacokin Biopharm 1989; 17:405–424.
15. Anissimov Y, Roberts MS. Diffusion modeling of percutaneous absorption kinetics. 1. Effects of flow rate, receptor sampling rate, and viable epidermal resistance for a constant donor concentration. J Pharm Sci 1999; 88:1201–1209.
16. Rougier A, Dupuis D, Lotte C, Roguet R, Schaefer H. In vivo correlation between stratum corneum reservoir function and percutaneous absorption. J Invest Dermatol 1983; 81:275–278.
17. Dupuis D, Rougier A, Roguet R, Lotte C, Kalopissis G. In vivo relationship between horny layer reservoir effect and percutaneous absorption in human and rat. J Invest Dermatol 1984; 82:353–356.

18. Rougier A, Dupuis D, Lotte C, Roguet R, Wester RC, Maibach HI. Regional variation in percutaneous absorption in man: measurement by the stripping method. Arch Dermatol Res 1986; 278:465–469.
19. Dupuis D, Rougier A, Roguet R, Lotte C. The measurement of the stratum corneum reservoir: a simple method to predict the influence of vehicles on in vivo percutaneous absorption. Br J Dermatol 1986; 115:233–238.
20. Stokes RP, Diffey BL. The water resistance of sunscreen and day-care products. Br J Dermatol 1999; 140:259–263.
21. Wester RC, Maibach HI, Bucks DA, Sedik L, Melendres J, Liao C, DiZio S. Percutaneous absorption of [14C]DDT and [14C]benzo[a]pyrene from soil. Fundam Appl Toxicol 1990; 15:510–516.
22. Billhimer WL, Berge CA, Englehart JS, Rains GY, Keswick BH. A modified cup scrub method for assessing the antibacterial substantivity of personal cleansing products. J Cosmet Sci 2001; 52:369–375.
23. Dessler W. Percutaneous absorption of hair dyes. In: Roberts MS, Walters KA, eds. Dermal Absorption and Toxicity Assessment. New York: Marcel Dekker, 1998:489–536.
24. Bucks DAW. Predictive Approaches II. In: Mass-Balance Procedure in Topical Drug Bioavailability, Bioequivalence and Penetration. New York: Plenum Press, 1993: 183–195.
25. Clarys P, Gabard B, Barel AO. A qualitative estimate of the influence of halcinonide concentration and urea on the reservoir formation in the stratum corneum. Skin Pharmacol Appl Skin Physiol 1999; 12:85–89.
26. McCarley KD, Bunge AL. Pharmacokinetic models of dermal absorption. J Pharm Sci 2001; 90:1699–1719.
27. Turpeinen M. Absorption of hydrocortisone from the skin reservoir in atopic dermatitis. Br J Dermatol 1991; 124:358–360.
28. Schaefer H, Redelmeier M. Skin Barrier. Basel: Karger, 1996:40–42.
29. Roberts MS, Walters KA. The relationship between structure and barrier function of skin. Dermal Absorp Toxic Assess 1998; 91:1–42.
30. Reddy MB, Guy RH, Bunge AL. Does epidermal turnover reduce percutaneous penetration? Pharm Res 2000; 17:1414–1419.
31. Benowitz NL, Lake T, Keller KH, Lee BL. Prolonged absorption with development of tolerance to toxic effects after cutaneous exposure to nicotine. Clin Pharmacol Ther 1987; 42:119–120.
32. Chambin-Remoussenard O, Treffel P, Bechtel Y, Agache P. Surface recovery and stripping methods to quantify percutaneous absorption of caffeine in humans. J Pharm Sci 1982; 11:1099–1101.
33. Yagi S, Nakayama K, Kurosaki Y, Higaki K, Kimura T. Factors determining drug residence in skin during transdermal absorption: studies on beta-blocking agents. Biol Pharm Bull 1998; 21:1195–1201.
34. Potard G, Laugel C, Schaefer H, Marty J-P. The stripping technique: in vitro absorption and penetration of five UV filters on excised fresh human skin. Skin Pharmacol Appl Skin Physiol 2000; 13:336–344.
35. Menczel E, Maibach HI. Chemical binding to human dermis in vitro testosterone and benzyl alcohol. Acta Derm Venereol 1972; 52:38–42.
36. Menczel E, Bucks D, Maibach H, Wester R. Malathion binding to sections of human skin: skin capacity and isotherm determinations. Arch Dermatol Res 1983; 275:403–406.
37. Bronaugh RL, Congdon ER. Percutaneous absorption of hair dyes: correlation with partition coefficients. J Invest Dermatol 1984; 83:124–127.
38. Lee AR, Tojo K. An experimental approach to study the binding properties of vitamin E (alpha-tocopherol) during hairless mouse skin permeation. Chem Pharm Bull (Tokyo) 2001; 49:659–663.
39. Baker JR, Christian RA, Simpson P, White AM. The binding of topically applied glucocorticoids to rat skin. Br J Dermatol 1977; 96:171–178.

40. Liu P, Higuchi WI, Ghanem AH, Good WR. Transport of beta-estradiol in freshly excised human skin in vitro: diffusion and metabolism in each skin layer. Pharm Res 1994; 11:1777–1784.
41. Borsadia S, Ghanem AH, Seta Y, Higuchi WI, Flynn GL, Behl CR, Shah VP. Factors to be considered in the evaluation of bioavailability and bioequivalence of topical formulations. Skin Pharmacol 1992; 5:129–145.
42. Walter K, Kurz H. Binding of drugs to human skin: influencing factors and the role of tissue lipids. J Pharm Pharmacol 1988; 40:689–693.
43. Singh P, Roberts MS. Effects of vasoconstriction on dermal pharmacokinetics and local tissue distribution of compounds. J Pharm Sci 1994; 83:783–791.
44. Roberts MS, Cross SE. A physiological pharmacokinetic model for solute disposition in tissues below a topical application site. Pharm Res 1999; 16:1394–1400.
45. Yourick JJ, Koenig ML, Yourick DL, Bronaugh RL. Fate of chemicals in skin after dermal application: does the vitro skin reservoir affect the estimate of systemic absorption? Toxical Appl Pharmacol 2004; 195:309–320.
46. Heard CM, Monk BV, Modley AJ. Binding of primaquine to epidermal membranes and keratin. Int J Pharm 2003; 257:237–244.
47. Miselnicky SR, Lichtin JL, Sakr A, Bronaugh RL. The influence of solubility, protein binding, and percutaneous absorption on reservoir formation in skin. J Soc Cosmet Chem 1988; 39(3):169–177.
48. Fang JY, Hwang TL, Leu YL. Effect of enhancers and retarders on percutaneous absorption of flurbiprofen from hydrogels. Int J Pharm 2003; 250:313–325.
49. Loden M, Buraczewska I, Edlund F. The irritation potential and reservoir effect of mild soaps. Contact Dermat 2003; 49:91–96.
50. Mueller B, Anissimov YG, Roberts MS. Unexpected clobetasol propionoate in human stratum corneum after topical application in vitro. Pharm Res 2003; 20:1835–1837.
51. Anissimov YG, Roberts MS. Diffusion modelling of percutaneous absorption kinetics: 3. Variable diffusion and partitioning coefficients. J Pharm Sci 2004; 93:470–487.
52. Hood HL, Wickett RR, Bronaugh RL. In vitro percutaneous absorption of the fragrance ingredient musk oil. Food Chem Toxicol 1996; 34:483–488.
53. Jung CT, Wickett RR, Desai PB, Bronaugh RL. In vitro and in vivo percutaneous absorption of catechol. Food Chem Toxicol 2003; 41:885–895.
54. Roberts MS, Anissimov YG, Cross SE. Factors affecting the formation of a skin reservoir for topically applied solutes. Skin Pharmacol Physiol 2004; 17(1):3–16.

15
Effects of Occlusion: Percutaneous Absorption

Hongbo Zhai and Howard I. Maibach
Department of Dermatology, School of Medicine, University of California, San Francisco, California, U.S.A.

I. INTRODUCTION

Occlusion means the skin covered by tape, gloves, impermeable dressings, or transdermal devices. Certain topical vehicles may also act as "occlusive dressings" if they contain fats or some polymer oils, reducing water loss to atmosphere. In healthy skin, the stratum corneum typically has water content of 10% to 20% and provides a relatively efficient barrier against percutaneous absorption of exogenous substances (1). Skin occlusion can increase stratum corneum hydration, and hence influence percutaneous absorption by altering partitioning between the surface chemical and the skin due to the increasing presence of water, swelling corneocytes and possibly altering the intercellular lipid phase organization, also by increasing the skin surface temperature, and increasing blood flow (2–4). Occlusion may enhance drug efficacy (5–10). Actually, skin occlusion is a complex event producing profound changes and influencing skin biology as well as wound healing processing (11–27). In general occlusion can, with exceptions (2,4,28,29), increase percutaneous absorption of topically applied compounds (30–42); even a short time (30 min) occlusion can result in significantly increased on penetration and horny layer water content (43). However, effects of occlusion on absorption may also depend on the anatomic site as well as vehicle and penetrant (32,37,44).

Transdermal drug delivery systems have a high level of interest; in practice, skin is not readily breached in the therapeutic level because of barrier resistance. Various approaches have been employed to enhance absorption. Occlusion, perhaps due to its simplicity and convenience, has been extensively adopted to increase absorption. This chapter focuses on the effect of occlusion on percutaneous absorption and summarizes related details.

II. PERCUTANEOUS ABSORPTION IN VITRO

Gummer and Maibach (30) examined the penetration of methanol and ethanol through excised, full thickness, guinea-pig skin in vitro at varying volumes and under

a variety of occlusive conditions over a period of 19 hours. Neither compound showed an increase in penetration with increasing dose volume. But occlusion significantly enhanced ($p < 0.01$) penetration of both when compared to non-occluded skin. The nature of the occlusive material significantly influenced the penetrated amounts of both compounds, and as well as the profiles of the amount penetrating per hour.

Hotchkiss et al. (31) evaluated absorption of model compounds, nicotinic acid, phenol and benzoic acid, and the herbicide triclopyr butoxyethyl ester (triclopyr BEE) with in vitro flow-through diffusion cells using rat and human skin. After application, the skin surface was non-occluded or covered with Teflon® caps as an occlusion device. The absorption of each compound across the skin and into the receptor fluid at 72 hours was calculated. Occlusion significantly ($p < 0.05$) enhanced absorption of the model compounds, but varying with the compound and the skin (rat or human) used. They observed the effect of vehicle and occlusion on the in vitro percutaneous absorption of [methylene-^{14}C]-benzyl acetate (1.7–16.6 mg/cm^2) in diffusion cells using full thickness skin from male Fischer 344 rats (32). When benzyl acetate in ethanol was applied to the skin and occluded with Parafilm®, the extent of absorption at 48 hours was not significantly different from non-occluded skin; but at 6 hours, as the ethanol content of the application mixture was increased, the absorption of benzyl acetate through occluded skin was enhanced proportionally ($r = 0.99$). With phenylethanol as a vehicle, the extent of the benzyl acetate absorption through occluded skin at 48 hours was significantly ($p < 0.05$) enhanced compared with non-occluded skin, but this did not correlate with the proportion of phenylethanol in the application mixture. With dimethylsulphoxide as a vehicle, the extent of benzyl acetate absorption through occluded skin at 48 hours was enhanced ($p < 0.05$) compared with non-occluded skin; when dimethylsulphoxide content of the application mixture was increased, the absorption of benzyl acetate was enhanced proportionally. They concluded that occlusion often significantly enhanced absorption, but the effect varied with time and vehicle.

Roper et al. (33) tested the absorption of 2-phenoxyethanol applied in methanol through non-occluded rat and human skin in vitro in two diffusion cell systems over 24 hours. 2-Phenoxyethanol was lost by evaporation with both non-occluded cells, but occlusion of the static cell reduced evaporation and increased total absorption to 98.8 ± 7.0%.

Treffel et al. (28) compared permeation profiles of two molecules with different physicochemical properties under occluded vs. non-occluded conditions in vitro over a period of 24 hours. Absorption was determined using human abdominal skin in diffusion cells under occluded and non-occluded conditions. Occlusion increased the permeation of citropten (a lipophilic compound; partition coefficient = 2.17) 1.6 times ($p < 0.05$) greater than the non-occluded permeation. But the permeation of caffeine (an amphiphilic compound; partition coefficient = 0.02) did not show significant differences ($p = 0.18$) between occlusive and nonocclusive conditions. They confirmed the view, i.e., occlusion does not necessarily increase the percutaneous absorption of all chemicals (2,4,29).

Brooks and Riviere (44) utilized an isolated perfused porcine skin flap (IPPSF) to determine the percutaneous absorption of ^{14}C-labeled phenol versus *p*-nitrophenol (PNP) at two concentrations (4 μg/cm^2 versus 40 μg/cm^2) in two vehicles (acetone versus ethanol) under occluded versus non-occluded dosing conditions over 8 hours Occlusion increased the absorption, penetration into tissues, and total recoveries of phenol when compared to non-occluded conditions. Absorption and penetration of phenol into tissues were greater with ethanol than with acetone under

non-occluded conditions, but the opposite was observed under occluded conditions. Phenol in acetone had a greater percentage of applied dose penetration into tissues with low-dose than high-dose, suggesting a fixed absorption rate. This was also seen for PNP, but only under occluded conditions. Neither phenol dose, vehicle, nor occlusion had a significant effect on the labeled phenol seen in the stratum corneum or on time of peak flux, a finding that limits the usefulness of noninvasive stratum corneum sampling to assess topical penetration. Neither PNP dose, vehicle, nor occlusion had a significant effect on total recovery of labeled PNP. They suggested that comparative absorption of phenol and PNP are vehicle, occlusion, and penetrant dependent.

III. PERCUTANEOUS ABSORPTION IN VIVO

A. Animals

Bronaugh et al. (34) measured the percutaneous absorption of cosmetic fragrance materials, safrole, and cinnamyl anthranilate, as well as of cinnamic alcohol and cinnamic acid, at occluded and non-occluded application sites over a 24-hours period. They determined the absorption in the rhesus monkey in vivo, and also measured the absorption value through excised human skin in diffusion cells system. Each radiolabeled compound was applied, in an acetone vehicle at a concentration of 4 $\mu g/cm^2$. Occlusion was accomplished by taping plastic wrap to skin application site for in vivo experiments and by sealing the tops of the diffusion cells with Parafilm. Occlusion of the application sites resulted in large increases in absorption, an effect consistent with the volatility of permeating molecules. When evaporation of the compounds was prevented, 75% of the applied cinnamic alcohol and 84% of the cinnamic acid were absorbed compared to 25% and 39%, respectively, without occlusion. In vitro experiments showed that the percutaneous absorption of these compounds was increased under occlusion in comparison to non-occlusion conditions (open to the air). The greatest difference between in vivo and in vitro absorption values occurred with safrole, which was the least well absorbed and the most volatile compound. Subsequently, they determined the percutaneous absorption of the fragrance benzyl acetate (octanol–water partition coefficient = 1.96) and five other benzyl derivatives (benzyl alcohol, octanol–water partition coefficient = 0.87; benzyl benzoate, octanol–water partition coefficient = 3.97; benzamide, octanol–water partition coefficient = 0.64; benzoin, octanol–water partition coefficient = 1.35; and benzophenone, octanol–water partition coefficient = 3.18) in vivo in rhesus monkeys and human models (39). Two occlusion methods (plastic wrap and glass chamber) were employed for 24 hours. In general, absorption through occluded skin was high. Differences in absorption were observed between the methods. The low percent absorbed for benzyl acetate was noted with plastic wrap compared to the non-occluded site, where glass chamber occlusion resulted in the greatest bioavailability. This discrepancy might be due to compound sequestration by the plastic. No correlations were found between skin penetration of these compounds and their octanol–water partition coefficients. Under non-occluded conditions skin penetration was reduced; there was great variability between compounds, possibly because of variations in the rates of evaporation from the application site.

Qiao et al. (35) described an in vivo in female weanling pigs model to quantify disposition of parathion (PA) and its major metabolites for human dermal risk assessment following ^{14}C PA topical (occluded and non-occluded dose of 300 μg,

40 μg /cm^2 on the abdomen and back) and intravenous (300 μg). Total ^{14}C PA and its major metabolites in plasma, urine, blood, stratum corneum, dosed tissues, dosing device, and evaporative loss were determined. Occlusion enhanced the partition of both PA and PNP into the stratum corneum from the dosed skin surface, and also slowed down the distribution of PA and PNP in the local dosed tissues. Occlusion also altered the first pass biotransformation of PA in the epidermis. They further analyzed this data, focusing on a quantitation of the effects of application site (back vs. abdomen) and dosing method (occluded vs. non-occluded) on in vivo disposition of both the parent PA and its sequential metabolites (36). They concluded that occlusion not only increased ^{14}C absorption and shortened the mean residence time in most compartments but also altered the systemic versus cutaneous biotransformation pattern. They investigated the effects of anatomical site and occlusion on the percutaneous absorption and residue pattern of total ^{14}C following topical application of PA onto four skin sites (300 μg/10 μCi; 40 μg /cm^2) in weanling swine using occluded and non-occluded dosing systems (37). Total excretion (% dose) of urinary and fecal was determined after 168-hour dosing onto the abdomen, buttocks, back, and shoulder ($N = 4$/site), and the % dose of excretion was 44%, 49%, 49%, and 29% in the occluded system; 7%, 16%, 25%, and 17% in the non-occluded system, respectively. The percutaneous absorption from the shoulder was much lower than that from the other three sites under occluded conditions. However, in the non-occluded system, absorption from the abdomen was the lowest, with shoulder and buttocks being similar, and the back the highest. They suggested that anatomic site may influence the effect of occlusion. They utilized the same model to determine the pentachlorophenol (PCP) dermal absorption and disposition from soil under occluded and non-occluded conditions for 408 hours (38). The absorption on occluded dosed site (100.7%) was significantly enhanced (by more than three times, $p < 0.0005$) when compared to non-occluded site (29.1%).

Mukherji et al. (40) evaluated the topical application of 2′,3′-dideoxyinosine (ddI), a nucleoside analog used for treating patients with acquired immunodeficiency syndrome. A dose of ddI (approximately 80 mg/kg) dispersed in approximately 1 g ointment base was applied to the back of high follicular density (HFD) and low follicular density (LFD) rats with or without occlusion. At 24 hours the experiment was terminated and skin sections at the application site removed. After 24-hours topical application, average plateau plasma levels of about 0.6 μg/mL were achieved within one to two hours and maintained for 24 hours. Occlusion gave a more uniform plasma profile but did not increase bioavailability. They thought that the transfollicular absorption route for ddI did not act as an important role due to the similar bioavailability in the HFD and LFD rats.

B. Man

Feldmann and Maibach (41) correlated the increased pharmacological effect of hydrocortisone (HC) by occlusive conditions with the pharmacokinetics of absorption. [^{14}C]-HC in acetone was applied to the ventral forearm. The application site was either non-occluded or occluded with plastic wrap. After 24-hours application, the non-occluded site was washed. At the occluded site, the wrap remained for 96 hours post application before washing the site. The percent of the applied dose excreted into the urine, corrected for incomplete renal elimination, was 0.46 ± 0.2 (mean ± SD) and 5.9 ± 3.5 under non-occluded and occluded conditions, respectively. The occlusive condition significantly increased (10-fold) the cumulative

absorption of HC (total excretion was occluded = 4.48% vs. non-occluded = 0.46%). They noted that the difference of application duration (24 hours exposure on non-occluded site vs. 96 hours exposure on occluded site) could influence the absorption as determined by the cumulative measurement of drug excreted into urine, but the significant difference in percent dose at 12 and 24 hours between non-occluded and occluded was not expected to be dependent upon differences in washing times. Malathion, a pesticide was intensively studied to determine the effect of duration of occlusion (45). In as little as one hour (13% of absorption) there was a significant increase in penetration, and in two hours 17%; in four hours this was 24% and in eight hours 39%.

Ryatt et al. (42) developed a human pharmacodynamic model to measure the enhanced skin penetration of hexyl nicotinate (HN) using laser Doppler velocimetry (LDV). Before applying HN, the application site was either untreated (control) or subjected to one of four 30-minute pretreatments: (a) occlusion with a polypropylene chamber; (b) occlusion [as in (a)] in the presence of 0.3 mL of the vehicle; (c) occlusion [as in (a)] in the presence of 0.3 mL of the vehicle containing 25% 2-pyrrolidone; (d) occlusion [as in (a)] in the presence of 0.3 mL of the vehicle containing 25% laurocapram (1-dodecylhexahydro-2*H*-azepin-2-one). The onset of action, time to peak, peak height, area under the curve (AUC), time-course, and magnitude of the LDV response were calculated. The onset of action and time to peak were significantly shortened, and the peak height and AUC significantly increased with pretreatments (a)–(d) (i.e., under occlusion conditions). Ryatt et al. (43) explored the relationship between increased stratum corneum hydration by occlusion and enhanced percutaneous absorption in vivo in man. Percutaneous absorption of HN was monitored noninvasively by LDV following each of three randomly assigned pretreatments: untreated control, 30-minute occlusion with a polypropylene chamber and 30-minute occlusion followed by exposure to ambient conditions for one hr. Stratum corneum water content after the same pretreatments was measured with the dielectric probe technique. The local vasodilatory effect of the nicotinic acid ester was quantified using LDV by the onset of increased blood flow, time of maximal increase in response, magnitude of the peak response and the area under the response–time curve. A 30-minute period of occlusion significantly shortened ($p < 0.05$) both the time of onset of the LDV-detected response to HN and the time to peak response when compared to the untreated controls. The stratum corneum water content values showed the same pattern, where the horny layer water content after 30-minute occlusion was significantly elevated ($p < 0.001$). There was a significant correlation between stratum corneum water content and area under the LDV response-time curve after 30-minute occlusion ($r = 0.8$; $p < 0.05$).

Bucks et al. (29) measured the percutaneous absorption of steroids (hydrocortisone, estradiol, testosterone, and progesterone) in vivo in man under occluded and "protected" (i.e., covered, but non-occlusive) conditions. The ^{14}C-labeled chemicals were applied in acetone to the ventral forearm of volunteers. After vehicle evaporation, the site was covered with a semirigid, polypropylene chamber for 24 hours. The intact chambers were employed as the occlusion condition and by boring several small holes through the chamber as the "protected" conditions (i.e., the roof of chamber was covered with piece of water permeable membrane). Urine was collected for seven days post application. Steroid absorption increased with increasing lipophilicity up to a point, but that penetration of progesterone (the most hydophobic analog studied) did not continue the trend and was presumably at least partly rate-limited by slow interfacial transport at the stratum corneum. Twenty-four-hour

occlusion significantly increased ($p < 0.01$) percutaneous absorption of estradiol, testosterone, and progesterone but did not effect the penetration of hydrocortisone. The more lipophilic steroids were enhanced by occlusion but not the most water-soluble (i.e., hydrocortisone).

Table 1 summarizes the brief data of the effect of occlusion on percutaneous absorption.

IV. DISCUSSION

Skin, particularly the stratum corneum, serves as a barrier that prevents or limits the entrance of substances from the environment and also modulates the balance of water loss from body fluids. Occlusion has the immediate effects of completely blocking diffusional water loss (22). The consequence is to increase stratum corneum hydration, thereby swelling the corneocytes, and promoting the uptake of water into intercellular lipid domains (2,4). Occlusion can increase stratum corneum water content from a normal range of 10% to 20% up to 50% and can increase the skin temperature from 32°C to 37°C (2,4). Occlusion also prevents the accidental wiping or evaporation (volatile compound) of the applied compound, in essence maintaining a higher applied dose (46). In addition, it has a reservoir effect of the drug in penetration rates as result of hydration (47). Initially, a drug enters the stratum corneum under occlusion. After the occlusive dressing is removed, and the stratum corneum dehydrates, the movement of drug slows and the stratum corneum becomes a reservoir (46,47). Hydration increased penetration of lipid-soluble, nonpolar molecules but had less effect on polar molecules (28,29). The absorption of more lipophilic steroids was enhanced by occlusion but not the most watersoluble (i.e., hydrocortisone) (29). It is implied that the rate-determining role of the sequential steps involved in percutaneous absorption can be revealed by experiments of the type described using related series of homologous or analogous chemicals. However, a trend of occlusion-induced absorption enhancement with increasing penetrant lipophilicity is apparent (28,29). An earlier report by Feldmann and Maibach (41) observed an increase in percutaneous absorption of hydrocortisone under occlusion conditions. Bucks et al. (2) and Bucks and Maibach (4) has explained this contrary data and suggested that may be due to an acetone solvent effect. Topical application of acetone can disrupt barrier function by extracting stratum corneum lipids (48,49). It is conceivable that 1 mL of acetone over an area of 13 cm^2 that might compromise stratum corneum barrier function and hence increased the penetration of hydrocortisone under occlusion condition. Experimental data is required to clarify this issue.

In practice, to increase of skin penetration rates of applied drug is far from simple. Skin barrier function can be ascribed to the macroscopic structure of the stratum corneum, which consists of alternating lipoidal and hydrophylic regions. For this reason, physicochemical characteristics of the drug, such as partition coefficient, structure, and molecular weight, play an important role in determining the facility of percutaneous absorption (50,51). Another factor to consider in transdermal drug delivery is the vehicle in which the drug is formulated as it acts on drug release from the formulation (32,44). Moreover, vehicles may also interact with human stratum corneum, thereby affecting its barrier function. Surfactants and penetration enhancers are well-known examples. Subsequently, dosing conditions, such as humidity, temperature, and occlusion, also have their impact on the actual input (rate) of drug through human skin.

Table 1 Summary on the Effect of Occlusion on Percutaneous Absorption

Models				
In vitro	In vivo			
	Animals	Humans	Compounds	Results and references
Guinea pig skin			Methanol and ethanol	Enhanced the penetration of both chemicals (30)
Human skin			Citropten and caffeine	Increased the permeation of citropten (lipophilic compound) but not the caffeine (amphiphilic compound) (43)
Rat and human skin			Nicotinic acid, phenol, benzoic acid, and triclopyr butoxyethyl ester	Significantly enhanced the percutaneous absorption of the compounds, but varying with the compound under study and the skin (rat or human) used (31)
Rats skin			Benzyl acetate in different vehicles (in ethanol, phenylethanol, and dimethylsulphoxide)	Significantly enhanced absorption, but the effect varied with time and vehicle (32)
Isolated perfused porcine skin flap			Phenol and PNP in two different vehicles (acetone and ethanol)	Increased the penetration on both compounds, but also affected by difference vehicles (44)
Rat and human skin			2-Phenoxyethanol applied in methanol	Reduced evaporation and increased total absorption (33)
Human skin	Rhesus monkeys		Safrole, cinnamyl anthranilate, cinnamic alcohol, and cinnamic acid	Resulted in greater permeation of all of the compounds (34)
	Weanling pigs		Parathion and its major metabolites	Increased the absorption and shortened the mean residence time; the effect of occlusion on

(*Continued*)

Table 1 Summary on the Effect of Occlusion on Percutaneous Absorption (*Continued*)

Models				
In vitro	In vivo			
	Animals	Humans	Compounds	Results and references
				percutaneous absorption affected by anatomical site difference (35–37)
	Weanling pigs		Pentachlorophenol	Absorption on occluded dosed site was significantly enhanced (by more than three times) when compared to non-occluded site (38)
	Rhesus monkeys	Humans	Benzyl acetate and five other benzyl derivatives	Increased the penetration with variability between compounds (39)
	Rats		2',3'-Dideoxyinosine	Gave a more uniform plasma profile but did not increase the bioavailability (40)
		Humans	Hydrocortisone	Significant increased the cumulative absorption (41)
		Humans	Hexyl nicotinate	Significantly increased the peak height and AUC and the onset of action and time to peak were significantly shortened; also showed a significant correlation between water content and area under the LDV response-time curve (42,43)
		Man	Hydrocortisone, estradiol, testosterone, and progesterone	Significantly increased percutaneous absorption of estradiol, testosterone, and progesterone but did not effect the penetration of hydrocortisone (29)

Abbreviations: AUC, area under the curve; LDV, laser Dappler velocimetry; PNP, *p*-nitrophenol.

In conclusion, occlusion increases the percutaneous absorption of many but not all compounds. The effect of occlusion on percutaneous absorption may be also affected by the physicochemical properties (such as volatility, partition coefficient, and aqueous solubility), anatomical site, and vehicle.

REFERENCES

1. Baker H. The skin as a barrier. In: Rook A, Wilkinson DS, Ebling FJG, eds. Textbook of Dermatology, 2d ed. Oxford: Blackwell Scientific Publications, 1972:249–255.
2. Bucks D, Guy R, Maibach HI. Effects of occlusion. In: Bronaugh RL, Maibach HI, eds. In Vitro Percutaneous Absorption: Principles, Fundamentals, and Applications. Boca Raton: CRC Press, 1991:85–114.
3. Haftek M, Teillon MH, Schmitt D. Stratum corneum, corneodesmosomes and ex vivo percutaneous penetration. Microsc Res Tech 1998; 43:242–249.
4. Bucks D, Maibach HI. Occlusion does not uniformly enhance penetration in vivo. In: Bronaugh RL, Maibach HI, eds. Percutaneous Absorption: Drug-Cosmetics-Mechanisms-Methodology. 3d ed. New York: Marcel Dekker, 1999:81–105.
5. Garb J. Nevus verrucosus unilateralis cured with podophyllin ointment. Arch Dermatol 1960; 81:606–609.
6. Scholtz JR. Topical therapy of psoriasis with fluocinolone acetonide. Arch Dermatol 1961; 84:1029–1030.
7. Sulzberger MB, Witten VH. Thin pliable plastic films in topical dermatological therapy. Arch Dermatol 1961; 84:1027–1028.
8. McKenzie AW. Percutaneous absorption of steroids. Arch Dermatol 1962; 86:91–94.
9. McKenzie AW, Stoughton RB. Method for comparing percutaneous absorption of steroids. Arch Dermatol 1962; 86:88–90.
10. Kaidbey KH, Petrozzi JW, Kligman AM. Topical colchicine therapy for recalcitrant psoriasis. Arch Dermatol 1975; 111:33–36.
11. Aly R, Shirley C, Cunico B, Maibach HI. Effect of prolonged occlusion on the microbial flora, pH, carbon dioxide and transepidermal water loss on human skin. J Invest Dermatol 1978; 71:378–381.
12. Rajka G, Aly R, Bayles C, Tang Y, Maibach HI. The effect of short-term occlusion on the cutaneous flora in atopic dermatitis and psoriasis. Acta Dermatol Venereol 1981; 61:150–153.
13. Faergemann J, Aly R, Wilson DR, Maibach HI. Skin occlusion: effect on pityrosporum orbiculare, skin P CO2, pH, transepidermal water loss, and water content. Arch Dermatol Res 1983; 275:383–387.
14. Alvarez OM, Mertz PM, Eaglstein WH. The effect of occlusive dressings on collagen synthesis and re-epithelialization in superficial wounds. J Surg Res 1983; 35:142–148.
15. Eaglstein WH. Effect of occlusive dressings on wound healing. Clin Dermatol 1984; 2:107–111.
16. Mertz PM, Eaglstein WH. The effect of a semiocclusive dressing on the microbial population in superficial wounds. Arch Surg 1984; 119:287–289.
17. Berardesca E, Maibach HI. Skin occlusion: treatment or drug-like device? Skin Pharmacol 1988; 1:207–215.
18. Silverman RA, Lender J, Elmets CA. Effects of occlusive and semiocclusive dressings on the return of barrier function to transepidermal water loss in standardized human wounds. J Am Acad Dermatol 1989; 20:755–760.
19. Agner T, Serup J. Time course of occlusive effects on skin evaluated by measurement of transepidermal water loss (TEWL). Including patch tests with sodium lauryl sulphate and water. Contact Dermatitis 1993; 28:6–9.

20. Matsumura H, Oka K, Umekage K, Akita H, Kawai J, Kitazawa Y, Suda S, Tsubota K, Ninomiya Y, Hirai, H, Miyata K, Morikubo K, Nakagawa M, Okada T, Kawai K. Effect of occlusion on human skin. Contact Dermatitis 1995; 33:231–235.
21. Berardesca E, Maibach HI. The plastic occlusion stress test (POST) as a model to investigate skin barrier function. In: Maibach HI, ed. Dermatologic Research Techniques. Boca Raton: CRC Press, 1996:179–186.
22. Kligman AM. Hydration injury to human skin. In: Van der Valk PGM, Maibach HI, eds. The Irritant Contact Dermatitis Syndrome. Boca Raton: CRC Press, 1996:187–194.
23. Leow YH, Maibach HI. Effect of occlusion on skin. J Dermatol Treat 1997; 8:139–142.
24. Denda M, Sato J, Tsuchiya T, Elias PM, Feingold KR. Low humidity stimulates epidermal DNA synthesis and amplifies the hyperproliferative response to barrier disruption: implication for seasonal exacerbations of inflammatory dermatoses. J Invest Dermatol 1998; 111:873–878.
25. Kömüves LG, Hanley K, Jiang Y, Katagiri C, Elias PM, Williams ML, Feingold KR. Induction of selected lipid metabolic enzymes and differentiation-linked structural proteins by air exposure in fetal rat skin explants. J Invest Dermatol 1999; 112:303–309.
26. Fluhr JW, Lazzerini S, Distante F, Gloor M, Berardesca E. Effects of prolonged occlusion on stratum corneum barrier function and water holding capacity. Skin Pharmacol Appl Skin Physiol 1999; 12:193–198.
27. Warner RR, Boissy YL, Lilly NA, Spears MJ, McKillop K, Marshall JL, Stone KJ. Water disrupts stratum corneum lipid lamellae: damage is similar to surfactants. J Invest Dermatol 1999; 113:960–966.
28. Treffel P, Muret P, Muret-D'Aniello P, Coumes-Marquet S, Agache P. Effect of occlusion on in vitro percutaneous absorption of two compounds with different physicochemical properties. Skin Pharmacol 1992; 5:108–113.
29. Bucks DA, McMaster JR, Maibach HI, Guy RH. Bioavailability of topically administered steroids: a "mass balance" technique. J Invest Dermatol 1988; 91:29–33.
30. Gummer CL, Maibach HI. The penetration of [^{14}C] ethanol and [^{14}C] methanol through excised guinea-pig skin in vitro. Food Chem Toxicol 1986; 24:305–309.
31. Hotchkiss SA, Hewitt P, Caldwell J, Chen WL, Rowe RR. Percutaneous absorption of nicotinic acid, phenol, benzoic acid and triclopyr butoxyethyl ester through rat and human skin in vitro: further validation of an in vitro model by comparison with in vivo data. Food Chem Toxicol 1992; 30:891–899.
32. Hotchkiss SA, Miller JM, Caldwell J. Percutaneous absorption of benzyl acetate through rat skin in vitro. 2. Effect of vehicle and occlusion. Food Chem Toxicol 1992; 30:145–153.
33. Roper CS, Howes D, Blain PG, Williams FM. Percutaneous penetration of 2-phenoxyethanol through rat and human skin. Food Chem Toxicol 1997; 35:1009–1016.
34. Bronaugh RL, Stewart RF, Wester RC, Bucks D, Mailbach HI, Anderson J. Comparison of percutaneous absorption of fragrances by humans and monkeys. Food Chem Toxicol 1985; 23:111–114.
35. Qiao GL, Williams PL, Riviere JE. Percutaneous absorption, biotransformation, and systemic disposition of parathion in vivo in swine. I. Comprehensive pharmacokinetic model. Drug Metab Dispos 1994; 22:459–471.
36. Qiao GL, Riviere JE. Significant effects of application site and occlusion on the pharmacokinetics of cutaneous penetration and biotransformation of parathion in vivo in swine. J Pharm Sci 1995; 84:425–432.
37. Qiao GL, Chang SK, Riviere JE. Effects of anatomical site and occlusion on the percutaneous absorption and residue pattern of 2,6-[ring-^{14}C] parathion in vivo in pigs. Toxicol Appl Pharmacol 1993; 122:131–138.
38. Qiao GL, Brooks JD, Riviere JE. Pentachlorophenol dermal absorption and disposition from soil in swine: effects of occlusion and skin microorganism inhibition. Toxicol App Pharmacol 1997; 147:234–246.

39. Bronaugh RL, Wester RC, Bucks D, Maibach HI, Sarason R. In vivo percutaneous absorption of fragrance ingredients in rhesus monkeys and humans. Food Chem Toxicol 1990; 28:369–373.
40. Mukherji E, Millenbaugh NJ, Au JL. Percutaneous absorption of 2′,3′-dideoxyinosine in rats. Pharm Res 1994; 11:809–815.
41. Feldmann RJ, Maibach HI. Penetration of ^{14}C hydrocortisone through normal skin: the effect of stripping and occlusion. Arch Dermatol 1965; 91:661–666.
42. Ryatt KS, Stevenson JM, Maibach HI, Guy RH. Pharmacodynamic measurement of percutaneous penetration enhancement in vivo. J Pharma Sci 1986; 75:374–377.
43. Ryatt KS, Mobayen M, Stevenson JM, Maibach HI, Guy RH. Methodology to measure the transient effect of occlusion on skin penetration and stratum corneum hydration in vivo. Br J Dermatol 1988; 119:307–312.
44. Brooks JD, Riviere JE. Quantitative percutaneous absorption and cutaneous distribution of binary mixtures of phenol and para-nitrophenol in isolated perfused porcine skin. Fundam Appl Toxicol 1996; 32:233–243.
45. Task Group on Occupational Exposure to Pesticides: Occupational Exposure to Pesticides. Washington, DC: Federal Working Group on Pest Management, 1974.
46. Wester RC, Maibach HI. Cutaneous pharmacokinetics: 10 steps to percutaneous absorption. Drug Metab Rev 1983; 14:169–205.
47. Ezzedeen FW, Stohs SJ, Kilzer KL, Makoid MC, Ezzedeen NW. Percutaneous absorption and disposition of iodochlorhydroxyquin in dogs. J Pharm Sci 1984; 73:1369–1372.
48. Elias PM. Epidermal lipids, barrier function, and desquamation. J Invest Dermatol 1983; 80:44–49.
49. Grubauer G, Feingold KR, Harris RM, Elias PM. Lipid content and lipid type as determinants of the epidermal permeability barrier. J Lipid Res 1989; 30:89–96.
50. Hostynek JJ, Magee PS, Maibach HI. QSAR predictive of contact allergy: scope and limitations. In: Elsner P, Lachapelle JM, Wahlberg JE, Maibach HI, eds. Prevention of Contact Dermatitis. Curr Probl Dermatol. Basel: Karger, 1996:18–27.
51. Wiechers JW. The barrier function of the skin in relation to percutaneous absorption of drugs. Pharma Week Sci Edit 1989; 11:185–198.

16

Variations of Hair Follicle Size and Distribution in Different Body Sites*

Nina Otberg, Heike Richter, Hans Schaefer, Ulrike Blume-Peytavi, Wolfram Sterry, and Jürgen Lademann
Humboldt University Berlin, Berlin, Germany

I. INTRODUCTION

The knowledge of permeation and penetration processes is a prerequisite for the development and optimization of drugs and cosmetics. In the past, percutaneous absorption was described as diffusion though the lipid domains of the stratum corneum. It was presumed that skin appendages, which mean hair follicles and sweat glands, play a subordinate role in absorption processes. The amount of appendages of the total skin surface was estimated to represent up to 0.1% (1). However, previous studies show higher absorption rates in skin areas with higher follicle density (2–6). On the other hand, hair follicle size and density and the amount of the absorbed drug have never been correlated. The variation in the thickness of the stratum corneum in different body areas was considered to be the main reason for the varying absorption rates. Feldman and Maibach (2) and Maibach et al. (3) found regional variations of percutaneous absorption in different skin areas. They assumed that the density and size of hair follicles might be the reason for their findings. More recent studies more strongly suggest that skin appendages play an important role in permeation and penetration processes of topically applied substances. Tenjarla et al. (4) and Hueber et al. (5,6) found significant differences in percutaneous absorption of appendage-free scarred skin and normal skin. Turner and Guy (7) found a significant iontophoretic drug delivery across the skin via follicular structures. Essa et al. (8) performed an in vitro Franz cell experiment for iontophoretic drug delivery. A new technique involving a stratum corneum/epidermis sandwich method was used for blocking the follicular orifice. A five times lower absorption rate was found when the potential shunt routes were blocked.

Moreover Hueber et al. (5,6) found a follicular reservoir of radiolabeled triamcinolone acetonide in human skin. Lademann et al. (9,10) found an amount of topically applied titanium dioxide microparticles located in the hair follicles of the

* Modified with permission from Journal of Investigative Dermatology (JID).

forearm. They showed that some follicles were open, whereas others were closed for the penetration process.

Hair follicle density has mainly been measured for terminal hair follicles on the scalp. Blume et al. (11) determined the vellus hair follicle density on the forehead, cheek, chest, and on the back by phototrichogram. Seago and Ebling (12) measured hair follicle density on the upper arm and thigh using a classical trichogram. Pagnoni et al. (13) used the cyanoacrylate technique for the measurement of hair follicle density in different regions of the face.

Hair follicles are the most important appendages in terms of surface area and skin depth. An exact knowledge of hair follicle densities, size of follicular orifices, follicular volume and follicular surface is necessary for the understanding of follicular penetration processes.

Therefore, our aim was to quantify characteristics of hair follicle sizes. This includes the measurement of the following parameters: density, size of follicular orifice, amount of orifice of the skin surface, hair shaft diameter, volume, and surface of the infundibula, in different regions of the body by using noninvasive cyanoacrylate skin surface biopsies and light microscopy. The volume of the follicle infundibula may represent the potential follicular reservoir for topically applied substances.

II. MATERIALS AND METHODS

The study was performed on six healthy volunteers (three females and three males) aged of 27 to 41 years with normal body mass indices (21–24). None of the volunteers suffered from any kind of skin disease, hormonal dysregulation, or adipositas.

All volunteers gave written informed consent and the protocol was approved by the institutional review board. The study was conducted according to the Declaration of Helsinki principles.

Cyanoacrylate surface biopsies were taken from each volunteer from seven different regions of the body (lateral forehead, back, thorax, upper arm, forearm, thigh, and calf region), just below the popliteal space, on the same day under the same conditions, which means same room temperature and humidity. Figure 1 shows the localization of the seven test regions. Hair follicle parameters were measured by light microscopy in combination with digital images. None of the volunteers showed terminal hair growth in the test regions.

Cyanoacrylate is a non-toxic, non-adherent, and optically clear adhesive, which polymerizes and bonds rapidly in the presence of small amounts of water and pressure (14). A drop cyanoacrylate (UHU® GmbH, Brühl, Germany) is placed on the untreated skin and covered with a glass slide under light pressure. After polymerization, which occurs in one minute, the glass slide can be removed. A thin sheet of horny cells, hair shafts and casts of the follicular infundibula are ripped off with the cyanoacrylate (15–17).

The surface biopsies were investigated using microscopy (Olympus® BX60M system-microscope, Tokyo, Japan) in combination with digital image analysis and a special software program (analySIS®, Soft Imaging System GmbH SIS, Münster, Germany). The follicular casts were counted in a marked area of one square centimeter. The diameter of the follicle orifice and of the hair shaft was measured directly. The percentage of orifices of the skin surface can easily be determined by adding all calculated circle areas of the follicular orifices in the labeled biopsy area.

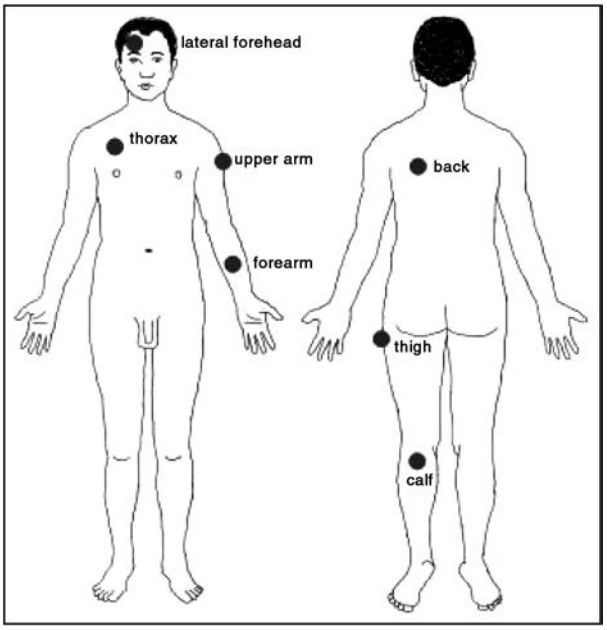


Figure 1 Localization of the seven test regions.

For the measurement of the surface and volume of the infundibula, a special three-dimensional image, extended focal image (EFI), was performed. With the module extended focal image of the software program analySIS microscope images can be taken in different focuses and can than be calculated to a three-dimensional picture. With the same software program length, height, and diameter of the infundibular casts can be measured. Every infundibular cast in the marked square centimeter was divided into truncated cones. Figure 2 explains the measurement of the

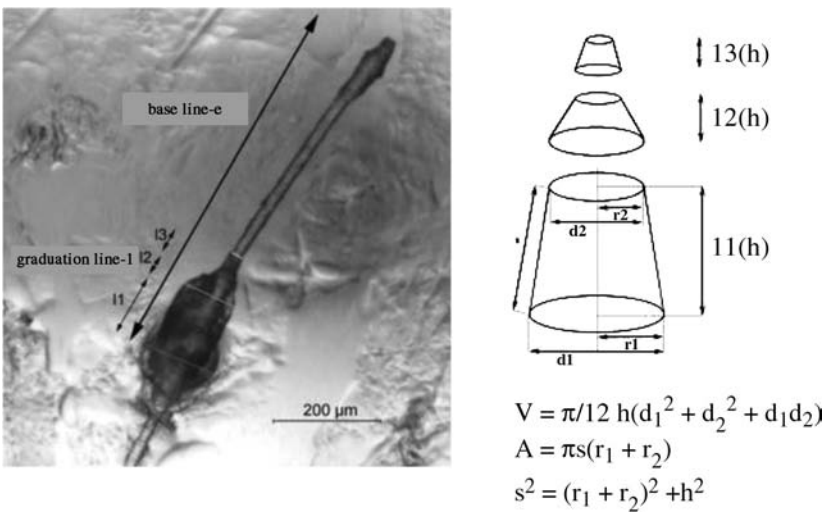


Figure 2 Cyanoacrylate skin surface biopsy with infundibular cast and vellus hair.

infundibular cast. It shows a cyanoacrylate skin surface biopsy from the lateral forehead. The volume (V) of each truncated cone was calculated with the following formula:

$$V_n = \pi/12 h_n \ (d_1^2 + d_2^2 + d_1 d_2) \quad (1)$$

where h is the height of the truncated cone and d is the diameter of the covers.

The whole infundibular volume per square centimeter was calculated by adding all single volumes and subtracting the hair shaft volumes. The hair shaft volume (V_{hs}) was calculated by the following formula:

$$V_{hsn} = \pi/4 \ d^2 \ h_n \quad (2)$$

where h is the height of the whole infundibulum and d is the hair shaft diameter.

The surface of the follicular infundibula was measured by calculating the curved surface (A) of the truncated cones by the following formulas:

$$A_n = \pi s(d_1/2 + d_2/2) \quad (3)$$

$$s^2 = (d_1/2 - d_2/2)^2 + h_n \quad (4)$$

where h is the height of the truncated cone and d is the diameter of the covers.

The follicular penetration surface was calculated by adding all curved surfaces within the marked area.

For statistical analysis, we utilized Mann and Whitney's U-test for the comparison of two variables and Kruskal and Wallis's h-test for the comparison of more than two variables and SPSS software (SPSS, Chicago, Illinois, U.S.A.). Data are expressed as mean $\pm$ SD with $p \leq 0.05$ considered significant, $p \leq 0.01$ considered very significant, and $p \leq 0.001$ considered highly significant.

III. RESULTS

Hair follicle density was measured on seven different body sites in six healthy volunteers. The samples were taken from corresponding areas in the different body areas of the volunteers. Figure 3 gives the average density with standard deviation for every test area. The average density was highest on the forehead [292 follicles/cm^2],

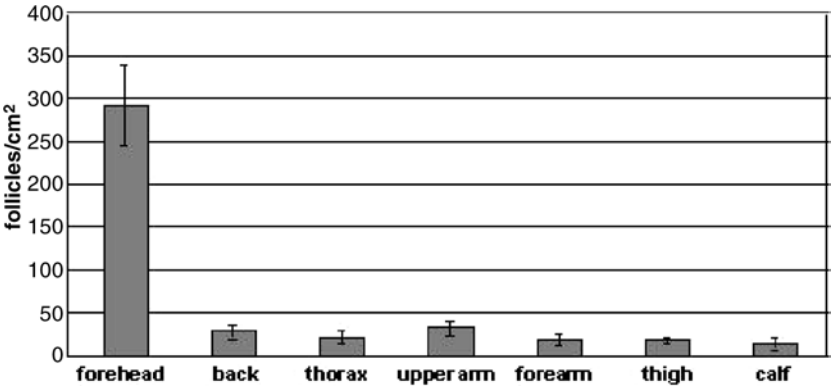


Figure 3 Hair follicle density on seven body sites.

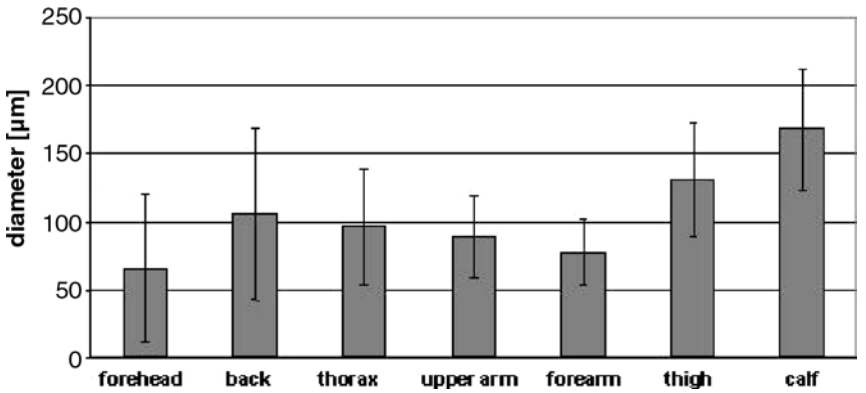


Figure 4 Diameter of hair follicle orifices on seven body sites.

significantly higher than in all other regions ($p \leq 0.001$). The skin regions on the back showed 29, on the thorax 22, on the upper arm 32, on the forearm 18, on the thigh 17, and on the calf region 14 follicles/cm^2 on average. Back and upper arm showed no significant differences in hair follicle density ($p > 0.05$).

Significant inter-site variations of the diameters of the follicular orifices could be found ($p \leq 0.001$). Thigh and calf showed no significant difference in diameters ($p > 0.05$). The diameters showed great variations in every body site (Fig. 4). High standard deviations were found, especially on the forehead and back. These areas belong to the seborrheic regions of the body, where small vellus hair follicles are found together with large sebaceous follicles. Comparing the mean values of diameters of the hair follicle orifices, the smallest diameters were found on the forehead with 66 µm and on the forearm with 78 µm. The calf region showed the largest diameter of the follicular orifices.

The percentage of follicular orifices on the skin surface is given in Table 1 for seven different test regions. The amount was calculated by adding all circle areas of the follicle orifices [calculated with the formula for circle areas: $A = \pi(d/2)^2$] in 1 cm^2 of the different test regions.

Although the forehead showed the smallest diameter, it also showed, due to the elevated hair follicle density, the highest percentage of follicular orifices on the skin surface. Significant inter-site variations of the percentage of the follicular orifices on the skin surface were found ($p \leq 0.001$). Thigh and calf showed no significant difference ($p > 0.05$).

Additionally, the hair shaft diameter was determined. Figure 5 gives the average hair shaft diameters with standard deviation for the seven measured body sites. The hairs on the thigh and calf region were significantly thicker compared to the other five regions ($p \leq 0.01$). Lateral forehead, back, thorax, upper arm, and forearm

Table 1 Percentage of Follicular Orifices on the Skin Surface in Seven Body Sites

Skin area	Forehead (%)	Back (%)	Thorax (%)	Upper arm (%)	Forearm (%)	Thigh (%)	Calf region (%)
Mean (±SD)	1.28 (±0.24)	0.33 (±0.15)	0.19 (±0.08)	0.21 (±0.09)	0.09 (±0.04)	0.23 (±0.12)	0.35 (±0.25)

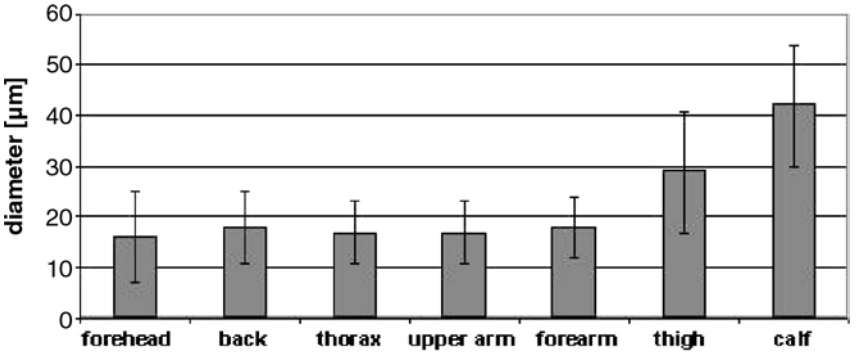


Figure 5 Hair shaft diameter on seven body sites.

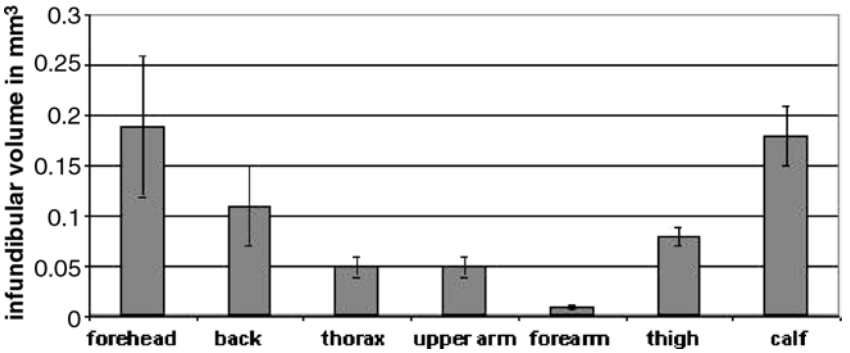


Figure 6 Volume of the follicular infundibula per square centimeter of skin on seven body sites.

showed no significant differences in hair shaft diameters ($p > 0.05$). The thigh showed hair shaft diameters of 29 µm, the calf region 42 µm.

The volume of the follicular infundibula was measured by dividing the casts on the surface biopsy in truncated cones, calculating each volume and adding all volumes within 1 cm^2 and subtracting the hair shaft volumes. The results of these measurements are given in Figure 6 related to 1 cm^2 skin surface. The forehead (0.19 mm^3/cm^2) and the calf regions (0.18 mm^3/cm^2) showed the highest volume with no significant difference ($p > 0.05$), although the hair follicle density is around 20 times higher on the forehead. The forearm shows the lowest volume at 0.01 mm^3/cm^2.

The potential surface for the penetration of topically applied drugs, and cosmetics has been estimated as the skin surface, disregarding the fact that substances penetrate into skin appendages (Fig. 7). The potential penetration surface of the hair follicles was calculated by measuring the curved surface of the follicular casts on the cyanoacrylate biopsy. Significant inter-site variations of the surface area were found ($p \leq 0.001$). The largest surface was found on the forehead with 13.7 mm^2 on average or 13.7% of the skin surface. The smallest surface was found on the forearm (0.95 mm^2), in accordance with the small follicles and the low follicle density.

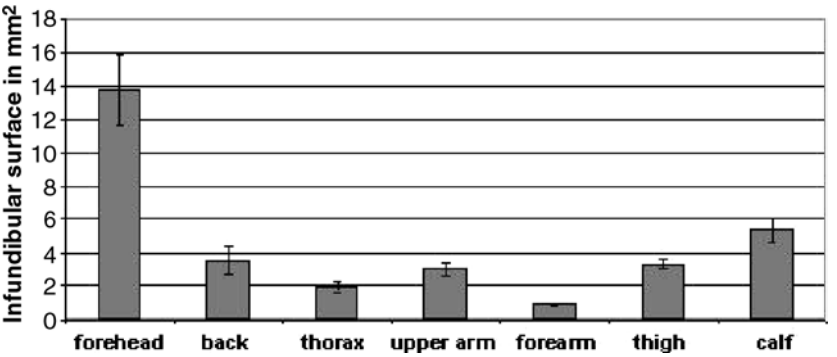


Figure 7 Surface of the follicular infundibula per square centimeter of skin on seven body sites.

IV. DISCUSSION

The knowledge of hair follicle density and size is important for the understanding and calculation of follicular penetration and permeation processes.

Only a few studies have been performed for the determination of the vellus hair follicle density on the human body. Blume et al. (11) determined the hair follicle density on the forehead, cheek, chest, and on the back. An average density of 423 follicles/cm^2 was found on the forehead and a mean density of 92 follicles on the back. Pagnoni et al. (13) found a density of 455 hair follicles on the lateral forehead and the highest density on the nasal wing with 1220 follicles/cm^2. These results show higher values, compared to our findings for the forehead (292 follicles/cm^2) and the back (29 follicles/cm^2). High standard variations as an expression of intraindividual variations occurred in every study. Even within the forehead region the hair follicle density can extremely differ to a high extent.

Seago and Ebling (12) measured the hair follicle density on the upper arm and thigh using a classical trichogram. They found a mean density of 18 follicles on the upper arm and 17 follicles in the skin area on the thigh, which correspond to our findings.

The mean hair follicle density depends on the skin area, because hair follicles are built in the early fetal period. After birth, the body proportions change and the hair follicles move apart according to the growth of body and skin. Because of the relatively lower growth of the head compared to the extremities, hair follicles are much more numerous on the scalp and in the face, than on arms and legs (12,13). Table 2 gives an overview of vellus hair follicle density found in literature compared to the presented results.

In spite of the fact that the size of hair follicles shows great intra- and inter-individual differences, hair shaft diameters showed relatively low variations. The thicker hair in the androgen-dependent areas on the thigh and calf, which were thicker than 30 μm, can be regarded as intermediate follicles. This means that these follicles are in a transitional stage between vellus and terminal hair (19).

Our findings show that the assumption of an appendage account of not more than 0.1% of the total skin surface (1) is valid for the forearm. The value of 0.1% corresponds well to our findings on the inner side of the forearm, which is most commonly used as an investigational area for skin penetration experiments. Skin areas with a higher follicle density, such as the forehead, or with larger follicle orifice,

Table 2 Review of Vellus Hair Follicle Density on Different Body Sites

	Results (by author)				
Body site	Own results (cm^{-2})	Pagnoni et al. (13) (cm^{-2})	Blume et al. (11) (cm^{-2})	Seago and Ebling (12) (cm^{-2})	Scott et al. (18) (cm^{-2})
Lateral forehead	292	455	414 ♀ 432 ♂	—	—
Tip of the nose	—	1112	—	—	—
Nasal wing	—	1220	—	—	—
Preauricular region	—	499	—	—	—
Back	29	—	93 ♀ 90 ♂	—	—
Thorax	22	—	—	—	—
Abdomen	—	—	—	—	6
Upper arm	32	—	—	17–19	—
Forearm	18	—	—	—	—
Thigh	17	—	—	14–20	—
Calf	14	—	—	—	—

such as the calf region, showed much higher values. A higher transfollicular absorption in these areas can be assumed.

The measurement of a potential follicular reservoir for topically applied substances showed extreme differences between the investigated body sites. The volume of the infundibula on the forehead was 0.19 mm^3. This is five times less than the volume of the stratum corneum, assuming that the stratum corneum shows a thickness of 10 μm with a volume of 1 mm^3/cm^2 skin surface. The determination of the reservoir function of the stratum corneum is part of recent studies. Lademann et al. (9,20) found that a topically applied substance is found mainly in the upper 20% of the stratum corneum. This means that we have an approximately comparable reservoir volume in the stratum corneum and in the follicles of the forehead, assuming that all follicles are open for the penetration process (10). In contrast to the forehead, the forearm shows a volume of 0.01 mm^3, which is 100 times less than the volume of the stratum corneum. It can be estimated that the hair follicles in this skin area play a minor reservoir function role.

The enlargement of the penetration surface through the follicular epithelium was measured by calculating the surface of the infundibular cast on the cyanoacrylate biopsy. The infundibular surface proved to be 13.7% on the forehead and only 1% on the forearm, thus only relatively low values for the enlargement of the potential penetration surface could be demonstrated.

A significantly higher amount of drug absorption in skin areas with high follicle densities or large follicles cannot be explained only by an enlargement of the penetration surface through the follicular epithelium. The reason for the better permeation through the hair follicles can likely be found in the ultra structure of the follicular epithelium and in the special environment of the follicular infundibulum. The hair follicle epithelium shows an epidermal differentiation in the infundibulum. The epithe-

lium of the uppermost parts shows no difference to the interfollicular epidermis, in the lower parts of the infundibular epithelium corneocytes are smaller and appears crumbly. This part of the follicular epithelium can be seen as an incomplete barrier for topically applied substances (21,22).

The present study shows a body region dependent hair follicle characteristics concerning follicular size and follicular distribution. Differential evaluation of skin penetration and absorption experiments and the development of new standards for the testing of topically applied drugs and cosmetics on different skin areas are mandatory. By knowing the differences of hair follicle size and density, we suggest to perform skin absorption experiment on human skin not only on the inner forearm but also in skin areas with other follicular properties, for example forehead or calf.

V. SUMMARY

For the evaluation and quantification of follicular penetration processes, the knowledge of variations of hair follicle parameters in different body sites is basic. Characteristics of follicle sizes and potential follicular reservoir were determined in cyanoacrylate skin surface biopsies, taken from seven different skin areas (lateral forehead, back, thorax, upper arm, forearm, thigh, and calf region). The highest hair follicle density, percentage of follicular orifices on the skin surface and infundibular surface were found on the forehead, while the highest average size of the follicular orifices was measured in the calf region. The highest infundibular volume and, therefore, a potential follicular reservoir were calculated for the forehead and for the calf region, although the calf region showed the lowest hair follicle density. The calculated follicular volume of these two skin areas was as high as the estimated reservoir of the stratum corneum. The lowest values for every other parameter were found on the forearm. The present investigation clearly contradicts former hypothesis that the amount of appendages of the total skin surface represents not more than 0.1%. Every body region disposes its own hair follicle characteristics, which, in the future, should lead us to a differential evaluation of skin penetration processes and a completely different understanding of penetration of topically applied drugs and cosmetics.

REFERENCES

1. Schaefer H, Redelmeier TE. In: Skin Barrier. In: Principles of Percutaneous Absorption. Basel: Karger, 1996:18.
2. Feldmann RJ, Maibach HI. Regional variation in percutaneous penetration of ^{14}C cortisol in man. J Invest Derm 1967; 48(2):181–183.
3. Maibach HI, Feldman RJ, Milby TH, Serat WF. Regional variation in percutaneous penetration in man. Arch Environ Health 1971; 23:208–211.
4. Tenjarla SN, Kasina R, Puranajoti P, Omar MS, Harris WT. Synthesis and evaluzation of *N*-acetylprolinate esters—Novel skin penetration enhancers. Int J Pharm 1999; 192:147–158.
5. Hueber F, Besnard M, Schaefer H, Wepierre J. Percutaneous absorption of estradiol and progesterone in normal and appendage-free skin of hairless rat: lack of importance of nutritional blood flow. Skin Pharmacol 1994; 7:245–256.
6. Hueber F, Schaefer H, Wepierre J. Role of transepidermal and transfollicular routes in percutaneous absorption of steroids: in vitro studies on human skin. Skin Pharmacol 1994; 7:237–244.

7. Turner NG, Guy RH. Visualization and quantification of iontophoretic pathways using confocal microscopy. J Invest Derm Proc 1998; 3:136–142.
8. Essa EA, Bonner MC, Barry BW. Possible role of shunt route during iontophoretic drug penetration. Perspect Percutan Penetration 2002; 8:54.
9. Lademann J, Weigmann HJ, Rickmeyer C, Bartelmes H, Schaefer H, Müller G, Sterry W. Penetration of titanium dioxide microparticles in a sunscreen formulation into the horny layer and the follicular orifice. Skin Pharmacol Appl Skin Physiol 1999; 12: 247–256.
10. Lademann J, Otberg N, Richter H, Weigmann HJ, Lindemann U, Schaefer H, Sterry W. Investigation of follicular penetration of topically applied substances. Skin Pharmacol Appl Skin Physiol 2001; 14(suppl 1):17–22.
11. Blume U, Ferracin J, Verschoore M, Czernielewski JM, Schaefer H. Physiology of the vellus hair follicle: hair growth and sebum excretion. Br J Dermatol 1991; 124:21–28.
12. Seago SV, Ebling FJ. The hair cycle on the human thigh and upper arm. Br J Dermatol 1995; 135:9–16.
13. Pagnoni AP, Kligman AM, Gammal SEL, Stoudemayer T. Determination of density of follicles on various regions of the face by cyanoacrylate biopsy: correlation with sebum output. Br J Dermatol 1994; 131:862–865.
14. Marks R, Dawber RPR. Skin surface biopsy: an improved technique for the examination of the horny layer. Br J Derm 1971; 84:117–123.
15. Plewig G, Kligman M. Sampling of sebaceous follicles by the cyanoacrylate technique. In: ACNE, Morphogenesis and Treatment. Berlin, Heidelberg, New York: Springer-Verlag, 1975:56.
16. Holmes RL, Williams M, Cunliffe WJ. Pilosebaceous duct obstruction and acne. Br J Derm 1972; 87:327.
17. Mills OH, Kligman AM. The follicular biopsy. Dermatologica 1983; 167:57–63.
18. Scott RC, Corrigan MA, Smith F, Mason H. The influence of skin structure on permeability: An intersite and interspecies comparison with hydrophilic penetrants. J Invest Derm 1991; 96(6):921–925.
19. Whiting DA. Histology of normal hair. In: Hordinsky MK, Sawaya ME, Scher RK, eds. Atlas of Hair and Nail. Philadelphia: Churchill Livingstone, 2000:9–18.
20. Lademann J, Weigmann HJ, Schaefer H, Müller G, Sterry W. Investigation of the stability of coated titanium micropartiles used in sunscreen. Skin Pharmacol Appl Skin Physiol 2000; 13:258–264.
21. Braun-Falko O, Plewig G, Wolff HH. Dermatologie und Venerologie. Berlin, Heidelberg, New York: Springer-Verlag, 1996.
22. Pinkus H, Mehregan AH. The pilar apparatus. In: A Guide to Dermatopathology. New York: Appleton-Century-Crofts, 1981:S22–S28.

17

Methodology: In Vivo Methods for Percutaneous Absorption Measurements

Ronald C. Wester and Howard I. Maibach
Department of Dermatology, School of Medicine, University of California, San Francisco, California, U.S.A.

I. INTRODUCTION

The rate-determining step for human risk assessment is bioavailability, that amount of chemical in the environment which gets into the human body. If the exposure includes skin, then skin permeability becomes a rate-determining step. Various methods are available to assess skin permeability. These include in vivo, in vitro, and computer model methods. Cost/benefit would favor the in vitro system (this is assumed) and certainly the computer calculated permeability is cost friendly (not to mention manpower friendly). The downside is that errors can cost money and human suffering. This presentation gives examples of the different methodologies, showing when they work and where validation points out method shortcomings.

II. METHOD ANALYSES: ATRAZINE

Table 1 gives the in vivo human percutaneous absorption of [^{14}C] atrazine. Two dose levels, 6.7 and 79 $\mu g/cm^2$, were applied to the ventral forearm of volunteers (from whom consent had been obtained) and total urinary and fecal radioactivity determined. A previous in vivo intravenous study in the rhesus monkey showed that all of the IV dose was excreted within seven days, and this was the case with the human volunteers with topical dose application. Total percent dose absorbed was 5.6 ± 3.0 and total dose accountability (absorbed plus washes) was $101.2 \pm 3.4\%$ for the 6.7 $\mu g/cm^2$ dose. Similar results were obtained for the higher dose. This is considered the gold standard for skin permeability. Definitive percent dose absorbed and flux are obtained and all of the applied dose is accounted for.

The in vivo urine samples were further validated. Split urine aliquots were analyzed by accelerator mass spectrometry (MS) (1). Data from these two methods (scintillation counting and accelerator MS) have a correlation coefficient of 0.998 for a linear plot of the entire sample set. Urinary metabolites were also determined using high-performance liquid chromatography (HPLC)–accelerator mass spectrometry (2).

Table 1 Atrazine Human In Vivo Percutaneous Absorption

	Dose A[a] ($n=4$) 6.7 μg/cm^2	Dose B[a] ($n=6$) 79 μg/cm^2
Excretion		
Urinary (%)	5.0 ± 2.9	1.1 ± 0.9
Fecal (%)	0.6 ± 0.3	0.1 ± 0.1
Total (%)	5.6 ± 3.0	1.2 ± 1.0
Dose absorbed (%)	5.6 ± 3.0	1.2 ± 10
Total dose accountability (%)	101.2 ± 3.4	92.3 ± 2.8
Flux (μg/cm^2/hr)	0.0156 ± 0.0084	0.0379 ± 0.0332
Half-life (hr) ^{14}C	17.5 ± 5.4	24.5 ± 9.0

Dose applied to ventral forearm, covered with non-occlusive raised patch for 24 hours, then dose side washed with soap and water.
[a]Mean ± SD.

Table 2 gives atrazine in vitro percutaneous absorption through human skin (3). The human skin was used under conditions that ensure skin viability (4) and atrazine metabolites were determined. In this in vitro study receptor fluid accumulation and skin content (at end of study) were determined for skin permeability. A basic question with in vitro methodology is does one use only receptor fluid content or both receptor fluid and skin content to determine skin permeability. Without knowledge of in vivo human absorption (Table 1), which is the proper choice?

Table 3 summarizes atrazine flux in humans using the in vivo data (0.0156 μg/cm^2/hr) and in vitro data (0.0081 μg/cm^2/hr for receptor fluid only and 0.038 μg/cm^2/hr using combined receptor fluid and skin content). For comparison purposes the flux was calculated using Guy and Potts (5) as 0.044 μg/cm^2/hr. All three-flux calculations are relatively in agreement.

Atrazine is a ''friendly'' chemical for these types of analysis because the molecular weight (215.69), water solubility (34.7 mg/L), and log P (octanol–water) of 2.61 are amendable to all systems. However, there are exceptions to the rule.

III. METHOD ANALYSES: BORATES

Boron is a ubiquitous element in rocks, soil, and water. A small amount of boron is essential to life. Borates come in contact with human skin in many ways (mining, detergent, fertilizer, wood treatment, and organic insecticide).

Table 2 Atrazine In Vitro Percutaneous Absorption Through Human Skin

Distribution	Percent dose absorbed
Receptor fluid	3.5 ± 0.3
Skin	12.8 ± 1.2
Surface wash	66.8 ± 6.9
Total recovery	83.0 ± 7.3

Note: Dose is 4.6 μg/cm^2. Each value: Mean ± SEM ($n=14$) for 20 hours.
Source: From Ref. 3.

Table 3 Atrazine Flux in Humans

Method	Flux ($\mu g/cm^2/hr$)[a]
In vivo human	0.016
In vitro	
Receptor fluid	0.008
Receptor fluid and skin	0.038
Calculated[b]	0.044

[a]Based on 6.7 μg/cm dose.
[b]From Ref. 5.

Table 4 gives the in vivo percutaneous absorption in human volunteers (from whom informed consent was obtained) for the borates 5% boric acid, 5% borax, and 10% disodium octaborate tetrahydrate (DOT). These dose concentrations are near water solubility limitation (6): The in vivo permeability constants (K_p) range from 1 to 2×10^{-7} for these borates. The human skin in vitro percutaneous absorption is in Table 5. Comparison of Tables 4 and 5 yields some interesting data relative to in vivo and in vitro methodology.

The in vitro permeability coefficient (K_p) for the 5% boric acid, 5% borax, and 10% DOT range from 0.8 to 2.9×10^{-4}. This is a 1000-fold increase over in vivo $K_p s$.

The in vivo studies were done with a dose of $2\,\mu L/cm^2$ (any more would run off the skin). The in vitro doses were at $1000\,\mu L/cm^2$. However one in vitro 5% boric acid was dosed at $2\,\mu L/cm^2$. Interestingly, the 5% boric acid K_p at $1000\,\mu L/cm^2$ was 2.9×10^{-4} while the 5% boric acid K_p at $2\,\mu L/cm^2$ was 1.4×10^{-6}, a 200-fold difference. The amount of vehicle (water) was the determining factor in boric acid in vitro human percutaneous absorption.

The relationship between flux and permeability coefficient (flux is concentration dependent while K_p is independent) was true for this in vitro study.

Table 4 In Vivo Absorption, Flux, and Permeability Content for ^{10}Boron as 5% Boric Acid, 5% Borax, and 10% DOT in Normal Human Volunteers

Dose	Dose ^{10}B (μg)	Percentage of dose	Flux ($\mu g/cm^2/h$)	Permeability constant K_p (cm/hr)
5% boric acid				
No treatment	14,200	0.226	0.00912	1.9×10^{-7}
SLS treatment	14,200	0.239	0.00966	2.0×10^{-7}
5% borax				
No treatment	9,270	0.210	0.00855	1.8×10^{-7}
SLS treatment	9,220	0.185	0.00746	1.5×10^{-7}
10% DOT				
No treatment	34,700	0.122	0.00975	1.0×10^{-7}
SLS treatment	34,800	0.107	0.00878	0.9×10^{-7}

Note: Dose was spread over 900-cm^2 area of the back.
Abbreviations: DOT, disodium octaborate tetrahydrate; SLS, sodium lauryl sulfate.
Source: From Ref. 6.

Table 5 In Vitro Percutaneous Absorption of Boron Administrated as Boric Acid, Borax, and DOT in Normal Human Skin

Dosing solution	Percentage of dose absorbed geometric mean (95% CI)	Flux ($\mu g/cm^2/hr$)	Permeability constant K_p (cm/hr)
Boric acid (w/v)			
5% at $2\,\mu L/cm^2$	1.75 (0.18–17)	0.07	1.4×10^{-6}
5% at $1000\,\mu L/cm^2$	0.70 (0.072–6.81)	14.58	2.9×10^{-4}
0.5% at $1000\,\mu L/cm^2$	0.28 (0.029–2.72)	0.58	1.2×10^{-4}
0.05% at $1000\,\mu L/cm^2$	1.20 (0.012–11.7)	0.25	5.0×10^{-4}
Borax			
5% at $1000\,\mu L/cm^2$	0.41 (0.042–3.99)	8.5	1.7×10^{-4}
DOT			
10% at $1000\,\mu L/cm^2$	0.19 (0.018–1.81)	7.9	0.8×10^{-4}

Abbreviations: CI, class interval; DOT, disodium octaborate tetrahydrate.
Source: From Ref. 6.

IV. SOLVENTS

Table 6 summarizes (PBPK) estimates for solvent human in vivo dermal absorption. Hand immersion involves the hand of a volunteer, who is sitting comfortably, being immersed in a bucket of water or soil containing one of the solvents. The volunteer wears a face mask. The volunteer inhales fresh air from an air tank. The mask has a special device that switches between inhalation and exhalation. Thus the volunteer exhales through a different pathway such that the exhaled breath goes to a tandem ion-trap mass spectrometer (MS/MS) coupled to a computer that records and can display real-time (every few seconds if wanted) solvent concentration in the exhaled breath (7–9).

Table 2 gives PBPK model estimates for the dermal absorption of trichloroethylene (TCE) in rats. Estimated permeability constants are listed. Generally, solvent dermal absorption is less for humans than for rats. In both species solvent absorption is less from soil than from water. This may be due to water's ability to retain solvent within a matrix on the skin better than with soil.

The combination of real-time breath analysis and PBPK modeling provides an opportunity to effectively follow the changing kinetics of uptake, distribution, and elimination phases of a compound throughout a dermal exposure. The sensitivity of the atmospheric-sampling glow discharge ionization (ASGDI)–MS/MS system

Table 6 (PBPK) Model Estimates for Human In Vivo Dermal Absorption

Solvent	Treatment	K_p (cm/hr)
Methylchloroform (TCA)	Water hand immersion	0.0063 ± 0.0006
Trichloroethylene (TCE)	Soil hand immersion	0.0015 ± 0.0005
	Water patch	0.019 ± 0.001
	Soil hand immersion	0.0074 ± 0.000
	Soil patch	0.0043 ± 0.002
Perchlorolthylene (PCE)	Soil hand immersion	0.0009 ± 0.0003

for exhaled-breath analysis is pivotal in enabling studies wherein human volunteers are exposed to low levels of compounds for short periods of time. This real-time, in vivo method is suitable for studying the percutaneous absorption of volatile chemicals and allows exposures to be conducted under a variety of exposure conditions, including occluded versus non-occluded, rat versus monkey versus human, and soil versus water matrices (10).

V. LIMITATIONS

Regulatory agencies have developed an affinity for a calculated permeability coefficient (K_p) for risk assessment. Permeability coefficients are easiest determined from the time course of chemical diffusion from a vehicle across the skin barrier into a receptor fluid. Table 7 compares in vitro diffusion receptor fluid absorption with in vivo percutaneous absorption. Receptor fluid accumulation for the higher log *P* chemicals (Table 8) is negligible. This is due to basic chemistry—the compounds are not soluble in the water based receptor fluid. Based on these receptor fluid accumulations these chemicals are not absorbed skin. Risk assessment would contain an extreme false negative component. That point where the diffusion system and receptor fluid

Table 7 In Vitro Receptor Fluid Vs. In Vivo Percutaneous Absorption

		Percent dose	
		In vitro	
Compound	Vehicle	Receptor fluid	In vivo
DDT	Acetone	0.08 ± 0.02	18.9 ±9.4
	Soil	0.04 ± 0.01	3.3 ± 0.5
Benzo[a]pyrene	Acetone	0.09 ± 0.06	51.0 ± 22.0
	Soil	0.01 ± 0.06	13.2 ± 3.4
Chlordane	Acetone	0.07 ± 0.06	6.0 ± 2.8
	Soil	0.04 ± 0.05	4.2 ± 1.8
Pentachlorophenol	Acetone	0.6 ± 0.09	29.2 ± 5.8
	Soil	0.01 ± 0.00	24.4 ± 6.4
PCBs (1242)	Acetone	—	21.4 ± 8.5
	TCB	—	18.0 ± 8.3
	Mineral oil	0.3 ± 0.6	20.8 ± 8.3
	Soil	0.04 ± 0.05	14.1 ± 1.0
PCBs (1254)	Acetone	—	14.6 ± 3.6
	TCB	—	20.8 ± 8.3
	Mineral oil	0.1 ± 0.07	20.4 ± 8.5
	Soil	0.04 ± 0.05	13.8 ± 2.7
2,4-D	Acetone	—	2.6 ± 2.1
	Soil	0.02 ± 0.01	15.9 ± 4.7
Arsenic	Water	0.9 ± 1.1	2.0 ± 1.2
	Soil	0.03 ± 0.5	3.2 ± 1.9
Cadmium	Water	0.4 ± 0.2	—
	Soil	0.03 ± 0.02	—
Mercury	Water	0.07 ± 0.01	—
	Soil	0.06 ± 0.01	—

Table 8 Octanol/Water Partition Coefficients of Compounds

Compounds	Log *P*
DDT	6.91
Benzo[a]pyrene	5.97
Chlordane	5.58
Pentachlorophenol	5.12
2,4-D	2.81
PCBs	Mixture
Aroclor 1242	High log *P*
Aroclor 1254	High log *P*

accumulation gives a true K_p or manufactures a false K_p has not been determined. Regulatory agents should have some in vivo validation before blindly accepting an in vitro K_p. Also, computer models based on in vitro data have the same risk.

VI. DISCUSSION

Human skin was developed during evolutionary history, basically designed as a physical barrier to the environment and to contain our water-based body chemistry. The industrial revolution introduced a new wave of chemicals for the skin to deal with. Considering skin's barrier properties, a lot of protection is provided. However, chemicals do permeate the skin barrier and human health requires knowledge and regulation to maintain safety. Skin permeability can best be determined in vivo in human volunteers (gold standard). In vitro diffusion methodology and predictive models can aid in predicting skin permeability, but they do have limitations. If these limitations are not vigorously defined and validated, the consequences can be severe. False positive errors can be financially costly and false negative errors can be deadly.

REFERENCES

1. Gilman SD, Gee SJ, Hammock BD, Vogel JS, Haack KW, Buchholz BA, Freeman SPHT, Wester RC, Hui X, Maibach HI. Analytical performance of accelerator mass spectrometry and liquid scintillation counting for detection of ^{14}C-labeled atrazine metabolites in human urine. Anal Chem 1998; 70:3463–3469.
2. Buchholz BA, Fultz E, Haack KW, Vogel S, Gilman SD, Gee SJ, Hammock BD, Hui X, Wester RC, Maibach HI. APLC—accelerator MS measurement of atrazine metabolites in human urine after dermal exposure. Anal Chem 1999; 71:3519–3525.
3. Ademola JI, Sedik LE, Wester RC, Maibach HI. In vitro percutaneous absorption and metabolism in man of 2-chloro-4-ethylamino-6-isopropylamine-5-triazine (Atrazine). Arch Toxicol 1993; 67:85–91.
4. Wester RC, Christopher J, Maibach HI, Forsell J. Human cadaver skin viability for in vitro T Hartway, N Poblete. Percutaneous absorption: storage and detrimental effects of heat-separation and freezing. Pharm Res 1998; 15:82–84.
5. Guy RH, Potts RO. Structure–permeability relationship in percutaneous penetration. J Pharm Sci 1992; 81:603–604.

6. Wester RC, Hui X, Haack KW, Poblete N, Maibach HI, Bell K, Schell MJ, Nortington DJ, Strong P, Culver BD. In vivo percutaneous absorption of boric acid, borax, and disodium octaborate tetrahydrate in humans compared to in vitro absorption in human skin from infinite and finite doses. Toxicol Sci 1998; 45:42–51.
7. Poet TS, Thrall KD, Corley RA, Hui X, Edwards JA, Weitz KK, Maibach HI, Wester RC. Utility of real time breath analysis and physiologically based pharmacokinetic modeling to determine the percutaneous absorption of methyl chloroform in rats and humans. Toxicol Sci 2000; 54:42–51.
8. Poet TS, Corley RA, Thrall KD, Edwards JA, Tanojo H, Weitz KK, Hui X, Maibach HI, Wester RC. Assessment of the percutaneous absorption of trichloroethylene in rats and humans using MS/MS real-time breath analysis and physiologically based pharmacokinetic modeling. Toxicol Sci 2000; 56:61–72.
9. Poet TS, Weitz KK, Gies RA, Edwards JA, Thrall KD, Corley RA, Tanojo H, Hui X, Maibach HI, Wester RC. PBPK modeling of the percutaneous absorption of perchlorolthylene from a soil matrix in rats and humans. Toxicol Sci 2002; 67:17–31.
10. Thrall KD, Poet TS, Corley RA, Tanojo H, Edwards JA, Weitz KK, Hui X, Maibach HI, Wester RC. A real-time in vivo method for studying the percutaneous absorption of volatile chemicals. Int J Occup Environ Health 2000; 6:96–103.

18

Determination of Percutaneous Absorption by In Vitro Techniques

Robert L. Bronaugh, Margaret E. K. Kraeling, and Jeffrey J. Yourick
Office of Cosmetics and Colors, Food and Drug Administration, Laurel, Maryland, U.S.A.

I. INTRODUCTION

In vitro percutaneous absorption methods have become widely used for measuring the absorption of compounds that come in contact with skin. Safety evaluations of toxic chemicals frequently rely on in vitro studies for human permeation data. Animal data must be used cautiously for estimating human absorption due to differences in barrier properties of animal and human skin (1).

In vitro absorption studies can also be used to measure skin metabolism of compounds if viable skin is obtained for the study and if the viability is maintained in the diffusion cells (2). The in vitro system allows for the isolation of skin so that metabolism by the organ can be distinguished from systemic metabolism.

Important considerations in conducting in vitro absorption studies are discussed in the following sections.

II. PRELIMINARY STEPS

It is useful in the planning of studies to know solubility and partitioning properties of the test compound. The log of the octanol/water partition coefficient (log P) has been used for years as an indicator of percutaneous absorption properties. Compounds need some lipid solubility in order to permeate through the lipid-enriched stratum corneum layer. Water solubility is also necessary for permeation through the more aqueous viable epidermal and dermal tissue. Diminished skin absorption may start to be observed with compounds of molecular weight above 500 Da (3).

III. DIFFUSION CELL

In vitro protocols generally allow the use of either the flow-through or static diffusion cell, but only the flow-through cell allows the maintenance of skin viability. The

flow-through cell provides the continual replacement of a nutrient medium necessary to maintain physiological conditions. Diffusion cells should be prepared from a material that is resistant to binding of test material such as glass or Teflon®.

IV. SOURCE OF SKIN

Human skin is generally recommended over animal skin for the most relevant data. When human skin cannot be obtained, animal skin is used for absorption and metabolism studies. Animal skin is more permeable than human skin; thus, its use results in a conservative estimate of skin penetration for safety assessments. The use of hairless animals is preferable since a section can be prepared with a dermatome. Metabolism of topically applied compounds by animal skin may be different than human skin (chap. 2).

V. VIABILITY OF SKIN

Viable skin more closely simulates in vivo conditions than nonviable skin. Skin metabolism can also be measured when viable skin is used in absorption studies. The skin is capable of biotransformations that can activate or deactivate an absorbed compound. The hydrolysis product of the ultimate carcinogen formed from benzo(a)pyrene was identified in the diffusion cell receptor fluid following topical application of benzo(a)pyrene to viable hairless guinea pig skin (4). The skin has also been shown to have significant capability for conjugating percutaneously absorbed compounds. The glycine conjugates of benzoic (5) and salicylic acid (6) were observed in hairless guinea pig skin after absorption of the parent compounds. Substantial amounts of absorbed benzocaine were found to be acetylated in human and hairless guinea pig skin (5,7). Viability of skin can be assessed by using glucose utilization techniques or the MTT assay (chap. 2). Cadaver skin is also acceptable for use in a skin absorption study. Cadaver skin must have satisfactorily passed an examination for barrier integrity. Since enzymatic activity is reduced or absent in cadaver skin, metabolism of the test compound must be unimportant or examined in another way (i.e., skin homogenate).

VI. PREPARATION OF SKIN

A split-thickness preparation of skin should be used in diffusion cells unless full-thickness skin can be justified. A dermatome section containing the epidermis and upper papillary dermal layer (200 μm) most closely simulates the barrier layer of skin (8). Full-thickness skin can artificially retain absorbed compounds that bind or diffuse poorly through it (most lipophilic chemicals) (9). Preparation of an epidermal layer by separation of the epidermis and dermis using heat is effective for non-hairy skin (10), but viability of skin is destroyed.

VII. RECEPTOR FLUID

A physiological buffer such as a balanced salt solution or tissue culture medium is needed to maintain viability of the skin for at least 24 hours (2). Bovine serum albumin is sometimes added to increase the solubility of lipophilic compounds. It is

preferable to use a physiological buffer even when metabolism is not measured to simulate in vivo conditions.

Some protocols use solubilizing agents (surfactants and organic solvents) in the receptor fluid so that skin absorption can be more easily determined by simply sampling the receptor fluid (9). Great care must be used with these solubilizing agents as the skin barrier can be damaged, particularly when split-thickness skin preparations are used. Further investigations are needed to assess the adequacy of solubilizing agents to adequately remove a wide variety of compounds from skin without damage to the barrier properties.

VIII. RECOVERY

Determination of total recovery of test compound lends credibility to experimental results. Normally recovery of radiolabeled compounds in percutaneous absorption experiments exceeds 90%. However, high recovery values cannot be obtained for volatile compounds unless the evaporating material is trapped.

IX. DETERMINATION OF ABSORPTION

The determination of systemic percutaneous absorption is sometimes a controversial issue in an in vitro diffusion cell study. Since the skin can sometimes serve as a reservoir for absorbed material, measurement of the absorbed compound appearing in the receptor fluid alone may not be an accurate determination of systemic skin absorption. Both skin and receptor fluid levels should be measured at the end of a study. If determination of systemic absorption is desired, it is not sufficient to simply measure only the receptor fluid levels. If significant amounts remain in skin, additional studies may be necessary to determine if the material in skin will eventually be systemically absorbed (see discussion below). Also, skin levels must be known in order to determine mass balance at the end of the experiment. Recoveries of at least 90% should be obtained unless the test compound is volatile.

Skin can be fractionated to observe localization in different layers. The stratum corneum layer can be removed from the surface of the skin by successive stripping with 10 or more pieces of cellophane tape (11). Individual variation has been reported in the number of strips necessary presumably due to differences in the pressure applied to the tape and differences in the tape itself. The epidermal and dermal layers can be separated with heat as previously described in the preparation of skin.

The guidelines for skin absorption studies recommended by the European Union's Scientific Committee for Cosmetics and Non-food Products (SCCNFP) require that material remaining in the viable skin levels (exclusive of stratum corneum) be considered as systemically absorbed (12). The Organization for Economic and Cultural Development (OECD) draft guideline for in vitro skin absorption studies states that all material remaining in skin (including the stratum corneum) may need to be considered as systemically absorbed unless additional studies show that there is no eventual absorption (13).

For example, the lipophilic fragrance ingredient, musk xylol, was shown to be absorbed through hairless guinea pig and human skin (14). However, substantial amounts of the fragrance were found in both types of skin at the end of the 24-hour studies (Table 1). An additional study showed that significant amounts of the material in the skin at 24 hours diffused into the receptor fluid in the next 48 hours.

Table 1 Percent Applied Dose of Musk Xylol Absorbed from O/W Emulsion and Methanol Vehicles in 24 Hours

	Hairless guinea pig skin[a]		Human skin[b]	
	O/W emulsion	Methanol	O/W emulsion	Methanol
Receptor fluid	32.1 ± 1.3	25.8 ± 1.2	4.1 ± 0.7	1.0 ± 0.2
Skin	22.9 ± 2.7	18.8 ± 2.2	17.3 ± 2.3	21.3 ± 0.8
Total absorbed	55.0 ± 2.1	44.6 ± 2.4	21.5 ± 3.0	22.3 ± 0.8
24-hr skin wash	24.9 ± 1.4	5.5 ± 0.3	46.9 ± 3.2	25.9 ± 1.3
Total recovery	80.5 ± 1.9	50.4 ± 2.5	68.5 ± 2.9	45.7 ± 3.3

[a]Values are the mean ± SE of four determinations in skin from each of three animals.
[b]Values are the mean ± SE of four to five determinations in skin from each of two human subjects.

These results suggest that 24-hour receptor fluid values alone do not adequately estimate systemic absorption of musk xylol.

X. EXPRESSION OF RESULTS

Studies are usually conducted by applying the test compound under conditions that simulate topical exposure. Sometimes an infinite dose is applied to the skin and absorption is expressed as a permeability constant (steady-state rate divided by applied concentration). Frequently exposure conditions require finite dosing and therefore a steady-state absorption rate is not achieved. Then absorption is usually expressed as a percent of the applied dose or as an absorption rate. These absorption values are for the specific dose applied and vehicle used and often cannot be easily extrapolated to other conditions of use.

XI. CONCLUSIONS

For the greatest acceptability of in vitro data, results from an in vitro method should come from a procedure that simulates in vivo conditions as closely as reasonably possible. We believe that viable skin is preferable but cadaver skin is acceptable since adequate supplies of viable human skin are sometimes difficult to obtain. Absorption values for compounds obtained from animal skin would likely exceed the permeability of these same compounds in human skin.

The use of solubilizing agents in the receptor fluid and/or the failure to include skin levels at the end of the study as percutaneously absorbed can lead to errors in percutaneous absorption measurements. Protocols following these procedures should be restricted to use in screening applications.

REFERENCES

1. Bronaugh RL, Stewart RF, Congdon ER. Methods for in vitro percutaneous absorption studies II. Comparison of human and animal skin. Tox Appl Pharmacol 1982; 62:481–488.
2. Collier SW, Sheikh NM, Sakr A, Lichtin JL, Stewart RF, Bronaugh RL. Maintenance of skin viability during in vitro percutaneous absorption/metabolism studies. Tox Appl Pharmacol 1989; 99:522–533.

3. Bos JD, Meinardi MMHM. The 500 dalton rule for the skin penetration of chemical compounds and drugs. Exp Dermatol 2000; 9:165–169.
4. Ng KME, Chu I, Bronaugh RL, Franklin CA, Somers DA. Percutaneous absorption and metabolism of pyrene, benzo(a)pyrene and di-(2-ethylhexyl)phthalate: comparison of in vitro and in vivo results in the hairless guinea pig. Tox Appl Pharmacol 1992; 115:216–233.
5. Nathan D, Sakr A, Lichtin JL, Bronaugh RL. In vitro skin absorption and metabolism of benzoic acid, p-aminobenzoic acid, and benzocaine in the hairless guinea pig. Pharm Res 1990; 7:1147–1151.
6. Boehnlein J, Sakr A, Lichtin JL, Bronaugh RL. Metabolism of retinyl palmitate to retinol (vitamin A) in skin during percutaneous absorption. Pharm Res 1994; 11:1155–1159.
7. Kraeling MEK, Lipicky RJ, Bronaugh RL. Metabolism of benzocaine during percutaneous absorption in the hairless guinea pig. Acetylbenzocaine formation and activity. Skin Pharmacol 1996; 9:221–230.
8. Bronaugh RL, Stewart RF. Methods for in vitro percutaneous absorption studies VI. Preparation of the barrier layer. J Pharm Sci 1986; 75:487–491.
9. Bronaugh RL, Stewart RF. Methods for in vitro percutaneous absorption studies III. Hydrophobic compounds. J Pharm Sci 1984; 73:1255–1258.
10. Bronaugh RL, Congdon ER, Scheuplein RJ. The effect of cosmetic vehicles on the penetration of N-nitrosodiethanolamine through excised human skin. J Invest Dermatol 1981; 76:94–96.
11. Kraeling MEK, Bronaugh RL. In vitro percutaneous absorption of alpha hydroxy acids in human skin. J Soc Cosmet Chem 1997; 48:187–197.
12. SCCNFP. Opinion concerning basic criteria for the in vitro assessment of percutaneous absorption of cosmetic ingredients. Adopted by the Scientific Committee on Cosmetic Products and Non-Food Products Intended for Consumers During the Plenary Session of 23 June 1999.
13. OECD. Environmental Health and Safety Publications: Draft Guidance Document for the Conduct of Skin Absorption Studies. Environment Directorate. Organisation for Economic Co-Operation and Development, Paris, December 2000.
14. Hood HL, Wickett RR, Bronaugh RL. The in vitro percutaneous absorption of the fragrance ingredient musk xylol. Fd Chem Toxicol 1996; 34:483–488.

19

The Fate of Cutaneous Levels of Absorbed Compounds

Robert L. Bronaugh, Margaret E. K. Kraeling, and Jeffrey J. Yourick
Office of Cosmetics and Colors, Food and Drug Administration, Laurel, Maryland, U.S.A.

I. INTRODUCTION

For some time it has been recognized that lipophilic compounds can present a problem in the in vitro measurement of percutaneous absorption. Compounds that are insoluble in water may not partition freely from excised skin into an aqueous receptor fluid. The problem was alluded to by Franz (1), who in selecting compounds for the study, omitted highly water-insoluble compounds to avoid results that were "artificially limited due to insolubility in the dermal bathing solution."

II. MODIFICATION OF RECEPTOR FLUID

Attempts have been made to overcome this problem by modifying the receptor fluid composition. Brown and Ulsamer (2) found that the skin permeation of the hydrophobic compound hexachlorophene increased twofold when normal saline was replaced with 3% bovine serum albumin (BSA) (in a physiological buffer) in the diffusion cell receptor fluid.

Other nonphysiological methods have been developed with surfactants and organic solvents. Bronaugh and Stewart (3) achieved more efficient receptor fluid partitioning of two fragrance ingredients by using the non-ionic surfactant polyethylene glycol oleyl ether (PEG-20 oleyl ether, Volpo 20). The studies were conducted with 6% PEG-20 oleyl ether and full-thickness rat skin. The permeation of a water-soluble control compound was unaffected by the addition of the surfactant to the receptor fluid. The authors concluded, however, that one receptor fluid would not be equally beneficial for all lipophilic compounds. Furthermore, they stated that for extremely lipophilic compounds insoluble in water, less than 50% of in vivo absorption values would probably be obtained by measuring receptor fluid contents. In subsequent studies with split-thickness skin, only 0.5% PEG-20 oleyl ether could be used in the receptor fluid without damage to the skin barrier (4).

III. SYSTEMIC ABSORPTION

An estimate of systemic absorption should no longer be obtained simply by measuring receptor fluid levels; skin levels must also be measured. Addition of solubilizing agents to the receptor fluid can improve partitioning of compounds from skin but effectiveness is variable. Surfactants and organic solvents destroy the viability of skin. Systemic absorption values should include absorbed material in the skin reservoir at the end of a study unless extended experiments have been conducted to determine the fate of that material remaining in the skin.

A review of the current status of in vivo and in vitro skin absorption methods and recommended protocols was prepared following a 1994 workshop (5). The report mentions that when material remaining in the skin was considered to be percutaneously absorbed, in vivo and in vitro correlations were usually improved.

The viability of skin can be maintained by using a balanced salt solution or a tissue culture medium. Addition of 4% BSA may be sufficient in some cases to enhance receptor fluid levels of applied compound without alteration of skin viability.

IV. SKIN RESERVOIR FORMATION

The methodological problem that a skin reservoir creates may not be limited to lipophilic compounds. Studies with alpha hydroxy acids (AHAs), such as glycolic acid and lactic acid, have shown us that very polar compounds can still be substantially retained in skin at the end of a 24-hours absorption study (6). The fate of the AHAs in terms of systemic absorption was not examined in these early studies.

V. FATE OF ABSORBED MATERIAL IN SKIN

The fate of test compounds that are extensively retained in skin after a 24-hours exposure has been examined in the following studies.

The percutaneous absorption of the fragrance ingredient musk xylol was evaluated in hairless guinea pig and human skin (7). The compound was applied to skin in an oil-in-water emulsion and in a volatile solvent (methanol). After 24 hours, the unabsorbed compound was removed from the surface of skin with a soap and water wash. Total absorption of musk xylol in hairless guinea pig skin was 55% from the emulsion vehicle and 45% from the methanol vehicle. In human skin, permeation of the fragrance from both vehicles was only 22% of the applied dose. A substantial percentage of the absorbed material remained in the skin at the end of the 24-hour absorption studies, particularly in the human skin.

An extended absorption study was conducted to assess the fate of the musk xylol remaining in human skin. Diffusion cells were assembled with human skin and dosed with musk xylol in an emulsion vehicle. At 24 hours, the skin in all cells was washed, and then half the cells were terminated and the receptor fluid and skin levels were measured (Fig. 1). Receptor fluid samples from the rest of the cells were collected for an additional six days, and the skin was then removed for analysis. Only about 25% of the musk xylol measured in skin at 24 hours remained in skin after seven days. Most of this material had diffused from skin into the receptor fluid during the 24 to 72–hour period following application. These data suggest that most of the absorbed musk xylol in skin at 24 hours would eventually be systemically absorbed in an in vivo study.

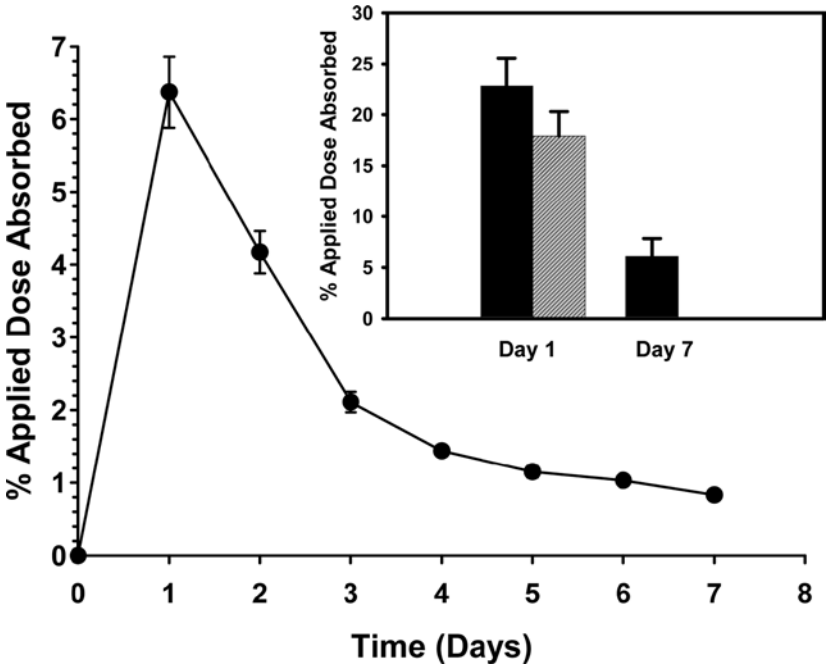


Figure 1 Time course of percutaneous absorption of musk xylol into the receptor fluid. Inset: Skin levels of musk xylol, ■ total skin ▨ and stratum corneum. Values are the means ± SE of determinations in two human subjects.

The fate of the skin reservoir formed during in vivo skin absorption studies was determined in hairless guinea pigs (8).[14]C-labeled phenanthrene, benzo(a)pyrene or di(2-ethylhexyl)phthalate was administered dermally in acetone to groups of four animals for each measurement. The absorption values for benzo(a)pyrene are presented in Table 1. At the end of 24 hours, unabsorbed test compound was removed from all animals with a soap and water wash. Some animals were sacrificed at 24 hours and the absorbed benzo(a)pyrene was determined in dosed skin, excreta, and carcass to give a value for total percutaneous absorption. The study was extended in other animals to totals of 48 hours or seven days after application of test compound. The amount of benzo(a)pyrene in skin decreased from 8.9% of the applied dose at 24 hours to only 1.4% when the study was continued for an additional 24 hours (for a total of 48 hours). After seven days, only 0.2% of the applied

Table 1 Bioavailability of Dermally Applied Benzo(a)pyrene

	Applied dose (%)		
Recovery site	24 hr	48 hr	7 days
Dosed skin	9.5 ± 4.1	1.4 ± 0.4	0.2 ± 0.2
Excreta	4.6 ± 2.5	11.2 ± 1.8	23.9 ± 6.0
Carcass	12.3 ± 3.8	11.4 ± 2.4	0.3 ± 0.1
Total	26.4 ± 6.2	24.0 ± 2.9	24.4 ± 5.9
Wash + cover	58.5 ± 10.9	53.0 ± 2.1	65.3 ± 10.4

Note: Values are the means ± SD from four hairless guinea pigs.

Table 2 DEA Viable Skin Penetration from Lotion Formulations in 24 hours

Consumer product (DEA dose/cm^2)	Applied dose penetrated (%)	
	Product E[a] [0.35 µg/cm^2]	Product F[b] [0.60 µg/cm^2]
Receptor fluid	0.6 ± 0.1[c]	1.2 ± 0.2[c]
Stratum corneum	4.8 ± 0.5[d]	2.3 ± 0.5[d]
Epidermis and dermis	10.0 ± 2.3	4.3 ± 1.6
Total in skin	14.8 ± 2.3	6.6 ± 1.2
Total penetration	15.4 ± 2.4	7.8 ± 1.4
Recovery	100.8 ± 4.3	96.1 ± 6.2

[a]Values are the mean and SEM of three to four replicates in each of seven subjects.
[b]Values are the mean and SEM of three to four replicates in each of three subjects.
[c]Receptor fluid values are significantly different (ANOVA followed by Tukey test, $p < 0.05$).
[d]Stratum corneum values are significantly different (ANOVA, $p < 0.05$).
Abbreviation: DEA, diethanolamine.

dose remained in skin. The results of the studies with all three compounds indicated that the amounts left in skin after surface washing eventually entered the systemic circulation and should be considered part of the total dose absorbed.

The skin absorption of diethanolamine (DEA) was determined from cosmetic formulations using excised human skin in diffusion cells (9). When ^{14}C-DEA was applied to skin in several commercially available lotions, only 0.6% to 1.2% of the applied dose was found in the receptor fluid at the end of 24 hour studies (Table 2). Most of the absorbed compound was found in the skin, with the greatest amounts

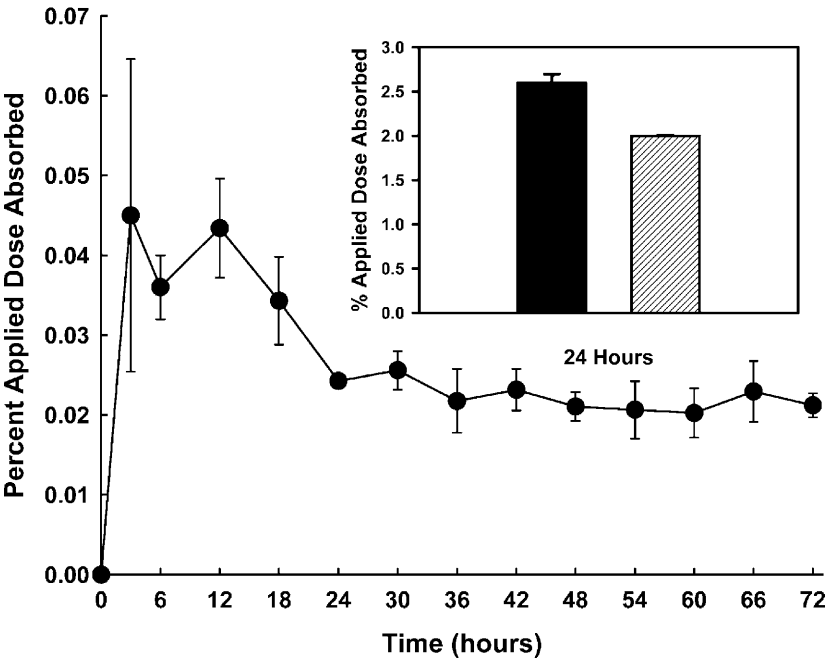


Figure 2 Time course of percutaneous absorption of DB1 into the receptor fluid. Inset: Skin levels of DB1, ■ total skin ▨ and stratum corneum. Values are the means ± SE of determinations in two rat studies.

penetrating through the stratum corneum into the deeper epidermal and dermal regions. An extended absorption study conducted with Product E for an additional 48 hours showed that no significant increases occurred in the DEA receptor fluid levels. The lack of additional partitioning of DEA into the receptor fluid could not be explained by poor water solubility. It appeared that DEA was binding to the skin and therefore the DEA in the skin reservoir was not available for systemic absorption.

The percutaneous absorption of Disperse Blue 1 (DB1) was determined through human skin from a semi-permanent hair dye vehicle (10). Only a small amount of the absorbed compound (0.2% of the applied dose) was found in the receptor fluid beneath the skin at the end of 24 hours (Fig. 2). The amount of DB1 absorbed in skin at 24 hours was 2.6%, with most of the compound in the stratum corneum (Fig. 2). The unabsorbed material was removed with soap and water from some cells and the studies were continued for an additional 48 hours (total 72 hours). Only a small amount of additional DB1 was found in the receptor fluid. It appeared that the DB1 in the skin reservoir was not available for significant percutaneous absorption.

Further studies are needed with additional compounds to more fully understand the fate of compounds that form a reservoir in skin during percutaneous absorption studies. This reservoir is likely formed in skin not only by lipophilic compounds, but also by polar and nonpolar compounds that bind to skin during the absorption process.

REFERENCES

1. Franz TJ. Percutaneous absorption. On the relevance of in vitro data. J Invest Dermatol 1975; 64:190–195.
2. Brown DWC, Ulsamer AG. Percutaneous penetration of hexachlorophene as related to receptor solutions. Food Chem Toxicol 1975; 13:81–86.
3. Bronaugh RL, Stewart RF. Methods for in vitro percutaneous absorption studies III. Hydrophobic compounds. J Pharm Sci 1984; 73:1255–1258.
4. Bronaugh RL, Stewart RF. Methods for in vitro percutaneous absorption studies VI. Preparation of the barrier layer. J Pharm Sci 1986; 75:487–491.
5. Howes D, Guy R, Hadgraft J, Heylings JHU, Kemper F, Maibach H, Marty J, Merk H, Parra J, Rekkas D, Rondelli I, Schaefer H, Tauber U, Verbiese N. Methods for assessing percutaneous absorption: the report and recommendations of the ECVAM workshop. ATLA 1996; 24:81–106.
6. Kraeling MEK, Bronaugh RL. In vitro percutaneous absorption of alpha hydroxy acids in human skin. J Soc Cosmet Chem 1997; 48:187–197.
7. Hood HL, Wickett RR, Bronaugh RL. The in vitro percutaneous absorption of the fragrance ingredient musk xylol. Food Chem Toxicol 1996; 34:483–488.
8. Chu I, Dick R, Bronaugh RL, Tryphonas L. Skin reservoir formation and bioavailability of dermally administered chemicals in hairless guinea pigs. Food Chem Toxicol 1996; 34:267–276.
9. Kraeling MEK, Yourick JJ, Bronaugh RL. Percutaneous absorption of diethanolamine in human skin in vitro. Food Chem Toxicol 2004; 1553–1561.
10. Yourick JJ, Koenig ML, Yourick DL, Bronaugh RL. Fate of chemicals in skin after dermal application: does the in vitro skin reservoir affect the estimate of systemic absorption? Toxicol Appl Pharamcol 2004; 195:309–320

20

Dermal Decontamination and Percutaneous Absorption

Ronald C. Wester and Howard I. Maibach
Department of Dermatology, School of Medicine, University of California, San Francisco, California, U.S.A.

Although decontamination of a chemical from the skin is commonly done by washing with soap and water, as it has been assumed that washing will remove the chemical, recent evidence suggests that often the skin and the body are unknowingly subjected to enhanced penetration and systemic absorption/toxicity because the decontamination procedure does not work or may actually enhance absorption. This chapter reviews some of the recent literature, then offers new in vitro and in vivo techniques to determine skin decontamination.

I. IN VIVO DECONTAMINATION MODEL

Figure 1 shows a skin decontamination model (1) where the time course of decontamination for several solvent systems can be tested. The illustration is for the abdomen of a rhesus monkey, but any large skin area can be used, including human. A grid of 1-cm^2 areas is marked on the skin. The illustration shows 24 separate blocks. As an example of use, the four blocks across the grid can represent four different decontaminating systems. The blocks down the abdomen can represent six time periods in which the skin is decontaminated. In our system we use a cotton applicator laden with washing solvent to wash the skin block area. This is illustrated with the following data.

Figure 2 shows glyphosate, a water-soluble chemical, removed from rhesus monkey skin with three successive soap-and-water or water-only washes. Approximately 90% of the glyphosate is removed with the washes, most in the first wash. There is no difference between soap-and-water and water-only washing. Figure 3 shows alachlor, a lipid-soluble chemical, also decontaminated with soap-and-water and water-only washes. In contrast to glyphosate, more alachlor is removed with soap-and-water than with water-only washes. Although the first alachlor washing removed a majority of chemical, successive washings contributed to the overall decontamination.

Figures 4 (glyphosate) and 5 (alachlor) illustrate skin decontamination with soap-and-water or water-only washes over a 24-hour dosing period, using the grid methodology from Figure 1, The three successive washes were pooled for each data

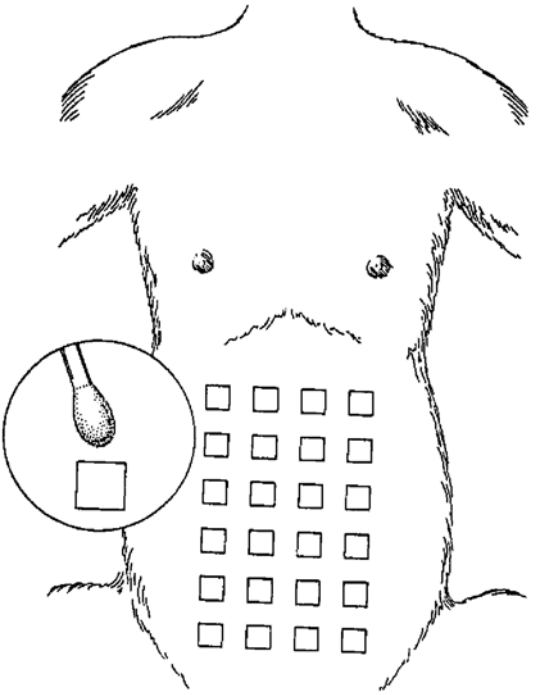


Figure 1 Illustration of grid method where multiple single doses are marked on rhesus monkey abdomen for skin decontamination with time using a cotton-tip applicator laden with appropriate solvent.

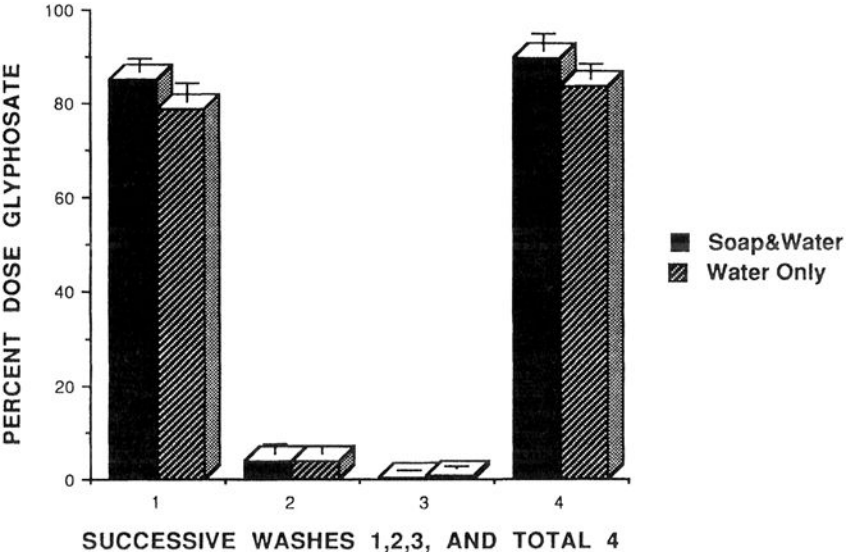


Figure 2 Glyphosate removal from rhesus monkey skin in vivo with successive washes. Note that water only and the addition of soap are equally effective. Glyphosate is water soluble.

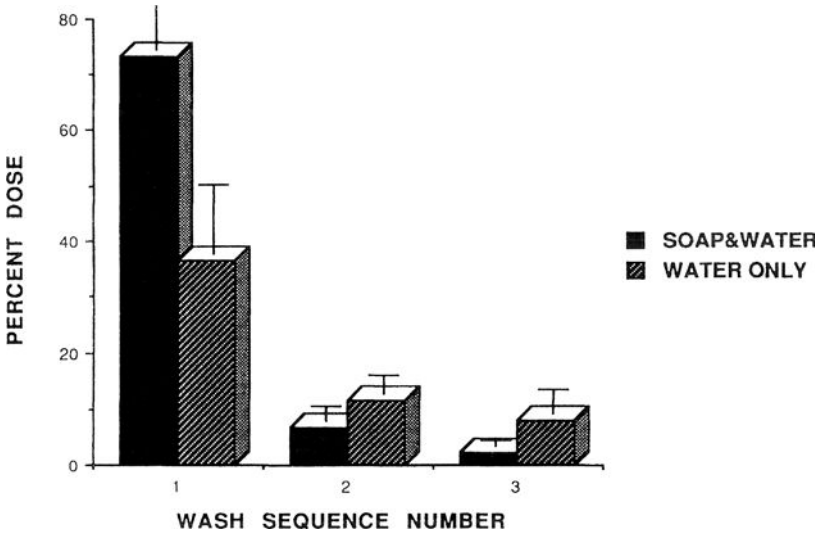


Figure 3 Alachlor removal from rhesus monkey skin in vivo with successive washes. Note that soap and water removes more alachlor than water only. Alachlor is lipid soluble.

time point. Certain observations are made. First, the amount recovered decreases over time. This is because this is an in vivo system and percutaneous absorption is taking place, decreasing the amount of chemical on the skin surface. There also may be some loss due to skin desquamation. Note that alachlor is more readily absorbed across skin than is glyphosate. The second observation is, again, that soap-and-water and water-only washes removed equal amounts of glyphosate, but alachlor is more readily removed with soap-and-water washing than with water only.

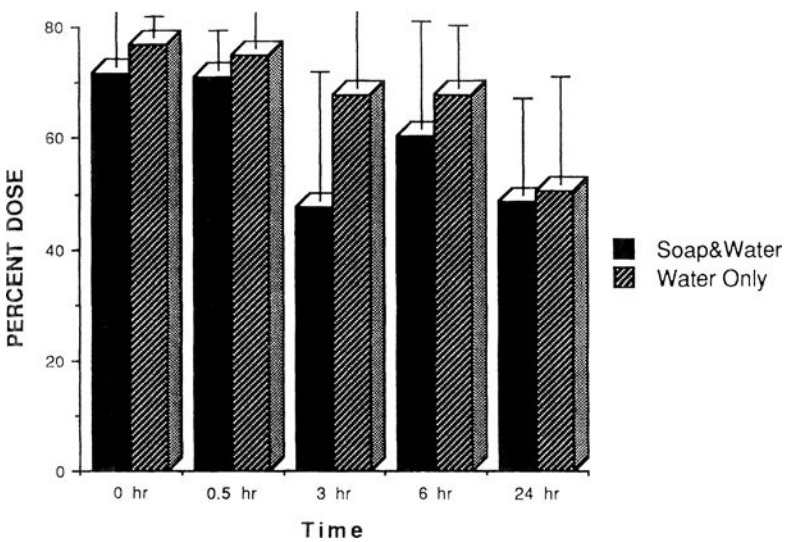


Figure 4 Time course, 0 to 24 hours, for in vivo glyphosate removal with skin washing. Over time, the ability to remove glyphosate decreases due to ongoing skin absorption. Soap-and-water and water-only washes were equally effective. Glyphosate is water soluble.

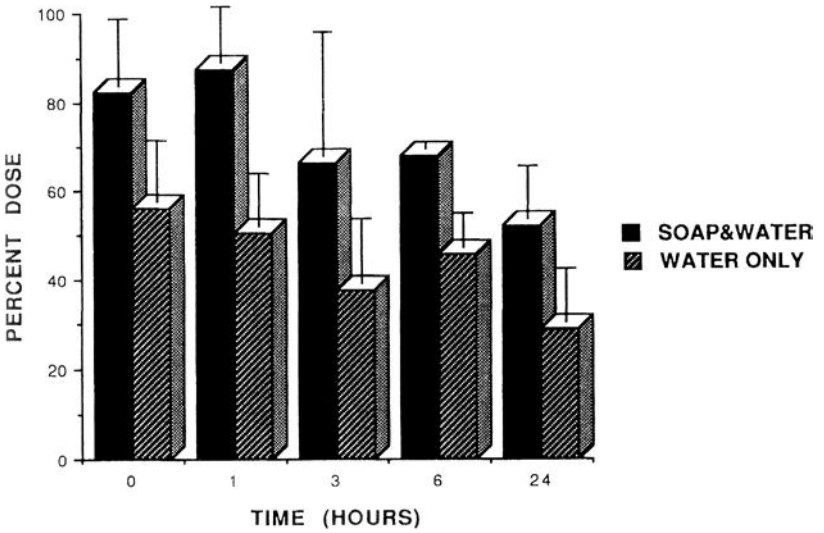


Figure 5 Time course, 0 to 24 hours for in vivo alachlor removal with skin washing. Over time the ability to remove alachlor decreases due to ongoing skin absorption. Soap and water was more effective than water only. Alachlor is lipid soluble.

The reason is that glyphosate is water soluble; thus, water is a good solvent for it. Alachlor is lipid soluble and needs the surfactant system for more successful decontamination (1,2).

Figure 6 shows alachlor skin decontamination at four dose concentrations washed with multiple successive soap-and-water applications. Most of the dose is removed with the first washing, and three successive washes are adequate to remove the dose.

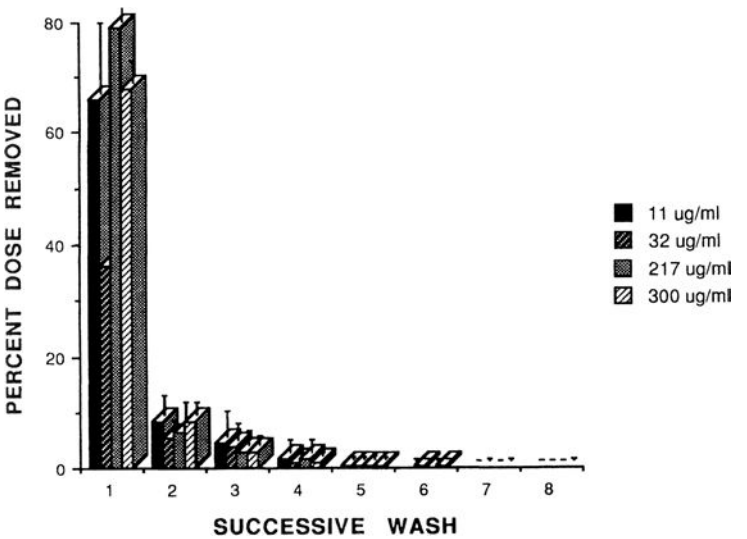


Figure 6 Alachlor soap-and-water skin decontamination with multiple successive washes. Three successive washes seem adequate for decontamination.

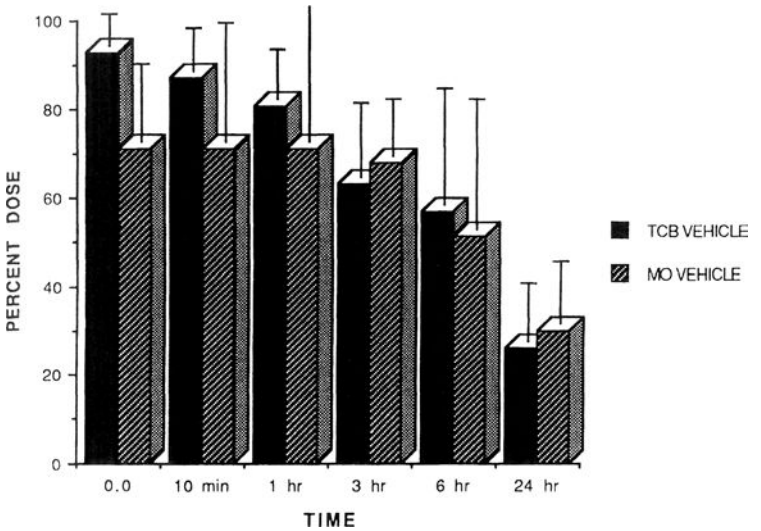


Figure 7 Polychlorinated biphenyls (PCBs) can be removed with soap and water; however, skin absorption of PCBs is high, and the chance to remove them from skin decreases with time. PCBs were applied to skin in either trichlorobenzene (TCB) or mineral oil (MO) vehicle.

Figure 7 shows 42% polychlorinated biphenyls (PCBs) applied in vivo in trichlorobenzene (TCB) or mineral oil (MO) to rhesus monkey skin and washed over a 24-hour period with soap and water. With time, the wash recovery of PCBs decreases due to the ongoing skin absorption. The PCBs can be removed from skin with soap and water if the decontamination is done soon enough after exposure (3).

The preceding discussion shows (Table 1) that there are two factors with in vivo skin decontamination. The first is the "rubbing effect" that removed loose surface stratum corneum due to natural skin desquamation. The second is the "solvent effect," which is related to chemical lipophilicity and was illustrated for glyphosate and alachlor.

II. IN VITRO DECONTAMINATION MODEL

In vitro skin mounted in diffusion cells can be decontaminated with solvents. A problem exists in that the mounted skin is fragile and cannot be rubbed, as naturally occurs with people washing their skin. Another in vitro technique that is easy to use for solvent efficiency in decontamination is with powdered human stratum corneum

Table 1 In Vivo Skin Decontamination

1.	*Rubbing effect*
	Removes "loose" surface stratum corneum
	"Loose" = natural desquamation
2.	*Solvent effect*
	Water only
	Soap and water
	Related to chemical lipophilicity

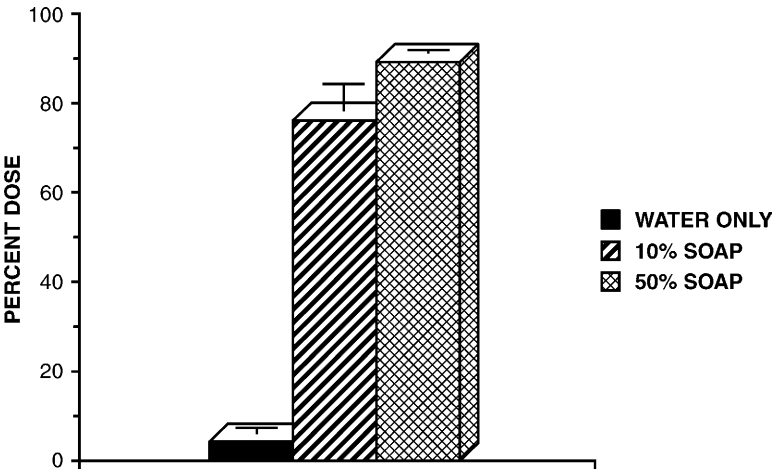


Figure 8 Alachlor was added to powdered human stratum corneum and then partitioned against water only or against water with 10% or 50% soap. Soap is required to remove alachlor, which is lipid soluble. This is a good in vitro model to screen potential decontamination vehicles.

(PHSC). Figure 8 shows results when alachlor was added to PHSC and then partitioned against water only or against water with 10% and 50% soap. Alachlor stayed with the PHSC when partioned against water-only; however, it readily partitioned to the solvents against 10% and 50% soap. These are the same confirming results shown in Figures 3, 5, and 6.

The PHSC is made according to Wester et al. (4). It is then mixed with [^{14}C]alachlor in Lasso formulation, allowed to set for 30 minutes, and then centrifuged. The alachlor, a lipid-soluble chemical, partitions ($90.3 \pm 1.2\%$) into the PHSC; $5.1 \pm 1.2\%$ remains in the Lasso formulation. Water-only wash (and subsequent centrifugation) removes only $4.6 \pm 1.3\%$ of the "bound" alachlor. However, when the bound alachlor–stratum corneum is washed with 10% and 50% soap and water (v/v), $77.2 \pm 5.7\%$ and $90.0 \pm 0.5\%$ of the alachlor is removed from the stratum corneum, respectively. Such a model would predict that alachlor in Lasso cannot be removed from the skin with water-only washing, but that the use of soap will decontaminate the skin. The "lipid" constituents of soap probably offer a more favorable partitioning environment for the alachlor.

III. EFFECTS OF OCCLUSION AND EARLY WASHING

Table 2 shows the effect of duration of occlusion on the rate of absorption of malathion (5). What is important from this table is that 9.6% of the applied malathion was absorbed during a zero-time duration. There was an immediate wash of the site of application with soap and water. Almost 10% of the applied dose was not washed off but, in fact, persisted on the skin through the wash procedure and was later absorbed into the body. Table 3 shows the short-term wash recovery for benzo[a]pyrene and DDT. Even when skin washing was initiated within 25 minutes of dosing, some benzo[a]pyrene and all of the DDT had absorbed sufficiently into the skin. Therefore, early washing after exposure is critical, but it may not provide complete decontamination (6).

Table 2 Effect of Duration of Occlusion on Percutaneous Absorption of Malathion in Humans

Duration (hr)	Absorption (%)
0[a]	9.6
0.5	7.3
1	12.7
2	16.6
4	24.2
8	38.8
24	6.8

[a]Immediate wash with soap and water.

Table 4 shows the effect of washing on the percutaneous absorption of hydrocortisone in a rhesus monkey. With a non-washing sequence between dose applications, the percentage dose absorbed was $0.55 \pm 0.06\%$ of applied dose. When a post-24-hour wash procedure was introduced, the percentage of dose absorbed statistically ($p < 0.05$) increased to $0.72 \pm 0.06\%$. The post-24-hour wash was supposed to remove the excess materials and thus decrease absorption. However, the soap-and-water wash hydrated the skin and the rate of absorption of hydrocortisone increased.

Table 5 shows dermal washing efficiency for PCBs in the guinea pig. When 42% PCB was applied to guinea pig skin and immediately washed, only 58.9% of the applied dose could be removed. The rest of the material was available for subsequent percutaneous absorption. When 42% PCB was applied to guinea pig skin and 24 hours later the site of application was washed, only 0.9% of the applied dose was removed. Thus, all the applied PCB was available for absorption or had already been absorbed into the body. When 54% PCB was applied to guinea pig skin and washed 24 hours post-application, 19.7% of the applied dose was removed. Thus, with 54% PCB, 80% of the applied dose could not be removed or had already been absorbed into the body. Subsequent examination of the rate of absorption of PCB showed that most was absorbed into the body. This study illustrates that the hypothesis that washing or bathing and any other application of water will remove all material from skin is wrong. Substantivity (the nonspecific absorption of material to skin) can be a strong force.

Table 3 Short-Term Wash Recovery for Benzo[a]pyrene and DDT: 25-minute Exposure Vs. 24-Hour Exposure

	Percent dose		
Chemical	Short exposure (25 min), in vitro receptor fluid	Skin	Long exposure (24 hr), in vivo
Benzo[a]pyrene	0.00 ± 0.00	5.1 ± 2.1	51.0 ± 22.0
DDT	0.00 ± 0.00	16.7 ± 13.2	18.8 ± 9.4

Note: In vitro the chemical in acetone vehicle was dosed on human skin then washed with soap and water after a 25-minute period. The in vivo studies were 24-hour exposure with acetone vehicle dosing.

Table 4 Effect of Washing on Percutaneous Absorption of Hydrocortisone in Rhesus Monkey

Treatment	Absorption (% ± SD)
No wash	0.55 ± 0.06
Post-24-hr wash[a]	0.72 ± 0.06

[a]Soap-and-water wash.

Figure 9 shows the percent dose absorbed per hour of a herbicide in the rhesus monkey (7). At 24 hours post-application, the site of absorption was washed with water and acetone sequentially. The time curve shows a "washing-in effect" following the 24-hour post-application wash. Thus, as we saw previously with hydrocortisone, there is definitely a washing-in effect. The application of water and acetone changed the barrier properties of skin and caused an increase in the rate of absorption of this herbicide. Moody and Nadeau (8) also recently showed the washing-in effect for 2,4-dichlorophenoxyacetic acid amine during in vitro percutaneous absorption studies in rat, guinea pig, and human skin.

It is generally assumed that pesticides and other chemicals can be easily removed from the skin. Another series of experiments by Feldman and Maibach (5) was designed to determine just how effective the removal is in terms of decreasing percutaneous absorption. The experimental variable was the removal of applied pesticide in different groups of subjects at varying times. Decontamination was attempted by a two-minute wash with soap and hot water. Data are presented in Table 6. Absorption of azodrin at a concentration of 4 $\mu g/cm^2$ on the human forearm was 14.7% if the site was not washed for 24 hours. Washing after four hours decreased absorption to 8% of the dose. Washing after only 15 minutes decreased penetration, but still 2.3% of the dose was absorbed. With similar experimental variables, ethion washing in 15 minutes decreased the penetration from the 24-hour time period from only 3.3% to 1.6%. Malathion decrease from the 24-hours to 15-minutes wash was from only 6.8% to 4.3%.

A similar relationship was maintained when the applied concentration was greatly increased. For instance, at a concentration of 4 $\mu g/cm^2$ of parathion, the penetration after washing at 24 hours was 8.6%; this was only decreased to 6.7% by washing in 15 minutes.

The effect of the anatomic site was also studied. On the palm, the penetration of parathion was 11.8% with washing at 24 hours. There was no significant decrease in penetration washing in 15 minutes; in fact, there was a slight increase. Thus, the very potent pesticide parathion absorbs to skin despite washing and is absorbed into the body.

Table 5 Dermal Wash Efficiency for Polychlorinated Biphenyls (PCBs) in Guinea Pig

PCB (%)	Wash time[a]	Dose removed (% ± SD)
42	Immediate	58.9 ± 7.5
42	Post-24-hr	0.9 ± 0.2
54	Post-24-hr	19.7 ± 5.5

[a]Wash procedure: twice with water, twice with acetone, and twice with water.

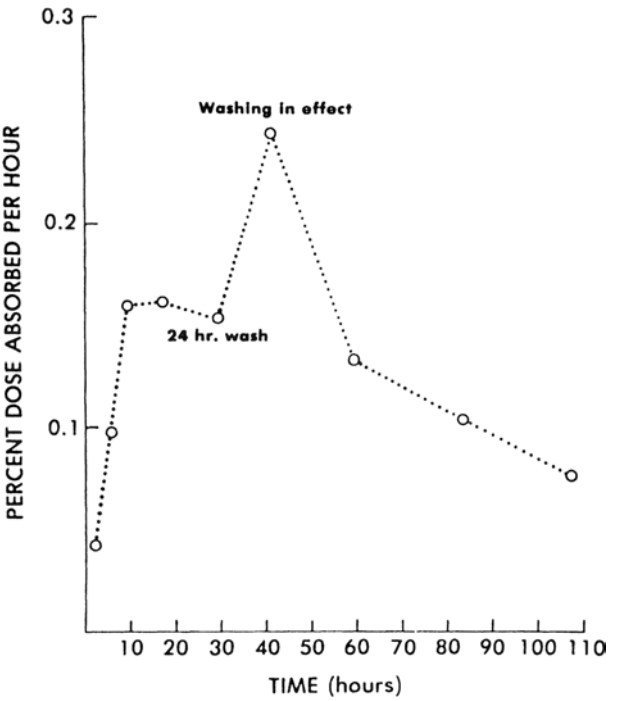


Figure 9 Effect of washing on absorption. Washing at 24 hours enhanced absorption, as shown by the peak effect at 48 hours.

Experiments with rubbing alcohol had similar results. When used with malathion, alcohol washing at four hours allowed 16.8% penetration and at 15 minutes, 17.7%. Penetration with parathion at four hours was 10.3%, and at 15 minutes, 8.2%. These data suggest that a careful examination be made of recommendations given to consumers and workers about when they can remove these substances from their skin and what materials should be used. It is obvious that protection from washing and bathing is not what had been predicted.

It was questioned whether a whole-body exposure to a solvent such as water might not be more effective at removing pesticides. For this reason a group of subjects was showered 4 hours after application instead of being washed locally with soap and water. The data for malathion, parathion, and Baygon are in Table 7. The shower was no more (and perhaps less) effective than the local application of soap and water. Showering does not appear to be a solution to the problem.

IV. TRADITIONAL SOAP AND WATER WASH AND EMERGENCY SHOWER

In the home and workplace, decontamination of a chemical from skin is traditionally done with soap-and-water wash; some workplaces may have an emergency water shower. It has been assumed that these procedures are effective, yet workplace illness and even death occur from chemical contamination. Water or soap-and-water washing may not be the most effective means of skin decontamination, particularly for fat-soluble materials. This study was undertaken to help determine whether there

Table 6 Effect of Washing on Percent Penetration

Compound, dose (μg/cm^2), and site	Minutes				Hours				
	1	5	15	30	1	2	4	8	24
Soap and water									
Azodrin, 4, arm			2.3				8.6		14.7
Ethion, 4, arm			1.6				2.9		3.3
Guthion, 4, arm									
Malathion									
4, arm	1.2		4.3	4.5	6.1	8.3	12.1		6.8
40, arm			4.7				6.8		
400, arm			1.4		2.0		4.7		
Parathion									
4, arm	2.8		6.7		8.4		8.0	15.8	8.6
40, arm			3.1				6.9		9.5
400, arm			2.2		2.3		4.2		4.8
4, forehead	8.4		7.1	12.2	10.5	20.1	27.7		36.3
4, palm		6.2	13.6	13.3	11.7	9.4	7.7		11.8
Lindane, 4, arm		1.7	1.8	4.2	3.9	6.7	5.1		9.3
Baygon, 4, arm	1.2		4.7	4.5	4.7	11.8	15.5	11.3	19.6
2,4-D									
4, arm	0.5		0.7	1.8	1.2	3.7	3.7		5.8
40, arm			0.7				2.8		
Rubbing alcohol									
Malathion, 4, arm			17.7		5.8		16.8		
Parathion, 4, arm			8.2		7.0		10.3		

are more effective means of removing methylene bisphenyl isocyanate (MDI), a potent contact sensitizer, from the skin. MDI is an industrial chemical for which skin decontamination using traditional soap-and-water washing and nontraditional polypropylene glycol, a polyglycol-based cleaner (DTAM), and corn oil was done in vivo in the rhesus monkey over eight hour. Water and soap-and-water (5% and 50% soap) washes were partially effective in the first hour, removing 51–69% applied dose. However, decontamination fell to 40% to 52% at four hours and 29% to 46% at eight hours (Fig. 10). Thus, the majority of MDI was not removed by traditional soap-and-water wash; skin tape stripping after wash confirmed that MDI was still on the skin (Fig. 11). In contrast, polypropylene glycol, DTAM, and corn oil removed 68% to 86% MDI in the first hour, 74% to 79% at four hour and 72% to 86% at

Table 7 Effect of Shower on Different Types of Removal at Four Hours

Compound	Absorption (%) after shower[a]		
	Arm	Forehead	Palm
Malathion	8.8 (12.1)	32.7	7.2
Parathion	16.5 (9.0)	41.9 (27.7)	13.4 (7.7)
Baygon	9.9 (15.5)	20.5	8.7

[a]Values in parentheses: after washing.

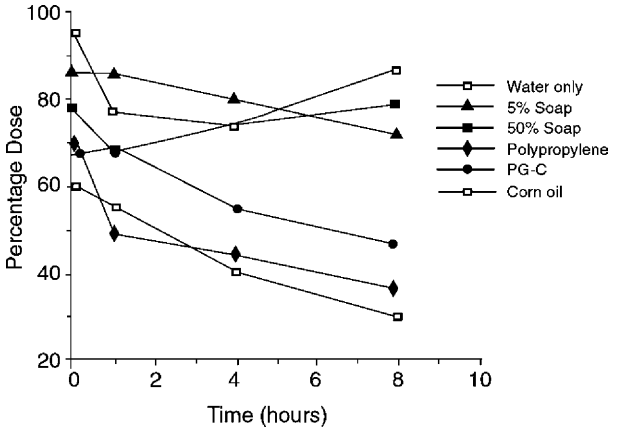


Figure 10 Mean percent applied dose of methylene bis phenyl isocyanate (MDI) removed with designated decontamination procedure at designated time period. Water and soap-and-water are the least effective, especially at four and eight hours.

eight hours. Statistically, polypropylene glycol, DTAM, and corn oil were all better ($p < 0.05$) than soap and water at four hours and eight hours after dose application. These results indicated that traditional soap-and-water wash and the emergency water shower are relatively ineffective at removing MDI from the skin. More effective decontamination procedures, as shown here, are available.

V. CONCLUSION: SUBSTANTIVITY

Substantivity has been defined as the nonspecific absorption of material from skin. It is obvious that the standard washing procedures do not always readily remove materials from skin. How important is this in terms of occupational exposure? Kazen et al. (9) did hexane hand rinsings on occupationally exposed people. They analyzed the

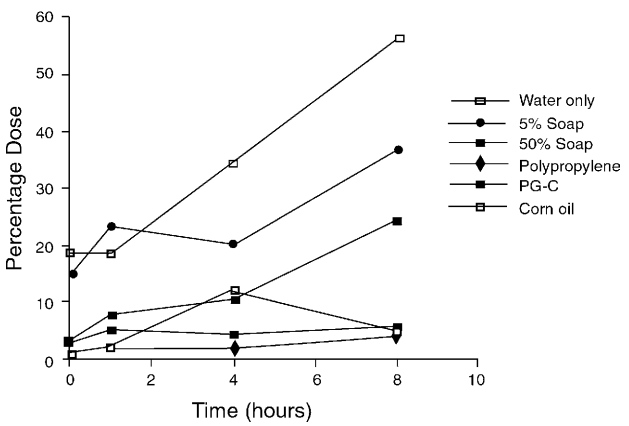


Figure 11 Mean percent applied dose of methylene bis phenyl isocyanate (MDI) removed by cellophane tape stripping following wash decontamination. This confirms that the MDI not removed by water and soap-and-water washes was still present on the skin.

rinsings by electron capture and flame photometric/gas–liquid chromatography for pesticide residues to determine whether or not these chemicals persisted on the skin long after exposure. Chlordane and dieldrin apparently persisted on the hands of a former pest control operator for at least two years. Methoxychlor, captan, and malathion persisted for at least seven days on the hands of a fruit and vegetable grower. Parathion was found on the hands of one man two months after his last known contact with this pesticide. Endosulfan, dichlorodiphenyl-dichloroethane (DDD), kelthane, decthal, trithijon, imidan, and guthion have persisted on the hands of some exposed workers from less than a day to 112 days after exposure (10–15).

In conclusion, washing is generally good, but it does not prevent penetration of some chemicals. Surely, the understanding of the mechanism and the development of more efficient removal systems must be a high priority for research.

REFERENCES

1. Wester RC, Melendres J, Sarason R, McMaster J, Maibach HI. Glyphosate skin binding, absorption, residual tissue distribution, and skin decontamination. Fundam Appl Toxicol 1991; 16:725–732.
2. Wester RC, Melendres J, Maibach HI. *In vivo* percutaneous absorption of alachlor in Rhesus monkey. J Toxicol Environ Health 1992; 36:1–2.
3. Wester RC, Bucks DAW, Maibach HI. Polychlorinated biphenyls (PCBs): dermal absorption, systemic elimination, and dermal wash efficiency. J Toxicol Environ Health 1984; 12:511–519.
4. Wester RC, Mobayen M, Maibach HI. *In vivo* and *in vitro* absorption and binding to powdered stratum corneum as methods to evaluate skin absorption of environmental chemical contaminants from ground and surface water. J Toxicol Environ Health 1987; 21:367–374.
5. Feldmann RJ, Maibach HI. Systemic absorption of pesticides through the skin of man. Occupational Exposure to Pesticides: Report to the Federal Working Group on Pest Management from the Task Group on Occupation Exposure to Pesticides. Appendix B, 120–127, 1974.
6. Wester RC, Maibach HI, Bucks DAW, Sedik L, Melenderes J, Liao C, Di Zio S. Percutaneous absorption of [^{14}C]-DDT and [^{14}C]-benzo(a)pyrene from soil. Fundam Appl Toxicol 1990; 15:510–5106.
7. Wester RC, Maibach HI. Advances in percutaneous absorption. In: Drill VA, Lazar P, eds. Cutanous Toxicity. New York: Raven Press, 1983:29–40.
8. Moody RP, Nadeau B. *In vitro* dermal absorption of two commercial formulations of 2,4-dichlorophenoxyacetic acid dimethylamide (2,4-D amine) in rat, guinea pig and human skin. Toxicol in vitro 1997; 11:251–262.
9. Kazen C, Bloomer A, Welch R, Oudbier A, Price H. Persistence of pesticides on the hands of some occupationally exposed people. Arch Environ Health 1974; 29:315–318.
10. Geno PW, Camann DE, Harding JH, Villalobos K, Lewis RG. Handwipe sampling and analysis procedure for the measurement of dermal contact with pesticides. Arch Environ Contam Toxicol 1996; 30:132–138.
11. Hewitt PG, Hotchkiss PG, Caldwell J. Decontamination procedures after in vitro topical exposure of human and rat skin to 4,4^{1}-methylenebis[2-chloroaniline] and 4,4^{1}-methylenedianiline. Fundam Appl Toxicol 1995; 26:91–98.
12. Kintz P, Tracqui A, Morgin P. Accidental death caused by the absorption of 2,4-dichlorophenol through the skin. Arch Toxicol 1992; 66:298–299.
13. Merrick MV, Simpson JD, Liddell S. Skin decontamination—A comparison of four methods. Br J Radiol 1982; 55:317–318.

14. Wester RC, Noonan PK, Maibach HI. Frequency of application of percutaneous absorption of hydrocortisone. Arch Dermatol 1997; 113:620–622.
15. Wester RC, Hui X, Landry T, Maibach HI. *In vivo* skin decontamination of methylene bisphenyl isocyanate (MDI): soap and water ineffective compared to polypropylene glycol, polyglycol-based cleanser, and corn oil. Toxicol Sci 1998; 48:1–4.

21

Chemical Partitioning into Powdered Human Stratum Corneum: A Useful In Vitro Model for Studying Interaction of Chemicals and Human Skin

Xiao-Ying Hui, Ronald C. Wester, Hongbo Zhai, and Howard I. Maibach
Department of Dermatology, School of Medicine, University of California, San Francisco, California, U.S.A.

I. INTRODUCTION

Chemical delivery/absorption into and through the skin is important in both dermato-pharmacology and dermato-toxicology. The human stratum corneum is the first layer of the skin and constitutes a rate-limiting barrier to the transport of most chemicals across the skin (1). Chemicals must first partition into the stratum corneum before entering the deeper layers of the skin, the epidermis, and the dermis to reach the vascular system. Chemical partitioning proceeds much faster than complete diffusion through the whole stratum corneum, and the process quickly reaches equilibrium. In addition to binding within the stratum corneum, a chemical can also be retained within the stratum corneum as a reservoir (2). Thus, understanding the process of chemical partitioning into the stratum corneum becomes important in developing an insight into its barrier properties and transport mechanisms.

Human stratum corneum has been used for decades as an in vitro model to explore both percutaneous absorption and the risks associated with dermal exposure (3–5). The human stratum corneum includes the horny pads of palms and soles (callus) and the membranous stratum corneum covering the remainder of the body (6). The traditional method of preparation is via physical–chemical and enzymological processes to separate the membranous layers of the stratum corneum from whole skin (Juhlin and Shelly 1977; Knufson et al. 1985). However, it is time consuming and, in some cases, difficult to control the size and thickness of a sheet of stratum corneum. Moreover, it is often difficult to locate a suitable skin source.

Powdered human stratum corneum (PHSC) prepared from callus (sole) is thus substituted for the intact membranous stratum corneum. Podiatrists routinely remove and discard PHSC from the human foot, so it is easily obtained. The callus can be cut easily and quickly into smaller pieces and ground with dry ice to form a powder. In our laboratory, PHSC particle sizes between 180 and 300 μm were selected

with the aid of a suitable sieve. Because a corneocyte is only about 0.5-μm thick and about 30 to 40-μm long, the selected PHSC contains both intact corneocytes and intercellular medium structures, and thus retains its original physical–biochemical properties. Moreover, the greater surface area of the PHSC enhances solute penetration. In a typical experimental procedure, a test chemical in a transport vehicle—water—is mixed with the PHSC, and the mixture is incubated. After a predetermined time period, a solution is separated from the PHSC by centrifugation, and samples are measured (7).

This chapter reviews PHSC as an in vitro model for studying chemical interaction with human skin, with reference to studies conducted in our laboratory over the last decades. The results demonstrate that PHSC (callus) offers an experimentally easy in vitro model for the determination of chemical partitioning into the SC and may be useful in many skin research areas.

II. PHSC AND PHYSICAL–CHEMICAL PROPERTIES OF STRATUM CORNEUM

The callus is derived from human stratum corneum (sc) and thus should retain some of its physical and chemical characteristics (8). Stratum corneum lipid plays an important role in the determination of skin functions. However, the average lipid content of the SC varies regionally, from 2.0, 4.3, 6.5 to 7.2 wt.% of dry stratum corneum from plantar, leg, abdomen, and face, respectively (9). Table 1 shows that the average lipid content of the dry PHSC samples derived from various regions were 2.29 and 0.25 wt.% after extraction. This result is consistent with that in human plantar as determined by Lampe et al. (9).

The water content of the SC is of importance in maintaining stratum corneum flexibility. Three possible mechanisms of water absorption and/or retention capacity of the SC have been suggested: (i) Imokawa et al. (10) suggested that stratum corneum lipids play a critical role because their removal by the application of acetone/ether decreased absorption/retention capacity. (ii) Friberg et al. (11), however, considered

Table 1 Lipid Content and Water Uptake of Powdered Human Stratum Corneum (PHSC)

Stratum corneum source	Lipid content (% w/w dry PHSC)	Water uptake (μg/mg dry PHSC)			
		Untreated PHSC	Delipidized PHSC		
			Lipid[a]	Protein[b]	Total
1	2.38	495.85	26.44	452.40	478.84
2	2.21	452.49	39.26	364.96	404.22
3	2.39	585.62	23.09	498.40	521.49
4	2.69	554.27	40.05	492.31	532.36
5	2.08	490.04	49.86	363.30	413.16
6	2.01	381.61	14.82	324.18	339.00
Mean	2.29	493.31	32.26	415.92	448.18
SD	0.25	72.66	12.97	74.50	75.47

[a]Lipid part extracted from the PHSC.
[b]Remaining part of the PHSC after lipid extraction.

that protein might also play an important role in stratum corneum water retention. They found that the additional water absorbed after re-aggregation of equilibrated lipids and proteins was equally partitioned between the protein and the natural lipid fraction of the human stratum corneum. (iii) Middleton (12) considered that water-soluble substances were responsible for water retention and for most of the extensibility of the corneum. He found that powdered stratum corneum—but not the intact corneum extracted by water—exhibited lower water retention capacity. He suggested that the powdering procedure ruptures the walls of the corneum cells and allows water to extract the water-soluble substances without a prior solvent extraction. We measured the water retention capacities of untreated PHSC, delipidized PHSC (as the protein fraction), and the lipid content by measuring the amount of [3H]-water (microgram equivalent) per milligram PHSC after equilibration. As shown in Table 1, no statistical differences ($p > 0.05$) were observed for untreated PHSC, delipidized PHSC, and the combination of delipidized PHSC and the lipid content. The PHSC can absorb up to 49% by weight of dry untreated PHSC (Table 1), which is consistent with literature reports. Middleton (12) found that the amount of water bound to intact, small pieces and powdered guinea-pig footpad stratum corneum was 40%, 40%, and 43% of dry corneum weight. Leveque and Rasseneur (13) demonstrated that the human stratum corneum was able to absorb water up to 50% of its dry weight. Our results (Table 1) suggest that the protein domain of the PHSC plays an important role in the absorption of water. Depletion of the PHSC lipid content did not affect water retention (14).

III. PHSC AND CHEMICAL PARTITIONING

Table 2 shows the effect of varying initial chemical concentrations on the partition coefficient (PC) PHSC/w of these compounds (14). Under fixed experimental conditions—two hour incubation time and 350°C incubation temperature—the concentration required to attain a peak value of the partition coefficient varied from chemical to chemical. After reaching the maximum, increases in the chemical concentration in the vehicle did not increase the PC value; rather, it slightly decreased or was maintained at approximately the same level. This is consistent with the results of Surber et al. (3,4) on whole stratum corneum. Chemical partitioning from the vehicle into the SC involves processes in which molecular binding occurs at certain sites of the SC, as well as simple partitioning. Equilibration of partitioning is largely dependent on the saturation of the chemical binding sites of the SC (3,15). The results also indicate that, under a given experimental conditions, the maximum degree of partitioning was compound specific. As the SC contains protein, lipids, and various lower molecular weight substances with widely differing properties, the many available binding sites display different selective affinities with each chemical. Thus, the degree of maximum binding or of equilibration varies naturally with molecular structure (15). This result demonstrated that the solubility limit of a compound in the SC was important in determining the degree of partitioning, as suggested by Potts and Guy (1993). On the basis of the solubility limit of a chemical, the absorption process of water soluble or lipid soluble substances was controlled by the protein domain or the lipid domain, respectively, or a combination of two (16). Since the lipophilicity of the lipid domain in the SC is much higher than that of water, a lipophilic compound would partition into the SC in preference to water. Thus, when water is employed as the vehicle, the PC PHSC/w increases with increasing lipophilicity of solute (17). Conversely, the protein domain

Table 2 Effect of Initial Aqueous Phase Chemical Concentration on Powdered Human Callus/Water Partition Coefficient

Chemical[a] (log $PC_{o/w}$)	Concentration (%, w/v)	Partition (mean)	Coefficient[b] (SD)
Dopamine (−3.40)	0.23	5.42	0.22
	0.46	6.04	0.28
	0.92	5.74	0.28
Glycine (−3.20)	0.05	0.36	0.01
	0.10	0.40	0.02
Urea (−2.11)	0.03	0.26	0.02
	0.06	0.15	0.02
	0.12	0.17	0.02
Glyphosate (−1.70)	0.02	0.79	0.04
	0.04	0.68	0.04
	0.08	0.70	0.01
Theophylline (−0.76)	0.18	0.37	0.02
	0.36	0.43	0.03
	0.54	0.42	0.02
Aminopyrine (0.84)	0.07	0.44	0.09
	0.14	0.46	0.03
Hydrocortisone (1.61)	0.09	0.37	0.01
	0.18	0.34	0.01
	0.36	0.29	0.02
Malathion (2.36)	0.47	0.50	0.09
	0.94	0.40	0.03
	1.88	0.53	0.04
Atrazine (2.75)	0.09	0.53	0.06
	0.14	0.59	0.07
	0.19	0.58	0.03
2,4-D (2.81)	0.27	7.52	0.81
	0.54	7.53	1.01
	0.82	8.39	1.67
Alachlor (3.52)	0.32	1.11	0.05
	0.64	1.08	0.04
	1.28	1.96	0.15
PCB (6.40)	0.04	1237.61	145.52
	0.08	1325.44	167.03
	0.16	1442.72	181.40

[a]PC PHSC/water represents the mean of each test ($n = 5$)$\pm$SD (14).
[b]Log PC (o/w) was cited in Hansch and Leo (1979).
Abbreviations: 2,4-D, 2,4-dichloro-phenoxyacetic adid; PC, partition coefficient; PCB, polychlorinated biphenyls; PHSC, powdered human stratum corneum

of the SC is significantly more polar than octanol and governs the absorption of hydrophilic chemicals (16). For very lipophilic compounds, low solubility in water rather than increased solubility in the SC can be an important factor (17). Moreover, in addition to partitioning into these two domains, some amount of chemicals may be taken into the SC as the result of water hydration. This is the "sponge domain," named by Raykar et al. (16). They assume that this water, having the properties of bulk water, carries an amount of solute into the SC equal to the amount of solute in the same volume of bathing solution. Therefore, for hydrophilic compounds and

Table 3 In Vivo Percutaneous Absorption of *p*-Nitroaniline in the Rhesus Monkey Following 30-minutes Exposure to Surface Water: Comparisons to In Vitro Binding and Absorption

Phenomenon	Percent dose absorbed/bound[a]
In vivo percutaneous absorption, rhesus monkey	4.1 ± 2.3
In vitro percutaneous absorption, human skin	5.2 ± 1.6
In vitro binding, powdered human stratum corneum	2.5 ± 1.1

[a]Each number represents the mean $\pm$ SD of four samples.

some lower lipophilic compounds, the partitioning process may include both the protein domain and sponge domain.

IV. PHSC AND PERCUTANEOUS ABSORPTION

To evaluate sensitivity of this in the in vitro PHSC model, we examined chemical partitioning into the PHSC as well as that in vitro percutaneous absorption in human skin, and in vivo percutaneous absorption in the rhesus monkey. Table 3 shows that the in vivo percutaneous absorption of nitroaniline from surface water following 30-minute exposure was 4.1% and 2.3% of the applied dose. This is comparable with the 5.2% and 1.6% for in vitro absorption with human cadaver skin and the 2.5% and 1.1% bound to PHSC. Wester et al. (8) suggest that this methodology—the systems tested, binding to PHSC, and in vitro and in vivo absorption—can be used to predict the burden on the human body imposed by bathing or swimming.

V. PHSC AND THE SKIN BARRIER FUNCTION

The barrier function of the stratum corneum is attributed to its multilayered wall-like structure, in which terminally differentiated keratin-rich epidermal cells (corneocytes) are embedded in an intercellular lipid-rich matrix. Any physical factor or chemical reagent that interacts with this two-compartment structure can affect the skin barrier function. Barry (6) described how certain compounds and mechanical trauma can easily dissociate callus cells and readily dissolve their membranes. Thus

Table 4 Protein Releasing from PHSC Following Chemical/Water Exposure

	Protein content (mg/4 mL)[a]		
Test chemicals	10 min	40 min	24 hr
Glycolic acid	0.093 (0.026)	0.175 (0.029)	0.173 (0.041)
Sodium hydroxide	0.419 (0.054)	0.739 (0.301)	5.148 (1.692)
Water	0.002 (0.014)	0.135 (0.043)	0.077 (0.021)

[a]Each number represents the mean (SD) of six samples.

the amount of protein (keratin) released from the stratum corneum after chemical exposure may be a measure of the solvent potential of the chemical. To evaluate this hypothesis, a test chemical in water is mixed with PHSC and incubated. After a predetermined time period, a solution is separated from the PHSC by centrifugation. The protein (keratin) content of the solution is then measured. Table 4 shows the amount of protein released from the PHSC after incubation with glycolic acid, sodium hydroxide, or water alone at different time points. Sodium hydroxide has a pronounced ability to release protein from PHSC. This ability increases with increasing incubation time. The results suggest that the PHSC model constitutes a vehicle to probe the barrier nature of the stratum corneum and the chemical interactions with the PHSC.

VI. PHSC AND DISEASED SKIN

The PHSC has potential application in medical treatment. For instance, a set of vehicles can be screened to determine which vehicle most readily releases a given drug into the stratum corneum. This information would assist in the determination of the most effective approaches to drug delivery via the skin. Furthermore, diseases involving the stratum corneum can be studied using PHSC. An example is Table 5, which is the partitioning of hydrocortisone from normal and psoriatic PHSC. In this case, we have shown that there is no difference in partitioning between normal and psoriatic PHSC. It should be noted that there is no difference between in vivo percutaneous absorption of hydrocortisone in normal volunteers and that in psoriatic patients (18).

VII. PHSC AND ENVIRONMENTALLY HAZARDOUS CHEMICALS

The leaching of environmentally hazardous chemicals from soil and their absorption by the skin of a human body is a major concern. Knowledge of the extent and degree of such absorption will aid in determining the potential health hazards of polluted soil. Our laboratory's interest is in the potential percutaneous absorption of contaminants from soil. Soil can be readily mixed with PHSC, but centrifugation does not separate the two. However, centrifugation readily separates PHSC from any liquid, to varying degrees. Thus, the partition coefficients of various liquids may

Table 5 Aqueous Partition Coefficient of Hydrocortisone with Normal and Psoriatic Stratum Corneum

	Partition coefficient[a]	
Stratum corneum type	Mean	SE
Normal sheet (abdominal)	1.04	0.88
Normal powdered (plantar)	1.70	0.47
Psoriatic	1.94	0.42

[a]No statistical significance ($p > 0.05$).

Table 6 Partition Coefficients of Four Environmental Hazardous Chemicals in PHSC/Water and Soil/Water

	Partition coefficient	
Test chemicals	PHSC	Soil
Arsenic	1.1×10^4	2.4×10^4
Cadmium chloride	3.6×10^1	1.0×10^5
Arodor 1242	2.6	1.7
Arodor 1254	2.9	2.0

Abbreviation: PHSC, Powdered human stratum corneum.

be determined relative to a common third liquid. These relative partitions can then be compared to those of other compounds and to skin absorption values (19–21) to evaluate the degree of hazard. We have determined such coefficients for several environmentally hazardous chemicals partitioning from soil into PHSC (Table 6).

VIII. PHSC AND CHEMICAL DECONTAMINATION

Our laboratory uses the PHSC model to determine which chemicals might be able to remove (decontaminate) hazardous chemicals from human skin. A contaminant chemical is mixed with PHSC, and the decontaminant effects of a series of possible decontaminants are measured. The liquid decontaminant is mixed with contaminated PHSC and, after a predetermined time period, a solution is separated from the PHSC by centrifugation. The content of the solution is a measure of decontaminant's potential. This is shown in Table 7, which demonstrates that alachlor readily contaminates PHSC. Water alone removes only a small portion of the alachlor. However, a 10% soap solution removes a larger portion of the alachlor, and a 50% soap solution removes most of it. Perhaps this is an elegant way to show that soapy water is effective in washing one's hands. However, it does illustrate the use of PHSC to determine the effectiveness of skin decontamination (Scheuplein and Blank 1973).

Table 7 Decontaminants Selection to Remove Environmental Hazardous Chemical (Alachlor) from Human Skin[a]

	[^{14}C]-alachlor (%)
PHSC	90.3 ± 1.2
Alachlor in Lasso supernatant	5.1 ± 1.2
Water-only wash of PHSC	4.6 ± 1.3
10% Soap-and-water wash	77.2 ± 5.7
50% Soap-and-water wash	90.0 ± 0.5

[a][^{14}C]-alachlor in Lasso EC formulation (1:20 dilution) mixed with powdered human stratum corneum, allowed to set for 30 minutes, then centrifuged. Stratum corneum wash with (1) water only, (2) 10% soap water, and (3) 50% soap and water.

Abbreviations: PHSC, powdered human stratum corneum.

Table 8 Effect of Two Polymers (L and H) on the Estradiol PC Between PHSC and Water

Test formulation and polymer concentration (%)	Log PC PHSC/water (mean ± SD, $n = 5$) estradiol concentration (μg/mL)		
	2.8	0.028	0.028
Polymer H (hydrophilic polymer)			
10	2.31 ± 0.22^a	2.36 ± 0.14^a	2.13 ± 0.07^a
5	1.93 ± 0.10^b	2.06 ± 0.21^b	1.94 ± 0.06^b
1	1.71 ± 0.10	1.61 ± 0.19	1.59 ± 0.26
Polymer L (lipophilic polymer)			
10	1.74 ± 0.10	1.65 ± 0.07	1.61 ± 0.14
5	1.70 ± 0.20	1.62 ± 0.17	1.65 ± 0.09
1	1.59 ± 0.19	1.57 ± 0.15	1.71 ± 0.07
Control (no polymer)	1.62 ± 0.14	1.68 ± 0.11	1.71 ± 0.13

[a]Statistically significantly different from control ($p < 0.01$).
[b]Statistically significantly different from control ($p < 0.05$).
Abbreviations: PC, partition coefficeint; PHSC, powdered human stratum corneum

IX. PHSC AND ENHANCED TOPICAL FORMULATION

Macromolecules have attracted interest as potential drug entities and as modulators to percutaneous delivery systems. Two macromolecular polymers [molecular weight (MW) 2081 and 2565] were developed to hold cosmetics and drugs to the skin surface by altering the initial chemical and skin partitioning. The effect of these polymers on the PC of estradiol with PHSC and water was determined in our laboratory. As shown in Table 8, the polymer L had no effect on the estradiol PC between PHSC and water. The polymer H, however, showed a significant increase ($p < 0.01$) in log PC for estradiol concentrations of 2.8 and 0.25 mg/mL. This increase was dependent upon the polymer concentration (22). The results suggest that the PHSC model can help in the development and selection of enhanced transdermal delivery systems.

X. PHSC AND QSAR PREDICTIVE MODELING

Many experiments have been conducted to predict chemical partitioning into the stratum corneum in vitro. However, most were based on quantitative structure-activity relationships (QSARs) or related chemicals to determine the partitioning process, and few studies focus on structurally unrelated chemicals (13). Since the range of molecular structure and physicochemical properties is very broad, any predictive model must address a broad scope of partitioning behavior.

This study assesses the relationship of a number of chemicals with a broad scope of physicochemical properties in the partitioning mechanism between PHSC and water. Uniqueness and experimental accuracy are added by using PHSC. The experimental approach is designed to determine how the PC PHSC/w is affected by (i) chemical concentration, (ii) incubation time, and (iii) chemical lipophilicity

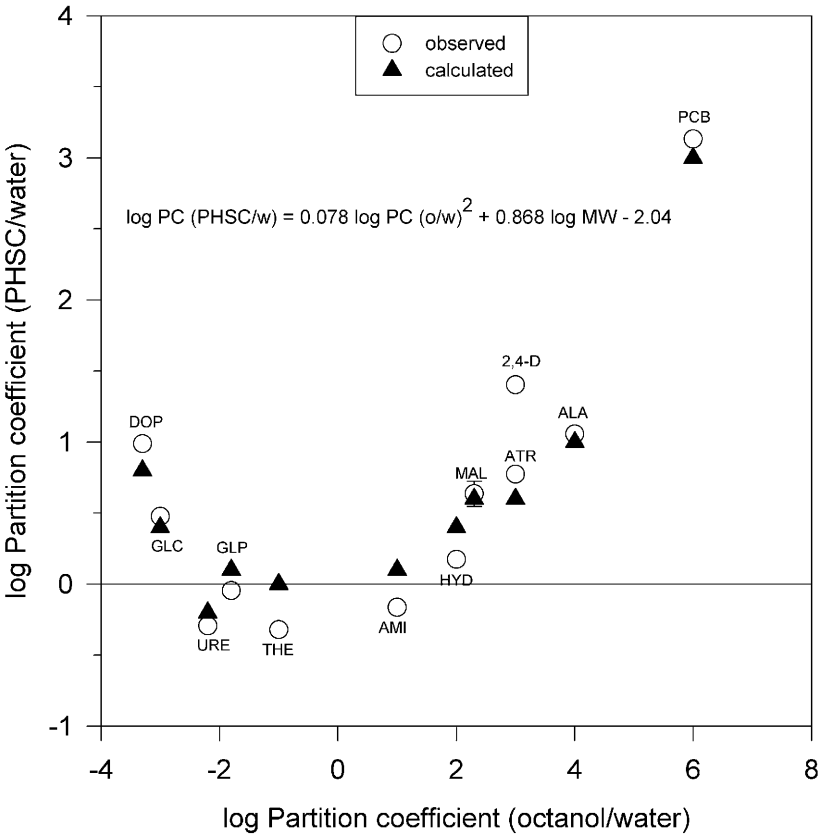


Figure 1 Correlation of the logarithm of stratum corneum/water partition coefficients (log PC sc/w) and logarithm of octanol/water partition coefficients of the 12 test chemicals. Open symbols express observed values and each represents the mean of a test chemical ± SD ($n = 5$). Closed symbols express calculated values by Equation (3). *Abbreviations:* DOP, dopamin; GLC, glycine; URE, urea; GLP, glyphosate; THE, theophylline; AMI, aminopyrine; HYD, hydrocortisone; MAL, malathion; ATR, atrazine; 2,4-D, 2,4-dichlorophenoxyacetic acid; ALA, alachlor; PCB, polychlorinated biphenyls.

(or hydrophilicity) and other factors. These parameters are used to develop an in vitro model that will aid in the prediction of chemical dermal exposure to hazardous chemicals.

Figure 1 describes a smooth, partially curvilinear relationship between the log PC PHSC/w and the log PC o/w of a number of chemicals. The lipophilicities and hydrophilicities of compounds were defined as log PC o/w larger or smaller than zero, respectively. For lipophilic chemicals, such as aminopyrine, hydrocortisone, malathion, atrazine, (2,4-dichloro phenoxyacetic acid), alachlor, and polychlorinated biphenyls (PCB), the logarithms of PHSC/water partition coefficients are proportional to the logarithms of the octanol/water partition coefficients:

$$\begin{aligned} &\log \text{PC PHSC/w} = 0.59\ \log \text{PC o/w} - 0.72 \\ &\text{Student-t values } 9.93 \\ &n = 7;\ r^2 = 0.95;\ S = 0.26;\ F = 98.61 \end{aligned} \tag{1}$$

For hydrophilic chemicals, such as theophylline, glyphosate, urea, glycine, and dopamine, the log PC PHSC/w values are approximately and inversely proportional to log PC o/w:

$$\log \text{PC PHSC/w} = -0.60 \log \text{PC o/w} - 0.27$$

$$\text{Student-t values: } -4.86 \tag{2}$$

$$n = 5;\ r^2 = 0.88;\ S = 0.26;\ F = 23.61$$

However, the overall relationship of the PC PHSC/w of these chemicals and their PC o/w is nonlinear. This nonlinear relationship is adequately described by the following equation:

$$\log \text{PC PHSC/w} = 0.078 \log \text{PC o/w}^2 + 0.868 \log \text{MW} - 2.04$$

$$\text{Student-t values: } -8.29 \qquad 2.04 \tag{3}$$

$$n = 12;\ r^2 = 0.90;\ S = 0.33;\ F = 42.59$$

The logarithm of MW gave a stronger correlation in this regression than MW ($t = 1.55$) itself. In Figure 4, the calculated log PC PHSC/w (Y estimate) values are compared to the corresponding observed values for these chemicals. As shown, the calculated values are acceptably close to the observed values. The correspondence with minimal scatter suggests that this equation would be useful in predicting in vitro partitioning in the PHSC for important environmental chemicals (14).

XI. DISCUSSION

A new in vitro model employing PHSC (callus) to investigate the interaction between chemicals and human skin has been developed in our laboratory. The PHSC (callus) offers an experimentally easy in vitro model for the determination of chemical partitioning from water into the SC. Due to the heterogeneous nature of the SC, the number and affinity of the SC binding sites may vary from chemical to chemical, depending upon molecular structure. For most lipophilic compounds, the PC PHSC/w was governed by the lipid domain, whereas PCs of the more hydrophilic compounds are determined by the protein domain and, possibly, by the sponge domain (16). These relationships can be expressed by the log PC PHSC/w of these chemicals as a function of the corresponding square of log PC o/w and log MW, Equation (3), which is useful in predicting various chemical partitionings into the SC in vitro. However, a disadvantage in using the human callus is that it may display some differences in water and chemical permeation when compared with membranous stratum corneum (6).

This chapter has summarized a variety of potential applications for PHSC, ranging from basic science to applications in medicine and environmental impact studies. The PHSC, imagination, and a balanced study design can add to scientific knowledge.

REFERENCES

1. Blank JH. Cutaneous barriers. J Invest Dermatol 1965; 45:249–256.
2. Zatz JL. Scratching the surface: rationale approaches to skin permeation. In: Zatz JL, ed. Skin Permeation Fundamentals and Application. Wheaten: Allured Publishing Co., 1993:11–32.
3. Surber C, Wilhelm KP, Hori M, Maibach HI, Guy RH. Optimization of topical therapy: partitioning of drugs into stratum corneum. Pharm Res 1990; 7(12):1320–1324.
4. Surber C, Wilhelm KP, Maibach HI, Hall L, Guy RH. Partitioning of chemicals into human stratum corneum: implications for risk assessment following dermal exposure. Fundam Appl Toxicol 1990; 15:99–107.
5. Potts RO, Guy RH. Predicting skin permeability. Pharm Res 1992; 9(5):663–669.
6. Barry BW. Structure, function, diseases, and topical treatment of human skin. In: Barry BW, ed. Dermatological Formulations: Percutaneous Absorption. NY: Marcel Dekker Inc., 1983:1–48.
7. Hui X, Wester RC, Maibach HI, Magee PS. Chemical partitioning into powdered human stratum corneum (callus). In: Maibach HI, ed. Toxicology of Skin. Philadelphia, PA: Taylor & Francis, 2000:159–178.
8. Wester RC, Mobayen M, Maibach HI. *In vivo* and *in vitro* absorption and binding to powdered stratum corneum as methods to evaluate skin absorption of environmental chemical contaminants from ground and surface water. J Toxicol Environ Health 1987; 21:367–374.
9. Lampe MA, Burlingame AL, Whitney J, Williams ML, Brown BE, Roitmen E, Elias PM. Human stratum corneum lipids: characterization and regional variations. J Lipid Res 1983; 24:120–130.
10. Imokawa G, Akasaki S, Hattori M, Yoshizuka N. Selective recovery of deranged water-holding properties by stratum corneum lipids. J Invest Dermatol 1986; 87(6):758–761.
11. Friberg SE, Kayali I, Suhery T, Rhein LD, Simion FA. Water uptake into stratum corneum: partition between lipids and proteins. J Dispersion Sci Technol 1992; 13(3): 337–347.
12. Middleton JD. The mechanism of water binding in stratum corneum. Br J Dermatol 1968; 80:437–450.
13. Leveque JL, Rasseneur L. Mechanical properties of stratum corneum: influence of water and lipids. In: Marks RM, Barton SP, Edwards C, eds. The Physical Nature of the Skin. Norwell, MA, USA: MTP Press Limited, 1988 Chapter 17.
14. Hui X, Wester RC, Maibach HI, Magee PS. Chemical partitioning into powdered human stratum corneum: a mechanism study. Pharm Res 1993; 10:S–413.
15. Rieger M. Factors affecting sorption of topically applied substances. In: Zatz JL, ed. Skin Permeation Fundamentals and Application. Wheten: Allured Publishing Co., 1993:33–72.
16. Raykar PV, Fung MC, Anderson BD. The role of protein and lipid domains in the uptake of solutes of human stratum corneum. Pharm Res 1998; 5(3):140–150.
17. Scheuplein RJ, Bronaugh RL. Percutaneous absorption. In: Goldsmith LA, ed. Biochemistry and Physiology of the Skin. Vol. 1. Oxford: Oxford University Press, 1983: 1255–1294.
18. Wester RC, Maibach HI. Dermatopharmacokinetics in clinical dermatology. Semin Dermatol 1983; 2(2):81–84.
19. Wester RC, Maibach HI, Sedik L, Melendres J, Di Zio S, Wade M. *In vitro* percutaneous absorption of cadmium from water and soil into human skin. Fundam Appl Toxicol 1992; 19:1–5.
20. Wester RC, Maibach HI, Sedik L, Melendres J, S, Wade M. *In vitro* percutaneous absorption and skin decontamination of arsenic from water and soil. Appl Toxicol 1993a; 20:336.

21. Wester RC, Maibach HI, Sedik L, Melendres J. Percutaneous absorption of PCBs from soil: *in vivo* rhesus monkey, *in vitro* human skin, and binding to powdered human stratum corneum. J Toxicol Environ Health 1993b; 39:375–382.
22. Wester RC, Hui X, Hewitt PG, Hostynet J, Krauser S, Chan T, Maibach HI. Polymers effect on estradiol coefficient between powdered human stratum corneum and water. J Pharm Sci 2002; in press.

22

Percutaneous Absorption of Hazardous Chemicals from Fabric into and Through Human Skin

Ronald C. Wester, Danyi Quan, and Howard I. Maibach
Department of Dermatology, School of Medicine, University of California, San Francisco, California, U.S.A.

Rebecca M. Wester
Methodist Health System, Dallas, Texas, U.S.A.

I. INTRODUCTION

The treated surface that is in most contact with skin is fabric. Consider clothes worn day and night, sheets and blankets, and fabric in rugs and upholstery. The fabric environment may have been assumed safe in the following exposure problems. Brown (1) and Armstrong et al. (2) reported separate cases of phenolic disinfectants in hospital laundry causing death of infants and sickening in others. Toxic compounds in clothing such as diapers were spread over a large surface area on a skin site with potential absorption. Both parameters (large surface area and application to the urorectal area) enhance absorption (3). If the diaper was covered with rubber pants or more clothing, this could enhance absorption. Dermatitis is reported for chemical finish in textiles (possible pesticides in raw cotton, chemicals in the manufacturing process, chemicals added for correct color and sheen). These must involve chemical transfer from fabric to skin. The clothing of field workers is filled with pesticides from spraying, the work of Snodgrass (4) suggesting that it may not launder out, but remain bioavailable. The pesticide "bomb" in the house settles on rugs, fabric chairs, etc., and the baby crawls over it. Finally, it should be noted that insecticide sprayed into the uniforms of Desert Storm personnel might have transferred from the fabric into and through the soldiers' skin. Both soldiers and civilians have the added threat of sprayed chemical warfare agents, which will settle on uniforms or clothing then diffuse to the skin and eventually into the body.

II. GLYPHOSATE (WATER-SOLUBLE HERBICIDE)

Tables 1 and 2 show the absorption profiles of 1% glyphosate through human skin and of glyphosate across cotton sheets into human skin. The zero-day treatment

Table 1 Percutaneous Absorption Parameters of Glyphosate Across Cotton Sheets into Human Skin Under Different Donor Conditions

Donor conditions	Treatment[a]	Flux (J) (μg/hr)	Permeability constant (P) (cm/hr)	Lag time (t) (hr)
1% glyphosate solution	None	4.12 ± 1.35	$4.59 \pm 1.56 \times 10^{-4}$	10.48 ± 1.23
Cotton–1% glyphosate solution	0 days	0.47 ± 0.08	$4.90 \pm 1.41 \times 10^{-5}$	5.00 ± 0.87
Cotton–1% glyphosate solution	1 day	0.05 ± 0.01	$5.21 \pm 0.69 \times 10^{-6}$	2.52 ± 0.53
Cotton–1% glyphosate solution	2 days	0.05 ± 0.01	$5.21 \pm 0.74 \times 10^{-6}$	1.31 ± 0.68
Cotton–1% glyphosate solution	Add water	0.23 ± 0.07	$2.40 \pm 0.54 \times 10^{-5}$	3.11 ± 1.02

Note: "Add water" means that the donor side included the treated cotton sheet and a certain amount of distilled water. Mean ± SEM ($n = 6$).
[a]A certain amount of 1% glyphosate aqueous solution was applied to cotton sheets, and the sheets were dried at room temperature for zero to two days.

means that cotton sheets were treated with glyphosate and immediately added to donor side while wet; the one- and two-day treatment means that treated cotton sheets were dried for one or two days, and "add water" means that the donor side included the treated cotton sheet and 300 μL distilled water or aqueous ethanol. Clearly, when the glyphosate-treated cotton sheets were used as a donor side, the absorbed amount of glyphosate was less than that of glyphosate solution (control). Comparison of the three treatments showed that zero day treatment caused two times higher skin absorption than did one- or two-day treatments. Table 1 gives the in vitro absorption parameters of glyphosate. The absorption of glyphosate under zero-day treatment showed about 10 times less than the control sample and 100 times less than one- or two-day treatments; the absorption (cm/hr) of control sample or zero-, one-, and two-day treatments were 4.59×10^{-4}, 4.90×10^{-5}, 5.21×10^{-6}, and 5.21×10^{-6}, respectively. Adding water to treated cotton sheets in

Table 2 Comparison of Percutaneous Absorption Profiles of Glyphosate Across Cotton Sheets into Human Skin Under Different Donor Conditions

Donor conditions	Treatment[a]	Absorbed amount across skin (%)	Residual amount on the skin (%)	Residual amount in the skin (%)
1% glyphosate solution	None	1.42 ± 0.25	—	0.56 ± 0.13
Cotton–1% glyphosate solution	0 days	0.74 ± 0.26	6.71 ± 2.80	4.32 ± 1.95
Cotton–1% glyphosate solution	1 day	0.08 ± 0.02	0.69 ± 0.07	0.23 ± 0.13
Cotton–1% glyphosate solution	2 days	0.08 ± 0.01	0.42 ± 0.18	0.06 ± 0.01
Cotton–1% glyphosate solution	Add water	0.36 ± 0.07	—	0.23 ± 0.13

Note: "Add water" means that the donor side included the treated cotton sheet and a certain amount of distilled water. Mean ± SEM ($n = 6$).
[a]A certain amount of 1% glyphosate aqueous solution was applied to cotton sheets, and the sheets were dried at room temperature for zero to two days.

a donor side resulted in an increase in absorption compared with that of one- or two-day treatment. This result indicated that cotton sheets played a protective role. Decreases in lag time of glyphosate were observed (Table 1) with the change of the donor-side conditions.

The residual amount of glyphosate in the skin or on the skin (after the cotton sheet is removed) after a 24-hour application is shown in Table 2. Note that zero-day treatment showed the highest residual amounts in the skin as well as on the skin (6.71% and 4.32%, respectively). A possible reason is that when the cotton sheets were treated with glyphosate solution and immediately applied to the skin, the glyphosate was not yet bound to the cotton sheet and continued to separate onto the skin surface (5).

III. MALATHION (LIPID-SOLUBLE PESTICIDE)

The absorption profiles of malathion under different treatments are given in Tables 3 and 4. The two-day treatment caused the lowest percutaneous absorption due the cotton absorption of the compound. However, zero-day treatment and adding solution to treated cotton sheets caused higher absorption. All the in vitro absorption parameters are listed in Table 3. Note that there were no great differences in the skin absorption of malathion among the control, zero-day treatment and adding solution to cotton sheets treatment (0.20, 0.14, and 0.20 cm/hr, respectively). The skin absorption of malathion under one- and two-day treatment was approximately six times less than under zero-day treatment. It was found the lag time of malathion was shorter than glyphosate except for the "add solution" samples.

From Table 4, it can be seen that the residual amount of malathion in the skin increased with the following order (listed as the donor conditions): adding solution to treated cotton sheets (9.4%) no cotton (control, 7.63%) > 0-day treatment (4.43%) > 1-day treatment (2.68%) > 2-day treatment (0.85%). The residual amounts of malathion in the skin were higher than the corresponding amounts of glyphosate (5).

Table 3 Percutaneous Absorption Parameters of Malathion Across Cotton Sheets into Human Skin Under Different Donor Conditions

Donor conditions	Treatment[a]	Flux (J)(μg/hr)	Permeability constant (P)(cm/hr)	Lag time (t)(hr)
1% malathion solution	None	2.40 ± 0.34	$2.03 \pm 0.65 \times 10^{-1}$	5.10 ± 1.24
Cotton–1% malathion solution	0 days	1.60 ± 0.18	$1.36 \pm 0.68 \times 10^{-1}$	4.26 ± 1.10
Cotton–1% malathion solution	1 day	0.26 ± 0.04	$2.20 \pm 0.71 \times 10^{-2}$	1.08 ± 0.28
Cotton–1% malathion solution	2 days	0.27 ± 0.01	$2.29 \pm 1.04 \times 10^{-2}$	1.12 ± 0.31
Cotton–1% malathion solution	Add solution	2.34 ± 0.54	$1.98 \pm 0.82 \times 10^{-1}$	5.60 ± 1.04

Note: "Add solution" means that the donor side included the treated cotton sheet and a certain amount of aqueous ethanol. Mean ± SEM ($n = 6$).

[a]A certain amount of 1% malathion–aqueous ethanol was applied to cotton sheets, and the sheets were dried at room temperature for zero to two days.

Table 4 Comparison of Percutaneous Absorption Profiles of Malathion Across Cotton Sheets into Human Skin Under Different Donor Conditions

Donor conditions	Treatment[a]	Absorbed amount across skin (%)	Residual amount on the skin (%)	Residual amount in the skin (%)
1% malathion solution	None	8.77 ± 1.43	—	7.63 ± 1.42
Cotton–1% malathion solution	0 days	3.92 ± 0.49	4.71 ± 1.27	4.43 ± 1.59
Cotton–1% malathion solution	1 day	0.62 ± 0.11	1.67 ± 0.77	2.68 ± 0.19
Cotton–1% malathion solution	2 days	0.60 ± 0.14	0.99 ± 0.08	0.85 ± 0.34
Cotton–1% malathion solution	Add solution	7.34 ± 0.61	—	9.40 ± 2.8

Note: "Add solution" means that the donor side included the treated cotton sheet and a certain amount of aqueous ethanol. Mean $\pm$ SEM ($n = 6$).
[a]A certain amount of 1% malathion–aqueous ethanol was applied to cotton sheets, and the sheets were dried at room temperature for zero to two days.

IV. PARATHION (LIPID-SOLUBLE PESTICIDE)

Parathion was the chemical of choice to use as a surrogate for VX. Actual data with VX would be best; however, little exists in the literature. To obtain radiolabeled VX and study it in the public domain is highly improbable. Parathion is in the same chemical class as VX (organophosphorus) and has the same functional group as VX. The structures of parathion and VX and physicochemical data that relate to percutaneous absorption are similar. The partition coefficients (log P octanol/water), molecular weights, and molecular volumes are close. Similar structure, log P, and molecular weight/molar volume suggest the potential for similar percutaneous absorption.

Table 5 gives the in vitro percutaneous absorption of parathion through naked human skin and skin protected by dry uniform material and wetted uniform material. Following this single-exposure and 96-hour absorption period, $1.78 \pm 0.41\%$ dose was absorbed through naked human skin, and $0.29 \pm 0.17\%$ and $0.65 \pm 0.16\%$ doses were absorbed through skin protected by dry and moist uniform, respectively. The absorption was continuous though the total exposure period. Therefore, an infinite dose was available through the 96-hour dosing period.

Statistically, naked skin absorption was greater than that protected by dry uniform ($p = 0.000$) and moist uniform ($p = 0.000$). Absorption through moist

Table 5 Barrier Properties of Dry and Moist Military Uniform to Parathion In Vitro Human Skin Absorption

Treatments	Percent dose absorbed (mean $\pm$ SD)	Permeability coefficient (K_p, cm/hr)
Skin ($n = 4$)[a]	1.78 ± 0.41	1.89×10^{-4}
Skin + dry uniform ($n = 6$)[b]	0.29 ± 0.17	2.04×10^{-5}
Skin + wetted uniform ($n = 5$)[c]	0.65 ± 0.16	6.16×10^{-5}

[a]Versus[b] $p = 0.000$.
[b]Versus[c] $p = 0.007$.
[c]Versus[c] $p = 0.000$.

Table 6 VX Systemic Absorption and Toxicity to Uniformed Military Personnel

Exposure time	Body exposure	Calculated VX systemic dose[a]	
		Compromised[b] (mg)	Protected[c] (mg)
1 hr	Head/neck[d]	4.16	4.16
	Arms and hands[d]	0.52	0.52
	Trunk	4.07	1.35
	Genital-s	0.45	0.15
	Legs	0.68	0.22
	Total	**9.87***	**6.40**
8 hr	Head/neck[d]	33.26*	33.26*
	Arms and hands[d]	4.16	4.16
	Trunk	32.52*	10.77*
	Genital-s	3.61	1.2
	Legs	5.42	1.8
	Total	**78.98***	**51.18***
96 hr	Head/neck[d]	399.16*	399.16*
	Arms and hands[d]	49.90*	49.90*
	Trunk	390.29*	129.25*
	Genital-s	43.37*	14.36*
	Legs	65.05*	21.54*
	Total	**947.76***	**614.21***

*Estimated systemic LD50 of VX is 6.5 mg (human, 70 kg). Systemic concentration is more than 50% lethality dose.
[a]4 $\mu g/cm^2$ on whole body area (1.8 cm^2).
[b]Uniform with perspiration.
[c]Dry uniform.
[d]Head/neck and arms and hands are unprotected.

uniform was statistically ($p = 0.007$) greater than through dry uniform. Table 6 shows the total body surface area of a uniformed soldier. Head, neck, and arms (including hands) are unprotected naked skin. The other body areas are covered with uniform. Calculated VX systemic absorption and toxicity to uniformed personnel. This is a one-time 4 $\mu g/cm^2$ VX exposure and resulting systemic dose occurs by skin absorption only (no respiratory and oral involvement). At one-hour post-exposure 50% lethality occurs with full-body exposure to the compromised sweated uniform, although the dry uniform is right at the threshold. At eight-hour postexposure to head and neck only, or trunk only, might cause lethality with both wet and dry uniform. At 96-hour post-exposure lethality occurs with exposure to any body part (6).

V. ETHYLENE OXIDE (COLORLESS GAS AT ORDINARY ROOM TEMPERATURE AND PRESSURE)

Ethylene oxide is used as a fumigant for textiles and foodstuffs, and to sterilize surgical instruments and hospital gowns. It is a highly reactive alkylating agent that can react directly with cellular macromolecules, including DNA, RNA, and protein, without prior metabolic activation (7). Data have been collected on genotoxicity of ethylene oxide in somatic and germ cells (8). Major et al. (9) have reported genotoxicological changes in nurses occupationally exposed to low-dose ethylene oxide. Studies

to assess ethylene oxide risk use inhalation and IV routes of administration (10). As ethylene oxide exposure of humans can occur through exposure of fabric/skin in the workplace (5), a study was done to determine the percutaneous absorption of [^{14}C] ethylene oxide from fabric into and through human skin. This study also serves as a model for exposure of fabric/skin to any potentially hazardous gas, be it under circumstances of war (5), the workplace, or some terrorist act, as recently occurred in Japan.

Table 7 gives the in vitro percutaneous absorption of [^{14}C] ethylene oxide from fabric through human skin. In cells where the fabric/skin surface area was open to the air, 0.72% and 0.85% of the applied dose accumulated in the receptor fluid and 0.62% and 0.32% in the skin. This gives percutaneous absorption values of 1.34% (receptor fluid accumulation plus skin content) and 1.17% of the dose (average 1.3% of the dose). Less than 10% residual radioactivity was recovered in fabric and washings.

In cells where the fabric/skin was occluded with double latex material, 46.16% and 39.54% of the dose was recovered in receptor fluid and 3.25% and 3.12% was in the skin. This gives percutaneous absorption values of 49.41% and 42.66% (average 46.0%). Less than 5% residual radioactivity was recovered in fabric and washings. It is assumed that the remainder of the [^{14}C] ethylene oxide was lost to the surrounding air.

Figure 1 shows the accumulation of radioactivity in receptor fluid. Almost all of the skin-absorbed radioactivity was in the first zero to four–hour interval.

Some receptor fluid accumulations from a non-radioactive study were quickly frozen and shipped to NAmSA laboratories (Irvine, California, U.S.A.) for assay. At a dose of 600 ppm, no ethylene oxide, ethylene chlorohydrin, or ethylene glycol was detected. At 3892 ppm, ethylene oxide represented 4.5% to 8.3% of the dose in the receptor fluid; no ethylene chlorohydrin or ethylene glycol was detected. The potential loss of ethylene oxide during analysis is not known; however, ethylene oxide is able to be absorbed unchanged across human skin (11).

VI. 2-BUTOXYETHANOL (VAPOR)

Jones et al. (12) conducted a human in vivo study using 2-butoxyethanol to investigate the influence of temperature, humidity, and clothing on the dermal absorption

Table 7 In Vitro Percutaneous Absorption of [^{14}C] Ethylene Oxide from Fabric Through Human Skin

		Percentage of dose	
Surface	Item assayed	Skin source 1	Skin source 2
Open to air	Receptor fluid (RF)	0.72	0.85
	Fabric	7.65	5.65
	Skin wash	0.03	0.03
	Skin rinse	0.001	0.001
	Skin content	0.62	0.30
	Average absorbed (RF + skin)		1.3
Occluded	Receptor fluid (RF)	46.16	39.54
	Fabric	3.62	3.62
	Skin wash	0.07	0.05
	Skin rinse	0.01	0.02
	Skin content	3.25	3.12
	Average absorbed (RF + skin)		46.0

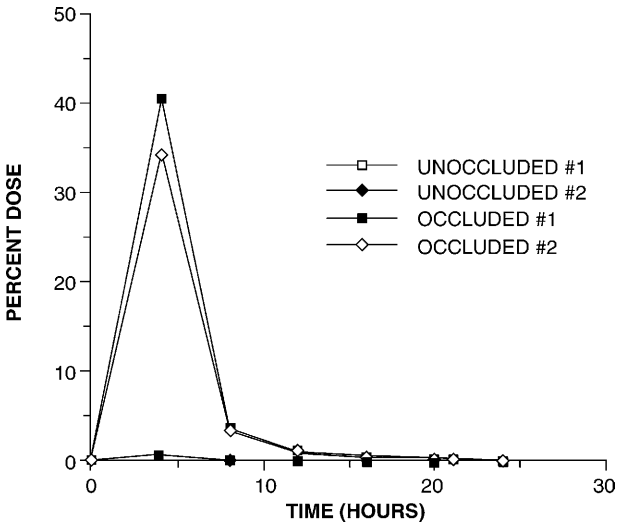


Figure 1 Ethylene oxide percutaneous absorption from fabric into human skin.

of vapors. The extent of dermal absorption was determined by biological monitoring to measure the resultant body burden of the chemical. The study showed that clothing had a minimal effect on the dermal contribution to total body burden with neither minimal clothing nor overalls having a significant effect on the amount absorbed through the skin. This could be because the rate of gas exchange through the clothing exceeds the absorption rate of 2-butoxyethanol through the skin.

Combining high temperature, high humidity, and the wearing of overalls had a significant impact on the percentage dermal absorption, resulting in a mean dermal contribution to total body burden of 39% (range 33–42%). This may be due to the overalls generating a micro-climate next to the skin where the environment is significantly hotter and more humid than the ambient environment.

The work showed that dermal absorption of vapors can be significant and that environmental conditions may affect the absorption. Some types of protective clothing may not be suitable to reduce absorption. The possibility of dermal absorption of vapors should be considered particularly for workers in high vapor concentration conditions where control of exposure relies on respiratory protection.

VII. DISCUSSION

Chemicals are introduced to fabric at many steps during manufacture and use. Cotton plants are treated with pesticides. Many chemical dyes and finishes are added to fabric during manufacture and these chemicals can cause human disease (13). The addition of chemicals (phenolic disinfectants) to fabric has caused human infant sickness and death (1,2). There are implications that the ''Gulf War Syndrome'' toxicity exhibited by soldiers may have been caused by interactions of insecticides and anti–nerve gas pills. The insecticides were impregnated into uniform fabric to ward off insects. This study and that of Snodgrass (4) show that chemicals in fabric will be absorbed from fabric into skin and then into the systemic circulation. Clothing and other fabric media (rugs and upholstery) must be considered repositories for

hazardous chemicals and these hazardous chemicals within fabric can be transferred to human skin. The threat of chemical warfare agents adds to the potential hazard of chemicals in clothing. Clothing seems to have minimal effect on vapors because the rate of gas exchange can exceed the rate of skin absorption.

REFERENCES

1. Brown BW. Fatal phenol poisoning from improperly laundered diapers. Am J Publ Health 1970; 60:901–902.
2. Armstrong RW, Eichner ER, Klein DE, Barthel WF, Bennett JV, Johnson V, Bruce H, Loveless LE. Pentachlorophenol poisoning in a nursery for newborn infants II. Epidemiologic and toxicologic studies. J Pediatr 1969; 75:317–325.
3. Wester RC, Maibach HI. Comparative percutaneous absorption. In: Maibach HI, Boisits E, eds. Neonatal Skin. New York: Marcel Dekker, 1982:137–147.
4. Snodgrass HL. Permethrin transfer from treated cloth to the skin surface: potential for exposure in humans. J Toxicol Environ Health 1992; 35:91–105.
5. Wester RC, Quan D, Maibach HI. In vitro percutaneous absorption of model compounds glyphosate and malathion from cotton fabric into and through human skin. Food Chem Toxicol 1996; 34:731–735.
6. Wester RM, Tanojo H, Maibach HI, Wester RC. Predicted chemical warfare agent VX toxicity to uniformed soldier using parathion in vitro human skin exposure and absorption. Toxicol Appl Pharmacol 2000; 168:149–152.
7. Brown CD, Wong BA, Fennell TR. In vitro and in vivo kinetics of ethylene oxide metabolism in rats and men. Toxicol Appl Pharmacol 1996; 136:8–19.
8. Preston RJ, Fennell TR, Leber AP, Sielken RL Jr, Swenberg RL. Reconsideration of the genetic risk assessment for ethylene oxide exposures. Environ Mol Mutagen 1995; 26:189–202.
9. Major J, Jakob MG, Tompa A. Genotoxicological investigation of hospital nurses occupationally exposed to ethylene oxide: 1. Chromosome aberrations, sister-chromatid exchanges, cell cycle kinetics, and UV-included DNA synthesis in peripheral blood lymphocytes. Environ Mol Mutagen 1996; 27:84–92.
10. Ehrenberg L, Törnquist M. The research background for risk assessment of ethylene oxide: aspects of dose. Mutat Res 1995; 330:41–54.
11. Wester RC, Hartway T, Serranza S, Maibach HI. Human Skin in vitro percutaneous absorption of gaseous ethylene oxide from fabric. Food Chem Toxicol 1997; 35:513–515.
12. Jones K, Cocker J, Dodd LJ, Fraser I. Factors affecting the extent of dermal absorption of solvent vapors: a human volunteer study. Ann Occup Hyg 2003; 47:145–150.
13. Hatch KL, Maibach HI. Textile chemical finish dermatitis. Contact Dermatitis 1986; 14:1–13.

23

Human Cadaver Skin Viability for In Vitro Percutaneous Absorption: Storage and Detrimental Effects of Heat-Separation and Freezing

Ronald C. Wester, Julie Christoffel, Tracy Hartway, Nicholas Poblete, and Howard I. Maibach
Department of Dermatology, School of Medicine, University of California, San Francisco, California, U.S.A.

James Forsell
Northern California Transplant Bank, San Rafael, California, U.S.A.

I. ABSTRACT

Purpose: For decades, human cadaver skin has been banked and utilized by hospitals for burn wounds and to study percutaneous absorption and transdermal delivery. Skin storage maintenance and confirmation of skin viability are important for both uses, especially for the absorption process where the in vivo situation is simulated.

Methods: Our system uses dermatomed human cadaver skin immediately placed in Eagles minimum essential media with Earles balanced salt solution (MEM–BSS) (In Vitro Scientific Products Corp., St Louis, Missouri, U.S.A.), and refrigerated after donor death, then transfered to the laboratory and placed in Eagles MEM–BSS with 50 μg/mL gentamicin at 4°C for storage.

Results: Skin viability, determined by anaerobic metabolism where glucose is converted to lactose, was highest ($P < 0.000$) during the first 18 hours of the first day after donor death, decreased some threefold by day two ($P < 0.000$), but then maintained steady-state viability through day eight. Viability then decreased by approximately one-half by day 13. Thus, using the above criteria, human skin will sustain viability for eight days following donor death in this system. Heat-treated (60°C water for one minute) and heat-separated epidermis and dermis lose viability.

Conclusion: Human skin viability can be maintained for absorption studies. It is recommended that this system be used, and that heat separation and skin freezing not be used, in absorption studies where skin viability and metabolism might be contributing factors to the study.

II. INTRODUCTION

Human cadaver skin is utilized in hospitals and research laboratories for various reasons. For nearly four decades, hospitals have banked skin for use as an effective temporary covering for burn wounds (1). Research laboratories also use cadaver skin to study the percutaneous absorption of drugs (2) and hazardous chemicals of environmental concern (3). Procedures such as heat treatment to separate epidermis from dermis are performed as part of the skin preparation for these studies. Human cadaver skin is not an easily obtained commodity, and storage for use becomes a necessity. Refrigerating and freezing skin are commonly done. With treatment and storage, skin viability has become a concern. This study determined human cadaver skin viability from point of death through time of storage, and the effect of heat and freezing treatment.

III. MATERIALS AND METHODS

Human cadaver skin was obtained from the Northern California Transplant Bank (San Rafael, California, U.S.A.). All donors were caucasian, aged 21 to 53 years, and both genders were represented. The time of a subject's death was recorded; skin was taken from the subject's thighs by use of a dermatome targeted to 500 micrometers. The skin was immediately placed in MEM-BSS and refrigerated at 4°C. The skin was then transported on ice to the laboratory and stored refrigerated at 4°C in Eagles MEM-BSS with 50 μg/mL gentamicin until used.

Dermatomed skin samples were mounted in an in vitro assembly consisting of flow-through design glass diffusion cells (Laboratory Glass Apparatus Inc., Berkeley, California, U.S.A.). Eagles MEM-BSS with gentamicin served as receptor fluid and flow rate was 1.5 mL/hr. The receptor fluid was at 37°C; skin surface temperature at 32°C. Eagles MEM contains glucose, and glucose metabolism to lactate in anaerobic energy metabolism was used as the measure of skin viability. Lactate production was determined using the Sigma Diagnostic Kit No. 826-UV (St. Louis, Missouri, U.S.A.) and a Hitachi spectrophotometer (San Jose, California, U.S.A.).

Dermatomed skin was used as stored in the refrigerator, frozen at −22 °C for storage, or heat separated (60°C water for one minute) into epidermis and dermis.

IV. RESULTS

Figure 1 shows lactate production from four human skin sources mounted in the diffusion system. Each data point represents four hour receptor fluid collection intervals over the 24-hour diffusion period. No chemical was dosed on the skin; just receptor fluid perfusing the skin. Lactate was produced by the skin sources over the full 24-hour period. The lactate curves rise in the early part of the period, where glucose is diffusing into the skin and lactate is diffusing out of the skin. Two skin sources reached steady-state at about 12 hours; lactate from the other two skin sources continued to rise until the process was stopped at 24 hours.

Table 1 and Figure 2 give the cumulative lactate produced (mmol/L) for the 24-hour perfusion period. Human skin was either dermatomed skin or heat-separated epidermis used within the time period of 0.75 to 13 days after donor death. The number of skin samples from the number of skin donors for each time period

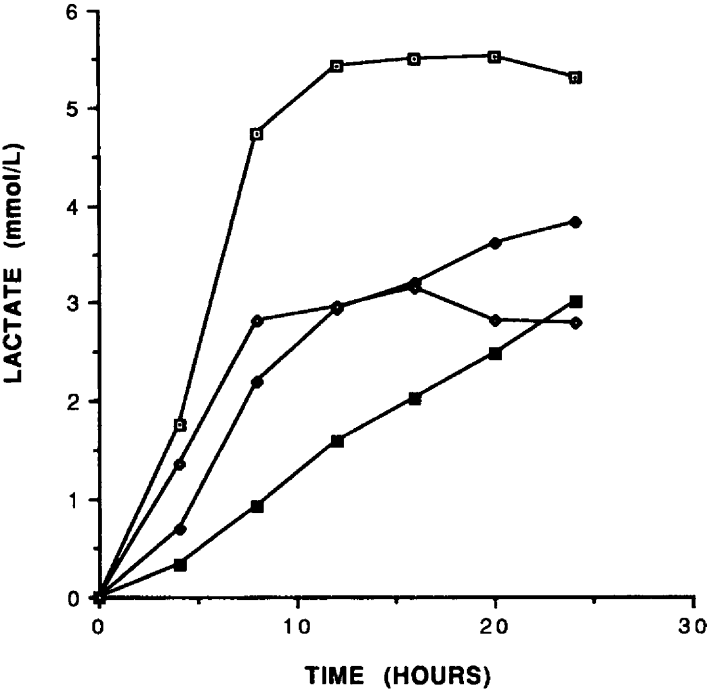


Figure 1 Lactate production from glucose (anaerobic energy metabolism) of four human skin sources perfused for 24 hour with Eagles minimum essential media (MEM)–Earle's balanced salt solution (BSS) with 50 μg/mL gentamicin. An initial time delay is noted where glucose absorbs into skin and lactose perfuses out of skin.

Table 1 In Vitro Human Skin Viability: Glucose Energy Metabolism to Lactate

	Dermatomed skin		Heat-separated epidermis	
Time after death (days)[a]	Lactate[b] (mmol/L/24 hr)	Number[c]	Lactate[b] (mmol/L/24 hr)	Number[c]
0.75	19.8 ± 8.9[d,e]	6/2	2.0 ± 1.1[e,f]	3/1
2	5.9 ± 4.1[d]	13/4	1.8 ± 0.8[f]	8/3
3	8.0 ± 4.8	8/3	0.6 ± 0.5	6/2
4	6.5 ± 1.7	9/3	0.7 ± 0.4	6/2
6	6.8 ± 3.0	11/3	0.2 ± 0.1	5/2
8	4.6 ± 2.3	6/2	0.2 ± 0.1	3/1
13	2.0 ± 0.6	3/1	0.9 ± 0.4	3/1

[a]Stored refrigerated in Eagles minimum essential media (MEM)–Earle's balanced salt solution (BSS) with 50 μm/mL gentamicin.
[b]Mean ± SD.
[c]Number of skin samples/number of human skin donors.
[d]$p < 0.000$.
[e]$p < 0.01$.
[f]$p < 0.007$.

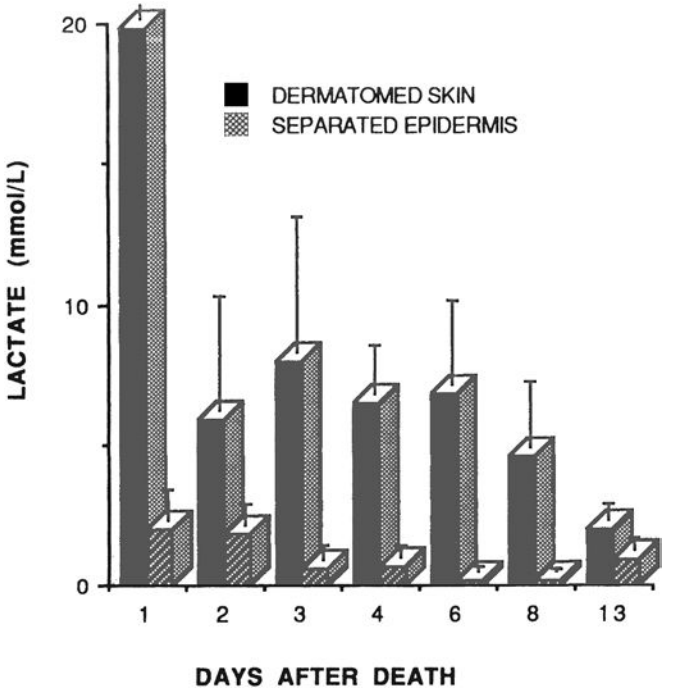


Figure 2 Viability of human skin stored refrigerated at 4°C in Eagles minimum essential media (MEM)–Earle's Earle's balanced salt solution (BSS) with 50 μg/mL gentamicin. Time indicated is that after donor's death.

are also listed. With dermatomed skin, refrigerated for only 0.75 day, the 24-hour cumulative lactate was a high of 19.8 ± 8.0 mmol/L. Lactate production decreased by day two ($p < 0.000$) and remained steady through day eight. Lactate production decreased further by approximately one half between day eight and day 13. Heat-separated epidermis lactate production was less than dermatomed skin ($p < 0.01$) at 2.0 ± 1.1 mmol/L. This level was maintained to the two-day period, then decreased ($p < 0.007$) at day three and remained less than 1 mmol/L through the 13-day test period.

Dermatomed skin was heat-treated at 60°C for one minute to simulate the heat-separation procedure to produce epidermis separated from dermis (but no

Table 2 Heat Effect on Human Skin Simulating Epidermis Heat-Separation Procedure

	Lactate (mmol/L) produced in 24 hr		
Source	Control dermatomed skin	Heat-treated skin[c]	Statistics
Number 1[a]	13.6 ± 1.5	1.5 ± 0.6	$p < 0.000$
Number 2[b]	7.4 ± 4.0	0.7 ± 0.14	$p < 0.04$

[a]Male, 21, thigh skin, used 69 hours after death ($n = 3$).
[b]Female, 30, thigh skin, used 39 hours after death ($n = 3$).
[c]Heated for 1 minute in 60°C water.

Table 3 Viability of Dermatomed Human Skin and Heat-Separated Epidermis and Dermis

	Lactate (mmol/L/24 hr) production		
Time (hr)	Dermatomed skin[a]	Epidermis[a]	Dermis[a]
29	9.7 ± 2.3[b]	1.5 ± 0.4[b]	0.9 ± 0.4[b]

Note: Note that epidermis plus dermis does not equal intact skin.
[a]Mean $\pm$ SD; male age 25, thigh skin. Epidermis and dermis separated after heat treatment for 1 minute in 60°C water.
[b]$p < 0.004$.

separation was performed) (Table 2). Lactate production decreased significantly ($p < 0.000$ and < 0.04) for both heat-treated skin samples. Therefore, heating to separate epidermis from dermis damages viability. In another study (Table 3) lactate production was determined in heat-separated epidermis and dermis. The cumulative lactate production was much less than intact dermatomed skin, again showing the detrimental effect of heat separation on skin viability.

Table 4 shows replicates from six dermatomed skin and heat-separated epidermis samples that were frozen at −22°C. The process of freezing was detrimental to skin viability of dermatomed skin ($p < 0.04$). Separated epidermis was not significantly different between refrigerated and frozen ($p > 0.05$) because the heat-separation process to get the epidermal layer had already been detrimental to skin viability.

V. DISCUSSION

It is logical that prolonged life and improved quality for stored skin is desirable for any transplant situation (4). During in vivo percutaneous absorption and transdermal delivery, the skin is viable and does metabolize glucose for energy, and metabolism does extend to other enzymes and other chemicals (5,6). Understanding and maintaining human cadaver skin viability places the skin use closer to the in vivo situation. This study shows that, in a sustaining media, skin can be energy viable for up to eight days. Harvesting the skin and use within a day of donor death gives

Table 4 Freezing Effect of Human Skin on Energy Metabolism

	Lactate production (mmol/L/24 hour)			
	Dermatomed skin		Heat-separated epidermis	
Skin sample	Refrigerated[a]	Frozen[a,b]	Refrigerated	Frozen[b]
1	12.2 ± 2.1	0.1 ± 0.1	1.0 ± 0.08	0.19 ± 0.13
2	2.4 ± 0.7	0.4 ± 0.3	1.5 ± 0.6	0.18 ± 0.13
3	7.4 ± 4.0	2.6 ± 0.4	–	–
4	9.7 ± 2.3	2.4 ± 0.5	1.5 ± 0.4	2.1 ± 0.2
5	9.5 ± 0.4	1.2 ± 0.04	0.2 ± 0.1	0.1 ± 0.05
6	27.5 ± 4.1	0.0	0.2 ± 0.1	0.0

[a]$p < 0.04$.
[b]Frozen 24 hours or longer.

the highest viability. Our system gets the skin quickly into sustaining media and refrigeration; it is not known if a delay from harvest to storage will affect viability. Common practices of freezing skin for storage, or heat treatment to separate epidermis from dermis, can destroy skin viability. The effect of enzymatically separating skin is not known. Bhatt et al. (7) also showed that heat treatment of hairless mouse skin for separation purposes eliminates viability.

Cadaver skin viability can be maintained and monitored. Glucose utilization can be measured by conversion of [^{14}C]glucose to $^{14}CO_2$ (8) or by lactate production (9) as shown here. The lactate production methodology does not require radioactivity use equipment.

ACKNOWLEDGMENTS

We thank the Northern California Transplant Bank who supplied the skin and made this study possible. Special acknowledgment to George Kositzin for the extra effort to obtain the skin samples.

REFERENCES

1. May SR, DeClement FA. Skin banking. Part III. Cadaveric allograft skin viability. J Burn Care Rehab 1981; 2:128–141.
2. Wester RC, Maibach HI. Percutaneous absorption of drugs. Clin Pharmacokinet 1992; 3:253–266.
3. Wester RC, Maibach HI, Sedik L, Melendres J, Wade M. Percutaneous absorption of PCBs from soil: in vivo rhesus monkey, in vitro human skin, and binding to powdered human stratum corneum. J Toxicol Environ Hlth 1993; 39:375–382.
4. Hurst LN, Brown DH, Murray KA. Prolonged life and improved quality of stored skin grafts. Plast Reconstr Surg 1984; 73:105–109.
5. Wester RC, Noonan PK, Smeach S, Kosobud L. Pharmacokinetics and bioavailability of intravenous and topical nitroglycerin in the rhesus monkey: estimate of percutaneous first pass metabolism. J Pharm Sci 1983; 72:745–748.
6. Bronaugh RL, Stewart RF, Storm JE. Extent of cutaneous metabolism during percutaneous absorption of xenobiotics. Toxicol Appl Pharmacol 1989; 99:534–543.
7. Bhatt RH, Micali G, Galinkin J, Palicharla P, Koch R, West DP, Solomon LM. Determination and correlation of in vitro viability for hairless mouse and human neonatal whole skin and stratum corneum/epidermis. Arch Dermatol Res 1997; 289:170–173.
8. Collier SW, Sheikh NM, Sakr A, Lichtin JL, Stewart RF, Bronaugh RL. Maintenance of skin viability during in vitro percutaneous absorption/metabolism studies. Toxicol Appl Pharmacol 1989; 99:522–533.
9. Kraeling MEK, Lipicky RJ, Bronaugh RL. Metabolism of benzocaine during percutaneous absorption in the hairless guinea pig: acetylbenzocaine formation and activity. Skin Pharmacol 1996; 9:221–230.

24

Interrelationships in the Dose–Response of Percutaneous Absorption

Ronald C. Wester and Howard I. Maibach
Department of Dermatology, School of Medicine, University of California, San Francisco, California, U.S.A.

In most medical and toxicological specialties the administered dose absorbed is defined precisely. This has not always been so in dermatoxicoiogy and dermatopharmacology. The absorbed dose is usually defined as percent applied dose absorbed, flux rate, and/or permeability constant. This may suffice for the person creating the data, but it is incomplete for the person judging the worthiness of the data. Chemical absorbed through skin is usually a low percentage of the applied dose. If 5% is absorbed, it is more than curiosity to question where the other 95% resides. Most critical is whether the remaining dose was in place during the course of the study and whether there is dose accountability. A second critical question is where the clinical or toxicological response lies in relationship to the topically applied dose, the standard safety and efficacy issue that a dose–response will provide. The third question is whether absorption is linear to administered dose, i.e. the dose–response.

This chapter defines our current, albeit far from perfect, understanding of the relation of applied dose to percutaneous absorption. The dose–response is a sound scientific principle and studies on percutaneous absorption need to apply this principle in some portion of a study.

I. DOSE–RESPONSE IN REAL TIME

Breath analysis is being used to obtain real-time measurements of volatile organics in expired air following exposure in rats and humans. The exhaled breath data is analyzed using physiologically based pharmacokinetic (PBPK) models to determine the dermal bioavailability of organic solvents. Human volunteers and animals breathe fresh air via a new breath-inlet system that allows for continuous real-time analysis of undiluted exhaled air. The air supply system is self contained and separated from the exposure solvent-laden environment. The system uses a Teledyne 3DQ Discovery ion trap mass spectrometer (MS/MS) equipped with an atmospheric sampling glow discharge ionization source (ASGDI). The MS/MS system provides an appraisal of individual chemical components in the breath stream in the single-digit parts-per-billion (ppb) detectable

range for compounds under study, while maintaining linearity of response over a wide dynamic range.

1,1,1-Trichlorethane [methyl chloroform (MC)] was placed in 4 L of water at 1%, 0.1%, and 0.01% concentration (MC is soluble at 0.1% and 0.01% concentrations) and volunteers placed a hand in the bucket of water containing the MC. Figure 1 gives the in vivo human dose–response. The analytical system measures MC in exhaled breath every four seconds and displays the amount in real time. For investigator "data analysis sanity," *75* four second data points are averaged each 5 minutes of elapsed time as

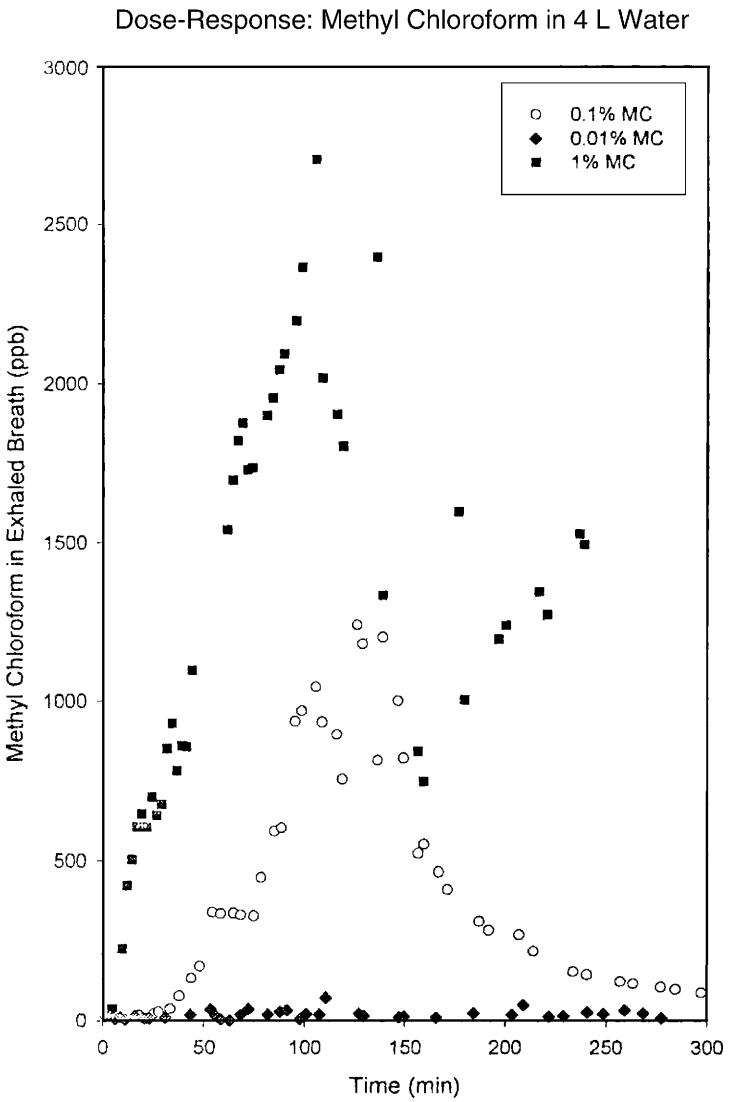


Figure 1 In vivo real-time absorption of the solvent methyl chloroform (MC) from human volunteers with a hand in 4 L of water containing 1%, 0.1%, or 0.01% solvent. The MC is soluble in water at 0.1% (note lag time) but exceeds solubility at 1% (note no lag time). The hand was removed from the solvent/water at 120 minutes.

presented in Figure 1. At 1% dose MC is immediately and rapidly absorbed through the skin, increasing to over 2500 ppb at two hours when the hand was removed from the solvent/water bucket. Breath MC levels then declined. The 0.1% dose (MC, which is completely soluble in water) peaked at approximately 1200 ppb at two hours when the hand was removed from the solvent/water exposure. There was an initial delay of 30 to 60 minutes in solvent absorption from the water soluble dose, not seen with the higher dose that exceeded solubility. The lowest dose, 0.01%, was near analytical limitation. These data are then analyzed for human body rate distribution using a PBPK model, and appropriate absorption and excretion rates produced (1).

II. PHARMACODYNAMIC DOSE–RESPONSE

Pharmacodynamics is a biologic response to the presence of a chemical. The chemical needs to be bioavailable for the response to happen, and a dose–response within the limits of the biological response can be measured. This can happen with in vivo human skin and an example is blood flow changes measured by laser Doppler velocimetry (LDV). Minoxidil is a direct-acting peripheral vasodilator originally developed for hypertension, but now available to promote hair growth. In a double-blind study, balding volunteers were dosed with 0%, 1%, 3%, and 5% minoxidil solutions once each day on two consecutive days and bloodflow was measured by LDV (Fig. 2). On day 1 an LDV dose–response showed the highest bloodflow from the 5% dose, followed by the 3% dose, with the 1% dose giving no response above control. Day 2 results clearly showed a pharmacodynamic response for the 5% solutions ($p < 0.0001$), but the other doses were near that of control (2).

This effect of concentration on percutaneous absorption also extends to the penetration of corticoids as measured by the pharmacodynamic vasoconstrictor assay. In this type of assay aibach and Stoughton (3) showed that, in general, there is a dose–response relationship, with increasing efficacy closely following increased dose. A several-fold difference in dose can override differences in potency between the halogenated analogues. If this applies to corticoids, it could also apply for other chemicals.

Biological response differs from straight chemical analyses (only limited by analytical sensitivity) in that a threshold is probably needed to initiate the response and there are probably limits to the extent that the biology can respond. However, within these parameters some dose–response should exist.

III. DOSE–RESPONSE INTERRELATIONSHIPS

The interrelationships of dose response in dermal absorption are defined in terms of accountability, concentration, surface area, frequency of application, and time of exposure. Accountability is an accounting of the mass balance for each dose applied to skin. Concentration is the amount of applied chemical per unit skin surface area. Surface area is usually defined in square centimeter of skin application or exposure. Frequency is either intermittent or chronic exposure. Intermittent can be one, two, and so on exposures per day. Chronic application is usually repetitive and on a continuing daily basis. Time of exposure is the duration of the period during which the skin is in contact with the chemical before washing. Such factors define skin exposure to a chemical and subsequent percutaneous absorption.

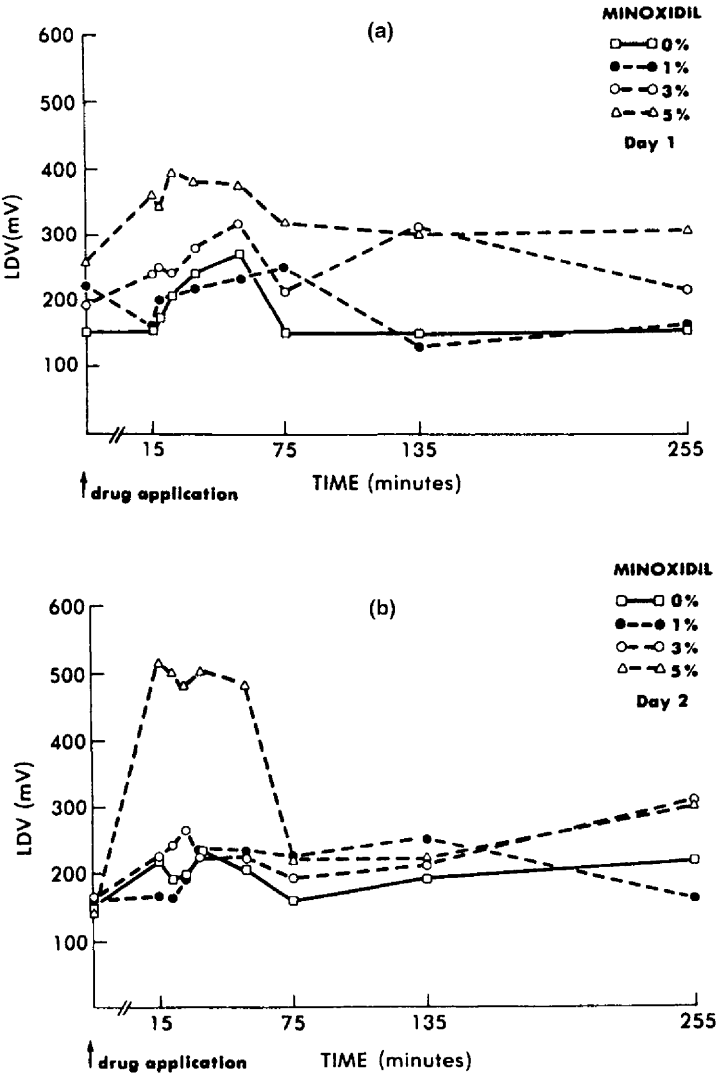


Figure 2 Pharmacodynamic laser Doppler velocimetry dose–response of minoxidil stimulating skin blood flow in the balding scalp of male volunteers.

IV. ACCOUNTABILITY (MASS BALANCE)

Table 1 gives the in vivo percutaneous absorption of dinoseb in the rhesus monkey and rat. The absorption in the rat over a dose range of 52 to 644 $\mu g/cm^2$ is approximately 90% for all of the doses (4). Conversely, absorption in the rhesus monkey for the dinoseb dose range of 44 to 3620 $\mu g/cm^2$ is approximately only 5%. There is an obvious difference because of species (rat and rhesus monkey). The question then becomes one of mass balance to determine dose accountability. (If dinoseb was not absorbed through skin, then what happened to the chemical?) Table 1 shows that at least 80% of the applied doses can be accounted for (rat and rhesus monkey) and that (Table 2) in the rhesus monkey the dinoseb remained on the skin (skin wash recovery 73.8 ± 6.8) and was not absorbed over the 24-hour application period.

Table 1 In Vivo Percutaneous Absorption of Dinoseb in Rhesus Monkey and Rat[a]

Applied dose ($\mu g/cm^2$)	Skin penetration (%)	Dose accountability (%)
Rat		
51.5	86.4 ± 1.1	87.9 ± 1.8
128.8	90.5 ± 1.1	91.5 ± 0.6
643.5	93.2 ± 0.6	90.4 ± 0.7
Rhesus monkey		
43.6	5.4 ± 2.9	86.0 ± 4.0
200.0	7.2 ± 6.4	81.2 ± 18.1
3620.0	4.9 ± 3.4	80.3 ± 5.2

[a]Rat = acetone vehicle; 72-hr application; Monkey—Premerge-3 vehicle; 24-hr application.

V. EFFECTS OF CONCENTRATION ON PERCUTANEOUS ABSORPTION

Maibach and Feldmann (5) applied increased concentrations of testosterone, hydrocortisone, and benzoic acid from 4 $\mu g/cm^2$ in three steps to 2000 $\mu g/cm^2$ (4 $\mu g/cm^2$ is approximately equivalent to the amount applied in a 0.25% topical application; 2000 $\mu g/cm^2$ leaves a grossly visible deposit of chemical). Increasing the concentration of the chemical always increased total absorption. These data suggest that as much as gram amounts of some compounds can be absorbed through normal skin under therapeutic and environmental conditions.

Wester and Maibach (6) further defined the relationship of topical dosing. Increasing concentration of testosterone, hydrocortisone, and benzoic acid decreased the efficiency of percutaneous absorption (percent dose absorbed) in both the rhesus monkey and man (Table 3), but the total amount of material absorbed through the skin always increased with increased concentration. Schuplein and Ross (7) also showed in vitro that the mass of material absorbed across skin increased when the applied dose was increased. The same relationship between dose applied and dose absorbed is also seen with the pesticides parathion and lindane in Table 4.

Wedig et al. (9) compared the percutaneous penetration of different anatomical sites. A single dose of a ^{14}C-labeled magnesium sulfate adduct of dipyrithione at concentrations of 4, 12, or 40 $\mu g/cm^2$ per site was applied for an eight-hour contact

Table 2 Percutaneous Absorption and Accountability of Dinoseb In Vivo Study in the Rhesus Monkey

	Applied dose ($\mu g/cm^2$)		
Disposition parameter	43.6	200.00	3620.0
	Applied dose accountability (%)		
Urine	3.3 ± 1.8	4.4 ± 23.9	3.0 ± 2.1
Feces	0.8 ± 0.5	1.0 ± 0.6	3.0 ± 1.7
Contaminated solids	0.03 ± 0.02	0.02 ± 0.02	0.07 ± 0.08
Pan wash	0.04 ± 0.03	0.8 ± 1.1	0.4 ± 0.3
Skin wash	81.1 ± 4.0	75.0 ± 22.9	73.8 ± 6.8
Total accountability	**86.0 ± 4.0**	**81.2 ± 18.1**	**80.3 ± 5.2**

Table 3 Percutaneous Absorption of Increased Topical Dose of Several Compounds in Rhesus Monkey and Man

	Totals for rhesus		Totals for man	
Compound ($\mu g/cm^2$)	%	Micrograms	%	Micrograms
Testosterone				
34	18.4	0.7	11.8	0.4
30	—	—	8.8	2.6
40	6.7	2.7	—	—
250	2.9	7.2	—	—
400	2.2	8.8	2.8	11.2
1600	2.9	46.4	—	—
4000	1.4	56.0	—	—
Hydrocortisone				
4	2.9	0.1	1.6	0.1
40	2.1	0.8	0.6	0.2
Benzoic acid				
3	—	—	37.0	1.1
4	59.2	2.4	—	—
40	33.6	134.4	25.7	102.8
2000	17.4	348.0	14.4	288.0

Source: From Refs. 5 and 6.

time to the forearm, forehead, and scalp of human volunteers. The results again indicated that, as the concentration increased, more was absorbed. Skin permeability for equivalent doses on different sites assumed the following order: forehead was equal to scalp, which was greater than forearm. The total amounts absorbed increased even when the percentage of dose excreted at two doses remained approximately the same. On the forehead, proportionately more penetrated from the 40 $\mu g/cm^2$ than from the 4 and 12 $\mu g/cm^2$ doses. On the scalp the difference was even more striking, with almost twice as much proportionately penetrating from 40 $\mu g/cm^2$

Table 4 Effect of Applied Topical Concentration on Human Percutaneous Absorption

	Total	
Compound ($\mu g/cm^2$)	%	(μg)
Parathion		
4	8.6	0.3
40	9.5	3.8
400	4.8	19.2
2,000	9.0	18.0
Lindane		
4	9.3	0.4
40	8.3	3.3
400	5.7	22.8
1000	3.4	34.0
2,000	4.4	88.0

Source: From Ref. 8.

than from 4 and 12 $\mu g/cm^2$. Thus, as the concentration of applied dose increased, the total amount of chemical penetrating the skin (and thus becoming systemically available) also increased for all the anatomical sites studied. Therefore, for exposure of many parts of the body, absorption can take place from all of the sites. As the concentration of applied chemical and the total body exposure increase, the subsequent systemic availability will also increase.

Although the penetration at these doses varied between anatomical sites, the percentage of the dose penetrating was similar at the three doses on the forearm and the forehead. However, on the occiput (of the scalp), there was an increasing percentage of penetration with increasing dosage. In other words, at the highest dose, the efficiency of penetration was the greatest.

Reifenrath et at. (10) determined the percutaneous penetration of mosquito repellents in hairless dogs. As the topical dose increased in concentration, the penetration in terms of percentage of applied dose was about the same (Table 5). However, the mean total amount of material absorbed increased dramatically. An application of 4 $\mu g/cm^2$ of *N,N*-diethyl-*m*-toluamide gave a 12.8% absorption resulting in a total absorption of 0.5 $\mu g/cm^2$. An increase in the dose to 320 $\mu g/cm^2$ decreased the percent absorbed to 9.4; however, the total amount of material absorbed was now up to 30.1 $\mu g/cm^2$, an increase of 60 times!

Roberts and Horlock (11) examined the effects of concentration and repeated skin application of percutaneous absorption. Following single-treatment application with 1%, 5%, and 10% ointments, the penetration fluxes for salicylic acid in hydrophilic ointment increased as the concentration increased (Table 6). With extended application (on a daily basis) a change in flux was also observed, the skin underwent a change, and subsequently the penetration flux changed.

Wester (unpublished observations) looked at percutaneous absorption of nitroglycerin. The topical concentration of nitroglycerin was increased stepwise from 0.01 to 10 mg/cm^2. The percentage dose absorbed remained basically the same between 0.01 and 1 mg/cm^2 (Table 7). But as this dose increased 10 times, the amount of material becoming systemically available increased 10 times. At 10 mg/cm^2 the percentage dose absorbed had markedly decreased. This suggests that the percentage of absorption could become saturated at a high concentration.

Howes and Black (12) determined the comparative percutaneous absorption of sodium and zinc pyrithione in shampoo through rat skin. As the concentrations

Table 5 Percutaneous Penetration and Total Absorption of Repellents in Relation to Dose of Chemical Applied to Hairless Dog

Compound	Topical Dose ($\mu g/cm^2$)	Penetration (% of applied dose)	Mean total absorbed ($\mu g/cm^2$)
Ethyl hexanediol	4	8.8	0.35
	320	10.3	33.0
N,*N*-diethyl-*m*-toluamide	4	12.8	0.51
	320	9.4	30.1
Sulfonamide[a]	100	9.1	9.1
	320	7.5	24.0
	1000	5.4	54.0

[a]*n*-Butane sulfonamide cyclohexamethylene.
Source: From Ref. 10.

Table 6 Mean Penetration Fluxes of Salicylic Acid in Hydrophilic Ointment Base Through Excised Rat Skin After Single Treatment

Salicyclic acid concentration (w/w)	Penetration flux of salicylic acid (mg/cm^2 hr, ± SE)
1	0.014 ± 0.002
5	0.061 + 0.003
10	0.078 ± 0.003

Source: From Ref. 11.

of material in shampoo increased from 0.1% to 2%, the penetration also increased from 0.7 to 1 $\mu g/cm^2$ (Table 8).

VI. CONCENTRATION AND NEWBORNS

Wester et al. (13) compared the percutaneous absorption in newborn versus adult rhesus monkeys. The total amount absorbed per square centimeter of skin again increased with increased applied dose and was further increased when the site of application was occluded. In the newborn the question of concentration may have special significance because surface area/body mass ratio is greater than in the adult. Therefore, the systemic availability per kilogram of body weight can be increased by as much as threefold.

VII. CONCENTRATION AND WATER TEMPERATURE

Cummings (14) determined the effect of temperature on rate of penetration on *n*-octylamine through human skin. Increasing the temperature increased the rate of penetration as evidenced by octylamine-induced wheal formation and erythema. The increase in cutaneous blood flow mainly involved areas of the wheal. The increase in cutaneous blood flow mainly involved areas of the epidermal factors. Therefore, increased temperature along with increased concentration will increase the percutaneous absorption.

Table 7 Percutaneous Absorption of Nitroglycerin: Topical Concentration Vs. Absorption for Neat Liquid Application

Topical nitroglycerin concentration (mg/cm^2)	Absorption	
	%	Total (μg)
0.01	41.8	0.004
0.1	43.5	0.04
1.0	36.6	0.4
7.0	26.6	1.9
10.0	7.8	0.8

Source: Wester (unpublished observations).

Table 8 The Effect of Concentration of Sodium Pyrithione in Shampoo on Absorption through Rat Skin

Concentration in shampoo (% w/v)	Total absorption (%)
0.1	0.07
0.5	0.27
1.0	0.62
2.0	1.02

Source: From Ref. 12.

VIII. CONCENTRATION AND DURATION OF CONTACT

Howes and Black (15) studied percutaneous absorption of trichlorcarbon in rat and humans. As the duration of contact increased, penetration increased.

Nakaue and Buhler (16) examined the percutaneous absorption of hexachlorophene in adult and weanling male rats at exposure times from 1.5 to 24 hours and determined the plasma concentrations of hexachlorophene. The plasma concentrations of hexachlorophene increased with time from a low of just a few ng/mL of plasma up to 80+ ng/mL.

Duration of occlusion enhances percutaneous absorption. The significance of time in occlusion was shown by Feldmann and Maibach (8), who concluded that the longer clothing occludes a pesticide, the greater the contamination potential becomes (Table 9).

IX. CONCENTRATION, DURATION OF CONTACT, AND MULTIPLE-DOSE APPLICATION

Black and Howes (17) studied the skin penetration of chemically related detergents (anionic surfactants) through rat skin and determined the absorption for multiple variables, mainly concentration of applied dose, duration of contact, and the effect of multiple-dose applications. With alcohol sulfate and alcohol ether sulfate, as the concentration of applied dose increased and the duration of contact increased, penetration increased. With multiple applications there was also an increase in

Table 9 Effect of Duration of Occlusion on Percutaneous Absorption of Malathion in Man

Duration (hr)	Absorption (%)
0[a]	9.6
0.5	7.3
1	12.7
2	16.6
4	24.2
8	38.8
24	62.8

[a]Immediate wash with soap and water.
Source: From Ref. 8.

Table 10 Concentration, Duration of Contact, and Multiple Application as Variables in Penetration of Anionic Surfactant Through Rat Skin

Variable	Penetration ($\mu g/cm^2$)
Concentration (% w/v)	
0.2	0.02
0.5	0.11
1.0	0.23
2.0	0.84
Duration of contact (min)	
1	0.25
5	0.47
10	0.69
20	0.97
Multiple application ($\times$ 5 min)	
1	0.14
2	0.25
4	0.36

Source: From Ref. 17.

penetration (Table 10). Therefore, again the systemic availability and potential toxicity of a chemical depend on many variables. One of these, the concentration, was discussed in the preceding paragraphs. Other variables, such as duration of contact and multiple application, are also important.

X. CONCENTRATION AND SURFACE AREA

Sved et al. (18) determined the role of surface area on percutaneous absorption of nitroglycerin. As the surface area of applied dose increased, the total amount of material absorbed and systemic availability of nitroglycerin increased. This was confirmed by the percutaneous absorption studies of Noonan and Wester (19), but there was no linear relationship between the size of the surface area and increase in absorption. However, the same information held. The surface area of applied dose determined systemic availability of the chemical.

XI. EFFECT OF APPLICATION FREQUENCY

Wester et al. (20,21) studied the effect of application frequency on the percutaneous absorption of hydrocortisone. Material applied once or three times a day showed a statistical difference ($p < 0.05$) in the percutaneous absorption. One application each 24 hours of exposure gave a higher absorption than material applied at a lower concentration but more frequently, namely, three times a day. This study also showed that washing (effect of hydration) enhanced the percutaneous absorption of hydrocortisone. This relationship between frequency of application and percutaneous absorption is also seen with testosterone.

The aforenoted studies used intermittent application per single day of application. Another consideration is extended versus short-term administration and the

Table 11 Incidence of Tumors After Application of Shale Oils

Shale Oil	Dose and frequency	Total dose per week (mg)	Number of animals with tumors
OCSO No. 6	10 mg, 4 times	40	2
	20 mg, 2 times	40	4
	40 mg, once	40	13
PCSO II	10 mg, 4 times	40	11
	20 mg, 2 times	40	17
	40 mg, once	40	19

Source: From Ref. 24.

subsequent effect on percutaneous absorption. Wester et al. (22) examined the percutaneous absorption of hydrocortisone with long-term administration. The work suggests that extended exposure had some effect on the permeability characteristics of skin and markedly increased percutaneous absorption.

With malathion, which apparently has no pharmacological effect on skin, the dermal absorption from day 1 was equivalent to day 8 application (23).

Therefore, for malathion, the single-dose application data are relevant for predicting the toxic potential for longer-term exposure.

XII. APPLICATION FREQUENCY AND TOXICITY

There is a correlation between frequency of application, percutaneous absorption, and toxicity of applied chemical. Wilson and Holland (24) determined the effect of application frequency in epidermal carcinogenic assays. Application of a single large dose of a highly complex mixture of petroleum or synthetic fuels to a skin site iacreased the carcinogenic potential of the chemical compared with smaller or more frequent applications (Table 11). This carcinogenic toxicity correlated well with the results of Wester et al. (20,21), in which a single applied dose increased the percutaneous absorption of the material compared with smaller or intermittent applications.

XIII. DISCUSSION

Many variables affect percutaneous absorption and subsequent dermal toxicity. Increased concentration of an applied chemical on skin increases the body burden, as does increasing the surface area and the time of exposure. The opposite also holds true, namely, dilution of a chemical will decrease the effects of the applied concentration, provided other factors do not change (such as diluting the chemical but spreading the same total dose over a larger surface area). The body burden is also dependent on the frequency of daily application and on possible effects resulting from long-term topical exposure. Dose accountability (mass balance) completes a dose–response study.

The current data provide a skeleton of knowledge to use in the design and interpretation of toxicological and pharmacological studies, to increase their relevance to the most typical exposures for man. In essence, we have just begun to define the complexity of the interrelationships between percutaneous absorption and

Table 12 Factors in the Dose–Response Interrelationships of Percutaneous Absorption

Concentration of applied dose ($\mu g/cm^2$)
Surface area of applied dose (cm^2)
Total dose
Application frequency
Duration of contact
Site of application
Temperature
Vehicle
Substantivity (nonpenetrating surface adsorption)
Wash-and-rub resistance
Volatility
Binding
Individual and species variations
Skin condition
Occlusion

Source: From Ref. 25.

dermatoxicology (Table 12) (25,26). Until an appropriate theoretical basis that has been experimentally verified becomes available, quantitating the various variables listed herein will greatly improve the usefulness of biologically oriented procedures such as laser Doppler velocimetry, transepidermal water loss, and real-time solvent assay in pulmonary breath exhalation, and will expand our knowledge of not only skin dose–response but the use of skin absorption and dynamics to better the human race.

REFERENCES

1. Wester RC, Hui X, Maibach HI, Thrall KD, Poet TS, Corley RA, Edwards JA, Weitz KK. Utility of real time breath analysis and physiologically based pharmacokinetic modeling to determine the percutaneous absorption of methyl chloroform in rats and humans. Toxicol Sci 2000; 54:42–51.
2. Wester RC, Maibach HI, Guy RH, Novak E. Minoxidil stimulates cutaneous blood flow in human balding scalps: pharmacodynamics measured by laser Doppler velocimetry and photopulse plethysmography. Invest Dermatol 1984; 82:515–517.
3. Maibach HI, Stoughton RB. Topical corticosteroids. Med Clin N Am 1973; 57: 1253–1264.
4. Shah PV, Fisher HL, Sumler MR, Monroe RJ, Chernoff N, Hall LL. A comparison of the penetration of fourteen pesticides through the skin of young and adult rats. J Toxicol Enviorn Health 1987; 21:353–366.
5. Maibach HI, Feldmann RJ. Effect of applied concentration on percutaneous absorption in man. Invest Dermatol 1969; 52:382.
6. Wester RC, Maibach HI. Relationship of topical dose and percutaneous absorption on Rhesus monkey and man. Invest Dermatol 1976; 67:518–520.
7. Scheuplein RJ, Ross LW. Mechanism of percutaneous absorption V. Percutaneous absorption of solvent-deposited solids. J Invest Dermatol 1974; 62:353–360.
8. Feldmann RJ, and Maibach HI. Systemic absorption of pesticides through the skin of man. In Occupational Exposure to Pesticides: Report to the Federal Working Group on Pest Management from the Task Group on Occupation Exposure to Pesticides. Appendix B, 1979; 120–127.

9. Wedig JH, Feldmann RJ, Maibach HI. Percutaneous penetration of the magnesium sulfate adduct of dipyrithione in man. Toxicol Appl Pharmacol 1977; 41:1–6.
10. Reifenrath WG, Robinson PB, Bolton VD, Aliff RE. Percutaneous penetration of mosquito repellents in the hairless dog: effect of dose on percentage penetration. Food Cosmet Toxicol 1981; 19:195–199.
11. Roberts MS, Horlock E. Effect of repeated skin application on percutaneous absorption of salicylic acid. J Pharm Sci 1978; 67:1685–1687.
12. Howes D, Black JG. Comparative percutaneous absorption of pyrithiones. Toxicology 1975; 5:209–220.
13. Wester RC, Noonan PK, Cole MP, Maibach HI. Percutaneous absorption of testosterone in the newborn Rhesus monkey: comparison to the adult. Pediatr Res 1977a; 11: 737–739.
14. Cummings EG. Temperature and concentration effects on penetration of *N*-octylamine through human skin in situ. J Invest Dermatol 1969; 53:64–79.
15. Howes D, Black JG. Percutaneous absorption of trichlorocarban in rat and man. Toxicology 1976; 6:67–76.
16. Nakaue HS, Buhler DR. Percutaneous absorption of hexachlorophene in the rat. Toxicol Appl Pharmacol 1976; 35:381–391.
17. Black JG, Howes D. Skin penetration of chemically related detergents. Soc Cosmet Chem 1979; 30:157–165.
18. Sved S, McLean WM, McGilveray IJ. Influence of the method of application on pharmacokinetics of nitroglycerin from ointment in humans. Pharm Sci 1981; 70:1368–1369.
19. Noonan PK, Wester RC. Percutaneous absorption of nitroglycerin. Pharm Sci 1980; 69:385.
20. Wester RC, Noonan PK, Maibach HI. Frequency of application on percutaneous absorption of hydrocortisone. Arch Dermatol Res 1977b; 113:620–622.
21. Wester RC, Noonan PK, Maibach HI. Variations in percutaneous absorption of testosterone in the Rhesus monkey due to anatomic site of application and frequency of application. Arch Dermatol Res 1980a; 267:299–335.
22. Wester RC, Noonan PK, Maibach HI. Percutaneous absorption of hydrocortisone increases with long-term administration. Arch Dermatol Res 1980b; 116:186–188.
23. Wester RC, Maibach HI, Bucks DAW, Guy RH. Malathion percutaneous absorption following repeated administration to man. Toxicol Appl Pharmacol 1983; 68:116–119.
24. Wilson JS, Holland LM. The effect of application frequency on epidermal carcinogenesis assays. Toxicology 1982; 24:45–54.
25. Wester RC, Maibach HI. Cutaneous pharmacokinetics: 10 steps to percutaneous absorption. Drug Metab Rev 1983; 14:169–205.
26. Wester RC, and Maibach HI. In vivo percutaneous absorption. In: Marzuui F, Maibach HI, eds. Dermatotoxicology, 2d ed. Washington: Hemisphere, 1982: 131–146.
27. Wester RC, Maibach HI, Guy RH, and Novak E. Pharmacodynamics and percutaneous absorption. In: Bronaugh R, Maibach H, eds. Percutaneous Absorption, New York: Marcel Dekker, Inc., 1985:547–560.

25

Blood Flow as a Technology in Percutaneous Absorption: The Assessment of the Cutaneous Microcirculation by Laser Doppler and Photoplethysmographic Techniques

Ethel Tur
Department of Dermatology, Sourasky Medical Center, Tel Aviv University, Tel Aviv, Israel

I. INTRODUCTION

Optical techniques for blood flow measurement were first introduced almost 70 years ago with the innovation of photoplethysmography (1), substantiated and expanded by Hertzman (2). Laser Doppler techniques came forth 40 years later (3), followed by the manufacture of commercial devices (4,5), which are used more frequently than photoplethysmography. These optical methodologies enable tracing of the movement of red blood cells in the skin. This is useful in following percutaneous penetration, when the penetrant has an effect on blood vessels or on blood flow. In addition, physiology and anatomy of the skin can be studied, as well as pathology. Moreover, laser Doppler flowmetry (LDF) measurements are applicable in the evaluation of internal diseases and conditions that affect the skin microvasculature.

The diverse application areas of the technique include tissues other than the skin, like the buccal, nasal, or rectal mucosa, as well as the intestine through an endoscope, and kidney, liver, or lung intra-operatively. This chapter exclusively deals with cutaneous LDF and reviews only investigations where this method was used to measure skin blood flow. In each field of LDF investigation knowledge has broadened in the last few years. In view of the large number of studies conducted in this area, it is impossible to review each and every one; therefore, we only attempt to demonstrate the possibilities of the technique.

After a review of some of the relevant basic considerations in experimental designs involving LDF, we discuss several conditions where LDF can be utilized. These include investigations of normal and diseased skin and the influence of the nervous system, environmental temperature, smoking, and pregnancy on skin blood flow. Studies of disease processes, severity, and treatment evaluation are then

discussed, including hypertension, peripheral vascular disease, diabetes mellitus, and Raynaud's phenomenon. We conclude with future possibilities and expectations.

II. THE METHOD OF LASER DOPPLER

A. Basic Principles

The LDF is a noninvasive method that continuously follows the flow of red blood cells (6). It operates on the Doppler principle, employing low power helium–neon laser emitting red light at 632.8 nm. The radiation is transmitted via an optical fiber to the skin. The radiation is diffusely scattered and its optical frequency is shifted by the moving red blood cells. The reflected light, being coherently mixed with another portion of the light scattered from static tissues, generates a Doppler beat signal in the photodetector output current. A quantitative estimation of the cutaneous blood flow derives from spectral analysis of the beat signal.

B. Advantages

As an objective, noninvasive and real-time measurement technique, LDF is an attractive practical tool for estimating the cutaneous blood flow. Besides, LDF is relatively simple, fast, and inexpensive, and can provide information that supplements the results of various other techniques.

C. Disadvantages

The LDF is inferior in quantitating blood flow as compared to other techniques, such as the ^{133}Xe washout technique. However, it is important to note that different methods measure different sections of the microvasculature. It is likely that the flux signal shown by the LDF represents the large volume of red blood cells moving within the larger blood vessels, particularly the subpapillary plexus, rather than the much smaller volume of red blood cells residing within the nutritive capillaries. The depth of laser penetration in the wavelengths used is approximately 1 mm. Therefore, in normal skin it is likely to include the subpapillary plexus, as well as the capillaries in the subpapillary dermis. In diseased skin it may measure a different body of vessels, for instance in psoriasis the epidermal ridges are elongated, and this may alter the relative contribution of superficial and deep blood flow to the laser Doppler signal. Another disadvantage of the LDF is that results obtained by various instruments or by the same instrument in different people cannot be compared.

D. Recent Developments

Improvements of the laser Doppler technique offer new possibilities and present new findings. Progressions are illustrated by refinements such as computerization and the design of a probe holder, which allows repeated measurements over the same site before and after manipulations to the skin through a multichannel LDF instrument, which allows simultaneous measurements of several sites (7). Another development is an integration-type LDF, equipped with a temperature-load instrument, allowing responses of the skin blood flow to cooling from 30 to 10°C to be evaluated (8). But the most substantial development is laser Doppler imaging (scanning LDF) (9–12), which records the tissue perfusion in several thousand measurement points. A map

of the spatial distribution of the blood flow is obtained in a short period of time. Unlike the LDF, which continuously records the blood flow over a single point, laser Doppler imaging maps the blood flow distribution over a specific area. Thus, the two methods do not compete with each other, but are rather complementary. The laser Doppler imaging has the advantage of operating without any contact with the skin surface, avoiding the influence of the pressure of the probe on the tissue perfusion. It can rapidly measure large areas of skin and allows simultaneous measurement of the extent of blood flow changes in abnormal areas of skin and estimates the area of these changes. Furthermore, objective evaluation of various interventions and therapeutic response may be obtained by serial scans.

III. CONCEPTS AND DESIGN OF EXPERIMENTAL STUDIES USING LDF

A. Planning and Performing LDF Blood Flow Measurements

Both static and dynamic LDF measurements can be used (13–15). Static studies, like baseline blood flow measurements, record only the steady-state blood flow, neglecting all transients. On the contrary, dynamic investigations can examine the competence of the blood vessels by following their response to triggers (12–14). Reactive hyperemia is an example for a dynamic test (12–14) recording the post occlusion time course of the blood flow. Other provocative methods examining the response to external triggers include: cognitive test (16), isotonic (17) and isometric tests (12), vasomotor reflexes (18,19), intracutaneous needle stimulation (20), topical vasodilators (21), and thermal test (12).

Some of these tests are vasoconstrictive (the isometric and cognitive tests and vasomotor reflexes), and some are vasodilative (the arterial postocclusive reactive hyperemia, intracutaneous needle stimulation, the thermal test, and the isotonic test).

To optimize skin blood flow response to the different tests, vasoconstrictive stimuli should be performed on a high blood flow site, whereas vasodilative stimuli should be performed on a low blood flow site. Consequently, the magnitude of the changes induced is maximized, providing a significant improvement in the quality of the data obtained. Moreover, vasoconstriction mediated by sympathetic stimulation, as in the cognitive test, should be provoked in the hands and feet, where the local blood supply is under a sympathetic vasoconstrictor control, and not in the face, which has a poor sympathetic vasoconstrictor supply (15).

Thus, to enhance the sensitivity of the measurements, the site tested should be carefully selected. For example, the fingers, being rich with microvascular arteriovenous anastomoses, are useful for vasoconstrictive tests, while the forearms are suitable for the vasodilative tests. The forearms have several advantages as a preferred site for vasodilative tests: (i) abundance of arterioles and capable of reactive hyperemia; (ii) a local effect, rather than thermoregulatory reflexes (22), is responsible for thermally induced vasodilatation; (iii) little inconvenience is experienced by the subjects tested.

The appropriate test should also be carefully selected in order to adequately probe the relevant topic. Before reaching a conclusion, one should bear in mind that differences in experimental settings might lead to different results. For instance, in order to study differences between young and old patients, different tests were used when addressing different questions. When aiming to study the thermoregulatory responses to cold stress, vasoconstrictor responses to inspiratory gasp, contralateral

arm cold challenge, and body cooling were measured (20), and differences were indeed found: elderly subjects had diminished sympathetic vasoconstrictor response. In contrast, in order to evaluate the penetration of drugs through aged skin, the erythema that results from topical application of methyl nicotinate was measured (23), and no differences were found between young and old subjects, indicating that microvascular reactivity to the applied stimulus was comparable.

1. Vasoconstrictive Test

Isometric Test. The site of blood flow measurement is the left middle fingertip. After establishing the baseline blood flow, it is continuously recorded when the subject squeezes a hard rubber ball in his right hand for 30 seconds. He then releases the grip and the maximum decrease in blood flow is recorded. The hemodynamic response to isometric hand grip exercise involves activation of the sympathetic nervous system, eliciting an increase in blood pressure, which is mainly dependent upon cardiac output (12).

Cognitive Test. The site of blood flow measurement is again the fingertip. The subject is requested to subtract seven sequentially from 1000 for a two minute period. Blood flow is monitored continuously. There is a rapid fall in the blood flow to the finger at the beginning of the mental arithmetic activity, and a rapid recovery at the end. The maximum decrease in blood flow is registered. This decrease is a manifestation of a sudden increase in sympathetic activity (15).

Venoarteriolar Response. The venoarteriolar reflex measures the ability to decrease flow during venous stasis (normally seen in the feet on dependency), and is assumed to be dependent on an intact sympathetic nerve function (24). The reflex occurs following increased venous pressure, which induces a constriction of the arterioles followed by a decrease in skin blood flow. An increase of venous pressure can be achieved by occlusion with a cuff (for instance at the base of the investigated finger) (25), or by lowering the leg below heart level (26–28). Usually, resting blood flow to the dorsum of the foot is measured with the patient resting in the supine position. Then standing flow is measured (or the flow after occlusion by a cuff), and the lowest reading over five minutes of standing is registered. The venoarteriolar reflex can be expressed as the percent decrease in skin blood flow on standing. The reaction is mediated by a sympathetic axon reflex, comprised of receptors in small veins and resulting in an increase in precapillary resistance.

Inspiratory Gasp. The subject is instructed to breathe in as deeply and quickly as possible and to hold his breath for 10 seconds. The percentage reduction from the resting flow is calculated. This procedure records the sympathetic vasoconstrictor reflex (29).

2. Vasodilative Tests

Cutaneous Postischemic Reactive Hyperemia Test. Blood flow in the middle part of the flexor aspect of the forearms (or sometimes the proximal part of the finger) is recorded. The arm is then clamped in a pneumatic cuff and inflated to greater than 40 mmHg above systolic pressure for a period of one to five minute during which blood flow measurements are continuously recorded. The cuff is then deflated resulting in an increase in blood flow, which is recorded continuously, usually until the blood flow returns to baseline values. Any of the following parameters can be measured: (i) baseline flow; (ii) peak flow above baseline flow; (iii) the time required

to reach the peak; (iv) the ratio between the peak flow and the time required to reach it, expressing the ability of the tissue to respond to fast external triggers; (v) the time required to return to the blood flow at rest; (vi) the area under the response–time curve (12–14).

Intracutaneous Needle Stimulation (Injection Trauma). Resting blood flow is recorded, and then a needle is inserted, usually in the center of the probe holder to a depth previously set by a needle guard. The blood flow reaches a peak within 15 minutes of injection, and then gradually returns to normal over several hours, depending on the degree of trauma (18).

Thermal Test. Resting blood flow is measured in the middle part of the flexor aspect of the left forearm, while the probe is mounted through a thermostated probe holder. The temperature setting of the thermistor is adjusted to 26°C. The temperature is maintained at 26°C for two minutes, before turning the setting to 28°C for the next two minute period. This 2°C step sequence is repeated every two minutes until the temperature reaches 44°C. Blood flow is recorded at the end of each two minute interval (12).

Axon Reflex Vasodilator Response. Vasoactive substances such as substance P, capsaicin, or histamine are administered topically or intradermally (30–32). Alternatively, acetylcholine is administered with the aid of electrophoresis (27). The extent of the response is measured at several distances from the site of administration. The same procedure is followed for measuring the response to direct stimulation with a firm mechanical stroke with a dermograph (Lewis triple response) (27).

Isotonic Test. The subject squeezes a partially inflated blood pressure cuff with maximum effort, at which the pressure is recorded, and one third of it is calculated. The subject is then instructed to grip the cuff at this value of one third of the maximum pressure. This isotonic exercise causes vasodilatation, and an increase in skin blood flow results (16).

B. Choosing Subjects

When comparing subjects or various groups of subject variations in population regarding sex (33,34), age (20), and race (35) should be taken into account. Assuring that subjects match for these variables will decrease the variance within the results.

IV. APPLICATIONS

The LDF may be used to study the time course of circulatory changes caused by physiological or pathological processes, including changes caused by pharmacological substances. Internal and external factors, skin conditions, and general conditions that affect the skin are all candidates for LDF investigations.

A. Skin Physiology, Pharmacology, and Pathology

1. Percutaneous Penetration

The LDF was applied for tracing the percutaneous penetration of vasoactive agents such as methyl nicotinate (6), prostacycline (36), or methadone (37), and for studying variations in normal skin (6,19). For instance, LDF assisted in evaluating the enhancement effect of ultrasound on skin penetration (38). Thus spatial variations (19), percutaneous penetration enhancers (39), vehicle effect on percutaneous absorption (40), the appendage contribution to penetration (41), age and racial differences

(42), were all studied with LDF. A decreased percutaneous penetration was recorded in black subjects at various skin sites (43). Circadian differences in penetration kinetics of methyl and hexyl nicotinate were also demonstrated by LDF (44). On the other hand, LDF is not suitable for studying the percutaneous penetration of vasoconstrictive agents such as glucocorticoids (45).

Transdermal delivery utilizing iontophoresis was studied at different sites of the forearms and hands, and vasodilatation was site dependent (46). It was shown that cutaneous vascular responses to iontophoresis of vasoactive agents comprise nonspecific, current-induced hyperemia, and specific effects of the administered drug (47).

2. *UVB-Induced Erythema*

The effect of ultraviolet (UV) may be evaluated by LDF, but the technique was not adequate for individuals with dark skin (48).

The UVB-induced skin blood flow was monitored using laser Doppler perfusion imaging technique. It was as sensitive as conventional LDF, but had the many advantages of measuring blood flow over large areas without contact with the skin surface (49). Laser Doppler perfusion imaging was also successfully used for phototesting (50).

3. *Inflammation and Contact Dermatitis*

Inflammation is well suited for LDF studies, because of its marked vasoactive component. An increase in blood flow indicated the induction of erythema by topical application of *Staphylococcus aureus* superantigen on intact skin (51). This occurred with both healthy subjects and patients with atopic dermatitis, suggesting that the superantigen may exacerbate and sustain inflammation. The UV-induced inflammation was increased following topical application of estrogen (52), while hypnotic suggestion attenuated UV inflammation (53).

The effect of various topical steroid formulations on UV-induced inflammation was measured by LDF, and it enabled grading of the potency of these topical corticosteroids (54).

The LDF was also used to assess the effect of systemic anti-inflammatory drugs, and it enabled grading of the effect of these drugs (55,56). Prick tests with allergens and histamine may also be evaluated by LDF (57). Regional variations in response to histamine should be taken into consideration (58).

The LDF is widely used for measuring the response to known irritants. Increased duration of exposure resulted in an increased response, and comparison between the back and forearm indicated a greater sensitivity on the back (59). Cumulative effect of subthreshold concentrations of irritants was indicated in studies with LDF (60). The vehicle effect on irritation was also studied by LDF, and the irritant effect depended on the vehicle (61).

The damage to the skin by repetitive washing (62), and the protective effect of barrier creams were also assessed by LDF (63), as well as the effect of treatment such as topical application of nonsteroidal anti-inflammatory drugs in various vehicles (thus studying the vehicle effect as well) (64). LDF measurements also suggested an improvement of acute ICD with twice daily application of cool compresses. No significant difference was found between the efficacy of physiologic saline or water compresses (65).

Non-immunologic contact urticaria induced by benzoic acid was followed and regional variations mapped by LDF (66), as was the suppressive effect of psoralen plus ultraviolet A (PUVA) treatment (67), and topical nonsteroidal anti-inflamma-

tory drugs (68). Regional variations, as well as age-related regional variations in the response to histamine were found (69).

Patch tests for allergic contact dermatitis may be objectively evaluated with LDF, as were patch tests with calcipotriol ointment in various patients, including psoriasis patients (70).

Laser Doppler imaging was more suitable for the quantification of allergic contact dermatitis than the regular LDF, as readings with the latter are time-consuming, and the laser Doppler imaging is valuable for measuring the area of response (71). Both allergic contact dermatitis and irritant contact dermatitis were studied with laser Doppler imaging (72). The technique allowed quantification of subclinical pattern of the allergic inflammation (73).

4. Psoriasis

Psoriasis, with its increased blood flow near the skin surface, is a natural candidate for LDF studies. Several investigators aimed at studying the disease process, whereas others were interested in the effect of several therapeutic modalities. A recent publication concentrated on the question whether cutaneous blood vessels in psoriasis possess a generalized inherently abnormal response to neuropeptides (74). Calcitonin gene-related peptide (CGRP) was intradermally injected in three concentrations to uninvolved skin of psoriatic patients and to healthy controls. This resulted in an increase in blood flow, which did not differ between the two groups, thus indicating that in uninvolved psoriatic skin the vasculature is not different than normal in its response to CGRP. Effects of treatment were assessed by LDF and compared to clinical evaluation methods (75).

Laser Doppler imaging allows rapid measurement of the area and the level of increase of blood flow in psoriatic plaques (9). Plaque severity can be assessed in terms of mean blood flow and area of increased blood flow simultaneously. The obtained scan image reveals the distribution and intensity of the rim of increased blood flow around the psoriatic plaque. This could be used in the study of early biochemical or immunological changes in the skin, before lesions become clinically observable. As an aid in evaluating phototherapy, a reduced sensitivity to both UVA and UVB was demonstrated in psoriasis plaques as compared to uninvolved skin, using the same instrument (10). The method also showed an improved response to PUVA treatment when calcipotriol was topically applied (76). Laser Doppler imaging was further used to demonstrate an abnormal thermal sensory response in psoriasis (77).

The application of LDF for the study of psoriasis, including evaluation of therapy was extensively reviewed (78).

5. Atopic Dermatitis

In a study of dermographism, a significant reduction in the intensity of hyperemia was found in atopic dermatitis patients following pressure on the skin (79). The role of acetylcholine in the etiology of pruritus in atopic dermatitis was studied by injecting acetylcholine and monitoring the vascular reaction. The reaction in the patients started earlier and was longer than the control group, suggesting an etiological role (80).

6. Age, Chronic Venous Insufficiency, and Cutaneous Ulcers

In comparison to the skin of adults (average age 34.6 years), the skin of small children (average age 3.5 years) demonstrated an increased cutaneous blood perfusion as measured by LDF (81).

Differences between elderly and younger individuals and between the forehead and cheek were found utilizing LDF during cooling from 30 to 10°C. In the forehead, the decrease in skin blood flow during cooling showed no marked quantitative change with age, but with aging, the rate of this decrease was reduced. In the cheek, on the other hand, the skin blood flow decreased markedly with aging, but no clear change was observed in the rate of this decrease (82).

Skin blood flow to the dorsum of the foot reduces with age, which might contribute to the attenuated cutaneous vasoreactivity to heat and ischemia in elderly people (83). Moreover, the response to heat is attenuated in the aged (84).

Laser Doppler flux is a product of the concentration of moving blood cells and the blood cell velocity. In an attempt to obtain more information about the cutaneous microcirculation in legs with venous ulcers and in healthy legs, the dynamics of the curves of the LDF, the concentration of moving blood cells, and the blood cell velocity were analyzed in patients with venous leg ulcers and in healthy subjects. The curves of the concentration of moving blood cells and the blood cell velocity were in opposite phase, reflecting the capillary blood flow. The greater amplitude of the LDF and the concentration of moving blood cells in legs with venous ulcers reflect the blood flow in anatomically altered capillaries in those legs (85).

The ability of the skin blood vessels to dilate in response to pilocarpin electrophoresis was assessed in patients with chronic venous insufficiency, but the microvasculature showed a normal capacity to vasodilate (86). The effect of external compression was also studied: compression increased the microcirculatory flow, which might be its mode of action in treating venous insufficiency (87).

In patients with venous ulcers, erythematous ulcer edges exhibited higher blood flow values than non-erythematous edges (88). Postural vasoregulation caused relative ischemia and reperfusion in venous leg ulcers, but the known mediators of reperfusion injury were not released, and therefore were not associated with the process (89). The LDF was also used to monitor the effect of prostanoids on ischemic ulcers (90), and the effect of Crystacide on chronic venous insufficiency and venous hypertension associated with ulcerations (91). It was also utilized to monitor the effect of Venoruton on the prevention and control of flight microangiopathy and edema in subjects with varicose veins flying for more than seven hours (92).

To evaluate different types of alternating pressure air mattresses for the prevention and treatment of pressure ulcers LDF was used on the sacrum, heels, trochanters, and buttock over at least two alternating cycles. Results indicated significant differences between the products (93).

For further examples of the use of LFD in peripheral vascular disease, please refer to Section IV.B.8.

7. Pigmentary Lesions and Melanoma

The LDF has a potential for use in oncology, being able to monitor the vascularization in tumors and adjacent skin. For instance, it may serve as an additional tool in the diagnosis of pigmentary skin lesions. Melanomas showed higher laser Doppler blood flow readings than basal cell carcinomas, and both showed higher readings than benign lesions (94). The LDF was higher in the center of melanomas than in

either the middle of melanocytic nevus or in neighboring healthy skin areas (95). Laser Doppler imaging was used to delineate the boundaries of pigmented lesions (96), and was able to monitor blood flow following photodynamic therapy of non-melanoma skin tumors (97).

8. Burns and Flaps

Surgical procedures such as liposuction (98) and flaps can be monitored (99) and their success predicted (100). Similarly, burn severity and treatment may be evaluated (101).

Laser Doppler perfusion imaging was used to measure the depth of burns (102). The instrument was useful if the effect of scanning distance, curvature of the tissue, thickness of topical wound dressings, and pathophysiological effects of skin color, blisters, and wound fluids were known and adjusted. Further studies proved it accurate to differentiate deep dermal from superficial partial thickness burns in the extremities (103) and to determine the need for excision and grafting in advance of clinical judgment (104).

B. General Conditions and Diseases

External factors, as well as certain general conditions and diseases, may affect the skin or have an effect on its blood flow even when the skin itself is healthy, as demonstrated by the effect of cellular phones on skin blood flow (105).

1. Nervous System

Skin blood flow is centrally controlled by the autonomic system, and takes part in the general regulatory mechanism. Autonomous activity was reflected in skin blood flow, which fluctuated in response to sympathetic modulation (106). Various vasodilating factors that control blood flow can be assessed by LDF (107).

Higher mental activity alters skin blood flow: During cognitive activity, skin blood flow to the finger decreases, but not to the molar region (15). The reason is that vasoconstriction in the finger is mediated by sympathetic stimulation, which controls the blood supply to the hands and feet, whereas the face has a poor sympathetic vasoconstrictor supply.

Sound stimuli also affect the skin microcirculation in sites rich with sympathetic innervations was demonstrated by LDF (108).

The effect of neural blockade at various spinal levels and general anesthesia was followed with LDF, and functions like respiratory movements were correlated (109).

The LDF measurements in acral regions ranked the role of alpha-1 and alpha-2 adrenoceptors in mediating sympathetic responses (110). Alpha-2 adrenoceptor was more potent in increasing the cutaneous microvascular resistance and reducing the perfusion.

To study the mechanism of pain relief by vasodilator agents, LDF measurements were conducted following intradermal injection of various vasodilators and compared to pain threshold (111). Pain threshold did not correlate with blood flow, indicating that the effect of vasodilators on primary afferent nociceptors is not related to the vasodilatory effect.

Laser Doppler measurement of patients with chronic fatigue syndrome showed peripheral cholinergic abnormalities in their vascular endothelium (112).

For further examples of the utilization of LDF for the study of the nervous system, please refer to sections 3, 4.2.2, and 4.2.9.

2. Environmental Temperature

Emotional stress induced vasoconstriction after prolonged heating to 34°C, whereas after prolonged cooling to 22°C vasodilatation was induced (113). The stress-induced decreased flow in warm subjects is probably neurally mediated, since it is preceded by increased skin sympathetic activity. But the increase of flow in cold subjects is more obscure. Different neural commands at different temperatures might be a possibility. Another possibility is that arteriovenous shunts receive a vasoconstrictor sympathetic input, whereas resistant vessels receive a vasodilator input. In cold subjects with high baseline vasoconstriction, the arteriovenous shunts are closed and unable to constrict any further, so only the vasodilatation in the resistance vessels is detected. In warm subjects, thermoregulatory activity is low, the basal flow is high, and the arteriovenous shunts are open. When the emotional stress occurs, the constrictor effect on the open arteriovenous shunts will be more pronounced and mask the vasodilatation in the resistance vessels. A study that examined effects of hyperoxia on thermoregulatory responses found that hyperoxia elicited an inhibitory effect on thermoregulatory skin blood flow (114).

Both LDF and laser Doppler imaging were utilized to correlate skin blood flow to temperature changes. The two did not correlate at sites with arteriovenous shunts (115).

Central thermoregulatory mechanisms affect the postural vasoconstrictor response. Following heating of the trunk with an electrical blanket, the postural fall in blood flow diminished in skin areas with relatively numerous arteriovenous shunts (plantar surface of the big toe) (116). In contrast, areas with only few or no arteriovenous shunts (dorsum of the foot) displayed similar postural flows before and after heating. Therefore, partial release of sympathetic vasoconstrictor tone associated with indirect heating appears to override the local postural control of cutaneous vascular tone in areas where arteriovenous anastomoses are relatively numerous. When measured at heart level, the indirect heating was accompanied by a significant increase in foot blood flow. Many experiments, utilizing both LDF and other techniques, support the view that this reflex thermoregulatory vasodilatation is mainly due to the release of sympathetic vasoconstrictor tone, induced by the elevated core temperature. The normal postural fall in foot skin blood flow was preserved within the skin temperature range of 26 to 36°C, but at higher temperatures it was markedly attenuated or even abolished (117). This might contribute to some of the problems of cardiovascular adaptations seen in hot environment.

The skin microcirculatory reaction to internally and externally applied cold stimuli was measured by LDF. Results showed a decrease in the microcirculation after external stimulation, while no reaction was detected in response to internal stimulations. Repetitive stimulations evoked slow habituation (118).

The influence of room temperature on peripheral flow in healthy subjects and patients with peripheral vascular disease was followed by LDF (119). The flow was very little affected when the room temperature was increased from 24 to 30°C; therefore, this range is suitable for skin blood flow studies. For temperatures higher than 30°C the peripheral circulation increased. The relationship between skin flow and room temperature was linear in room temperatures between 23 and 30°C, whereas between 30 and 35°C it was curvilinear.

3. Flushing and Facial Pallor

Flushing, a transient reddening of the face and other body sites, is caused by vasodilatation, which may be provoked by many pharmacologic and physiologic reactions. Emotionally provoked blushing was recorded in the forehead by LDF. There was a sudden increase of blood flow, which returned to baseline value after approximately three minutes (120).

Other provoking factors are alcohol and conditions such as menopause, carcinoid, mastocytosis, or drugs, like nicotinic acid (121). Flushing occurs after orchidectomy for carcinoma of the prostate, and LDF measurements correspond closely to the intensity of the attacks as experienced by the patients and also to the measurement of sweating by evaporimetry (122).

The LDF technique is appropriate for quantitative assessment of alcohol-provoked flushing. Comparing LDF to the change in molar thermal circulation index, a linear correlation was found between the two methods. Moreover, the LDF method was more specific and more sensitive (123). The effects of various therapeutic modalities for facial flushing and rosacea were thus studied.

Systemic administration of nicotinic acids produces a generalized cutaneous erythema, partially mediated by prostaglandin biosynthesis. To further examine the mechanism, local cutaneous vasodilatation was studied following topical application of methyl nicotinate (124). Pretreatment with prostaglandin inhibitors (indomethacin, ibuprofen, and aspirin) significantly suppressed the erythemal response, while doxepin had no effect on this response. Arginine vasopressin was infused in high levels, comparable to those attained during physical stress, and a marked facial pallor in healthy men resulted (125). The pallor was objectively verified by LDF measurements, consistent with a fall in nutritional blood flow to the skin. In contrast, blood flow to the finger rose, indicating an increased blood flow through arteriovenous shunts. Thus, LDF assisted in determining that arginine vasopressin has a selective vasoactive effect in the skin.

4. Physical Activity

Cutaneous microvascular blood flow on the dorsum of the hand (non-glabrous skin) and on the finger pulp (glabrous skin) was measured by LDF. Endothelium-dependent vasodilation was assessed by an iontophoretic application of acetylcholine on the dorsum of the hand and by an induction of post-occlusive reactive hyperemia on the finger pulp. Endothelium-independent vasodilation was assessed on the dorsum of the hand by iontophoretically applied sodium-nitroprusside. The acetylcholine-evoked increase in LDF was significantly greater in the group of cyclists as compared with controls. In contrast, sodium-nitroprusside produced a significantly smaller response in the group of cyclists. Thus, a greater vasodilator capacity of endothelium in glabrous as well as in non-glabrous skin was demonstrated in the group of physically trained subjects. In addition, regular physical activity also modified the reactivity of vascular smooth muscle cells (126). Another study using similar methods (acetylcholine, sodium nitroprusside, and post-occlusive reactive hyperemia) found that athletes have higher endothelial activity than less trained individuals (127).

Another study found that postischemic LDF was significantly lower in nonathletic subjects than in athletes. In both groups the hyperemic stimulus significantly increased LDF. The flow reserve, estimated as peak/basal LDF, was significantly lower in control subjects than in athletes (128).

5. Smoking

Studies suggest an abnormality in capillary blood flow and its regulation in the skin as an immediate result of cigarette smoking, and a chronic effect as well (13).

Cigarette smoking triggers the release of vasopressin: A significant correlation was found between the skin blood flow response to cigarette smoking and the plasma vasopressin levels after smoking (129). The vasopressin released may mediate some of the vasoconstriction, since pretreatment with a vasopressin antagonist reduced the nicotine-induced vasoconstriction in the skin while vasopressin antagonist alone had no effect.

Calcium ions may play a role in the pathogenesis of the vasoconstriction caused by acute smoking. Elderly habitual smokers were given the calcium-channel blocker-nifedipine, and calcitonin—a hypocalcemizing hormone that has a vasoactive action. Both drugs prevented the LDF measured vasoconstriction induced by cigarette smoking, indicating that the process is calcium mediated (130).

The vasodilatory response of the skin microvasculature was impaired in subjects who have smoked cigarettes for many years, involving both endothelium-dependent and endothelium-independent responses. Both acetylcholine- and sodium-nitroprusside–induced skin-blood-flow increases were significantly attenuated in comparison with nonsmokers. Heart rate was also significantly blunted (131). Vascular responsiveness is altered even in light smokers compared to control subjects. The total hyperaemic response was approximately 45% smaller in smokers compared to nonsmoker controls (132).

These and other studies illuminate some of the mechanisms involved in the changes of the microvascular bed in the skin of habitual smokers, and reveal both acute and chronic changes. Chronic changes occur relatively early in a person's smoking history, but later they become more severe. It would be interesting to assess the correlation between these skin blood flow changes and the future development of peripheral vascular disease in a long-term study.

6. Pregnancy and Gestational Hypertension

Both normal and hypertensive pregnancy manifest microvascular changes. In gestational hypertension baseline blood flow on the fingertip was lower than in normal pregnancy, but this measurement could not discriminate between these subjects and nonpregnant healthy controls (12). Provocative tests were then used (isometric test, cognitive test, reactive hyperemia test, and thermal test), and the isometric test gave the most discriminative results. The control group showed a larger decrease than both the normal pregnancy group and the gestational hypertension group. Gestational hypertension showed a larger decrease than the normal pregnancy group. The cognitive test and the postischemic reactive hyperemia allowed some degree of discrimination, whereas the thermal test did not show any abnormality in the pregnant groups. Thus LDF recording of the response to vasoactive stimuli may differentiate between groups of subjects with normal or hypertensive pregnancy and nonpregnant subjects. Normal pregnancy modifies the response of the skin microvasculature to some vasoactive stimuli, whereas gestational hypertension pushes that response back toward the nonpregnant state. However, the method cannot yet be applied as a diagnostic tool for the individual patient.

7. Hypertension

Hypertension is associated with, or even originates from, an increased total peripheral resistance. The skin microvasculature plays a role in this peripheral resistance, hence the importance of its investigation in hypertension.

The decrease of skin blood flow that follows smoking of two cigarettes was measured in hypertensive habitual smokers (133). The same measurements were done before any treatment and following intravenous administration of alpha-1 inhibition with doxazosin and beta-1-blockade with atenolol. Skin blood flow decreased under all the above conditions, but the decrease was attenuated by doxazosin compared to atenolol. These findings indicate that selective alpha-1 adrenoceptors have a major effect on smoking-induced cutaneous vasoconstriction. In this respect doxazosin is preferable to atenolol for the antihypertensive treatment of patients who smoke.

In hypertensive patients both the resting flow and the standing flow to the feet were significantly lower, but increased after nifedipine treatment (24). The venoarteriolar reflex was lower in hypertensive patients, improving after nifedipine treatment, but still below normal.

Side effects of treatments and their mechanisms may be studies by LDF. Following nifedipine treatment, a weaker venoarteriolar reflex was observed in patients who developed ankle edema, whereas before treatment their response did not differ from those who did not develop edema (134). In another study, calcium channel blockers of different chemical origins antagonized postural vasoconstriction in the skin of the dorsum of the foot, indicating altered postural capillary blood flow regulation (135). Fluid filtration to the extravascular compartment may then eventuate, which may explain ankle edema during treatment with calcium channel blockers.

The cutaneous postischemic reactive hyperemia response does not seem to differentiate between hypertensive patients and normotensive controls (14,136). Thus, a few provocative tests were able to detect differences between hypertensive patients and controls, while other tests could not.

8. Peripheral Vascular Disease

The adequacy of skin blood flow in the ischemic extremity is an important determinant in the assessment of the severity of peripheral vascular disease. Old and young healthy volunteers were compared to patients with lower limb atherosclerosis and intermittent claudication and patients with lower limb atherosclerosis and critical ischemia (137). Elderly controls had higher flux values in the toe compared with claudicators, while claudicators had higher perfusion values than patients with critical ischemia.

Using the ratio between toe and finger flows narrows the range of the results, eliminating differences in cardiac output that occur from patient to patient; this method was able to distinguish between a group of healthy controls and a group of patients with peripheral vascular disease (138). The same technique was useful for evaluating patients with peripheral arterial disease and for distinguishing different etiologies of the disease (25). Patients with intermittent claudication, patients with rest pain and those with critical foot ischemia had a significantly lower resting flow than normal. Healthy controls showed a reduction of skin blood flow on standing, which was smaller in patients with severe claudication. Patients with rest pain had higher skin blood flow values when standing, indicating a loss of the vasomotor tone and an increase of flow determined by gravity. The inverse effect of an increase

in blood flow with standing was associated with the clinical improvement when the patients lowered their limbs (25).

Microcirculatory alterations in limbs with claudication were found, with early occurrence of microcirculatory compensation to atherosclerotic disease of increasing severity (139). The skin perfusion increased with dependency, which explains why patients obtain relief of pain with dependency.

Skin blood flow is an important determinant of healing of ulcers or an inevitable amputation. The baseline skin blood flow in patients with peripheral vascular disease was significantly lower than normal, and the pulse waves attenuated or absent (140). In indeterminate cases, the accuracy of the LDF method could be enhanced by the use of reactive hyperemia.

Using provocative tests, there was a correlation between the impairment of the LDF results and the gravity of the clinical picture, significant differences being recorded between limbs with no sign of necrosis and limbs affected by slight necrosis (141). In patients with pain at rest, postischemic hyperemia was absent. Following therapy with intraarterial administration of naftidrofuryl, a statistically significant improvement in several LDF assessed parameters was achieved, and treatment of four limbs with percutaneous transluminal angioplasty resulted in a completely normal test, matching the disappearance of all the symptoms caused by the peripheral occlusive arterial disease.

A reduction in the postischemic reactive hyperemia was found in patients with leg ulcers, with a sensitivity comparable to the measurements of distal systolic blood pressure (142). The healing effect of peripheral sympathectomy and pain relief were also monitored by LDF (143).

These studies again demonstrate that appropriate physiologic tests like hydrostatic pressure loading and postischemic reactive hyperemia test, are more indicative of abnormalities than are static parameters like resting flow. LDF can also provide explanations to therapeutic effects, like that of CO_2 baths in occlusive arterial disease, where an increased skin blood flow and increased oxygen utilization were observed (144).

The microcirculation under compression bandages has been assessed by LDF, demonstrating flow changes related to the cuff pressure, making it possible to assess the microcirculation through intact bandages, without the need to place any sensors at the skin–bandage interface (145).

9. *Diabetes Mellitus*

Diabetes mellitus is the most illustrative disease for the application of skin blood flow measurements, its microangiopathic changes serving as a natural target for LDF application to probe the disease's various aspects. Skin blood flow is affected in diabetes, either directly or via the nervous system, as exemplified by deficient responses in the fingertip that resembles premature aging (146). LDF was widely used in studying the process of diabetes mellitus and the etiology of its various complications, in grading disease severity, predicting its outcome, and following treatment. Damage to the microcirculation in diabetes mellitus is responsible for a great number of its grave complications. The neuropathy that further affects the microcirculation adds to the diversity and complexity of the disease, making the exposure of its yet unsolved aspects even more intriguing and rewarding. An understanding of the mechanisms responsible for microvascular complications may help in developing new treatment modalities. Furthermore, detection of early functional

changes in the microcirculation might identify patients at risk at a reversible stage. The possibility of using the skin as a model for diabetic microangiopathy, and its correlation to retinopathy and nephropathy are still under investigation.

Insulin-Dependent Diabetes Mellitus (IDDM). A normal physiological fall in cutaneous blood flow following food ingestion was demonstrated by LDF measurements. This fall was attenuated in IDDM. These abnormalities of vasoconstriction in the peripheral microcirculation were present after eight years of diabetes and preceded the development of clinically apparent neuropathy or vascular disease (147).

Using a thermal probe for provocation, blood flow values were lower than normal at 35°C, and this difference was even more pronounced at 44°C (148). Retinopathy and nephropathy were also associated with such a decrease.

Sympathetic neural dysfunction was indicated by reduction of vasoconstrictor responses to contralateral arm cold challenge and body cooling, and also to inspiratory gasp (20). Vascular disturbances measured on the dorsum of the hand seemed to be exaggerated by parasympathetic neuropathy (149).

Skin microvascular vasodilator response to both injection trauma and local thermal injury was impaired in IDDM, unrelated to diabetic control (18). This impairment in response to injury may be an important factor in the development of foot ulceration that often follows minor trauma. In order to investigate the mechanisms underlying the impaired hyperemia to local injury, substance P was intradermally injected and a reduced peak response was achieved in IDDM patients as compared to controls, whereas the response to capsaicin was the same (150). Following histamine blockade with chlorpheniramine, the response to capsaicin remained unaltered, while the response to substance P was reduced in both groups. Therefore, impaired skin hyperemia may represent decreased vascular reactivity to locally released substance P from peripheral nerve fibers.

Structural pathology in early diabetic neuropathy is best correlated to peroneal-motor conduction velocity (151). Transcutaneous oxygen and LDF measurements were correlated with peroneal-motor conduction velocity in IDDM patients, suggesting that hypoxia generates diabetic peripheral neuropathy, and that in early neuropathy, therapeutic measures to improve blood flow might arrest its progress. Indeed, pentoxifylline treatment (400 mg three times daily) increased the skin blood flow in the lower extremity, as measured after three and six months of therapy (152).

Nociceptive C fibers were evaluated by measuring the axon reflex vasodilatation of the foot in response to electrophoresis of acetylcholine, to direct mechanical stroke with a dermograph, and to a deep inspiratory gasp (27). The flare was reduced only in patients with foot complications, and it correlated with the clinical diminution of pain sensation, both are components of nociceptive C fiber function. Reduction of the flare indicated an impairment of neurogenic inflammatory response, which, along with an impairment of the protective pain sensation, may be a contributory factor in the poor and slow healing of foot lesions of diabetic patients. Since sympathetic vasoconstrictor reflexes were present in most diabetic patients with foot ulceration, the role of autonomic neuropathy in ulcer development is questioned.

Similar results were obtained by measuring the flare induced by acetylcholine iontophoresis at various current strengths (153). Maximum flare response was reduced in neuropathic patients, especially those with a previous history of foot ulceration, suggesting that small fiber neuropathy affects ulcer development. The flare was also reduced in some patients with retinopathy without neuropathy, suggesting an early loss of small nociceptor C fibers, preceding large fiber neuropathy. The curve of the hyperemic response plotted against current strength did

not show a rightward shift, indicating that the abnormal response was due to axonal loss rather than to dysfunction. The flare did not correlate with the cardiac autonomic function.

Non-insulin-dependent Diabetes Mellitus (NIDDM). Subjects at risk of developing NIDDM who have fasting hyperglycemia exhibited decreased microvascular hyperemia, positively correlated with insulin sensitivity and negatively correlated with fasting plasma insulin concentrations (154). Thus, hyperinsulinemia as a result of insulin resistance may affect the microvascular function in the prediabetic state.

Noncritically ischemic feet have a higher hyperemic response in comparison with critically ischemic feet (155).

The venoarteriolar response was lower in diabetic patients than in healthy controls, and lowest in patients with neuropathy (26). Both the increased skin blood flow and the impaired venoarteriolar reflex are causes of edema and may contribute to the thickening of capillary basement membranes detected in diabetes.

A hyperthermal LDF was developed to quantify autonomic dysfunction in the skin (156). The technique measures the time to induction of an increase of microcirculation following hyperthermia. Autonomic dysfunction was found in diabetic patients even with a short disease duration, suggesting that it was an early complication of NIDDM, even when the disease was well controlled.

Investigations of the sympathetic nervous function in NIDDM showed that deep breathing induced a decrease in skin blood flow (157). Many other neurovascular functional tests in experimental and human diabetes were studied (158).

Diabetes induces functional microvascular disturbances in the forearms. The cutaneous postischemic reactive hyperemia response was significantly lower than in nondiabetic controls (14). Retinopathy was a further factor in achieving more abnormal results. Evaluation of beraprost sodium treatment revealed a decreased effect when the severity of retinopathy and nephropathy increased (159).

Evaluation of Treatment. A variety of treatment modalities were assessed by LDF, starting with simple physical measures like elastic stockings, through old and new medications, to evaluation of a combined kidney and pancreas transplantation. Elastic stockings repressed the deterioration of the microcirculation, as was shown by LDF studies (160). The effect of an angiotensin converting enzyme inhibitor, captopril, was studied on IDDM (161). It improved skin blood flow, as measured with LDF using postocclusive reactive hyperemia response, and this was independent of its hypotensive effect.

In NIDDM, during insulin infusion foot blood flow was redistributed with an increase in capillary flow relative to arteriovenous shunt flow (162). Since blood that passes through arteriovenous shunts does not enter the capillary bed and plays no role in skin nutrition, this represents an improvement in the skin nutrition.

Hypoglycemia, but not hyperinsulinemia, caused a regional skin vasodilatation in healthy control subjects. Following a hyperinsulinemic euglycemic clamp, hypoglycemia was induced by a stepwise reduction in the intravenous glucose infusion. The increase in blood flow that was observed in healthy controls was absent in patients with non-insulin-dependent diabetes mellitus (163).

Defibrotide, an oral profibrinolytic drug, was given to non-insulin-dependent diabetic patients with microangiopathy. The microcirculation was evaluated by the venoarteriolar response and by the rise in skin blood flow following local heating, both decreased in diabetic patients. Following six months of treatment, patients in the new drug treatment group improved their microcirculatory parameters

(venoarteriolar reflex) in association with an improvement in signs and symptoms (164). Calcium channel blockers were also evaluated with LDF (165).

A combined kidney and pancreas transplantation improved the skin microvascular reactivity; therefore, the possibility that transplantation could reverse or halt diabetic complications was studied (23). Skin blood flow at rest, postischemic reactive hyperemia and venoarteriolar reflex at 2 and 38 months following transplantation were measured. The rest blood flow was higher 38 months following transplantation as compared to two months, but the delayed time to peak during hyperemia was even more impaired at 38 months. This is probably due to a disturbed function of the smooth muscle cells of the vessel wall, and might indicate a progress of structural changes in spite of an improved metabolism. The veno-arteriolar reflex was also impaired at both time points, probably due to neuropathy, since this reflex depends on an intact sympathetic nerve function. A trend for improvement in four out of five patients with the most impaired reflex was observed, but it did not reach statistical significance, still might be indicating that diabetic neuropathy can be improved after transplantation (23). Laser Doppler perfusion imaging of patients with diabetic neuropathy showed skin vasodilation following topical application of methyl nicotinate at the forearm and foot levels, suggesting a potential of methyl nicotinate to increase blood flow and to prevent diabetic foot problems (166).

These and other studies indicate that LDF can be useful in the investigation of some diabetes pathophysiological mechanisms, disease severity, and the efficacy of its control.

10. Raynaud's Phenomenon

The intermittent blanching that occurs in Raynaud's phenomenon believably results from an active microvascular vasoconstriction and emptying. Therefore, LDF is useful for the investigation of the pathophysiological mechanisms underlying Raynaud's phenomenon and for evaluating treatments.

To clarify the etiology of Raynaud's phenomenon three vasodilators were intravenously administered, and the response of CGRP was compared with that of endothelium-dependent adenosine triphosphate and the endothelium-independent prostacyclin (167). The first vasodilator induced an increase in blood flow in the hands of patients but not in healthy controls, which may reflect a deficiency of endogenous CGRP release in Raynaud's phenomenon.

The role of the histaminergic and peptidergic axes in primary Raynaud's phenomenon was also studied (29,30). Digital blood flow response to intradermal injections of saline, histamine, histamine-releasing agent (compound 48/80), substance P, and CGRP was measured. No evidence of local deficiency in histamine release or in the response to histamine was found (30), even at low temperatures (29), and the patients reacted normally to the neuropeptides substance P (29,30) and CGRP (30), providing a rationale for treating Raynaud's phenomenon with vasoactive peptides.

Digital skin blood flow of both hands was measured during local heating of only one hand. Patients with Raynaud's phenomenon showed a decreased digital blood flow during stepwise cooling in both hands, but the reaction in the cooled hand was more pronounced and more consistent (168).

Patients with Raynaud's phenomenon had an abnormal vascular response to temperature change (32). Studying the hyperemic response to local skin warming, the patients showed vasodilatation at lower skin temperatures than normal, independent

of central sympathetic control. Knowledge of skin temperature is therefore important for the interpretation of blood flow studies in Raynaud's phenomenon. Provocative testing (occlusion) under different degrees of finger and body cooling detected an increase in the number of fingers of patients exhibiting vasospasm as the severity of cooling increased (169).

Occupational exposure to vibrations causes Raynaud's phenomenon. For prevention and treatment of vibration syndrome, an objective test was developed, combining LDF with finger cooling (170). It enabled the demonstration of significant differences among four groups: subjects without vibration exposure, subjects with exposure but with no signs of white fingers, subjects with few attacks, and subjects with frequent attacks.

In patients with Raynaud's phenomenon suffering from scleroderma, blood flow decrease during cooling was similar to healthy controls, but the patients had a longer rewarming period (171). In such patients, when resting blood flow was very low, the postischemic reactive hyperemia response was absent (172). After warming the hand in warm water, the hyperemic response was restored and its magnitude corrected, but its time course was longer, with a delay to achieving maximum flow as compared to controls. This may be related to changes in the vessels themselves, or to connective tissue sclerosis limiting the rate of response.

Provocative tests, which evoke sympathetic tone, like the isometric test, were studied in addition to temperature measurements in groups of patients with primary Raynaud's phenomenon, systemic sclerosis, and undifferentiated connective tissue disease as compared to a control group (173). Considerable differences were found in both the level of vessels involved and the relative importance of local finger temperature and discrimination between various etiologies of Raynaud's phenomenon was possible.

Cutaneous post-occlusive reactive hyperemia enabled grading obstructive vascular disease in groups of patients with Raynaud's phenomenon, but could not discriminate among individuals in the subgroups (174). Another provocative test, the cognitive test, detected two subgroups within the patients with Raynaud's phenomenon (175). The first subgroup showed a reduction in blood flow similar to healthy controls, whereas the second showed a paradoxical increase, suggesting an organic etiology.

The LDF was used to evaluate various treatment modalities in Raynaud's phenomenon. Thus, a single topical application of minoxidil 5% solution to the fingers was ineffective (176). Ketanserin, an antagonist of the serotonin-2-(5-HT-2)-receptor, was given to nine patients with generalized scleroderma (177). Finger systolic pressure and LDF after cooling and rewarming of the finger did not improve. Thus, ketanserin in the doses used (20 mg three times a day in the first week and 40 mg three times a day for four weeks) was not effective in the treatment of Raynaud's phenomenon in generalized scleroderma. When given to patients with primary Raynaud's phenomenon, ketanserin normalized digital blood flow (178). Pretreatment with alpha-adrenoceptor antagonists did not abolish this effect, suggesting that in contrast to the effects on the systemic circulation, the mechanism underlying digital vasodilatation after ketanserin does not involve alpha-adrenoceptor antagonism.

Application of the vasodilator hexyl nicotinate at various sites on the upper limb resulted in an increase in blood flow both in patients with Raynaud's phenomenon (13 with primary Raynaud's disease and 12 with systemic sclerosis and

Raynaud's phenomenon) and in normal subjects (179). Moreover, increasing the drug concentration increased flow rate.

The effect of nifedipine on perniosis was also studied. An increase in blood flow to a finger or a toe adjacent to a diseased one could be demonstrated after the drug intake (180).

11. Other Diseases

Several diseases, like leprosy, have distinct skin lesions, which may be followed up by LDF. Blood flow in lesions of leprosy paralleled the clinical appearance and histopathology of the lesions during treatment (181,182). The amount of hyperemia was useful in monitoring the early changes of reversal reaction during chemotherapy. The LDF was also valuable to evaluate peripheral autonomic function in leprosy (183). The skin overlying Kaposi's sarcoma was also studied by LDF (184).

The LDF was also used to investigate microvascular physiology in patients with sickle-cell disease (185). Large local oscillations in skin blood flow to the arm were demonstrated, occurring simultaneously at sites separated by 1 cm, suggesting a synchronization of rhythmic flow in large domains of microvessels. The periodic flow may be a compensatory mechanism to offset the deleterious altered rheology of erythrocytes in sickle-cell disease.

Changes in skin microvascular reactivity were demonstrated in hypertriglyceridemia (186), and even in Alzheimer's disease (187,188).

In a study involving very low cardiovascular risk female population of 862 healthy females screened for cardiovascular risk factors, a significant correlation was observed between the weight of cardiovascular risks and the impairment of postischemic forearm skin reactive hyperemia. Thus, skin LDF may represent a valuable, simple, and noninvasive tool to assess and monitor microvascular function in future prospective observational and interventional studies (189).

V. CONCLUSION AND FUTURE PROSPECTS

The LDF method allows real-time analysis of a wide range of physiological and pathological processes, as well as pharmacological processes and percutaneous penetration. It provides objective numerical data at various time points or at various skin sites. However, results obtained by LDF should not be interpreted as absolute values, but should rather serve as relative estimates. It should be noted that results obtained by different instruments or by the same instrument in different subjects cannot be compared. Furthermore, biological variations within the disease state can also produce discord between different studies. There is a need, therefore, for technical improvements, for calibration standards, better probe designs, and more reproducible measuring procedures before LDF turns into a useful clinical tool. Improvements may lead to a wider use in the area of skin pharmacology, which naturally requires accuracy and repeatability.

An important development was the laser Doppler imaging (scanning LDF) (28), which, quickly and sequentially, remotely scans the tissue perfusion in several-thousand-measurement points. A map of the spatial distribution of the blood flow is thus obtained. Unlike regular LDF, which continuously records the blood flow over a single point, the laser Doppler imaging maps the blood flow distribution over a specific area. Thus, the two methods do not compete with each other, but are rather

complementary. The laser Doppler imaging has the advantage of operating without any contact with the skin surface, and, therefore, it does not disturb the local blood flow. A software module was implemented in the laser Doppler imaging, resulting in a duplex mode for recording both spatial and temporal blood perfusion components (190). Another new device combines laser Doppler perfusion imaging and digital photography, with many clinical applications like evaluating grafts or treatment of leg ulcers (191). It has also been used for mapping the vulvar skin blood flow in psoriasis or lichen sclerosus with invasive neoplasia, demonstrating increased perfusion in vulvar cancer (192).

Other improvements in laser Doppler are the introduction of advanced computerization and the development of new probes, such as multisite probes allowing simultaneous measurements at several sites, multi-subject probes allowing simultaneous measurements of several subjects. These developments are accompanied by multichannel LDF instruments capable of simultaneous collection of data from many independent probes. Finally, a new probe holder design (7) permits repeated measurements over the same site before and after manipulations to the skin.

Technical innovations have improved the accuracy and repeatability of LDF, making it useful as a clinical tool. The multitude of published reports of the last years clearly indicates an increased interest in LDF and its multiple uses in diverse clinical and investigational areas.

REFERENCES

1. Molitor H, Kniazuk M. A new bloodless method for continuous recording of peripheral circulatory changes. J Pharmacol Exp Ther 1936; 57:6–18.
2. Hertzman AB. Photoelectric plethysmography of the fingers and toes in man. Proc Soc Exp Biol Med 1937; 37:529–534.
3. Stern MD. In vivo evaluation of microcirculation by coherent light scattering. Nature 1975; 254:56–58.
4. Holloway GA, Watkins DW. Laser Doppler measurement of cutaneous blood flow. J Invest Dermatol 1977; 69:306–309.
5. Nilsson GE, Tenland T, Oberg PA. A new instrument for continuous measurement of tissue blood flow by light beating spectroscopy. IEEE Trans Biomed Eng 1980; 27: 12–19.
6. Tur E. Cutaneous blood flow: laser Doppler velocimetry. Int J Dermatol 1991; 30: 471–476.
7. Braverman IM, Schechner JS. Contour mapping of the cutaneous microvasculature by computerized laser Doppler velocimetry. J Invest Dermatol 1991; 97:1013–1018.
8. Nagashima Y, Yada Y, Suzuki T, Sakai A. Development and clinical application of an integration type laser Doppler flowmeter equipped with temperature-load instrument for skin blood flow. Jpn J Appl Physiol 2001; 31:295–304.
9. Wardell K, Naver HK, Nilsson, GE, Wallin BG. The cutaneous vascular axon reflex characterized by laser Doppler perfusion imaging. J Physiol 1993; 460:185–199.
10. Speight EL, Essex TJH, Farr PM. The study of plaques of psoriasis using a scanning laser–Doppler velocimeter. Br J Dermatol 1993; 128:519–524.
11. Speight EL, Farr PM. Erythemal and therapeutic response of psoriasis to PUVA using high-dose UVA. Br J Dermatol 1994; 131:667–672.
12. Liu D, Svsanber K, Wang I, Andersson-Engels S, Svanberg S. Laser Doppler perfusion imaging: new technique for determination of perfusion of splanchnic organs and tumor tissue. Lasers Surg Med 1997; 20:473–479.

13. Tur E, Tamir A, Guy RH. Cutaneous blood flow in gestational hypertension and normal pregnancy. J Invest Dermatol 1992; 99:310–314.
14. Tur E, Yosipovitch G, Oren-Vulfs S. Chronic and acute effects of cigarette smoking on skin blood flow. Angiology 1992; 43:328–335.
15. Tur E, Yosipovitch G, Bar-On Y. Skin reactive hyperemia in diabetic patients. Diabetes Care 1991; 14:958–962.
16. Wilkin JK, Trotter K. Cognitive activity and cutaneous blood flow. Arch Dermatol 1987; 123:1503–1506.
17. Weinstein L, Janjan N, Droegemueller W, Katz MA. Forearm plethysmography in normotensive and hypertensive pregnant women. South Med J 1981; 74:1230–1232.
18. Low PA, Neumann C, Dyck PJ, Fealey RD, Tuck RR. Evaluation of skin vasomotor reflexes by using laser–Doppler velocimetry. Mayo Clin Proc 1983; 58:583–592.
19. Allen J, Frame JR, Murray A. Microvascular blood flow and skin temperature changes in the fingers following a deep aspiratory gasp. Physiol Meas 2002; 23:365–373.
20. Rayman G, Williams SA, Spencer PD, Smaje LH, Wise PH, Tooke JE. Impaired microvascular hyperaemic response to minor skin trauma in type I diabetes. Br Med J 1986; 292:1295–1298.
21. Mayrovitz NH, Smith J, Delgado M. Variability in skin microvascular vasodilatory responses assessed by laser Doppler imaging. Ostomy Wound Manage 1997; 43:66–70.
22. Khan F, Spence VA, Belch JJF. Cutaneous vascular responses and thermoregulation in relation to age. Clin Sci 1992; 82:521–528.
23. Roskos KV, Bircher AJ, Maibach HI, Guy RH. Pharmacodynamic measurements of methyl nicotinate percutaneous absorption: the effect of aging on microcirculation. Br J Dermatol 1990; 122:165–171.
24. Shami SK, Chittenden SJ. Microangiopathy in diabetes mellitus: II Features, complications and investigation. Diabetes Res 1991; 17:157–168.
25. Jorneskog G, Tyden G, Bolinder J, Fagrell B. Skin microvascular reactivity in fingers of diabetic patients after combined kidney and pancreas transplantation. Diabetologia 1991; 34:S135–S137.
26. Cesarone MR, Laurora G, Belcaro GV. Microcirculation in systemic hypertension. Angiology 1992; 43:899–903.
27. Belacro G, Nicolaides AN. Microvascular evaluation of the effects of nifedipine in vascular patients by laser–Doppler flowmetry. Angiology 1989; 40:689–694.
28. Belacro G, Nicolaides AN. The venoarteriolar response in diabetics. Angiology 1991; 42:827–835.
29. Parkhouse N, Le Quesne PM. Impaired neurogenic vascular response in patients with diabetes and neuropathic foot lesions. N Engl J Med 1988; 318:1306–1309.
30. Wardell K, Naver HK, Nilsson GE, Wallin BG. The cutaneous vascular axon reflex characterized by laser Doppler perfusion imaging. J Physiol 1993; 460:185–199.
31. Bunker CB, Foreman JC, Dowd PM. Vascular responses to histamine at low-temperatures in normal digital skin and Raynaud's phenomenon. Agents Actions 1991; 33:197–199.
32. Bunker CB, Foreman JC, Dowd PM. Digital cutaneous vascular responses to histamine and neuropeptides in Raynaud's phenomenon. J Invest Dermatol 1991; 96:314–317.
33. Maurel A, Hamon P, Macquin-Mavier I, Largue G. Cutaneous microvascular flow studied by laser–Doppler. Presse Med 1991; 20:1205–1209.
34. Walmsley D, Goodfield MJD. Evidence for an abnormal peripherally mediated vascular response to temperature in Raynaud's phenomenon. Br J Rheumatol 1990; 29:181–184.
35. Gean CJ, Tur E, Maibach HI, Guy RH. Cutaneous responses to topical methyl nicotinate in black, oriental and caucasian subjects. Arch Dermatol Res 1989; 281:95–98.
36. Belch JJ, Mclaren M, Lau CS, Mackay IR, Bancroft A, McEwen J, Thompson JM. Cicaprost, an orally active prostacycline analogue: its effects on platelet aggregation and skin blood flow in normal volunteers. Br J Clin Pharmacol 1993; 35:643–647.

37. Drummond PD, de Silva-Rossdeutscher E. Transcutaneous iontophoresis of methadone provokes local flushing and thermal hyperalgesia. Inflamm Res 2003; 52:366–371.
38. McElnay JC, Benson HA, Harland R, Hadgraft J. Phonopheresis of methyl nicotinate: a preliminary study to elucidate the mechanism of action. Pharm Res 1993; 10:1726–1731.
39. Ryatt KS, Stevenson JM, Maibach HI, Guy RH. Pharmacodynamic measurement of percutaneous penetration enhancement in vivo. J Pharmacol Sci 1986; 75:374–377.
40. Guy RH, Tur E, Schall LM, Elamir S, Maibach HI. Determination of vehicle effects on percutaneous absorption by laser Doppler velocimetry. Arch Dermatol Res 1986; 278:500–502.
41. Tur E, Maibach HI, Guy RH. Percutaneous penetration of methyl nicotinate at three anatomical sites: evidence for an appendageal contribution to transport? Skin Pharmacol 1991; 4:230–234.
42. Guy RH, Tur E, Bjerke S, Maibach HI. Are there age and racial differences to methyl nicotinate-induced vasodilatation in human skin? J Am Acad Dermatol 1985; 12: 1001–1006.
43. Berardesca E, Maibach HI. Racial differences in pharmacodynamic response to nicotinates in vivo in human skin: black and white. Acta Derm Venereol 1990; 70:63–66.
44. Reinberg AE, Soudant E, Koulbanis C, Bazin R, Nicolai A, Mechkouri M, Touitou Y. Circadian dosing time dependency in the forearm skin penetration of methyl and hexyl nicotinate. Life Sci 1995; 57:1507–1513.
45. Noon JP, Evans CE, Haynes WG, Webb DJ, Walker BR. A comparison of techniques to assess skin blanching following the topical application of glucocorticoids. Br J Dermatol 1996; 134:837–842.
46. Gardner-Medwin JM, Taylor JY, Macdonald IA, Powell RJ. An investigation into variability in microvascular skin blood flow and the responses to transdermal delivery of acetylcholine at different sites in the forearm and hand. Br J Clin Pharmacol 1997; 43:391–397.
47. Grossmann M, Jamieson MJ, Kellogg DL Jr, Kosiba WA, Pergola PE, Crandall CG, Shepherd AM. The effect of iontophoresis on the cutaneous vasculature: evidence for current-induced hyperemia. Microvasc Res 1995; 50:444–452.
48. Kollias N, Bager A, Sadiq I. Minimum erythema dose determination in individuals of skin types V and VI with diffuse reflectance spectroscopy. Photodermatol Photoimmunol Photomed 1994; 10:249–254.
49. Youn JI, Park SB, Park BS, Han WS. Comparative quantitative analysis of ultraviolet B-induced skin blood flow change using laser Doppler perfusion imaging technique. Photodermatol Photoimmunol Photomed 2000; 16:167–171.
50. Falk M, Ilias MA, Wardell K, Anderson C. Phototesting with a divergent UVB beam in the investigation of anti-inflammatory effects of topically applied substances. Photodermatol Photoimmunol Photomed 2003; 19:195–202.
51. Strange P, Skov L, Lisby S, Nielsen PL, Baadsgaard O. Staphylococcal enterotoxin B applied on intact normal and intact atopic skin induces dermatitis. Arch Dermatol 1996; 132:27–33.
52. Jemec GB, Heideheim M. The influence of sex hormones on UVB induced erythema in man. J Dermatol Sci 1995; 9:221–224.
53. Zacharie R, Oster H, Bjerring P. Effects of hypnotic suggestions on ultraviolet B radiation-induced erythema and skin blood flow. Photdermatol Photoimmunol Photomed 1994; 10:154–160.
54. Bjerring P. Comparison of the bioactivity of monetasone furoate 0.1% fatty cream, betamethasone dipropionate 0.05% cream and betamethasone valerate 0.1% cream in humans. Inhibition of UV-B-induced inflammation monitored by laser Doppler blood flowmetry. Skin Pharmacol 1993; 6:187–192.
55. Duteil L, Queille C, Poncet M, Czernielewski J. Processing and statistical analysis of laser Doppler data applied to the assessment of systemic anti-inflammatory drugs. J Dermatol Sci 1991; 2:376–382.

56. Denham KJ, Boutsiouki P, Clough GF, Church MK. Comparison of the effects of desloratadine and levocetirizine on histamine-induced wheal, flare and itch in human skin. Inflamm Res 2003; 52:424–427.
57. Nyren M, Ollmar S, Nicander I, Emtestam L. An electric impedance technique for assessment of wheals. Allergy 1996; 51:923–926.
58. Tur E, Aviram G, Zeltser D, Brenner S, Maibach HI. Regional variations of human skin blood flow responses to hitamine. Curr Probl Dermatol 1995; 22:50–66.
59. Dykes PJ, Black DR, York M, Dickens AD, Marks R. A step-wise procedure for evaluating irritant materials in normal volunteer subjects. Hum Exp Toxicol 1995; 14:204–211.
60. Tur E, Eshkol Z, Brenner S, Maibach HI. Cumulative effect of subthreshold concentrations of irritants in humans. Am J Contact Dermatitis 1995; 6:216–220.
61. Agner T. An experimental study of irritant effects of urea in different vehicles. Acta Derm Venereol (Stockh) 1992; 177:S44–S46.
62. Grunewald AM, Gloor M, Gehring W, Kleesz P. Damage to the skin by repetitive washing. Contact Dermatitis 1995; 32:225–232.
63. Marks R, Dykes PJ, Hamami I. Two novel techniques for the evaluation of barrier creams. Br J Dermatol 1989; 120:655–660.
64. Poelman MC, Piot B, Guyon F, Deroni M, Leveque JL. Assessment of topical non-steroidal anti-inflammatory drugs. J Pharm Pharmacol 1989; 41:720–722.
65. Levin CY, Maibach HI. Do coll water or physiplogic saline compresses enhance resolution of experimentally induced irritant contact dermatitis? Contact Dermatitis ; 45: 146–150.
66. Shriner DL, Maibach HI. Regional variations of non-immunologic contact urticaria. Functional map of the human face. Skin Pharmacol 1996; 9:312–321.
67. Larmi E. PUVA treatment inhibits non-immunologic immediate contact reactions to benzoic acid and methyl nicotinate. Int J Deramatol 1989; 28:609–611.
68. Johansson J, Lahti A. Topical non-steroidal anti-inflammatory drugs inhibit non-immunologic immediate contact rections. Contact Dermatitis 1988; 19:161–165.
69. Tur E. Age-related regional variations of human skin blood flow response to histamine. Acta Derm Venereol 1995; 75:451–454.
70. Fullerton A, Avnstorp C, Agner T, Dahl JC, Olsen LO, Serup J. Patch test study with calcipotriol ointment indifferent patient groups, including psoriatic patients with and without adverse dermatitis. Acta Derm Venereol 1996; 76:194–202.
71. Quinn AG, McLelland J, Esex T, Farr PM. Quantification of contact allergic inflammation: a comparison of existing methods with a scaning laser Doppler velocimeter. Acta Derm Venereol 1993; 73:21–25.
72. Quinn AG, McLelland J, Esex T, Farr PM. Measurement of cutaneous inflammatory reactions using a scaning laser Doppler velocimeter. Br J Dermatol 1991; 125:30–37.
73. Stucker M,Auer T, Hoffman K, Altmeyer P. Two-dimensional blood flow determinations in allergic reactions using laser Doppler scanning. Contact Dermatitis 1995; 33:299–303.
74. Artemi P, Seale P, Satchell P, Ware S. Cutaneous vascular response to calcitonin gene-related peptide in psoriasis and normal subjects. Australas J Dermatol 1997; 38:73–76.
75. Zachariae R, Oster H, Bjering P, Kragballe K. Effects of psychological intervention on psoriasis: a preliminary report. J Am Acad Dermatol 1996; 34:1008–1015.
76. Speight EL, Farr PM. Calcipotriol improves the response of psoriasis to PUVA. Br J Dermatol 1994; 130:79–82.
77. Yosipovitch G, Chan YH, Tay YK, Goh CL. Thermosensory abnormalities and blood flow dysfunction in psoriatic skin. Br J Dermatol 2003; 149:492–497.
78. Tur E, Tamir A, Tamir G, Brenner S. Psoriasis. In: Berardesca E, Elsner P, Maibach HI, eds. Bioengineering of the Skin: Cutaneous Blood Flow and Erythema. Part 2: Laser Doppler Velocimetry and Photoplethysmography. Boca Raton, Florida: CRC Press, 1995:123–131.

79. Hornstein OP, Boissevain F, Wittmann H. Non-invasive measurement of the vascular dynamics of dermographism—comparative study in atopic and non-atopic subjects. J Dermatol 1991; 18:79–85.
80. Vogelsang M, Heyer G, Hornstein OP. Acetylcholine induces different cutaneous sensations in atopic and non-atopic subjects. Acta Derm Venereol 1995; 75:434–436.
81. Fluhr JW, Pfisterer S, Gloor M. Direct comparison of skin physiology in children and adults with bioengineering methods. Pediatr Dermatol 2000; 17:436–439.
82. Nagashima Y, Yada Y, Suzuki T, Sakai A. Evaluation of the use of an integration-type laser–Doppler flowmeter with a temperature-loading instrument for measuring skin blood flow in elderly subjects during cooling load: comparison with younger subjects. Int J Biometeorol 2003; 47:139–147.
83. Van den Brande P, von Kemp K, De Coninck A, Debing E. Laser Doppler flux characteristics at the skin of the dorsum of the foot in young and in elderly healthy human subjects. Microvasc Res 1997; 53:156–162.
84. Kenney WL, Morgan AL, Farquhar WB, Brooks EM, Pierzga JM, Derr JA. Decreased active vasodilator sensitivity in aged skin. Am J Physiol 1997; 272:H1609–H1614.
85. Malanin K, Havu VK, Kolari PJ. Dynamics of cutaneous laser Doppler flux with concentration of moving blood cells and blood cell velocity in legs with venous ulcers and in healthy legs. Angiology 2004; 55:37–42.
86. Shami SK, Cheatle TR, Chittenden SJ, Scurr JH, Coleridge-Smith PD. Hyperaemic response in the skin microcirculation of patients with chronic venous insufficiency. Br J Surg 1993; 80:433–435.
87. Abu-Own A, Shami SK, Chittenden SJ, Farrah J, Scurr JH, Smith PD. Microangiopathy of the skin and the effect of leg compression in patients with chronic venous insufficiency. J Vasc Surg 1994; 19:1074–1083.
88. Schemeller W, Roszinski S, Huesmann M. Tissue oxygenation and microcirculation in dermatoliposclerosis with different degrees of erythema at the margins of venous ulcers. A contribution to hypodermitis symptoms. Vasa 1997; 26:18–24.
89. He CF, Cherry GW, Arnold F. Postural vasoregulation and mediators of reperfusion injury in venous ulceration. J Vasc Surg 1997; 25:647–653.
90. Gschwandtner ME, Koppensteiner R, Maca T, Minar E, Schneider B, Schnurer G, Ehringer H. Spontaneous laser Doppler flux distribution in ischemic ulcers and the effect of prostanoids: a crossover study comparing the acute action of prostaglandin E1 and iloprost vs saline. Microvasc Res 1996; 51:29–38.
91. Belcaro G, Cesarone MR, Nicolaides AN, Geroulakos G, Di Renzo A, Milani M, Ricci A, Brandolini R, Dugall M, Ruffini I, Cornelli U, Griffin M. Improvement of microcirculation and healing of venous hypertension and ulcers with Crystacide. Evaluation of free radicals, laser Doppler flux and PO2. A prospective-randomaized-controlled study. Angiology 2003; 54:325–330.
92. Cesarone MR, Belcaro G, Geroulakos G, Griffin M, Ricci A, Brandolini R, Pellegrini L, Dugall M, Ippolito E, Candiani C, Simeone E, Errichi BM, Di Renzo A. Flight microangiopathy on long-haul flights: prevention of edema and microcirculation alterations with Venoruton. Clin Appl Thromb Hemost 2003; 9:109–114.
93. Rithalia SV. Evaluation of alternating pressure air mattresses: one laboratory-based strategy. J Tissue Viability 2004; 14:51–58.
94. Tur E, Brenner S. Cutaneous blood flow measurements for the detection of malignancy in pigmented skin lesions. Dermatology 1992; 184:8–11.
95. Junger M, Steins A, Schlagenhauff B, Rassner G. Microcirculation of cutaneous melanoma. Hautarzt 1999; 50:848–852.
96. Ilias MA, Wardell K, Stucker M, Anderson C, Salerud EG. Assessment of pigmented skin lesions in terms of blood perfusion estimates. Skin Res Technol 2004; 10:43–49.
97. Wang I, Andersson Engels S, Nilsson GE, Wardell K, Svanberg K. Superficial blood flow following photodynamic therapy of malignant non-melanoma skin tumors measured by laser Doppler perfusion imaging. Br J Dermatol 1997; 136:184–189.

98. Gupta SC, Khiabani KT, Stephenson LL, Zamboni WA. Effect of liposuction on skin perfusion. Plast Reconstr Surg 2003; 112:1965.
99. Ribuffo D, Muratori L, Antoniadou K, Fanini F, Martelli E, Marini M, Messineo D, Trinci M, Scuderi N. A hemodynammic approach to clinical results in the TRAM flap after selective delay. Plast Reconstr Surg 1997; 99:1706–1714.
100. Place MJ, Witt P, Hendricks D. Cutaneous blood flow patterns in free flaps determined by laser Doppler flowmetry. J Reconstr Microsurg 1996; 12:355–358.
101. Niezgoda JA, Cianci P, Folden BW, Ortega RL, Slade JB, Storrow AB. The effect of hyperbaric oxygen therapy on a burn wound model in human volunteers. Plast Reconstr Surg 1997; 99:1620–1625.
102. Droog EJ, Steenbergen W, Sjoberg F. Measurement of depth of burns by laser Doppler perfusion imaging. Burns 2001; 27:561–568.
103. Riordan CL, McDonough M, Davidson JM, Corley R, Perlov C, Barton R, Guy J, Nanney LB. Non-contact laser Doppler imaging in burn depth analysis of the extremities. J Burn Care Rehabil 2003; 24:177–186.
104. Jeng JC, Bridgeman A, Shivnan L, Thornton PM, Alam H, Clarke TJ, Jablonski KA, Jordan MH. Laser Doppler imaging determines need for excision and grafting in advance of clinical judgment: a prospective blinded trial. Burns 2003; 29:665–670.
105. Monfrecola G, Moffa G, Procaccini EM. Non-ionizing electromagnetic radiations, emitted by a cellular phone, modify cutaneous blood flow. Dermatology 2003; 207:3–5.
106. Bernardi L, Hayoz D, Wenzel R, Passino C, Calciati A, Weber R, Noll G. Synchronous and baroceptor-sensitive oscillations in skin microcirculation: evidence for central autonomic control. Am J Physiol 1997; 273:H1867–H1878.
107. Ozbebit FY, Esen F, Gulec S, Esen H. Evaluation of forearm microvascular blood flow regulation by laser Doppler flowmetry, iontophoresis, and curve analysis: contribution of axon reflex. Microvasc Res 2004; 67:207–214.
108. Kolev OI, Nilsson G, Tibbling L. Influence of intense sound stimuli on skin microcirculation. Clin Auton Res 1995; 5:187–190.
109. Kano T, Shimoda O, Higashi K, Sadanaga M. Effects of neural blockade and general anesthesia on the laser Doppler skin blood flow waves recorded from the finger or toe. J Auton Nerv Syst 1994; 48:257–266.
110. Willette RN, Hieble JP, Sauermelch CF. The role of alpha adrenoceptor subtypes in sympathetic control of the acral-cutaneous microcirculation. J Pharmacol Exp Therap 1991; 256:599–605.
111. Mashimo T, Pak M, Choe H, Inagaki Y, Yamamoto M, Yoshiya I. Effects of vasodilators guanethidine, nicardipine, nitroglycerine, and prostaglandin E1 on primary afferent nociceptors in humans. J Clin Pharmacol 1997; 37:330–335.
112. Khan F, Kennedy G, Spence VA, Newton DJ, Belch JJ. Peripheral cholinergic function in humans with chronic fatigue syndrome, Gulf War syndrome and with illness following organophosphate exposure. Clin Sci (Lond) 2004; 106:183–189.
113. Elam M, Wallin BG. Skin blood flow responses to mental stress in man depend on body temperature. Acta Physiol Scan 1987; 129:429–431.
114. Yamashita K, Tochihara Y. Effects of hyperoxia on thermoregulatory responses during feet immersion to hot water in humans. J Physiol Anthropol Appl Human Sci 2003; 22:181–185.
115. Bornmyr S, Svensson H, Lilja B, Sundkvist G. Skin temperature changes and changes in skin blood flow monitored with laser Doppler flowmetry and imaging; a methodological study in normal humans. Clin Physiol 1997; 17:71–81.
116. Hassan AA, Rayman G, Tooke JE. Effect of indirect heating on the postural control of skin blood flow in the human foot. Clin Sci 1986; 70:577–582.
117. Hassan AA, Tooke JE. Effect of changes in local skin temperature on postural vasoconstriction in man. Clin Sci 1988; 74:201–206.
118. Kolev OI. Cutaneous microcirculatory reaction to externally and internally applied cold caloric stimuli and its habituation. Clin Auton Res 2003; 13:295–297.

119. Winsor T, Haumschild DJ, Winsor D, Mikail A. Influence of local and environmental temperatures on cutaneous circulation with use of laser Doppler flowmetry. Angiology 1989; 40:421–428.
120. Steurer J, Hoffman U, Bollinger A. Skin hyperemia in a habitual blusher. Vasa 1997; 26:135–136.
121. Tur E, Ryatt KS, Maibach HI. Idiopathic recalcitrant facial flushing syndrome. Dermatologica 1990; 181:5–7.
122. Frodin T, Alund G, Varenhorst E. Measurement of skin blood flow and water evaporation as a means of objectively assessing hot flushes after orchidectomy in patients with prostate cancer. The Prostate 1985; 7:203–208.
123. Wilkin JK. Quantitative assessement of alcohol-provoked flushing. Arch Dermatol 1986; 122:63–65.
124. Wilkin JK, Fortner G, Reinhardt LA, Flowers OV, Kilpatrick SJ, Streeter WC. Prostaglandins and nicotinate-provoked increase in cutaneous blood flow. Clin Pharmacol Ther 1985; 38:273–277.
125. Wiles PG, Grant PJ, Davies JA. The differential effect of arginine vasopressin on skin blood flow in man. Clin Sci 1986; 71:633–638.
126. Lenasi H, Strucl M. Effect of regular physical training on cutaneous microvascular reactivity. Med Sci Sports Exerc 2004; 36:606–612.
127. Kvernmo HD, Stefanovska A, Kirkeboen KA. Enhanced endothelial activity reflected in cutaneous blood flow oscillations of athletes. Eur J Appl Physiol 2003; 90:16–22.
128. Vassalle C, Lubrano V, Domenici C, L'Abbate A. Influence of chronic aerobic exercise on microcirculatory flow and nitric oxide in humans. Int J Sports Med 2003; 24:30–35.
129. Waeber B, Schaller MD, Nussberger J, Bussien JP, Hofbauer KG, Brunner HR. Skin blood flow reduction induced by cigarette smoking. Role of vasopressin. Am J Physiol 1984; 247:H895–H901.
130. Nicita-Mauro V. Smoking, calcium, calcium antagonists, and aging. Exp Gerontol 1990; 25:393–399.
131. Pellaton C, Kubli S, Feihl F, Waeber B. Blunted vasodilatory responses in the cutaneous microcirculation of cigarette smokers. Am Heart J 2002; 144:269–274.
132. Noble M, Voegeli D, Clough GF. A comparison of cutaneous vascular responses to transient pressure loading in smokers and non-smokers. J Rehabil Res Dev 2003; 40:283–288.
133. Lecerof H, Bornmyr S, Lilja B, De Pedis G, Hulthen UL. Acute effects of doxazosin and atenolol on smoking-induced peripheral vasoconstriction in hypertensive habitual smokers. J Hypertens Suppl 1990; 8:S29–S33.
134. Salmasi AM, BelcaroG, Nicolaides AN. Impaired venoarteriolar reflex as a possible cause for nifedipine-induced ankle oedema. Int J Cardiol 1991; 30:303–307.
135. Iabichella ML, Dell'Omo G, Melillo E, Pedrinelli R. Calcium channel blockers blunt postural cutaneous vasoconstriction in hypertensive patients. Hypertension 1997; 29:751–756.
136. Orlandi C, Rossi M, Finardi G. Evaluation of the dilator capacity of skin blood vessels of hypertensive patients by laser Doppler flowmetry. Microvasc Res 1988; 35:21–26.
137. Kvernebo K, Slagsvold CE, Stranden E, Kroese A, Larsen S. Laser Doppler flowmetry in evaluation of lower limb resting skin circulation. A study in healthy controls and atherosclerotic patients. Scand J Clin Lab Invest 1988; 48:621–626.
138. Winsor T, Haumschild DJ, Winsor D, Mikail A. Influence of local and environmental temperatures on cutaneous circulation with use of laser Doppler flowmetry. Angiology 1989; 40:421–428.
139. Cisek PL, Eze AR, Comerota AJ, Kerr R, Brake B, Kelly P. Microcirculatory compensation to progressive atherosclerotic disease. Ann Vasc Surg 1997; 11:49–53.
140. Karanfilian RG, Lynch TG, Lee BC, Long JB, Hobson RW. The assessment of skin blood flow in peripheral vascular disease by laser Doppler velocimetry. Am Surg 1984; 50:641–644.

141. Leonardo G, Arpaia MR, Del Guercio R. A new method for the quantitative assessment of arterial insufficiency of the limbs: cutaneous postischemic hyperemia test by laser Doppler. Angiology 1987; 38:378–385.
142. Kristensen JK, Karlsmark T, Bisgaard H, Sondergaard J. New parameters for evaluation of blood flow in patients with leg ulcers. Acta Derm Venereol 1986; 66:62–65.
143. Koman LA, Smith BP, Pollock FE Jr, Smith TL, Pollock D, Russel GB. The microcirculatory effects of peripheral sympathectomy. J Hand Surg Am 1995; 20:709–717.
144. Hartmann BR, Bassenge E, Pittler M. Effect of carbon dioxide-enriched water and fresh water on the cutaneous microcirculation and oxygen tension in the skin of the foot. Angiology 1997; 48:337–343.
145. Melhuish JM, Krishnamoorthy L, Bethaves T, Clark M, Williams RJ, Harding KG. Measurement of the skin microcirculation through intact bandages using laser Doppler flowmetry. Med Biol Eng Comput 2004; 42:259–263.
146. Stansberry KB, Hill MA, Shapiro SA, McNitt PM, Bhatt BA, Vinik AI. Impairment of peripheral blood flow responses in diabetes resembles an enhanced aging effect. Diabetes Care 1997; 20:1711–1716.
147. Rossi M, Lall K, Standfield N, Dornhorst A. Impaired vasoconstriction of peripheral cutaneous blood flow in Type 1 diabetic patients following food ingestion. Diabet Med 1998; 15:463–466.
148. Rendell M, Bergman T, O'Donnell G, Drobny E, Borgos J, Bonner F. Microvascular blood flow, volume and velocity measured by laser Doppler techniques in IDDM. Diabetes 1989; 38:819–824.
149. Bornmyr S, Svensson H, Lilja B, Sundkvist G. Cutaneous vasomotor responses in young type I diabetic patients. J Diabetes Complicat 1997; 11:21–26.
150. Boolell M, Tooke JE. The skin hyperaemic response to local injection of substance P and capsaicin in diabetes mellitus. Diabetic Med 1990; 7:898–901.
151. Young MJ, Veves A, Walker MG, Boulton AJM. Correlations between nerve function and tissue oxygenation in diabetic patients: further clues to the aetiology of diabetic neuropathy. Diabetologia 1992; 35:1146–1150.
152. Rendell M, Bamisedun O. Skin blood flow and current perception in pentoxifylline-treated diabetic neuropathy. Angiology 1992; 43:843–851.
153. Walmsley D, Wiles PG. Early loss of neurogenic inflammation in the human diabetic foot. Clin Sci Colch 1991; 80:605–610.
154. Jaap AJ, Shore AC, Tooke JE. Relationship of insulin resistance to microvascular dysfunction in subjects with fasting hyperglycemia. Diabetologia 1997; 40:238–243.
155. Wall B. Assessment of ischemic feet in diabetes. J Wound Care 1997; 6:32–38.
156. Koltringer P, Langsteger W, Lind P, Klima G, Wakonig P, Eber O, Reisecker F. Autonomic neuropathies in skin and its incidence in non-insulin-dependent diabetes mellitus. Horm Metabol Res 1992; 26:S87–S89.
157. Valensi P, Smagghue O, Paries J, Velayoudon P, Nguyen TN, Attali JR. Peripheral vasoconstrictor responses to sympathetic activation in diabetic patients: relationship with rheological disorders. Metabolism 1997; 46:235–241.
158. Westerman RA, Low AM, Widdop RE, Neild TO, Delaney CA. Non-invasive tests of neurovascular function in human and experimental diabetes mellitus. In: Molinatti GM, Bar RS, Belfiore F, Porta M, eds. Endothelial Cell Function in Diabetic Microangiopathy. Problems in Methodology and Clinical Aspects, Vol 9, Karger, Basel, 1990:127.
159. Aso Y, Inukai T, Takemura Y. Evaluation of microangiopathy of the skin in patients with non-insulin-dependent diabetes mellitus by laser Doppler Flowmetry; microvasculatory responses to beraprost sodium. Diabetes Res Clin Pract 1997; 36:19–26.
160. Belcaro G, Laurora G, Cesarone MR, Pomante P. Elastic stockings in diabetic microangiopathy. Long-term clinical and microcirculatory evaluation. Vasa 1992; 21: 193–197.
161. Yosipovitch G, Schneiderman J, Erman A, Chetrit A, Milo G, Boner G, van Dijk DJ. The effect of an angiotensin converting enzyme inhibitor on skin microvascular

hyperemia in microalbuminuric insulin-dependent diabetes mellitus. Diabet Med 1997; 14:235–241.
162. Flynn MD, Boolell M, Tooke JE, Watkins PJ. The effect of insulin infusion on capillary blood flow in the diabetic neuropathic foot. Diabet Med 1992; 9:630–634.
163. Aman J, Berne C, Ewald U, Tuvemo T. Cutaneous blood flow during a hypoglycaemic clamp in insulin-dependent diabetic patients and healthy subjects. Clin Sci Colch 1992; 82:615–618.
164. Belcaro G, Marelli C, Pomante P, Laurora G, Cesarone MR, Ricci A, Girardello R, Barsotti A. Fibrinolytic enhancement in diabetic microangiopathy with defibrotide. Angiology 1992; 43:793–800.
165. Rendell MS, Shehan MA, Kahler K, Bailey KL, Eckermann AJ. Effect of calcium channel blockade on skin blood flow in diabetic hypertension: a comparison of isradipine and atenolol. Angiology 1997; 48:203–213.
166. Caselli A, Hanane T, Jane B, Carter S, Khaodhiar L, Veves A. Topical methyl nicotinate-induced skin vasodilation in diabetic neuropathy. J Diabetes Complications 2003; 17:205–210.
167. Shawket S, Dickerson C, Hazleman B, Brown MJ. Selective suprasensitivity to calcitonin-gene-related peptide in the hands in Raynaud's phenomenon. Lancet 1989; 2: 1354–1357.
168. Suichies HE, Aarnoudse JG, Wouda AA, Jentink HW, de Mul FF, Greve J. Digital blood flow in cooled and contralateral finger in patients with Raynaud's phenomenon. Comparative measurements between photoelectrical plethysmography and laser Doppler flowmetry. Angiology 1992; 43:134–141.
169. Allen JA, Devlin MA, McGrann S, Doherty CC. An objective test for the diagnosis and grading of vasospasm in patients with Raynaud's syndrome. Clin Sci 1992; 82:529–534.
170. Kurozawa Y, NasuY, Oshiro H. Finger systolic blood pressure measurements after finger cooling. Using the laser–Doppler method for assessing vibration-induced white finger. J Occup Med 1992; 34:683–686.
171. Kristensen JK, Englhart M, Nielsen T. Laser Doppler measurement of digital blood flow regulation in normals and in patients with Raynaud's phenomenon. Acta Derm Venereol 1983; 63:43–47.
172. Goodfiled M, Hume A, Rowell N. Reactive hyperemic responses in systemic sclerosis patients and healthy controls. J Invest Dermatol 1989; 93:368–371.
173. Engelhart M, Seibold JR. The effect of local temperature versus sympathetic tone on digital perfusion in Raynaud's phenomenon. Angiology 1990; 41:715–723.
174. Wollersheim H, Reyenga J, Thien T. Postocclusive reactive hyperemia of fingertips, monitored by laser Doppler velocimetry in the diagnosis of Raynaud's phenomenon. Microvasc Res 1989; 38:286–295.
175. Martinez RM, Saponaro A, Dragagna G, Santoro L, Leopardi N, Russo R, Tassone G. Cutaneous circulation in Raynaud's phenomenon during emotional stress. A morphological and funcitonal study using capillaroscopy and laser Doppler. Int Angiol 1992; 11:316–320.
176. Whitmore SE, Wigley FM, Wise RA. Acute effect of topical minoxildil on digital blood flow in patients with Raynaud's phenomenon. J Rheumatol 1995; 22:50–54.
177. Engelhart M. Ketanserin in the treatment of Raynaud's phenomenon associated with generalized scleroderma. Br J Dermatol 1988; 119:751–754.
178. Brouwer RM, Wenting GJ, Schalekamp MA. Acute effects and mechanism of action of ketanserin in patients with primary Raynaud's phenomenon. J Cardiovasc Pharmacol 1990; 15:868–876.
179. Bunker CB, Lanigan S, Rustin MHA, Dowd PM. The effects of topically applied hexyl nicotinate lotion on the cutaneous blood flow in patients with Raynaud's phenomenon. Br J Dermatol 1988; 119:771–776.

180. Rustin MHA, Newton JA, Smith NP, Dowd PM. The treatment of chilblains with nifedipine: the results of a pilot study, a double-blind placebo-controlled randomized study and a long-term open trial. Br J Dermatol 1989; 120:267–275.
181. Agusni I, Beck JS, Potts RC, Cree IA, Ilias MI. Blood flow velocity in cutaneous lesions of leprosy. Int J Lepr Other Mycobact Dis 1988; 56:394–400.
182. Abbot NC, Beck JS, Feval F, Weiss F, Mobayen MH, Ghazi-Saidi K, Dowlati Y, Velayati AA, Stanford JL. Immunotherapy with Mycobacterium vaccae and peripheral blood flow in long-treated leprosy patients, a randomised, placebo-controlled trial. Eur J Vasc Endovasc Surg 2002; 24:202–208.
183. Wilder Smith A, Wilder Smith E. Electrophysiological evaluation of peripheral autonomic function in leprosy patients, leprosy contacts and controls. Int J Lepr Other Mycobact Dis 1996; 64:433–440.
184. Leu AJ, Yanar A, Jost J, Hoffman U, Franzeck UK, Bollinger A. Microvascular dynamics in normal skin versus skin overlying Kaposi's sarcoma. Microvasc Res 1994; 47:140–144.
185. Rodgers GP, Schechter AN, Noguchi CT, Klein HG, Nienhuis AW, Bonner RF. Periodic microcirculatory flow in patients with sickle-cell disease. N Engl J Med 1984; 311:1534–1538.
186. Tur E, Politi Y, Rubinstein A. Cutaneous blood flow abnormalities in hypertriglyceridemia. J Invest Dermatol 1994; 103:597–600.
187. Algotsson A, Nordberg A, Almkvist O, Winblad B. Skin vessel reactivity is impaired in Alzheimer's disease. Neurobiol Aging 1995; 16:577–582.
188. Maltz JS, Eberling JL, Jagust WJ, Budinger TF. Enhanced cutaneous vascular response in AD subjects under donepezil therapy. Neurobiol Aging 2004; 25:475–481.
189. Vuilleumier P, Decosterd D, Maillard M, Burnier M, Hayoz D. Postischemic forearm skin reactive hyperemia is related to cardovascular risk factors in a healthy female population. J Hypertens 2002; 20:1753–1757.
190. Wardell K, Nilsson GE. Duplex laser Doppler perfusion imaging. Microvasc Res 1996; 52:171–182.
191. Bornmyr S, Martensson A, Svensson H, Nilsson KG, Wollmer P. A new device combining laser Doppler perfusion imaging and digital photography. Clin Physiol 1996; 16:535–541.
192. Saravanamuthu J, Seifalian AM, Reid WM, Maclean AB. A new technique to map vulva microcirculation using laser Doppler perfusion imager. Int J Gynecol Cancer 2003; 13:812–818.

26
Drug Concentration in the Skin

Christian Surber and Fabian P. Schwarb
Institut für Spital-Pharmazie, Universitätskliniken, Kantonsspital, Basel, Switzerland

Eric W. Smith
College of Pharmacy, University of South Carolina, Columbia, South Carolina, U.S.A.

Howard I. Maibach
Department of Dermatology, School of Medicine, University of California, San Francisco, California, U.S.A.

I. INTRODUCTION

An understanding of the pharmacodynamics and pharmacokinetics of a drug is essential for its safe use. A therapeutic effect of a drug and its appropriate dosage regimens are based upon the relationships of time and drug concentration at the active site (target organ or biophase) and the resultant drug response. For reasons of feasibility, correlation of drug effects and drug concentration in blood or urine are most often monitored for systemically acting agents. The three factors that are generally assessed are: (a) the area under the serum concentration versus time curve, (b) the peak serum concentration, and (c) the time to peak serum concentration. Analytical difficulties sometimes preclude the measurement of drug or metabolite levels in the body fluids, in which case drug effects are assessed by observing an appropriate pharmacologic response (1,2). Pharmacokinetics are the current mainstay parameters of bioequivalence assessments because blood and urine assays are available for nearly all drugs, and because pharmacokinetic methods are generally well understood. The key assumption is that equivalent pharmacokinetic parameters indicate equivalent therapeutics—or, more precisely, that observed differences in pharmacokinetic parameters between formulations are predictive of differences in clinical performance of the two formulations. However, little attempt to verify this key assumption is made (3–5).

For topical drug products, such as ointments, creams, and gels (as distinguished from transdermal delivery systems), bioavailability studies paralleling those of orally administered drugs are often difficult to carry out and may provide an inappropriate measure of topical bioequivalence. Furthermore, topical doses tend to be so small that drug concentrations in blood and/or urine are often undetectable using current assay techniques. Moreover, systemic availability may not properly reflect cutaneous bioavailability for medications intended to treat local skin disorders since

systemically detected drug is no longer at its intended site of action and is, additionally, subjected to complex central compartment pharmacokinetics.

Assessment of bioavailability or bioequivalence of topical formulations may be made by taking one of several possible approaches. Bioavailability or bioequivalence may be established through a well-controlled clinical trial or through an easily monitored pharmacological endpoint. Establishing that the concentration of drug within the treated tissue correlates with clinical performance or to some relevant pharmacological endpoint is another approach to bioavailability or bioequivalence that is currently being debated. Similarly, some in vitro methods and animal studies that correlate with clinical performance are being investigated.

At present a well-controlled clinical trial is the only uncontested, generally acceptable procedure for demonstrating bioavailabilty and bioequivalence of topical drug products. It is highly desirable to develop alternative in vivo (and in vitro) procedures because of the high costs of conducting clinical trials. The purposes of this chapter are: (a) to discuss some methods for the direct determination of drug concentration in the skin compartment, (b) to review the relationships between the drug concentration in the skin and a clinical or pharmacological effect, and (c) to point out some difficulties in the interpretation of the results from these models.

II. SAMPLING TECHNIQUES

A. Suction Blister Technique

The development of a defined suction blister that separates the skin strata subepidermally was first described by Kiistala (6–8). Kiistala's method uses a special dome-shaped Dermovac cap (Instrumentarium Corp., Espoo, Finland) with several small holes of 6 mm diameter. Suction blisters can also be developed using a plane block with holes of similar diameter (8 mm) (9). In a typical suction blister induction with a Dermovac cap, a consistent suction of about 200 mm Hg (2.66 Pa) below the atmospheric pressure is employed for a two- to three-hours period, after which 50 to 150 μL suction blister fluid and small stratum corneum–epidermal sheets can be harvested. The blister fluid corresponds roughly to the interstitial fluid. In contrast to the alternative cantharidin-induced blister fluid (10), the suction blister fluid is free of white cells for the first five hours, after which leukocytes begin to appear (11). The protein content of suction blisters is 60% to 70% of the corresponding serum value (9). Secretion of fluid into the capsule of the Dermovac with and without bursting of the blister roof is often observed. In diseased skin, blisters cannot be raised uniformly, and standardization of the methodology in diseased skin has not been possible.

For pharmacokinetic studies up to 20 small blisters are formed; drug is administered systemically or topically (either before or after blister raising), and the blister fluid and blister roof are harvested at various time intervals for subsequent analysis.

Only limited reports exist where the suction blister technique has been used to study topical drug delivery (12–17). Treffel et al. (12) studied transepidermal absorption of citropten and bergapten from two different cosmetic tanning products (oil/water emulsion, oil) into suction blister fluid. The drug concentrations determined by high-pressure liquid chromatography were 37 and 51 ng/mL (water/oil emulsion) and 26 and 23 ng/mL (oil), respectively, for citropten and bergapten.

A number of studies have been published concerning 8-methoxypsoralen (8-MOP) absorption. Using the suction blister technique, Huuskonen et al. (13) studied absorption of 8-MOP during psoralen plus ultraviolet A (PUVA) bath

therapy. More recently, Averbeck et al. (14) compared the photobiological activity (18) and the concentration of 5-MOP (bergapten) after topical application. They observed that the photobiological activity of 5-MOP in the suction blister fluid was more effective when it was delivered from an ethanolic solution than from a bergamot oil with the same 5-MOP content. From these experiments it can be concluded that the suction blister technique is useful not only for pharmacokinetic studies but also for pharmacodynamic evaluations, making it possible to study the biological activity of a drug and its metabolites at the level of the target organ.

Surber et al. (16) and Laugier et al. (17) compared acitretin (retinoid) concentration in the skin after topical and systemic administration using the suction blister technique, and two other skin biopsy techniques. These data are discussed in Section II.H.

B. Cantharidin Blister Technique

Large sheets of stratum corneum and blister fluid can be obtained with some discomfort to the subjects using the cantharidin blister technique (10). Many samples can be obtained from different regions of the same person with little effort and with the advantage of not leaving a permanent scar, although abnormal skin pigmentation at the site of application may persist for several months after harvest. Use is made of the capacity of cantharidin, a substance extracted from "Spanish fly" to produce an intraepidermal blister (in humans only). For most body areas a 0.2% solution of cantharidin in acetone is satisfactory, and for sites where the stratum corneum is thick and dense the concentration is increased to 0.5%. The cantharidin–acetone solution is placed into a glass or metal cylinder and the acetone is evenly evaporated to dryness under a stream of air. A layer of wet cloth is placed over and beyond the application site and fastened occlusively to the skin by impervious plastic tape. From 8 to 10 hours later, the turgid clear blister can be punctured using an insulin syringe in order to collect the blister fluid. Subsequently the blister itself can be excised with scissors. Remnants of epidermis clinging to the underface of the horny layer are removed by firm rubbing with a cotton-tipped applicator. Circular sheets of stratum corneum as large as 4 cm in diameter can be prepared in this manner, and the volume of blister fluid is dependent on the size of the blister raised. Cantharidin blisters can also be obtained by the various cantharidin plasters described in old pharmacopoeias. The cantharidin blister fluid is an inflammatory exudate, containing 650 to 12,700 white cells/μL (19,20) and its albumin concentration significantly exceeds that of suction blister fluid (70–80% of the respective serum level) (21).

The blisters (suction blister and cantharidin blister) contain a fluid reservoir that is continuous with the intravascular fluid and the skin surface such that an immediate representation of the tissue concentration of a drug can be assumed. However, alterations of the composition of the blister fluid and the morphology of the blister base or blister roof may influence drug penetration into the blister fluid. The induction of an inflammatory response, for example, may result in a slower or enhanced passage of drug from the capillaries into the blister. The preservation of the barrier function of the stratum corneum following blister formation has also been questioned since the stratum corneum is then in an abnormally stretched state (15).

C. Related Techniques

If the intention of the experimentation is to gain better access to the interstitial fluid as an investigative or analytical medium, then the surface layers of the skin may be removed by suction blistering and subsequent excision or by dermabrasion, in order to obtain a skin window exposing the epidermal tissue. A chamber filled with saline solution or prewetted disks may subsequently be applied to the exposed skin window. At various time intervals, the fluid or the disks are removed from the skin window and are refilled with isotonic saline or replaced by new disks (22,23). The method of dermabrasion leads to an acute inflammatory reaction, and large numbers of granulocytes and albumin are found in the skin chamber fluid. Similarly, access to other peripheral compartments may be achieved by using different experimental "devices" that allow the collection of specific tissue fluids. Pertinent methods include the implantation of tissue cages, fibrin clots, and nylon or cotton threads (24–28).

D. Surface Recovery

Percutaneous absorption may be determined by the loss of material from the application surface as the drug penetrates into skin. Drug recovery from an ointment or a solution application is difficult because total recovery of compound from the skin can never be assured. The technique is usually applicable only in cases where a large amount of drug is absorbed from the applied formulation. In contrast, with the topical application of a transdermal delivery device, the entire unit can be removed from the skin and the residual amount of drug in the device can be determined. It is assumed that the difference between applied dose and residual dose is the amount of drug absorbed. It is also possible to monitor the disappearance of radioactivity from the surface of skin using an external Geiger–Müller counter (29). The limitation of this methodology is that the disappearance is due both to the movement of ^{14}C-labeled chemical into the skin and to the quenching effect of the skin on the β-rays incident on the instrument detector. The degree of quench radiolabeled chemicals in the various cell layers of the skin has not been defined. Lee et al. (30) recently developed a new methodology using ^{19}F magnetic resonance spectroscopy (MRS) to measure the in vivo percutaneous absorption of flurbiprofen through hairless rat skin. A 2% w/v flurbiprofen gel containing isopropyl alcohol, water, and propylene glycol was used. Gel was applied within a rubber O-ring to the skin of the lower back of an anesthetized hairless rat and occluded with a plastic cover slip. The animal was placed on a magnetic resonance surface coil, and measurements were taken continuously over approximately three hours at 10-minuts intervals with a 2 T GE CSI nuclear magnetic resonance (NMR) spectrometer in order to measure the disappearance of magnetic resonance signal intensity per time interval. This assessment relates directly to the percent of drug disappearance over time and can be converted to a flux value.

Related to the surface recovery technique, Phillips et al. (31–34) and Peck et al. (35) developed transcutaneous drug collection device. The device consists of a salt-impregnated absorbent pad [e.g., 0.3 g agarose, 0.5 g activated carbon, 9.2 g 10% saline per 10 g (36)], which is covered by water-impermeable tape. Drug is assessed in the pad at continuous time intervals. The technique has been proposed as a method for studying drug disposition in subjects in a fashion that is less intrusive than currently available techniques and that may be suited to the surveillance of drug exposure in ambulatory individuals. In particular, continuous transcutaneous drug collection (CTDC) has been proposed for the estimation of ethanol intake in drinking

subjects (32) and for the monitoring of patient compliance with a drug regimens (36,37).

Peck et al. (35) have extensively analyzed the theoretical basis for the use of the CTDC device in assessing various aspects of drug pharmacokinetics. The time course of drug accumulation in the CTDC device was simulated using standard pharmacokinetic and mathematical techniques. The influences and implications of single and polyexponential drug disposition kinetics and back transfer of drug from the collection device were investigated. Their interpretation of the results suggest two principal factors that affect the utility of this technique: first, the degree of back transfer of drug from the CTDC device into the body and second, the duration of transcutaneous drug collection relative to the elimination rate of the drug from the body. In their theoretical treatment they excluded the notion that the rate of drug transfer into the CTDC device is somehow dependent upon the sweat secretion rate. They were aware of the fact that an occlusive dressing such as a CTDC device surely alters the skin permeability relative to unoccluded skin. However, they assume that the temperature and the hydration of the skin under the dressing become stabilized. Furthermore, their analyses suggested that the utility of a CTDC device is severely restricted when back transfer from the collection device is substantial. The ability to minimize or even exclude back transfer by binding the effused target chemical irreversible would promote the use of this promising tool for assessing the systemic amount of drug exposure.

E. Skin Stripping and Related Techniques

The skin stripping and related techniques are discussed in chapter 23.

F. Sebum Collection

Sebaceous glands are largest and most numerous on the forehead, face, in the ear, and on the midline of the back. Sebum is a complex mixture of lipids. Its principal components are glycerides, free fatty acids, wax esters, squalene, cholesterol, and cholesterol esters. Sebum is miscible with water and allows water and polar and nonpolar materials to penetrate. The length of time required for sebum to be produced and move from the base of the sebaceous gland to the skin surface is less than 10 days (38–41). Several functions have been ascribed to sebum, such as controlling water loss and protecting the skin from fungal and bacterial infection; however, these claims have been questioned. Sebum collection has been used extensively to study the changes of the lipid composition during therapies with retinoids.

Sebum is normally collected by swabbing the forehead, nose, cheeks, and midback with a sponge soaked in an organic solvent (e.g., isopropylalcohol or hexane). The sebum is extracted from the sponge for a subsequent analysis. With other techniques a cigarette paper, a special tape, or a ground-glass plate is pressed onto the skin site of interest to adsorb the surface sebum (42–44).

Attempts have also been made to detect different drugs in the sampled lipid mixture. Tetracycline and minocycline are well referenced and are clinically considered to be effective drugs in the treatment of acne and other infectious dermatosis. However, documentation of skin pharmacokinetic data for these antibiotics is sparse and controversial. Rashleigh et al. (45) showed that tetracycline detected by a fluorometric method accumulated in sebum after oral administration. Significant quantities of tetracycline (3–18 μg/g sebum lipid) were detected in the surface film taken

from the forehead after four to five days. However, they did not measure tetracycline levels within the pilosebaceous lumens, the focal point for acneform lesions. There was no direct relationship found between the dose applied, blood levels, and concentration of the drug in the sebum. They stated that from their experimental design and data a firm conclusion on the route of tetracycline penetration into the skin cannot be drawn. Using a microbiologic method that required approximately 1 g of skin from each subject, Gould and Richtie (46) showed indirectly that 70% of dosed terramycin was present in the skin when compared with the serum terramycin level. Aubin et al. (47) dosed 10 volunteers with minocycline (200 mg/day) for four weeks but were not able to detect minocycline in the skin by using high-performance liquid chromatography (HPLC) (C_{18}) at a detection limit of 0.3 ng/mL. However, Luderschmidt et al. (48) reported that they successfully detected approximately 40 μg minocycline per 6 cm^2 area by HPLC on day 6 of treatment in patients administered 100 mg minocycline/day. With the exception of Rashleigh et al. (45), none of the investigators discussed the pathway of the drug penetration into the skin, and from the experiments carried out it is purely hypothetical whether tetracyclines accumulate in the sebaceous glands.

The knowledge of the drug concentration in sebum is mainly derived from the examination of surface samples collected from anatomical sites rich in sebaceous glands. An alteration of drug (and sebum) between the site of biosynthesis and the skin surface is highly probable since the corresponding lag time is about eight to nine days (40,41). During that delay a number of factors could contribute to an alteration of the initial sample, such as (a) biotransformation by microorganisms or by enzymes released from the microorganisms; (b) dilution and/or reaction with other endogenous or exogenous species such as epidermal lipids; (c) adsorption or binding to other media such as hair; or (d) alteration through environmental aggressions such as temperature, light, oxygen, and humidity. Isolation of sebaceous glands (49) from humans or animals during drug treatment is possible and may therefore be an alternative sebum collection procedure.

G. Hair and Nail Collection

The use of hair or nails is advantageous in that xenobiotics are maintained unchanged for long periods of time in these easily sampled tissues. It is thus possible to monitor the intake of drugs and poisons or to follow the chronology of an intoxication by analysis of hair or nail content. The detection of arsenic in hair is probably the most well known of these techniques for forensic purposes. As a result of better analytical equipment, the detection of a variety of drugs such as phencyclidine, phenobarbital, opiates, amphetamines, tricyclic antidepressants, methadone, and nicotine in this matrix has been made possible (50–55). These advances have mainly been made in forensic medicine, while little effort has been made in dermatology to detect drugs (e.g., antimycotics) in the hair after systemic dosing (56).

In a series of papers, Walters and Flynn (57–61) developed the basic concepts of the permeability of the human nail plate and thus created a better understanding of the toxicity potentials and therapeutic possibilities of substances applied to the nail. The collective physicochemical and clinical observations point to one general conclusion, namely, that the nail is permeable to a variety of chemicals ranging from small polar and nonpolar nonelectrolytes and salts to large complex drug molecules. Collectively analyzed, these studies indicate that the nail plate is intrinsically up to one thousand times more permeable to water than is stratum corneum, given that the ratio of

nail to stratum corneum thickness is about 100. Information from systematic investigations on penetration of various antifungals into the nail from topical formulations and the influence of the corresponding vehicles are still infrequent and incomplete (62–64).

It is generally understood that in the planning of a drug regimen with, for example, an oral antibiotic for the treatment of an infection, it is necessary to know the pattern of serum and tissue levels following drug administration. When considered in parallel with information concerning the bactericidal levels of an antibiotic, it is possible to plan an appropriate oral dosage, application frequency, and duration of therapy. Although in the past there has been a lack of similar relevant information concerning drugs used to treat disease of the nail plate, the same principles should apply. In a recent study with humans (65), plasma terbinafine levels directly correlated with oral dose, and distal nail levels correlated with plasma levels. Terbinafine was generally detected earlier in proximal nail plate than in distal nail clippings, and the persistence of the drug in the nail plate paralleled plasma levels. Based on this data it should be possible to design a therapeutic regimen based on an optimal oral dose and duration of therapy (66).

H. Skin Biopsy

The most invasive—but still practicable—method to access skin compartments is the excision of skin tissue. In contrast to the other methods described, the punch and shave biopsies allow direct ingress into the compartment of interest. After removal (optional) of the stratum corneum from skin with an appropriate technique (tape stripping or adhesive), the punch biopsy will contain parts of the subcutaneous tissues, dermis, and epidermis, and the shave biopsy will mainly contain epidermis and some dermis. Parts of the stratum corneum may remain on the epidermis depending on the method used for stratum corneum removal. Subcutaneous tissue can mechanically be divided from the dermis, and the latter can be separated from the epidermis by heating techniques (67). Human skin samples larger than 100 mg are difficult to obtain, and the usual amount harvested is less than 50 mg.

Surber et al. (16) and Laugier et al. (17) compared the acitretin concentration (synthetic retinoid) in human skin after oral and topical dosing using three different skin sampling techniques: punch biopsy, shave biopsy, and suction blister. All three techniques have been used by various investigators to quantitate drugs and xenobiotics in the skin. Each technique gives access to distinctive skin compartments (Fig. 1).

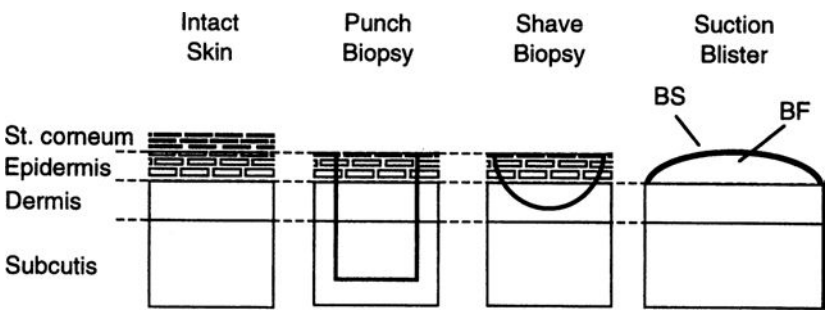


Figure 1 Schematic diagram of intact skin (*left*) and the skin specimens taken using three sampling techniques. (For details see text). *Abbreviations*: BS, blister skin; BF, blister fluid.

Table 1 Total Drug Concentration in Skin After Oral and Topical Administration of Acitretin

Sample	Total drug concentration, ng/g wet tissue	
	Oral application	Topical application
Punch biopsy	275	160
Shave biopsy	160	360
Suction blister fluid	200	90
Suction blister skin	460	3,800

Source: Data from Refs. 16 and 17.

The acitretin concentration in the skin after systemic application in a steady-state situation was comparable with the drug concentration reached after a single 24-hour topical application of a saturated acitretin/isopropylmyristate formulation (Table 1). However, no beneficial effects have so far been observed in psoriasis and other disorders of keratinization by the topical administration of acitretin. Similar observations have been made with methotrexate and cyclosporin (67,68). One may postulate that drug concentration at a particular site within the skin following the two routes of administration could be different due to the direction of the drug concentration gradient. This hypothesis has also been postulated and illustrated by Parry et al. (69) when comparing the clinical efficacy of topical and oral acyclovir. Model predictions and in vivo data agree that topical administration of acyclovir results in a much greater total epidermal drug concentration than that after oral administration. However, mathematical modeling of the acyclovir concentration gradient through the epidermis revealed that the drug concentration in the target site of the herpes simplex infection, the basal epidermis, was two to three times less after topical administration than after oral administration. Furthermore, one may postulate that drug metabolism could be different depending on the route of administration. Data supporting this hypothesis are still incomplete. Despite skilled experimentators, sophisticated sampling techniques, and instrumentation, the formation gained from these tissue samples is probably only an estimate of the chemical distribution within the skin. Accurate and specific information on drug localization within a particular skin compartment following both routes of administration is not obtained by these methods, possibly because of interlaminate drug contamination.

The following two techniques have been used to obtain skin sections parallel to the outer skin surface to a depth of about 300 to 600 μm.

1. Semiautomated Skin Sectioning Technique

With this approach the skin tissue from a punch biopsy is placed onto a cryomicrotome table and 10 to 40 μm sections are cut parallel to the skin surface. This technique is summarized in the form of an excellent standard operating procedure by Schaefer and Lamund (70) and Schaefer et al. (71). When the cylinder-shaped punch biopsy is placed, dermis side down, on the microtome chuck maintained at −17°C it is essential that the stratum corneum surface is parallel to the cutting plane. This can be accomplished by placing several metal rings of internal diameter and composite thickness slightly greater than that of the skin sample around the tissue and filling the rings with embedding medium. Subsequently a flat, precooled surface (glass slide)

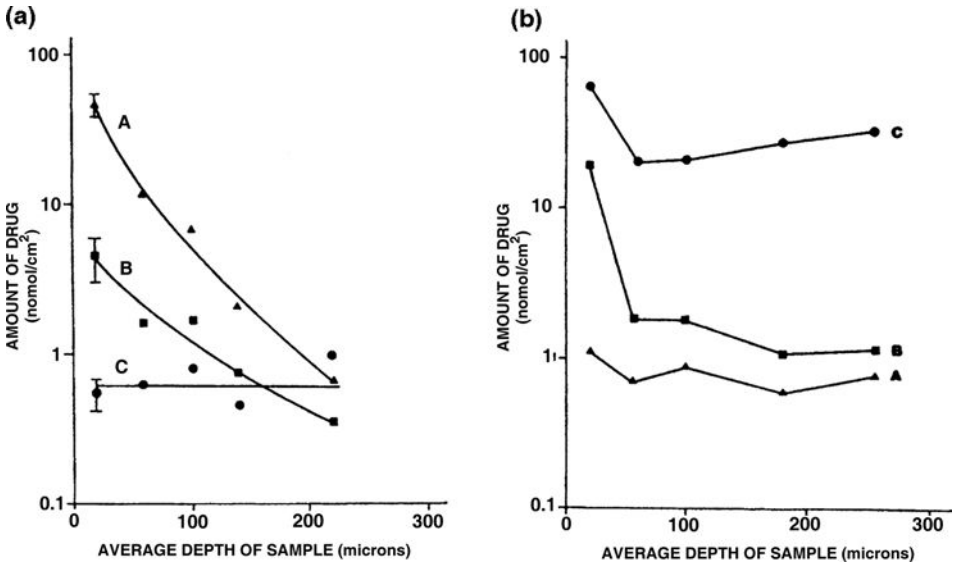


Figure 2 The concentration profile of the diester (**A**), monoester (**B**), and salicylate (**C**) as a function of the depth within human skin either grafted to athymic mice (**a**) or in vitro (**b**). Results were obtained after 24 hours of topical drug application. *Source*: From Ref. 73.

is pressed against the stratum corneum, resulting in a flat outer surface, and the whole assembly is then rapidly frozen and can be stored. The technique does not take into account the dermal papillae, and a clear separation of histologically distinct compartments is not possible. The method has predominately been used to characterize the pharmacokinetic and metabolic behavior of topically applied drugs (72,73).

Using excised human skin and tissue grafted to athymic mice, the in vitro and in vivo concentration profiles of salicylic acid and salicylate esters were obtained for the outer several hundred microns of the skin (73). The results show significant differences in the extent of enzymatic cleavage and distribution of metabolites between in vitro and in vivo studies. The data also suggest that in vitro results may overestimate metabolism because of increased enzymatic activity and/or decreased capillary removal of biotransformed products (Fig. 2).

2. *Manual Skin Sectioning Technique*

With the development of the skin sandwich flap model (74), Pershing and Kruegar (75) proposed a new manual skin sectioning technique by which the disposition of test compounds may be examined after topical administration. Their technique requires the use of radiolabeled compound and fresh skin that has not been frozen. Briefly (Fig. 3), a 2-mm skin punch biopsy is sectioned into 115-μm-thick sections by dipping the stratum corneum end of the biopsy into cyanoacrylate adhesive (step 1) and fixing this end of the biopsy cylinder to a microscope slide. Two 115-μm-thick microscope cover slips, which act as cutting guides, are positioned on either side of the biopsy and are held in place on the microscope slide with tape (step 2). A single-edged razor blade is used to shave the adhering stratum corneum side of the punch from the remainder of the biopsy. The outermost stratum of the removed

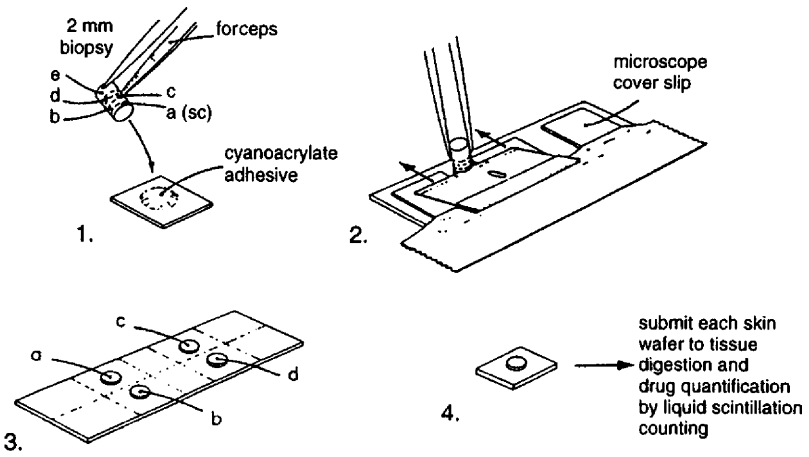


Figure 3 Manual sectioning technique of the punch biopsies. For details see text. *Source*: From Ref. 79.

biopsy segment is then dipped in the cyanoacrylate adhesive again and fixed in a new location on the microscope slide (b) prior to sectioning in an identical manner using the cover slips as cutting guides. The remainder of the skin biopsy is sectioned similarly, producing multiple 115-μm sections (c–d) on an individual microscope slide (step 3). After complete sectioning of the skin biopsy, the various skin wafers on the microscope slide are individually digested with tissue solublizer and submitted to liquid scintillation counting for drug quantification. Subsequently, a concentration gradient and disposition profile of the test compound in the skin is constructed. The authors also reported that freezing the 2-mm biopsy results in redistribution of the drug from the stratum corneum to the middle sections (400–600 μm depth) of the skin biopsy, thereby portraying an inaccurate distribution profile in the skin, unfortunately, this statement is not documented further, since this redistribution phenomenon may also be relevant for a 4 to 6 mm biopsy, even though it was only described for a 2-mm biopsy. This observation makes it necessary to carefully reevaluate the skin preparation procedure.

I. Microdialysis

Microdialysis is a sampling technique that allows continuous, real-time drug monitoring and causes minimal tissue damage or physiological alterations in the test subject. Further advantages of microdialysis sampling include the fact that once a molecule crosses the dialysis membrane, enzymatic degradation or protein binding is eliminated and that the tissue can be directly sampled without causing significant tissue fluid loss. Additionally, thermal and hydrolytic degradation of the compounds of interest can be minimized by optimizing the microdialysis sampling rate and the nature of the dialysis medium (76,77). A significant reduction in the number of animals required to perform dermal and transdermal drug delivery research may be possible. A single animal can be used for the continuous real-time study of drug concentration in the skin with microdialysis, compared to numerous animals required for each time point by other currently accepted methods.

The initial questions regarding the feasibility of this technique and the impact of the probe implantation on the flux of drug through the skin were addressed by studies using a commercially available probe implanted into full-thickness rat skin in vitro (78). Results of the initial feasibility studies necessitated the development of a novel probe system based on minimal probe dimensions. While a coated probe of linear geometry has been used previously, a biocompatible silicone coating on a cellulose dialysis fiber for implantation into skin has been designed and validated by the same group (79). Following topical application of 5-fluorouracil cream (Efudex), the implanted dermal microdialysis probe successfully monitored the drug concentration in the skin in vivo. Edema, inflammation, and tissue scarring around the site of implantation assessed by histological examination appeared to be minimal during the first 24 to 36 hours after implantation. The histological studies revealed lymphocyte infiltration into the area of implantation after six hours and scar-tissue formation around the probe after 72 hours. While the problem of tissue damage due to probe implantation is a disadvantage of any invasive procedure, the extent of tissue damage determined by histological examination and drug perfusion studies was minimal.

In a recent report, Matsuyama et al. (80) successfully demonstrated that the intradermal implantation of a microdialysis probe in vivo was practical in order to study percutaneous absorption of methotrexate and to assess changes in drug concentrations following coapplication of an enhancer.

This simple method for determining drug concentration in the skin in vivo provides previously inaccessible information about drug transport in the skin and may, in the future, serve as a reliable technique for studying topical bioavailability and skin pharmacokinetics in order to guide drug development and patient therapy.

III. ANALYTICAL TECHNIQUES

A. Autoradiography

Autoradiography is a photographic technique used to detect the localization of radioactive materials in specimens. The technique itself is over 100 years old, but its application to skin research has increased greatly during the last 30 years. The methodology has improved rapidly, and application of the technique has progressed not only from a tissue level to cell level, but also to a subcellular level (81). In the process of drug delivery to the skin, the localization of the penetrating/permeating compounds in the skin layers and the identification of transport pathways is essential. Only a few approaches to quantify the compound in the different skin layers and appendages have been reported. An important contribution to the quantitative evaluation was made by Schaefer et al. (71) and Schalla et al. (82), who introduced the skin sectioning method discussed earlier. To overcome certain disadvantages of their technique, they supplemented their findings with qualitative histoautoradiography. Thus the combination of histoautoradiography and skin sections may indicate predominating permeation routes.

In a recent investigation (83) the development of an intracutaneous depot for drugs was studied using a new pharmaceutical ingredient, diethylene glycol monoethyl ether (Transcutol). A qualitative assessment revealed that the distribution pattern of hydrocortisone (model drug studied) was dependent on the vehicle used. In the control group (treated with hydrocortisone without Transcutol) the distribution was not uniform, whereas in the treatment group (treated with hydrocortisone with

Transcutol) the hydrocortisone was uniformly distributed in the skin and the amount of radioactivity present in the skin was higher in the treatment group relative to the control group.

In an autoradiographic study on percutaneous absorption of five ^{14}C-labeled oils in the guinea pig, a decreasing "absorbability" in the following order was found: isopropyl myristate, glyceryl trioleate, *n*-octadecane, decanoxydecane, and 2-hexyldecanoxyoctane (84). The skin irritation potentials (macroscopic observation of erythema) of these oils were in agreement with the absorption observed by microautoradiography, although isopropyl myristate produced much more severe irritation than 2-hexyldecanoxyoctane.

Estradiol retention in the skin was investigated by Bidmon et al. (85) using dry-mount autoradiography. [^{3}H]Estradiol-17β in dimethyl sulfoxide, ethylene glycol, or sesame oil was applied to shaved rat skin in the dorsal neck region. The results of the experimental demonstrate that dry-mount autoradiography provides both regional and cellular resolution for specific tissues and indicates the penetration routes of the diffusible compound. Since embedding and melting of tissue are avoided and permanent contact with photographic emulsion is obtained, translocation of labeled compound during the preparation of the autoradiograms is excluded and the cellular and subcellular resolution is high. After 2 hours of topical treatment with [^{3}H]Estradiol-17β dissolved in dimethyl sulfoxide a distinct cellular distribution was apparent. Accumulation of radioactivity was found in the epidermis, sebaceous glands, dermal papillae of hair, and fibroblasts. The stratum corneum accumulated and retained radioactivity, apparently forming a depot for the hormone. Marked concentration and retention of hormone were observed in the sebaceous glands for more than 24 hours, suggesting that sebaceous glands serve as second storage sites for the hormone. In all autoradiograms, two penetration pathways to the dermis were visible: one through the stratum corneum and epidermis, and the other through the hair follicles. The same permeation routes and sites of deposition and retention are recognizable for female and male rats, independent of whether dimethyl sulfoxide, ethylene glycol, or sesame oil was used as the vehicle. It is important to note that low topical doses of drug reveal information on specific drug binding in target cells with cellular and subcellular resolution. Higher doses provide the advantage of visualizing permeation routes, gradients, and vehicle effects in the various skin compartments (Fig. 4).

By means of a microcomputer-based image-analyzing autoradiographic method, it was possible to measure and visualize the effects of carriers and application time on the localization in the rate skin of two lipophilic compounds, tetrahydrocannabinol, and oleic acid (86). It was found that both compounds, dissolved in Transcutol, show similar penetration profiles after two hours. No significant difference was found between the concentration in the epidermis and that in the appendages, either for tetrahydrocannabinol or for oleic acid. However, a dramatic effect of formulation composition on the localization of tetrahydrocannabinol was observed (Fig. 5) after 24 hours when polyethylene glycol 400, diethylene glycol monoethyl ether, or propylene glycol/ethanol was used.

These data document a first effort in quantitative autoradiography, and the information is well conformed with previously reported results of skin permeation behavior of tetrahydrocannabinol (87).

Autoradiographic approaches are also used to study the effect of topically applied compounds (e.g., retinoic acid, Azone, and tetradecane) on epidermal growth using [^{3}H]thymidine (88–90). In a recent study (91), autoradiographic and immunohistochemical techniques were combined to analyze minoxidil localization

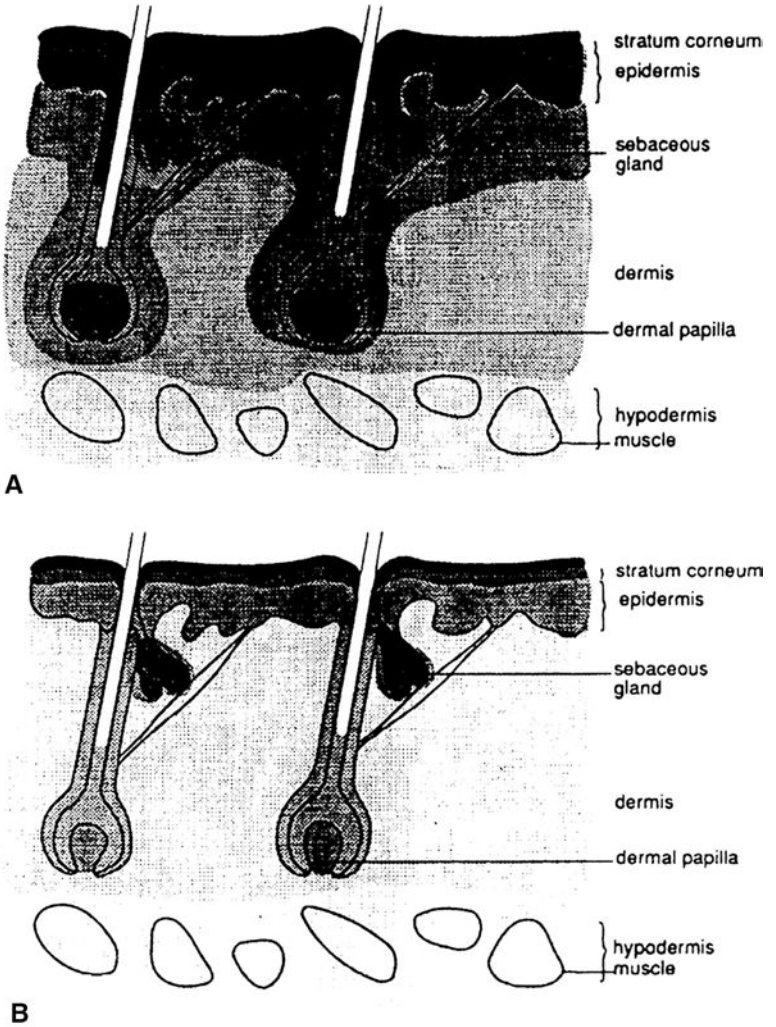


Figure 4 Scheme of distribution of radiolabeled estradiol (**A**) two hours and (**B**) 24 hours after topical application of 301 pmol/cm^2. The penetration gradients through the epidermis and the hair follicles are visible, as well as the enhanced uptake of radioactivity in sebaceous glands and dermal papillae. The highest amount of radioactivity is on top of the stratum corneum and in the stratum corneum (**B**). The different grey levels reflect the different silver grain densities. *Source*: From Ref. 85.

in cultured vibrissa follicles, revealing incongruent findings. The data suggest that minoxidil is not covalently bound to a cellular receptor in the hair follicle. Therefore, minoxidil's site of activity for stimulation of the hair follicle still remains to be elucidated.

B. Fluorescence

Fluorescent or fluorescence-labeled substances permit the use of the fluorescence microscope for qualitative localization within the skin strata. In 1957 Borelli and

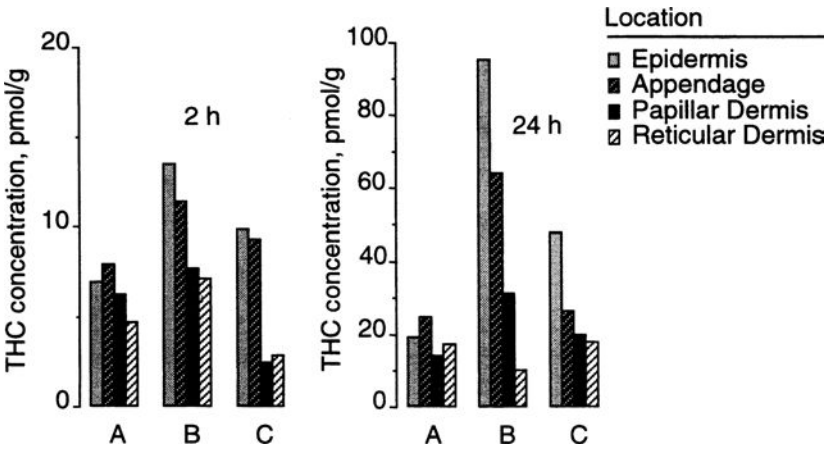


Figure 5 In vivo effect of vehicle and vehicle composition on the localization of tetrahydrocannabinol (THC) in the epidermis, appendages, and dermis of the hairless rat skin after 2 hour and 24 hours application. Vehicles: (**A**) polyethylene glycol 400, (**B**) diethylene glycol monoethyl ether (Trancutol), and (**C**) propylene glycol:ethanol (7:3). *Source*: redrawn from Ref. 86.

Metzger (92) studied the in vitro percutaneous absorption of the fluorescent dye "acridinorange" incorporated into various topical preparations commonly used at that time, using domestic pig and human skin. Using fluorescence microscopy they observed qualitative different penetration characteristics of the dye into the skin depending on the preparations used. The addition of a nicotinic acid ester enhanced penetration of the dye into deeper skin structures. Follicles contributed significantly to the penetration of the dye. Similarly, Meyer et al. (93) observed percutaneous absorption of tetracycline derivatives incorporated in various vehicles. Using semisolid formulations, antibiotic penetration into deeper regions of the skin was minimal, while with fluid formulations containing enhancers (dodecan, tetradecan), the penetration into the skin was greater. Fricker et al. (94) investigated the absorption of an intact oligopeptide in rat and dog small intestine using a stable somatostatin analog. The octapetide, also a potential candidate for iontophoretic topical deliver, was coupled to 4-nitrobenzo-2-oxa-1, 3-diazol to have a fluorescent label for direct vizualization. The labeled peptide was successfully used to investigate the existence of preferential absorption sites in the small intestine. However, even though the biological qualities of the labeled and nonlabeled peptide may be comparable, the derivatization of a molecule does change its physiochemical qualities. Therefore, such molecules are only suitable for studying selected aspects of drug transport through the skin.

C. Sample Collection and Drug Analysis: Critical Parameters

With a few exceptions, tissue collection procedures do involve a high degree of invasiveness and inconvenience and are therefore often impractical. Furthermore, ethical considerations (95) in conducting human studies render it necessary to carefully select the site for sampling, sample size, and frequency of sampling. Hence analytical assays and drug extraction procedure have to meet high demands.

Most of the already mentioned methods yield samples that reflect an instantaneous state of the drug in the tissue. However, changes of drug concentration in a

specific compartment are necessary for a pharmacokinetic characterization of a drug. Analytical assays should be done according standardized guidelines, such as HPLC (high performance liquid chromatography) Assays for Bioavailability, Bioequivalence and Pharmacokinetic Studies, a consensus of a symposium held in Washington, DC, in December 1990 (96). There is an important and unsolved problem with the determination of the completeness of drug recovery by extraction from the skin. In order to determine the extraction recovery from the skin tissue, an in vitro experiment is usually performed where excised tissue is spiked with the drug. However, the in vivo drug distribution into skin is different from the in vitro process and the laboratory information is probably only of limited value. The homogenization of certain tissues has been recognized as a major problem in drug analysis, and several methods are available for this purpose (potter, dissolution with strong acids or bases, or enzymatic degradation). Skin tissue is one of the most difficult tissue structures to homogenize. We have evaluated several procedures and found that a homoginizer that combines mechanical and shock cavitation forces successfully breaks up the skin tissue structures without adding to the sample treatment procedure other problems, such as isomerization or metabolizing of the compounds of interest (17,97,98).

IV. C^* CONCEPT: RELATIONSHIP OF SKIN TARGET SITE FREE DRUG CONCENTRATION (C^*) TO THE IN VIVO EFFICACY

A novel method based on the measurement of free drug concentration (C^*), or thermodynamic activity of drug, at the skin target site has been developed by Imanidis, Higuchi, Lee, and co-workers (99,100) to assess bioavailability and to predict efficacy for antivirals and other dermatological formulations. To measure C^* following the administration of a topical formulation initially entailed the establishment of a correlation between the steady-state dermal drug flux and an elicited efficacy. This was accomplished by a novel animal model in which hairless mice were infected at a small site at the lumbar skin area with cutaneous herpes simplex virus type 1. Three days postinoculation, this induced a narrow band of skin lesion development along the peripheral neural path toward the spinal cord. Taking advantage of this unique pattern of lesion development, an antiviral agent, such as acyclovir, was applied to an Azone-pretreated skin area, dorsal to the virus inoculation site and in the predicted path of lesion development. Five days after virus inoculation, the lesion development was scored for each mouse and two different antiviral efficacy parameters were separately assessed: (a)''topical'' (local) efficacy measured the antiviral activity of acyclovir delivery topically to the skin area directly under the drug application site, and (b) ''systemic'' efficacy measured the antiviral activity of acyclovir delivery via systemic circulation to the target site, presumably the epidermal basal layer (101). To quantify drug flux, a transdermal delivery system was developed in this animal model, and the amount of acyclovir delivered to each infected animal could be controlled during the time period of drug therapy through a rate-controlling membrane. The actual (experimental) flux was determined at the end of each in vivo experiment by carrying out an extraction of the residual acyclovir in the transdermal delivery system. This extraction assay served to validate the expected (theoretical) flux or, alternatively, provided the bounds of uncertainty to the drug flux in the particular experiment. The results clearly showed a quantitative relationship between the antiviral efficacy and the experimental flux of acyclovir obtained

from in vivo experiments. Topical efficacy increased with increasing acyclovir flux in the range of 10 to 100 $\mu g/cm^2/day$. Based on the relatively high precision of topical efficacy results, it is believed that the quantitative nature of this animal model should be valuable in the screening of new antiviral agents for topical treatment of cutaneous herpes virus infections and the optimization of topical formulations. Two factors may limit the applicability of this elegant approach to other classes of dermatological formulations. First, the drug was delivered from a transdermal delivery system at a constant rate over several days. With semisolid formulations, formulation application and formulation changes are difficult to control. Recently Mehta et al. (102) confirmed these results with a series of semisolid formulations using acyclovir as a model drug. However, the same group also showed that while predictions based on the C^* concept may correlate well with the in vivo efficacy for acyclovir, that may not be the case for other drugs such as bromovinyldeoxyuridine (103). Bolger et al. (104) recently reported that the concentration of acyclovir in plasma attained following topical administration was effective in reducing mortality associated with herpes infection of hairless mice. These findings have important ramifications for the use of not only the hairless mouse, but also other small-animal models for investigating the topical therapy of cutaneous herpes infections in which the area is large enough to produce significant antiviral drug concentrations in the blood. Therefore, effective systemic delivery of a topically applied drug might falsely indicate the analysis of its therapeutic potential in small animal models of herpes simplex infection. The possibility of both local and systemic modes of drug action should thus be taken into account in the evaluation of topical drugs when using small-animal models. Second, unfortunately the target sites for many dermatological agents (including acyclovir when treating cutaneous herpes simplex virus type 1) are still unknown.

V. CONCLUSION

In terms of the availability of topical drugs, the measurement of primary interest is the concentration of therapeutic agent within the skin or within a specific tissue layer of the skin. While some of the techniques described here show considerable promise and recent evidence suggests that drug concentration in the skin correlates with measures of drug effect in skin, the techniques still require substantial further development and validation (105,106). For this reason, current regulatory bioequivalence judgements have not been based on dermatopharmacokinetic studies. While it might be argued that acceptance of the method should require documentation of a good correlation to an observed clinical effect, this documentation has never been required for oral dosage forms to assess bioequivalence.

REFERENCES

1. Smolen VF, Williams EJ, Kuehn PB. Bioavailability and pharmacokinetic analysis of chlorpromazine in humans and animals using pharmacological data. Can J Pharm 1975; 10:95–106.
2. Queille-Roussel C, Poncet M, Schaefer H. Quantification of skin-colour changes induced by topical corticosteroid preparations using the Minolta Chroma Meter. Br J Dermatol 1991; 124:264–270.
3. Somberg JC. Bioequivalence or therapeutic equivalence. J Clin Pharmacol 1986; 26:1.

4. Dettelbach HR. A time to speak out on bioequivalence and therapeutic equivalence. J Clin Pharmacol 1986; 26:307–308.
5. Lamy PP. Generic equivalents: Issues and concerns. J Clin Pharmacol 1986; 26:309–316.
6. Kiistala U. Suction blister device for separation of viable epidermis from dermis. J Invest Dermatol 1968; 50(2):129–137.
7. Kiistala U. Dermal–epidermal separation. II. External factors in suction blister formation with special reference to the effect of temperature. Ann Clin Res 1972; 4:236–246.
8. Kiistala U. Dermal–epidermal separation. I. The influence of age, sex and body region on suction blister formation in human skin. Ann Clin Res 1972; 4:10–22.
9. Schreiner A, Helium KB, Digranes A, Bergman I. Transfer of penicillin G and ampicillin into human skin blisters induced by suction. Scand J Infect Dis 1978; 14(suppl): 233–237.
10. Miescher G. Beiträge zur Ekzemfrage. I. Zur Frage der Spezifität der ekzematösen Hautreaktion. Arch Derm Syph 1936; 173:119–154.
11. Kiistala U, Mustakallio KK, Rorsman H. Suction blister in the study of cellular dynamics of inflammation. Acta Derm Venereol (Stockh) 1967; 47:150–153.
12. Treffel P, Makki S, Faivre B, Humbert P, Blanc D, Agache P. Citropten and bergapten suction blister fluid concentrations after solar product application in man. Skin Pharmacol 1991; 4:100–108.
13. Huuskonen H, Koulu L, Wilen G. Quantitative determination of methoxalen in human serum, suction blister fluid and epidermis by gas chromatography mass spectrometry. Photodermatology 1984; 1:137–140.
14. Averbeck D, Averbeck S, Blais J, Moysan A, Huppe G, Morliere B, Prognon P, Vigny P, Dubertret L. Suction blister fluid: its use for pharmacodynamic and toxicological studies of drugs and metabolites in vivo in human skin after topic or systemic administration. In: Maibach HI, Lowe NJ, eds. Models in Dermatology. New York: S. Karger AG, 1989:5–11.
15. Agren MS. Percutaneous absorption of zinc from zinc oxide applied topically to intact skin in man. Dermatologica 1990; 180:36–39.
16. Surber C, Wilhelm KP, Berman D, Maibach HI. In vivo skin penetration of acitretin in volunteers using three different sampling techniques. Pharm Res 1993; 10(9):1291–1294.
17. Laugier JP, Surber C, Bun H, Geiger JM, Wilhelm KP, Durand A, Maibach HI. Determination of acitretin in the skin, in the suction blister, and in plasma of human volunteers after multiple oral dosing. J Pharm Sci 1994; 83(5):623–628.
18. Dubertret L, Averbeck D, Prognon P, Blais J, Vigny P. Photobiological activity of the suction blister fluid from patients treated with 8-methoxypsoralen. Br J Dermatol 1983; 109:421–427.
19. Allison JH, Bettley FR. Investigations into cantharidin blisters raised on apparently normal skin in normal and abnormal subjects. Br J Dermatol 1958; 58:330–339.
20. Findlay CD, Wise R, Allcock JE, Durham SR. The tissue penetration as measured by a blister technique and pharmacokinetics of cefsulodin compared with carbenicillin and ticarcillin. J Antimicrob Chemother 1981; 7:637–642.
21. Simon C, Malerczyk V, Brahmstaedt E, Toeller W. Cefazolin, ein neues Breit-bandspektrum-Antibiotikum. Dtsch Med Wochenschr 1973; 98:2448–2450.
22. Frongillo RF, Galuppo L, Moretti S. Suction skin blister, skin window, and skin chamber techniques to determine extravascular passage of cefotaxime in humans. Antimicrob Agents Chemother 1981; 19(1):22–28.
23. Shyu WC, Quintiliani R, Nightingale CH. An improved method to determine interstitial fluid pharmacokinetics. J Infect Dis 1985; 152(6):1328–1331.
24. Raeburn JA. A review of experimental models for studying the tissue penetration of antibiotics in man. Scand J Infect Dis 1978; 14(suppl):225–227.
25. Ryan DM, Hodges B, Spencer GR, Harding SM. Simultaneous comparison of three methods for assessing ceftazidime penetration into extravascular fluid. Antimicrob Agents Chemother 1982; 22(6):995–998.

26. Hoffstedt B, Walder M. Penetration of ampicillin, doxycycline and gentamycin into interstitial fluid in rabbits and of penicillin V and pivampicillin in humans measured with subcutaneously implanted cotton threads. Infection 1981; 9:7–11.
27. Holm SE. Experimental models for studies on transportation of antibiotics to extravasal compartments. Scand J Infect Dis 1978; 13(suppl):47–51.
28. Wise R. Methods of evaluating the penetration of beta lactam antibiotics into tissues. Rev Infect Dis 1986; 8(suppl 3):325–332.
29. Marty JP, Bucks DAW, Maibach HI. Noninvasive radioisotope counting on skin: Surface or external counting?. In: Bronaugh RL, Maibach HI, eds. Percutaneous absorption: Mechanisms—Methodology—Drug delivery. New York: Marcel Dekker, 1989:435–442.
30. Lee DJ, Burt CT, Koch RL. Percutaneous absorption of flurbiprofen in the hairless rat measured in vivo using ^{19}F magnetic resonance spectroscopy. J Invest Dermatol 1992; 99:431–434.
31. Phillips M. Sweat-patch test for alcohol consumption: rapid assay with an electrochemical detector. Alcohol Clin Exp Res 1982; 6(4):532–534.
32. Phillips M, McAloon MH. A sweat-patch test for alcohol consumption: evaluation in continuous and episodic drinkers. Alcohol Clin Exp Res 1980; 4(4):391–395.
33. Phillips ELR, Little RE, Hillman RS, Labbe RF, Campbell C. A field test of the sweat patch. Alcohol Clin Exp Res 1984; 8(2):233–237.
34. Phillips M. An improved adhesive patch for long-term collection of sweat. Biomater Med Dev Art Org 1980; 81(1):13–21.
35. Peck CC, Lee K, Becker CE. Continuous transepidermal drug collection: basis for use in assessing drug intake and pharmacokinetics. J Pharmacokinet Biopharmacol 1981; 9(1):41–58.
36. Peck CC, Conner DP, Bolden BJ, Almirez RG, Kingsley TE, Mell LD, Murphy GM, Hill VE, Rowland LM, Ezra D, Kwiatkowski TE, Bradley CR, Abdel-Rahim M. Outward transcutaneous chemical migration: implications for diagnostics and dosimetry. Skin Pharmacol 1988; 1:14–23.
37. Conner DP, Almirez RG, Rhyne P, Zamani K, Bolden BJ, Peck CC. Transcutaneous collection of theophylline: constancy and linearity of skin permeability. Skin Pharmacol 1989; 2:155–161.
38. Downing DT, Stewart ME, Wertz PW, Colton SW, Abraham W, Strauss JS. Skin lipids: an update. J Invest Dermatol 1987; 88:2s–6s.
39. Rieger MD. Skin lipids and their importance to cosmetic science. Cosmet Toiletries 1987; 102:36–49.
40. Epstein EH, Epstein WL. New cell formation in human sebaceous glands. J Invest Dermatol 1966; 46:453–458.
41. Downing DT, Strauss JS, Ramasastry P, Abel M, Lees CW, Pochi PE. Measurements of the time between synthesis and the surface excretion of sebaceous lipids in sheep and man. J Invest Dermatol 1975; 64:215–219.
42. Faergemann J, Zehender H, Jones T, Maibach HI. Terbinafine levels in serum, stratum corneum, dermis-epidermis (without stratum corneum), hair, sebum and eccrine sweat. Acta Derm Venereol (Stockh) 1991; 71(4):322–326.
43. Nordstrom KM, Schmus HG, McGinley KJ, Leyden JJ. Measurement of sebum output using a lipid absorbent tape. J Invest Dermatol 1986; 87:260–263.
44. Saint-Leger D, Bague A. A simple and accurate routine procedure for qualitative analysis of skin surface lipids in man. Arch Dermatol Res 1981; 271:215–222.
45. Rashleigh PL, Rife E, Goltz RW. Tetracycline levels in skin surface film after oral administration of tetracycline to normal adults and to patients with acne vulgaris. J Invest Dermatol 1967; 49(6):611–615.
46. Gould JC, Richtie HD. The terramycin content of human skin during therapy: a comparison with serum and urine levels. Br J Plast Surg 1952; 5:208–212.

47. Aubin F, Blanc D, Guinchard C, Agache P. Absence de passage de la minocycline dans le sebum? Ann Dermatol Venereol 1988; 115:977.
48. Luderschmidt C, Nissen, H-P, Neubert U, Knuechel M. Newer methods for measuring therapeutic response in acne. In: Cullen SI, ed. Focus on Acne Vulgaris; March; Athens. London: Royal Society of Medicine Services Ltd. 1983; Congress and Symposim Series no. 95:131–140.
49. Kellum RE. Isolation of human sebaceous glands. Arch Dermatol 1966; 93:610–612.
50. Suzuki O, Hattori H, Asano M. Nails as useful materials for detection of methamphetamine or amphetamine abuse. Forens Sci Int 1984; 24:9–16.
51. Ochsendorf FR, Runne U, Schofer H, Schmidt K, Raudonat HW. Sequential chloroquine concentrations in human hair represent ingested dose and duration of therapy—Human hair as a pharmacologic and toxicologic tachograph. Arch Dermatol 1989; 281:121.
52. Balabanova S, Wolf HU. Determination of methadone in human hair by radioimmunoassay. Z Rechtsmed 1989; 102:1–4.
53. Ishiyama I, Nagai T, Toshida S. Detection of basic drugs (methamphetamine, antidepressants and nicotine) from human hair. J Forens Sci 1983; 28(2):380–385.
54. Smith FP, Liu RH. Detection of cocaine metabolite in perspiration stain, menstrual bloodstrain, and hair. J Forens Sci 1986; 31(4):1269–1273.
55. Balabanova S, Brunner H, Nowak R. Radioimmunological determination of cocaine in human hair. Z Rechtsmed 1987; 98:229–234.
56. Van Cutsem J, Van der Flaes M, Thienpont D, Dony J, Hörig C. Quantitative Bestimmung von Ketoconazol in den Haaren oral behandelter Ratten und Meerschweinchen. Mykosen 1980; 23(8):418–425.
57. Walters KA, Flynn GL, Marvel JR. Physicochemical characterization of the human nail: permeation pattern for water and the homologous alcohols and differences with respect to the stratum corneum. J Pharm Pharmacol 1983; 35:28–33.
58. Walters KA, Flynn GL, Marvel JR. Physioehemical characterization of the human nail: solvent effects on the permeation of homologous alcohols. J Pharm Pharmacol 1985; 37:771–775.
59. Walters KA, Flynn GL, Marvel JR. Penetration of the human nail plate: the effects of the vehicle pH on the permeation of miconazole. J Pharm Pharmacol 1985; 37:498–499.
60. Walters KA, Flynn GL. Permeability characteristics of the human nail plate. Int J Cosmetic Sci 1983; 5:231–246.
61. Walters KA, Flynn GL, Marvel JR. Physiochemical characterization of the human nail: I. Pressure sealed apparatus for measuring nail plate permeability. J Invest Dermatol 1981; 76(2):76–79.
62. Stüttgen G, Bauer E. Bioavailability, skin and nail penetration of topically applied antimycotics. Mykosen 1982; 25(2):74–80.
63. Pittrof F, Gerhards J, Erni W, Klecak G. Loceryl® nail lacquer—realization of a new galenical approach to onychomycosis therapy. Clin Exp Dermatol 1992; 17(suppl 1):26–28.
64. Roncari G, Ponelle C, Zumbrunnen R, Guenzi A, Dingemanse J, Jonkman JHG. Percutaneous absorption of amorolfine following a single topical application of an amorolfine cream formulation. Clin Exp Dermatol 1992; 17(suppl 1):33–36.
65. Dykes PJ, Thomas R, Finlay AY. Determination of terbinafine in nail samples during systemic treatment for onychomycoses. Br J Dermatol 1990; 123:481–486.
66. Surber C, Wilhelm K-P, Hori M, Maibach HI, Guy RH. Optimization of topical therapy: Partitioning of drugs into stratum corneum. Pharm Res 1990; 7(12):1320–1324.
67. Fry L, McMinn RMH. Topical methotrexate in psoriasis. Arch Dermatol 1967; 96:483–488.
68. Surber C, Itin P, Bilchner S. Clinical controversy on the effect of topical cyclosporin A: what is the target organ. Dermatology 1992; 185(4):242–245.

69. Parry, GE, Dunn P, Shah VP, Pershing LK. Acyclovir bioavailability in human skin. J Invest Dermatol 1992; 98:856–863.
70. Schaefer H, Lamaud E. Standardization of experimental models. In: Shroot B, Schaefer H, eds. Skin Phamacokinetics. New York: Karger, 1987:77–80. (Shroot B, Schaefer H., series editors. Pharmacology and the Skin; vol. 1.).
71. Schaefer H, Stütten G, Zesch A, Schalla W, Gazith J. Quantitative determination of percutaneous absorption of radiolabled drugs in vitro and in vivo by human skin. Curr Probl Dermatol 1978; 7:80–94.
72. Zesch A, Schafer H. Penetrationskinetik von radiomarkierten Hydrocortisone aus verschiedenartigen Salbengrundlagen in die menschliche Haut. Arch Derm Forsch 1975; 252:245–256.
73. Guzek DB, Kennedy AH, McNeill SC, Wakshull E, Potts RO. Transdermal drug transport and metabolism. I. Comparison of in vitro and in vivo results. Pharm Res 1989; 6(1):33–39.
74. Wojciechowski Z, Pershing LK, Huether S, Leonard L, Burton SA, Higuchi WI, Krueger GG. An experimental skin sandwich flap on an independent vascular supply for the study of percutaneous absorption. J Invest Dermatol 1987; 88:439–446.
75. Pershing LK, Krueger GG. Human skin sandwich flap model for percutaneous absorption. In: Bronaugh RL, Maibach HI, eds. Percutaneous Absorption. New York: Marcel Dekker, 1989:397–414.
76. Scott DO, Bell MA, Lunte CE. Microdialysis-perfusion sampling for the investigation of phenol metabolism. J Pharm Biomed Analysis 1989; 7(11):1249–1259.
77. Lunte CE, Scott DO, Kissinger PT. Sampling living systems using microdialysis. Anal Chem 1991; 63:773A–780A.
78. Ault, JM, Lunte CE, Meltzer NM, Riley CM. Microdialysis sampling for investigation of dermal drug transport. Pharm Res 1992; 9(10):1256–1261.
79. Ault, JM, Lunte CE, Meltzer NM, Riley CM. Microdialysis as a dermal sampling technique for percutaneous absorption. In: Brain KR, James VJ, Walters KA, eds. Prediction of Percutaneous Penetration. Cardiff: STS Publishing, 1993:44–48.
80. Matsuyama K, Nakashima M, Nakaboh Y, Ichikawa M, Yano T, Satoh S. Application of in vivo microdialysis to transdermal absorption of methotrexate in rats. Pharm Res 1994; 11(5):684–686.
81. Fukuyama K. Autoradiography. In: Skerrow D, Skerrow CJ, eds. Methods in Skin Research. London: Wiley, 1985:71–89.
82. Schalla W, Jamoulle J-C, Schaefer H. Localization of compounds in different skin layers and its use as an indicator of percutaneous absorption. In: Bronaugh RL, Maibach HI, eds. Percutaneous Absorption: Mechanism—Methodology—Drug delivery. 2d ed. New York: Marcel Dekker, 1989:283–312.
83. Ritschel, WA, Panchagnula R, Stemmer K, Ashraf M. Development of an intracutaneous depot for drugs. Skin Pharmacol 1991; 4:235–245.
84. Suzuki M, Asaba K, Komatsu H, Mochizuka M. Autoradiographic study on percutaneous absorption of several oils useful for cosmetics. J Soc Cosmet Chem 1978; 29:265–282.
85. Bidmon H-J, Pitts JD, Solomon HF, Bondi JV, Stumpf WE. Estradiol distribution and penetration in rat skin after topical application, studies by high resolution autoradiography. Histochemistry 1990; 95:43–54.
86. Fabin B, Touitou E. Localization of lipophilic molecules penetrating rat skin in vivo by quantitative autoradiography. Int J Pharm 1991; 74:59–65.
87. Touitou E, Fabin B, Dany S, Almog S. Transdermal delivery of tetrahydrocannabinol. Int J Pharm 1988; 43:9–15.
88. Plewig G, Fulton JE. Autoradiographische Untersuchungen an Epidermis und Adnexen nach Vitamin A-Säure-Behandlung. Hautarzt 1974; 23(3):128–136.
89. Klein JA, McCullough JL, Weistein GD. Topical tritiated thymidine for epidermal growth fraction determination. J Invest Dermatol 1986; 86(4):406–409.

90. Motoyoshi K, Ito M, Sakamoto F, Sato Y. A time course study of the proliferation of sebaceous glands induced by topically applied tetradecane in rabbit pinna skin. Autoradiography and electron microscopy. J Dermatol 1987; 14:9–14.
91. Zelei BV, Walker CJ, Sawada GA, Kawabe TT, Knight KA, Buhl AE, Johnson GA, Diani AR. Immunohistochemical and autoradiographic findings suggest that minoxidil is not localized in specific cells of vibrissa, pelage, or scalp follicles. Cell Tissue Res 1990; 262:407–413.
92. Borelli S, Metzger M. Fluorescenzmikroskopische Untersuchungen über die perkutane Penetration fluorescierender Stoffe. Hautarzt 1957; 8(6):261–266.
93. Meyer F. Örtliche Andwendung von Tetracyclinen. Arch Pharmakol Exp Pathol 1966; 225:47–48.
94. Fricker G, Bruns C, Munzer J, Briner U, Albert R, Kissel T, Vonderscher J. Intestinal absorption of octapeptide SMS 201–995 visualized by fluorescence derivatization. Gastroenterology 1991; 100:1044–1552.
95. Svensson CK. Ethical considerations in the conduct of clinical pharmacokinetic studies. Clin Pharmacokinet 1989; 17(4):217–222.
96. Shah VP, Midha KK, Dighe S, McGilveray IJ, Skelly JP, Yacobi A, Layloff T, Viswanathan CT, Cook CE, McDowall RD, Pittman KA, Spector S. Analytical methods validation: bioavailability, bioequivalence and pharmacokinetic studies. Pharm Res 1992; 9(4):588–592.
97. Wagener HH, Voegtle-Junkert U. Zur Auswertung von Wirkstoffkonznetrationen in Geweben nach perkutaner Andwendung von nicht-steroidalen Antirheumatika. Arzneim-Forsch/Drug Res 1996; 46(1,3):299–301.
98. Panus, PC, Tober-Meyer B, Ferslew KE. Tissue extraction and high-performance liquid chromatographic determination of ketoprofen. J Chromatogr 1998; 705:295–302.
99. Imanidis G, Song W, Lee PH, Su MH, Kern ER, Higuchi WI. Estimation of skin target site acyclovir concentrations following controlled (trans)dermal drug delivery in topical and systemic treatment of cutaneous HSV-1 infections in hairless mice. Pharm Res 1994; 11(7):1035–1041.
100. Lee PH, Su MH, Kern ER, Higuchi WI. Novel animal model for evaluating topical efficacy of antiviral agents: flux verus efficacy correlations in acyclovir treatment of cutaneous herpes simplex virus type 1 (HSV-1) infections in hairless mice. Pharm Res 1992; 9(8):979–989.
101. Price RW. Neurobiology of human herpes virus infections. Crit Rev Clin Neurobiol 1986; 2:61–123.
102. Mehta SC, Afouna MI, Ghanem A-H, Higuchi WI, Kern ER. Relationship of skin target site free drug concentration (C^*) to the in vivo efficacy: an extensive evaluation of the predictive value of the C^* concept using acyclovir as a model drug. J Pharm Sci 1997; 86(7):797–801.
103. Afouna MI, Mehta SC, Ghanem A-H, Higuchi WI, Kern ER. Absence of correlation between C^* predictions and in vivo topical antiviral efficacy in hairless mice for bromovinyldeoxyuridine (BVDU). Pharm Res 1997; 14(11): S-35 (abstr. 1105).
104. Bolger GT, Allen T, Garneau M, Lapeyre N, Lird F, Jaramillo J. Cutaneouly applied acyclovir acts systemically in the treatment of herpetic infection in the hairless mouse. Antivir Res 1997; 35:157–165.
105. Caron D, Queille-Roussel C, Shah VP, Schaefer H. Correlation between the drug penetration and the blanching effect of topically applied hydrocortisone creams in human beings. J Am Acad Dermatol 1990; 23:458–462.
106. Pershing LK, Silver BS, Krueger GG, Shah VP, Skelly JP. Feasibility of measuring the bioavailability of topical betamethasone dipropionate in commercial formulations using drug in skin and a skin blanching bioassay. Pharm Res 1992; 9(1):45–51.

27

Stripping Method for Measuring Percutaneous Absorption In Vivo

André Rougier
Laboratoire Pharmaceutique, La Roche-Posay, Courbevoie, France

Didier Dupuis and Claire Lotte
Laboratoires de Recherche Fondamentale, L'Oréal, Aulnay sous Bois, France

Howard I. Maibach
Department of Dermatology, School of Medicine, University of California, San Francisco, California, U.S.A.

From a practical viewpoint, it remains difficult to draw valid conclusions from the literature concerning the absorption level of a given compound. This is essentially due to the diversity of techniques used, animal species (1,2), anatomical location (3,4), duration of application (1), dose applied (5,6), and vehicle used (1,7). Furthermore, because this kind of research has interested scientists from widely differing disciplines, each worker has chosen or adapted the methodology to elucidate a particular problem.

From a theoretical viewpoint, over the two past decades, considerable attention has been paid to the understanding of the mechanisms and routes by which chemical compounds may penetrate the skin. Without considering the different interpretation about mechanisms acting on percutaneous absorption, it is well established that the main barrier is the stratum corneum (3,8,9), which also acts as a reservoir for topically applied molecules (10,11). Moreover, it is likely that at the early step of the absorption process the interaction between the physicochemical properties of the drug, the vehicle, and the horny layer plays an important role in total absorption.

In the first part of this chapter, we hypothesize that the amount of chemical present in the stratum corneum at the end of application may represent the stratum corneum vehicle partitioning and could also reflect the rate of penetration of the chemical.

In the second part, we ascertain that this hypothesis is independent of the main factors likely to modify the absorption level of a compound, that is, contact time, dose applied, vehicle used, anatomical site involved, and animal species chosen.

I. IN VIVO RELATIONSHIP BETWEEN STRATUM CORNEUM CONCENTRATION AND PERCUTANEOUS ABSORPTION

We chose to test, on the hairless rat, 10 radiolabeled molecules having very different physicochemical properties and belonging to different chemical classes.

For each compound, a group of 12 female hairless Sprague-Dawley rats, aged 12 weeks, weighing 200 ± 20 g was used. The molecules, dissolved in ethanol/water mixtures (chosen according to the solubility of the chemical), were applied on 1 cm^2 of dorsal skin during 30 minutes. The standard dose applied was 200 nmol cm^2. At the end of application, the excess product on the treated area was rapidly removed by two washings with ethanol/water (95:5), followed by two rinsings with distilled water, and light drying with cotton wool.

The 12 animals were then divided into two groups (Fig. 1). The animals of group 1, wearing collars to prevent licking, were placed individually in metabolism cages for four days. Urinary excretion was established by daily sampling of the urine and liquid scintillation counting (Packard Instruments 460 C). The feces were collected daily, pooled and counted by liquid scintillation after lyophilization, homogenization, and combustion of the samples with an Oxidizer 306 (Packard Instruments).

After four days, the animals were sacrificed and series of six strippings were carried out on the treated area to determine the amount of product not penetrated within 96 hours. The remaining skin of the treated area (epidermis and dermis) was sampled and counted by liquid scintillation after digestion in Soluene 350 (United Technology Packard). The carcasses were lyophilized, homogenized, and samples

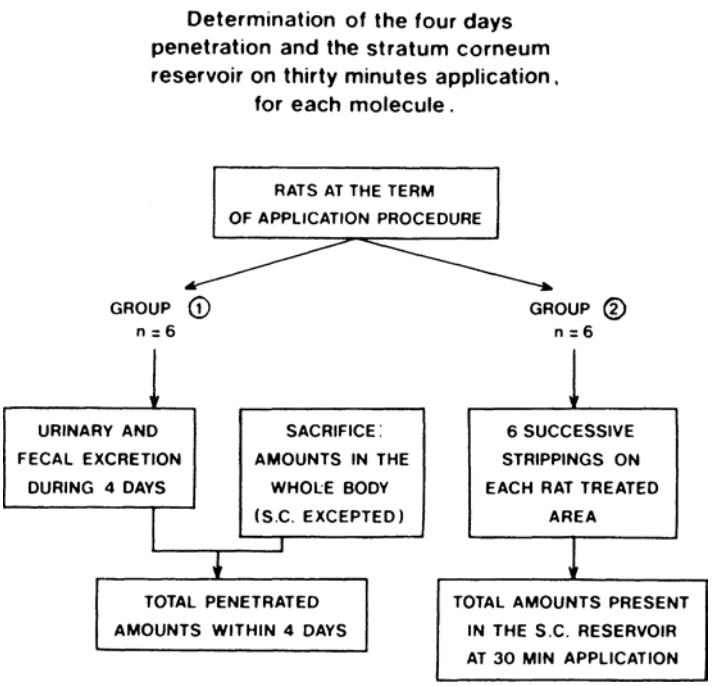

Determination of the four days penetration and the stratum corneum reservoir on thirty minutes application, for each molecule.
RATS AT THE TERM OF APPLICATION PROCEDURE
GROUP ①
n = 6
GROUP ②
n = 6
URINARY AND FECAL EXCRETION DURING 4 DAYS
SACRIFICE: AMOUNTS IN THE WHOLE BODY (S.C. EXCEPTED)
6 SUCCESSIVE STRIPPINGS ON EACH RAT TREATED AREA
TOTAL PENETRATED AMOUNTS WITHIN 4 DAYS
TOTAL AMOUNTS PRESENT IN THE S.C. RESERVOIR AT 30 MIN APPLICATION

Figure 1 Procedures for determining total percutaneous absorption, within four days, and the stratum corneum reservoir at the end of application. *Source*: From Ref. 12.

were counted by liquid scintillation after combustion. The total amount of chemical penetrating within four days was then determined by adding the amounts found in the excreta (urine plus feces), in the epidermis and dermis of the application area, and in the whole animal body.

At the end of application and washing, the stratum corneum of the treated area of the animals from the second group was removed by six stoppings, using 3M adhesive tape. The radioactivity on each strip was measured after complete digestion of the keratinic material in Soluene 350 (United Technology Packard), addition of Dimilume 30 (United Technology Packard), and liquid scintillation counting.

In our experimental conditions, the capacity of the stratum corneum reservoir for each compound has been defined as the sum of the amounts found in the first six strippings.

The percutaneous absorption results show (Fig. 2) that after 96 hours there are large differences in the amounts of substances that have penetrated through the skin. Thus, one can observe that the most penetrating molecule, benzoic acid, penetrates 50 times more than dexamethasone.

When the compounds benzoic acid, acetylsalicylic acid, dehydroepiandrosterone, sodium salicylate, testosterone, hydrocortisone, and dexamethasone are classified according to a decreasing order of penetration rate, we observe that this order is similar to that found in the literature concerning studies in humans (13,14). Likewise, it is established that acetylsalicylic acid and salicylic acid have similar penetrating properties (14), whereas their sodium salts exhibit diminished penetration (8) and, indeed, we observed that sodium salicylate penetrates less than acetylsalicylic acid.

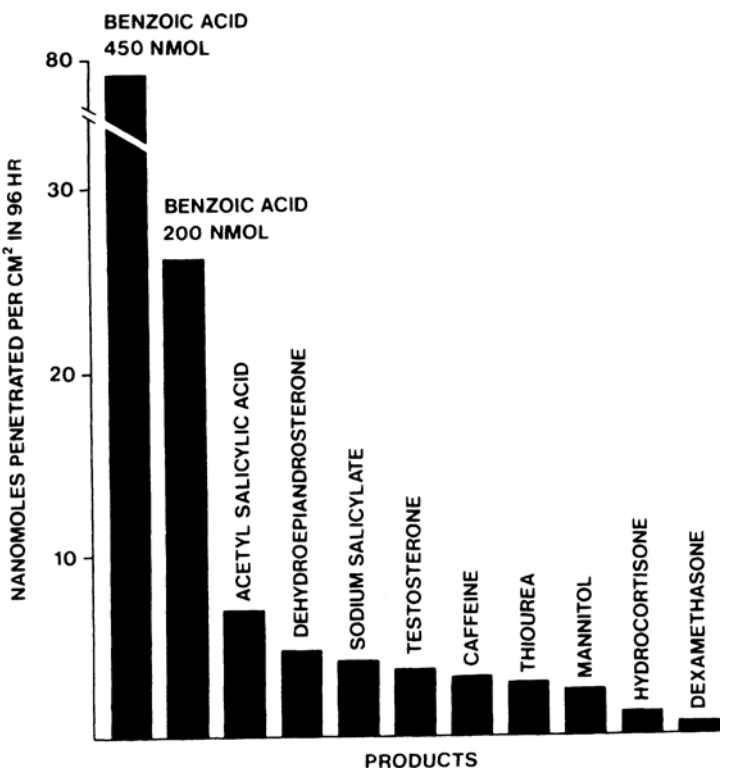


Figure 2 Percutaneous absorption levels of the tested compounds, four days after their topical administration in the hairless rat. *Source*: From Ref. 12.

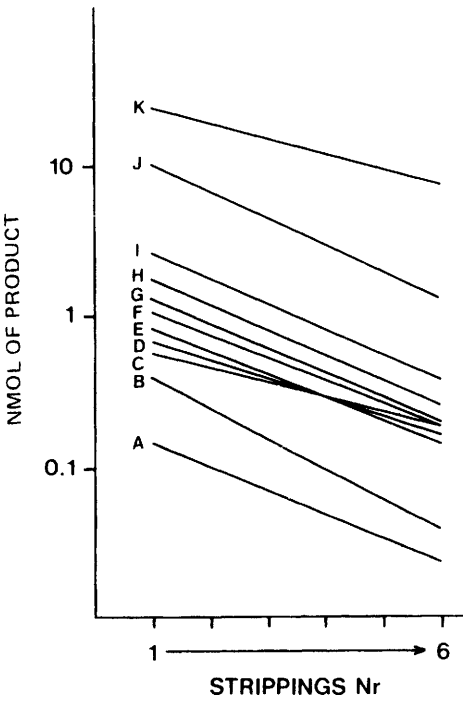


Figure 3 Distribution of the tested molecules within the horny layer of the dosed area, 30 minutes after their administration in the hairless rat: (**A**) dexamethasone, (**B**) hydrocortisone, (**C**) dehydroepiandrosterone, (**D**) testosterone, (**E**) mannitol, (**F**) thiourea, (**G**) caffeine, (**H**) sodium salicylate, (**I**) acetylsalicylic acid, (**J**) benzoic acid (200 nmol), and (**K**) benzoic acid (450 nmol). *Source*: From Rougier, Dupuis, Lotte, and Roguet, unpublished data (1983).

Figure 3 shows the concentrations of compounds present on each stripping of the dosed area of the animals of group 2, at the end of application procedures. It is worth noting that, as in the in vitro results (15), in vivo, the substance concentration decreases inside the stratum corneum, following an exponential relation. Considering the diversity of the compounds tested, it seems that this observation can be outlined as one of the factors governing percutaneous absorption.

As shown in Figure 4, independent of the physicochemical nature of the tested agent, there exists a highly significant linear correlation between the total amount of chemical penetration within four days (y) and the amount present in the stratum corneum at the end of application time (x, 30 minutes; $r=0.98$, $p < 0.001$).

From a theoretical viewpoint, this correlation sheds some light on a possible explanation of the stratum corneum barrier effect. A weak reservoir capacity would correspond to a weak penetration and therefore a strong barrier. Inversely, a high reservoir capacity corresponds to a high penetration and therefore a weak barrier effect. As a consequence, it is possible that barrier and reservoir functions of the horny layer may reflect the same physiological reality. From a practical viewpoint, the simple measurement of the amount of a chemical within the stratum corneum at the end of a 30-minute application gives a good predictive assessment of the total amount penetrating within four days.

As previously mentioned, the absorption level of molecules has been proved to be dependent on their application conditions. It was therefore important to ascertain

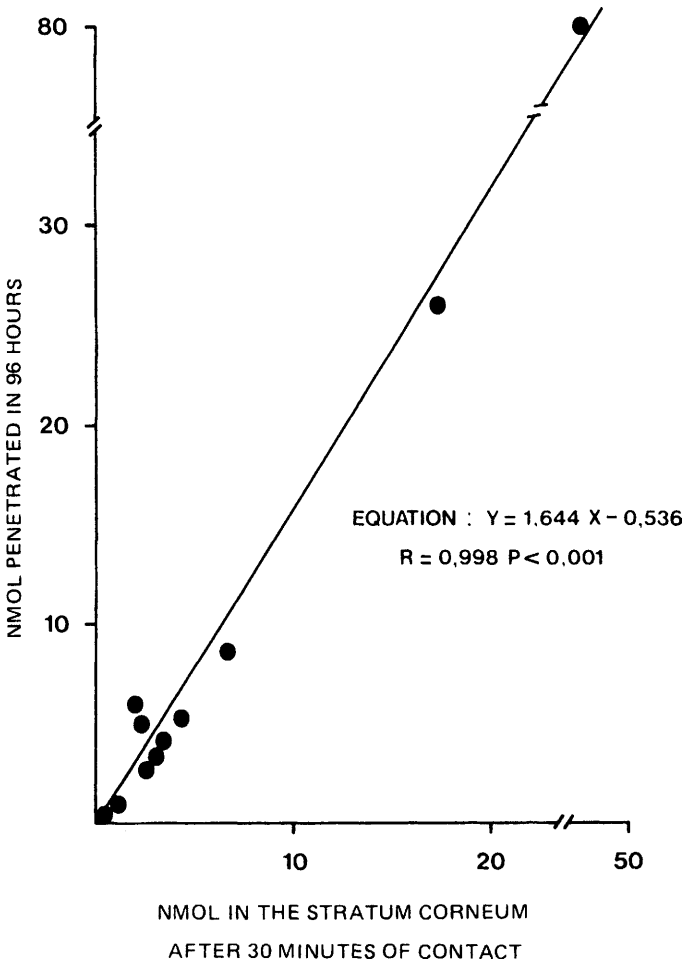


Figure 4 Relationship between the penetration level of the tested compounds after four days ansd their concentrations in the stratum corneum at the end of application (30 min). *Source*: From Ref. 12.

that the "stripping method" was independent of the main factors able to modify the penetration level of a chemical, that is, application time, dose applied, vehicle used, and anatomical site involved.

II. INFLUENCE OF APPLICATION CONDITIONS ON THE RELATIONSHIP BETWEEN STRATUM CORNEUM CONCENTRATION AND PERCUTANEOUS ABSORPTION

A. Influence of Application Time

The duration of application of a compound may considerably influence the total amount absorbed. Moreover, the time of application of a substance may be closely related to its field of use.

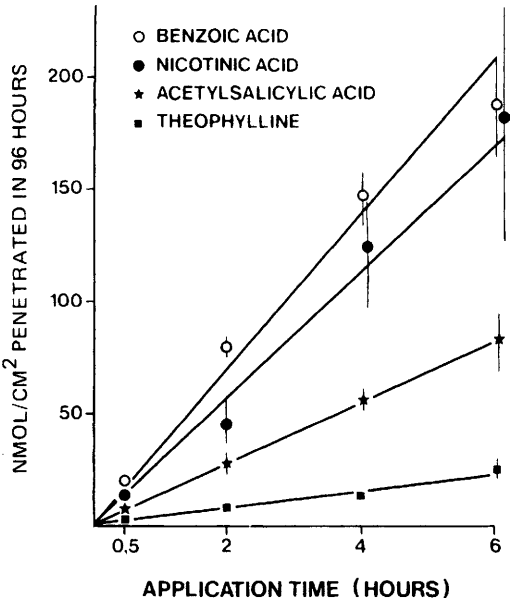


Figure 5 Relationship between the penetration levels of the tested compounds and the application time in the hairless rat. *Source*: From Ref. 18.

Percutaneous absorption of four radiolabeled compounds—theophylline, nicotinic acid, acetylsalicylic acid, and benzoic acid—was studied in the hairless rat. One thousand nanomoles of each compound was applied onto 1 cm^2 of dorsal skin during 0.5, 2, 4, and 6 hours, thus covering most of the usage conditions of the compounds topically applied. Total percutaneous absorption within four days for each compound and each application time was carried out as described in the foregoing section. The stratum corneum reservoir was assessed for each compound, after an application time fixed at 30 minutes by stripping the treated area.

As shown in Figure 5, the penetration rate of the tested compounds is strictly proportional to the duration of application ($r = 0.98$, $p < 0.001$). From a theoretical viewpoint, this relationship provides evidence that, as in the in vitro studies (16,17), a constant flux of penetration really does exist in vivo. This type of correlation having been found for four compounds with widely different physicochemical properties, it is reasonable to assume that it may constitute one of the laws of the in vivo percutaneous absorption phenomena. From a practical viewpoint, this linear relationship implies that the knowledge of the four-day penetration of a compound applied for only 30 minutes has a predictive value for penetration resulting from longer times of application.

As discussed in the preceding section, with a 30-minute application, the total amount of compound recovered within the horny layer is strictly correlated with the amount that penetrated in a 4-day period. Figure 6 shows that this correlation is confirmed ($r = 0.99$, $p < 0.001$) for the four agents tested in this experiment. The total percutaneous absorption of a compound being directly linked to the duration of application (Fig. 5), the simple knowledge of the reservoir effect of the stratum corneum for a chemical applied for 30 minutes allows the predictive assessment of its penetration resulting from longer times of application. Thus, this only mildly

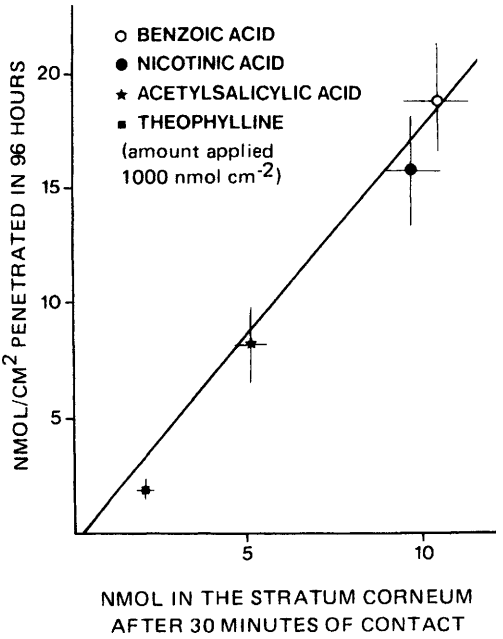


Figure 6 Correlation between the amount of chemical in the stratum corneum at the end of application (30 minutes) and its overall penetration within four days in the hairless rat. *Source*: From Ref. 18.

invasive method offers the advantages, when applied to humans, of reducing skin exposure and of immobilizing subjects only for a short period.

B. Influence of Dose Applied

In most medical and toxicological specialties, the administered dose is defined precisely. This has not always been the case in dermatotoxicology and dermatopharmacology. It is, however, well known that an increased concentration of an applied chemical on the skin increases percutaneous penetration (5,6,19), as does increasing the surface area treated or the application time. This question of concentration may have special significance in infants because the surface/body weight ratio is greater than in adults.

Percutaneous absorption of four radiolabeled compounds—theophylline, nicotinic acid, acetylsalicylic acid, and benzoic acid, dissolved in ethylene glycol/Triton X-100 (90:10)—was studied in the hairless rat. For each compound, increasing doses from 125 to 1000 nmol were applied onto 1 cm^2 of dorsal skin for 30 minutes. For each compound and each dose, total percutaneous absorption within four days and the stratum corneum reservoir at the end of application time were assessed as described in the preceding section.

As shown in Figure 7, within the limits of the concentrations used, there exists a linear dose–penetration relationship ($r = 0.98, p < 0.001$). However, it has been shown by Skog and Wahlberg (20) that when the applied concentration was increased, penetration was increased up to a certain point, at which a plateau was reached. Within the range of concentration used in the present study, this phenomenon does not appear. This tends to indicate that the horny layer is unaffected by the concentrated solutions, with the permeability constant being unaltered over the entire concentration range.

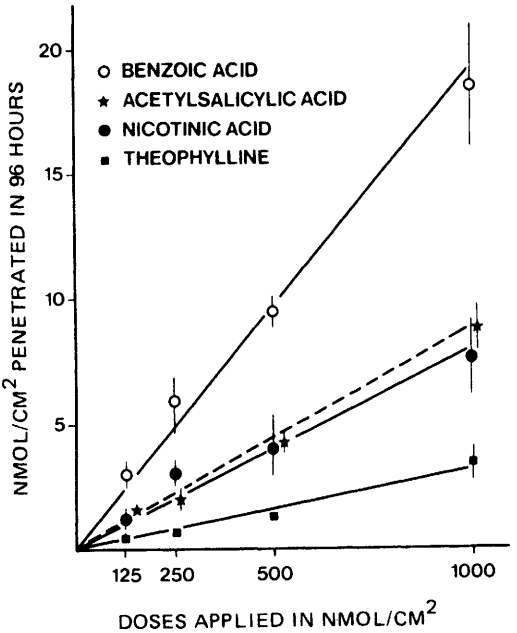


Figure 7 Relationship between dose applied and penetration rate of the tested compounds in the hairless rat. *Source*: From Rougier et al., unpublished data.

When one considers the differences in physicochemical properties of the tested compounds, it seems that, at least for a range of concentration, the linear relationship existing between dose applied and percutaneous absorption level might be taken as a general law.

Independently of the physicochemical nature of the chemical and whatever dose was administered, there is (Fig. 8) a highly significant correlation between the total amounts that penetrated over a four-day period and the amounts recovered in the stratum corneum at the end of application time ($r = 0.98$, $p < 0.001$). From a toxicological viewpoint, the influence of applied concentration on the overall penetration of a drug can therefore be easily predicted using the stripping method. From a pharmacological viewpoint, Sheth et al. (21) have shown that the therapeutic efficacy of increasing doses of an antiviral (iododeoxyuridine) on herpes simplex infection can be predicted by the use of the stripping method.

C. Influence of Vehicle

In recent years, increasing attention has been devoted to the influence that the components of a vehicle may have on enhancing or hindering skin absorption of drugs. The effects of vehicles have been reviewed in detail by several authors (22–25). It is now well established that substances added to formulations as excipients and other factors, such as the physical form of the drug, affect not only its release and absorption, but also its action. Unfortunately, few techniques can be used routinely to elucidate rapidly the role that a vehicle or a component in a vehicle may have on the overall absorption of a drug in vivo.

The influence of nine vehicles on the in vivo percutaneous absorption of [^{14}C]benzoic acid was studied in the hairless rat using the stripping method. Twenty

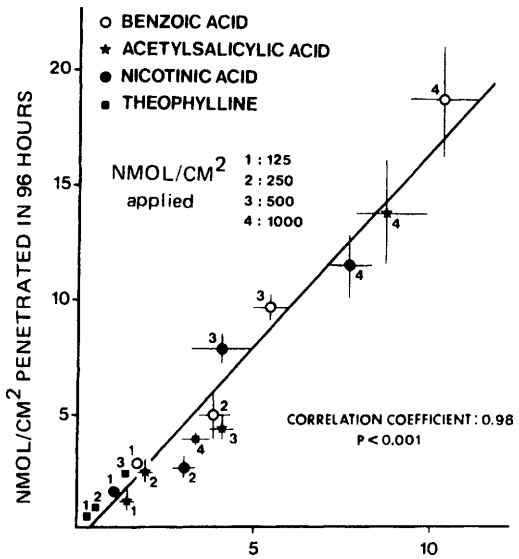


Figure 8 Influence of dose applied on the relationship between the level of penetration of the tested compounds after four days and their concentration in the stratum corneum at the end of application (30 min). *Source*: From Rougier, Lotte, and Dupuis, unpublished data.

microliters of each vehicle, containing 200 nmol of benzoic acid, were applied to 1 cm^2 of dorsal skin during 30 minutes. After this time, total percutaneous absorption and stratum corneum reservoir were assessed as previously described.

As shown in Figure 9, although the vehicles used were simple in composition, the total amount of benzoic acid that penetrated over four days varied by a factor of 50, once more demonstrating the importance of vehicle in skin absorption. Figure 9

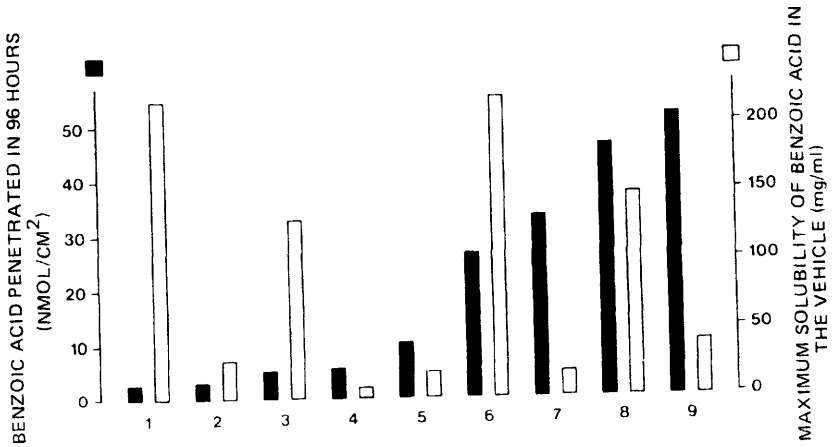


Figure 9 Comparative values of solubility of benzoic acid in the vehicles and corresponding percutaneous absorption levels: (**1**) propylene glycol/Triton X-100 (90:10), (**2**) glycerol/Triton X-100 (90:10), (**3**) ethylene glycol/Triton X-100 (90:10), (**4**) ethylene glycol/Triton X-100; 90:10)/water (40:60), (**5**) (propylene glycol/Triton X-100; 90:10)/water (40:60), (**6**) ethanol/water (95:5), (**7**) methanol/water (40:60), (**8**) ethanol/water (60:40), and (**9**) ethanol/water (40:60). *Source*: From Ref. 28.

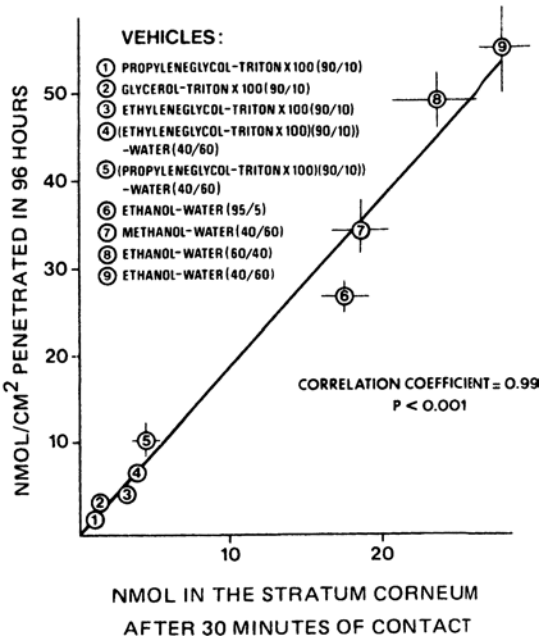


Figure 10 Influence of the tested vehicles on the relationship between the penetration level of benzoic acid within four days and its concentration in the stratum corneum at the end of application (30 min). *Source*: From Ref. 28.

also shows the maximum solubility values (mg/ mL) of benzoic acid in each vehicle. It is generally admitted that the release of a compound can be favored by the selection of vehicles having low affinity for that compound or by one in which it is least soluble (26,27). As may be seen, the solubility of benzoic acid differed by a factor 30 between the least and the most efficient solvent medium (vehicles 4 and 6). However, we can see that there is a weak relationship between penetration level and maximum solubility of benzoic acid. For instance, the greatest penetration is not obtained with the vehicle in which benzoic acid is least soluble, and vice versa.

Applied vehicles have the potential to either increase or decrease the quantity of water in the horny layer and, thereby, to increase or decrease penetration (29). It is interesting that the penetration of benzoic acid is enhanced by increasing the water content of the vehicles, whatever the organic phase (vehicles 1 and 5, and 6, 8, and 9).

As shown in Figure 10, independently of the vehicles composition, the amount of benzoic acid found within the horny layer at the end of application and the amount penetrating in four days are linearly correlated ($r = 0.99$, $p < 0.001$). The influence of the vehicle composition on the in vivo penetration level of a chemical can therefore be easily predicted by simply stripping the treated area and measuring the amount engaged in the stratum corneum at the end of application.

D. Influence of Anatomical Site

Although all authors agree on the importance of anatomical location in percutaneous absorption, the literature contains relatively little information on the subject. Furthermore, generaly reviews dealing with this topic, among others (24,30,31),

often give contradictory explanations of the differences in permeability observed from one site to another. Moreover, if it is clear that both in vitro (31) and in vivo (32–34) the anatomical location is of great importance, the connection between the differences observed, the structure of the skin, and the physicochemical nature of the penetrant, remain obscure.

Percutaneous absorption of four radiolabeled compounds—acetylsalicylic acid, benzoic acid, caffeine, and benzoic acid sodium salt—was measured in humans on four body sites, using the stripping method. For each substance and each location, a group of six to eight male Caucasian informed volunteers, aged 28 $\pm$ 2 years, was used. One thousand nanomoles of each compound were applied to an area of 1 cm^2, in 20 μL of ethylene glycol/ water/Triton X-100 mixtures, the composition of which was chosen according to the solubility of each compound. After 30 minutes of contact, the excess substance in the treated area was rapidly removed as described earlier for the rat. On each patient, two strictly identical applications were performed in an interval of 48 hours. The first application, designed to measure the total penetration of the chemical involved, was made on the right-hand side of the body. For technical convenience, the compounds chosen for the test were ones that are quickly eliminated in the urine. By using data from the literature on the kinetics of urinary excretion of these substances (14,35,36), administered by different routes in various species, the total amounts penetrating within the following four days were deduced, after liquid scintillation counting, from the amounts excreted in the first 24-hour urine. These were, respectively, 75%, 50%, 75%, and 31% of the total quantities of benzoic acid sodium salt, caffeine, benzoic acid, and acetylsalicylic acid absorbed.

At the end of the second application, performed on the left-hand side of the body (contralateral site), the stratum corneum of the treated area was removed by 15 successive strippings (3M adhesive tape), and the radioactivity present in the horny layer was measured as previously described for the rat.

To make comparisons easier, Figure 11 expresses the permeability of each site to the various compounds in relation to that of the arm to benzoic acid sodium salt. This representation offers the advantage of simultaneously showing differences in permeability due to both the physicochemical properties of the penetrants and to the structural peculiarities of the areas where they were applied.

Skin permeability appears to be as follows: arm $\leq$ abdomen $<$ postauricular $<$ forehead. It is worth noting that whatever the compound applied, the forehead is about twice as permeable as the arm or the abdomen. It may be pointed out that this average ratio agrees well with those reported for the same areas with other compounds (32,33).

A possible explanation of the higher penetration in areas where there are more sebaceous glands, such as the forehead, could be that absorption occurs through the follicles, rather than through the epidermis. In our opinion, it is difficult to reconcile the great disproportion, a factor of 50 to 100, existing between the number of sebaceous glands of the arm and the forehead (37,38) and the relatively weak difference, a factor of two to three, observed in skin permeability between these two sites. As a consequence, if it is reasonable to assume that the follicular pathway plays a role in percutaneous absorption, it has to be reevaluated.

In the past, the sebum was believed to reduce absorption of hydrophilic compounds (39). This theory has since been disproved (40). As our results show (Fig. 11), the same ratio, a factor of two, exists between permeability levels of areas such as the forehead, which is rich in sebum, and the arm, which has very little, to compounds with totally different lipid/water solubility, such as benzoic acid and its sodium salt.

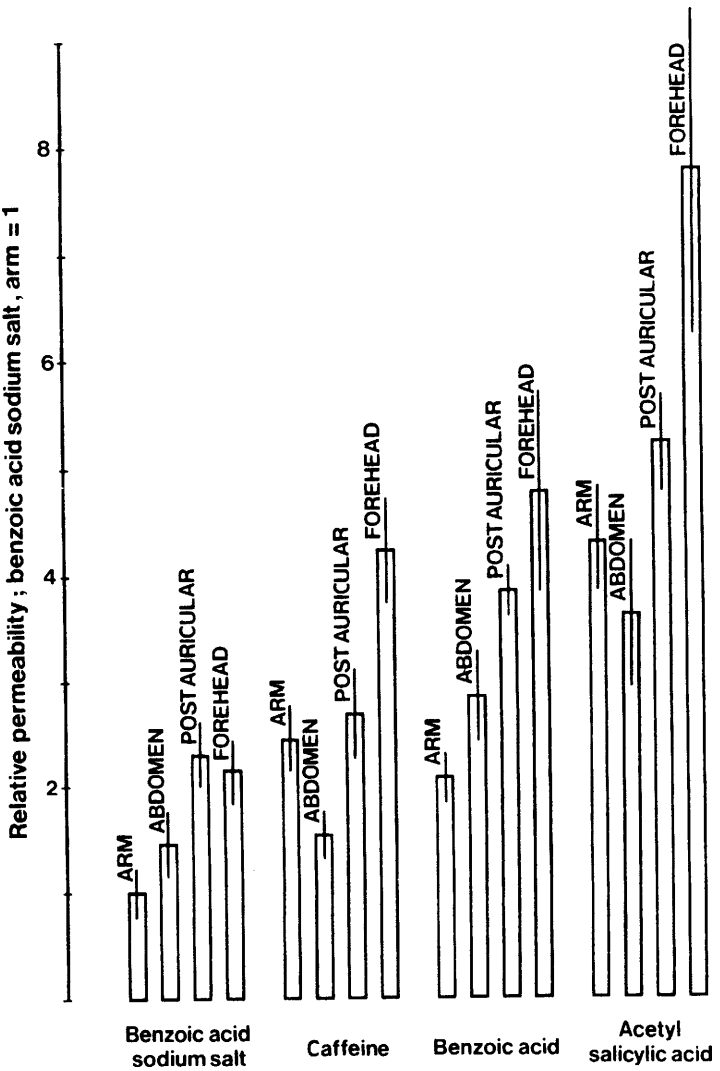


Figure 11 Influence of anatomical site on the total percutaneous absorption of the tested compounds (values expressed relatively to that of benzoic acid sodium salt applied on the arm). *Source*: From Ref. 41.

Among the numerous applications of studies on the relationship existing between skin permeability and anatomical site, considerable attention has been given in recent years to finding favorable "windows" for transdermal treatment of systemic diseases. For various reasons, the postauricular area has been studied most often for scopolamine transdermal drug delivery (42,43). According to Taskovitch and Shaw (44), in this area the closeness of the capillaries to the surface of the skin may promote resorption of substances and give the postauricular skin its good permeability. As our results show (Fig. 11), whatever the compound applied, this area has a high level of permeability. Apart from caffeine, it is statistically higher than that of the arm or abdomen and often similar to that of the forehead.

As Figure 12 shows, the correlation between the amount of substance present in the stratum corneum at the end of a 30-minute application and the total amount absorbed within four days is confirmed in humans, whatever the factors involved in differences of permeability between sites ($r = 0.97$, $p < 0.001$). As a consequence, by simply measuring the quantity *(x)* of a chemical present in the stratum corneum at the end of application, it is now possible to predict the total quantity *(y)* absorbed over a four-day period. It should also be mentioned that this correlation curve is similar to that established in the rat (see sec. I), thus demonstrating that the relationship between reservoir function of the horny layer and percutaneous absorption is independent of the animal species.

The consequences of such findings are obvious and far-reaching. They would make it easier to screen new drugs in animals and, thus, predict their toxicological or pharmacological implications. They would also circumvent some ethical difficulties of human experiments, particularly those using potentially toxic agents. It is self-evident that in vivo investigations with animals, and particularly humans, are preferable to in vitro methods. It is also obvious that the experimentor has a higher degree of responsibility when performing in vivo percutaneous absorption studies in humans. Moreover, the blood and urine analyses generally used in the in vivo methods involve severe technical problems because of the low concentrations that must be assayed. Radiolabeled compounds are detected with high sensitivity but

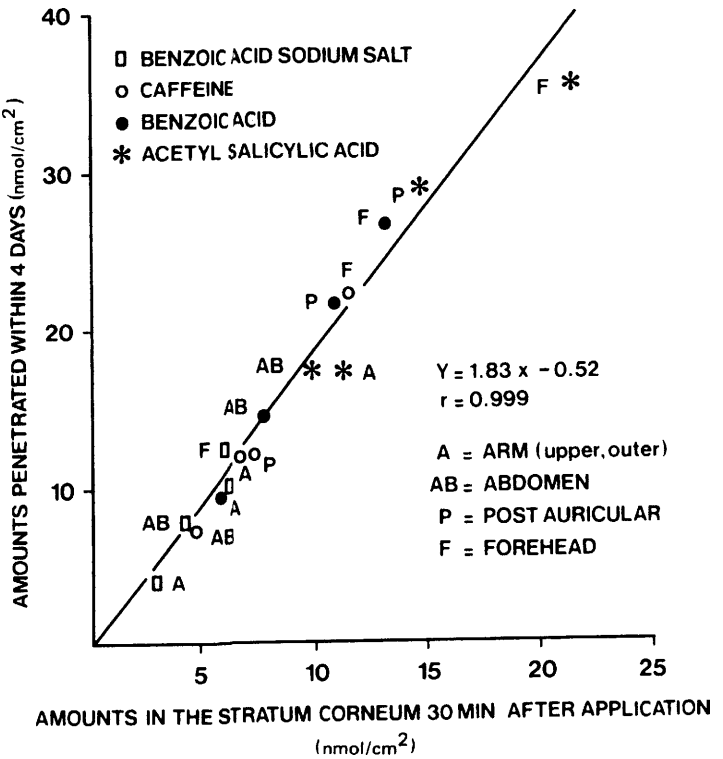


Figure 12 Correlation between total percutaneous absorption within four days and the amounts present in the stratum corneum at the end of application time (30 min), for each compound and each anatomical site. *Source*: From Ref. 24.

imply ethical problems when applied to humans. For technical convenience, labeled compounds were used in our experiments. However, because of the relatively large amount of substance present in the stratum corneum at the end of application, it should be possible, with the stripping method, to measure percutaneous absorption in both animals and humans by appropriate nonradioactive analytical techniques. When it is, nevertheless, essential to use labeled substances, this method makes it possible both to substantially reduce the level of radioactivity administered and to limit contact time.

REFERENCES

1. Tregear RT. The permeability of skin to molecules of widely differing properties. In: Rook A, Champion RH, eds. Progress in Biological Sciences in Relation to Dermatology. 2nd ed. London: Cambridge University Press, 1964:275–281.
2. Winkelmann RK. The relationship of structure of the epidermis to percutaneous absorption. Br J Dermatol 1969; 81(suppl 4):11–22.
3. Marzulli FN. Barrier to skin penetration. J Invest Dermatol 1962; 39:387–393.
4. Lindsey D. Percutaneous penetration. In: Pillsbury DM, Livingood CS, eds. Proceedings of the 12th International Congress of Dermatology. Amsterdam: Exerpta Medica, 1963; 407–415.
5. Maibach HI, Feldmann RJ. Effect of applied concentration on percutaneous absorption in man. J Invest Dermatol 1969; 52:382.
6. Wester RC, Maibach HI. Relationship of topical dose and percutaneous absorption in rhesus monkey and man. J Invest Dermatol 1976; 67:518–520.
7. Poulsen BJ. Design of topical drug products: biopharmaceutics. In: Ariens EJ, ed. Drug Design. Vol. IV. New York: Academic Press, 1973:149–190.
8. Malkinson FD, Rothman S. Percutaneous absorption. In: Marchionini A, Spier HW, eds. Handbuch der Haut und Geschlecht Skrauberten, Normale und Pathologische de Haut, Vol. 1. Part 1. Berlin-Heidelberg: Springer-Verlag, 1963:90–156.
9. Stoughton RB. Percutaneous absorption. Toxicol Appl Pharmacol 1965; 7(Suppl 2):1–6.
10. Stoughton RB, Fritsh WF. Influence of dimethyl sulfoxide (DMSO) on human percutaneous absorption. Arch Dermatol 1964; 90:512–517.
11. Vickers CFH. Existence of a reservoir in the stratum corneum. Arch Dermatol 1963; 88:20–23.
12. Rougier A, Dupuis D, Lotte C, Roguet R, Schaefer H. In vivo correlation between stratum corneum reservoir function and percutaneous absorption. J Invest Dermatol 1983; 81:275–278.
13. Feldmann RJ, Maibach HI. Percutaneous penetration of steroids in man. J Invest Dermatol 1969; 52:89–94.
14. Feldmann RJ, Maibach HI. Absorption of some organic compounds through the skin in man. J Invest Dermatol 1970; 54:399–404.
15. Schaefer H, Stuttgen G, Zesch A, Schalla W, Gazith J. Quantitative determination of percutaneous absorption of radiolabeled drugs in vitro and in vivo in human skin. In: Mali JWH, ed. Current Problems in Dermatology. Basel: S. Karger, 1978:80–94.
16. Scheuplein RJ. Mechanism of percutaneous absorption: II. Transient diffusion and relative importance of various routes of skin absorption. J Invest Dermatol 1967; 48:79–88.
17. Treherne JE. Permeability of skin to some electrolytes. J Physiol 1956; 13:171–180.
18. Rougier A, Dupuis D, Lotte C, Roguet R. The measurement of the stratum corneum reservoir: a predictive method for in vivo percutaneous absorption studies: influence of application time. J Invest Dermatol 1985; 84:66–68.
19. Scheuplein RJ, Ross LW. Mechanism of percutaneous absorption of solvents deposited solids. J Invest Dermatol 1974; 62:353–360.

20. Skog E, Wahlberg JE. A comparative investigation of the percutaneous absorption of lethal compounds in the guinea pig by means of the radioactive isotopes ^{51}Cr, ^{58}Co, ^{65}Zn, ^{110m}Ag, ^{115m}Cd, ^{203}Hg. J Invest Dermatol 1964; 43:187–192.
21. Sheth NV, Keough MB, Spruance SL. Measurement of the stratum corneum drug reservoir to predict the therapeutic efficacy of topical iododeoxyuridine for herpes simplex virus infection. Annual Meeting of the American Federation of Clinical Research, Washington, DC, May 1986.
22. Barr M. Percutaneous absorption. J Pharm Sci 1962; 57:395–408.
23. Idson B. Biophysical factors in skin penetration. J Soc Cosmet Chem 1971; 22:615–620.
24. Idson B. Percutaneous absorption. J Pharm Sci 1975; 64:901–924.
25. Rothman S. Physiology and Biochemistry of the Skin. Chicago: University of Chicago Press, 1990.
26. Blank HI, Scheuplein RJ. The epidermal barrier. In: Rook A, Champion RH, eds. Progress in Biological Sciences in Relation to Dermatology. 2nd ed. London: Cambridge University Press, 1964:245–261.
27. Schutz E. Der Einflub von polyäthylenglycol 400 auf die percutan resorption von wirkstoffen. Archiv Exp Pathol Pharmakol 1957; 232:237–240.
28. Dupuis D, Rougier A, Roguet R, Lotte C. The measurement of the stratum corneum reservoir: a simple method to predict the influence of vehicles on in vivo percutaneous absorption. Br J Dermatol 1986; 115:233–238.
29. Shelley WB, Melton FM. Factors accelerating the penetration of histamine through normal intact skin. J Invest Dermatol 1949; 13:61–64.
30. Barry BW. Dermatological formulations: percutaneous absorption. In: Swarbrick J, ed. Drugs and Pharmaceutical Sciences. Vol. 18. New York: Marcel Dekker, 1983.
31. Scheuplein RJ. Site variation in diffusion and permeability. In: Jarrett A, ed. Physiology and Pathophysiology of the Skin. New York: Academic Press, 1979:1731–1752.
32. Feldmann RJ, Maibach HI. Regional variations in percutaneous penetration of ^{14}C cortisol in man. J Invest Dermatol 1967; 48:181–183.
33. Maibach HI, Feldmann RJ, Milby TH, Serat WF. Regional variations in percutaneous penetration in man. Arch Environ Health 1971; 23:208–211.
34. Wester RC, Maibach HI, Bucks DA, Aufrere MB. In vivo percutaneous absorption of paraquat from hand, leg and forearm of humans. J Toxicol Environ Health 1984; 14:759–162.
35. Bridges JW, French WR, Smith RL, Williams RT. The fate of benzoic acid in various species. Biochem J 1970; 118:47–51.
36. Bronaugh RL, Stewart RR, Congdon ER, Giles AL. Methods for in vitro percutaneous absorption studies. I. Comparison with in vivo results. Toxicol Appl Pharmacol 1982; 62:474–480.
37. Benfenati A, Brillanti F. Sulla distribuzione delle ghiandole sebaceenella cute del corpo umano. Arch Ital Dermatol 1939; 15:33–42.
38. Szabo, G. The regional frequency and distribution of hair follicles in human skin. In: Montagna W, Ellis RA, eds. The Biology of Hair Growth. New York: Academic Press, 1958:33–38.
39. Calvery HO, Draize JH, Lang EP. Metabolism and permeability of normal skin. Physiol Rev 1946; 26:495–540.
40. Blank HI, Gould E. Penetration of anionic surfactants into the skin. II Study of mechanisms which impede the penetration of synthetic anionic surfactants into skin. J Invest Dermatol 1961; 37:311–315.
41. Rougier A, Lotte C, Maibach HI. In vivo percutaneous penetration of some organic compounds related to anatomic site in man: predictive assessment by the stripping method. J Pharm Sci 1987.
42. Shaw JE, Chandrasekaran SK, Michaels AS, Taskovitch L. Controlled transdermal delivery, in vitro and in vivo. In: Maibach HI, ed. Animal Modes in Human Dermatology. Edinburgh, London: Churchill-Livingstone, 1975:136–146.

43. Shaw JE, Chandrasekaran SK, Campbell PS, Schmitt LG. New procedures for evaluating cutaneous absorption. In: Drill VA, Lazar P, eds. Cutaneous Toxicity. New York: Academic Press, 1977:83–94.
44. Taskovitch L, Shaw JE. Regional differences in morphology of human skin. Correlation with variations in drug permeability. J Invest Dennatol 1978; 70:217.

28
Tape-Stripping Technique

Christian Surber and Fabian P. Schwarb
Institut für Spital-Pharmazie, Unicersitätskliniken, Kantonsspital, Basel, Switzerland

Eric W. Smith
College of Pharmacy, University of South Carolina, Columbia, South Carolina, U.S.A.

I. INTRODUCTION

Tape stripping is a technique that has been found useful in dermato-pharmacological research for selectively and, at times, exhaustively removing the skin's outermost layer, the stratum corneum. Typically, an adhesive tape is pressed onto the test site of the skin and is subsequently abruptly removed. The application and removal procedure may be repeated 10 to more than 100 times (1,2).

Skin that has been stripped in this manner has been used as standardized injury in wound healing research. The technique has been adapted for studying epidermal growth kinetics (3–7), and it may also be useful as a diagnostic tool in occupational dermatology to assess the quality of the stratum corneum (8,9).

The observation that the skin may serve as a reservoir for chemicals was originally reported by Malkinson and Ferguson (10). The localization of this reservoir within the stratum corneum was later demonstrated for corticosteroids by Vickers (11) and has been confirmed by others (12–15). The introduction of the tape-stripping method to further investigate the reservoir and barrier function of the skin gave a significant expansion to experimental tools in skin research (16–18).

Differences in the permeability of intact and fully stripped skin have provided information about the diffusional resistance of the various dermal strata (19). It has been recognized that complete removal of the stratum corneum was not possible even after 30 to 40 strippings (20), and a certain barrier function in the tissue so treated remains (21,22). Öhman and Vahlquist (2) showed that after 100 tape strippings the entire stratum corneum could be removed (Fig. 1); however, no permeation data through such completely stripped skin exist.

II. APPLICATION OF THE TAPE-STRIPPING TECHNIQUE IN DERMATOPHARMACOLOGY

The presumption that factors that improve percutaneous absorption also result in an increase in the stratum corneum reservoir (11,15) made the tape-stripping

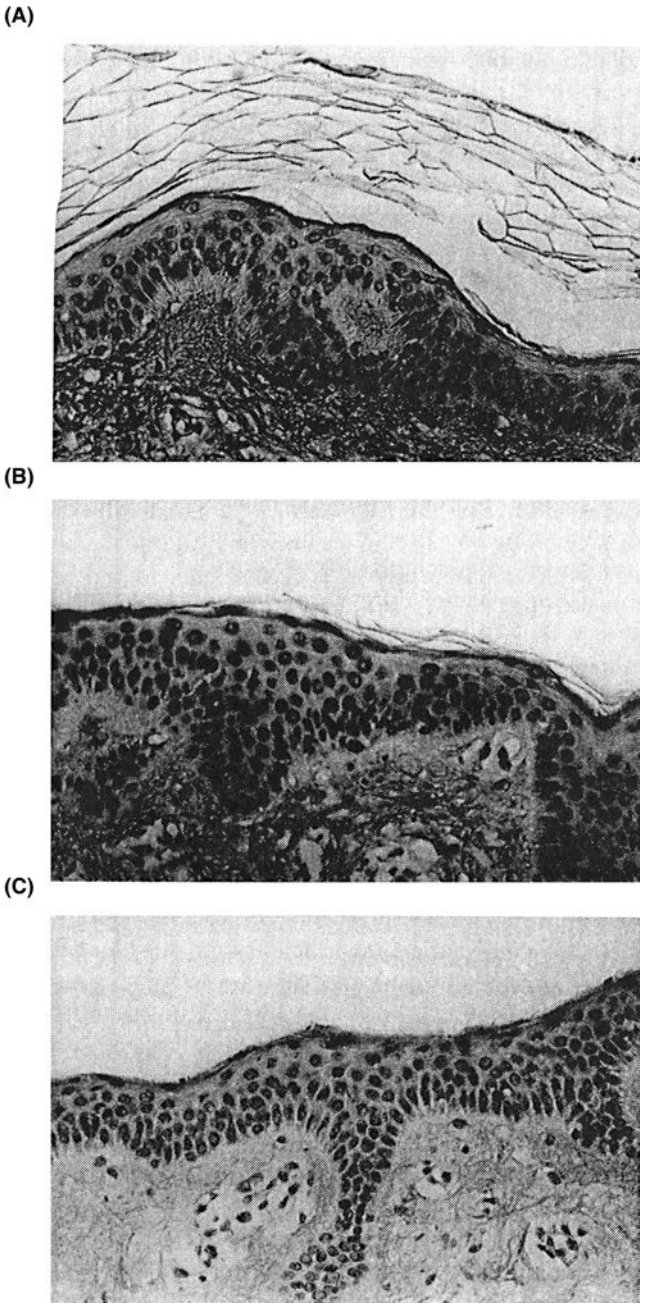


Figure 1 Skin that is (**A**) intact, (**B**) 50 times stripped, and (**C**) 100 times stripped
Source: From Ref. 2.

methodology a promising tool for selecting or comparing vehicles for topical drugs. Data from tape-stripping experiments were therefore related to (a) chemical penetration into skin, (b) chemical permeation through skin, (c) chemical elimination from the skin, (d) pharmacodynamic parameters, and (e) clinical parameters.

In a series of in vitro and in vivo investigations using the tape-stripping technique, it could be shown that drug penetration into stratum corneum, determined by quantification of radiolabeled chemical on the removed tape, was clearly vehicle dependent. In vitro drug penetration into the stratum corneum was usually higher than in vivo, whereas penetration into deeper tissues was higher in vivo. In vivo drug permeation through the skin, determined as drug excreted in the urine, was found to be vehicle independent. It was noted that different vehicles may bring about different therapeutic drug concentrations into the skin, but similar or different systemic burdens were produced (e.g., corticosteroids and salicylic acid) (16,23–26).

Dupuis, Lotte, Rougier, and coworkers (27–31) standardized the methodology of the tape-stripping technique. Their stripping method determines the concentration of chemical in the stratum corneum at the end of a short application period (30 minutes). They found a linear relationship between the stratum corneum reservoir content and in vivo percutaneous absorption (total amount of drug permeated in four days) using the standard urinary excretion method (32–34). They could also show, for a variety of simple pharmaceutical vehicles, that percutaneous absorption of benzoic acid is vehicle dependent and can be predicted from the amount of drug within the stratum corneum at 30 minutes after application. They stated that the major advantages of their validated tape-stripping protocol are the subsequent elimination of urinary and fecal excretion to determine absorption, and the applicability to non-radiolabeled determination of percutaneous absorption because the skin strippings contain adequate chemical concentrations for non-labeled assay methodologies (Table 1). Despite the fact that the assay provides reliable prediction of total absorption for a group of selected compounds, mechanistic interpretations are still rare. Based on the data of Rougier et al. Auton (35) presented an initial first mathematical approach that may help to explain some of the above observations.

The tape-stripping technique has also been used to analyze biological activity, thus taking into account binding, decomposition, and metabolism of a given drug. From a skin area treated with various griseofulvin formulations, stratum corneum was stripped onto tapes, sterilized, and then inoculated with *Trichophyton mentagrohytes* spores. Under controlled in vitro conditions the degree of growth of the spores in the stratum corneum was graded. Various formulations of topical griseofulvin were tested for activity and duration of effect with this method. The antifungal effect

Table 1 Comparison of Drug Strength, Amount of Drug on the Skin (A), Amount of Drug Absorbed When 2 mg of a Topical Dermatological Dosage Form at Various Strengths Is Spread Over an Area of 1 cm^2 Assuming a 5% Absorption of the Dose Applied (B), and Amounts When Further Assuming that 90% of the Dose Absorbed Will Be Retained in the Total Skin (C) and that From that Amount 80% Will Be Retained in the Stratum Corneum (D)

Strength (%)	A, dose applied ($\mu g/cm^2$) on the skin surface	B, dose absorbed ($\mu g/cm^2$), 5% of dose applied	C, dose absorbed ($\mu g/cm^2$) as 90% of B in total skin	D, dose absorbed (ng/cm^2) as 80% of C in the stratum corneum
1	20	1,000	900	720
0.1	2	100	90	72
0.01	0.2	10	9	7.2

Note: From these columns, it is obvious that quantification of a drug may be difficult (e.g., corticosteroids/high-performance liquid chromatography).

of griseofulvin in the cream base was weak and of short duration, whereas the antifungal formulated into a dimethylacetamide vehicle was effective for 24 hours and could be detected 96 hours after one application (36).

A direct study evaluating whether differential drug uptake of topical 2% miconazole and 2% ketokonazole from cream formulations in to human stratum corneum correlated with differential pharmacological activity (100-fold) against *Candida albicans* was recently done (37). After removal of the residue from a single 24-hours topical dose of the two antifungals, the stratum corneum of the test sites was removed by tape stripping. The tapes were extracted for drug quantification [high-performance liquid chromatography (HPLC)] and bioactivity against *C. albicans* growth in vitro. Topical ketaconazole produced significantly higher drug concentrations in stratum corneum than miconazole at one, four and eight hours after a single topical dose. However, after 24 hours the concentrations were similar. Tape disk extracts from the ketaconazol-treated skin sites demonstrated significantly greater bioactivity in the bioassay than miconazole, due to the fact that the stratum corneum can easily be sampled, drug activity can be evaluated directly in the target tissue. Data from such experiments are more relevant than the standard in vitro minimal inhibition concentration (MIC) methods. The combination of a pharmacokinetic and a pharmacodynamic method offers a more comprehensive approach with which to identify optimized topical vehicle formulations for antifungal delivery to the skin and to determine bioequivalence between topical antifungal products.

Sheth et al. (1) compared the concentration of iododeoxy-uridine in the stratum corneum of the guinea pig skin by tape stripping at different points, after single and multiple topical doses of the drug, in various simple formulations. These results were correlated with the efficacy of topical iododeoxyuridine against an experimental cutaneous herpes simplex virus. The results showed an excellent correlation between the quantity of iododeoxyuridine in the stratum corneum and the reduction in lesion severity. Both formulation composition and dosing frequencies had an effect on the iododeoxyuridine concentration in the stratum corneum and on the corresponding clinical efficacy.

Data from in vitro and in vivo human skin model systems indicated that significantly higher acyclovir concentrations were achieved in stratum corneum (tape-stripping/cyanoacrylate method) (38) after topical application as compared to oral administration. However, mathematical modeling of in vitro and in vivo skin biopsy data and sectioning experiments demonstrated that the drug concentration at the target site, the basal epidermis, is two to three times less lower after topical administration than after oral administration (39).

Penetration of two chemicals d*l*-alpha-tocopherol nicotinate and L440, an anti-inflammatory substance [L440 $\rightarrow$ 2-(*t*-butyl)-4-cyclohexylphenylnicotinate *N*-oxide], into human stratum corneum (by a tape-stripping method) (40) from two liposomal gels was significantly higher than from conventional formulations (oil/water, water/oil bases). Only a slight dependence of the extent of penetration into stratum corneum on liposome diameter was observed. The anti-inflammatory effect of L440 was determined by the arachidonic acid-induced ear edema in the male NMR mouse. A significant clinical effect of L440 was observed with the liposomal formulation and with the oil-in-water (o/w) base. An insignificant effect of L440 in the water-in-oil (w/o) base was detected (41).

Attenuated total reflectance infrared spectroscopy (ATR-IR) can quantitate the appearance of a drug or vehicle in the skin from human volunteers. However, it will only work for the outer regions of the epidermis, and it requires compounds with an

unique infrared spectrum. The ATR-IR has been used to study the effect of oleic acid on the percutaneous absorption of *p*-cyanophenol in vivo (42). Higo et al. (43) recently showed that the amount of *p*-cyanophenol in the stratum corneum was highly correlated with depth ($r^2 = 0.84$–0.93) depending on application time. In this study drug determination was carried by ATR-IR and by direct ^{14}C analysis of *p*-cyanophenol following progressive removal of tissue by tape stripping.

Pershing et al. (44–47) simultaneously compared a skin blanching bioassay with drug content in human stratum corneum following topical application of commercial 0.05% betamethasone dipropionate formulations. The rank order of the betamethasone dipropionate formulation potency was found to be is similar between by the visual skin blanching assay and the tape-stripping assessments and by monitoring with the a-scale of the Minolta chromameter. The rank correlation between the tape-stripping method and the skin blanching response was moderate to good.

Usually drug uptake is assessed by applying test and reference products simultaneously to multiple skin sites in a single study subject. Stratum corneum samples are obtained at sequentially increasing times intervals from the time of application. In a similar manner, to assess drug elimination, test and reference products are applied for a specific period of time at multiple sites and removed. The stratum corneum samples are collected at sequentially increasing times after drug formulation removal. Additionally, drug elimination studies after the drug concentration has reached a plateau in the stratum corneum have been proposed (48,49). These data support the application of dermato-pharmacokinetic principles to bioavailability and bioequivalence determinations of topical dermatological products (48–50).

III. THE POTENTIAL OF THE TAPE-STRIPPING METHODS

Recently, Shah et al. (51) summarized the essential of an international expert panel that presented a series of invited contributions at the American Association of Pharmaceutical Scientists (AAPS)/Food and Drug Administration (FDA) workshop on Bioequivalence of Topical Dermatological Dosage Forms—Methods for Evaluating Bioequivalence, held in September 1996. The workshop explored the possibility that dermato-pharmacokinetic characterization might provide an alternative approach to clinical trials for the determination of bioequivalence of topical dermatological products in a parallel manner, analogous to the use of concentration–time curves for systemically administered drugs. If accepted, this approach might allow dermatopharmacokinetic studies to replace clinical trials as a means of documenting bioequivalence of selected topical drug products. Among a variety of models presented (e.g., microdialysis, confocal laser scanning microscopy, or transepidermal water loss), the tape-stripping method seems to have the greatest potential for dermatopharmacokinetic characterization of selected topical drug products.

IV. PROTOCOL OUTLINE FOR A TAPE-STRIPPING EXPERIMENT

The following outlines an example of procedural steps involved in a tape-stripping experiment:

- Apply the test and/or the reference drug products concurrently at multiple sites.

- After an appropriate interval, remove the excess drug by wiping with tissue or cotton swab. Appropriate time duration should be determined in a pilot study.
- Apply the adhesive tape with uniform pressure; remove and discard the first stripping, as this is believed to represent unabsorbed drug on the skin surface. Repeat this procedure if one tape strip is not sufficient to remove all excess/unabsorbed drug from the skin surface.
- Apply (at the same site), remove, and collect 9 to 20 successive tape strippings from each application site. Repeat the procedure for each site at other designated time points.
- Extract the drug from single or combined tape strippings and determine the concentration in the extract solution using an appropriate analytical methods (cave extraction recovery).
- Express the results as amount of drug per square centimeter area of the adhesive tape (e.g., ng/cm^2) or by another adequate means (e.g., ng/protein content).

This procedure will provide information about the drug uptake in the stratum corneum.

To determine a drug elimination phase from the stratum corneum, apply the drug product concurrently at multiple sites, allow sufficient exposure periods until an apparent steady-state level is achieved, and remove excess drug from the skin surface as described above. After predetermined time intervals (e.g., 1, 3, 5, and 21 hours after drug removal), collect skin samples using 9 to 20 successive tape strips, and analyze them for drug content.

V. UNANSWERED QUESTIONS AND CONCERNS

Despite the fact that the tape-stripping method has been used in dermato-pharmacological research for several decades, several experimental details have not been addressed and the technique still awaits rigorous validation.

First, in bioequivalence evaluations the vehicle components of a test and a reference product may be different and may variably influence both the adhesive properties of the tape as well as the cohesion of the corneocytes. Hence dermato-pharmacokinetic characterization may become extremely complex and susceptible to error. As described previously by Surber et al. (52), the vehicle may significantly change the cohesion of the corneozytes. It was shown in this chapter that the removal of corneocytes can be highly dissimilar, and dermato-pharmacokinetic characterization based on a concentration profile within the stratum corneum is not possible (Fig. 2). A similar observation was made by van der Molen et al. (53). They showed that normal tape stripping of human stratum corneum yields cell layers that originate from various depths because of furrows in the skin.

Second, the material and methods sections of most research papers that used a tape-stripping technique rarely describe the use of a template to assure consistent removal of stratum corneum from the exact treatment area. Without such a template, consistency in terms of the stratum corneum removal area is not assured and, hence, dermato-pharmacokinetic characterization may become questionable. The recent AAPS/FDA workshop report (51) addresses this issue and recommends also the use of such demarcating templates (52).

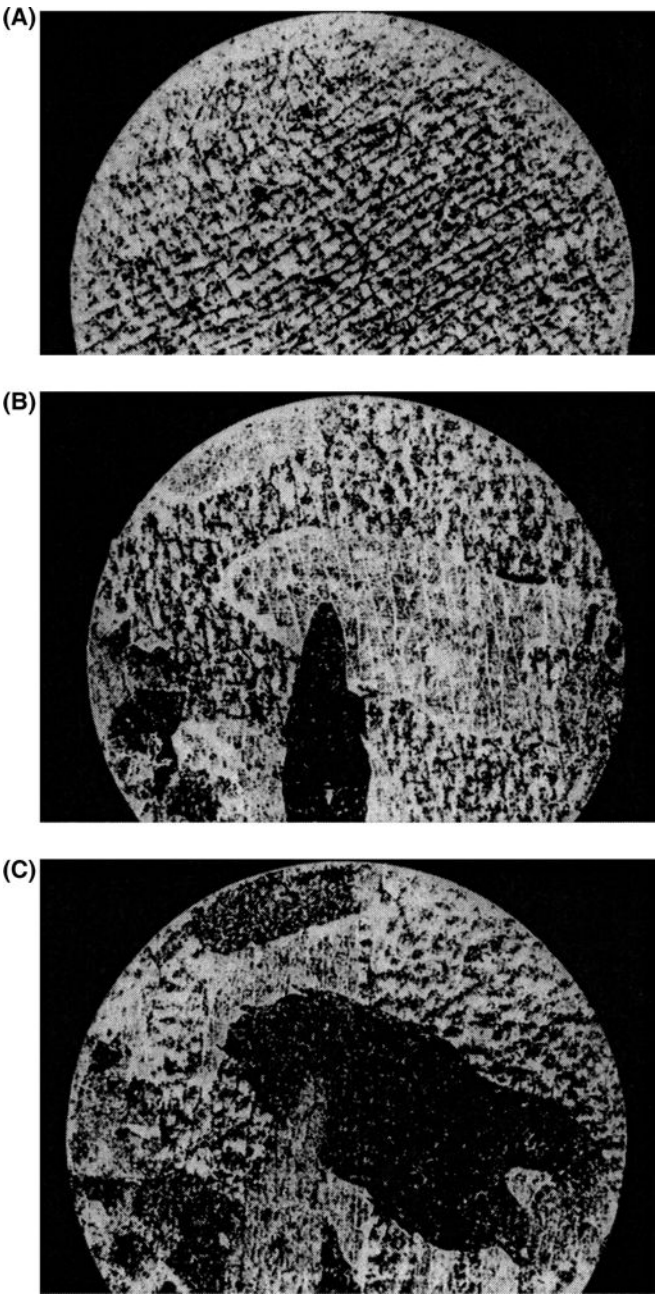


Figure 2 (**A**) Strip 7 taken from untreated skin, (**B**) Strip 7, and (**C**) 8 taken from a skin site three hours after the application of a w/o cream base.

Third, the tape-stripping method has primarily been applied in experimental in vivo settings. However the technique has also been used to remove stratum corneum from skin that has been used for in vitro experiments. Depending on the skin origin (human and animal) and source (surgery and morgue), skin storing conditions, and the duration of the in vitro experiment, the integrity of the skin may vary and will

markedly influence the amount of stratum corneum that is being removed with each tape strip. As seen in Figure 3, freshly prepared hairless rat skin used in an in vitro experiment will separate at the basal membrane approximately three hours after the start of the experiment. Subsequent tape stripping removes the entire epidermis, including the stratum corneum.

Fourth, as previously stated by several experts, the major advantage of the tape-stripping technique is the applicability to non-radiolabeled determination of percutaneous absorption because the skin strippings contain adequate chemical concentrations for non-labeled assay methodologies. However, using realistic doses of topical dermatological dosage forms on the skin (usually less than 2 mg/cm^2); the quantification of the drug in the skin strippings may become a major analytical challenge (low concentration in the strippings and difficult extraction from the tapes). Table 1 may illustrate this issue.

Lastly, even though tape-stripping is considered to be essentially noninvasive, stripped sites in certain dark-skinned individuals may remain pigmented for several months after healing. This effect must be communicated to the volunteers before entering a study.

VI. RELATED TECHNIQUES

The surface biopsy and skin scraping techniques have also been used to remove stratum corneum from the skin.

The skin surface biopsy technique using cyanoacrylate contact cement adhesive was first used to remove the stratum corneum for diagnostic and investigative purposes in superficial mycosis infections. The glue is applied to a glass slide and pressed onto the skin surface. The slide is subsequently removed after the glue has polymerized with the stratum corneum (54,55). This technique allows also the quantification of drug found in the stratum corneum after various application times (56). However, a distinction between the transepidermal and the transfollicular routes of absorption is not possible because the hair follicle content is also removed with this method.

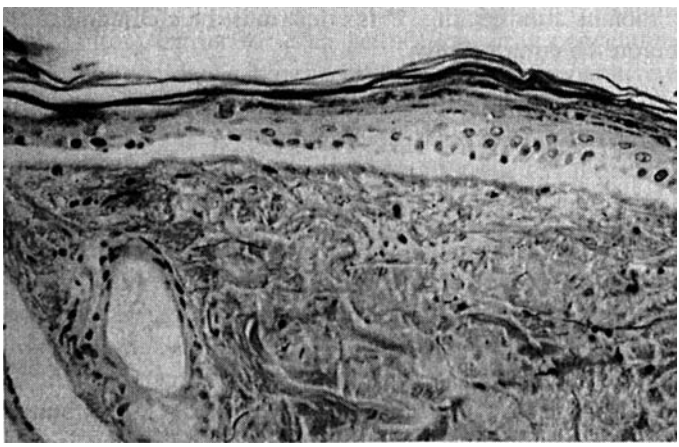


Figure 3 Separation of epidermis from dermis three hours after the start of an in vitro percutaneous absorption experiment with rat skin.

Large amounts of corneocytes can be harvested by scrapping the stratum corneum from the surface with an open dermal steel curette. Usually superficial ($< 20\,\mu m$ depth) and, with more vigorous scraping, mid-level (20–40 μm depth) stratum corneum can be collected in this manner (57,58). This technique has also been successfully employed by Faergemann et al. (59–61) to determine drug concentration (terbinafine, fluconazole) in the stratum corneum. However, the degree of superficial sebum and sweat contamination of the stratum corneum may influence the amount of drug found in this tissue.

VII. CONCLUSIONS

The skin-stripping method has potential for being a specific dermato-pharmacokinetic method that assesses drug concentration in stratum corneum as a function of time. Both drug uptake and drug elimination profiles may be evaluated to determine traditional pharmacokinetic metrics, such as AUC, C_{max}, and T_{max}.

Currently two general views on the potential applicability of the skin-stripping technique are expressed. Some researchers are of the opinion that only diseases in which stratum corneum is the site of action are amenable to this method of analysis, because only the drug concentration in the stratum corneum is measured (i.e., antifungal or corticosteroid classes of topical dermatological drugs). Others contend that regardless of how far through the skin layers the drug needs to permeate (stratum corneum–epidermis–dermis), the active moiety needs to pass through the stratum corneum first before reaching the deeper skin layers. Since the stratum corneum is the rate-limiting barrier for drug permeation, drug concentrations in this layer may also provide meaningful information for comparative evaluation of topical dosage forms intended for dermal, subdermal, or systemic action.

Despite the application of the tape-stripping methods in dermatopharmacological research for several decades, the technique still awaits rigorous validation in order to become a viable, robust, and reproducible method for bioequivalence evaluation of topical dermatological drug products.

REFERENCES

1. Sheth NV, McKeough MB, Spruance SL. Measurement of stratum corneum drug reservoir to predict the therapeutic efficacy of topical iododeoxyuridine for herpes simplex. J Invest Dermatol 1987; 89:598–602.
2. Ohman H, Vahlquist A. *In vivo* studies concerning a pH gradient in human stratum corneum and upper epidermis. Acta Derm Venereol (Stockh) 1994; 74:375–379.
3. Eriksen G, Lamke L. Regeneration of human epidermal surface and water barrier function after stripping. Acta Derm Venereol (Stockh) 1971; 51:169–178.
4. Wilhelm D, Elsner P, Maibach HI. Standardized trauma (tape-stripping) in human vulvar and forearm skin. Acta Derm Venereol (Stockh) 1991; 71:123–126.
5. Downes AM, Matoltsy AG, Sweeney TM. Rate of turnover of the stratum corneum in hairless mice. J Invest Dermatol 1967; 49(4):400–405.
6. Pinkus H. Examination of the epidermis by the strip method of removing horny layers. I. Observations on thickness of the horny layer, and on mitotic activity after stripping. J Invest Dermatol 1951; 16:383–386.

7. Pinkus H. Examination of the epidermis by the strip method of removing horny layers. II. Biometric data on regeneration of human epidermis. J Invest Dermatol 1951; 16: 431–447.
8. Piérard GE, Piérard-Franchimont C, Saint-Léger D, Kligman AM. Squamometry: the assessment of xerosis by colorimetry of D-Squame® adhesive discs. J Soc Cosmet Chem 1992; 47:297–305.
9. Schatz H, Kligman AM, Manning S, Stoudemayer T. Quantification of dry (xerotic) skin by image analysis of scales removed by adhesive discs (D- Squame®). J Soc Cosmet Chem 1993; 44:53–63.
10. Malkinson FD, Ferguson EH. Percutaneous absorption of hydrocortisone- 4-^{14}C in two human subjects. J Invest Dermatol 1955; 25:281–285.
11. Vickers CFH. Existence of reservoir in the stratum corneum. Arch Dermatol 1963; 88:20–23.
12. Stoughton RB. Dimethyl sulfoxide (DMSO) induction of a steroid reservoir in human skin. Arch Dermatol 1965; 91:657–660.
13. Carr RD, Wieland RG. Corticosteroid reservoir in the stratum corneum. Arch Dermatol 1966; 94:81–84.
14. Carr RD, Tarnowski WM. The corticosteroid reservoir. Arch Dermatol 1966; 94: 639–642.
15. Munro DD. The relationship between percutaneous absorption and stratum corneum retension. Br J Dermatol 1969; 81(suppl 4):92–97.
16. Lücker P, Nowak H, Stüttgen G, Werner G. Penetrationskinetik eines Tritium-markierten 9 alpha-Fluor-16 methylen-prednisolonesters nach epicutaner Applikation beim Menschen. Arzneim-Forsch /Drug Res 1968; 18:27–29.
17. Tsai J-C, Cappel MJ, Flynn GL, Weiner ND, Kreuter J, Ferry J. Drug and vehicle deposition from topical applications: use of *in vitro* mass balance technique with minoxidil solutions. J Pharm Sci 1992; 81(8):736–743.
18. Tojo K, Lee AC. A method for predicting steady-state rate of skin penetration *in vivo*. J Invest Dermatol 1989; 92:105–108.
19. Moon KC, Wester RC, Maibach HI. Diseased skin models in the hairless guinea pig: *in vivo* percutaneous absorption. Dermatologica 1990; 180:8–12.
20. Holoyo-Tomoka MT, Kligman AM. Does cellophane tape stripping remove the horny layer? Arch Dermatol 1972; 106:767–768.
21. Malkinson FD. Studies on the percutaneous absorption of ^{14}C labelled steroids by use of glass-flow cell. J Invest Dermatol 1958; 31:19–28.
22. Feldman RJ, Maibach HI. Penetration of ^{14}C hydrocortisone through normal skin: effect of stripping and occlusion. Arch Dermatol 1965; 91:661–666.
23. Zesch A, Schafer H. Penetrationskinetik von radiomarkierten Hydrocortisoner aus verschiedenartigen Salbengrundlagen in die menschliche Haut. Arch Derm Forsch 1975; 252:245–256.
24. Zesch A, Schaefer H, Hoffmann W. Barriere- und Reservoirfunktion der einzelnen Hornschichtlagen der menschlichen Haut für lokal aufgetragene Arzneimittel. Arch Derm Forsch 1973; 246:103–107.
25. Zesch A. Reservoirfunktion der Hornschicht. In: Klaschka F, ed. Stratum corneum: Struktur und Funktion. Berlin: Grosse Verlag, 1981:63–76.
26. Schwarb FP, Gabard B, Rufli T, Surber C. Percutaneous absorption of salicylic acid in man after topical administration of three different formulations. Dermatology 1999; in press.
27. Dupuis D, Rougier A, Roguet R, Lotte, C, Kalopissis G. *In vivo* relationship between horny layer reservoir effect and percutaneous absorption in human and rat. J Invest Dermatol 1984; 82(4):353–356.
28. Dupuis D, Rougier A, Roguet R, Lotte C. The measurement of the stratum corneum reservoir: a simple method to predict the influence of vehicles *in vivo* percutaneous absorption. Br J Dermatol 1986; 115:233–238.

29. Rougier A, Lotte C, Maibach HI. The hairless rat: a relevant animal model to predict *in vivo* percutaneous absorption in humans? J Invest Dermatol 1987; 88(5):577–581.
30. Rougier A, Lotte C, Dupuis D. An original predictive method for *in vivo* percutaneous absorption studies. J Soc Cosmet Chem 1987; 38:397–417.
31. Rougier A, Rallis M, Krien P, Lotte C. In vivo percutaneous absorption: a key role for stratum corneum/vehicle partitioning. Arch Dermatol Res 1990; 282:498–505.
32. Feldmann RJ, Maibach HI. Percutaneous penetration of steroids in man. J Invest Dermatol 1969; 52(l):89–94.
33. Feldmann RJ, Maibach HI. Absorption of some organic compounds through the skin in man. J Invest Dermatol 1970; 54:399–404.
34. Feldmann RJ, Maibach HI. Percutaneous penetration of some pesticides and herbicides in man. Toxicol Appl Pharmacol 1974; 28:126–132.
35. Auton TR. Skin stripping and science: a mechanistic interpretation using mathematical modelling of skin deposition as a predictor of total absorption. In: Scott RC, Guy RH, Hadgraft J, Boddé HE, eds. Prediction of Percutaneous Penetration. London: IBC Technical Services Ltd., 1990:558–576.
36. Knight AG. The activity of various topical griseofulvin preparations and the appearance of oral griseofulvin in the stratum corneum. Br J Dermatol 1974; 91:49–55.
37. Pershing LK, Corlett J, Jorgensen C. *In vivo* pharmacokinetics and pharmacodynamics of topical ketoconazole and miconazole in human stratum corneum. Antimicrob Agents Chemother 1994; 38(1):90–95.
38. Pershing LK, Krueger GG. Human skin sandwich flap model for percutaneous absorption. In: Bronaugh RL, Maibach HI, eds. Percutaneous Absorption. New York: Marcel Dekker, 1989:397–414.
39. Parry GE, Dunn P, Shah VP, Pershing LK. Acyclovir bioavailability in human skin. J Invest Dermatol 1992; 98:856–863.
40. Bredthauer D. Vergleichende Untersuchung zur Hornschicht-Penetration von Lichtschutzmitteln: Abrissmethode versus photoakustische Spektroskopie. Göttingen: Georg-August Universität, 1990.
41. Michel C, Purmann T, Mentrup E, Seiller E, Kreuter J. Effect of liposomes on percutaneous penetration of lipophilic materials. Int J Pharm 1992; 84:93–105.
42. Mak VHW, Potts RO, Guy RH. Percutaneous penetration enhancement in vivo measured by attenuated total reflectance infrared spectroscopy. Pharm Res 1990; 7:835–841.
43. Higo N, Naik A, Bommannan BD, Potts RO, Guy RH. Validation of reflectance infrared spectroscopy as a quantitative method to measure percutaneous absorption *in vivo*. Pharm Res 1993; 10(10):1500–1506.
44. Pershing LK, Silver BS, Krueger GG, Shah VP, Skelly JP. Feasibility of measuring the bioavailability of topical betamethasone dipropionate in commercial formulations using drug in skin and a skin blanching bioassay. Pharm Res 1992; 9(1):45–51.
45. Pershing LK, Lambert LD, Shah VP, Lam SY. Variability and correlation of chromameter and tape-stripping methods with the visual skin blanching assay in quantitative assessment of topical 0.05% betamethasone dipropionate bioavailability in humans. Int J Pharm 1992; 86:201–210.
46. Pershing LK, Corlett JL, Lambert LD, Poncelet CE. Circadian activity of topical 0.05% betamethasone dipropionate in human skin *in vivo*. J Invest Dermatol 1994; 102: 734–739.
47. Pershing KL, Lambert L, Wright ED, Shah VP, Williams RL. Topical 0.05% betamethasone dipropionate: pharmacokinetic and pharmacodynamic dose-response studies in humans. Arch Dermatol 1994; 130:740–747.
48. Lücker PW, Beubler E, Kukovetz WR, Ritter W. Retention time and concentration in human skin bifonazole and clotrimazole. Dermatologica 1984; 169(suppl l):51–56.
49. Shah VP, Pershing LK. The stripping technique to assess bioequivalence of topical applied formulations. In: Brain KR, James VJ, Walters KA, eds. Prediction of Percutaneous Penetration. London: IBC Technical Services Ltd., 1990:473–476.

50. von Hattingberg HM, Brockmeier D. Drug concentration control and pharmacokinetic analysis during long term therapy with desk top computers. In: Gladtke E, Heimann G, eds. Pharmacokinetics: A 25 year old discipline; 1978 Nov; Cologne. New York: Fischer, 1980:165–179.
51. Shah VP, Flynn GL, Yacobi A, Maibach HI, Bon C, Fleischer NM, Franz TJ, Kaplan SA, Kawamoto J, Lesko LJ, Marty J-P, Pershing LK, Schaefer H, Sequeira JA, Shrivastava WJ, Williams RL. Bioequivalence of topical dermatological dosage forms—Methods of evaluation of bioequivalence. Pharm Res 1998; 15(2):167–170.
52. Surber C, Henn U, Bieli E, Schwarb FP, Gabard B, Rufli T. Skin tape- stripping: is this technique adequate to explore principles of dermatopharmacokinetics? Dermatology 1999, in preparation.
53. van der Molen RG, Spies F, van't Noordende JM, Boelsma E, Mommaas AM, Koerten HK. Tape stripping of human stratum corneum yields cell layers that originate from various depths because of furrows in the skin. Arch Dermatol Res 1997; 289:514–518.
54. Whiting DA, Bisset EA. The investigation of superficial fungal infections by skin surface biopsy. Br J Dermatol 1974; 91:57–65.
55. Marks R, Dawber RPR. Skin surface biopsy: an improved technique for examination of the horny layer. Br J Dermatol 1971; 84:117–123.
56. Finlay A, Marks R. Determination of corticosteroid concentration profiles in stratum corneum using the skin surface biopsy technique. Br J Dermatol 1982; 107(suppl 22):33.
57. Epstein WL, Shah VP, Riegelman S. Griseofulvin levels in stratum corneum. Study after oral administration in man. Arch Dermatol 1972; 106:344–348.
58. Wallace SM, Shah VP, Epstein WL, Greenberg J, Riegelman S. Topically applied antifungal agents. Arch Dermatol 1977; 113:1539–1542.
59. Faergemann J, Zehender H, Denouel J, Millerioux L. Levels of terbinafine in plasma, stratum corneum, dermis-epidermis (without stratum corneum), sebum, hair and nails during and after 250 mg terbinafine orally once per day for four weeks. Acta Derm Venereol (Stockh) 1993; 73(4):305–309.
60. Faergemann J, Zehender H, Jones T, Maibach HI. Terbinafine levels in serum, stratum corneum, dermis-epidermis (without stratum corneum), hair, sebum and eccrine sweat. Acta Derm Venereol (Stockh) 1991; 71(4):322–326.
61. Faergemann J, Laufen H. Levels of fluconazole in serum, stratum corneum, epidermis-dermis (without stratum corneum) and eccrine sweat. Clin Exp Dermatol 1993; 18(2): 102–106.

29

Percutaneous Drug Delivery to the Hair Follicle

Andrea C. Lauer
Senior Clinical Scientist/Global Medical Marketing, South San Francisco, California, U.S.A.

I. INTRODUCTION

Unique biochemical and immunological events dictate the complex cyclic growth and differentiation patterns of hair follicles and their associated sebaceous glands (1), structures that are collectively referred to as pilosebaceous units. Once regarded as mere evolutionary remnants, hair follicles and sebaceous glands have been recognized increasingly as significant pathways for percutaneous transport (2). Percutaneous transport routes via the lipoidal domains of the stratum corneum have been well established (3,4), whereas comparatively less is known about the specific roles of hair follicles and sebaceous glands. Determination of the roles of these structures is complicated by the lack of adequate animal models and methodologies that can distinctly distinguish follicular and stratum corneum pathways. Moreover, it may be possible that a topically applied compound traverses more than one pathway simultaneously.

The stratum corneum is acknowledged not only as the main barrier to skin penetration, but also as the major permeation pathway. The tightly packed, semicrystalline intercellular lipid domains and the extremely compact corneocytes of the stratum corneum create a barrier highly resistant to percutaneous transport (3,4). Modulation of stratum corneum lipid fluidity by topical agents has been thoroughly studied and is generally acknowledged as the major mechanism of percutaneous delivery (5). Passive percutaneous transport depends on several factors, including penetrant lipophilicity, charge, and molecular size (6). The upper limit of molecular size for permeation through the stratum corneum is still unknown.

Early suggestions of a follicular pathway were based on the hypothesis that hair follicles act as shunts, resulting in the rapid transport of ions and large polar molecules. Scheuplein (7) and Scheuplein et al. (8) first described transient follicular delivery for small polar molecules and large polar steroids that ordinarily would not be expected to traverse the skin rapidly due to their charge or restrictive molecular size. Feldmann and Maibach (9) and Maibach et al. (10) observed increases in percutaneous transport through skin areas with greatest follicular densities in both animals and humans, which also hinted at the possibility of follicular delivery.

Later studies incorporated fluorescence microscopy, autoradiography, radiolabel deposition, confocal laser scanning microscopy, and other techniques, yielding data that have further supported this route for a wide range of drug molecules and vehicles (2). Specific particulate systems including liposomes (11–19) and synthetic microspheres (20,21) have been found to localize in follicular and sebaceous areas that act as drug reservoirs for compounds with varying physicochemical characteristics.

In several studies, hair follicles have been shown to act as channels, though not necessarily depots, for the iontophoretic flux of several molecules. Iontophoresis may be particularly useful in systemic delivery of ionic, polar compounds and high-molecular-weight peptides, which are slowly transported passively (22,23). Although the importance of follicular routes for iontophoretic flux should not be disregarded, a full discussion of iontophoresis is beyond the scope of this chapter, which is confined to passive follicular delivery.

II. CONSIDERATIONS FOR EXPERIMENTAL DESIGN

Careful consideration of several factors is necessary in designing an experimental approach to assess follicular permeation:

- Hair follicle and sebaceous gland anatomy (i.e., drug targets)
- Drug delivery goal: localized or systemic?
- Animal models
- Quantitative and qualitative analysis methods
- Physicochemical properties of permeants and vehicles

III. HAIR FOLLICLE AND SEBACEOUS GLAND ANATOMY

The structure of the stratum corneum and its function in percutaneous transport are closely intertwined (3–5). Analogously, an understanding of the anatomy and physiology of the hair follicles and sebaceous glands is equally important, especially with regard to targeting specific therapeutic sites within the hair follicle. A simplified diagram of a vertically cross-sectioned mammalian pilosebaceous unit is illustrated in Figure 1. The hair follicle is an invagination of the dermis and is continuous with the epidermis, which offers less resistance to transport than the stratum corneum. Dermal matrix cells overlying the follicular papilla give rise to the hair shaft and the inner root sheath, whereas the outer root sheath, which is continuous with the epidermis, is likely of epithelial origin (24,25). It is not unlikely that the tightly compacted cells of the inner root sheath beneath the hair follicle infundibulum (opening) may physically restrict transport deep within the hair follicle.

The pilosebaceous unit is a dynamic structure that undergoes cyclic growth phases: anagen (active), catagen (resorption), and telogen (resting) (24). Cotsarelis et al. (26) have described a mid-follicle ''bulge area'' that exhibits one of the fastest rates of cell division in mammals. It is thought that diffusable growth factors from the follicular papilla cause proliferation of the normally slow-cycling bulge cells in early anagen. However, during telogen, the bulge area is most responsive to topically applied carcinogens (26), suggesting that follicular delivery may vary depending on hair cycle stage. Hair cycle activity in humans occurs in a mosaic pattern, with a random distribution of neighboring hair follicles in varying growth stages, whereas hair cycle activity in most animals is in a wave pattern of synchronized adjacent hair follicles.

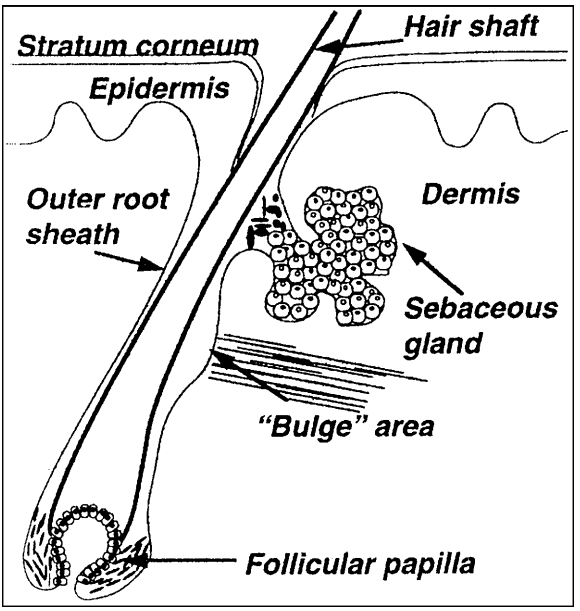


Figure 1 Simplified diagram of a mammalian hair follicle and sebaceous gland.

Although located deep in the dermis, sebaceous glands are appendages of the epidermis that secrete sebum into the follicular canal, leading to the skin surface (24). Sebum flows into the follicular canal as a result of lysed sebocytes within sebaceous glands, creating a lipophilic environment that may favor transport for some molecules, but may also act as a chemical and physical barrier for others. Analysis of skin surface lipids of several species has shown tremendous variation in sebum composition among species. Human sebum is rich in squalene, wax esters, triglycerides, cholesterol, cholesterol esters, and free fatty acids (27). Androgenic hormones influence sebaceous gland size by stimulating rate of cell division and lipid accumulation (24,27). Targeting the sebaceous glands with agents to decrease androgen activity could be useful in the treatment of dermatologic disorders such as acne.

Several epithelial cell types, specialized structures, receptors, and immunocompetent cells reside within the pilosebaceous units. Hormones, growth factors ultraviolet radiation, and drugs interact at various levels of the hair follicle (24). Greater understanding of the molecular signals that control the onset and duration of hair follicle growth and development, which still are not fully understood, may enable rational design of targeted follicular delivery systems. Obvious therapeutic targets exist within the pilosebaceous unit, which may offer promising treatments for acne, male pattern baldness, alopecia areata, and some skin cancers (24). Besides localized delivery, systemic delivery via the hair follicle may also be achieved due to the large capillary networks associated with the pilosebaceous unit (28).

IV. ANIMAL MODELS

A. Hairless Animals

As stated previously, the choice of animal models for assessing follicular delivery is currently limited. A hairless rodent model may seem an obvious, convenient choice

to represent the nonfollicular pathway; however, these animals only appear macroscopically hairless and do indeed possess abnormal hair follicles (19,29). In Figure 2, the gross historical differences between CRL CD hairless rat skin and Sprague–Dawley hairy rat skin are shown by light-microscopy viewing of hematoxylin- and eosin-stained 5 μm vertical cross-sections of untreated dorsal skin (19). The stratum corneum of hairless rodent skin is typically hyperkeratinized, the hair follicles and sebaceous glands are enlarged and cysts frequently are present in the epidermis, dermis, and hair follicles (19,29).

Despite the known histological differences, hairless rodents continue to be widely used as models for percutaneous penetration of a wide variety of molecules. In some studies, the hairless rat has been more accurately depicted as a follicular model, and has been compared to a follicle-free model developed by scarring hairless rat skin (20,21,30–34). Illel and Schaefer (30) induced follicle-free skin in hairless rats by immersing anesthetized rats into 60°C water for one minute, followed by removal of epidermis and healing for three months. At this point, transepidermal water loss evaluations indicated normal barrier function, and histological analysis showed a complete absence of hair follicles and sebaceous glands. Preliminary in vitro studies by Illel and Schaefer (30) found that the steady-state flux and total diffusion of [^{3}H]hydrocortisone were 50-fold greater for hairless rat skin compared to follicle-free hairless rat skin after 24 hours. Several additional studies followed comparing the percutaneous transport profiles of intact hairless rat skin and the scarred, follicle-free

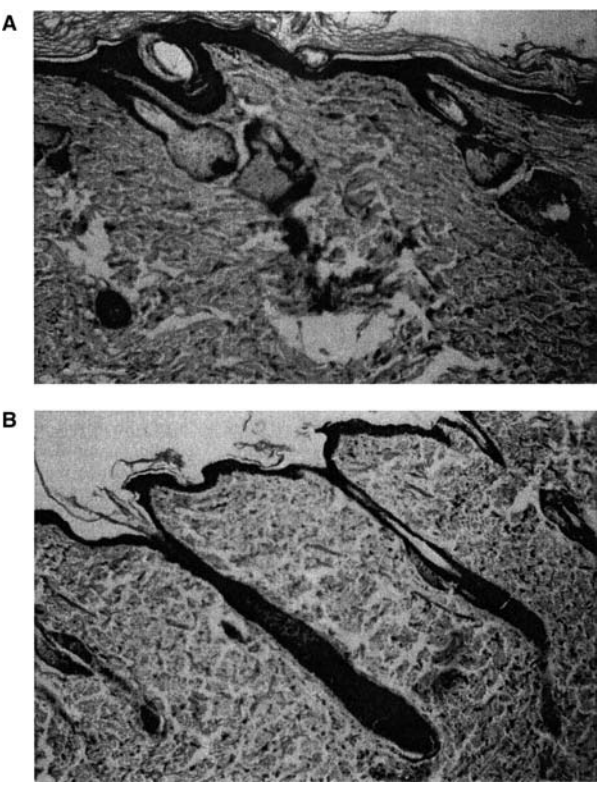


Figure 2 Light microscopy photographs (70X) showing hematoxylin- and eosin-stained 5 μm vertical skin sections of (**A**) untreated hairless rat skin and (**B**) untreated hairy rat skin.

hairless rat skin (20,21,31–34). In vitro studies showed that permeation of a wide range of compounds—tritiated caffeine, niflumic acid, and *p*-aminobenzoic acid—was approxi-mately three times greater through hairless rat skin compared to the follicle-free model (31). Hueber et al. (32) confirmed these findings with in vivo studies using radiolabled hydrocortisone, progesterone, estradiol, and progesterone. The overall conclusion of these studies using intact hairless rat skin and scarred hairless rat skin was that follicular transport, especially via sebaceous glands, was significant for a wide range of topically applied compounds. Although this induced follicle-free model has offered some insight into follicular delivery, it is somewhat imperfect due to an incomplete assessment of the overall effects of heat-induced scarring on the hairless rat stratum corneum.

In addition, it has been shown that hairless rat skin does not exhibit typically normal absorption patterns, for both polar and nonpolar compounds, when compared to animals with fully developed hair follicles. In vivo permeability profiles of CRL CD hairless rat and Sprague–Dawley hairy rat skin have been investigated for up to 12 hours using small polar and lipophilic molecules in various vehicles (19). Hairy rat skin was closely clipped with an electric clipper at least 12 hours prior to the study in order to allow close skin contact with applied formulation. Aqueous [^{14}C]mannitol solution was applied for specified time periods to the dorsal surface of a 4-cm^2 skin area, followed by euthanization and preparation for radiolabel assay. Excised skin was tape-stripped to remove stratum corneum completely, followed by assay of tape strips and remaining epidermis/dermis (viable skin) for radiolabel by liquid scintillation counting. As shown in Figure 3, in vivo topical application of aqueous [^{14}C]mannitol solution to hairless rat skin resulted in significant systemic accumulation in the urine, whereas systemic levels were negligible for hairy rat ($p < 0.05$). Mannitol deposition into both hairless and hairy rat viable skin (Fig. 4),

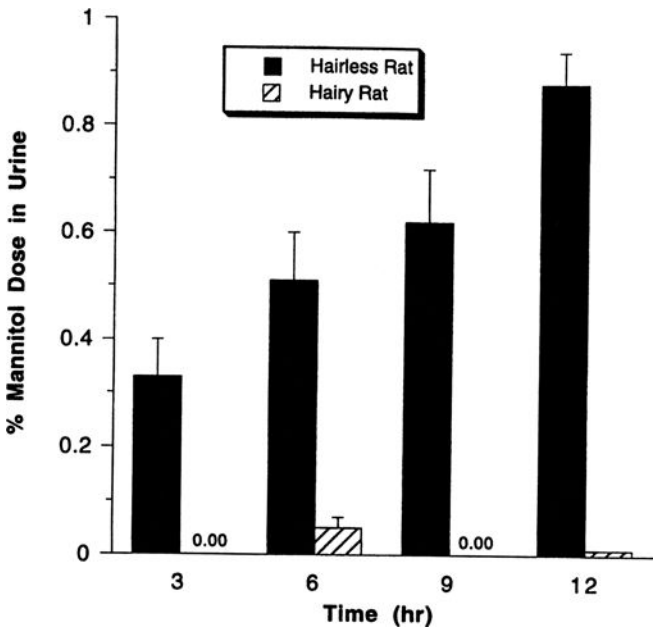


Figure 3 Urinary deposition of mannitol. In vivo deposition of [^{14}C]mannitol after topical application of aqueous solution to hairless and hairy rat skin (n = 3–6, mean ± SEM).

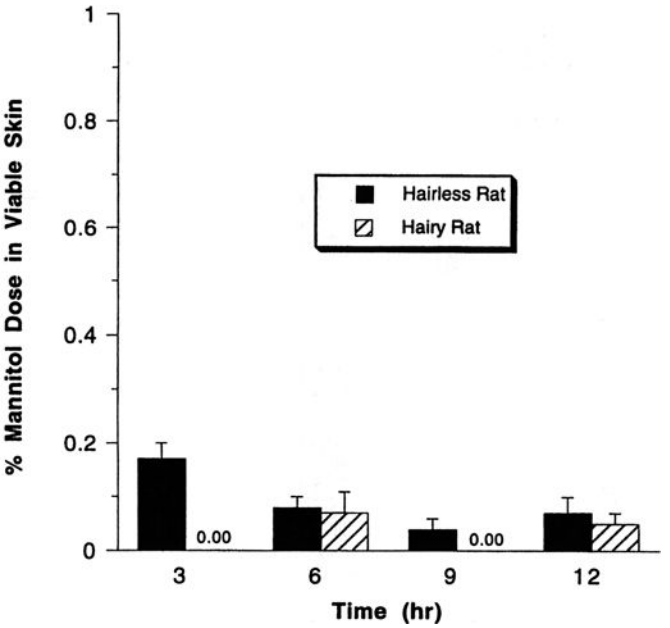


Figure 4 Viable skin deposition of mannitol. In vivo deposition of [^{14}C]mannitol after topical application of aqueous solution to hairless and hairy rat skin (n = 3–6, mean ± SEM).

which is defined as the epidermal and dermal layers remaining following complete tape stripping of the stratum corneum, was $< 0.2\%$ of the applied dose at all time points. The results suggest that hairless rat skin acted as a sieve to aqueous mannitol solution, whereas hairy rat skin provided a sufficient barrier to this extremely polar molecule that is not expected to permeate the stratum corneum easily. In a similar study, a hydroalcoholic solution containing [^{3}H]progesterone was topically applied to hairless and hairy rat skin in vivo. Figure 5 shows that after 12 hours, progesterone deposition into hairless rat skin was approximately sixfold greater than that in hairy rat skin. Systemic levels of progesterone in the hairless rat were approximately twice the levels found in hairy rat urine. The data suggest that lipophilic compounds may be retained in the extensive depots of hairless rat skin provided by the numerous large sebaceous glands present in this species.

Hisoire and Bucks (35) observed similar permeability differences for hairless and hairy guinea pig skin following in vitro topical application of 0.025% retinoic acid in an ethanolic gel formulation. Histological analysis also indicated ultrastructural abnormalities in hairless guinea pig skin, including cysts and follicular aberrations. Although the authors concluded that the results were a consequence of stratum corneum differences between the two models, the possible influence of abnormal hair follicles and sebaceous glands cannot be excluded. Collectively, the results of these studies indicate that hairless animals are probably inappropriate models for topical absorption due to the presence of abnormal hair follicles, cysts, and other aberrations that result in a leaky barrier for polar compounds while acting as a lipophilic depot for nonpolar compounds (19,35).

The newborn rat also represents a follicle-free skin model until the age of three to four days, which is when hair follicles begin to develop. Illel et al. (31) found a fivefold greater flux of [^{3}H]hydrocortisone through newborn rat skin five days after

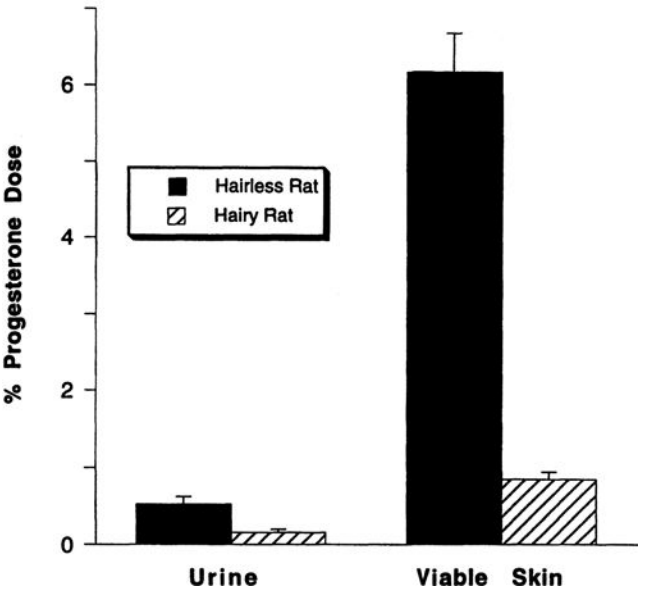


Figure 5 In vivo deposition of [^{3}H]progesterone from hydroalcoholic solution (60% v/v) into hairless and hairy rat skin after 12 hours of topical application ($n = 3$, mean ± SEM).

birth compared to 24 hours after birth. Although the newborn rat lacks hair follicles, the possibility of barrier impairment due to underdeveloped stratum corneum cannot be eliminated since this skin has yet to be fully characterized.

B. Follicle-Free Area of Guinea Pig Skin

The skin behind the ears of guinea pigs is completely devoid of hair follicles and sebaceous glands, which may provide a potential model that excludes follicular routes. However, investigations are limited by the extremely small surface area at this site and the possibility of site-specific lipid composition varying from other sites. Wahlberg (36) used surface radiation disappearance measurements to quantify in vitro and in vivo percutaneous absorption using aqueous and organic solutions of $HgCl_2$ and NaCl applied to hairy and hair follicle-free guinea pig skin. Although no clear differences were found in this study, it should be noted that systemic absorption was not assessed.

C. Syrian Hamster Ear

The ventral side of the Syrian hamster ear, which is rich in large sebaceous glands, was developed by Plewig and Lunderschmidt (37) as a model for sebaceous gland deposition based on its structural similarity to human sebaceous glands. Matias and Orenfreich (38) developed a method in which formulation is applied to the ventral surface of the ear and after a specified time point, the animal is euthanized and the ear is stratified into anatomical layers to allow for scraping of sebaceous contents. Sebaceous contents can then be quantitatively analyzed by several methods, depending on the applied permeant. A wide range of molecules in various vehicles, many of which were liposomal preparations, have been shown to be absorbed in appreciable amounts into hamster ear sebaceous glands (11,14,17).

D. Macaque Monkey

The perfect animal model for clearly defining contributions of the stratum corneum and follicular routes remains elusive, but at present, the study of an animal model possessing true, fully developed hair follicles may be the best option. The macaque monkey may be one of the most physiologically correct models, especially for studying follicular targeting to prevent androgenic baldness. This animal exhibits a species-specific frontal scalp baldness that coincides with puberty, and may be a particularly relevant model for the study of human androgenic alopecia since the hormonal and genetic factors that induce baldness closely parallel those causing baldness in humans. Uno and Kurata (39) found that topical application of hypertrichotic drugs, minoxidil and diazoxide, resulted in significant follicular enlargement and hair regrowth in bald macaques. In another study, topical application of an antiandrogen that inhibits 5α-reductase resulted in prevention of baldness in preadolescent macaques (40).

E. In Vitro Histocultures with Hair Follicles

Histocultured skin containing fully developed hair follicles may be a promising alternative to in vivo animal models. Li et al. (41) developed an in vitro three-dimensional histoculture using a collagen–sponge–gel support system to maintain tissue viability of mouse skin. Early anagen hair follicles in this model developed into full-grown anagen follicles and produced pigmented hair shafts in vitro. Similar mouse and human histocultures with well-developed hair follicles were used in vitro to assess follicular delivery of liposomal formulations containing calcein (12), melanin (13), or high-molecular-weight DNA (18). In limited cases, human skin can be assessed in vivo if follicular biopsy methods are used (42). Although in vitro methods have been improved, the potential effects of excessive hydration on excised skin and the lack of functioning circulatory networks surrounding the pilosebaceous units should still be considered.

V. METHODOLOGIES TO ASSESS FOLLICULAR PERMEATION

In the absence of a completely appropriate animal model, recently improved methodologies for quantifying and visualizing topical permeation routes may offer the best hope in more clearly defining these pathways. Following topical application of an agent for a specified time, the skin must be carefully excised and processed in at least one of several ways in order to assess drug deposition. If a thin cross-sectioning technique for microscopic visualization is chosen, care should be taken to avoid harsh fixatives and cross-contamination during sectioning.

A. Radiolabel Deposition

A frequently used method to assess topical drug deposition quantitatively, especially if a radiolabeled compound is available, is the tape-stripping method (43). At the end of the application time, excised skin is cellophane tape-stripped until stratum corneum removal is complete, as indicated by the glistening appearance of the residual viable skin (remaining epidermis and dermis) and lack of visible cellular components on tape strips. Tape strips and the residual viable skin can be analyzed

for radiolabel by liquid scintillation counting after soaking in scintillation cocktail for several hours. Major organs should also be analyzed for radiolabel content to determine systemic absorption. The tape-stripping method is somewhat subjective, however, resulting in artificially high marker levels in the residual skin if stratum corneum removal is incomplete. Conversely, tape stripping may not be ideal for assessing follicular delivery since follicular contents may be stripped away, thereby underestimating follicular deposition. This method may be most useful for assessing follicular deposition when combined with other techniques such as visualization by microscopic methods. Deposition of topically applied radiolabeled agents can be assessed in hamster ear sebaceous glands by using the scraping technique, as described earlier in the animal model discussion, in combination with tape stripping.

B. Autoradiography

Autoradiography has been used previously to show localized drug deposition into the hair follicles (44,45). Nicolau et al. (44) combined microscopic autoradiography and liquid scintillation counting to assess in vivo follicular delivery of viprostol, a synthetic prostaglandin E_2 analog, in a petrolatum base. In mouse skin, distribution of radioactivity was evident in the stratum corneum and hair follicles 30 minutes after topical application. After 12 hours, viprostol was localized in the stratum corneum, epidermis and lower hair follicle of monkey and mouse skin. Drug retention occurred only in follicular structures after 72 hours, suggesting a depot function for this structure. Bidmon et al. (45) found dose and vehicle dependencies using an improved dry-mount autoradiography technique to detect [^{3}H]estradiol-17β in hairy rat skin. Drug localization was visualized in the epidermis, sebaceous glands and follicular papilla following a two-hour topical application of the drug in dimethyl sulfoxide (DMSO), ethylene glycol, or sesame oil formulations. After 24 hours, autoradiograms indicated that hair follicles and sebaceous glands continued to act as drug depots.

C. Fluorescence Microscopy

Several investigators have visualized follicular deposition using simple fluorescence microscopy, and have combined these data with quantitative data for a follicular pathway (11,21,46). Topically applied fluorescent molecules can be visualized in skin structures after carefully cryosectioning skin into thin slices or in follicular biopsies. Fluorescence-labeled polymeric microspheres and microspheres loaded with fluorescent molecules have been visualized in follicular structures by simple epifluorescence microscopy and by scanning electron microscopy (20,21). The use of epifluorescence microscopy is limited by the requirement of extremely thin skin slices and the potential uncertain interpretation of data due to skin and hair follicle autofluorescence.

D. Confocal Laser Scanning Microscopy

Confocal laser scanning microscopy (CLSM) allows direct visualization of permeating fluorescent markers within hair follicles while minimizing detection skin and hair follicle autofluorescence. Importantly, CLSM does not require harsh fixation procedures, and relatively thick specimens can be viewed by collecting a series of images at regular focus intervals. CLSM minimizes the detection of autofluorescence by directly a single beam of laser light to the sample, resulting in a clearly defined fluorescent area that is much brighter than autofluorescent areas (47). With CLSM, a

stack of optical sections from varying depths can be combined to reveal three-dimensional fluorescent marker distributions within the skin. Besides offering excellent qualitative visualization, the data can also be processed by computer interface to show quantitative site-dependent fluorescent intensities. CLSM has been used previously to visualize localization of topically applied fluorescent markers within the hair follicles and sebaceous glands (20,48).

E. Immuno-histochemistry

Immunostaining and immunofluorescence techniques may be used to visualize topically applied agents that localize in follicular structures. Balsari et al. (15) used an immuno-histochemistry technique to evaluate the in vivo percutaneous penetration of liposome-encapsulated monoclonal antibody to doxorubicin (MAD11) in 10-day-old rats. Following a 30-minute application of formulation, the rats were euthanized and tissue samples were removed for cryosectioning. The immunoperoxidase technique was performed with an avidin–biotin–peroxidase complex (ABC) kit, followed by staining with diaminobenzidine and counterstaining with hematoxylin. Staining observed by light microscopy indicated localization of MAD 11 in the stratum corneum, epidermis, and deep in the dermis surrounding follicular structures. The qualitative data obtained in this study via immunostaining were further supported with radiolabel penetration studies.

Yarosh et al. (16) quantitatively assessed the localization of topically applied DNA repair enzymes within mouse skin via immunocytology using antibodies against the DNA repair enzymes. After termination of the in vivo study, skin was sectioned and stained with antibodies against T4 endonuclease V and fluorescein Bothiocyanate (FITC) linked secondary antibodies. After a one-hour topical application period, immunostaining indicated that enzymes were found in the epidermis in the cells surrounding the follicular root sheath and the sebaceous glands.

F. Follicular Biopsies

Follicular casting methods have been used to remove follicular contents by applying a quick-setting cyanoacrylate adhesive on a glass slide to the skin surface (20,42,49,50). Drug deposition in the follicular casts pulled from the skin can be analyzed by microscopy or by various analytical techniques following extraction in solvents. Bojar et al. (50) investigated follicular deposition of a topically applied azelaic acid cream, 20% w/w, in human back and forehead skin. After five hours, surface drug was removed followed by follicular biopsy and detection of azelaic acid in follicular cast supernatant by high-performance liquid chromatography (HPLC) analysis. The investigators explained the findings of lower drug concentrations in forehead follicular casts as a consequence of rapid removal from the richly vascularized sebaceous glands at that site. Follicular casting has previously been combined with microscopic analysis by fluorescence and scanning electron microscopy to assess deposition of drug-loaded microspheres into follicular structures (20).

G. Pharmacological Effect

The ability of a topically applied agent to elicit a pharmacological response that is specific to the pilosebaceous unit may be useful in supporting a follicular delivery hypothesis. Although this is not an absolute indicator of a follicular route, combined

with additional data it can support the hypothesis. Balsari et al. (15) observed that a topically applied liposomal anti-doxorubicin monoclonal antibody, MAD11, was able to prevent alopecia in 31 of 45 young rats treated intraperitoneally with doxorubicin. While these data alone suggest a follicular route, the investigators also used radiolabel deposition and immunohistochemistry visualization techniques.

Lieb et al. (14) used a quantitative bioassay to assess in vivo follicular delivery of topically applied [^{3}H]cimetidine to hamster ear sebaceous glands. Various vehicles containing 3% cimetidine were applied to the ventral side of hamster ears twice daily for four weeks. Since cimetidine is known to have antiandrogenic activity, the basis of the assay was to measure changes in sebaceous gland sized as observed by phase-contrast microscopy. Drug deposition into sebaceous glands, as apparent by sebaceous gland size reduction, was greatest with ethanol and nonionic lipid-based formulations at pH values when cimetidine was mostly unionized.

Several pharmacological responses may be measured that suggest activity at the follicular level via transfollicular delivery, but systemic follicular delivery following transdermal delivery via the stratum corneum must be ruled out as an explanation. Hormonal effects on hair growth and acne are also examples of the therapeutic responses that occur at the follicular level.

H. Laser Doppler Flowmetry

Regional variations in cutaneous blood flow following topical application of agents can be measured by laser Doppler flowmetry (LDF). Tur et al. (51) measured skin blood flow by LDF following topical application of methyl nicotinate, a vasodilator, to human skin on the forearm, forehead, and palm. The measured LDF responses indicated the greatest response at the forehead, an intermediate response at the forearm, and the least response through the palm. The investigators concluded that a preferential permeation route exists in areas of high follicular density, but conceded that other factors may have been influential such as potential skin lipid differences.

I. Gene Expression

Gene delivery to target sites within the hair follicles and sebaceous glands is currently an exciting development that may yield interesting new therapies. Investigators in recent studies have assessed follicular delivery of topically applied viral and nonviral vectors, as measured by gene expression at the follicular level. Li and Hoffman (52) demonstrated that a topically applied phospholipid (egg phosphatidylcholine) liposome preparation containing the lacZ reporter gene resulted in selective expression of the gene in hair bulb matrix cells and bulge area cells in mouse skin. Lu et al. (53) have shown that topically applied viral vectors can be used to transfer genes into various strata of the skin. Following a two-day topical treatment of mouse skin in vivo with an adenovirus vector in phosphate-buffered saline, the skin was excised and stained with X-gal. The resulting blue staining of the sectioned skin indicated gene localization in the epidermis and some hair follicles. It may be important to note that ethanol pretreatment and tape stripping of the skin three to four times may have compromised the barrier function of the stratum corneum, thereby enhancing gene delivery from aqueous solution into the deeper skin strata.

VI. FORMULATION EFFECTS ON FOLLICULAR DEPOSITION

The presence of sebum in the follicular canal may restrict or enhance the transport of molecules into the follicle, depending on the physicochemical characteristics of the drug and vehicle. Dissolving the permeant in lipoidal solvents such as ethanol or acetone (3–5), which may reorganize or delipidize sebum, may thereby open the passageway for drug deposition within the follicle. Wetting agents (e.g., sodium lauryl sulfate) may be useful in decreasing the interfacial tension between polar drugs and sebum, which may promote mixing in the form of an emulsion, providing a more favorable environment for drug partitioning and absorption.

Bamba and Wepierre (33) assessed formulation effects on follicular deposition of [^{14}C]pyridostigmine bromine in a 72-hour in vitro study using hairless rat and scarred (follicle-free) hairless rat skin. Greatest drug deposition into hair follicles was achieved by an ethanol vehicle during the first 24 hours, whereas Azone and Nerol vehicles delivered pyridostigmine preferentially via a transepidermal route. The authors explained these results as a consequence of ethanol miscibility with sebum, which allowed more favorable drug deposition into sebaceous glands. The use of two other vehicles, dimethyl sulfoxide and propylene glycol, also resulted in significant drug delivery through the follicular routes.

Paniculate delivery systems, including liposomes and polymeric microspheres, have yielded especially interesting data supporting a follicular route. These systems have been compared to conventional formulations and simple drug solutions, with particular emphasis on liposomal lipid composition and microbead particle size (11–21).

A. Liposomes

Liposomal systems, upon dehydration following topical application, may yield a fluid liquid-crystalline state in which bilayers containing drug can partition and pack into the follicular openings. Follicular delivery of hydrophilic molecules may be facilitated via association with polar head groups of liposomal bilayers. Results from recent studies have suggested that this mechanism of action is not dependent on the extent of hydrophilic drug entrapment (11), in that empty liposomes along with "free" aqueous solution exhibit similar absorption profiles. Following dehydration, extent of entrapment may be inconsequential due to the establishment of a new equilibrium between the drug and bilayers. Several studies have also shown facilitated follicular delivery of lipophilic molecules carried by liposomal formulations (11–19).

Lieb et al. (11) used an in vitro hamster ear model to quantitatively assess follicular deposition of a low-molecular-weight hydrophilic dye, carboxyfluorescein. Ears cut at the base were mounted ventral side up on Franz diffusion cells containing 1-(2-hydroxyethyl) piperazine-1-ethanesulfonic acid (HEPES) isotonic buffer, pH 7.4. Various formulations containing carboxyfluorescein, 100 μg/mL, were studied: (a) isotonic HEPES buffer, (b) 5% propylene glycol, (c) 10% ethanol in HEPES, (d) 0.05% sodium lauryl sulfate (SLS) in HEPES, (e) multilamellar (MLV) egg phosphatidylcholine (PC):cholesterol (CH):phosphatidylserine (PS) liposomes, and (f) a non-bilayer suspension of the same lipid mixture (MIX). After a 24-hour in vitro study, quantitative fluorescence microscopy and fluorescence spectroscopy were used to visualize and quantitate carboxyfluorescein deposition into sebaceous glands. The dermal side of the ear was examined by epifluorescence microscopy, and images of several sebaceous glands were digitally processed and quantitated for fluorescence,

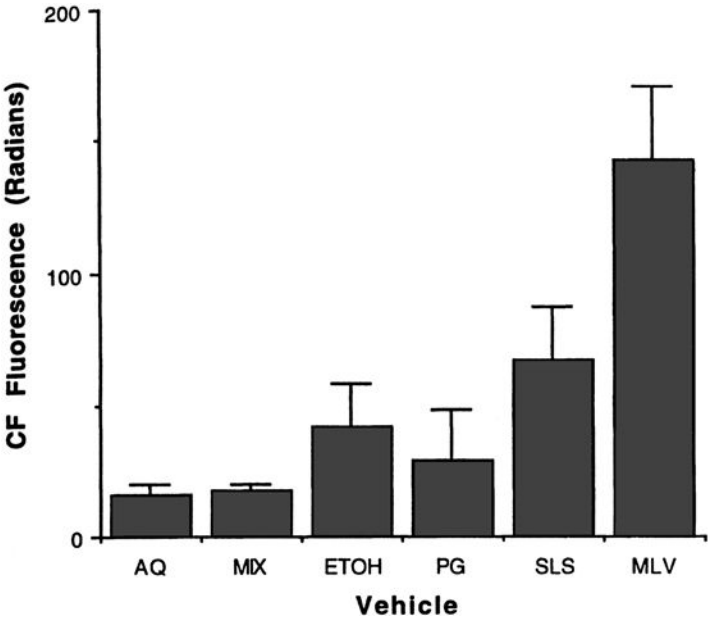


Figure 6 Formulation effects on deposition of carboxyfluorescein (CF) in hamster ear sebaceous glands, as determined by quantitative fluorescence microscopy after 24 hours of in vitro topical application ($n = 4$, mean $\pm$ SEM). *Abbreviations*: AQ, aqueous; MIX, lipid mixture; ETOH, ethanol; PG, propylene glycol; SLS, sodium lauryl sulfate; MLV, multilamellar liposomes. *Source*: From Ref. 11.

as measured in radians. Phospholipid liposomes were superior to all formulations, as shown in Figure 6. Data obtained from the scraping technique (not shown) correlated strongly with the quantitative fluorescence microscopy data. The data suggest that liposomes can enhance follicular delivery of small polar molecules, which are not ordinarily expected to penetrate the stratum corneum or sebaceous glands.

In a study of specific liposomal formulation effects, Niemiec et al. (17) compared peptide deposition from phospholipid (PC/CH/PS) liposomes and nonionic liposomes into hamster ear sebaceous glands. Nonionic liposomes consisted of glyceryl dilaurate, cholesterol, and polyoxyethylene 10-stearyl ether at a weight percent of 57:15:28, respectively. Topical application of [^{125}I]-α-interferon or [^{3}H]cyclosporine in various formulations was followed by the previously described scraping technique. Nonionic liposomes provided the greatest follicular deposition for both peptides, with deposition approximately fourfold greater than that achieved by phospholipid liposomes. Relatively low amounts of either drug were found in the dermis, suggesting that nonionic liposomes are capable of delivering peptides with varying physicochemical characteristics into sebaceous glands.

Li et al. (12) used CLSM to visualize the follicular localization of a liposome-entrapped fluorescent hydrophilic dye, calcein, in mouse skin histocultures. After a 20-minute incubation period, liposomes made with egg PC delivered calcein deeper into the hair follicle than those made with dipalmitoyl PC or aqueous calcein. The results suggested that formulation factors may have determined follicular deposition, based on differences in phase transition temperatures for the liposomal lipids. Egg PC liposomes were in a liquid-crystalline state at 37°C, whereas dipalmitoyl PC liposomes were in a gel phase. Another study by Li et al. (13), using liposomally entrapped

melanin in a 12-hour mouse skin histo-culture, showed similar results. Follicular delivery of melanin from egg PC liposomes was superior to that from aqueous melanin solution, as indicated by fluorescence microscopy visualization of thin skin slices.

Enhancement of percutaneous transport of [^{14}C]mannitol via liposomes into follicular structures of the Sprague–Dawley hairy rat has been shown in vivo (19). As shown earlier in Figure 2, hairless rat skin is a leaky barrier to aqueous mannitol solution, whereas hairy rat skin is relatively impenetrable to aqueous mannitol solution. However, as shown in Figure 7, appreciable amounts of liposomal mannitol are deposited into hairy skin following topical application for up to 12 hours, with negligible systemic accumulation in the urine or feces (data not shown) (19). Conversely, hairless rat skin is also a leaky barrier to liposomal mannitol, with negligible amounts remaining in the viable skin, but relatively high urinary levels comparable to those attained following topical application of aqueous mannitol (data not shown). In a similar study, CLSM was used to visualize the deposition of a topically applied small polar fluorescent compound, carboxyfluorescein, at 100 μg/mL in aqueous or liposomal systems. With this technique, a 20 μm-thick vertical cryosection of treated hairy rat skin was viewed, showing upper follicular deposition of liposomal carboxyfluorescein up to 72 hours (48), whereas aqueous solution resulted in fluorescence appearing only on the stratum corneum. Fluorescence was visualized only in the stratum corneum of hairless rat skin, regardless of formulation, at this time point. The results collectively suggest that fully developed follicular structures may act as depots for molecules in an appropriate carrier system, such as liposomes.

Most remarkably, liposomes have been shown to target macromolecules into the hair follicle. Li et al. (18) targeted liposomally entrapped high-molecular-weight DNA into hair follicles of histocultured mouse skin. Egg PC liposomes were loaded

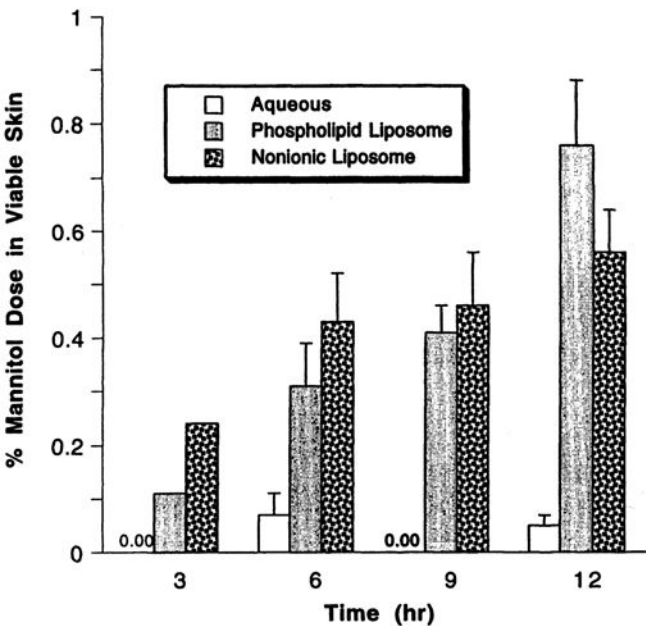


Figure 7 In vivo deposition of [^{14}C]mannitol into viable skin or hairy rats after topical application of phospholipid-based liposomes and nonionic lipid-based liposomes (n = 3–6, mean ± SEM).

with [^{35}S]-dATP-labeled DNA that was isolated from a mouse genomic DNA library. Mouse skin histo-cultures were incubated with liposomal DNA or free DNA solution for 44 hours. With liposomal DNA, autoradiography indicated radiolabel presence in the cell membranes and cytoplasm of hair follicle cells, whereas no radiolabel was found after incubation with free DNA solution. In another study discussed previously, Li and Hoffman (52) also demonstrated follicular deposition of other macromolecules (genes) using liposomal formulations. Follicular delivery of such macromolecules seems unlikely via lipoidal pathways of the stratum corneum due to probable size restrictions.

As discussed previously, Balsari et al. (15) topically applied liposomal MAD11, resulting in the prevention of systemic doxorubicin-induced alopecia in young rats. Phospholipid-based liposome formulations were compared with aqueous MAD11 solution and empty liposomes, using radiolabel deposition and immunochemistry histological studies. High dermal levels of radiolabeled antibody combined with immunostaining in follicular structures suggest that this macromolecule was able to be delivered via liposomes into the hair follicles, which exerted a protective effect against alopecia. Again, considering the large molecular size of MAD11 ($>$150 kDa), a transport route through the stratum corneum lipids into the hair follicle seems unlikely.

B. Polymeric Microspheres

Results from a series of studies using topically applied polymeric microspheres have indicated that particle size and vehicle composition may be important factors determining the extent of follicular deposition. Schaefer et al. (20) investigated follicular deposition of fluorescent polystyrene microbeads, with diameters ranging from approximately 1 to 47 μm, suspended in aqueous or lipophilic vehicles. Microbeads were topically applied to hairless rat skin (in vivo) or human skin (in vitro) for 15 minutes, including a 5-minute massage time period, after which follicular biopsies were performed and viewed with fluorescence microscopy. The 7-μm-diameter microbeads were found to be optimally sized, as indicated by fluorescence deep within hair follicles of both species. Suspension of these beads in a lipophilic vehicle, Miglyol, yielded best results for follicular deposition into hairless rat skin. Microbead localization deep within the hair follicle was also shown by scanning electron microscopy. Similar particle size and vehicle effects were also observed using poly-β-alanine microbeads labeled with dansyl chloride in an aqueous gel, hydroalcoholic gel, and a silicone oil. Microbeads with 5 μm diameter preferentially targeted the hair follicle, which was best achieved in the most lipophilic vehicle, silicone oil. Rolland et al. (21) used similar studies with polymeric microspheres loaded with adapalene, a fluorescent antiacne drug, and suspended in aqueous gel. Adapalene was visualized deep within hairless rat (in vivo) and human (in vitro) hair follicles by fluorescence microscopy following up to 5 hours of topical application of the microsphere formulation. The microspheres were subsequently visualized by scanning electron microscopy deep within the hair follicle, with optimum delivery occurring with 5-μm microspheres. The results of these studies collectively suggest that particulate systems can be designed to specifically target follicular structures based on particle diameter and vehicle composition.

VII. SUMMARY

Passive follicular delivery may be a larger component of topical delivery than was previously assumed. As more knowledge is gained about the structure and function of hair follicles and sebaceous glands, the relevance of therapeutic targeting to specific areas may be better defined. The development of improved animal models and methodologies to assess follicular delivery may enable a better understanding of the kinetics of follicular transport. Follicular delivery is likely dependent on the physicochemical characteristics of both the drug and vehicle. Results from several studies have shown that particulate systems, including liposomes and polymeric microsphere systems, preferentially localize in pilosebaceous units. Manipulation of particle size and other formulation factors, such as lipid ratios and composition, may be useful in achieving a greater extent of delivery to the follicles and sebaceous glands. The potential of liposomes to deliver localized pharmacological agents and macromolecules such as genes into hair follicles and sebaceous glands may have a great impact on future treatments of follicular disorders.

REFERENCES

1. Hardy MH. The secret life of the hair follicle. Trends Genet 1992; 8:55–61.
2. Lauer AC, Lieb LL, Ramachandran C, Flynn GL, Weiner ND. Transfollicular drug delivery. Pharm Res 1995; 12:179–186.
3. Elias PM. Epidermal lipids, barrier function and desquamation. J Invest Dermatol 1983; 80:44–49.
4. Downing DT. Lipid and protein structures in the permeability barrier of mammalian epidermis. J Lipid Res 1992; 33:301–313.
5. Williams AC, Barry BW. Skin absorption enhancers. Crit Rev Ther Drug Carrier Sys 1992; 9:305–353.
6. Kasting GB, Smith RL, Cooper ER. Effect of lipid solubility and molecular size on percutaneous absorption. In: Shroot B, Schaefer H, eds. Skin Pharmacokinetics. Basel: Karger, 1987:138–153.
7. Scheuplein RJ. Mechanism of percutaneous absorption. 1. Routes of penetration and the influence of solubility. J Invest Dermatol 1965:334–346.
8. Scheuplein RJ, Blank IH, Brauner GJ, MacFarlane DJ. Percutaneous absorption of steroids. J Invest Dermatol 1969; 52:63–70.
9. Feldmann JR, Maibach HI. Regional variation in percutaneous penetration of ^{14}C-cortisol in man. J Invest Dermatol 1967; 48:181–183.
10. Maibach HI, Feldmann RJ, Hilby TH, Serat WF. Regional variation in percutaneous penetration in man. Arch Environ Health 1971; 23:208–211.
11. Lieb LM, Ramachandran C, Egbaria K, Weiner ND. Topical delivery enhancement with multilamellar liposomes via the pilosebaceous route: I. In vitro evaluation using fluorescent techniques with the hamster ear model. J Invest Dermatol 1992; 99:108–113.
12. Li L, Margolis LB, Lishko VK, Hoffman RM. Product-delivering liposomes specifically target hair follicles in histocultured intact skin. In Vitro Cell Dev Biol 1992; 28A: 679–681.
13. Li L, Lishko VK, Hoffman RM. Liposomes can specifically target entrapped melanin to hair follicles in histocultured skin. In Vitro Cell Dev Biol 1993; 29A:192–194.
14. Lieb L, Ramachandran C, Flynn G, Weiner N. Follicular (pilosebaceous unit) deposition and pharmacological behavior of cimetidine as a function of formulation. Pharm Res 1994; 11:1419–1423.

15. Balsari AL, Morelli D, Ménard S, Veronesi U, Colnaghi MI. Protection against doxorubicin-induced alopecia in rats by liposome-entrapped monoclonal antibodies. FASEB J 1994; 8:226–230.
16. Yarosh D, Bucana B, Cox P. Localization of liposomes containing a DNA repair enzyme in murine skin. J Invest Dermatol 1994; 103:461–468.
17. Niemiec S, Ramachandran C, Weiner N. Influence of nonionic liposomal composition on topical delivery of peptide drugs into pilosebaceous units: An invivo study using the hamster ear model. Pharm Res 1995; 12:1184–1188.
18. Li L, Lishko VK, Hoffman RM. Liposome targeting of high molecular weight DNA to the hair follicles of histocultured skin: a model for gene therapy of the hair growth processes. In Vitro Cell Dev Biol 1993; 29A:258–260.
19. Lauer AC, Elder JT, Weiner ND. Evaluation of the hairless rat as a model for in vivo percutaneous absorption. J Pharm Sci 1997; 86:13–18.
20. Schaefer H, Watts F, Brod J, Illel B. Follicular penetration. In: Scott RC, Guy RH, Hadgraft J, eds. Prediction of Percutaneous Penetration, Methods, Measurements, Modelling. London: IBC Technical Services, 1990:163–173.
21. Rolland A, Wagner N, Chatelus A, Shroot B, Schaefer H. Site-specific drug delivery to pilosebaceous structures using polymeric microspheres. Pharm Res 1993; 10:1738–1744.
22. Green PG, Hinz RS, Kim A, Szoka FC, Guy RH. Iontophoretic delivery of a series of tripeptides across the skin in vitro. Pharm Res 1991; 8:1121–1127.
23. Cranne-van Hinsberg WH, Verhoef JC, Bax LJ, Junginger HE, Boddé HE. Role of appendages in skin resistance and iontophoretic peptide flux: human versus snake skin. Pharm Res 1995; 12:1506–1512.
24. Bertolino AP, Klein LM, Freedberg IM. Biology of hair follicles. In: Fitzpatrick TB, Eisen AZ, Wolff K, Freedberg IM, Austen KF, eds. Dermatology in General Medicine, 4th ed. Vol. I. New York: McGraw-Hill, 1993:289–293.
25. Philpott MP, Sanders DA, Kealey T. Whole hair follicle culture. Dermatol Clin 1996; 14:595–607.
26. Cotsarelis G, Sun T, Lavker RM. Label-retaining cells reside in the bulge area of pilosebaceous unit: implications for follicular stem cells, hair cycle and skin carcinogenesis. Cell 1990; 61:1329–1337.
27. Steward ME, Downing DT. Chemistry and function of mammalian sebaceous lipids. Adv Lipid Res 1991; 24:263–301.
28. Ryan TJ. Cutaneous circulation. In: Goldsmith LA, ed. Physiology, Biochemistry and Molecular Biology of the Skin. Oxford: Oxford Press, 1991:1019–1084.
29. Hanada K, Chiyoya S, Suzuki K, Hashimoto I, Hatayama I. Study of the skin of a new hairless rat mutant. J Dermatol 1988; 15:257–262.
30. Illel B, Schaefer H. Transfollicular percutaneous absorption: Skin model for quantitative studies. Acta Derm Vernerol 1988; 68:427–430.
31. Illel B, Schaefer H, Wepierre J, Doucet O. Follicles play an important role in percutaneous absorption. J Pharm Sci 1991; 80:424–427.
32. Hueber F, Wepierre J, Schaefer H. Role of transepidermal and transfollicular routes in percutaneous absorption of hydrocortisone and testosterone: In vivo study on hairless rat. Skin Pharmacol 1992; 5:99–107.
33. Bamba FL, Wepierre J. Role of the appendageal pathway in the percutaneous absorption of pyridostigmine bromine in various vehicles. Eur J Drug Metab Pharmacokinet 1993; 18:339–348.
34. Hueber F, Besnard M, Schaefer H, Wepierre J. Percutaneous absorption of estradiol and progesterone in normal and appendage-free skin of the hairless rat: lack of importance of nutritional bloodflow. Skin Pharmacol 1994; 7:245–256.
35. Hisoire G, Bucks D. An unexpected finding in percutaneous absorption observed between haired and hairless guinea pig skin. J Pharm Sci 1997; 86:398–400.
36. Wahlberg JE. Transepidermal or transfollicular absorption? Acta Derm Venereol 1968; 48:336–344.

37. Plewig G, Lunderschmidt C. Hamster ear model for sebaceous glands. J Invest Dermatol 1977; 68:171–176.
38. Matias JR, Orentreich N. The hamster ear sebaceous glands. I. Examination of the regional variation by stripped skin planimetry.. J Invest Dermatol 1983; 81:43–46.
39. Uno H, Kurata S. Chemical agents and peptides affect hair growth. J Invest Dermatol 1993; 101:143S–147S.
40. Uno H. Quantitative models for the study of hair growth in vivo. Ann NY Acad Sci 1991; 642:107–124.
41. Li L, Paus R, Slominski A, Hoffman RM. Skin histoculture assay for studying the hair cycle. In Vitro Cell Dev Biol 1992; 28A:695–698.
42. Mills OH, Kligman AM. The follicular biopsy. Dermatologica 1983; 167:57–63.
43. Rougier A, Lotte C. Predictive approaches. I. The stripping technique. In: Shaw VP, Maibach HI, eds. Topical Drug Bioavailability, Bioequivalence and Penetration. New York: Plenum Press, 1993:163–182.
44. Nicolau G, Baughman RA, Tonelli A, McWilliams W, Schiltz J, Yacobi A. Deposition of viprostol (a synthetic PGE_2 vasodilator) in the skin following topical administration to laboratory animals. Xenobiotica 1987; 17:1113–1120.
45. Bidmon HJ, Pitts JD, Solomon HF, Bondi JV, Stumpf WE. Estradiol distribution and penetration in rat skin after topical application, studied by high resolution autoradiography. Histochemistry 1990; 95:43–54.
46. Kao J, Hall J, Hellman G. In vitro percutaneous absorption in mouse skin: influence of skin appendages. Toxicol Appl Pharmacol 1988; 94:93–103.
47. Matsumoto B, Kramer T. Theory and applications of confocal microscopy. Cell Vision 1994; 3:190–198.
48. Lauer A. In Vivo Deposition of Polar Molecules from Various Topical Formulations into Hairless and Hairy Rat Skin. Ph.D. dissertation, University of Michigan, Ann Arbor, 1996.
49. Mills OH, Kligman AM. A human model for assaying comedelytic substances. Br J Dermatol 1982; 107:543–548.
50. Bojar RA, Cutcliffe AG, Graupe K, Cunliffe WJ, Holland KT. Follicular concentrations of azelaic acid after a single topical application. Br J Dermatol 1993; 129:399–402.
51. Tur E, Maibach HI, Guy RH. Percutaneous penetration of methyl nicotinate at three anatomic sites: evidence for an appendageal contribution to transport? Skin Pharmacol 1991; 4:230–234
52. Li L, Hoffman RM. The feasibility of targeted selective gene therapy of the hair follicle. Nature Med 1995; 1:705–706.
53. Lu B, Federoff HJ, Wang Y, Goldsmith LA, Scott G. Topical application of viral vectors for epidermal gene transfer. J Invest Dermatol 1997; 108:803–808.

30

In Vivo Percutaneous Absorption in Human Volunteers: Exhaled Breath Analysis

Karla D. Thrall and Angela D. Woodstock
Battelle, Pacific Northwest Laboratory, Richland, Washington, U.S.A.

I. INTRODUCTION

In general, evaluations of dermal uptake of a chemical are made using animal skin (in vitro or in vivo) or human skin in vitro. However, studies conducted in our laboratory have illustrated that analysis of exhaled breath presents a useful methodology to assess dermal absorption of volatile compounds in human volunteers (1,2). Exhaled breath data is particularly useful when evaluated using some form of a kinetic model, such as a physiologically based pharmacokinetic (PBPK) model, to describe the changing kinetics over time. A PBPK model is ideally suited for integrating a variety of data, including exhaled breath measurements, to determine the penetration rate of chemicals through the skin. For instance, a PBPK model can be used to assess dermal exposures under non-steady-state conditions, where the transdermal flux is a function of the permeability coefficient (K_p), the area exposed, and the changing concentration gradient across the skin (3). The integration of real-time exhaled breath measurements and a PBPK model to determine dermal absorption has been successfully used for a number of compounds, including methyl chloroform, trichloroethylene, benzene, and toluene (1,2,4).

This chapter describes the use of exhaled breath analysis and PBPK modeling to evaluate the percutaneous absorption of aqueous toluene and *o*-xylene in human volunteers. A PBPK model developed to describe the dermal exposure to these aqueous compounds in rats was expanded to apply to humans and used to estimate a single permeability coefficient to describe all individual data sets.

II. MATERIALS AND METHODS

A. Chemicals

The high-performance liquid chromatography (HPLC)–grade xylene, as the ortho-isomer (98% purity), and toluene (99% purity) were obtained from Sigma–Aldrich (Milwaukee, Wisconsin, U.S.A.).

Table 1 Demographic Information on Volunteers

ID no.	Sex	Age	Race	Body weight (kg)	Body height (cm)	Surface area exposed (cm^2)
Toluene						
T1	M	57	Caucasian	83.9	173	20,126
T2	M	24	Caucasian	88.4	180	20,123
T3	F	48	Caucasian	48.5	163	15,060
T4	M	21	Caucasian	99.8	185	22,841
T5	F	23	Caucasian	97.5	170	21,259
T6	M	39	Caucasian	95.2	168	20,852
Xylene						
X1	M	58	Caucasian	83.9	173	1990
X2	F	49	Caucasian	48.5	165	1503
X3	F	26	Caucasian	80.7	175	1972

B. Human Subjects

Human studies were conducted under approval from the Battelle Memorial Institutional Review Board (IRB) in accordance with the terms and conditions of Federal Regulation 45 CFR 46 under the authority of Multiple Project Assurance M1221. Demographic information, including sex, age, race, body weight, and height, is given in Table 1. No volunteers reported chronic cardiovascular, hepatic, central nervous system, renal, hematological, gastrointestinal, or dermatological problems. Volunteers provided and wore their own swimsuits during the study.

C. Human Exposure Conditions

Human dermal exposures were conducted by either submersion in tap water to neck level (toluene) or submersion of the lower legs (*o*-xylene) in a 397-L stainless steel hydrotherapy tub (Whitehall Manufacturing Industry, California, U.S.A.) containing an initial target concentration of approximately 500 μg/L toluene or *o*-xylene. The target concentrations were selected to stay below the Washington State Drinking Water Guidelines and the U.S. Environmental Protection Agency (EPA) Federal Drinking Water Guidelines of maximum contaminant levels (5). The tub was connected to a municipal hot and cold water supply and water inflow was adjusted to fill the tub at approximately 38°C. The hydrotherapy tub was filled with roughly 80 gal (300 L) tap water; total water volume in the tub was measured during filling using a calibrated electronic digital flow meter/accumulator (Great Plains Industries, Wichita, Kansas, U.S.A.). To quantitate total exposure, triplicate water samples (5 mL) were collected from the hydrotherapy tub prior to the addition of the compound, immediately upon addition of the compound to the bathwater, and at five-minute intervals throughout the exposure phase. These samples were analyzed by a gas chromatographic (GC) headspace method. Water temperature was measured using a digital thermometer (Fluka, Everett, Washington, U.S.A.) and recorded at the same time intervals as the collection of aliquots for analysis. Water temperature stayed relatively constant (within ± 1°C) throughout each study.

The study protocol entailed monitoring background exhaled breath for each volunteer for two to five minutes prior to entry into the tub. Throughout the study,

the water was continually mixed using a 0.5 horsepower turbine agitator. During the exposure phase, each volunteer was either submerged to neck level or immersed their lower legs in the tub for 10 to 30 minutes while continually providing exhaled breath for real-time analysis. A weighed quantity of neat material, prepared in a separate room, was added to the water near the agitator after the volunteer was comfortably situated in the hydrotherapy tub, and during the ongoing analysis of exhaled breath. The addition of the compound to the bathwater was designated as time zero for water analysis. At the end of the monitoring period the volunteer left the tub, briefly towel dried, and provided 10 to 30 minutes of post-exposure exhaled breath for real-time analysis. Purified breathing air (medical grade) was continually provided to the volunteer throughout the study to isolate inhalation of any volatilized compound in the room.

D. Real-Time Breath Analysis System

The exhaled breath monitoring system utilized during the human studies consisted of a breath inlet device connected to a Discovery II (LGC Inc., Los Gatos, California, U.S.A.) ion trap tandem mass spectrometer (MS/MS) equipped with an atmospheric sampling glow discharge ionization (ASGDI) source and has been described previously (4). Volunteers wore a Hans Rudolph (Kansas City, Missouri, U.S.A.) face mask containing two one-way non-rebreathing valves. Purified breathing air was supplied by a gas cylinder to a 15-L foil-lined buffer bag to provide air to the volunteer on demand. Expired air was passed through a large-diameter Teflon tube into a heated glass-mixing chamber (1.3-L volume). Breath samples entered the mixing chamber through a tube that bent off to one side, and exited the mixing chamber via a tube bent in the opposite direction, thus ensuring that samples were well mixed by turbulent flow. The ASGDI-MS/MS system continually drew air samples from the center of the mixing chamber at a calibrated rate of 12 L/hr to provide a new data point every 4.6 seconds. Excess exhaled air was vented from the mixing chamber via a large bore hole exit tube with negligible flow restriction.

Intensity data from the mass spectrometer were converted to concentration (ppb) using external gas standards prepared in Tedlar bags (Supelco Inc., Bellefonte, Pennsylvania, U.S.A.) and a calibration curve. A new calibration curve was generated each day of operation. The ASGDI-MS/MS methodology had detection limits in the 2 to 10 ppb range for both toluene and *o*-xylene, and calibrations were linear to 57 ppm (57,000 ppb).

E. PBPK Model

The dermal PBPK model (Fig. 1) has been used to successfully describe the dermal absorption of aqueous toluene in the rat (1). Anatomical compartments in the model were used to describe the distribution of toluene into the rapidly perfused, slowly perfused, fat, liver, and skin compartments. The skin compartment in the model represented exposed skin; nonexposed skin was included in the slowly perfused compartment. Total skin, with a volume of 10% of the body weight, was assumed to receive 5% of the cardiac output. The exposed skin volume and blood flow rate were calculated as described by Jepson and McDougal (3).

Model parameters specific to human physiology, partition coefficients, and metabolism were taken from the literature (Table 2). To simulate dermal exposures, the rate of change in the concentration of compound in the skin compartment (C_{sk}, μg/mL) was related to the rate of penetration through the skin (the flux) and the rate

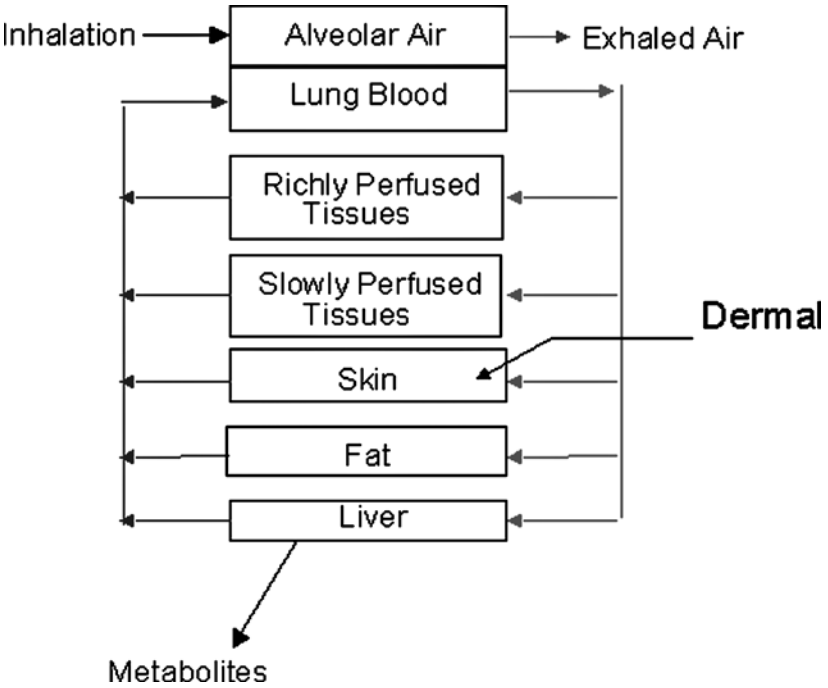


Figure 1 Schematic representation of a generic physiologically based pharmacokinetic (PBPK) model used to describe dermal absorption.

Table 2 Physiologically Based Pharmacokinetic (PBPK) Model Parameters

Parameter	Toluene[a]	*o*-Xylene[b]
Blood flow (% cardiac output)		
Liver	25	25
Fat	6	6
Rapidly perfused	49	49
Slowly perfused	15	15
Tissue volume (% body weight)		
Liver	4	4
Fat	20	20
Rapidly perfused	5	5
Slowly perfused	52	52
Metabolic constants		
Vmax (mg/kg/hr)	4.68	8.4
Km (mg/L)	0.55	0.2
Partition coefficients[c]		
Saline:air	1.75	2.6
Blood:air	13.9	34.0
Liver:air	83.5	129
Fat:air	1021	2105
Muscle:air	27.7	74.8
Skin:air	43.0	65.4

[a]Adapted from Ref. 2.
[b]Adapted from Ref. 7.
[c]Adapted from Ref. 15.

of delivery due to blood flow and arterial concentration (the perfusion) as described previously (4). In the PBPK model, this is written as:

$$V_{sk}\frac{dC_{sk}}{dt} = K_p A\left(C_{liq} - \frac{C_{sk}}{P_{sk/liq}}\right) + Q_{sk}\left(C_a - \frac{C_{sk}}{P_{sk/b}}\right)$$

where V_{sk} is the volume of the skin exposed (mL), K_p the permeability coefficient (cm/hr), A the exposed surface area (cm^2), Q_{sk} the blood flow rate to the exposed skin (mL/hr), C_a the arterial concentration (μg/mL), C_{sk} the skin concentration (μg/mL), C_{liq} the liquid chemical concentration (μg/mL), $P_{sk/b}$ the compound-specific skin to blood partition coefficient (unitless; calculated by dividing the solubility ratio of skin:air by blood:air), and $P_{sk/liq}$ is the compound-specific skin to water partition coefficient (dimensionless; calculated by dividing the solubility ratio of skin:air by water:air).

The skin permeability coefficient (K_p) for each volunteer was estimated from this equation based on the kinetics of absorption as described by the exhaled breath. A maximum likelihood search algorithm in SimuSolv (Version 3.0; Dow Chemical Co., Midland, Michigan, U.S.A.) was used to vary the K_p coefficient until an optimal fit was achieved that described the time-course data. The percent variability explained for all optimized values was always $\geq$80%. The use of these routines has been described previously (6).

III. RESULTS

A representative toluene exhaled breath profile from a single volunteer exposed to aqueous toluene by the dermal route is given in Figure 2 (points). The exhaled breath data clearly showed toluene to be rapidly absorbed, with peak concentrations achieved within seconds following the addition of the compound to the water. Upon

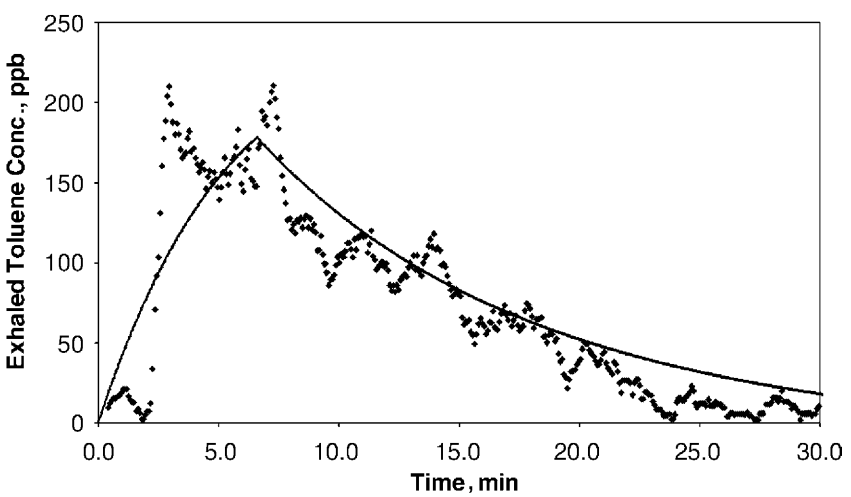


Figure 2 Exhaled breath profile (*points*) for a human volunteer (T5, Table 1) dermally exposed to an initial toluene water concentration of 496.9 μg/L in a 265-L hydrotherapy tub and physiologically based pharmacokinetic (PBPK) model prediction (*line*) describing the data. The volunteer was a 23-year-old Caucasian female, 97.5 kg body weight, 170 cm height, with an exposed surface area of 21,259 cm^2.

exit from the hydrotherapy tub, the concentration of toluene in the exhaled breath rapidly declined. By five minutes post-exposure, there was essentially no detectable toluene in the expired air. For $n = 6$ volunteers, toluene was found in the exhaled breath at peak levels of approximately 100 to 200 ppb under initial exposure concentrations ranging from 455 to 550 μg/L (Table 3). No measurable toluene was detected in the pre-exposure exhaled breath samples in any of the volunteers.

The exhaled breath profile for each volunteer was analyzed using the toluene PBPK model as described previously, with physiological parameters set for humans. The changing concentration of toluene in the water over the exposure period was represented as loss from the exposure system (Kloss). For simplicity, the PBPK model assumed that all subjects had the same body weight-proportional blood flow, ventilation, and metabolism rates. A representative example of the model simulation of the exhaled breath profile is provided in Figure 2 (line). The optimized K_p for human dermal absorption of toluene in water was found to range from 0.003 to 0.020 cm/hr. A single averaged K_p value of 0.012 ± 0.007 cm/hr (average ± SD, $n = 6$) was found to adequately describe all the individual dermal exposure data sets.

A representative *o*-xylene exhaled breath profile from a human volunteer is given in Figure 3 (points). As observed with toluene exposures, the human exhaled breath data indicated rapid absorption, with *o*-xylene initially appearing in the exhaled breath within seconds of addition of the compound to the hydrotherapy tub. At initial exposure concentrations ranging from 469 to 481 μg/mL, *o*-xylene was found in the exhaled breath at peak levels of approximately 75 to 100 ppb (Table 3). No measurable *o*-xylene was detected in two-minute pre-exposure breath samples in any of the volunteers.

The exhaled breath profile for each volunteer was analyzed using the PBPK model described for toluene, with metabolic and partition coefficient parameters set specific for *o*-xylene (Table 2). A comparison of the PBPK model prediction (line) and exhaled breath data (points) for a human volunteer is illustrated in Figure 3. The optimized K_p for human dermal absorption of *o*-xylene in water was found to range from 0.004 to 0.005 cm/hr. A single averaged K_p value of 0.005 ± 0.001 cm/hr

Table 3 Analytical and Physiologically Based Pharmacokinetic (PBPK) Model Results for Human Exposures

Subject ID no.	Initial water concentration (μg/L)	K_p (cm/hr)	Peak exhaled breath concentration (ppb)
Toluene			
T1	545.6	0.020	200
T2	549.6	0.011	125
T3	454.9	0.004	120
T4	490.7	0.003	100
T5	496.9	0.020	200
T6	503.5	0.011	200
Average	506.9 ± 35.8	0.012 ± 0.007	157 ± 47
o-Xylene			
X1	481.2	0.004	75

(*Continued*)

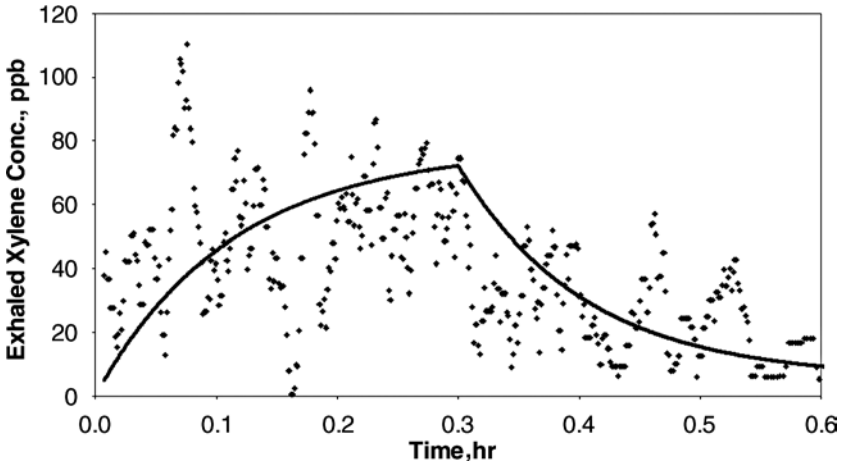


Figure 3 Exhaled-breath profile (*points*) for a human volunteer (X2, Table 1) dermally exposed to an initial *o*-xylene water concentration of 469.1 μg/L in a 322-L hydrotherapy tub and physiologically based pharmacokinetic (PBPK) model prediction (*line*) describing the data. The volunteer was a 49-year-old Caucasian female, 48.5 kg body weight, 165 cm height, with an exposed surface area of 1503 cm^2.

(average ± S.D., $n = 3$) was found to adequately describe all the individual dermal exposure data sets.

IV. DISCUSSION

In recent studies conducted using PBPK modeling and exhaled breath analysis from dermal exposures in F344 male rats, the permeability coefficients (K_p) for aqueous toluene and *o*-xylene were found to be 0.074 ± 0.005 cm/hr (1) and 0.058 ± 0.009 cm/hr (7), respectively. In comparison, the human values determined here of 0.012 ± 0.007 cm/hr for toluene and 0.005 ± 0.001 cm/hr for *o*-xylene are 6 to 12 times lower than the rat. The magnitude of this difference is consistent with the results of previous studies comparing rat and human toluene vapor exposures, where the rat in vivo K_p of 0.72 cm/hr (8) is roughly five times greater than the in vivo human value of 0.14 cm/hr for hand and forearm vapor exposures (9). Numerous investigators have shown that the dermal absorption of a variety of compounds is greater in rats than in humans, although the extent of the differences appears to vary by compound (3,8,10,11).

Due to differences in exposure conditions, it is difficult to directly compare the permeability coefficients determined here to literature estimates. For example, the U.S. EPA (11) human K_p value for aqueous toluene was estimated to be 1 cm/hr based on flux data reported in 1968 (12). However, in this earlier study the amount of toluene absorbed was quantified by measuring the loss of the compound from the donor solution, and steady-state conditions were not verified. Permeability may be overestimated when assuming that the rate of chemical loss from the exposure solution represents the average flux into the skin (3). For xylene, on the other hand, Kezic et al. (13) conducted brief (three minutes) exposures to neat liquid *m*-xylene in human volunteers and reported a flux of 46 ± 17 nmol/cm^2/min (0.29 mg/cm^2/hr). Simulation of the Kezic et al. (13) exhaled breath data using the *o*-xylene PBPK model described here

indicates a K_p value of 0.005 cm/hr appropriately described the data. This value is identical to the average human K_p value for aqueous *o*-xylene exposures determined in the present study. A U.S. EPA estimate of dermal absorption of *o*-xylene was not available.

Dermal flux is an integral part of a dermal exposure risk assessment, and can be considered an index of percutaneous absorption (14). The form of the flux equation used in the PBPK model assumes that the concentration inside the skin is uniform, which is not precisely correct. Unfortunately, flux equations that take into account the concentration of the chemical in the skin with respect to distance in the skin requires the solution of partial differential equations (3). Partial differential equations have parameters which cannot be directly measured, and therefore have to be fit or estimated. Thus, using a partial differential equation description forces the model to be descriptive, rather than predictive. However, the simple homogeneous model, as described here, has been shown experimentally to accurately describe the penetration of chemicals such as dibromomethane and bromochloromethane (3). Although the current model simulations focused on optimization of the permeability coefficient to describe the data, there is always the danger of misinterpretation of the data based on the ability of the model to access which parameters are crucial. A sensitivity analysis indicated that parameters associated with the ability to describe the exhaled breath profiles were most sensitive to parameters that relate to permeability, including the surface area exposed, the permeability coefficient, the dermal exposure concentration, and to a lesser extent, the breathing rate. On the other hand, sensitivity analyses indicate that the model is not sensitive to parameters such as partition coefficients and metabolic rate constants.

In summary, the experiments on volunteers reported here provided definitive data for assessing the absorption of aqueous toluene and *o*-xylene through human skin. Furthermore, the utilization of sensitive, real-time instrumentation allowed for controlled exposures to be conducted under a realistic bath-water scenario. Analysis of the resultant exhaled breath data using a PBPK model estimated an average K_p values for dermal absorption of aqueous toluene and *o*-xylene of 0.012 ± 0.007 cm/hr and 0.005 ± 0.001 cm/hr, respectively. Although a comparative human value for *o*-xylene was not located in the literature, the U.S. EPA (11) estimate for toluene absorption in the human of 1 cm/hr is in sharp contrast to the data reported here and suggests that a reevaluation of human dermal absorption may be warranted.

ACKNOWLEDGMENTS

This work was supported by Grant Number 1-P42-ES10338–01 from the National Institute of Environmental Health Sciences (NIEHS), National Institutes of Health (NIH), with funds from the EPA. The contents of this manuscript are solely the responsibility of the authors, and do not necessarily represent the official views of NIEHS, NIH, or EPA.

REFERENCES

1. Thrall KD, Woodstock AD. Evaluation of the dermal absorption of aqueous toluene in F344 rats using real-time breath analysis and physiologically based pharmacokinetic modeling. J Toxicol Environ Health A 2002; 65:2087–2100.

2. Thrall KD, Weitz KK, Woodstock AD. Use of real-time breath analysis and physiologically based pharmacokinetic modeling to evaluate dermal absorption of aqueous toluene in human volunteers. Toxicol Sci 2002; 68:280–287.
3. Jepson GW, McDougal JN. Physiologically based modeling of nonsteady state dermal absorption of halogenated methanes from an aqueous solution. Toxicol Appl Pharmacol 1997; 144:315–324.
4. Thrall KD, Poet TS, Corley RA, Tanojo H, Edwards JA, Weitz KK, Hui X, Maibach HI, Wester RC. A real-time in vivo method for studying the percutaneous absorption of volatile chemicals. Int J Occup Environ Health 2000; 6:96–103.
5. U.S. EPA. Drinking Water Standards and Health Advisories. EPA 822-B-00–001. Office of Water, U.S. Environmental Protection Agency, Washington DC, 2000.
6. Agin GL, Blau GE. Application of Dow Advanced Continuous Simulation Language (DASCL) to the design and application of chemical reactor systems. Am Inst Chem Eng Symp Ser 1982; 78(214):108–118.
7. Thrall KD, Woodstock AD. Evaluation of the dermal bioavailability of aqueous xylene in F344 rats and human volunteers. J Toxicol Environ Health A 2003; 66:1267–1281.
8. McDougal JN, Jepson GW, Clewell HJ III, Gargas ML, Andersen ME. Dermal absorption of organic chemical vapors in rats and humans. Fundam Appl Toxicol 1990; 14: 299–308.
9. Kezic S, Monster AC, Kruse J, Verberk MM. Skin absorption of some vaporous solvents in volunteers. Int Arch Occup Environ Health 2000; 73:415–422.
10. Bronaugh RL. Current issues in the in vitro measurement of percutaneous absorption. In: Roberts MS, Walters KW, eds. Dermal Absorption and Toxicity Assessment. New York: Marcel Dekker, 1998:155–160.
11. U.S. EPA. Dermal Exposure Assessment: Principles and Applications. EPA/600/8-91/011B, U.S. Environmental Protection Agency, Washington DC, 1992.
12. Dutkiewicz T, Tyras H. Skin absorption of toluene, styrene, and xylene by man. Br J Ind Med 1968; 25:243.
13. Kezic S, Monster AC, van de Gevel IA, Krüse J, Opdam JJG, Verberk MM. Dermal absorption of neat liquid solvents on brief exposures in volunteers. Am Ind Hygiene Assoc J 2001; 62:12–18.
14. Fiserova-Bergerova V, Pierce JT, Droz PO. Dermal absorption potential of industrial chemicals: criteria for skin notation. Am J Ind Med 1990; 17:617–635.
15. Thrall KD, Gies RA, Muniz J, Woodstock AD, Higgins G. Route-of-entry and brain tissue partition coefficients for common Superfund contaminants. J Toxicol Environ Health A 2002; 65:2075–2086.

31

Relative Contributions of Human Skin Layers to Partitioning of Chemicals with Varying Lipophilicity

Tatiana E. Gogoleva, John I. Ademola, Ronald C. Wester, Philip S. Magee, and Howard I. Maibach

Department of Dermatology, School of Medicine, University of California, San Francisco, California, U.S.A.

I. INTRODUCTION

The skin is an organized, heterogeneous, multilayered organ. The stratum corneum (SC), epidermis (SCE), and dermis (D), together with the appendages and the vasculatures, constitute the living protective system around the body. Percutaneous absorption of surface applied agents is the sum of the penetration and permeation of a chemical into and through the stratum corneum, epidermis, and some part of the dermis (1–5). In this investigation, the contribution of three skin layers to stratum corneum percutaneous absorption was evaluated by quantifying partitioning of model compounds between skin layers and vehicles [water and isopropyl myristate (IPM)]. The influences of drug concentrations, equilibration time, vehicle hydrophilicity, lipophilicity, and pH of the vehicle on partitioning behavior of model compounds were examined.

II. MATERIALS AND METHODS

A. Radioisotopes and Chemicals

The following chemicals were obtained from Radiochemical Center, Amersham, Illinois, U.S.A.: [^{3}H]propranolol hydrochloride (specific activity 17.1 Ci/mmol), 3-[5(n)-^{3}H]-indolacetic acid (specific activity 29.6 Ci/mmol), and [^{3}H]-8-methoxypsoralen (specific activity 85 Ci/mmol). Atrazine[ring-^{14}C] (specific activity 7.8 mCi/mmol) and 4-acetamidophenol[ring-UL-^{14}C] (specific activity 7.3 mCi/mmol) were purchased from Sigma Chemical Company (St. Louis, Missouri, U.S.A.). [^{14}C]Salicylic acid (specific activity 56.6 mCi/mmol) was received from NEN Research Products (Wilmington, Delaware, U.S.A.) and theophylline [8-^{14}C] from American Radiolabeled Chemicals Inc. (St. Louis, Missouri, U.S.A.). Propranolol base was prepared from [^{3}H]propranolol HC1 (specific activity 17.1 Ci/mmol) as follows: 0.1 mL of propranolol hydrochloride was evaporated,

and water and sodium hydroxide were added (pH 8). Propranolol base was extracted three times by ethyl acetate. The radiochemical purity determined by thin-layer chromatography (TLC) was $> 98\%$ for all compounds. Unless otherwise specified the experiments were performed with the addition of cold compounds. 4-Acetamidophenol, indolacetic acid, 8-methoxypsoralen, propranolol hydrochloride, salicylic acid, and theophylline were purchased from Sigma Chemical Company. Atrazine was received from Monsanto Agricultural Company (St. Louis, Missouri, U.S.A.).

B. Skin Source

Skin samples were taken from the upper thigh of human cadavers (School of Medicine, University of California, San Francisco, California, U.S.A.). The skin was dermatomed to targeted 0.5 mm thickness (Dermatome model B; Padgett, Kansas City, Missouri, U.S.A.) and refrigerated at 4°C in phosphate-buffered saline prior to separation of skin layers. The skin was used within two days, postmortem.

C. Separation of Skin Layers

To separate dermis from epidermis, the tissue was submerged in phosphate buffered saline for 30 seconds at 60°C. The epidermis was peeled from the dermis with dissection forceps. Thin sheets of epidermis were placed dermal side down on a filter paper saturated with 0.0001% trypsin solution (pH 7.6, Sigma Chemical Company). After digestion of the viable epidermis, the sheets of stratum corneum were rinsed thoroughly with deionized water. The skin samples were dried at 37°C for 24 hours in the incubator and stored in the desiccator (6,7).

Model compounds were placed in borosilicate glass tubes, secured with Teflon, and equilibrated for 3 hours at room temperature. Aliquots taken from each vial were analyzed by liquid scintillation counting to obtain the initial concentration of compounds in each solution. Accurately weighed individual skin layer samples were then placed in each vial and the mixture equilibrated with occasional gentle agitation for 0.25 to 24 hours at 20°C. The hydrated skin samples were then removed from the vials, blotted on filter paper, weighed, and dissolved in Soluene 350 (Packard Instrument Company, Downers Grove, Illinois, U.S.A.). The weights of stratum corneum, epidermis, and dermis were 2.1 ± 0.3, 3.7 ± 0.7, and 12.2 ± 6.4 mg, respectively. The surface area of the skin samples was approximately 1 cm^2. The weight of the skin layers (mg) and the volume of the vehicle were chosen so that concentrations of the compounds in the vehicle would not exceed their solubility.

The amount of radiolabeled compound in the vehicle and dissolved skin sample was determined by liquid scintillation counting (TriCarb, model 1500; Packard Instrument Company). All experiments were performed in triplicate.

D. Skin Membrane/Water Partition Coefficient Determination

The partition coefficient (PC) of compounds between skin layers and vehicle was defined as the ratio of concentrations of radiolabeled chemicals revealed in the skin layers and in the vehicle (6,7). The skin membrane/vehicle partitioning was defined as:

$$\mathrm{PC} = \frac{\text{mg solute}/1000\text{ mg skin}}{\text{mg solute}/1000\text{ mg vehicle}}$$

E. Data Relations

The correlation matrix and linear relationships were derived using the MINITAB statistical package, Version 6.1, from MINITAB Inc. (State College, Pennsylvania, U.S.A.).

III. RESULTS

A. Partitioning Studies

The partitioning of model compounds in human stratum corneum, epidermis, and dermis as a function of equilibration time is shown in Figures 1–3. In stratum corneum and epidermis the lipophilic chemicals—propranolol, atrazine, and salicylic acid—reached equilibrium in three to six hours. The most hydrophilic compound, theophylline, required 12 hours to achieve equilibrium. However, in the dermis/water system, equilibrium was reached in 3 hours, which can be explained by the ease of dermal hydration. The partition coefficient time profile of MOP is different than that for the other compounds. The skin layers were not saturated up to 24 hours after the drug exposure, although the partition coefficient continued to increase with contact time.

The values of partition coefficient for lipophilic compounds are different in the three skin layers. The PCs of more lipophilic compounds such as propranolol, salicylic acid, and atrazine are higher in stratum corneum than epidermis and dermis. However the PC values of hydrophilic theophylline remained relatively constant in the three skin layers.

Table 1 shows the influence of drug concentration on PC of the model compounds. In all experiments the PC values decreased as drug concentration increased. This may be due to the saturation of available "binding sites" in the skin

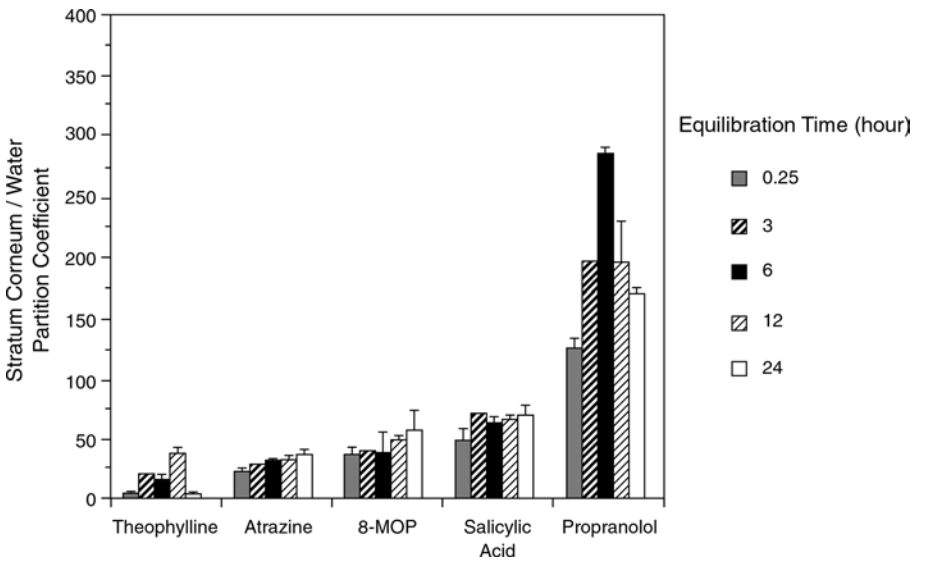


Figure 1 Stratum corneum/water partition coefficient (mean ± SD, $n = 3$) of model compounds as a function of equilibrium time. In the stratum corneum the lipophilic chemicals propranolol, atrazine, and salicylic acid reached equilibrium in three to six hours. The hydrophylic compound theophylline required 12 hours to achieve equilibrium. Solutions of chemicals used were at saturation solubility concentrations.

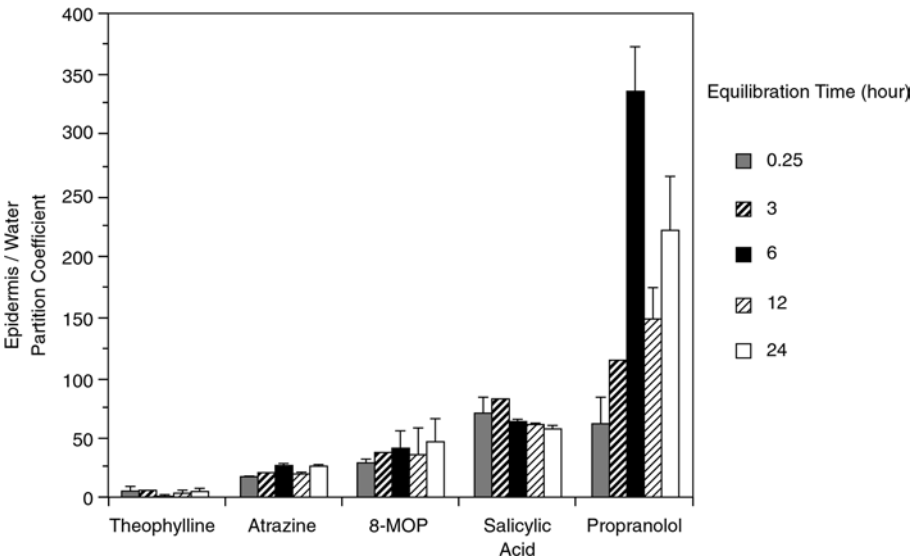


Figure 2 Epidermis/water partition coefficient (mean ± SD, $n = 3$) of model compounds as a function of equilibration time. Partitioning profiles of the tested chemicals follow the trend observed in the stratum corneum. For the lipophilic compounds propranolol, atrazine, and salicylic acid it required three to six hours to achieve equilibrium. Solutions of chemicals used were at saturation solubility concentrations.

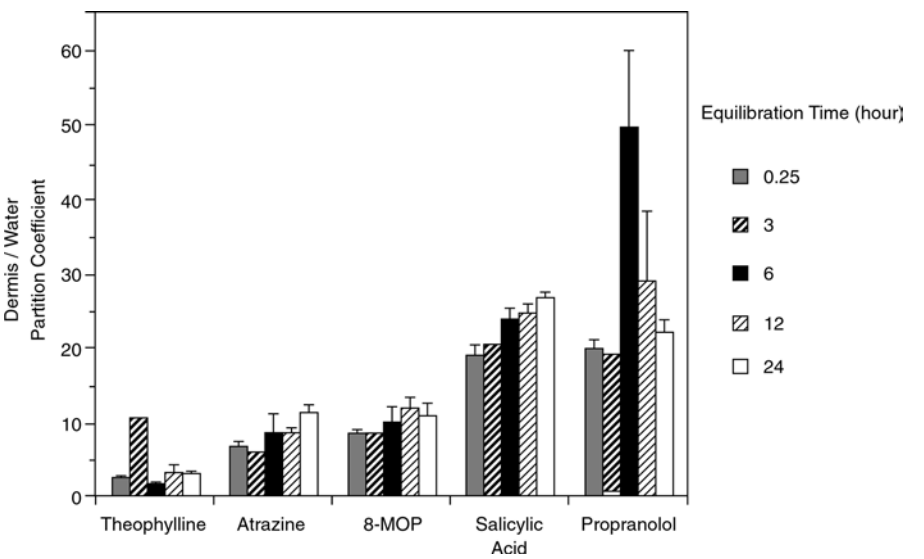


Figure 3 Dermis/water partition coefficient (mean ± SD, $n = 3$) of model compounds as a function of equilibration time. In the dermis/water system, equilibrium for hydrophilic theophylline was reached in three hours. Solutions of chemicals used were at saturation solubility concentrations.

Table 1 Effect of Aqueous Phase Model Compound Concentrations (C, μg/cm^3) on Skin Layers' Water Partition Coefficient (PC) (Mean ± SD; $n = 3$)

Propranolol				Atrazine			
	PC				PC		
C	SC	SCE	D	C	SC	SCE	D
0.1	804 ± 86	691 ± 76	224 ± 60	1.5	110 ± 39	74 ± 16	45 ± 17
0.3	707 ± 88	433 ± 11	116 ± 59	2.9	111 ± 16	57 ± 17	12 ± 1.1
0.5	462 ± 103	321 ± 24	65 ± 11	5.8	70 ± 11	32 ± 1.8	16 ± 8.1
0.9	336 ± 21	235 ± 55	43 ± 6.3	12	59 ± 13	35 ± 1.8	10 ± 4.2
1.8[a]	271 ± 50	150 ± 17	22 ± 1.8	23[a]	37 ± 4	29 ± 1.1	11 ± 1.1

8-MOP				Salicylic Acid			
	PC				PC		
C	SC	SCE	D	$C \times 10^2$	SC	SCE	D
1.1	69 ± 12	60 ± 0.2	15 ± 1.5	1.3	150 ± 62	16 ± 4.3	6.6 ± 0.5
2.2	57 ± 14	56 ± 9.1	13 ± 3.8	2.6	194 ± 41	101 ± 32	7.0 ± 0.6
4.4	52 ± 11	40 ± 11	11 ± 1.4	5.8	182 ± 38	108 ± 31	9.8 ± 1.0
8.8	56 ± 3.2	46 ± 15	10 ± 1.7	12	91 ± 21	85 ± 41	16 ± 1.3
17[a]	56 ± 18	48 ± 19	11 ± 1.6	24[a]	68 ± 10	60 ± 3.2	27 ± 0.8

Indolacetic Acid				Acetaminophen				Theophylline			
	PC				PC				PC		
C	SC	SCE	D	$C \times 10^2$	SC	SCE	D	$C \times 10^3$	SC	SCE	D
3.2	31 ± 0.7	14 ± 1.4	11 ± 1.5	1.1	27 ± 2.2	13 ± 1.5	13 ± 0.53	0.6	12 ± 0.9	11 ± 0.9	4.4 ± 0.7
6.3	16 ± 3.1	9.7 ± 0.4	5.8 ± 0.8	2.2	15 ± 0.5	8 ± 0.9	7.8 ± 3.1	1.1	11 ± 0.3	9.4 ± 1.6	4.2 ± 0.6
13	11 ± 1.0	6.0 ± 1.4	5.6 ± 1.1	4.4	22 ± 8.6	8 ± 1.2	5.1 ± 0.7	2.2	8.3 ± 0.3	7.1 ± 2.9	5.1 ± 0.6
25	8.2 ± 0.8	4.2 ± 0.4	3.2 ± 0.8	8.8	14 ± 2.8	4.7 ± 0.8	5.8 ± 1.9	4.4	6.7 ± 1.3	8.1 ± 1.7	3.3 ± 0.5
50[a]	6.8 ± 0.3	4.4 ± 0.3	3.8 ± 0.6	17[a]	17 ± 2.6	6.3 ± 0.9	6.4 ± 0.7	8.8[a]	4.6 ± 0.5	7.1 ± 2.4	3.0 ± 0.4

Note: The data demonstrate the influence of drug concentration on PC of the model compounds. As the concentration of the chemical increases, the PC values inversely decrease. Equilibration time was 24 hours.

[a]Saturation solubility concentrations (μg/cm^3) are as follows: propranolol (1.8), atrazine (23), 8-MOP (17), salicylic acid (2.4×10^3), indolacetic acid (50), acetaminophen (1.7×10^3), theophylline (8.8×10^3).

layers. As the number of moles available for binding and partitioning increases, the binding sites become saturated, while the concentration of unbound compound increases. Hence this process will continuously decrease the values of partition coefficient.

The PC values of these model compounds are comparable with the octanol/water PCs from the literature, summarized in Table 2. The IPM is often used in PC studies because of its presumed similarities to the properties of skin lipids (8). In the skin layers the PCs of the model compounds in water and IPM are inversely related, while partition coefficients between octanol/water, skin layers/water, and IPM/water are related directly. Note that in the SC/IPM system the PC values for lipophilic compounds (propranolol and atrazine) resemble the PC values of the more hydrophilic compounds (acetaminophen and theophylline). This is not surprising, given the complexity of the stratum corneum composition. It is likely that in SC in the presence of a lipophilic vehicle (IPM), the hydrophilic model compounds more readily partitioned into the protein domain of the stratum corneum.

The pH of the vehicle determines the degree of partitioning of salicylic acid. The data (Table 2) demonstrate that at pH 2.4 the PC values are higher than at pH 5.0 in all skin layers. The pH of the solvent determines the degree of ionization according to the Henderson–Hasselbach equation (9). The pK_a of salicylic acid is 3.0 (10). At pH 2.4 80% of molecules of salicylic acid exist in protonated or unionized form. Their permeation across the lipid membrane occurs more readily. At pH 5.0, 99% of the drug is unprotonated or in the ionized form, which is poorly soluble in lipids. The PC values in the skin decrease. The partitioning behavior of unionized and ionized salicylic acid between octanol and water is similar to partitioning of model compounds in the skin layers studied.

B. Data Relations

The correlation matrix was used to select the highest correlation for each of the experimental log P values. As experimental error is substantial and the data set is small ($n = 8$), no attempt was made to achieve higher correlations by multiple regression on two or more descriptors.

The simple linear relations are justified by the T value of the coefficient, the explained variance (r^2), and the Fisher distribution (F). The standard deviation around the equation line (point scatter) is represented by s. The correlation coefficient (r) is shown in the following equations in parentheses next to the explained variance, $r^2(r)$. The weakest expressions are significant at 96.3% confidence level (CL). The others range from 98.4% to 99.9% CL. The equations are arranged from highest to lowest significance, with w indicating water and o indicating oil:

$$\log P(\mathrm{SC/w}) = 1.01 \log P(\mathrm{SCE/w}) + 0.125$$
$$T = 8.05$$

$$n = 8 \quad s = 0.184 \quad r^2 = 0.915(0.957) \quad F = 64.8$$

$$\log P(\mathrm{SC/IPM}) = 1.00 \log P(\mathrm{SCE/IPM}) + 0.164$$
$$T = 3.92$$

$$n = 7 \quad s = 0.505 \quad r^2 = 0.755(0.869) \quad F = 15.40$$

Table 2 Partition Coefficient (log *P*) of Model Compounds

Model compound	Log *P* octanol/water	Log *P*IPM/water	Stratum corneum		Stratum corneum/epidermis		Dermis	
			Log *P*SC/water	Log *P*SC/IPM	Log *P*SCE/water	Log *P*SCE/IPM	Log *P*D/water	Log *P*D/IPM
Propranolol	3.09	0.18	2.43	1.74	2.17	1.68	1.34	1.55
Atrazine	2.75	0.55	1.57	2.87	1.46	2.67	1.04	2.66
8-MOP	2.53	0.89	1.75	0.67	1.68	0.59	1.03	0.28
Salicylic acid, pH 2.4	2.26	0.68	1.83	0.14	1.77	0.16	1.43	0.72
Salicylic acid, pH 5	1.74	0.37	1.05	NA	0.91	NA	0.85	NA
Indolacetic acid	1.41	−0.68	0.83	1.05	0.64	1.29	0.58	1.44
Acetaminophen	0.32	−0.81	1.23	1.42	0.01	1.51	0.81	0.11
Theophylline	−0.78	−0.65	0.66	2.23	0.85	1.07	0.89	1.95

Note: The measures skin layers/water, skin layers/IPM, and IPM/water partition coefficients are compared with the octanol/water PC values from the literature. Equilibration time was 24 hours. Solution of the chemicals used were at saturation solubility concentrations.
Abbreviation: NA, not available.

$$\log P(\mathrm{SC/w}) = 0.358 \log P(\mathrm{o/w}) + 0.823$$
$$T = 3.32$$

$$n = 8 \quad s = 0.376 \quad r^2 = 0.648(0.805) \quad F = 11.05$$

The equations show equal patterns of behavior of model compounds in isolated stratum corneum and epidermis in aqueous and organic vehicles. Apparently, there is no effect from water soluble epidermal tissue. Log P(SC/w) versus log P(o/w) has a lot of scatter; nevertheless, this relationship allows the approximation of log P(SC/w) for any compound for which log P(o/w) is known.

IV. CONCLUSION

The data presented here are compatible with physicochemical properties of the chemicals used in the study and previous literature observations. The calculated partition coefficients of model compounds as a function of equilibration time, chemical concentration, and nature of the solvent may be valuable in prediction of in vivo and in vitro transport of drugs and environmental agents through human skin.

Raykar et al. (11) suggested that two domains exist in the stratum corneum: The uptake of highly lipophilic compounds (log P values near 3.0) may be governed by the lipid domain of stratum corneum, while partitioning of the more hydrophilic solutes occurs in the protein domain. Theophylline partitions relatively equally into the stratum corneum, epidermis, and dermis; therefore, the retention of theophylline in those skin layers could be due to the binding to the protein domain of the skin. The data presented here are comparable with earlier observations and probably correspond to the 6 to 24–hour period of hydration of stratum corneum (12–14).

REFERENCES

1. Schalla W, Jamoulle J, Schaefer H. Localization of compounds in different skin layers and its use as an indicator of percutaneous absorption. In: Bronaugh RL, Maibach HI, eds. Percutaneous Absorption. New York: Marcel Dekker, 1989:283–312.
2. Elias PM, Cooper ER, Korc A, Brown BE. Percutaneous transport in relation to stratum corneum structure and lipid composition. J Invest Dermatol 1981; 76:297.
3. Noonan PK, Wester RC. Cutaneous metabolism of xenobiotics. In: Bronaugh RL, Maibach HI, eds. Percutaneous Absorption. New York: Marcel Dekker, 1989:53–75.
4. Hansch C, Leo A. Substituent Constants for Correlation Analysis in Chemistry and Biology. Chapter 4. New York: Wiley, 1979.
5. Hansch C, Dunn WJ III. Linear relationships between lipophilic character and biological activity of drugs. J Pharm Sci 1972; 61:1.
6. Surber C, Wilhelm KP, Hori M, Maibach HI, Guy RH. Optimisation of topical therapy: partitioning of drugs into stratum corneum. Pharm Res 1990; 7:1320–1324.
7. Surber C, Wilhem KP, Maibach HI, Hall LL, Guy RH. Partitioning of chemicals into human stratum corneum: implications for risk assessment following dermal exposure. Fundam Appl Toxicol 1990; 15:99–107.
8. Hadgraft J, Ridout G. Development of model membranes for percutaneous absorption measurements. I. Isopropyl myristate. Int J Pharm 1989; 39:149–156.

9. Lee G, Swarbrick J, Kiyohara G, Payling DW. Drug permeation through human skin. III. Effect of pH on the partitioning behavior of chromone-2 carboxylic acid. Int J Pharm 1985; 23:43–54.
10. Katzung BG. Basic and Clinical Pharmacology. 4th ed. (city): Appleton and Lange, 1982:2–3.
11. Raykar PV, Fung M, Anderson BD. The role of protein and lipid domains in the uptake of solutes by human stratum corneum. Pharm Res 1988; 5:140–149.
12. Idson B. Vehicle effects in percutaneous absorption. Drug Metab Rev 1983; 14:2, 207–222.
13. Bronaugh RL, Congdon ER. Percutaneous absorption of hair dyes: correlation with partition coefficients. J Invest Dermatol 1984; 83:124–127.
14. Chadrasekaran SK, Campbell PS, Watanabe T. 1. Application of the "dual sorption" model to drug transport through skin. Polym Eng Sci 1980; 20:36–39.

32

Effect of Single vs. Multiple Dosing in Percutaneous Absorption

Ronald C. Wester and Howard I. Maibach
Department of Dermatology, School of Medicine, University of California, San Francisco, California, U.S.A.

I. INTRODUCTION

Standard pharmacokinetic practice is to first do a single-dose application to determine bioavailability. This standard application is no different for percutaneous absorption and most absorption values are for single doses. But think of topical application (or any drug dosing) and the procedure is repeated, whether once per day for several days (or longer) or multiple times during the day, which also can go on for several days (or longer). There are few one-dose magic bullets in pharmaceutics. Therefore, it becomes important to view multiple topical dosing, especially if that is the standard procedure with which a topical drug is used, or if such exposure occurs for a hazardous environmental chemical.

A. Single Daily Dose Application Over Many Days: Human

Figure 1 illustrates the method used in this type of study (1,2). [^{14}C]malathion was applied to the skin of human volunteers on day 1. For days 2 to 7, nonradioactive malathion was applied once per day to the same skin site. The radioactivity excretion curve for days 1 to 7 represents the single first daily dose. On day 8, the [^{14}C] malathion was applied again (note that malathion had been applied the previous seven days). The radioactivity-excretion curve for days 8 to 14 represents the multiple daily dose. Figure 1 shows no difference in the percutaneous absorption of malathion in man for single daily dose (exposure) over several days. This same method was used by Bucks et al. (3) to study several steroids in man. Table 1 shows no difference in the absorption of a single daily topical steroid dose over several days. The results are exactly like that with malathion (Fig. 2).

There is an exception to the clear results above. Azone® (l-dodecylazacycloheptan-2-one) is an agent that has been shown to enhance the percutaneous absorption of drugs. Azone is believed to act on the stratum corneum (SC) by increasing fluidity of the lipid bilayers. Because Azone is nonpolar, it is thought to act by partitioning into the lipid bilayers, thereby disrupting the structure, and potentially allowing drug

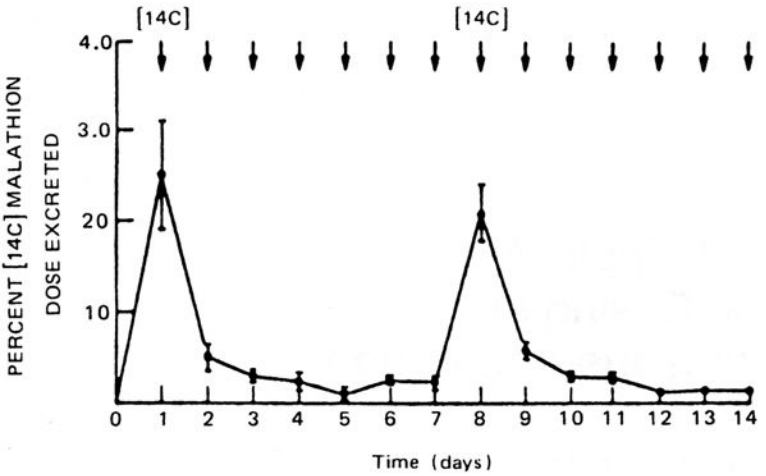


Figure 1 Percutaneous absorption of [^{14}C]malathion after single and repeated topical application (5 mg/cm^2) to the ventral forearm of man. Arrow represents application of malathion, and ^{14}C represents when [^{14}C]malathion was applied.

penetration to increase. Previous clinical studies with single-dose administration show neat Azone percutaneous absorption to be $< 1\%$. A short-term, four day dosing sequence gave absorption of $3.5 \pm 0.3\%$. However, the effect of long-term multiple dosing of Azone on the percutaneous absorption of Azone has never been assessed. A study such as this is important because the mechanism of Azone, disruption of the lipid bilayer structure, suggests a potential for enhanced percutaneous absorption with chronic administration.

Excretion from days 1 to 7 topical application gave a single-dose percutaneous absoprtion of $1.84 \pm 1.56\%$ dose. Percutaneous absorption from days 8 to 15 skin application was $2.76 \pm 1.91\%$, and the absorption from days 15 to 21 skin application

Table 1 Percutaneous Absorption of Steroids in Humans

	Mean % applied dose absorbed (±SD)	
	Non-protected	Occlusion
Hydrocortisone		
Single application	2 ± 2	4 ± 2
Multiple application		
First dose	3 ± 1	4 ± 1
Eighth dose	3 ± 1	3 ± 1
Estradiol		
Single application	11 ± 5	27 ± 6
Multiple application		
First dose	10 ± 2	38 ± 8
Eighth dose	11 ± 5	22 ± 7
Testosterone		
Single application	13 ± 3	46 ± 15
Multiple application		
First dose	21 ± 6	51 ± 10
Eighth dose	20 ± 7	50 ± 9

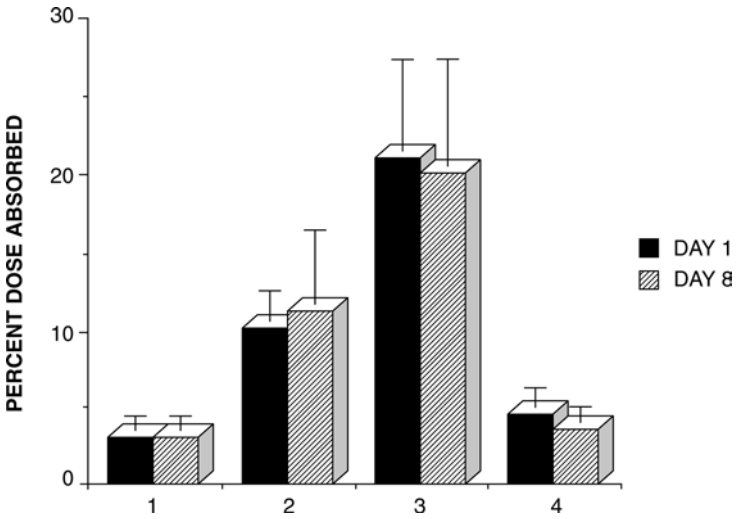


Figure 2 Skin absorption single (day 1) and multiple (day 8) dose in human.

was 2.72 ± 1.21%. Statistical analysis showed a significant difference for day 1 dosing versus day 8 dosing ($p < 0.001$) and for day 1 dosing versus day 15 dosing ($p < 0.008$). No difference was observed in percutaneous absorption for day 8 versus day 15 dosing (Fig. 3). The daily excretion patterns show that peak excretion occurred at 24 or 48 hours following topical application. The results show that an increase occurs in the absorption of Azone with long-term multiple application, but that this enhanced self-absorption occurs early in use, and a steady-state absorption amount is established after the initial enhancement (4).

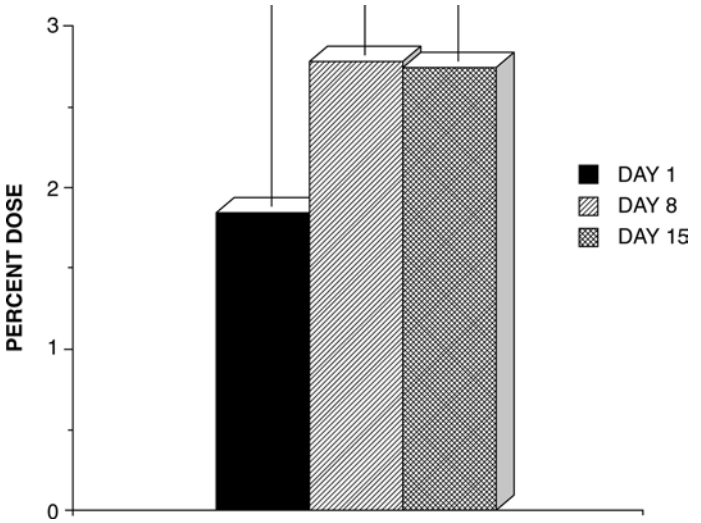


Figure 3 Azone multiple dosing in human volunteers.

B. Triple Daily Dose Application: Hydrocortisone

1. Study design

The study was specifically designed to compare a single low dose (13.33 μg/cm^2) to a single larger dose (40.0 μg/cm^2; three times the amount) and to three multiple-application therapy (13.33 μg/cm^2 × 3 = 40.0 μg/cm^2) treatments. Student two-tailed, paired *t*-tests were employed to compare the percentage of the applied dose absorbed and observed mass absorbed per square centimeter between each of the treatments:

- Treatment 1 — one bolus application of 1.0 μCi/13.33 μg/cm^2 on the right arm, 3 in from the antecubital fossa. The dose was exposed to the skin for 24 hours, followed with removal by washing.
- Treatment 2 — one bolus application of 1.0 μCi/40.0 μg/cm^2 on the left arm, 3 in from the antecubital fossa. The dose was exposed to the skin for 24 hours, followed with removal by washing.
- Treatment 3 — Three repeat applications of 1.0 μCi/13.33 μg/cm^2 on the left ventral forearm, 1 in from the antecubital fossa. One dose was applied, followed by identical doses 5 and 12 hours after the initial dose. The site was washed 24 hours after the initial dose was applied.

Treatment	Dose per application (μgc/cm^2)	Cumulative dose (μgc/cm^2)	Total vehicle volume (μL)	
			Acetone	Cream
1[a]	13.33	13.33	20	100
2[b]	40.00	40.00	20	100
3[c]	13.33	40.00	60	100

[a]Single dose of 13.33 μg/cm^2, administered in 20 μL of vehicle.
[b]Single dose of 40.00 μg/cm^2, administered in 20 μL of vehicle.
[c]Three serial 13.33 μg/cm^2 doses, each administered in 20 μL of vehicle (total 60 μL).

C. Hydrocortisone Dosing Sequence

Figures 4 and 5 show the predicted and observed hydrocortisone in vivo percutaneous absorption in acetone or cream vehicles dosed at 13.3 μg/cm^2 x 1 (single low dose), 40.0 μg/cm^2 × 1 (single high dose, and an amount three times that of the low dose), and 13.3 μg/cm^2×3 (multiple dose, which is three times the single low dose and equal in total amount to the 40 μg/cm^2 in the single high dose). The predicted amounts are multiples (three times) of that of the observed single dose value.

With acetone vehicle 0.056 ± 0.073 μg/cm^2 hydrocortisone was absorbed for the low dose. The single high-dose absorption was 0.140 ± 0.136 μg/cm^2 a value near its predicted linear amount of 0.168. The multiple-dose absorption should have been the same predicted 0.168; however, the absorption was 0.372 ± 0.304 μg/cm^2, a value statistically ($p < 0.05$) greater than that of the single high dose (Fig. 4).

With the cream vehicle, the same pattern emerged. The single high-dose absorbed [0.91 ± 1.66 μg/cm^2] was three times that of the low dose absorbed 0.31 ± 0.43 μg/cm^2).

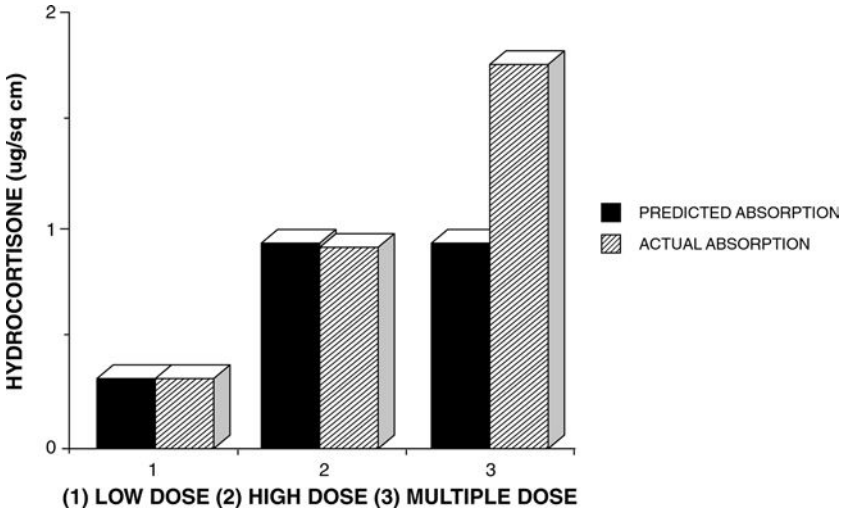


Figure 4 Hydrocortisone in vivo human skin absorption in cream vehicle.

The multiple dose absorbed (1.74 ± 0.93 μg/cm^2) exceeded the predicted amount and was statistically ($p < 0.006$) greater than that of the single high dose.

Table 2 gives the predicted and observed in vitro hydrocortisone percutaneous absorption. The receptor fluid accumulations (absorbed amounts) show the same trend as that seen in vivo. In vitro studies also allowed the human skin to be assayed for hydrocortisone content following the 24-hour dosing interval. The skin content values markedly reflect those seen with the receptor fluid values. Only three observations were made per dosing sequence, so statistically no differences exist. The same human skin sources were used for both acetone and cream vehicles, so these absorption amounts can be compared. Hydrocortisone absorption is greater with the acetone vehicle (5,6).

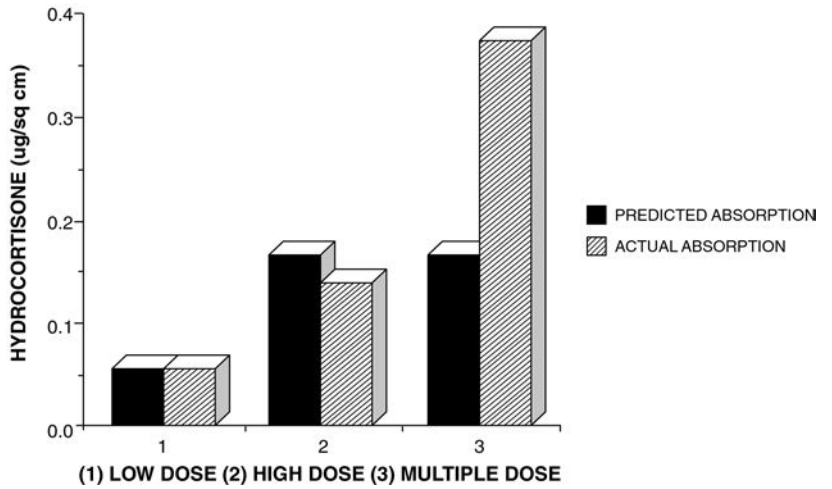


Figure 5 Hydrocortisone in vivo human skin absorption in acetone vehicle.

Table 2 Predicted and Observed Hydrocortisone Absorption: In Vitro

		Hydrocortisone ($\mu g/cm^2$)			
		Receptor fluid		Skin	
Vehicle	Dosing sequence	Predict	Observe	Predict	Observe
Acetone[a]	13.3 $\mu g/cm^2 \times 1$	—	0.13 ± 0.05	—	0.87 ± 0.23
	40.0 $\mu g/cm^2 \times 1$	0.39[b]	0.35 ± 0.22	2.61[b]	2.21 ± 2.05
	13.3 $\mu g/cm^2 \times 3$	0.39	0.55 ± 0.75	2.61	2.84 ± 2.05
Cream[a]	13.3 $\mu g/cm^2 \times 1$	—	$0.053 + 0.029$	—	0.30 ± 0.24
	40.0 $\mu g/cm^2 \times 1$	0.16[b]	0.23 ± 0.03	0.90[b]	0.86 ± 0.53
	13.3 $\mu g/cm^2 \times 3$	0.16	0.27 ± 0.21	0.90	1.19 ± 0.43

[a] $n = 3$; mean $\pm$ SD.
[b] 0.39 $\mu g/cm^2$ is three times the measured value of 0.13 $\mu g/cm^2$; 2.61 $\mu g/cm^2$ is three times the measured value of 0.87 $\mu g/cm^2$; 0.16 $\mu g/cm^2$ is three times the measured value of 0.053 $\mu g/cm^2$; 0.90 $\mu g/cm^2$ is three times the measured value of 0.30 $\mu g/cm^2$.

Little information is available on the most effective topical corticosteroid or other topical formulation dosing regimen regarding the number of skin applications in one day. Multiple applications for an ambulatory patient with a readily accessible skin site are common practice. However, for hospitalized patients, or patients where multiple dosing would be difficult, a single effective dose of hydrocortisone will eventually do the task.

D. Triple Daily Dose Application: Diclofenac

Diclofenac, a nonsteroidal anti-inflammatory drug, has been widely used in the treatment of rheumatoid arthritis and osteoarthritis. However, oral delivery of this drug poses certain disadvantages, such as fast first-pass metabolism and adverse side effects (including gastrointestinal reactions and idiosyncratic drug reactions). Therefore, alternative routes of administration have been sought. The skin has become increasingly important to this effect, and many drugs have been formulated in transdermal delivery systems, including diclofenac itself. However, diclofenac sodium is not easily absorbed through the skin due to its hydrophilic nature. Much work has concentrated on using percutaneous absorption enhancers or cosolvents to increase penetration. A new diclofenac sodium lotion named Pennsaid has been developed for topical application. Pennsaid includes the absorption enhancer dimethylsulfoxide (DMSO). It is expected that the addition of DMSO may increase the in vivo permeation rate of diclofenac through the skin into the deeper target tissues beneath the skin.

Tables 3 and 4 show that multiple doses of Pennsaid lotion (2 $\mu g/cm^2$ and 5/d/cm^2 3x/day) delivered a total of 40.1 ± 17.6 µg and 85.6 ± 41.4 µg diclofenac, respectively at 48 hours, compared to only 9.4 ± 2.9 µg and 35.7 ± 19.0 µg absorbed after topical appliation of diclofenac as an aqueous solution ($P < 0.05$). A single-dose study showed no statistical difference between diclofenac delivered in Pennsaid lotion or an aqueous solution. Over 48 hours the total absorption for Pennsaid lotion was 10.2 ± 6.7 and 26.2 ± 17.6 µg (2 and 5 $\mu L/cm^2$, respectively), compared to 8.3 ± 1.5 and 12.5 ± 5.7 µg from an aqueous solution. Both single doses of Pennsaid lotion and aqueous diclofenac showed decreased diclofenac absorption into the

Table 3 In Vitro Percutaneous Absorption of Diclofenac from Pennsaid Lotion and Aqueous Solution in Viable Human Skin

	Dosing Regimen	Diclofenac absorbed ($\mu g/cm^2$)[a]
A	30 $\mu g/cm^2$ single-dose Pennsaid	10.2 ± 6.7
B	75 $\mu g/cm^2$ single-dose Pennsaid	26.2 ± 17.6
C	30 $\mu g/cm^2$ single-dose aqueous	8.3 ±1.5
D	75 $\mu g/cm^2$ single-dose aqueous	12.3 ± 5.6
E	240 $\mu g/cm^2$ multidose Pennsaid	40.1 ± 17.6
F	600 $\mu g/cm^2$ multidose Pennsaid	85.6 ± 41.4
G	240 $\mu g/cm^2$ multidose aqueous	9.4 ± 2.9
H	600 $\mu g/cm^2$ multidose aqueous	35.7 ± 19.0

Note: Absorbed, cumulative, in receptor fluid plus skin.
[a]Mean ± SD ($n = 4$ or 5).

receptor fluid between 12 and 24 hours. However, when applied multiple times, absorption from Pennsaid lotion was continually increasing up to 48 hours (7). Clinically, Pennsaid lotion has been shown to be effective in a multidose regimen.

The above studies with hydrocortisone and diclofenac show enhanced human skin absorption from a multidose (defined as three times per day application) regimen. The key for diclofenac is the Pennsaid formulation and, probably, the inclusion of the penetration enhancer DMSO. For hydrocortisone it may simply be the continuing application of vehicle that "washes" the drug through the skin.

E. Animal Models

There are several multidose studies in the literature using animals (8–12), which give mixed results when compared to subsequent human studies. A key animal study is

Table 4 Statistical Summary: Diclofenac Absorption in Viable Human Skin

Treatment	Statistic[a] ($p=$)
Pennsaid lotion	
A vs. B—single dose	0.09[b]
E vs. F—multiple doses	0.05[c]
A vs. E—single vs. multiple	0.007[c]
B vs. F—single vs. multiple	0.02[c]
Aqueous solution	
C vs. D—single dose	0.16[b]
G vs. H—multiple doses	0.02[c]
C vs. G—single vs. multiple	0.42[b]
D vs. H—single vs. multiple	0.03[c]
Pennsaid lotion vs. aqueous solution	
A vs. C—single dose	0.57[b]
B vs. D—single dose	0.13[b]
E vs. G—multiple doses	0.005[b]
F vs. H—multiple doses	0.04[c]

[a]Student's *t*-test.
[b]Non-significant.
[c]Statistically significant.

that by Bucks et al. (13), where percutaneous absorption of malathion multidose in the guinea pig is similar to multidose in man except where skin washing is introduced into the study design. Skin washing enhances multidose malathion percutaneous absorption. In human studies skin washing is not a consideration because bathing is an everyday event. In animal experiments treatment of skin may compromise skin integrity (application of keratolytic agents soap and water washing) and this can result in altered percutaneous absorption.

II. DISCUSSION

Percutanous absorption with single-dose regimens are generally the only types of studies done to determine typical bioavailability. Tradition and regulatory requirements are probably the driving forces. In actual clinical use, the multidose regimen is probably the more widely practiced treatment. Two types of experimental designs have been tested. The one of a single daily dose over the course of a few weeks probably does not affect percutaneous absorption unless the skin is compromised by disease (14), or if some key ingredient in the formulation is an absorption enhancer, such as Azone, and Azone seems to have only influenced the early part of the dosing period. The more intriguing multidose regimen is the multiple dose application during a single day. Both formulation (as seen with hydrocortisone) and formulation ingredients (DMSO in Pennsaid lotion) can enhance skin absorption. The combined (and relevant) study of multidoses within each day over several days dosing has not been done. Neither have longer term studies using multidose daily regimens been done to assess percutaneous absorption and diseased skin, and the potential compromise of keratolytic agents such as salicylic acid and hydrocortisone.

REFERENCES

1. Wester RC, Maibach HI, Bucks DAW, Guy RH. Malathion percutaneous absorption after repeated administration to man. J pharm Sci 1983; 65:116–119.
2. Wester RC, Maibach HI, Bucks DAW, Guy RH. Malathion percutaneous absorption after repeated administration to man. Toxicol Appl Pharmacol 1983; 68:116–119.
3. Bucks DAW, Maibach HI, Guy RH. In vivo percutaneous absorption: effect of repeated application versus single dose. In: Bronaugh R, Maibach H, eds. Percutaneous Absorption. 2d ed. New York: Marcel Dekker, 1989:633–651.
4. Wester RC, Melendres J, Sedik L, Maibach HI. Percutaneous absorption of Azone following single and multiple doses to human volunteers. J Pharm Sci 1994; 83:124–125.
5. Melendres J, Bucks DAW, Camel E, Wester RC, Maibach HI. In vivo percutaneous absorption of hydrocortisone: multiple-application dosing in man. Pharm Res 1992; 9:1164–1167.
6. Wester RC, Melendres J, Logan F, Maibach HI. Triple therapy: multiple dosing enhances hydrocortisone percutaneous absorption in vivo in humans. In: Smith E, Maibach H, eds. Percutaneous Penetration Enhancers. Boca Raton, FL: CRC Press, 1995:343–349.
7. Hewitt PG, Poblete N, Wester RC, Maibach HI, Shainhouse JZ. In vitro cutaneous disposition of a topical diclofenac lotion in human skin: effect of a multi-dose regimen. Pharm Res 1998; 15(7): 988–992.
8. Roberts MS, Horlock E. Effect of repeated skin application on percutaneous absorption of salicylic acid. J Pharm Sci 1978; 67:1685–1687.
9. Wester RC, Noonan PK, Maibach HI. Frequency of application on percutaneous absorption of hydrocortisone. Arch Dermatol 1997; 113:620–622.

10. Wester RC, Noonan PK, Maibach HI. Variations in percutaneous absorption of testosterone in the Rhesus monkey due to anatomic site of application and frequency of application. Arch Dermatol Res 1980a; 267:229–235.
11. Wester RC, Noonan PK, Maibach HI. Variations in percutaneous absorption of hydrocortisone increases with long-term administration: In vivo studies in the Rhesus monkey. Arch Dermatol Res 1980b; 116:186–188.
12. Courtheoux S, Pechnenot D, Bucks DA, Marty JPL, Maibach H, Wepierre J. Effect of repeated skin administration on in vivo percutaneous absorption of drugs. Br J Dermatol 1986; 115:49–52.
13. Bucks DAW, Marty JPL, Maibach HI. Percutaneous absorption of malathion in the guinea pig: effect of repeated skin application. Food Chem Toxic 1958; 23:919–922.
14. Wester RC, Maibach HI. Percutaneous absorption in diseased skin. In: Maibach H, surber C, eds. Topical Corticosteroids. Basel: Karger, 1992:128–141.

33

Electrical Enhancement of Transdermal Delivery of Ultradeformable Liposomes

Ebtessam A. Essa, Michael C. Bonner, and Brian W. Barry
University of Bradford, Bradford, U.K.

I. INTRODUCTION

Human skin, the largest single organ of the body (up to 16% of body weight), provides the formulator with a wide and easily accessible area for drug application. It is a complex, layered structure, forming a barrier between the body and the outside environment. The percutaneous route for drug administration has many advantages over other pathways, including avoidance of gut and hepatic first pass effects, continuous drug delivery, fewer side effects, and improved patient compliance. Unfortunately, the protective function of the skin makes it difficult for most drugs to penetrate into and through the skin. The outermost layer of the skin (stratum corneum) provides the principal barrier to permeation and consists of corneocytes embedded in a highly organized lipid matrix. Several approaches have been developed to disorganize the lipid bilayers, thereby enhancing the penetration of drugs (1).

Because of its important barricade function, the lipid region of the skin has been extensively characterized over the last 20 years. Freeze–fracture electron microscopic studies revealed the presence of lipid lamellae in the intercellular regions. The lipid can be crystalline, gel, liquid crystalline, or liquid (2,3). Because of its predominantly semisolid character, the resistance to drug penetration is further increased in these lamellar phases.

In order to broaden the spectrum of drugs that can be delivered via the skin, and to increase systemic delivery efficiency, there is a continuing demand to increase the skin permeability. Many techniques have been developed to overcome the barrier; including chemical (e.g., enhancers and liposome encapsulation) and physical (e.g., iontophoresis and electroporation) methods. This chapter summarizes our present knowledge of means by which lipid vesicles under iontophoresis, electroporation, and combinations of these electrical methods can alter drug transport through skin.

A. Ultradeformable Liposomes

Liposomes are lipid vesicles that fully enclose aqueous domains. The lipid molecules are usually phospholipids with or without cholesterol, and the lipid may arrange into

one or more bilayers. Liposomes can entrap hydrophilic molecules within their aqueous regions, or they can incorporate lipophilic molecules within the membrane. The use of liposomes as drug carriers for topical and/or transdermal delivery has been recently reviewed (4,5).

Although it has been generally accepted that vesicles normally increase drug transport across the skin, questions arise about the mechanism of action of these formulations. Many researchers suggested that phospholipid vesicles administered on the skin first disintegrate, then small fragments or lipid monomers diffuse through the barrier (6). Liposomes may first adsorb and fuse with the skin surface and their constituents then change the ultrastructure of the intercellular regions in the deeper layers of the stratum corneum, thus producing a penetration enhancing effect (7). Other workers believe that some vesicles (called transfersomes) are deformable enough to pass through the intact stratum corneum and reach the systemic circulation as intact structures (8,9). Similar vesicles accumulate in channel-like regions in the stratum corneum (10,11).

Transfersomes are highly deformable liposomes (also designated as ultradeformable, ultraflexible, or elastic). These vesicles incorporated an edge activator, a surfactant molecule such as sodium cholate or deoxycholate that gives the membrane its characteristic deformablity or elasticity owing to its high radius of curvature (12,13). A typical transfersome formulation comprised phospholipid (e.g., phosphatidylcholine) as the main ingredient with 10 to 24 wt.% of a surfactant added, with the vesicles suspended in an aqueous vehicle containing 3% to 10% v/v ethanol. The inventors claimed that such vesicles squeeze through pores in the stratum corneum that are less than one-tenth the liposome's diameter when applied non-occlusively. The driving force for penetration is claimed to be the skin's hydration gradient. Thus, sizes up to 200 to 300 nm could potentially penetrate intact to the deep layers of the skin and may progress far enough to reach the systemic circulation. Such ultradeformable liposomes are the subject of this chapter.

B. Electrical Methods for Enhancing Skin Delivery

Electrotransport (iontophoresis and electroporation) is a technique originally designed to deliver compounds through the skin that pose significant challenges, such as ionized compounds and hydrophilic macromolecules. The method has now been extended to particulate delivery, i.e. liposomes.

1. Iontophoresis

Iontophoresis in the present context can be defined as the facilitated movement of molecules across a membrane using low, physiologically acceptable electric current. Usually, an electrode of the same polarity as the drug contacts the drug and skin. A grounding electrode completes the circuit (14–16). The method is based on the general principle that like charges repel each other and opposite charges attract. Thus, to deliver a negatively charged molecule across the skin, it is placed under the negative electrode (cathode), where it is repelled towards a positive electrode (anode) placed elsewhere on the body, and vice versa for a drug cation. Thus ions on either side of the skin will migrate in the direction dictated by their charges. Their migration speeds are determined by their physicochemical characteristics and the properties of the diffusion media (17,18). The sum of individual ion fluxes must equal the current supplied by the power source; thus all ions compete to carry the charge.

The technique has been used clinically for delivering medication to surface tissue for several decades. However, its potential has been rediscovered for transdermal systemic delivery of ionic drugs, including peptides and oligonucleotides that are normally difficult to administer except by the parenteral route (15).

Iontophoresis enhances drug delivery not only by electro-repulsion, but also by electro-osmosis—a bulk solvent flow across a membrane under an electric potential gradient. At normal pH, skin is negatively charged and fluid flows in the direction of cation flux. Such flow either enhances the transport of cations or retards anion movement. The contribution of electro-osmotic flux to the overall transport of charged compounds is likely to be small, as fluid flow is estimated at μL/hr (19). One further transport possibility is that the electric current may disorganize somewhat the intercellular lipids structure of the stratum corneum, thus producing a more permeable skin (20).

Iontophoresis is believed to transport drug primarily through preexisting pathways such as skin appendages (21,22) and intercellular routes (23), but also via induced new aqueous pores (24). The dominant iontophoretic pathway depends on the physicochemical properties of the permeant and its affinity to the environment available, where lipophilic permeants favor the intercellular route and hydrophilic compounds mainly penetrate through the appendageal pathway (25).

2. Electroporation

An electrical enhancement technique that could work alone or in conjunction with iontophoresis is electroporation. Electroporation (or electropermeabilization) is a long established technique for permeabilizing biological membranes, and is widely used to introduce genetic material into bacterial cells. High-voltage pulse(s) (usually from 100 to 1000 V) applied for a very short duration (from micro- to milliseconds) create transient aqueous pores in lipid bilayers. These pores provide pathways for drug penetration through the horny layer of the skin (26–29). Localized heating of lipids, causing a phase transition, forms the pores (30). Drug transport through these transient pores can also be facilitated by electrophoresis during the pulse "on" time, or by simple diffusion through these aqueous domains that remain open for some time after pulsing. Unlike iontophoresis, electroosmotic solvent flow is much less significant (31–33).

In spite of the marked increase in transdermal drug infiltration under an applied electomotive force (EMF), safety is a major concern, although several reports indicated that skin damage is usually mild and reversible (20,33,34).

II. LIPOSOMES UNDER ELECTRICAL POTENTIAL

The potential benefits of modifying the packing of the intercellular bilayer lipids of the skin to promote penetration, together with electrically driving vesicles across the skin is attractive, and takes advantage of two dissimilar mechanisms of action (35).

A. Iontophoresis and Ultradeformable Liposomes

Combining lipid vesicles with iontophoresis is a somewhat recent approach, and few reports have been published of this mode of transdermal drug delivery. Here, we briefly review their conjoint use.

While there are numerous reports on the use of liposomes for penetration enhancement, the combination of liposomes and iontophoresis has received little attention, though it could offer some additional benefits. A charge can effectively be imparted to neutral drugs by encapsulating them in charged liposomes, thus enhancing their iontophoretic delivery. To prepare charged liposomes, stearylamine is commonly used to induce positive charges, while dicetyl phosphate yields negative charges (15). An early report of the combined use of iontophoresis and traditional liposomes in skin delivery was for enkephalin entrapped in positive or negative vesicles (36). Iontophoresis increased liposomal enkephalin penetration compared to the control solution. During transport, enkephalin degraded, but to a lesser extent in the liposomes, reflecting a protective effect of the vesicles for the encapsulated drug. Iontophoretic delivery of neutral colchicine encapsulated in positively charged liposomes increased the drug flux by four to five times compared to free colchicine (37).

The effect of different liposomal formulations on the iontophoretic transport of enoxacin through rat skin in vitro has also been investigated (38). The iontophoretic penetration of enoxacin increased with a decrease in the fatty acid chain length of the phospholipid, explained as due to the decrease in the phase transition temperature of the lipid.

The effects of zwitterionic lipids [phosphatidylcholine (PC) and distearoyl phosphatidylcholine (DSPC)], cationic lipid (stearylamine) and the penetration enhancer azone on the iontophoretic transdermal flux of neutral mannitol through human skin in vitro, were examined (39). The skin was pretreated with the placebo lipid suspensions or Azone® solution, all containing 32% ethanol, prior to iontophoresis. For the lipid suspensions, only PC increased mannitol flux compared to control (without pretreatment). Interestingly, the authors found that the combination of PC and electric current increased mannitol flux almost as effectively as the potent penetration enhancer azone, suggesting a synergistic effect between PC and electric current.

More recently, the combined use of iontophoresis and ultradeformable (ultraflexible or elastic) liposomes has been studied. Offering the potential to stabilize therapeutic agents undergoing iontophoresis, surfactant-based elastic vesicles (composed of octaoxyethylene laurate ester, sucrose laurate ester, and cholesterol sulfate) were used to deliver apomorphine through human skin in vitro (40).

Transfersomes (PC: sodium cholate; 86:14% w/w) are negatively charged ultradeformable vesicles due to the edge activator (cholate anion). Using human epidermal membranes, cathodic iontophoresis (0.2–0.8 mA/cm^2 constant current) increased the delivery of estradiol compared to the control (saturated estradiol aqueous solution), even though the vesicles were delivered against electro-osmotic flow (41). The steroid flux rose linearly with the applied current, confirming the ability of iontophoresis to provide controlled drug delivery.

The enhancement in estradiol flux from liposomes compared to control (up to 15-fold at 0.8 mA/cm^2) was attributed to the augmented effect of both electric field and phospholipids released from the lipid vesicles. Both processes modulated the intercellular lipid lamellae of the stratum corneum, increasing membrane permeability. It was also suggested that under such conditions of a permeabilized skin structure, intact vesicles might penetrate someway down the stratum corneum because of their flexibility. Importantly, iontophoresis induced tritium exchange of the ^3H-labeled estradiol with water, and had to be allowed for so as not to falsely elevate the flux data. Tritium exchange increased with increasing current density and time of

application. Interestingly, the liposomal structure shielded the drug against the effect, producing a protective action (41).

To estimate the role of vesicle deformability on the enhanced drug penetration from ultradeformable vesicles, iontophoresis (six hours of 0.8 mA/cm^2) of estradiol from the same ultradeformable vesicles (containing sodium cholate as edge activator) was compared with that from traditional liposomes (i.e., without edge activator). The prototype nonrigid pure PC and membrane-stabilized (PC: cholesterol; 1:1 molar ratio) formulations were used. All preparations improved skin delivery of estradiol in terms of flux and skin deposition, compared with control solution, with ultradeformable liposomes being the most effective. Nevertheless, there was no strong evidence that such higher results were due to any special capability of transfersomes to deform. Moreover, by comparing the zeta potentials of the three liposomal formulations with their flux values, it was concluded that the highest result obtained from transfersomes was because of the greater electrophoretic repulsion force imposed by the current acting on the more charged vesicles (42).

Despite the encouraging data in these studies, the question arises whether or not the relatively high current density of 0.8 mA/cm^2 is suitable for practical application, knowing that most reports recommend a maximum of 0.5 mA/cm^2, for clinical relevance (34). To probe the safety of iontophoresis using such a relatively high current, an in vitro experimental protocol was designed to examine skin barrier integrity before and after current application. The same transfersome formulations and saturated drug solution were used (41). This protocol involved three consecutive four-hour stages; a first passive diffusion stage, then iontophoresis (0.8 mA/cm^2), and finally a second passive regime, applied to the same piece of the skin. This sequence of drug delivery thus assessed the effect of current on the skin barrier properties. Theoretically, if skin barrier modulation due to iontophoresis is a reversible process, estradiol passive penetration following current termination would be similar to that of the first passive stage. The transepidermal estradiol fluxes from ultradeformable liposomes and control at different stages, as shown in Figure 1, indicated that iontophoresis reversibly changed the skin barrier. The passive flux after iontophoresis was similar to that before current application, for both solution and liposomes, suggesting the suitability of such current density for in vitro application. For clinical usage, of course, we would also need to do in vivo studies.

There is considerable debate about the pathways taken by ions traversing the skin during iontophoresis. However, there is general agreement that a low-resistance route is involved. The current flows via domains of low resistance and these are clearly provided by the shunt route (comprising hair follicles and sweet glands). Attempts to assess the contribution of various transport pathways during iontophoresis from the literature are difficult given the diversity of the experimental protocols used. With ultradeformable liposomes, the shunt route was shown to contribute minimally to passive delivery, and the intercellular lipid domain was suggested to be the main pathway (43,44). Therefore, we investigated the role of shunt route in the skin penetration of estradiol during occluded passive and iontophoretic (0.5 mA/cm^2) delivery of the drug from saturated solution and negatively charged transfersomes (45). The technique of using a stratum corneum/epidermis (SC/Ep) sandwich designed by El Maghraby et al. (44) was employed (Fig. 2). The study monitored the delivery of estradiol through human epidermal membrane compared to that through a sandwich of stratum corneum and epidermis. In the SC/Ep sandwich, the additional stratum corneum formed the top layer. Because skin shunts occupy only about 0.1% of skin surface area, it was assumed that the top

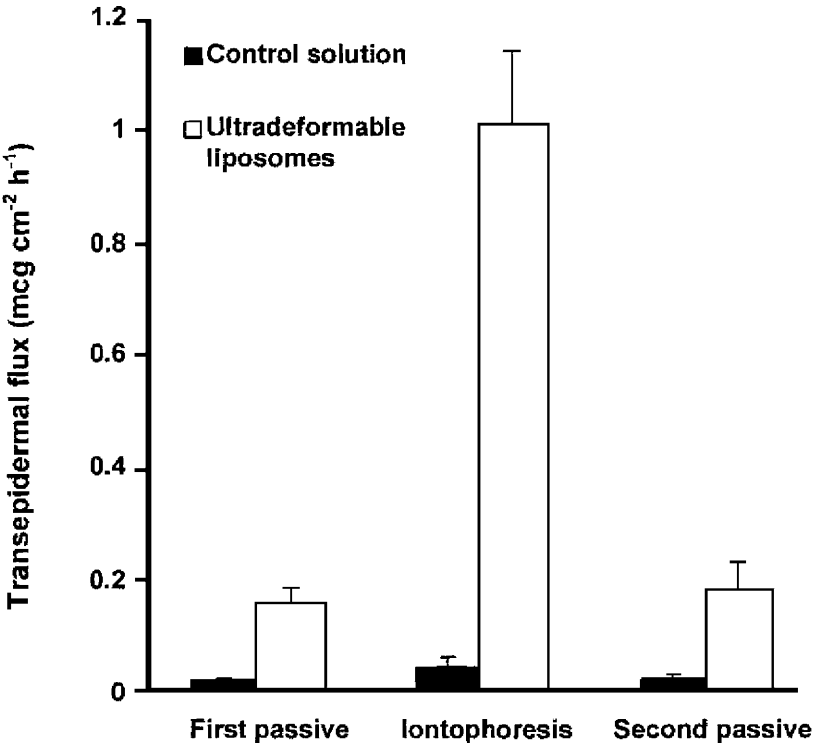


Figure 1 In vitro iontophoretic estradiol fluxes through human epidermis from control saturated solution and ultradeformable liposomes using the three four-hour stages protocol; first passive, iontophoresis (0.8 mA/cm^2) then second passive ($n = 5–6$).

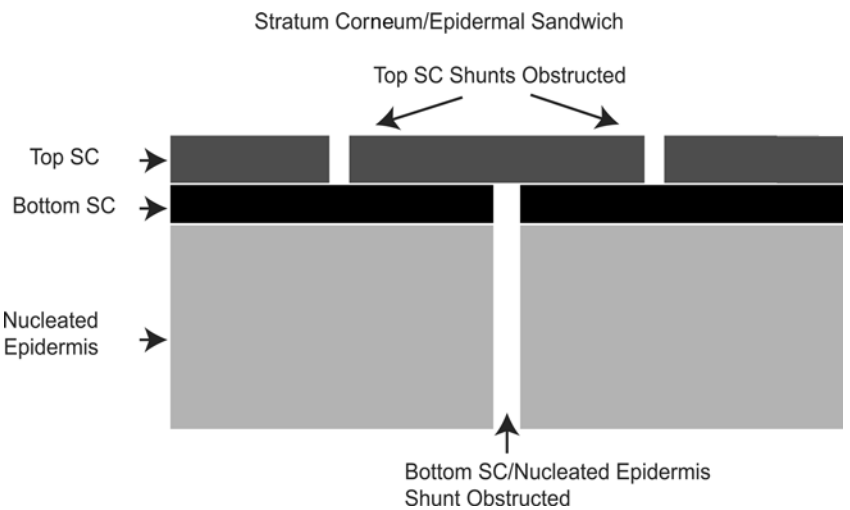


Figure 2 Diagrammatic representation of the skin sandwich (not to scale).

layer of the stratum corneum would essentially block all shunts available in the bottom membrane. The presence of the top layer of stratum corneum effectively doubles the thickness of the skin barrier. This doubling should reduce the transepidermal flux by half compared to that through epidermal membrane alone, if the shunt route was unimportant for drug penetration (46). A much greater reduction in flux would indicate a major shunt contribution to estradiol penetration.

The reduction in the iontophoretic flux of the steroid indicated an important role for the shunt route, which was estimated to represent up to about 50% of the total iontophoretic pathway. In spite of their lipophilic nature and relatively large size [126 ± 4.2 (SD) nm], ultradeformable liposomes were capable of penetrating at least some way down the shunts under the effect of iontophoresis. The data also suggested that anatomical shunts were not the only possible iontophoretic pathway, as due to disorganization of the intercellular lipid lamella under electrical treatment, some additional pores formed.

B. Electroporation and Ultradeformable Liposomes

During electroporation, any elevated transdermal penetration can result from several features; the increased permeability of the skin due to electrical breakdown, electrophoresis (repulsion force between the applied current and the entity of the same polarity) and/or—but less likely—from electro-osmosis. The mechanism of pore formation was reported to be due to a temperature rise within the stratum corneum intercellular lipids to above their phase transition temperature. The temperature rises in localized regions known as local transport regions (LTRs) (30,47). Additionally, the bulk of stratum corneum is not homogenous but exhibits defects, so it is likely that at least temporary aqueous pathways exist, e.g., in desmosomes or protein structures between adjacent corneocytes. The electric field can force electrolytes into such areas, expanding them so that stratum corneum resistance reduces markedly (48).

Published research on the combined use of liposomes and electroporation is sparse. For example, the effect was investigated of electroporation (pulses of 250 V, 20 ms, 10 pulses/min for five minutes) on the epidermal delivery of colchicine encapsulated in positively charged standard liposomes (DSPC: cholesterol; 1:0.5 molar ratio) (49). The total charge and cumulative amount of colchicine delivered over 24 hours were less than that after iontophoresis ($0.5\,mA/cm^2$) for six hours. Interestingly, the authors proposed that intact vesicles could penetrate through such a potentially modified skin structure.

For the first time, skin delivery of highly deformable liposomes (PC: sodium cholate; 86:14% w/w) under, electroporation has been investigated (50). Five pulses (100 V, 100 ms, and one minute spacing) were applied to negatively charged vesicles containing estradiol dosed on to human epidermal membranes, with saturated solution as control. Although electroporation markedly increased skin penetration and deposition over eight hours from control solution (about 16-fold relative to passive diffusion), when ultradeformable liposomes were delivered electrically drug penetration parameters were not enhanced over those of simple occluded passive delivery from the same vesicles. Such low penetration was unexpected for ultradeformable liposomes, as it would be reasonable to assume that the combination of the two accelerent strategies (released phospholipids acting as chemical enhancer and electroporation as a physical force) would augment each other, increasing penetration. This surprising result was attributed in part to the possible attenuated effect of the electrical pulses on the skin due to voltage/liposomes interaction.

Nevertheless, as liposomes were suspended in saturated (non-entrapped) estradiol solution, it would be logical to expect a result at least similar to that of control or even higher due to the well-accepted enhancing effect of liposomes. Therefore, a possible role of PC (present in liposomes but not in solution) in restoring some of the skin's barrier properties was suggested.

To delineate this effect of PC on the skin barrier after electroporation, a two-stage protocol was designed so as to introduce the same number of pores within the skin using the same pulsing regimen detailed above. Membranes were dosed with empty liposome suspension (i.e., without estradiol) with or without edge activator for 30 minutes, while control membranes were treated with water. After washing the donor chambers, penetration from estradiol solution through control and treated skin was followed for 2.5 hours (Stage I). To examine further the skin integrity, another set of pulses was applied while estradiol solution remained in the donor (Stage II), and penetration was followed for a further two hours (50).

The results are displayed as cumulative amount penetrated versus time plots in Figure 3.

The graph displays a steady increase in estradiol penetrated during Stage I, with control (water-treated) showing the highest penetration rate. After the second pulsing (Stage II), drug penetration was once again increased, with the control showing a marked rise compared to that through skin treated with the two types of empty vesicles. It was therefore suggested that during skin electroporation using

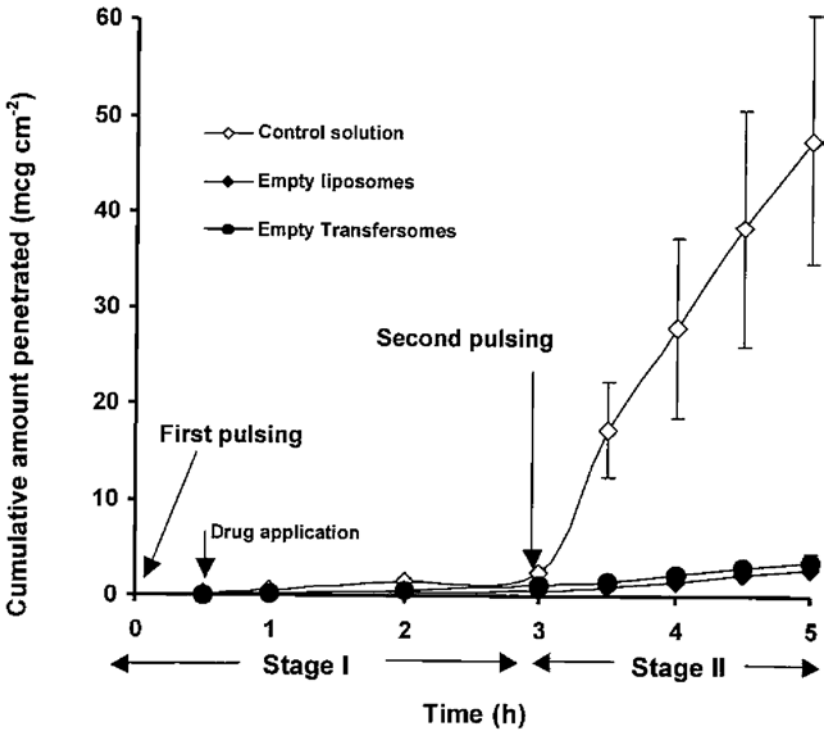


Figure 3 Two-stage in vitro human epidermal penetration of estradiol from saturated aqueous solution after two sets of pulses (five pulses, 100 V, 100 ms, and one minute spacing) through control (water-treated) and empty liposome (with or without cholate)–treated skin ($n = 6$–10).

liposomes, PC molecules released from liposomes at the highly altered skin sites could improve skin repair. The PC monomers reaching the site of high skin perturbation (LTRs) would replace some of water molecules at these particular regions. Although in a liquid–crystalline state, PC microdomains would be more resistant to molecular penetration than are water molecules. Thus, such new liquid crystalline microdomains acted in opposition to the more usual penetration enhancing effect of phospholipids operating particularly at gel regions of the intercellular lipid. Accordingly, under such conditions, phospholipids would act as penetration retardants, in reasonable agreement with Fang et al. (51) who also reported a retardation of flurbiprofen permeation through mice skin in vitro when phospholipids were mixed with cellulose hydrogel.

C. Combined Physical Methods and Ultradeformable Liposomes

The combined use of electroporation and iontophoresis in improving trans-epidermal drug delivery was first investigated a decade ago (52). Transport of luteinizing hormone-releasing hormone in solution through human skin in vitro was enhanced by the combination by 5 to 10 times the corresponding iontophoretic flux (52). However, more recent reports gave outcomes where the combined techniques were less encouraging (53,54).

A recent study investigated the delivery of liposomally encapsulated estradiol (42). Transdermal fluxes and skin deposition from solution and ultradeformable vesicles under iontophoresis, electroporation and the two electric methods are shown in Figure 4.

The histograms reveal that under passive and iontophoretic deliveries ultradeformable liposomes improved drug penetration and deposition, compared to the control saturated solution. Under electroporation, only the solution improved drug penetration parameters compared to passive penetration, while liposomes did not markedly increase penetration as compared to solution, due to the possible retarding effect of the phospholipid. While electroporation alone did not improve estradiol parameters from cholate-containing ultradeformable liposomes over passive delivery, two hours of iontophoresis ($0.8\,mA/cm^2$) after skin pulsing (five pulses, 100 V, 100 ms, and one minute spacing) increased drug flux by 17-fold compared to passive delivery.

Together, the barrier distorting factors (electroporation, iontophoresis, and phospholipids) may have disturbed more of the stratum corneal lipid domain. However, the penetration data were still low. While iontophoretic delivery enhanced estradiol flux from ultradeformable vesicles by up to about 15-fold compared to control, combined electroporation and iontophoresis raised the flux by only 2.5-fold. This low ratio suggested an increased skin barrier towards estradiol penetration, a result that supports the earlier finding of the penetration retarding effect of PC monomers when present during skin electroporation. Thus, the overall results supported the concept that PC protects the skin after high-voltage pulses. The dramatic fall in skin deposition value to 0.46-fold compared to control solution further emphasizes the protective effect of PC monomers against estradiol diffusion into, and through, the skin.

III. CONCLUDING REMARKS

Chemical and electrical penetration enhancement strategies have been well established for the improvement of drug penetration through the skin. A charge

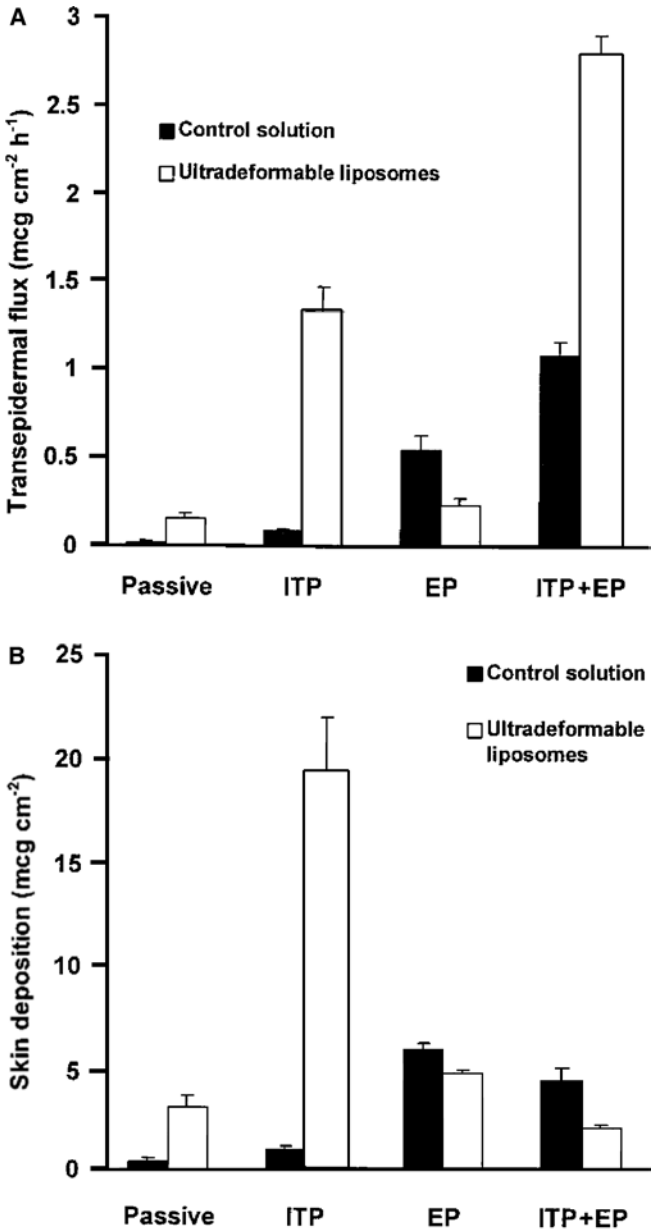


Figure 4 Transepidermal estradiol fluxes (**A**) and skin deposition (**B**) after iontophoresis (ITP), electroporation (EP), and combined electroporation and iontophoresis (EP+ITP) delivery from saturated aqueous solution and ultradeformable liposomes, through human epidermal membranes in vitro ($n = 6$–12).

can effectively be applied to neutral molecules by their entrapment in a charged vesicle, with the intention of maximizing its skin delivery by electrical enhancement. Studies have indicated that iontophoresis of such vesicles can indeed augment the penetration of entrapped drugs, irrespective of the flexibility of the liposome. Efforts

to deliver liposomally entrapped drugs by means of high voltage pulsing (electroporation) have, however, produced surprisingly low levels of drug penetration. This recent finding indicates that phospholipid components of such vesicles may act as penetration retardants, attenuating enhancement effects of the electrical treatment.

REFERENCES

1. Barry BW. Novel mechanisms and devices to enable successful transdermal delivery. Eur J Pharm Sci 2001; 14:101–104.
2. White SH, Mirejovsky D, King GI. Structure of lamellar lipid domains and corneocytes envelops of murine stratum corneum. An X-ray diffraction study. Biochemistry 1988; 27:3725–3732.
3. Bouwstra JA, Gooris GS, van der Spek JA, Lavrijsen S, Bras W. The lipid and protein structure of mouse stratum corneum: a wide and small angle diffraction study. Biochim Biophys Acta 1994; 1212:183–192.
4. Bouwstra JA, Honeywell-Nguyen PL. Skin structure and mode of action of vesicles. Adv Drug Del Rev 2002; 45:S41–S55.
5. Bouwstra JA, Honeywell-Nguyen PL, Groois GS, Ponec M. Structure of the skin barrier and its modulation by vesicular formulations. Prog Lipid Res 2003; 42:1–36.
6. Schreier H, Bouwstra JA. Liposomes and niosomes as topical drug carriers: dermal and transdermal drug delivery. J Control Rel 1994; 30:1–15.
7. Hofland HEJ, Bouwstra JA, Boddé HE, Spies F, Junginger HE. Interactions between liposomes and human stratum corneum *in-vitro:* freeze fracture electron microscopical visualization and small angle X-ray scattering studies. Br J Dermatol 1995; 132:853–856.
8. Cevc G, Blume G. Lipid vesicles penetrate into intact skin owing to the transdermal osmotic gradient and hydration force. Biochim Biophys Acta 1992; 1104:226–232.
9. Cevc G, Schätzlein A, Richardsen H. Ultradeformable lipid vesicles can penetrate the skin and other semi-permeable barriers un-fragmented. Evidence from double label CLSM experiments and direct size measurements. Biochim Biophys Acta 2002; 1564:21–30.
10. Honeywell-Nguyen PL, Frederik PM, Bomans PHH, Junginger HE, Bouwstra JA. Transdermal delivery of pergolide from surfactant-based elastic and rigid vesicles: characterisation and in vitro transport studies. Pharm Res 2002; 19:991–997.
11. Honeywell-Nguyen PL, Groenink HWW, de Graaff AM, Bouwstra JA. The in vivo transport of elastic vesicles into human skin: effects of occlusion, volume and duration of application. J Control Rel 2003; 90:243–255.
12. Cevc G, Gebauer D, Stieber J, Schätzlein A, Blume G. Ultraflexible vesicles, Transfersomes, have an extremely low pore penetration resistance and transport therapeutic amounts of insulin across the intact mammalian skin. Biochim Biophys Acta 1998; 1368:201–215.
13. Cevc G, Blume G. New, highly efficient formulation of diclofenac for topical, transdermal administration in ultradeformable drug carriers, Transfersomes. Biochim Biophys Acta 2001; 1514:191–205.
14. Green PG, Flanagan M, Shroot B, Guy RH. Iontophoretic drug delivery, In: Walters KA, Hadgraft J, eds. Pharmaceutical Skin Penetration Enhancement. New York: Marcel Dekker Inc., 1993:311–333.
15. Banga AK. In: Electrically Assisted Transdermal and Topical Drug Delivery. London: Taylor and Francis, 1998.
16. Guy RH. Iontophoresis-recent developments. J Pharm Pharmacol 1998; 50:371–374.
17. Sage BH, Riviere JE. Model system in iontophoresis transport efficacy. Adv Drug Deliv Rev 1992; 9:265–237.
18. Phipps JB, Padmanabhan RV, Lattin GA. Iontophoretic delivery of model inorganic and drug ions. J Pharm Sci 1989; 78:365–369.

19. Pikal MJ, Shah S. Transport mechanisms in iontophoresis. III. An experimental study of the contributions of electroosmotic flow and permeability change in transport of low and high molecular weight solutes. Pharm Res 1990; 7:222–229.
20. Jadoul A, Bouwstra J, Préat V. Effect of iontophoresis and electroporation on the stratum corneum. Adv Drug Deliv Rev 1999; 35:89–105.
21. Cullander C, Guy RH. Sites of iontophoretic current flow into the skin: identification and characterisation with the vibrating probe electrode. J Invest Derm 1991; 97:55–64.
22. Cullander C. What are the pathways of iontophoretic current flow through mammalian skin? Adv Drug Deliv Rev 1992; 9:119–135.
23. Monteiro-Riviere NA, Inman AO, Riviere JE. Identification of the pathway of iontophoretic drug delivery: light and ultrastructural studies using mercuric chloride in pigs. Pharm Res 1994; 11:251–256.
24. Graaff AM, Li GL, van Aelst AC, Bouwstra JA. Combined chemical and electrical enhancement modulates stratum corneum structure. J Control Rel 2003; 90:49–58.
25. Turner NG, Guy RH. Iontophoretic transdermal pathways: dependence on penetrant physicochemical properties. J Pharm Sci 1997; 86:1385–1389.
26. Pliquett UF, Zewert TE, Chen T, Langer R, Weaver JC. Imaging of fluorescent molecules and small ion transport through human stratum corneum during high voltage pulsing: localised transport regions are involved. J Biophys Chem 1996; 58:185–204.
27. Prausnitz MR, Lee CS, Liu CH, Pang JC, Singh TP, Langer R, Weaver JC. Transdermal transport efficiency during skin electroporation and iontophoresis. J Control Rel 1996; 38:205–217.
28. Higuchi WI, Li SK, Ghanem AH, Zhu HG, Song Y. Mechanistic aspects of iontophoresis in human epidermal membrane. J Control Rel 1999; 62:13–23.
29. Prausnitz MR. A practical assessment of transdermal drug delivery by skin electroporation. Adv Drug Del Rev 1999; 35:61–76.
30. Pliquet UF, Gusbeth CA. Perturbation of human skin due to application of high voltage. J Bioelectrochem 2000; 51:41–51.
31. Pliquett U, Weaver JC. Electroporation of human skin: simulation measurement of changes in transport of two fluorescent molecules and in the passive electrical properties. Bioelectrochem Bioenerget 1996; 39:1–12.
32. Vanbever R, Morre ND, Préat V. Transdermal delivery of fentanyl by electroporation. II Mechanisms involved in drug transport. Pharm Res 1996; 13:1359–1365.
33. Vanbever R, Leroy MA, Préat V. Transdermal penetration of neutral molecules by skin electroporation. J Control Rel 1998; 54:243–250.
34. Curdy C, Kalia YN, Guy RH. Non-invasive assessment of the effects of iontophoresis on human skin in vivo. J Pharm Pharmacol 2001; 53:769–777.
35. Williams AC. Transdermal and Topical Drug Delivery. London and Chicago: Pharmaceutical Press, 2003.
36. Vutla NB, Betageri GV, Banga AK. Transdermal iontophoretic delivery of enkephalin formulated in liposomes. J Pharm Sci 1996; 85:5–8.
37. Kulkarni SB, Banga AK, Betageri GV. Transdermal iontophoretic delivery of colchicine encapsulated in liposomes. Drug Del 1996; 3:245–250.
38. Fang J, Sung KC, Lin H, Fang C. Transdermal iontophoretic delivery of enoxacin from various liposome-encapsulated formulations. J Control Rel 1999; 60:1–10.
39. Kirjavainen M, Urtti A, Monkkonen J, Hirvonen J. Influence of lipid on the mannitol flux during transdermal iontophoresis in vitro. Eur J Pharm Sci 2000; 10:97–102.
40. Li GL, Danhof M, Bouwstra JA. Effect of elastic liquid state vesicle on apomorphine iontophoresis transport through human skin in vitro. Pharm Res 2001; 11:1627–1630.
41. Essa EA, Bonner MC, Barry BW. Iontophoretic estradiol skin delivery and tritium exchange in ultradeformable liposomes. Int J Pharm 2002; 240:55–66.
42. Essa EA, Bonner MC, Barry BW. Electrically assisted skin delivery of liposomal estradiol; phospholipid as damage retardant. J Control Rel 2004; 95:535–546.

43. Cevc G, Gebauer D, Stieber J, Schätzlein A, Blume G. Ultraflexible vesicles, Transfersomes, have an extremely low pore penetration resistance and transport therapeutic amounts of insulin across the intact mammalian skin. Biochim Biophys Acta 1998; 1368:201–215.
44. El Maghraby GMM, Williams AC, Barry BW. Skin hydration and possible shunt route penetration in controlled estradiol delivery from ultradeformable and standard liposomes. J Pharm Pharmacol 2001; 53:1311–1322.
45. Essa EA, Bonner MC, Barry BW. Human skin sandwich for assessing shunt route penetration during passive and iontophoretic drug and liposome delivery. J Pharm Pharmacol 2002; 54:1481–1490.
46. Barry BW. Drug delivery routes in skin: a novel approach. Adv Drug Deliv Rev 2002; 54:31–40.
47. Pliquett UF, Martin GT, Weaver JC. Kinetics of the temperature rise within human stratum corneum during electroporation and pulsed high voltage iontophoresis. Bioelectrochem 2002; 57:65–72.
48. Boddé HE, van den Brink I, Koerten HK, de Haan FHN. Visualization of in vitro percutaneous penetration of mercuric chloride transport through intercellular space versus cellular uptake through desmosomes. J Control Rel 1991; 15:227–236.
49. Badkar AV, Betageri GV, Hofmann GA, Banga AK. Enhancement of transdermal iontophoretic delivery of a liposomal formulation of colchicine by electroporation. Drug Deliv 1999; 6:111–115.
50. Essa EA, Bonner MC, Barry BW. Electroporation and ultradeformable liposomes; human skin repair by phospholipid. J Control Rel 2003; 92:163–172.
51. Fang JY, Hwang TL, Leu YL. Effect of enhancers and retarders on percutaneous absorption of furbiprofen from hydrogels. Int J Pharm 2003; 250:313–325.
52. Bommannan D, Tamada J, Leung L, Potts RO. Effect of electroporation on transdermal iontophoretic delivery of luteinizing hormone releasing hormone (LHRH) in vitro. Pharm Res 1994; 11:1809–1814.
53. Badkar AV, Banga AK. Electrically enhanced transepidermal delivery of a macromolecule. J Pharm Pharmacol 2002; 54:907–912.
54. Fang JY, Hwang TL, Huang YB, Tsai YH. Transepidermal iontophoresis of sodium nonivamide acetate V. Combined effect of physical enhancement methods. Int J Pharm 2002; 235:95–105.

34

In Vitro Release from Semisolid Dosage Forms—What Is Its Value?*

Vinod P. Shah
Food and Drug Administration, Rockville, Maryland, U.S.A.

I. INTRODUCTION

A key aspect of any new drug product is its safety and efficacy as demonstrated in controlled clinical trials. The time and expense associated with such trials make them unsuitable as routine quality control methods to reestablish comparability in quality and performance following a change in formulation or method of manufacture. Therefore, in vitro and in vivo surrogate tests are often used to assure that product quality and performance are maintained over time. In addition, an appropriate in vitro dissolution test is used as a market release test to assure batch-to-batch consistency for product performance. The focus of this chapter is the application of in vitro release approaches in the documentation of performance of semisolid dosage forms.

In vitro approaches, such dissolution, are standard methods used to assess performance characteristics of a solid oral dosage formulation. It has evolved as a critical test method in the field of drug development. In vitro dissolution is used specifically to guide formulation development, monitor manufacturing process, batch-to-batch quality and possibly predict in vivo performance. When used as a quality control procedure, in vitro dissolution testing can signal an inadvertent change in drug and/or excipient characteristics or in the manufacturing process. Dissolution tests are used to provide biowaiver for drug products containing highly soluble, highly permeable drug substances with rapid dissolution characteristics and for lower strength dosage forms under certain conditions.

Extension of in vitro dissolution methodology to semisolid dosage forms (topical dermatological drug products such as creams, ointments, gels, and lotions) has been the subject of both substantial effort and debate. A simple, reliable, reproducible, relevant, and generally acceptable in vitro method to assess drug release from a semisolid dosage form would be highly valuable for the same reasons that such

* The chapter reflects scientific opinion of the author and does not necessarily reflect the policies of the FDA agency.

methodology has proved valuable in the development, manufacture, and batch-to-batch quality control of solid oral dosage forms.

Present quality control tests to assure the identity, strength, quality, purity, and potency for semisolid dosage forms include identification, assay, homogeneity, viscosity, specific gravity, particle size, microbial limits, and impurity profile. These tests may provide little or no information about drug release properties of the product, stability of the product, or effects of manufacturing and processing variables on the performance of the finished dosage form. A drug release test for topical products, analogous to a dissolution test for a solid oral dosage form, is therefore of interest. Such a test should be able to detect formulation and manufacturing process changes that affect performance of the drug product in vivo. Ultimately, it would be desirable to demonstrate that in vitro performance of a topical formulation correlates in some way with in vivo performance of the formulation. Pending development of such data, a drug release test may be used to assess batch-to-batch drug release uniformity and quality of the product, just as in vitro dissolution is now used for solid oral dose forms.

II. IN VITRO RELEASE TESTING

In vitro release is one of several methods used to characterize performance characteristics of a finished topical dosage form. Important changes in the characteristics of a drug product or in the thermodynamic properties of the drug substance in the dosage form should be manifested as a difference in drug release. Drug release is theoretically proportional to the square root of time when the drug release from the formulation is rate limiting. A plot of the amount of drug released per unit area (mcg/cm^2) against the square root of time yields a straight line, the slope of which represents the release rate. This release rate measure is formulation specific and can be used to monitor product quality. As summarized in a Food and Drug Administration (FDA) guidance document (1), recommended methodology for in vitro release studies is as follows:

- Diffusion cell system: a static diffusion cell system with a standard open cap ground glass surface with 15 mm diameter orifice, and total diameter of 25 mm (Fig. 1)
- Synthetic membrane: appropriate inert, porous, and commercially available synthetic membranes such as polysulfone, cellulose acetate/nitrate mixed ester, or polytetrafluoroethylene 70 μm membrane of appropriate size to fit the diffusion cell diameter (e.g., 25 mm in the preceding case)
- Receptor medium: appropriate receptor medium such as aqueous buffer for water-soluble drugs or a hydro-alcoholic medium for sparingly water-soluble drugs or another medium with proper justification
- Number of samples: a minimum of six samples is recommended to determine the release rate (profile) of the topical dermatological product.
- Sample applications: about 300 mg of the semisolid preparation is placed uniformly on the membrane and kept occluded to prevent solvent evaporation and compositional changes. This corresponds to an infinite dose condition.
- Sampling time: multiple sampling times (at least five times) over an appropriate time period to generate an adequate release profile and to determine the drug release rate (a six-hour study period with not less than five samples, i.e., at 30 minutes and 1, 2, 4, and 6 hour) is suggested. The sampling times may have to be varied depending on the formulation. An aliquot of

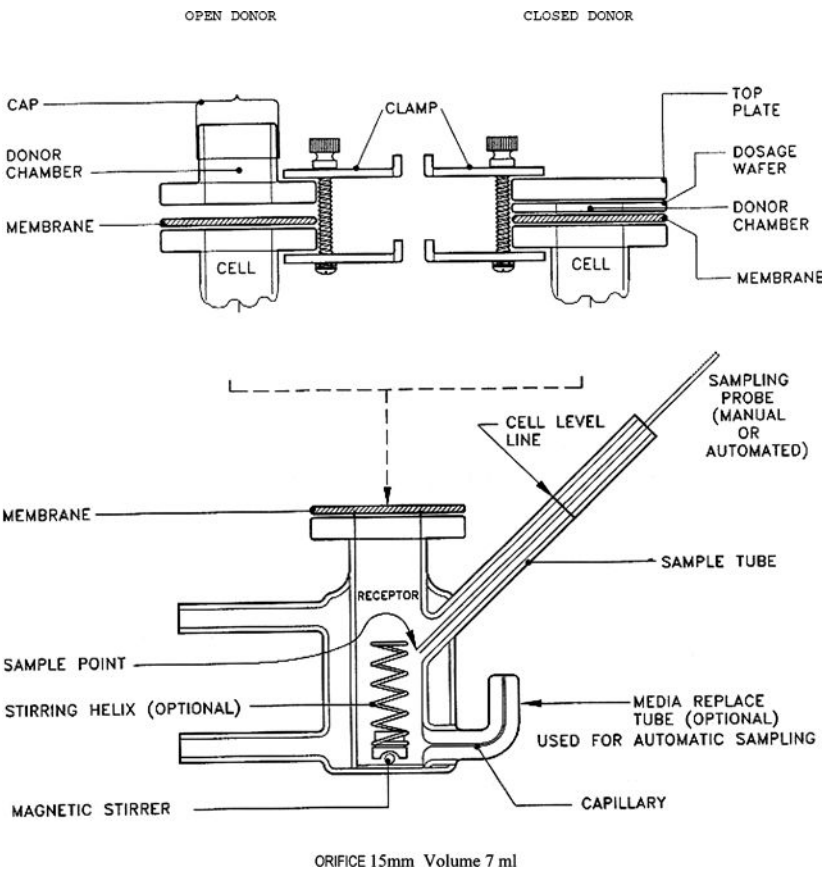


Figure 1 Schematic of diffusion cell assembly used for in vitro release measurement.

the receptor phase is removed at each sampling interval and replaced with fresh aliquot, so that the lower surface of the membrane remains in contact with the receptor phase over the experimental time period.

- Sample analysis: appropriate validated, specific, and sensitive analytical procedure, generally high-pressure liquid chromatography (HPLC), is used to analyze the samples and to determine the drug concentration and the amount of drug released.
- In vitro release rate: a plot of the amount of drug released per unit membrane area (mcg/cm^2) versus square root of time should yield a straight line. The slope of the line (regression) represents the release rate of the product. An X-intercept typically corresponding to a small fraction of an hour is a normal characteristic of such plots.
- Automation: the in vitro release test system can be completely automated.

III. DISCUSSION

When drugs are applied topically, a pharmacologically active agent must be released from its carrier (vehicle) before it can contact the epidermal surface and be available

for penetration in the stratum corneum and lower layers of the skin (2). A topical formulation is a complex drug delivery system, and the dynamics of drug release from a vehicle have been a subject of debate and investigation for many years (3–14). A simple and reproducible method, generally applicable to all topical dermatological dosage forms has been developed to measure in vitro drug release from the dosage form using a vertical diffusion cell and a synthetic membrane (3–5). This in vitro release test is gaining importance as a product performance and quality control test. Scientific workshops on scale-up of a semisolid disperse system (6) and on the value of in vitro drug release (7) have resulted in recommendations on the use of in vitro release tests as a measure of in-process control and also as a finished product specification for creams, ointments, and gels. In addition, the cited workshop report also recommends the use of in vitro release test for monitoring product reproducibility during component and compositional changes, manufacturing equipment and process changes, scale-up, and/or transfer to another manufacturing site (6,7). These recommendations (use of in vitro release test) are the basis of assuring product sameness after Scale-up and Post-approval changes (SUPAC)-related changes (1).

A relatively simple methodology has been developed to assess drug release characteristics from topical dermatologic formulations. This methodology employs a vertical static diffusion cell system, commonly referred to as the Franz cell, a commercially available polysulfone synthetic membrane, and an aqueous receptor phase (Fig. 1). To determine in vitro drug release, an infinite amount of drug is applied on the donor chamber. Aliquots of the receptor media are removed at 30-, 60-, 120-, 240-, and 360-minute intervals, analyzed, and the cumulative amount of drug released, expressed in $\mu g/cm^2$, is plotted against square root of time ($minute^{0.5}$). The relationship between drug release and square root of time has been shown to be linear and valid for topical formulations as long as the percentage of drug release is less than 30% of the drug applied in the donor chamber (4,5). This relationship holds true for topical formulations with either fully dissolved or suspended drug. The release rate or the slope of the line is obtained by linear regression analysis and is considered to be the property of the formulation. The polysulfone synthetic membrane serves as a support membrane. The support membrane should be chemically inert to the experimental formulations and should not react with the drug or the receptor medium; should be permeable to the drug, and should not be rate limiting in the drug release process (8,11).

Selection of an appropriate receptor medium is important to maintain sink conditions during in vitro release studies. In addition, it must be determined that the receptor medium should not react with the membrane or alter the dosage form by back diffusion through the membrane. The receptor medium selected should be compatible with the analytical (HPLC) method such that the analysis can be carried out by direct injection of the receptor medium onto HPLC system. Either aqueous buffer or a water miscible organic solvent mixture of 30% ethanol in water was determined to be optimum receptor medium for the study of in vitro release of corticosteroid drug products (9).

IV. IN VITRO RELEASE-CORTICOSTEROIDS

Extensive research carried out on the drug release of hydrocortisone from a cream matrix concluded the value and utility of simple in vitro release test. It also established that the release rate is highly reproducible, concentration dependent and is

the characteristic of the formulation (13). In vitro release of marketed corticosteroids using polysulfone membrane and 30% alcohol as a receptor medium for creams and alcohol: isopropyl myristate: water in ratios of 85:10:5 as a receptor medium for ointments was evaluated. The results confirmed the inert nature of the support membrane and wide application of the procedure (8–14). The release rate from two 0.05% of betamethasone dipropionate cream formulations, Diprolene (potency category 2), and Diprosone (potency category 3) was rank orderly related to the potency of the product. In vitro release experiments using different agitation/mixing speeds and different lot numbers of synthetic membranes showed no significant difference in release rate, establishing the ruggedness of the simple test procedure (12). In vitro release rate measurements performed over two years and from different batches of a given manufacturer also showed no important differences in results. Other experiments clearly show that the release rate is formulation sensitive and is reproducible. Figure 2 shows the release rate of nine marketed miconazole nitrate cream products. The release rate falls into two distinct groups, which corresponds to two distinct groups of formulations (formulation information derived from Physicians' Desk Reference book). These experiments establish the ruggedness and reproducibility of the in vitro release methodology and support its use in quality control/quality assurance. Unpublished work in our laboratory indicates that in vitro release methodology is also applicable to other groups of dermatological dosage forms such as antifungal, antiviral, and antiacne drug products intended for topical administration. Overall, these results demonstrate the versatility and utility of the in vivo release test methodology. In a recent report on dissolution/in vitro release of novel/special dosage forms, in vitro release studies using vertical diffusion cell system, as described in this chapter, is being recommended as the method of choice for semisolid dosage forms (15).

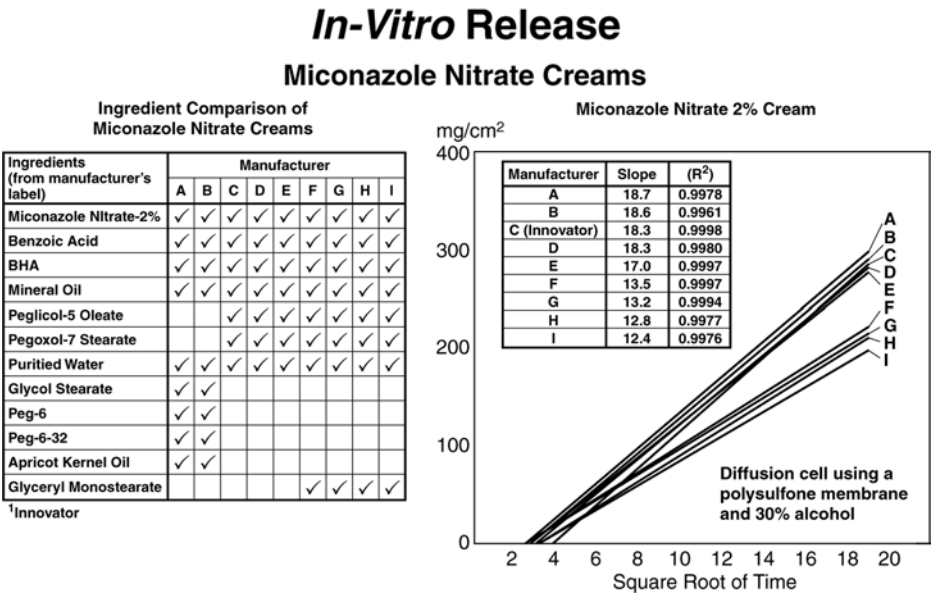

In-Vitro Release
Miconazole Nitrate Creams
Ingredient Comparison of Miconazole Nitrate Creams
Ingredients (from manufacturer's label)
Manufacturer
A B C D E F G H I
Miconazole Nitrate-2% ✓ ✓ ✓ ✓ ✓ ✓ ✓ ✓ ✓
Benzoic Acid ✓ ✓ ✓ ✓ ✓ ✓ ✓ ✓ ✓
BHA ✓ ✓ ✓ ✓ ✓ ✓ ✓ ✓ ✓
Mineral Oil ✓ ✓ ✓ ✓ ✓ ✓ ✓ ✓ ✓
Peglicol-5 Oleate ✓ ✓ ✓ ✓ ✓ ✓ ✓ ✓
Pegoxol-7 Stearate ✓ ✓ ✓ ✓ ✓ ✓ ✓ ✓
Purified Water ✓ ✓ ✓ ✓ ✓ ✓ ✓ ✓ ✓
Glycol Stearate ✓ ✓
Peg-6 ✓ ✓
Peg-6-32 ✓ ✓
Apricot Kernel Oil ✓ ✓
Glyceryl Monostearate ✓ ✓ ✓ ✓
[1]Innovator
Miconazole Nitrate 2% Cream
mg/cm2
Manufacturer Slope (R2)
A 18.7 0.9978
B 18.6 0.9961
C (Innovator) 18.3 0.9998
D 18.3 0.9980
E 17.0 0.9997
F 13.5 0.9997
G 13.2 0.9994
H 12.8 0.9977
I 12.4 0.9976
A B C D E F G H I
Diffusion cell using a polysulfone membrane and 30% alcohol
400
300
200
100
0
2 4 6 8 10 12 14 16 18 20
Square Root of Time

Figure 2 In vitro release of nine marketed miconazole cream products.

V. APPLICATIONS

Application of in vitro release testing in drug development and its value in topical drug products quality assurance was discussed extensively in scientific workshop entitled Assessment of Value and Applications of In Vitro Testing of Dermatological Drug Products (7). The report indicates that in vitro release methodology is based on sound scientific principles and is of value in assessing product quality. It also indicates that the in vitro release should not be used to compare fundamentally different types of topical formulations such as creams, ointments, and gels. Further, the report indicates that release rate by itself should not be used as a measure of bioavailability/bioequivalence (BA/BE) of these complex formulations. Nonetheless, in vitro release test can serve as a valuable tool for initial screening of experimental formulations in the product development area and can serve to signal possible bioinequivalence. In vitro release testing may find a future use as a quality control tool to assure batch-to-batch uniformity, just as the dissolution test is used to assure quality and performance of solid oral dosage forms.

A. SUPAC-SS

In May 1977, the FDA released a guidance for industry entitled SUPAC-SS—Nonsterile Semisolid Dosage Forms—Scale-Up and Post-approval Changes: Chemistry, Manufacturing, and Controls; In Vitro Release Testing and In Vivo Bioequivalence Documentation (1). The guidance relies on in vitro release testing to assure product sameness between prechange (approved, reference) product and post-change (SUPAC-related changes, test) product. Release rates are considered similar when the ratio of the median release rate for the post-change (test) product over the median release rate for the pre-change (reference) product is within the 90% confidence interval limits of 75 % to 133.33%. The release rate is regarded as a "final quality control" test that can signal possible inequivalence in performance, thus comprising in the aggregate a number of physicochemical tests that might be performed individually.

B. Waivers for Lower Strength

For solid oral dosage forms, biowaivers for generic products are generally granted in situations where the formulations of lower strength(s) product(s) are proportionately similar and the dissolution profile is also similar [21 CFR 320.22 (d) (2)]. Using these same principles, bioequivalence waivers for lower strength(s) of topical dermatological drug products might also be granted based on in vitro release rate measurements. For a request of biowaiver for lower strength, the product must meet the following criteria:

- Formulations of the two strengths should differ only in the concentration of the active ingredient and equivalent amount of the diluent.
- No differences should exist in manufacturing process and equipment between the two strengths.
- For a generic application, that is, an abbreviated new drug application (ANDA), the reference listed drug (RLD) should be marketed at both higher and lower strengths.

- For an ANDA, the higher strength of the test product should be bioequivalent (BE) to the higher strength of RLD.

In vitro drug release rate studies should be measured under the same test conditions for all strengths of both the test and RLD products. The in vitro release rate should be compared between (a) the RLD at both the higher (RHS) and lower strengths (RLS) and (b) the test (generic) products at both higher (THS) and lower strengths (TLS). Using the in vitro release rate, the following ratios and comparisons should be made:

$$\frac{\text{Release rate of RHS}}{\text{Release rate of RLS}} \sim \frac{\text{Release rate of THS}}{\text{Release rate of TLS}}$$

The ratio of the release rates of the two strengths of the test products should be about the same as the ratio of the release rate of reference products.

C. Biowaivers for Simple Gel Preparations

Drug products containing highly soluble and highly permeable active ingredients exhibiting rapid dissolution characteristics are now subject to biowaivers. These formulations are considered to behave like solutions and are granted biowaivers under certain conditions (16). Similarly, it is anticipated that topical dermatological preparations such as gels can also be subject to biowaivers as long as they meet certain in vitro release criteria.

VI. CONCLUSION

In vitro release rate methodology for topically applied locally acting drug products can reflect the combined effect of several physical and chemical parameters, including solubility and particle size of the active ingredient and rheological properties of the dosage form. In most cases, in vitro release rate is a useful test to assess product sameness between pre-change and post-change semisolid products such as creams, gels, lotions, and ointments. The release test appears to be formulation specific and is a property of the formulation and its method of manufacture.

REFERENCES

1. Guidance for Industry: SUPAC-SS Nonsterile Semisolid Dosage Forms. Scale-Up and Post-approval Changes: Chemistry, Manufacturing, and Controls; In Vitro Release Testing and In Vivo Bioequivalence Documentation. US Department of Health and Human Services, Food and Drug Administration, Center for Drug Evaluation and Research, May 1997.
2. Guy RH, Guy AH, Maibach HI, Shah VP. The bioavailability of dermatological and other topically administered drugs. Pharm Res 1986; 3:253–262.
3. Shah VP, Elkins J, Lam SY, Skelly JP. Determination of in vitro drug release from hydrocortisone creams. Int J Pharm 1989; 53:53–59.
4. Guy R, Hadgraft J. On the determination of drug release rates from topical dosage forms. Int J Pharm 1990; 60:R1–R3.
5. Higuchi WI. Analysis of data on the medicament release from ointments. J Pharm Sci 1962; 51:802–804.

6. Van Buskirk GA, Shah VP, Adair D, Arbit HM, Dighe SV, Fawzi M, Feldman T, Flynn GL, Gonzalez MA, Gray VA, Guy RH, Herd AK, Hem SL, Hoiberg C, Jerussi R, Kaplan AS, Lesko LJ, Malinowski HJ, Meltzer NM, Nedich RL, Pearce DM, Peck G, Rudman A, Savello D, Schwartz JB, Schwartz P, Skelly JP, Vanderlaan RK, Wang JCT, Weiner N, Winkel DR, Zatz JL. Workshop report: scale-up of liquid and semisolid disperse systems. Pharm Res 1994; 11:1216–1220.
7. Flynn GL, Shah VP, Tanjarla SN, Corbo M, DeMagistris D, Feldman TG, Franz TJ, Miran DR, Pearce DM, Sequeira JA, Sawrbrick J, Wang JCT, Yacobi A, Zatz JL. Workshop report: assessment of value and applications of in vitro testing of topical dermatological drug products. Pharm Res 1999; 16:1325–1330.
8. Shah VP, Elkins JS. In vitro release from corticosteroid ointments. J Pharm Sci 1995; 84:1139–1140.
9. Shah VP, Elkins JS, Williams RL. In vitro drug release measurement of topical glucocorticoid creams. Pharm Forum 1993; 19:5048–5059.
10. Corbo M, Schultz TW, Wong GK, Van Buskirk GA. Development and validation of in vitro release testing methods for semisolid formulations. Pharm Technol 1993; 17(9): 112–128.
11. Zatz JL. Drug release from semisolids: effect of membrane permeability on sensitivity to product parameters. Pharm Res 1995; 2:787–789.
12. Shah VP, Elkins JS, Williams RL. Evaluation of the test system used for in vitro release of drugs for topical dermatological drug product. Pharm Dev Technol 1999; 4(3): 377–385.
13. Pillai RK, Shah VP, Abriola L, Caetano P Flynn GL. Release of hydrocortisone from a cream matrix: dependency of release on suspension concentration and measurement of solubility and diffusivity. Pharm Dev Technol 2001; 6(3):373–384.
14. Shah VP, Elkins J, Shaw S, Hanson R. In vitro release: comparative evaluation of vertical diffusion cell system and automated procedure. Pharm Dev Technol 2003; 8(1):97–102.
15. Siewart M, Dressman J, Brown CK, Shah VP. FIP/AAPS Guidelines to dissolution/in vitro release testing of novel/special dosage forms. AAPS Pharm Sci Tech 2003; 4(1): 43–52.
16. Guidance for Industry: Waiver of In Vivo Bioavailability and Bioequivalence Studies for Immediate-Release Solid Oral Dosage Forms Based on a Biopharmaceutics Classification System. US Department of Health and Human Services, Food and Drug Administration, Center for Drug Evaluation and Research, Aug 2000.

35

Chemical Warfare Agent VX Penetration Through Military Uniform and Human Skin: Risk Assessment and Decontamination

Rebecca M. Wester
Methodist Health System, Dallas, Texas, U.S.A.

Howard I. Maibach and Ronald C. Wester
Department of Dermatology, School of Medicine, University of California, San Francisco, California, U.S.A.

I. INTRODUCTION

Most well-known warfare chemicals have similar molecular structures as the organophosphorus compounds. One of these, parathion, has been shown to exhibit body regional variation in human skin absorption (1). The exposed head and neck region ($\times 4$), trunk ($\times 3$), and genital area ($\times 12$) absorb more chemical than arms and hands, and legs and feet. In agricultural use, parathion has caused human death. Permeability constants (K_p) (potential chemical absorbed through human skin per unit area and time) indexed to regional variation gives the mass of chemical absorbed through a region of the human body and the total body absorption when summed over all regions. The further overlap of toxicity data to absorption can be used to estimate potential lethality.

Percutaneous absorption and regional variation form the final barrier between the "outside" and the "inside" of the body where toxicity occurs. Percutaneous absorption is influenced by moisture and certainly a soldier or civilian will sweat, and it does rain. Clothing also affects percutaneous absorption because material can act as both a barrier and a skin delivery system (2). Sweating, clothing, and skin absorption are thus interrelated.

Our objective of this study was to determine the percutaneous absorption of parathion when applied to naked human skin and uniformed skin with and without sweat, and predict potential human absorption and lethality of the structurally related chemical warfare agent (CWA) VX. A discussion as to skin decontamination of chemical warfare agents follows the absorption study.

II. METHODOLOGY

A soldier wearing standard field uniform will have both naked skin (head, neck, arms, and hands) and uniform covered skin exposed during a chemical warfare incident. And, in military encounters, the soldier has no choice but to wear that same uniform for an extended period.

The study design was to dose, in a single exposure, naked skin and uniform protected skin to the chemical warfare agent stimulant parathion and continue the exposure and absorption period over 96 hours. Uniforms can become wet from sweating and rain, so both wet and dry uniform material were included.

[^{14}C]parathion (specific activity 9.2 mCi/mmol) was obtained from Sigma (St. Louis, Missouri, U.S.A.) Uniform material was standard army issue coat, hot weather woodland camouflage, combat pattern, 50% nylon and 50% cotton (American Apparel Inc.).

The in vitro assembly consisted of flow-through design glass skin diffusion cells (LG-1084-LCP, Laboratory Glass Apparatus Inc., Berkeley, California, U.S.A.). Human cadaver skin was treated with dermatome to a thickness of 500 μm. Skin backs from two different donors (white male, age 71, and white male, age 60) were used. The skin specimens were mounted in the diffusion cells, with an available skin area of 1 cm^2. The excised skin used in this study is of similar thickness (dermatoned) and obtained from the donors within 24 hours postmortem. A visual barrier integrity check was performed prior to the study.

Uniform material was placed over the skin before the skin samples were clamped into the diffusion cell. The receiver side of the diffusion cell consisted of continuous flow Eagles MEM-BSS with gentamicin at a 3 mL/hr flow rate (3). A single dose of [^{14}C]parathion (4 μg containing 1 μCi) was applied to each naked skin or uniform covered skin cell. Those uniformed cells, which were wetted received a 20 μL water dose each of the four-day experiment. The receiver cells were placed over magnetic stirrers, and all the absorption experiments were carried out at 37°C, using a recirculating constant temperature water bath. At designated intervals, samples were automatically collected into scintillation vials (4).

A. Surrogate Model

Parathion was the chemical of choice to use as a surrogate for VX. Actual data with VX would be the best; however, little exists in the literature. To obtain radiolabeled VX and study it in the public domain is highly improbable. Parathion is in the same chemical class as VX (organophosphorus), and has the same functional groups as VX. Table 1 gives the structures of parathion and VX, and physicochemical data, which relate to percutaneous absorption. The partition coefficients (log P octanol/water), molecular weights, and molecular volumes are close. Similar structure, log P, and molecular weight/molar volume suggest the potential for similar percutaneous absorption.

Table 1 Structure and Physicochemical Comparisons of Parathion and VX

	Parathion	VX
Parathion coefficient (log P octanol/water)	3.83	2.22
Molecular weight	291.26	267.37
Molar volume	219.5 ± 3.0	262.5 ± 3.0

Table 2 Barrier Properties of Dry and Moist Military Uniform to Parathion In Vitro Human Skin Absorption

Treatments	Percent dose absorbed (Mean ± SD)	Permeability coefficient (K_p, cm/hr)
Skin ($n = 4$)[a]	1.78 ± 0.41	1.89×10^{-4}
Skin + dry uniform ($n = 6$)[b]	0.29 ± 0.17	2.04×10^{-5}
Skin + wetted uniform ($n = 5$)[c]	0.65 ± 0.16	6.16×10^{-5}

[a]Versus[b] $p = 0.000$.
[b]Versus[c] $p = 0.007$.
[a]Versus[c] $p = 0.000$.

B. Data Calculations

Parathion percutaneous absorption and permeability coefficients for naked skin and uniform (dry and wet) were obtained by experimentation. The permeability coefficient for VX (1.6×10^{-3} cm/hr) was calculated from Potts and Guy (5). Relative differences in permeability due to wet and dry uniform were then applied to the volumetric solution (VS) permeability coefficient. These in turn were applied to regional difference in human skin absorption (6) and predicted VX systemic concentration by skin absorption for each body region and total body exposure were calculated. Toxic 50% lethality of VX was obtained from Refs. 7 and 8.

III. RESULTS

Table 2 gives the in vitro percutaneous absorption of parathion through naked human skin and skin protected by dry uniform material and wetted uniform material. Following this single exposure and 96-hour absorption period, $1.78 \pm 0.41\%$ dose was absorbed through naked human skin, and $0.29 \pm 0.17\%$ and $0.65 \pm 0.16\%$ doses through skin protected by dry and moist uniform, respectively. The absorption was continuous though the total exposure period. Therefore, an infinite dose was available through the 96-hour dosing period. Statistically, naked skin absorption was greater than that protected by dry uniform ($p = 0.000$) and moist uniform ($p = 0.000$). Absorption through moist uniform was statistically ($p = 0.007$) greater than through dry uniform (statistics done only on percent absorbed dose—the raw data).

Table 3 gives calculated VX systemic absorption and toxicity to uniformed personnel. This is a one-time $4\,\mu g/cm^2$ VX exposure and resulting systemic dose occurs by skin absorption only (no respiratory and oral involvement). At one hour post-exposure 50% lethality occurs with full body exposure to the compromised sweated uniform, although the dry uniform is right at the threshold. At eight hours post-exposure to head and neck only, or trunk only, might cause lethality with both wet and dry uniform. At 96-hours post-exposure lethality occurs with exposure to any body part (4).

IV. DISCUSSION

A. Percutaneous Absorption

Chemical warfare agents are easily and inexpensively produced, and are a significant threat to military forces and to the public. The VX as well as other CWAs sarin and

Table 3 The VX Systemic Absorption and Toxicity to Uniformed Military Personnel

Exposure time	Body exposure	Calculated VX systemic dose[a]	
		Compromised[b] (mg)	Protected[c] (mg)
1 hr	Head/neck[d]	4.16	4.16
	Arms and hands[d]	0.52	0.52
	Trunk	4.07	1.35
	Genital-s	0.45	0.15
	Legs	0.68	0.22
	Total	**9.87***	**6.40**
8 hr	Head/neck[d]	33.26*	33.26*
	Arms and hands[d]	4.16	4.16
	Trunk	32.52*	10.77*
	Genital-s	3.61	1.2
	Legs	5.42	1.8
	Total	**78.98***	**51.18***
96 hr	Head/neck[d]	399.16*	399.16*
	Arms and hands[d]	49.90*	49.90*
	Trunk	390.29*	129.25*
	Genital-s	43.37*	14.36*
	Legs	65.05*	21.54*
	Total	**947.76***	**614.21***

*Estimated systemic LD50 of VX is 6.5 mg (human, 70 kg). Systemic concentration is more than 50% lethality dose.
[a]4 $\mu g/cm^2$ on whole body area (1.8 m^2).
[b]Uniform with perspiration.
[c]Dry uniform.
[d]Head/neck and arms and hands are unprotected.

soman belong to the chemical class of organophosphorus compounds along with well-known pesticides parathion, malathion, fenitrothion, chlorpyrifos, and diazinon. Parathion was used as a CWA simulant and by experimentation gave relative bioavailabilty permeability coefficients between naked skin and skin wearing sweated or dry uniform. Risk assessment for VX was then determined using the bioavailability relative to uniformed and naked skin, and the regional variation of human percutaneous absorption. Since risk is for clothed humans, these factors need to be included in the assessment. These absorption factors combined with an assessment of VX toxicity show how deadly VX can be from just skin exposure.

Risk assessment for chemicals requires a bioavailability component to determine how much of an exposure gets into the body. In vivo bioavailability is usually available for animals, and sometimes for man. In vitro data have been substituted for in vivo data. This normal course of events changes when dealing with VX and other chemical warfare agents. The deadly nature of the compounds precludes them from normal scientific inquiry, and any data, which may be available with a government, remain under the control of the government. However, risk potential for the military and the public is real and risk assessment needs to be done with the information at hand.

The Potts–Guy equation provides estimates for the permeation of pure molecules. The condition is for infinite application, generally but not necessarily aqueous.

Parathion (neat) was applied to the skin in an amount that would be infinite for 96 hours. The proof of an infinite dose is the ever-increasing cumulative amount of permeation (Fig. 1), which would have reached a plateau if the dose was finite. Also, only 1.78%, 0.29%, and 0.65% of applied doses were absorbed for the three treatments (Table 2). The dosing vehicle was toluene, which will evaporate immediately upon contact (9). Some water would be available from the circulating receptor fluid (diffusion) and, of course, moisture was added as one of the experimental treatments. The K_p for parathion in this study was 1.89×10^{-4} cm/hr for dermatoned skin. The calculated K_p in epidermis (the Potts–Guy equation) for parathion is 1.59×10^{-2} cm/hr. The calculated K_p for VX is 1.6×10^{-3} cm/hr (epidermis), which falls right between the two K_p (research-dermatoned skin and calculated-epidermis) for parathion.

Craig et al. (10) reported the percutaneous absorption of VX in subjects (U.S. Army enlisted men) using a cholinesterase inhibition assay. Subjects dosed on the forearm at 18°C room temperature for six hours had a penetration of $0.60 \pm 0.19\%$. Applying the Potts–Guy equation used in this study for a 4 μg dose over six hours gives a penetration of 0.96%, very similar to the empirical data of Craig et al. (10). They showed regional variation (cheek higher than forearm) justifying our use of regional variation for risk assessment. They also showed higher VX penetration with higher room temperature (46°C), suggesting sweat/moisture involvement as with this current study.

Chemicals in cloth cause cutaneous effects. Hatch and Maibach (11) reported that chemicals added to cloth in 10 finish categories (dye, wrinkle resistance, water repellency, soil release, and so on) caused irritant and allergic contact dermatitis, atopic dermatitis exacerbation, and urticarial and phototoxic skin responses. This is qualitative information that chemicals will transfer from cloth to skin in vivo in humans. Quantitative data are lacking. Snodgrass (12) studied permethrin transfer from treated cloth to rabbit skin in vivo. Transfer was quantitative but less than expected. Interestingly, permethrin remained within the cloth after detergent laun-

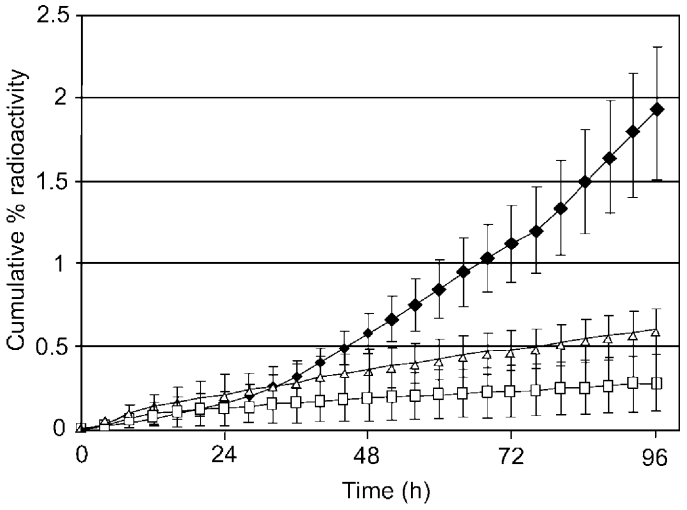


Figure 1 Percutaneous absorption of parathion across excised human skin (◆) without clothing; (■) with clothing; (▲) with clothing and sweat simulation. Values are means ± SD for each 4-hour time point.

Table 4 Effect of Washing (Soap and Water) In Vivo Human

	Percent penetration								
	Min				Hr				
$\mu g/cm^2$	1	5	15	30	1	2	4	8	24
Parathion, 4 arm	2.8		6.7		8.4		8.0	15.8	8.6
Parathion, 40			3.1				6.9		9.5
Parathion, 400 arm			2.2		2.3		4.2		4.8
Parathion, 4 forehead	8.4		7.1	12.2	10.5	20.1	27.7		36.3
Parathion, 4 palm		6.2	13.6	13.3	11.7	9.4	7.7		11.8

dering. Wester et al. (2) showed in vitro percutaneous absorption of glyphosate and malathion through human skin decreased when added to cloth (the cloth then placed on skin). When water was added to glyphosate/cloth and water/ethanol to malathion/cloth, the percutaneous absorption increased (malathion to levels from solution). This perhaps reflects clinical situations where dermatitis occurs most frequently in human sweating areas (axilla and crotch).

One insecticide used widely in the Persian Gulf is the alipathic chlorinated hydrocarbon permethrin. The military has done extensive studies on the use of permethrin-treated uniforms as a protective agent against insect-borne diseases. In the Gulf, military personnel were supplied cans of 0.5% permethrin and told to spray their own uniforms because the military did not have pretreated uniforms in stock. The dose recommended, $125\,\mu g/cm^2$, far exceeded the permethrin dose used in agriculture (i.e., 0.1–0.2 kg/ha or $2\,\mu g/cm^2$). The result was that personnel who wore treated uniforms were subjected to dermal exposure via a massive dose of the insecticide for their entire period of service in Gulf. This has been suggested as

Table 5 Decontamination of [^{14}C]-MDI as Percent Dose in Skin Washes Following Topical Administration in Rhesus Monkey

	Percent dose recovered [mean (±SD)]			
Washing methods	5 min	1 hr	4 hr	8 hr
Water	60.0	56.7	40.2	29.2
	(11.1)	(10.1)	(8.9)	(9.7)
5% soap	71.2	51.1	46.1	36.6
	(5.2)	(14.1)	(8.2)	(12.8)
50% soap	67.3	68.6	54.4	45.7
	(9.6)	(16.0)	(5.2)	(6.6)
Polypropylene glycol	88.9	86.0	78.9	71.6
	(13.5)	(14.1)	(16.4)	(19.7)
PG-C	85.3	67.7	73.7	77.9
	(9.5)	(24.6)	(3.0)	(20.6)
Corn oil	95.1	77.2	73.2	86.2
	(9.0)	(24.2)	(17.4)	(10.0)

Abbreviations: MDI, methylene bisphenyl isocyanate.

a contributing cause to the Gulf War Syndrome (13). This paper and that of Snodgrass (12) and Wester et al. (2) show that chemicals, including permethrin, can be absorbed into and through skin from cloth.

Time following exposure is most critical. Exposed clothing needs to be removed and skin decontaminated. It is imperative that the decontamination procedure not in itself enhance skin absorption (14). This applies to public as well as military situations. Society has a system of first responders for emergency incidents. Civilian chemical warfare agent exposure has proved to be such an incident. First responders include police, firefighters, paramedics and other medical personnel, and good Samaritans. All but the firefighters will be wearing uniforms or civilian clothing similar in composition and design to that used in this bioavailability study. First responders have suffered the same fate as initial intended civilian targets, so their knowledge of this potential skin and clothing involvement is of importance.

These data refer directly to a model penetrant in an in vitro study, and predicts in vivo toxicity for one of the chemical warfare agents. Although we do not wish to over generalize, the practical importance of this toxicological arena mandates broader study, such as model in vivo studies and examination of other fabrics and other chemical warfare agents model compounds, as well as the agents themselves.

B. Skin Decontamination

Recent events have brought forth concerns for weapons of mass destruction of which CWA are included. The military has its protective and decontamination equipment, but little of this is privy to citizens. In the event of CWA civilian exposure, guidelines include:

1. concern and essence of time following exposure,
2. remove contaminated clothing from victim,
3. hose (water) exposed skin,
4. transport to hospital facilities.

From the percutaneous absorption and risk assessment presented here, numbers 1 and 2 are well justified. The essence of time is especially important. Number 3 presents a problem. Table 4 (15) shows in vivo human percutaneous absorption of parathion after soap and water wash. In a matter of minutes, certainly in the first hour, a large dose of parathion is absorbed. Time of effective response is very limited.

Table 5 (16) shows in vivo skin decontamination of methylene bisphenyl isocyamate (MDI). Water (alone) is fairly ineffective. This suggests that hosing victims of CWA attack is limited in effectiveness. Soap and water washing improved decontamination some, but as in Table 4 is not as effective as the public may believe. Two glycol-based cleaners were more effective than soap and water, as was off-the-shelf corn oil.

REFERENCES

1. Maibach HI, Feldmann RJ, Milby TH, Sert WR. Regional variation in percutaneous penetration in man. Arch Environ Health 1971; 23:208–211.
2. Wester RC, Quan D, Maibach HI. In vitro percutaneous absorption of model compounds glyphosate and malathion from cotton fabric into and through human skin. Food Chem Toxicol 1996; 34:731–735.

3. Wester RC, Christoffel J, Hartway T, Poblete N, Maibach HI, Forsell J. Human cadaver skin viability for in vitro percutaneous absorption: storage and detrimental effects of heat-separation and freezing. Pharma Res 1998; 15:82.
4. Wester RM, Tanojo H, Maibach HI, Wester RC. Predicted chemical warfare agent VX toxicity to uniformed soldier using parathion in vitro human skin exposure and absorption. Toxicol Appl Pharmacol 2000; 168:149–152.
5. Potts RO, Guy RH. Predicting skin permeability. Pharm Res 1992; 9:663–669.
6. Guy RH, Maibach HI. Calculations of body exposure from percutaneous absorption data. In: Bronaugh R, Maibach HI, eds. Percutaneous Absorption. New York: Marcel Dekker, 1985:461–466.
7. Somani SM, Solana RP, Dube SN. Toxicology of nerve agents. In: Somani SM, ed. Chemical Warfare Agents. San Diego: Academic Press, 1992:76.
8. Sidell FR. Nerve agents. In: Sidell FR, Takafuji ET, Franz DR, eds. Medical Aspects of Chemical and Biological Warfare. Textbook of Military Medicine, Part I: Warfare, Weaponry, and the Casualty. Washington DC: Borden Institute, 1995:141.
9. Wester RC, Maibach HI. Benzene percutaneous absorption: dermal exposure relative to other benzene sources. Int J Occup Environ Health 2000; 6:122–126.
10. Craig FN, Cummings E, Sim VM. Experimental temperature and the percutaneous absorption of a cholinesterase inhibitor, VX. J Invest Dermatol 1977; 68:357–361.
11. Hatch KL, Maibach HI. Textile chemical finish dermatitis. Contact Dermatitis 1996; 14:1–13.
12. Snodgrass HL. Permethrin transfer from treated cloth to the skin surface: potential for exposure in humans. J Toxicol Environ Health 1992; 35:912–915.
13. Plapp FW. Permethrin and the gulf war syndrome. Arch Environ Health 1999; 54:312.
14. Wester RC, Maibach HI. Advances in percutaneous absorption. In: Drill V, Lazar P, eds. Cutaneous Toxicity. New York: Raven Press, 1984:29–40.
15. Maibach HI, Feldmann R. Systemic absorption of pesticides through the skin of man. n: Occupational Exposure to Pesticides. Federal Working Group on Pest Management. Washington, DC. Appendix B, 1974:120–127.
16. Wester RC, Hui H, Andry LT, Maibach HI. In vivo skin decontamination of MDI: soap and water ineffective compared to propylene glycol, polyglycol-based cleanser, and corn oil. Toxicol Sci 1999; 48:1–4.

36

Transepidermal Water Loss Measurements for Assessing Skin Barrier Functions During In Vitro Percutaneous Absorption Studies

Avinash Nangia
ALZA Corporation, Palo Alto, California, U.S.A.

Bret Berner
Cygnus, Redwood City, California, U.S.A.

Howard I. Maibach
Department of Dermatology, School of Medicine, University of California, San Francisco, California, U.S.A.

I. INTRODUCTION

In the course of performing in vitro percutaneous absorption studies, it is important to ensure the integrity of the stratum corneum. In vitro assessment of the permeability of chemicals is often preceded by studying the rate of penetration of tritiated water (1,2). However, this technique has several limitations. For example, it results in hydrated stratum corneum, possibly affecting the penetration of the compound under investigation. This method cannot be used if the test compound is tritium labeled. In addition, it is time-consuming and requires a license and facilities to handle radioactive materials. In practice, the repetitive measurement of tritiated water in laboratories is accomplished by determining the fraction of the dose applied absorbed at a fixed time. Selection of that fixed time is difficult without a priori knowledge of the permeability, and improper selection can lead to an erroneous assessment of the barrier properties of skin. Recently an alternate technique, which measures the electrical resistance across the skin slices, has also been proposed for this purpose (3). Based on the initial results, this technique appears to have some advantages, but more studies are required to validate it.

Transepidermal water loss (TEWL) measurements with an evaporimeter, under controlled environmental conditions, are predictive of altered barrier functions (4). Measurement of TEWL with an evaporimeter has been used to evaluate the competency of the skin barrier in vivo (5,6). Investigators have also addressed the possibility of using this technique in vitro (7,8). In a study by Moloney, an evaporimeter was

used to investigate the structural requirements of lipids, which are capable of altering the barrier functions and thus promoting skin permeability. Subtle changes in the skin barrier were observed with this device, suggesting TEWL usefulness in detecting damaged skin. The TEWL is also a relevant and sensitive indicator in vivo and in vitro for prediction of percutaneous absorption of various chemicals (9,10).

Measurement of TEWL by an evaporimeter is a continuous measurement of water permeation through skin under gradient conditions. In contrast, tritiated water permeation is a cumulative measurement over time. With increasing time, finite-dose tritiated water permeation methods reflect the dose absorbed and not the permeability of the tissue. Assuming a negligible time lag for water permeation (10–15 minutes), from mass balance we find that:

$$\frac{dC}{dt} = -APC/V$$

where C is the concentration of tritiated water in the donor solution, t the time, A the surface area, V the volume of tritiated water applied and is assumed to be constant, and P is the permeability of skin. By integrating, the fraction absorbed may be obtained as:

$$\text{fraction absorbed} = 1 - \exp\left[-(A/V)\int_o^t dt\ P\right]$$

for constant P at short times ($APt/V \ll 1$)

$$\text{fraction absorbed} = APt/V$$

and the tritiated water permeation reflects the permeability of skin. However, in general, even for constant P:

$$\text{fraction absorbed} = 1 - \exp(-APt/V)$$

At long times, particularly, the fraction absorbed of tritiated water equals unity because it does not depend on the permeability. In contrast, TEWL is a measure of the skin permeability at all times.

II. METHODS

In our laboratory, we have examined the relationship between TEWL and skin barrier functions that have been damaged to varying extents by different techniques. After altering the skin barrier, tritiated water flux measurements were also obtained and correlated with the TEWL measurements. The TEWL results were then further analyzed to study the relationship between water loss and in vivo primary skin irritation caused by various chemicals.

In vitro skin permeation studies were performed using the flow-through diffusion cell through the heat-separated human epidermis. Using physiological saline (containing 0.01% w/v gentamicin sulfate) and a 1.0-cm^2 permeation area (maintained at 32°C), the donor side of the epidermis was subjected to various physical and chemical pretreatments to create various damaged skin models. In the first category, epidermis was delipidized with a chloroform:methanol (C:M) mixture (2:1% v/v) for different time intervals under occlusion. In the second category, different concentrations of sodium lauryl sulfate (SLS) were exposed for various time intervals. In the third category, five basic compounds (norephedrine, antipyrine,

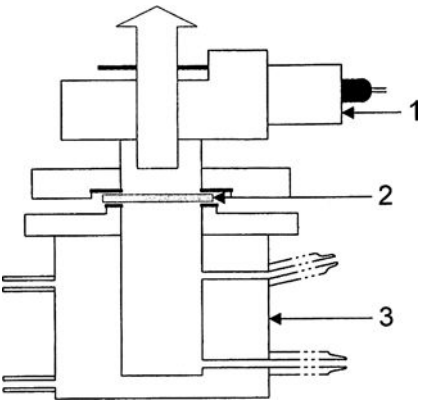


Figure 1 Schematic diagram of the diffusion cell coupled to an evaporimeter: (**1**) evaporimeter probe; (**2**) skin slice; (**3**) diffusion cell.

imipramine, naphazoline, and mecamylamine) of different basicity (pK_a) were applied for in different concentration for 24 hours. In the last category, mechanical insults to the skin slices were induced by either abrading it with sandpaper or a sharp needle or by stripping with adhesive tape. The extent of barrier function perturbation was assessed by observing for changes in TEWL values from the baseline as well as by quantitating the tritiated water flux. The TEWL measurements were made by placing a collard probe on top of the upper half of the permeation cell (Fig. 1) and leaving it there until a constant value was established. An unstirred column of 2.5 cm above the skin provided little resistance to water permeation. Only skin samples with a baseline TEWL reading between 1.0 and 6.0 $g/m^2/hr$ were used. Details of these procedures have been previously reported by Nangia et al. (11,12).

An in vivo skin irritation study was also conducted to correlate with the in vitro data and to establish that the in vitro technique has clinical application. To 12 healthy female volunteers were applied plastic chambers containing aqueous or ethanolic solutions of five basic permeants in a random order, in longitudinal rows on both the left and right interscapular areas of the back. Chambers containing water and ethanol served as vehicle controls. After 24 hours, the patches were removed and the test sites were marked. Thirty minutes later, the sites were graded for erythema and edema, using a zero to five visual irritation scoring system (11). The TEWL values were measured using the evaporimeter.

III. RESULTS AND DISCUSSION

Exposure to the C:M mixture resulted in a rapid and irreversible damage to the barrier properties. The extent of damage increased with the contact time (Fig. 2). An exposure of three minutes had a pronounced effect and resulted in a TEWL of 22.1 ± 8.0 $g/m^2/hr$, which was approximately five times higher than the baseline values. Damage to the water barrier of the excised skin was most effective when the skins were exposed for 10 minutes with a TEWL value of 29.9 ± 8.0 g/m^2 hr. This value was similar to that of an uncovered cell filled with water (27.5 ± 5.7 $g/m^2/hr$), suggesting that 10 minutes of exposure to C:M mixture is adequate to completely destroy the water barrier of the skin. Treatment for 60 minutes did not exhibit further damage. The C:M treatment also resulted in an increased fraction of tritiated

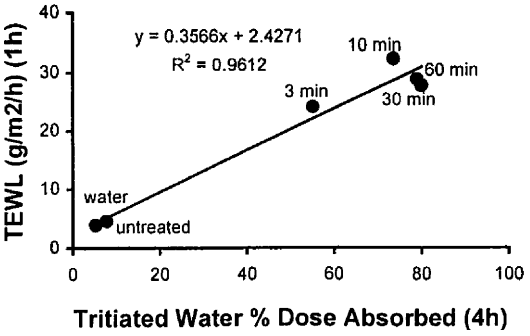


Figure 2 Linear correlation between transepidermal water loss (TEWL) (measured after one hour) and the fraction of the dose of tritiated water absorbed (in four hours) after chloroform–methanol treatment is applied to excised human skin.

water absorbed in four hours; these results were consistent with the trend for TEWL. The correlation between the effects of C:M treatment on TEWL and the fraction of tritiated water absorbed was found to be excellent ($r^2 = 0.96$). In a similar type of study in our laboratory, Abrams et al. (13) evaluated the effect of topical exposure to various organic solvents for various time intervals on the barrier functions of excised human skin. After exposure to various solvents, the contents of the donor compartment of the cell were analyzed for various lipids. By measuring the TEWL with an evaporimeter, various solvents were ranked for their ability to alter skin barrier integrity. The C:M exposure for 12 minutes was found to extract the maximum quantity of stratum corneum lipids and also induced greatest TEWL change, further confirming our results, and demonstrated that an evaporimeter is a useful tool to evaluate skin barrier functions.

The concentration-dependent increases in TEWL and tritiated water absorbed by SLS treatment are shown in Figure 3. A good correlation between the two was observed ($r^2 = 0.98$). Treatment with SLS resulted in a significant increase in TEWL at all concentrations. A concentration below the critical micelle concentration (CMC) (i.e., 0.125% w/v) caused the least damage to the skin. However, the extent of damage observed with concentrations higher than the CMC was more severe. A linear dependence of TEWL on surfactant concentration between 0.125% and 2% w/v

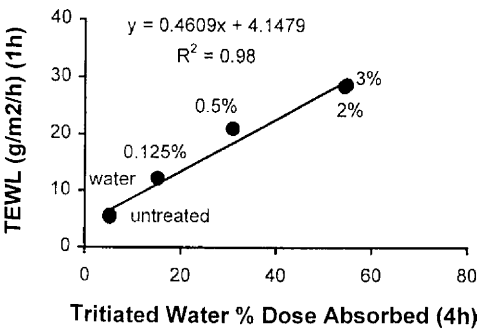


Figure 3 Linear correlation between transepidermal water loss (TEWL) (measured after one hour) and the fraction of the dose of tritiated water absorbed (in four hours) at various concentrations of sodium lauryl sulfate (SLS) (after four hours) applied to excised human skin.

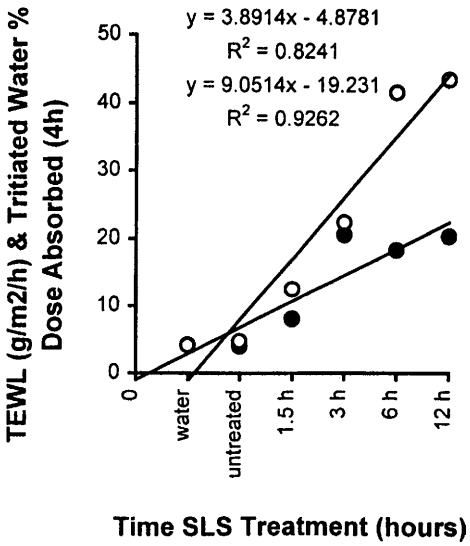


Figure 4 Linear correlation between transepidermal water loss (TEWL) (measured after one hour) and the fraction of the dose of tritiated water absorbed (in four hours) after different durations of sodium lauryl sulfate (SLS) treatment are applied to excised human skin. •, TEWL; ○, tritiated water absorbed.

was observed. No further increase in TEWL was evident at 3% w/v, suggesting that 2% w/v SLS solution caused maximum possible damage to the skin.

At a fixed concentration (2% w/v) of SLS, the time dependence of the effect of SLS on the barrier function was characterized. The extent of damage, as reflected by either TEWL or the fraction of tritiated water absorbed, increased linearly with contact time (Fig. 4) ($r^2 = 0.82$ and 0.93 for TEWL and tritiated water measurements, respectively).

Of the three acute physical injuries created, abrasion with sandpaper inflicted the greatest damage, while a needle had little effect on the increase in TEWL and

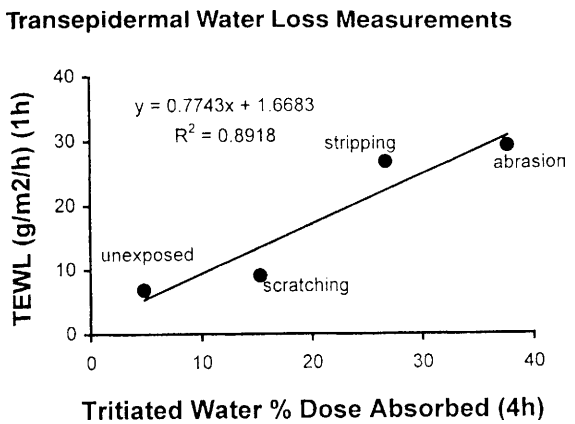


Figure 5 Linear correlation between transepidermal water loss (TEWL) (measured after one hour) and the fraction of the dose of tritiated water absorbed (in four hours) after various physical injuries are applied to excised human skin.

Table 1 Irritation Induced by Basic Compounds with Increasing pK_a Values

Compound[a]	pK_a	TEWL values[b] ($g/m^2/hr$)	Dose $^3H_20$ absorbed (% absorbed in 20 hr)	Erythema score[c]
Antipyrine	1.4	4.8 ± 0.8	30.0	0.00 ± 0.00
Norephedrine	9.0	5.2 ± 1.6	45.2	1.03 ± 0.43
Imipramine	9.5	9.8 ± 0.6	55.0	2.30 ± 1.70
Naphazoline	10.9	13.8 ± 4.1	90.5	2.50 ± 1.70
Mecamylamine	11.2	28.4 ± 6.2	88.7	2.83 ± 1.14
Water	—	4.6 ± 1.3	28.2	0.08 ± 0.19
Ethanol	—	7.7 ± 1.2	43.6	0.50 ± 0.61

[a]Antipyrine and norephedrine solutions were in distilled water, while the remaining bases were in ethanol.
[b]Transepidermal water loss (TEWL) values were measured in vitro after one hour, using the evaporimeter.
[c]Scored using a zero to five visual irritation scoring system: (0) no erythema; (1) very slight erythema—barely perceptible; (2) well-defined uniform erythema; (3) moderate to severe erythema; (4) severe erythema to slight eschar formation; (5) severe erythema with edema.

tritiated water permeation (Fig. 5). For these acute injuries, TEWL correlated well with results for water permeation ($r^2 = 0.89$; Fig. 5).

Table 1 shows the TEWL values after exposure to five basic permeants. Application of the antipyrine solution (p$K_a = 1.4$, nonirritant control) for 24 hours did not cause any damage to the skin, and the TEWL was similar to that for control water-treated skin. All the remaining four basic compounds, norephedrine (p$K_a = 9$), imipramine (p$K_a = 9.5$), naphazoline (p$K_a = 10.9$), and mecamylamine (p$K_a = 11.2$), resulted in an increase in TEWL and the fraction of tritiated water absorbed, with the maximum effect seen with mecamylamine, followed by naphazoline, imipramine, norephedrine, and antipyrine. The rank for the bases was in accordance with their pK_a values; that is, TEWL increases with higher pK_a values. Mecamylamine, with the highest pK_a of 11.2, perturbed the skin barriers completely. The maximum percentage of tritiated water absorbed through cadaver skin also ranked the permeants in a manner similar to that of TEWL, and the correlation between TEWL and water permeation was found to be reasonably good ($r^2 = 0.71$).

Deviations occurred for large fractions of water absorbed, because in that regime this measurement no longer reflects water permeation. Comparison of the results between in vitro TEWL values and the visual irritation score further validates this technique for in vitro toxicological studies.

From these studies, it is quite clear that TEWL measurement with an evaporimeter, under controlled environmental conditions, is a simple and rapid method of screening the integrity of the barrier functions of skin in vitro and can thus be routinely used as an alternative to tritiated water permeation.

REFERENCES

1. Bronaugh RL, Stewart RF. Methods for in vitro percutaneous absorption studies. VI. Use of excised human skin. J Pharm Sci 1986; 75:1094–1097.
2. Scott RC, Dugard PH, Doss AW. Permeability of abnormal rat skin. J Invest Dermatol 1986; 86:201–207.

3. Lawrence JN. Electric resistance and tritiated water permeability as indicators of barrier integrity of in vitro human skin. Toxicol In Vitro 1997; 11:241–249.
4. Pinnagoda J, Tupker RA, Agner T, Serup J. Guidelines for transepidermal water loss (TEWL) measurement. Contact Dermatitis 1990; 22:164–178.
5. Leveque JL, Garson JC, de Rigal J. Transepidermal water loss from dry and normal skin. J Soc Cosmet Chem 1979; 30:333–343.
6. Roskos K, Guy RH. Assessment of skin barrier functions using transepidermal water loss: effect of age. Pharm Res 1989; 6:949–953.
7. Wilson DR, Maibach HI. A review of transepidermal water loss. In: Maibach HI, Boisits EK, eds. Neonatal Skin: Structure and Function. New York: Marcel Dekker, 1982:83–100.
8. Moloney SJ. Effect of exogenous lipids on in vitro transepidermal water loss and percutaneous absorption. Arch Dermatol Res 1988; 280:67–70.
9. Murahata RI, Crowe DM, Roheim JR. The use of transepidermal water loss to measure and predict the irritation response to surfactants. Int J Cosmet Sci 1986; 8:225–231.
10. Lotte C, Rougier A, Wilson DR, Maibach HI. In vivo relationship between transepidermal water loss and percutaneous penetration of some organic compounds in man: effect of anatomic site. Arch Dermatol Res 1987; 279:351–356.
11. Nangia A, Camel E, Berner B, Maibach HI. Influence of skin irritants on percutaneous absorption. Pharm Res 1993; 10:1756–1759.
12. Nangia A, Anderson PH, Berner B, Maibach HI. High dissociation constants (pK_a) of basic permeants are associated with in vivo skin irritation in man. Contact Dermatitis 1996; 34:237–242.
13. Abrams K, Harvell JD, Shriner D, Wertz P, Maibach H, Maibach HI, Rehfeld SJ. Effect of organic solvents on in vitro human skin water barrier function. J Invest Dermatol 1993; 101:609–613.

37

Assessment of Microneedles for Transdermal Drug Delivery

Mark R. Prausnitz
Schools of Chemical and Biomedical Engineering, Georgia Institute of Technology, Atlanta, Georgia, U.S.A.

I. INTRODUCTION

Drugs can be delivered into the body using a variety of different routes (1,2). The oral route is generally most popular, due largely to convenience for the patient. However, many drugs are degraded in the gastrointestinal tract or by first-pass effects of the liver or are simply not absorbed across the intestinal epithelium. The usual alternative is delivery across the skin, typically using a hypodermic needle. Although the needle is highly effective to deliver drugs, it is often inconvenient and painful for patients.

Transdermal drug delivery from a patch attempts to address limitations of both the oral route and the use of needles (3,4). Transdermal patches can avoid the drug degradation associated with oral delivery and the pain and inconvenience associated with injection. Delivery across skin also lends itself naturally to slow-release drug delivery over time. However, transdermal delivery has been severely limited by poor drug absorption across skin. Those few drugs that have optimal physicochemical properties and are effective at low doses are currently the only candidates for transdermal delivery. At a steady rate over the past 25 years, approximately a dozen such drugs have received Food and Drug Administration (FDA) approval, but the impact of transdermal delivery on medical practice has been limited.

This limited impact is due largely to the fact that the vast majority of drugs cannot cross the skin at therapeutic rates due to the skin's barrier properties regulated by the stratum corneum, skin's outer 10 to 15 μm (5). Stratum corneum provides such an effective barrier because it is made of a brick-and-mortar structure containing flattened keratinocytes filled with cross-linked keratin surrounded by an extracellular matrix of multi-lamellar lipid bilayers. Effective methods to safely overcome this barrier could make transdermal delivery a viable option for many more drugs and thereby reduce the need for hypodermic needles.

A. Creating Nanometer Pathways to Increase Skin Permeability

Until recently, most attempts to increase skin permeability have employed the use of chemical agents to alter the molecular structure of stratum corneum and thereby

create nanometer-scale pathways for drug transport (6,7). Chemical enhancers can act by disrupting the structured environment of the stratum corneum lipids, extracting skin lipids, increasing drug solubility in stratum corneum, or other mechanisms. Because chemical enhancers disrupt stratum corneum on the molecular scale, their enhancement of skin permeability to small drugs is generally modest. Chemical enhancement of macromolecule transport across skin has been even less successful, with some recent exceptions (8). Moreover, the effects of chemical enhancers are not localized to the stratum corneum and therefore can often cause irritation and toxicity deeper in the skin.

Physical methods to disrupt stratum corneum structure on the nanometer scale have also received attention and offer potential advantages over chemical approaches (9,10). Electric fields or ultrasound, for example, can rearrange molecular structures in a manner that is localized to the stratum corneum. Moreover, the pathways created are somewhat larger than those generated by chemical enhancers and therefore have had greater success delivering macromolecules across skin. A limitation of these physical methods is that they require an energy source, which increases the expense, size, and complexity of a drug delivery system compared to a conventional patch.

B. Creating Micron Pathways to Increase Skin Permeability

Recent studies suggest that chemical and physical approaches to create nanometer pathways of molecular dimensions have, in a sense, been too gentle. Pathways of micron, i.e., cellular dimensions, should be much more effective, because they are orders of magnitude larger than the nanometer dimensions of drugs, including macromolecules. From a safety perspective, micron pathways are still one or more orders of magnitude smaller than the holes made by hypodermic needles, which are well tolerated by the skin and have found essentially universal clinical acceptance.

Micron pathways can be generated in the skin by a variety of methods, including heat (11), dermabrasion (12), the combination of certain chemical enhancers and electric fields (13), and microneedles (14). Although proof-of-concept for each of these approaches has been established, more studies, especially through clinical trials, are needed to fully assess both safety and efficacy. These approaches of micron-scale disruption have had promising results and may represent the most effective compromise between pathways large enough to deliver macromolecules across skin, but small enough for good patient compliance and safety.

II. MICRONEEDLES FOR TRANSDERMAL DELIVERY

This review focuses on microneedles as a novel method to create micron pathways across skin for transdermal drug delivery. Microneedles are generally hundreds of microns long, 1 to 10-μm wide at the tip, and on the order of 100-μm wide at the base. They are typically used as multi-needle arrays and can be solid or hollow. An advantage of microneedles over other physical methods to increase skin permeability is that they require no power supply and should be simple to use to create micron-scale pathways for delivery.

A. Microneedle Delivery Scenarios

Microneedles can be applied for drug delivery in a variety of ways. The ''poke and patch'' approach involves inserting (and possibly immediately removing) an array of

solid microneedles into the skin to create a set of holes and placing a drug-loaded patch onto the skin over the holes. Similar to a conventional transdermal patch, drug is released from the patch and diffuses through the highly permeable skin over time.

As an alternative related to, for example, smallpox vaccine delivery using bifurcated needles (15), the "coat and poke" approach involves coating solid microneedles with drug, inserting the needles into the skin, and leaving them there until the drug rapidly or slowly dissolves away. A "dip and scrape" method can also be used, where an array of blunt-tipped microneedles is dipped into a drug solution and scraped across the skin to create and deposit drug in micro-troughs along the skin surface.

Finally, hollow microneedles can be inserted into skin and left in place. Using an "insert and infuse" approach, drugs can then be delivered through the needle bores from a patch-like reservoir or actively pumped through the needles for a rapid injection or slow delivery, similar to drug infusion pumps.

B. Microneedle Fabrication

Needles of micron dimensions can be fabricated by a variety of methods, but the approach that lends itself best to reliable and inexpensive mass production involves leveraging the tools of the microelectronics industry (16,17). This technology, often called microfabrication or micro-electromechanical systems (MEMS), uses lithography, plasma etching, and other techniques to produce structures typically of micron dimensions, although submicron structures are possible. Using microfabrication, microneedle arrays can probably be mass produced for less than a dollar, and for the simplest designs, less than 10 cents (data not shown).

A variety of fabrication techniques have been used to make microneedles with various geometries (18–28). Figure 1 shows some representative examples from our laboratory. Most emphasize a sharp tip to facilitate insertion into the skin and a shaft that at least partially tapers to a wider base to provide structural strength. The tips on hollow needles are often less sharp, due to the presence of the hollow bore. The first needles were made of silicon, but metal and polymer needles are gaining increasing attention.

C. Drug Delivery Using Solid Microneedles

Solid microneedles have been used primarily to pierce micron holes in the skin and thereby provide pathways for drug transport. Figure 2A shows a histological cross section of skin with needles from a section of a microneedle array embedded in the skin. This image shows that microneedles can be inserted into the skin of, in this case, a hairless rat in vivo (29). As a companion image, Figure 2B shows skin pierced with microneedles, after which a dye solution was placed onto the skin surface. Dye entered the skin wherever each needle inserted, demonstrating the creation of micron transport pathways in the skin (29).

The size of transdermal transport pathways made by microneedles is assessed in Figure 3A. Small molecules, macromolecules, and even nanoparticles can be delivered across the skin with permeabilities at least three orders of magnitude greater than intact skin in vitro (19,26). Mechanistically, it is, perhaps, not surprising that compounds of nanometer dimensions readily pass through micron holes created by microneedles. However, for applications, these increases in skin permeability are dramatic and significant.

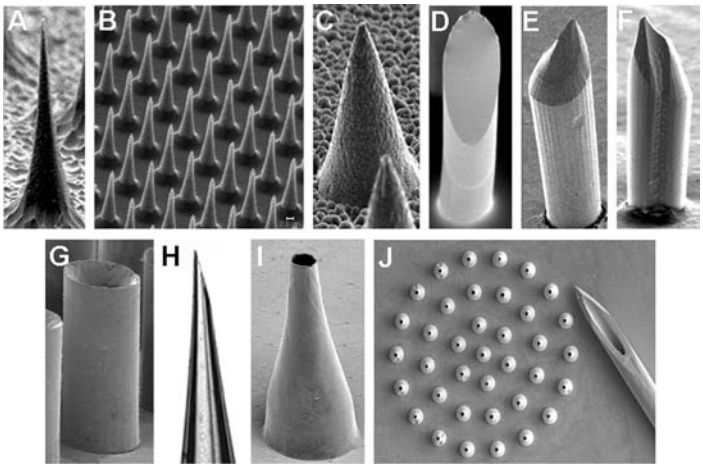


Figure 1 Solid and hollow microneedles fabricated out of silicon, polymer, metal, and glass imaged by optical and scanning electron microscopy. Solid microneedles: (**A**) silicon microneedle (150-μm tall), from a 400-needle array; (**B**) section of an array containing 160,000 silicon microneedles (25-μm tall); (**C**) metal microneedle (120-μm tall) from a 400-needle array. Biodegradable polymer microneedles with beveled tips from 100-needle arrays; (**D**) flat-bevel tip made of polylactic acid (400-μm tall); (**E**) curved-bevel tip made of polyglycolic acid (600-μm tall); (**F**) curved-bevel tip with a groove etched along the full length of the needle made of polyglycolic acid (400-μm tall). Hollow microneedles; (**G**) straight-walled, metal microneedle (200-μm tall) from a 100-needle array; (**H**) tip of a tapered, beveled, glass microneedle (900-μm length shown); (**I**) tapered, metal microneedle (500-μm tall) from a 37-needle array; (**J**) array of tapered, metal microneedles (500-μm height) shown next to the tip of a 26-gauge hypodermic needle. *Source*: From Ref. 26.

Results from a representative in vivo study are shown in Figure 3B. After treatment with an array of microneedles, an insulin solution was placed on the skin of a diabetic, hairless rat (29). Over the four-hour delivery period, the rat's blood glucose level dropped steadily, indicating delivery of bioactive insulin at "therapeutic" rates. After the insulin solution was removed from the skin, the blood glucose level stabilized. These effects were remarkably different from control animals exposed to insulin without microneedles and were bounded by the effects of subcutaneous injection of 0.05 and 0.5 U of insulin using a hypodermic needle. Further study showed that changing the insulin formulation and microneedle parameters could be used to modify insulin pharmacokinetics and pharmacodynamics (29).

Additional studies have addressed in vivo delivery of a variety of other compounds. For example, a number of other peptides and proteins have been delivered across the skin using microneedles, such as desmopressin (30), human growth hormone (31), bovine serum albumin (26), and ovalbumin (32), which was used as an antigen to elicit an immune response. Genetic material has also been delivered using microneedles, including oligonucleotides (33) and DNA, either as a reporter gene (34) or as a vaccine (35).

D. Drug Delivery Using Hollow Microneedles

Hollow microneedles offer additional opportunities, because they can be used for pressure-driven injection for active drug delivery using a syringe or micro-pump. Figure 4A shows a histological cross section of skin pierced with hollow microneedles.

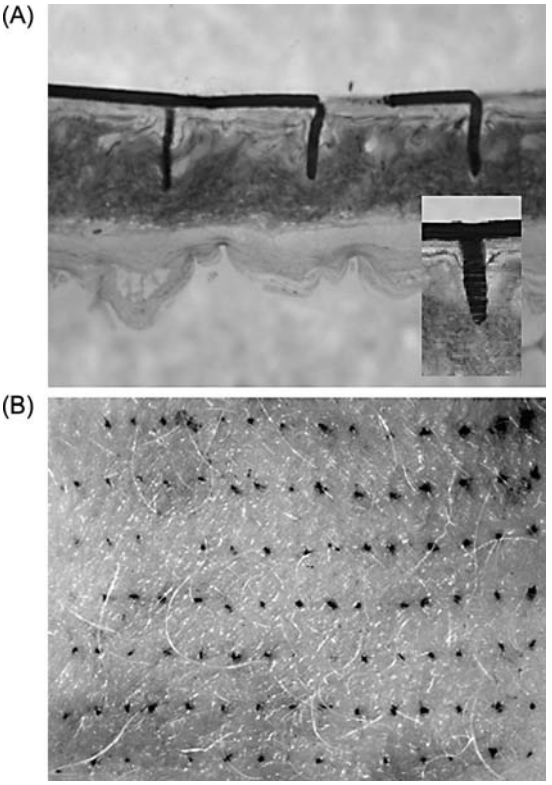


Figure 2 Light microscopy images of solid microneedles inserted into hairless rat skin in vivo. (**A**) Cross section of microneedles inserted into skin in vivo and imaged after biopsy, fixation, staining, and sectioning. The dark structures are the 1000-μm long needles, piercing vertically into the skin, and the base plate of the array, aligned horizontally along the skin surface. The lightly stained tissue corresponds to the epidermis and the thicker darkly stained tissue below corresponds to the dermis. The inset shows a side view of a single microneedle sectioned at an angle rotated 90° relative to the main image. (**B**) Surface of skin after insertion and removal of microneedles in vivo, followed by topical staining with a tissue-marking dye. Each dark spot corresponds to the site of microneedle penetration into the skin. *Source*: From Ref. 29.

These microneedles penetrated across the epidermis and into the superficial dermis, but did not insert to their full depth. This is because the tips of these hollow microneedles are not as sharp as those achieved in solid microneedles (Fig. 1).

As an example of in vivo drug delivery, microneedles were used to inject insulin to diabetic hairless rats. As shown in Figure 5, a 30-minute infusion of insulin caused a steady reduction in blood glucose level over a five-hour period, which corresponded to a drop of up to 70% from pre-infusion levels (26). A dose-dependent response was observed, where infusion at larger pressure caused a larger drop in blood glucose. Subcutaneous injection of 0.05 and 0.5 U insulin bracketed the response seen using microneedles.

III. PAIN, SAFETY, AND CONVENIENCE OF MICRONEEDLES

The micron-scale size of microneedles has been proposed to achieve a balance between transport pathways large enough to deliver drugs, but small enough to avoid

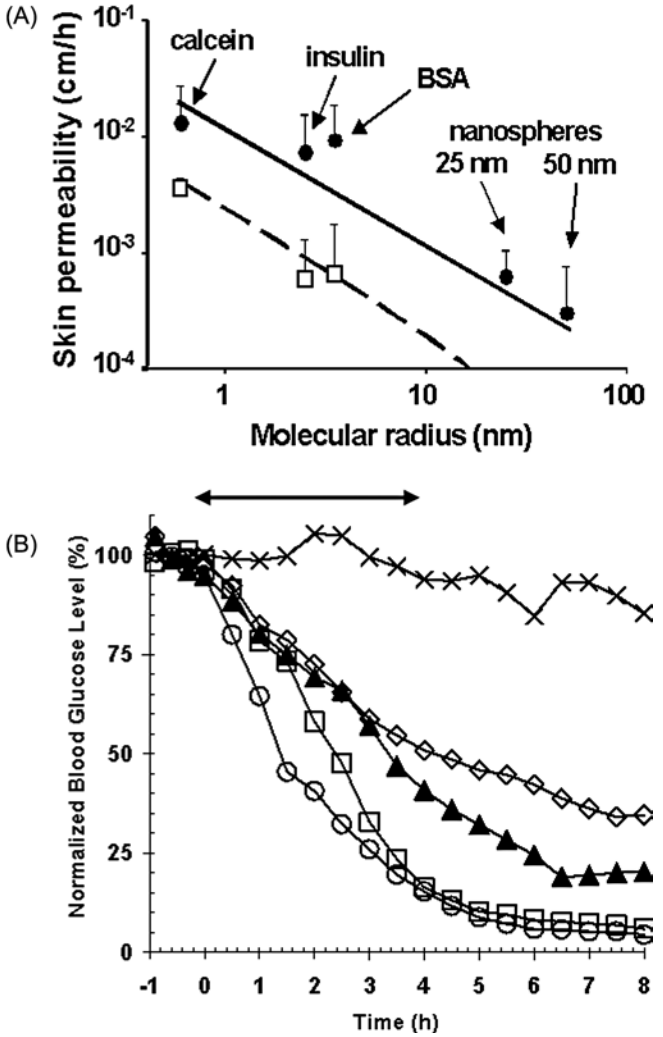


Figure 3 Transdermal delivery using solid microneedles. (**A**) The permeability of human cadaver epidermis was increased by orders of magnitude with a 400-needle array (Fig. 1A) inserted (□) and after the array was removed (•) for calcein, insulin, bovine serum albumin (BSA), and latex nanospheres of 25- and 50-nm radius. In the absence of microneedles, permeability to all compounds was below their detection limits on the order of 10^{-6}–10^{-4} cm/hr (data not shown). Predictions are shown for needles inserted (*dashed line*) and needles removed (*solid line*) using a theoretical model (26). (**B**) Changes in blood glucose level in diabetic, hairless rats after insulin delivery using microneedles (▲), subcutaneous hypodermic injection of 0.05 U (◇), 0.5 U (□), or 1.5 U (○) of insulin, or passive delivery across untreated skin (×). Microneedles were inserted into skin for 10 minutes and then removed. Insulin solution was applied to the skin immediately after microneedle insertion and left on the skin for four hours. Subcutaneous injections took a few seconds to perform. *Source*: From Refs. 26 and 29.

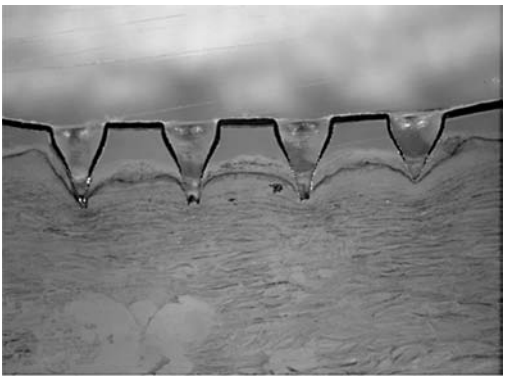


Figure 4 Cross section of hollow microneedles inserted into human cadaver skin imaged by light microscopy after fixation, staining, and sectioning. The dark structures are the cross sections of the hollow-bored microneedles. The epidermis corresponds to the darker band along the skin surface and the dermis is below. These needles inserted just across the epidermis, but did not insert to their full needle length of 500 μm.

clinical complications and promote patient satisfaction. Although this hypothesis has not yet been fully tested, there is information to assess its validity.

A. Avoidance of Pain by Microneedles

Microneedles have been put forward as a painless way to deliver drugs across skin. Certainly, needles that pierce only into the stratum corneum are unlikely to cause sensation, because there are no nerves located in stratum corneum (5). However, it

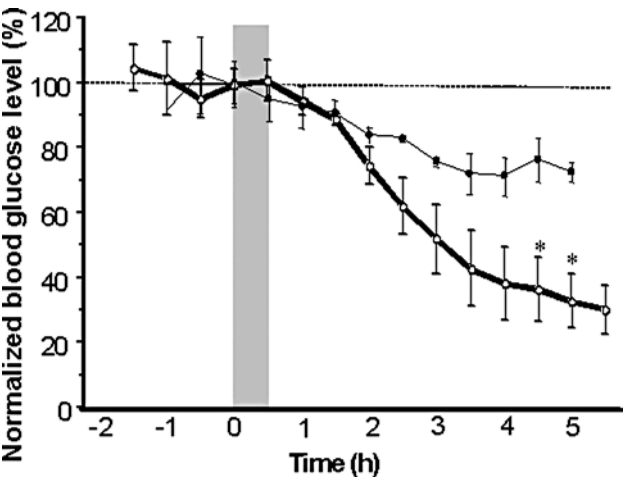


Figure 5 Transdermal delivery using hollow microneedles. Blood glucose levels in diabetic, hairless rats shown as a function of time before and after microinjection of insulin solution at 10 psi (●) or 14 psi (○). Insulin was microinjected through a hollow, glass microneedle (Fig. 1H) inserted into rat skin for 30 minutes (*shaded region*). As a negative control, microinjection of saline did not cause significant changes in blood glucose levels (data not shown). *Source*: From Ref. 26.

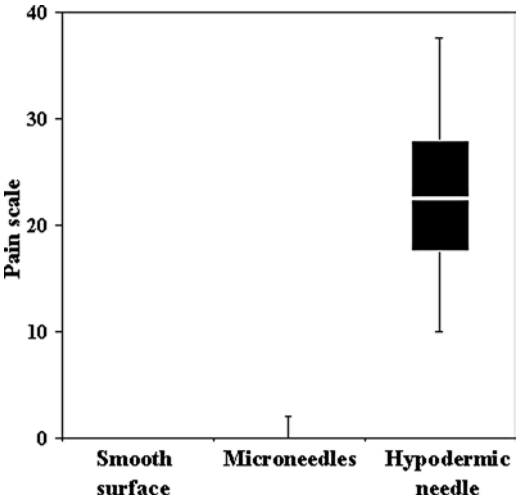


Figure 6 Box plot showing visual analog pain scores from a blinded comparison among (i) a smooth silicon surface, (ii) a 400-microneedle array (Fig. 1A), and (iii) a 26-gauge hypodermic needle (large needle in Fig. 1J) inserted into the forearm of human subjects. For each treatment, the 5th, 25th, 50th, 75th, and 95th percentiles are shown. *Source*: From Ref. 36.

is extremely difficult to insert a needle just 10 to 15 μm into the skin; there are no data in the literature to suggest that this has been accomplished.

Although there are nerves located below the stratum corneum, microneedle insertion into the viable epidermis and even into the superficial dermis can nonetheless avoid pain, probably due to the small diameter, and relatively short length of microneedles. For example, when an array of 400 microneedles measuring 150 μm in length were inserted into the skin of blinded human subjects, the subjects were unable to distinguish between the microneedles inserted into the skin and a smooth surface pressed against the skin surface (Fig. 6) (36). In contrast, insertion of a 26-gauge hypodermic needle into the skin caused significantly greater levels of pain. Additional studies examined the effect of increasing microneedle length over the range of 500 to 1500 μm. Pain levels increased with increasing needle length, although all microneedle pain scores were many-fold lower than the pain of a hypodermic needle (data not shown).

B. Safety of Microneedles

Microneedles are also expected to be safe. The risk of disease transmission is reduced by the fact that microneedle are typically bloodless. Moreover, their expected low cost makes microneedles suitable as disposable devices, thereby eliminating the risk associated with repeated use (37). The increased permeability that persists after microneedle application could increase the risk of bacterial or viral infection. However, preliminary data suggest that although increased permeability is maintained under occlusion, non-occluded skin reseals within minutes (data not shown). Anecdotal data from our laboratory show that after many hundreds of microneedle insertions into human subjects, no associated infections have been reported.

Intentional reuse is also difficult with microneedles, which is of interest in developing countries and to intravenous drug abusers (37). Reuse of solid microneedles should

generally be of little interest, since simply increasing skin permeability is of little value. Hollow microneedles will probably be incorporated into commercial products as single-use, application-specific devices that cannot be reused. Repeated use is further hindered by the fact that needle tips become increasingly dull after reuse, making needle insertion into the skin more difficult. Finally, if microneedles are made of polymer, they can be easily destroyed by incineration or biodegradation.

Complications associated with the possibility of needles breaking off in the skin are reduced by a number of factors. First, microneedles can be fabricated using a variety of biocompatible biomaterials. Moreover, microneedles can be made very strong, especially when made of metal (38,39). If needles break, they can be sloughed off during normal epidermal renewal or may be expelled from the skin by normal healing processes, although a residual needle tip could cause, for example, a granuloma (5). Finally, needles made of biodegradable polymer can safely degrade in the skin.

C. Convenience of Microneedles

Microneedle-based drug delivery is expected to be convenient for patients and thereby increase patient compliance. For example, microneedle devices could be similar in size to current transdermal patches, because microneedle arrays are typically less than 1-mm thick and less than 1 cm^2 in area. They could also be used in a manner similar to patches, were a microneedle device is placed on the skin and left to deliver drug for many hours or days.

As a "trailing edge" technology that builds off advances in the microelectronics industry, microneedle fabrication costs are expected to be sufficiently low that microneedle devices could be inexpensive and disposable (40). The cost is also kept low by not requiring the use of a power supply, in contrast to most other physical methods to enhance skin permeability. The likely simplicity of microneedle device design should reduce the chance for device failure or operator error, which is appealing to both patients and the FDA.

IV. CONCLUSIONS

There is growing interest to increase transdermal delivery via micron-scale disruptions of stratum corneum microstructure. Microneedles provide an attractive method to increase skin permeability in this way because of their expected effectiveness, safety, simplicity to use, and low cost to manufacture. Applicable to a variety of delivery scenarios, microneedles have been shown to deliver drugs, proteins, DNA, and vaccines in vitro and in vivo. Microfabrication technology can produce solid and hollow needles with a variety of sizes, shapes, and materials. Studies indicate that microneedles can be painless. Evidence to date has not shown significant safety concerns. Rapidly expanding research and development activity in industry and academia suggests that microneedle-based delivery systems may soon become commercial products that impact medical practice.

ACKNOWLEDGMENTS

I thank Mark Allen, Shawn Davis, Harvinder Gill, Shilpa Kaushik, Wijaya Martanto, Devin McAllister, Jung-Hwan Park, Hubert Vesper, and Ping Wang for valued

collaboration and helpful discussions. This work was supported in part by the National Institutes of Health and the Georgia Tech/CDC Collaborative Research Program.

REFERENCES

1. Park K, ed. Controlled Drug Delivery: Challenges and Strategies. Washington, DC: American Chemical Society, 1997.
2. Langer R. Drug delivery and targeting. Nature 1998; 392:5–10.
3. Prausnitz MR, Mitragotri S, Langer R. Current status and future potential of transdermal drug delivery. Nat Rev Drug Discov 2004; 3:115–124.
4. Purdon CH, Azzi CG, Zhang J, Smith EW, Maibach HI. Penetration enhancement of transdermal delivery—current permutations and limitations. Crit Rev Ther Drug Carrier Syst 2004; 21:97–132.
5. Champion RH, Burton JL, Burns DA, Breathnach SM, eds. Textbook of Dermatology. London: Blackwell Science, 1998.
6. Smith EW, Maibach HI, eds. Percutaneous Penetration Enhancers. Boca Raton, FL: CRC Press, 1995.
7. Williams AC, Barry BW. Penetration enhancers. Adv Drug Deliv Rev 2004; 56:603–618.
8. Karande P, Jain A, Mitragotri S. Discovery of transdermal penetration enhancers by high-throughput screening. Nat Biotechnol 2004; 22:192–197.
9. Banga AK. Electrically-Assisted Transdermal and Topical Drug Delivery. London: Taylor & Francis, 1998.
10. Prausnitz MR. Overcoming skin's barrier: the search for effective and user-friendly drug delivery. Diab Technol Ther 2001; 3:233–236.
11. Bramson J, Dayball K, Evelegh C, Wan YH, Page D, Smith A. Enabling topical immunization via microporation: a novel method for pain-free and needle-free delivery of adenovirus-based vaccines. Gene Ther 2003; 10:251–260.
12. Herndon TO, Gonzalez S, Gowrishankar T, Anderson RR, Weaver JC. Transdermal microconduits by microscission for drug delivery and sample acquisition. BMC Med 2004; 2:12.
13. Ilic L, Gowrishankar TR, Vaughan TE, Herndon TO, Weaver JC. Spatially constrained skin electroporation with sodium thiosulfate and urea creates transdemal microconduits. J Control Release 1999; 61:185–202.
14. Prausnitz MR. Microneedles for transdermal drug delivery. Adv Drug Deliv Rev 2004; 56:581–587.
15. Baxby D. Smallpox vaccination techniques: from knives and forks to needles and pins. Vaccine 2002; 20:2140–2149.
16. Madou MJ. Fundamentals of Microfabrication: the Science of Miniaturization. Boca Raton, FL: CRC Press, 2002.
17. McAllister DV, Allen MG, Prausnitz MR. Microfabricated microneedles for gene and drug delivery. Annu Rev Biomed Eng 2000; 2:289–313.
18. Chen J, Wise KD. A multichannel neural probe for selective chemical delivery at the cellular level. IEEE Trans Biomed Eng 1997; 44:760–769.
19. Henry S, McAllister DV, Allen MG, Prausnitz MR. Microfabricated microneedles: a novel approach to transdermal drug delivery. J Pharm Sci 1998; 87:922–925.
20. Reed ML, Wu C, Watkins KJS, Vorp DA, Nadeem A, Weiss LE, Rebello K, Mescher M, Smith AJC, Rosenblum W, Feldman MD. Micromechanical devices for intravascular drug delivery. J Pharm Sci 1998; 87:1387–1394.
21. Brazzle J, Papautsky I, Frazier AB. Micromachined needle arrays for drug delivery or fluid extraction. IEEE Eng Med Biol Mag 1999; 18:53–58.
22. Lin L, Pisano AP. Silicon processed microneedles. J MEMS 1999; 8:78–84.
23. Smart WH, Subramanian K. The use of silicon microfabrication technology in painless blood glucose monitoring. Diab Technol Ther 2000; 2:549–559.

24. Griss P, Enoksson P, Tolvanen-Laakso HK, Merilainen P, Ollmar S, Stemme G. Micromachined electrodes for biopotential measurements. J MEMS 2001; 10:10–16.
25. Gardeniers JGE, Luttge R, Berenschot JW, de Boer MJ, Yeshurun Y, Hefetz M, van't Oever R, van den Berg A. Silicon micromachined hollow microneedles for transdermal liquid transport. J MEMS 2003; 6:855–862.
26. McAllister DV, Wang PM, Davis SP, Park J-H, Canatella PJ, Allen MG, Prausnitz MR. Microfabricated needles for transdermal delivery of macromolecules and nanoparticles: fabrication methods and transport studies. Proc Natl Acad Sci USA 2003; 100: 13755–13760.
27. Zahn JD, Deshmukh A, Pisano AP, Liepmann D. Continuous on-chip micropumping for microneedle enhanced drug delivery. Biomed Microdevices 2004; 6:183–190.
28. Kim K, Park DS, Lu HM, Che W, Kim K, Lee J-B, Ahn CH. A tapered hollow metallic microneedle array using backside exposure of SU-8. J Micromech Microeng 2004; 14:597–603.
29. Martanto W, Davis S, Holiday N, Wang J, Gill H, Prausnitz M. Transdermal delivery of insulin using microneedles in vivo. Pharm Res 2004; 21:947–952.
30. Cormier M, Johnson B, Ameri M, Nyam K, Libiran L, Zhang DD, Daddona P. Transdermal delivery of desmopressin using a coated microneedle array patch system. J Control Release 2004; 97:503–511.
31. Cormier M, Daddona PE. Macroflux technology for transdermal delivery of therapeutic proteins and vaccines. In: Rathbone MJ, Hadgraft J, Roberts MS, eds. Modified-Release Drug Delivery Technology. New York: Marcel Dekker, 2003:589–598.
32. Matriano JA, Cormier M, Johnson J, Young WA, Buttery M, Nyam K, Daddona PE. Macroflux microprojection array patch technology: a new and efficient approach for intracutaneous immunization. Pharm Res 2002; 19:63–70.
33. Lin W, Cormier M, Samiee A, Griffin A, Johnson B, Teng C, Hardee GE, Daddona P. Transdermal delivery of antisense oligonucleotides with microprojection patch (Macroflux) technology. Pharm Res 2001; 18:1789–1793.
34. Chabri F, Bouris K, Jones T, Barrow D, Hann A, Allender C, Brain K, Birchall J. Microfabricated silicon microneedles for nonviral cutaneous gene delivery. Br J Dermatol 2004; 150:869–877.
35. Mikszta JA, Alarcon JB, Brittingham JM, Sutter DE, Pettis RJ, Harvey NG. Improved genetic immunization via micromechanical disruption of skin-barrier function and targeted epidermal delivery. Nat Med 2002; 8:415–419.
36. Kaushik S, Hord AH, Denson DD, McAllister DV, Smitra S, Allen MG, Prausnitz MR. Lack of pain associated with microfabricated microneedles. Anesth Analg 2001; 92: 502–504.
37. Simonsen L, Kane A, Lloyd J, Zaffran M, Kane M. Unsafe injections in the developing world and transmission of blood borne pathogens: a review. Bull World Health Organ 1999; 77:789–800.
38. Davis SP, Landis BJ, Adams ZH, Allen MG, Prausnitz MR. Insertion of microneedles into skin: measurement and prediction of insertion force and needle fracture force. J Biomech 2004; 37:1155–1163.
39. Yang M, Zahn JD. Microneedle insertion force reduction using vibratory actuation. Biomed Microdevices 2004; 6:177–182.
40. Greystone Associates. Microneedle Drug Delivery: Technology, Markets, and Prospects. Amherst, NH: Greystone Associates, 2004.

38

Human Percutaneous Absorption and Transepidermal Water Loss (TEWL) Correlation

Ronald C. Wester and Howard I. Maibach
Department of Dermatology, School of Medicine, University of California, San Francisco, California, U.S.A.

I. INTRODUCTION

Percutaneous absorption is defined as the rate and extent that a chemical is absorbed into and through the skin and into the systemic circulation. A major variable in percutaneous absorption is regional variation, where some body sites show extensive skin absorption, while the other sites show less absorption. Also, we are a world of individuals and percutaneous absorption will vary by individual, as well as anatomic site. Where percutaneous absorption is the passage of chemicals from the outside environment into and through skin, transepidermal water loss (TEWL) is the passage of water in the other direction, from the body through the skin into the outside environment. The question is whether percutaneous absorption and TEWL correlate and are predictable of one another.

A. Percutaneous Absorption

The first occupational disease in recorded history was scrotal cancer in chimney sweepers. The historical picture of a male worker holding a sweeper and covered from head to toe with black soot is vivid. But why the scrotum? Percutaneous absorption in man and animals varies depending on the area of the body in contact with a chemical. This is called regional variation. When a certain skin area if exposed, any effect of the chemical will be determined by how much skin is absorbed through the skin. Where systemic drug delivery is desired, such as transdermal delivery, a high-absorbing area may be desirable to deliver sufficient drug. Scopolamine transdermal systems are supposedly placed in the postauricular area (behind the ear) because at this skin site the percutaneous absorption of scopolamine is sufficiently enhanced to deliver effective quantities of the drug. A different example is with estimating human health hazard effects of environmental contaminants. This could be a chemical warfare agent on exposed parts of the skin (head, face, neck, and hands)

and trying to determine the amount of chemical that might be absorbed into the body. The estimate for skin absorption is an integral part of the estimate for potential hazard, thus, accuracy of estimate is very relevant.

B. Regional Variation in Humans

Feldmann and Maibach (1) were the first to systemically explore the potential for regional variation in percutaneous absorption. The first absorption studies were done with ventral forearm, because this site is convenient to use; however, skin exposure to chemicals exists over the entire body. They first showed regional variation with the absorption of parathion (Fig. 1). The fact that the scrotum was the highest absorbing skin site (scrotal) cancer in chimney sweeps is the key. Among other body sites, skin absorption was lowest for the foot area, and higher around the head and face area.

Data in Table 1 illustrates the influence of anatomical region on the percutaneous absorption of two common pesticides, parathion and malathion, in humans (2). There are two major points in this study. First, regional variation was confirmed with the different chemicals; note that parathion and malathion are chemically related to some chemical warfare agents. Second, those skin areas that would be exposed to the pesticides, the head and face, were of the higher absorbing sites. The body areas most exposed to environmental contaminants are the areas with the higher skin absorption.

Table 2 gives site variability for parathion skin absorption with time. Soap and water wash in the first few minutes after exposure is not a perfect decontaminant. Site variation is apparent early in skin exposure (3).

Van Rooy et al. (4) applied coal tar ointment to various skin areas of volunteers and determined absorption of polycyclic aromatic hydrocarbons (PAH) by surface disappearance of PAH and the excretion of urinary I-OH pyrene. Using PAH disappearance skin ranking (highest to lowest) was shoulder > forearm > fore-

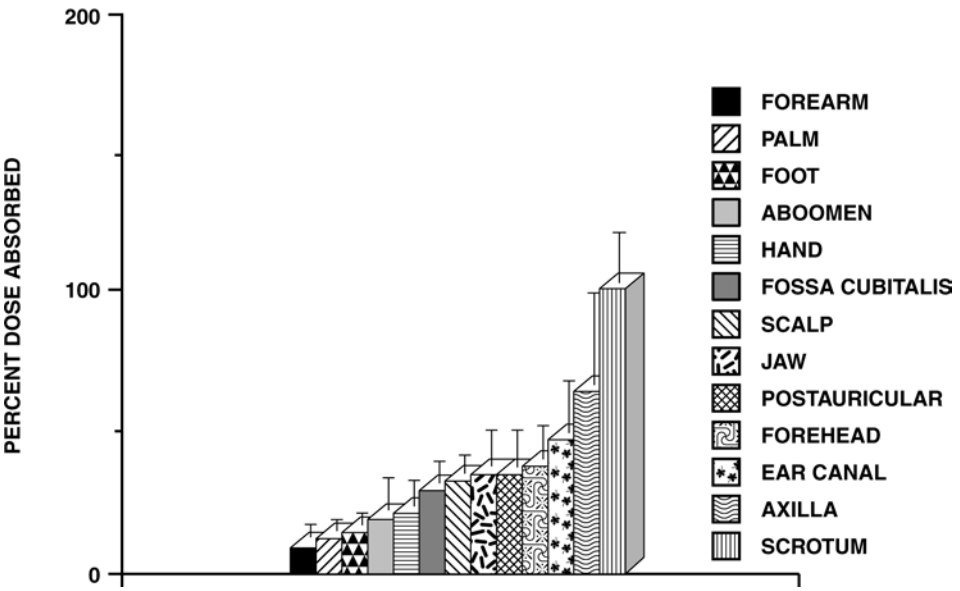


Figure 1 Anatomic regional variation with parathion percutaneous absorption.

Table 1 Effect of Anatomical Region on In Vivo Percutaneous Absorption of Hydrocortisone and Two Pesticides, Parathion and Malathion, in Humans In Vivo

	Dose absorbed (%)		
Anatomical region	Hydrocortisone	Parathion	Malathion
Forearm	1.0	8.6	6.8
Palm	0.8	11.6	5.8
Foot, ball	0.2	13.5	6.8
Abdomen	1.3	18.5	9.4
Hand, dorsum	—	21.0	12.5
Forehead	7.6	36.3	23.2
Axilla	3.1	64.0	28.7
Jaw angle	12.2	33.9	69.9
Fossal cubitalis	—	28.4	
Scalp	4.4	32.1	
Ear canal	—	46.6	
Srotum	36.2	101.6	

head > groin > hand (palmar) > ankle. Using I-OH pyrene excretion skin ranking (highest to lowest) was neck > calf > forearm > trunk > hand. Table 3 compares their results with Guy and Maibach (5).

Rougier et al. (6) examined the influence of anatomical site on the relationship between total penetration of benzoic acid in humans and the quantity present in the stratum corneum (SC) 30 minutes after application. Figure 2 shows total penetration of benzoic acid according to anatomical site. Figure 3 shows correlation between the level of penetration of benzoic acid within four days and its level in the SC after a 30-minute application relative to anatomical site.

Wertz et al. (7) determined regional variation in permeability through human and pig skin and oral mucosa. In the oral mucosa of both species, permeability ranked floor of mouth > buccal mucosa > palate. Skin remains a greater barrier; absorption some 10-fold less than oral mucosa.

The barrier properties of skin relative to the oral mucosa have been a benefit for longer term transdermal delivery. Nitroglycerin buccal tablets are effective for about 20 minutes, due to rapid buccal absorption. In contrast, transdermal nitrogly-

Table 2 Site Variation and Decontamination Time for Parathion

Skin residence time before soap and water wash[a]	Parathion dose absorbed (%)[a]		
	Arm	Forehead	Palm
1 min	2.8	8.4	
5 min			6.2
15 min	6.7	7.1	13.6
30 min		12.2	13.3
1 hr	8.4	10.5	11.7
4 hr	8.0	27.7	7.7
24 hr	8.6	36.3	11.8

[a]Each time is a mean for four volunteers. The fact that there were different volunteers at each time point accounts for some of the variability with time for each skin site.

Table 3 Absorption Indices of Hydrocortisone and Pesticides (Parathion/Malathion) Calculated by Guy and Maibach (5) Compared with Absorption of Pyrene and Polycyclic Aromatic Hydrocarbons (PAH) for Different Anatomical Sites by Van Rooy et al. (4)

	Absorption			
Anatomical site	Hydrocortine	Pesticides	Pyrene	PAH
Genitals	40	12	–	–
Arms	1	1	1	1
Hand	1	1	0.8	0.5
Leg/ankle	0.5	1	1.2	0.8/0.5
Trunk/shoulder	2.5	3	1.1	/2.0
Head/neck	5	4	/1.3	1.0

cerin is prescribed for 24 hours continuous dose delivery. The transdermal nitroglycerin patch is placed on the chest more for psychological reasons than that related to scientific regional variation skin absorption. Some transdermal systems take advantage of regional variations in skin absorption and some do not (Table 4).

Shriner and Maibach (8) studied skin contact irritation and showed that areas of significant response were neck > perioral > forehead. The volar forearm was the least sensitive of eight areas tested. This is in contrast to the commonly held belief that the forearm is one of the best locations to test for immediate contact irritation.

C. Individual Variation

It is well understood that chemical trials are designed with multiple volunteers to account for individual subject variation. This extends to in vivo percutaneous absorption where individual subject variability has been demonstrated. This subject variation also extends to in vitro human skin samples (9). Table 5 shows the in vitro percutaneous absorption of vitamin E acetate through human skin in vitro. Percent doses absorbed for two formulations, A and B, are shown for 24-hour receptor fluid accumulation and for skin content (skin digested and assayed at 24-hour time point). Assay of skin surface soap and water wash at the end of the 24-hour period gives dose accountability.

The two formulations were the same except for slight variation in pH. Statistically, there was no difference in absorption between the two formulations. How-

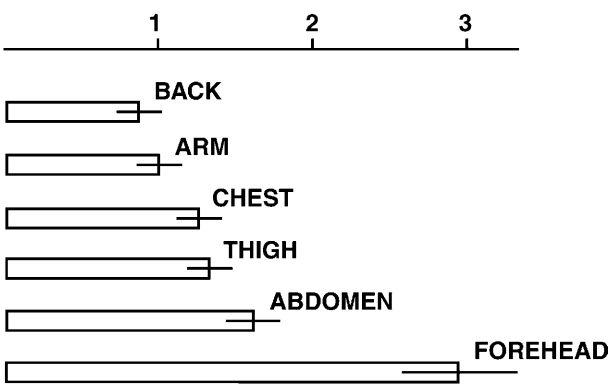


Figure 2 Relative permeability, ARM=1

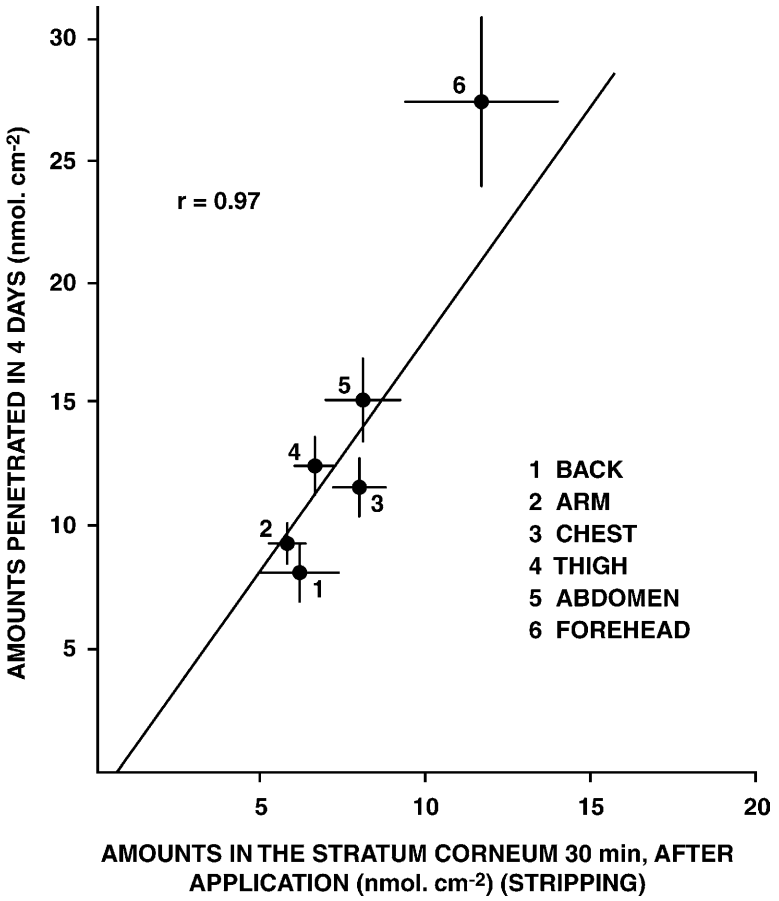


Figure 3 Human percutaneous absorption and transepidermal water loss.

Table 4 Site Variation in Transdermal Delivery

Transdermal	Body site	Reason
Nitroglycerin	Chest	Psychological: the patch is placed over the heart
Scopolamine	Postauricular	Scientific: behind the ear was found to be the best absorbing area
Estradiol	Trunk	Convenience: easy to place, and out of view
Testosterone	Scrotum	Scientific: highest skin absorbing area
Testosterone	Trunk	Scientific/convenience: removal from trunk skin is easier than scrotal skin

Table 5 In Vitro Percutaneous Absorption of Vitamin E Acetate into and Through Human Skin

	Percent dose absorbed		
	Receptor fluid	Skin content	Surface wash
Formula A:			
Skin source 1	0.34	0.58	74.9
Skin source 2	0.39	0.66	75.6
Skin source 3	0.47	4.08	89.1
Skin source 4	1.30	0.96	110.0
Mean ± SD	0.63 ± 0.45[a]	1.56 ± 1.69[b]	87.4 ± 16.4
Formula B:			
Skin source 1	0.24	0.38	–
Skin source 2	0.40	0.64	107.1
Skin source 3	0.41	4.80	98.1
Skin source 4	2.09	1.16	106.2
Mean ± SD	0.78 ± 0.87[a]	1.74 ± 2.06[b]	103.8 ± 5.0

[a] $p = 0.53$ (non-significant; paired t-test)
[b] $p = 0.53$ (non-significant; paired t-test)

ever, a careful examination of the individual values in Table 5 shows consistency within individuals. Analysis of variance (ANOVA) for individual variation showed statistical significance for receptor fluid ($p = 0.02$) and skin content ($p = 0.000$); therefore, when comparing treatments for in vitro percutaneous absorption, it is recommended that each treatment be a part of each skin source.

II. TRANSEPIDERMAL WATER LOSS

Water comprises about 60% of adult human body weight. The body obtains water from the intake of foods and fluids and leaves the body visibly via urine, sweat, and feces. Additionally, the body loses water continuously by evaporation from the respiratory passages and skin surface—termed insensible water loss, since we do not feel that we are actually losing water all the time. The amount of water that is leaving the body at rest is about 700 mL/day at an ambient temperature of 20°C (10,11). The average water loss by diffusion through the skin is 300 to 400 mL/day, even in a person who is born without sweat glands (11) or whose sweat glands are inactivated (12). In other words, the water molecules themselves actually diffuse across the skin (11). This invisible natural process of water diffusion is called TEWL (10).

The TEWL has been related to the skin barrier function by a series of investigations. For instance, studies in the past have established that washing the skin surface with fat solvents did not increase the rate of water loss, but light sandpapering of skin surface (13) or tape stripping of the whole SC (14,15) resulted in increased TEWL. As the permeation rate of water across full thickness skin, epidermis or SC turned out to be approximately the same, it was realized that SC acts as the principal barrier to TEWL (16). Furthermore, a high rate of TEWL has been detected by patients with SC disorders, like psoriasis or ichthyosis (17). The TEWL is therefore taken as a measure of the skin barrier integrity which mainly resides in the SC.

Anatomical skin site is an important variable with respect to baseline TEWL, which can be ranked from the highest to the lowest values: palm > sole

> forehead = postauricular skin = dorsum of hand > forearm = upper arm = thigh = chest = abdomen = back (18). It can actually be related to the SC thickness of the particular body regions (19). Studies of different areas of the forearms showed the differences between three sites: (i) the site close to the wrist showed the highest values in all cases; (ii) the nearest elbow region showed a slightly higher value than the median site; (iii) the median site (20,21). Statistically, only the wrist region differed significantly form the other sites. The fact that the sweat gland density and activity varied on the forearm increasing towards the wrist could be one, but not the only, explanation for the higher value of the wrist region (22). Another hypothesis is that the wrist region is more exposed to mechanical and atmospheric influences than the others and the SC there could be more easily and regularly irritated, leading to increased TEWL values (22). An emotional influence on the wrist region was also suggested to play a role.

A. Correlation of Percutaneous Absorption and TEWL

Percutaneous absorption can be performed in vivo with human volunteers and animals. It can also be done in vitro with cadaver skin, human and animal, in a diffusion system. Percutaneous absorption is by passive diffusion only, from a higher concentration progressively to a lower concentration. The TEWL has a passive diffusion component where water from the body (high concentration) passes out through the skin to a lower concentration, the environment. This would be baseline TEWL. The TEWL also has an active component, the release of water through sweat glands for heat dissipation or nervous response. In vivo TEWL studies would contain both passive and active water transport; however, cadaver skin in in vitro studies would only have the passive transport.

Lotte et al. (23) studied the relationship between the percutaneous penetration of four chemicals and TEWL in vivo in man as a function of anatomic site. The findings showed an appreciable difference in the permeability of the skin from one site to another with regard to both water loss and chemical penetration. In addition, independent of the physicochemical properties of the molecules administered, there was a linear relationship between TEWL and penetration. Table 6 gives the results for the four anatomic sites (arm, abdomen, postauricular, and forehead) and the four test chemicals (benzoic acid sodium salt, caffeine, benzoic acid, and acetylsalicylic acid). Figure 4 illustrates the correlation between percutaneous absorption and TEWL. Correlations ranged from $r = 0.62$ to 0.73, which are good for an in vivo human study. These data confirm both the importance of anatomic site in the degree of permeability of the cutaneous barrier and the utility of determination of TEWL and percutaneous absorption in the evaluation of its functional condition.

Aalto-Karte and Turpeinen (24) studied in vivo percutaneous absorption of hydrocortisone in three children and six adults with widespread dermatitis after the application of 1% hydrocortisone cream. Before application of the cream, the TEWL was measured in six skin areas. A highly significant correlation was found between the post-application rise in plasma cortisol level and the mean TEWL.Figure 5 shows the relationship where the correlation coefficient r was a significant ($p < 0.001$) 0.991.

The TEWL and percutaneous absorption can also be correlated using in vitro diffusion systems. This removes the influence of active water production (sweaty palms) but an in vitro system can have its own particular problems. Nangia et al. (25) demonstrated linear correlation between tritiated water absorbed and TEWL for various sodium lauryl sulfate treatments and for various physical injuries applied

Table 6 Percutaneous Absorption and Transepidermal Water Loss (TEWL) Values According to Anatomic Site

n	Anatomic site	Amount in urine after 24 hour[a]	Total amount penetrated within 4 days[b]	TEWL[c]	Relative permeability to arm	
					Penetration	TEWL
Compound: benzoic acid sodium salt, vehicle A						
6	Arm (upper, outer)	3.02[d] (0.34)[e]	4.02 (0.45)	6.06 (0.36)	1	1
6	Abdomen	5.73 (0.54)	7.65 (0.72)	5.37 (0.46)	1.9	0.9
6	Postauricular	7.54 (0.62)	10.06 (0.82)	7.72 (0.64)	2.5	1.3
8	Forehead	9.31 (1.76)	12.32 (2.30)	12.29 (0.96)	3.1	2
Compound: caffeine, vehicle B						
7	Arm (upper, outer)	6.04 (0.92)	12.09 (1.84)	7.04 (0.95)	1	1
6	Abdomen	3.76 (0.67)	7.53 (1.34)	6.05 (0.43)	0.6	0.9
7	Postauricular	5.87 (0.52)	11.72 (1.05)	8.74 (0.62)	1	1.2
6	Forehead	11.17 (1.20)	23.35 (2.39)	12.77 (1.05)	1.9	1.8
Compound: benzoic acid, vehicle A						
8	Arm (upper, outer)	6.87 (0.75)	9.15 (1.01)	4.24 (0.35)	1	1
7	Abdomen	10.88 (1.23)	14.52 (1.64)	4.40 (0.51)	1.6	1
8	Postauricular	16.87 (3.85)	22.49 (5.14)	8.35 (0.41)	2.5	1.9
7	Forehead	20.10 (2.39)	26.80 (3.19)	10.34 (0.70)	2.9	2.4
Compound: acetylsalicylic acid, vehicle A						
7	Arm (upper, outer)	5.27 (0.18)	17.00 (0.37)	5.08 (0.79)	1	1
6	Abdomen	5.34 (1.03)	17.20 (3.35)	5.16 (0.43)	1	1
6	Postauricular	11.04 (2.50)	29.17 (5.37)	9.04 (0.84)	2.1	1.8
6	Forehead	10.89 (1.02)	35.14 (3.29)	11.22 (0.96)	2.1	2.2

[a]24 hour urinary accumulation.
[b]Calculated from urinary excretion: (b)= (a)/0.75.
[c]Measured just before the application, expressed in $g/m^2/hr$.
[d]Expressed in $nmol/cm^2$.
[e]SD.
Abbreviations: Vehicle A, (ethyleneglycol/triton × 100) (90/10); Vehicle B, (ethyleneglycol/triton × 100) (90/10)/(H_2O)(50/50).

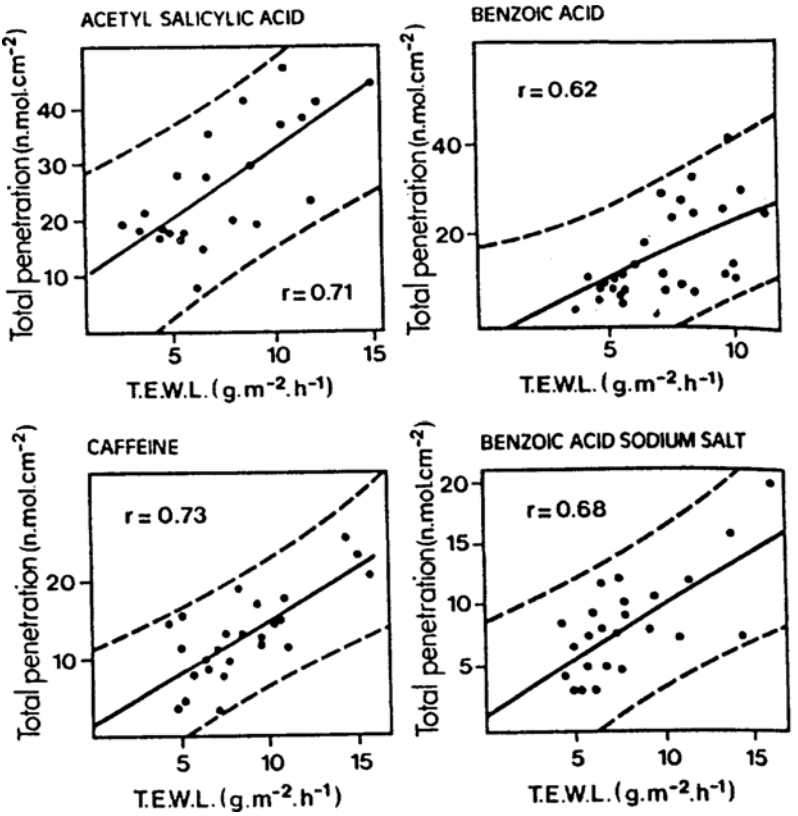


Figure 4 In vivo relationship between transepidermal water loss (TEWL) and percutaneous absorption of different compounds according to the anatomic site in man.

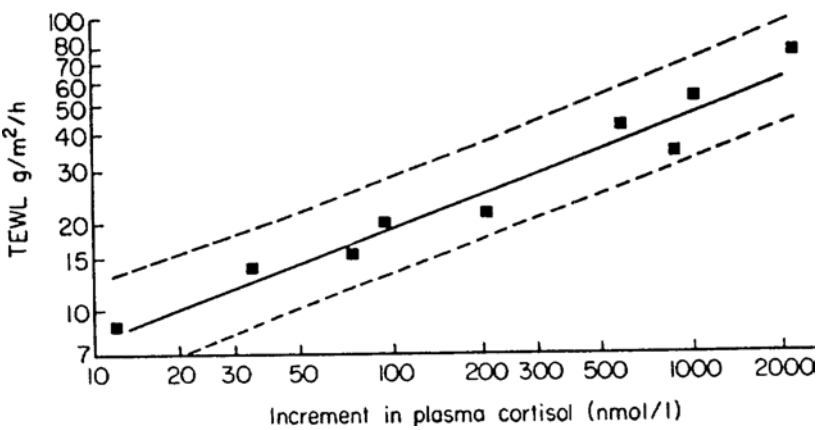


Figure 5 Relation between TEWL and the increment in plasma cortisol in the percutaneous absorption test, in nine patients with widespread dermatitis. Log_{10} scales have been used to normalize the skewed distributions of the two variables. 95% confidence limits are give. The regression line is: $\log_{10}$ TEWL=0.39 $\log_{10}$ plasma cortisol+0.51. Spearman's rank correlation coefficient r_s is 0.991 ($p < 0.001$: 95% confidence limits for r_s 0.955-0.998).

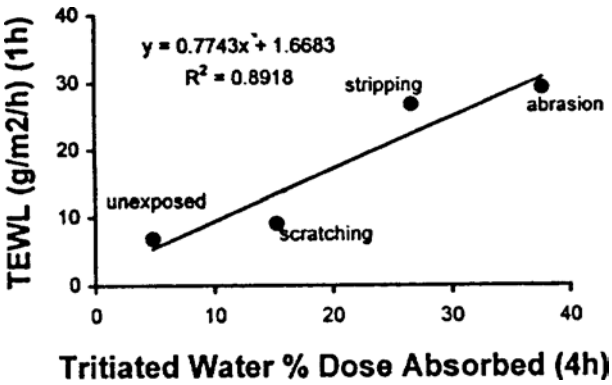


Figure 6 Linear correlation between TEWL (measured after 1 h) and the fraction of the dose of tritiated water absorbed (in 4 h) after various physical injuries applied to excised human skin.

to the excised skin (Fig. 6). Chilcott et al. (26) on the other hand found no correlation between basal TEWL rates and the permeability of human epidermal membranes to ^3H_2O ($p = 0.72$) or sulfur mustard ($p = 0.74$). Similarly, there was no correlation between TEWL rates and the ^3H_2O permeability of full-thickness pig skin ($p = 0.68$). There was no correlation between TEWL rate and ^3H_2O permeability following up to 15 tape strips ($p = 0.64$) or up to four needle-stick punctures ($p = 0.13$).

Punnagoda et al. (18) summarized the individual-related variables to TEWL Table 7

Table 7 Individual-Related Variables to Transepidermal Water Loss (TEWL)

Age.	Baseline TEWL is, for the most part of the range, independent of age. Premature infants have increased TEWL during their first weeks, and elderly skin may show decreased TEWL.
Sex.	Sex as a factor has no apparent effect on baseline TEWL.
Race.	There is no apparent difference in baseline TEWL between different human races.
Anatomic sites.	Anatomic site is an important variable with respect to baseline TEWL, which can be ranked as follows: palm > sole > forehead = postauricular skin = nail = dorsum of hand > forearm = upper arm = thigh = chest abdomen = back.
Intra- and inter-individual variation.	The intra-individual variation of baseline TEWL values is considerably less than the inter-individual variation by sites and by days.
Sweating.	Physical, thermal, or emotional sweating are important variables to control for in making accurate TEWL measurements.
Vascular effects.	TEWL does not appear to be influenced by simple vasoconstriction and vasodilatation.
Skin surface temperature.	Skin temperature is important for TEWL and preconditioning of the test person is required (see "Sweating" above). Skin surface temperature should be measured and reported in publications, particularly if ambient room air temperature deviates from 20 to 22°C.

Source: From Ref. 18.

III. DISCUSSION

Human skin has barrier properties designed through evolution to protect the inner body from the environment. This barrier property is not absolute and chemicals on the skin can pass into and through the skin by passive diffusion. These same barrier properties are also leaky to the body's water content and water escapes, through the skin, also by passive diffusion. This two way passive travel through the same membrane suggests a correlation between percutaneous absorption and TEWL, especially in the same individual. Science involves seeking a truth amongst a multitude of variables. Despite the many variables in both percutaneous absorption and TEWL, some statistically positive correlations have been determined between the two. This is not absolute, and negative reports do exist. The TEWL also has the added variable of active water exchange for heat dissipation.

REFERENCES

1. Feldmann RJ, Maibach HI. Regional variation in percutaneous penetration of [14C] cortisol in man. J Invest Dermatol 1967; 48:181–183.
2. Maibach HI, Feldmann RJ, Milby TH, Sert WF. Regional variation in percutaneous penetration in man. Arch Environ Health 1971; 23:208–211.
3. Wester RC, Maibach HI. In vivo percutaneous absorption and decontamination of pesticides in humans. J Toxicol Environ Health 1985; 16:25–37.
4. Van Rooy TGM, De Roos JHC, Bodelier-Bode MD, Jongeneelen FJ. Absorption of polycyclic aromatic hydrocarbons through human skin: differences between anatomic sites and individuals. J Toxicol Environ Health 1993; 38:355–368.
5. Guy RH, Maibach Hl. Calculations of body exposure from percutaneous absorption data. In: Bronaugh R, Maibach H, eds. Percutaneous Absorption. New York: Marcel Dekker, 1985:461–466.
6. Rougier A, Dupuis D, Lotte C, Roquet R, Wester RC, Maibach HI. Regional variation in percutaneous absorption in man: measurement by the stripping method. Arch Dermatol Res 1986; 278:465–469.
7. Wertz PW, Swartzendruber DC, Squier CA. Regional variation in the structure and permeability of oral mucosa and skin. Adv Drug Deliv Rev 1993; 12:1–12.
8. Shriner DL, Maibach HI. Regional variation of nonimmunological contact urticaria. Skin Pharmacol 1996; 348:1–11.
9. Wester RC, Maibach HI. Individual and regional variation with in vitro percutaneous absorption. In: Bronaugh R, Maibach H, eds. Vitro Percutaneous Absorption. Boca Raton, FL: CRC Press, 1991:25–30.
10. Rothman S. Insensible water loss. In: Rothman S, ed. Physiology and Biochemistry of the Skin. Chicago: The University of Chicago Press, 1954:233–243.
11. Guyton AC. Textbook of Medical Physiology. Philadelphia, WB: Saunders Co, 1991:274–275.
12. Pinson EA. Evaporation from human skin with sweat glands inactivated. Am J Physiol 1942; 137:492–503.
13. Winsor T, Burch GE. Different roles of layers of human epigastric skin on diffusion rate of water. Arch Int Med 1944; 74:428–436.
14. Blank IH. Factors which influence the water content of the stratum corneum. J Invest Dermatol 1952; 18:433–440.
15. Blank IH. Further observations on factors which influence the water content of the stratum corneum. J Invest Dermatol 1953; 21:259–269.
16. Kligman AM. The biology of the stratum corneurn. In: Montagna W, Lobitz WCJ, eds. The Epidermis. New York: Academic Press, 1964:387–433.

17. Frost P, Weinstein GD, Bothwell JW, Wildnauer R. Icthyosiform dermatoses III. Studies of transepidermal water loss. Arch Dermatol 98:230–233.
18. Punnagoda J, Tupker RA, Agner T, Serup J. Guidelines for transepidermal water loss (TEWL) measurement. A report from the standardization group of the European Society of Contact Dermatitis. Contact Dermat 1990; 22:64–178.
19. Baker H, Kligman AM. Measurement of transepidermal water loss by electrical hygrometry. Instrumentation and responses to physical and chemical insults. Arch Dermatol 1967; 96:441–452.
20. Martini MC, Cotte J. Influence des produits hygroscopiques et occlusifs sur l'evaporation in vivo de l'eau du stratum corneum. Lab Pharma Probl Technol 1982; 30:547–553.
21. Panisset F, Treffel P, Faivre B, Lecomte PB, Agache P. Transepiermal water loss related to volar forearm sites in humans. Acta Derm Vencreol (Stockh) 1994; 72:4–5.
22. Sam VV, Passet J, Maillois H, Guillot B, Guillot JJ. TEWL measurement standardization: kinetic and topographic aspects. Acta Derm Venereol (Stockh) 1994; 74:168–170.
23. Lotte C, Rougler A, Wilson DR, Maibach HI. In vivo relationship between transepidermal water loss and percutaneous penetration of some organic compounds in man: effect of anatomic site. Arch Dermatol Res 1987; 279:351–356.
24. Aalto-Korte K, Turnpeinen M. Transepidermal water loss and absorption of hydrocortisone in widespread dermatitis. Br J Dermatol 1993; 128:633–635.
25. Nangia A, Berner B, Maibach HI. Transepidermal water loss measurements for assessing skin barrier function during in vitro percutaneous absorption studies. In: Bronaugh R, Maibach H, eds. Percutaneous Absorption, 3d ed. New York: Marcel Dekker, 1999:587–594.
26. Chilcott RP, Dalton CH, Emmanuel AJ, Allen CE, Bradley ST. Transepidermal water loss does not correlate with skin barrier function in vitro. J Invest Dermatol 2002; 118:871–875.

39

Natural Nano-Injectors as a Vehicle for Novel Topical Drug Delivery

Tamar Lotan
NanoCyte, Inc., Research Center, Jordan Valley, Israel

I. INTRODUCTION

The stratum corneum (SC) is the main obstacle for topical drug delivery. To overcome this tough thick barrier and to improve the permeability of the skin, a variety of vehicles and technologies have been developed. We looked at nature, seeking biological structures that can easily penetrate the SC.

The main parameters for selecting such a biological structure were:

1. proven ability to penetrate the SC,
2. a human-safe structure,
3. availability of the biological structure,
4. self-activation – no need for an active device operation,
5. compatibility with drugs and active compounds.

A biological structure fulfilling all the above criteria is the Cnidaria nano-injector. This structure has a capability to penetrate the skin at 40,000 $\times$ g using a sophisticated nano-injection system. The Cnidaria phylum, consisting of hydra, sea anemone, coral, and jellyfish, is one of the most primitive multicellular organisms dated 700 million years ago. The cnidarians are characterized by their stinging cells that serve various functions such as prey capture, defense, and locomotion. The stinging cells manufacture intracellular structure known as cnidocyst, which is composed of a capsule containing a folded nano-injector. The Cnidaria nano-injection structure has the capability to penetrate the hard cuticule of arthropod as well as human skin. There are more than 10,000 members in the Cnidaria phylum; several, such as the jellyfish, are highly toxic to humans, but most members are harmless to humans (1). The cells consisting of the nano-injectors are being continuously reproduced, and can count up to 45% of the total Cnidaria cells (2,3). The nano-injectors can operate independently, outside the living cells and, thus, can be isolated and kept as a powder. In the following the nano-injector structure is described and its implication for topical drug delivery is demonstrated.

II. PRINCIPLE OF OPERATION

Cnidocysts have been a subject for research since the 18th century. Leeuwenhoek, in 1703, was the first one to observe the cnidocysts in the hydra, but it took another 40 years to discover their ability to discharge and inject out the nano-injector (4).

The basic structure of the cnidocyst consists of a capsule, a nano-injector, and a matrix. The assembly of the capsule is a three-step process, which is done in the post-Golgi vacuole (5). First, the capsule is formed; secondly, a long tubule starts to grow and elongates outside the capsule. Once the capsule reaches its final size the tubule connects with the capsule wall and invaginates into the capsule to form the folded nano-injector. As the length of the nano-injector can reach up to 50 times the capsule dimension, the nano-injector is highly packed within the capsule (Fig. 1).

At the last stage the capsule is sealed by a specific cover and is filled with high concentrations of poly-γ-glutamate matrix (6,7). This type of condensed structure requires the capsule wall to have a high tensile strength, nearly that of steel (8,9). The wall of the capsule as well as the nano-injector is made of fibrils of short collagen known as minicollagen (10). The distribution of the fibrils along the capsule provides the tensile strength necessary to withstand the high osmotic pressure in the capsule. Nevertheless, the capsule wall is permeable to solutions and essentially performs like a porous net, thus permitting free movement of small molecular weight solutions (11), whereas within the capsules, a large matrix of poly γ glutamate is trapped.

The high internal pressure that develops within the capsule is a result of an interaction between the poly γ glutamate and a high concentration of divalent or monovalent cations. It was demonstrated that the cationic content of the capsule can be changed without impairing the functionality of the capsule. However, divalent cations result in lower internal pressure than monovalent cations (2,12,13).

In nature the capsule is embedded within the cytoplasm of the cell and only upon combined chemical and mechanical stimuli of the cell, the capsule will discharge and inject the nano-injector (14,15). During the activation process the condensed packaging of the poly γ glutamate dissociates and the internal osmotic pressure increases to 150 bar, generating high water flow into the capsule. As a result the cover of the one opening of the capsule flaps open, giving way to the racing nano-injector

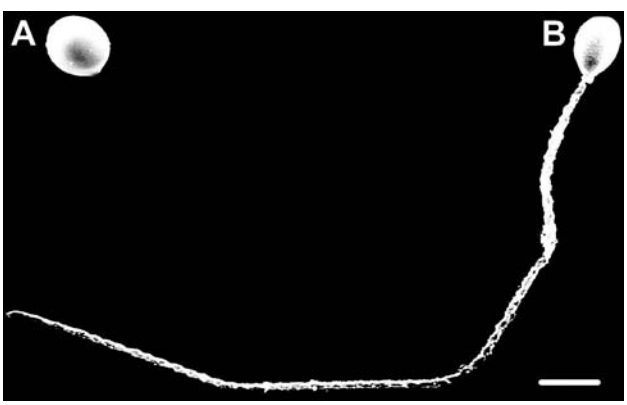


Figure 1 Electron micrograph of capsule before and after activation. The long nano-injector is highly folded within the capsule (**A**). After the nano-injector is released its length is about 20 times the diameter of the capsule (**B**). Scale bar, 10 μm.

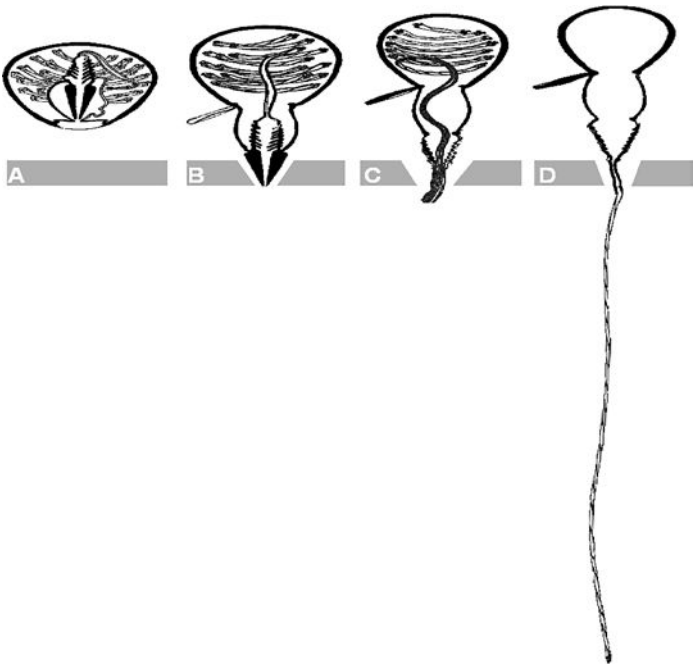


Figure 2 Capsule mode of operation. (**A**) The capsule at the inactive state. (**B**) High internal pressure of 150 bar is built in the microcapsule. (**C**) With 40,000 × g of acceleration, the nano-injector penetrates the skin. (**D**) The drug is delivered through the nano-injector into the epidermis/dermis. *Source:* Modified from Tardent and Holstein 1982 (17).

(Fig. 2). Using high-speed cinematography it was shown that the nano-injector is injected at high acceleration of 40,000 × g. The discharge process is completed in about three milliseconds and is considered to be one of the fastest events in cell biology (16).

Among the different Cnidaria species there are about 30 types of capsules; all act according to a common principle, but differ in their size, shape, and length of the nano-injector (3) (Fig. 3). These vary from 50 to 800 μm in length and up to 1 or 2 μm in diameter, enabling painless and accurate penetration to different layers of skin. With these physical characteristics the nano-injector is an optimal vehicle for drug delivery.

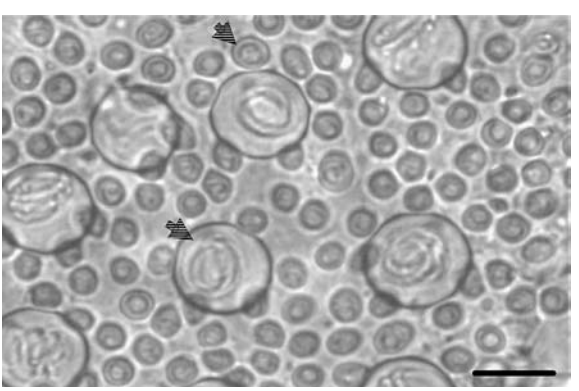


Figure 3 Round-shaped capsules of 15 and 3 μm diameter. The arrow points to the folded nano-injector within the capsule. Scale bar, 10 μm.

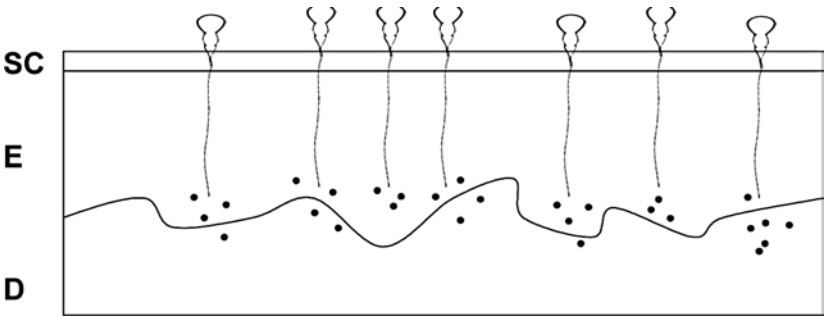


Figure 4 Schematic model of capsules penetrating the skin and delivering the drug directly to the epidermis. The drug is pumped through the capsule to the nano-injector and is released in the epidermis.

III. TOPICAL FORMULATION AND APPLICATION

The capsules can be isolated from the living cells, purified, and sterilized without impairing their injection and penetration capability. Due to their high-condensed content, the capsules' density is higher than regular cells. Once the tissue surrounding the capsules is loosened, the capsules can be purified based on their high density. The purified capsules can be sterilized by ethanol, UV or γ radiation. At the end of the process they can be kept as a powder or in formulation. The nano-injector structure can be formulated in various forms, including suspension, lotion, cream, or stick, and it can also be attached to an adhesive patch. Nevertheless, in order to keep the structure active the formulation should be water-free. When the nano-injectors are applied to the skin they are at the inactive state. Activation occurs as a result of wetting the dried, waterless capsules. This is done while adding the drug in a solution/gel over the capsules (Fig. 4).

As the activation process is immediate, the entire application is completed in less then five minutes. The formulation is a key issue in the application of the nano-injector structure as it should keep the capsules in contact with the skin and in a ready-to-operate state.

IV. HUMAN SAFETY

Sea anemone was targeted as a known safe-to-human prototype specie.

Anemones' capsules were extracted and formulated in oil-ethanol liquid formulation for the safety studies.

A. Dermal Irritation

The nano-injectors were tested in a single-patch primary dermal irritation study in 100 volunteers (total 16 males and 84 females). The human volunteers were patched on the back for 48 hours. Application sites were graded for dermal response at 1, 24, and 48 hours after removal of test material, using a scoring structure ranging from zero (negative and normal skin) to four (a bullous reaction). All sites were graded at all time points as zero.

B. Sensitization Test

A repeat insult patch test was done with 30 human volunteers (four males and 26 females). Each of 30 human volunteers was repeatedly (10 applications) occlusively patched with the test material for 24 consecutive hours. After the 10th application, no response indicative of either a contact dermal irritation or sensitization was seen at 20 minutes or 24 or 48 hours after patch removal in any of the individuals tested.

The above results showed no potential for either cumulative contact irritation or sensitization in humans.

V. IMMEDIATE DELIVERY

Because of the high internal pressure that develops in the capsule, water is pumped into the capsule up to the point when the capsule injects the nano-injector. Therefore, during the activation of the nano-injector structure the drug is delivered from the surrounding application to the capsule, triggering the opening of the capsule cover and ending up injecting through the nano-injector to the skin. To demonstrate immediate delivery into the skin the nano-injector structure was tested with a blue dye for visual results. The nano-injectors were applied in vivo on the backs of rabbits (Fig. 5). The dye solution was put over control skin and nano-injector applied skin. After one minute the skin was thoroughly washed and wiped. The results demonstrated that while the dye was completely washed from the control site, the nano-injector structure penetrated the skin and delivered the blue dye *trans*-cutaneously.

Immediate delivery of active compounds is commonly associated with syringes. However, with the Cnidaria nano-injector structure it is possible to immediately deliver an active to the epidermis via topical formulation.

VI. INDUCTION OF LOCAL ANESTHESIA

The induction of immediate local anesthesia by topical application is sought by surgeons. Therefore, we tested the nano-injector vehicle with lidocaine-HCl. The physiological effect was evaluated using a prick test. The nano-injector structure

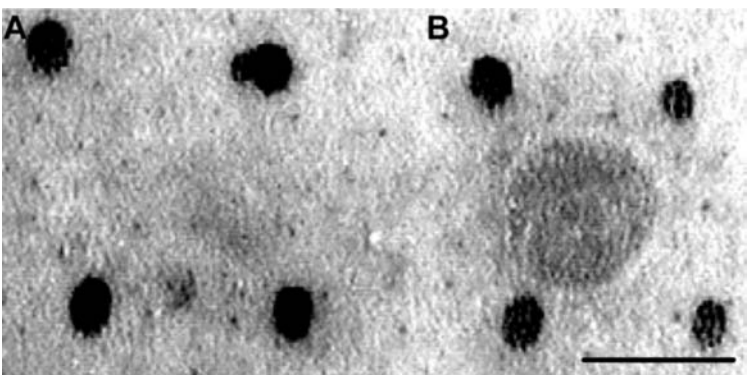


Figure 5 Immediate delivery of dye into the skin. Dye with or without capsules application was applied for one minute on the back of a rabbit, washed thoroughly, and photographed. (**A**) Control—application of dye to the skin. (**B**) Test application of dye with capsules. Scale bar, 1.0 cm.

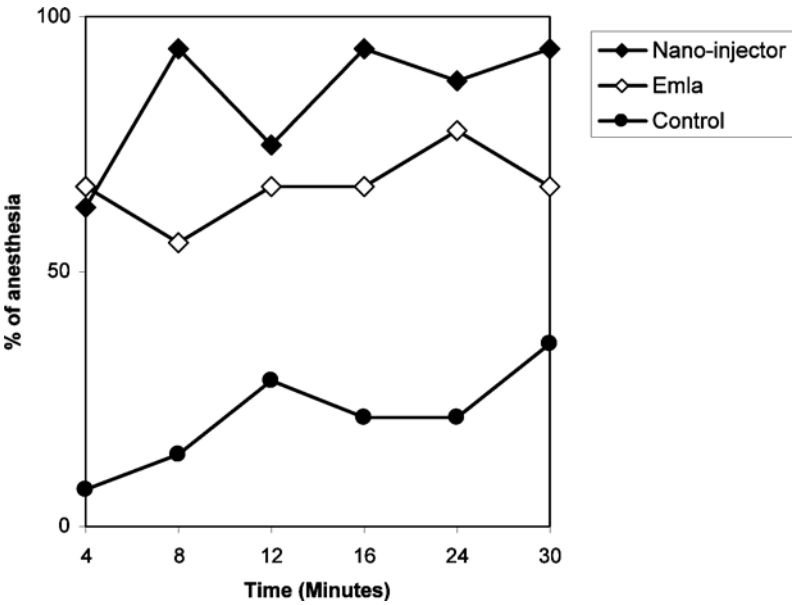


Figure 6 Induction of immediate anesthesia. Time (minutes) from capsules application versus percent of cases resulting in anesthesia, $n \geq 9$. Emla was put one hour before anesthesia was tested.

was compared to emla, a combination of 2.5% lidocaine and 2.5% prilocaine topical cream. However, emla was applied one hour before the experiment commenced, in line with the product guidance. The nano-injectors were applied over the skin and activated with 2% lidocaine-HCl. Two minutes after application, the sites were rinsed with water and wiped. Anesthesia was tested every 4 minutes up to 30 minutes (Fig. 6). The results demonstrated that the nano-injector structure was effective after four minutes of application, similar to emla that required 60 minutes of application prior to inducing local anesthesia.

VII. DISCUSSION

The nano-injection structure is a novel delivery platform derived from a biological source. Initial safety and efficacy was shown with the structure. The compatibility of the structure with hydrophilic compounds is attractive as these are the most difficult molecules to penetrate the skin. The ability to induce immediate local anesthetics is intriguing as well as the potential to deliver locally chemotherapic drugs. The power of the nano-injectors in penetrating hard surfaces as well as the possibility to choose the length of the nano-injector make it an attractive vehicle to deal with severe dermatology conditions.

REFERENCES

1. Lotan A, Fishman L, Loya Y, Zlotkin E. Delivery of a nematocyst toxin. Nature 1995; 375:456.
2. Tardent P. The cnidarian cnidocyte, a high-tech cellular weaponry. Bioessays 1995; 17:351–362.

3. Kass-Simon G, Scappaticci AA. The behavioral and developmental physiology of nematocysts. Can J Zool 2002; 80:1772–1794.
4. Hessinger DA, Lenhoff HM, eds. The Biology of Nematocysts. San Diego, CA: Academic Press Inc., 1988.
5. Engel U, Pertz O, Fauser C, Engel J, David CN, Holstein TW. A switch in disulfide linkage during minicollagen assembly in Hydra nematocysts. EMBO J 2001; 20:3063–3073.
6. Weber J. Ploygamma-glutamic acids are the major constiuents of nematocysts in hydra (hydrazoa, cnidaria). J Biol Chem 1990; 265:9664–9669.
7. Szczepanek S, Cikala M, David CN. Poly-gamma-glutamate synthesis during formation of nematocyst capsules in Hydra. J Cell Sci 2002; 115:745–751.
8. Holstein TW, Benoit M, Herder GV, Wanner G, David CN, Gaub HE. Fibrous minicollagens in hydra nematocysts. Science 1994; 265:402–404.
9. Ozbek S, Engel U, Engel J. A switch in disulfide linkage during minicollagen assembly in hydra nematocysts or how to assemble a 150-bar-resistant structure. J Struct Biol 2002; 137:11–14.
10. Kurz EM, Holstein TW, Petri BM, Engel J, David CN. Mini-collagens in hydra nematocytes. J Cell Biol 1991; 115:1159–1169.
11. Lubbock R, Amos WB. Removal of bound calcium from nematocyst contents causes discharge. Nature 1981; 290:500–501.
12. Weber J. Nematocysts (stinging capsules of Cnidaria) as Donnan-potential-dominated osmotic systems. Eur J Biochem 1989; 184:465–476.
13. Hidaka M, Afuso K. Effects of calcium on the mechanical properties of the capsule wall of isolated nematocysts from *calliactis polypus*. Comp Biochem Physiol A 1994; 107A: 31–36.
14. Watson GM, Hessinger DA. Cnidocyte mechanoreceptors are tuned to the movements of swimming prey by chemoreceptors. Science 1989; 243:1589–1591.
15. Muir Giebel GE, Thorington G, Lim RY, Hessinger D. Control of cnida discharge: II. Microbasic p-mastigophore nematocysts are regulated by two classes of chemoreceptors. Biol Bull 1988; 175:132–136.
16. Holstein T, Tardent P. An ultrahigh-speed analysis of exocytosis: nematocyst discharge. Science 1984; 223:830–833.
17. Tardent P, Holstein T. Morphology and morphodynamics of the stenotele nematocyst of Hydra attenuata Pall. (Hydrozoa, Cnidaria). Cell Tissue Res. 1982; 224:269–290.

40

Human Risk Assessment of Chemical Warfare Agents from Skin Exposure*

Ronald C. Wester, Hanafi Tanojo, Xiao-Ying Hui, Hongbo Zhai, and Howard I. Maibach
Department of Dermatology, School of Medicine, University of California, San Francisco, California, U.S.A.

Eugene Olajos and Harry Salem
Aberdeen Proving Grounds, Aberdeen, Maryland, U.S.A.

I. ABSTRACT

The objective was to perform analysis on existent dermal absorption data on selected organophosphorus (OP) compounds including chemical warfare agents (CWA)—sarin (GB), soman (GD), and VX—and develop a postulate of critical factors in observed regional differences in toxicant uptake/absorption by human skin. Body contours for skin absorption and lethality were developed. Parathion and malathion exposed head and neck region (×4), trunk (×3) and genital area (×12) absorb more chemical than arms and hands, and legs and feet. In field userparathion has caused human death, while malathion is considered safe. Human skin is more permeable to parathion than malathion. Permeability constants (Kp) (potential chemical absorbed through human skin per unit area and time) indexed to regional variation gives the mass of chemical absorbed through all regions of the human body. Further overlap of toxicity data to the constant showed lethality with parathion but not for malathion. VX has a high Kp and is also the most toxic; 50% lethality is reached when exposure is to any single region of the body. Sarin and soman are less toxic percutaneously than VX and they have the same toxicity level. However, soman has greater skin absorption than sarin. Estimate of 50% lethality is only reached for sarin at the 24-hour exposure level, whereas the 50% lethality estimate for soman is reached in the first hour.

Chemical warfare agents are a serious threat to human life. In order to minimize or prevent the hazard of these agents, an understanding of the way that these chemicals get on to and into the human body is needed for both military function and protection of life.

* Government sponsorship of the research upon which this publication is based does not constitute endorsement of the results or conclusions presented here.

II. INTRODUCTION

Percutaneous absorption is defined as the rate and extent that a chemical is absorbed into and through the skin and into the systemic circulation. Definitive percutaneous absorption models are needed to understand the exposure time course of absorption and toxicity of chemical warfare agents (CWA). These models are needed for response personnel, be it targeted military or first responders such as police, firefighters, medical emergency and good Samaritans. In all cases, the skin, be it fully exposed (head, arms, and hands) or clothed, is assaulted and the chemical will absorb through the skin. The skin forms the final barrier between the "outside" and the "inside" of the body. Model design needs a comprehensive understanding of body contours and percutaneous absorption. The objective was to review and perform data analysis/reduction on existent dermal absorption data on various chemicals including organophosphates and selected chemical warfare agents—such as GB, GD, VX, and sulfur mustard (HD)—and develop a postulate regarding the role of critical factors in the observed regional differences in toxicant uptake/absorption by the skin. Variables to the analyses are reviewed and a model system showing percutaneous absorption and toxicity are presented.

A. Regional Variation Human Percutaneous Absorption

The first occupational disease in recorded history was scrotal cancer in chimney sweepers (1). The historical picture of a male worker holding a sweeper and covered from head to toe with black soot in vivid. But why the scrotum? Percutaneous absorption in man and animals varies depending on the areas of the body in contact with a chemical. This is called regional variation. When a certain skin area is exposed, any effect of the chemical will be determined by how much is absorbed through the skin. Feldmann and Maibach (2) first showed regional variation with the absorption of parathion. The scrotum was the highest-absorbing skin site (leading to scrotal cancer in chimney sweeps). Among other body sites, skin absorption was lowest for the foot area, and higher around the head and face area (Table 1).

Table 1 Effect of Anatomical Region on In Vivo Percutaneous Absorption of Hydrocortisone and the Two Pesticides Parathion and Malathion in Human Volunteers

	Dose absorbed (%)		
Anatomical region	Hydrocortisone	Parathion	Malathion
Forearm	1.0	8.6	6.8
Palm	0.8	11.6	5.8
Foot, ball	0.2	13.5	6.8
Abdomen	1.3	18.5	9.4
Hand, dorsum	—	21.0	12.5
Forehead	7.6	36.3	23.2
Axilla	3.1	64.0	28.7
Jaw angle	12.2	33.9	69.9
Fossal cubitalis	—	28.4	
Scalp	4.4	32.1	
Ear canal	—	46.6	
Scrotum	36.2	101.6	

Parathion and malathion are chemically related to some chemical warfare agents, and those skin areas that would be exposed openly to the pesticides, the head and face, were of the higher absorbing sites. Guy and Maibach (3) took the hydrocortisone and parathion/malathion data and constructed penetration indices for five anatomical sites. The indices can be used with total body surface areas to estimate systemic availability relative to body exposure sites. Other studies have confirmed regional variation in man as well as in animals (4).

B. Percutaneous Absorption from Chemicals in Clothing

Military and civilian alike will be wearing some form of clothing during chemical warfare exposure. Basic question is whether clothing is protective, semi-protective, or a conduit for chemical deliveries to the skin. Chemicals in cloth cause cutaneous effects; for example, Hatch and Maibach (5) reported that chemicals added to cloth in 10 finish categories (dye, wrinkle resistance, water repellency, soil release, and so on) caused irritant and allergic contact dermatitis, atopic dermatitis exacerbation, and urticarial and phototoxic skin responses. This is qualitative information that chemicals will transfer from cloth to skin in vivo in humans. Snodgrass (6) studied permethrin transfer from treated cloth to rabbit skin in vivo. Transfer was quantitative but less than expected. Interestingly, some permethrin remained within the cloth after detergent laundering. In other studies (7), In vitro percutaneous absorption of glyphosate and malathion through human skin were decreased when added to cloth (the cloth then placed on skin) and this absorption decreased as time passed over 48 hr. When water was added to glyphosate/cloth and water/ethanol to malathion/cloth, the percutaneous absorption increased (malathion to levels from solution). This perhaps reflects clinical situations where dermatitis occurs most frequently in human sweating areas (axillia and crotch). Wester et al. (8) further showed that a CWA simulant (parathion) will diffuse through army uniform into and through skin, and the diffusion is enhanced with moisture (rain and sweating).

C. Chemical Warfare Agents

The CWA are comprised of incendiary mixtures, smokes, or irritant burning, poisonous, or asphyxiating gases that have a long history of use since World War I in 1917 (9). The field behavior of CWA is dependent on weather variable such as wind, temperature, air stability, humidity, and precipitation. The CWA may appear in the field in different forms: vapors, aerosols, or liquids. One classification as used by the U.S. Army are: (a) blood agents, (b) nerve agents, (c) choking agents, (d) blister agents, (e) incapacitating agents, (f) tear gases, and (g) vomiting gas (9). The CWA are also subdivided into non-persistent and persistent agents. Persistent agents such as HD pose a threat for many days after release. The HD exists normally as an oily liquid that is vaporized by explosive blasts and persists in the environment for a prolonged period, dependent on climatic factors. HD is highly potent cytotoxic alkylating agent that is strongly vesicating (9–13). Topical exposure to HD results in erythema appearing within hours followed by edema, blistering, and ulceration. Systemic toxicity from HD may contribute to the high incidence of secondary infections and it may be fatal (9). Because HD is an important vesicant (blister) agent, it has found widespread use as a CWA. HD has reemerged as a major threat around the world in recent years; therefore, most studies have focused on prevention of HD injuries (9–18).

Non-persistent volatile agents such as nerve agents produce casualties in inadequately protected personnel. These CWA are OP chemicals. Organophosphorous chemicals were developed for agricultural use as pesticides. Parathion and malathion have a long history of use; malathion is still used for pest control (19). The extremely potent organophosphorous chemicals, tabun (GA), GD, GB, and VX found potential use as CWA. These nerve agents achieve their primary effects by phosporylating or phosphonylating the serine hydroxyl at the active site of the enzyme AchE, producing irreversible inhibition of the enzyme with consequent elevation of Ach levels. Acetylcholine accumulates in the peripheral and central nervous system leading to cholinergic manifestations. At high doses, there is depression of the respiratory center in the brain, followed by peripheral neuromuscular blockade, causing respiratory paralysis and death.

D. Structure and Toxicity

Table 2 gives the structures and toxicity of nerve agents and related compounds. Sarin and soman are organophosphorous compounds with a similar chemical structures, as are mipafox, dimefox, and DFP (Table 2). Slight modification in molecular structure can have a profound effect on toxicity. For example, in the mouse IPR test, sarin is more toxic that mipafox (×32), dimfox (×3), and DFP (×5.8) (20–25).

Table 3 shows the molecular structure of VX and other organophosphorous compounds. Again, the toxicity of each compound will vary in toxicity relative to its chemical structure. Note that parathion and malathion are in this group, two chemicals for which human regional variation percutaneous absorption was previously discussed. Parathion is considered to be of high toxicity while malathion is considered to be of low toxicity. These two organophosphorous compounds of similar molecular structure and divergent level of toxicity are of the same class as the organophosphorous chemical warfare agents (26–43).

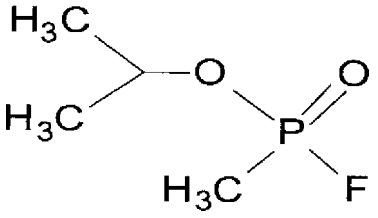
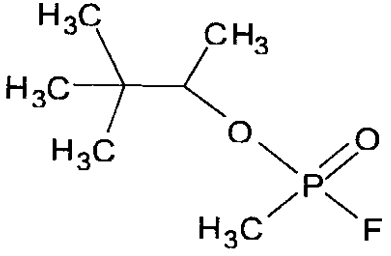
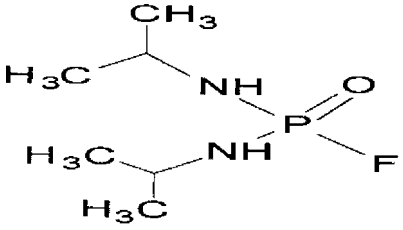
E. Structure and Percutaneous Absorption

The toxic effectiveness of a chemical warfare agent is dependent upon the inherent toxicity of the molecular structure and its bioavailability. Bioavailability is defined as the rate and amount of a chemical that is delivered to the biological site of action.

Bioavailability can be from many routes of exposure. This paper is limited to the skin route, percutaneous absorption.

Tables 4 and 5 show the molecular structure of the chemical warfare agents and related compounds, and lists percutaneous absorption data for each, including a derived permeability coefficient. The permeability coefficients (Kp) is a flux value, normalized for concentration, that represents that rate at which the chemical penetrates the skin (cm/hr). Kp values are laboratory (in vitro experiment and/or computer derived) and represent an average value; they do not take human regional percutaneous absorption into account. Where P is the octanol:water partition coefficient expressed as log base 10 and gives the lipophiiicity of a chemical of a chemical. log P of sarin is 0.45, meaning three molecules reside in octanol for each one in water. Soman is more lipophilic; log P of 1.78 = a 60:1 ratio. VX is still more lipophillic, log P of 2.22 = 166:1 ratio. Very lipophilic chemicals such as DDT with a log P of 6.91 have an 8 million to one ratio. As a general rule, lipophilicity with some water solubility equates to good percutaneous absorption. The human stratum corneum is lipophilic. The epidermis become progressively less lipophilic, to hydrophilic

Table 2 Toxicity of Organophosphorus Compounds Similar to Sarin and Soman

Structure	Name	Toxicity
	Sarin (GB); isopropyl methylphosphonofluoridate; Mol. wt.: 140.09	Human: LCt50:100 mg min/m^3; LD50 (skin); 12.5 mg/70-kg (44). Mouse: IPR LD50: 0.42 mg/kg.
	Soman (GD); pinacolyl-methylphosphonofluoridate; Mol. wt.: 182.17	Human: LCt50: 50 mg min/m^3; LD50 (skin); 12.5 mg/70-kg (44).
	Mipafox; *N*, *N*′-*bis*(1-methylethyl)-phosphordiamidic fluoride; CAS: 371-86-8; Mol. wt.: 182.18	Mouse: IPR LD50: 13.5 mg/kg (20) Rat: IPR LD50: 105.7 mg/kg (20) Chicken: IPR LD50: 35.4 mg/kg (20).

(*Continued*)

Table 2 Toxicity of Organophosphorus Compounds Similar to Sarin and Soman (*Continued*)

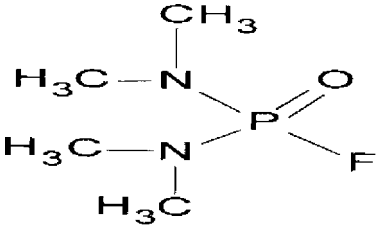
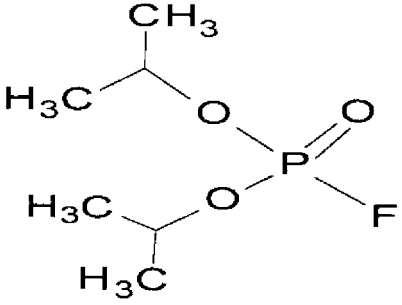
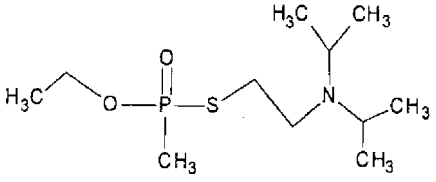
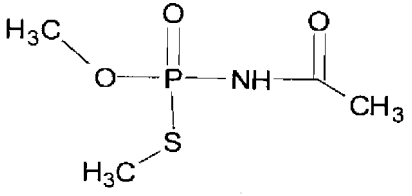
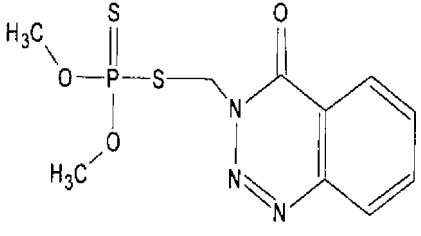
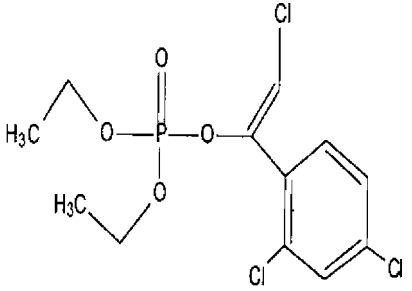
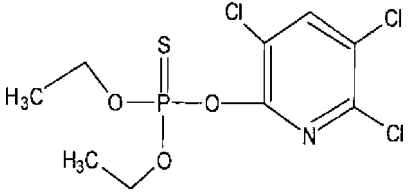
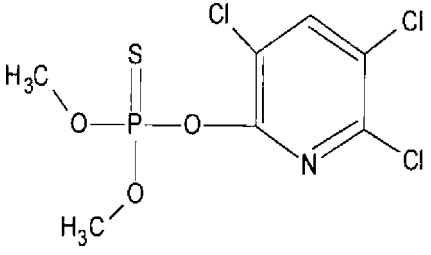
Structure	Name	Toxicity
	Dimefox; tetramethylphosphoro-diamidic fluoride; Mol. wt.: 154.12; CAS: 115-26-4	Rat: oral LD50: 7.5 mg/kg (21); other strain 1.8 mg/kg (22); IPR LD50: 5 mg/kg (21,23). Mouse: IPR LD50: 1.4 mg/kg (21,23). Guinea pig: IPR LD50: 2.5 mg/kg (21,23). Dog: IPR LD50: 5–10 mg/kg (21,23).
	DFP; DIFP; Diisopropyl fluorophosphate; Mol. wt.: 184.15	Rat: oral LD50: 5 mg/kg; IPR LD50: 1.280 mg/kg; SCU LD50: 1.440 mg/kg; IMS LD50: 1.800 mg/kg (24,25). Mouse: oral LD50: 2 mg/kg; IHL LC50: 440 mg/$m^3$10 min; skin LD50: 72 mg/kg; IPR LD50: 2.450 mg/kg; SCU LD50: 3 mg/kg. Rabbit: oral LD50: 4 mg/kg; SCU LD50: 1 mg/kg; IVN LD50: 0.300 mg/kg.

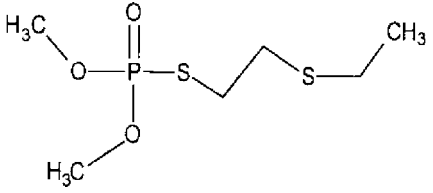
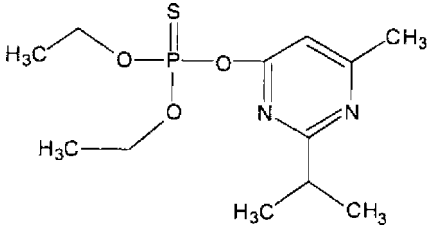
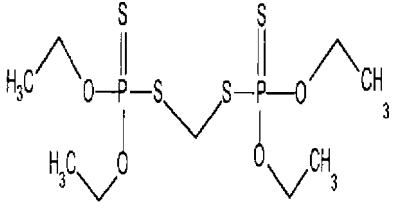
Table 3 Study of Organophosphorus Compounds Similar to VX

Structure	Name	Toxicity
	VX; S-[2-[*bis*(1-methylethyl) amino]ethyl) -*O*-ethyl; Mol. wt.: 267.37 C11 H26 N O2 P S	Human: LCt50: 10 mg min m^3; LD50 (skin) 6.5 mg/70-kg (44).
	Acephate; O,S-Dimethyl *N*-acetylphosphoramidothioate; CAS: 30560-19-1; Mol. wt.: 183.17; RTECS #: TB4760000	Rat: oral LD50: 700 mg/kg (26); skin LD50: >2500 mg/kg. Mouse: oral LD50: 233 mg/kg. Rabbit: skin LD50: 2000 mg/kg.
	Azinphos-methyl; O,O-Dimethyl S-[4-oxo-1,2,3-benzotriazin-3(4H)-yl)-methyl phosphorodithioate; CAS: 86-50-0; Mol. wt.: 317.33; RTECS #:TE 1925000	Rat: oral LD50: 7 mg/kg (27); IHL LC50: 69 mg/m3/1hr; skin LD50: 88 mg/kg; IPR LD50: 4900 ug/kg; IVN LD50: 7500 ug/kg; UNR LD50: 15 mg/kg. Mouse: oral LD50: 8600 µg/kg; Skin LD50: 65 mg/kg; IPR LD50: 4 mg/kg. Guinea pig: Oral LD50: 80 mg/kg; skin LD50: >280 mg/kg; IPR LD50: 40 mg/kg.

(*Continued*)

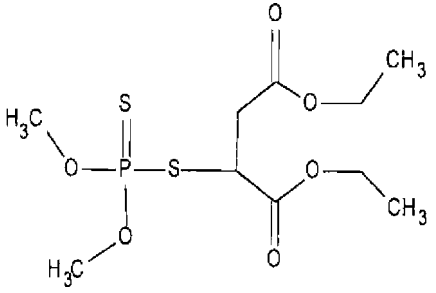
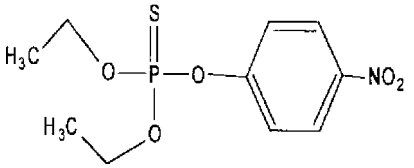
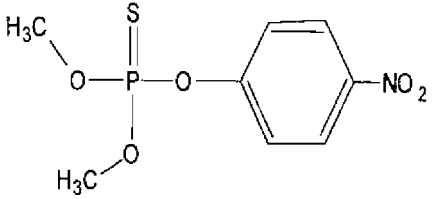
Table 3 Study of Organophosphorus Compounds Similar to VX (*Continued*)

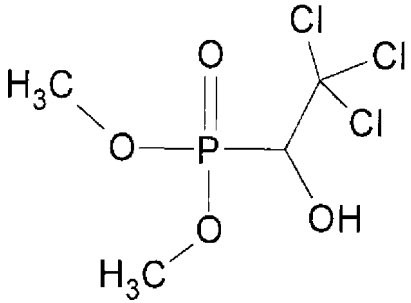
Structure	Name	Toxicity
	Chlorfenvinphos 2-Chloro-1-(2,4-dichlorophenyl)vinyl diethyl phosphate, CAS: 470-90-6; Mol. wt.: 359.57; RTECS #: TB8750000	Rat: oral LD50: 10 mg/kg (28); IHL LC50: 50 mg/m^3/4hr; skin LD50: 26.400 mg/kg; IPR LD50: 8.500 mg/kg; SCU LD50: 7 mg/kg; IVN LD50: 6.600 mg/kg. Mouse: oral LD50: 65 mg/kg; skin LD50: 336 mg/kg; IPR LD50: 87 mg/kg; SCU LD50: 339 mg/kg; IVN LD50: 87 mg/kg. Dog: oral LD50:1200 mg/kg; IVN LD50: 51 mg/kg. Rabbit: oral LD50: 300 mg/kg; skin LD50: 400 mg/kg
	Chlorpyrifos; *O,O*-Diethyl *O*-3,5,6-trichloro-2-pyridyl phosphorothioate; CAS: 2921-88-2; Mol. wt.: 350.59; RTECS #: TF6300000	Rat: oral LD50: 82 mg/kg (29); IHL LC50: > 200 mg/m3/4hr; skin LD50: 202 mg/kg. Mouse: oral LD50: 60 mg/kg; skin LD50: 120 mg/kg; IPR LD50: 192 mg/kg. Rabbit: oral LD50: 1,000 mg/kg; skin LD50: 2,000 mg/kg
	Chlorpyriphos-methyl *O,O*-Dimethyl *O*-(3,5,6-trichloro-2-pyridinyl) phosphorothioate; CAS: 5598-13-0; Mol. wt.: 322.54; RTECS #: TG0700000	Rat: oral LD50: 1828 mg/kg (30); IHL LC50: > 670 mg/m^3/4hr; skin LD50: 3,713 mg/kg; SCU LD50: 6,900 mg/kg; IVN LD50: 710 mg/kg. Mouse: oral LD50: 2032 mg/kg; skin LD50: > 2,800 mg/kg; IPR LD50: 2,325 mg/kg; SCU LD50: 23,800 mg/kg. Rabbit: oral LD50: 2 g/kg; skin LD50: > 2 g/kg. Guinea Pig: oral LD50: 2,250 mg/kg.

	Demeton-S-methyl; S-2-ethylthioethyl *O,O*-dimethyl phosphorothioate (25); CAS: 919-86-8; Mol. wt.: 230.29; RTECS® TG1750000	Oral-RAT LD50: 30 mg/kg (31); IHL-RAT LC50: 500 mg/m^3/4hr; skin-RAT LD50: 85 mg/kg; IPR-RAT LD50: 7,500 mg/kg; IVN-RAT LD50: 65 mg/kg.
	Diazinon *O,O*-Diethyl *O*-(2-isopropyl-6-methyl-4-pyrimidinyl) phosphorothioate; CAS: 333-41-5; Mol. wt.: 304.34	Rat: oral male LD50: 235–435 mg/kg (32–34); Oral female LD50: 285 mg/kg (3); Oral both LD50: 300–1,250 mg/kg (35,36); skin male LD50: 900 mg/kg (37); skin female LD50: 455 mg/kg (37); skin both LD50: $>$2,150 mg/kg (37).
	Ethion; *O,O,O,O,*-Tetraethyl S,S-methylene *bis*-(phosphorodithioate); CAS: 563-12-2; Mol. wt.: 384.48; RTECS®: TE4550000	Rat: oral LD50: 13 mg/kg; IHL LC50: 864 mg/m^3; skin LD50: 62 mg/kg; IPR LD50: 26 mg/kg; UNR LD50: 55 mg/kg. Mouse: oral LD50: 40 mg/kg; IPR LD50: 35 mg/kg. Guinea Pig: oral LD50: 40 mg/kg; skin LD50: 915 mg/kg (39). Rabbit: skin LD50: 915 mg/kg (29)

(*Continued*)

Table 3 Study of Organophosphorus Compounds Similar to VX (*Continued*)

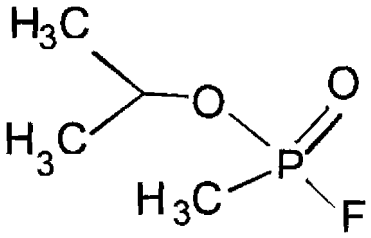
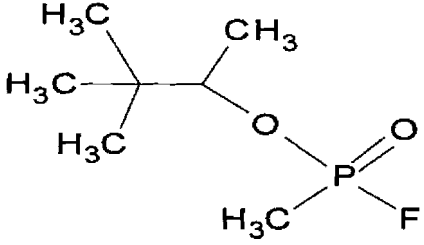
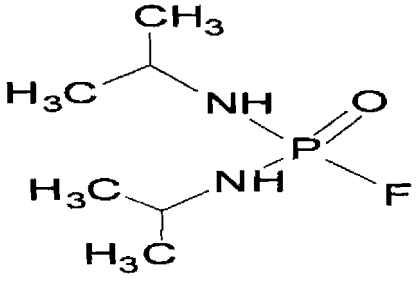
Structure	Name	Toxicity
	Malathion; *O,O*-Dimethyl S-1,2-*bis*(carbethoxyethyl) phosphorodithioate; CAS: 121-75-5; Mol. wt.: 330.36 RTECS #: WM8400000	Man: oral LDLO: 471 mg/kg. Woman oral LDLO: 246 mg/kg. Rat: oral LD50: 290 mg/kg; IHL LC50: 43790 ug/m3/4hr; skin LD50: >4444 mg/kg; IPR LD50: 250 mg/kg; SCU LD50: 400 mg/kg; IVN LD50: 50 mg/kg. Mouse: oral LD50: 190 mg/kg; skin LD50: 2330 mg/kg; IPR LD50: 193 mg/kg; SCU LD50: 221 mg/kg; IVN LD50: 184 mg/kg. Rabbit: skin LD50: 4100 mg/kg; SCU LD50: 280 mg/kg. Guinea Pig: Oral LD50: 570 mg/kg; skin LD50: 6700 mg/kg; IPR LD50: 271 mg/kg; SCU LD50: 450 mg/kg (40).
	Parathion; Parathion-ethyl; *O,O*-Diethyl O-(4-nitrophenyl) phosphorothioate; CAS: 56-38-2; Mol. wt.: 291.26 C10H14NO5PS	Rat: oral male LD50: 13–15 mg/kg (37,41); Oral female LD50: 3–3.6 mg/kg (37,41); skin Male LD50: 21 mg/kg (37); skin female LD50: 6.8 mg/kg (37).
	Parathion-methyl; *O,O*-Dimethyl O-(4-nitrophenyl) phosphorothioate; Mol. wt.: 263.21	Rat: oral male LD50: 14 (45)– 20 (34) mg/kg; Oral female LD50: 24 mg/kg (37); skin male LD50: 67 mg/kg (37); skin female LD50: 67 mg/kg (37). Mouse: SCU LD50: 30 mg/kg (42).

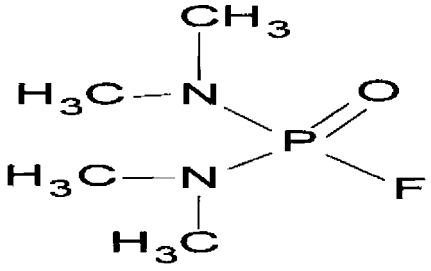
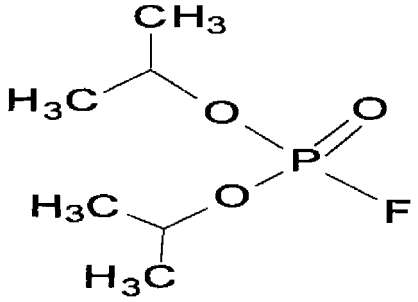


Trichlorfon; Metrifonate; Dimethyl 2,2,2-trichloro-1-hydroxyethylphosphonate; CAS: 52-68-6; Mol.wt: 257.44 RTECS #: TA0700000

Rat: oral LD50: 560 mg/kg; IHL LC50: 1,300 mg/m^3; skin LD50: 2,000 mg/kg; IPR LD50: 160 mg/kg; SCU LD50: 400 mg/kg; IMS LD50: 395 mg/kg. Mouse: oral LD50: 300 mg/kg; skin LD50: 1,710 mg/kg; IPR LD50: 196 mg/kg; SCU LD50: 267 mg/kg; IVN LD50: 290 mg/kg. Mammalian: Skin LD50: $>$2,800 mg/kg.

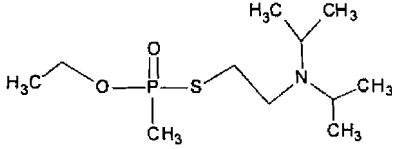
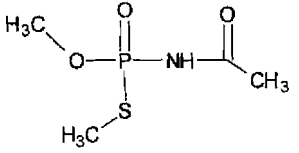
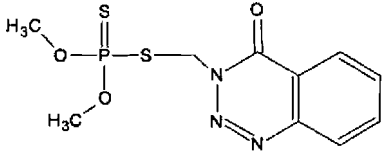
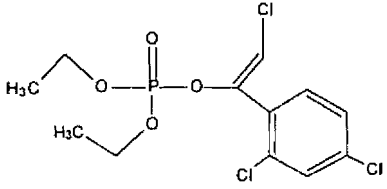
Table 4 Skin Absorption Data of Organophosphorus Compounds Similar to Sarin and Soman

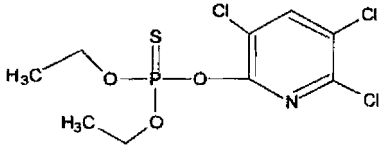
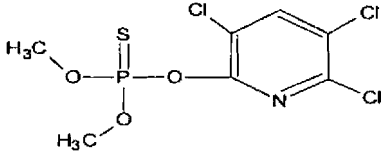
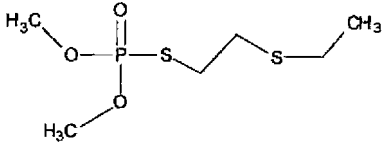
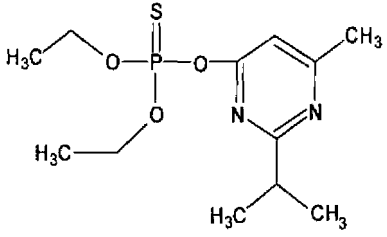
Structure	Name	Skin absorption	kp (cm/h)[a]	Log $P(K_{ow})$[b]
	Sarin (GB); isopropyl methylphosphonofluoridate; Mol. wt.: 140.09	Upon contact, 15–20 min asymptomatic interval before onset of effects (87)	5.31×10^{-4}	0.45
	Soman; pinacolyl-methylphosphonofluoridate; CAS: 96-64-0; Mol. wt.: 182.17	Upon contact, 15–20 min asymptomatic interval before onset of effects (87)	2.59×10^{-3}	1.78
	Mipafox; *N*,*N*'-*bis*(1-methylethyl)-phosphordiamidic fluoride; CAS: 371–86–8; Mol. wt.: 182.18		2.26×10^{-4}	0.29 (est 46)

	Dimefox; tetramethylphosphoro-diamidic fluoride; CAS: 115-26-4; Mol. wt.: 154.13		1.03×10^{-4}	− 0.43 (est.46)
	DFP; DIFP; Diisopropyl fluorophosphate; CAS: 55-91-4; Mol. wt.: 184.15	Absorption through skin is not tested, but systemic absorption through eye cornea is low (47–49)	8.69×10^{-4}	1.13 (est. 46)

[a]Based on the formula: $\log kp = -2.74 + [0.71 \times \log P(K_{ow})] - (0.0061 \times MW)$, where kp=permeability coefficient, $P(K_{ow})$ = partition coefficient in octanol compared to water, MW = molecular weight.
[b]$P(K_{ow})$ = partition coefficient in octanol compared to water.
(*Source*: From Ref. 68.)

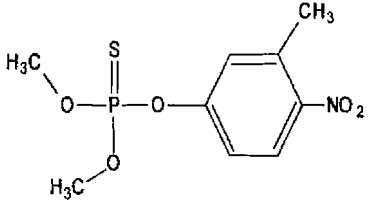
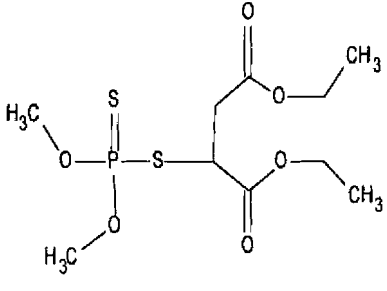
Table 5 Skin Absorption Data of Organophosphorus Compounds Similar to VX

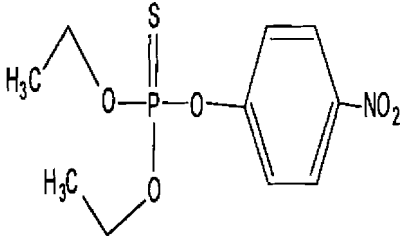
Structure	Name	Skin absorption	*k*p (cm/h)[a]	Log $P(K_{ow})$[b]
	VX; S-[2-[*bis*(1-methylethyl)amino]ethyl]-*O*-ethyl; CAS: 50782-69-9; Mol. wt.: 267.37		1.60×10^{-3}	2.22
	Acephate; *O*,*S*-Dimethyl *N*-acetylphosphoramidothioate; EC: 250-241-2; CAS: 30560-19-1; Mol. wt.: 183.17; RTECS #: TB4760000		3.24×10^{-5}	−0.89
	Azinphos-methyl; *O*,*O*-Dimethyl *S*-(4-oxo-1,2,3-benzotriazin-3(4H)-yl)-methylphosphorodithioate; CAS: 86-50-0; Mol. wt.: 317.33; RTECS #: TE1925000	Human: (forearm solvent) acetone 16%, 5 days (excretion analysis) (5)	2.67×10^{-3}	2.96
	Chlorfenvinphos; 2-Chloro-1-(2,4-dichlorophenyl)vinyl diethyl phosphate; CAS: 470-90-6; Mol. wt.: 359.57; RTECS #: TB8750000	Rabbit: non-irritating to skin and eyes (29)	6.31×10^{-3} 1.16×10^{-2}	3.85 (Z-isomer) 4.22 (E-isomer)

	Chlorpyrifos; *O,O*-Diethyl *O*–3,5,6-trichloro-2-pyridyl phosphoroth ioate; CAS: 2921-88-2; Mol. wt.: 350.59; RTECS #: TF6300000	Mouse (dermal) solvent: acetone (51)	2.87×10^{-2}	4.7
	Chlorpyriphos-methyl *O,O*-Dimethyl *O*-(3,5,6-trichloro-2-pyridinyl) phosphorothioate; CAS: 5598-13-0; Mol. wt.: 322.54; RTECS #: TG0700000	Irritation data rabbit: skin 500 mg/24h mild (52)	2.01×10^{-2}	4.24
	Demeton-*S*-methyl; *S*-2-ethylthioethyl *O,O*-dimethyl phosphorothioate (53); CAS: 919-86-8; Mol. wt.: 230.29; RTECS#: TG 1750000	Acute percutaneous LD50 for male rats 302 mg/kg (29)	6.20×10^{-4}	1.32
	Diazinon *O,O*-Diethyl O-(2-isopropyl-6- methyl-4-pyrimidinyl) phosphorothioate; CAS: 333-41-5; Mol. wt: 304.34	Rat male (dermal); solvent: THF; up to 144 hr; 1 mg/kg, t50 = 11.8 hr; 10 mg/kg, t50 = 10.2 hr (54). Rat female (dermal); solvent: THF; up to 144 hr; 1 mg/kg, t50 = 5.2 hr; 10 mg/kg, t50 = 5.3 hr (54). Sheep (shaved back); solvent: acetone; 3 days, 40 mg/kg (55,56). Human (ventral	5.58×10^{-3}	3.30

(*Continued*)

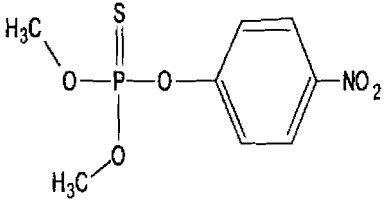
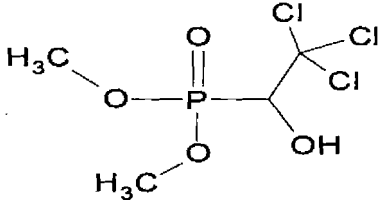
Table 5 Skin Absorption Data of Organophosphorus Compounds Similar to VX (*Continued*)

Structure	Name	Skin absorption	*k*p (cm/h)[a]	Log $P(K_{ow})$[b]
		forearm or abdomen); solvent: acetone (2 ug cm2) or lanolin wool grease (1.47 ug/cm2) 24 hr; only 3–4% absorbed (57)		
	Fenitrothion *O*,*O*-Dimethyl *O*-(3-methyl-4-nitrophenyl) phosphorothioate; CAS: 122-14-5; Mol. wt.: 277.24	Rhesus monkey (forehead) 49% (urinary excretion half-life 14 hr); Rhesus monkey (ventral forearm) 21% (urinary excretion half-life 17 hr); Rats (middorsal) 84% (urinary excretion half-life 20 hr). (58). DEET increased the absorption through rat skin (32% vs. 15% control in acetone) and monkey skin (9.7% vs. 3.2% control) (59).	6.49×10^{-3}	3.16
	Malathion; *O*,*O*-Dimethyl *S*-1,2- *bis*(carbethoxyethyl) phosphorodithioate; CAS: 121-75-5; Mol.wt.: 330.36; RTECS #: WM8400000	Human (forearm); solvent: acetone; 8%, 5 days (excretion analysis) (50); Human: solvent acetone; forearm 6.8%, palm 5.8%, foot 6.8%, abdomen 9.4%, hand, dorsum 12.5%, forehead 23.2%, axilla 28.7%, jaw 69.9% (60);	1.58×10^{-3}	2.75

		Mouse (dermal); no solvent; 1.4%, 11 hr (excretion analysis) (61); Mouse (dermal) solvent: acetone; 25%, 1 hr (patch) (57). Human ventral forearm 1st appl. 4.4%, 2nd. appl. 3.5% (62)		
	Parathion; Parathion-ethyl; *O*,*O*-Diethyl *O*-(4-nitrophenyl) phosphorothioate; CAS: 56-38-2; Mol. wt.: 291.26	Human (forearm); solvent acetone; 10%, 5 days (excretion analysis) (50). Mouse (dermal); no solvent; 1.4%, 1 hr (excretion analysis) (61). Mouse (dermal); solvent: acetone; 32%, days (patch) (3). Rat (dermal); solvent: acetone; 59%, 1 hr (patch) (63). Roach (dermal); solvent: acetone; 14%, 1 hr (patch) (64). Hornworm (dermal); solvent: acetone; 8%, 1 hr (patch) (64). Quail (dermal); solvent: acetone; 40%, 1 hr (patch) (64). Frog (dermal); solvent: acetone; 33%, 1 hr (patch) (64). Human: solvent acetone; forearm 8.6%, palm 11.8%, foot 13.5%, abdomen 18.5%, hand, dorsum 21.0% forehead 36.3%, axilla 64.0%, jaw	1.59×10^{-2}	3.83

(*Continued*)

Table 5 Skin Absorption Data of Organophosphorus Compounds Similar to VX (*Continued*)

Structure	Name	Skin absorption	*k*p (cm/h)[a]	Log $P(K_{ow})$[b]
		33.9%, fossal cubitalis 28.4%, scalp 32.1%, ear canal 46.6%, scrotum 101.6% (60)		
	Parathion-methyl; *O*,*O*-Dimethyl *O*-(4-nitrophenyl) phosphorothioate; Mol. wt.: 263.21	Human (abdomen, in vitro); solvent: acetone (3.01 µmol/mL], 24–48 hr, absorp. rate: 0.04 nmol/cm^2/hr, Kp: 4.4×10^{-4} cm/hr, dose absorbed 24 hr: 1.35%, 48 hr: 3.58%. (65). Human (abdomen, in vitro); solvent: aqueous formulation [4.2 umol/mL], 24–48 hr, absorp. rate: 0.16 nmol/cm^2/hr, *K*p: 14.2×10^{-4} cm/hr, dose absorbed 24 hr: 5.20%, 48 hr: 8.99% (62)	4.11×10^{-3}	3.0
	Trichlorfon; Metrifonate; Dimethyl 2,2,2-trichloro-1-hydroxyethylphosphonate; CAS: 52–68-6; Mol. wt.: 257.44; RTECS #: TA0700000	Irritation data: rabbit: eye 120 mg/6 day-1 mild (66)	9.88×10^{-5}	0.43 (20EC)

[a]Based on the formula: log *k*p = −2.74 + [0.71 × log $P(K_{ow})$]−(0.0061 × MW), where *k*p = permeability coefficient, $P(K_{ow})$ = partition coefficient in octanol compared to water, MW = molecular weight.

[b]$P(K_{ow})$=partition coefficient in octanol compared to water.

(*Source:* From Ref. 68.)

in the upper dermis and circulatory blood. The nerve agents require percutaneous absorption to achieve their toxic end point via skin exposure.

Mustard gas has a long history, having been initially used in World War I as an effective chemical weapon. Mustard gas was called *schwefellost* or *gelbes Kreuz cross* by Germans and *yperite* by the French. Mustard gas was used against the allies on the Western front in July 1917, near Ypres, Belgium. Of all the chemical warfare agents used, mustard gas was the greatest producer of casualties. Sulfur and nitrogen mustards are also referred to as blister agents. The immediate organs affected on exposure to sulfur mustard include the eyes, lungs, and skin—the eyes being the most sensitive target organ. Sulfur mustard has also been reported to be a potent carcinogen. Table 6 shows the toxicity and percutaneous absorption of mustard.

F. Theoretical Constructs of Percutaneous Absorption and Toxicity

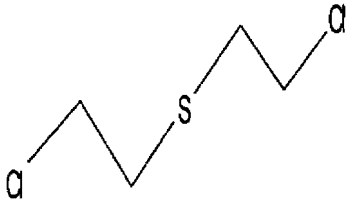
The exposure dose is defined as a continuous/infinite monolayer of $4\,\mu g/cm^2$. The $4\,\mu g/cm^2$ is the amount of chemical deposited on the skin from a thin film of 0.25% solution. It is also the experimental amount of chemical used to determine the human regional variation of skin absorption used in this analysis. The monolayer is that layer which is immediate to the skin and readily available for percutaneous absorption. Continuous/infinite means the monolayer is continually maintained at $4\,\mu g/cm^2$. As the chemical is absorbed from the monolayer, it is replaced at the immediate skin surface. This can account for larger chemical doses and larger volumes exposed to the skin. The continuous/infinite monolayer is used where exposure can be from an infinite source and be variable, such as soil or water. Chemical warfare exposure by its own nature will be highly variable, and the exposure area will be beyond the immediate surface of the skin.

Figure 1 illustrates the total body surface of a human male with 18,000 cm^2 of body surface ($1.8\,m^2$). The head and neck region totals 9% ($0.16\,m^2$), and arms and hands 18% ($0.32\,m^2$), trunk 36% ($0.65\,m^2$), legs and feet 36% ($0.65\,m^2$), and genitals 1% ($0.018\,m^2$). The percentages (9,18), and (36) of the sections, except genitals, are multiples of 9, giving to the ''rule of 9'' when discussing body surface sections. Human risk assessment is traditionally done with the naked body, because knowledge of the effect of clothing was never determined. This will first be done here, with clothing introduced later.

Figure 2 shows parathion systemic absorption when $4\ \mu g/cm^2$ is deposited on the human body for one hour. The $4\,\mu g/cm^2$ is the parathion dose used to determine human regional variation. This $4\,\mu g/cm^2$ was determined to be the amount deposited from a thin film of 0.25% solution. This human body construct shows parathion systemic absorption for each region of the body; total systemic absorption is for total body exposure. Values are calculated from the $4\,\mu g/cm^2$ does in $10\mu L/cm^2$ formulation absorbed according to the permeability constant (*K*p) and then adjusted for regional variation using the following index:

head and neck	$\times 4$
arms and hands	$\times 1$
trunk	$\times 3$
genitals	$\times 12$
legs and feet	$\times 1$

Table 6 Toxicity and Percutaneous Absorption of Mustard

Structure	Name	Toxicity
	Mustard; HD 2,2′-dichloroethylsulfide; CAS: 505-60-2; Mol. wt.: 159.08; RTECS: WQ0900000	Human: LD50(skin) 100 mg/70 kg (44)

Structure	Name	Skin absorption	kp (cm/h)[a]	Log $P(K_{ow})$[b]
	Mustard; HD 2,2′ dichloroethylsulfide; CAS: 505–60–2; Mol. wt.: 159.08; RTECS: WQ0900000	Human: rapid absorption, can be completely removed after 2–3 min, partially after 10–15 min (67).	5.38×10^{-3}	2.03

[a]Based on the formula: $\log k\text{p} = -2.74 + [0.71 \times \log P(K_{ow})] - (0.0061 \times \text{MW})$, where kp = permeability coefficient, $P(K_{ow})$ = partition coefficient in octanol compared to water; MW = molecular weight.
[b]$P(K_{ow})$ = partition coefficient in octanol compared to water.
(*Source*: From Ref. 68)

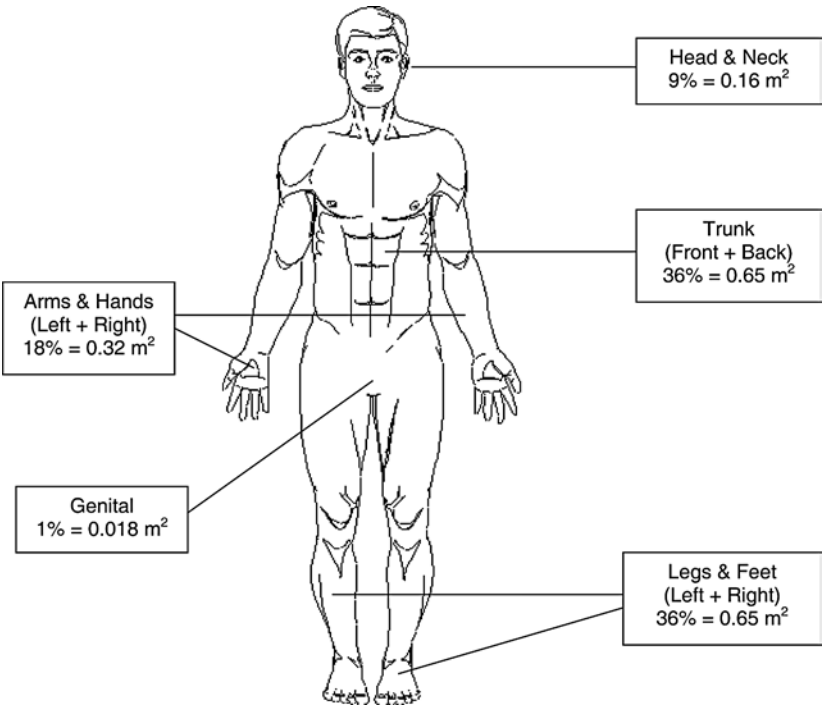
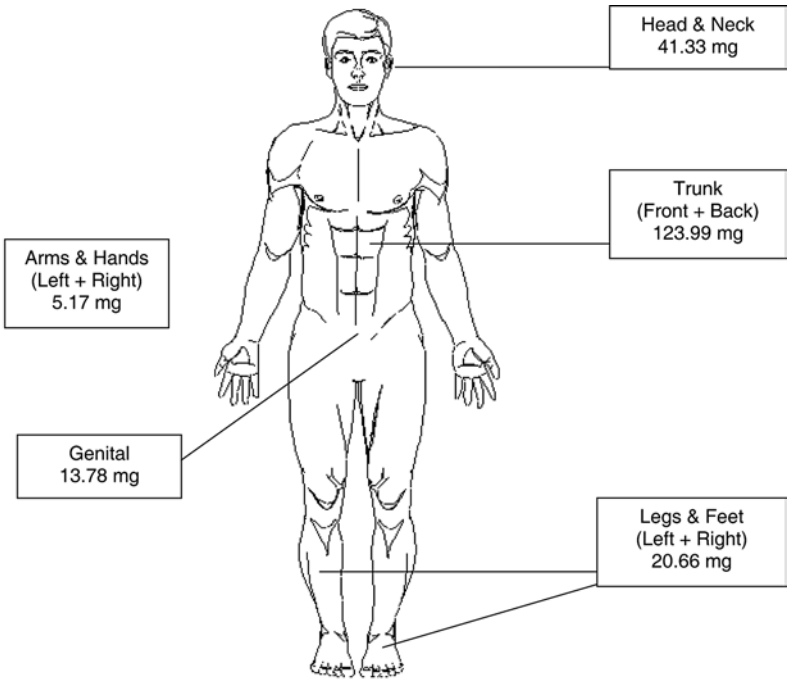


Figure 1 Human body surface contours defined as percent and area. Adult: 1.8 m^2.

This is the actual regional variation index for parathion in humans. The basic permeability constant has a value of $\times 1$ (forearm). Body regions such as the head and neck absorbed fourtimes the basic value, so this $4\times$ value was calculated for the head and neck region rate of absorption. Since the structures of the chemical warfare agents sarin, soman, and VX are similar to organophosphorous chemicals, this index was used for these CWA. Exposure time periods (''continuous/infinite dose application'' means that the total dose was in place for the full time periods) show that percutaneous absorption is time dependent. The longer the chemical is in contact with the skin, the more chemical that will be absorbed. The reverse is also true in that the sooner exposed chemical is removed from the skin, less chemical will be absorbed.

Table 7 summarizes systemic absorption (mg) after total body exposure of 4 $\mu g/cm^2$ for malathion, parathion, sarin, soman, VX, and mustard. Indicated 50% lethality dose is for a 70 kg human. The LD50 for parathion is 14 mg/kg. Given a body weight of 70 kg, then systemic absorption of 980 mg would result in 50% mortality. Thus, parathion lethal toxicity levels can be reached at eight hours and longer exposures. Less malathion is absorbed through human skin than parathion and malathion (LD50 = 290 mg/kg) is $20\times$ less toxic than parathion. Thus, no systemic toxicity is noted in the malathion construct.

Sarin and soman have a similar toxicity level (12.5 mg/70 kg) but soman has greater human skin absorption. Thus, estimates of 50% lethality are only reached for sarin at the 24-hour exposure level, whereas the 50% lethality estimate for soman is reached in the first hour. VX is the most lethal of the CWA's and requires an hour or less time to reach lethality. Mustard is better known for its external hazardous



Skin exposure dose:	4 μg/cm^2 continuous/infinite on whole body area (1.8 m^2) with 1hr exposure time.
Total systemic absorption:	204.93 mg.
Head, neck and arms:	46.50 mg.
Estimated systemic LD50 of parathion:	980 mg (human, 70 kg).

Figure 2 Distribution of parathion systemic absorption for human body required contours.

Table 7 Percutaneous Absorption of Chemical Warfare Agents on Whole (Unprotected) Body Area (1.8 m^2)

		Total systemic absorption (mg) after exposure time		
Compound	Estimated LD50[a] (mg)	1 (hr)	8 (hr)	24 (hr)
Malathion	20300	20.24	161.94	485.83
Parathion	980	204.92	1639.00[b]	4918.00[b]
Sarin (GB)	12.5	6.82	58.58[b]	163.73[b]
Soman (GB)	12.5	33.23[b]	265.84[b]	797.53[b]
VX	6.5	20.62[b]	164.93[b]	494.79[b]
Mustard (HD)	100	69.16	553.32[b]	1659.95[b]

Skin exposure dose: 4 µg/cm^2 continuous/infinite.
[a]Estimated systemic LD50 of 70 kg human.
[b]Indicates 50% lethality dose.

Table 8 Partial Body Exposure with Predicted Percutaneous Absorption and Toxicity for 24-hour Exposure

		Systemic absorption (mg)	
Anatomical region	Sarin	Soman	VX
Head and neck	33.02[a]	160.85[a]	99.79[a]
Arms and hands	4.13	20.11[a]	12.47[a]
Trunk (front and back)	99.06[a]	482.54[a]	299.37[a]
Legs and feet	16.51[a]	80.42[a]	49.9[a]
Genital-s	11.01	53.62[a]	33.26[a]

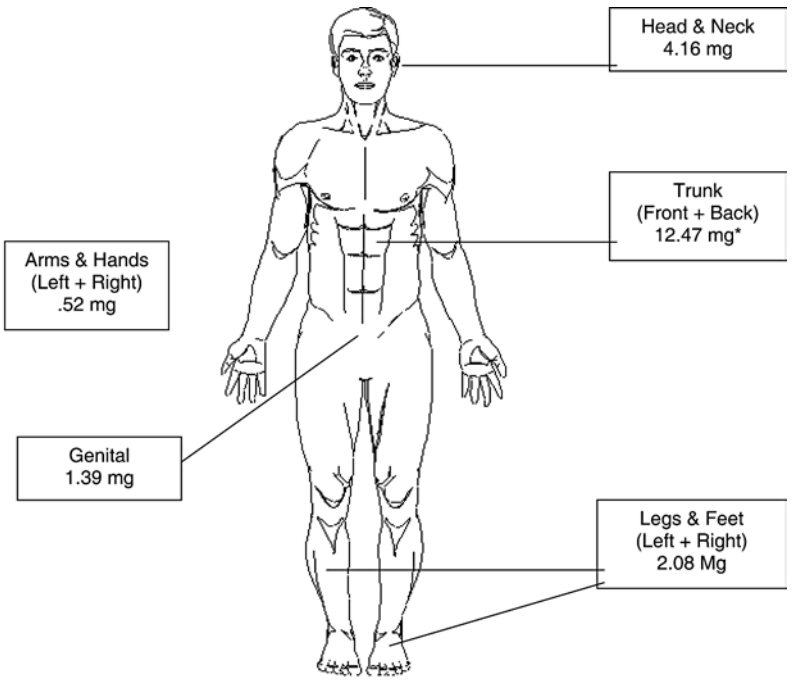
Skin exposure dose: 4 μg/cm^2 continuous/infinite to specific anatomic region.
[a]Indicates 50% lethality dose.

toxicity, but systemic mustard toxicity can also occur. Mustard's toxicity constructs shows this happening at the eight-hour exposure period.

Table 8 shows CWA percutaneous absorption and toxicity for 24-hour exposure to Individual body sections. Partial body exposure will lead to lethality. Toxicity to partial body exposure will also occur for less exposure time periods. Figure 3 shows the body contour for VX at 1 hour. Any body section combination of systemic dose adding up to the estimated systemic LD50 will have dire consequences. This is true for soman and sarin as well as VX.

The above analysis was done using standard application of percutaneous absorption and toxicity estimate to human skin. People (military and civilian) will be clothed in an actual CWA exposure. Wester et al. (8) predicted CWA VX toxicity to uniformed soldiers using parathion in vitro skin exposure and absorption. A soldier wearing field uniform will have both naked skin (head, neck, arms, and hands) and uniform covered skin exposed during a chemical warfare incident. And, in military encounters, the soldier has no choice but to wear that same uniform for an extended period. The study design was to dose, in single exposure, naked skin and uniform protected skin to the chemical warfare agent simulant parathion and continue the exposure and absorption period over 96 hours. Uniforms can become wet from sweating and rain, so both wet and dry uniform materials were included. Parathion was the chemical of choice to use as a surrogate for VX. Actual data with VX would be the best, however, little exists in the literature. Parathion is in the same chemical class as VX (organophosphorus), and has the same functional groups as VX. The partition coefficients (log P octanol/water) are similar (3.83 for parathion; 2.22 for VX), as are molecular weight (291.26 for parathion; 267 for VX) and molar volume (219.5 for parathion; 262.5 for VX). Similar structure, log p, and molecular weight/molar volume suggest the potential for similar percutaneous absorption (8).

The in vitro percutaneous absorption of parathion was determined through naked human skin and skin protected by dry uniform material and wetted uniform material. The uniform material was standard army issue coat, hot weather woodland camouflage, combat pattern: 50% nylon and 50% cotton (8). Following the single exposure and 96-hour absorption period, 1.78 $\pm$ 0.41% dose was absorbed through naked human skin, and 0.29 $\pm$0.17% and 0.65 $\pm$ 0.16% doses through skin protected by dry and moist uniform, respectively. The absorption was continuous through the total exposure period, an infinite dose was available through the 96-hour dosing period. Statistically, naked skin absorption was greater than that protected by dry



Skin exposure dose:	4 μg/cm^2 continuous/infinite on whole body area (1.8 m^2) with one hour exposure time.
Total systemic absorption:	20.62 mg.
Head, neck and arms:	4.68 mg.
Estimated systemic LD50 of VX:	6.5 mg (human, 70 kg).

* indicates 50% lethality dose.

Figure 3 Distribution of VX systemic absorption of human body regional contours.

uniform ($p = 0.000$) and moist uniform ($p = 0.000$). Absorption through moist uniform was statistically ($p = 0.007$) greater than through dry uniform. Table 9 gives calculated VX systemic absorption and toxicity to uniformed personnel. This is an one time 4 μg/cm^2 VX exposure and resulting systemic dose occurs by skin absorption only (no respiratory and oral involvement). At one hour post exposure, 50% lethality occurs with full body exposure to the compromised sweated uniform, although the dry uniform is right at the threshold. At eight hours post exposure to head and neck only, or trunk only, might cause lethality with both wet and dry uniform. At 96 hours post exposure, lethality occurs with exposure to any body part.

III. DISCUSSION

Some comparison can be done between calculated fluxes and literature values. Blank et al. (67) determined the rate of sarin penetration into human skin using an in vitro diffusion system. Human cadaver skin was clamped between a base unit and a top

Table 9 VX Systemic Absorption and Toxicity to Uniformed Military Personnel

Exposure time	Body exposure	Calculated VX systemic dose	
		Compromised (mg)	Protected (mg)
1 hr	Head/neck	4.16	4.16
	Arms and hands	0.52	0.52
	Trunk	0.47	1.35
	Genital-s	0.45	0.15
	Legs	0.68	0.22
	Total	**9.87**[a]	**6.40**
8 hr	Head/neck	33.26[a]	33.26[a]
	Arms and hands	4.16	4.16
	Trunk	32.52[a]	10.77[a]
	Genital-s	3.61	1.2
	Legs	5.42	1.8
	Total	**78.98**[a]	**51.18**[a]
96 hr	Head/neck	399.16[a]	399.16[a]
	Arms and hands	49.90[a]	49.90[a]
	Trunk	390.29[a]	129.25[a]
	Genital-s	43.37[a]	14.36[a]
	Legs	65.05[a]	21.54[a]
	Total	**947.76**[a]	**614.21**[a]

Skin exposure dose: 4 μg/cm^2 continuous/infinite on whole body area (1.8 m^2); head/neck and arms and hands are unprotected. Compromised: uniform with perspiration. Protected: dry uniform.
Estimated systemic LD50 of VX is 6.5 mg (human, 70 kg).
[a]Indicates that the systemic concentration is more than 50% lethality dose.
Source: From Ref. 8.

cylinder. The cylinder was filled with [^{32}P]sarin (10–100 μL/3 cm^3; 1 μL = approximately 1000 μg) and the top sealed (sarin has high vapor pressure). No liquid circulated under the skin (i.e., no skin conditions), but a pledget of cotton moistened with water was kept in the base unit to prevent the skin from drying out.

Penetration was determined on the separated dermis using colorimetric and radioactivity assays. Sarin is not stable in aqueous solutions. The radioactivity represents total chemical penetration and colomietric represents surviving intact active sarin. Colorimetric assay was some three times less sensitive than radioactivity. The data in Table 10 are calculated from eight samples from three skin sources (cadavers). There was a 10-fold variation in individual penetration which the author called human biological variability. It should be noted that the dose of 10 to 100 μL/3 cm^3 is artificially contained over the skin. Normal liquid which exceeds 10 μL/cm^2 will run off the skin. The in vitro system has a cylinder over the skin where the chemical is poured in and maintained over the skin. The calculated mean fluxes for sarin (understanding there is a 10-fold variability) were 35.6 (radioactivity assay) and 10.8 (colorimetric) μg/cm^2 hr. A calculated flux for human skin using the Potts and Guy (68) method is an agreeable 8.5 μg/cm^2 hr using the same large dose. Blank et al. (67) also showed that trauma increased skin penetration as did increased temperature. Liquid sarin penetrated human skin four times greater than as vapor, and all of the vapor sarin broke down in the skin.

Fredriksson (69) determined time to death by sarin dosed to living cats. Dosing was by intravenous and percutaneous administration. For percutaneous absorption

Table 10 Experimental and Calculated Nerve Chemical Warfare Agent Skin Flux

Chemical	Dose (per cm^2 area)		Skin flux ($\mu g/cm^2$ hr)	
	Mass (μg)	Volume (μL)	Calculated (human)	Experimental
Sarin				
Human (radioactivity)	16,000	16	8.5[d]	35.6[a]
Human (colorimetric)	16,000	16	8.5[d]	10.8[a]
Human	4	1	0.002[d]	
Cat (time to death)	16,000	16	8.5[d]	60–120[b]
Soman				
Human	4	1	0.01[d]	
Cat (time to death)	16,000	16	41.4[d]	16.2[c]
VX				
	Human	4	1	0.006[d]

Note: An artificial mass and volume were contained above skin in the Blank and Fredriksson studies, resulting in unrealistic skin fluxes. Normal skin will support 2–10 $\mu L/cm^2$ volume before running over. A more practical exposure in spray configuration would be 4 $\mu g/10\ \mu L/cm^2$.

[a]Blank et al. (67). Calculated mean rate of penetration for colorimetric (active) and radioactive (total) from Table 1, page 303. The difference between radioactivity and colorimetric is due to sarin hydrolysis.

[b]Fredriksson (69), page 36.

[c]Fredriksson (70), page 488.

[d]Calculated for human according to Potts and Guy (68).

a cylindrical ring (3.1 cm^2) was glued to the skin and a volume (50 μL) of sarin placed in the cylinder [analogous to the in vitro system of Blank, et al. (67)] The time to death was then determined. Using a ratio of time to death for percutaneous and IV. dosing, Fredriksson determined a sarin skin flux in the cat of 60 to 120 $\mu g/cm^2$ hr. This is greater than that determined by Blank et al. (67) or calculated according to Potts and Guy (68) (Table 9).

Fredriksson (69) also determined the flux of soman in the cat to be 16.2 $\mu g/cm^2$/hr. This is almost three times that predicted by Potts and Guy (68) (Table 10). Percutaneous absorption in the cat relative to man is not known. Generally, absorption in animals is greater than in man (57).

It should be noted that in the above studies by Blank et al. (67) and Fredriksson (69,70) that the dosing situation was an artificial system in that a dose was contained above the skin that would normally run off the skin if it was not contained. A more practical estimation of an amount deposited on skin is 4 $\mu g/cm^2$, and amount deposited from a thin film of a 1/4% solution (71). Terrorist delivery of a CWA might be in some form of a spray resulting in thin film coating on the skin. The studies of Blank et al. (67) and Fredriksson (69,70) were done at high doses for short periods of time. In reality, the dose will be less. Survival will depend on a lesser dose inflicted on a proportion of the body, either protected or not protected. But, as Fredriksson showed, these chemicals are deadly.

Craig et al. (72) reported the percutaneous absorption of VX in subjects (U.S. Army enlisted men) using a cholinesterase inhibition assay. Subjects dosed on the

Table 11 Skin Decontamination with Soap and Water Wash

	Percent dose absorbed, wash time following topical application								
	Minutes				Hours				
Pesticide ($\mu g/cm^2$)	1	5	15	30	1	2	4	8	24
Malathion (4), arm	1.3		4.3	4.5	6.1	8.3	12.1		6.8
Malathion (40), arm			4.7				6.8		
Malathion (400), arm			1.4		2.0		4.7		
Parathion (4), arm	2.8		6.7		8.4		8.0	15.8	8.6
Parathion (40), arm			3.1				6.9		9.5
Parathion (400), arm			2.2		2.3		4.2		4.8
Parathion (4), forehead	8.4		7.1	12.2	10.5	20.1	27.7		36.3
Parathion (4), palm		6.2	13.6	13.3	11.7	9.4	7.7		11.8

Source: Maibach and Feldmann (71) and Wester and Maibach (74).

forearms at 18°C room temperature for six hours had a penetration of $0.60 \pm 0.19\%$. Applying the Potts-Guy (68) equation used in this study for a $4\,\mu g/cm^2$ dose over six hours gives a penetration of 0.96%, very similar to the empirical data of Craig et al. (72). They showed regional variation (cheek higher than forearm) justifying the use of regional variation for risk assessment. They also showed higher VX penetration with higher room temperature (46°C), suggesting sweat/moisture involvement as with the study by Wester et al. (8).

Time following exposure is most critical. Exposed clothing needs to be removed and skin decontaminated. It is imperative that the decontamination procedure in itself not enhance skin absorption. This applies to public and well as military situations. Society has a system of first responders to emergency incidents. First responders include police, firefighters, paramedics, and other medical personnel, and good Samaritans. All but the firefighters will be wearing uniforms or civilian clothing similar in composition and design to that used in the military uniform bioavailability study (8). First responders in Japan's subway gas attack in 1995 have suffered the same fate as initial intended civilian targets, so their knowledge of this potential skin and clothing involvement is important.

The emergency procedure for CWA exposure is to remove contaminated clothing and then wash with soap and water. Removing the contaminated clothing as soon as possible is important since the clothing is a continuing source of CWA exposure (8). However, washing with soap and water probably is less effective than thought in removing the CWA. Table 11 (71,74) gives the skin decontamination of various dose levels of parathion and malathion in human volunteers. Removal was attempted by a two-minute wash with soap and hot water. As early as one minute after dosing, some chemical was not removed with washing. The amounts absorbed during the first hour before washing are significant, some not much different than at 24 hours. Showering at four hours also had little decontamination effect. Soap and water wash decontamination has been shown to be less than believed for other chemicals (75). Some other washing methods have been shown to work where soap and water does not, but these would need to be tested for CWAs (75). Some of these new methods involve readily available household material as well as commercial material.

CWA attacks can be isolated such as the Aum Shinrikyo attacks on the Tokyo subway in 1995, and dealt with accordingly. The Iraqis attack on Halabja in 1988 Northern Iraq (Kurdish) were continual air chemical bombardment over several days with chemical ''cocktails" containing sarin, tabun, VX, mustard, and cyanide. This resulted in both immediate deaths and longer term casualties. This emphasizes the need for knowledge and careful planning towards these multiple agents (76).

REFERENCES

1. Wester RC. Twenty absorbing years. In: Surber C, Elsner P, Bircher AJ, eds. Exogenous Dermatology. Karger: Basel, 1995:112–123.
2. Feldmann RJ, Maibach HI. Regional variation in percutaneous penetration of [^{14}C] cortisol in man. J Invest Dermatol 1967; 48:181–183.
3. Guy RH, Maibach HI. Calculations of body exposure from percutaneous absorption data. In: Bronaugh R, Maibach H, eds. Percutaneous Absorption. New York: Marcel Dekker, 1985:461–466.
4. Wester RC, Maibach HI. Regional variation in percutaneous absorption. In: Bronaugh R, Maibach H, eds. Percutaneous Absorption. 3d ed. New York: Marcel Dekker, 1999:107–116.
5. Hatch KL, Maibach HI. Textile chemical finish dermatitis. Contact Dermatitis 1986; 14:1–13.
6. Snodgrass HL. Permethrin transfer from treated cloth to the skin surface: potential for exposure in humans. J Toxicol Environ Health 1992; 35:912–915.
7. Wester RC, Quan D, Maibach HI. In vitro percutaneous absorption of model compounds glyphosate and malathion from cotton fabric into and through human skin. Food Chem Toxicol 1996; 34:731–735.
8. Wester RM, Tanojo H, Maibach HI, Wester RC. Predicted chemical warfare agent VX toxicity to uniformed soldier using parathion In vitro human skin exposure and absorption. Toxicol Appl Pharmacol 2000; 168:149–152.
9. Smith KJ. The prevention and treatment of cutaneous injury secondary to chemical warfare agents. Application of these finding to other dermatologic conditions and wound healing. Dermatol Clin 1999; 17:41–60.
10. Smith KJ, Hurst CG, Moeller RB, Skelton HG, Sidell FR. Sulfur mustard: its continuing threat as a chemical warfare agent, the cutaneous lesions induced, progress in understanding its mechanism of action, its long-term health effects, and new developments for protection and therapy. J Am Acad Dermatol 1995; 15:133–138.
11. Yourick JJ, Dawson JS, Mitcheltree LW. Reduction of erythema in hairless guinea pigs after cutaneous sulfur mustard vapor exposure by pretreatment with niacinamide, promethazine and indomethacin. J Appl Toxicol 1995; 15:133–138.
12. Casillas RP, Smith KJ, Castrejon LR, Tezak-Reid T, Lee RB, Stemler FW. Effect of topical applied drugs against HD-induced cutaneous injury in the mouse ear edema model. Med Defense Biosci Rev 1996; 2:801–809.
13. Wormser U, Brodsky B, Green BS, Arad-Yellin R, Nyska A. Protective effect of povidone-iodine ointment against skin lesions induced by sulfur and nitrogen mustards and by non-mustard vesicants. Arch Toxicol 1997; 71:165–170.
14. Zhang Z, Riviere JE, Monteiro-Riviere NA. Evaluation of protective effects of sodium thiosulfate, cysteine, niacinamide and indomethacin on sulfur mustard-treated isolated perfused porcine skin. Chem Biol Interac 1996:249–262.
15. Kwong CD, Segers DP, Reynolds RC, Truss JW, Thomas-Updike LD, Hacklex BE Jr. Efforts directed toward the development of a reactive topical skin protectant against CEES. Med Defense Biosci Rev 1996; 2:871–881.

16. Sawyer TW, Hancock JR, D'Agostino PA. L-thiocitrulline: a potent protective agent against the toxicity of sulfur mustard in vitro. Toxicol Appl Pharmacol 151:340–346.
17. Sawyer TW. Modulation of sulfur mustard toxicity by arginine analogues and related nitric oxide synthase inhibitors in vitro. Toxicol Sci 1998; 46:112–123.
18. Sawyer TW. Synergistic protective effects of selected arginine analogues against sulphur mustard toxicity in neuron culture. Toxicol Appl Pharmacol 1999; 155:169–176.
19. Wester RC, Maibach HI, Bucks DAW, Guy RH. Malathion percutaneous absorption after repeated administration to man. Toxicol Appl Pharmacol 1983; 68:116–119.
20. Chattopadhyay DP, Dighe SK, Nashikkar AB, Dube DK. Species differences in the in vitro inhibition of brain acetylcholinesterase and carboxylesterase by mipafox, paraoxon and soman. Pestic Biochem Physiol 1986; 26:202–208.
21. Okinaka AJ, Doull J, Coon JM, DuBois KP. Studies on the toxicity and pharmacological actions of bis(dimethylamido) fluorophosphate (BFP). J Pharmacol Exp Ther 1954; 112:231–245.
22. Sanderson DM, Edson EF. Oxime therapy in poisoning by six organophosphor insecticides in the rat. J Pharm Pharmacol 1959; 11:721–728.
23. DuBois KP, Coon JM. Toxicology of organic phosphorus-containing insecticides to mammals. Arch Ind Hyg Occup Med 1952; 6:9-13.
24. Cohen SD. Mechanisms of toxicological interactions involving organophosphate insecticides. Fundam Appl Toxicol 1984; 4:315–324.
25. Wilson BW, Walker CR. Regulation of newly synthesized acetylcholinesterase in muscle cultures treated with diisopropylfluorophosphate. Proc Natl Acad Sci USA 1974; 71:3194–3198.
26. Registry of Toxic Effects of Chemical Substances (RTECS) #: TB4760000. US Dept. Health and Human Services. NIOSH. Cincinnati, Ohio.
27. Registry of Toxic Effects of Chemical Substances (RTECS) #: TE1925000. US Dept. Health and Human Services. NIOSH. Cincinnati, Ohio.
28. Registry of Toxic Effects of Chemical Substances (RTECS) #: TB8750000. US Dept. Health and Human Services. NIOSH. Cincinnati, Ohio.
29. Tomilin CDS ed. The Pesticide Manual. UK: British Crop Protection Committee, Survey, 1997.
30. Registry of Toxic Effects of Chemical Substances (RTECS) #: TG0700000. US Dept. Health and Human Services. NIOSH. Cincinnati, Ohio.
31. Registry of Toxic Effects of Chemical Substances (RTECS)# TG1750000. US Dept. Health and Human Services. NIOSH. Cincinnati, Ohio.
32. Gasser R. Regarding a new insecticide with a broad spectrum of action. Z. Naturforsch. B: Anorg Chem Org Chem Biochem Biophys Biol 1953; 8:225–232. in German.
33. Gaines TB. Acute toxicity of pesticides. Toxicol Appl Pharmacol 1969; 14:515–534.
34. Shaffer CB, West B. The acute and subacute toxicity of technical *O*,*O*-diethyl *S*-2 diethylaminoethyl phosphorothioate hydrogen oxalate (Tetram®). Toxicol AppI Pharmacol 1960; 2:1-13.
35. Piccirillo VJ. Hazeiton Laboratories America, Inc., Vienna, Virginia. Unpublished report submitted to WHO by Ciba-Geigy Ltd, Basel, 1978.
36. Kuhn JO. Stillmeadow Inc., Houston, Texas. Unpublished report submitted to WHO by Ciba-Geigy Ltd, Basel, 1989.
37. Gaines TB. The acute toxicity of pesticides to rats. Toxicol Appl Pharmacol 1960; 2:88–99.
38. Bathe R. Ciba Geigy Ltd, Basel, Switzerland. Unpublished Report, 1972.
39. Registry of Toxic Effects of Chemical Substances (RTECS) #: TE4550000. US Dept. Health and Human Services. NIOSH. Cincinnati, Ohio.
40. Registry of Toxic Effects of Chemical Substances (RTECS) #: WM8400000. US Dept. Health and Human Services. NIOSH. Cincinnati, Ohio.

41. DuBois KP, Doull J, Salerno PR, Coon JM. Studies on the toxicity and mechanism of action of *p*-nitrophenyl diethyl thionophosphate (parathion). J Pharmacol Exp Ther 1949; 95:79–91.
42. Holmstedt B. Structure-activity relationship of the organiphosphorus anticholinesterase agents. Handb Exp Pharmacol 15 (suppl) 1963; 428–485 (in German).
43. Registry of Toxic Effects of Chemical Substances (RTECS) #: TA0700000. US Dept. Health and Human Services. NIOSH. Cincinnati, Ohio.
44. Somani SM, Solana RP, Dube SN. Toxicodynamics of nerve agents. In: Somani SM, ed. Chemical Warfare Agents. San Diego, California: Academic Press, 1992:67–123.
45. Moody RP, Benoit FM, Riedel D, Ritter L. Dermal absorption of the insect repellent Deet (N,N-diethyl-m-toluamide) in rats and monkeys: effect of anatomic site and multiple exposure. J Toxicol Environ Health 1998; 26(2):137–147.
46. Meyian WM, Howard PH. Atom/fragment contribution method for estimating octanol-water partition coefficients. J Pharm Sci 1995; 84(1):83–92.
47. Marr WG. The clinical use of di-isopropyl fluorophosphate (DFP) in chronic glaucoma. Am J Ophthalmol 1947; 30:423–426.
48. Leopold IH, Comroe JH. Effect of diisopropyl fluorophosphate (DFP) on the normal eye. Arch Ophthalmol (Chicago) 1946; 36:17–32.
49. Leopold IH, McDonald PR. Diisopropyl fluorophosphate (DFP) in treatment of glaucoma. Arch Ophthalmol (Chicago) 1948; 40:176–188.
50. Feldman RJ, Maibach HI. Percutaneous penetration of some pesticides and herbicides in man. Toxicol Appl Pharmacol 1974; 28:126.
51. Shah PV, Montoe RJ, Guthrie FE. Comparative rates of dermal penetration of insecticides in mice. Toxicol Appl Pharmacol 1981; 59:414–423.
52. Registry of Toxic Effects of Chemical Substances (RTECS) #: TG0700000. US Dept. Health and Human Services. NIOSH. Cincinnati, Ohio.
53. IPCS (International Programme on Chemical Safety)/IOMC. Demeton-S-Methyl. Environmental Health Criteria, ed. Vol. 197. World Health Organization, Geneva, 1997.
54. Ballantine L. Advanced product chemistry percutaneous absorption of 2o-^{14}C-diazinon in rats. Ciba Geigy Corp., Greensboro, North Carolina. Unpublished report No. ABR-84011 submitted to WHO by Ciba-Geigy Ltd, Basel, 1984.
55. Capps TM. Ciba Geigy Corp., Greensboro, North Carolina. Unpublished report No. ABR-90014 submitted to WHO by Ciba-Geigy Ltd Basel, 1990.
56. Pickles M. Ciba Geigy Corp., Greensboro, North Carolina. Unpublished report submitted to WHO by Ciba-Geigy Ltd Basel, 1990.
57. Wester RC, Maibach HI. Cutaneous pharmacokinetics: 10 steps to percutaneous absorption. Drug Metab Rev 1983; 14:169–205.
58. Moody RP, Franklin CA. Percutaneous absorption of the insecticides fenitronthion and aminocarb in rats and monkeys. J Toxicol Environ Health 1987; 20:209–218.
59. Moody RP, Riedel D, Ritter L, Franklin CA. The effect of DEET (N,N-diethyl-m-toluamide) on dermal persistence and absorption of the insecticide fenitronthion in rats and monkeys. J Toxicol Environ Health 1987; 22:471–479.
60. Maibach HI, Feldmann RJ, Milby T, Serat W. Regional variation in percutaneous penetration in man. Arch Environ Health 1987; 22:471–479.
61. Marty JP. Fixation des substances chimiques dans les structures superficielles de la peau: Importance dans les problemes de decontamination et de biodisponibilite. Ph.D. Thesis, University of Paris-Sud, Paris.
62. Wester RC, Maibach HI, Bucks DAW, Guy RH. Malathion percutaneous absorption after repeated administration to man. Toxicol Appl Pharmacol 1983; 68:116–119.
63. Knaak JB, Yee K, Ackerman CR, Zweig G, Foy DM, Wilson BW. Percutaneous absorption and dermal dose cholinesterase response studies with parathion and carbaryl in the rat. Toxicol Appl Pharmacol 1983; 76:252–263.
64. Shah PV, Montoe RJ, Guthrie FE. Comparative penetration of insecticides in target and non-target species. Drug Chem Toxicol 1983; 6:155–179.

65. Sartorelli P, Aprea C, Bussahi R, Novelli MT, Orsi D, Sciarra G. In vitro percutaneous penetration of methyl-parathion from a commercial formulation through the human skin. Occup Environ Med 1997; 54:524–525.
66. Registry of Toxic Effects of Chemical Substances (RTECS) #: TA0700000. US Dept. Health and Human Services. NIOSH. Cincinnati, Ohio.
67. Blank IH, Criesemer RD, Gould E. The penetration of an anticholinesterase agent (sarin) into skin. I. Rate of penetration into excised human skin. J Invest Dermatol 1957; 29:299–309.
68. Potts RO, Guy RH. Structure-permeability relationships in percutaneous penetration. J Pharma Sci 1992; 81:603–604.
69. Fredriksson T. Studies on the percutaneous absorption of sarin and two allied organophosphorus cholinesterase inhibitors. Acta Dermato-Venereol 1958; 38(41):9–83.
70. Fredriksson T. Studies on the percutaneous absorption of sarin and two allied organophosphorus cholinesterase inhibitors. Acta Derm-Venereol 1969; 49:484–489.
71. Maibach HI, Feldmann RJ. Systemic absorption of pesticides through the skin of man in occupational exposure to pesticides: report to the federal working group on pest management for the task group on occupational exposure to pesticides. Appendix B 120–127. US Government Printing Office, Washington DC, 1975; 0-551-026.
72. Craig FN, Cummings EG, Sim VM. Experimental temperature and the percutaneous absorption of a cholinesterase inhibitor, VX. J Invest Dermatol 1977; 68:357–361.
73. Wester RC, Maibach HI. Advances in percutaneous absorption. In: Drill V, Lazar P, eds. Cutaneous Toxicity. New York: Raven Press, 1984:29–40.
74. Wester RC, Maibach HI. In vivo percutaneous absorption and decontamination of pesticides in humans. J Toxicol Environ Health 1985; 16:25–37.
75. Wester RC, Hui HI, Landry T, Maibach HI. In vivo skin decontamination of methylene bisphenyl isocyanate (MDI): soap and water ineffective compared to propylene glycol, polyglycol-based cleanser, and corn oil. Toxicol Sci 1999; 48:1–4.
76. Testimony of Dr. Christine M. Gosden before the Senate Judiciary Subcommittee on Technology, Terrorism and Government, and the Senate Select Committee on Intelligence on April 22,1998.

41

The Relationship Between In Vivo Dermal Penetration Studies in Humans and In Vitro Predictions Using Human Skin

Simon C. Wilkinson
Health Protection Agency, Newcastle upon Tyne, U.K.

Faith M. Williams
University of Newcastle, Newcastle upon Tyne, U.K.

I. INTRODUCTION

There has been a reluctance to accept in vitro derived dermal penetration data due to the limited number of parallel in vitro and in vivo absorption studies in humans or animals, which can be used to confirm the validity of the data. This was the situation in 2000 (1) when the Organisation for Economic Cooperation and Development (OECD) considered guidelines on skin absorption. These guidelines and guidance notes are now accepted (2). There have been a number of recent comparative studies that have helped to place the in vitro results in context. In this chapter we will consider the value of data obtained from in vitro studies for the prediction of percutaneous absorption in humans in vivo. In vitro studies considered include those using excised skin from either surgical waste or cadavers, taken from various anatomical sites (breast, abdomen, and thigh), and used either full- or split-thickness (dermatomed, otherwise reduced in thickness, or epidermal membranes). In vivo studies considered include human volunteer studies in which the test compound has been applied topically and absorption has been assessed by the monitoring of blood, urine, feces and/or exhaled air, and microdialysis studies. Earlier comparative reports measuring in vivo absorption in primates are also included, as are relevant studies using pigs and rodents. Data are presented as percent dose applied measured in the different compartments (unabsorbed, membrane, and absorbed) and/or as flux. Permeability coefficient (k_p) values are only presented when an infinite dose was applied (i.e., the maximum absorption rate was achieved). In the summaries below "absorbed" refers to material entering the systemic circulation in vivo or receptor fluid (plus the receiver chamber wash, where described) in vitro. Data are expressed as means $\pm$ SEM unless otherwise stated. It should be noted that many of the published studies are of limited use as not all information is presented, making comparisons difficult. A database has been established of in vitro and in vivo dermal

penetration studies from peer-reviewed journals in which the quality of such details was considered. Only about 50% of the entries satisfy the criteria laid down (2a).

II. STUDIES COMPARING IN VITRO ABSORPTION IN EXCISED SKIN WITH HUMAN VOLUNTEERS OR PRIMATES IN VIVO

A. The Influence of the Physicochemical Properties of the Test Compound

Some of the earlier studies in which human skin was used in vitro to predict absorption in vivo (in human volunteers or in some cases model primates) tended to report lower absorption in vitro than in vivo, though this was not always the case. Underestimation of in vivo absorption by in vitro models has often been explained by the fact that lipophilic compounds (with a log octanol/water partitioning coefficient ($\log k_{OW}$) greater than three) are not sufficiently soluble in the receptor fluid used, thus absorption of these compounds is limited in the in vitro system. To overcome this problem, researchers have added surfactants such as polyethylene glycol 20-oleyl ether (PEG 20) to increase the solubility of lipophilic materials in the receptor fluid, or proteins such as bovine serum albumin (BSA) that will bind the test compound, thus increasing the sink capacity of the receptor fluid for the test compound. Bronaugh et al. (3) compared percutaneous absorption of two lipophilic compounds, safrole ($\log k_{OW}$ 3.45) and cinnamyl anthranilate ($\log k_{OW}$ 4.74), and two amphipathic compounds cinnamic acid ($\log k_{OW}$ 2.13) and cinnamic alcohol ($\log k_{OW}$ 1.95) through human skin in vitro with percutaneous absorption in rhesus monkeys in vivo. In vitro studies used dermatomed human skin in static and flow through cells with saline as receptor fluid. The PEG 20 (at 6% w/v) was added to the receptor fluid for the two more lipophilic compounds. The dose site was washed after 24-hour exposure and experiments were continued until 48 to 72 hours after dosing (when "absorption was complete"). In vivo studies involved application of the test compounds to the abdomen of Rhesus monkeys in metabolic chairs. The dose was removed by a soap wash at 24 hours and biological monitoring continued for a further four days. Data were corrected for absorption by other routes using a parenterally administered reference dose. In both studies, 4 $\mu g/cm^2$ of each test compound was applied in acetone in either occluded or non-occluded conditions. In a separate in vitro study, addition of PEG 20 to saline receptor fluid significantly increased absorption of cinnamyl anthranilate and safrole applied in acetone vehicles, yet surprisingly, absorption of testosterone ($\log k_{OW}$ 3.32) in a petroleum vehicle was no different from normal saline. In non-occluded studies, cinnamyl anthranilate absorption in vivo ($26.1 \pm 3.3\%$ after five days) was quite well predicted by the in vitro model ($24.0 \pm 5.1\%$ after 48 hours) when PEG 20 was present in receptor fluid, as was cinnamic alcohol ($25.4 \pm 4.4\%$, compared with 33.0 ± 7.9 % in vitro, normal saline receptor fluid). Surprisingly, absorption of safrole in vivo ($4.1 \pm 0.8\%$) was significantly overpredicted in vitro ($15.0 \pm 2.0\%$). In occluded conditions, only safrole was significantly different in vitro ($38.4 \pm 2.4\%$) than in vivo ($13.3 \pm 2.3\%$). The difference between models for safrole was attributed to the fact that it is a volatile liquid (the other substances studies are solid at skin temperature); the authors assumed that a lower degree of evaporation of the dose occurred in vitro than in vivo.

Bronaugh and Maibach (4) studied the absorption of a range of nitroaromatic compounds ($\log k_{OW}$ values ranged from 0.53 to 2.17) applied to human and monkey skin in vitro (using normal saline as receptor fluid) and in monkeys

(abdomen skin) in vivo, corrected for other routes by IV dosing. They compared their findings with previously obtained human volunteer data. All compounds were applied in acetone at 4 $\mu g/cm^2$. The remaining dose was washed off the skin surface at 24 hours, and absorption was followed for a five-day period in total. There were non-significant increases in absorption of all compounds (except nitrobenzene) through monkey skin in vivo and in vitro compared with human skin in vitro. Only with nitrobenzene were there significant differences between the values determined by the four methods. For this compound, absorption in human volunteers was significantly lower than in vitro with human skin and monkey skin (both in vitro and in vivo), though the authors noted that the volunteer study was not directly comparable. Absorption of nitrobenzene was also significantly higher through human skin in vitro ($7.8 \pm 1.2\%$) than in monkey in vivo ($4.2 \pm 0.5\%$). The poor penetration of nitrobenzene in vivo was attributed to its high volatility.

Bronaugh and Franz (5) reported the absorption of benzoic acid (log k_{OW} 1.83), caffeine (log k_{OW} 0.01) and testosterone (log k_{OW} 3.32) from petrolatum, water-based gel and ethylene glycol-based gel in vitro (dermatomed human abdomen skin in flow through diffusion cells, with normal saline as receptor fluid) and volunteers (male adult abdomen), corrected using an IV reference dose in monkey. Material was kept on the skin for 24 to 36 hours. With benzoic acid, there was a trend towards lower absorption in the in vitro studies; absorption of benzoic acid (0.5 $\mu g/cm^2$ in petrolatum) was $46.5 \pm 5.9\%$ in vitro, compared with $60.6 \pm 10.7\%$ in vivo. Absorption of testosterone (2 $\mu g/cm^2$) was significantly lower in vitro than in vivo from petrolatum (39.4% compared with 49.5%) and ethylene glycol gel vehicles (23.7% compared with 36.3%). Absorption of the most hydrophilic compound, caffeine, was similar or greater in vitro than in vivo from both petrolatum and water gel. The choice of receptor fluid (saline) almost certainly contributed to the lower absorption in vitro for the more lipophilic compounds. The delay before establishment of the maximum rate was longer in in vivo studies, due to differences in pharmacokinetic parameters.

Even addition of surfactants to receptor fluids may not be sufficient to overcome solubility limitations for highly lipophilic compounds. For example, Wester et al. (6) compared percutaneous absorption of the polychlorinated biphenyls (PCBs) aroclor 1242 (log k_{OW} 4.11) and aroclor 1254 (log k_{OW} 6.30) with human skin in vitro with rhesus monkey in vivo. In vitro studies were carried out using dermatomed human cadaver skin in flow through cells with saline supplemented with 6% (w/v) PEG 20 as receptor fluid. The PCBs were applied in mineral oil at 1 to 2$\mu g/cm^2$. Comparable in vivo studies were carried out using aroclor 1242 (4.1 $\mu g/cm^2$ in mineral oil or 4 $\mu g/cm^2$ in trichlorobenzene) and 1254 (4.8 $\mu g/cm^2$ in min oil or 4.78 $\mu g/cm^2$ in trichlorobenzene), applied to abdomen skin of rhesus monkeys in metabolic chairs, with absorption corrected for other routes by IV reference dose. The experimental period in vivo was 30 days. In vitro data (less than 1% of the applied dose in each case) greatly underestimated absorption in vivo: $20.4 \pm 8.5\%$ of arochlor 1242 was absorbed with the mineral oil vehicle, compared with $18.0 \pm 3.8\%$ with trichlorobenzene, while $20.8 \pm 8.3\%$ of applied arochlor 1254 was absorbed with the mineral oil vehicle and $14.6 \pm 3.6\%$ with trichlorobenzene. The authors attributed this to the lack of partitioning of the highly lipophilic PCBs from skin into receptor fluid, even with PEG 20 in receptor fluid. The majority of the PCBs in the in vitro system remained unabsorbed or were recovered from the epidermis and upper dermis, confirming that solubility of these compounds was limiting in the in vitro system.

Wester et al. (7) studied the percutaneous absorption of isofenphos (log k_{OW} 4.12) in human male volunteers (13.2 μg/cm^2 in acetone, applied to ventral forearm and washed off at 24 or 72 hours). In a separate study, the ventral forearm was marked into a grid composed of 6×1 cm^2 areas, each dosed with 16.6 μg/cm^2 and washed with soap and water at various time intervals. The dose was unoccluded for eight hours after application, then clothing could be worn. Comparable in vitro studies used dermatomed human thigh skin from one donor in flow through cells using plasma as receptor fluid over 24 hours. The surface wash in vitro contained much more test compound [79.7 ± 2.2 (SD) %] after 24 hours than after the same time in vivo (0.75 ± 0.93%). Tape strips contained very little dose material in vivo (not done in vitro). Mean percentage absorbed in vivo (corrected using IV reference dose in rhesus monkey) was 3.63 ±3.58%, compared with 2.5 ± 2.0% in vitro. However, considerable evaporation of the applied dose in vivo was, again, not replicated in vitro, a limitation of comparative studies.

Wester et al. (8) compared the percutaneous absorption of the organophosphate diazinon (log k_{OW} 3.81) using dermatomed human cadaver abdomen skin in vitro (0.25 μg/cm^2 in acetone, using PBS as receptor fluid), with that in human volunteers applied to forearm or abdomen in acetone (2 μg/cm^2) or lanolin (1.5 μg/cm^2). In vivo absorption was corrected for other routes using an IV reference dose in rhesus monkey. In vivo human diazinon absorption (calculated from urinary disposition) ranged from 2.87 ± 1.16% to 3.85 ± 2.16%, and was not significantly affected by vehicle. In vitro, 14.1 ± 9.2% of the applied dose was absorbed from an applied loading of 0.25 μg/cm^2, with the same absolute amount being absorbed in vivo and in vitro (0.035 μg/cm^2). Total recovery was approximately 60% in both systems. Pentachlorophenol (PCP, log P 5.12) absorption was compared in human cadaver skin in vitro and rhesus monkey in vivo by Wester et al. (9). The PCP was applied in soil (0.7 μg/cm^2) or acetone vehicle (0.8 μg/cm^2) to human cadaver skin in vitro in flow through cells (dose in contact for 15 hours, human plasma used as receptor fluid) and rhesus monkey abdomen in vivo (dose in contact 24 hours with a non-occlusive cover, then washed off and urine collected for a further 13 days). In vitro absorption as percent applied dose (4.1–4.3% in acetone, 0.15–0.18% in soil) greatly underestimated in vivo monkey (24.4 ± 6.4% in soil, 29.2 ± 5.8% in acetone, a non-significant vehicle effect). The authors suggested that the underestimation in vitro resulted from the interaction between soil and skin in vitro and to the low solubility of PCP in plasma.

For certain, highly lipophilic compounds, ethanol/water mixtures have been used as receptor fluids in in vitro systems. Pershing et al. (10) compared the flux of beta estradiol (10 μg/mL, log k_{OW} 4.01) through dermatomed human skin in vitro (using 75% ethanol/PBS as vehicle and receptor fluid) with that through human dermatomed skin grafted to athymic rats (known as a human skin sandwich flap). The flux obtained in vitro (6.5 ± 1.1 μg/cm^2/hr) compared well with that obtained in vivo (8.4 ± 1.8 μg/cm^2/hr). Solubility of beta estradiol in 75% ethanol/PBS was unlikely to be limiting. Addition of 5% (v/v) oleic acid to donor and receiver solutions increased in vitro flux to 40.7 ± 36.4 μg/cm^2/hr (sixfold increase), but addition of oleic acid to the donor solution did not greatly influence flux in vivo, or the apparent kp (the solubility of the test compound decreased to 6.1 μg/mL in oleic acid–treated vehicle). In vitro permeation (normalized for dose concentration) with 75% ethanol/PBS in receiver chamber showed no significant enhancement effect of oleic acid, as did concentrations of oestradiol in skin biopsies. Enhanced beta estradiol permeation

with oleic acid was tissue concentration dependent, and increased in vitro only when skin was equilibrated with oleic acid.

Percutaneous absorption of fluazifop butyl (FB, log k_{OW} 4.50, 2.5–250 $\mu g/cm^2$, in aqueous dilutions of emulsifiable concentrate) was studied in vitro in rat and human skin and in human volunteers and rats in vivo by Ramsey et al. (11). In vitro studies employed epidermal membranes in static diffusion cells with various receptor fluids, with the dose in contact for 24 hours (human) or 72 hours (rat). In in vivo studies, the dose was applied to back skin of human volunteers (dose washed off after eight hours, shower at 24 hours, monitored in blood and urine) and to the dorsolumbar skin of rats (dose in place for up to 72 hours). The use of aqueous ethanol (50% v/v) receptor fluid with rat skin in the in vitro system resulted in an overprediction of absorption (in terms of amounts of substance) compared with in vivo in rat while tissue culture medium (with or without polyethylene glycol 20 oleyl ether) underpredicted absorption. However the factor of difference was within three, regardless of receptor fluid, and was largest at earlier timepoints. In contrast, absorption of FB with in vitro human skin membranes with aqueous ethanol receptor fluid closely matched in vivo data for all the concentrations tested, while the other receptor fluids tested underpredicted by up to a factor of 24. Considering possible loss of dose in human volunteers between 8 and 24 hours compared with the in vitro model, absorption could theoretically be lower in vivo than in vitro. Clark et al (12) demonstrated metabolism of FB by acid hydrolysis to fluazifop acid (FA) in rat and human skin post mitochondrial fractions, and FA was detected (whilst FB was not) in the receptor fluid of flow through diffusion cells containing rat and, to a much lesser extent, human skin treated with FB in acetone (156 $\mu g/cm^2$). A reservoir of FB was measured in vitro in both rat (about 34% after 24 hours) and human skin (about 37%); a substantial portion of this was recovered from the stratum corneum of rat skin ($31.3 \pm 6.6\%$ of the applied dose). No FA was detected in tape strippings, skin extracts or surface washes. In comparison, Ramsey et al. (11) recovered up to 91% of the applied dose of FB in the tape strips from rat skin in vivo; unfortunately comparable data from the human volunteer study were not available. The fact that no parent compound was measured in receptor fluid by Clark et al. (12) suggested that metabolism was required before absorption into receptor fluid could occur, though given the findings of the later study by Ramsey et al. (11), the use of an aqueous receptor fluid without additions almost certainly limited solubility of the parent compound.

Dick et al. (13) compared the percutaneous absorption of chloroform (16.1 $\mu g/cm^2$) in aqueous solution (applied to human volunteer ventral mid-forearm covered by charcoal-containing device) with in vitro absorption (female abdomen skin dermatomed to 300 μm) dosed with aqueous chloroform in low (0.62 $\mu g/cm^2$) or high (70.3 $\mu g/cm^2$) loading. In in vivo studies, the dose was removed by washing at eight hours after application. Exhaled air was monitored and urine collected for three days post exposure. Tape stripping was also carried out at three days post exposure. In vitro studies were carried out with charcoal occlusion chambers using Hanks balanced salt solution (HBSS) as receptor fluid, and were terminated at four hours. Dose recovery from in vivo studies was poor (48.4%), but better in in vitro studies (84.1% and 95.8% in low and high dose, respectively). In vivo percent dose absorbed (total excretion) after eight hours was 8.2%, similar to in vitro penetration (perfusate plus skin) after four hours (7.1% from the higher dose application). In vivo, pulmonary excretion after 48 hours was 7.8%, which was in good agreement with in vitro perfusate alone after four hours (7%).

Split thickness skin (dermatomed or epidermal membranes) is regarded as the best type of skin for use in in vitro studies [OECD (2)], especially for lipophilic compounds, as the aqueous layers of the dermis can provide a significant barrier to the diffusion of lipophilic materials. Beckley-Kartey et al. (14) compared the absorption and metabolism of coumarin (1,2-benzopyrone) (log k_{OW} 1.39) in vitro in flow through cells using both rat and human skin (full thickness) with that in vivo (rats and human volunteers). The dose in vitro was 3.7 $\mu g/cm^2$ in ethanol and was in contact for 72 hours. HBSS was used as receptor fluid. The in vivo dose (applied to dorsal skin of rats and humans) was 20 $\mu g/cm^2$ in 70% ethanol/water vehicle and occluded for six hours prior to removal by washing. Coumarin absorption in human skin occluded in vitro ($66.0 \pm 8.3\%$) gave good estimate of that in vivo ($59.7 \pm 4.5\%$, $n = 3$). This was also the case in the rat ($60.4 \pm 8.3\%$, cf. 69.3% in vivo, $n = 2$). In both types of study, coumarin absorption was rapid and extensive (human in vivo peak blood concentration was measured 30 to 60 minutes after application, while, in vitro, most of absorbed dose was found in receptor fluid within 24 hours of exposure). Coumarin remained metabolically unchanged during absorption in vitro and was not metabolised by freshly isolated human epidermal keratinocytes, or by whole skin homogenates of human, rat or mouse skin. Metabolism of coumarin was not studied in vivo in humans or rats; detection was achieved through administration of a radiolabelled analogue to volunteers.

Wester et al. (15) studied the percutaneous absorption of boric acid (5% w/v), borax (5% w/v) and disodium octaborate tetrahydrate (10% w/v) in a water vehicle, as well as the influence of pretreatment with a chemical irritant on in vivo absorption. Human volunteer studies involved application of test compounds to back skin (2 $\mu L/cm^2$), with and without pre-irritation [24-hour application of (2%) SLS]. The dosing site was protected with a T-shirt for 24 hours, with no washing allowed. The T-shirt was then removed and the dose site washed. Each subject was dosed twice and measured twice. Comparable in vitro studies used human thigh cadaver skin in flow through cells supported with PBS, and the dose removed by washing after 24 hours. In vitro studies used either a dose matched to the in vivo study or an infinite dose (1000 $\mu L/cm^2$). In vivo absorption of all three compounds was low (less than 0.3%) but measurable. The SLS pretreatment did not result in measurable irritation (by TEWL) and there was no significant effect on absorption. Flux from boric acid in vitro at the matched dose was almost tenfold higher than in the in vivo study, and 1000-fold greater with the infinite dose. The percutaneous absorption of Mexoryl SX, another lipophilic compound, in vitro (0.16% of the applied dose) also over estimated systemic absorption in human volunteers (0.014% of the applied dose estimated from urinary excretion) under identical exposure conditions (16).

Van de Sandt et al. (17) compared the percutaneous absorption of propoxur (2-isopropoxyphenyl N-methyl carbamate) in several in vitro models (''rocked static'' system, rat dorsal and human ''viable'' whole abdomen skin and epidermal membranes, and a perfused porcine ear (PPE) model) with that in vivo (rat dorsal and human volar forearm). In all experiments, dose was 150 $\mu g/cm^2$ in 60% (v/v) aqueous ethanol and the exposure time was four hours. Tissue culture medium containing 10% foetal bovine serum was used as receptor fluid for the viable skin membranes and saline plus 3% BSA was used with epidermal membranes. The in vivo percutaneous absorption rate was calculated from blood concentrations after dosing using linear-system dynamics and point area deconvolution methods. In vitro parameters (absorbed dose and maximum flux) almost always overestimated those obtained in vivo in human volunteers. There were also considerable differences

between models. Absorbed dose after 24 hours was overestimated by in vitro experiments by a factor of two to eight, and maximum flux by one to seven. The overprediction was greatest with rat (then human) epidermal membranes and lowest with viable skin. Absorption in the PPE model was intermediate between these. The potential absorbed dose (dose applied minus dose recovered from application site) was the best predicted parameter with a maximum overestimation of 2.5-fold. Differences in absorption at 24 hours and maximum flux between in vivo and in vitro systems were minimal when viable membranes were used. In vivo absorption differed greatly between rats and humans. This was reflected in the difference in time to peak plasma concentration in rats (0.5-hr post-administration) and humans (approximately seven hours post-administration). A subsequent study (18) compared percutaneous absorption of *ortho*-phenylphenol in human volunteers (volar forearm) with both full thickness viable skin and epidermal membranes in static diffusion cells (receptor fluids were the same as those used in the propoxur study). Standardised conditions of dose ($120\,\mu g/cm^2$ in 60% (v/v) aqueous ethanol) and exposure time (four hours) were used throughout. Parallel studies were carried out with rats and rat skin. In human volunteers, the potential absorbed dose was $105\,\mu g/cm^2$, and about 27% of the applied dose was excreted in urine within 48 hours. This parameter was accurately predicted by the in vitro models using human skin, and a reasonable estimate was made of the amount systemically available when full thickness membranes were used in the in vitro model. However, maximum flux and k_p were underestimated by full thickness membranes, as would be expected for a lipophilic compound (log p 3.28). Human epidermal membranes ($12.8\,\mu g/cm^2/hr$) gave a good representation of flux in human volunteers ($11.0\,\mu g/cm^2/hr$), though predictions of the amount absorbed were overestimated by epidermal membranes approximately 3.5-fold after 48 hours.

A number of in vivo in vitro comparative studies were carried out during the EDETOX project, a three-year European Union funded research program into the evaluation of dermal absorption of toxic chemicals, which ran from January 2001 to April 2004 (final report in preparation). Researchers at TNO compared the percutaneous absorption of caffeine absorption using excised human skin (unpublished data) with that in human volunteers (19). Caffeine was applied to split thickness human abdomen skin in static diffusion cells (with saline as receptor fluid) or to the volar forearm in water vehicle at either 10 or $100\,\mu g/cm^2$; the exposure time was four hours in each case, after which the test compounds were removed by washing.

Monitoring of blood, urine and feces or receptor fluid continued for 72 hours after dosing. Amounts of caffeine measured in receptor fluid correlated well with the amount excreted in urine and faeces in vivo, especially at the lower dose. In both models, relative absorption was markedly reduced with the higher dose level, and the species difference in vitro at this dose was much less marked than in vivo. A marked skin reservoir was measured in rat skin, especially in vivo. But this was not detected with human skin.

B. Variability—Relationship Between In Vitro and In Vivo

If in vitro studies are to be useful in predicting absorption in vivo, they must reflect inter-individual variability. Jakasa et al. (20) reported the dermal absorption of neat and aqueous solutions of 2-butoxyethanol (BE) applied to volar forearm in volunteers (50% (v/v), 90% (v/v) BE in water or neat BE, $0.2\,mL/cm^2$ for four hours), as part of the EDETOX project. An inhalation exposure with known input rate and duration was used as a reference dose in vivo, and dermal absorption parameters

were calculated from excretion of total (free plus conjugated) butoxyacetic acid (BAA) in urine and BE in blood. Percutaneous absorption of BE from aqueous solutions exceeded that of neat BE. The time weighted average flux (calculated from cumulative BAA excretion) was (mean ± SD) 1.34 ± 0.49, 0.92 ± 0.60, and $0.26 \pm 0.17\,mg/cm^2/hr$ for 50%, 90%, and neat BE, respectively. The time weighted average flux from neat BE could not be calculated from BE concentrations in blood. Inter-individual variation in dermal flux with 50% BE (performed twice on each volunteer) was approximately twice as great as intra-individual variation, regardless of whether blood or urine data were used to calculate flux. These findings were compared with in vitro studies carried out by nine laboratories participating in EDETOX under comparable exposure conditions (21). All laboratories studied absorption of 50% (v/v) BE in water using static or flow through cells and either full thickness or split thickness human skin; the experiment was carried out three times in each laboratory. Selected laboratories also studied 75% (v/v) BE in water and neat BE. The exposure time was four hours and the volume applied was $0.2\,mL/cm^2$. The average maximum flux values of BE from a 50% (v/v) aqueous solution measured by each laboratory ranged from 0.5 to $2.8\,mg/cm^2/hr$ [average 1.4 ± 0.9 (SD) $mg/cm^2/hr$] which compared very well with the human volunteer data. Flux with neat BE measured in vitro ($0.29 \pm 0.12\,mg/cm^2/hr$) also compared well with human volunteer data. Wagner et al. (22) established a method in which skin samples used for in vitro studies were taken from volunteers previously studied in in vivo experiments. The lipophilic drug flufenamic acid was applied in a wool alcohol ointment (under infinite dose conditions) to the skin that was planned for excision in human volunteers at different timepoints prior to surgery. After anaesthetisation and disinfection of the area to be excised, the treated area of skin was cut off and immediately frozen to prevent further diffusion of the drug; the remaining flap of excised skin was used for in vitro studies. At the end of in vivo and in vitro studies, the skin was sectioned horizontally (into stratum corneum and deeper layers) and the test compound extracted and quantified. A poor correlation was found between amounts of drug in the stratum corneum in vivo and in vitro, perhaps because of the varying amounts of disinfectant used. However, direct linear correlations were found between penetration and permeation in vitro and in vivo in deeper skin layers. This design of study represents the "ultimate" in vitro–in vivo correlation, in which variability in both types of study is controlled by paired samples. The importance of inter- and intra-laboratory variation in in vitro percutaneous absorption studies has been identified by van de Sandt et al. (23). The variation arising from different skin donors was a considerable contributor to variation between studies, even within laboratories, along with the thickness of the skin used.

C. The Skin Reservoir In Vitro and In Vivo

The lower solubility of lipophilic chemicals in aqueous receptor fluids can result in the development of a reservoir of test compound in the skin or in the stratum corneum in vitro which may not be formed in comparable in vivo studies. It is very difficult to study the skin reservoir in vivo using human volunteers (although this has been done in experimental animals), though the stratum corneum can be sampled in vivo using tape stripping. Dick et al. (24,25) compared absorption of lindane through human skin in vitro with that in human volunteers. Lindane was applied in either acetone (120 mg/mL) or a white-spirit based formulation (3 mg/mL) to dermatomed human skin in static diffusion cells (with 50% aqueous ethanol as receptor fluid) or

to the ventral forearm, protected by a lightweight, non-occlusive guard (13.3 $\mu L/cm^2$ in each case). In vivo, the unabsorbed surface dose was removed by washing at six hours after dosing, and two corners of the dose site were tape stripped. The guard was removed after eight hours and replaced by a cloth gauze. The two remaining corners were tape stripped at 24 hours. Blood and urine analysis continued for 72 hours after dosing (the parent compound was not detected in urine, only conjugates of chlorinated phenols). Two sets of diffusion cells were run in parallel for the in vitro experiments, which were washed to remove the surface dose at six hours and tape stripped at either 6 or 24 hours after dosing. The proportion of the dose remaining unabsorbed after six hours was very similar between comparative studies with both the acetone vehicle ($79.3 \pm 6.3\%$ in vivo, $76.0 \pm 1.3\%$ in vitro) and the formulation ($10.5 \pm 1.5\%$ in vivo, $8.5 \pm 0.9\%$ in vitro). With the acetone vehicle, the proportion of the dose recovered from tape stripping after six hours in vivo ($14.3 \pm 2.5\%$) was comparable with the in vitro study ($14.2 \pm 4.8\%$) though this was not the case after 24 hours ($0.03 \pm 0.01\%$ in vivo, $27.5 \pm 11.4\%$ in vitro). When applied in formulation, lindane recovery in tape strips was significantly higher in vitro ($60.4 \pm 10.5\%$ at 6 hours, $39.7 \pm 6.2\%$ at 24 hours) than in vivo ($29.9 \pm 5.4\%$ after six hours, $3.0 \pm 0.7\%$ after 24 hours). These data suggested that any stratum corneum reservoir of lindane was more rapidly depleted in vivo than in vitro, though this could have been partly due to loss of some the applied material to the cloth gauze and clothing in the in vivo study, or by desquamation, processes that could not be replicated in vitro. Griffin et al. (26) compared their in vitro data for the organophosphate chlorpynfos log k_{OW}4.69) though full thickness human skin, with 50% ethanol/water as receptor fluid, applied in a commercial concentrate diluted in water (2086 nmol/cm^2) with a previous human volunteer study using the same concentrate in water (1046 nmol/cm^2) (27). Absorption into receptor fluid was much greater as a proportion of the applied dose (19.7%) than that excreted in vivo as dialkylphosphate metabolites (1.0%), though as with the lindane studies (24,25), the proportion of the dose recovered from the dose site by washing was very similar (56.8% in vitro, 52.6% in vivo) under similar conditions of occlusion. The authors commented that the results could be explained by chlorpyrifos partitioning into subcutaneous fat and being slowly released, resulting in low concentrations below the analytical limit of the method, or by the use of the ethanol/water receptor fluid, which may have altered the permeability of the skin, resulting in overestimation of absorption. A considerable reservoir of chlorpyrifos remained in the skin in vitro (15.6% of the applied dose) after 24 hours, despite the ethanol:water receptor fluid, though unfortunately no tape stripping was carried out in this study. More recently, Roberts et al. (28) demonstrated that a reservoir of steroid existed in the stratum corneum in vivo, by the reactivation of the vasoconstrictor effect of a steroid, both by occlusion and by application of a placebo cream, some time after the original topical application of the steroid. This indicates that the stratum corneum reservoir effect is not an artefact of the in vitro system for all chemicals.

The fate of material penetrating the skin but not reaching the receptor fluid in vitro has been an area of discussion in recent years; there has been much debate about whether such material is available for systemic absorption (''absorbable'') or whether it remains in the skin or is lost from the stratum corneum through desquamation. A recent study (29) on dihydroxyacetone (DHA), 7-(2H-naphtho[l,2-d]triazol-2-yl)-3-phenylcoumarin (7NTPC), and disperse blue 1 (DB1) considered the fate of the fraction of these compounds present in the skin after 24-hour exposure in the 48 hours following termination of exposure, to determine whether this reservoir was available

for further systemic absorption. In the case of DHA and DB1, very little of the compound penetrating the skin after 24 hours was available for further absorption. 7NPTC was found to be distributed throughout the epidermis and dermis, especially around hair follicles, and the authors recommended that this compound be investigated further. A study of the percutaneous absorption of catechol in human and rat skin in vitro and in vivo in rats concluded that the skin reservoir of this compound at 24 hours did not contribute to systemic absorption during the following 48 hours (30).

III. MICRODIALYSIS STUDIES IN VOLUNTEERS AND IN VITRO

Microdialysis as a means of measuring percutaneous penetration in vivo has been reviewed by Groth (31). The potential for microdialysis as a means of correlating in vivo and in vitro skin penetration data was noted by Boelsma et al. (32), who compared percutaneous absorption of methyl nicotinate (MN) through excised human skin and reconstructed epidermis with that in human volunteers (volar forearm). The in vivo study suffered from higher analytical thresholds than in the in vitro study; MN was only detectable in vivo after application of 100 mM MN for 10 minutes, compared with 25 mM for one minute with excised human skin. However, few studies have been performed in which percutaneous absorption through human skin in vitro has been compared with microdialysis human volunteers under comparable conditions, though some animal studies have been reported (33). There are some recognized difficulties with microdialysis, such as calibration of the probes (determination of the relative recovery of the test compound in the skin), and the affinity of the certain lipophilic chemicals for the probe itself (31). Measurement of the relative recovery may be performed in vitro by immersing the probe in solutions of the test compound, though in vivo methods have been developed, to provide a better estimate of the amount of unbound test compound in the extracellular space (34). As part of the EDETOX project, Korinth et al. (35) assessed the utility of microdialysis for measuring percutaneous absorption of BE, as 90% (v/v) or 50% (v/v) aqueous solutions, in human volunteers applied at a volume of 0.2 mL/cm^2. The BE concentrations were measured in dialysate (saline) as were concentrations of BAA in urine. Average flux values based on BAA levels in urine, calculated using data from a reference inhalation exposure, were similar to those obtained by Jakasa et al. (20), though the amount of BE recovered in the dialysate was considerably lower than that absorbed systemically. The authors then assessed the relative recovery of BE in dialysate in vitro using human skin in static cells, in which dialysis probes had been carefully inserted, compared with the amount measured in receptor fluid beneath the skin. These studies confirmed that only a fraction of the amount of BE entering the systemic circulation was recovered in the dialysis tubing, and underlined the need for careful calibration of the probes in an appropriate manner. The potential for microdialysis as a tool for in vivo/in vitro comparisons remains, as the technique is noninvasive and may enable the direct measurement of metabolites resulting from enzyme activities within the skin.

IV. CONCLUSIONS

A. The Design of In Vitro and In Vivo Studies

After many years of research and several studies in which data from human volunteer studies and from in vitro studies with human skin were compared under similar

conditions, we believe that the receptor fluid and thickness of the skin section used in in vitro studies are critical for certain compounds (see Ref. 36) if absorption in vivo is not to be underestimated in vitro. Similarly, in vivo and in vitro studies should be carefully designed to avoid differential loss of material, especially with volatile compounds, which can lead to an apparent overestimation of absorption by in vitro studies. Total recovery of the applied dose is essential in vitro (2) and should be carefully considered in vivo. Inter-individual differences in permeability of skin used in in vitro studies also appear to be critical variables (24,37), though a multi-center study in which skin was replaced by an artificial membrane, in order to eliminate this source of error reported a fourfold variation between highest and lowest average flux values from 16 different laboratories, when saturated aqueous methyl paraben was used as a model penetrant (38). It seems likely that the differences in temperature of the different parts of the diffusion cell, which may influence both diffusion rates and the concentration of the penetrant in the donor phase, may have varied considerably between laboratories. The importance of this parameter in finite dose studies is yet to be determined. However, the design of the diffusion cell itself (static or flow through) does not appear to be a significant source of variation. As regards in vivo studies, it appears that inherent variation in skin permeability between individuals may be at least as important as the design of the study in determining variability.

B. Does the Closeness of Predictions Vary with Lipophilicity of Chemicals?

Historically, some comparisons involving lipophilic compounds have been characterized by an underestimation in vitro of the degree of systemic absorption in vivo, and there have been concerns that the reservoir of such compounds measured in vitro in the stratum corneum and/or lower layers of the epidermis and dermis was not a true reflection of the situation in vivo for some chemicals. Conversely, in vitro measurements of more hydrophilic compounds have been either close to in vivo findings or have overestimated absorption, whilst predictions of absorption of volatile compounds in vitro have, in some cases, overestimated in vivo results, due to differential loss of the dose material from the skin surface. Correct design of in vitro studies (as described above) may reduce some of the problems associated with underestimation of absorption of some lipophilic compounds, though for highly lipophilic materials, use of an ethanol/water receptor fluid maybe necessary to ensure that percutaneous absorption is not limited by solubility. There are concerns that this may influence the permeability of excised skin over time. It is also clear that the use of such receptor fluids does not necessarily preclude the formation of a skin reservoir in vitro. In an in vitro system using a 50% ethanol:water receptor fluid, a considerable proportion (about 32%) of the applied dose of oxadiazon (log k_{OW} 5.08) in acetone (six-hour exposure terminated by a surface wash) was found in the stratum corneum of dermatomed human skin 24 hours after application of the test compound (39). It must also be made clear that reservoir effects are not limited to lipophilic compounds; generic protein binding and binding to receptors may also result in reservoir effects. Although the stratum corneum and skin reservoirs may play a role for certain chemicals in vivo, it is not yet clear how well in vitro studies predict the importance of this reservoir effect in vivo. Maintenance of skin viability in vitro, and careful design of studies to demonstrate the fate of these reservoirs in the longer term, are key factors.

C. Importance of Metabolism

There have been very few reported studies comparing the dermal metabolism of topically applied chemicals in human volunteers with that measured in excised human skin in vitro. This is understandable, as some of the enzyme activities in human skin are known to be unstable in time and under frozen storage, so freshly excised human skin should be used; this has attendant logistic problems, and animal skin has often been used as a model. Furthermore, measurement of dermal metabolism in human volunteers (and indeed in any whole animal) is complicated by the hepatic metabolism of test compounds. As mentioned above, microdialysis may provide a means of assessing dermal metabolism in human volunteers, and hence may provide a comparison with corresponding in vitro studies.

D. Final Remarks

If in vitro studies are well designed and well controlled, in vitro approaches using human skin can predict absorption in vivo, and the OECD's acceptance of in vitro data obtained under such conditions is welcome. However, loss of the applied dose material through desquamation cannot be easily replicated in vitro, and reservoir effects may differ between in vivo and in vitro systems, depending on the chemical.

REFERENCES

1. OECD. Draft guidance document for the conduct of skin absorption studies. OECD environment health and safety publications, Series on Testing and Assessment no. 28, December 2000.
2. OECD Guideline for Testing of Chemicals. Guideline 428: Skin Absorption: In Vitro Method. (Original Guideline, adopted 13th April 2004). OECD, Paris, 2004.
2a. www.edetox.ncl.ac.uk.
3. Bronaugh RL, Stewart RF, Wester RC, Bucks DAW, Maibach HI. Comparison of percutaneous absorption of fragrances by humans and monkeys. Food Chem Toxicol 1985; 23:111–114.
4. Bronaugh RL, Maibach HI. Percutaneous absorption of nitroaromatic compounds: in vivo and in vitro studies in the human and the monkey. J Invest Dermatol 1984; 84:180–183.
5. Bronaugh RL, Franz TJ. Vehicle effects on percutaneous absorption: in vivo and in vitro comparison with human skin. Br J Dermatol 1986; 115:1–11.
6. Wester RC, Maibach HI, Bucks DAW, McMaster JR. Percutaneous absorption and skin decontamination of skin PCBs: in vitro studies with human skin and in vivo studies in the rhesus monkey. J Toxicol Environ Health 1990; 31:235–246.
7. Wester RC, Maibach HI, Melendres J, Sedik L, Knaak J, Wang R. In vivo and in vitro percutaneous absorption and skin evaporation of isofenphos in man. Fundam Appl Toxicol 1992; 19:521–526.
8. Wester RC, Sedik L, Melendres J, Logan F, Maibach HI, Russell I. Percutaneous absorption of diazinon in humans. Food Chem Toxicol 1993; 8:569–572.
9. Wester RC, Maibach HI, Sedik L, Melendres J, Wade M, DiZio S. Percutaneous absorption of pentachlorophenol from soil. Fundam Appl Toxicol 1993; 20:68–71.
10. Pershing LK, Parry G, Lambert LD. Disparity of in vitro and in vivo oleic acid-enhanced beta-oestradiol percutaneous absorption across human skin. Pharm Res 1993; 10:1745–1750.

11. Ramsey JD, Woolen BH, Auton TR, Scott RC. The predictive accuracy of in vitro measurements for the dennal absorption of a lipophilic penetrant (fluazifop butyl) through rat and human skin. Fundam Appl Toxicol 1994; 23:230–236.
12. Clark NWE, Scott RC, Blain PG, Williams FM. Fate of fluazifop butyl in rat and human skin in vitro. Arch Toxicol 1993; 67:44–48.
13. Dick D, Ng KME, Sauder DN, Chu I. In vitro and in vivo percutaneous absorption of 14C-chloroform in humans. Hum Exp Toxicol 1995; 14:260–265.
14. Beckley-Kartey SAJ, Hotchkiss SAM, Capel M. Comparative in vitro absorption and metabolism of coumarin (1,2-benzopyrone) in human, rat and mouse. Toxicol Appl Pharmacol 1997; 145:34–42.
15. Wester RC, Hui X, Hartway T, Maibach HI, Bell K, Schell MJ, Northington DJ, Strong P, Culver BD. In vivo percutaneous absorption of boric acid, borax and disodium octaborate tetrahydrate in humans compared to in vitro absorption in human skin from infinite and finite doses. Toxicol Sci 1998; 45:42–51.
16. Benech-Kieffer F, Meuling WJA, Leclerc C, Roza L, Leclaire J, Nohynek G. Percutaneous absorption of Mexoryl SX (R) in human volunteers: comparison with in vitro data. Skin Pharmacol Appl Skin Physiol 2003; 16:343–355.
17. van de Sandt JJM, Meuling WJA, Elliott GR, Cnubben NHP, Hakkert BC. Comparative in vitro-in vivo percutaneous absorption of the pesticide propoxur. Toxicol Sci 2000; 58:15–22.
18. Cnubben NHP, Elliott GR, Hakkert BC, Meuling WJA, van de Sandt JJM. Comparative in vitro-in vivo percutaneous penetration of the fungicide ortho-phenylphenol. Regul Toxicol Pharmacol 2002; 35:198–208.
19. Meuling WJA, van de Sandt JJM, Roza L. Percutaneous penetration of [14C]-caffeine in human volunteers: a mass balance approach. In: Brain KR, Walters KA, eds. Perspectives in Percutaneous Penetration. Vol. 8A. Cardiff: STS Publishing, 2002:105.
20. Jakasa I, Mohammadi N, Kruse J, Kezic S. Percutaneous absorption of neat and aqueous solutions of 2-butoxyethanol in volunteers. Int Arch Occup Environ Health 2003; 77:79–84.
21. Kezic S. Human in vivo studies of dermal penetration: their relation to in vitro predictions. In: Perspectives in Percutaneous Penetration Vol 9A (Brain KR, Walters KA, eds) STS Publishing, Cardiff, 2004; 8.
22. Wagner H, Kostka KH, Lehr CM, Schaefer UF. Human skin penetration of flufenamic acid: In vivo/in vitro correlation (deeper skin layers) for skin samples from the same subject. J Invest Dermatol 2002; 118:540–544.
23. van de Sandt JJM, van Burgsteden JA, Cage S, Carmichael PL, Dick I, Kenyon S, Korinth G, Larese F, Limasset JC, Maas WJM, Montomoli L, Nielsen, JB, Payan J-P, Robinson E, Sartorelli P, Schaller KH, Wilkinson SC, Williams FM. In vitro predictions of skin absorption of caffeine, testosterone, and benzoic acid: a multi-centre comparison study. Regul Toxicol Pharmacol 2004; 38:271–281.
24. Dick IP, Blain PG, Williams FM. The percutaneous absorption and skin distribution of lindane in man. I. In vivo studies. Hum Exp Toxicol 1997; 16:645–651.
25. Dick IP, Blain PG, Williams FM. The percutaneous absorption and skin distribution of lindane in man. II. In vitro studies. Hum Exp Toxicol 1997; 16:652–657.
26. Griffin P, Payne M, Mason H, Freedlander E, Curran AD, Cocker J. The in vitro percutaneous absorption of chlorpyrifos. Hum Exp Toxicol 2000; 19:104–107.
27. Griffin P, Mason H, Heywood K, Cocker J. Oral and dermal absorption of chlorpyrifos: a human volunteer study. Occup Environ Med 1999; 56:10–13.
28. Roberts MS, Cross SE, Anissimov YG. Factors affecting the formation of a skin reservoir for topically applied solutes. Skin Pharmacol Physiol 2004; 17:3–16.
29. Yourick JJ, Koenig ML, Yourick DL, Bronaugh RL. Fate of chemicals in the skin after dermal application: does the in vitro skin reservoir affect the estimate of systemic absorption. Toxicol Appl Pharmacol 2004; 195:309–320.

30. Jung CT, Wickett RR, Desai PB, Bronaugh RL. In vitro and in vivo percutaneous absorption of catechol. Food Chem Toxicol 2003; 41:885–895.
31. Groth L. Cutaneous microdialysis – methodology and validation. Acta Dermato-Venereol 1996; 76:1–65.
32. Boelsma E, Anderson C, Karlsson AMJ, Ponec M. Microdialysis technique as method to study the percutaneous penetration of methyl nicotinate through excised human skin, reconstructed epidermis and human skin in vitro. Pharm Res 2000; 17:141–147.
33. Kreilgaard M. Assessment of cutaneous drug delivery using microdialysis. Adv Drug Deliv Rev 2002; 54:S99–S121.
34. Kreilgaard M. Dermal pharmacokinetics of microemulsion formulations determined by microdialysis. Pharm Res 2001; 18:367–373.
35. Korinth G, Wellner T, Jakasa I, Kezic S, Kruse J, Schaller KH. Assessment of percutaneous absorption of 2-butoxyethanol by microdialysis in volunteers. In: Brain KR, Walters KA, eds. Perspectives in Percutaneous Penetration. Vol. 9A. Cardiff: STS Publishing, 2004:100.
36. Wilkinson SC, Maas WJM, Nielsen JB, Greaves LC, van de Sandt JJM, Williams FM. Influence of skin thickness on percutaneous penetration in vitro. In: Perspective in Percutaneous Penetration Vol 9A (Brain KR, Walters KA, eds) STS Publishing, Cardiff, 2004; 83.
37. Lee FW, Earl L, Williams FM. Interindividual variability in the percutaneous penetration of testosterone through human skin in vitro. Toxicology 2001; 168:63.
38. Chilcott RP, et al. Inter- and intra-laboratory variation of in vitro diffusion cell measurements: an international multi-centre study using quasi-standardised methods and materials. J Pharma Sci 2004; 94:632–638.
39. Dick IP, Williams FM. In vitro models for the prediction of dermal absorption of chemicals. Health and Safety Executive Research Report CRR 178/1998, HSE U.K., 1998.

42

Permethrin Bioavailability and Body Burden for a Uniformed Soldier

Ronald C. Wester and Howard I. Maibach
Department of Dermatology, School of Medicine, University of California, San Francisco, California, U.S.A.

Rebecca M. Wester
Methodist Health System, Dallas, Texas, U.S.A.

I. ABSTRACT

The purpose of this study was to determine the bioavailability and body burden of permethrin for a soldier wearing permethrin impregnated uniform and access to a spray can of permethrin. Historically, disease bearing insects have spread illness and death to military personnel. Starting with DDT, insecticides have been used to control the situation. The safety of insecticide use to the soldier is of most importance.

Permethrin molecular weight (391.29) is of a size which will absorb through human skin. Permethrin water solubility is very low at 0.006 mg/L with a log P of 6.5. The low water solubility can inhibit skin absorption when using in vitro diffusion systems with a water-based receptor fluid. The diffusing permethrin will not be soluble in the water; therefore, no accumulation in the receptor fluid. This is just basic chemistry. Therefore, in vitro permethrin diffusion data were not used in this analysis (produce false results). In vivo rhesus monkey data were used. Rhesus monkey in vivo skin absorption is relative to and predictive of man in vivo.

Permethrin, being extremely lipophilic, with log P of 6.5, one would assume the compound would distribute widely to the layers of the body, resulting in high clearance and a long half-life. The half-life is actually short, about a day (rat and rhesus monkey). This suggests extensive permethrin metabolism and removal from the body.

The regional human body surfaces for a uniformed soldier are covered with either 125 $\mu g/cm^2$ permethrin in uniform material, or 4 $\mu g/cm^2$ permethrin from a single spray, or probably both. Percutaneous absorption as a base value of 8.7% (0.087 index) which is multiplied by the index for each body region, was used. Permethrin, in the uniform, partitions from uniform material to skin before skin absorption takes place. This uniform partition is estimated at 0.29. The time period for a soldier to wear the same uniform is for one day or longer. Total body burden is estimated at 1.24 mg/kg. If the permethrin spray is used more often, the body burden will increase proportionally.

II. INTRODUCTION

The purpose of this study was to determine the bioavailability and body burden of permethrin for a soldier wearing permethrin impregnated uniform, and has access to a spray can of permethrin.

Clothing treated with the insecticide permethrin offers near complete protection against insect vectors when used in conjunction with topical insect repellents. Of concern is the leaching of permethrin from the military battle dress uniform (BDU) and the potential for skin absorption by the wearer. Historically, disease bearing insects have spread illness and death to military situation. The safety of insecticide use to the soldier is of most importance. Suggestion of permethrin involvement in Gulf War syndrome necessitates a careful analysis of permethrin and body burden relative to permethrin toxicity.

III. PERMETHRIN

CAS number: 052645–53–1
C_{21} $H_{20}Cl_2O_3$
Molecular weight: 391.29
Water solubility: 0.006 mg/L
log *P* (octanol:water partition coefficient): 6.50
Isomers: Of the four possible isomers, the IR, *trans* and the IR, *cis*-isomers are the two esters primarily responsible for insecticidal activity. Technical material is a mixture of approximately 60% *trans*- and 40% *cis*-isomers.

Sources: Merck Index 11th edition 1989
SRC Phys Prop Database

Some of the above physical and chemical parameters have a bearing on the human percutaneous absorption of permethrin. The molecular weight (391.29) is of a size which will absorb through human skin. The Dalton Rule of 500 has an arbitrary top level of MW 500 (1).

Permethrin water solubility is very low at 0.006 mg/L with a log *P* of 6.5. The low water solubility can inhibit skin absorption when using in vitro diffusion systems with a water-based receptor fluid. Therefore, in vitro permethrin diffusion data were not used in this analysis (produce false results). In vivo rhesus monkey data were used. Rhesus monkey in vivo skin absorption is relative to and predictive of to man in vivo (2). In vivo human skin contains a lipophilic outer stratum corneum which is a more compatible environment for permethrin. The skin becomes less lipophilic at the epidermis:dermis barrier where absorption occurs. The log *P* of 6.5 means an octanol:water partition of 3,162,278:1 ($10^{6.5}$) for permethrin.

IV. PERMETHRIN PHARMACOKINETICS

Anadon et al. (3)
Sprague–Dawley rat
Elimination half-life
IV 8.67 hours (plasma)
oral 12.37 (plasma)

Clearance (plasma)
0.058 L/hr (not influenced by dose concentration or route)
Oral bioavailability 60.69%

Sidon et al. (4)
Sprague–Dawley rat and rhesus monkey
Elimination half-life
IM 0.8 to 1.1 days (urinary) both species

Permethrin is extremely lipophilic, log *P* of 6.5. One would assume the compound would distribute widely to the layers of the body, resulting in high clearance and a long half-life. The half-life is actually short, about a day (rat and rhesus monkey). This suggests extensive permethrin metabolism and removal from the body (5).

V. SOURCE FOR BIOAVAILABILITY AND BODY BURDEN CALCULATIONS

Human Body Surface Areas
USEPA (6)

Permethrin Dose
The targeted dose for permethrin in the uniform is 125 $\mu g/cm^2$ (7). The dose of 4 $\mu g/cm^2$ is the estimated amount of chemical deposited from a thin film of 0.25% solution applied to human skin (8). This is the spray dose.

Percutaneous Absorption
Table 1 from Ref. 4. In vivo percutaneous absorption of *cis* and *trans* isomers of permethrin dosed to ventral forearm for 24 hours.

Body Region Index
Skin from different parts of the human body absorbed chemicals at different rates and amounts. This is called regional variation. Guy and Maibach (9) devised an index to account for regional variation.

Uniform Effect
Permethrin in the uniform must leach out to the skin to be absorbed into the body. Table 2 shows the only three chemicals deposited on cloth, on human skin for which the percutaneous absorption was determined. Index

Table 1 Index Calculation: Permethrin Percutaneous Absorption in Forearm

Isomer/radiolabel position[a]	Dose absorbed (%)
cis-^{14}C-alcohol	8.7
cis-^{14}C-cyclopropyl	8.7
trans-^{14}C-alcohol	12.2
trans-^{14}C-cyclopropyl	5.0
Average	8.7
Index	0.087

All rhesus monkey in vivo forearm.
[a]Molecular site of ^{14}C-label.
Source: From Ref. 4.

Table 2 Index Calculation: Dose Partition of Permethrin from Uniform to Human Skin

Chemical	Dose absorbed (%)	Difference
Parathion[a]		
Human skin only	1.78	
Dry cloth	0.29	0.163
Wet cloth	0.65	0.365
Glyphosate[b]		
Human skin only	1.42	
Dry cloth	0.08	0.056
Wet cloth	0.36	0.254
Malathion[b]		
Human skin only	8.77	
Dry cloth	0.60	0.068
Wet cloth	7.34	0.837
Overall percent difference = index[c]		0.29

[a]Wester et al. (10) standard army issue uniform 50% cotton/50% nylon.
[b]Wester et al. (11) T-shirt 100% cotton.
[c]The index is the proportional difference in skin absorption without and with the added layer of cloth.

is based on absorption with and without (deposited directly on skin) cloth. The index is an average for these three chemicals. Wet is cloth was wetted with 20 μg/cm water (glyphosate and paratheon) or 50:50 water:ethanol (malathion).

The "wet" is to simulate a soldier's sweating and wet atmospheric conditions. In the few chemicals studied, the wetted cloth situation shows increased skin absorption compared to the dry situation (10,11).

A. Risk Assessment

Table 3 gives the bioavailability and body burden of permethrin for a uniformed soldier. The regional human body surfaces for a uniformed soldier are covered with either 125 $\mu g/cm^2$ permethrin in uniform material or 4 $\mu g/cm^2$ permethrin from a single spray. Percutaneous absorption as a base value of 8.7% (0.087 index) which is multiplied by the index for each body region. Permethrin in the uniform partitions from material to skin before skin absorption takes place. This uniform effect/partitioning is estimated at 0.29. The time period is for a soldier to wear the same uniform for one day or longer. Total body burden is estimated at 1.24 mg/kg. If the permethrin spray is used more often, the body burden will increase proportionally (Table 4).

Oral subacute and subchronic toxicity studies of permethrin have been performed in rats and mice at dose level up to 10,000 mg/kg diet and for 14 days to 26 weeks in duration. Changes detected at the higher level were an increase in liver/body weight ratio, hypertrophy in the liver, and clinical signs of poisoning such as tremor. The no-observed-effects levels (NOEL) in rats ranged from 20 mg/kg diet (in studies lasting 90 days or six months) to 1500 mg/kg diet (in six-month studies). The NOEL values in dogs ranged from 5 mg/kg body weight in three-month studies to 250 mg/kg body weight in six-month studies. In long-term studies in mice and rats, an increase in liver weight was found which was considered to be associated

Table 3 Permethrin Bioavailability and Body Burden for Uniformed Soldier

Human part	Body surface area[a](cm^2)	Perimethrin dose[b] (μg/cm^2)	Percutaneous absorption[c]	Body region index[d]	Uniform effect[e]	Total (μg)
Head	1,180	4	0.087	×4	1	1,642.56
Neck	420	4	0.087	×4	1	584.64
Trunk	5,690	125	0.087	×3	0.29	53,834.51
Arms	2,280	125	0.087	×1	0.29	7,190.55
Hands	840	4	0.087	×1	1	292.32
Genitals	180	125	0.087	×12	0.29	6,812.10
Legs	5,050	125	0.087	×1	0.29	15,926.44
Feet	1,120	4	0.087	×1	1	389.76
			Total (μg)			86,672.88
			Total (mg)			86.67
			Total body burden (mg/70 kg soldier)			1.24 mg/kg

[a]USEPA (1992).
[b]Uniform = 125 μg/cm^2 (7) spray open skin = 4 μg/cm^2.
[c]8.7% (0.087) permethrin dose absorbed—calculated from Ref. 4.
[d]Region body absorption index from Ref. 9.
[e]Calculated from Refs. 10 and 11. The 0.29 is 29% absorption from cloth relative to open skin (index).

Table 4 Permethrin Bioavailability and Body Burden with Multiple Spray

Permethrin spray[a]	Total body burden (mg/kg)
$1 \times 4\,\mu g/cm^2 = 4$	1.24
$5 \times 4\,\mu g/cm^2 = 20$	1.40
$10 \times 4\,\mu g/cm^2 = 40$	1.61

[a]1:1 spray use from spray can in 24 hours; 5:5 spray uses; 10:10 spray uses.

with an induction of the liver microsomal enzyme system. The NOEL in a two-year rat study was 100 mg/kg diet, corresponding to 5.0 mg/kg body weight. There were indications, from three long-term mouse studies, of oncogenicity in the lungs of one strain of mouse (females only) at the highest dose level (5 g/kg diet). Studies in rats revealed no oncogenic potential in either sex. Permethrin was not mutagenic in vivo or in vitro studies (12).

An NRC subcommittee (7) concluded that soldiers who wear permethrin-impregnated battle-dress uniforms are unlikely to experience adverse health effects at the suggested permethrin exposure levels (0.125 mg/cm^2). Concern has been raised where permethrin is used in conjunction with other neurotoxic agents (pyridostigmine bromide, DEET), the combination showing toxicity (13).

VI. DISCUSSION

The permethrin percutaneous absorption chosen for this analysis was that of Sidon et al. (4), studies done in vivo in the rhesus monkey. The rhesus monkey in an animal model relevant to man for percutaneous absorption (2,14). The high log *P*

chemicals are not soluble in the water-based perfusion fluids that are used, leading to false negative conclusions as to permethrin skin absorption (15,16). Other high log *P* compounds which have negligible in vitro absorption but significant in vivo absorption include DDT (log *P* 6.91), benzo[a]pyrene (log *P* 5.97), chlordane (log *P* 5.58), pentachlorophenol (log *P* 5.12) and the PCBs.

Snodgrass (17) determined the percutaneous absorption of permethrin (*cis* and *trans* mix) impregnated cotton and NYCO/50/50 nylon–cotton blend dyed woodland camouflage fabric in rabbits. Depending on environment of fabric type, the percutaneous absorption was 1% to 3% of applied dose. Expressed as percent of applied dose the estimate from this analysis for the arm (Table 3) is as follow:

$$\text{percent dose absorption} = \frac{7190.55\,\mu g}{2280\,cm^2 \times 125\,\mu g/cm^2} \times 100 = 2.5\%$$

These percent dose absorptions are in agreement, even given the variability of species where the rabbit is a higher skin absorbing species than man. This suggests that the controlling step is the release of permethrin from fabric to skin.

The amount of permethrin in uniform fabric is targeted to 125 $\mu g/cm^2$, and factory processed uniforms would has some quality assurance for this. However, this is not the only source. Packets containing permethrin are available with directions to soak the uniform in a tub of water containing the packet's contents, then hang up to dry. The amount of permethrin in the uniforms from packet treatment would be expected to vary relative to those produced with some quality assurance.

The permethrin body burden estimate from uniform and one spray application is 1.24 mg/kg for the soldier wearing the uniform for a least one day and for a few days after that (Table 3). Permethrin exposure from the one uniform would decrease with wear. The half-life of permethrin is about one day so body accumulation would not be expected. Variables such as undergarments (T-shirt and shorts) would probably decrease exposure while excessive use of a permethrin spray can will increase exposure (Table 4). Wet condition (humidity, rain, and sweating) and elevated temperature will increase permethrin absorption. The NOEL estimates from animal studies at 5 mg/kg, giving a fivefold safety margin (12), which is the only safety net from co-exposure to other neurotoxic agents.

REFERENCES

1. Bos JD, Meinarde MMHM. The 500 Dalton rule for the skin penetration of chemical compounds and drugs. Exp Dermatol 2000; 9:165–169.
2. Wester RC, Maibach HI. Percutaneous absorption in the Rhesus monkey compared to man. Topicol Appl Pharmacol 1975; 32:394–398.
3. Anadon A, Martinez-Garranaga MR, Drag MJ, Bungas P. Toxicokinetics of permethrin in the rat. Toxicol Appl Pharmacol 1991; 110:1–8.
4. Sidon EW, Moody RP, Franklin Ca. Percutaneous absorption of cis - and trans - permethrin in Rhesus monkeys and rats: anatomic site and interspecies variation. J Toxicol Environ Health 1998; 23:207–216.
5. Gaughan LC, Unai I, Casida JE. Permethrin metabolism in rats. J Agric Food Chem 1977; 25:9–17.
6. USEPA. Dermal exposure assessment: principles and applications. Interim Report EPA/600/8-91/011B, 1992.

7. National Research Council. Health effects of permethrin impregnated army battle-dress uniforms. NRC Committee on Toxicology Govt. Reports Announcements and Index (GRA & I), Issue 24, 1994.
8. Maibach HI, Feldmann RJ. Systemic absorption of pesticides through the skin of man. In: Occupational Exposure to Pesticides: Report to the Federal Working Group on Pest Management from the Task Group on Occupational Exposure to Pesticides, Appendix B, 1974:120–127.
9. Guy RH, Maibach HI. Calculations of body exposure from percutaneous absorption data. In: Bronaugh R, Maibach H, eds. Percutaneous Absorption. New York: Marcel Dekker Inc., 1985:461–466.
10. Wester RM, Tanojo H, Maibach HI, Wester RC. Predicted chemical warfare agent VX toxicity to uniformed soldier using parathion in vitro human skin exposure and absorption. Toxicol Appl Pharmacol 2000; 168:149–152.
11. Wester RC, Quan D, Maibach HI. In vitro percutaneous absorption of model compound glyphosate and malathion from cotton fabric into and through human skin. Food Chem Toxicol 1996; 34:731–735.
12. WHO. TA: Environmental Health Criteria PG, 1990; 125 IP: 94 V1.
13. Abou-Donia MB, Wilmath KP, Jensen KF, Oehme FW, Kurt TL. Neurotoxicity resulting from coexposure to pyridostigmine bromide, DEET and permethrin: implications of Gulf War chemical exposure. J Toxicol Environ Health 1996; 48:35–56.
14. Wester RC, Maibach HI. Toxicokinetics: dermal exposure and absorption of toxicants. In: Bond G, ed. Comprehensive Toxicology Vol.1 General Principles. New York: Pergamon Press, 1997:99–114.
15. Franz TJ, Lehman PA, Franz SF, Guin JD. Comparative percutaneous absorption of lindane and permethrin. Arch Dermatol 1996; 132:9–17.
16. Baynes RE, Hailing KB, Riviere JE. The influence of diethyl-*m*-toluamide (DEET) on the percutaneous absorption of permethrin and carbaryl. Toxicol Appl Pharmacol 1997; 144:332–339.
17. Snodgrass HL. Permethrin transfer from treated cloth to the surface skin: potential for exposure in humans. J Toxicol Environ Health 1992; 35:91–105.

43

The Correlation Between Transepidermal Water Loss and Percutaneous Absorption: An Overview

Jackie Levin and Howard I. Maibach
Department of Dermatology, School of Medicine, University of California, San Francisco, California, U.S.A.

I. ABSTRACT

Independently both TEWL and percutaneous absorption measurements accurately gauge stratum corneum (SC) skin water barrier integrity. Both TEWL and percutaneous absorption rates increase when the integrity of the SC barrier is compromised. Experiments to discern a quantitative and/or qualitative correlation between the two indicators has resulted in controversy. This paper reviews some major studies investigating this correlation.

II. INTRODUCTION

A. TEWL

Transepidermal water loss (TEWL) is the outward diffusion of water through skin (1). TEWL measurements are used to gauge skin water barrier function. An increase in TEWL reflects impairment of the water barrier (2). TEWL measurements allow parametric evaluation of the effect of barrier creams against irritants and characterization of skin functionality in clinical dermatitis and in irritant and allergic patch test reactions (3). An evaporimeter determines TEWL by measuring the pressure gradient of the boundary layer resulting from the water gradient between the skin surface and ambient air. TEWL measurements can be affected by the anatomical site, sweating, skin surface temperature, inter- and intra-individual variation, air convection, ambient air temp, ambient air humidity, and instrument related variables to name a few. Although TEWL is influenced by many variables, experiments show that evaporimeter measurements are reproducible in vitro and in vivo (3,4).

B. Percutaneous Absorption

Percutaneous absorption refers to the rate of absorption of a topically applied chemical through the skin. A compound's absorption rate is important for determining the effectiveness and/or potential toxicity of topically applied compounds. Since many topical formulations are used on diseased skin, where the integrity of the permeability barrier is in doubt, the dose absorbed into the body could vary greatly (5). One rate limiting step of a compound's absorption through the skin is the rate of diffusion through the SC. The rate of absorption in vivo through the SC cannot be described by a zero or first order mathematical rate equation because the SC is a complex system variable in its penetration properties. Many factors contribute to the percutaneous absorption of a given chemical. This review discusses three main categories that give rise to percutaneous absorption rate variation; methodology (including the effects of application time, method of measurement, and physicochemical properties of the topical compound), inter-individual variation (including the effects of skin condition, age of individual, and blood flow), and intra-individual variation (including the differences between anatomic sites) (6,7).

C. Why Do We Want to Correlate TEWL and Percutaneous Absorption?

The extensive procedure required to measure percutaneous absorption versus TEWL enhances the desire to find a correlation between the two measurements in order to more easily assess skin barrier function. Experimentation investigating the correlation between TEWL and percutaneous absorption has resulted in studies concluding significant quantitative correlation and a few concluding no quantitative correlation. Yet despite the significant quantitative correlation demonstrated in some experiments, the precise qualitative relationship between percutaneous absorption and TEWL remains unsettled. Is the quantitative correlation just a coincidence or have we not discovered the link between the two indicators?

We review some major studies defining the correlation between TEWL and percutaneous absorption and discuss major assumptions made in these experiments.

D. Main Review Correlation Studies

Oestmann, et al. investigated correlations between TEWL and hexyl nicotinate penetration parameters in man. Hexyl nicotinate (HN) penetration was indirectly measured by means of laser-Doppler flowmetry (LDF), which quantifies the increase in cutaneous blood blow (CBF) caused by penetration of HN, a vasoactive substance. Lipophilic HN was chosen over hydrophilic methyl nicotinate because HN is a slower penetrant, hence, making it easier to distinguish an intact barrier from an impaired barrier.

The LDF parameters t_0 and t_{max} were compared with corresponding TEWL values and a weak quantitative negative correlation was made ($r = -0.31$, $r = -0.32$). This correlation suggests that when an individual's response time, t_0, was fast, the skin barrier was impaired. The weak negative correlation found may be due to the percutaneous absorption method used. The LDF method has some negative attributes and is not as reproducible as other methods. Further research should investigate this weak correlation between TEWL and penetration of HN.

Lamaud et al. investigated whether permeability changes of hydrophilic compounds (TEWL) are correlated to those of lipophilic compounds (hydrocortisone).

Penetration of 1% hydrocortisone and TEWL rates were recorded for the hairless rats in vivo before and after UV irradiation (660 J/cm^2). Both the before and after UV irradiation results correlated well with the TEWL values for application periods up to 1 hour. In part two of the experiment drug penetration was evaluated by urinary excretion five days after a single 24 hours application on normal, stripped, or UV-irradiated skin of hairless rats. The quantity of drug eliminated correlated with the level of TEWL for up to two days. These results suggest that TEWL can predict the changes of skin permeability to lipophilic drugs in normal and some damaged skin.

Oestmann et al. characterized the SC barrier function in patients with various keratinization disorders using two non invasive methods: measuring outward transport of water through skin by evaporimetry (TEWL) and the vascular response to HN penetration into the skin determined by LDF. Three of the five types of keratinization disorders studied autosomal dominant ichthyosis vulgaris (ADI), X-linked recessive ichthyosis (XRI), and autosomal recessive congenital ichthyosis (CI) have impaired barrier function and are a type of icthyosis while the other two keratinization disorders studies, dyskeratosis follicularis (DD), and erythrokeratoderma variabilis (EKV), have no prior information available on barrier impairment. In this experiment the two methods of barrier function assessment, TEWL and LDF, were correlated.

The TEWL measurements and the LDF parameter, t_0, showed a high negative correlation in the patient group ($r = -0.64$) and a weaker negative correlation among the control group ($r = -0.39$). Because TEWL reflects the SS-flux of a compound across SC and parameter t_0 is a function of the duration of the lag phase (non-SS), this study suggests that these two methods should not be considered as exchangeable alternatives but rather as complementary tests. Each method reflects a different aspect of the barrier function.

This paper concludes that TEWL and HN penetration injunction are suitable methods to monitor skin barrier function in keratinization disorders and are helpful in discriminating between some of these disorders.

Rougier et al. attempt to establish the relationship between the barrier properties of the horny layer (percutaneous absorption and TEWL) and the surface area of the corneocytes according to anatomic site, age, and sex in man. The penetration of benzoic acid (BA) was measured in vivo at seven human anatomic sites and compared to its TEWL measurement taken on the contralateral site. The amount of BA penetrated was measured through urinary extraction up to 24 hours after application. It was discovered that irrespective of anatomic site and gender a linear relationship ($r = 0.92$, $p < 0.001$) exists between total penetration of BA and TEWL.

Comparing corneocytse surface area to permeability the study found a general correlation of increasing permeability for both H_20 and BA with decreasing corneocyte size. The smaller the volume of the corneocyte, the greater the intercellular space available to act as a reservoir for topically applied molecules (8). This thinking is in accord with other studies who have shown that the smaller the capacity of the reservoir, the less the molecule is absorbed (8–12). However certain anatomic sites where corneocyte size was similar (980–1000 μm^2) and there were large differences in permeability suggest that while corneocyte surface area appears to be an important phenomena, it only partly explains the difference in permeability observed according to anatomic site and age.

This study demonstrates that percutaneous absorption and TEWL are indeed quantitatively correlated yet corneocyte size partially explains the difference in permeability between the different anatomic sites and age of the skin. It seems that other factors may be when corneocyte area is less than 600 μm^2 or more than 1000 μm^2.

Lotte et al. examine the relationship between the percutaneous penetration of four chemicals (acetyl-salicylic acid, benzoic acid, caffeine, and the sodium salt of benzoic acid) and TEWL in man as a function of anatomic site. The amount of chemical penetrated was measured by urinary excretion for up to 24 hours after application. For a given anatomic site the permeability varies widely in relation to the nature of the molecule administered due to the physicochemical interactions which occur between the molecule, vehicle, and SC. For all anatomic sites investigated, irrespective of physicochemical properties of the molecules administered, there was a linear relationship between TEWL and percutaneous absorption.

Aalto-Korte and Turpeinen attempted to find the precise relationship between TEWL and percutaneous absorption of hydrocortisone in patients with active dermatitis. Percutaneous absorption of hydrocortisone and TEWL were studied in three children and six adults with dermatitis. All the subjects had widespread dermatitis covering at least 60% of the total skin area. Plasma cortisol levels were determined first and 2 and 4 hours after hydrocortisone application by radioimmunoassay. The TEWL was measured in six standard skin areas immediately before application of the hydrocortisone cream. Each individual TEWL value was calculated as a mean of these six measurements.

The concordance between the post-application increment in plasma cortisol and the mean TEWL was highly significant resulting in a correlation coefficient of $r = 0.991$ ($p < 0.001$). In conclusion this study found a highly significant correlation between TEWL and percutaneous absorption of hydrocortisone.

Tsai et al. investigates the relationship between permeability barrier disruption and the percutaneous absorption of various compounds with different lipophilicity values. Acetone treatment was used on in vivo hairless mice to disrupt the normal permeability barrier and in vivo TEWL measurements used to gauge barrier disruption. The hairless mouse skin was then excised and placed in diffusion cells for the in vitro percutaneous absorption measurements of five model compounds. The permeability and lipophilicity of the all the compounds tested on the barrier disrupted hairless mouse is summarized in Table 1.

The permeability barrier disruption by acetone treatment and TEWL measurements significantly correlated with the percutaneous absorption of the hydrophilic and lipophilic drugs sucrose, caffeine, and hydrocortisone. However acetone treatment did not alter the percutaneous penetration of the highly lipophilic compounds estradiol and progesterone, hence suggesting that there is not a correlation between TEWL and the percutaneous absorption of highly lipophilic compounds. The results imply the need to use both TEWL and drug lipophilicity to predict alterations in skin permeability.

Table 1 Summarizes the Permeability and Lipophilicity of all the Compounds Tested on the Barrier Disrupted Hairless Mouse in the Study by Tsai et al. (13)

Compound	Partition coefficient ($K_{o/w}$)	Correlation coefficient (r)
Sucrose	−3.7	0.82
Caffeine	−0.02	0.86
Hydrocortisone	1.5	0.82
Estradiol	2.7	0.72
Progesterone	3.9	0.01

Chilcott et al. investigated the relationship between TEWL and skin permeability to tritiated water ($^3H_20$) and the lipophilic sulfur mustard (^{35}SM) in vitro. No correlation was found between basal TEWL rates and the permeability of human epidermal membrane to $^3H_20$ ($p = 0.72$) or sulfur mustard ($p = 0.74$). Similarly, there was no correlation between TEWL rates and the $^3H_20$ permeability of full thickness pig skin ($p = 0.68$). There was no correlation between TEWL rates and $^3H_20$ permeability following up to 15 tape strips ($p = 0.64$) or up to four needle stick punctures ($p = 0.13$). These data indicate that under these experimental circumstances TEWL cannot be used as a measure of skin's permeability to topically applied compounds.

III. DISCUSSION

The majority of studies investigating TEWL and percutaneous absorption correlation observe a quantitative correlation. It is our hypothesis that the papers which did not observe a quantitative correlation (13,14) or observed a weak correlation (1,15) do so as a result of assumptions made in the experiment's design. Many of the experiments investigating TEWL and percutaneous absorption make large assumptions which could affect the results of experimentation and hence be the source of the controversy. For example, Tsai et al., and Chilcott et al. assume that an in vitro measurement of TEWL and percutaneous absorption are equivalent to in vivo measurements, while Lamaud et al. assume that animal skin may serve as a permeability model for human skin. Great sources of error and variation can also be induced depending on the measurement method and type of absorption compound used in obtaining percutaneous absorption rates. Because we do not completely understand the qualitative relationship between TEWL and percutaneous absorption, it is hard to determine which assumptions made during the experiment could be affecting the correlation results. This section investigates the probable causes that could influence the results of the correlation experiments. Table 2 provides a summary of the major assumptions made by the studies discussed.

A. Using In Vitro Methods to Model In Vivo Experiments

Skin permeation can be measured in living humans or in vitro by using excised skin in diffusion cells. In theory, studies using excised skin are feasible models for in vivo experiments because passage through the skin is a passive diffusion process and the stratum corneum is composed of non-living tissue. Many studies comparing in vivo and in vitro TEWL and percutaneous absorption measurements have been conducted and the results from those experiments support the contention that reliable measurements can be obtained from in vitro methodology (6,16–22).

While the consensus is that in vitro experiments are reasonable models for in vivo human experiments, some experiments note significant differences between these methods for measuring skin permeation. The most significant study by Bronaugh and Stewart (20) found that the effects of UV irradiation could not be duplicated using an in vitro experimentation model, hence suggesting that in vitro experiments examining the TEWL and percutaneous absorption after barrier damage may not be an acceptable model for in vivo experimentation. In vitro damage to the SC barrier may not be an accurate model to in vivo SC damage

Table 2 A summary of the Major Assumptions Made by the Studies Discussed in this Review

Reference	In vivo vs. in vitro (prec abs)[c]	Skin type	Percutaneous absorption measurement method	Type of absorption compound[b]	Healthy skin vs. damaged skin	Correlation results
Ref. 1	Vivo	Human	LDF	Lipophilic	Healthy	Yes
Ref. 29	Vivo	Animal	Urinary	Lipophilic	Both	Yes
Ref. 15	Vivo	Human	LDF	Lipophilic	Damaged	Yes
Ref. 30	Vivo	Human	Urinary	Lipophilic hydrophilic and	Healthy	Yes
Ref. 28	Vivo	Human	Urinary plasma cortisol level	Lipophilic	Healthy	Yes
Ref. 31	Vivo	Human		Lipophilic hydrophilic and	Damaged	Yes
Tsai et al. 2001[a](a)	Vitro	Animal	Diffusion cell	Lipophilic	Damaged	Yes
Tsai et al. 200l[a](b)	Vitro	Animal	Diffusion cell	Highly lipophilic hydrophilic and	Damaged	No
Ref. 14	Vitro	Both	Diffusion cell	Lipophilic	Both	No

[a]Note: Tsai et al. (13) was divided into two experiments in this table since the study found a correlation between TEWL's and percutaneous absorption with some compounds and no correlation with others.
[b]Type of absorption compound was determined by their octanol-water partition coefficient, $K_{o/w}$. Value less than one is hydrophilic and more than three is very lipophilic.
[c]Since TEWL in vivo and in vitro measurements are considered equivalent, we are only concerned with how percutaneous absorption measurements were taken.

because in vivo exposure to skin irritants results in a cascade of reactions that do not occur in human cadaver skin (16).

Chilcott et al. investigated TEWL and percutaneous absorption correlation in vitro after inducing different types of barrier damage. This was also one of the only studies reviewed which did not observe a correlation between TEWL and percutaneous absorption. It is possible that using in vitro methodology in the experimental design may be the cause for this studies inability to show correlation after damage.

B. Using Animal Skin to Model Human Skin

Comparing the skin morphology and chemical absorption of human vs. animal skin, it is clear that human skin is unique in both aspects and should be used for the most meaningful results (23). Yet an experiment by Bronaugh et al. (22) found that

depending on the compound of interest and the vehicle used, permeability values obtained using animal skin can be well within an order of magnitude of the permeability values for human skin.

Independently, in vitro methods and animal skin models prove to be reliable models for human in vivo absorption. Therefore, it seems logical to assume that in vitro and animal methods may be used in unison to accurately model in vivo human absorption. However [2]Rougier et al. document a distinct difference between animal studies done in vivo versus animal studies done in vitro when compared to human absorption. This experiment compares the skin permeability of humans to the hairless rat (24) and the hairless mouse (19) using molecules of widely different physicochemical properties. The results show that, in vivo, for whatever the molecule tested the permeability ratios remain relatively constant while in vitro they do not. Therefore when application conditions are strictly identical in humans and in animals it may be possible to model human in vivo absorption by measuring in vivo animal absorption but not using in vitro animal absorption. The inaccurate results obtained when conducting experiments in vitro using animal skin may have affected the results studies by Tsai et al. and Chilcott, et al. which were the only two papers to conclude no correlation between TEWL and percutaneous absorption and only the two papers using in vitro animal methodology.

C. Percutaneous Absorption Measurement Methods

A major factor affecting percutaneous absorption measurements is methodology (25,26). All methods for percutaneous absorption measurements are not equal and hence can give different results. Table 2 column 3 summarizes of the percutaneous absorption methods used in these correlation studies.

The most common method for determining percutaneous absorption in vivo is measuring the radioactivity of excreta following topical application of a labeled compound. Determination of percutaneous absorption from urinary radioactivity does not account for metabolism by skin but has been proven to be a reliable method for absorption measurement and is widely accepted as the "gold standard" when available.

The most commonly used in vitro technique involves placing a piece of excised skin in a diffusion chamber, applying radioactive compound to one side of the skin, and then assaying for radioactivity in the collection vessel on the other side (27). The advantages of using this in vitro technique are that the method is easy to use and that the results are obtained quickly. The disadvantage is that the fluid in the collection bath which bathes the skin is saline, which may be appropriate for studying hydrophilic compounds, is not suitable for hydrophobic compounds. If the parent compound is not adequately soluble in water then determining in vitro permeability into a water receptor fluid will be self-limiting.

When conducting in vitro experiments animal skin is often substituted for human skin. Because animal skin has different permeability characteristics than human skin, one should be careful which type of animal skin is used (see Sec 2.2). In addition, proper care should be taken in skin preparation of excised skin to make sure not to damage skin barrier integrity. Anatomical site is also important as well as using many different skin samples. The only two experiments which did not find a correlation between TEWL and percutaneous absorption, Tsai et al. and Chilcott et al. were experiments that measured percutaneous absorption in vitro. Perhaps using a diffusion cell to measure percutaneous absorption is the reason for not finding a correlation.

Oestmann et al. and Lavrijsen et al. used LDF to measure HN penetration. The LDF measures the increase in CBF caused by the penetration of HN, a vasoactive substance. One problem with this method is that LDF measurements are not only dependant on the amount of HN absorbed but the individual's vasoreactivity, gender, and age. This may be the reason that Oestmann et al. and Lavrijsen et al. obtained only a weak correlation between TEWL and percutaneous absorption of HN. Another disadvantage of this method is LDF measurement's many sources of variation which make it difficult to compare inter-laboratory results. If an attempt should be made note that LDF parameters t_o, and t_{max} are a function of HN concentration, the vehicle used, and the application time and the LDF parameters LDF_{base} and LDF_{max} are relative values depending on the type of LDF used.

D. Type of Compound

The percutaneous absorption rate and/or total absorption of a compound varies greatly depending on the compound and its lipophilicity yet, many of the papers reviewed did not consider how lipophilicity of the test compound would affect percutaneous absorption and hence correlation results. Feldmann and Maibach (17) measured both the total absorption and max absorption rate for 20 different compounds of different lipophilicities. The range for total absorption for the 20 compounds tested was greater than 250 times while the difference in maximum absorption rate was greater than 1000 fold (17). Because of the extreme range of absorption for topically applied compounds it seems reasonable to assume that the correlation between TEWL and percutaneous absorption may not be independent of the physicochemical properties of the compound applied. Namely, can TEWL measurements predict the skin barrier's permeability changes to both hydrophilic and very lipophilic compounds?

Correlation results from main studies Oestmann et al., Lamaud et al., Lavrijsen et al., Lotte et al., Aalto-Korte et al., and Tsai et al. suggest that TEWL can predict the changes in skin permeability to hydrophilic and slightly lipophilic topical drugs. Tsai et al. also discovered that the percutaneous absorption of highly lipophilic compounds does not correlate with TEWL.

The highly lipophilic compounds were the compounds that did not show evidence of a correlation between percutaneous absorption and TEWL while the moderately lipophilic compounds such as hydrocortisone and benzoic acid did. This should be further investigated. In the future it may be necessary to use both TEWL and drug lipophilicity to predict alterations in skin permeability.

E. Exploring the Qualitative Reasoning for the Correlation Between Percutaneous Absorption and TEWL

Experiments investigating the correlation between TEWL and percutaneous absorption have found a quantitative correlation between the two skin barrier indicators, yet have failed to find their precise qualitative relationship. Most experiments looking for an explanation of skin permeability examine and compare trends in physical aspects of the skin such as SC membrane thickness, corneocyte size, area of the horny layer, transcorneal routes, sebum lipid film, and intercellular volume to include a few. Yet we remain clueless about the structure function relationship of the SC because there is no one morphology aspect that explains the permeability of the SC. Skin has particular features which combine together in varying degree to

produce different experimental values of TEWL and percutaneous absorption (28). Further investigation needs to be done investigating the relationship between TEWL and percutaneous absorption in terms of skin structure and morphology.

IV. CONCLUSION

Although it is not certain why studies by Tsai et al. and Chilcott et al. showed no quantitative correlation we can postulate some estimations. Tsai et al. is the only paper demonstrating a clear distinction between highly lipophilic compounds and slightly lipophilic compounds when correlating percutaneous absorption and TEWL. Acetone treatment could affect a certain aspect of the skin barrier that mostly affects and interacts with hydrophilic compounds hence having no effect on the highly lipophilic compounds such estradiol and progesterone. It would be interesting to ascertain if the same results were obtained when selecting a different form of barrier damage such as physical tape stripping, etc. Or it could be the fact that the lipophilic compounds chosen were even more hydrophobic than those used in other experiments and indeed TEWL and percutaneous absorption of highly lipophilic compounds are not correlated.

It is difficult to understand why Chilcott et al. found no correlation between TEWL and percutaneous absorption. The results could have been affected by the fact that the experiment was done in vitro, partly on animal skin, using an extremely lipophilic compound, sulfur mustard. It would be interesting to ascertain if TEWL and percutaneous absorption of sulfur mustard correlated with the results up to one hour after application.

Taken together, the weight of evidence confirms a relationship between TEWL (water transport) to percutaneous penetration, yet much remains before this can fully be generalized and the mechanism understood. Future experiments should take into consideration the effects modeling realistic situations using alternative methods to the ideal.

REFERENCES

1. Oestmann E, Lavrijsen APM, Hermans J, Ponec M. Skin barrier function in healthy volunteers as assessed by transepidermal water loss and vascular response to hexyl nicotinate: intra- and inter-individual variability. Br J Dermatol 1993; 128:130–136.
2. Nilsson GE. Measurement of water exchange through skin. Med Biol Eng Comput 1977; 15:209–218.
3. Pinnagoda J, Tupker R, Agner T, Serup J. Guidelines for transepidermal water loss (TEWL) measurement. Contact Derm 1990; 22:164–178.
4. Pinnagoda J, Tupker R, Coenraads PJ, Nater JP. Comparability and reproducibility of the results of water loss measurements: a study of 4 evaporimeters. Contact Derm 1989; 20:241–246.
5. Bronaugh R, Weingarten D, Lowe N. Differential rates of percutaneous absorption through the eczematous and normal skin of a monkey. J Invest Dermatol 1986; 87:451–453.
6. Noonan P, Gonzalez M. Pharmacokinetics and the variability of percutaneous absorption. J Toxicol 1990; 9(2):511–516.
7. Wester RC, Maibach HI. 1993. Chair's summary: percutaneous absorption - in vitro and in vivo correlations. In: Dermatology Progress & Perspectives. The Proceedings of the

18th World Congress of Dermatology, New York, June 12–18, 1993. New York: The Parthenon Publishing Group., 1993: 1149–1151.
8. Dupuis D, Rougier A, Roguet R, Lotte C, Kalopissis G. In vivo relationship between-horny layer reservoir effect and percutaneous absorption in human and rat. J Invest Dermatol 1984; 82:353–356.
9. Rougier A, Dupuis C, Lotte R, Roguet R, Schaefer H. In vivo correlation between stranum corneum reservoir function and percutaneous absorption. J Invest Dermatol 1983; 81:275–278.
10. Rougier A, Lotte C, Maibach HI. In vivo percutaneous penetration of some organic compounds related to anatomic site in man: predictive assessment by the stripping method. J Pharm Sci 1987; 76:451–454.
11. Rougier A, Dupuis D, Lotte C, Roguet R. The measurement of the stratum corneum reservoir. A predictive method for in vivo percutaneous absorption studies: influence of application time. J Invest Dermatol 1985; 84:66–68.
12. Rougier A, Lotte C, Maibach HI. The hairless rat: a relevant model to predict in vivo percutaneous absorption in humans? J Invest Dermatol 1987; 88:577–581.
13. Tsai, Sheu, Hung, Cheng. Effect of barrier disruption by acetone treatment on the permeability of compounds with various lipophilicities: implications for the permeability of compromised skin. J of Pharm Sci 2001; 90:1242–1254.
14. Chilcott RP, Dalton CH, Emmanuel AJ, Allen CE, Bradley ST. Transepidermal water loss does not correlate with skin barrier function in vitro. J Invest Dermatol 2002; 118(5):871–875.
15. Lavrijsen APM, Oestmann E, Hermans J, Bodde HE, Vermeer BJ, Ponec M. Barrier function parameters in various keratinization disorders: transepidermal water loss and vascular response to hexyl nicotinate. Br J Dermatol 1993; 129:547–554.
16. Nangia A, Camel E, Berner B, Maibach HI. Influence of skin irritants in percutaneous absorption. Pharm Res 1993; 10:1756–1759.
17. Feldmann R, Maibach HI. Absorption of some organic compounds through the skin in man. J Invest Dermatol 1970; 54:399–404.
18. Franz TJ. The finite dose technique as a valid in vitro model for the study of percutaneous absorption in man. Curr Probl Dermatol 1978; 7:58–68.
19. Bronaugh R, Stewart R. Methods for in vitro percutaneous absorption studies VI: preparation of the barrier layer. J Pharm Sci 1986; 75:487–491.
20. Bronaugh R, Stewart R. Methods for in vitro percutaneous absorption studies V: permeation through damaged skin. Future experiments should take into consideration the effects of modeling realistic situations using alternative methods to the ideal. J Pharm Sci 1985; 74:1062–1066.
21. Bronaugh R, Stewart R. Methods for in vitro Percutaneous absorption studies III; hydrophobic compounds. J of Pharm Sci 1983; 73:1255–1258.
22. Bronaugh R, Stewart R, Congdon E. Methods for in vitro percutaneous absorption studies II. Animal models for human skin. Toxicol Applied Pharm 1982; 62:481–488.
23. Bronaugh R, Franz TJ. Vehicle effects on percutaneous absorption: in vivo and in vitro comparisons with human skin. Br J Dermatol 1986; 115:1–11.
24. Walker W, Dugard PH, Scoot RC. In vitro percutaneous absorption studies: a comparison of human and laboratory species. Hum Toxicol 1983; 2:561–565.
25. Bronaugh R, Maibach HI. Percutaneous Absorption. 2nd ed. New York: Marcel Dekker, 1989.
26. Wester RC, Maibach HI. Percutaneous absorption in diseased skin. In: Maibach, Surber, eds. Topical Corticosteriods. Basel: Karger, 1992:128–141.
27. Bronaugh R, Maibach HI. In Vitro Percutaneous Absorption. Boca Raton: CRC Press, 1991.
28. Lotte C, Rougier A, Wilson DR, Maibach HI. In vivo relationship between transepidermal water loss and percutaneous penetration of some organic compounds in man: effect of anatomic site. Arch Dermatol Res 1987; 279:351–356.

29. Lamaud E, Lambrey B, Schalla W, Schaefer H. Correlation between Transepidermal water loss and penetration of drugs. J Invest Dermatol 1984; 82:556.
30. Rougier A, Lotte C, Corcuff P, Maibach HI. Relationship between skin permeability and corneocyte size according to anatomic site, age and sex in man. J Soc Cosmet Chem 1988; 39:15–26.
31. Aalto-Korte K, Turpeinen M. Transepidermal water loss and absorption of hydrocortisone in widespread dermatitis. Br J Dermatol 1993; 128:663–635.
32. Dupuis D, Rougier A, Roguet R, Lotte C. The measurement of the stratum corneum reservoir: a simple method to predict the influence of vehicles on in vivo percutaneous absorption. Br J Dermatol 1986; 115:233–238.

44

Percutaneous Penetration as It Relates to the Safety Evaluation of Cosmetic Ingredients

Jeffrey J. Yourick and Robert L. Bronaugh
Office of Cosmetics and Colors, Food and Drug Administration, Laurel, Maryland, U.S.A.

I. INTRODUCTION

Exposure of consumers to cosmetic products mainly occurs via the dermal route. Once a chemical contacts skin, absorption begins. Diffusion into and through the stratum corneum typically is the rate limiting step in percutaneous absorption. However, the rate-limiting barrier to absorption is dependent upon the specific chemical. For a cosmetic chemical that is applied to skin, the accuracy of the risk assessment can be improved by basing the potential systemic exposure on an estimate of the dermal exposure that has been corrected with skin absorption data (1). Dermal exposure to a cosmetic ingredient is a function of the concentration of chemical contacting skin and the duration of skin contact. Leave-on cosmetic products would represent the category of products resulting in large dermal exposures, while rinse-off product use results in dermal exposures that are brief and discontinuous.

Percutaneous absorption of cosmetic ingredients, including fragrances, can represent a major route of ingredient uptake and subsequent systemic exposure. There are many factors that alter the extent of percutaneous absorption of cosmetic ingredients such as physicochemical properties of the ingredient, hydration state of skin, duration of product contact, vehicle/formulation effects, and area of application to name a few. To generate data that will be useful in the risk assessment, the absorption study design should attempt to incorporate testing conditions that approximate consumer use conditions.

In this chapter, we will discuss how percutaneous absorption data can be used to refine the risk assessment process, especially the exposure estimate, for cosmetic ingredients. We will discuss various issues regarding the safety/risk assessment for both non-carcinogenic and carcinogenic cosmetic ingredients.

II. HAZARD IDENTIFICATION

The evaluation of cosmetic safety begins with the identification of a hazard. Hazard identification may be defined as a determination of whether exposure to a cosmetic ingredient or impurity in the ingredient can lead to an increased incidence of an adverse health effect and the relative strength of the evidence for biologic causation. Hazard identification can arise from many different sources. Consumer use of products can result in adverse health effects that are reported to physicians, the Food and Drug Administration (FDA), or the company that produced the product. Animal toxicity testing of chemicals can also raise concerns about the safety of chemicals. Toxicology (short term and subchronic) and carcinogenesis testing, such as that performed at the National Toxicology Program, is one means to identify potential hazardous chemicals. Reports published in the open literature are another source to identify hazardous chemicals. These types of reports may range from human patch testing of cosmetic chemicals for sensitization or irritation to animal toxicity testing.

During the process of hazard identification it is important to identify toxicity studies that define doses of the chemicals that are toxic and ideally doses at which no toxicity was found. The dosage level at which no adverse effects were observed is referred to as the NOAEL. It is not usually the case that a human NOAEL for a cosmetic finished product or cosmetic raw ingredient will be available. For most toxicity testing, a NOAEL is derived from an animal study that administered the chemical by one of several possible routes such as feed, gavage, drinking water, or skin painting. Therefore, to evaluate human safety from animal data requires some method of extrapolation. For cosmetics the extrapolation from animal data to human safety involves many different factors including the species of animals, body weights, body surface area, quality and length of animal test, and sensitive human populations, just to name a few (2).

III. EXPOSURE ESTIMATE

Once a potential hazard has been identified, the next step in the process of safety evaluation is to estimate human exposure. Generally, exposure to a cosmetic ingredient is via the dermal route. The dermal exposure to a cosmetic ingredient is the amount of that ingredient that is applied to the skin. However, the systemic exposure to that cosmetic ingredient may be much lower given the barrier properties of skin. Furthermore, systemic exposure will also be dependent upon the duration of skin contact. For an accurate estimate of systemic exposure for a specific dermally applied chemical it is important also to know the extent of skin absorption. Once the percent of applied dermal dose absorbed is determined experimentally, refinement of the systemic exposure estimate can be made from the applied dermal dose. In the absence of any skin absorption data, it should be assumed that all (i.e., 100%) of the chemical that is applied to skin is absorbed (conservative approach).

A. Dermal Exposure

To estimate dermal exposure to a cosmetic ingredient, it is important to know the use conditions for the specific product(s) containing the ingredient of interest. From the product use instructions, it is possible to determine many factors pertinent to the exposure calculation, such as the approximate frequency of product use, volume/weight of

product used, duration of exposure, and other conditions of exposure (e.g., apply heat or cover application area with plastic). An ingredient could be contained in one product intended for leave-on usage (e.g., moisturizing lotion) or in a different product intended as a rinse-off formulation (e.g., hair dye product or shampoo). All these use conditions must be defined and utilized in the exposure estimate.

An important piece of information necessary for the dermal exposure estimate is the concentration of the ingredient in the finished product. However, this product information is proprietary and difficult to obtain. The FDA's Cosmetic Technology Branch occasionally conducts surveys that directly measure ingredient concentrations in finished cosmetic products. These data are used in the exposure estimate.

The initial dermal exposure estimate is calculated from as many of the above-mentioned exposure conditions as are deemed pertinent to include. When actual data are unavailable for a specific parameter, an estimate of the parameter must be used. However, any estimates used in the calculation should be clearly noted in the exposure estimate summary. This is important since uncertainties in the exposure estimate will affect the final safety assessment. It is desirable to calculate an exposure in units of ingredient weight/kg body weight/day. This facilitates comparison of dermal exposure to a NOAEL obtained from a dietary or parental administration study.

B. Percutaneous Absorption

Percutaneous absorption is measured in fresh, viable human and/or animal skin using in vitro flow-through diffusion cell methodology. These techniques are described in detail in Chapter 18 of this book and by Bronaugh and Collier (3). A variety of receptor fluids may be used, the composition of which will depend upon the specific chemical being tested. The application of chemicals should be made in a manner that approximate consumer use conditions as closely as possible to generate data providing realistic exposure estimates.

Skin absorption is dependent on many factors including; lipid solubility of the chemical, duration of skin contact, location of skin contact, vehicle for the chemical, environmental conditions, occlusion of the dosing area by clothing, surface area of skin application, and the age of the individual. These factors must be considered when attempting to accurately define the exposure estimate.

Skin absorption studies should be conducted under conditions that approximate specific product use/abuse conditions. A well-designed absorption study should take into account the relevant experimental conditions necessary to replicate consumer use conditions. A typical experimental design should consider the dosing vehicle, the dosing concentration, and the duration of exposure, to simulate use conditions. To simulate a leave-on product the dosing solution may be left on the skin for 24 hours, whereas for a rinse-off product the dosing solution may be removed after one to two minutes. The percent of applied dose absorbed is determined experimentally and is used in estimating systemic exposure to the chemical.

IV. SAFETY ASSESSMENTS

A. Non-carcinogenic Cosmetic Ingredient Safety Evaluation: Assume a Threshold for Toxicity

One approach for extrapolating data from animal studies to human hazard/safety is the safety factor approach. The safety factor approach implies that there is a threshold

dose for a toxic effect. If the NOAEL is considered as the threshold dose, then the NOAEL is divided by a safety factor (usually 100; 10 for interspecies and 10 for intraspecies variability) to determine a safe human dose or an "acceptable daily intake" (ADI) (4).

1. Exposure Estimate: Acute and Chronic Exposure

The systemic exposure estimate for a single exposure to a cosmetic ingredient is a function of the amount applied to skin, the concentration of the ingredient in the product, the duration of skin contact, and the extent of percutaneous absorption. If no data are available for these specific exposure conditions, then these parameters must be estimated. The volume of the product used is the typical amount of product applied to the skin. If the volume of the product applied is not available, then it is possible to use a typical application rate, such as milligram product applied to skin per centimeter square, for specific cosmetic product categories (e.g., a lotion is typically applied at $2\,mg/cm^2$). The amount of a cosmetic ingredient systemically absorbed can be estimated as follows:

Amount absorbed/kg body weight =
application rate × concentration of ingredient in product
× duration of exposure × surface area exposed
× % skin absorption / weight of individual

The estimated daily dose is an exposure estimate based on chronic usage of a specific product. The amount absorbed per kg body weight is multiplied by the estimated frequency of use throughout a lifetime, divided by the total number of days represented by a lifetime of use:

Estimated daily dose = amount absorbed/kg body weight
× estimated frequency of use over a lifetime/
toal number of days represented by a lifetime of use

2. Safety Assessment

If an NOAEL for the Ingredient Is Available.

Acceptable daily intake = NOAEL /safety factor
Margin of safety = NOAEL /estimated daily dose

If an NOAEL for the Ingredient Is Not Available. It is sometimes the case when a toxicology study is completed that all experimental doses caused an adverse effect such that an NOAEL is not determined, but the lowest experimental dose was identified as the lowest observed adverse effect level (LOAEL). It is possible to divide the LOAEL by an additional safety factor to estimate the NOAEL (4). This estimated NOAEL can then be used in the calculation of acceptable daily intake and margin of safety as present above.

Assessment. The safety assessment is reviewed and after a qualitative evaluation of the uncertainties inherent in the exposure estimate, a decision is made by the risk managers as to whether there is a potential safety problem with exposure to a specific cosmetic ingredient or finished product. Furthermore, risk managers will

ultimately be responsible for making decisions on any corrective actions that might be necessary.

B. Carcinogenic Cosmetic Ingredient Safety Evaluation

The safety assessment of a cosmetic ingredient suspected to be carcinogenic (determined, e.g., from open literature publications, National Toxicology Program reports, IARC reports, and unpublished studies, etc.) in either animals or humans is currently conducted using a different approach. An initial exposure estimate is completed as outlined in the preceding section to derive an estimated daily dose. Since it may not be appropriate to consider a threshold for carcinogenic potential, quantitative risk assessment calculations are used to determine the relative lifetime cancer risk resulting from the potential exposure. A mathematical model is used to perform the linear regression for the low-dose estimate of cancer risk. The procedure for the cancer risk estimation has been outlined (4). Briefly, a direct method (linear-at-low dose approach) for low-dose cancer risk estimation is used. A straight line is drawn from a point on the dose-response curve to the point of origin. The slope of the straight line is used as an index of carcinogenic potency. The upper limit estimate of relative cancer risk (4) is then:

$$[\ \text{risk} \leq \text{slope} \times \text{dose}\ ]$$

C. Risk Management

Risk management deals with identifying and considering the range of regulatory options and then making a decision about which approach to use. Risk managers review the risk assessment and consider all other legal, economic, social, ethical, and political issues that may arise from a risk management decision (5). A set of decision options is formulated to address the specific risk assessment findings. The risk managers must then decide on the nature of any corrective actions required to protect the public health.

V. CASE STUDY—EXPOSURE ESTIMATE FOR THE DERMALLY APPLIED FRAGRANCE MUSK XYLOL

Musk xylol is a fragrance ingredient used in a variety of cosmetic and household products. It accumulates in the environment and levels have been measured in worldwide bodies of water (6). The fragrance was found to be carcinogenic in a rodent bioassay (7). Mutagenicity testing, both mammalian and bacterial, has indicated that musk xylol is not genotoxic (8). We have reported that 22% of musk xylol was absorbed through human skin after topical application in a cosmetic emulsion vehicle (9). In addition to absorption data, a determination of the daily amount applied to skin is needed to estimate systemic exposure. The amount of musk xylol applied to skin is difficult to determine because the fragrance is found in a number of product categories that might be used simultaneously by consumers.

Musk xylol, as a component of the perfume, is contained in many different types of cosmetic products. Therefore, for any determination of the total amount of musk xylol applied to skin, it is necessary to estimate the amount of musk xylol

on skin from use of each product type. There are many exposure parameters that need to be defined and estimated prior to calculating musk xylol on skin for each product type. First, it is necessary to estimate the total amount of each product type that will be used daily by consumers. This is represented as "product usage" and is estimated in grams of product applied per day (Table 1). However, only a small percentage of the actual finished cosmetic product is perfume. Furthermore, the perfume component of most finished cosmetic products is composed of many different fragrances. Therefore, the perfume concentration ("Perfume conc. (%)," Table 3) and the percentage of the fragrance that is musk xylol (Table 2) can be estimated. The "Retention factor" (Table 3) adjusts the exposure estimate to musk xylol based on either the volatility of the applied product or whether the product is a wash-off or leave-on type product. The amount of "Perfume retained (mg/day)" (Table 3) is estimated from "Perfume concentration," "Retention factor," and "Product usage." The "Musk xylol on skin (μg/day)" for each product type (Table 3) is then calculated from the "Perfume retained" and the percentage of perfume attributed to the fragrance, musk xylol. The "Musk xylol in perfume (%)" (Table 3) was estimated by Monte Carlo simulation (see the following discussion) using the data from Table 2. The "Musk xylol on skin (μg/day)" (Table 3) is estimated from "Perfume retained" and "Musk xylol in perfume." The "Total amount of musk xylol applied to skin (mg/day)" (Table 4) was estimated by 2000 iterations of the Monte Carlo simulation (see the following discussion). Finally, the amount of musk xylol available for systemic absorption is estimated from "Musk xylol on skin" (Table 4, 90th percentile) and the percent of musk xylol absorbed through skin (22%) .

A. RIFM Dermal Exposure Estimate

An exposure estimate for musk xylol was prepared by the Research Institute for Fragrance Material (RIFM) in 1993 (RIFM, unpublished data, 1993) using the point

Table 1 Product Usage (g/day) from Cosmetic Toiletry and Fragrance Association Survey[a]

Product type	50th percentile	90th percentile
Bath preparations	1.81	9.50
Colognes	0.55	0.93
Perfumes	0.10	0.40
Shampoos, rinses	12.02	29.40
Hair sprays	0.93	2.13
Other hair preps	5.09	13.04
Soaps	2.47	3.72
Deodorants	0.42	0.67
Cleansing creams	1.04	2.60
Face, body preps	3.08	5.99
Moisturizers	0.45	0.87
Other skin preps	2.57	6.13
Suntan preps	2.00	4.00
Air fresheners	2.50	5.74
Household detergents	61.12	140.31

[a]Survey by The Cosmetic, Toiletry, and Fragrance Association, unpublished, 1983.

Table 2 Musk Xylol in Perfumes (%) from Research Institute for Fragrance Materials (RIFM) Survey[a]

Product type	50th percentile	90th percentile
Bath preparations	0.3	2.5
Colognes	0.1	1.5
Perfumes	0.2	0.5
Shampoos, rinses	1.5	2.0
Hair sprays	1.5	1.7
Other hair preps	1.5	2.3
Soaps	1.5	3.8
Deodorants	0	1.5
Cleansing creams	0.4	1.5
Face, body preps	0.4	1.5
Moisturizers	0.4	1.4
Other skin preps	0.4	1.3
Suntan preps	0.4	2.5
Air fresheners	0	1.1
Household detergents	0.8	4.1

[a]RIFM, unpublished, 1993.

estimate approach. Estimate of total daily musk xylol applied to skin was based on product usage (Table 1) and percent musk xylol (Table 2) in 15 different categories of commercial products (13 cosmetics and two households). For the point exposure estimate, RIFM summed the exposures to all categories of products and established four exposure levels based on the amount of product usage and the musk xylol con-

Table 3 Musk Xylol Retained on Skin

Product type	Product usage (g/day)[a]	Perfume conc. (%)[b]	Retention factor[b]	Perfume retained (mg/day)	Musk xylol in perfume (%)[a]	Musk xylol on skin (μg/day)
Bath preps	1.78	2	0.01	0.36	0.57	2.04
Colognes	0.67	5	0.9	30.1	0.31	92.0
Perfumes	0.088	18	0.9	14.2	0.28	39.9
Shampoos	6.47	0.5	0.2	6.47	0.44	28.3
Hair sprays	0.88	0.15	0.3	0.40	1.22	4.85
Other hair preps	10.9	0.5	0.2	10.9	0.93	101.2
Soaps	1.81	1.2	0.2	4.33	2.85	123.7
Deodorants	0.47	0.75	1	3.51	0.27	9.44
Cleansing creams	0.87	0.5	1	4.37	0.79	34.4
Face, body preps	1.90	0.5	1	9.52	0.47	45.1
Moisturizers	0.18	0.5	1	0.91	0.58	5.27
Other skin preps	4.28	0.5	1	21.4	0.58	123.5
Suntan preps	1.43	0.4	1	5.72	1.07	61.2
Air freshners	1.35	1.75	0.01	0.24	0.097	0.23
Household detergents	48.7	0.25	0.001	0.12	2.26	2.75

[a]Monte Carlo simulation estimates from one iteration of the modeling.
[b]Data from Research Institute for Fragrance Materials, unpublished, 1993.

Table 4 Total Amount of Musk Xylol Applied to Skin (mg/day)[a]

Minimum	0.34
Mean	0.84
Maximum	1.5
Fiftieth percentile	0.82
Ninetieth percentile	1.1

[a]Final results from the Monte Carlo simulation (2000 iterations) of musk xylol dermal exposure (compilation of results like that found in Table 3).

centration in the product. The RIFM selected, as a more realistic exposure estimate, the 50th percentile level, which was 0.5 mg/day, not the 90th percentile value of 3.9 mg/day. To provide the exposure estimate a margin of safety, RIFM doubled the 0.5 mg/day exposure estimate and used 1.0 mg/day as the estimated daily exposure for its safety assessment.

B. Dermal Exposure Estimates Using Monte Carlo Simulation

A different approach for estimating certain exposure parameters is to estimate product usage and percent musk xylol in perfume using survey data and Monte Carlo simulation techniques. The Divisions of Biotechnology and GRAS Notice Review (DBGNR) and Petition Review (DPR) of the Office of Food Additive Safety at FDA have adapted Monte Carlo simulation techniques to estimate exposures to food additives contained in multiple food sources. We have applied this simulation approach to estimate the total amount of musk xylol applied to skin since musk xylol is contained in multiple cosmetic product categories and these products might be used simultaneously by consumers. The Monte Carlo simulation approach is a quantitative method that is able to summarize an exposure condition (i.e., product usage or percent musk xylol in perfume for our example) as a probability distribution. This simulation method can generate a distribution of possible outcomes by a number of model iterations and for each iteration, uses a different randomly selected set of input values [e.g., the distribution input values for "Bath Preparations" from the CTFA Survey of Product Usage (Table 1) were: 0 at the zero percentile, 1.81 at the 50th percentile, and 9.5 at the 90th percentile]. The Monte Carlo simulation results will give the range of probabilities of possible outcomes for the exposure parameter. It is then possible to use the simulation results to examine estimates of probable exposure parameters at any desired exposure level (e.g., 90th percentile estimate of total amount of musk xylol applied to skin) from a number of exposure pathways, i.e., cosmetic product categories.

Monte Carlo simulations of musk xylol exposure parameters were conducted using the PC-based software program, @RISK (Palisade Corporation, Newfield, New York, U.S.A.) within the Excel (Microsoft Corporation, Redmond, Washington, U.S.A.) spreadsheet program. Monte Carlo sampling techniques with 2000 iterations were used to generate probability distributions of product usage and percent musk xylol in perfume for each cosmetic or household product. Each distribution [TRIANG (min, most likely, and max)] was created by input of the minimum (0), most likely 50 percentile, and maximum values (90th percentile), for (i) product usage (Table 1) and (ii) percent musk xylol in perfume (Table 2). The Monte Carlo

derived estimates of product usage (column one, Table 3) and percent musk xylol in perfume (column five, Table 3) were multiplied by RIFM estimates of perfume concentration and retention of topically applied product on skin to estimate musk xylol on skin (column six, Table 3). The 90th percentile estimate of total amount of musk xylol applied to skin (1.1 mg/day) (Table 4) was selected as the dermal exposure for use in the systemic exposure estimate.

C. Potential Systemic Exposure Estimate

Potential systemic exposure is the total amount of musk xylol applied to skin multiplied by the fraction of musk xylol absorbed through the skin [from percutaneous absorption study, 0.22 (9)]. The potential systemic exposure to musk xylol based on the Monte Carlo simulation estimate follows:

$$1.1\,\text{mg/day} \times\ 0.22 = 0.24\,\text{mg musk xylol/day}$$

VI. CONCLUSION

Determination of ingredient usage in products can be difficult when the ingredient is contained in many different commercial product categories at various concentrations within each product category. A consumer is likely to be exposed to a cosmetic ingredient by using products in several different categories. An individual might use a product from each musk xylol-containing product category over a short-time period, but it is probably not realistic to assume an individual would use all categories of products over a lifetime. An overestimate of exposure will occur by assuming that the consumer is simultaneously using products from all product categories. This was the case with the exposure estimate for musk xylol done by RIFM. They assumed that a consumer would use a product daily from each product category that contains musk xylol. The RIFM calculated both the 50th and 90th percentile levels of exposure. The RIFM chose an intermediate exposure level of 1.0 mg/day (50th percentile value of 0.5 mg/kg/day $\times$ 2) for use in its safety assessment.

A second approach for estimating musk xylol exposure was done by using Monte Carlo simulation techniques to estimate certain exposure parameters. The Monte Carlo simulation method is useful in simulating exposure from a number of pathway sources. This simulation approach can evaluate models where at least one input value (e.g., product usage) can be defined by a distribution of values. Each iteration of the simulation uses a set of input values sampled from the distribution of possible input values to calculate the outcome of the model as a single result. @RISK generates an output probability distribution by consolidating single results from each individual iteration. The advantage of this approach is that an exposure at any desired percentile can be derived from the outcome probability function. It was found by using the Monte Carlo simulation approach, that the 90th percentile exposure estimate for musk xylol was 1.1 mg/day.

A comparison of the RIFM and Monte Carlo simulation approaches found that the estimates of daily dermal exposure to musk xylol with the two approaches were quite close (1.0 mg/day for the RIFM estimate vs. 1.1 mg/day for the estimate using Monte Carlo simulations). However, to obtain its estimate, RIFM chose to use the 50th percentile exposure value (0.5 mg/day) multiplied by two, without providing any theoretical basis for selecting these parameters, rather than using the 90th

percentile exposure. The RIFM approach (using a summation of all product categories) estimated a 90th percentile exposure to musk xylol of 3.9 mg/day, while the approach using Monte Carlo simulations estimated a 90th percentile exposure of 1.1 mg/day. This represents a greater than threefold difference in the 90th percentile exposure estimates to musk xylol using the two different approaches. The RIFMs assertion that use of the 50th percentile exposure value and a safety factor of two provided a more realistic exposure estimate is confirmed by the exposure estimate obtained using Monte Carlo simulations. However, without a theoretical basis to justify its selection of parameters (50th percentile exposure and a safety factor of two), the extrapolation of the RIFM approach to other exposure estimates is questionable. Monte Carlo simulations provide modeling of the available exposure data for product usage and ingredient concentration, rather than simply summing the exposure to the ingredient across all product categories, which probably leads to an overestimate of exposure. As shown by the musk xylol exposure estimate, use of this technique provides a more realistic estimate of exposure parameters, especially for the higher percentile exposures, than using a single point estimate approach. Therefore, the use of Monte Carlo simulations to estimate certain exposure parameters represents an improvement in our ability to provide realistic estimations of consumer exposure to cosmetic ingredients, especially for ingredients that are contained in multiple product categories.

REFERENCES

1. ECETOC: Percutaneous Absorption. Monograph No. 20. Brussels. 1993.
2. Faustman EM, Omenn GS. Risk assessment. In: Klaassen CD, ed. Casarett & Doull's Toxicology: The Basic Science of Poisons. 5th ed. New York: McGraw-Hill, 1996:75–88.
3. Bronaugh RL, Collier SW. Protocol for in vitro percutaneous absorption studies. In: Bronaugh RL, Maibach HI, eds. In Vitro Percutaneous Absorption: Principles, Fundamentals, and Applications. Boston: CRC Press, 1991:237–241.
4. Kokoski CJ, Henry SH, Lin CS, Ekelman KB. Methods used in safety evaluation. In: Branen AL, Davidson PM, Salminen S, eds. Food Additives. New York: Marcel Dekker, 1990:579–615.
5. NRC: Understanding Risk: Informing Decisions in a Democratic Society. Stern PC, Fineburg HV, eds. Washington DC: National Academy Press, 1996:33–34.
6. Rimkus GG, Wolf M. Nitro musk fragrances in biota from freshwater and marine environment. Chemosphere 1995; 30:641–651.
7. Maekawa A, Matsushima Y, Onodera H, Shibutani M, Ogasawara H, Kodama Y, Kurokaea Y, Hayashi Y. Long-term toxicity/carcinogenicity of musk xylol in B6C3F_1 Mice. Fd Chem Toxicol 1990; 8:581–586.
8. Nair J, Ohshima H, Malaaveille C, Friesen M, O'Neill IK, Hautefeuille A, Bartsch H. Identification, occurance and mutagenicity in *Salmonella tryphimurium* of two synthetic nitromusks, musk ambrette and musk xylene, in Indian chewing tobacco and betal quid, Fd. Chem Toxicol 1986; 24:27–31.
9. Hood HL, Wickett RR, Bronaugh RL. In vitro percutaneous absorption of the fragrance ingredient musk xylol. Fd Chem Toxicol 1996; 34:483–488.

45
Percutaneous Absorption of Hair Dyes

Jeffrey J. Yourick and Robert L. Bronaugh
Office of Cosmetics and Colors, Food and Drug Administration, Laurel, Maryland, U.S.A.

I. INTRODUCTION

Consumer hair dye products can be divided into three product types; permanent, semi-permanent, and temporary. Permanent or oxidation hair colors are the most widely used hair dye products. Oxidation hair dye products contain a solution of dye intermediates which form hair dyes by chemical reactions on the hair, and preformed dyes that are added as toning agents to attain the intended shades. The dye solution and the hydrogen peroxide solution (developer) are mixed just prior to hair application. The applied mixture causes the hair shaft to swell. The dye intermediates (and toning dyes) penetrate the hair shaft to some degree before they have chemically reacted with the hydrogen peroxide to form the final colored hair dye. Semi-permanent and temporary hair coloring products are typically solutions of several hair dyes, which bind to the hair shaft to differing degrees. Temporary hair colors need to be reapplied after each shampooing.

The Food and Drug Administration (FDA) regulates cosmetic products under the authority of the Federal Food, Drug, and Cosmetic (FD&C) Act. This law is designed to assure that products under FDA jurisdiction are safe under intended conditions of use and properly labeled. The FDA however, does not have the authority to approve cosmetic products, their formulations or their labeling. Under the provisions of the FD&C Act, a cosmetic is deemed to be adulterated if, among other things, it bears or contains a poisonous or deleterious substance which may render it injurious to users under the conditions of use as prescribed in the labeling or under such conditions of use as are customary or usual. Coal-tar hair dyes are exempt from adulteration provisions of the FD&C Act, provided the product label bears the caution statement described in section 601(a) of the Act. Additional information regarding the safety and regulation of hair dyes can be found at Ref. 1.

Certain coal-tar hair dyes, such as 4-chloro-*m*-phenylenediamine, 2,4-toluenediamine, 2-nitro-*p*-phenylenediamine (2NPPD), 4-amino-2-nitrophenol, and disperse blue 1(DB1), have been reported to cause tumors in at least one animal species in lifetime feeding studies. For this reason, the public health risk resulting from consumer use of certain hair dyes needs to be evaluated. The focus of this chapter will be to describe the skin absorption of certain hair dyes with potential safety issues.

The following definitions are used when referring to dermal/skin absorption and dermal/skin penetration. Skin/dermal/percutaneous absorption represents the amount of topically applied chemical that is ultimately determined to be systemically available. This would constitute receptor fluid content plus skin content if it is determined that material remaining in the skin ultimately partitions into the receptor fluid. Therefore, it must be determined individually whether the stratum corneum and/or viable epidermal/dermal content should be considered as systemically available. Skin/dermal/percutaneous penetration represents the total amount of topically applied chemical that is found in the receptor fluid plus the skin at the end of a study. However, not all of this material may be systemically available for absorption.

II. SKIN ABSORPTION AND METABOLISM OF 2-NITRO-*P*-PHENYLENEDIAMINE

A. Introduction

The 2NPPD is a "coal-tar dye" used in semipermanent (nonoxidative) and permanent (oxidative) hair dye formulations. The 2NPPD is not an oxidation dye, but is present in oxidation formulations as a color tinting agent. The Cosmetic Ingredient Review Expert Panel concluded that 2NPPD is safe as a hair dye ingredient at current concentrations (up to 1%) of use (1a). The mutagenicity and carcinogenicity of 2NPPD have been investigated in several different experimental systems. The 2NPPD was mutagenic in Ames testing (2) and in several different mammalian tests (1a,3). Hair dye formulations containing 2NPPD are mutagenic to some strains of *Salmonella typhimurium* (1a). The urine of rats was also found to be mutagenic when tested after topical application of hair dyes containing 2NPPD (1). In long-term carcinogenicity feeding studies with 2NPPD, mixed results have been found in rodents. An increase in hepatic carcinomas and adenomas was noted in female mice fed 2NPPD, but not male mice or rats (4). In a two mouse strain chronic skin-painting study using a semipermanent hair dye formulation containing 2NPPD, there was a reduced time-to-tumor and an increased number of tumors noted in one strain of mice. In a chronic rat skin-painting study with a hair dye containing 1.1% 2NPPD, there was no increase in gross lesion numbers (1a).

Because of the genotoxicity, potential for carcinogenicity reported for 2NPPD, and the lack of skin metabolism information in previous studies, the in vitro skin absorption and metabolism of 2NPPD were investigated.

B. 2NPPD Materials and Methods

1. Chemicals

^{14}C-2NPPD (specific activity: 25.6 mCi/mmol) was synthesized by Research Triangle Institute (Research Triangle, North Carolina, U.S.A.) with a radiochemical and chemical purity of >99% as determined by thin-layer chromatography (TLC) and high-performance liquid chromatography (HPLC). Nonradiolabeled 2NPPD was obtained from Sigma Chemical Co. (St. Louis, Missouri, U.S.A.). Several potential 2NPPD metabolites were used as HPLC standards and were obtained from Aldrich Chemical Co. (Milwaukee, Wisconsin, U.S.A.). Triaminobenzene was obtained from Arcos (Arcos Organics, New Jersey). The HPLC-grade solvents were obtained from J.T. Baker Chemical Co. (Phillipsburg, New Jersey, U.S.A.). HEPES-buffered Hanks'

balanced salt solution (HHBSS; dry powder packets prepared by Gibco BRL, Life Technologies, Grand Island, New York, U.S.A.) was prepared fresh prior to each study. The structure of N4-acetyI-2NPPD was verified by NMR and mass spectroscopy.

2. Animal and Human Skin

Female fuzzy (Hsd:Fuzzy-fz) rats (Harlan Sprague Dawley Inc., Indianapolis, Indiana, U.S.A.), 3 to 10 months of age, were used in these experiments. Fresh, viable human skin was obtained as a result of abdominoplasty procedures from a local cosmetic surgeon.

3. 2NPPD Dosing Solutions

The 2NPPD percutaneous absorption was determined by using four dosing vehicles; ethanol, a semipermanent hair dye formulation, a permanent-oxidative hair dye formulation, or a permanent-control (water substituted for hydrogen peroxide). The permanent hair dye formulation was tested only on rat skin. All dosing solutions were applied to the epidermal surface of the skin for 30 minutes and contained amounts of 2NPPD estimated to come in contact with skin during actual product usage (sec. 3). The skin was then washed and receptor fluid was collected for 24 hours. The semipermanent hair dye formulation (a commercial product obtained from a local cosmetics store) contained approximately 0.7% unlabeled 2NPPD as determined by HPLC. The semipermanent formulation was spiked with ^{14}C-2NPPD so that approximately 0.5 μCi or 4.7 μg/cm^2 of ^{14}C-2NPPD was applied per cell. The semipermanent formulation was applied at a dosage rate of 7.8 mg/cm^2. The permanent-oxidative hair dye formulation (a commercial product obtained from a local cosmetics store) was applied after a 1:1 dilution of the dye base with either a developing lotion (containing 6% hydrogen peroxide) or water (oxidative-control). The permanent formulation was spiked with ^{14}C-2NPPD so that approximately 0.5 μCi or 4.7 μg/cm^2 of ^{14}C-2NPPD was applied per cell. The permanent formulation was immediately applied to the skin in the diffusion cell after the 1:1 dilution at a dosage rate of 18.2 mg/cm^2.

4. Percutaneous Absorption Studies

Percutaneous absorption studies were done as described in Reference 5 using flow-through diffusion cells. Barrier integrity of human skin discs were verified by using the 20-minute tritiated water test (6). The amount of 2NPPD remaining in the skin after 24 hours was determined by liquid scintillation counting (LSC).

5. Liquid Chromatography Method

The 2NPPD and 2NPPD metabolites in receptor fluid or skin were determined by HPLC using a modified method of Nakao et al. (7). The chromatography column consisted of a C_{18} guard column connected to a 5 μm-C_{18}, 4.6 × 250 mm (Alltech Associates, Deerfield, Illinois, U.S.A.) column. Composition of the mobile phase was 20% acetonitrile and 80% HPLC-grade water run under isocratic conditions at a flow rate of 1.0 mL/min. The analyte in the eluate was monitored first by ultraviolet absorption at 238 nm and second by a radioisotope detector (Radiomatic, Packard Instrument Co., Downers Grove, Illinois, U.S.A.). The HPLC result reported for each peak in the metabolism studies is the individual peak area divided

by the total ^{14}C peak area for each sample run: expressed as a percent of the total ^{14}C peak area. Percent of peak areas reported are the mean ± SE from three rat ($n = 3$) or two human studies ($n = 2$).

6. Data Analysis

Values reported are the means ± SE for the rat studies, $n = 3$ for each vehicle tested. Values reported are the means ± SD for the human studies, $n = 2$ for each vehicle tested. Each individual rat/human skin piece was used to prepare 8 to 10 skin discs for placement into individual diffusion cells. Usually each absorption study (i.e., derived from one rat or human subject) was performed using two vehicles. Each vehicle was tested on four to five diffusion cells (replicates). For each vehicle, the four to five replicate cell absorption values were averaged to give a single absorption value for each rat/human subject. Statistical (SigmaStat® Statistical Software, SPSS Inc., Chicago, Illinois, U.S.A.) differences were determined using either a Student's *t*-test ($p < 0.05$) or analysis of variance (ANOVA, $p < 0.05$) followed by a posteriori multiple comparisons of group means by the Tukey test ($p < 0.05$).

C. Results—Skin Penetration

The percutaneous absorption of radiolabeled 2NPPD through fuzzy rat skin into the receptor fluid with four dosing vehicles is depicted in Figure 1. The 2NPPD rapidly penetrated rat skin with the peak in absorption noted at the three-hour time point with all vehicles tested (percent applied dose absorbed ranged from approximately 0.9 to 3.1). When comparing the four vehicles tested for 2NPPD absorption, there were no significant differences between the various vehicles over the time points examined. However, it is interesting to note that absorption of 2NPPD from the oxidative-permanent hair dye formulation tended to be lower than the other dosing vehicles.

Table 1 summarizes 2NPPD percutaneous absorption in fuzzy rat skin 24 hours after application. No difference was seen in the amount of 2NPPD absorbed over 24 hours into the receptor fluid from the different dosing vehicles tested. A similar amount of 2NPPD remained in the skin (2.9–2.2% of the applied dose absorbed) for all the hair product formulations, although a higher amount of 2NPPD was found in skin dosed with an ethanol vehicle. When considering the total (receptor fluid + skin) percent applied dose absorbed after 24 hours, a similar amount of 2NPPD was absorbed from both the hair product formulations. A significantly higher amount of 2NPPD was absorbed with the ethanol vehicle than with the permanent (oxidative) formulation. After 30 minutes, approximately 67% (range: 59.1–72.8%) of the 2NPPD was recovered in the washes for all vehicles tested. The average recovery of 2NPPD at the end of the experiment (after 24 hours) was 73.2% (range: 68.4–78.8%) of the total percent of the applied dose. These low recovery values were potentially due to 2NPPD binding to the wooden stick of the applicators. Recovery values were improved by changing the applicator type from a wooden stick with a cotton swab to a plastic stick with a cotton swab. Since 2NPPD is not a volatile chemical, we would not predict that the lower recoveries were due to evaporative loss of 2NPPD. It is possible that 2NPPD was bound to the walls of the diffusion cell.

Absorption of 2NPPD through human skin for a 30-minute application of the dosing vehicles is shown in Figure 2. Percutaneous absorption of 2NPPP peaked at

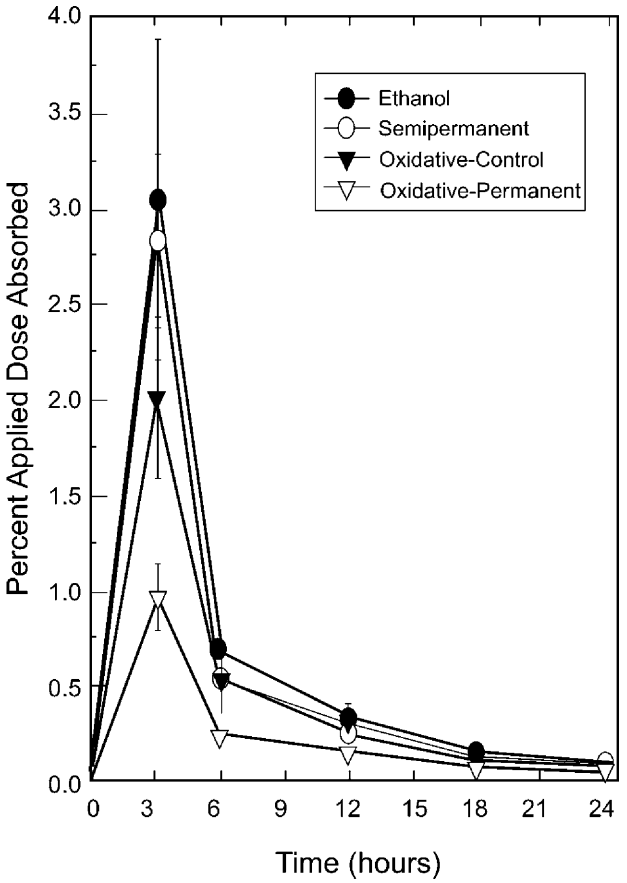


Figure 1 Percent applied 2NPPD dose absorbed over 24 hours in receptor fluid from fuzzy rat skin. Absorption values are the mean ± SE from three individual rat studies ($n = 3$). Each single absorption value was determined by averaging 4–5 replicate measurements for each time interval point and dosing solution. *Source*: From Ref. 5.

three hours in the receptor fluid for both the ethanol and semipermanent vehicles tested. There was no difference in the absorption measured between the two vehicles. Similar to the results in fuzzy rat skin, human skin 2NPPD absorption was rapid, peaked at 3 hours, and there was no difference between the dosing vehicles.

A summary of 2NPPD absorption in human skin using an ethanol or semipermanent hair dye formulation is presented in Table 2. No significant differences between the absorption were noted when the two vehicles were compared across the categories listed in Table 2. The total percent of applied 2NPPD dose absorbed was 9.2 ± 5.75 and 9.5 ± 3.16 for the ethanol and semipermanent formulations, respectively. The approximate total penetration of 9% of the applied dose absorbed is represented by about 6% absorption into the receptor fluid and approximately 3% 2NPPD remaining in the skin.

D. Results—Rat Skin Metabolism

The extent of 2NPPD metabolism and the metabolic profile changed dependent upon the tissue and dosing vehicle used in the fuzzy rat studies (Fig. 3). When

Table 1 Summary of 2NPPD Absorption in Fuzzy Rat Skin[a]

	Percent of applied dose			
	Ethanol	Semipermanent	Control-permanent	Permanent
Receptor fluid	4.3 ± 1.07[b]	3.8 ± 0.98	3.1 ± 0.52	1.53 ± 0.19
Skin content	4.9 ± 0.47[c]	2.9 ± 0.61	2.2 ± 0.21	2.7 ± 0.14
Total applied dose penetrated	9.3 ± 1.17[d]	6.9 ± 1.15	5.3 ± 0.53	4.2 ± 0.08
Wash	59.1 ± 2.69	72.8 ± 7.00	66.3 ± 10.30	69.8 ± 8.30
Recovery	68.4 ± 3.69	78.8 ± 6.69	71.6 ± 9.90	74.0 ± 8.70

[a]All values represent data 24 hours after 2NPPD application.
[b]Values are the means ± SE of four to five replicate measurements for three rats.
[c]Ethanol vehicle group is significantly (ANOVA followed by Tukey test, $p < 0.05$) greater than all other skin receptor fluid groups.
[d]Ethanol vehicle group is significantly (ANOVA followed by Tukey test, $p < 0.05$) greater than the permanent vehicle group.
Source: From Ref. 5.

an ethanol dosing vehicle was used on rat skin, 2NPPD was approximately 85% metabolized. The majority (65%) of 2NPPD was metabolized to N4-acetyl-2NPPD, while lesser amounts were metabolized to triaminobenzene (17%) and a potential sulfated metabolite (3%). When a semipermanent hair dye formulation was used as the dosing vehicle, approximately 47% of the 2NPPD was metabolized upon absorption. Approximately 20% of the absorbed 2NPPD was metabolized to N4-acetyl-2NPPD and triaminobenzene and about 6% was potentially sulfated. The profile of metabolism in skin was altered by the dosing vehicle. When comparing the dosing vehicles in skin, greater metabolism of 2NPPD was noted with the ethanol dosing vehicle and the major metabolite formed was the acetylated metabolite. Less 2NPPD was metabolized with the product vehicle and a smaller amount of acetylated 2NPPD was formed, while a larger percentage of metabolized 2NPPD was pushed toward the formation of triaminobenzene and the sulfated metabolite.

E. Human Skin Metabolism

The in vitro metabolism of 2NPPD in human skin was also investigated (Fig. 4). When 2NPPD was applied to human skin in ethanol almost complete metabolism of the absorbed material to N4-acetyl-2NPPD (90%) was seen. A small amount (7%) of triaminobenzene was formed and a smaller amount (3%) of unmetabolized 2NPPD was also found. When 2NPPD was applied to human skin in a semipermanent formulation, less 2NPPD (60%) was metabolized and approximately equal amounts of N4-acetyl-2NPPD and triaminobenzene were formed (Fig. 4). In human skin, unlike the rat, there was no sulfation of 2NPPD.

III. DISCUSSION

The in vitro percutaneous absorption and metabolism of the hair dye ingredient 2NPPD were determined in human and fuzzy rat skin. The 2NPPD was applied

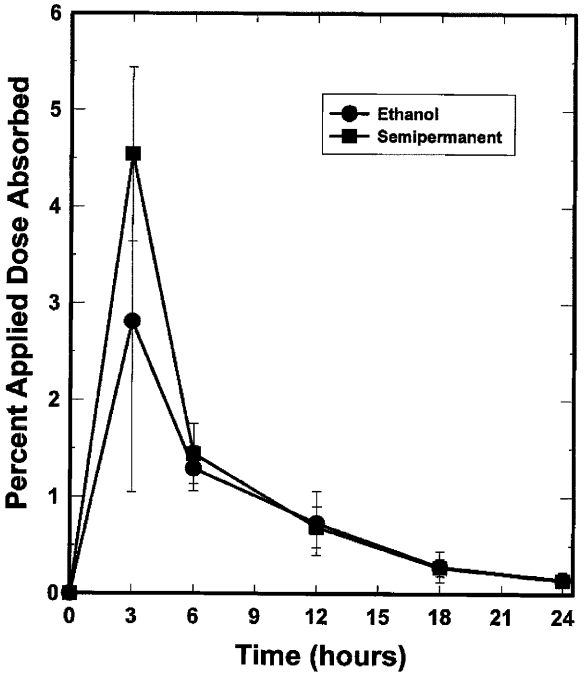


Figure 2 Percent applied 2NPPD dose absorbed over 24 hours in receptor fluid from human skin. Absorption values are the mean ± SD from two individual human donor studies ($n = 2$). Each single absorption value was determined by averaging four to five replicate measurements for each time interval point and dosing solution. *Source*: From Ref. 5.

to skin for 30 minutes, then removed to simulate consumer exposure to a typical hair dye product. Thus, the extent of absorption was limited by the relatively short application (i.e., exposure) time. Ethanol, when used as the dosing vehicle, can be considered as a test condition free from formulation constituent and other dye interactions. When ethanol was used as the dosing vehicle, a significant portion of the 2NPPD was absorbed and found in the receptor within three hours. The rapid percutaneous penetration of 2NPPD can be explained by its solubility properties. The extent of percutaneous penetration for a chemical is determined by its inherent physicochemical properties (8). Partition coefficients for 2NPPD have been reported in octanol/water and stratum corneum/water of 3.4 and 13.0, respectively (9). When an infinite dose of 2NPPD was applied in aqueous solution, a permeability constant of 5.0×10^{-4} cm/hr was determined (9). 2NPPD has both lipophilic and hydrophilic solubility properties and a relatively low molecular weight of 153.1 g, which all contribute to its rapid skin penetration properties. Also, small rapidly penetrating molecules may result in similar absorption values between human and rat skin as found in this study with 2NPPD.

The absorption of 2NPPD from the semipermanent and permanent formulations was reduced by the presence of several dyes and dye intermediates (2-methylresorcinol, 4-amino-2-hydroxytoluene, *N*,*N*-*bis*(2-hydroxyethyl)-*p*-phenylenediamine sulfate, *p*-aminophenol, *p*-phenylenediamine, and resorcinol) in the product and further reduced in the oxidative-permanent formulation by the addition of hydrogen peroxide. One explanation for the lower 2NPPD absorption from this formulation is

Table 2 Summary of 2NPPD Absorption in Human Skin Using an Ethanol and Semipermanent Hair Dye Formulation[a]

	Percent of applied dose	
	Ethanol	Semipermanent formulation
Receptor fluid	5.3 ± 2.57[b]	7.1 ± 1.56
Skin content	3.9 ± 3.17	2.5 ± 1.6
Total applied dose absorbed	9.2 ± 5.75	9.5 ± 3.16
Wash	63.4 ± 4.44	54.2 ± 3.47
Recovery	72.6 ± 1.27	63.8 ± 0.31

[a]All values represent data 24 hours after 2NPPD application.
[b]Values are the means ± SD of four to five replicate measurements for two human subjects.
Source: From Ref. 5.

that 2NPPD is chemically changed by oxidation due to the hydrogen peroxide. For example, the extent of HC Yellow No. 4 absorption was reduced if a dosing vehicle was applied that contained a formulation with seven other semipermanent hair dyes when compared with a formulation containing solely HC Yellow No. 4 (10). Mixtures of several dyes contained in one product formulation may change the solubility properties of the individual dyes. Furthermore, mixtures of dyes in formulations may result in the formation of dye aggregates through hydrogen bonding that could change the partition coefficient and molecular volume of the individual dyes (11). These dye-to-dye interactions are expected to slow the percutaneous penetration of an individual dye component.

The metabolism of 2NPPD after dermal application to human and rat skin can currently be summarized in Figure 5. In human and rat skin, it appears that 2NPPD is being metabolized via two pathways. The major pathway consists of N4-acetylation of the corresponding amine group. The second pathway consists of nitro reduction of the 2-nitro group to an amine. This was demonstrated by the presence of 1,2,4-triaminobenzene in the receptor fluid. In rat skin, but not human skin, a sulfated metabolite of 2NPPD was also detected, but the identity of the metabolite was not pursued. There is evidence to suggest it is possible to directly sulfate amine groups (12), indicating that sulfation potentially could have occurred on 2NPPD, acetylated-2NPPD, and/or triaminobenzene in rat skin.

The percutaneous absorption of 2NPPD obtained in this study is compared to a previous in vivo study (13). Our present results indicate that 5.4 μg 2NPPD per cm^2 was absorbed (based on 48.2 g of a semipermanent hair dye formulation containing 0.7% 2NPPD, 9.5% absorption, scalp skin surface area of 650 cm^2, and 10% of the applied formulation contacts the scalp skin) after a 30-minute application over 24 hours. In the Wolfram and Maibach study, approximately 3.4 μg 2NPPD per cm^2 was absorbed (based on 48.2 g formulation containing 1.36% 2NPPD, 0.143% absorption, and scalp surface area of 650 cm^2). The value of 3.4 $\mu g/cm^2$ 2NPPD absorbed in the in vivo human application study (13) compares well with the value of 5.4 $\mu g/cm^2$ found in the present in vitro human skin study, even though different hair dye formulations were used. In the present study, the actual amount applied to the skin was based on the estimated amount that would actually contact the scalp skin (approximately 10% of the product applied). This resulted in a higher relative

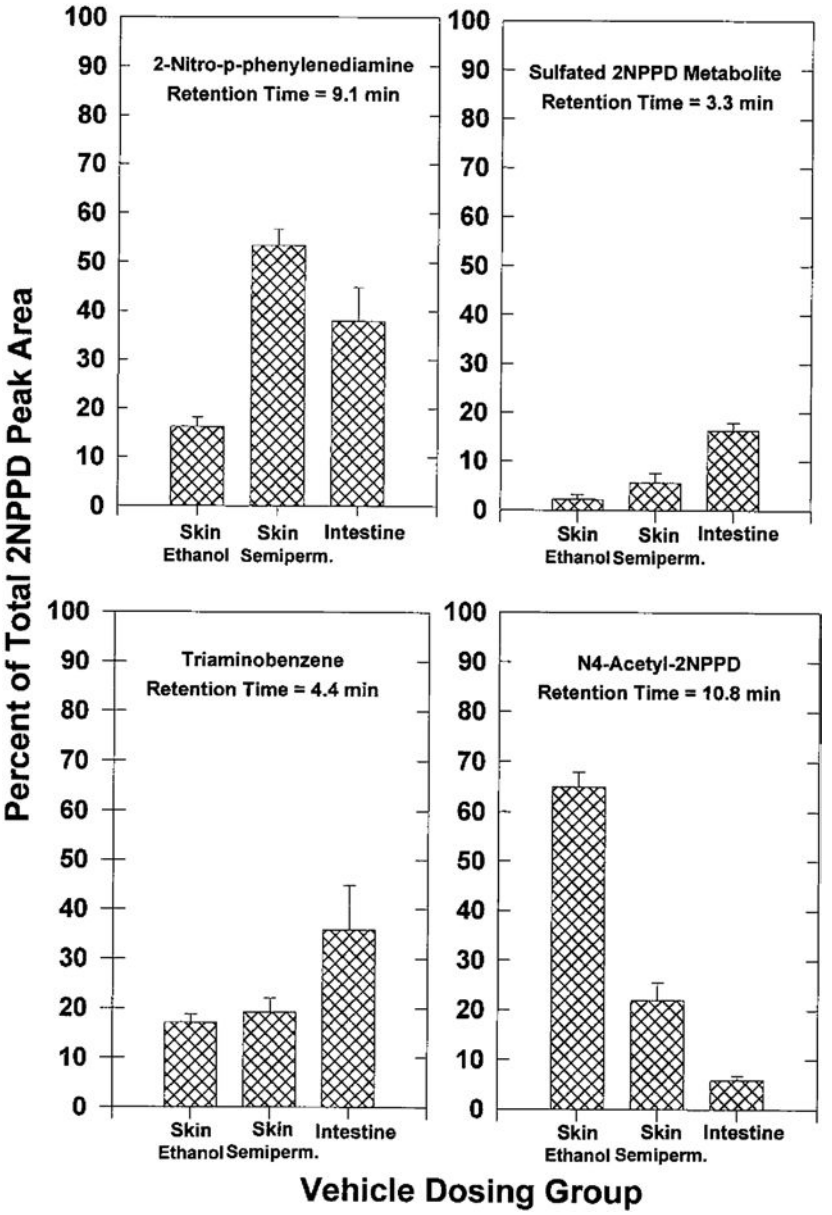


Figure 3 Metabolism of 2NPPD upon absorption through rat skin and intestinal tissue. The 2NPPD and metabolites were determined in receptor fluid fractions from three-hour skin and one-hour intestinal samples. Total ^{14}C-peak area was determined for each chromatogram. Then a percent of the total ^{14}C-peak area was calculated for each peak. Percent of peak areas reported are the mean $\pm$ SE from three individual rat studies ($n = 3$). Each single percent of peak area value was determined by averaging four to five replicate cell fractions from each rat study. *Source*: From Ref. 5.

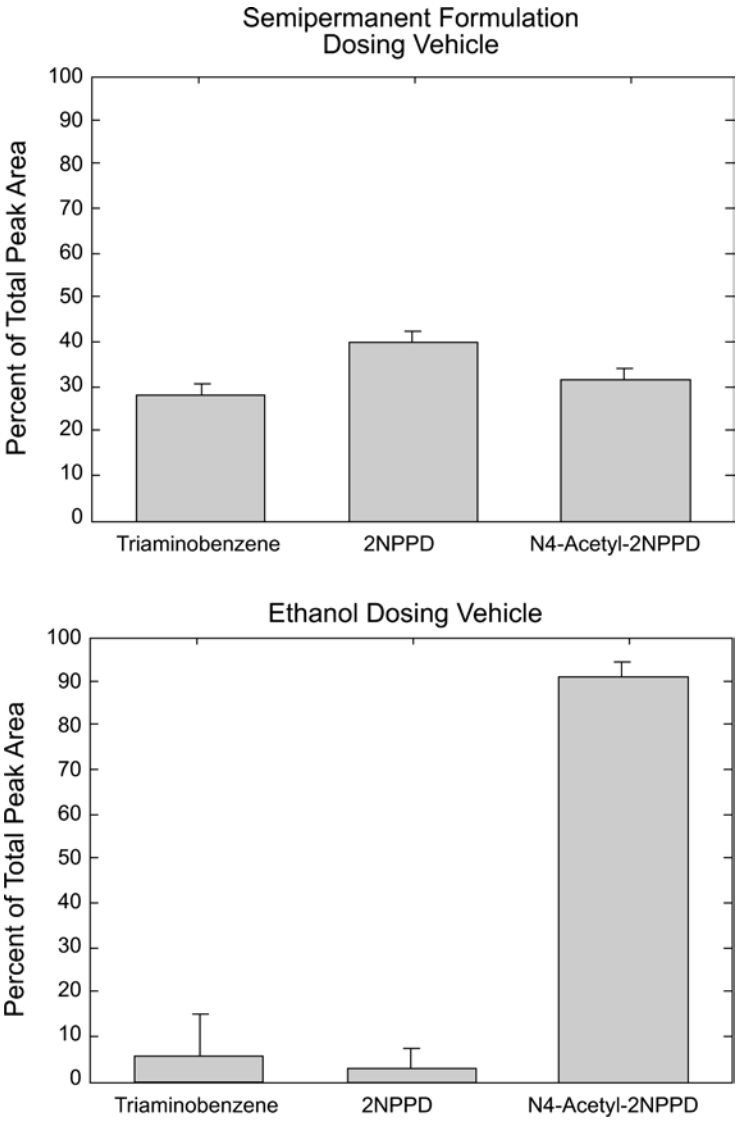


Figure 4 Metabolism of 2NPPD upon absorption through human skin using ethanol and a semipermanent dosing vehicle. The 2NPPD and metabolites were determined in receptor fluid fractions from the three hour time point. Total ^{14}C-peak area was determined for each chromatogram. Then a percent of the total ^{14}C-peak area was calculated for each peak. Percent of peak areas reported are the mean $\pm$ SD from two human studies ($n = 2$). Each single percent of peak area value was determined by averaging four to five replicate cell fractions from each human study. *Source*: From Ref. 5.

percentage of applied dose absorbed when compared with the Wolfram and Maibach (13) study.

In summary, these studies indicate that 2NPPD rapidly penetrates both human and rat skin. Under conditions that simulate normal consumer use conditions, approximately 5% to 10% of the 2NPPD that contacts the skin would be expected to be absorbed. We found extensive metabolism of 2NPPD upon absorption. The

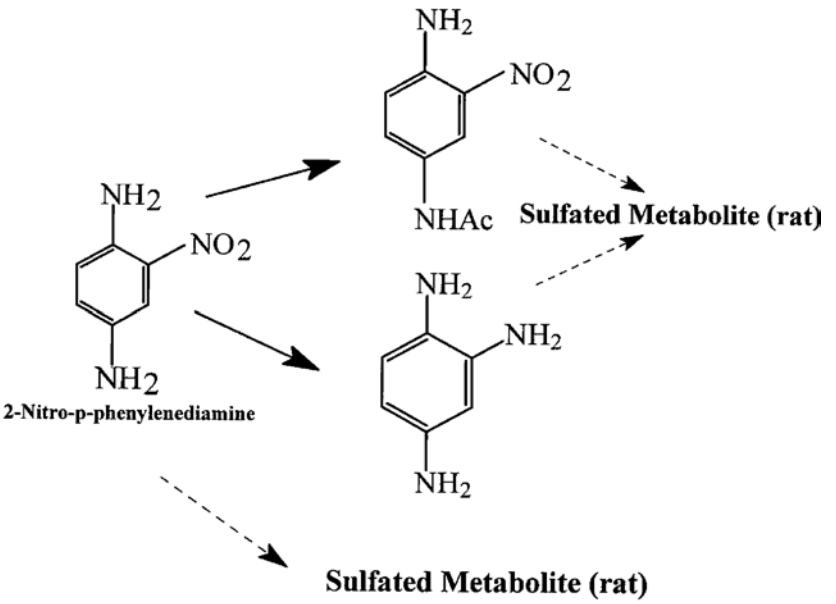


Figure 5 A proposed pathway for the metabolism of 2NPPD upon percutaneous absorption through human and rat skin. Metabolism of 2NPPD to sulfated metabolites was only observed in the rat. *Source*: From Ref. 5.

extent of metabolism and the metabolic profile were found to be both species and dosing vehicle dependent. Even though no sulfation of 2NPPD was seen in human skin, unmetabolized 2NPPD that is systemically absorbed after dermal application, could potentially be sulfated in other tissues (e.g., liver). The metabolism information will be useful in predicting the extent of 2NPPD and/or metabolite systemic absorption relative to a dermal exposure, which will improve the health hazard assessment of 2NPPD.

IV. SKIN ABSORPTION OF DISPERSE BLUE 1

A. Introduction

The DB1 (1,4,5,8-tetraaminoanthraquinone) is a dye with a tetraaminoanthraquinone structure possessing a blue–black color. The DB1 is used in temporary and semipermanent (nonoxidative) hair dyes, colors, and rinses. The DB1 is mutagenic in certain strains of *S. typhimurium* both with and without S9 activation (14). Positive tests are also noted with DB1 using several different mammalian mutagenicity assays (15). In a National Toxicology Program (NTP-TR-299) rodent carcinogenicity feeding study with DB1, there was "clear evidence of carcinogenicity for male and female F344/N rats." The DB1 administration resulted in "equivocal evidence of carcinogenicity in male B6C3F1 mice" and "no evidence of carcinogenicity in female B6C3F1 mice" (16). Due to the carcinogenicity of DB1 in rodents after oral administration, the potential for DB1 skin absorption was investigated.

The skin absorption of DB1 and the fate of the material remaining in the skin at the end of a 24 hour in vitro absorption study were investigated. An extended absorption study was conducted with DB1 to more thoroughly determine systemic

availability of the dye. Absorption studies were conducted in a manner that attempted to determine absorption of the dye using realistic exposure conditions that could be easily applied to human exposure situations.

B. Disperse Blue 1—Materials and Methods

1. Chemicals

^{14}C-DB1 (specific activity; 39.7 mCi/mmol) was synthesized by Research Triangle Institute (Research Triangle, North Carolina, U.S.A.) and had a radiochemical and chemical purity of $>98\%$. HPLC-grade solvents were obtained from J.T. Baker Chemical Co. (Phillipsburg, New Jersey, U.S.A.). HEPES-buffered Hanks' balanced salt solution (HHBSS; dry powder packets prepared by Gibco BRL, Life Technologies, Grand Island, New York, U.S.A.) was prepared fresh prior to each study.

2. Animal and Human Skin

Female fuzzy (Hsd:Fuzzy-fz) rats (Harlan Sprague Dawley Inc., Indianapolis, Indiana, U.S.A.), 3 to 10 months of age, were used in these experiments. Fresh, viable human skin was obtained as a result of abdominoplasty procedures from a local cosmetic surgeon.

3. Disperse Blue 1 Skin Dosing Solutions

Both an ethanol and a spiked semipermanent hair color formulation were used as test vehicles. A DB1 semipermanent formulation, a representative dye base formulation containing DB1 and ^{14}C-DB1, was formulated for these skin absorption studies. The formulation contained a concentration of DB1 that would be relevant to an estimated human dermal exposure during actual product usage. The total DB1 content (nonradiolabeled and radiolabeled) of the test semipermanent formulation was 0.52%. The DB1 ethanol solution was prepared by adding nonradiolabeled DB1 to pure ethanol so that a concentration of 0.52% DB1 was achieved. The nonradiolabeled DB1 dosing vehicles were spiked with ^{14}C-DB1 such that approximately 2 μg of radiolabeled DB1 was applied to skin in each diffusion cell. The dosage rate for the ethanol vehicle was 15 $\mu L/cm^2$ and the dosage rate for the semipermanent formulation was 7.8 mg/cm^2. All dosing vehicles were applied to skin for 30 minutes. The actual radiolabeled DB1 dose applied was determined by LSC.

4. Absorption Studies

Percutaneous absorption studies were done as described in Yourick et al. (17) using flow-through diffusion cells. Barrier integrity of human skin discs were verified by using the 20-minute tritiated water test (6). The amount of DB1 remaining in the skin after 24 hours was determined by LSC.

5. Data Analysis

Values reported are the mean $\pm$ SE for the human and rat studies. DB1 absorption was tested in human donor skin ($n=4$) and rat skin ($n=3$) using 0.52% DB1 in a semipermanent hair dye formulation and 0.52% DB1 in an ethanol solution. Each vehicle was tested on three to five diffusion cells (replicates). For each vehicle, the

three to five replicate diffusion cell absorption values were averaged to give a single absorption value for each human subject or rat (i.e., $n = 1$). Statistical (SigmaStat Statistical Software, SPSS Inc., Chicago, Illinois, U.S.A.) differences were determined using either a Student's t-test ($p < 0.05$) or analysis of variance (ANOVA, $p < 0.05$) followed by a posteriori multiple comparisons of group means by the Tukey test ($p < 0.05$).

C. Dermal Penetration and Absorption of Disperse Blue 1

The percutaneous absorption of DB1 through human skin into the receptor fluid with ethanol and the semipermanent dosing vehicles is depicted in Figure 6. The DB1 slowly penetrated human skin with relatively constant absorption over the course of 24 hours. In human skin ($n = 4$), the percentages of applied dose absorbed over 24 hours into the receptor fluid were 0.2 ± 0.04 ($X \pm SE$) and 0.2 ± 0.02 for the ethanol and semipermanent vehicles, respectively, with approximately 11% and 3% remaining in skin, respectively (Table 3). There was no effect of the vehicle on the absorption of DB1 into the receptor fluid, however, there was a significant increase in the amount of DB1 that remained in the skin in an ethanol vehicle compared to the semipermanent formulation vehicle. This resulted in a significantly lower total penetration of DB1 into human skin when the semipermanent hair dye vehicle was compared to the ethanol vehicle. The amount of DB1 that was absorbed into the receptor fluid was significantly lower in human skin when compared with rat skin

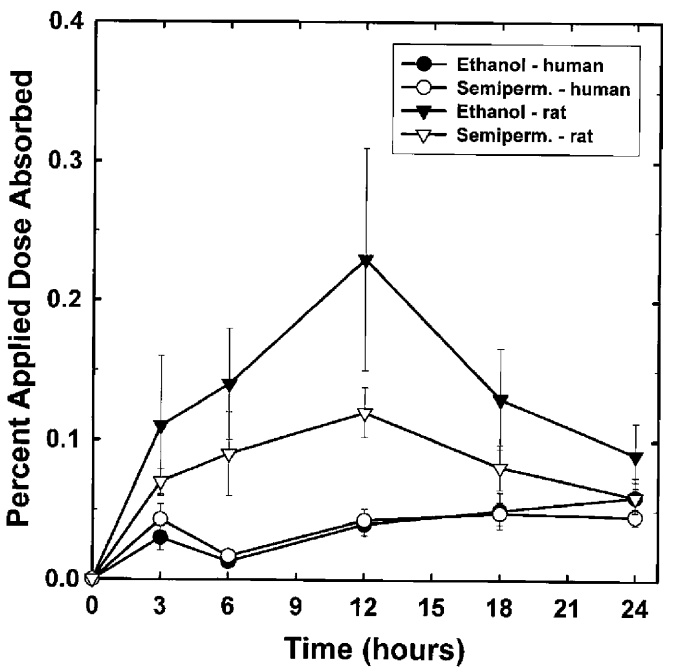


Figure 6 Percent applied DB1 dose absorbed over 24 hours in receptor fluid from human and rat skin. Absorption values are the $X \pm SE$ from four separate human studies ($n = 4$) and three individual rat studies ($n = 3$). Each individual absorption value within a study was determined by averaging four to five replicate diffusion cell measurements for each time interval point and dosing solution. *Source*: From Ref. 17.

Table 3 Summary of DB1 Penetration in Human and Fuzzy Rat Skin[a]

	Percent of applied dose	
	Dosing vehicle	
Skin type	Ethanol	Semipermanent
Receptor fluid		
Rat	0.7 ± 0.23[b]	0.4 ± 0.074
Human	0.2 ± 0.04[d]	$0.2 + 0.02$[d]
Skin content		
Rat	8.8 ± 1.64	2.6 ± 0.13[c]
Human	11.1 ± 1.30	3.1 ± 0.28[c]
Total penetrated (Receptor fluid + skin)		
Rat	9.5 ± 1.55	3.0 ± 0.20[c]
Human	11.3 ± 1.34	3.3 ± 0.30[c]
Wash		
Rat	74.2 ± 3.37	80.9 ± 8.62
Human	76.1 ± 5.37	88.2 ± 2.21
Recovery		
Rat	83.5 ± 1.95	83.9 ± 8.82
Human	87.4 ± 5.83	91.5 ± 2.50

[a]All values represent data 24 hours after DB1 application.
[b]Values are the $X \pm$ SE for rat ($n = 3$) and human ($n = 4$) skin.
[c]Significantly different from the ethanol dosing vehicle.
[d]Significantly different from rat skin.
Source: From Ref. 17.

(Table 3). In addition, no human skin metabolism of DB1 was found by HPLC analysis of skin or receptor fluid.

Dermal absorption of DB1 through fuzzy rat skin into the receptor fluid over 24 hours is shown in Figure 6. DB1 also slowly diffused across fuzzy rat skin, similar to human skin, with relatively constant absorption over the course of 24 hours. In rat skin ($n = 3$), the percentages of applied dose absorbed over 24 hours into the receptor fluid were 0.7 ± 0.23 and 0.4 ± 0.07 for the ethanol and product vehicles, respectively, with approximately 9% and 3% remaining in skin, respectively (Table 3). The localization of the substantial amount of DB1 remaining in skin was investigated. The majority of DB1 (approximately 80%) was found in the stratum corneum with the remainder contained in the viable epidermis/dermis layer (data not shown). To examine the fate of DB1 from the skin reservoir, an absorption study in rat skin was extended to 72 hours (Fig. 7). The extended absorption study (skin washed after 24 hours) revealed that little (0.16% of the applied dose) of the DB1 that penetrated skin within 24 hours (2.6% of the applied dose; Table 3) moves through the skin to be absorbed into the receptor fluid over 72 hours. No rat skin metabolism of DB1 was found by HPLC analysis of skin or receptor fluid.

D. Discussion

In summary, the skin reservoir can often contribute to the amount of material considered absorbed in diffusion cell studies. When the skin reservoir is significant

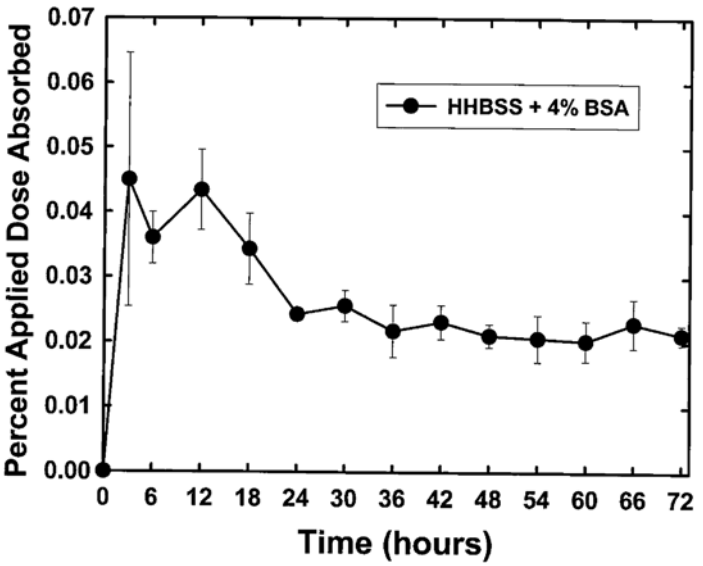


Figure 7 Extended DB1 absorption study in fuzzy rat skin. Absorption values are the $X \pm$ SE from two separate rat studies. Each individual absorption value within a study was determined by averaging three to four replicate diffusion cell measurements for each time interval point. *Source*: From Ref. 17.

compared to levels in receptor fluid, the contribution of the skin reservoir to systemic absorption should be examined. Therefore, it is important to determine the fate of chemicals remaining in the skin at the end of a typical 24 hour in vitro absorption study. An extended (72 hours) absorption study demonstrated that the DB1 remaining in the skin did not appreciably move into the receptor fluid beyond the extent measured after 24 hours. The barrier property of skin in diffusion cell studies has been shown to remain intact for 72 hours (18). Therefore, it seems reasonable to disregard the skin content as absorbed material. For exposure assessment purposes, the amount of DB1 considered systemically bioavailable would simply be the DB1 absorbed in the receptor fluid at 24 hours. With further investigation of the skin reservoir, we found it was not appropriate to add the skin levels of DB1 to the receptor fluid levels to characterize the total of absorbed material. This essentially reduced the percent of applied dose absorbed being considered for exposure estimates from 3.3% to 0.2% for DB1.

V. HAIR DYE ABSORPTION: CORRELATION WITH PARTITION COEFFICIENTS

Percutaneous absorption through human skin of a homologous series of hair dyes was investigated (9). The hair dyes studied were *p*-phenylenediamine, *o*-phenylenediamine, 2NPPD, 2-amino-4-nitrophenol, 4-chloro-*m*-phenylenediamine, and 4-amino-2-nitrophenol. A compound's oil and water solubility properties affect its ability to diffuse across the epidermal membrane. The permeability constants for these dyes were compared to the octanol/water and skin membrane/water

Table 4 Percutaneous Absorption of Hair Dyes and Correlation with Partition Coefficients

Compound	pKa	Octanol/water partition coefficient	Stratum corneum/water partition coefficient	Permeability constant (cm/hr)[a]
p-Phenylenediamine	6.3	0.5	ND	2.4×10^{-4}
o-Phenylenediamine	4.8	1.4	6.9	4.5×10^{-4}
2-Nitro-*p*-phenylenediamine	3.9	3.4	13.0	5.0×10^{-4}
2-Amino-4-nitrophenol	7.1	13.5	ND	$< 3.0 \times 10^{-5}$ (6.6×10^{-4})
4-Chloro-*m*-phenylenediamine	4.1	7.0	ND	2.1×10^{-3}
4-Amino-2-nitrophenol	7.8	9.1	13.0	8.6×10^{-5} (2.8×10^{-3})

[a]Values were obtained with a borate buffer (pH 9.7) as the vehicle. Numbers in parentheses were obtained in water to prevent ionization. Results are the mean of three to seven determinations.
Source: From Ref. 9. *Abbreviations*: ND not determined

partition coefficients (Table 4). The permeability constants determined for these dyes were in the same rank order as the octanol/water partition coefficients, with the exception of 4-chloro-*m*-phenylenediamine. Stratum corneum/water partition values correlated in a reverse order when compared with skin permeability constant values. It was apparent that once binding of the hair dye to the membrane was saturated, the partition coefficients more closely correlated with the rank order of the permeability constants. It was concluded that the prediction of percutaneous absorption of the homologous series of hair dyes was most closely associated with the oil/water partition coefficient, but this may be confounded by the capacity of the dye to bind to skin components.

VI. CONCLUSION

In summary, the skin absorption of representative hair dye ingredients is presented in this chapter. The 2NPPD rapidly penetrates both human and rat skin. We found extensive metabolism of 2NPPD upon absorption. The extent of metabolism and the metabolic profile were found to be both species and dosing vehicle dependent. The DB1 slowly penetrates human and rat skin and was not metabolized. An extended (72 hours) DB1 absorption study demonstrated that DB1 remaining in the skin did not appreciably move into the receptor fluid beyond the extent measured after 24 hours. It was also shown with a series of homologous hair dyes that prediction of dermal absorption is most closely associated with the oil/water partition coefficient, but skin binding must also be considered. Extended absorption studies in conjunction with additional information on skin localization, skin binding studies, and vehicles effects can help to determine the fate of hair dye ingredients in skin. Additional investigation and characterization of the skin reservoir will provide data that can be used to realistically refine the exposure assessment for hair dye chemicals.

REFERENCES

1. http ://www.cfsan.fda.gov/~dms/cos-toc.html.
1a. Elder RL. Final report on the safety assessment of 2-nitro-*p*-phenylenediamine and 4-nitro-*o*-phenylenediamine. J Amer Coll Toxicol 1985; 4:161–197.
2. Ames BN, Kammen HO, Yamasaki E. Hair dyes are mutagenic: identification of a variety of mutagenic ingredients. Proc Nat Acad Sci USA 1975; 72:2423–2427.
3. IARC. IARC Monographs on the Evaluation of the Carcinogenic Risk of Chemicals to Humans. 1,4-Diamino-2-nitrobenzene (2-nitro-para-phenylenediamine). Vol. 57. Lyon: France, 1993:85–200.
4. National Cancer Institute (NCI). Bioassay of 2-Nitro-*p*-Phenylenediamine for Possible Carcinogenicity (CAS No. 5307-14-2), Technical Report Series No. 169. NCI Publication NCI-CG-TR-169. US Department of Health and Human Services, Public Health Services, National Institutes of Health, 1979.
5. Yourick JJ, Bronaugh RL. Percutaneous penetration and metabolism of 2-nitro-*p*-phenylenediamine in human and fuzzy rat skin. Toxicol Appl Pharmacol 2000; 166:13–23.
6. Bronaugh RL, Stewart RF, Simon M. Methods for in vitro percutaneous absorption studies VII: use of excised human skin. J Pharm Sci 1986; 75:1094–1097.
7. Nakao M, Gotoh Y, Matsuki Y, Hiratsuka A, Watabe T. Metabolism of the hair dye component, nitro-*p*-phenylenediamine, in the rat. Chem Pharm Bull 1987; 35:785–791.
8. Flynn GL. Mechanism of percutaneous absorption from physicochemical evidence. In: Bronaugh RL, Maibach HI, eds. Percutaneous Absorption: Mechanisms-Methodology-Drug Delivery. New York: Marcel Dekker, 1985:17–42.
9. Bronaugh RL, Congdon ER. Percutaneous absorption of hair dyes: correlation with partition coefficients. J Invest Dermatol 1984; 83:124–127.
10. Dressler WE, Azri-Meehan S, Grabarz R. Utilization of in vitro percutaneous penetration data in the safety assessment of hair dyes. In: Lisanski SG, Macmillan R, Dupris J, eds. Alternatives to Animal Testing. Proceedings of an International Scientific Conference. Newbury, U.K.: CPL Press, 1996:269.
11. Dressler WE. Percutaneous absorption of hair dyes. In: Roberts MS, Walters KA, eds. Dermal Absorption and Toxicity Assessment. New York: Marcel Dekker Inc., 1998:518.
12. Parkinson A. Biotransformation of xenobiotics. In: Klaassen CD, ed. Casarett & Doull's Toxicology: The Basic Science of Poison. 5th ed. New York: McGraw-Hill, 1996: 168–170.
13. Wolfram LJ, Maibach HI. Percutaneous penetration of hair dyes. Arch Dermatol Res 1985; 277:235–241.
14. Zeiger E, Anderson B, Haworth S, Lawlor T, Mortelmans K. Salmonella mutagenicity tests. IV. Results from the testing of 300 chemicals. Environ Molec Mutagen 2004; 11(Suppl 12):1–158.
15. Pang SNJ. Final Report on the Safety Assessment of Disperse Blue 1. J Am Coll Toxicol 1995; 14(6):433–451.
16. NTP-TR- 299. National Toxicology Program. Technical Report Series No. 299. Toxicology and Carcinogenesis Studies of C.I. Disperse Blue 1 (CAS No. 2475-45-8) in F344/N Rats and B6C3F_1 Mice (Feed Studies). NIH Publication No. 86-2555. National Toxicology Program, Research Triangle Park, NC, and Bethesda, MD, 1986:241.
17. Yourick JJ, Koenig ML, Yourick DL, Bronaugh RL. Fate of chemicals in skin after dermal application: does the in vitro skin reservoir affect the estimate of systemic absorption? Toxicol Appl Pharmacol 2004; 195(3):309–320
18. Kraeling ME, Jung CT, Yourick JJ, Bronaugh RL. In vitro percutaneous absorption of diethanolamine (DEA) in human skin. Toxicol Sci 2002; 66(1-S):Abstract #807:166.

46
Hair Dye Penetration in Monkey and Man

Leszek J. Wolfram
Clairol, Inc., Stamford, Connecticut, U.S.A.

Howard I. Maibach
Department of Dermatology, School of Medicine, University of California, San Francisco, California, U.S.A.

Hair dyes have been in use for decades, yet even recent studies of their skin penetration potential have been restricted primarily to their evaluation in rats and dogs (1–6). Although undoubtedly useful, the results of these experiments are difficult to extrapolate to man and to relate to the percutaneous absorption that occurs under conditions of practical usage of fully formulated products. Sporadic attempts have been made to single out individual ingredients for studies in man (7,8), but these could not be readily quantitated.

A thorough study by Wester et al. (9), comparing the percutaneous absorption in man and different animal species while pointing to the experimental advantages of using animal models, stresses the need for frequent checks at each stage of the penetration process. The authors conclude that both in vivo and in vitro studies of the skin of the rhesus monkey approximate the permeability characteristics of human skin.

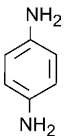
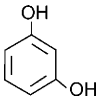
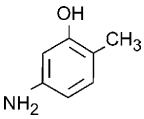
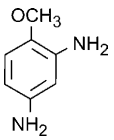
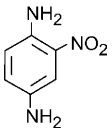
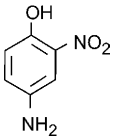
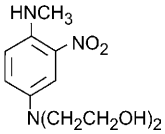
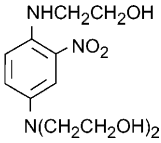
We recently initiated (10) a comprehensive evaluation of skin penetration potential of hair dyes from both permanent and semipermanent color categories. This chapter summarizes our results. The investigation focuses on man, although in most cases a comparison study also has been carried out using rhesus monkey as the animal model. The methodology is, in general, patterned after the procedure developed by Feldmann and Maibach (11) for measurement of percutaneous absorption in man. This method involves quantifying absorption on the basis of the percentage of radioactivity excreted in the urine following application of a known amount of the labeled compound.

I. EXPERIMENTAL

A. Hair Dyes

Commercially available hair dye products, representatives of permanent and semipermanent hair color categories (Nice 'n Easy and Loving Care formulations, respectively) were individually labeled with radioactive materials. The radioactively labeled

Table 1 Dyes Studied in This Work

Dye structure	Dye	Species and yield of urinary recovery from parenteral (P) or oral (O) administration
	*p*-Phenylenediamine (PPD)	Man, 72% (P)
	Resorcinol	Rhesus monkey, 79% (P)
	4-Amino-2-hydroxytoluene	Man, 94% (O)
	2,4-Diaminoanisole (DAA)	Rhesus monkey, 61% (P)
	2-Nitro-PPD	Rhesus monkey, 56% (P)
	2-Nitro-4-aminophenol	Rhesus monkey, 68% (P)
	HC Blue No. 1	Man, 94% (O)
	HC Blue No. 2	Man, 51% (O)

dyes together with their urinary recoveries following parenteral (P) or oral (O) administration are listed in Table 1.

B. Dyeing Procedure

Process instructions, specific for each hair color product, were followed. Net weights of single-application hair coloring products vary between 3 (semipermanent dyes) and 4 fl oz (oxidative and permanent dyes). While this is sufficient to color up to 120 g of hair, the average weight of female scalp hair 4-in long is about 60 g. The

ratio of lotion to hair commonly operative during hair coloring is thus 1.5 to 2.0, and the latter value was chosen to arrive at the quantity of the dye mixture that was used in the studies with rhesus monkey.

1. Human Volunteers

The coloring was performed with one subject at a time. The subject was seated in a chair having his head rested on a specially constructed sink support for comfort and easy collection of rinse water. The dye mixture was applied to dry hair and worked gently into the hair mass over a period of five to eight minutes and left on the hair for an additional 20 (permanent color) or 30 (semipermanent color) minutes. In the latter case, a plastic turban was wrapped around the hair for the dyeing period. The dyed hair was thoroughly rinsed, towel blotted, dried, and either clipped with an electric clipper or left on (see below).

2. Rhesus Monkeys

Animals were tranquilized with 0.2 mL of ketamine and placed comfortably in a supine position on a laboratory bench top. The head of each monkey was rested on a specially designed sink support to facilitate the coloring process and to assure quantitative collection of the rinse water. The dye lotion (total of 5 g, in the case of oxidative dyes consisting of 2.5 g of the dye solution and 2.5 g of 6% aqueous hydrogen peroxide) was worked into the dry scalp hair until all the dye mixture was used (~3 minutes). The operator wore vinyl disposable gloves. Twenty minutes was allowed for the dyeing process to proceed (30 minutes in the case of semipermanent dye, where a plastic turban was also used). After dyeing, the hair was rinsed with a microshower until the rinsing water was free of color. The excess water remaining on the hair was blotted with a paper towel and dyed hair was cut off with electric clippers.

C. Urine Collection

1. Human Volunteers

The subjects were given plastic urine containers for each time period: 0 to 4, 4 to 8, 8 to 12, and 12 to 24 hour and then for every 24-hour period for as long as required.

2. Rhesus Monkeys

After the dyeing procedure was completed, all the monkeys were restrained in ophthalmological chairs, thus preventing the animals from touching the scalp area. Urine samples were collected at 6, 12, and 24 hours and from then on at 24-hour intervals for seven days. For both species and for each time period, total urine weights were recorded and an aliquot removed for analysis.

D. Radioactivity Determination in Urine

All urine samples were filtered and assayed in PPD/Triton/toluene with a liquid scintillation spectrometer. A [^{14}C]toluene internal standard (100,000 cpm) was added to each counting vial to determine the extent of quenching. The counting cocktail was 81% efficient and the background was 22 cpm. Most specimens were also counted by the wet ashing method (11). The assay values listed in the tables have been corrected for incomplete excretion from internal application. For the latter, (Table 1).

E. Radioactivity Determination in Dyed Hair and Stratum Corneum

Samples of hair or of the horny layer were digested overnight in counting vials, each containing 1 mL of Unisol. The digested samples were decolorized by the addition of 50% hydrogen peroxide and each was diluted with 15 mL of Unisol complement. Clear samples were equilibrated in the counting chamber at 4°C before counting on a Packard Tricarb liquid scintillation spectrometer. Three samples were analyzed for each hair lot and one of the stratum corneum, with three radioactivity determinations for each sample.

II. RESULTS

Two methodological approaches (denoted "Application Only" and "Application and Wear"), reflecting different experimental objectives, have been developed in the course of this study. In the first one, the hair was removed immediately following the completion of the coloring procedure; in the other, the hair was left on. The first approach allowed us to evaluate the extent of skin penetration by hair dyes resulting from the hair coloring procedure alone. The second approach recognized that (a) people color their hair to wear it as such, and (b) the dyed hair represents a reservoir of dye moieties that through a variety of routes, may become bioavailable.

A. Application Only

The data on total excretion of radiolabeled dye ingredients are given in Table 2. In most cases, they reflect the counts obtained over 144 hours following application of the dye; occasionally a time span of 96 hours was used if the counts at longer times were at the background level.

Two entries of Table 2, namely ($T_{1/2}$) and total dose excretion, should be clarified. It was found that the urinary excretion followed satisfactory first-order kinetics and thus, time required for 50% excretion ($T_{1/2}$) was employed as an additional quantifying parameter. Regarding the dose, bear in mind that in the process of hair coloring, the product is usually applied in the form of a viscous lotion and uniformly distributed within the hair mass. Clearly, only the product that is in contact with the scalp serves as a dye reservoir available for skin penetration. The quantity available depends on the retention of the product by hair, which in turn is a function of total surface area of the hair mass and the viscosity of the product. Unless the product is applied sparingly (product/hair ratio much less than one—a situation that is unlikely to be encountered in hair dyeing), the thickness of the product film present on the scalp is at least 5 to 10 times that of the horny layer of the scalp; and under such conditions, the quantity of the absorbed dye reaches a limiting value and is independent of the quantity of lotion used (6). Throughout this work, every attempt was made to maintain a constant ratio of product to hair weight (~2) and thus to make the dose excretion values intercomparable.

From the five dyes that were concurrently evaluated on both man and the rhesus monkey, three of them (DAA, PPD, and HC Blue No. 1) show striking equivalence in cutaneous absorption between these two species. This parallels the earlier finding of Wester et al. (9) and Bartek and LaBudde (12), who noted a similar pattern for absorption of benzoic acid, testosterone, and hydrocortisone. Two remaining dyes (2-nitro-PPD and resorcinol), representing the semipermanent and

Table 2 Parameters of Percutaneous Absorption of Hair Dyes

Hair color category	Labeled ingredient	Species	Number of subjects	Total dose excretion [% (±SD)]	$T_{1/2}$ of Urinary excretion (hr)
Permanent (oxidative)	2,4-Diaminoanisole (DAA)	Man	3	0.022 (0.01)	18
		Rhesus monkey	2	0.032	20
	Resorcinol	Man	3	0.076 (0.03)	31
		Rhesus monkey	3	0.177 (0.03)	31
	4-Amino-2-hydroxytoluene	Man	3	0.20 (0.10)	24
	p-Phenylenediamine (PPD)	Man	5	0.190 (0.06)	16
		Rhesus monkey	3	0.182 (0.06)	22
Semipermanent	2-Nitro-PPD	Man	3	0.143 (0.04)	24
		Rhesus monkey	3	0.551 (0.10)	24
	4-Amino-2-nitrophenol	Man	3	0.235 (0.08)	10
	HC Blue No. 1	Man	5	0.151 (0.12)	18
		Rhesus monkey	3	0.127 (0.03)	40

Table 3 Flux of Hair Dyes Through Human Scalp

Dye	Flux (mol/cm^2 hr)
DAA	9.2×10^{-11}
Resorcinol	2.2×10^{-10}
4-Amino-2-hydroxytoluene	4.5×10^{-10}
2-Nitro-PPD	4.7×10^{-10}
HC Blue No. 1	4.9×10^{-10}
PPD	6.3×10^{-10}
4-Amino-2-nitrophenol	8.3×10^{-10}

permanent categories, respectively, do not follow this pattern. Both dyes show greater absorption for rhesus monkey than man, although the $T_{1/2}$ values are identical in both species.

The results also indicate that except for DAA, the dyes appear to penetrate the skin to a similar extent. This is in spite of substantial differences in the chemical structure of the dyes, in the nature of the dye bases, and in the reaction pathways responsible for color formation. The observed effect is, however, somewhat fortuitous because the various dyes are present in their respective formulations at different concentrations. A better perception of their penetration potential can be deduced from the flux values, which were calculated for individual dyes from the 24-hour excretion data, normalizing the quantity applied in each case to 10 μM/cm^2 (Table 3).

There is approximately a 10-fold spread in the flux, with DAA being at the low end of the scale and 4-amino-2-nitrophenol exhibiting the highest potential. No apparent correlation to either molecular weight or the chemical structure is evident, but the spread in molecular weight is relatively small (it varies between 100 and 250), and all the dyes are unchanged under dyeing conditions. It is also interesting that the flux ranking of dyes is not reciprocated by their solubility characteristics. The membrane/vehicle partition coefficients (which reflect the solubility properties of materials in media of differing polarities) are considered to be important factors in determining the flux of materials through the stratum corneum but, surprisingly, their utility in this case is minimal (Table 4).

Table 4 Partition Coefficients of Hair Dyes Between Octanol/Water and Guinea Pig Stratum Corneum/Water

	Partition coefficients		
Dye	Octanol/water	Intact stratum corneum/water	Delipidized sratum corneum/water
DAA	0.7	—	—
Resorcinol	7.0	3.6	7.7
4-Amino-2-hydroxytoluene	25.4	8.0	21.1
2-Nitro-PPD	3.6	13.2	28.9
HC Blue No. 1	10.8	2.8	7.3
PPD	0.2	4.0	7.3
4-Amino-2-nitrophenol	10.1	5.0	9.1

The octanol/water partition coefficients seem to be at odds as well with those determined for stratum corneum/water with no evidence of a pattern that could be persuasively interpreted. The data all but imply that the lipid domains in the horny layer are the unlikely sites for retention of lipophilic dyes. That the distribution of dyes in the stratum corneum is highly complex is further evidenced by the fact that the delipidization of stratum corneum by chloroform/methanol increases the values of partition coefficients of dyes irrespective of whether they are hydrophilic or prefer a nonpolar environment. Clearly, the removal of the lipids augments the reservoir capacity of the horny layer. It would be presumptuous, however, to assume that such an increase would simply translate into faster or more extensive diffusion, since the latter is likely to be critically dependent on the binding of the dyes to the stratum corneum and there is no information about how delipidization affects the binding characteristics.

An additional and useful insight into the mechanism of scalp penetration by hair dyes can be gained from the $T_{1/2}$ values of urinary excretions. The results of monitoring the urinary recoveries of dyes administered by parenteral injection

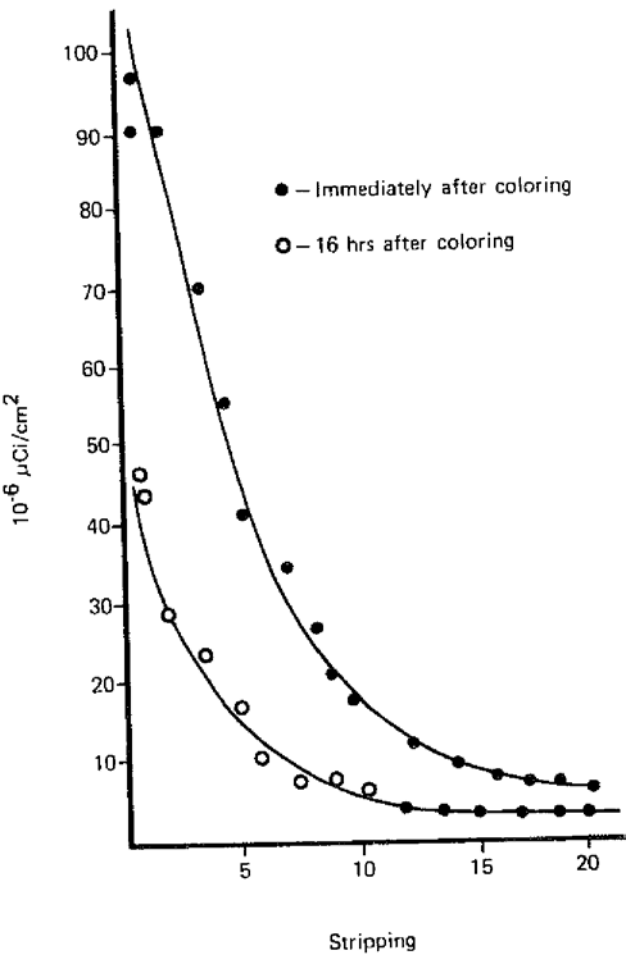


Figure 1 Distribution of radioactive PPD in the horny layer.

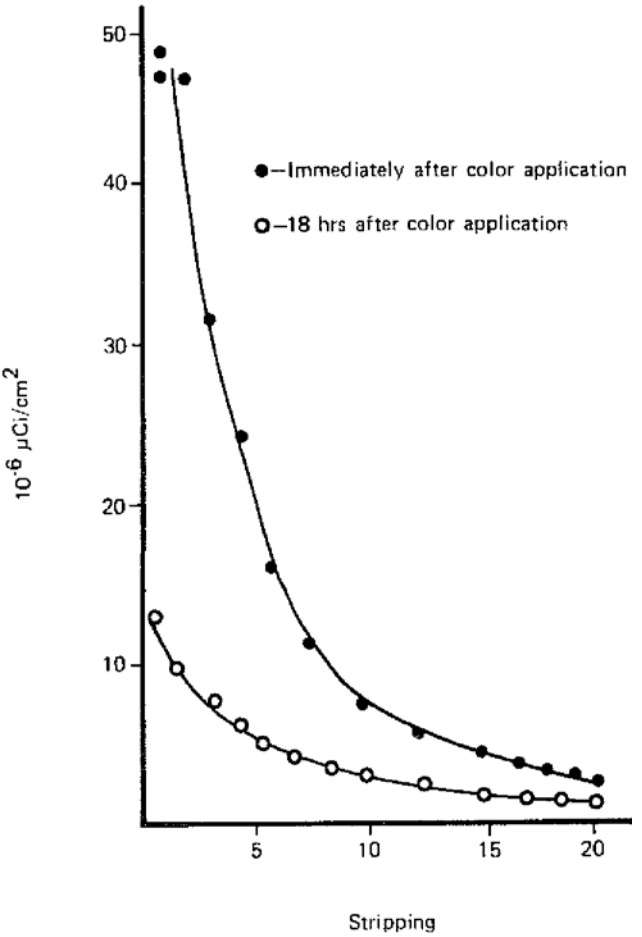


Figure 2 Distribution of radioactive HC Blue No. 1 in the horny layer.

or orally show that elimination of those materials from the organisms of either rhesus monkey or man is rapid, yielding $T_{1/2}$ values of four hours or less. That is clearly not the case with the urinary dye recoveries following hair dyeing, where $T_{1/2}$ values vary from 10 to 40 hours, suggesting that only trivial amounts of dye penetrate the stratum corneum during the actual process of hair coloring. It follows that the bulk of the urine-recovered dye must have been taken up into the horny layer and then slowly released into the circulation. Some penetration of hair follicles and/or sweat ducts might also have occurred, but this shunt mechanism—judging again by high $T_{1/2}$ values—seems to be of less importance. A direct experimental support for the magnitude of the horny layer reservoir has been obtained by applying a measured quantity of dye formulation to forearms of human volunteers, mimicking the dyeing procedure, and then removing sequential layers of stratum corneum all the way to the glistening layer by stripping with adhesive tape. The application areas were large enough to allow for stripping adjacent regions 16 or 18 hours after the color application. Figures 1 and 2 illustrate the results obtained in the case of PPD and HC Blue No. 1, respectively. The change in the concentration profiles of both dyes with time is a dramatic demonstration of their mobility in the horny layer and serves as an

Table 5 Dose Absorption of Hair Dyes in Man Under Conditions of Use (Application +30 Days Wear)

Dye	Number of subjects	Cumulative dose absorption (%) 1st day	10th day	20th day	30th day	(±SD)	$T_{1/2}$ (hr)
PPD	3	0.19	0.31	0.34	0.34	(0.12)	26
2-Nitro-PPD	4	0.19	0.42	0.62	0.75	(0.30)	150
HC Blue No. 1	4	0.15	0.28	0.30	0.50	(0.15)	138
HC Blue No. 2	4	0.01	0.07	0.094	0.094	(0.02)	52

independent confirmation of the observed kinetics of scalp penetration. It is worth adding that the calculations based on the reservoir potential in both cases strongly suggest that the urinary excretion values, which are the measure of the extent of dye penetration, can be satisfactorily accounted for by the dye absorbed within the stratum corneum.

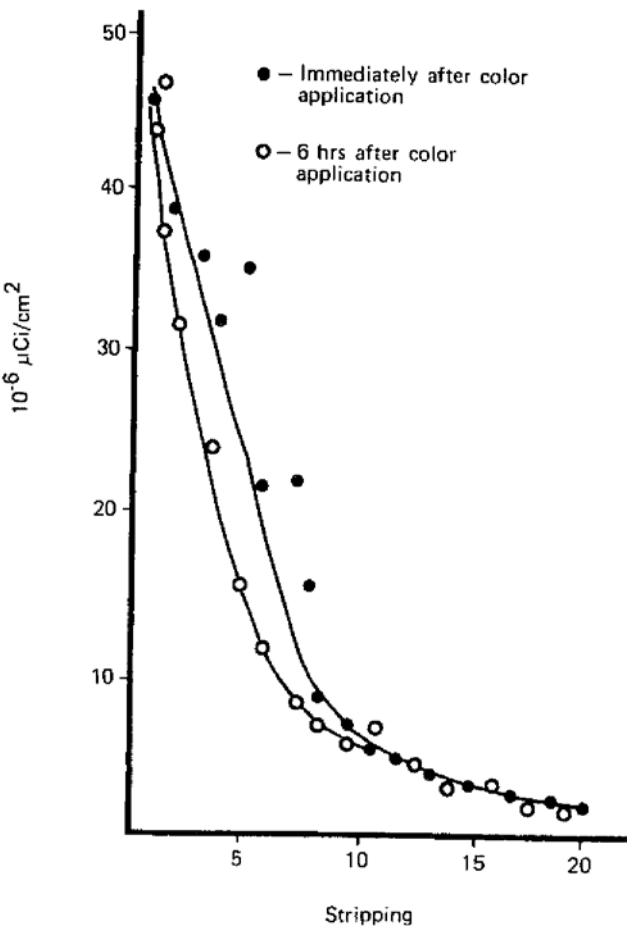


Figure 3 Distribution of radioactive HC Blue No. 1 in the horny layer.

B. Application and Wear

The hair coloring procedures employed in this study were identical to those described earlier, however, the collections of urine and their radioactive assays continued for as long as 30 days following the dye application. The results of the assays, both total and interim, are given in Table 5. The half-times ($T_{1/2}$) of urinary excretions are also included as informative guides.

The results fall into a pattern that one would anticipate from the mechanism of hair coloring that is characteristic for a given class of dyes. In the case of oxidative (permanent) dyes (based on PPD and its couplers), the color-forming reactions convert the small, mobile, and colorless molecules into much bulkier dye moieties trapped within the structure of the hair. There is little chance for these materials to diffuse out of the hair, even when it becomes fully swollen during shampooing. On the other hand, the semipermanent dyes do not undergo any changes in size upon their deposition in the fiber, and they retain a high degree of mobility, which translates into a potential for outward diffusion. Thus, while the hair acts as a repository for both types of dye, their bioavailabilities are clearly different. The latter finds its experimental verification in the urinary excretion data. There is only

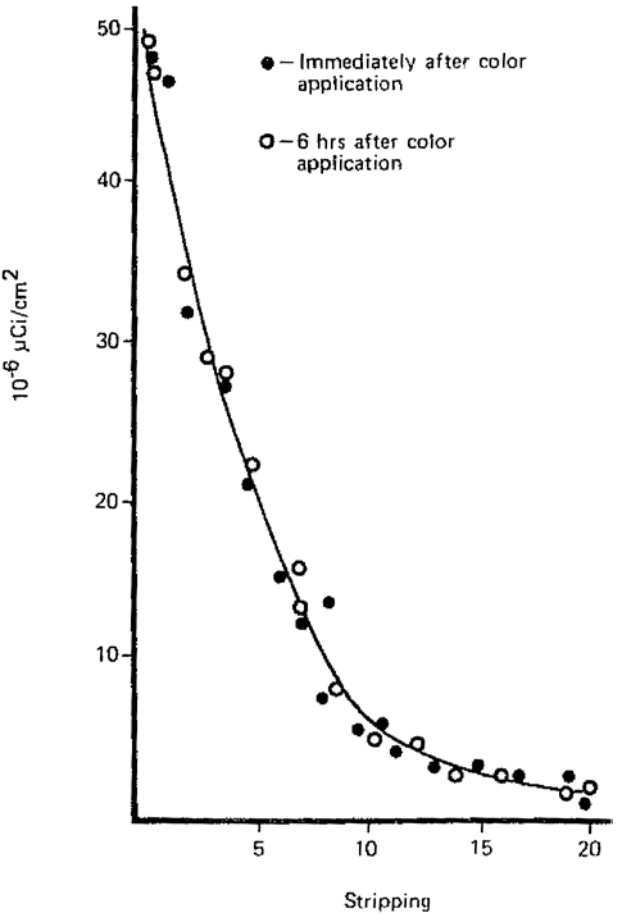


Figure 4 Distribution of radioactive HC Blue No. 2 in the horny layer.

a marginal increase in the dosage absorption of PPD when compared to the "Application Only" values, with most of the increase generated within two days of color application. HC Blue No. 1 and 2-nitro-PPD, on the other hand, register a four- to fivefold increase with measurable absorption values spread over several weeks. This trend is also reflected in the $T_{1/2}$ values of urinary excretion—a trivial change for PPD, but a substantial increase for both HC Blue No. 1 and 2-nitro-PPD.

The excretion data of Table 5 reflect not only scalp penetration but also include dye that has become bioavailable through other ports of entry (dermal as well as oral)—a real-life situation. In this sense, the $T_{1/2}$ values do not have the same meaning as those of Table 2, where they referred exclusively to scalp permeation.

The higher mobility of semipermanent dyes when compared to their oxidative counterparts implies faster depletion of the hair "reservoir." This is fully attested to by the results of the radioactive assays of the dyed hair. Over the 30-day wear period, the hair colored with permanent dyes lost approximately 10% of its original dye content, while losses of well over 60% were recorded for hair dyed with semipermanent dyes.

Table 5 contains one entry (HC Blue No. 2) that appears to be at odds with the remainder of the data. This dye is strikingly similar in its chemical structure to HC Blue No. 1, it remains unaltered during the dye-out, yet in its skin permeation characteristics it does not behave like a semipermanent. The octanol/water partition coefficient for HC Blue No. 2, at 1.6, is much lower than that of HC Blue No. 1, and the dye partitions poorly into the stratum corneum from water. A clue to the unusual behavior of this dye was furnished by the skin stripping experiments. Figures 3 and 4 are the dye content profiles of human stratum corneum stripped from the forearms dyed with components containing either HC Blue No. 1 or No. 2. The stripping was done immediately upon dyeing and again six hours later. The radioactivities of the dye lotions were almost identical, and so were the assays of stratum corneum strips harvested right after dyeing (29.7×10^{-4} μCi for HC Blue No. 1, and 30.3×10^{-4} μCi for HC Blue No. 2). Obviously, both dyes were diffusing at comparative rates while the dye lotions were on. The assays of the six-hour strips revealed, however, that while the activity of the skin dyed with HC Blue No. 1 decreased to 24.5×10^{-4} μCi (16% loss), that of tissue dyed with HC Blue No. 2 remained unchanged. The HC Blue No. 2 is thus obviously bound much more strongly to the stratum corneum than HC Blue No. 1, yet such a conclusion would hardly be arrived at on the basis of its partition coefficient.

There is little doubt that an increase in the tenacity of binding is inversely related to the dye mobility within the horny layer and thus adversely affects the diffusion of the dye into viable epidermis. With the diffusion process markedly slowed down, the natural process of desquamation attains an important role. The bulk of the dye reservoir is located in a few uppermost layers of the stratum corneum, and their loss by desquamation can lead to a rapid and precipitous drop in the quantity of the bioavailable dye, hence in the total extent of skin penetration. It appears from the results presented here that HC Blue No. 2 exemplifies such a behavior.

REFERENCES

1. Frenkel EP, Brody F. Percutaneous absorption and elimination of an aromatic hair dye. Arch Envir Health 1973; 27:401–404.
2. Howes D, Black JG. Percutaneous penetration of 2-nitro-*p*-phenylenediamine. Int J Cosmet Sci 1983; 5:215–226.

3. Hruby E. The absorption of p-toluenediamine by the skin of rats and dogs. Cosmet Toxicol 1977; 15:595–599.
4. Hruby E. Cutaneous resorption of 2,4-diaminoanisole in the rat and dog. SGAE Report AOO37, March 1979.
5. Nakao M, Takeda Y. Body distribution, excretion and metabolism of *p*-phenylenediamine in rats. J Pharm Soc Japan 1979; 99:1149–1153.
6. Tsomi V, Kalopissis G. Cutaneous penetration of some hair dyes in the hairless rat. Toxicol Eur Res 1982; 4:119–127.
7. Kiese M, Rauscher M. The absorption of *p*-toluenediamine through human skin in hair dyeing. Toxicol Appl Pharmacol 1968; 13:325–331.
8. Maibach HI, Leaffer MA, Skinner WA. Percutaneous penetration following use of hair dyes. Arch Dermatol 1975; 111:1444–1445.
9. Wester RC, Noonan P, Maibach HI. Recent advances in percutaneous absorption using the rhesus monkey model. J Soc Cosmet Chem 1979; 30:297–307.
10. Maibach HI, Wolfram LJ. Percutaneous penetration of hair dyes. J Soc Cosmet Chem 1981; 32:223–229.
11. Feldmann RJ, Maibach HI. Absorption of some organic compounds through the skin of man. J Invest Dermatol 1970; 54:399–404.
12. Bartek MJ, LaBudde JA. Animal models in dermatology: relevance to human dermatopharmacology and dermatotoxicology. In: Maibach HI, ed. London: Churchill-Livingstone, 1975:103–120.

47

In Vitro Percutaneous Absorption of Triethanolamine in Human Skin

Margaret E. K. Kraeling and Robert L. Bronaugh
Office of Cosmetics and Colors, Food and Drug Administration, Laurel, Maryland, U.S.A.

I. INTRODUCTION

Triethanolamine (TEA) is widely used as an ingredient in cosmetic products, household cleaning products, textiles, herbicides, and pharmaceutical ointments. The most widespread human exposure to TEA occurs in cosmetics where it is used in combination with fatty acids as an emulsifying agent and also as a thickening agent, fragrance ingredient, and pH adjuster. The TEA was reported to be used in cosmetic creams and lotions at a concentration between 1% and 2% (1). In 1983, the Cosmetic Ingredient Review (CIR) Expert Panel concluded that the use of TEA was safe in cosmetic rinse-off formulations, and should not exceed a concentration of 5% in leave-on products (2). Acute toxicity studies in animals demonstrated that prolonged or repeated exposure to TEA can cause severe skin irritation or impairment of vision (3). Chronic application of high dermal doses of TEA can lead to systemic toxicity (3). The National Toxicology Program (NTP) examined TEA carcinogenicity by the dermal route because of its widespread use and because of the potential for its conversion to *N*-nitrosodiethanolamine. The NTP concluded in 1999 that its preliminary findings of liver carcinogenicity in mice were invalid because of the presence of a *Helicobacter hepaticus* infection that complicated the interpretation of the study (4).

The in vivo skin penetration of TEA was reported in mice following topical and intravenous administration (5). The authors concluded that TEA was extensively absorbed through mouse skin. Since no human skin absorption data was available, the following studies were conducted using cosmetic formulations relevant to consumer exposures.

II. MATERIALS AND METHODS

A. Materials

[^{14}C]TEA (specific activity 19.1 mCi/mmol) was synthesized by Research Triangle Institute (Research Triangle, North Carolina, U.S.A.) with a radiochemical and

chemical purity of 99% as determined by thin-layer chromatography (TLC) analyzed on a Bioscan 200 Imaging Scanner and GC. Non-radiolabeled TEA and other reagents were obtained from Sigma Chemical Co. (St. Louis, Missouri, U.S.A.). [^{3}H]Water (specific activity, 55.5 mCi/mmol; 97% purity) was purchased from New England Nuclear Corp. (Boston, Massachusetts, U.S.A.). Solvents used were HPLC-grade and obtained from J.T. Baker Chemical Co. (Phillipsburg, New Jersey, U.S.A.). Hepes-buffered Hanks' balanced salt solution (HHBSS; dry powder packets of Hanks' balanced salt solution prepared by Gibco BRL, Life Technologies, Grand Island, New York, U.S.A.) was prepared fresh prior to each study.

B. Oil-in-Water Emulsion Formulations

Oil-in-water (O/W) emulsions were prepared containing TEA and stearic acid as the emulsifying agents. The formulations for both the 1% and 5% TEA products are listed in Table 1. The oil phase (Part 1) and aqueous phase (Part 2) were heated separately to 75°C and then mixed by adding Parts 2 to 1 while stirring Part 1 vigorously with an electric stirrer. Stirring was continued while the emulsion remained in the water bath at 75°C. The emulsion was transferred to an Omnimixer (Sorvall Inc., Newtown, Connecticut, U.S.A.) and stirred until the emulsion cooled to room temperature. Aliquots of the 1% and 5% TEA emulsions were each spiked with a radiotracer dose of 0.5 μCi [^{14}C]TEA (3.9 μg) and thoroughly mixed prior to the studies. The initial pH of the 1% and 5% TEA emulsions were 8.0 and 8.2, respectively. Further absorption studies were conducted with these emulsions after adjusting the pH of each emulsion to 7.0 with 3 M hydrochloric acid.

The stearate and salicylate salts of [^{14}C]TEA were prepared by mixing equal molar amounts of either stearic or salicylic acid with a radiotracer dose of 0.64 μCi [^{14}C]TEA (5 μg TEA) and incorporating the mixture into a stock O/W emulsion. A

Table 1 Compositions of O/W Emulsions Containing 1% TEA, pH 8.0, and 5% TEA, pH 8.2

Parts of emulsion	(1% TEA) grams per 100 grams emulsion	(5% TEA) grams per 100 grams emulsion
Part I		
Glyceryl monostearate (Lipo Chemicals, Paterson, NJ)	3	3
Isopropyl myristate (Lipo Chemicals, Paterson, NJ)	3	3
Stearic acid (Lipo Chemicals, Paterson, NJ)	5	10.5
Mineral oil (light) (Penreco, Karns City, PA)	5	5
Propyl paraben (Pfaltz & Bauer Inc., Stamford, CT)	0.15	0.15
Cetearyl alcohol (Henkel Corp., Hoboken, NJ)	1	1
Part 2		
Triethanolamine (Sigma Chemical Co., St. Louis, MO)	1	5
Propylene glycol (Aldrich Chemical Co., Milwaukee, WI)	5	5
Methyl paraben (Pfaltz & Bauer Inc., Stamford, CT)	0.15	0.15
Water	76.7	67.2

Table 2 Composition of O/W Emulsion for TEA Salts

Parts of emulsion	Grams per 100 grams emulsion
Part I	
Polyglyceryl-3 distearate (BASF Corp., Parsippany, NJ)	3
Mineral oil (light) (Penreco, Karns City, PA)	10
Cetearyl alcohol (Henkel Corp., Hoboken, NJ)	3.0
Part 2	
Propylene glycol (Aldrich Chemical Co., Milwaukee, WI)	5
Water	78.0
Part 3	
Methyl paraben (Pfaltz & Bauer Inc., Stamford, CT)	0.5
Propyl paraben (Pfaltz & Bauer Inc., Stamford, CT)	0.5

modified formula (Table 2) containing polyglyceryl-3 distearate as the emulsifying agent (instead of TEA and stearic acid) was used for the [^{14}C]TEA stearate and salicylate studies to prevent exchange of ^{14}C-labeled TEA with unlabeled TEA after incorporation of the salts into the formulation. The procedure for preparing the emulsion was the same as described earlier, except that after Part 2 was incorporated into Parts 1 and 3 (the preservatives listed in Table 2) was added to the mixture and stirred for an additional 20 minutes. Aliquots of the formulation were spiked with the [^{14}C]TEA stearate salt or the [^{14}C]TEA salicylate salt and mixed thoroughly. The final concentration of TEA in the formulations containing the TEA salts was 0.25%.

C. Percutaneous Absorption Experiments

In vitro percutaneous absorption studies were conducted based on methods previously described in detail for viable skin in flow-through diffusion cells (6,7). Human skin was freshly obtained from abdominoplasty procedures. Subcutaneous fat was removed, the skin was gently washed with a 10% soap solution, and then the skin was cut with a Padgett dermatome (Padgett Instruments, Dermatome Division, Kansas City, Missouri, U.S.A.) to a thickness of 200 to 300 μm. Skin discs were placed stratum corneum side up in flow-through diffusion cells (8). The skin surface temperature was maintained at 32°C by water circulated through the aluminum holding blocks for the diffusion cells. The viability of the skin was maintained by perfusing the diffusion cells with a receptor fluid of HHBSS for the duration of the 24 hour studies (9). Receptor fluid was collected at six-hours intervals for 24 hours. The integrity of the barrier of skin in each diffusion cell was verified by a 20-minute exposure to [^{3}H]water and subsequent determination of the percent absorption of the radiolabel (10).

The emulsion was applied to skin in the diffusion cells at a concentration of 3 mg/cm^2 (exposed skin = 0.64 cm^2). The emulsion contained approximately 0.5–0.64 μCi of test compound. At the end of each experiment the skin surface was washed three times with 0.3 mL of a 10% soap solution and rinsed three times with 0.3 mL of distilled water to remove unabsorbed material remaining on the surface of the skin. The skin was removed from the diffusion cell and tape-stripped with Scotch Magic™ cellophane tape (Commercial Office Supply Division, St. Paul, Mimesota, U.S.A.) 10 times to remove the stratum corneum. The viable epidermis and dermis were cut into thin strips with a razor and digested with tissue solubilizer.

D. Extended Studies

In order to determine the fate of the TEA that remained in the skin, penetration studies with TEA in the emulsion formulations were extended to 72 hours. The skin in the diffusion cells was washed at 24 hours according to the procedure described in section C and then removed from the diffusion cells at 72 hours. Receptor fluid sampling times were extended to 30, 36, 42, 48, 54, 60, 66, and 72 hours. Hydration of the skin prevented separation of the stratum corneum from the epidermis by tape-stripping at 72 hours. Therefore, the whole skin (stratum corneum, epidermis, and dermis) was removed from the diffusion cell and cut into thin strips with a razor and digested with tissue solubilizer.

III. ANALYSIS

The percutaneous penetration of TEA for the 24- and 72-hours studies was determined by measuring the absorbed radioactivity in the six-hours interval receptor fluid fractions and in the skin layers using liquid scintillation counting (Minaxibeta Tri-Carb® 4000 Series liquid scintillation counter, Packard Instrument Co., Downers Grove, Illinois, U.S.A.) using Ultima Gold™ (Packard Instrument Co., Meriden, Connecticut, U.S.A.) liquid scintillation cocktail.

IV. DATA

The results (mean $\pm$ SEM) of two to four replicates from two to three subjects were determined and expressed as the percent of the applied dose of TEA penetrated. In these studies, the term "absorption" was defined as the amount of test chemical representing in vivo systemic absorption and was determined as the amount of test chemical in the receptor fluid. The term "penetration" was defined as the total amount of test compound entering the skin and was determined as the sum of the test compound in the receptor fluid and skin.

Statistical analyses (SigmaStat Statistical Software, SPSS Inc., Chicago, Illinois, U.S.A.) of differences between pairs was conducted using the student's *t*-test ($p < 0.05$).

V. RESULTS

The TEA absorption from an O/W emulsion was examined at a commonly used TEA concentration of 1% (1) and at the CIR recommended upper limit (5%) for TEA in leave-on products (2). Only about 1% of the applied dose was found in the receptor fluid when either concentration of TEA was applied (Table 3). Lowest levels were usually found in the first six hours, frequently followed by similar absorption of TEA in collection fractions during the remainder of the study (Fig. 1). Substantial amounts of TEA were found in the stratum corneum and the viable epidermal and dermal layers at the end of the 24-hour studies. Most of the TEA was removed in the 24-hour wash and recoveries of radioactivity were approximately 100%.

The pH values for the O/W TEA emulsions were determined to be 8.0 at 1% TEA and 8.2 at 5% TEA. However, the pH values of commercial TEA-containing cosmetic lotions were observed to be approximately 7.0 (data not shown). The extent of ionization of TEA at different pH values was calculated from the

Table 3 The TEA Human Skin Penetration from an O/W Emulsion at pH 8

	Applied dose (%)	
Recovery site[a]	1% TEA[b]	5% TEA[c]
Receptor fluid	1.1 ± 0.3	1.2 ± 0.6
Stratum corneum	6.7 ± 3.1	5.5 ± 1.5
Epidermis and dermis	14.2 ± 3.0	9.6 ± 2.9
Total in skin	20.9 ± 0.3	15.4 ± 2.4
Total penetration	22.0 ± 0.4	16.5 ± 2.9
Wash	79.6 ± 3.9	82.1 ± 4.3
Total recovery	101.6 ± 3.8	98.6 ± 2.9

Values are the mean ± SEM of three to four replicates in each of three subjects. No significant difference was found between values obtained from 1% to 5% TEA emulsions (*t*-test, $p < 0.05$).
[a]Recovery after 24 hours.
[b]pH 8.0.
[c]pH 8.2.

Henderson–Hasselbach equation (Table 4). The ionization of TEA at pH 8.0 (38.7%) or pH 8.2 (28.5%) is substantially lower than at pH 7.0 (86.3%). Therefore, the percutaneous absorption of TEA would be expected to be lower at a lower pH.

Skin absorption studies were repeated at the 1% and 5% TEA concentrations with the pH of the O/W emulsions adjusted to pH 7.0 to more closely simulate the pH of commercial TEA-containing cosmetic products. Percutaneous absorption of TEA was substantially reduced at this lower pH (Table 5). The 24 hour receptor fluid levels were approximately 50% lower than the corresponding values obtained at pH

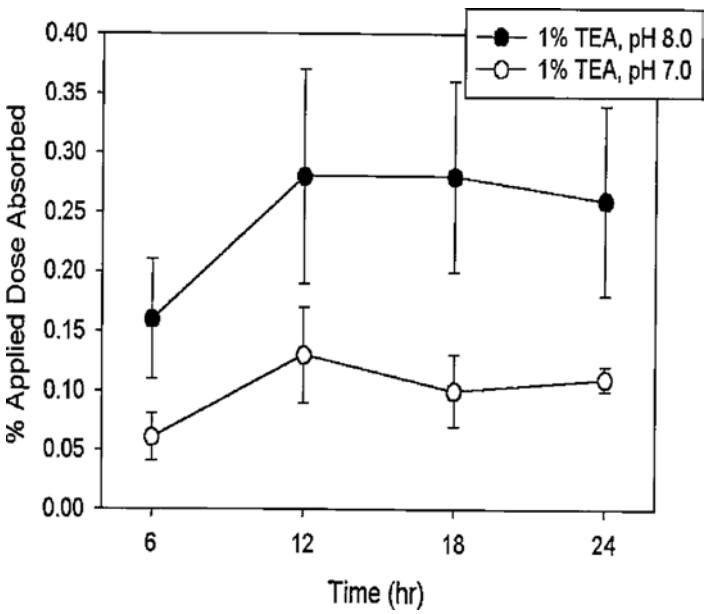


Figure 1 TEA absorption profiles from the receptor fluid samples in 24 hour absorption studies in flow-through diffusion cells. The values are the mean ± SEM of three to four replicates in each of three subjects (1% TEA, pH 8.0) or three to four replicates in each of two subjects (1% TEA, pH 7.0).

Table 4 Effect of pH on the Percent Ionization of TEA

pH	Ionization[a] (%)
8.2	28.5
8.0	38.7
7.0	86.3
6.8	90.9

[a]Values calculated using the Henderson–Hasselbach equation.

8.0 and 8.2. Skin levels of TEA were also reduced by two- to three-fold. The profile of absorption into the receptor fluid was similar with the emulsion at pH 7.0 or 8.0 (Fig. 1).

Substantial amounts of TEA remained in skin at the end of the 24-hour studies. Therefore, additional experiments were conducted for 72 hours (with a 24-hour skin wash) to determine if additional TEA diffused into the receptor fluid from skin. Only minimal additional amounts of TEA diffused into the receptor fluid during the additional 48 hours (Table 5). Histological examination of the skin at 72 hours indicated that viability was not maintained in these extended studies (data not shown) but the diffusional barrier should remain intact. In percutaneous absorption studies of diethanolamine (DEA) using freshly obtained human skin, the barrier properties of the skin remained intact after 72 hours based on tritiated water absorption data (11).

The TEA salicylate salt has been found to be readily absorbed through skin and possibly useful for local analgesia (12). All of the TEA in a TEA/stearic acid emulsion presumably exists as the TEA stearate salt since an excess of stearic acid was used. The ratio of stearic acid to TEA in the 1% TEA formulation was 5:1 and in the 5% TEA formulation it was about 2:1 (Table 1). The absorption of the salicylate and stearate salts of TEA was compared in a simplified emulsion (Table 2). Similar absorption results were seen with both ^{14}C-labeled TEA salts (Table 6). Receptor fluid levels were small and similar at the two pH levels tested. Almost 30% of the applied dose was found in skin at the end of the 24-hour studies

Table 5 Extended Study of TEA Human Skin Penetration from an O/W Emulsion at pH 7.0

	Applied dose (%)			
Recovery site	1% TEA[a] 24 hr	1% TEA[a] 72 hr	5% TEA 24 hr	5% TEA 72 hr
Receptor fluid	0.43 ± 0.11	0.68 ± 0.26	0.28 ± 0.01	0.60 ± 0.10
Stratum corneum	4.9 ± 1.3	—	2.4 ± 0.2	—
Epidermis and dermis	4.4 ± 0.1	—	3.1 ± 0.4	—
Total in skin	9.3 ± 1.2	8.9 ± 0.8	5.5 ± 0.3	6.3 ± 0.7
Total penetration	9.7 ± 1.1	9.6 ± 0.6	5.8 ± 0.3	6.9 ± 0.8
Wash	88.9 ± 1.4	87.9 ± 3.1	88.0 ± 0.02	89.8 ± 0.8
Total recovery	98.7 ± 2.5	97.5 ± 3.6	93.7 ± 0.3[b]	96.7 ± 0.02[b]

Values are the mean ± SEM of 3 to 4 replicates in each of two subjects.

[a]No significant difference was observed between values obtained at 24 and 72 hours with a 1% TEA emulsion (student's t-test, $p < 0.05$).

[b]Significant difference between values obtained at 24 and 72 hours with 5% TEA emulsion (student's t-test, $p < 0.05$).

Table 6 The TEA Salt Human Skin Penetration from an O/W Emulsion

Recovery site[a]	Applied dose (%)			
	TEA-stearate pH 7.0	TEA-stearate pH 8.2	TEA-salicylate pH 7.0	TEA-salicylate pH 8.2
Receptor fluid	0.46 ± 0.16	0.51 ± 0.15	0.58 ± 0.30	0.33 ± 0.03
Skin	29.1 ± 2.4	50.1 ± 2.3	28.2 ± 7.4	49.6 ± 2.1
Total penetration	29.5 ± 2.5	50.6 ± 2.2	28.8 ± 7.7	49.9 ± 2.1
Wash	66.5 ± 0.3	47.9 ± 0.9	66.3 ± 5.3	47.3 ± 2.6
Recovery	96.0 ± 2.9	98.5 ± 3.1	95.1 ± 2.4	97.2 ± 4.7

Values are the mean ± SEM of 2 to 4 replicates in each of two subjects.
[a]Recovery after 24 hours.

at pH 7.0. Greater penetration into the skin was observed at pH 8.2 compared to pH 7.0, as seen in the 1% and 5% TEA studies (Table 3).

VI. DISCUSSION

The TEA has previously been found to be rapidly absorbed through mouse or rat skin (in vivo) when applied in large doses (1000–2000 mg/kg) either directly to the skin or in an acetone vehicle (5). Over 50% of the applied dose was excreted in the urine during the 24- and 48-hour studies. Less absorption would be expected through human skin using formulations relevant to cosmetic exposure. Human skin is generally less permeable than rodent skin and the TEA exposure dose will be smaller from cosmetic products. Also, release of TEA from cosmetic product formulations and penetration into the skin will be dependent on the ionization of TEA.

The extent of TEA ionization in a cosmetic product depends on the pH of the formulation. Therefore, percutaneous penetration of TEA and the TEA stearate or salicylate salt may also depend on the formulation pH since the solubility properties of a compound are known to affect skin absorption. Ionization of TEA should reduce absorption by increasing the polarity of the molecule. The skin absorption obtained at pH 7.0 (86% ionization) resulted in lower absorption and skin penetration values (Table 5). The faster absorption and more extensive penetration of radiolabeled TEA at pH 8.0 to 8.2 (Table 3) may reflect primarily the penetration of un-ionized TEA since most of the TEA is un-ionized and incapable of salt formation.

Less than 1% of the applied dose of TEA at pH 7.0 was absorbed through the skin into the receptor fluid. Most of TEA penetrating the skin remained in the skin at the end of the 24-hour studies (Table 5). Additional extended studies (72 hours) were conducted to determine the fate of this material in the skin reservoir. The extended absorption studies showed only a minimal increase in receptor fluid levels (Table 5). These results suggest that the TEA contained in the skin reservoir was not available for systemic absorption. We have recently observed a similar large skin reservoir of DEA in human skin absorption studies (11).

The absorption of another salt of TEA (TEA salicylate) was studied in canine and human skin (12). Higher skin, fascia, and muscle levels of salicylic acid were achieved in dogs at or below the site of application of a TEA salicylate-containing

cream (10%) than when oral salicylic acid was administered. A comparison of the penetration of radiolabeled TEA stearate and TEA salicylate shows very similar penetration both at pH 7.0 and at pH 8.2 (Table 6). The data suggests that the penetration rate of the TEA molecule determines the penetration of its salts. Also, the high skin levels observed with TEA salts in these studies are consistent with the high local levels of salicylates previously observed in vivo (12).

In conclusion, the absorption of TEA through human skin is low under conditions that simulate exposure from cosmetic usage (1–5% TEA emulsion vehicle, pH 7.0). Systemic absorption of TEA was estimated to be less than 1% of the applied dose following a 24-hour exposure period.

REFERENCES

1. Furches BJ. Alkanolamines in creams and lotions. Cosmet Toiletries 1980; 95:63–66.
2. Cosmetic Ingredient Review. Final report on the safety assessment of triethanolamine, diethanolamine, and monoethanolamine. J Am Coll Toxicol 1983; 7:183–235.
3. Melnick RL, Tomaszewski KE. Triethanolamine. In: Buhler DR, Reed DJ, eds. Ethel Browning's Toxicity and Metabolism of Industrial Solvents. Vol. 2. 2nd ed. Nitrogen and Phosphorous Solvents, New York: Elsevier Science Publishers, 1990:441–450.
4. National Toxicology Program Technical Report, TR-449, Toxicology and Carcinogenesis Studies of Triethanolamine in F344 Rats and B6C3F1 Mice. NIH Pub. No. 00–3365, 1999:1–296.
5. Stott WT, Waechter JM Jr, Rick DL, Mendrala AL. Absorption, distribution, metabolism, and excretion of intravenously and dermally administered triethanolamine in mice. Fd Chem Toxicol 2000; 38:1043–1051.
6. Bronaugh RL, Hood HL, Kraeling MEK, Yourick JJ. Determination of percutaneous absorption by in vitro techniques. In: Bronaugh RL, Maibach HI, eds. Percutaneous Absorption: Drugs-Cosmetics-Mechanisms-Methodology. New York: Marcel Dekker, Inc., 1999:157–161.
7. Kraeling MEK, Bronaugh RL. In vitro percutaneous absorption of alpha hydroxy acids in human skin. J Soc Cosmet Chem 1997; 48:187–197.
8. Bronaugh RL, Stewart RF. Methods for in vitro percutaneous absorption studies IV: the flow-through diffusion cell. J Pharm Sci 1985; 74:64–67.
9. Collier SW, Sheikh NM, Sakr A, Lichtin JL, Stewart RF, Bronaugh RL. Maintenance of skin viability during in vitro percutaneous absorption/metabolism studies. Toxicol Appl Pharmacol 1989; 99:522–533.
10. Bronaugh RL, Stewart RF, Simon M. Methods for in vitro percutaneous absorption studies VII: use of excised human skin. J Pharm Sci 1986; 75:1094–1097.
11. Kraeling MEK, Yourick JJ, Bronaugh RL. In vitro human skin penetration of diethanolamine. Fd Chem Toxicol 2004; 42:1553–1561.
12. Rabinowitz JL, Feldman ES, Weinberger A, Schumacher HR. Comparative tissue absorption of oral ^{14}C-aspirin and topical triethanolamine ^{I4}C-salicylate in human and canine knee joints. J Clin Pharmacol 1982; 22:42–48.

48

Nail Penetration—Enhance Topical Delivery of Antifungal Drugs by Chemical Modification of the Human Nail

Xiao-Ying Hui, Ronald C. Wester, Sherry Barbadillo, and Howard I. Maibach
Department of Dermatology, School of Medicine, University of California, San Francisco, California, U.S.A.

I. INTRODUCTION

The human nail, equivalent to claws and hooves in other mammals, acts as a protective covering for the delicate tips of the fingers and toes against trauma, enhances the sensation of fine touch, and enables one to retrieve and manipulate objects. The nail is also used for scratching and grooming, as a cosmetic organ, and by some to communicate social status. The appearance of the nail plate is a thin, hard, yet slightly elastic, translucent, and convex structure (1).

Disorders of the nail resulting from a variety of conditions such as infections or physical–chemical damage can result in painful and debilitating states, and often change the appearance of the nail plate. Onychomycosis is the most common nail plate disorder (2). It thickens the nail, makes it white and opaque, and causes pain while wearing shoes. Onychomycosis is a fungal infection of the nail plate—usually caused by the species *Epidermophyton*, *Microsporum*, and *Trichophyton*—and affects 14% of the human population. Aging increases the incidence significantly, with the rate estimated to be 48% in persons 70 years of age (3).

To cure the infection, the patient is obliged to take oral systemic medication for an extended period, generally months, or undergo surgical nail removal (4). These treatments have adverse effects such as pain (surgery) and systemic side effects (oral treatment). Thus, topical therapy is the most desirable approach, but has met with limited success to date. Topical therapy is limited by the infection's deep-seated nature, and by the ineffective penetration of the deep nail plate by topically applied drugs (5,6).

How can topical drugs be delivered effectively into the nail? And, perhaps as importantly, how can the drug content in the human nail be assessed in order to validate nail drug delivery? Our challenge was to develop a system to assay drug content in the inner nail bed in which the infection resides. We developed a micrometer-controlled drilling instrument that removes and collects from the inner nail bed a

powder sample from which—by mass balance recovery—we can determine the amount of penetrated radiolabeled drug. With such an assay procedure, the effectiveness of topical nail drug delivery can be assessed (7,8). This paper reviews the results of studies undertaken with the drilling instrument.

II. REVIEW OF NAIL PHYSICAL AND CHEMICAL PROPERTIES THAT AFFECT TOPICAL PENETRATION

The human nail anatomy consists of nail plate, nail bed, and nail matrix. The nail plate consists of three layers: the dorsal and intermediate layers derived from the matrix, and the ventral layer from the nail bed (9,10). The upper (dorsal) layer, is only a few cell layers thick, and consists of hard keratin. It constitutes the main barrier to drug diffusion into and through the nail plate. The intermediate layer constitutes three quarters of the whole nail thickness, and consists of soft keratin. Below the intermediate layer is the ventral layer of soft keratin—a few cells thick—that connects to the underlying nail bed, in which many pathological changes occur. Thus, in the treatment of nail diseases, achieving an effective drug concentration in the ventral nail plate is of great importance. The nail bed consists of non-cornified soft tissue under the nail plate. It is highly vascularized. Beneath the nail bed is the nail matrix, which is a heavily vascularized thick layer of highly proliferative epithelial tissue that forms the nail plate.

The human nail is approximately 100 times thicker than the stratum corneum, and both are rich in keratin. However, they exhibit some physical and chemical differences (11,12). The nail possesses high sulfur content (cystine) in its hard keratin domain, whereas the stratum corneum does not. The total lipid content of the nail ranges from 0.1% to 1%, as opposed to approximately 10% for the stratum corneum. This suggests that the role of the lipid pathway in the nail plate is probably of much less importance than that in the stratum corneum. The human nail acts like a hydrophilic gel membrane, while the stratum corneum acts like a lipophilic partition membrane.

Under average conditions, the nail contains 7% to 12% water, in comparison to 25% in the stratum corneum. At 100% relative humidity, the maximal water content in the nail is approximately 25%, in sharp contrast to the stratum corneum that can increase its water content to 200% to 300%. The rate of chemical penetration into/through the human nail depends upon its water solubility (11), and its molecular size (12).

Topical therapy for onychomycosis has been largely ineffective, and this failure may be due to poor penetration of drugs into the nail plate (13). The nail's unique properties, particularly its thickness and relatively compact construction, make it a formidable barrier to the entry of topically applied agents (14). The concentration of an applied drug across the nail dropped about 1000-fold from the outer surface to the inner surface (15). As a result, the drug concentration presumably had not reached a therapeutically effective level in the inner ventral layer. The existing clinical evidence suggests that a key to successful treatment of onychomycosis by a topical antifungal product lies in effectively overcoming the nail barrier. Currently available topical treatments have limited effectiveness, possibly because they cannot sufficiently penetrate the nail plate to transport a therapeutically sufficient quantity of antifungal drug to the target sites (16) and eradicate the infection.

To achieve an effective chemical concentration into/through the human nail plate, penetration enhancers that tend to promote diffusion through the skin's horny

layer have been studied. However, these studies were conducted on a few limited nail penetration models that may not provide an intimate contact between the receptor compartment and the nail surface, and the nail plate can be easily hydrated beyond normal levels (6,11,12,16,17). Moreover, nail samples prepared with scalpel or sand paper are time consuming, and may be not accurate (10,18).

III. METHODOLOGY

We devised two experiments to evaluate drug penetration through the human nail, using radiolabeled drugs. In the first experiment we sampled the ventral/intermediate layers to determine the penetration of each of four drugs in a test formulation with a penetration enhancer and, for comparison purposes, in a saline control. In a second experiment, we used only one drug in one test formulation with a penetration enhancer and also in a saline control, but we measured the amount of that drug recovered at various depths from the nail surface to the support bed.

A. Formulations

Nails have a high content of disulfide bonds (10.6% vs. 1.2% for human skin) which make the nails both strong and impenetrable. To deliver a therapeutically sufficient quantity of an antifungal drug to fungally infected sites, such as nail plate, bed, and matrix, a suitable carrier is needed to enhance drug penetration through the nail barrier. In the case of the antifungal drugs urea, ketoconazole and salicylic acid, a lotion (Pennsaid lotion, Dimethaid Research Inc., Markham, Ontario, Canada. Pennsaid is a registered trademark of Dimethaid Research Inc.) containing the penetration enhancer dimethylsulfoxide (DMSO) had previously been shown to enhance skin penetration (7,8,19). To test these three drugs, we prepared three formulations with [^{14}C]-urea, [^{3}H]-ketoconazole, and [^{14}C]-salicylic acid at 0.002%, 0.1%, and 0.07%, respectively, and corresponding saline controls with each drug at the same concentrations.

For the antifungal drug econazole, we used a nail lacquer formulation, which is a popular choice for topical antifungal treatment. Nail lacquer contains a film-forming agent and a solvent, in addition to the antifungal drug and, possibly, a penetration enhancer. Once the lacquer is applied, it forms a thin, water-insoluble film containing the supersaturated antifungal drug. This provides a chemical gradient to drive drug flux as the drug is released. Thus, a lacquer formulation is suitable for topical treatment of nail diseases. We selected a commercial lacquer formulation, EcoNail (EcoNail is a trademark of MacroChem Corporation, Massachusetts, U.S.A.). The components of this lacquer formulation include econazole with penetration enhancer, 2-*n*-1,3-nonyl-dioxolane (18%) were assembled into a test formulation in the lab prior to use (8). The control is the same formulation minus 2-*n*-1,3-nonyl-dioxolane.

To summarize, we prepared four test formulations and four corresponding saline controls—one pair for each drug. We measured the nail penetration of urea, ketoconazole, and salicylic acid from a commercial lotion. We measured the nail penetration of econazole from a commercial nail lacquer.

B. Compounds

In each of these studies reported, a radiolabeled compound [^{3}H or ^{14}C] was used, and chemical content was determined by radioactivity scintillation counting.

C. Human Finger Nail Plates

Nail plates were collected from adult human cadavers and stored in a closed container at 0°C. Before each experiment, nail samples were gently washed with normal saline to remove any contamination, and then rehydrated by placing them for three hours on a cloth wetted with normal saline. Nail samples were randomly selected and allocated to test groups. Nail thickness was measured before testing in order to determine the drilling depth for each nail. Five nails were used for each formulation tested.

D. Dosing and Surface Washing Procedures

A 10-μL dosing aliquot of each of the test formulations was applied to the surface of a nail plate with a microsyringe twice daily approximately eight hours apart for 14 days. Starting on the second day, each morning before dosing, the surface of the nail was washed with cotton tips in a cycle as follows to simulate daily bathing: a dry tip, then a tip wetted with 50% Ivory liquid soap (Ivory is a registered trademark of Procter & Gamble, Cincinnati, Ohio, U.S.A.), then a tip wetted with distilled water, then another tip wetted with distilled water, then a final dry tip. The nails treated with lacquer also received an alcohol wash to remove residual lacquer that was insoluble in soap and water. The samples from each cycle from each nail were pooled and collected by breaking off the cotton tip into scintillation glass vials. An aliquot of 5.0 mL methanol was added to each vial to extract the test material. The radioactivity of each sample was measured in a liquid scintillation counter.

E. Nail Incubation

To keep the nail at physiological levels of temperature and humidity, we incubated it in a Teflon one-chamber diffusion cell (Permegear Inc., Hellertown, Pennsylvania, U.S.A.). The nail surface (top center) was open to air and the inner surface made contact with a small cotton ball acting as a nail supporting bed (Fig. 1). The cotton ball was wetted by normal saline. The incubation period started 24 hours prior to the first dose, and ended 24 hours after the final dose. A small cotton ball wetted with 0.1 mL normal saline was placed in the chamber beneath the nail plate to serve as a ''nail bed'' and provide moisture for the nail plate, and the degree of hydration was monitored and controlled during the experiment (7,8).

F. Nail Sampling Procedure

The objective was to determine drug concentration within the nail where the disease resides. Treatment dosing is applied to the surface of the nail. The drilling system samples the inner core of the nail without disturbing the nail surface. The two parts (surface and inner core) can be assayed separately. The surface contains only residual drug after washing. The drilled out core (from the ventral side) is thus a true drug measurement at the target site where the disease resides. Drug penetration into the nail was sampled by a unique micrometer-controlled nail sampling instrument that enabled finely controlled drilling into the nail and collection of the powder created by the drilling process. The nail sampling instrument (Fig. 2) has two parts, a nail sample stage and a drill. The nail sampling stage consists of a copper nail holder, three adjustments, and a nail powder capture. The three adjustments control vertical

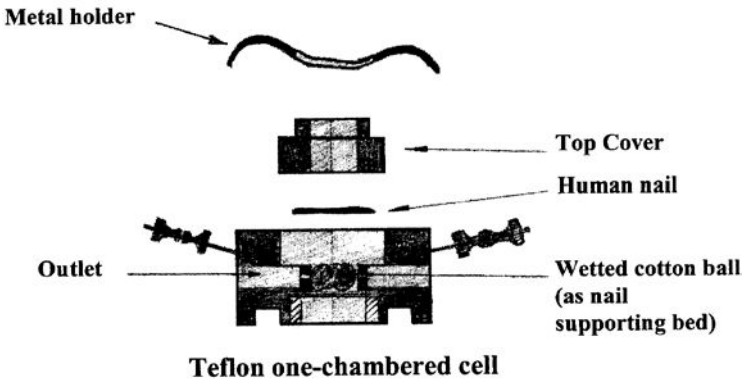


Figure 1 Nail support and incubation system. *Source:* From Ref. 7.

movement. The first coarse adjustment (on the top) is for changing the copper cell and taking powder samples from the capture. The other two adjustments (lower) are used in sampling. The second coarse adjustment allows movement of 25 mm while the fine adjustment provides movement of 0.20 mm. The nail powder capture is located between the copper cell and the cutter. The inner shape of the capture is an inverted funnel with the end connected to a vacuum pump. By placing a filter paper inside the funnel, nail powder samples can be captured on the filter paper during sampling. The nail is fastened in a cutting holder below the cutter and surrounded by a funnel containing a filter paper. The funnel is attached to a vacuum pump. During drilling, the vacuum draws the powder debris onto the filter paper so it can be collected and measured.

After completion of the dosing and incubation phase, the nail plate was transferred from the diffusion cell to a clean cutting holder for sampling. The nail plate was secured in position so that the ventral surface faced the cutter and the

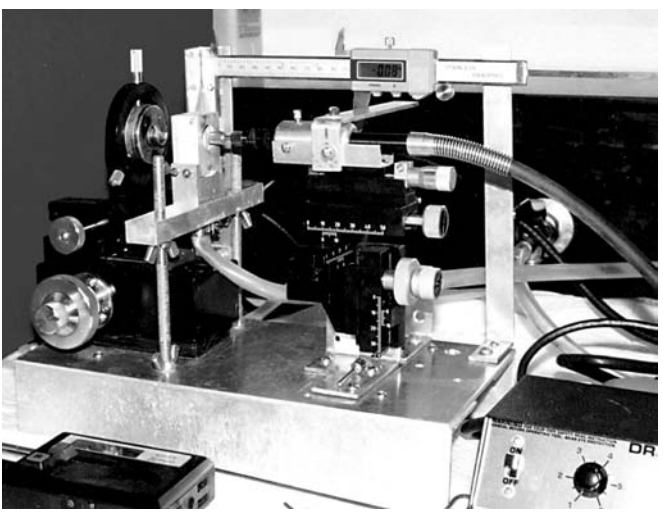


Figure 2 The sampling system.

dorsal-dosed surface faced the holder. The cutting holder was moved to bring the plate surface just barely in contact with the cutter tip. The drill was then turned on and a fine adjustment moved the stage toward the cutter tip, removing a powder sample from the nail. In this way, a hole approximately 0.3 to 0.4 mm in depth and 7.9 mm in diameter was drilled in each nail, enabling the harvest of powder sample from the center of each nail's ventral surface. We will refer to these samples as having been taken from the "ventral/intermediate nail plate."

After the nail had delivered its ventral/intermediate nail plate powder samples, it was removed from the sampling instrument. The nail outside the dosing area was cut away and discarded. The nail within the dosing area but outside the sampling area was trimmed away and saved; we refer to this as the "remainder nail plate." It surrounds the dorsal layer above the sampling area where the powder samples were taken; we refer to this as the "sampling area dorsal nail plate." The ventral/intermediate nail plate powdered samples, the sampling area dorsal nail plate and the remainder nail plate were individually collected into a glass scintillation vial and weighed. The nail samples were then dissolved by adding 5.0 mL of a Packard Soluene-350 (Packard Instrument Company, Meriden, Connecticut, U.S.A.). The total mass of nail collected was measured by the difference in weight of the plate before and after drilling (7,8).

IV. RESULTS

Table 1 shows that the averages of hydration of the wetted cotton balls 109 ± 6.2 AU that resembles the average hydration of human nail bed, 99.9 ± 8.9 AU measured from fresh human cadavers, where AU is arbitrary units, a digital expression of capacitance. During the experiment, the holding tank temperature was $25 \pm 2°C$ and relative humidity was $44 \pm 8\%$. Thus, there was no statistical difference between hydration conditions for nails treated with either the test formulation or the saline control. The advantage of this incubation device is that it is non-occlusive and hydration controlled, and approximate normal physical condition is reached.

The advantage of the micrometer-controlled drilling and nail powder removal system is the accuracy of the sampling process. The sampling instrument allowed well-controlled, accurate, and reproducible sampling of the inside of the nail. Table 2 shows that the average depth of nail sampling from the inner center surface was

Table 1 Hydration of Nail Plate and Nail Bed[a]

Measurement[b]			Hydration (AU)[c]	
Source	*N*	Time	Nail plate	Nail bed
Human cadavers	6	24-hr post mortem	7.6 ± 0.9	99.9 ± 8.9
Diffusion cells	8	Twice/day for 7 days	8.5 ± 2.4	109.9 ± 6.2

[a]During the experiment, the holding tank temperature was $25 \pm 2°C$ and relative humidity was $44 \pm 8\%$.
[b]Hydration of the nail plate and the supporting cotton bed was measured with a Corneometer CM 820 (Courage & Khazaka, Cologne, Germany).
[c]AU is arbitrary units, a digital expression of capacitance.

Table 2 Nail Core Sampled from the Ventral (Inner) Surface Center of the Human Nail Plate

		Nail core sampled from the ventral (inner) surface center of the nail plate[a]			
Test number	Whole nail thickness (mm)	Depth of core (mm)	Whole nail thickness (%)	Total core sample removed (mg)	Powder sample collected (mg)
Urea (control)	0.65 (0.09)	0.25 (0.03)	39.52 (8.05)	16.4 (4.3)	5.2 (0.8)
Urea (test)	0.71 (0.07)	0.27 (0.03)	37.97 (2.69)	17.6 (4.3)	6.4 (1.3)
Ketoconazole (control)	0.68 (0.05)	0.28 (0.03)	41.88 (1.16)	14.3 (6.7)	6.7 (2.6)
Ketoconazole (test)	0.73 (0.03)	0.28 (0.02)	38.62 (2.69)	14.1 (5.1)	4.3 (1.6)
Salicylic acid (control)	0.77 (0.07)	0.25 (0.08)	32.62 (9.38)	12.1 (2.4)	6.0 (0.5)
Salicylic acid (test)	0.60 (0.12)	0.21 (0.06)	35.03 (6.45)	23.4 (8.3)	4.7 (0.8)
Average	0.69 (0.09)	0.26 (0.05)	37.61 (6.20)	16.3 (6.2)	5.5 (1.6)

[a]Nail sample, approximately 0.24 mm in depth and 7.9 mm in diameter, was drilled from the center of the ventral surface of the nail. The amount of nail sample removed was measured by difference in weight and depth of the drilled area before and after sampling. Each number represents mean (SD) of five samples.
Source: From Ref. 7.

well controlled at 0.26 ± 0.05 mm, which was close to the expected depth of 0.24 mm. The weight of the nail samples collected was consistent for all experiments.

Table 3 summarizes the penetration of ketoconazole, urea, salicylic acid, and econazole into the human inner nail plate. Each test formulation contained a drug delivery enhancer (7,8) and was compared to a control formulation without any penetration enhancer. In each case the test formulation enhanced drug delivery ($p < 0.05$).

Table 4 summarizes the econazole mass balance recovery following the 14-day nail treatment. Overall recovery of applied dose was $90.8 \pm 16.4\%$ for the test formulation and $96.4 \pm 7.3\%$ for the saline control, indicating that essentially the entire dose was accounted for.

Table 4 also indicates what happens to chemicals put on the nail in this experiment. Approximately 72% was washed from the surface. The dose absorbed from the surface of the nail penetrated to the sampling area dorsal nail plate (11.4%), the ventral/intermediate nail plate (1.4%) and the supporting bed (0.7%), which is the cotton ball upon which the nail rested. Notice that econazole recovery in the test formulation is greater for both the ventral/intermediate nail plate and the supporting bed, which is an effect of the drug delivery enhancer. Now notice that at the sampling area dorsal nail plate, there is more econazole from the saline control because the dose remained on the nail surface.

Table 3 Radiolabeled Drug Penetration into Human Nail from a Test Formulation Containing a Penetration Enhancer Vs. a Control Without a Penetration Enhancer

		Radioactivity content in ventral/intermediate center layer of the nail plate[a]			
Drugs	Penetration enhancer	Unit[b]	Test formulation	Control formulation	*p* value (*t*-test)
Ketoconazole	Dimethylsulfoxide	μg Eq/g	53.9 (10.6)	34.0 (15.9)	0.048
Urea	Dimethylsulfoxide	μg Eq/g	0.35 (0.15)	0.2 (0.09)	0.039
Salicylic acid	Dimethylsulfoxide	μg Eq/g	10.2 (0.6)	70. (1.1)	0.008
Econazole	2-*n*-nonyl-1,3-dioxolane	μg Eq/mg	11.2 (2.6)	1.8 (0.3)	0.008

[a]The data represent the mean (SD) of five samples per formulation group. The nail sample drilled as powder from ventral/intermediate layer of human nail plate.
[b]μg Eq/g or μg Eq/mg = microgram equivalents drug per gram (or mg) of nail sample. Because radioactivity is used, the drug mass is referred to as "equivalents" because radioactivity was measured, not the drug itself.
Source: From Refs. 7 and 8.

V. DISCUSSION

Topical therapy for onychomycosis is not yet maximally effective, and this failure may be due to poor penetration of drugs into the nail plate. The nail's unique properties, particularly its thickness and relatively compact construction, make it a formidable barrier to the entry of topically applied agents. The concentration of an applied drug across the nail drops about 1000-fold from the outer surface

Table 4 Mass Balance Recovery of Econazole Following 14-Day Human Nail Treatment with a Test Formulation Containing a Penetration Enhancer and a Control Without a Penetration Enhancer[a]

	Carbon-14 recovery as percent of dose	
Sampling area	Test formulation	Control formulation
Dorsal/intermediate nail plate	11.38 (3.59)	20.11 (2.95)
Ventral/intermediate nail plate (powdered samples)	1.35 (1.10)	0.22 (2.95)
Remainder nail plate	5.63 (3.86)	3.22 (2.32)
Supporting bed (cotton ball)	0.72 (0.33)	0.00 (0.00)
Surface washes	71.75 (12.48)	72.81 (5.12)
Total	90.83 (16.42)	96.36 (7.31)

[a]The data represent the mean (SD) of each group ($n = 5$). The test formulation group contains 18% 2-*n*-nonyl-1,3-dioxolane and the control formulation contains no 2-*n*-nonyl-1,3-dioxolane.
Source: From Ref. 8.

Table 5 Comparison of Econazole Concentration and Relative Antifungal Efficacy with a Test Formulation Containing a Penetration Enhancer or a Control Without a Penetration Enhancer[a]

Parameter	Test formulation	Control formulation	*p* value (*t*-test)
Econazole in the deeper layer ($\mu g/cm^3$)[b]	14,830 (341)	2,371 (426)	0.0079
Efficacy coefficient *E* (MIC = 1 μg/mL)	14,830 (341)	2,371 (426)	0.0079
Efficacy coefficient *E* (MIC = 100 μg/mL)	148 (3.4)	23.7 (4.3)	0.0079
Flux of the deeper layer ($\mu g/cm^2/hr$)[c]	1.58 (0.32)	0.21 (0.04)	0.0001
Efficacy coefficient *E* (MIC = 1 μg/mL)	1.58 (0.32)	0.21 (0.04)	0.0001

[a]The data represent the mean (SD) of each group ($n = 5$). The test formulation group contains 18% 2-*n*-nonyl-1,3-dioxolane and the control formulation contains no 2-*n*-nonyl-1,3-dioxolane.
[b]The deeper layer is the center of the ventral/intermediate layer of the nail plate. The data represent the amount of drug in the sample after a 14-day dosing period.
[c]The deeper layer is the center of the ventral/intermediate layer of the nail plate. The flux ($\mu g/cm^2/hr$) was computed from the average of the cumulative amount of econazole permeated into the deeper layer of the nail (dorsal/intermediate layer and cotton ball supporting bed).
Source: From Ref. 8.

to the inner surface. As a result, the drug concentration presumably does not reach a therapeutically effective level in the ventral/intermediate layers.

Minimum inhibitory concentration (MIC) is a laboratory index in the determination of antifungal potency. For econazole, the range of MIC for *Dermatophytes* species is 0.1 to 1.0 μg/mL and for yeast species it is 1.0 to 100 μg/mL (20). After 14 days of exposure, the econazole content measured in the test group was 11.15 ± 2.56 μg/mg for the ventral/intermediate layers. This content multiplied by the density of the nail sample (1.332 mg/cm^3, measured under current experimental conditions) yields $14{,}830 \pm 340$ $\mu g/cm^3$ of econazole, almost 15,000 times the MIC for most *Dermatophytes* species, and 150 times that for most yeast species (Table 5).

Martin and Lippold (11) introduced an efficacy coefficient *E* to better estimate and compare the relative efficacy of antifungal agents. The efficacy coefficient *E* is the ratio of the flux of an antimycotic drug through the nail plate to the MIC. The flux of econazole into the deep layer of human nail is 1.58 ± 0.32 $\mu g/cm^2$/hour in test group, compared to only 0.21 ± 0.04 $\mu g/cm^2$/hour in the control group. If the MIC value is 1.0 μg/mL, the efficacy coefficient *E* calculated from the test group is 1.58, which is sixfold greater than that in the control group. The results suggest that the enhanced level of econazole in the ventral/intermediate layers and supporting bed dramatically exceeds the MIC of econazole for most common onychomycosis organisms.

The intermediate nail plate has remained a barrier against drugs, as exhibited by the failure of topical nail therapy for nail infections. The intermediate nail plate can now be scientifically studied, and with proper formulation one can deliver a variety of chemicals, be they drugs or nail modifiers (cosmetics). The nail is now ready

for serious attention and treatment just as hair and skin have been in the past. The nail barrier can be breached.

These findings presumably relate to delivery of cosmetic agents for the management of nail abnormalities, such as nails that are peeling or fragile. The research and development on these agents will be simplified when the rules describing the relationship of physical chemistry to flux are developed for the nail, as they have been in part for the skin.

REFERENCES

1. Murdan S. Drug delivery to the nail following topical application. Int J Pharm 2002; 236(1–2):1–26.
2. Dorlands Illustrated Medical Dictionary, 27th ed. Philadelphia: WB Saunders Company, 1988.
3. Elewski B, Charif MA. Prevalence of onychomycosis in patients attending a dermatology clinic in northeastern Ohio for other conditions. Arch Dermatol 1997; 133:1172–1173.
4. Niewerth M, Korting HC. Management of onychomycosis. Drugs 1999; 58(2):283–296.
5. Meisel CW. The treatment of onychomycosis. In: Nolting S, Korting HC, eds. Onychmycoses—Local Antimycotic Treatment. New York: Springer-Verlag, 1990:12–28.
6. Walters KA, Flynn GL. Permeability characteristics of the human nail plate. Int J Cosmet Sci 1983; 5:231–246.
7. Hui X, Shainhouse JZ, Tanojo H, Anigbogu A, Markus G, Maibach HI, Wester RC. Enhanced human nail drug delivery: nail inner drug content assayed by new unique method. J Pharm Sci 2002; 91:189–195.
8. Hui X, Barbadillo S, Lee C, Maibach HI, Wester RC. Enhanced econazole penetration into human nail by 2-N-nonyl-1,3-dioxane. J Pharm Sci 2003; 92:142–148.
9. Runne U, Orfanos CE. The human nail—structure, growth and pathological changes. Curr Probl Dermatol 1981; 9:102–149.
10. Kobayashi Y, Miyamoto M, Sugibayashi K, Morimoto Y. Drug permeation through the three layers of the human nail plate. J Pharm Pharmacol 1999; 51:271–278.
11. Martin D, Lippold BC. In vitro permeability of the human nail and a keratin membrane from bovine hooves: influence of the partition coefficient octanol/water and the water solubility of drugs on their permeability and maximum flux. J Pharm Pharmacol 1997; 49:30–34.
12. Martin D, Lippold BC. In vitro permeability of the human nail and a keratin membrane from bovine hooves: prediction of the penetration rate of antimycotics through the nail plate and their efficacy. J Pharm Pharmacol 1997; 49:866–872.
13. Meisel CW. The treatment of onychomycosis. In: Nolting S, Korting HC, eds. Onychmycoses—Local Antimycotic Treatment. New York: Springer-Verlag, 1990:12–28.
14. Walters KA, Flynn GL. Permeability characteristics of the human nail plate. Int J Cosmet Sci 1983; 5:231–246.
15. Stüttgen G, Bauer E. Bioavailability, skin- and nail-penetration of topically applied antimycotics. Mykosen 1982; 25(2):74–80.
16. Walters KA, Flynn GL, Marvel JR. Physicochemical characterization of the human nail: solvent effects on the permeation of homologous alcohols. J Pharm Pharmacol 1985; 37:771–775.
17. Walters KA, Flynn GL, Marvel JR. Physiocochemical characterization of the human nail: I. Pressure sealed apparatus for measuring nail plate permeabilities. J Invest Dermatol 1981; 76:76–79.
18. Polak A. Kinetic of amorolfine in human nails. Mycoses 1993; 36:101–103.

19. Hui X, Hewitt HG, Poblete N, Maibach HI, Shainhouse JZ, Wester RC. In vivo bioactivity and metabolism of topical diclofenac lotion in human volunteers. Pharm Res 1998; 15:1589–1595.
20. Thienpont D, Cutsem JV, Nueten JMV, Niemegeers CJE, Marsboom R. Biological and toxicological properties of econazole, a broad-spectrum antimycotic. Arzneimittelforschung 1975; 25:224–231.

49

Topical Dermatological Vehicles: A Holistic Approach

Eric W. Smith
College of Pharmacy, University of South Carolina, Columbia, South Carolina, U.S.A.

Christian Surber
Institut für Spital-Pharmazie, Universitätskliniken, Kantonsspital, Basel, Switzerland

Howard I. Maibach
Department of Dermatology, School of Medicine, University of California, San Francisco, California, U.S.A.

I. INTRODUCTION

The broad spectrum of topical preparations in use today vary in their physicochemical nature from powders through semisolids to liquids. While early topical formulations were often crude mixtures of chemicals, the optimized drug delivery systems common today achieve a balance between the physicochemical requisites for stability of active and inactive constituents, preservation against microbial spoilage, and, most importantly, presentation of the drug to the skin in a system that will allow appropriate release of the active to the stratum corneum. This is in addition to ensuring the elegance and user acceptability of the formulation. It is clear, therefore, that topical vehicle formulation is not a facile process, and as many of the desirable properties of the formulation as possible must be fulfilled in this process. Obviously, the synthetic and semisynthetic formulation constituents that are available today make this task somewhat easier than the formulation techniques of yesterday that utilized predominantly natural products.

In dermatology, the drug is rarely applied to the skin in the form of a pure chemical but, instead, is normally incorporated into a suitable carrier system—the vehicle. The term *vehicle* in this context is relatively new and was developed only when it became possible to designate a specific (therapeutic) effect to a chemical substance. Thereby it became possible to distinguish between ''active'' and ''inactive'' ingredients in a formulation. In crude terms, the vehicle or base may be regarded as the sum of the ingredients in which the drug is presented to the skin. In practical terms, the vehicle is not only the sum of the formulation ingredients but also (in most cases) represents the existence of a physical, structured matrix comprised of the vehicle constituents. This structural matrix can be monophasic (e.g., a simple lipid),

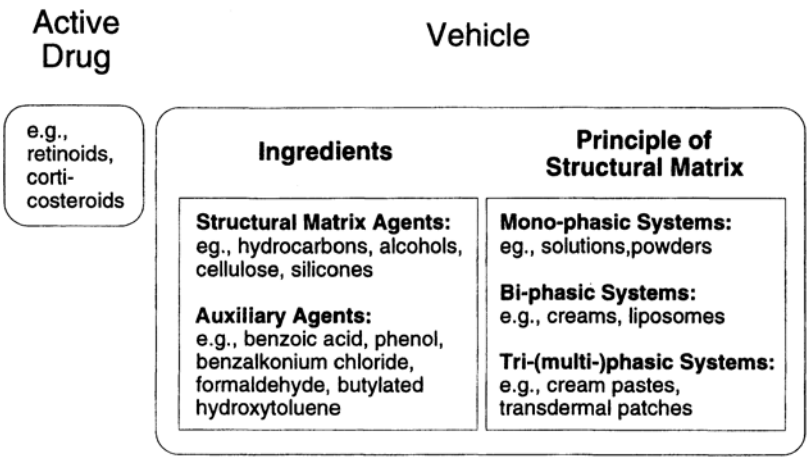

Active Drug
Vehicle
e.g., retinoids, corti-costeroids
Ingredients
Principle of Structural Matrix
Structural Matrix Agents: eg., hydrocarbons, alcohols, cellulose, silicones
Auxiliary Agents: e.g., benzoic acid, phenol, benzalkonium chloride, formaldehyde, butylated hydroxytoluene
Mono-phasic Systems: eg., solutions,powders
Bi-phasic Systems: e.g., creams, liposomes
Tri-(multi-)phasic Systems: e.g., cream pastes, transdermal patches

Figure 1 Principle of topical preparations.

biphasic (e.g., a cream), or tri- or multiphasic systems (e.g., multiple emulsions, pastes, and patch systems) into which a drug is incorporated (Fig. 1).

II. CLASSIFICATION OF TOPICAL VEHICLES

The simplest classification of topical vehicles consists of an initial division of the preparation into liquid, semisolid, or solid classes (Table 1). It is obvious that this is a simplification of the diversity of external formulations and does not account for many of the newer formulations (e.g., liposomes and microcapsules). Although a comprehensive classification has been proposed for isolated dermatological vehicles (1), clinical textbooks tend to combine the pharmaceutical nomenclature, the character of the structural matrix, and the formulation performance when attempting to classify the topical vehicles available for therapy.

Modern vehicles are frequently tailor-made and developed as carefully as the drug that they are intended to contain. Formulator research and development are extensive in terms of the stability, compatibility, and patient or consumer acceptability of the vehicle. More recently, it has become obvious that the type of vehicle or the nature of the excipients can markedly affect (or negate) the percutaneous absorption of a drug. This realization has added another, essential, dimension to the formulation development process. Several studies have demonstrated how markedly different drug delivery potentials are achieved by incorporating the same concentration of the same drug into topical vehicles of different physicochemical composition (2) or by incorporation into identical vehicles where the microstructure of the vehicle matrix is altered by micronization (3). Typically for most topically delivered drugs, the greatest delivery rates of the actives are achieved from alcoholic solutions, which have marked drug dissolution and skin barrier modification potential, and from lipid ointments, which tend to be occlusive in nature. Recent scientific research in this field has demonstrated that the delivery vehicle may have a marked effect on the barrier potential of the stratum corneum. Thus, modern pharmaceutical (and cosmetic) formulation development is based upon the stability and compatibility of excipients and active drug(s), cosmetic or aesthetic acceptability of the vehicle, and bioavailability of the drug(s).

Table 1 Simple Classification System for Topical Dermatological Vehicles

System	Monophasic	Diphasic	Multiphasic
Liquid	Nonpolar solution, often designated as oil	Emulsion (o/w, w/o), often designated as milk, lotion, shake, etc.	Emulsion (o/w/o, w/o/w), often designated as milk, lotion, shake, etc.
	Polar solution, often designated as paint, lotion, etc.	Suspension, often designated as paint, shake, etc.	Suspension, often designated as paint, shake, etc.
Semisolid	Anhydrous, nonpolar ointment, and polar ointment	Emulsion (o/w, w/o), often designated as washable (o/w), nonwashable (w/o), or amphiphilic (o/w, w/o) creams	Emulsion (o/w, w/o), with powder, often designated as cream pastes
	Hydrous, nonpolar gel, and polar gel	Suspension, often designated as paste	
Solid	Powder	Transdermal patch	Transdermal patch

III. THE IDEAL VEHICLE

The ''ideal'' vehicle should fulfill many different functions, all of which need to be addressed in the development process. It should be easy to apply and remove, and be nontoxic, nonirritant, nonallergenic, chemically stable, homogeneous, bacteriostatic, cosmetically acceptable, pharmacologically inert, and should readily release the drug to the stratum corneum (Table 2). In topical dermatological treatment, formulators, producers, legislators, prescribers, and consumers perceive both the performance of the structural matrix and the performance of the ingredients of the topical preparations to be important. These requirements have led to extensive discussions on the ''vehicle effect,'' where different interest groups have different conceptions of the delivery vehicle and different expectations of its role. The effect of the vehicle on the topical drug availability is probably much greater in topical drug delivery than in any other route of drug administration. It is common knowledge that potent molecules may be made clinically ineffective or that enhanced efficacy may be generated with weaker molecules, depending upon the vehicle used (4,5). Despite the wishes of many formulators, there is no universal vehicle; each drug, at each concentration, requires a unique vehicle for optimized therapy.

In attempting to design a topical delivery vehicle, one should bear in mind that this is a situation of constant dynamic equilibrium; the constituents of the formulation will interact with one another and will interact with the skin once the product has been applied. Katz and Poulsen (6) have listed the interactions that may occur between the vehicle, drug, and skin as:

- vehicle–drug interactions,
- vehicle–skin interactions,
- drug–skin interactions,
- vehicle–drug–skin interactions.

Vehicle–drug interactions include all physical and chemical reactions that may take place between the drug molecules and the combined molecules of all the other

Table 2 Selection Criteria for Topical Vehicles

Pharmaceutical, technological criteria for pharmaceutical semisolid
Stability of active drugs
Stability of ingredients
Rheological properties—consistency, extrudability
Loss of water and other volatile components
Phase changes—homogeneity/phase separation, bleeding
Particle size and particle size distribution of dispersed phase
Apparent pH
Microbial contamination/sterility (in unopened containers and under conditions of use)
Enhanced or controlled drug release from the vehicle
Cosmetic and usage criteria for topical vehicles
Visual appearance of product
Odor and color
Sampling and dispensing characteristics: ease of removal from container
Application properties, texture (stiffness, grittiness, greasiness, and adhesiveness)
Residual impression after application, permanency on the skin
Biopharmaceutical criteria for topical vehicles
Enhanced drug delivery and drug retention in the skin
Controlled drug delivery and drug retention in the skin
Targeted drug delivery and drug retention in the skin

formulation constituents. Solubility is of primary importance here, in that this parameter will define the physical state of the drug molecule in the vehicle (solution, suspension, ionized, or nonionized) and will define the magnitude of the concentration gradient for passive diffusion.

Vehicle–skin interactions include the broad spectrum of physical and chemical events that may take place once the vehicle comes into contact with the stratum corneum. The formulation constituents all have potential to partition from the applied vehicle and enter the stratum corneum. If one considers the holistic, classical approach to dermatological therapy, then the partitioning of the ancillary, formulation substances into the skin have an important function in fulfilling the emollient, tactile, and rubifacient functions of the formulation. Modern topical delivery theory may suggest that the partitioning of the ancillary formulation chemicals is unimportant in the therapeutic goal unless such partitioning interferes with the delivery or diffusion of the active drugs. Recent technology has made use of this phenomenon in the form of penetration enhancer chemicals that are specifically designed to penetrate the stratum corneum from the applied vehicle and facilitate transport of the active drug principal through the barrier layer. Generally, penetration enhancers are vehicle components that interact with the stratum corneum to bring about changes in drug solubility or drug diffusion or both (7,8).

Drug–skin interactions include cutaneous metabolism and binding of the drug by the skin strata. Although it was classically believed that the stratum corneum was a ''dead'' layer of cells, we are now only beginning to understand the complex metabolic activity that is possible in this tissue and the potential for using this phenomenon in terms of prodrug diffusion through the skin. Similarly, it has been long established that a depot of topically delivered drug is rapidly established in the stratum corneum and that the active agent may be delivered from this binding site for days or weeks after initial application of the vehicle to the skin (9).

Formulations in which significant vehicle–drug–skin interactions occur are probably the most common. Many pharmaceutical solvents, propylene glycol, for example, are known to have modest effects on reducing the skin barrier function (thereby altering the diffusivity of the drug through the skin) as well as influencing the solubility of the drug in the delivery vehicle (increasing the concentration gradient across the barrier layer) and changing the partitioning of the drug from the vehicle into the stratum corneum.

IV. THE CHOICE OF VEHICLE

Depending on environmental conditions, ethnic origin (10,11), gender, age, localization, and state of disease, different skin conditions are treated with respect to oiliness or humidity. The choice of a vehicle in a particular disease or in a specific patient often follows recommendations that are either based on a classification of topical preparations (12–15) or follow a few simple assessment parameters. It is a basic dermatological concept that the more acute the dermatosis, the blander the treatment should be. The principle of "wet-on-wet" and the use of occlusive ointments for dry or chronic dermatoses has become commonplace. As the condition improves, a "wet" dermatosis may subsequently be treated with either a drying paste or an oil-in-water cream, and a "dry" dermatosis may have a hydrous ointment, water-in-oil cream, or even an occlusive ointment applied (12,16). The capability of vehicles to alter the condition of the skin surface can be attributed to their influence on the lipid and water content of the skin or lipid composition (17–19). Vehicles with hydrophilic properties are suitable for oily and normal skin conditions, whereas vehicles with lipophilic properties are more suitable for dry skin conditions because of their emollient action.

There are several anatomical issues that need to be considered in the choice of an appropriate vehicle. Chemicals applied to different regions of the body permeate to varying extents. Most importantly from a clinical perspective, the reactivity of the same dermatosis to the same dose of formulation at different anatomical locations may vary markedly. Table 3 gives an overview of current prescribing practices. Similarly, topical preparations are tested in the pharmaceutical and cosmetic industries with respect to stability under various carefully defined climatic conditions (20). Practical assessments of the stability problems of vehicles or vehicle constituents encountered during use are rarely available. Preparations formulated for certain geographical climates are often inappropriate in more extreme climatic conditions. Hence, the final conditions of usage of the topical preparation should be kept in mind when selecting an appropriate vehicle.

Cosmetic or aesthetic criteria such as visual appearance, odor, application properties, or permanency of vehicle and drug on the skin are also important factors that influence patient acceptance of a topical preparation and compliance with a prescribed regimen of therapy. Commercially, these aspects are also important in maintaining customer loyalty. Ointments are often associated with adhesiveness by users and prescribers and are usually used for more severe diseases; creams or lotions are easier to apply and have a cooling effect and are usually preferred by patients.

Table 3 Localization, Skin Status, and Vehicle Used in Different Locations

Localization	Status	Dosage forms used
Hairy skin	Dry	Solutions, w/o cream
	Oily	Solution, gel
Face	Dry	w/o cream
	Oily	Solution, o/w cream
Ear	Oily	o/w cream
Body/extremities	Dry	Ointment, w/o cream
	Oily	o/w cream
Intertrigenous area	Humid	Drying pastes, o/w cream
Hand/feet	Dry	During the day: o/w or w/o cream
	Oily	During the night: ointment, w/o cream
Nail	Dry	Solutions, lacquer

V. CONCLUSION

As outlined here, many factors influence the development, the choice, the performance, and hence the clinical effectiveness of the vehicle. These factors are often viewed from different perspectives by patients, chemists, formulators, and clinicians. Due to this complexity, no uniform and comprehensive recommendations and guidelines are available for the development and the use of semisolid formulations, and it seems unlikely that this can be achieved in the future. Dermatological vehicle treatment may therefore remain an "art" gleaned by personal experience, rather than a defined, textbook science.

REFERENCES

1. Juch RD, Rufli T, Surber C. Pastes: what do they contain? How do they work? Dermatology 1994; 189:373–377.
2. Wall DS, Abel SR. Therapeutic-interchange algorithm for multiple drug classes. Am J Health-Syst Pharm 1996; 53:1295–1296.
3. Wilhelmsen L. Ethics of clinical trials—The use of placebo. Eur J Clin Phar macol 1979; 16:295–297.
4. Hadgraft J. Formulation of anti-inflammatory agents. In: Hensby C, Lowe NJ, eds. Nonsteroidal Anti-Inflammatory Drugs. New York: S. Karger, 1989:21–43.
5. Polano MK, Bonsel J, Van der Meer BJ. The relation between the effect of topical irritants and the ointment bases in which they are applied to the skin. Dermatologica 1950; 101:69–80.
6. Katz M, Poulsen BJ. Absorption of drugs through skin. In: Brodie BB, Gillete JR, eds. Handbook of Experimental Pharmacology. Vol. 28. New York: Springer, 1971:103–174.
7. Barry BW. Mode of action of penetration enhancers in humans skin. J Control Release 1987; 6:85–97.
8. Walters KA, Hadgraft J. Pharmaceutical Skin Penetration Enhancement. New York: Marcel Dekker, 1993.
9. Woodford R, Haigh JM, Barry BW. Possible dosage regimens for topical steroids, assessed by vasoconstrictor assays using multiple applications. Dermatologica 1983; 166:136–140.
10. Schlossmann ML. Formulating ethnic makeup products. J Cosmet Toilet 1995; 110: 59–63.

11. Sugino K, Imokawa G, Maibach HI. Ethic difference of stratum corneum lipid in relation to stratum corneum function. J Invest Dermatol 1993; 100:597–601.
12. Griffiths WAD, Wilkinson JD. Topical therapy. In: Rook A, Wilkinson DS, Ebling FJG, Champion RH, Burton JL, Ebling FJG, eds. Textbook of Dermatology. London: Blackwell Scientific Publications, 1992:3037–3084.
13. Thoma K. Dermatika. München: Werbe- und Vertriebsgesellschaft Deutscher Apotheker, 1983.
14. Hundeiker M. Grundlagen der Therapie mit äusserlichen Arzneimittelzuber- eitungen. Zentrlbl Hautkr 1982; 148:683–697.
15. Katz M. Design of topical drug products: pharmaceutics. In: Ariëns EJ, ed. Drug Design. New York: Academic Press, 1973:93–148.
16. Barry BW. Dermatologic Formulations. New York: Marcel Dekker, 1983.
17. Gabard B. Testing the efficacy of moisturizers. In: Elsner P, Berardesca E, Maibach HI, eds. Bioengineering of the Skin: Water and Stratum Corneum. Boca Raton, FL: CRC Press, 1994:147–170.
18. Lodén M. The increase in skin hydration after application of emolients with different amounts of lipids. Acta Derm Venereol (Stockh) 1992; 72:327–330.
19. Choudhury TH, Marty JP, Orecchini AM, Seiller M, Wepierre J. Factors in the occlusivity of aqueous emulsions. Influence of humectants. J Soc Cosmet Chem 1985; 36: 255–269.
20. Grimm W. International harmonization of stability tests for pharmaceuticals. The ICH tripartite guideline for stability testing of new substances and products. Eur J Pharm Biopharm 1995; 41(3):194–196.

50

Measurements of Drug Penetration Using Non-invasive Methods: Fourier Transform Infrared Spectroscopy

S. Wartewig
Institute of Applied Dermatopharmacy, Martin-Luther-University Halle-Wittenberg, Halle (Saale), Germany

Reinhard H. H. Neubert
Department of Pharmacy, Institute of Pharmaceutics and Biopharmacy, Martin-Luther-University Halle-Wittenberg, Halle (Saale), Germany

I. INTRODUCTION

Noninvasive one-line monitoring of topical drug delivery is an important topic in dermatopharmaceutical research. It has been proved that infrared (IR) spectroscopy is a versatile tool in such studies of drug diffusion in artificial membranes and in biological systems such as stratum corneum. The IR spectroscopy exhibits the big advantage of being non-destructive.

The IR spectra provide images of vibrations of the atoms of a compound. An IR spectrum is obtained by passing IR radiation through a sample and determining what fraction of the incident radiation is absorbed at particular frequency. In other words, IR spectroscopy is based on the absorption of electromagnetic radiation by a molecular system. In IR spectroscopy, it is common to use the wavenumber unit $\tilde{\nu}$, which is expressed in cm^{-1}, instead of the frequency ν. This is the number of wave in a length of one centimetre, the reciprocal wavelength, and is given by the following relationship:

$$\tilde{\nu} = \frac{1}{\lambda} = \frac{v}{c} \tag{1}$$

where λ is the wavelength and c is the velocity of light in vacuum (2.997925×10^8 m/sec). The wavenumber unit has the advantage of being linear with frequency or energy.

The vibrations of a polyatomic molecule can be considered as a system of oscillators. If there are N atomic nuclei in the molecule, there will be a total of $3N$ degrees of freedom of motion for all the nuclear masses in the molecule. Subtracting the pure translations and rotations of the entire molecule leaves ($3N$-6) vibrational degrees of

freedom for a nonlinear molecule and (3*N*-5) vibrational degrees of freedom for a linear molecule. These internal degrees of freedom correspond to the number of independent normal modes of vibration. A normal mode is called IR active, if this mode alters the electric dipole moment of the molecule. Thus, as a rule of thumb, strong IR bands are related to polar functional groups.

The vast majority of molecules exhibit IR bands in the mid-IR region between 400 and 4000 cm^{-1}. The position and intensity of a vibrational band are characteristic of the underlying molecular motion and consequently of the atoms participating in the chemical bond, their conformation and immediate environment. Thus, a certain submolecular group produces bands in a characteristic spectral region. These characteristic bands form the empirical basis for the interpretation of vibrational spectra.

The reader interested in details of the basic principles of IR spectroscopy and the interpretation of vibrational spectra is referred to relevant books (1–3).

The objective of this paper is to review new developments in applications of IR spectroscopy to study penetration of drugs into membranes. Prior to that, it is useful to give a short introduction to the concept of Fourier transform (FT) technique and to briefly explain the principles of attenuated total reflection (ATR) and photoacoustic spectroscopy (PAS) as well as microscopic methods. In this context, we will mainly discuss systems studied by our research group.

II. INSTRUMENTATION

A. Fourier Transform Technique

In the past decades, Fourier transform-infrared (FT-IR) spectrometers have almost entirely replaced dispersive instruments because of their better performance in nearly all respects. The application of the FT technique has improved the acquisition of IR spectra dramatically. The heart of the optical hardware in such FT spectrometers is the interferometer. The most common set-up used is the classic two-beam Michelson interferometer shown schematically in Figure 1. It consists of two mutually perpendicular plane mirrors, a fixed mirror and a movable one. A semi-reflecting mirror, the beam splitter, bisects the planes of these two mirrors. A beam emitted by a source is split in two by the beam splitter. The reflected part of the beam travels to the fixed mirror, is reflected there and hits the beam splitter again. The same happens to the transmitted radiation. Since the two split beams are spatially coherent, they interfere on recombination. The beam, modulated by the movement of the mirror, leaves the interferometer and is finally focussed on the detector. The signal actually registered by the detector, the interferogram, is thus the radiation intensity of the combined beams as a function of the position of the movable mirror. Generally, it is difficult to understand an interferogram, because it is a function of time and, traditionally, we are used to think in the frequency (or wavenumber) domain, namely in terms of spectra. The mathematics of the conversion of an interferogram into a spectrum is the Fourier transformation. Based on fully developed software the computer performs this transformation.

The essential steps for obtaining an FT-IR spectrum are to produce an interferogram with and without a sample in the beam and then to transform these interferograms into spectra of the source with sample absorption and the source without sample absorption. The ratio of the former and the latter is the IR transmission

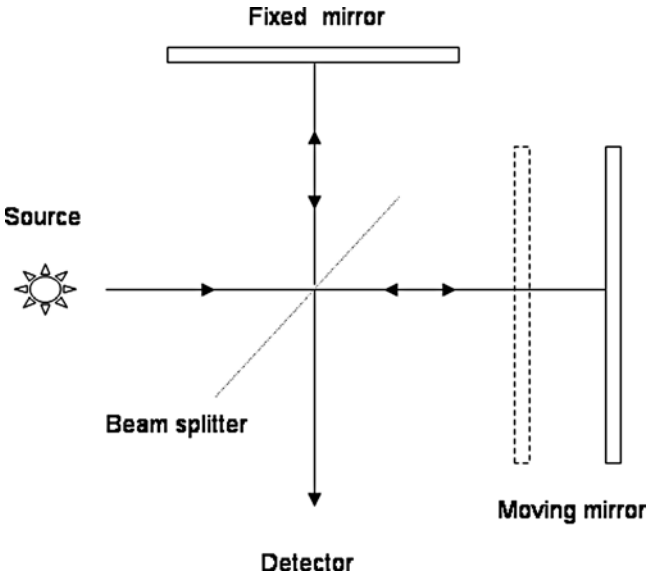


Figure 1 The scheme of a Michelson interferometer.

spectrum of the sample. The sample is usually placed between interferometer and detector.

B. Attenuated Total Reflection

In ATR, the sample is placed in optical contact against a special crystal, termed ATR crystal, which is composed of a material with a high index of refraction, e.g., zinc selenide (ZnSe). The IR beam from the spectrometer is focused onto the bevelled edge of the ATR element by a set of mirrors, reflected through the crystal, and then directed to the detector by another set of mirrors.

The use of ATR in spectroscopy is based upon the fact that although completed internal reflection occurs at the sample–crystal interface, radiation does in fact penetrate a short distance into the sample (Fig. 2). This penetration is termed the

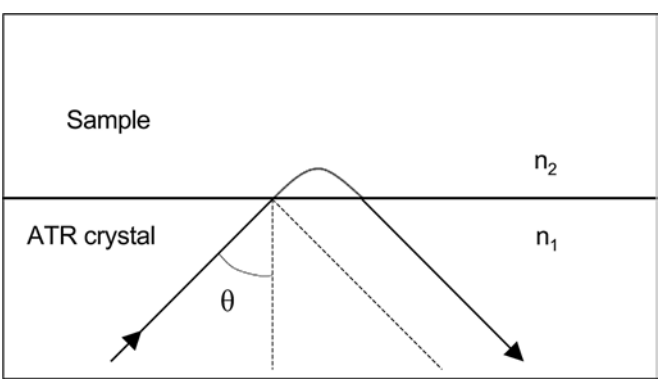


Figure 2 The scheme of the attenuated total reflection (ATR).

evanescent wave. The sample interacts with the evanescent wave resulting in the absorption of radiation by the sample, which closely resembles the transmission spectrum for the same sample. However, the ATR spectrum will depend upon several parameters, including the angle of incidence for the incoming radiation, the wavelength of the radiation, and the refractive indices of the sample and the ATR crystal.

The penetration depth, d_p, of the evanescent wave, defined as the distance required for the electrical field amplitude to fall to $1/e$ of its value at the interface, is given by (4):

$$d_p = \frac{\lambda}{2\pi n_1 \sqrt{sin^2\theta - (n_2/n_1)^2}} \tag{2}$$

where λ is the wavelength, n_1 and n_2 are the refractive indices of the ATR crystal and the sample, respectively, and θ is the angle of incidence. Obviously, the penetration depth of the beam depends on the wavelength. For a sample with $n_2 = 1.6$, typical of a polymeric material, placed on a ZnSe element ($n_1 = 2.4$) with a 45° angle of incidence, the penetration depth is in the range from 2.8 to 1.4 μm for the spectral range from 1000 to 2000 cm^{-1}. Furthermore, Equation (2) shows that total reflection occurs when the angle of incidence is larger than the critical angle:

$$\theta_{cr} = \sin^{-1}(n_2/n_1)$$

The ATR is a quick and non-destructive sampling technique for obtaining the IR spectrum of a material's surface. Samples examined by FT-IR-ATR generally require minimum, or no, sample preparation, but an intimate optical contact between the sample and the ATR crystal is crucial. Unfortunately, the crystal element itself can be the Achilles heel of the ATR technique: the crystal will degrade with surface scratching and cracking. Recently, very reasonable, interchangeable Fresnel ATR elements with a surface area diameter of 20 mm are commercially available.

C. Photoacoustic Spectroscopy: FT-IR–PAS

In PAS, intensity modulated radiation impinges on the sample, is absorbed and generates heat waves within the sample. In turn, after diffusion to the sample surface, these thermal waves generate pressure modulation (i.e., sound) in the surrounding transfer gas, usually helium. A sensitive microphone coupled to the acoustic chamber detects the sound signal that provides information about the properties of the sample (Fig. 3). The prerequisite for a photoacoustic experiment is to apply modulated light. In the case of an FT-IR spectrometer, it is already available in form of the interferogram. In other words, using FT-IR–PAS, the interferogram is recorded by an acoustic detector.

Due to the acoustic way of detection, both optical and thermal properties of the sample determine the photoacoustic signal. Therefore, it is necessary to differentiate between optically transparent and optically opaque as well as thermally thin and thermally thick samples. For a thermally thick sample without saturation effect, the theory (5) predicts that the acoustic signal, S_{PAS}, is given by the expression:

$$S_{PAS} = \frac{\alpha(\tilde{\nu}) I_o}{4\pi\rho C f} \tag{3}$$

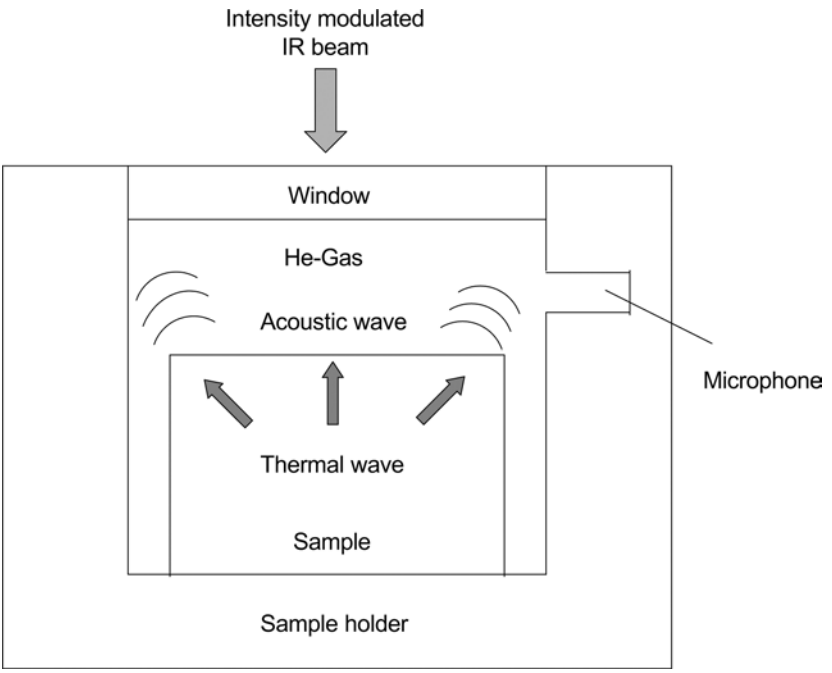


Figure 3 The scheme of a photoacoustic cell.

where $\alpha(\tilde{\nu})$ is the spectral optical absorption coefficient, I_o the intensity of the incident IR beam, ρ the density, C the specific heat, and f is the modulation frequency. Furthermore, for an optically and thermally homogeneous material, the depth L_S from which the signal arises, the thermal diffusion length, is described mathematically as:

$$L_s = \sqrt{\frac{\kappa}{\pi\rho C f}} = \sqrt{\frac{\alpha}{\pi f}} \tag{4}$$

where κ is the thermal conductivity of the sample and $\alpha = \kappa/\rho C$ is the thermal diffusivity. Based on this relationship, it is possible to select various sampling depths by choosing appropriate modulation frequencies.

Advanced FT spectrometers allow recording an interferogram using the step-by-step mode with phase modulation. In such step-scan experiments, the moving mirror of the interferometer oscillates about the stopping position with selected modulation frequency and modulation amplitude. In this way, the phase modulation of the radiation is provided. The demodulation of the PA signal with the modulated IR beam as reference is ensured by the acquisition processor. The fact that the step-scan technique in conjunction with phase modulation (6) provides a uniform modulation frequency for all wavenumbers and consequently a uniform probing depth represents the most important advantage of this method. It gives the ability to carry out controllable depth profiling of the sample. Hence, applying a sequence of several modulation frequencies in repeated manner, it is possible to obtain data from various probing depths in the course of the penetration process.

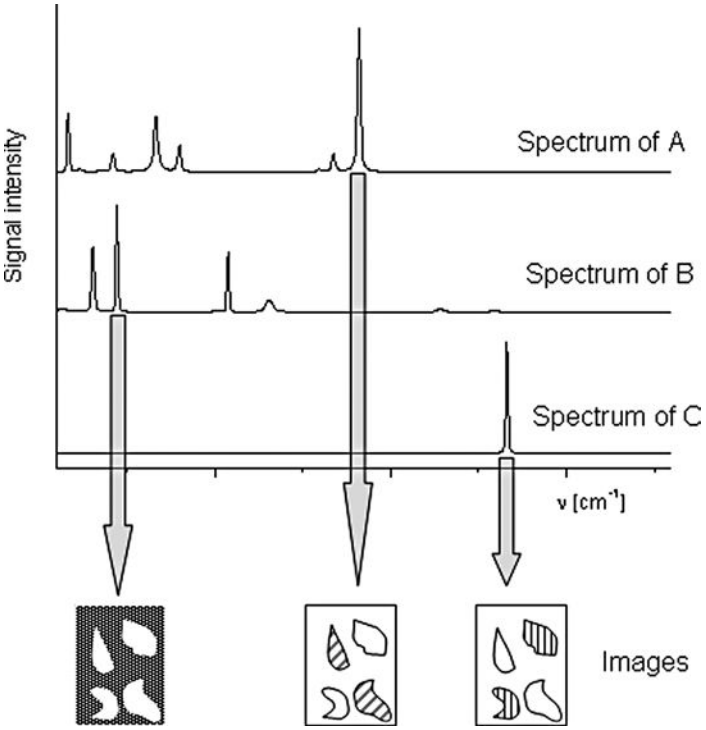


Figure 4 The principle of vibrational spectroscopic imaging.

D. IR Microspectroscopy

In the last decade, IR microscope has gained increasing acceptance as analytical tools for microsampling of heterogeneous systems (7). The collection of vibrational spectra through microscope optics and the visualization of the spectral data by imaging represent a relatively new technique, which uses spectral features as a native intrinsic contrast mechanism. An advantage of imaging is that the information is present in a form readily comprehensible to non-spectroscopists and is comparable with the output of other microscopic techniques.

Using a research-grade instrument, it is possible to perform chemical visualization. Once the spectral data at different areas of the sample in a grid pattern have been collected, they can be reduced and presented using software packages as three-dimensional surface projection, band intensity ratio maps, chemicals maps or even as outputs from multivariate analysis. The prime advantage in using the imaging function is that the distribution of molecular species within a matrix can be determined quickly and at high lateral resolution. As schematically illustrated in Figure 4, the spatial distribution of the molecular compounds present in the specimen can be mapped out separately.

From the experimental point of view, there are two strategies of visualization, namely mapping and imaging. In the mapping mode of operation, spectra are sequentially (in time) collected by point-to-point measurements with a computer-controlled motorized XY stage attached to the microscope facility. Generally, mapping experiments are time consuming and tedious.

In the imaging mode of operation, thousands of spatially resolved spectra may be collected simultaneously from analytes distributed within the sample. The IR imaging (8) is performed using focal-plane arrays as multichannel detectors. At present, commercial IR imaging spectrometers are equipped with array detectors in 64×64 or 128×128 pixels format. Therefore, in the course of an analysis, 4096 or 16,384 spatially encoded interferograms are recorded simultaneously, which are subsequently transformed to the same number of spectra. Although one might expect this to be time consuming, processing this huge amount of data occupies about three to five minutes for each sample. The principal difference is that each pixel of the IR data contains a complete spectrum, not just intensity data at a single wavenumber. From the microscopic point of view, the aperture used for spatial isolation in a conventional IR microscope is replaced by an individual pixel on the array. For the standard 64×64 array, the pixels are $60 \times 60\,\mu m$, which, when imaged to the sample position, translates into a sample area of $6 \times 6\,\mu m$.

The FT-IR images can be obtained in transmission, reflection or ATR mode. For IR transmission microspectroscopy, the major requirement is that the sample be sufficiently thin and non-scattering. A general rule of thumb is that the desired sample thickness for most common materials should be on the order of $10\,\mu m$. Once the sample has been suitably thinned, it is usually mounted on a support that is transparent to both IR and visible light. For most systems, such as native stratum corneum or tissue, the sample can be supported by BaF windows.

III. PENETRATION OF DRUGS INTO MEMBRANES STUDIED BY FT-IR–ATR

The FT-IR–ATR is now a well-established technique employed to monitor the penetration of drugs into and the permeation of drugs across membranes, which are used to simulate the stratum corneum, as well as to determine diffusion coefficients of the diffusants. The first experiments of this kind were performed in order to investigate the diffusion of small molecules through polymer films (9–13). In the early 1990s, the pharmacists have introduced the ATR technique into drug delivery studies and numerous reports on this subject can now be found in the literature (14–23).

In the simplest case of such experiments, an appropriate artificial or natural membrane, e.g., stratum corneum, acting as acceptor is sandwiched between an impermeable ATR crystal and a reservoir of penetrant, the donor (Fig. 5). The donor can be an ointment or another semisolid formulation. The membrane is initially devoid of penetrant. As diffusion through the membrane occurs, there will be a build up of penetrant concentration at the interface between membrane and crystal, which can be monitored on-line by the appearance and increase of drug-specific IR bands as a function of time. Of course, it is favorable if the penetrant under investigation exhibit an IR band that can be distinguished from the IR spectrum of the membrane.

As an example, Figure 6 show the FT-IR–ATR spectra acquired at various times of the penetration process of urea into a glycerol–collodion membrane; thereby, the donor used was a formulation of 10% urea in a carboxymethylcellulose hydrogel. It is obvious that several changes in the spectral features appear due to the diffusion of urea, in particular the increasing intensity of the isolated IR band at $1460\,cm^{-1}$, which belongs to the antisymmetric CN stretching mode. The integrated absorbance of this urea band, plotted in Figure 7 as a function of the penetration time, can be used as measure of the urea concentration at the interface between membrane and ATR crystal.

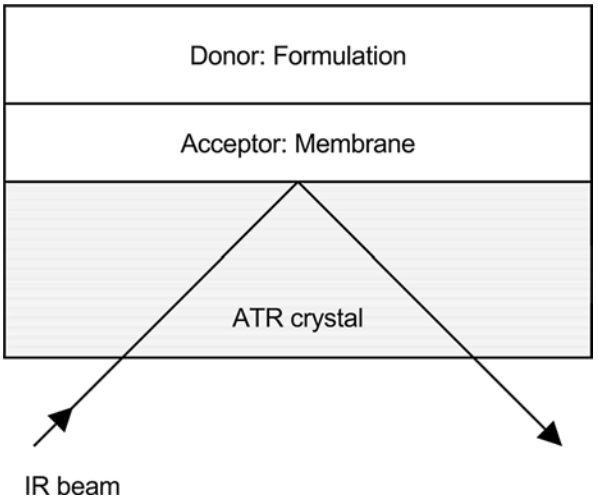


Figure 5 The sample arrangement for the drug penetration experiment using attenuated total reflection (ATR) technique.

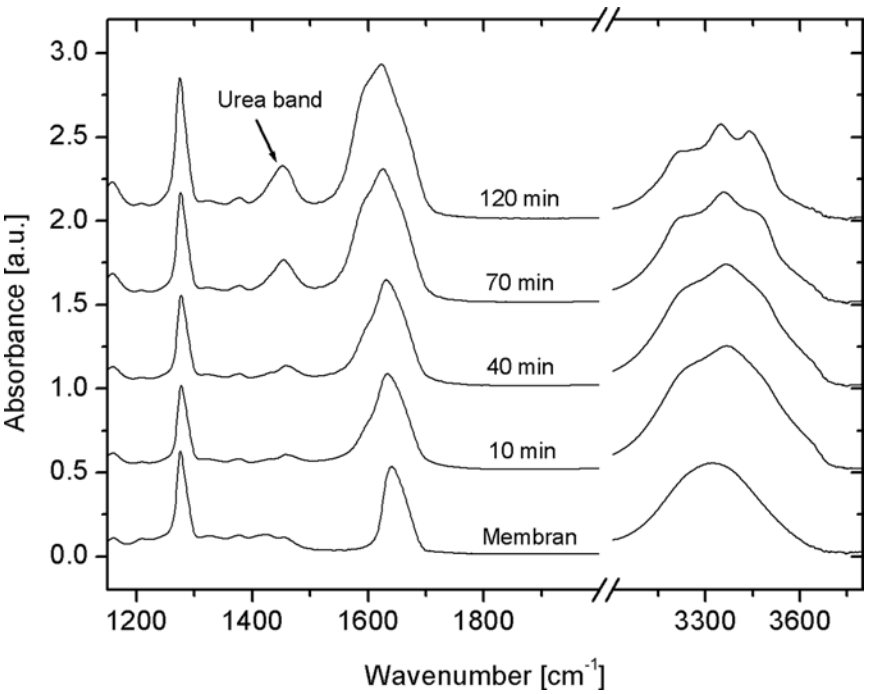


Figure 6 The FT-IR-ATR spectra for the glycerol–collodion membrane/urea/carboxycellulose hydrogel system recorded at various times of the penetration experiment.

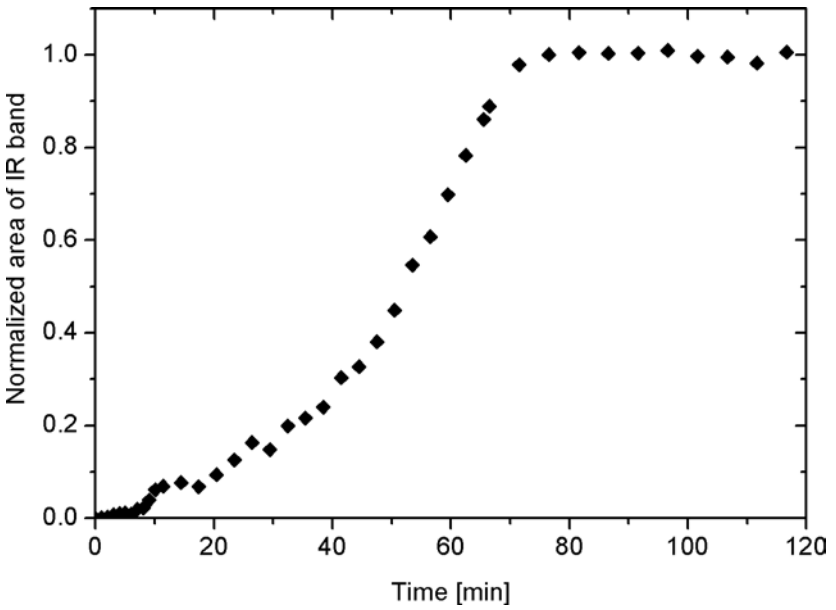


Figure 7 Penetration of urea into a glycerol–collodion membrane: intensity of the urea band at 1460 cm^{-1} as a function of penetration time.

The penetration of the drug from the formulation, in most cases a suspension, into the membrane occurs sequentially, i.e., (i) the solid drug particles dissolve in the liquid phase of the formulation, (ii) dissolved drug molecules diffuse in the donor, (iii) the drug crosses the interface between donor and membrane, and finally (iv) the drug diffuses in the acceptor. In order to simplify the mathematical model, it is often assumed that the saturation concentration of drug in the liquid phase of the formulation ($c_{\mathrm{d\ sat}}$) does exist during the entire penetration process. This assumption implies that the first step is not essential and the diffusion of the drug inside the donor system is negligible. The drug diffusion in the acceptor obeys Fick's second law for the one-dimensional case, i.e:

$$\frac{\partial c_{\mathrm{a}}}{\partial t} = D\frac{\partial^2 c_{\mathrm{a}}}{\partial x^2} \tag{5}$$

where c_{a} is the drug concentration in the acceptor and D is a concentration-averaged effective diffusion coefficient taken as constant. Equation (5) has to be solved for the following initial and boundary conditions:

$$\text{at } t = 0, \quad c_{\mathrm{a}} = 0 \quad \text{for } \ 0 < x < L \tag{6}$$

$$\text{at } t \geq 0, \quad c_{\mathrm{a}}(x = L) = kc_{\mathrm{dsat}} = c_{\mathrm{a\ sat}} = \text{const} \tag{7}$$

and:

$$\frac{\partial c_{\mathrm{a}}}{\partial x} = 0 \ \text{ for } \ x = 0 \tag{8}$$

where L is the thickness of the membrane (Fig. 8), $c_{\mathrm{a\ sat}}$ is the saturation concentration of the drug in the acceptor membrane, and k is the partition coefficient between

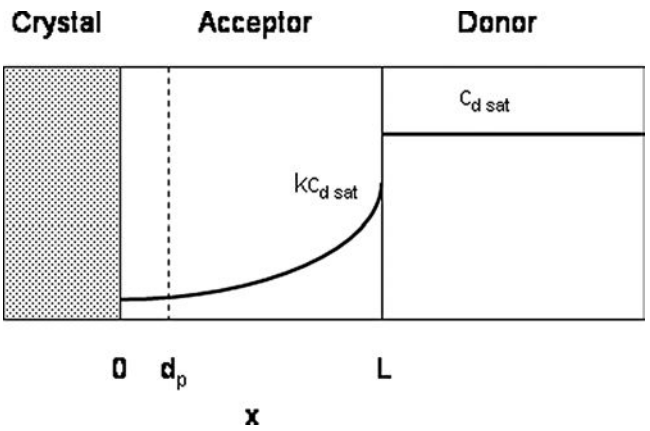


Figure 8 Model of the drug concentration profile for a penetration experiment using attenuated total reflection (ATR) technique.

formulation and membrane. The boundary condition (7) indicates that the drug concentration on the right edge of the membrane remains constant during the entire penetration process. The condition for zero flow [Eq. (8)] implies that no drug can traverse the left membrane boundary.

The solution to Equation (5) with these boundary and initial conditions is (24):

$$\frac{c_a}{c_{a\ sat}} = 1 - \frac{4}{\pi}\sum^{n=0}\frac{(-1)^n}{2n+1} \times \exp\left[\frac{-D(2n+1)^2\pi^2 t}{4L^2}\right] \times \cos\left[\frac{(2n+1)\pi x}{2L}\right] \tag{9}$$

Equation (9) can be related to the experimental IR absorption data with the use of the ATR differential form of the Beer–Lambert law (4):

$$A = \int_O^L \varepsilon c E_0^2 \exp\left(\frac{-2x}{d_p}\right) dx \tag{10}$$

where A is the ATR absorbance, ε is an effective extinction coefficient, and E_0 is the electric field strength at $x = 0$ (interface sample/ATR crystal). Substituting Equation (9) into the absorbance expression, with assumptions of weak IR absorption and negligible changes in the sample refraction index, results in:

$$\frac{A_t}{A_{eq}} = 1 - \frac{8}{\pi d_p(1 - e^{-2L/d_p})}\sum^{n=0}\frac{e^g\{fe^{-2L/d_p} + (-1)^n(2/d_p)\}}{(2n+1)(4/d_p^2 + f^2)} \tag{11}$$

where:

$$g = \frac{-D(2n+1)^2\pi^2 t}{4L^2} \tag{12}$$

$$f = \frac{(2n+1)\pi}{2L} \tag{13}$$

A_t is the integrated IR absorbance of the diffusing penetrant at time, t, and A_{eq} is its value at equilibrium ($t \to \infty$). In the case that the membrane is much thicker than the penetration depth of the IR beam $L \gg d_p$, the Equation (2) becomes:

$$\frac{A_t}{A_{eq}} = 1 - \frac{4}{\pi}\sum^{n=0}\frac{(-1)^n}{2n+1}\exp\left[-\frac{(2n+1)^2\pi^2 Dt}{4L^2}\right] \tag{14}$$

The effective diffusion coefficient can be determined by regressing the experimental data to Equations (11) and (14), respectively. Another procedure is the numerical solution of the partial differential equation (5) in conjunction with a non-linear least-squares data fitting (25).

A point of debate is whether this simplified mathematical model is applicable to the real experiment. As emphasized above, it is essential to ensure intimate contact between membrane and ATR crystal over the entire penetration process. In some cases, however, this requirement is not fulfilled. It is not unusual when the intensity of membrane bands decreases during the experiment while that of permeant bands increases (see, e.g., Ref. 17). Thus, in order to quantify the drug uptake, the absorption value of interest has to be normalized against a spectral parameter of the membrane. To be quite certain, it is also necessary to calibrate the uptake of drug within the membrane using another analytical method. But, that is often not an easy task. Further, the above model implies that the optical properties of the membrane remain constant in the course of the experiment. However, it is well known that the vehicle itself can penetrate into the membrane changing their biophysical properties. If swelling of the membrane occurs in the course of the penetration process, it should be considered within the mathematical model (13).

From this point of view, it is preferable to use an experimental set-up with a well-defined acceptor, which means a Franz type diffusion cell adapted for the ATR technique. As schematically shown in Figure 9, an appropriate liquid as acceptor ensures the contact of the system with the ATR crystal. It is also advantageous that the calibration of the IR spectra of the liquid/drug solution can be performed in a separate experiment.

The FT-IR–ATR technique can also be applied to study the drug release in formulations (26,27).

IV. PENETRATION OF DRUGS INTO MEMBRANES STUDIED BY FT-IR–PAS

For the penetration experiment using FT-IR–PAS, the schematic arrangement of the donor and acceptor (artificial membrane or the isolated stratum corneum) with respect to the IR input beam is shown in Figure 10. The handling is rather easy; the topical formulation is loaded in a brass cup that fits into the sample holder of the PAS cell and the appropriate membrane is placed on the ointment surface. Of course, prior to the start of the penetration experiment, a certain handling time, from our experience, approximately five minutes, is required and the PAS cell must be purged with helium for about 30 seconds.

Employing the step-scan FT-IR–PAS with phase modulation, Schendzielorz et al. (25) and Hanh et al. (28) investigated the penetration of several drugs (clotrimazole, dithranol, and methoxsalen) from semisolid vaseline formulation into

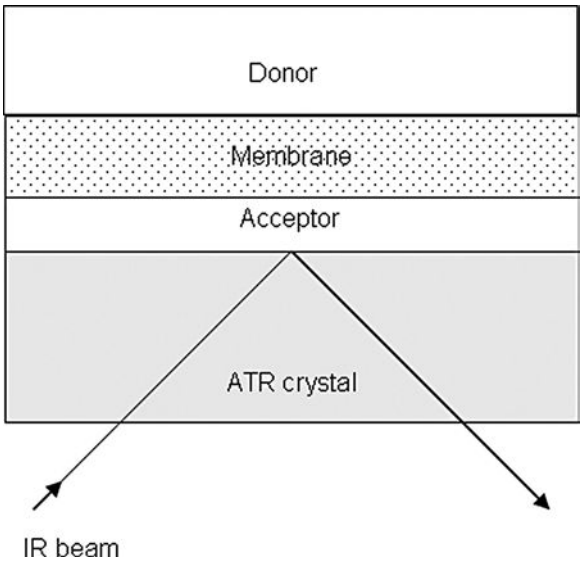


Figure 9 The sample arrangement of a Franz type diffusion cell adapted to the attenuated total reflection (ATR) technique.

a lipophilic dodecanol–collodion membrane. Typical examples of FT-IR-PA spectra in the spectral range of interest for the membrane/vaseline/dithranol system during the penetration experiment are depicted in Figure 11. The increase of the integral intensity of a selected drug IR band was determined, in the case of dithranol, it is the band at 1614 cm^{-1}. For the FT-IR–PAS experiment carried out with a sequence of several modulation frequencies, the relative increase of the drug signal intensity versus the penetration time is shown in Figure 12, thereby, the results of the ATR experiment are included for the purpose of comparison. Assuming a thermal diffusivity of $\alpha = 9 \times 10^{-4}$ cm^2/sec, a typical value for an organic material, and using

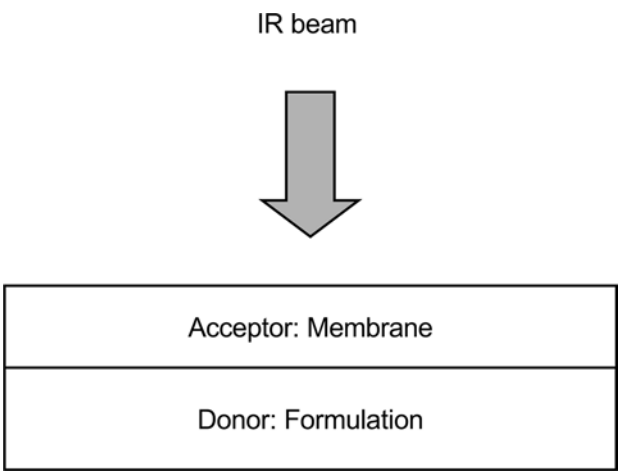


Figure 10 The sample arrangement for drug penetration experiment using Photoacoustic Spectroscopy (PAS).

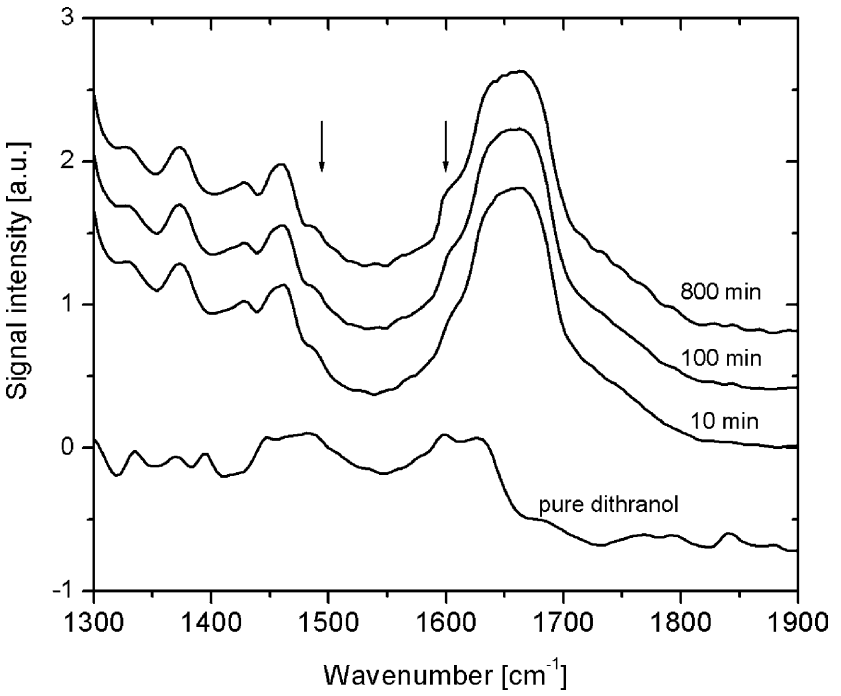


Figure 11 The Fourier transform-infrared (FT-IR) photoacoustic spectra in the spectral range 1300 to 1900 cm^{-1} for the dodecanol–collodion membrane/vaseline/dithranol system recorded at various times of the penetration experiment. The photoacoustic spectrum of the pure dithranol is also shown. Bands due to the drug are marked by arrows.

Equation (3), the modulation frequencies applied (54, 112, and 418 Hz) correspond to sampling depths of 23, 16, and 8 μm, respectively, whereas in the case of ATR, the sampling depth amounts to 1.7 μm. The curve profiles thus obtained in the time interval up to about 200 minutes clearly indicate the distance-dependent distribution of the drug in the membrane and that a lag-time can be observed for sampling depths shorter than 10 μm.

The experimental findings indicated that it was necessary to consider a layered structure of the membrane. Therefore, in the mathematical model applied, it was assumed that the diffusion coefficient is a function of distance within the membrane. So, according to the experimental conditions, i.e., various sampling depths chosen, the membrane was divided into virtual layers and each layer (i) was characterized by an effective diffusion coefficient, D_i. The partial differential equation (5) was numerically solved for the appropriate initial and boundary conditions (28). The spectroscopic data were used as an input data set for the mathematical modeling of the drug diffusion in the membrane. In this manner, the depth-dependent diffusion coefficients were determined. Furthermore, as a result of this modelling, the drug concentration–distance profile at various times and the drug concentration–time profile at various positions in the membrane were calculated.

Continuing this research, Hanh et al. (29) studied the penetration of the lipophilic model permeant, 1-cyanodecane, into isolated human SC. The experiments yielded that the effective diffusion coefficient for 1-cyanodecane in SC is depth-dependent; in the inner region of the SC, this coefficient is approximately 1.6-fold

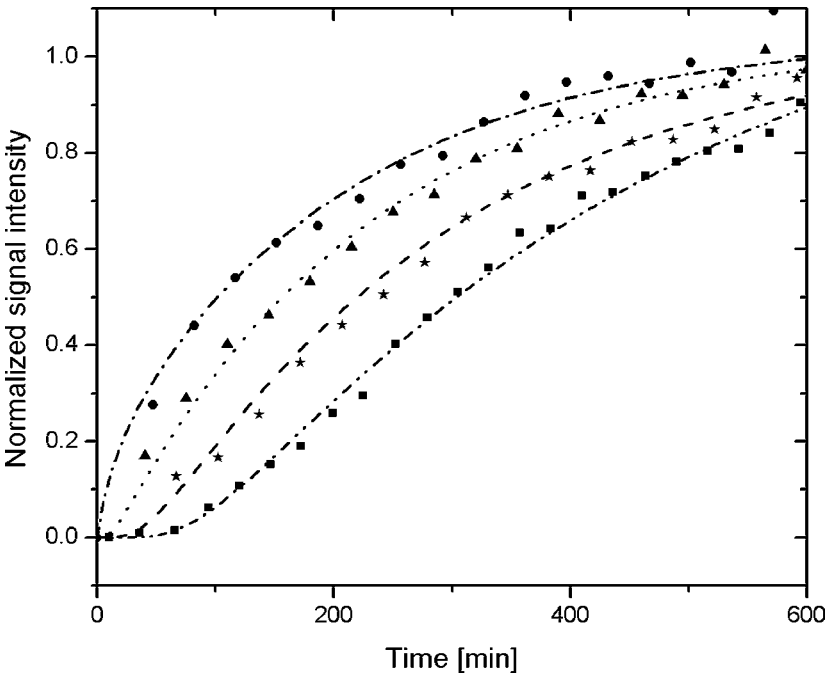


Figure 12 The increase of the normalized signal intensity of dithranol versus the penetration time determined by step-scan Fourier transform-infrared–photoacoustic spectroscopy (FT-IR–PAS) with phase modulation frequencies of 54 (•), 112 (▲), and 418 (⋆) Hz, and FT-IR–ATR (■).

that measured in the outer region. This finding is not unexpected and can be explained by the inherent, not uniformly homogeneous structure of the SC.

Recently, the penetration of nitroglycerin from Nitro-Dur (Schering-Plough Ltd., U.K.) transdermal drug patches into a poly(ethylene) glycol 400 impregnated microfiber filter used as acceptor was followed by using the rapid-scan FT-IR–PAS (30). In the continuous-scan mode of operation, each wavenumber, $\tilde{\nu}$, is modulated at a different frequency given by $f = 2\nu\tilde{\nu}$, where ν is the mirror velocity. That means monitoring different IR bands, in the case of nitroglycerin at 752, 852, 1276, and 1643 cm^{-1}, allows probing different sampling depth. The authors argue that this property is advantageous for the measurement of drug penetration into membranes. According to our experience, we would prefer the step-scan mode of operation because of the clearer experimental condition.

V. LATERAL DRUG DIFFUSION STUDIED BY IR MICROSPECTROSCOPY

Up to now, there are only a few investigations of lateral drug diffusion using FT-IR mapping or imaging. Rafferty and Koenig (31) have studied the diffusion of nicotine in ethanol/water mixtures into an ethylene-vinyl acetate (EVA) copolymer membrane by FT-IR imaging. The concentration profiles extracted from the images showed that segregation occurs during diffusion. Nicotine diffuses into EVA ahead

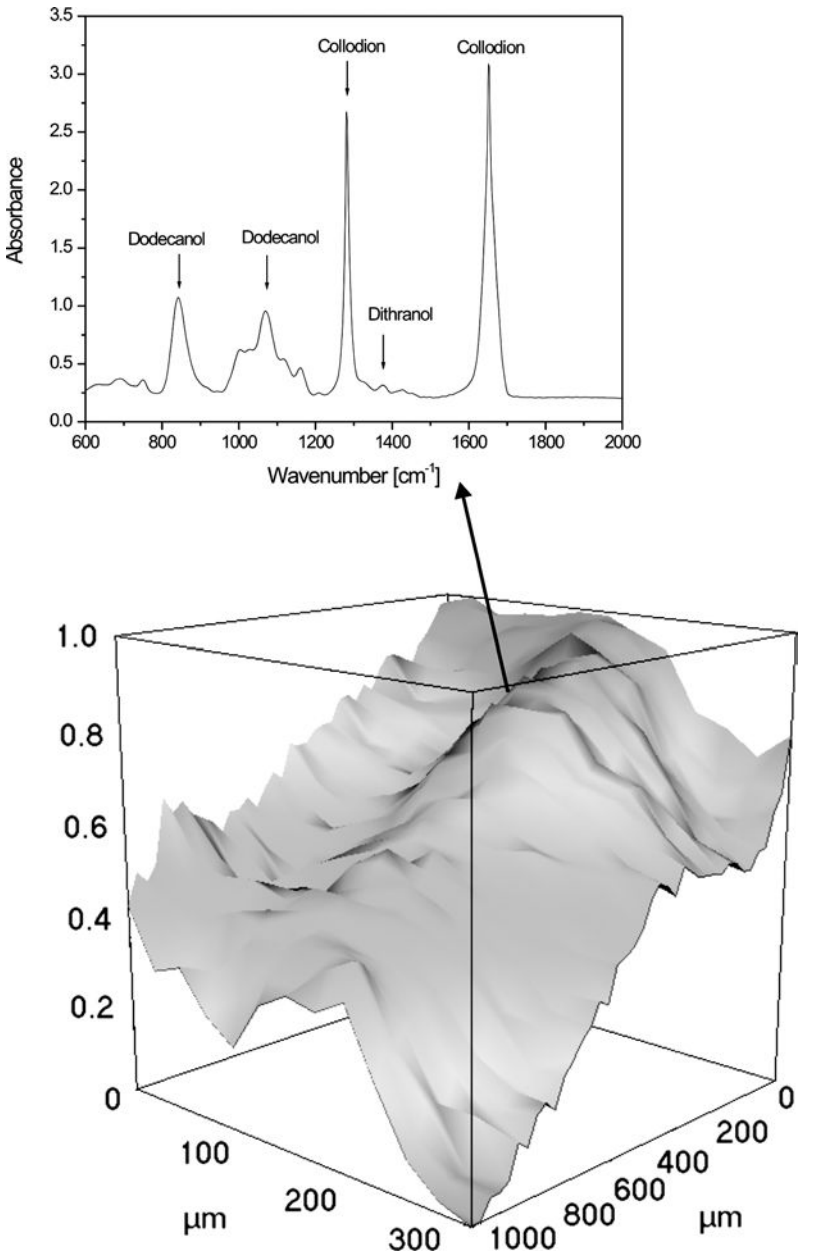


Figure 13 The Fourier transform-infrared (FT-IR) mapping of the lateral diffusion of dithranol in vaseline formulation into a dodecanol–collodion membrane (thickness 12 µm). To extract the drug concentration profile the integrated intensity of the dithranol band in the spectral range 1398 to 1472 cm^{-1} was used. The IR absorbance spectrum at the location (175 and 350) is shown on the top.

of the solvent for 0 to 60 wt.% ethanol/water mixtures; for the 80 wt.% ethanol solvent, D_2O leads the diffusion front, and for the 100 wt.% ethanol solvent, ethanol diffuses into EVA first. The initial swelling rates were calculated from the concentration profiles, and an exponential trend with increasing ethanol concentration in the

solvent was observed. The concentration profiles were also used to calculate average diffusion coefficients for the overall solution and specifically for nicotine.

Preliminary FT-IR mapping results of the lateral diffusion of dithranol in vaseline formulation into a dodecanol–collodion membrane (thickness 12 μm) are presented in Figure 13. The IR transmission experiment was performed with a Bruker spectrometer IFS 66 equipped with an IR microscope, IR-Scope II, and a computer-controlled motorized XY stage. Each spectrum was recorded with 20 scans at a spectral resolution of 2 cm^{-1} and a lateral resolution of 25 μm. To scan under these conditions a sample area of 300 × 1000 μm, the measuring time amounts to 2.5 hour. To extract the drug concentration profile, the integrated intensity of the dithranol band in the spectral range 1398 to 1472 cm^{-1} was chosen (Fig. 13). The concentration profiles show that there is a heterogeneous distribution of dithranol particles in the formulation, which results in a non-uniform drug diffusion front in the membrane.

VI. CONCLUSION

Nowadays, FT-IR–ATR is a well-established standard method to study drug penetration, influence of penetration modifiers and drug release. The FT-IR–PAS has been applied to determine drug penetration into artificial membranes and into biological systems such as isolated stratum corneum. The possibility of spectral depth profiling is the big advantage of this technique. However, FT-IR–PAS is limited to in vitro investigations so far.

Over the last years, there has been tremendous technical improvement in IR microspectroscopy. This unique technique offers completely new possibilities to study lateral diffusion of drugs in relevant polymeric systems, in semisolid formulations, in artificial membranes, and, in the future, maybe in biological systems.

ACKNOWLEDGMENTS

We have benefited enormously from the substantial effort of our students and collaborators. In particular, we would like to thank Dr. Bui Duc Hanh for performing the investigations of the lateral drug diffusion.

REFERENCES

1. Colthup NB, Daly LH, Wiberley SE. Introduction to Infrared and Raman Spectroscopy. 3d ed. San Diego: Academic Press, 1990.
2. Chalmers J, Griffiths PR. eds. Handbook of Vibrational Spectroscopy. Vols. 1–5. Chichester: Wiley, 2001.
3. Günzler H, Heise HM, Gremlich H-U. IR Spectroscopy. Weinheim: Wiley-VCH, 2002.
4. Mirabella FM. Principles, theory, and practice of internal reflection spectroscopy. In: Mirabella FM, ed. Internal Reflection Spectroscopy: Theory and Applications. New York: Marcel Dekker, 1993:17–52.
5. Rosencwaig A. Photoacoustics and Photoacoustic Spectroscopy. New York: Wiley, 1980.
6. Smith MJ, Manning CHJ, Palmer RA, Chao JL. Step scan interferometry in the mid-infrared with photothermal detection. Appl Spectr 1988; 42:546–555.

7. Sommer AJ. Mid-infrared transmission microscopy. In: Chalmers J, Griffiths PR, eds. Handbook of Vibrational Spectroscopy. Vol. 2. Chichester: Wiley, 2001:1369–1385.
8. Kidder LH, Hake AS, Lewis EN. Instrumentation for FT-IR imaging. In: Chalmers J, Griffiths PR, eds. Handbook of Vibrational Spectroscopy. Vol. 2. Chichester: Wiley, 2001:1386–1403.
9. Trifonov A, Nikolov P, Kolev D, Tsenov I. An investigation of liquid penetration through solid phase by ATR. Phys Stat Solidi (a) 1975; 27:135–140.
10. Brand H. Determination of diffusion specific parameters by means of IR-ATR spectroscopy. Exp Tech Phys 1985; 33:423–431.
11. Hemmelmann K, Brandt H. Investigation of diffusion and sorption properties of polyethylene films for different liquids by means of IR-ATR spectroscopy. Exp Tech Phys 1986; 34:439–446.
12. Brandt H, Hemmelmann K. On the evidence of non-linear sorption at the surface polyethylene/ATR-element for the diffusion of ethyl acetate in polystyrene films. Exp Tech Phys 1987; 35:349–358.
13. Hörnig K, Hemmelmann K, Brandt H, Hergeth W-D, Wartewig S. Monomers in polymer dispersions. III. Diffusion of monomers in poly(vinyl-acetate) films. Acta Polymerica 1991; 42:601–604.
14. Wurster DA, Buraphacheep V, Patel JM. The determination of diffusion coefficients in semisolids by Fourier transform infrared (FT-IR) spectroscopy. Pharm Res 1993; 10:616–620.
15. Farinas KC, Doh L, Venkatraman S, Potts RO. Characterisation of solute diffusion in a polymer using ATR-FTIR spectroscopy and bulk transport techniques. Macromolecules 1994:5220–5221.
16. Reinl HM, Hartinger A, Dettmar P, Bayerl TM. Time resolved infrared ATR measurements of liposome transport kinetics in human keratinocyte cultures and skin reveals a drastic dependence on liposome size and phase state. J Invest Dermatol 1995; 105:291–295.
17. Tralhão AML, Watkinson AC, Brain KR, Hadgraft J, Armstrong NA. Use of ATR-FTIR spectroscopy to study the diffusion of ethanol through glycerogelatin films. Pharm Res 1995; 12:572–575.
18. Harrison JE, Watkinson AC, Green DM, Hadgraft J, Brain K. The relative effect of Azone® and Transcutol® on permeant diffusivity and solubility in human stratum corneum. Pharm Res 1996; 13:542–546.
19. Pellet MA, Watkinson AC, Hadgraft J, Brain KR. Comparison of permeability data from traditional diffusion cell and ATR-FTIR spectroscopy. Part I. Synthetic membranes. J Control Rel 1997; 154:205–215.
20. Pellet MA, Watkinson AC, Hadgraft J, Brain KR. Comparison of permeability data from traditional diffusion cell and ATR-FTIR spectroscopy. Part II. Determination of diffusional pathlengths in synthetic membranes and human stratum corneum. J Control Rel 1997; 154:217–227.
21. Nardviriyakul N, Wurster DE, Donovan MDD. Determination of diffusion coefficients of sodium ρ-aminosalicylate in sheep nasal mucosae and dialysis membranes by Fourier transform infrared horizontal attenuated total reflectance spectroscopy. J Pharm Sci 1997; 86:19–25.
22. Cantor AS. Drug and excipient diffusion and solubility in acrylate adhesives measured by infrared-attenuated total reflectance (IR-ATR). J Control Rel 1999; 61:219–231.
23. Dias M, Rahagan SL, Hadgraft J. ATR-FTIR spectroscopic investigations on the effect of solvents on the permeation of benzoic acid and salicylic acid through silicone membranes. Int J Pharm 2001; 216:51–59.
24. Crank J. The Mathematics of Diffusion. Oxford: Clarendon Press, 1956.
25. Schendzielorz A, Hanh BD, Neubert R, Wartewig S. Penetration studies of clotrimazole from semisolid formulation using step-scan FT-IR photoacoustic spectroscopy. Pharm Res 1999; 16:42–45.

26. Hanh BD, Neubert R, Wartewig S. Investigations of drug release from suspensions using FT-ATR technique. Part I. Determination of effective diffusion coefficient of drugs. Int J Pharm 2000; 204:145–150.
27. Hanh BD, Neubert R, Wartewig S. Investigations of drug release from suspensions using FT-ATR technique. Part II. Determination of effective dissolution coefficient of drugs. Int J Pharm 2000; 204:151–158.
28. Hanh BD, Neubert R, Wartewig S, Christ A, Hentzsch C. Drug penetration as studied by non-invasive methods: FT-ATR, FTIR and UV photoacoustic spectroscopy. J Pharm Sci 2000; 89:1106–1113.
29. Hanh BD, Neubert R, Wartewig S, Lasch J. Penetration of compounds through human stratum corneum as studied by Fourier transformed infrared photoacoustic spectroscopy. J Control Rel 2001; 70:393–398.
30. Nakamura O, Lowe RD, Mitchem L, Snook RD. Diffusion of nitroglycerin from drug delivery patches through micro-fiber filters using Fourier transform infrared photoacoustic spectroscopy. Anal Chim Acta 2001; 427:63–73.
31. Rafferty D-W, Koenig J-L. FTIR imaging for the characterization of controlled-release drug delivery applications. J Control Rel 2002; 83:29–39.

51
Percutaneous Absorption of Sunscreens

Kenneth A. Walters
Control Delivery Systems, Inc., Watertown, Massachusetts, U.S.A.

Michael S. Roberts
Department of Medicine, University of Queensland, Princess Alexandra Hospital, Woolloongabba, Queensland, Australia

I. INTRODUCTION

Ultraviolet radiation causes sunburn, premature aging of skin, and skin cancer. There is a considerable body of evidence that suggests that actinic keratosis, basal cell and squamous skin cancer, malignant melanoma, and cutaneous lupus erythematosis are exacerbated or triggered by sun exposure (1). Cancer prevention organizations (including the American Academy of Dermatology) have undertaken major efforts to educate the public to avoid unnecessary exposure to solar radiation. For these reasons, it is now common practice for manufacturers to include sunscreen active ingredients in many traditional cosmetic products (e.g., lipsticks, foundations, and moisturizers) as well as so-called ''beach sunscreens.''

Sunscreens have been used to protect against solar ultraviolet radiation (UVR) for more than a century with broad spectrum UVA and UVB sunscreens now widely available. The U.S. Food and Drug Administration (FDA) defines a sunscreen active ingredient as one that ''absorbs, reflects, or scatters radiation in the ultraviolet range at wavelengths of 290–400 nm'' (2). Most sunscreen actives (e.g., octyl salicylate and octyl methoxycinnamate) absorb in the UVB spectrum (290 to 320 nm). Some sunscreen actives absorb in both the UVA and UVB range (e.g., benzophenone-3; 200 to 350 nm). The sunscreens approved for consumer use vary widely between countries (3). Some examples of commonly used sunscreen actives approved for products throughout the world are shown in Table 1.

An understanding of the potential for human systemic exposure is an integral part of the safety assessment of sunscreen actives used in consumer products (4,5). There is, however, little published data in the scientific literature regarding the skin penetration of topically applied sunscreen actives. Although mathematical modeling from physicochemical data has suggested that the percutaneous absorption of certain sunscreen actives may be significant (6), it is important to appreciate that under conditions of actual exposure the rates of percutaneous absorption of such compounds will not be constrained solely by

Table 1 Some Examples of Commonly Used Sunscreen Actives

Chemical names	Other names
Homomenthyl salicylate	Homosalate
2-Ethylhexyl salicylate	Octyl salicylate
p-Aminobenzoic acid	PABA
Octyl dimethyl-*p*-aminobenzoate	Octyl dimethyl PABA, padimate O
2-Hydroxy-4-methoxy benzophenone	Benzophenone-3, oxybenzone
2-Hydroxy-4-methoxy benzophenone-5-sulfonic acid	Benzophenone-4, sulisobenzone
2-Ethylhexyl-*p*-methoxycinnamate	Octyl methoxycinnamate
Butyl methoxydibenzoylmethane	Avobenzone

Abbreviation: PABA, *p*-aminobenzoic acid.
Source: From Ref. 57.

physicochemical properties but may also be strongly influenced by the nature and properties of the vehicle in which they are applied (5,7). Percutaneous absorption of sunscreens needs also to be examined from the viewpoint of the relative risk and benefits of not using a sunscreen when the use of a sunscreen is warranted. This chapter examines both the data on skin permeation of sunscreens, the prediction of sunscreen penetration and the relative risks and benefits of using sunscreens when their use may be warranted.

II. SKIN PERMEATION OF SUNSCREENS

A. Data from In Vivo Human Studies

The amount of published literature concerning the percutaneous absorption of sunscreens in human subjects in vivo from commercial products is limited. Noting considerable variability in absorption between subjects (Fig. 1), Hayden et al. (8) found between 1% and 2% benzophenone-3 absorption 12 hours after application to human skin. Benzophenone-3 has also been detected in breast milk of humans (9) following dermal application. More recently, Gustavsson Gonzalez et al. (10) applied 40 g of a commercially available SPF14 lotion, containing 4% benzophenone-3, to the whole body (except scalp and genital regions) of 11 volunteers and monitored urine excretion of total (free + conjugates) benzophenone-3 over 48 hours. They reported that about 10 mg or ~0.5% of the applied amount was recovered in the urine over that time period.

Treffel and Gabard (11,12) examined the permeation of benzophenone-3, 2-ethylhexyl-4-methoxycinnamate, and 2-ethylhexyl salicylate (octyl salicylate) from a commercial vehicle (emulsion gel) and petroleum jelly, through human skin both in vivo and in vitro. Sunscreen formulations were applied to the skin surface in amounts reflective of consumer use (~2 mg/cm^2) and samples were taken at intervals up to a maximum exposure of six hours. For the in vivo study, samples of the stratum corneum of the treated area (back) were taken by tape stripping at 0.5, 2, and 6 hours following application of the formulations. Although there were no statistical differences in the amount of individual sunscreen agents found in the stratum corneum following 0.5-hour exposure, there was a significant vehicle effect in that the agents applied in the emulsion gel generated considerably higher stratum corneum levels than when applied in petroleum jelly (Fig. 2). These data were reflected in the in vitro study where epidermal levels of the sunscreen

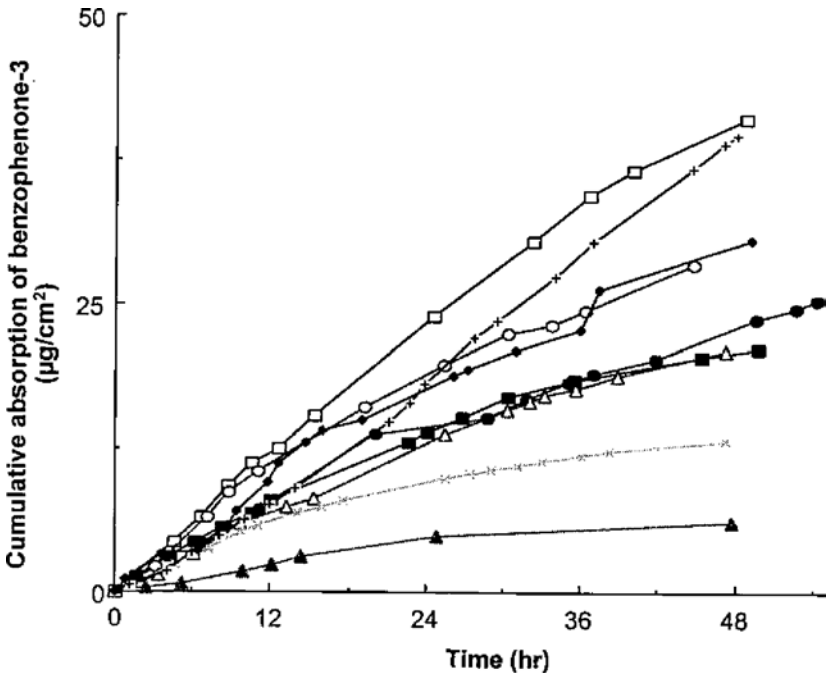


Figure 1 Skin absorption of benzophenone-3 following topical application of the sunscreen agent in a commercial formulation. Data calculated from urinary recovery of the sunscreen agent and its metabolites. *Source*: From Ref. 8.

agents were, for the most part, higher following application in the emulsion gel. In most cases, levels in the dermis and receptor fluid were below the level of quantification, except for benzophenone-3 (the least lipophilic sunscreen agent). Although higher levels of benzophenone-3 were found in the dermis and receptor fluid following application in petroleum jelly, permeation to the receptor fluid also occurred from the emulsion gel. These data indicated that when applied in petroleum jelly approximately 5% of the applied dose of benzophenone-3 permeated through human skin within six hours. The in vitro data generated in this study should, however, be viewed with caution since the skin was obtained from only two donors. Furthermore, all three sunscreen agents were detectable in samples of dermal tissue after only two minutes of exposure, which suggests possible contamination during the biopsy procedure.

Early work by Feldman and Maibach (13) indicated that a significant amount of *p*-aminobenzoic acid (PABA) applied to human skin (at a dose of 4 $\mu g/cm^2$) was excreted in the urine over five days (approximately 28% of the applied dose). It is important to appreciate, however, that these data were obtained under conditions in which the permeant was applied as a solvent deposited solid. This application method can generate higher absorption values than those that would be obtained using more conventional application techniques. For example, Arancibia et al. (14) applied PABA in three different formulations (a hydroalcoholic gel, an oil-in-water emulsion at pH 4.2, and an oil-in-water emulsion at pH 6.5, each containing 5% PABA) to the face, neck, arms and trunk of human males (20-g application) and subsequently measured urinary excretion over 48 hours. There was no discernible difference in absorption between vehicles, although there was a large variation in the amount absorbed (1.6–9.6% of the applied dose).

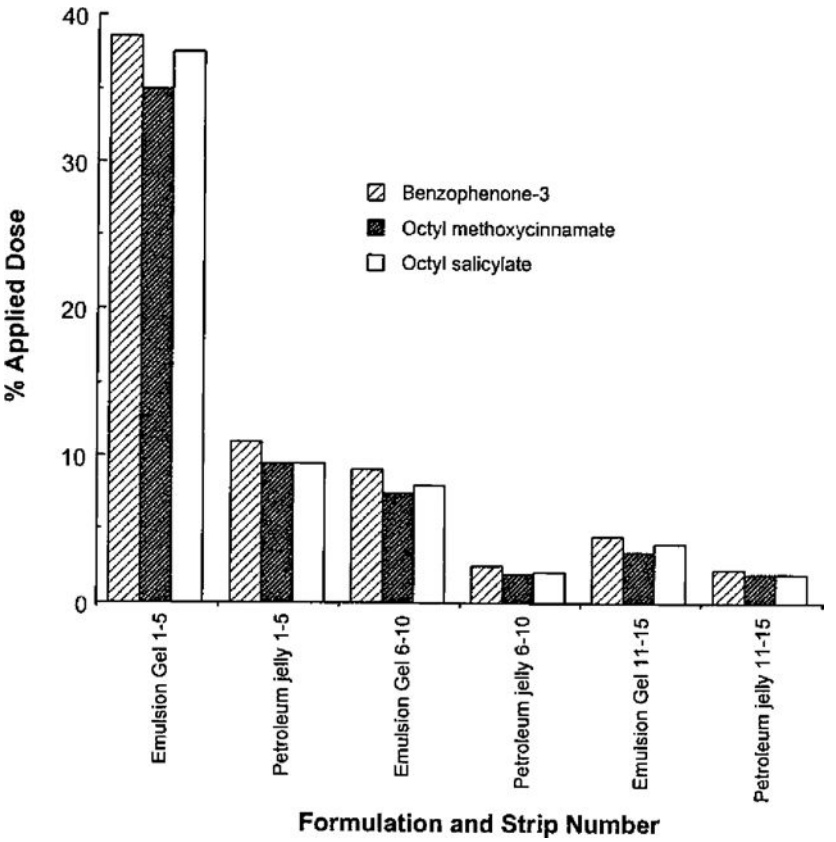


Figure 2 Effect of formulation on the amount of sunscreen agent recovered from stratum corneum tape strips following 30-minute exposure. *Source*: From Ref. 14.

Sunscreen absorption rates based on disappearance measurements after application to the skin may be used wrongly to describe the extent of systemic absorption. Studies on commercial sunscreen products applied to human skin have shown that, whilst the more lipophilic sunscreen actives penetrate the stratum corneum, they do not tend to permeate through into the epidermis (15) and may be eventually lost by desquamation. In contrast, the more polar benzophenone-3 is less tightly bound by the stratum corneum, may permeate further, and thus may be available for systemic absorption (15). These observations are pertinent to the interpretation of the data of Hagerdorn-Leweke and Lippold (16) who determined the human skin permeation of several sunscreen actives in vivo. Each active (octyl dimethyl PABA, 4-isopropyl-dibenzoylmethane, 3-(4-methyl-benzylidine), isoamyl-4-methoxycinnamate, and camphor and benzophenone-3) was applied as a saturated solution in 30% propylene glycol–water, to the skin of the upper arm using glass chambers. Reduction of the permeant in the donor vehicle was assessed hourly for six hours. The calculated maximum flux ranged from $0.53\,\mu g/cm^2$/hour for octyl dimethyl PABA (octanol–water $\log P = 5.75$) to $4.93\,\mu g/cm^2$/hour for isoamyl-4-methoxycinnamate (octanol–water $\log P = 4.83$). There was a correlation between $\log P$ values and skin flux such that maximum flux decreased with increasing lipophilicity. These data were then used to estimate the amount of absorption of a saturated solution

following total body exposure (surface area 1.8 m^2) for one hour. The predicted values ranged from 10 mg for octyl dimethyl PABA to 89 mg for isoamyl-4-methoxycinnamate. It is important to point out, however, that such estimates can be very misleading and not particularly relevant for safety assessment. In this case for example, the estimates were made using data obtained from repetitive infinite doses, of maximum thermodynamic activity, under fully occluded conditions. These conditions constitute an unlikely scenario during actual consumer use of sunscreen products.

Benech-Kieffer et al. (17) evaluated the systemic absorption of a new sunscreen (Mexoryl SX®, terephthalylidine dicamphor sulphonic acid) following application to human skin in an emulsion formulation for four hours and determined a urine recovery of 0.014%. The corresponding in vitro absorption over a period of 24 hours after an application of four hours was 0.16% of the applied dose. The authors canvassed issues such as washing, semi-occlusive properties of the vehicle, the need to use finite "in use" conditions, European Union (EU) safety considerations, and effect of clothing. Solid lipid nanoparticles have been reported to reduce oxybenzone penetration into stratum corneum (18).

The lateral spreading of topically applied compounds through the stratum corneum in vivo is well known. It has been suggested that such spreading may reduce the extent of absorption (19), presumably by reducing the effective concentration gradient for penetration. Jacobi et al. (20) suggested that 3% to 4% and 8% to 15% of a sunscreen (4-methylbenzylidene camphor in an emulsion) had spread outside the area of application after one and six hours, respectively. Tape stripping has been used by a number of other authors to quantify absorption of suncreens in humans in vivo (21,22).

Microfine titanium dioxide (TiO_2) particles are gaining acceptance as a UV filter in sunscreen formulations. Lademann et al. (23) evaluated the penetration of the microparticles into human stratum corneum and follicles using a novel method that allowed exact location of the material following exposure. Briefly, this technique involved a tape-stripping protocol coupled with UV–Vis spectroscopic and X-ray fluorescent measurement to determine distribution of TiO_2 throughout the stratum corneum. An oil-in-water emulsion containing the TiO_2 was applied to the volar forearm of volunteers in multiple doses over three days. As would be expected, the largest concentration of TiO_2 was located in the outer layers of the stratum corneum. Space-resolved Raman spectroscopic measurements allowed determination of TiO_2 in follicular areas. Microparticles were found to be associated in the pilosebaceous orifice regions. The overall conclusions were that no TiO_2 particles permeated completely through the stratum corneum although there was some penetration into the hair follicles.

Similar data were obtained by Bennat and Müller-Goymann (24) who also noted a formulation dependence on TiO_2 distribution. Although there was very little penetration into the deeper layers of the stratum corneum from an aqueous dispersion sunscreen formulation, preparation in an oily dispersion resulted in deeper penetration into skin. The latter effect was attributed to the presence of octyl palmitate in the oily preparation. More recently Pflucker et al. (25), using microscopic analysis of skin punch biopsies after an application of three TiO_2 formulations to the forearm for six hours, revealed that the pigments were located exclusively on the outermost layer of the stratum corneum.

B. Data from In Vitro Human Studies

Data from in vitro human studies should be interpreted carefully. Most such studies use isolated epidermis or dermatomed human skin and artificial receptor solutions.

The choice of receptor conditions may greatly affect the observed extent of absorption and should be made with due consideration to the physicochemical nature of the permeant (7).

Similarly, the composition of the formulation vehicle may also significantly affect penetration. For example, the in vitro skin penetration of padimate O (octyl dimethyl *p*-aminobenzoate) from an alcoholic formulation was greater than from a lotion (26). It was postulated that evaporation of volatile components of the vehicle contributed to the fourfold difference in penetration. Confirmation of the influence of the vehicle of application on the extent of penetration of sunscreen actives has been presented by Marginean Lazar et al. (27). These researchers evaluated the in vitro human skin permeation of octyl methoxycinnamate and butyl methoxy dibenzoylmethane from a series of five emulsion vehicles (a conventional oil-in-water emulsion, an emulsifier-free oil-in-water preparation, a water-in-oil emulsion, a water-in-silicone emulsion, and an oil-in-water emulsion with lamellar liquid crystals). Whereas no sunscreen active was found in receptor solutions following eight-hour exposure to 2% butyl methoxy dibenzoylmethane (irrespective of the vehicle), 8% octyl methoxycinnamate was detected at varying levels depending upon the vehicle. The greatest amount of octyl methoxycinnamate was found following application in an emulsifier-free oil-in-water preparation. The oil-in-water emulsion containing lamellar liquid crystals and the water-in-silicone formulation resulted in the slowest permeation rates of the sunscreen active.

Jiang et al. (28) have reported the in vitro human skin permeation of the commonly used sunscreen active, octyl salicylate (2-ethylhexyl salicylate). Their data, obtained using infinite dose application of the sunscreen at high concentrations in liquid paraffin, indicated relatively low permeation. Furthermore, evidence of self-association of octyl salicylate, at high vehicle concentrations, was presented. This group, using an inert membrane as a reference, showed that the permeation of benzophenone-3 through human skin from different solvents could be attributed to differential effects of the vehicle on activity of the sunscreen in the vehicle and on the intrinsic permeability of the skin (29). They also evaluated the in vitro human skin penetration of sunscreen actives from commercial products intended for use by either adults or children (15). In this study, the penetration into and permeation across isolated epidermal membranes of sunscreen actives (benzophenone-3, octocrylene, octyl salicylate, octyl methoxycinnamate, and butyl methoxydibenzoylmethane) were determined following application of a finite dose (2.0–2.5 mg formulation/cm^2). Only benzophenone-3 was detectable in the receptor phase (4% bovine serum albumin in phosphate buffered saline) and the data indicated that approximately 10% of the applied dose had permeated over the eight-hour exposure period. Significant amounts (5–25 $\mu g/cm^2$, representing 3–14% applied dose) of each of the sunscreen actives were recovered from the epidermal membranes following exposure (Fig. 3). It is interesting to note that penetration of benzophenone-3 through the skin was not significantly different for products intended either for adult use or for child use (Fig. 4). This latter observation is important since the skin surface-body weight ratio is higher in children than in adults and thus the potential systemic load following an equivalent applied dose would be expected to be higher in children than in adults.

Walters et al. (30) have reported the in vitro human skin permeation of octyl salicylate from two vehicles (an oil/water emulsion and a hydro-alcoholic formulation) that were representative of typical commercial sunscreen products. Human abdominal skin obtained at autopsy was heat separated to yield epidermal membranes (comprising stratum corneum and viable epidermis) and mounted in

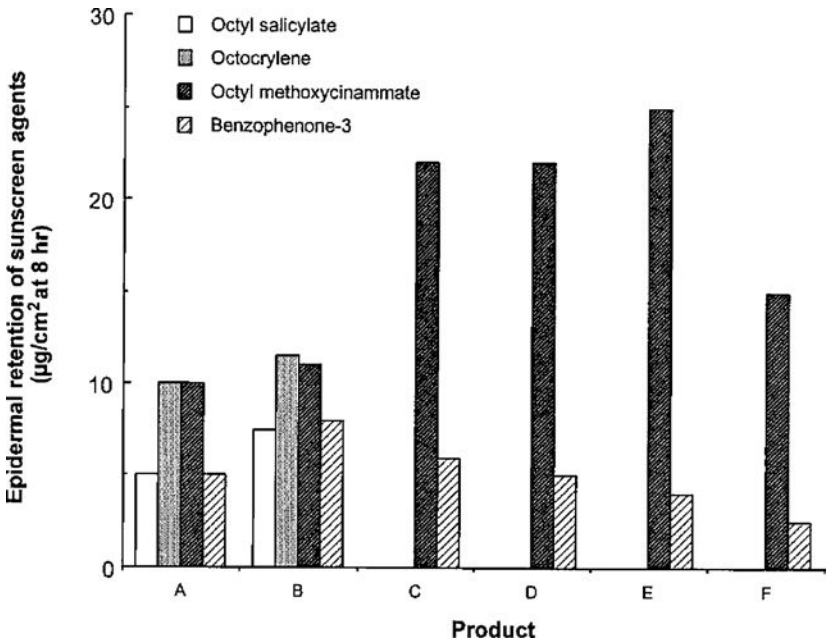


Figure 3 Amount of sunscreen agent recovered from human skin epidermal membranes following eight-hour exposure to several commercial sunscreen products. *Key*: A, Product 1 (adult); B, Product 1 (child); C, Product 2 (adult); D, Product 2 (child); E, Product 3 (adult); F, Product 3 (child). *Source*: From Ref. 15.

glass horizontal-type diffusion cells. Receptor phase solutions consisted of phosphate-buffered saline, pH 7.4, containing 6% Volpo N20 (polyoxyethylene-20-oleyl ether). A finite dose of the oil/water emulsion formulation (5 mg/cm^2) and hydro-alcoholic lotion (5 μL/cm^2) was applied to the skin surface. Permeation of ^{14}C-labeled octyl salicylate was determined by analysis of samples taken from the receptor phase at intervals over 48 hours. The data (Table 2) clearly show that the skin permeation of octyl salicylate from typical sunscreen vehicles was low (<1% over 48 hours), although higher than predicted from physicochemical data. The cumulative percutaneous permeation of ^{14}C-labeled material was very similar in each case (1.58 μg/cm^2 over 48 hours), although the amount of applied material remaining in the epidermal membranes at 48 hours was slightly higher for the hydro-alcoholic solution (32.8%) than the oil/water emulsion (17.2%) (Fig. 5).

Since it might reasonably be expected that vehicles of the type used by Walters et al. (30) would have a greater influence on the cumulative amount of permeant appearing in the receptor phase, these data reflect the importance of the use of final formulations (rather than simple solutions) in the risk assessment of substances intended for topical exposure. However, these data should also be interpreted cautiously. The amount of ^{14}C-labeled material recovered from the skin in vitro may not be truly predictive of the quantity of octyl salicylate remaining within the stratum corneum or epidermis, under user-like conditions, since the surface rinsing procedure used here was not particularly rigorous. Moreover, sunscreen products are typically formulated so as to provide a high degree of skin substantivity (i.e., the sunscreen active is delivered preferentially to the skin surface, where it remains in or on the upper layers of the stratum corneum).

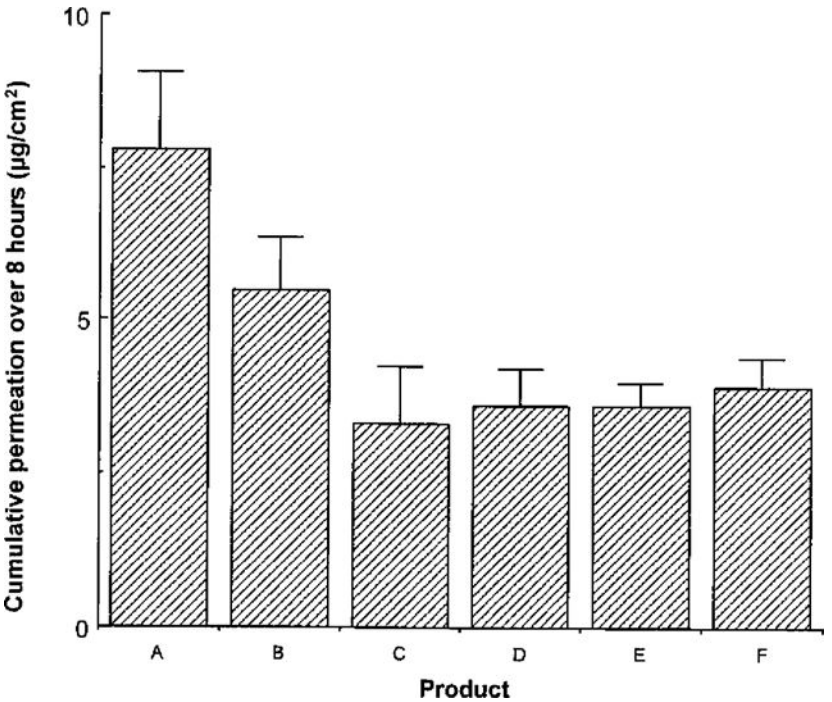


Figure 4 Amount of benzophenone-3 permeated through human skin epidermal membranes following eight-hour exposure to several commercial sunscreen products. *Key*: A, Product 1 (adult); B, Product 1 (child); C, Product 2 (adult); D, Product 2 (child); E, Product 3 (adult); F, Product 3 (child). *Source*: From Ref. 15.

The extent to which various sunscreen agents (octyl methoxycinnamate, benzophenone-4, benzophenone-3, octyl triazone, and octocrylene) were either retained in the stratum corneum or able to permeate through the viable epidermis following application in an oil-in-water emulsion has been evaluated by Potard et al. (31). In general, only a limited amount of all sunscreens, other than benzophenone-3, permeated across the skin. Using the tape-stripping technique, the authors determined that greater than 94% of the applied sunscreen agent was found in the first eight tape strips. The retention of sunscreens in the stratum corneum at 30 minutes and at 16 hours were highly correlated and were in the order: octocrylene, octyl methoxycinnamate $>$ octyl triazone, and benzophenone-3 $>$ benzophenone-4.

Table 2 Permeation and Recovery Data for Octyl Salicylate after Application as a Finite Dose

Parameter	Hydroalcoholic lotion	O/W emulsion
Total permeated at 48 hr ($\mu g/cm^2$)	1.58 ± 0.25[a]	1.58 ± 0.36
Total % absorption at 48 hr	0.59 ± 0.09	0.65 ± 0.16
Recovery in wash (%)	36.21 ± 5.98	36.66 ± 5.31
Recovery in skin (%)	32.77 ± 4.74	17.18 ± 1.28
Total recovery (%)	69.57 ± 6.84	54.50 ± 5.47

[a]Data are means $\pm$ SE (n=9–11).
Source: From Ref. 30

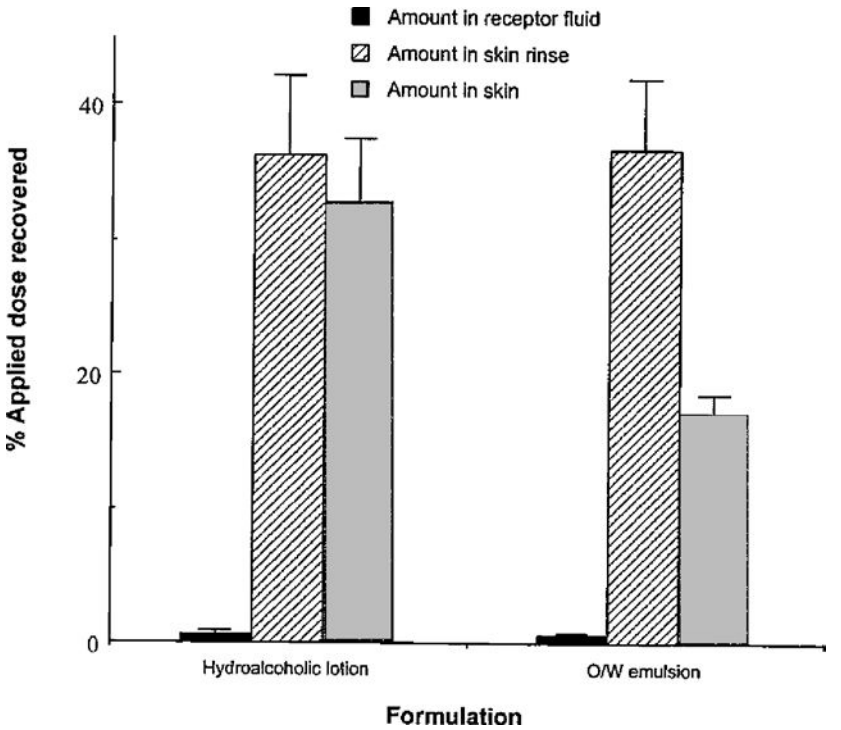


Figure 5 Recovery of octyl salicylate from various compartments following 48-hour exposure to two different formulations. Human skin epidermal membranes. *Source*: From Ref. 30.

Recently, Cross et al. (32) examined the effect of viscosity on the human skin penetration of sunscreens using infinite dosing and in-use applications. The authors found that, whereas increasing the viscosity of the vehicle decreased penetration fluxes under infinite dosing conditions, fluxes following in-use (or finite) doses had the opposite effect (Fig. 6A). It was suggested that the reduced penetration in the infinite dosing case reflects a diminished diffusivity of sunscreen in the vehicle. In contrast, a high-viscosity product under "in-use" conditions was postulated to have promoted penetration via a greater stratum corneum hydration relative to lower viscosity products (Fig. 6B). The results emphasised and supported the need for skin permeation studies to be conducted under "in-use" conditions in order to more closely represent application conditions used in practice. Risk assessment for a UV filter in the EU is based on an amount of $2\,mg/cm^2$ of a sunscreen product typically being applied to the skin (33). Table 3 gives a summary of some of the studies on human skin permeation of sunscreen actives.

C. Animal Models

In evaluating the significance of the results from studies utilizing animal models, it is very important to appreciate that, in the majority of cases, permeation data obtained, using small animal skin (e.g., rat, mouse, and guinea pig) gives much higher absorption values than that obtained using human skin (34). Any data from studies using animal models should, therefore, be extrapolated to the human situation only with great caution.

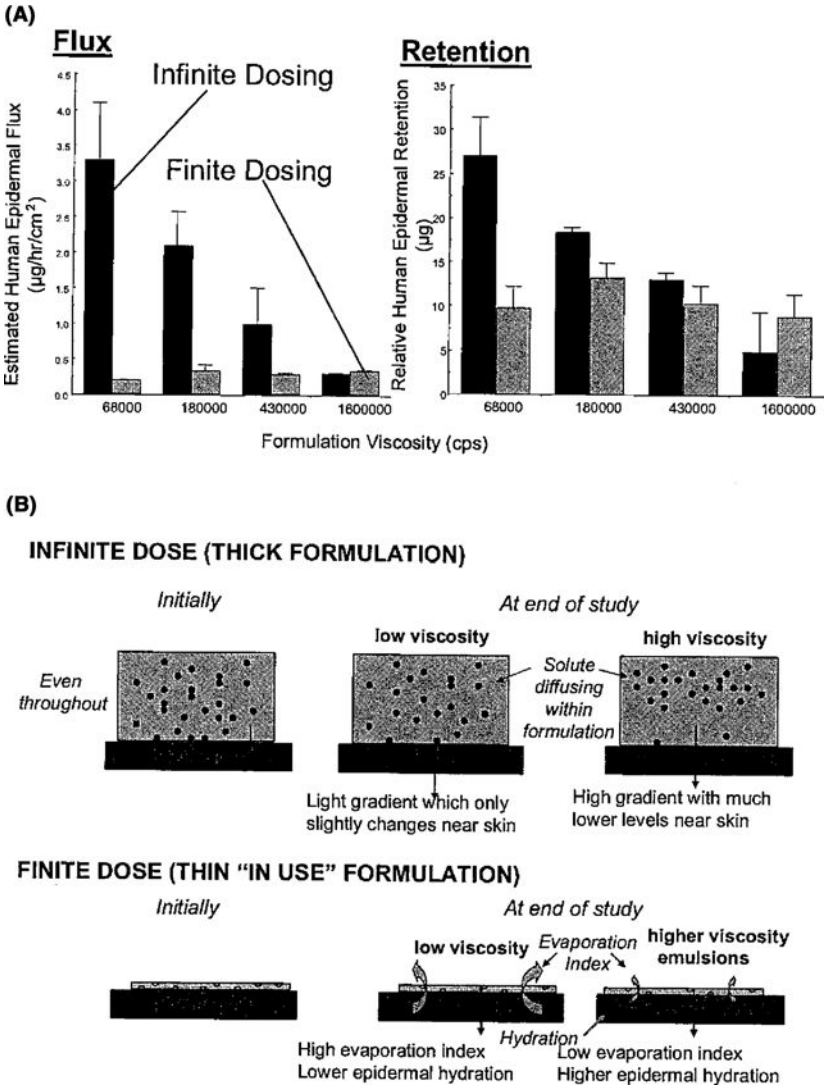


Figure 6 (**A**) Effect of formulation viscosity on epidermal flux and retention of oxybenzone. (**B**) Diagrammatic representation of possible processes involved. *Source*: From Ref. 32.

Following dermal application of up to 800 μg/cm^2 of benzophenone-3 to rats, urinary, and fecal excretion (collected over 72 hours) amounted to 13.2% to 39.2% and 3.71% to 6.67% of the applied dose, respectively (35). Benzophenone-3 was shown to readily cross rat skin (36). In contrast, quaternary ammonium benzophenones showed no detectable skin penetration over 45 hours when applied to hairless mouse skin in vitro (37).

Brinon et al. (38) evaluated the effect of formulation vehicle on the permeation of benzophenone-4 across full-thickness hairless rat skin following application of an infinite dose. Using an aqueous solution of benzophenone-4 as the control, steady-state flux was determined over 48 hours from a series of emulsions prepared using different surfactant systems. The results showed variation in steady-state flux between 10 ± 6 and 86 ± 7 μg/cm^2/hour (aqueous solution control: 32 ± 24 μg/

Table 3 Reported Human Skin Absorption of Sunscreen Actives

Sunscreen	Type of test	Dose absorbed (%)	Exposure time (hr)	Flux ($\mu g/cm^2/hr$)	Vehicle	Other	References
p-Aminobenzoic acid	In vivo	1.6–9.6	48		Hydroalcoholic gel o/w emulsion		(14)
	In vivo	28.37 urine	120		Solvent deposited solid radiolabel		(13)
Benzophenone-3 (oxybenzone)	In vivo	Loss from donor	6	4.44	Propylene glycol	Permeability: 0.053 cm/hr	(15)
	In vitro	5.3–6.4	6		o/w emulsion gel and petrolatum		(11)
	In vitro	5–10 receptor, 4–12 skin	8		Commercial formulations		(15)
	In vivo	1–2 urine	10		Commercial formulation		(8)
	In vivo	0.5 urine	48		Commercial formulation		(10)
Homosalate	In vivo	1.08–4.43	24		8% lotion		(58)
2-Hydroxy-4-methoxybenzo-phenone-5-sulphonic acid	In vivo	6	16		o/w emulsion radiolabel		(16)
Isoamyl-*p*-methoxy-cinnamate	In vivo	Loss from donor	6	3.16	Propylene glycol	Permeability: 0.105 cm/hr	(16)
4-Isopropyl-dibenzoylmethane	In vivo	Loss from donor	6	0.85	Propylene glycol	Permeability: 0.277 cm/hr	(16)
3-(4-methylbenzyl-idene)-camphor	In vivo	Loss from donor	6	2.11	Propylene glycol	Permeability: 0.091 cm/hr	(16)
Octyl dimethyl PABA	In vivo	Loss from donor	6	0.53	Propylene glycol	Permeability: 0.259 cm/hr	(16)
Octyl methoxy-cinnamate	In vitro	10	16		o/w emulsion		(40)
	In vitro	1.6–9.3	6		o/w emulsion gel and petrolatum	In skin only, none in	(11)

(*Continued*)

Table 3 Reported Human Skin Absorption of Sunscreen Actives (*Continued*)

Sunscreen	Type of test	Dose absorbed (%)	Exposure time (hr)	Flux ($\mu g/cm^2/hr$)	Vehicle	Other	References
						receptor	
	In vitro	7–17	8		Commercial formulations	In skin only, none in receptor	(15)
Octyl salicylate	In vitro	1.9–7.7	6		o/w emulsion gel and petrolatum	In skin only, none in receptor	(11)
	In vitro	0.59–0.65	48		Alcoholic and o/w emulsion	Cum. absorption 1.58 $\mu g/cm^2$	(30)
	In vitro	5–7	8		Commercial formulations	In skin only, none in receptor	(15)
TEA salicylate	In vivo	0.8–26.8 urine	24		10% cream		(58)

Note: Exposure periods and application condition vary.

cm^2/hour) depending on the surfactant system used. The data indicated that flux of the sunscreen active from simple emulsion systems was low compared to that from more complex liquid crystalline emulsions. It should be pointed out, however, that the concentration of benzophenone-4 in all systems was kept constant (2.5%) and it is possible that solubility of the sunscreen in the formulation may have varied resulting in differences in thermodynamic activity of the permeant within the formulation. Nonetheless, these data suggest that manipulation of the formulation vehicle may be a means of reducing the percutaneous absorption of sunscreen actives. Subsequent to this work, Brinon et al. (39) measured the permeation of benzophenone-4 and octyl methoxycinnamate from several surfactant solutions through pig skin in vitro. The latter results showed variation in the steady-state flux of benzophenone-4 from 0.8 ± 0.2 to 32 ± 9 $\mu g/cm^2$/hour and that of octyl methoxycinnamate from 0.1 ± 0.1 to 0.6 ± 0.1 $\mu g/cm^2$/hour dependent on the surfactant system. The authors concluded that it was possible that the liquid crystalline phases modified either the vehicle-stratum corneum partition coefficient or the properties of the stratum corneum.

More relevant results (i.e., pertinent to actual product use) were presented by Benech-Keiffer et al. (40) who applied a finite dose of the oil soluble sunscreen active, octyl methoxycinnamate, and the water soluble, benzophenone-4, in an oil-in-water emulsion formulation to fuli-thickness and split-thickness human and pig skin in vitro. They suggested that the majority of the applied dose of the two sunscreens remained on the skin surface after 16 hours of exposure and that the amount penetrating into the receptor solution was low. They concluded that pig skin may be used as an alternative to human skin for the prediction of in vivo systemic exposure.

Gupta et al. (41) emphasised the influence of formulation effects on skin absorption by determining the permeation and skin distribution of octyl methoxycinnamate and benzophenone-3, from either a hydro-alcoholic or an oil based vehicle, using pig skin in vitro. Permeation was measured from systems containing either the two sunscreens individually or in combination. Permeation of sunscreen through the skin and into the receptor fluid was low in all cases, but was somewhat higher when applied in the hydro-alcoholic vehicle (but still less than 0.5% of the applied dose in most cases). This latter observation presumably the result of altered vehicle-skin partitioning induced by sunscreen solubility changes as the alcohol evaporated. On the other hand, when the amount of sunscreen found in the viable epidermal tissue was taken into account, penetration increased to approximately 12.5% and approximately 3% of the applied dose for the hydro-alcoholic and oil based vehicles, respectively. Interestingly, when applied in combination, the two sunscreens tended to slightly reduce overall penetration of each other when applied in the hydro-alcoholic vehicle, but this was reversed for the oily vehicle. Furthermore, the authors found that there was an increased stratum corneum to penetrated ratio for the combination products (which occurred for both vehicles but was more apparent for the oily vehicle). This observation is of fundamental importance to the function of sunscreens where the basic requirement is for broad spectrum UV protection coupled with high retention of sunscreen in the stratum corneum. Fernandez et al. (42) used pig skin to show that minimal penetration of oxybenzone into the skin was facilitated using vehicles with a higher oxybenzone solubility and a low polarity. Fernandez et al. (22) then compared the penetration of benzophenone-3 from a range of vehicles using excised pig skin and human subjects in vivo. They suggested similar results for the two types of skin and significant differences in stratum corneum benzophenone-3 concentrations for the different vehicles used. Godwin

et al. (43), using hairless mouse skin in vitro, suggested that the penetration enhancer Transcutol® CG increased the skin accumulation of the UV absorbers oxybenzone and cinnamate without affecting the epidermal permeation rate.

III. PREDICTION OF THE SKIN PENETRATION OF SUNSCREENS

Watkinson et al. (6) have predicted the skin penetration of various sunscreen agents based on mathematical modeling. The model took into account the physicochemical characteristics of each permeant in approximating several parameters important in the prediction of percutaneous absorption: (a) partition of the permeant from vehicle into stratum corneum; (b) passive diffusion of the permeant across stratum corneum; (c) partitioning of the permeant at the junction between stratum corneum and viable tissue; (d) uptake into systemic blood circulation and elimination of the permeant; (e) potential return of the permeant into vehicle from stratum corneum; (f) potential return of the permeant to stratum corneum from viable tissue; (g) potential return of the permeant to viable tissue from blood.

As for any mathematical modeling of permeation, several assumptions were made in the generation of rate constants. These included (a) the first-order rate constant described the partitioning from vehicle into stratum corneum (k_a which is dependent on diffusion through the vehicle); (b) partitioning into skin was a ratio of k_a and k_r (the rate constant for diffusion from stratum corneum back into vehicle); (c) diffusion across stratum corneum was predicted from molecular weight (M)($k_1 = D/h^2$, where D is the diffusion coefficient and h is the path length for diffusion); (d) partitioning from the stratum corneum into the viable tissue was determined from the molecular weight and the octanol-water partition coefficient (calculated by the Hansch group contribution method) as the ratio k_2/k_3 (k_2 is the rate constant from stratum corneum into viable tissue; k_3 is the rate constant from viable tissue back into stratum corneum); (e) permeants with melting points below ambient temperatures were assumed to possess very large stratum corneum solubilities; (f) the applied dose was assumed as $40\,\mu g/cm^2$; (g) exposure time was 12 hours; (h) the area of application was $1.4\,m^2$ estimated as 75% of the total average skin surface area.

Thus, estimation of k_1 from molecular weight (M), for $M < 740$ and estimation of the diffusion across viable tissue, k_2 were made using:

$$k_1(h^{-1}) = 0.91M^{-\gamma_3}$$

$$k_2(h^{-1}) = 14.4M^{-\gamma_3}$$

and estimation of partitioning between the stratum corneum and viable tissue, where K_{oct} is the octanol–water partition coefficient was made using:

$$k_3 = k_2 K_{oct}/5$$

Estimation of stratum corneum solubility was made using melting point (M_p):

$$\log[SC] = 1.911 \times 10^3/M_p - 2.956$$

Although, based on their predictions, the authors suggest that systemic absorption of some sunscreen actives across large areas of skin may occur at significant levels after long periods of exposure, only minor amounts of the most lipophilic compounds were expected to penetrate. For example, octyl salicylate had a calculated

Table 4 Relationship Between Predicted Human Skin Absorption and Calculated Octanol-Water Partition Coefficients (log *P*) for Selected Sunscreen Agents

Compound	Absorption[a] μg/1.4 m^2	Calculated log P[b]
2-Ethylhexyl salicylate	0.50	6.19
p-Aminobenzoic acid	21,000	1.00
4-lsopropyl-dibenzoylmethane	61	4.06
2-Hydroxy-4-methoxy benzophenone	100	3.87
2-Ethylhexyl-*p*-methoxycinnamate	0.75	6.40

[a]Predicted total body absorption in six hours.
[b]Calculated using Hansch group contribution method.
Source: Ref. 6.

systemic availability over 12 hours from an application to 1.4 m^2 of 3.3 μg in total. Examples of predicted values for dermal absorption of typical sunscreen agents using this model are given in Table 4. It is important to appreciate, however, that predictive estimates of the extent of skin absorption are of limited value unless the estimates and assumptions within the model are rigorous. Models of this type often ignore the potential for biotransformation or degradation that may modify the dermal penetration characteristics and toxicity profile of the original chemical. Furthermore, many variables associated with actual product use will alter the extent of skin penetration of sunscreen actives. For example, frequent reapplication (as is recommended), vehicle release and formulation excipients may affect skin permeability. It is essential, therefore, that for risk assessment purposes more accurate determinations of skin permeation are obtained (44).

IV. RISKS AND BENEFITS ASSOCIATED WITH TOPICAL SUNSCREEN USE

The penetration of certain sunscreen agents into the skin and the subsequent potential systemic absorption needs to be examined in the context of the widespread use of these agents to protect against sunburn, photo-ageing, and skin cancer. Although applied to large areas of the body, in some cases on a very frequent basis, few adverse reactions appear to be evident. Generally, sunscreens have already undergone vigorous cytotoxicity, phototoxicity, photogenotoxicity, and ocular/cutaneous screening in accordance with guidelines laid down by regulatory authorities (4,33). Nohynek and Schaefer (33) point out that the hazards of not using sunscreens far outweigh any hazards associated with their use. They quote data showing skin cancer has an incidence of 780 per 100,000 in the United States and about 2000 per 100,000 people in subtropical Australia. The corresponding melanoma incidences are 14.2 per 100,000 in the United States and 55.8 per 100,000 in subtropical Australia. They further suggest that inappropriate claims about sunscreen toxicity is dangerous if they lead to a reduced use and a subsequent increase in UV-induced skin damage and skin cancers.

Poorly expressed outcomes can wrongly suggest that sunscreens are inappropriate. For instance, the human data (8,10) strongly contradicts the statement by Felton et al. (45) that "a number of commonly used UV absorbers ... have been

shown to rapidly penetrate the skin and reach the systemic circulation, leaving the skin unprotected against the harmful radiation of the sun.'' Hayden et al. (8) and Gustavsson et al. (10) have shown that, based on urinary excretion, the amount of actual sunscreen absorbed in human volunteers after topical application is less than 2% of the applied amount. A somewhat higher penetration of between ~2% and ~5% absorption is deduced from human skin stripping studies (11).

Sunscreens have been associated with photocontact allergic reactions (47–49). However, the incidence of allergy in the exposed population is rare (50). Xu et al. (51) have suggested that sunscreens may lead to phototoxicity in melanocytes but not keratinocytes. However, recent data from Hayden et al. (52) suggests that when the extent of ''binding'' of sunscreens is accounted for in the comparison of epidermal penetration and toxicity of sunscreens to cultured keratinocytes, the concentrations required to cause such toxicity is several orders of magnitude greater than the actual concentrations likely to be present in the viable epidermis.

Perhaps a greater concern associated with the use of sunscreens is their potential to enhance the absorption of other applied compounds, especially for those sunscreens included in barrier products. Their penetration enhancement potential has been recognized as a benefit in facilitating therapeutic action of topically applied drugs (53). Octyl salicylate was reported to increase testosterone skin permeation 6.3-fold, whereas padimate 0 increased that of testosterone, estradiol, and progesterone by 2.4, 3.5, and 9.3-fold, respectively, relative to controls (53). However, sunscreens have also been shown to promote the skin penetration of some potentially hazardous agents applied to the skin. Brand et al. (54) and Brand and colleagues (55) showed that the application of sunscreen formulations 30 minutes prior to application of the herbicide 2,4-dichlorophenoxyacetic acid significantly increased the hairless mouse skin penetration of the herbicide from six of the nine commercially available products. The greatest enhancement ratio found for any of the sunscreens was 2.1. However, recognizing the unique sensitivity to enhancement of hairless mouse skin and the innate variability in human skin, it is unlikely that the reported enhancement will prove to be of any greater concern than that already associated with topical exposure to 2,4-dichlorophenoxyacetic acid. Interestingly, Gupta et al. (41) has suggested that co-administration of octyl methoxycinnamate to pig skin reduces the penetration of topically applied oxybenzone.

V. CONCLUSIONS

In most countries, the marketing of sunscreen products is subject to significant regulatory controls. Following extensive review of safety and efficacy, only certain sunscreen actives are permitted for use within allowable concentration ranges. In addition, combination of individual actives within the same product is also highly controlled. Because of the ingenuity of formulators and the careful use of combinations of sunscreen actives, today's sunscreen products contain lower concentrations of active ingedients than ever before. Despite the widespread use of sunscreens, only small numbers of adverse reactions, mainly consisting of contact or photocontact allergies, have been reported. Sunscreen products provide protection against skin cancer and guard against sunburn and many cumulative, suberythemal forms of skin damage. As such, sunscreen products may be assumed to be amongst the safest of consumer products. Nevertheless, as new information on the toxicological properties of individual sunscreen actives emerges, it may be necessary to conduct a

risk assessment of the safety of sunscreen products. Under these circumstances, it may be useful to evaluate the percutaneous absorption of sunscreens (see, e.g., Refs. 6 and 56).

It may be concluded from the examples described here that there are two factors in particular that are important when considering the skin penetration and permeation of sunscreen actives: (a) that the vehicle of application can markedly influence the rate, skin distribution and extent of percutaneous absorption and (b) that those sunscreen actives with high lipophilicity will possess a greater affinity for the stratum corneum which will tend to reduce diffusion to deeper layers of the skin. However, studies on the percutaneous penetration of octyl salicylate from representative sunscreen formulations through human skin in vitro (30) illustrate that although it is possible to predict the penetration of sunscreen agents and to speculate how penetration may be modulated by various types of vehicle, there is no substitute for conducting finite-dose experiments using human skin and actual formulations of interest when the data is to be used for risk assessment of substances intended for topical exposure. The influence of formulation vehicle and quantification of penetration rates and skin distribution using experiments designed to mimic actual product use are essential prerequisites to the generation of realistic risk assessment values.

ACKNOWLEDGMENTS

The authors are indebted to Cameron Hayden for his unreserved advice and assistance in the preparation of this chapter. We also grateful to Sheree Cross for drawing and providing Figure 6 and to Eloise Larsen for assistance in literature searching. MSR thanks the NHMRC (Australia) and the PAH Research Foundation for their support.

REFERENCES

1. Naylor MF, Farmer KC. The case for sunscreens. A review of their use in preventing actinic damage and neoplasia. Arch Dermatol 1997; 133:1146–1154.
2. Ting WW, Vest CD, Sontheimer R. Practical and experimental consideration of sun protection in dermatology. Int J Dermatol 2003; 42:505–513.
3. Hayden CJG, Roberts MS, Benson HAE. Sunscreens; are Australians getting the good oil? Aust NZ J Med 1998; 28:639–646
4. Federal Register Sunscreen drug products for over-the-counter human use; final monograph. Fed Reg 1999; 64:27666 (May 21).
5. Hayden CGJ, Benson HAE, Roberts MS. Sunscreens: toxicological aspects. In: Roberts MS, Walters KA, eds. Dermal Absorption and Toxicity Assessment. New York: Marcel Dekker, 1998:537–599.
6. Watkinson AC, Brain KR, Walters KA, Hadgraft J. Prediction of the percutaneous penetration of ultra-violet filters used in sunscreen formulations. Int J Cosmet Sci 1992; 14:265–275.
7. Gettings SD, Howes D, Walters KA. Experimental design considerations and use of in vitro skin penetration data in cosmetic risk assessment. In: Roberts MS, Walters KA, eds. Dermal Absorption and Toxicity Assessment. New York: Marcel Dekker, 1998: 459–487.

8. Hayden CGJ, Roberts MS, Benson HAE. Systemic absorption of sunscreen after topical application. Lancet 1997; 350:863–864.
9. Hany J, Nagel R. Detection of sunscreen agents in human breast milk. Dtsch Lebensm Rundsch 1995; 91:341–345.
10. Gustavsson GH, Farbrot A, Larko O. Percutaneous absorption of benzophenone-3, a common component of topical sunscreens. Clin Exp Derm 2002; 27:691–694.
11. Treffel P, Gabard B. Vehicle influence on the in vitro skin penetration of ultra-violet filters used in sunscreen formulations. In: Brain KR, James VJ, Walters KA, eds. Prediction of Percutaneous Penetration. Vol. 4b. Cardiff: STS Publ, 1996:178–181.
12. Treffel P, Gabard B. Skin penetration and sun protection factor of ultra-violet filters from two vehicles. Pharm Res 1996; 13:770–774.
13. Feldman R, Maibach H. Absorption of some organic compounds through the skin in man. J Invest Dermatol 1970; 54:399–404.
14. Arancibia A, Borie G, Cornwell E, Medrano C. Pharmacokinetic study on the percutaneous absorption of p-amino-benzoic acid from 3 sunscreen preparations. Farmaco Ed Prat 1981; 36:357–365.
15. Jiang R, Roberts MS, Collins DM, Hoffmann NV, Benson HAE. Absorption of sunscreens into human skin: an evaluation of a number of commercial products. Br J Clin Pharmacol 1998; 48:635–637.
16. Hagedorn-Leweke U, Lippold BC. Absorption of sunscreens and other compounds through human skin in vivo: derivation of a method to predict maximum fluxes. Pharm Res 1995; 12:1354–1360.
17. Benech-Kieffer F, Meuling WJA, Leclerc C, Roza L, Leclaire J, Nohynek G. Percutaneous absorption of Mexoryl SX® in human volunteers: comparison with in vitro data. Skin Pharmacol Appl Skin Physiol 2003; 16:343–355.
18. Wissing SA, Muller RH. Solid lipid nanoparticles as carrier for sunscreens: in vitro release and in vivo skin penetration. J Contr Rel 2002; 81:225–233.
19. Ashworth J, Watson WS, Finlay AY. The lateral spread of clobetasol 17-propionate in the stratum corneum in vivo. Brit J Pharmacol 1998; 119:351–358.
20. Jacobi U, Weigmann HJ, Baumann M, Reiche AI, Sterry W, Lademann J. Lateral spreading of topically applied UV filter substances investigated by tape stripping. Skin Pharmacol Physiol 2004; 17:17–22.
21. Couteau C, Perez Cullel N, Connan AE, Ciffard LJM. Stripping method to quantify absorption of two sunscreens in human. Int J Pharm 2001; 222:153–115.
22. Fernandez C, Marti-Mestres G, Ramos J, Maillots H. LC analysis of benzophenone-3: II application to determination of 'in vitro' and 'in vivo' skin penetration from solvents, coarse and submicron emulsions. J Pharm Biomed Anal 2000; 24:155–165.
23. Lademann J, Weigmann HJ, Rickmeyer C, Barthelmes H, Schaefer H, Mueller G, Sterry W. Penetration of titanium dioxide microparticles in a sunscreen formulation into the horny layer and the follicular orifice. Skin Pharmacol Appl Skin Physiol 1999; 12: 247–256.
24. Bennat C, Müller-Goymann CC. Skin penetration and stabilization of formulations containing microfine titanium dioxide as physical UV filter. Int J Cosmet Sci 2000; 22: 271–283.
25. Pflucker F, Wendel V, Hohenberg H, Gartner E, Will T, Pfeiffer S, Wepf R, Gers-Barlag H. The human stratum corneum layer: an effective barrier against dermal uptake of different forms of topically applied micronised titanium dioxide. Skin Pharmacol Appl Skin Physiol 2001; 14(supp 1):92–97.
26. Kenney G, Sakr A, Lichtin J, Chou H and Bronaugh R. In vitro skin absorption and metabolism of padimate O and a nitrosamine formed in padimate O–containing cosmetic products. J Soc Cosmet Chem 1995; 46:117–127.
27. Marginean Lazar G, Baillet A, Fructus AE, Arnaud-Battandier J, Ferrier D, Marty JP. Evaluation of in vitro percutaneous absorption of UV filters used in sunscreen formulations. Drug Cosmet Ind 1996; 158:50–62.

28. Jiang R, Roberts MS, Prankerd RJ, Benson HAE. Percutaneous absorption of sunscreen agents from liquid paraffin: selt association of octyl salicylate and effects on skin flux. J Pharm Sci 1997; 86:791–796.
29. Jiang R, Benson HAE, Cross SE, Roberts MS. In vitro human epidermal and polyethylene membrane and penetration of the sunscreen benzophenone-3 from a range of solvents. Pharm Res 1998; 15:1863–1868.
30. Walters KA, Brain KR, Howes D, James VJ, Kraus AL, Teetsel NM, Toulon M, Watkinson AC, Gettings SD. Percutaneous penetration of octyl salicylate from representative sunscreen formulations through human skin in vitro. Fd Chem Toxicol 1997; 35: 1219–1225.
31. Potard G, Laugel C, Schaefer H, Marty JP. The stripping technique: In vitro absorption and penetration of five UV filters on excised fresh human skin. Skin Pharmacol Appl Skin Physiol 2000; 13:336–344.
32. Cross SE, Jiang R, Benson HAE, Roberts MS. Can increasing the viscosity of formulations be used to reduce the human skin penetration of the sunscreen oxybenzone? J Invest Dermatol 2001; 117:147–150.
33. Nohynek GJ, Schaefer H. Benefit and risk of organic ultraviolet filters. Reg Toxicol Pharmacol 2001; 33:285–299.
34. Walters KA, Roberts MS. Veterinary applications of skin penetration enhancers. In: Walters KA, Hadgraft J, eds. Pharmaceutical Skin Penetration Enhancement. New York: Marcel Dekker, 1993:345–364.
35. El Dareer S, Kalin J, Tillery K, Hill D. Disposition of 2-hydroxy-4-methoxybenzophenone in rats dosed orally, intravenously, and topically. J Toxicol Environ Health 1986; 19:491–502.
36. Okereke CS, Abdel-Rahman MS, Friedman MA. Disposition of benzophenone-3 after dermal administration in male rats. Toxicol Lett 1994; 73:113–122.
37. Monti D, Saettone MF, Centini M, Anselmi C. Substantivity of sunscreens— in vitro evaluation of the transdermal permeation characteristics of some benzophenone derivatives. Int J Cosmet Sci 1993; 15:45–52.
38. Brinon L, Geiger S, Alard V, Tranchant JF, Pouget T, Couarraze G. Influence of lamellar liquid crystal structure on percutaneous diffusion of a hydrophilic tracer from emulsions. J Cosmet Sci 1998; 49:1–11.
39. Brinon L, Geiger S, Alard V, Doucet J, Tranchant JF, Couarraze G. Percutaneous absorption of sunscreens from liquid crystalline phases. J Contr Rel 1999; 60:67–76.
40. Benech-Keiffer F, Wegrich P, Schwarzenbach R, Klecak G, Weber T, Leclaire J, Schaefer H. Percutaneous absorption of sunscreens in vitro: interspecies comparison, skin models and. reproducibility aspects. Skin Pharmacol Appl Skin Physiol 2000; 13: 324–335.
41. Gupta PK, Zatz JL, Rerek M. Percutaneous absorption of sunscreens through micro-Yucatan pig skin in vitro. Pharm Res 1999; 16:1602–1607.
42. Fernandez C, Marti–Mestres G, Mestres JP, Maillols H. LC analysis of benzophenone-3 in pigskin and in saline solution: Application to determination of in vitro skin penetration. J Pharm Biomed Anal 2000; 22:393–402.
43. Godwin DA, Kim N, Felton LA. Influence of Transcutol^{R} CG on the skin accumulation and transdermal permeation of ultraviolet absorbers. Eur J Pharm Biopharm 2002; 53: 23–27.
44. Gettings SD, Azri-Meehan S, Demetrulias JL, Dressier WE, Kasting GB, Kelling CK, Howes D. The use of in vitro skin penetration data in the safety assessment of cosmetic formulations. In: Brain KR, James VJ, Walters KA, eds. Prediction of Percutaneous Penetration. Vol. 3b. Cardiff: STS Publ, 1993:621–637.
45. Felton LA, Wiley CJ, Godwin DA. Influence of hydroxypropyl-beta-cyclodextrin on the transdermal permeation and skin accumulation of oxybenzone. Drug Dev Ind Pharm 2002; 28:1117–1124.

46. Wissing SA, Muller RH. Solid lipid nanoparticles as carrier for sunscreens: in vitro release and in vivo skin penetration. J Contr Rel 2002; 81:225–233.
47. Schauder S, Ippen H. Contact and photocontact sensitivity to sunscreens. Review of a 15-year experience of the literture. Contact Dermatitis 1997; 37:221–232.
48. Carrotte-Lefebvre I, Bonnevalle A, Segard M, Delaporte E, Thomas P. Contact allergy to octocrylene. First 2 cases. Contact Dermatitis 2003; 48:45–55.
49. Zhang XM, Nakagawa M, Kawai K, Kawai K. Erythema-multiforme-like eruption following photoallergic contact dermatitis from oxybenzone. Contact Dermatitis 1998; 38:43–44.
50. Mancel E, Drouet M, Sabbah A, Avenal-Audran M. Allergy to sunscreens. Allerg Immunol 1999; 31:195–199.
51. Xu C, Green A, Parisi A, Parsons PG. Photosensitization of the sunscreen octyl p-dimethylaminobenzoate by UVA in human melanocytes but not keratinocytes. Photochem Photobiol 2001; 73:600–604.
52. Hayden CGJ, Cross SE, Anderson C, Saunders NA, Roberts MS. Sunscreen human skin penetration and related human keratinocyte toxicity after topical application. Skin Pharmacol Physiol 2005; 18:170–174.
53. Morgan TM, Reed BL, Finnin BC. Enhanced skin permeation of sex hormones with novel topical spray vehicles. J Pharm Sci 1998; 87:1213–1218.
54. Brand RM, Spaulding M, Mueller C. Sunscreens can increase dermal penetration of 2,4-dichlorophenoxyacetic acid. J Toxicol Clin Toxicol 2002; 40:827–832.
55. Pont AR, Charron AR, Brand RM. Active ingredients in sunscreens act as topical penetration enhancers for the herbicide 2,4-dichlorophenoxyacetic acid. Toxicol Appl Pharmacol 2004; 195:348–354.
56. Agin P, Anthony FA, Hermensky S. Oxybenzone in sunscreen products. Lancet 1998; 351:525.
57. Klein K, Steinberg D. Encyclopedia of UV absorbers. In: Sun Products, Protection and Tanning. Carol Stream: Allured Publishing Corporation, 1998:11–65.
58. Federal Register. Sunscreen drug products for over the counter human drug use: establishment of a monograph. Fed Reg 1978; 43:38206 (Aug 25).

52

Use of Microemulsions for Topical Drug Delivery

Sandra Heuschkel, Anuj Shukla, and Reinhard H. H. Neubert
Department of Pharmacy, Institute of Pharmaceutics and Biopharmaceutics, Martin-Luther-University Halle-Wittenberg, Halle (Saale), Germany

I. INTRODUCTION

During the past several years great efforts have been made in dermatopharmaceutical research for the development of new drug delivery systems having a colloidal phase as key prerequisite for their effectiveness. Among micelles, mixed micelles, nanoparticles, and liposomes, microemulsions (MEs) play the most important role and represent a promising alternative to conventional formulations.

MEs are formed combining appropriate amounts of a hydrophilic and a lipophilic phase as well as a surfactant. Mostly a cosurfactant is required additionally. Depending on the oil-to-water ratio and the physicochemical features of the surfactants, contained in the ME, a characteristic microstructure of either small oil droplets in an aqueous surrounding (o/w) or water droplets in an oil continuous matrix (w/o) exists. However, bicontinuous structures are also possible.

MEs exhibit the following properties:

- thermodynamic stability
- very low surface tension of $<10^{-3}$ N/m
- optical isotropy
- transparency or slight opalescence
- low viscosity
- particle size of the colloidal phase in the range of 10 to 200 nm
- highly dynamic structures due to fluctuating surfaces.

Due to these special features several advantages in terms of preparation and pharmaceutical use of MEs result, such as:

- spontaneous formation without energy input,
- long-term stability,
- high variability of the composition depending on the surfactant system used,
- high solubilization capacity for hydrophilic and lipophilic drugs,
- improvement of both dermal and transdermal drug delivery,
- drug localizer effect depending on the components.

Basic research interests are development, characterization, and drug delivery potential of MEs. The latter provides a wide range of pharmaceutical applications that ensure improved topical and systemic drug availability, such as in oral, parenteral, dermal, and ophthalmic administration (1–4).

The purpose of this chapter is to give an overview about selected methods for the physicochemical characterization of MEs and current developments in the field of cutaneous application.

II. CHARACTERIZATION

Basic components in a physicochemical characterization of ME systems are:

1. phase stability and phase behavior,
2. microstructure, dimension (size and distribution), shape (or conformation), and surface features (specific area, charge, and distribution),
3. local molecular arrangements, interactions, and dynamics.

Among these properties, particle size, interactions, and dynamics are of fundamental importance since they control many of the general properties of MEs. In particular, the size distribution of MEs gives essential information for a reasonable understanding of the mechanism governing both the stability and the penetration into the skin (5,6). Many technologies such as scattering techniques (static light scattering, dynamic light scattering, small angle neutron scattering, and small angle X-ray scattering) as well as transmission electron microscopy, and nuclear magnetic resonance have been in growing use in particle characterization. Other methods, e.g., electrokinetic chromatography, conductance, viscosity, electrical birefringence, infrared spectroscopy, and calorimetry are also employed for investigating the internal physicochemical states of MEs (7–11).

Since among all these techniques used for structure elucidation of MEs microscopy, viscosity measurements, and scattering experiments are of most practical relevance, their applications are discussed in detail in this chapter.

A. Microscopy

Optical isotropy is one important feature of MEs. Unlike lamellar or hexagonal liquid crystals, isotropic structures do not cause birefringence between crossed polarizers. Therefore, polarization microscopy is applied to detect this behavior.

Freeze fracture electron microscopy (FFEM) is a method to visualize the microstructure of colloidal systems, mainly size and shape of the ME droplets. The sample is rapidly frozen, applying cooling rates of about 10^4 K/sec, and subsequently fractured. It is possible to etch the frozen and fractured sample, which yields an amplification of the characteristic relief by lyophilization of the frozen water along the fractured surface. In either case the surface is shadowed in 45° angle with a thin layer of platinum and then immediately in vertical angle with carbon providing a mechanical stabilization. After a washing procedure the resulting replica can be observed in a transmission electron microscope (TEM). Due to shadowing in transversal angle, the platinum layer thickness depends on the surface structure, which causes light–dark contrasts in the micrographs (12). Instead of platinum, gold, or tantalum-wolfram can be used as shadow materials, showing the advantage of decoration effects only on the oil fracture face. Therefore, it is possible to differentiate between water and oil fractions within the specimen (13).

A negative aspect of this method is that only replica can be observed, never the sample itself. Furthermore, formation of artifacts by cryofixation cannot always be excluded. For example, ice decoration is a frequently occurring artifact in FF-TEM (15). According to Jahn and Strey, high cooling rates, a limited number of components, large and slowly reorganizing structures as well as detailed structural knowledge from other experimental techniques are essential to minimize these effects (13).

Schulman et al. applied electron microscopy to get structural information of MEs. In this case, visualization was attained by staining the double bonds in the oil phase with osmium tetroxide (14).

Among other techniques electron microscopy studies were carried out by Alany et al. in order to characterize colloidal structures of two pseudoternary phase diagrams and to identify phase transitions between the colloidal phases formed (15). The studied systems composed of a lipophilic phase, water, and a surfactant blend either with or without the cosurfactant 1-butanol. In the cosurfactant-free phase diagram a ME region and a phase of lamellar liquid crystals were identified, whereas the 1-butanol containing system showed only an increased ME area without any other structures. Electron micrographs enabled the visualization of the structural differences between droplet and bicontinuous MEs as well as lamellar phases.

B. Viscosimetry

Determination of rheological behavior and viscosity of MEs is used for obtaining different kinds of information. In many cases, shear rate and shear stress are proportional which means that these MEs exhibit Newtonian flow. The results of such measurements can carry structural information (16).

Ktistis investigated the viscosity of o/w MEs containing isopropyl myristate (IPM), polysorbate 80, sorbitol, and water, varying oil-volume fraction φ, total surfactant concentration, and surfactant/cosurfactant mass ratio in order to determine their effect on the hydration of the dispersed droplets (17). The increase of the relative viscosity η_{rel} with increasing φ could be described by the following equation:

$$\eta_{rel} = \exp[a\varphi/(1 - K\varphi)] \quad (1)$$

where a is the constant with a theoretical value of 2.5 for solid spheres and K is the hydrodynamic interaction coefficient. Decrease in polysorbate/sorbitol mass ratio as well as increasing total surfactant concentration yielded an increase of a and a decrease of K. The deviation of the obtained a values from the theoretical value for spheres was attributed to the hydration of the droplets. The ratio of bound solvent layer to droplet core radius was calculated, resulting in an increase of this parameter with increasing total surfactant concentration due to a greater hydrodynamic volume of the droplets.

Primorac et al. studied the rheological behavior of o/w MEs with different emulsifying agents and observed an increase in viscosity with decreasing HLB of coemulsifiers (18). All systems studied behaved as Newtonian fluids indicating the existence of spherical particles, but it is also reported about non-Newtonian properties of MEs, e.g., pseudoplastic and thixotropic flow (19).

The aforementioned studies of Alany et al. demonstrated that rheological behavior could be used to differentiate between MEs that change from droplet to bicontinuous systems (15). Although both exhibit Newtonian flow, only the viscosity

of the latter was independent of the water volume fraction. Additionally, it was possible to distinguish between MEs and lamellar liquid crystals. Because of their geometrically ordered and rigid structure, lamellar phases show a higher viscosity and pseudoplastic flow.

Rheological characteristics are important features for the development of innovative pharmaceutical dosage forms, in particular for special administration routes. Lecithin based o/w MEs for parenteral use were studied in terms of their rheological properties dependent on the oil phase content, the total surfactant concentration, and the polysorbate 80/lecithin weight ratio K_m (20). It was shown that an increase in the amount of surfactant and oil, respectively, resulted in a change of the rheological behavior from non-Newtonian into Newtonian flow and rising viscosity values, whereas K_m influenced these properties only marginally. The results of this method in combination with particle size analysis led to the selection of a Newtonian ME system containing 10% oil (IPM), 30% surfactant blend, and 60% water, which was further tested in terms of stability and acute toxicity. From the results the authors concluded that lecithin-based o/w MEs are valuable technological alternatives for intravenous administration of low water soluble drugs.

C. Light and Neutron Scattering

Elucidation of the ME microstructure, although important for a specific development of these drug delivery systems, can be very complex. Below, the application of three scattering techniques is explored in some depth. These methods involve only weak perturbation and hence are readily used to monitor particle size and size distribution in the ME non-destructively. The aspects are discussed by recalling the theoretical background and illustrating the potential of the techniques with experimental results.

1. Light Scattering from Microemulsion Droplets

Interaction of light with matter can be used to obtain important information about structure and dynamics of matter. Investigation of this interaction is possible by light scattering experiments, which offer two ways of gleaning information. The first method, called dynamic light scattering (DLS), monitors fluctuations in scattered light as a function of time $I(t)$. The second method, called static light scattering (SLS), observes interparticle interference patterns of scattered light by measuring the time average intensity as a function of angle $\langle I(\theta)\rangle$.

SLS from Microemulsion Droplets. For MEs, time-average (or "total") intensity of the scattered light arises from concentration fluctuation of the droplets of the dispersed phase. The scattering intensity $\langle I\rangle$ at a selected scattering angle θ can be written as (21):

$$\langle I(q)\rangle = kV\phi P(q)S(q) \tag{2}$$

where q is the scattering wave vector with $q = \left(\frac{4\pi n}{\lambda}\right)\sin\frac{\theta}{2}$, depending on the wavelength λ of the incident light, the refractive index n of the ME, and the scattering angle θ. K is a constant characteristic of the instrument, V the ME droplet volume, ϕ the droplet volume fraction, P the form factor of an isolated colloidal particle, and S the structure factor which carries all the information about correlations among colloidal particles. Often, ME droplets have a small radius R compared to

the wavelength of the light λ, and $qR << 1$. In this case, scattering intensity is independent of the scattering angle, and for spherical droplets Equation (2) can be rewritten as (22):

$$\frac{\phi}{\langle I \rangle} \approx G \frac{1}{R^3} \left(\frac{\partial n}{\partial \phi} \right)^{-2} (1 + K_I \phi) \tag{3}$$

where G is the constant for all samples, and K_I describes perturbation due to thermodynamic effects and is therefore related to the interaction potential. For hard sphere potential $K_I = 8$. The coefficient K_I becomes smaller if there are supplementary attractive interactions, and larger in case of additional repulsive interaction.

If the studied systems are ideal mixtures, $(\partial \mathrm{n}/\partial \phi)$ is constant and $(\phi/\langle I \rangle)$ should be a linear function of ϕ provided that droplet size does not vary significantly over the concentration range. By extrapolating the linear plot of $(\phi/\langle I \rangle)$ to $\phi = 0$, the radius of ME droplets R can be obtained if a calibration has been made by applying samples of known size (23). By the slope of the linear plot of $(\phi/\langle I \rangle)$ versus ϕ, determination of interdroplet interaction is possible. From this interaction potential, parameters describing stability, i.e., coagulation time of systems can be estimated (24).

DLS from Microemulsion Droplets. Brownian motion of the ME droplets within the continuous phase causes time-dependent fluctuations of the scattered light intensity dependent on the hydrodynamic properties of the system. In DLS, the autocorrelation function of the scattered light $\mathrm{g}_2(\tau) = \langle I(t) I(t+\tau) \rangle_t$ is detected. Since the normalized field autocorrelation function $g_1(\tau)$ is a quantity of basic interest in DLS and carries the information about droplet motions in a system, it has been derived from the measured scattered intensity autocorrelation function $g_2(\tau)$ via Siegert relation (25):

$$g_1(\tau) = C\sqrt{1 - g_2(\tau)} \tag{4}$$

where the constant C is in the order of unity, dependent on instrumental conditions and the amount of background scattering from solvent, etc.

For dense polydisperse interacting systems of ME droplets, $g_1(\tau)$ can be represented as the sum of two exponentials, provided that the extent of polydispersity is not too large (26):

$$g_1(\tau) = \frac{A_1}{A_1 + A_2} \exp(-D_c q^2 \tau) + \frac{A_2}{A_1 + A_2} \exp(-D_s q^2 \tau) \tag{5}$$

The two exponentials in Equation (5) are attributed to the existence of two relaxation modes: fast mode is due to collective diffusion D_c (i.e., total number of density fluctuations), whereas slow mode is due to self-diffusion D_s (i.e., concentration fluctuations that decay by the exchange of species by single droplet diffusion). $A_1/(A_1 + A_2)$ and $A_2/(A_1 + A_2)$ are the intensities of their exponentials. Relative amplitude of slower decaying mode, $A_2/(A_1 + A_2)$, can be used as measure of the size polydispersity index $\sigma_\mathrm{s} = \sqrt{\frac{\langle R^2 \rangle}{\langle R \rangle^2}} - 1$ (26–28).

Average hydrodynamic radius of scattering droplets R_h can be determined from the free particle diffusion coefficient D_0 using the Stokes–Einstein equation:

$$R_\mathrm{h} = \frac{k_\mathrm{B} T}{6\pi\eta D_0} \tag{6}$$

where k_B is the Boltzmann's constant, T is the absolute temperature, and η is the coefficient of the continuous phase viscosity. For spherical particles, interacting through essentially hard sphere or excluded-volume forces, D_0 can be deduced from

Table 1 Particle Size Parameters of Microemulsions

	DLS		SANS		
ME	R_h (nm)	σ_s	R_{core} (nm)	R_{shell} (nm)	σ_s
IPP	9.58	0.156	7.75	11.49	0.174
Eutanol	9.01	0.180	7.98	10.81	0.209

Note: Errors are smaller than ±2% for the radii and ±10% for the size polydispersity index σ_s).
Source: From Ref. 29.

the collective diffusion coefficient D_c by means of the droplet volume fraction ϕ following (25):

$$D_c = D_0(1 + 1.56\phi + 0.91\phi^2 + \cdots) \tag{7}$$

The results of this kind of double exponential fit for o/w MEs consisting of Poloxamer 331/Tagat® O2 as surfactants, water/propylene glycol as continuous phase and two different pharmaceutical oils [Eutanol® G and isopropyl palmitate (IPP)] studied by Shukla et al. are summarized in Table 1. The obtained values are close to the results deducted by approximate analysis of small angle neutron scattering and indicate that the kind of oil (comparable molecular size provided) only marginally influences the droplet size of a ME (29).

In diluted regions, the difference between D_c and D_s is expected to be small. Therefore, resolution of the measured autocorrelation function by a sum of two exponentials will be difficult. In this case, analyzing the obtained normalized field autocorrelation function $g_1(\tau)$ by a single exponent (30) (for monodisperse systems) or cumulants (31) (for polydisperse systems) gives an apparent diffusion coefficient D_{app}. D_0 can be identified with D_{app} when $\phi \rightarrow 0$ and is used for the calculation of R_h.

Shukla et al. investigated o/w MEs by means of DLS using a dilution procedure in the region of the phase diagram where surfactant-covered oil droplets were formed (32). Aim of the studies was to determine information about diffusion coefficient, droplet size, interparticle interaction, and polydispersities from experimental data applying cumulant fitting. By a suitable model, scattering data were corrected for interparticle interactions that occur in concentrated non-ideal systems. The results indicate a considerable increase in coagulation time due to the observed particle–particle interaction compared with rapid coagulation that happens when there is no interaction between particles except a sharp attraction by touching each other. These stability results were consistent with the observed long-term stability of the studied MEs.

2. *Neutron Scattering from Microemulsion Droplets*

The principle of neutron scattering can be understood due to the similarities to light scattering. The scattering intensity of thermal neutrons from soft-matter can also be expressed by Equation (2) (Ref. 33). In the case of light, the interaction is between the electric field of the radiation and the electronic charges. Neutrons, having no electrical charge, interact in almost all situations via their scattering length with the nuclei exclusively. Their penetration is very large and allows the study of materials containing heavy elements. The typical wavelength associated with thermal neutrons is in the order of 1–10 Å, which means an increased resolution. Considering the droplet sizes present in colloidal systems, it can be deduced that neutrons are very often the

more appropriate way of studying their structure. Mostly small scattering angles are applied. This constitutes the technique of small angle neutron scattering or SANS.

Shukla et al. used core shell sphere form factor with an internal core of radius R_{core} and a scattering length density ρ_{core} surrounded by a shell with an outer radius R_{shell} and a scattering length density ρ_{shell} (34) for fitting their data. A useful expression of the structure factor $S(q)$ for hard spheres is obtained from the Percus–Yevick approximation (35).

Applying the aforementioned procedure, the authors obtained size and polydispersity index of the two o/w MEs already investigated by DLS (Table 1) (29). In their computation, a Schultz size distribution function was used and the fits were generated by allowing R_{core}, ρ_{shell}, and σ_s to vary. As shown in Figure 1, R_{core} radius corresponds to the size of the oil droplet (dark black part:pure oil and residue:penetration of surfactant tails into the oil), whereas R_{shell} describes the distance between the center of the particle and a position in the surface film where the difference in scattering length density has its maximum. As expected, the outer radius incorporates looser-bounded surfactant molecules and is substantially bigger than the hydrodynamic radius R_h, obtained by DLS. The latter is supposed to consist of the oil core and a stronger bounded surfactant film, perhaps containing some solvent molecules too.

Although ME structure elucidation by SANS has been advanced by several workers (e.g., Refs. 36–39) there are still many complications. First, the scattering length density of the attached surfactant layer is usually of the value between those of adsorbed molecules comprising the layer and solvent molecules, as a consequence of penetration or adsorption of solvent into the attached layer. Second, for other than hard sphere potentials, SANS data analysis, incorporating polydispersity, may not be straightforward due to complexity in the structure factor.

Nevertheless, scattering techniques are valuable tools for structure determination of colloidal systems.

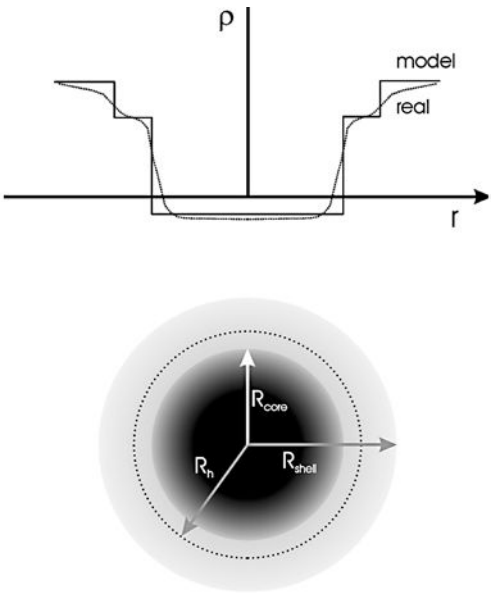


Figure 1 Model of an o/w microemulsion droplet as core shell sphere. *Source*: From Ref. 29.

III. DERMAL AND TRANSDERMAL DRUG DELIVERY USING MICROEMULSIONS

MEs are known to be promising drug delivery systems. In particular in the field of dermatopharmacy these colloidal systems have attracted interest due to their improving effect on percutaneous penetration of the so-called problematic drugs.

In the case of lipophilic substances, application of conventional vehicles such as ointments often causes formation of a drug depot in stratum corneum. This phenomenon is attributed to the high affinity of these drugs to the lipophilic structure of the outermost skin layer. MEs are capable of increasing their permeation extent. On the other hand, stratum corneum hampers the transport of hydrophilic drugs into skin. Incorporation into MEs helps to overcome this barrier. Due to their hydrophilic and lipophilic domains, it can be suggested that MEs are able to interact with both, the lipid and the polar pathway by entering the stratum corneum via the intercellular route. Altering the lipid bilayer as well as hydration of the horny layer may lead to an increased permeability. Therefore, MEs can be applied to improve dermal as well as transdermal drug delivery. Basic advantages are the reduction of systemic side effects and first-pass metabolism that occur frequently after oral application.

In the past, the crucial point of topical administration in therapy was the high surfactant content needed to stabilize the colloidal phase of MEs. Hence, a lot of research work was focused on both, diminishing their concentration and searching for well-tolerated surfactants. Taking into account that MEs can be applied in treatment of skin diseases, an amount of 20% to 30% of surfactants appears to be the threshold of acceptance in dermal use. Employing surfactants from native origin such as phospholipids or alkyl polyglycosides seems to generate mild and non-aggressive ME systems. Besides, polymeric surfactants such as the even for parenteral application admitted poloxamers appear to be useful as well.

During the past several years, improving effect of MEs on dermal drug delivery has been demonstrated in several in vitro, ex vivo, and in vivo studies, investigating the influence of different factors on the enhancing activity.

Already in the 1980s, Ziegenmeyer and Fuehrer performed in vitro experiments with skin membranes, studying the penetration behavior of tetracycline hydrochloride incorporated in a cream, a gel, and a ME (40). Penetration enhancing activity of the ME was shown by the distinct increase in diffusion rate compared to the conventional vehicles.

The influence of prilocaine hydrochloride and lidocaine incorporation into MEs on both drug flux through excised rat skin using Franz type diffusion cells (41) and dermal drug delivery potential in rats by means of microdialysis assay (42), compared to conventional formulations was studied by Kreilgaard et al. All the investigations resulted in a significant benefit of the low skin irritant MEs. Drug flux and in vivo penetration rate were increased for the hydrophilic as well as for the lipophilic model drug compared to commercial products. These effects were found to be due to the high drug solubilization capacity of MEs, causing a larger concentration gradient towards the skin, and could be related mainly to the drug mobility in the vehicle dependent on the internal ME structure as studied by NMR. Remarkably, an increased surfactant content yielded lower permeation coefficients. Applying a pharmacokinetic model that provides reliable estimation of cutaneous absorption coefficient and lag time from microdialysis data, a good correlation was found

between the obtained in vivo data and previous in vitro results using Franz-type diffusion cells.

Further investigations were carried out by the same author in order to estimate dermal drug delivery of lidocaine from MEs and an o/w emulsion based cream in volunteers using minimal invasive microdialysis technique and determination of the pharmacodynamic effect, respectively (43). Applying the ME, the mean absorption coefficient of the local anesthetic drug was shown to increase about threefold and the lag time entering the dermis was reduced considerably compared to the conventional vehicle. However, the anesthetic effect did not diverge significantly between the two formulations.

Kriwet and Mueller-Goymann obtained different colloidal structures like liposomes, MEs, and lamellar liquid crystals by varying the mass ratio of the compounds of a ternary system containing phospholipids, diclofenac diethylamine, and water (44). In this case, the amphiphilic drug takes part essentially in forming the microstructure. In vitro drug release studies as well as permeation studies through excised human stratum corneum exhibited a dependence of diffusion behavior on the colloidal structure. Whereas in liposomes and lamellar phases strongly bound drug and phospholipids hamper the interaction with the horny layer, incorporation into MEs leads to enhanced stratum corneum permeability.

Niflumic acid was incorporated into sucrose fatty acid ester-stabilized bicontinuous MEs by Bolzinger-Thevenin et al. (45). Anti-inflammatory effect of a ME system which was saturated with the drug (1%) was comparable to that from a commercially available 3% o/w emulsion. Occurring lag time was attributed to the accumulation of niflumic acid in the interfacial film of the ME, which could control the drug release.

In an in vivo model using rabbits, Kemken et al. studied the pharmacodynamic effect of several β-blockers that were included into water-free ME pre-formulations (46). The vehicles were saturated with the drugs and, after application under occlusion, water uptake from the skin occurred leading to in situ formation of water containing MEs with decreasing solubility of the lipophilic drugs and therefore a supersaturation. The observed high pharmacodynamic effects were assumed to be due to rising thermodynamic activity as driving force for enhanced dermal drug uptake.

In vitro skin permeation studies with felodipine investigating the effect of the oil phase of o/w MEs were carried out by Trotta et al. (47). Keeping the amount of the other phases nearly constant, it was shown that drug flux depends on the composition of the lipophilic phase. The ME system with the highest solubility for the drug could be favored in permeability, probably due to the droplets of the internal phase acting as effective drug reservoir.

Schmalfuß et al. described the possibility of controlling the penetration behavior of a hydrophilic model drug by means of ex vivo penetration studies on human skin, analyzing the drug concentration in different skin layers (48). Administration of a standard w/o ME resulted in an accumulation of diphenhydramine hydrochloride (DPH) in the dermis. Addition of cholesterol as penetration enhancer caused a generally higher penetration rate and a shift of the drug towards the epidermis. Cholesterol was assumed to loosen the stratum corneum lipid bilayers enabling an increased hydration of the polar headgroups and therefore, facilitating penetration of DPH along the polar route. This mechanism is proposed for hydrophilic substances. Unlike this, incorporation of oleic acid as enhancer did not change

penetration rate or concentration profile, probably because it influences only the lipophilic pathway by altering the ceramide chains mobility.

Cationic MEs containing piroxicam and a piroxicam-ß-cyclodextrin inclusion complex, respectively, were developed by Dalmora et al. (49,50). These systems, exhibiting a remarkably increased solubility of the drug compared to simple solutions, demonstrated in in vitro drug release studies a reservoir effect for piroxicam. The following in vivo assessment of anti-inflammatory activity on rats resulted in significantly inhibited inflammatory reactions after topical application relative to control and an improved effect of the MEs after subcutaneous administration compared to a buffered solution of the drug. Moreover a prolonged pharmacological activity after subcutaneous application confirmed the potential of modifying dermal drug delivery by ME systems.

Stable and well skin tolerated o/w MEs stabilized by a polymeric surfactant (Poloxamer 331) and either macrogol-sorbitan-fatty acid ester or macrogol-glycerol-fatty acid ester were developed and characterized by Krause (51,52) and Jahn (29,32,53,54). Several oils could be incorporated such as IPP and oleic acid. In one case, the drugs themselves (eutectic mixture of lidocaine and prilocaine) were used as lipophilic phase. Studies with hydrocortisone (HC) as lipophilic model drug were carried out (51). In vitro drug release experiments by means of a multilayer membrane system resulted in good releasing properties of the MEs as well as for commercially available vehicles indicating that drug release is not the rate-limiting factor in penetration. Using Franz-type diffusion cells, the penetration behavior of HC from the innovative ME was subsequently compared to that of an o/w cream (Nubral® 4HC), which has already been proven to be effective in treatment of dermatologic diseases. Drug content in different layers of human breast skin as well as in the acceptor solution was analyzed after 30 and 300 minutes, respectively. Application of the conventional vehicle yielded a considerable accumulation of HC in the stratum corneum and only small amounts of drug were detected in lower skin layers and the acceptor. Unlike this, HC penetration from the ME caused inferior drug depot in the horny layer whereas the amount permeated in the acceptor increased significantly. The results clearly demonstrate a transdermal drug delivery effect and confirm the ability of MEs to transport drugs in a greater extent through the main permeability barrier, the stratum corneum.

Jahn succeeded in developing cyclosporine A (Cs A) containing o/w MEs of therapeutic importance (53,54). In the past, several conventional topical formulations for the immunosuppressive drug were shown to be ineffective in treatment of psoriasis compared to systemic or intradermal application. Because of its strong lipophilicity and a high molecular weight of 1202 g/mol, only an accumulation in the stratum corneum with a slow transport towards lower skin regions was detected. But T-cell as target structures are localized in the dermoepidermal junction region and in the upper dermis layer. In ex vivo penetration studies on human breast skin using Franz-type diffusion cells, higher concentrations of Cs A were detected in viable epidermis and dermis layers following the application of an o/w cream than MEs. But the conventional vehicle was not able to transport the drug through all the skin layers, whereas 20% to 30% of the applied dose from the ME reached the acceptor (Figs. 2 and 3). This amount of drug is assumed to be responsible for a pharmacological effect.

Clinical relevance of the modern colloidal systems in topical treatment of psoriasis could be confirmed by an in vivo study including 10 patients sufferingfrom chronic plaque-type psoriasis. A Cs A-ME was shown to be comparable to

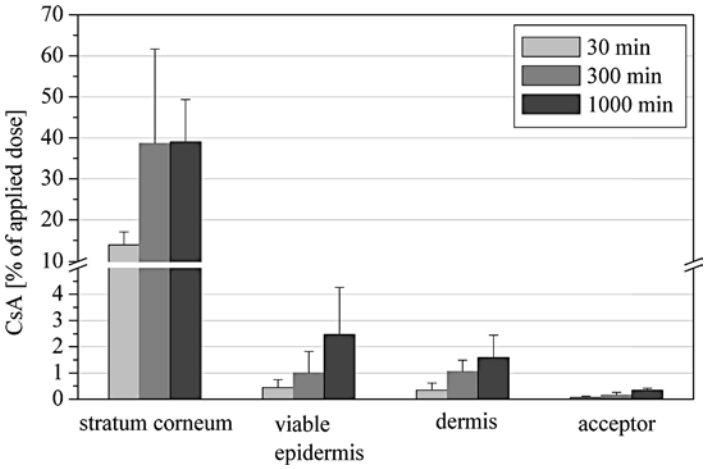


Figure 2 Penetration of cyclosporine A (Cs A) from an o/w cream into human skin ex vivo after 30, 300, and 1000 minutes (mean ± SD, $n = 3$). *Source*: From Ref. 53.

commercially available creams containing calcipotriol and betamethasone-17-valerate, which are commonly used in psoriasis therapy. The slight advantage of a system with DMSO as enhancer in addition to oleic acid as lipophilic phase in preceding penetration studies could not be established in vivo. Application of this ME on chronic-inflammatory skin caused irritant effects and is therefore concluded not to be suited for the treatment of damaged skin.

Lehmann et al. tested an o/w and a w/o ME for their suitability in dermatological use (55). In hen's egg test on chorioallantoic membrane (HET-CAM) both formulations, containing either sucrose esters or Tagat® S/Plurololeat® WL1173 as nonionic surfactants and IPM as lipophilic phase, were classified as non-irritant. But an in vivo test on human subjects demonstrated a significant increase in transepidermal water loss (TEWL) by the MEs compared to untreated control sites.

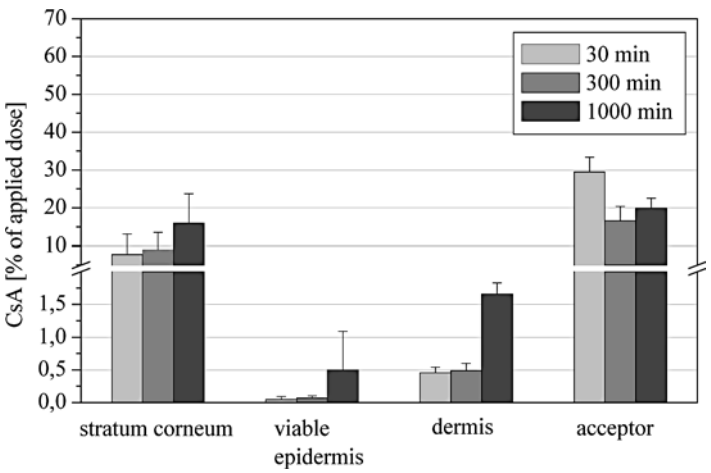


Figure 3 Penetration of cyclosporine A (Cs A) from an o/w microemulsion (ME) into human skin ex vivo after 30, 300, and 1000 min (mean ± SD, $n = 3$). *Source*: From Ref. 53.

The water-continuous system caused dehydration of stratum corneum additionally. Furthermore, the influence of the MEs on HC penetration compared to an amphiphilic cream was evaluated in terms of a skin-blanching test. Despite the observed enhanced drug penetration from the colloidal systems, neither ME confers benefit in HC therapy because irritant effects of the formulations outbalance the improved penetration of the anti-irritant drug. The authors concluded that use of MEs as drug delivery systems is more valuable when irritant effects are negligible.

Good human skin tolerability of a lecithin-based o/w ME compared to conventional vehicles (o/w and w/o cream, and gel) was observed by Paolino et al. (56). It could be demonstrated that incorporation of 1% oleic acid into the ME was significantly less irritant than an oleic acid dispersion of the same concentration. This effect was supposed to be due to the incorporation of oleic acid in the ME microstructure and the impossibility to strongly perturb the stratum corneum lipids. For the same reason, the oleic acid containing ME exhibited poor additional enhancing activity on skin permeation of ketoprofen, but both MEs clearly improved transdermal delivery with respect to the conventional vehicles.

Rhee et al. developed an optimized o/w ME for topical application of the same drug (57). Basic ingredients were Labrasol®/Cremophor® RH 40 as surfactant blend, oleic acid, in this case found to enhance the drug permeation, and water. The authors carried out permeation experiments on excised rat skin in order to investigate the influence of oil and surfactant content on transdermal transport. With increasing surfactant content a 12- to 23-fold decrease in permeation rate was detected, which was probably caused by a lower thermodynamic activity at higher surfactant amounts. At surfactant concentrations of 30% and 55%, respectively, an optimum oil content of 6% was found. Incorporating several terpenes as enhancer, only limonene exhibited improved permeation properties.

Transdermal transport of hydrophilic and lipophilic drugs such as lidocaine free base, lidocaine hydrochloride, estradiol, and diltiazem hydrochloride from w/o and o/w MEs composed of IPM, polysorbate 80, water, ethanol as well as *N*-methyl-pyrrolidone (NMP), and oleyl alcohol as enhancer was studied by Lee et al. (58). For all the drugs a considerable improved transport by MEs compared to the solution in either water or IPM was observed, with a significantly better flux from the o/w system than from w/o. The results suggest that transport from the aqueous phase is the most important factor for both kinds of drugs, whereas the oil phase serves as a drug depot. This could be confirmed by removing surfactant and oil from the system. The flux from the remaining water phase components was comparable to that from the o/w ME. It was concluded that presence of NMP increases the partition of the lipophilic drugs into the water phase, hence making them available for the transport across the skin.

Baroli et al. studied cutaneous accumulation potential as well as percutaneous delivery of the photoactive drug 8-methoxsalen (8-MOP) incorporated in several ME systems at saturation level, varying the amount of surfactant, IPM, and water (59). All MEs exhibited an increase in both parameters compared to saturated IPM solution and a clinical used aqueous solution on newborn pig skin in vitro. However, the quotient of accumulated to delivered drug could be modified by changing the ratio of the ingredients. Since 8-MOP is effective in psoriasis therapy, retaining of the drug in the skin is required and can be realized by the MEs. Due to low viscosity and surface tension occurring desquamation plaques might be reached easily. Limiting factor in therapy seems to be the surfactant content. For clinical use well-tolerated

surfactants in low concentrations are essential, even for administration on damaged skin.

In vitro investigations on pig skin regarding transdermal delivery of methotrexate (MTX) were carried out by Alvarez-Figueroa and Blanco-Méndez (60). Topical application of this drug is problematic because of its hydrophilic character, the high molecular weight, and the high dissociation degree at physiological pH. The authors found incorporation of MTX in MEs to be more effective compared to simple solutions. However, iontophoretic delivery from solutions exceeded the ME results, probably due to the lower solubility of MTX in MEs than in aqueous solutions.

The suitability of thickened w/o MEs for transdermal absorption of apomorphine was examined on hairless mouse skin by Peira et al. (61). In order to improve the permeation properties of the drug, lipophilic apomorphine–octanoate ion pairs were formed. An estimation of the in vivo steady-state plasma concentration from the obtained in vitro steady-state flux led to a promising result with regard to future in vivo application.

Changez and Varshney developed w/o MEs made of AOT (sodium *bis*(2-ethyl hexyl) sulfosuccinate), IPM, and water for topical application of the local anesthetic drug tetracaine hydrochloride (62). The local analgesic response as a measure for the therapeutic potential was evaluated on rats. The optimal formulation exhibited an eightfold enhancement of this parameter compared to an aqueous solution of the drug. It was assumed that AOT as anionic surfactant is able to soften the stratum corneum. Furthermore, the safety of the MEs as transdermal carrier systems could be confirmed by histopathological, irritation, and oxidative stress investigations on mice.

Transdermal application of estradiol is a frequently used way for increasing systemic bioavailability by avoiding the first pass metabolism that occurs after oral treatment. In vitro permeation experiments through human cadaver skin demonstrated that MEs are appropriate vehicles for this purpose (63). The observed 200- to 700-fold increase in steady-state flux compared to a saturated solution in phosphate buffered saline was assumed to be due to the improved solubility in the MEs and the resulting increased concentration gradient towards the skin. Considering therapeutic plasma concentration and estradiol clearance, pharmacological effects can be expected by topical application of the systems.

As has been shown, numerous studies confirm MEs as potential vehicles for dermal drug delivery. Their superior penetration behavior is attributable to a variety of factors depending on the composition and the resulting microstructure of the ME. The high solubilization capacity of the vehicles for hydrophilic and lipophilic drugs leads to a large concentration gradient towards the skin, which is, combined with a high thermodynamic activity, the driving force for drug transport. The very low interfacial tension ensures an excellent contact to the skin surface, where the good spreading is additionally supported by the low viscosity. Hence, the formulation is capable to enter the skin easily. Due to the dynamic structure with continuously and spontaneously fluctuating interfaces high drug mobility is acquired, further enhancing the drug diffusion process (3,41).

Most MEs require a relatively large amount of surfactants that are able to alter the structure of the stratum corneum and facilitate drug diffusion or increase the drugs partition into skin, respectively. In some cases, penetration enhancer like oleic acid, which is also used as lipophilic phase, *N*-methyl-pyrrolidone, dimethylsulfoxide, and terpenes as well as solubilizer such as β-cyclodextrin are incorporated additionally (Table 2). Nevertheless, the necessity of these ingredients is still contentious because of the superior penetration properties of the vehicle ME itself.

Table 2 Penetration Modifier and Solubilizer in Microemulsions

Penetration modifier/solubilizer	References
Cholesterol, oleic acid	(48)
β-Cyclodextrin	(49,50)
Dimethylsulfoxide	(51,53,54)
Oleic acid[a]	(53,54,56)
N-methyl pyrrolidone, oleyl alcohol	(58)
Terpenes	(57)

[a]Also used as oil phase

However, the full drug diffusivity potential of MEs can also be hampered by their composition and microstructure, e.g., due to adsorption of drug molecules to the surfactant film, encapsulation, or unfavorable partitioning of the drug between formulation and skin (3,41). Investigating the transdermal permeation of glucose as hydrophilic model drug from MEs through human cadaver skin, Osborne et al. found a relationship between drug flux and water content in the ME. Presence of free water was shown to be essential for glucose transport into skin. At lower water contents, all molecules are used for hydrating the surfactant headgroups, thus being not available for partitioning into the skin (64).

In a previous study, the same authors performed a pretreatment of the skin with either the surfactant dioctyl sodium sulphosuccinate, the cosurfactant octanol, or a mixture of both, and compared the measured transdermal water flux with the one obtained by applying a ME containing these ingredients (65). Whereas pretreatment with the single substance had marginal influence, the combination of both was as effective in increasing the water flux as the ME itself. Therefore, it was concluded that the enhancing activity of the ME is a result of the synergism between surfactant and cosurfactant, independent of the formulations microstructure. Similar to that, pretreatment with a w/o ME increased the percutaneous absorption of the subsequently applied cetyl alcohol included in a cream and a lotion, respectively (66).

Delgado-Charro et al. presented a model of multiple factors influencing transdermal drug delivery (67). Main part are different partitioning processes between ME droplets, continuous phase, and skin. Resulting penetration represents the sum of the drugs relative activities in these fractions. Additionally, diffusion of single ME constituents into the skin is possible, which may reduce the barrier function of the stratum corneum by diverse interactions and consequently improves penetration properties. Another option is that the formulation extracts some horny layer components and a new physical entity, realizing drug release now, may result by losing the original ME structure.

Considering the aforementioned facts, a number of influencing factors on the MEs penetration behavior could be found. Nevertheless, more research work is required for a detailed clarification of the penetration mechanism.

IV. CONCLUSION

In summary, a lot of studies could confirm the benefit of MEs as drug delivery systems, in particular in the field of dermatopharmacy. In addition to the ease of preparation and long-term stability as practical advantages, the high solubilization

capacity for hydrophilic as well as lipophilic drugs has to be emphasized. These substances, causing several problems in dermal and transdermal administration due to their physicochemical properties, were shown to be effectively transported to their target region in the skin or blood circulation, respectively.

Moreover, the growing use of non-irritant ingredients, mainly surfactants, leads to the creation of ME systems that are suitable for dermal application. Tolerability studies are basically required for future clinical use. Since they are often missing or have been performed applying animal models, such tests have to be carried out on human skin in vivo. These investigations in conjunction with the variety of available characterization methods offer the opportunity for the development of optimized colloidal formulations and a better understanding of the drug delivery mechanism from MEs.

REFERENCES

1. Tenjarla S. Microemulsions: an overview and pharmaceutical applications. Crit Rev Ther Drug 1999; 16:461–521.
2. Jahn K, Krause A, Janich M, Neubert RHH. Colloidal drug carrier systems. In: Bronaugh RL, Maibach HI, eds. Topical Absorption of Dermatological Products. New York: Marcel Dekker, 2002:483–493.
3. Kreilgaard M. Influence of microemulsions on cutaneous drug delivery. Adv Drug Del Rev 2002; 54(suppl 1):S77–S98.
4. Vandamme TF. Microemulsions as ocular drug delivery systems: recent developments and future challenges. Prog Retin Eye Res 2002; 21:15–34.
5. Constantinides PP, Yiv SH. Particle size determination of phase-inverted water-in-oil microemulsions under different dilution and storage conditions. Int J Pharm 1995; 115:225–234.
6. Mueller BW, Mueller RH. Particle size distributions and particle size alterations in microemulsions. J Pharm Sci 1984; 73:919–922.
7. Mrestani Y, El-Mokdad N, Rüttinger HH, Neubert RHH. Characterization of partitioning behavior of cephalosporins using microemulsion and micellar electrokinetic chromatography. Electrophoresis 1998; 19:2895–2899.
8. Mrestani Y, Neubert RHH, Krause A. Partition behaviour of drugs in microemulsions measured by electrokinetic chromatography. Pharm Res 1998; 15:799–801.
9. Kumar P, Mittal KL, eds. Handbook of Microemulsion Science and Technology. New York: Marcel Dekker, 1999.
10. Attwood D. Microemulsions. In: Kreuter J, ed. Colloidal Drug Delivery Systems. New York: Marcel Dekker, 1994:31–71.
11. Moulik SP, Paul BK. Structure, dynamics and transport properties of microemulsions. Adv Colloid Interface Sci 1998; 78:99–195.
12. Junginger H, Heering W. Darstellung kolloider Strukturen von Salben, Cremes, Emulsionen und Mikroemulsionen mittels Gefrierbruch-Ätztechnik und TEM. Acta Pharm Technol 1983; 29:85–96.
13. Jahn W, Strey R. Microstructure of microemulsions by freeze fracture electron microscopy. J Phys Chem 1988; 92:2294–2301.
14. Schulman JH, Stoeckenius W, Prince LM. Mechanism of formation and structure of micro emulsions by electron microscopy. J Phys Chem 1959; 63:1677–1680.
15. Alany RG, Tucker IG, Davies NM, Rades T. Characterizing colloidal structures of pseudoternary phase diagrams formed by oil/water/amphiphile systems. Drug Dev Ind Pharm 2001; 27:31–38.

16. Gradzielski M, Hoffmann H. Rheological properties of microemulsions. In: Kumar P, Mittal KL, eds. Handbook of Microemulsion Science and Technology. New York: Marcel Dekker, 1999:357–386.
17. Ktistis G. A viscosity study on oil-in-water microemulsions. Int J Pharm 1990; 61: 213–218.
18. Primorac M, Stupar M, Vuleta G, Vasiljević D. Rheological properties of oil/water microemulsions. Pharmazie 1992; 47:645–646.
19. Primorac M, Daković LJ, Stupar M, Vasiljević D. The influence of temperature on the rheological behaviour of microemulsions. Pharmazie 1994; 49:780–781.
20. Moreno MA, Ballesteros MP, Frutos P. Lecithin-based oil-in-water microemulsions for parenteral use: pseudoternary phase diagrams, characterization and toxicity studies. J Pharm Sci 2003; 92:1428–1437.
21. Langevin D, Rouch J. Light scattering of microemulsion systems. In: Kumar P, Mittal KL, eds. Handbook of Microemulsion Science and Technology. New York: Marcel Dekker, 1999:387–410.
22. Cazabat AM, Langevin D. Diffusion of interacting particles: light scattering study of microemulsions. J Chem Phys 1981; 74:3148–3158.
23. Gan LM, Ng SC, Ong SP, Chew CH, Koh LL. A light scattering study of the influence of poly(ethylene glycol) on the droplet size and the interdroplet interaction in a water-in-oil microemulsion. Colloid Polym Sci 1989; 267:1087–1095.
24. Verwey EJW, Overbeek JThG. Theory of the stability of lyophobic colloids. New York: Elsevier Publishing, 1948:164–185.
25. Pusey PN. Diffusion of spherical particles in concentrated dispersion. In: Degiorgio V, Corti M, eds. Physics of Amphiphiles: Micelles, Vesicles and Microemulsions. Amsterdam: Elsevier, 1995:152–159.
26. Yan YD, Clarke JHR. Dynamic light scattering from concentrated water-in-oil microemulsions: The coupling of optical and size polydispersity. J Chem Phys 1990; 93: 4501–4509.
27. Shukla A. Characterization of Microemulsions Using Small Angle Scattering Techniques. Ph.D. dissertation, Martin-Luther-University, Halle-Wittenberg, Germany, 2003.
28. Kops-Workhoven MM, Fijnaut R. Dynamic behavior of silica dispersions studied near the optical matching point. J Chem Phys 1982; 77:2242–2253.
29. Shukla A, Janich M, Jahn K, Krause A, Kiselev MA, Neubert RHH. Investigation of pharmaceutical oil/water microemulsions by small-angle scattering. Pharm Res 2002; 19:881–886.
30. Pusey PN, Tough RJA. Particle interaction. In: Pecora R, ed. Dynamic Light Scattering. New York: Plenum Press, 1985:85–179.
31. Koppel DE. Analysis of macromolecular polydispersity in intensity correlation spectroscopy: the method of cumulants. J Chem Phys 1972; 57:4814–4820.
32. Shukla A, Janich M, Jahn K, Neubert RHH. Microemulsions for dermal drug delivery studied by dynamic light scattering: effect of interparticle interactions in oil-in-water microemulsions. J Pharm Sci 2003; 92:730–738.
33. Kotlarchyk M, Chen SH. Analysis of small angle neutron scattering spectra from polydisperse interacting colloids. J Chem Phys 1983; 79:2461–2469.
34. Chen SH. Small angle neutron scattering studies of the structure and interaction in micellar and microemulsion systems. Ann Rev Phys Chem 1986; 37:351–399.
35. Percus JK, Yevick GJ. Analysis of classical statistical mechanics by means of collective co-ordinates. Phys Rev 1958; 110:1–13.
36. Kotlarchyk M, Chen SH, Husang JS, Kim MW. Structure of three-component microemulsions in the critical region determined by small-angle neutron scattering. Phys Rev A 1984; 29:2054–2069.
37. Kotlarchyk M, Chen SH, Husang JS. Temperature dependence of size and polydispersity in a three-component microemulsion by small-angle neutron scattering. J Phys Chem 1982; 86:3273–3276.

38. Husang JS, Safran SA, Kim MW, Grest GS, Kotlarchyk M, Quirke N. Attractive interactions in micelles and microemulsions. Phys Rev Lett 1984; 53:592–595.
39. Lisy V, Brutovsky B. Interpretation of static and dynamic neutron and light scattering from microemulsion droplets: Effect of shape fluctuations. Phys Rev E 2000; 61: 4045–4053.
40. Ziegenmeyer J, Fuehrer C. Mikroemulsionen als topische Arzneiform. Acta Pharm Technol 1980; 26:273–275.
41. Kreilgaard M, Pedersen EJ, Jaroszewski JW. NMR characterisation and transdermal drug delivery potential of microemulsion systems. J Control Release 2000; 69:421–433.
42. Kreilgaard M. Dermal pharmacokinetics of microemulsion formulations determined by in vivo microdialysis. Pharm Res 2001; 18:367–373.
43. Kreilgaard M, Kemme MJB, Burggraaf J, Schoemaker RC, Cohen AF. Influence of a microemulsion vehicle on cutaneous bioequivalence of a lipophilic model drug assessed by microdialysis and pharmacodynamics. Pharm Res 2001; 18:593–599.
44. Kriwet K, Mueller-Goymann CC. Diclofenac release from phospholipid drug systems and permeation through excised human stratum corneum. Int J Pharm 1995; 125:231–242.
45. Bolzinger-Thevenin MA, Carduner C, Poelman MC. Bicontinuous sucrose ester microemulsion: a new vehicle for topical delivery of niflumic acid. Int J Pharm 1998; 176:39–45.
46. Kemken J, Ziegler A, Mueller BW. Investigations into the pharmacodynamic effects of dermally administered microemulsions containing β-blockers. J Pharm Pharmacol 1991; 43:679–684.
47. Trotta M, Morel S, Gasco MR. Effect of oil phase composition on the skin permeation of felodipine from o/w microemulsions. Pharmazie 1997; 52:50–53.
48. Schmalfuß U, Neubert R, Wohlrab W. Modification of drug penetration into human skin using microemulsions. J Control Release 1997; 46:279–285.
49. Dalmora MEA, Oliveira AG. Inclusion complex of piroxicam with ß-cyclodextrin and incorporation in hexadecyltrimethylammonium bromide based microemulsion. Int J Pharm 1999; 184:157–164.
50. Dalmora ME, Dalmora SL, Oliveira AG. Inclusion complex of piroxicam with ß-cyclodextrin and incorporation in cationic microemulsion. In vitro drug release and in vivo topical anti-inflammatory effect. Int J Pharm 2001; 222:45–55.
51. Krause SA. Entwicklung und Charakterisierung von Mikroemulsionen zur dermalen Applikation von Arzneistoffen. Ph.D. dissertation, Martin-Luther-University, Halle-Wittenberg, Germany, 2001.
52. Shukla A, Krause A, Neubert RHH. Microemulsions as colloidal vehicle systems for dermal drug delivery. Part IV: Investigation of microemulsion systems based on a eutectic mixture of lidocaine and prilocaine as the colloidal phase by dynamic light scattering. J Pharm Pharmacol 2003; 55:741–748.
53. Jahn K. Moderne galenische Zubereitungen zur dermalen Anwendung von Ciclosporin A und Mycophenolatmofetil. Ph.D. dissertation, Martin-Luther-University, Halle-Wittenberg, Germany, 2002.
54. Wohlrab J, Neubert R, Jahn K. Arzneiformulierung, enthaltend Ciclosporin A und deren Verwendung. PCT/EO 01/14749, 2002.
55. Lehmann L, Keipert S, Gloor M. Effects of microemulsions on the stratum corneum and hydrocortisone penetration. Eur J Pharm Biopharm 2001; 52:129–136.
56. Paolino D, Ventura CA, Nisticó S, Puglisi G, Fresta M. Lecithin microemulsions for the topical administration of ketoprofen: percutaneous adsorption through human skin and in vivo human skin tolerability. Int J Pharm 2002; 244:21–31.
57. Rhee YS, Choi JG, Park ES, Chi SC. Transdermal delivery of ketoprofen using microemulsions. Int J Pharm 2001; 228:161–170.
58. Lee PJ, Langer R, Shastri VP. Novel microemulsion enhancer formulation for simultaneous transdermal delivery of hydrophilic and hydrophobic drugs. Pharm Res 2003; 20:264–269.

59. Baroli B, López-Quintela MA, Delgado-Charro MB, Fadda AM, Blanco-Méndez J. Microemulsions for topical delivery of 8-methoxsalen. J Control Release 2000; 69: 209–218.
60. Alvarez-Figueroa MJ, Blanco-Méndez J. Transdermal delivery of methotrexate: iontophoretic delivery from hydrogels and passive delivery from microemulsions. Int J Pharm 2001; 215:57–65.
61. Peira E, Scolari P, Gasco MR. Transdermal permeation of apomorphine through hairless mouse skin from microemulsions. Int J Pharm 2001; 226:47–51.
62. Changez M, Varshney M. Aerosol-OT microemulsions as transdermal carriers of tetracaine hydrochloride. Drug Dev Ind Pharm 2000; 26:507–512.
63. Peltola S, Saarinen-Savolainen P, Kiesvaara J, Suhonen TM, Urtti A. Microemulsions for topical delivery of estradiol. Int J Pharm 2003; 254:99–107.
64. Osborne DW, Ward AJI, O'Neill KJ. Microemulsions as topical drug delivery vehicles: in-vitro transdermal studies of a model hydrophilic drug. J Pharm Pharmacol 1991; 43:451–454.
65. Osborne DW, Ward AJI, O'Neill KJ. Microemulsions as topical drug delivery vehicles. I. Characterization of a model system. Drug Dev Ind Pharm 1988; 14:1203–1219.
66. Linn EE, Pohland RC, Byrd TK. Microemulsion for intradermal delivery of cetyl alcohol and octyl dimethyl PABA. Drug Dev Ind Pharm 1990; 16:899–920.
67. Delgado-Charro MB, Iglesias-Vilas G, Blanco-Méndez J, López-Quintela MA, Marty JP, Guy RH. Delivery of a hydrophilic solute through the skin from novel microemulsion systems. Eur J Pharm Biopharm 1997; 43:37–42.

53

Solid Lipid Nanoparticles (SLN) and Nanostructured Lipid Carriers (NLC) for Dermal Delivery

R. H. Müller, W. Mehnert, and E. B. Souto
Department of Pharmacy, Free University of Berlin, Berlin, Germany

I. INTRODUCTION

There are different approaches to modulate the penetration of active ingredients into the skin, i.e., either to increase the penetration or to minimize it. In general, increase in penetration is desired in case of pharmaceutical actives, either focusing the drug in the upper skin layer for local treatment or to achieve permeation of the skin leading to systemic absorption. A classical example for the latter case is nitroglycerine creams, finally leading to the development of transdermal patches. For cosmetic actives, the penetration to only a limited degree is desired to ensure that the active creates only cosmetic effects and do not lead to a pharmaceutical treatment of the skin. In case of sunscreen formulations, the penetration should be minimized to avoid irritations of the skin or other side effects, such as allergic reactions (1,2). Therefore, depending on the purpose of the topical formulation different requirements might be fulfilled by the dermal formulation.

A very simple approach to increase penetration is the use of occlusive formulations. Occlusion can be created by placing a plastic foil with low water permeability onto the skin, and—apart from other effects—the drug molecules are expelled in the same way as it is done in modern transdermal patches. Occlusion can also be created using water impermeable hydrocarbon bases, such as petrolatum. However, the aesthetic appearance of these formulations is not appealing. To reduce its fatty character one can produce water-in-oil (w/o) emulsions, realized in highly occlusive cosmetic night creams. Concerning oil-in-water (o/w) emulsions, they possess the desired ''lighter character'' but are distinctly less occlusive.

Another approach to improve penetration of drugs is the use of particulate carriers in the broadest sense, which means covering liposomes and solid particles, such as nano- and microparticles made from polymers or natural macromolecules. Phospholipid vesicles have already been described in the 20s of the last century (3) and were rediscovered as a dermal carrier system by Bangham (4) about 30 years ago. Despite intensive investigations of the liposomes in the cosmetic and the pharmaceutical area,

the question of penetration into the skin is still partially controversially discussed. At least it can be summarized that not any liposome will penetrate, once it seems to depend on its size and chemical composition, e.g., transfersomes (5). For solid particulate carriers a penetration of the intact particle through the stratum corneum can be excluded for those having a micrometer size, but also for most nanoparticles due to their size and rigidity of the carrier itself. However, in case of particles in the lower nanometer range, the diffusion into the gap surrounding hair follicles might be possible. Depending on the hair type, human hair follicles have a mean diameter ranging from 10 to 70 μm (6), therefore, theoretically particles can enter through these hair follicles and release the active compound in the vicinity of the hair shaft and bulb. However, transfollicular absorption is mainly considered as a minor route.

Another approach to increase penetration is the use of absorption enhancers, classical examples are the dimethylsufoxide (DMSO) and alcohols. The DMSO is a regulatorly accepted excipient used in preparations to treat herpes zoster (e.g., Virunguent® Salbe, Hermal, Germany). Another dermal absorption enhancer is cholic acid (7). The principle of action of absorption enhancers consists on their interaction with the lipid surface of the skin, changing its fluidity, and solubility for the cosmetic active, facilitating its absorption. Fatty acids such as lauric acid and also surfactants can act as absorption enhancers, therefore surfactant-rich dermal formulations will also benefit from an absorption enhancer effect. Microemulsions are such surfactant-rich systems, containing up to 30 % to 40% surfactant or surfactant mixture (8,9). Another important principle to modulate penetration of actives from microemulsions is their water content and the degree of saturation of the drug in the system. In case the active compound is dissolved in the microemulsion distinctly below its saturation solubility, penetration, and preferential location in the epidermis will take place. If the active concentration is close to or at its saturation solubility, increased systemic absorption will occur. This phenomenon is explained by formation of a supersaturated system after application of the microemulsion to the skin. There will be water uptake by the microemulsion from the skin, changing the solubility of the active molecules in the microemulsion, which in general is reduced with increasing water content. Thus, the system transfers from a saturated microemulsion to a supersaturated microemulsion due to the reduction of the solubility of the active compound. As a consequence, these latter try to leave the system, occurring in vitro leading to formation of crystals, but in vivo the drug leaves the microemulsion by penetrating into the skin (increased thermodynamic activity) (10–13).

A novel dermal delivery system with absorption increasing effects, such as occlusion, penetration enhancement, and controlled release of cosmetic and pharmaceutical actives are the solid lipid nanoparticles (SLN). This system is the first generation of lipid nanoparticles consisting of a solid matrix, which were developed at the beginning of the 1990s in parallel by the research group of Müller and Lucks (14) in Germany and Gasco (15) in Italy. The second generation, the so-called nanostructured lipid carriers (NLC) were developed at the turn of the millennium (16). This chapter describes the lab and large-scale production of these two lipid particles, the production of final formulations for dermal application and also discusses the various effects on the skin highlighting potential applications.

II. DEFINITIONS

The lipid nanoparticles are derived from o/w emulsions replacing the liquid lipid (oil) by a lipid being solid both at room and body temperature. The characteristic

is that the particle matrix is in a solid state, and its melting temperature can be adjusted by the choice of the lipid. Depending on the kind of application, it varies between 50°C (122°F) and up to almost 100°C (212°F).

SLN: these particles are the first generation of the lipid nanoparticles, consisting of a matrix, which is produced from a solid lipid. The lipid can be a highly pure lipid, e.g., tristearin (17–21) or a less defined mixture of acylglycerols, such as Compritol® (22–26) or Imwitor® (27–29).

NLC: these particles are produced from a lipid blend, consisting of a mixture of a solid lipid with a liquid lipid (oil). This mixture is chosen in order to obtain a particle matrix, which is in a solid state at the anticipated melting point. Relatively high amounts of oil can be incorporated when choosing a mixture with a high melting lipid, e.g., blending the oil Miglyol®812 (medium chain triacylglycerols) with Carnauba wax [melting point between 80–90°C (176–194°F)]. Up to above two-third of oil can be admixed but still remaining the melting point above 50°C (122°F) (30).

What is the special trick to use lipid blends in NLC? When producing a lipid particle from a solid lipid only (SLN), especially in case of highly pure lipids such as tristearin, the particles can form relatively perfect lipid crystals, then recrystallizing after being prepared by a hot homogenization process, or during precipitation when using the microemulsion technique. This means that the loading capacity of these carriers can be limited, especially when high drug loadings are required. Mixing especially very different molecules, such as long chain acylglycerols of the solid lipid with short chain acylglycerols of the liquid lipid, creates crystals with many imperfections.

Apart from localizing drug in between fatty acid chains or lipid lamellae, these imperfections provide a space for additional loading of active molecules. These latter can be incorporated in the particle matrix in a molecular dispersed form, or be arranged in amorphous clusters. High-resolution X-ray analysis can be used to determine the type of drug incorporation. For example, for cyclosporine it was found that the drug is located in between the fatty acid chains (54.6 Å) (31).

The type of the selected lipids used for preparation of nanoparticles also seems to be responsible for their physical shape. In case of highly pure lipids, such as tristearin or cetyl palmitate, the nanoparticles have a more cubic shape (32). On the contrary, in case of using rather polydispersed mixtures, which are preferentially used for cosmetic products, the lipid nanoparticles obtained a nice spherical shape (Fig. 1). When using identical lipid molecules the cubic shape occurs because they can build up a crystal-like a dense brick wall. In case of larger and smaller, and simultaneously differently shape ''stones'' (crystallizing molecules), the creation of a spherical structure is possible.

III. PRODUCTION OF LIPID NANOPARTICLES

There are different methods described in the literature to prepare lipid nanoparticles. The major technologies are the preparation by the high-pressure homogenization technique (33) and by the hot microemulsion technique (15). Other methodologies used by single research groups are precipitation of lipid particles using water-immiscible organic solvents, such as cyclohexane (34,35), chloroform (35), or methylene chloride (36), or semi-polar water-miscible solvents, such as ethanol, acetone, or methanol (37,38), or applying a solvent diffusion method using a partially water soluble solvent, such as benzyl alcohol (29) or tetrahydrofuran (39). These

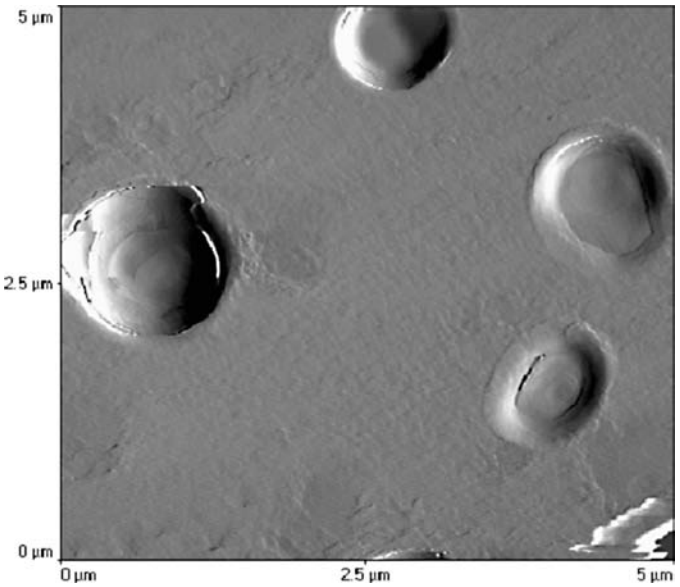


Figure 1 Atomic force microscopy (AFM) picture of lipid nanoparticles. *Source:* From Ref. 32.

latter three methodologies are comparable to solvent-based preparation methods for polymeric nano- or microparticles. All these methods, apart from high-pressure homogenization, require the use of organic solvents. This is less desired regarding the need to remove the solvent after particle production and potential solvent residues in the obtained product. Therefore, the high-pressure homogenization seems to be the most suitable technology for production of lipid nanoparticles.

There are two high-pressure homogenization technologies that can be applied for production of lipid nanoparticles, the so-called hot homogenization and cold homogenization techniques. When applying the hot homogenization process, the lipid is melted and the active compound is dissolved in the melted lipid. A typical temperature is 5°C above the melting temperature of the lipid. In the next step, the active-containing lipid melt is dispersed in a surfactant-stabilizer solution at identical temperature using a high-speed stirrer, i.e., a rotor–stator, such as the Ultra-Turrax (IKA, Staufen, Germany). A pre-emulsion is obtained with a mean droplet diameter typically somewhere between 2 and 5 µm. The pre-emulsion is then passed through a high-pressure homogenizer. Typical production conditions are a pressure of 250 to 500 bar and one to a maximum of three homogenization cycles. For most dermal formulations one cycle and 250 bar are sufficient. In the cold homogenization process, the active-containing lipid melt is solidified, grounded to microparticles, which are suspended in a cold surfactant-stabilizer solution. In this case a pre-suspension is homogenized, i.e., the lipid microparticles will be reduced to lipid nanoparticles in a solid state. This method is applied in certain cases to produce a homogeneous particle matrix with evenly molecularly dispersed drug. The production conditions affect the resulting inner structure of the lipid particles (for details see Ref. 40).

For the homogenization process a piston-gap homogenizer or a jet-stream homogenizer (microfluidizer type) can be used. For some technical reasons (temperature

control, cost of large-scale equipment, and availability in industry) the piston-gap homogenizers are typically preferred, e.g., equipment from APV Gaulin (www.apv.-com) or Avestin (www.avestin.com). Lab scale production can be performed using either a Micron LAB40 (APV, batch size 40 mL or for even smaller volumes) or an Avestin B3 (minimum batch size of approximately 3.5 mL). For larger volumes the continuous version of the LAB40 can be applied being equipped with product containers having a capacity of up to 500 mL (minimum volume of approximately 200 mL due to the dead volume of 50 mL). The LAB60 has a homogenization capacity of 60 L/hr and can be used for first technical batches. The LAB60 can be purchased with fitted product containers of up to 10 L (approximately 10 kg suspension). The minimum batch size in the continuous mode by circulating the product is about 2 kg. The maximum batch size is 10 kg when running the LAB60 in the discontinuous mode, which means passing the product three times through the homogenizer. The production times are 10 and 20 minutes, respectively (homogenization time). The Gaulin 5.5 has been successfully employed for large-scale production, having a homogenization capacity of 150 L/hr. Running a product with only one homogenization cycle will lead to about half a ton of particle suspension within three hours homogenization time. Larger machines are the Rannie 118 with up to 2 tons/hr (APV systems) or the Avestin 1000 with the capacity of 1 ton/hr (Avestin). Scaling up is easily possible when moving from 40 g dispersion (Micron LAB40) to, e.g., 40 kg batches produced with the Gaulin 5.5 (scalling up factor 1000). Running products on the larger machines leads even to a better product quality, i.e., more homogeneous size distribution and smaller particle sizes in less homogenization cycles. The obtained highest quality is due to the fact that larger machines are much better temperature controlled. In contrast to the LAB40, larges machines possess two homogenization valves in series and the valve design and geometry is identical or at least very similar. In addition, the larger machines are multi-plunger equipped, avoiding, or minimizing pulsating of the homogenization pressure as it occurs with the one-plunger homogenizer (e.g., LAB40).

IV. PRODUCTION OF FINAL TOPICAL FORMULATIONS

A. Incorporation into Creams and Gels

Identical to other carriers, such as liposomes, polymeric nanoparticles, and microsponge systems, the lipid nanoparticles can be added to cream formulations or gels. The smart feature of this approach is the fact that the addition of lipid nanoparticles to an already existing cream or gel formulation will combine the advantages of the well-established topical formulation with the special features of the lipid nanoparticles. Therefore, it is highly attractive to further improve an existing formulation on the market by a simple addition of lipid nanoparticles.

Incorporation of lipid nanoparticles into a cream is a very simple process. Ideally, the lipid nanoparticles are added as a highly concentrated suspension, i.e., with 50% solid (particle) content. In this case, addition of 10 g lipid particle suspension to 90 g cream leads to a lipid particle concentration of 5% in the final cream formulation. This concentration is sufficient to create an occlusive effect (41) or to load a cream with chemically unstable compounds, which are stabilized by incorporation in lipid nanoparticles. A typical example is retinol (final retinol concentration in cream 0.1% and retinol concentration in lipid particles 3.3%, see Ref. 42). Incorporation can be performed during or after the production of the o/w cream. In the first case, a part of the water in the cream formulation is replaced by a highly

concentrated lipid nanoparticle suspension, than the production process is run as usual. The lipid nanoparticles are sufficiently stabilized avoiding their coalescence with the oil droplets of the emulsion. If the production process of the emulsion is performed at a temperature higher than the melting point of the lipid nanoparticles, these latter will melt but will recrystallize during the cooling at the end of the process. A more elegant approach is the addition of concentrated lipid nanoparticle suspension after the production of the cream. The cream is produced as usual, but with reduced water content in order to compensate the water added with the lipid nanoparticle suspension. After production of the cream, the concentrated lipid nanoparticle suspension is admixed by stirring at room temperature. This process avoids the melting of the nanoparticles, a process, which can be accompanied by an undesired change of the internal particle structure. Note that the inner particle structure is very important, e.g., to adjust in a controlled way the desired release profile of the actives.

The addition of lipid nanoparticle suspension to gels is even simpler. The gel compounds can be mixed, and a concentrated nanoparticle suspension added before the gelation process is performed. However, it should be noted that electrolytes could destabilize the lipid nanoparticle suspension, as they do to any suspension. The zeta potential is reduced leading to aggregation of suspended particles. This phenomenon should be considered when, e.g., adding electrolytes in form of sodium hydroxide for the preparation of polyacrylic acid gels. It was found that the kind of neutralizing agent affects the dispersity of the lipid nanoparticles. Aggregation could be avoided or minimized when using Tristan® and Neutrol® TE as neutralizing agents (42). As soon as the gel has been formed, aggregation is not an issue any more because the particles are entrapped in the gel network and physically stabilized. It was found that in general lipid particle suspensions, which are unstable because of suboptimal surfactant combination, are perfectly stable after incorporation into gels. This opens the opportunity to use stabilizers, which are not that efficient in providing a long-term stability of the suspension, but are regulatory accepted. The lipid nanoparticle suspensions need to be stable only for the few hours until they are incorporated into the gel. Then they are stabilized by the gel network. This makes the system highly flexible to comply with the regulatory requirements, facilitating the entry of the product into the pharmaceutical or cosmetic market.

B. Preparation of Lipid Nanoparticle Gels

Topical formulations can be produced consisting of lipid nanoparticles only. This approach has certain advantages, such as the release of actives being only controlled by the lipid nanoparticle matrix. The desired properties can be adjusted in a very controlled way by attenuating the lipid nanoparticle features. The preparation process is again simple. A lipid nanoparticle suspension is prepared, then the gelling agent is added, preferentially non-electrolyte agents, such as cellulose derivatives (42). For many gel preparations a lipid nanoparticle content somewhere between 4% and 10% is sufficient. To make production most economic, a concentrated particle suspension (e.g., 50%) should be prepared and then diluted to the desired final concentration. Based on this purpose, 100 kg of stock nanoparticle suspension can be diluted by a factor 10 to 1000 kg (one ton) of final product to be gellified.

C. Preparation of Lipid Nanoparticle Creams

According to the SLN patent, the lipid concentration is between 0.1% up to a maximum of 30.0%. The reason behind was based on the fact that when applying higher lipid concentrations, ointments with a bicontinuous structure will be formed (Fig. 2). However, when developing the NLC system it was discovered that even when going to concentrations up to 50% or 60% the homogenization process leads to definite particles and not to an ointment-like system (Fig. 3).

This discovery opened new perspectives to produce creams (or more precisely: suspensions) of lipid nanoparticles in a high concentration. The viscosity of the preparations increases with the lipid concentration, i.e., at about 40% to 45% the preparations are cream-like, above 50% they become paste-like and when going up to a solid content of 80% or 90% the preparations are solid and can be cut with a knife. These solid preparations are not suitable for dermal application, but of high interest for oral administration of lipid particles to exploit the absorption enhancing effect of lipids (45). Of course, it can be asked: How can such highly concentrated lipid particle suspensions be prepared? Again, the trick is very simple. From food industry the preparation of highly concentrated mayonnaises (o/w systems) is well known. Commercial products contain up to 80% oil (being dispersed in an outer water phase). The trick to prepare a mayonnaise is to add the oil phase stepwise, which is exactly done when preparing highly concentrated lipid nanoparticle suspensions. First, a stock suspension is prepared by high-pressure homogenization containing, e.g., 50% lipid nanoparticles. Then stepwise additional melted lipid is added and dispersed again building a concentration of up to 80% or 90% of solid content. In the melted state, the preparation is still liquid and hence it has a relatively low viscosity. After cooling down—depending on the lipid content—the system becomes cream-like, paste-like, or even solid (Fig. 4).

Creams prepared from SLN only were investigated regarding their rheological properties. It could be shown that they are similar in viscosity and viscoelasticity to standard cream and ointment formulations of the European Pharmacopoeia (47). Thus, it

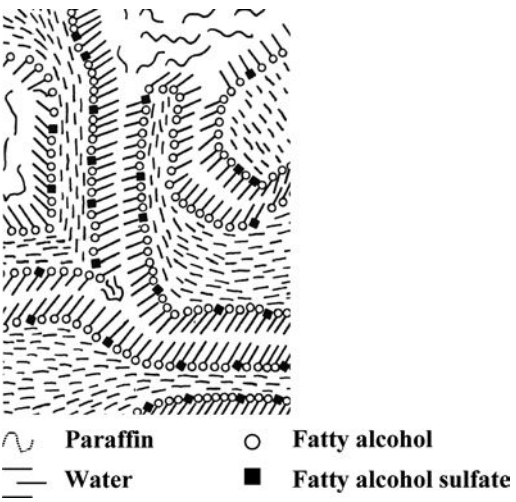


Figure 2 Structure of a bi-continuous cream. *Source:* Modified from Ref. 43.

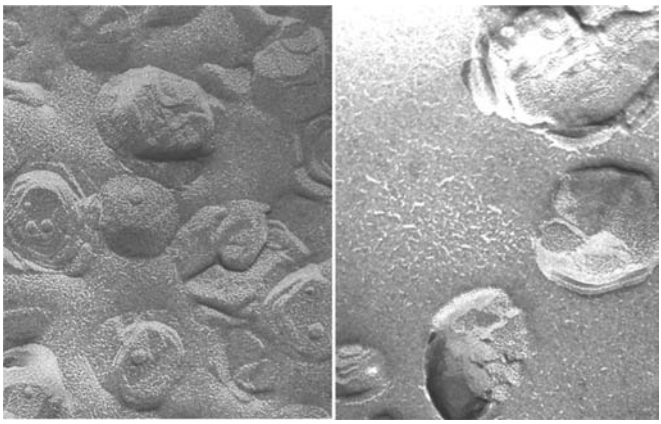


Figure 3 Electron micrograph of a 35% lipid particle dispersion before (*left*) and after (*right*) dilution with water to a 10% of lipid concentration. The mean photon correlation spectroscopy (PCS) particle size is 260 nm (1 bar = 1 μm). *Source:* Modified from Ref. 44.

can be concluded that by using a relatively high-lipid particle content and modifying its concentration, certain rheological properties can be adjusted in a controlled way.

V. PROPERTIES OF LIPID PARTICLES AND EFFECTS ON SKIN

A. Stabilization of Chemically Labile Actives

A solid matrix has the basic advantage that it is able to stabilize chemically labile actives against degradation by other species, e.g., water or oxygen. This effect has already been described for polymeric particles (48) and it is also valid for the lipid nanoparticles. The stability of retinol could be enhanced by incorporating it in NLC made from a mixture of Compritol 888 ATO and Miglyol 812 (32). The same effect was described for coenzyme Q10. This latter compound is relatively stable

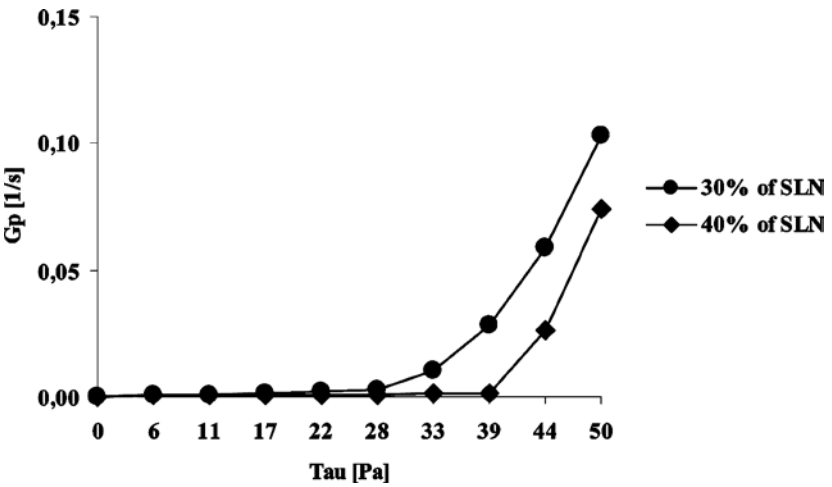


Figure 4 Effect of increasing concentration of lipid nanoparticles, ranging from 30% to 40% in the rheological properties of a hydrophilic cream. *Source:* Modified from Ref. 46.

when incorporated in a protective packaging, but it degrades fast when exposed to light, especially when stressing it by artificially lighting leading to a bi-exponential degradation behavior (32,49).

B. Lightening Effect in Creams

According to market studies, appearance is an important factor for a cosmetic to be sold, i.e., not only the packaging should be attractive but also appearance of the product itself. White products are preferred by the consumers. Compounds like coenzyme Q10 are colored (yellow) leading to a yellowish appearance of the cream. The coloration can be weakened by addition of the white lipid nanoparticle suspension.

This whitening effect is of special interest for actives, which are degraded with degradation products possessing a color. An example is vitamin C, which turns to an intermediate colored product, but the final degradation product is again white. In case such coloration occurs, even if it is weak, it will be associated by the consumer to a spoiled product—despite the percentage of such degradation products might be not relevant and not impair the product quality. Addition of lipid nanoparticles can avoid or minimize such effects.

C. Occlusion

The general property of ultrafine particle is their adhesiveness to surfaces, e.g., described for polymeric nanoparticles. It is also known that liposomes adhere to the skin. The same is valid for the lipid nanoparticles. It was calculated that approximately 4% of lipid nanoparticles with a diameter of approximately 200 nm should form theoretically a monolayer film when ca. 4 mg of formulation is applied per square centimeter (41).

The occlusion factor can be determined in vitro using the test by de Vringer (50). A beaker with water is covered with a cellulose acetate filter to which the formulation is applied and then the evaporation of water is determined as a function of time. A beaker covered with the filter paper only is used as reference. An occlusion factor can be calculated, being zero in case no occlusion occurs and water evaporation of sample and reference are identical, being 100 when maximum occlusive effect occurs. It could be shown that the occlusion factor of lipid microparticles ($>1\,\mu m$ diameter) was only 10%, compared to a factor of 50% when using lipid nanoparticles of approximately 200 nm (32,51). This result can be explained by the different structure of the adhesive microparticle/nanoparticle layer on the skin. The space filled with air in a particle layer of optimal packing density is independent on the particle size (which is 24% assuming a three-dimensional hexagonal packing of ideal spherical particles). However, the dimensions of the air channels are much larger in a layer of microparticles compared to a layer of nanoparticles; therefore, the larger pores in the microparticle layer favor hydrodynamically water evaporation. In addition, when applying the nanoparticle suspension to a surface/skin the pressure leads to fusion of the particles and finally to a dense film. This fusion is further promoted by capillary forces involved during the water evaporation process (similar to coating tablets with Eudragit® nanoparticle dispersions). Figure 5 shows a scanning electron microscopy (SEM) picture of such a nanoparticle film.

D. Skin Hydration and Elasticity

In vitro occlusion tests showed nicely the superiority of lipid nanoparticle films compared to lipid microparticle films. However, the question is how relevant are

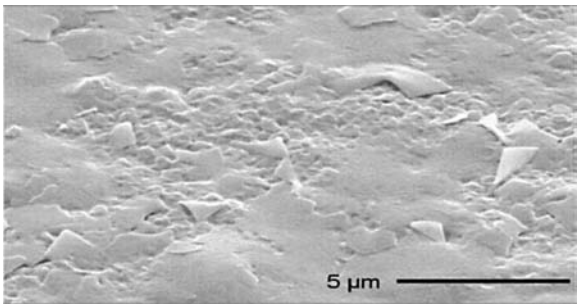


Figure 5 Scanning electron microscopy (SEM) picture of a solid lipid nanoparticle film applied to a surface after evaporation of water leading to a dense, poreless film. *Source:* From Ref. 52.

the in vitro data for the in vivo situation, i.e., will lead the film to a significant increase in hydration of the skin, eventually to an increase in skin elasticity?

A double-blind study was performed using a well-established day cream from the cosmetic market. It was a high-quality product, i.e., the reference was of high standard. In this formulation a part of the oil was replaced by SLN (final formulation having 4% lipid nanoparticle solid content). The formulation was applied to the alveolar forearms of the volunteers. Skin hydration was measured with a Corneometer CM 825 and skin elasticity with a Cutometer SEM 575. In order to assess the condition of the skin before the treatment, measurements were taken before the beginning of the study. The analyses were then performed within two and four weeks after administration of tested formulations. Figure 6 shows that there is no change in skin hydration in non-treated controls. Skin hydration was distinctly increased to about 24% (arbitrary units of the corneometer and modification is based on measuring the dielectric constant). The SLN-loaded day cream had a further increase to about 32%. The results were statistically significant when applying the

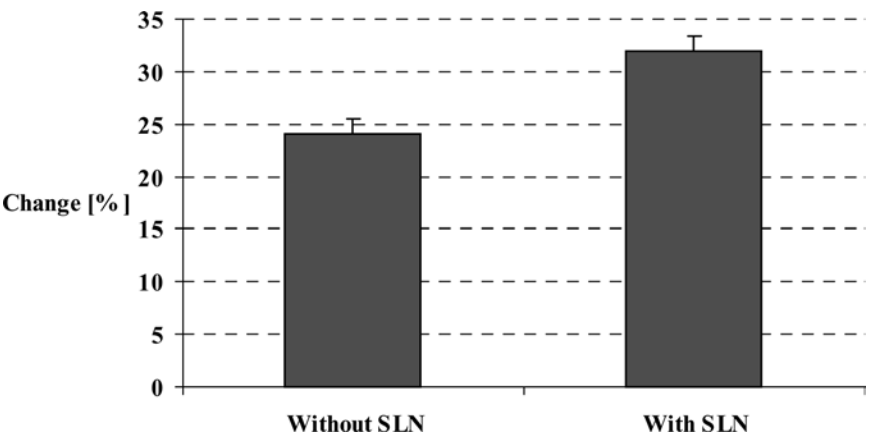


Figure 6 Increase in skin hydration after application of a commercial day cream (without SLN) and the same day cream containing lipid nanoparticles (with SLN) with identical lipid content in comparison to untreated controlled groups. *Abbreviation*: SLN, solid liquid nanoparticles. *Source:* Modified from Ref. 54.

Wilcoxon test (53). It should be emphasized, that this increase was achieved by running the SLN formulation against a high-quality market product. Despite this, SLN addition improved skin hydration further. However, when applying the cosmetic night cream higher occlusion factors can be achieved. But in this case, the smart approach is to increase the occlusion effect and maintaining simultaneously the light character of the day cream. Elasticity was also measured, however, in this study no increase was found. The reason for this observation was due to the fact that the study was performed with students aged 26 ± 3 years, and they still have a highly elastic skin. Further improvement is, therefore, not possible. Currently, a study is planned with older volunteers.

E. Modulation of Release and Creation of Supersaturation

Depending on the method of preparation (hot homogenization vs. cold homogenization), the composition of the formulation (i.e., content of surfactant/stabilizer), the solubilizing properties of the surfactant for the incorporated active and the TX-solubility diagrams, SLN with a different structure will be obtained. Basically, there are three types of SLN:

1. Homogeneous type
2. Core-shell type with active-enriched core
3. Core-shell type with active-enriched shell

For example, production applying the hot homogenization technique at higher temperatures and using higher surfactant concentration leads to the core-shell type with active-enriched shell. A typical example is coenzyme Q10. It could be shown by AFM measurements that most of the active is located in the outer shell (55), results that were also confirmed by another research group using acyclovir as a model drug (56). Details of these models can be found in Refs. 24 and 40. Depending on the matrix structure, the release profiles will vary from very fast release, medium release, or extremely prolonged release (Fig. 7).

It should be noted that the release profiles were obtained by in vitro assays, applying the patent method of the U.S. Pharmacopoeia (USP 24), which means in the absence of any lipid degradation enzymes. Release in vivo will be superposition of drug diffusion from the lipid matrix (corresponds to an in vitro release) and simultaneously particle degradation by lipases. The degradation of lipid nanoparticles was intensively studied as a function of the chemical nature of the lipid, the nature of the stabilizing surfactant and the particle size using lipase/co-lipase (57–60). Due to the microbial flora of the skin, a contribution of enzymatic degradation to the drug release cannot be excluded, appears rather likely (10). It is perfectly clear that release over weeks is not interesting for in vivo topical delivery, but the obtained in vitro release data emphasize the capacity of the lipid nanoparticle system to modulate drug release, i.e., to adapt it to the therapeutic needs.

Modulation of drug release into certain layers of the skin and, therefore, drug penetration across skin membranes can also be achieved as a consequence of the creation of a supersaturated system (11). These systems can be created by incorporation of lipid nanoparticles into topical formulations (creams, ointments, emulsions, and gels). The increase in saturation solubility will lead to an increased diffusion pressure of drug into the skin. Figure 8 depicts the phenomenon of triggered drug release and supersaturation effect of NLC into a dermal preparation. During storage, the drug remains in the NLC because these particles preserve their

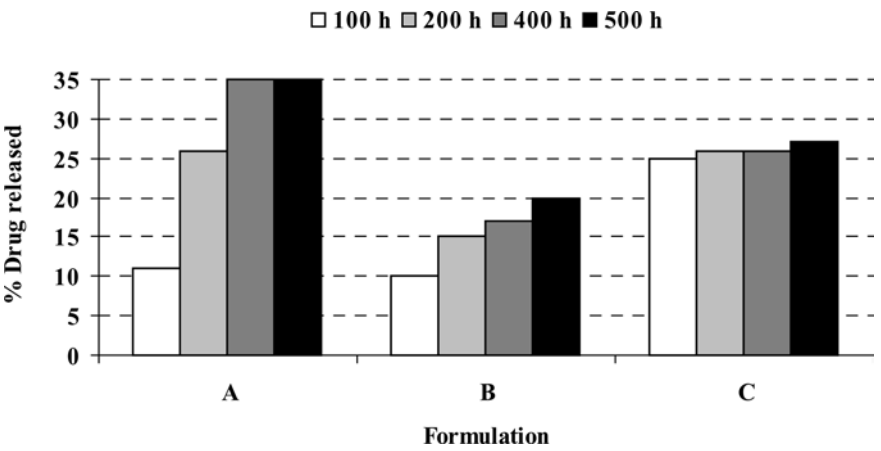


Figure 7 Release of prednisolone after 100, 200, 400, and 500 hour from lipid nanoparticles prepared by different lipid compositions and methods: (**A**) Cholesterol solid lipid nanopart (SLN) by cold homogenization technique, (**B**) Compritol SLN by cold homogenization technique, and (**C**) Compritol SLN by hot homogenization technique. *Source:* Modified from Refs. 24 and 55.

polymorphic form. After application of NLC-loaded cream onto the skin, and due to an increase in temperature and water evaporation, the lipid matrix of NLC transforms from a more unstable polymorph to a more ordered polymorph leading to drug expulsion. The drug is expelled from the lipid matrix into the emulsion already saturated with drug and thus creating a supersaturation effect. This phenomenon increases the thermoactivity and leads to drug penetration into the skin.

F. Penetration of Actives

The penetration of various interesting cosmetic actives into dermal route has been studied (32,53,61,62). For instance, coenzyme Q10 was applied onto the skin dissolved

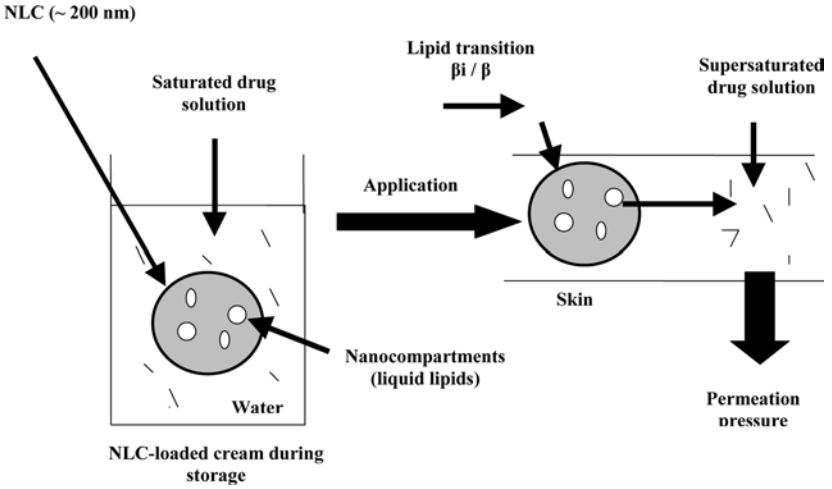


Figure 8 Supersaturation effect and triggered drug release. *Source:* From Ref. 11.

in liquid paraffin, isopropanol, and incorporated in a lipid nanoparticle formulation (32). The cumulative amount penetrated was determined using the Tesa™-stripping test. After five strips, the cumulative amounts were 1%, 28%, and 53%, respectively, for the three formulations, showing clearly the superiority of the SLN formulation. Interesting was also the comparison between the penetration of coenzyme Q10 from lipid microparticles (4.5 μm diameter) and lipid nanoparticles (200 nm diameter, PCS). Figure 9 shows increased penetration when applying the nanoparticle system to the skin, which is attributed to an occlusive effect and differences in release profiles of the two formulations.

The penetration of drugs via the topical route has been intensively studied by the research group of Schäfer–Korting, in Berlin (42,63–67). Prednicarbate (PC) was incorporated in SLN of different lipid composition and the penetration into human skin was studied using Franz flow-through diffusion cells (68). Figure 10 shows the penetration of PC into excised human skin after application of drug-loaded SLN prepared with glycerol behenate in comparison to a cream, after 6 hours (Fig. 10A) and 24 hours (Fig. 10B). After incorporation of PC into SLN, an improved in drug uptake ($2.50 \pm 0.66\%$, percentage of applied dose) could be observed in comparison to the cream ($0.84 \pm 0.13\%$, percentage of applied dose), leading to an accumulation in the first skin slice without reaching the corium, and therefore, avoiding skin atrophy which is the main side effect of topical corticosteroids. These findings support the targeting ability of lipid nanoparticles, where the drug must be incorporated and not adsorbed to the surface of the particle. Furthermore, it could also be observed that dilution of PC-SLN with an o/w cream did not decrease the targeting effect to the superficial layers of the skin.

It was also studied to which extent lipid nanoparticles can penetrate into the skin, using fluorescence labeled particles (69). The results could be summarized that SLN obviously do not penetrate intracellularly between the corneocytes of the stratum corneum, especially there is no paracellular transport. However, interestingly it was found that the lipid nanoparticles diffuse into the hair follicle, precisely into the

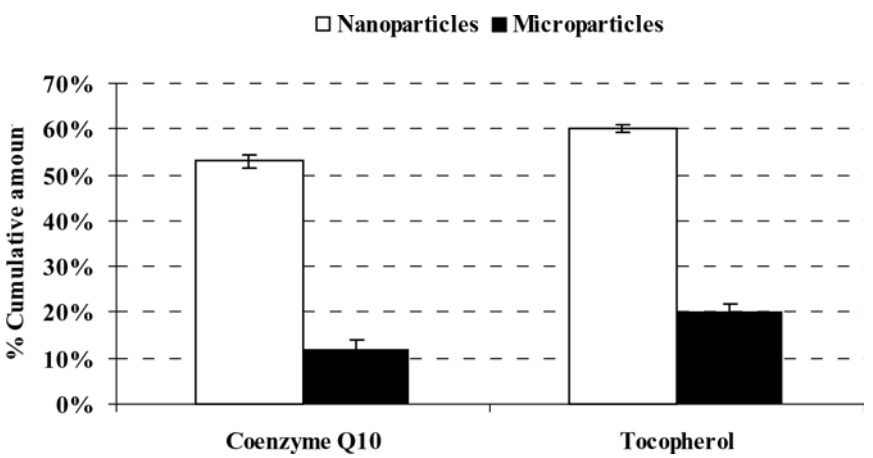


Figure 9 Total amount of coenzyme Q10 and α-tocopherol penetrated after five strips when the drug is administered after incorporation into lipid nanoparticles Versus. lipid microparticles (Tesa-stripping test, cumulative amount). *Source:* Modified from Ref. 32.

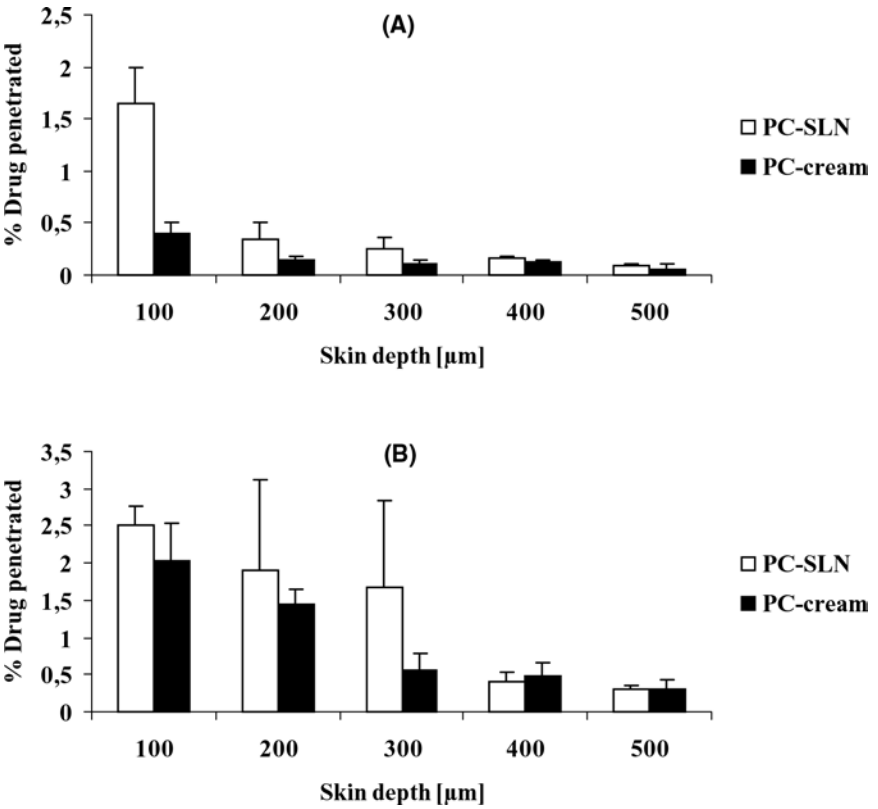


Figure 10 Penetration of prednicarbate into excised human skin following administration of 125 µg of drug incorporated in SLN (PC-SLN) in comparison to a conventional cream (PC-cream), after 6 hours (**A**) and 24 hr (**B**). *Source:* Modified from Ref. 68.

gap surrounding the hair. This opens the opportunity to target drugs specifically to the hair follicle for special treatments, such as alopecia.

To summarize: these data show that lipid nanoparticles applied to the skin can increase the penetration of incorporated drugs. Obviously, the penetration profiles differ from active to active, and they are also affected by the matrix morphology of the particles. In addition, there seems to be special interactions of the lipids of the particle matrix with the lipids of the stratum corneum, resulting in a pronounced effect on the penetration profile. However, these effects are not yet fully understood and are under intensive investigation. Furthermore, the lipid nanoparticles offer the opportunity to provide a moderate increase of the penetration as required for cosmetics (which need to avoid deep penetration and to avoid a pharmaceutical effect) but also increased penetration/permeation as desired for pharmaceutical actives. Note that these latter should be localized into the skin either for local treatment or penetrate deeply for systemic effects.

G. Prolonged Release of Actives—Sunscreens

There are cosmetic and skin care applications in which just the opposite to an increase of penetration is desired, achieving prolonged release with little penetration as possible. Typical examples are sunscreens loaded with particulate and molecular

UV blockers. A side effect of molecular UV blockers is penetration into the skin leading to skin irritation or even allergic reactions (70). Particulate UV blockers frequently used are titanium dioxide particles. There is also an ongoing controversial discussion whether and how to which extent titanium dioxide particles penetrate into the skin (71,72), where they can potentially interact with the immune system (1). Lipid nanoparticles were prepared loaded with molecular UV blockers (53,62,73) and also loaded with titanium dioxide particles (74).

After incorporation of molecular UV blockers into lipid nanoparticles, a synergistic effect of the UV scattering caused by the SLN themselves and the UV absorbance of the molecular sunscreen was observed (75). This opens the perspective to reduce the concentration of the molecular sunscreen, and simultaneously its potential side effects, but also maintaining the UV protective level. Apart from reduction of side effects, this result is of commercial interest in case of expensive UV blockers. In addition, it was found that penetration of molecular sunscreens into the skin was reduced when comparing SLN to a traditional o/w emulsion system (76). A Tesa-stripping test was performed with volunteers, observing that the cumulative amount after seven strips was 4% and 6%, respectively. Using SLN formulations the sunscreen penetration decreased about 40%, in comparison to the tested o/w emulsion.

From the results discussed above, it can be said that the lipid nanoparticles appear as an attractive system to formulate sunscreens products with lower and medium sun protection factor (SPF). To achieve high SPF values (higher than 30), relatively high concentrations of molecular sunscreens in combination with titanium dioxide are required. Typical examples are 10 to 20% of molecular sunscreens (e.g., ethylhexyltriazone and ethylhexylmethoxycinnamate) and 1 to 3% of titanium dioxide (74).

Concerning the drug loading capacity of lipid nanoparticles, it ranges from about 1% (e.g., for prednisolone) up to 25% (e.g., vitamin E and cyclosporine) or even up to 50% and more, in case of well lipid miscible lipophilic actives (e.g., vitamin E) (percentages calculated on the total particle mass, i.e., lipid plus active). "Super-loaded" NLC were developed having a sunscreen loading of 70%. This was achieved by using the liquid sunscreen as oil component in the NLC formulation, and cetyl palmitate was added to create a solid matrix (74). At the same time, 2% of titanium dioxide particles were incorporated into the lipid nanoparticles. This opens the opportunity to produce also topical sunscreens formulations with higher SPF values. However, it should be kept in mind that, in case of too high loadings, the release of sunscreen from the nanoparticles might be accelerated, approaching again the release from emulsions. If there is too little matrix material (solid lipid) in the nanoparticle, there will be only little prolongation in release.

H. Prolonged Release of Actives—Scents/Perfumes

Other interesting compounds for prolonged release are perfumes and insect repellents. At present there is a tendency to create prolonged release perfume formulations by incorporating the perfumes into o/w emulsions. There is a slower release from emulsions compared to Eau de Toilettes. The release can be further slowed down by incorporating the perfume in a solid lipid nanoparticle instead in a liquid lipid particle (oil droplet). This was nicely shown for the perfume Allure. In the first 3 hr the release of the perfume from lipid nanoparticles was similar to the emulsion, which attributed to release of perfume from the outer layers of the particles. During the remaining 10 hours the release from the SLN was prolonged. After 6 hours 100%

of perfume was released from the emulsion, but only 75% was released from the SLN suspension (16,53,77). This demonstrates the principle usage of the lipid nanoparticles for prolonged perfume release, in order to create a once a day application with continuing sent over at least 12 hours. Prolonged release was also observed for insect repellents, such as lemon oil (53,78–80).

VI. CONCLUSIONS AND PERSPECTIVES

Lipid nanoparticles (SLN and NLC) are an interesting system for the delivery of cosmetic and pharmaceutical actives. Similar to emulsions they are composed of accepted excipients, i.e., all cosmetic and pharmaceutical excipients with accepted status in products or GRAS (generally regarded as safe) substances can be used, and can be produced on large industrial scale, using an established and low cost homogenization process. The lipid nanoparticles possess additionally the advantages of a solid particle matrix similar to polymeric nanoparticles, having the ability to protect chemically labile ingredients and to modulate release (from very fast to extremely prolonged release). They can easily be incorporated into existing, well-established products combining the advantages of these products with the special features of the lipid nanoparticle technology. Physical stability of the nanoparticles has been shown i.e., for the required storage periods in cosmetics.

It has also been observed that optimized aqueous lipid particle suspensions are stable up to three years. From this it can be summarized that lipid nanoparticles represent an interesting carrier for topical formulations and they have the perspective to be introduced to the market in a number of products.

First products are already on the market by the company Yamanouchi (e.g., Nanobase® in Poland). However, in this case the lipid nanoparticles are active-free (because only active-free particles are covered by the Yamanouchi patent, see Ref. 50). In case actives are present they are dissolved in the disperse aqueous phase. These products exploit the special features of placebo SLN, such as good application properties and adhesion leading to skin hydration. If the lipid particle creams contain actives in the water phase, the penetration should be improved. It is expected that more products based on SLN and NLC will follow, both in cosmetic and pharmaceutical area, when looking at the strongly increase number of research groups in the last 10 years starting to work with this delivery system (33,81).

ACKNOWLEDGMENTS

The authors would like to acknowledge Prof. Dr. C. C. Müller-Goymann, from the Institute of Pharmaceutical Technology of the Technical University of Braunschweig for taking the electron microscopy graphs.

REFERENCES

1. Hagedorn-Leweke U, Lippold BC. Accumulation of sunscreens and other compounds in keratinous substrates. Eur J Pharm Biopharm 1998; 46:215–221.
2. Ricci C, Pazzaglia M, Tosti A. Photocontact dermatitis from UV filters. Contact Dermaititis 1989; 38:343–344.

3. Lehmann O. Neue Untersuchungen über Flüssige Kristalle. II. Teil, in Carl Winter's Universitätsbuchhandlung Heidelberg, 1912.
4. Bangham AD. Membrane models with phospholipids. Prog Biophys Mol Biol 1968; 18:29–95.
5. Cevc G. Lipid vesicles and other colloids as drug carriers on the skin. Adv Drug Deliv Rev 2004; 56:675–711.
6. Lauer AC, Lieb LM, Ramachandran C, Flynn GL, Weiner ND. Transfollicular drug delivery. Pharm Res 1995; 12:179–186.
7. Funke AP. Transdermale Absorption von Hochlipophilen, Basischen Antiestrogenen aus Flüssigformulierungen und Matrix-Transdermalsystemen. Ph.D. thesis, Free University of Berlin, 2000.
8. Bourrel M, Schechter RS. In: Microemulsions and related systems. Formulation, Solvency, and Physical Properties, Vol. 30. New York, Basel, Hong-Kong: Marcel Dekker Inc., 1988.
9. Attwood D. Microemulsions. In: Kreuter J, ed. Colloidal Drug Delivery Systems. New York, Basel, Hong-Kong: Marcel Dekker Inc., 1994:31–71.
10. Müller RH, Wissing SA. Lipopearls for topical delivery of active compounds and controlled release. In: Rathbone MJ, Hadgraft J, Roberts MS, eds. Modified-Release Drug Delivery Systems. New York, Basel, Hong-Kong: Marcel Dekker Inc., 2003:571–587.
11. Müller RH, Radtke M, Wissing SA. Solid lipid nanoparticles (SLN) and nanostructured lipid carriers (NLC) in cosmetic and dermatological preparations. Adv Drug Deliv Rev 2002; 54(suppl):S131–S155.
12. Müller RH, Radtke M, Wissing SA. Nanostructured lipid matrices for improved microencapsulation of drugs. Int J Pharm 2002; 242:121–128.
13. Radtke M. Nanostructured lipid carriers (NLC): Untersuchungen zur Struktur, Wirkstoffinkorporation und Stabilität. Ph.D. thesis, Freie Universität Berlin, 2003.
14. Müller RH, Lucks JS. Arzneistoffträger aus festen Lipidteilchen, Feste Lipidnanosphären (SLN), EP 0605497, 1996.
15. Gasco MR. Methods for producing solid lipid microspheres having a narrow size distribution, USP Patent 5 250 236 (1993).
16. Müller RH, Mäder K, Lippacher A, Jenning V. Fest-flüssige (halbfeste) Lipidpartikel und Verfahren zur Herstellung hochkonzentrierter Lipidpartikeldispersionen, PCT/EP00/04565 (2000).
17. Siekmann B, Westesen K. Submicron-sized parenteral carrier systems based on solid lipids. Pharm Pharmacol Lett 1992; 1:123–126.
18. Westesen K, Bunjes H. Do nanoparticles prepared from lipids solid at room temperature always possess a solid lipid matrix? Int J Pharm 1995; 115:129–131.
19. Bunjes H, Westesen K, Koch MHJ. Crystallization tendency and polymorphic transitions in triglyceride nanoparticles. Int J Pharm 1996; 129:159–173.
20. Radomska A, Dobrucki R, Müller RH. Chemical stability of the lipid matrices of solid lipid nanoparticles (SLN) development of an analytical method and determination of long-term stability. Pharmazie 1999; 54:903–909.
21. Bunjes H, Koch MHJ, Westesen K. Effect of particle size on colloidal size solid triglycerides. Langmuir 2000; 16:5234–5241.
22. zur Mühlen A, zur Mühlen E, Niehus H, Mehnert M. Atomic force microscopy studies of solid lipid nanoparticles. Pharm Res 1996; 13:1411–1416.
23. Ahlin P, Kristl J, Šmid-Kobar J. Optimization of procedure parameters and physical stability of solid lipid nanoparticles in dispersions. Acta Pharm 1998; 48:259–267.
24. zur Mühlen A, Mehnert W. Drug release and release mechanism of prednisolone loaded solid lipid nanoparticles. Pharmazie 1998; 53:552–555.
25. Pinto JF, Müller RH. Pellets as carriers of solid lipid nanoparticles (SLN) for oral administration of drugs. Pharmazie 1999; 54:506–509.
26. Videira MA, Almeida AJ, Botelho MF, Santos AC, Gomes C, Pedroso Lima JJ. Lymphatic uptake radiolabelled solid lipid nanoparticles administered by the pulmonary route. Eur J Nucl Med 1999; 26:PS-462.

27. Zimmermann E, Müller RH. Electrolyte- and pH-stabilities of aqueous solid lipid nanoparticles (SLN™) dispersions in artificial gastrointestinal media. Eur J Pharm Biopharm 2001; 52:203–210.
28. Schöler N, Hahn H, Müller RH, Liesenfeld O. Effect of lipid matrix and size of solid lipid nanoparticles (SLN) on the viability and cytokine production of macrophages. Int J Pharm 2002; 231:167–176.
29. Trotta M, Debernardi F, Caputo O. Preparation of solid lipid nanoparticles by a solvent emulsification-diffusion technique. Int J Pharm 2003; 257:153–160.
30. Fischer-Carius A. Untersuchungen an Extrudierten und Sphäronisierten Matrixpellets mit Retardierter Wirkstofffreigabe. Ph.D. Thesis, Freie Universität Berlin, 1998.
31. Runge SA. Feste Lipidnanopartikel (SLN®) als Kolloidaler Arzneistoffträger für die Orale Applikation von Cyclosporin A. Ph.D. thesis, Freie Universitär Berlin, 1998.
32. Dingler A. Feste Lipid-Nanopartickel als Kolloidale Wirkstoffträgersysteme zur Dermalen Applikation. Ph.D. thesis, Freie Universität Berlin, 1998.
33. Müller RH, Mehnert W, Lucks JS, Schwarz C, zur Mühlen A, Weyhers H, Freitas C, Rühl D. Solid lipid nanoparticles (SLN)—an alternative colloidal carrier system for controlled drug delivery. Eur J Pharm Biopharm 1995; 41:62–69.
34. Sjöström B, Bergenståhl B. Preparation of submicron drug particles in lecithin-stabilized o/w emulsions. I. Model studies of the precipitation of cholesteryl acetate. . Int J Pharm 1992; 88:53–62.
35. Siekmann B, Westesen K. Investigations on solid lipid nanoparticles prepared by precipitation in o/w emulsions. Eur J Pharm Biopharm 1996; 43:104–109.
36. Reithmeier H, Herrmann J, Göpferich A. Development and characterization of lipid microparticles as a drug carrier for somatostatin. Int J Pharm 2001; 218:133–143.
37. Schubert MA, Müller-Goymann CC. Solvent injection as a new approach for manufacturing lipid nanoparticles—evaluation of the method and process parameters. Eur J Pharm Biopharm 2003; 55:125–131.
38. Dubes A, Parror-Lopez H, Abdelwahed W, Degobert G, Fessi H, Shahgaldian P, Coleman AW. Scanning electron microscopy and atomic force microscopy imaging of solid lipid nanoparticles derived from amophiphilic cyclodextrins. Eur J Pharm Biopharm 2003; 55:279–282.
39. Shahgaldian P, Gualbert J, Aïssa K, Coleman AW. A study of the freeze-drying conditions of calixarene based solid lipid nanoparticles. Eur J Pharm Biopharm 2003; 55: 181–184.
40. zur Mühlen A, Schwarz C, Mehnert W. Solid lipid nanoparticles (SLN) for controlled drug delivery—drug release and release mechanism. Eur J Pharm Biopharm 1998; 45:149–155.
41. Wissing SA, Lippacher A, Müller RH. Investigations on the occlusive properties of solid lipid nanoparticles (SLN). J Cosmet Sci 2001; 52:313–324.
42. Jenning V, Schäfer-Korting M, Gohla S. Vitamin A-loaded solid lipid nanoparticles for topical use: drug release properties. J Control Release 2000; 66:115–126.
43. Bauer KH, Frömming KH, Führer C. Lehrbuch der Pharmazeutischen Technologie, Wissenschaftliche Verlagsgesellschaft mbH, Stuttgart, 1999:276.
44. Lippacher A, Müller RH, Mäder K. Liquid and semisolid SLN™ dispersions for topical application: rheological characterization. Eur J Pharm Biopharm 2004; 58:561–567.
45. Müller RH, Keck CM. Challenges and solutions for the delivery of biotech drugs—a review of drug nanocrystal technology and lipid nanoparticles. J Biotechnol 2004; 113: 151–170.
46. Souto EB, Müller RH. Rheological and in vitro release behaviour of clotrimazole-containing aqueous SLN dispersions and commercial creams. Int J Pharm (submitted).
47. Lippacher A, Müller RH, Mäder K. Preparation of semisolid drug carriers for topical application based on solid lipid nanoparticles. Int J Pharm 2001; 214:9–12.

48. Sakuma S, Suzuki N, Sudo R, Hiwatari K, Kishida A, Akashi M. Optimized chemical structure of nanoparticles as carriers for oral delivery of salmon calcitonin. Int J Pharm 2002; 239:185–195.
49. Müller RH, Dingler A. Feste lipid-nanopartikel (Lipopearls™) als neuartiger carrier für kosmetische und dermatologische wirkstoffe. Pharm Zeit Dermo 1998; 49:11–15.
50. de Vringer T. Topical preparation containing a suspension of solid lipid particles, European Patent No. 91200664 (1992).
51. Müller RH, Dingler A. The next generation after the liposomes: solid lipid nanoparticles (SLN, Lipopearls) as dermal carriers in cosmetics. Eurocosmetics 1998; 7–8:19–26.
52. Wissing SA, Müller RH. A novel sunscreen system based on tocopherol acetate incorporated into solid lipid nanoparticles (SLN). Int J Cosmet Sci 2001; 23:233–243.
53. Wissing SA. SLN als Innovatives Formulierungskonzept für Pflegende und Protective Dermale Zubereitungen. Ph.D. thesis, Free University of Berlin, 2002.
54. Wissing SA, Müller RH. The influence of solid lipid nanoparticles (SLN) on skin hydration and viscoelasticity—in vivo study. Eur J Pharm Biopharm 2003; 56:67–72.
55. zur Mühlen A. Feste Lipid—Nanopartikel mit prolongierter Wirkstoffliberation: Herstellung, Langzeitsabilität, Charakterisierung, Freisetzungsverhalten und Mechanismen. Ph.D. thesis, Free University of Berlin, 1996.
56. Lukowski G, Werner U, Pflegel P. Surface investigation and drug release of drug-loaded solid lipid nanoparticles. Proceedings 2nd World Meeting APGI/APV, Paris, 1998: 573–574.
57. Müller RH, Olbrich C. Solid lipid nanoparticles: phagocytic uptake in vitro cytotoxicity and in vitro biodegradation. 1st communication. Pharm Ind 1999; 61:462–467.
58. Müller RH, Olbrich C. Solid lipid nanoparticles: phagocytic uptake, in vitro cytotoxicity and in vitro biodegradation. 2nd Communication. Drugs made in Germany 1999; 42: 75–79.
59. Olbrich C, Müller RH. Enzymatic degradation of SLN—effect of surfactants and surfactant mixtures. Int J Pharm 1999; 180:31–39.
60. Lbrich C, Kayser O, Müller RH. Lipase degradation of Dynasan 114 and 116 solid lipid nanoparticles (SLN)—effect of surfactants, storage time, and crystallinity. Int J Pharm 2002; 237:119–128.
61. Jenning V. Feste Lipid-Nanopartikel (SLN) als Trägersystem für die Dermale Applilkation von Retinol. Ph.D. thesis, Freie Universität Berlin, 1999.
62. Wissing SA, Müller RH. Solid lipid nanoparticles (SLN)—a novel carrier for UV blockers. Pharmazie 2001; 56:783–786.
63. Gysler A, Lange K, Korting HC, Schäfer-Korting M. Prednicarbate biotransformation in human foreskin keratinocytes and fibroblasts. Pharm Res 1997; 14:793–797.
64. Lange K, Gysler A, Bader M, Kleuser B, Korting HC, Schäfer-Korting M. Prednicarbate versus conventional topical glucocorticoids: pharmacodynamic characterization in vitro. Pharm Res 1997; 14:1744–1749.
65. Gysler A, Kleuser B, Sippl WE, Lange K, Korting HC, Höltje HD, Schäfer-Korting M. Skin penetration and metabolism of topical glucocorticoids in reconstructed epidermis and excised human skin. Pharm Res 1999; 16:1386–1391.
66. Maia CS, Mehnert W, Schläfer-Korting M. Solid lipid nanoparticles as drug carriers for topical glucocorticoids. Int J Pharm 2000; 196:165–167.
67. Jenning V, Gysler A, Schäfer-Korting M, Gohla S. Vitamin A-loaded solid lipid nanoparticles for topical use: occlusive properties and drug penetration into porcine skin. Eur J Pharm Biopharm 2000; 49:211–218.
68. Santos Maia C, Mehnert W, Schaller M, Korting HC, Gysler A, Haberland A, Schäfer-Korting M. Drug targeting by solid lipid nanoparticles for dermal use. J Drug Target 2002; 10:489–495.
69. Münster U, Nakamura C, Haberland A, Jores K, Mehnert W, Rummel S, Schaller M, Korting HC, Zouboulis ChC, Blume-Peytavi U, Schäfer-Korting M. RU 58841-

myristate—prodrug development for topical treatment of acne and androgenetic alopecia. Pharmazie 2004; 60:8–12.
70. Mariani E, Neuhoff C, Bargagna A, Bonina F, Giacchi M, De Guidi G, Velardita A. Synthesis, in vitro percutaneous absorption and phototoxicity of new benzylidene derivatives of 1,3,3-trimethyl-2-oxabicyclo[2.2.2]octan-6-one as potential UV sunscreens. Int J Pharm 1998; 161:65–73.
71. Bennat C. Lichtschutz mit Mikropigmenten—Beitrag zur Physikochemischen Charakterisierung, Galenischen Stabilisierung und Untersuchung des Penetrationsverhaltens von Mikrofeinen Titandioxid und Zinkdioxid. Ph.D. thesis, TU Braunschweig, 1999.
72. Bennat C, Müller-Gowmann CC. Skin pebetration and stabilization of formulations containing microfine titanium dioxide as physical UV filter. Int J Cosmet Sci 2000; 22:271–283.
73. Wissing SA, Müller RH. The development of an improved carrier system for sunscreens formulations based on crystalline lipid nanoparticles. Int J Pharm 2002; 242:373–375.
74. Saupe A. Pharmazeutisch-Kosmetische Anwendungen Nanostrukturierter Lipidcarrier (NLC): Lichtschutz und Pflege. Ph.D. Thesis, Free Universität Berlin, 2004.
75. Müller RH, Mäder K, Wissing S. Mittel mit UV-Strahlung absorbierender und/oder reflektierender Wirkung zum Schutz vor gesundheitsschädlicher UV-Strahnung und Stärkung dern natürlichen Hautbarriere, Deutsche -Patentenanmeldung Nr 199 32 156.6 (P 51102). PCT-application PCT/EP00/06534 (P 53516).
76. Wissing SA, Müller RH. In vitro and in vivo skin permeation of sunscreens from solid lipid nanoparticles (SLN™), supercooled melts and emulsions. Proceedings of the 4th World Meeting APGI/APV, Florence, 2002:1135–1136.
77. Wissing SA, Mäder K, Müller RH. Solid lipid nanopartices (SLN™) as a novel carrier system offering prolonged release of the perfume Allure (Chanel). Proc Int Symp Control Release Bioact Mater 2000; 27:1–12.
78. Wissing SA, Mäder K, Müller RH. Prolonged efficacy of the insect lemon oil by incorporation into solid lipid nanoparticles (SLN™). Proceedings of the 3rd World Meeting APGI/APV, Berlin, 2000:439–440.
79. Yaziksiz-Iscan Y, Wissing SA, Müller RH, Hekimoglu S. Different production methods for solid lipid nanoparticles (SLN) containing the insect repellent DEET. Proceedings 4th World Meeting APGI/APV, Florence, 2000:789–790.
80. Yaziksiz-Iscan Y, Hekimoglu S, Sargon MF, Kas S, Hincal AA. In vitro release and skin permeation of DEET incorporated solid lipid nanoparticles in various vehicles. Proceedings of the 4th World Meeting APGI/APV, Florence, 2000:1183–1184.
81. Müller RH, Mäder K, Gohla S. Solid lipid nanoparticles (SLN) for controlled drug delivery—a review of the state of art. Eur J Pharm Biopharm 2000; 50:161–177.

54
Transdermal Transport by Phonophoresis

Laurent Machet
Department of Dermatology, Université François-Rabelais, University Hospital of Tours, Tours, France

Alain Boucaud
Université François-Rabelais, Laboratoire Ultrasons Signaux Instrumentation (CNRS FRE 2448), University Hospital of Tours, Tours, France

I. ABSTRACT

We present the main data published with low-, medium-, and high-frequency ultrasound over the last two decades, and to discuss the mechanisms involved in ultrasound-induced transdermal transport. Specific attention is paid to the biological effects of ultrasound on living skin which might be significant for tolerance and practical use in human applications.

II. INTRODUCTION

Phonophoresis or sonophoresis is the term given to the use of ultrasound as a physical enhancer of percutaneous absorption of drugs. The skin provides an essential barrier function that effectively limits exchanges with the external environment in both directions: reduction of penetration of exogenous compounds and reduction of transepidermal losses. The main barrier property of the skin is due to the stratum corneum (SC), the outermost layer of the skin, that is a 10 to 20 μm thick membrane composed of compact stacking of cornified keratinocytes that are separated by highly ordered intercellular lipid bilayers.

Topical or systemic administration of drugs through the skin needs to overcome this barrier. However, significant transdermal transport of high molecular weight molecules is quite impossible with conventional chemical enhancers. Physical enhancers have therefore been investigated to create wider pathways through the epidermis, using electric voltage, a process known as electroporation (1), or by using ultrasound, a process referred to as phonophoresis (or sonophoresis). On the other hand, the use of powerful techniques to overcome the skin barrier is limited by potential damage to the skin (2).

The use of ultrasound as a transdermal transport enhancer, i.e., sonophoresis or phonophoresis, became very popular in sports medicine for local treatment of minor

injuries, and is believed both to accelerate functional recovery and to increase transdermal transport of topically applied drug, especially non-steroidal anti-inflammatory drugs (3,4). However the extent of the drug transport enhancement still remains fairly low or is not even significant in some studies. The feasibility of making the skin permeable to treatments such as insulin (5–7) or low molecular weight heparin (8), by using low frequency ultrasound, reported in recent years has increased the interest for the application of this non-invasive method in human medicine.

III. PHYSICAL CHARACTERISTICS OF ULTRASOUND

Ultrasound is generated by a piezoelectric crystal transducer which converts electric power into a mechanical oscillation generating an acoustic wave. After its emission, the wave is transmitted in an aqueous coupling medium (air or gas are bad transmitter media for ultrasound) placed between the transducer and the skin. This wave is partially reflected by the skin, while the other part penetrates and propagates through the skin with a direction parallel to the direction of oscillation. During its propagation, the wave is partially scattered and absorbed by the medium, resulting in attenuation of the emitted wave. An increase in temperature of the exposed medium is thus induced by the conversion of the ultrasound energy into heat.

The effects of ultrasound on the skin in terms of tolerance and efficacy of transdermal transport are directly related to the different ultrasound parameters, i.e., frequency, intensity, and mode and time of application of the emitted wave.

A. Frequency

The frequency f of the emitted wave depends on the size and the geometry of the ultrasound transducer. The frequency range of ultrasound is generally defined as higher than 20 kHz. In-depth penetration of the acoustic wave into the skin is inversely proportional to the frequency, hence the biological effects of high frequency ultrasound are mainly located at the skin surface (i.e., stratum corneum and epidermis), while low frequency ultrasound may interact with deeper located structures (i.e., dermis, hypodermis, and muscles). Frequencies ranging from 0.8 to 2 MHz were first used (3,9), then higher frequencies ranging from 3 to 20 MHz were investigated, with the idea of concentrating the acoustic energy on the SC (10,11). Finally, more recently low frequency ultrasound (20–150 kHz) has been shown to enhance transdermal transport more effectively (5,6,12).

B. Mode

The ultrasound waves can be emitted continuously (continuous mode) or in a sequential mode, for example 0.1 second applied every second (discontinuous or pulsed mode). Pulsed mode is used in preference to continuous mode in order to avoid faster and more intense rises in temperature in/or at the skin surface.

C. Intensity

Intensity I is equal to $I = c \times E$, where E is the emitted acoustic energy (E) and c is the speed of the ultrasound wave in the medium. In human soft tissues the value of c is ~ 1500 m/sec. The energy E depends on the density of the propagation medium

(ρ), the total pressure (P) equal to the sum of the atmospheric pressure and the pressure created by the ultrasonic wave: $E = P^2/\rho c^2$. The intensity usually used in sonophoresis ranges from 0.5 to 2 W/cm^2 and the increase in pressure is approximately 0.2 bar with an intensity of 1 W/cm^2 in water (13).

IV. ULTRASOUND-ENHANCED PERCUTANEOUS ABSORPTION: PHARMACOKINETIC DATA

A. Medium (0.8–2 MHz) and High Frequency (3–20 MHz) Phonophoresis

1. In Vitro Studies

In vitro studies have been performed in the last two decades, to quantify the increase in cutaneous permeability induced by ultrasound (Table 1). Differences between studies are related to ultrasound conditions (frequency, continuous or pulse mode, duration, intensity), monitoring (or not) of the increase in temperature induced by ultrasound within the donor compartment, control (or not) of the integrity of the skin by clinical and histological studies , and the origin of the membranes used (isolated epidermis, controlled skin thickness using a dermatome, or full thickness skin). It can be concluded that the increase in percutaneous flux still remains moderate (enhanced-ratio generally between one and five) when ultrasound is applied over a short time (5–15 min) (14,15). Increasing the exposure time from 10 to 60 minutes has been reported to result in a two- to fivefold increase in transdermal diffusion of prednisolone in vitro with continuous application of 1 MHz ultrasound at 4.3 W/cm^2 (16). Interestingly, in the latter study no ultrasound induced transdermal transport was found after removing the SC, demonstrating that ultrasound modified SC permeability. With more longer exposure of skin to ultrasound (up to 20 hours), providing periodic replacement of donor and receptor compartment solutions to ensure sufficient dissolved gas concentrations and hence to maintain the cavitation activity, permeability may be increased across isolated epidermal sheets from 1 to 13 (17,18). This was explained by the enhancement of diffusivity of the drug within the SC rather than an increase in the partition coefficient (19). However, it must be emphasized that these latter in vitro operating conditions are far from being applicable in vivo.

2. In Vivo Studies

Studies conducted with various animal species have generally shown a significant effect of ultrasound on transdermal transport (Table 2). The technique became very popular in humans in the United States (9) and phonophoresis is currently used in sports medicine (3).

The efficacy of the technique overall is believed to be explained both by the physical effect of ultrasound itself on subcutaneous injured tissues and by enhancement of transdermal transport (4). However, in vivo controlled studies have provided conflicting results (20) (Table 3).

In summary, it is clear that high and medium frequency ultrasound can increase both in vitro and in vivo transdermal transport of medium sized molecules ($<$500 Da) that are currently used in clinical practice without ultrasound. Increasing loco-regional diffusion of non-steroidal anti-inflammatory drugs 2- to 10-fold in synovial tissue or muscles may be specifically helpful in sports medicine. However, when it does exist, such enhancement remains moderate or needs long time exposure

Table 1 In Vitro Studies of High- and Medium- Frequency Phonophoresis Across Rat, Mice, or Human Skin

References	F (kHz)	I (W/cm^2)	Mode	Duration (min)	Molecule	Membrane	Effect
(68)	20,000	3	P	15	Diclofenac	Mice skin	× 2–30 enhancement
(33)	3,300	3	C	10	Digoxine	Hairless mice skin	Flux × 3 but heating resulted in the same effect
(15)	3,300 1,100	2.25	C	240	Hydrocortisone	Rat skin	× 2.2 enhancement × 1.8
(63)	1,100 ???	2	C	5	Sucrose Mannitol Hydrocortisone	Rat skin	× 4.5 enhancement × 4.1 × 7.7
(34)	1,100	1.5	C	20	Azydothymidine	Human skin	Flux × 1 with a cooling coil
(16)	1,100	4.3	C	10–30	Prednisolone	Hairless mouse skin	× 2-5
(35)	1,100	1.5	C	20	Mannitol Estradiol Hydrocortisone	Hairless mice skin Human skin	Flux ×1 with a cooling coil Flux × 1 with a cooling coil
(32)	1,000	1	C	240	Ibuprofene	Human epidermis	× 3 enhancement
(17)	1,000	2	C	300	Seven molecules	Human epidermis	Flux × 13 estradiol, × 5 testosterone, × 4 cortisol, × 1.5 butanol, × l.2 caffeine.
(18)	1,000	1.4	C	1,440	Four molecules with chemical enhancer	Human epidermis	Flux × 1 à × 75
(19)	1,000	2	C	300	Five molecules	Human stratum corneum	× 2–15 enhancement

Table 2 In Vivo Studies of High- and Medium- Frequency Phonophoresis in Animals

Refs.	F (kHz)	I (W/cm^2)	Mode	Duration min	Molecule	Animal	Effect
(68)	20,000	3	P	15	Diclofenac	Rats	Reduction in provoked paw edema
(10)	2,000	0.2	C	20	Salicylic acid	Cobayes	Urinary excretion increase at 10 MHz (× 4) and 16 MHz (× 2.5) but not at 2
	10,000						
	16,000						
(69)	1,000	1–3	C	5	Cortisol	Swine	Intramuscular concentration ×3
(70)	1,000	1.5	C	3	D-mannitol	Rats	Increased diffusion × 5–20
	1,000	3	P	5			
(42)	1,000	1–2.5	P	10–19	Indomethacin	Rats	Mild increase in blood concentrations
			C	10			

to ultrasound, making the use of this range of frequency for systemic transdermal delivery questionable.

B. Low Frequency Sonophoresis (20–150 kHz)

This range of frequency has been investigated more intensively in recent years in vitro (Table 4), in some animal species in vivo (Table 5) and in humans (Table 6).

1. In Vitro

Using a 20 kHz ultrasound probe, diffusion of low molecular weight molecules across epidermal sheets was increased from 2- to 5000-fold (21). Moreover, the synergistic action of a chemical enhancer such as sodium lauryl sulfate has been shown with low molecular weight molecules (22). Although statistically significant, the enhancement ratio remains relatively low in some in vitro studies performed on mouse skin (23) especially for hydrophilic drugs (24). A significant increase was also demonstrated using 350 μm thickness human dermatomed skin including the epidermis and upper dermis, with enhancement ratios of 4 and 34 for caffeine and fentanyl, respectively, during sonication and the lag time was shortened (25). Moreover, by using 20 kHz ultrasound, it was shown that large size molecules such as poly 1-lysine (51 kDa) could be delivered through human heat stripped skin with an exponentially enhancement of the drug transport with ultrasound exposure time (26).

2. In Vivo

Enhancement of low-weight molecule has been demonstrated with higher order of magnitude than that observed with medium or high frequency ultrasound (Table 5). Moreover particular attention was drawn by Tachibana who first demonstrated

Table 3 In Vivo Studies of High- and Medium- Frequency Phonophoresis in Humans

Refs.	F (kHz)	I (W/cm^2)	Mode	Duration (min)	Molecule	Number of patients	Effect
(71)	3,000	1	C	5	Nicotinates	10	Non significant
(72)	3,000	1	C	5	Nicotinate	10	Vasodilatation × 1.7
(73)	750–3,000	1–1.5	C P	5	Prilocaine Lignocaine	11	Significant increase in duration of anesthesia
(74)	750–3,000	1.5	C	5	Benzydamine	10	Non significant
(75)	1,100	0.25	C	5	Anaesthetic drugs	6	Non significant
(76)	1,000	0–3	C	5	Hydrocortisone	102	Reduced pain (68% vs. 28%)
(77)	1,000	1.5	P	5	Salicylate	40	Non significant
(4)	1,000	1.5	C	5	Ketoprofen	10	× 10 enhancement transport in synovial tissue, however no enhancement in fat
(20)	870	2	P	5	Lignocaine	10	Non significant
(78)	870	2	P	5	Fluocinolone acetonide	12	Non significant

the transdermal diffusion of a macromolecule (insulin, 6 kDa) across hairless mice skin exposed to 48 kHz ultrasound applied for five minutes in vivo, resulting in marked decrease (80%) in glycemia (5). In vivo transdermal delivery of insulin was then confirmed by Mitragotri in 1995 using a 20 kHz ultrasound probe applied for 60 minutes (6) and by our group with a shorter application time of 15 minutes in hairless rats (Fig. 1) (7). Using a home-made ultrasound device (cymbal arrays), Smith et al. (27) recently reported 70% decrease in blood glucose concentration in Sprague Dawley rats exposed to insulin and 20 kHz ultrasound at 100 W/cm^2 for 60 minutes. Transdermal delivery of macromolecules with conserved biological activity was confirmed with ultrasound-induced transdermal delivery of low-molecular-weight-heparin (8), demonstrating measurable systemic antiXa activity.

In summary, low-frequency ultrasound is able to overcome skin barrier, and could ultimately contribute to valuable therapeutic devices. The extent of enhancement is greater with passively low-penetrating drugs, suggesting that ultrasound interacts with the lipid bilayers of the SC (see sec.V.A.) (17). Another field of application for ultrasound-induced skin permeability is the non-invasive quantitative assessment of blood concentration of glucose using reverse skin permeability of glucose (28). After the exposure of the skin of diabetic patients to 20 kHz ultrasound at 10 W/cm^2 for two minutes (50% duty cycle), fairly good correlation was found between

Table 4 In Vitro Studies of Low-Frequency Phonophoresis Across Rat, Mice, or Human Skin

References	F (kHz)	I (W/cm^2)	Mode	Duration (min)	Molecule	Membrane	Effect
(12)	150	0.111	C	60	Nine molecules	Hairless rat skin	Flux × 2–15
(62)	150	0.111	C	60	Benzoate sodium	Hairless rat skin	× 7 enhancement
					Deuterium oxyde		× 4 enhancement
(24)	40	0.44	C	240	Caffeine	Hairless mice skin	× 4 enhancement
					Morphine		× 10 enhancement
(17)	20	0.125	P	300	Seven molecules	Human epidermis	Flux × 3 (oestradiol), × 80 (cortisol), × 113 (water), × 400 (Salicylic acid), × 5000 (sucrose)
(79)	20	0.2	P	120	Vasopressine	Human epidermis	$Kp = 1/10^{-5}$ cm/hr with ultrasound $Kp = 0$ without ultrasound
(23)	20	0.1–0.3	P	240	Clobetasol 17-propionate	Hairless mice	× 1.9–4 enhancement
			C	240			× 1.5–5.9 enhancement
(57)	20	1.6–14	P	90	Mannitol	Pig skin	× 10 enhancement
(8)	20	7	P	10	Low-molecular-weight heparin	Pig skin	× 21 enhancement
(25)	20	2.5	P	60	Caffeine	Human skin	× 4 enhancement
					Fentanyl		× 34
	20	2.5	C	10	Caffeine		× 1
					Fentanyl		× 4

Table 5 In Vivo Studies in Animals of Low- Frequency Phonophoresis

References	F (kHz)	I (W/cm^2)	Mode	Duration (min)	Molecule	Animal	Effect
(80)	48	0.17	C	5	Lidocaïne	Mice	Increased pain threshold
(6)	20	0.225	P	60	Insuline	Rats	Marked decreased in blood glucose level
(17)	20	0.125	P	300	Salicylic acid	Rats	Flux × 300
(81)	20	7	P	2	Manitol Inulin Glucose	Rats	× 33 enhancement × 20 enhancement × 65 enhancement
(8)	20	7	P	2	Dalteparin	Rats	Anti-Xa activity
(7)	20	2.5	P	15	Insulin	Rats	Marked decrease in blood glucose level
(27)	20	0.1	P	20 60	Insulin	Rats	Marked decrease in blood glucose level

Table 6 In Vivo Studies of Low-Frequency Phonophoresis in Humans

Refs.	F (kHz)	I (W/cm^2)	Mode	Duration (min)	Molecule	Number of patients	Effect
(4)	100	20% duty cycle	P	5	Ketoprofen	9	× 14 Enhancement transport in synovial tissue, but no enhancement in fat
(29)	20	10	P	2	Glucose	7	Increased reverse transport of glucose

glucose concentrations found in extracted fluids and in blood (29), using a vacuum pump to extract dermal interstitial fluid.

V. MECHANISM OF ACTION OF ULTRASOUND ON TRANSDERMAL TRANSPORT

The main modes of action of ultrasound-enhanced transport can briefly summarized as follows: the propagation of ultrasonic waves in a medium induces two main physical consequences, i.e., heating and cavitation. These mechanisms are linked as cavitation may provoke local heating (30). Moreover, cavitation itself can create violent micro jets that can dramatically affect adjacent material as metal, and in the present case the SC. Overall the consequence is an increase in skin permeability by increasing fluidity of intercellular lipids, and by partial removal of intercellular fluid and possibly some corneocytes, resulting in enlarged intercellular spaces and in the creation of

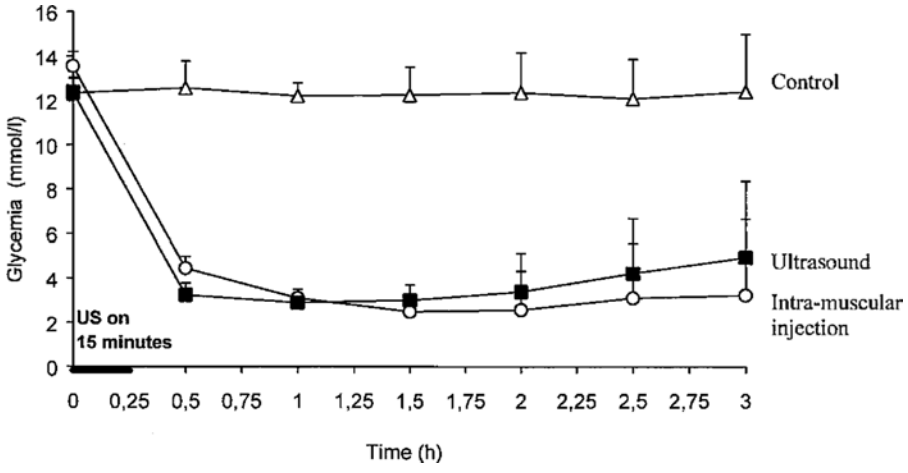


Figure 1 In vivo sonophoresis of insulin (20 kHz, pulsed mode, 2.5 W/cm^2, 15 minutes): decrease in glycemia of rats exposed to ultra sound is similar to the decrease in glycemia of rats treated with 0.5 IU intramuscular injection of insulin (mean values and SD, four animals in each curve). *Source*: Redrawn from Ref. 7.

aqueous channels though the SC. The nature of these aqueous channels and their persistence after the end of sonication remain to be clarified.

A. Heating

Several phenomena explain the increase in temperature within and at the skin surface exposed to ultrasound. Increase in temperature may be excessive and it is possible to use an aqueous gel which decreases reflection or to use an ultrasound-pulsed mode or a low focused ultrasound wave, which decreases energy density, and to decrease the length and/or the intensity of the sonication.

1. Heating at the Skin Surface

Using 1 MHz ultrasound, Miyazaki et al. (31) showed a rise of 6°C for a fairly low intensity of 0.25 W/cm^2 and 12°C for an intensity of 0.75 W/cm^2. Moreover, despite the use of a cooling coil, an 11 °C increase occurred in the donor compartment using 1 MHz ultrasound in continuous mode for four hours (32). We obtained increases of 15 to 30°C at intensities ranging from 1 to 3 W/cm^2 (33). Moreover, when heating with an electric resistance, we obtained an equivalent increase in percutaneous flow (Fig. 2). Our findings obtained with a cooling system did not show any significant increase in percutaneous diffusion rates of various molecules with molecular weight of 138 to 781 Da (azidothymidine, digoxine, hydrocortisone, mannitol, estradiol, and salicylic acid) (34,35). Increase in temperature is thus one of the major factors, which can explain the increase in percutaneous absorption in the frequency range from 1 to 3 MHz and in continuous mode. However, a threefold increase was observed with a larger molecule, vasopressin V-2 antagonist (molecular weight 1014 Da) (36), demonstrating that heating is not the only mechanism of action of medium frequency.

Using lower frequency ultrasound (20 kHz, 10–30 W/cm^2) and monitoring the temperature, percutaneous flow of hydrocortisone was quadrupled though cellulose

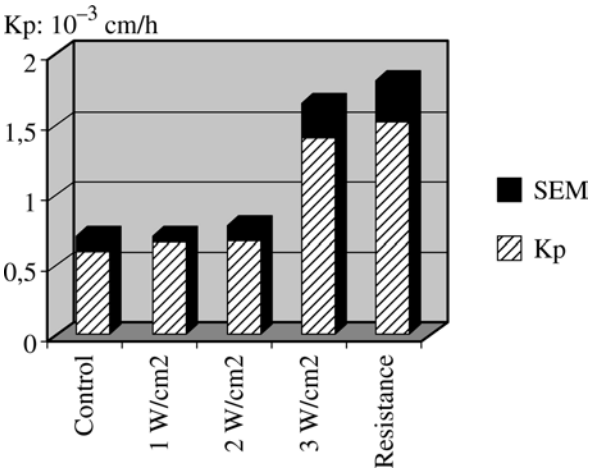


Figure 2 High-frequency phonophoresis of digoxin. Ultrasound (3.3 kHz, 3 W/cm^2) provoked an increase both in transdermal transport and temperature in donor compartment. Similar heating outside the skin with an electrical resistance resulted in similar increase in transdermal transport. *Source*: Redrawn from Ref. 33.

membranes and the temperature was increased threefold (25–75°C), whereas the diffusion flux measured was close to that of controls at similar temperatures (37). By contrast, using lower intensities on hairless rat skin (12) and in isolated epidermal sheets (6), the rise in temperature in the donor compartment was less and cannot explain the 10- to 100-fold increases in percutaneous absorption. Merino et al. (38) reported an increase in temperature of 20°C of mannitol solution exposed to 20 kHz at 15 W/cm^2 for two hours. However, only 25% of the transdermal transport enhancement was attributable to this rise in temperature. The same group also studied the migration of a hydrophilic tracer (calcein) by using confocal microscopy and compared with adequate heating control, again showing a greater efficicacy of 20 kHz ultrasound than simple heating (39).

2. Heating Within the Skin

When an ultrasound wave penetrates through the skin or other structure, it decreases gradually as it propagates. This phenomenon of attenuation is explained by three mechanisms i.e., absorption, reflection, and dispersion, and it depends on the frequency of the wave and the density and heterogeneity of the structure. Part of this ultrasound energy is finally converted into heat. Due to its heterogeneity, the attenuation coefficient of the skin is four times higher than that of other soft tissues (40,41). It is known that in-depth penetration of ultrasound is inversely proportional to frequency: 50% of energy penetrates up to 10 cm beneath SC using 90 kHz ultrasound, whereas the same amount of energy only penetrates to 2 cm using 1 MHz ultrasound. In-depth transmission might support vasodilatation of dermal capillaries allowing systemic diffusion. Asano et al. (42) showed an increase of 6°C at 1 W/cm^2 and an increase of 11°C at 2 W/cm^2 by introducing a thermal probe beneath the skin of rats exposed to ultrasound (1 MHz, 1–2 W/cm^2, continuous mode). Using a 20 kHz ultrasound probe, the intradermal temperature measured in vivo just beneath sonicated skin increases only by a few degrees/centigrade during sonication (2,43).

B. Cavitation

1. Description

Cavitation is the production of microbubbles in a liquid, when a large negative pressure is applied to it. When a medium is exposed to ultrasound, the transmitted waves alternatively compress and stretch its molecular structure. If a sufficiently large negative pressure is applied to the liquid so that the distance between the molecules exceeds the critical molecular distance necessary to hold the liquid intact, the liquid will break down and voids will be created, i.e., cavitation bubbles will form. Acoustic cavitation can easily be observed in liquid media, especially under high ultrasound intensity and low frequency conditions. During the negative phase, bubbles grow around their equilibrium radius. However, the pressure in the medium increases during the positive phase, causing reduction in the bubble radius size. There are two forms of cavitation: stable and unstable. Stable cavitation corresponds to bubbles that oscillate many times around its equilibrium radius (resonance radius R_r expressed in μm). The R_r is roughly related to frequency (F in kHz) by the following equation: $F \times R_r = 3000$.

Thus the resonance radius is 3 μm with 1 MHz and 150 μm with 20 kHz. The size of observed bubbles may be greater in living tissue (44). Unstable cavitation exists for a very short length of time, during which the gas cavity grows very quickly and then

implodes producing a local rise in temperature. When implosion occurs near an interface, it creates a shock wave and violent micro jets that can damage adjacent structures, even as resistant as metal. Growth and decrease in bubble size and their life span, depend on several parameters including intensity and frequency of the ultrasound field, external pressure, viscosity, gas content, and temperature of the coupling medium. The occurrence of cavitation in water is facilitated by the presence of dissolved gas and needs to increase intensity when increasing frequency (13,45).

The occurrence and consequences of cavitation have been studied in living cells and tissues (46,47) with possible applications for destruction of cancers (48,49) and permeation of cell membranes (50).

2. *Implications in Transdermal Transport*

The major role played by cavitation in ultrasound mediated transdermal transport is supported by a series of experiments conducted in vitro:

1. The need to keep dissolved gas in the medium to form nuclei of cavitation (17)
2. The possibility of permeating cell membranes in vitro (51) is enhanced in the presence of artificial cavitation nuclei
3. The demonstration of possible pores created at the skin surface by ultrasound (35), and within the SC (43,52)
4. The demonstration of multiple pits induced by bubble implosion on aluminium foils exposed to ultrasound and the correlation with intensity and skin conductivity (53,54)
5. Dose–response curves of skin conductivity enhancement with cavitation (55)

Cavitation Outside the Skin. Implosion of bubbles near the SC surface induced by cavitation can create localized damage, justifying systematic morphological studies. Small cavities of a few micrometer in size, that could correspond to impact of cavitation bubbles on the SC surface , have indeed been shown using scanning electron microscopy (Fig. 3) (35). Crater-like images of 5 to 15 μm size were also reported in hairless mice exposed to 1 MHz ultrasound at 4.3 W/cm^2 in vitro (16). Scanning electron microscopic examination of rat skin after in vivo exposure to

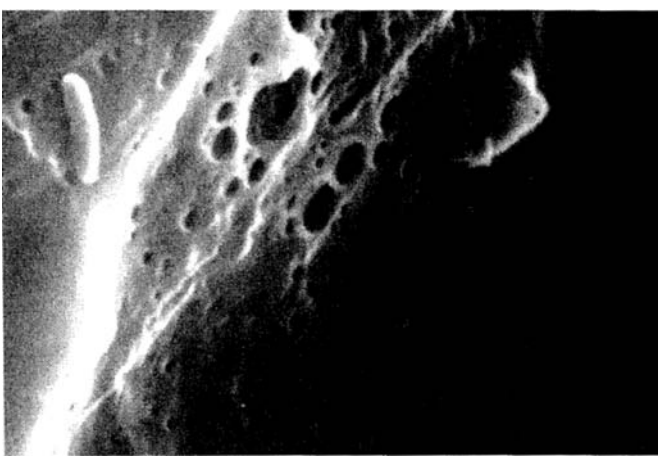


Figure 3 Numerous holes at the stratum corneum surface corresponding to cavitation occurring at skin interface.

150 kHz ultrasound, demonstrated 100 to 150 μm lesions on the SC surface (56), corresponding to the size of the bubbles induced by stable cavitation at 20 kHz (13). Similarly pits provoked by 20 kHz ultrasound application on aluminum foil (53,57) probably corresponded to the same phenomenon, and interestingly, the numbers of pits increased with intensity and reduction in the distance between the skin and the probe. Cellular membrane disruption and inter- and intracytoplasmic vacuolae have been demonstrated in fish without significant increase in temperature within the skin (58) and these lesions were not observed when cavitation in the donor compartment was suppressed using degassed water, indicating that these lesions originate from cavitation outside the skin.

Cavitation Within the Skin. Indirect proof of cavitation has been demonstrated in isolated epidermis in vitro, after incubating the epidermis with fluorescein resulting in bleaching of fluorescence, probably secondary to production of hydroxyl radicals induced by cavitation (17). Theoretically, cavitation is possible within the SC because of the presence of dissolved oxygen and nitrogen and the presence of lacunae between corneocytes (59). The aqueous contents of sweat channels, whose diameter is approximately 5 μm, makes it highly probable that cavitation could occur within it in vivo with medium frequency ultrasound, but this is less probable with low frequency ultrasound because of the greater size of the bubbles. The existence of dissolved gas at depth in living tissue can allow the development of cavitation bubbles (44). We demonstrated epidermal and dermal damage using low frequency ultrasound, including muscles and vessels necrosis (see sec. VI.C) (2), highly suggestive of undesirable in-depth cavitation, using ultrasound parameters that are not far from those used in sonophoresis.

C. Miscellaneous

Independently of cavitation and heating, ultrasound waves provoke a rise in pressure in liquid medium in the donor compartment. The relative contribution of this flow has been estimated to represent 0.02 % at1 W/cm^2 and 2% at 100 W/cm^2 and is thus negligible (13). Recently phonophoresis of mannitol across pig skin in vitro was found to be the same when ultrasound was applied before application of mannitol or simultaneously, suggesting no significant effect of convection in ultrasound-induced transdermal transport (57). On the other hand, we did not evidence any changes in glucose blood levels of rats when ultrasound was applied before application of insulin, while marked hypoglycemia was observed, when ultrasound and insulin were applied simultaneously (7).

In conditions of negligible temperature rise and absence of cavitation, mechanical stress, has shown evidence of intercellular widening induced by transverse (shear) waves (60, see sec. VI.A).

The boundary layer of water immediately adjacent to membranes in studies carried out in vitro, is less well mixed and constitutes an additional resistance to diffusion through the skin. This can be reduced by acoustic streaming (13).

VI. BIOLOGICAL CONSEQUENCES OF ULTRASOUND APPLICATION ON SKIN

The SC lipids are essential to skin barrier integrity. Hence, it is attempting to hypothesize that ultrasound can affect lipid fluidity either by heating, shock waves or microjets and moreover provokes partial removal of lipids from SC.

A. Removal or Modification of Stratum Corneum Lipids

In a model of lipid bilayers using low frequency ultrasound, defects were observed using an atomic force microscope, with diameters of 10 to 100 nm (61). Intercellular lipid content was measured in hairless rat skin in vitro after ultrasound exposure (150 kHz) in a surfactant solution (Tween 20), Lipid release from the skin was demonstrated and this increased with length of time of exposure to 150 kHz ultrasound. Lipid release was correlated with increased skin conductivity and enhanced transport of polar molecules (62). Similarly, sebaceous gland debulking was demonstrated on histological sections of hairless rat skin exposed to low-intensity ultrasound (63). Moreover, removal of 30% of the total amount of SC lipids was demonstrated using 20 kHz ultrasound (15 W/cm^2 , duty cycle 0.1–0.9 for two hours) in pigs, a species with less prominent sebaceous glands (39).

B. Imaging Pathway of Sonophoretic Transport

As seen above (sec. IV.B.2.) pits secondary to cavitation on the skin surface have been shown with both medium and low frequency ultrasound (16,35,43). Nevertheless, whether these crater-like lesions are a possible pathway for transdermal transport remains uncertain. The following section will report on evidence for possible in depth pathways.

1. High- and Medium- Frequency Ultrasound

The migration of a tracer (lanthanum) has been demonstrated between intercorneocyte spaces after exposure to high frequency ultrasound (10–16 MHz) and the tracer reached the dermis (11). Widening of intercellular spaces was observed (64), with some desmosomal alteration, but these modifications were transient. The assumption that intercellular cavities were secondary to cavitation is doubtful since the occurrence of cavitation is uncertain at the frequency and intensity used (13). It is thus more likely that widening of intercellular space was secondary to mechanical stress causing disruption of the lipid bilayers. This is supported by a further study carried out on fish below the cavitional threshold at 3 MHz and 2 W/cm^2 which demonstrated intensity dose-dependent intercellular widening, while cavitation was undetectable (60). The maximum disorganization affecting the outer layers of epidermis was found with a 45° angle of the incidence radiation, suggesting a role of a transverse wave in the occurrence of cell to cell disruption.

2. Low-Frequency Ultrasound

Human SC exposed to 168 kHz at 1.2 W/cm^2 for 15 minutes was examined with epifluorescence microscopy: 20 μm cavities were seen, and considered to be the consequence of cavitation. As expected, the attenuation coefficient of SC was increased and assumed to be induced by multiplication of cell-to-cell interfaces, intercellular lipids and entrapped air pockets (52). Confocal images were recently used to trace sonophoresis (20 kHz) of a hydrophobic and fluorescent compound and showed a marked but spatially discontinuous increase in transepidermal transport. The areas made permeable could not be identified to detect the anatomic structure but there was focal in depth penetration of the tracer whereas, despite being located within ultrasound field, adjacent areas did not display any penetration of the tracer. These modifications were restricted to a 1 cm^2 surface below the ultrasound probe (39).

C. Skin Tolerance to Ultrasound

Ultrasound is used to treat and destroy tumors (64), or to fragment hard concretions in the treatment of urinary stone disease (65). Moreover, while earlier research on sonophoresis used intensities less than 2 W/cm^2, recent studies performed on excised skin have used intensities greater than 15 W/cm^2. Therefore, special attention has to be paid to tolerance of skin exposed to medium and low frequency ultrasound in the conditions used in transdermal transport studies. As seen above, parameters such as intensity, frequency, mode and duration of ultrasound exposure are of importance since it is expected that cavitation again can be a key issue in damaging living cells. With medium and high frequency ultrasound (1–3 MHz) and intensities ranging from 2 to 3 W/cm^2, we observed macroscopic changes in human skin in vitro (33). Histological studies have shown multiple keratinocyte necrosis, with epidermal detachment, edema and degeneration of collagen fibers in the upper part of dermis whereas heating alone produced no histological alterations (33,42,63). Transmission electron microscopy additionally revealed alterations of intracytoplasmic organites (33) and holes could be demonstrated on the skin surface using scanning electron microscopy (cf. sec.VI.A) (16).

In vitro experiments using hairless mice skin exposed to low frequency ultrasound (20 kHz continuous mode for four hours) showed epidermal and dermal lesions despite relatively low intensity (0.2 W/cm^2). Lesions were less marked using pulsed mode (23). Using human skin in vitro we observed normal appearance of skin exposed to 2.5 W/cm^2 and dose-dependent severity of skin lesions, again greater with continuous mode, from 4 to 20 W/cm^2. Similarly, a dose-dependent increase in temperature in the donor compartment was measured, varying from 33 to 65°C (2). Comparable findings were reported in dogs (43). Experiments were also carried out in vivo with hairless rat skin exposed to 2.5 W/cm^2 Immediately after sonication, macroscopic and microscopic appearance was normal. However, overt macro and microscopic lesions occurred 24 hours later, thus demonstrating delayed constitution of ultrasound-induced lesions (Fig. 4) (2). These lesions were not expected to be induced by heating of the donor compartment since increase was moderate Moreover similar heating with an electrical resistance produced no lesions. Additionally, lesions were not provoked by diffusion of heated water through the skin since the same ultrasound protocol, applied with a plastic film interposed between the ultrasound and the skin resulted in the same epidermal and dermal lesions. Finally the increase in temperature was moderate (+3°C), contrasting with the severity of vessel and muscle necrosis, suggesting probable in depth cavitation (2). However hairless mouse skin, and particularly the SC, is thinner than human skin and this could explain why the human skin threshold tolerance to ultrasound is higher in vitro, and probably also in vivo, since preliminary findings in two human volunteers showed absence of immediate or delayed cutaneous lesions after sonication (5 W/cm^2, pulse duration 1.6 seconds, 25% duty cycle, 15 minutes) (66). Moreover, we know that ultrasound exposure (20 kHz, 10 W/cm^2, 50% duty cycle, two minutes) was well tolerated in seven diabetic patients in vivo (29).

VII. STABILITY OF DRUGS EXPOSED TO ULTRASOUND

Possible degradation of drugs due to ultrasound has been checked in vitro using ultrasound at high intensity, and no degradation occurred with poly 1-lysine (26), insulin (7), fentanyl, or caffeine (25). Persistent in vivo biological activity of insulin

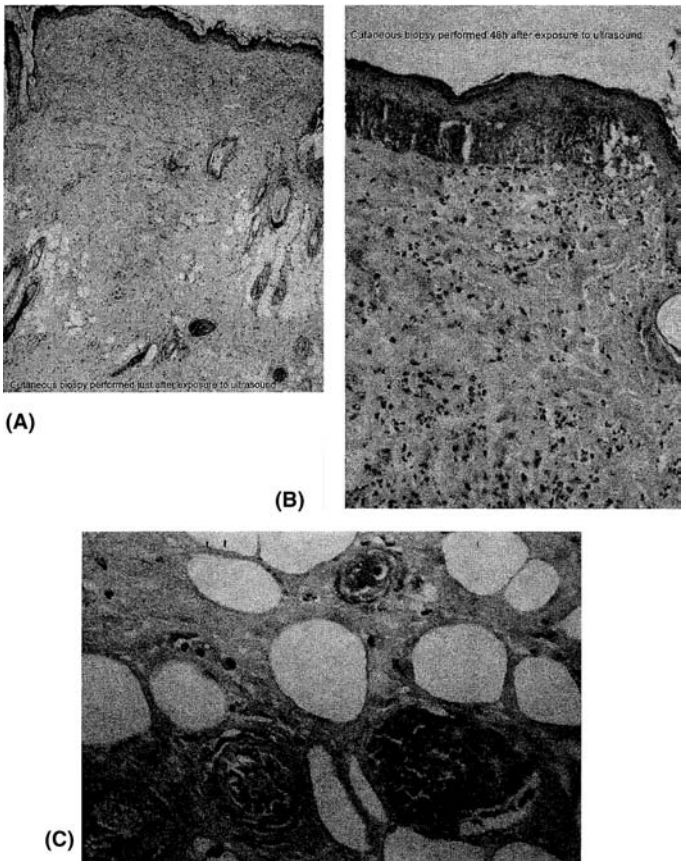


Figure 4 Histologic examination of cutaneous biopsies taken in hairless mice exposed to 20 kHz ultrasound at 2.5 W/cm^2. (**A**) Normal aspect just after exposure to ultrasound, (**B**) epidermal necrosis 48 hour after exposure to ultrasound, and (**C**) lesions of vessels deeply located within hypodermis.

and low-molecular-weight heparin is also in accordance with the absence of significant degradation in the conditions used (6–8).

VIII. PROSPECTS: IS PAINLESS NEEDLE-FREE INJECTION A REALISTIC GOAL?

There is no doubt that ultrasound can markedly increase transdermal transport (66,67). Findings published to date are encouraging, especially for diabetes therapy: it is possible to decrease glucose blood levels in animals in vivo (6) that can be monitored using inverse sonophoresis (29). The daily dose of insulin required to treat an adult diabetic patient is usually between 30 and 60 IU, and the amount delivered to animals is about 0.5 to 1 IU for a short period. Thus repeated pulses over the day would theoretically make possible the administration of a daily dose. However, eight years after Mitragotri's first paper, no human in vivo study has been yet published, maybe because (i) human barrier skin is more difficult to overcome with ultrasound than animal skin, (ii) sonicating 1 cm^2 of a rat weighing 500 g is expected to be much

more effective than sonicating 1 cm^2 of a 60 kg human, and (iii) there are technology problems to proposing a small ultrasound device powerful enough to deliver the ultrasound intensity necessary to achieve drug delivery. Other problems include short and long-term safety in humans, reproducibility, standardization of the process, extension of sonicated area, and cost. Thus there is no doubt that further studies are required (66,67).

REFERENCES

1. Lombry C, Dujardin N, Preat V. Transdermal delivery of macromolecules using skin electroporation? Pharm Res 2000; 17:32–37.
2. Boucaud A, Montharu J, Machet L, Arbeille B, Machet MC, Patat F, Vaillant L. Clinical, histologic, and electron microscopy study of skin exposed to low-frequency ultrasound. Anat Rec 2001; 264:114–119.
3. Byl NB. The use of ultrasound as an enhancer for transcutaneous drug delivery: phonophoresis. Phys Ther 1995; 75:539–553.
4. Cagnie B, Vinck E, Rimbaut S, Vanderstraten G. Phonophoresis versus topical application of ketoprofen: comparison between tissue and plasma levels. Phys Ther 2003; 83:707–712.
5. Tachibana K, Tachibana S. Transdermal delivery of insulin by ultrasonic vibration. J Pharm Pharmacol 1991; 43:270–271.
6. Mitragotri S, Blankschtein D, Langer R. Ultrasound-mediated transdermal protein delivery. Sciences 1995; 269:850–853.
7. Boucaud A, Garrigue MA, Machet L, Vaillant L, Patat F. Effect of sonication parameters on transdermal delivery of insulin to hairless rats. J Control Release 2002; 81:113–119.
8. Mitragotri S, Kost J. Transdermal delivery of heparin and low-molecular weight heparin using low frequency ultrasound. Pharm Res 2001; 18:l151–1156.
9. Pottenger FJ, Karalfa BL. Utilization of hydrocortisone phonophoresis in United States army physical therapy clinics. Military Med 1989; 154:355–358.
10. Bommannan D, Okuyama H, Stauffer P, Guy RH. Sonophoresis I. The use of high-frequency ultrasound to enhance transdermal drug delivery. Pharm Res 1992; 9:559–64.
11. Bommannan D, Menon GK, Okuyama H, Elias PM, Guy RH. Sonophoresis. II. Examination of the mechanism(s) of ultrasound-enhanced transdermal delivery. Pharm Res 1992; 9:1043–1047.
12. Ueda H, Sugibayashi K, Morimoto Y. Skin penetration-enhancing effect of drugs by phonophoresis. J Control Release 1995; 37:291–297.
13. Simonin, JP. On the mechanisms of in vitro and in vivo phonophoresis. J Control Release 1995; 33:125–141.
14. Meidan VM, Walmsley AD, Irwin WJ. Phonophoresis- is it a reality? Int J Pharm 1995; 118:129–149.
15. Meidan VM, Docker MF, Walmsley AD, Irwin WJ. Phonophoresis of hydrocortisone with enhancers: an acoustically defined model. Int J Pharm 1998; 170:157–168.
16. Hikima T, Hirai Y, Tojo K. Effect of ultrasound application on skin metabolism of prednisolone 21-acetate. Pharm Res 1998; 15:1680–1683.
17. Mitragotri S, Blankschtein D, Langer R. A Mechanistic study of ultrasonically-enhanced transdermal drug delivery. J Pharm Sci 1995; 84:697–706.
18. Johnson M, Mitragotri S, Patel A, Blankschtein, D, Langer, R. Synergistic effects of chemical enhancers and therapeutic ultrasound on transdermal drug delivery. J Pharm Sci 1996; 85:670–679.
19. Mitragotri S. Effect of therapeutic ultrasound on partition and diffusion coefficient in human stratum corneum. J Control Release 2001; 71:23–29.

20. McElnay, JC, Matthews MP, Harland R, McCafferry DF. The effect of ultrasound on the percutaneous absorption of lignocaine. Br J Clin Pharmacol 1985; 20:421–424.
21. Mitragotri S, Blankschtein D, Langer R. Transdermal drug delivery using low-frequency sonophoresis. Pharm Res 1996; 13:411–420.
22. Mitragotri S, Ray D, Farell H, Tang H, Yu B, Kost J, Blankstein D, Langer R. Synergistic effect of ultrasound and sodium lauryl sulfate on transdermal drug delivery. J Pharm Sci 2000; 89:892–900.
23. Fang JY, Fang CL, Sung KC, Chen HY. Effect of low frequency ultrasound on the in vitro percutaneous absorption of clobetasol 17-propionate. Int J Pharm 1999; 191:33–42.
24. Monti D, Gianelli R, Chetoni P, Burgalassi S. Comparison of the effect of ultrasound and of chemical enhancers on transdermal permeation of caffeine and morphine through hairless mouse skin in vitro. Int J Pharm 2001; 229:131–137.
25. Boucaud A, Machet L, Arbeille B, Machet MC, Sournac M, Mavon A, Patat F, Vaillant L. In vitro study of low-frequency ultrasound-enhanced transdermal transport of fentanyl and caffeine across human and hairless rat skin. Int J Pharm 2001; 228:69–77.
26. Weimann LJ, Wu J. Transdermal delivery of poly 1-lysine by sonomacroporation. Ultrasound Med Biol 2002; 28:1173–1180.
27. Smith NB, Lee S, Shung KK. Ultrasound-mediated transdermal in vivo transport of insulin with low-profile cymbal arrays. Ultrasound Med Biol 2003; 29:1205–1210.
28. Mitragotri S, Coleman M, Kost J, Langer R. Transdermal extraction of analytes using low-frequency ultrasound. Pharm Res 2000; 17:466–470.
29. Kost J, Mitragotri S, Gabbay R, Pisko M, Langer R. Transdermal monitoring of glucose and other analytes using ultrasound. Nature Med 2000; 6:347–350.
30. Holt RG, Roy RA. Measurements of bubble-enhanced heating from focused MHz-frequency ultrasound in a tissue-mimicking material. Ultrasound Med Biol 2001; 27:1399–1412.
31. Miyasaki S, Mizuoka H, Oda M, Takada M. External control of drug release and penetration: enhancement of the transdermal absorption of indomethacin by ultrasound irradiation. J Pharm Pharmacol 1991; 43:115–116.
32. Brucks R, Nanavaty M, Jung D, Siegel F. The effect of ultrasound on ibuprofen through human epidermis. Pharm Res 1989; 6:697–701.
33. Machet L, Pinton J, Patat F, Arbeille B, Pourcelot L, Vaillant L. In vitro phonophoresis of digoxin across hairless mice and human skin: thermal effect of ultrasound. Int J Pharm 1996; 133:39–45.
34. Pelucio-Lopes C, Machet L, Vaillant L, Patat F, Letiecq M, Furet Y, Lorette G. Phonophoresis of azidothymidine (AZT) ex vivo across human and hairless mice skin. Int J Pharm 1993; 96:249–252.
35. Machet L, Cochelin N, Patat F, Arbeille B, Machet MC, Lorette G, Vaillant L. In vitro phonophoresis of mannitol, oestradiol and hydrocortisone across hairless mouse and human skin. Int J Pharml 1998; 65:169–174.
36. Machet L, Cochelin N, Patat F, Pelucio-Lopes C, Pourcelot L, Lorette G, Vaillant L. Phonophoresis of vasopressin ex vivo across hairless mouse and human skin. Eur J Dermatol 1995; 5:441.
37. Julian TN, Zentner GM. Mechanism for ultrasonically enhanced transmembrane solute permeation. J Control Release 1990; 12:77–85.
38. Merino G, Kalia YN, Delagado-Charro, MB, Potts RO, Guy RH. Frequency and thermal effects on the enhancement of transdermal transport by sonophoresis. J Control Release 2003; 88:85–94.
39. Alvarez-Roman R, Merino G, Kalia YN, Naik A, Guy RH. Skin permeability enhancement by low frequency sonophoresis: lipid extraction and transport pathways. J Pharm Sci 2003; 92:1138–1146.
40. Goss SA, Fritzell L, Dunn F. Comprehensive compilation of empirical ultrasonic properties of mammalian tissues. J Acoust Soc Am 1978; 64:423–457.

41. Goss SA, Johnson RL, Dunn F. Ultrasonic absorption and attenuation of high frequency sound in mammalian tissue. Ultrasound Med Biol 1979; 5:181–186.
42. Asano J, Suisha F, Takada M, Kawasaki N, Myasaki S. Effect of pulsed output ultrasound on the transdermal absorption of indomethacin from an ointment in rats. Biol Pharm Bull 1997; 20:288–291.
43. Singer AJ, Homan CS, Church AL, McClain SA. Low-frequency sonophoresis: pathologic and thermal effects in dogs. Acad Emerg Med 1998; 5:35–40.
44. Ter Haar GR, Daniels S. Evidence for ultrasonically induced cavitation in vivo. Phys Med Biol 1981; 26:1145–1149.
45. Esche R. Untersuchungen der Schwingungskavitation in Flüssigkeiten. Acustica 1952; 2:208–218.
46. Carstensen, EL, Gracewski S, Dalecki D. The search for cavitation in vivo. Ultrasound Med Biol 2000; 26:1377–1385.
47. Poliachik SL, Chandler WL, Mourad PD, Ollos RJ, Crum LA. Activation, aggregation and adhesion of platelets exposed to high-intensity focused ultrasound. Ultrasound Med Biol 2001; 27:1567–1576.
48. Huber PE, Debus J. Tumor toxicity in vivo and radical formation in vitro depend on the shock wave- induced cavitation dose. Radiat Res 2001; 156:301–309.
49. Cochran, SA, Prausnitz MR. Sonoluminescence as an indicator of cell membrane disruption by acoustic cavitation. Ultrasound Med Biol 2001; 27:841–851.
50. Liu J, Lewis TN, Prausnitz MR. Non-invasive assessement and control of ultrasound-mediated membrane permeabilization. Pharm Res 1998; 15:918–924.
51. Greenleaf WJ, Bolander ME, Sarkar G, Goldring MB, Greenleaf JF. Artificial cavitation nuclei significantly enhance acoustically induced cell transfection. Ultrasound Med Biol 1998; 24:587–595.
52. Wu J, Chappelow J, Yang J, Weimann L. Defects generated in human stratum corneum specimens by ultrasound. Ultrasound Med Biol 1998; 24:705–710.
53. Tehara T, Mitragotri S, Kost J, Langer R. Dependance of low-frequency sonophoresis on ultrasound parameters; distance of the horn and intensity. Int J Pharm 2002; 235:35–42.
54. Tang H, Wang CC, Blankschtein D, Langer R. An investigation of the role of cavitation in low-frequency ultrasound-mediated transdermal drug delivery. Pharm Res 2002; 19:l 160–1169.
55. Tezel A, Sens A, Mitragotri S. Investigations of the role of cavitation in low-frequency sonophoresis using acoustic spectroscopy. J Pharm Sci 2002; 91:444–453.
56. Yamashita N, Tachibana K, Ogawa K, Tsujita N, Tmita A. Scanning electron microscopic evaluation of the skin surface after ultrasound exposure. Anat Rec 1997; 247:455–461.
57. Mitragotri S, Farell J, Tang H, Terahara T, Kost J, Langer R. Determination of threshold energy dose for ultrasound-induced transdermal transport. J Control Release 2000; 63:41–52.
58. Frenkel V, Kimmel E, Iger Y. Ultrasound-cavitation damage to external epithelia of fish skin. Ultrasound Med Biol 1999; 25:1295–1303.
59. Menon GK, Elias PM. Morphologic basis for a pore-pathway in mammalian stratum corneum. Skin Pharmacol 1997; 10:235–246.
60. Frenkel V, Kimmel E, Iger Y. Ultrasound-induced intercellular space widening in fish epidermis. Ultrasound Med Biol 2000; 26:473–480.
61. Malghnani MS, Yang J, Wu J. Generation and growth of bilayer defects induced by ultrasound. J Acoust Soc Am 1998; 103:1682–1685.
62. Ueda H, Ogihara M, Sugibayashi K, Morimoto Y. Change in the electrochemical properties of skin and the lipid packing in stratum corneum by ultrasonic irradiation. Int J Pharm 1996; 37:217–224.
63. Meidan VM, Docker MF, Walmsley AD, Irwin WJ. Low intensity ultrasound as a probe to elucidate the relative follicular contribution to total transdermal absorption. Pharm Res 1998; 15:85–92.

64. Menon GK, Bommannan DB, Elias PM. High-frequency sonophoresis: permeation pathways and structural basis for enhanced permeability. Skin Pharmacol 1994; 7:130–139.
65. Coleman AJ, Saunders JE. A review of the physical properties and biological effects of the high amplitude acoustic fields used in extracorporeal lithotripsy. Ultrasonics 1993; 31:75–89.
66. Machet L, Boucaud A. Phonophoresis: efficiency, mechanisms and skin tolerance. Int J Pharm 2002; 243:1–15.
67. Merino G, Kalia YN, Guy RH. Ultrasound-enhanced transdermal transport. J Pharm Sci 2003; 92:1125–1137.
68. Vyas SP, Singh R, Asati RK. Liposomally encapsulated diclofenac for sonophoresis induced systemic delivery. J Microencapsulation 1995; 12:149–154.
69. Griffin, JE, Touchstone JC. Ultrasonic movement of cortisol into pig tissue. I–Movement into skeletal muscle. Am J Phys Med 1963; 42:77–85.
70. Levy L, Kost J, Meshulam Y, Langer R. Effect of ultrasound on transdermal drug delivery to rats and guinea pigs. J Clin Invest 1989; 83:2074–2078.
71. Benson HAE, Me Elnay JC, Harland R, Hargraft J. Influence of ultrasound on the percutaneous absorption of nicotinates esters. Pharm Res 1991; 8:204–209.
72. McElnay JC, Benson HAE, Harland R, Hadgraft J. Phonophoresis of methyl nicotinate: a preliminary study to elucidate the mechanism of action. Pharm Res 1993; 10: 1726–1731.
73. Benson HAE, Mc Elnay JC, Harland R. Phonophoresis of lignocaine and prilocaine from Emla cream. Int J Pharm 1988; 44:65–69.
74. Benson HAE, Mc Elnay JC, Harland R. Use of ultrasound to enhance percutaneous absorption of benzydamine. Phys Ther 1989; 69:113–118.
75. Williams AR. Phonophoresis: an in vivo evaluation using three topical anaesthetic preparations. Ultrasonics 1990; 28:137–141.
76. Griffin JE, Echternach JL, Price RE, Touchstone JC. Patients treated with ultrasonic driven hydrocortisone and with ultrasound alone. Phys Ther 1967; 47:595–601.
77. Ciccone CD, Leggin BG, Callamaro JJ. Effects of ultrasound and trolamine salicylate phonophoresis on delayed-onset muscle soreness. Phys Ther 1991; 71:666–678.
78. McElnay JC, Kennedy TA, Harland R. Enhancement of the percutaneous absorption of fluocinolone using ultrasound. Br J Clin Pharmac 1986; 21:609–610.
79. Zhang I, Shung KK, Edwards DA. Hydrogels with enhanced mass transfer for transdermal drug delivery. J Pharm Sci 1996; 85:1312–1316.
80. Tachibana K, Tachibana S. Use of ultrasound to enhance the local anesthetic effect of topically applied lidocaine. Anesthesiology 1993; 78:1091–1096.
81. Mitragotri S, Kost J. Low-frequency sonophoresis: an non invasive method of drug delivery and diagnostics. Biothechnol Prog 2000c; 16:488–492.

55

Percutaneous Penetration of Oligonucleotide Drugs

Hongbo Zhai and Howard I. Maibach
Department of Dermatology, School of Medicine, University of California, San Francisco, California, U.S.A.

Myeong Jun Choi
Charmzone Research and Development Center, 1720-1 Taejang 2-dong, Wonju, Kangwon-do, Korea

I. INTRODUCTION

Antisense oligonucleotides (ONs) technology uses single stranded DNA to modulate gene expression. Antisense ONs with base sequences complementary to a specific mRNA can selectively modulate gene expression (1). Thus, antisense ONs may have potential as therapeutic agents against systemic and local diseases (2). Carcinoma, melanoma, psoriasis, xeroderma pigmentation, and viral diseases are potential candidates.

Despite major research and development efforts in topical systems and the advantages of the topical route, low stratum corneum (SC) permeability remains a major problem limiting the usefulness of the topical approach (3–5). To increase permeability, chemical, and physical approaches have been examined to lower SC barrier properties.

Physical approaches for skin penetration enhancement, such as tape stripping (6–8), intradermal injection (8,9), iontophoresis (7,10), and electroporation (7,11,12) have been evaluated. In addition, vehicles systems had been used to enhance permeability (13,14).

Topical antisense therapy may offer advantages over systemic therapy; ready access to argeted tissue, intervention in the case of toxicity, and the use of powerful and convenient animal model such as grafted skin on SCID and nude mice (8,15). This method should decrease cost, enhance patient compliance and, in some cases, improve pharmacokinetics. In addition, the method provides a simple and convenient delivery system (13,16). Clinical applications of antisense ONs depend on the development of new approaches to delivery. Improvement of ONs administration can be achieved either by chemical modifications of ONs or by utilizing carrier systems. This chapter reviews percutaneous delivery methods of antisense ONs and summarizes recent data.

II. SKIN BARRIER AND FUNCTIONS

The SC is a permeability barrier that depends upon the presence of a unique mixture of lipids in the SCs intercellular domains. The SC comprises nonviable cornified cells (corneocytes) embedded in lipid-rich intercellular domains (intercorneocyte spaces). Intercellular domains comprise ceramides (CER), cholesterol (CHOL), and free fatty acid (FFA), with smaller amounts of cholesteryl sulfate, sterol, triglycerides, squalene, *n*-alkanes, and phospholipids. The composition of the SC intercellular lipids is unique in biological systems. These lipids exist as a continuous lipid phase; occupying about 20% of the SC volume, and arranged in multiple lamellar structures. All CER and fatty acids found in SC are rod and cylindrical in shape; this physical attribute makes them suitable for the formation of highly ordered gel phase membrane domains. The CHOH is capable of either fluidizing membrane domains or of enhancing rigidity, depending on the physical properties of the other lipids and the proportion of CHOH relative to the other component (17). Intracellular lipids that form the only continuous domain in the SC are required for a competent skin barrier. Based on electron microscopic and x-ray diffraction studies, the lipids appear arranged as lamellar structures, the organization of which is strongly dependent on lipid composition (18).

Skin barrier functions vary in skin conditions such as atopic dermatitis, psoriasis, and Gaucher's disease (5,19). Some skin barrier functions are reduced in atopic dermatitis and psoriasis. Hence, larger and charged molecules can penetrate into SC of some diseased skin. White et al. (5) observed that ON penetrated into psoriatic but not normal skin. When ONs are applied to skin, these lamellar structures prevent penetrating ON. Methods to overcome this barrier are required to develop ON drugs against systemic and local skin diseases.

III. SKIN INTERACTION OF OLIGONUCLEOTIDES

When ONs are applied, they can interact with skin components and be destroyed by skin enzymes. Regnier et al. (3) reported the affinity of various ONs with SC components. Passive accumulation of the phosphorothioate (PS) ON in the SC was much higher than 3′-end modified phosphodiester (3′-PO) ON accumulation (Table 1). Immediately after pulsing (electroporation), the accumulation of PS on the SC was significantly higher than the accumulation of 3′-PO and the quantity of PS was almost unchanged in the SC during four hours incubation after pulsing, one-third of the quantity of 3′PO was found in the SC. In the viable skin, the transport of 3′-PO was more efficient than that of PS at immediately after pulsing (Table 1). These results indicate a stronger interaction of the PS with the SC components. The PS and 3′-PO were stable in the skin, while the non-protected PO exhibited significant degradation within the viable skin. Hence, 3′-PO with high stability and low SC retention may be a good candidate for antisense ON therapy.

White et al. (8) found that ON in aqueous solution and gel does not significantly penetrate normal human skin grafts on athymic mice. The lack of penetration of ON across normal SC was consistent with the finding of Butler et al. (20) but in contrast to those of others (13,14). Mehta et al. (13) and Valssov et al. (14) found that ON crossed the SC of human skin grafts and mouse skin after application in a cosmetic cream and lotion. Because the cosmetic cream and lotion contained penetration enhancers, ON had different penetration properties. Others reported that ONs/DNA penetrated the skin through follicular ducts (21,22).

Table 1 Effect of Oligonucleotide (ON) Types on the ON Affinity for the Stratum Corneum (SC) of Intact Skin and on the Ability of the ON to Penetrate into Intact Skin After Pulsing

		Accumulation after pulsing (pmol/cm^2)[b]			
	Passive diffusion ON concentration	Stratum corneum		Viable tissue	
Type of ONs	in the SC (μM)[a]	5 min	4 hr	5 min	4 hr
PS[c]	100 μM ± 10	225 ± 12.5	180 ± 10	23	33 ± 2
3′-PO[d]	25 μM ± 3	200 ± 10	75 ± 3	71 ± 4	39 ± 2

[a]Effect of the ON types on the ON affinity for the stratum corneum of intact skin after four hours passive diffusion. Donor solution: ON 3.2 μM, EDTA 1 mM, sucrose 8% in 0.04 M Hepes buffer, pH 7.
[b]Mean quantity of PS or 3′-end modified PO oligonucleotide (pmol/cm^2) recovered from the SC and viable skin of hairless rat skin immediately or four hour after pulsing. Donor solution: ON 3.2 μM, EDTA 1 mM, sucrose 8% in 0.04 M Hepes buffer, pH 7.
[c]Sequence of ON is 5′-ACC AAT CAG ACA CCA-3′ and molecular weight and net electric charge are 4727 and -14, respectively. Non-bridging oxygen of the phosphodiester backbone is replaced by sulfur.
[d]Sequence of ON is 5′-ACC AAT CAG ACA C∗C∗A∗-3′ and molecular weight and net electric charge are 4593 and –14, respectively. Hydrogen at the deoxyribose 2′ position is replaced by hydroxymethyl group at three base (C∗C∗A∗) of 3′-end.
Abbreviations: PO, phosphodiester; PS, phosphorothioate.

IV. OLIGONUCLEOTIDES MODIFICATION

Antisense ONs are short synthetic fragments of genes that inhibit gene expression. Antisense ONs consist in natural PO compounds. These compounds have poor stability in nuclease enzyme in vitro and in vivo and minimal skin penetrating properties. To improve stability, chemical modifications have focused on the PO backbone and/or the sugar moiety (23).

Replacement of the non-bridging oxygen of the PO backbone by sulfur results in a PS with enhanced stability to enzymatic degradation. Replacement of the non-bridging oxygen by a methyl group results in increased hydrophobicity due to the loss of the negative charge. Replacement of hydrogen at the deoxyribose 2′ position with a hydroxymethyl group converts the sugar to a modified ribose. One modification replaces the deoxyribose phosphate backbone as in peptide nucleic acids (24).

Although chemical modifications provide improved stability and penetration, they have also resulted in non-antisense activities such as an aptameric effect (25,26), clotting and complement system (27), and immunomodulation property (28). Thus, an alternative strategy to the use of chemically modified ONs would be the association of natural PO molecules (including 3′-end modification) with a drug carrier such as liposomes that might provide increased stability and transport.

V. TAPE STRIPPING

Topically applied ON does not penetrate normal human SC. But, removal by tape stripping lead to extensive penetration of ON throughout the epidermis. Stripping increased the penetration of ONs in the viable skin. Regnier et al. (3) compared penetration through intact and stripped skin. After four hour passive diffusion, between 15 and 25 pmol/cm^2 of ONs were found in the SC and 0.5 and 3 pmol/cm^2 found in the viable skin. In contrast, stripping increased ON concentration in the viable skin by one or two orders of magnitude. Table 2 shows the effect of tape

Table 2 Influence of Stripping and Electroporation on Oligonucleotides (ON)Topical Delivery

		ON concentration in the skin (after 4 hr)	
		Passive diffusion (μM)	Electroporation (μM)
Intact skin	Stratum corneum	9–25[a]	30–70
	Viable tissues	0.003–0.05[b]	0.5–0.6
Stripped skin	Viable tissues	0.5–1.2	2.5–3.5

[a]Average ON concentration in the stratium corneum (SC) was calculated by based on a stratum thickness of 14 μm. Mean quantities of ON recovered from the SC of intact skin four hours passive diffusion. Donor solution: ON 3.2 μM, EDTA 1 mM, sucrose 8% in 0.04 M Hepes buffer, pH 7.
[b]Average ON concentration in the viable skin was calculated by based on a tissue thickness of 0.65 mm. Mean quantities of ON recovered from the viable skin four hours after passive diffusion. Donor solution: ON 3.2 μM, EDTA 1 mM, sucrose 8% in 0.04 M Hepes buffer, pH 7.
Abbreviations: EDTA,

stripping on ON penetration. In addition, topical application of a high concentration of ON (500 nmol) to human skin grafts over 24 hour resulted in localization of the ON in the SC, with no penetration into viable epidermis. In contrast, when 5 nmol of ON was topically applied after tape stripping (10 times with Scotch Crystal®), ON could be detected in all epidermal layers. Stripping of the human skin or skin grafts resulted in a significant change in penetration of ON into the lower epidermis and ultimately keratinocyte ON uptake. In addition to ON, tape stripping increased the penetration of peptide and DNA antigens into viable skin. Hence, tape stripping has been used to disrupt the skin barrier before percutaneous peptide and DNA vaccines (29–31).

VI. ELECTROPORATION AND IONTOPHORESIS

Electroporation is a phenomenon in which lipid bilayers exposed to high intensity electric field pulses are temporarily destabilized and permeated (12,32). The most common use of high voltage pulsing is the introducing of DNA into isolated cells and for introducing (ONs) into cells. In addition, this technique enhances the topical ON delivery and facilitates ON uptake by skin cells (33–35).

Iontophoresis enhances ON across hairless skin in vitro (36). In contrast to electroporation, iontophoresis is not believed to permeate the cells of the treated tissue. Oldenburg et al. (10) investigated the effect of pH, salt concentration, current density, and ON structure by iontophoretic delivery across hairless mouse skin. Brand et al. (37) evaluated 16 biologically relevant PS ONs with lengths from 6 to 40 bases for their iontophoretic transport across hairless mouse skin. The base located at the 3′-end impacted the ability of an ON to be iontophoretically transported.

Electroporation and iontophoresis for the transdermal delivery of drugs were compared by Banga et al. (38). Electroporation applies a high voltage pulse of short duration to permeate the skin barrier, while iontophoresis applies a small low voltage with constant current to push charged drug into the skin. The ON transport across the SC was primarily transcellular during electroporation and paracellular during iontophoresis. In addition, electroosmosis is important in delivering ON in iontophoresis but electroporation is not. Compared with the passive diffusion, electroporation and iontophoresis increased the topical delivery of the macromolecule

greater than one order of magnitude. Table 2 shows the effect of electroporation on ON delivery. Regnier et al. (11) also compared electroporation with that of iontophoresis for ON delivery; ON was delivered to the viable skin tissue equally by both. This result was inconsistent with Regnier and Preat (7) who reported electroporation less efficient than iontophoresis to deliver ON in the viable tissues of intact skin.

The most important advantage of topical delivery of antisense ON by skin electroporation is the rapid cellular and nuclear uptake of antisense compounds by the keratinocytes. Advantages of skin electroporation are: (1) reducing ON exposure to the nuclease present in both extracellular fluids and endocytic compartments,(2) shortening the time of onset of the antisense effect, and (3) lowering the threshold ON concentration necessary to achieve such an effect. Iontophoresis facilitates the transport of charged and high molecular compounds, which cannot be normally delivered by passive delivery. Iontophoresis provides rapid onset of action, since the lag time is of the order of minutes, as compared to hours in passive transport. Disadvantages of iontophoresis are a slight feeling of tingling or itch. Transient erythema and local vasodilatation are two common side effects associated with iontophoresis (39,40). However, with rapid and significant advances in the area of biotechnology resulting in increased number of peptide, protein, ON, and DNA drugs, iontophoresis, and electroporation provide unique opportunities for non-invasive, safe, convenient, effective, and patient-controlled delivery of such drugs.

McAllister et al. (41) developed micro-scale projections that penetrate only the outermost layers of the skin using micro-electrical mechanical system (MEMS)-based fabrication. With this device, Mikszta et al. (42) improved genetic immunization via micro-fabricated silicon projections, termed micro-enhancer arrays (MEAs), to mechanically disrupt the skin barrier and targeted epidermal delivery of genetic vaccines. The MEA-based delivery enabled topical gene transfer resulting in reporter gene activity up to 2800-fold above topical controls in a mouse model. This technology may be applicable to targeted therapy of epidermal disorders and skin cancer. Skin is a privileged target for antisense ON given its accessibility; many have thought that electroporation, iontophoresis, and MEA technology, which enhance SC and keratinocyte permeability, might be a useful method for their topical delivery.

VII. ANTISENSE OLIGONUCLEOTIDES SEMISOLID FORMULATIONS

Vlassov et al. (14) first reported ON penetration through skin. They applied ON lotion on mouse ear and recovered intact ON from blood and pancreas. Subsequently, several methods were developed to deliver ON into skin. C-5 propyne modified antisense ON in aqueous solution penetrated psoriatic SC, but not normal skin. This result suggests that ONs can be topically applied to psoriatic skin in simple topical formulations and efficiently reach the basal epidermis fully intact. Thus, simple formulation including cream and lotion might be used to treat psoriasis. In contrast to systemic ON injection, there was no apparent degradation of the ON after topical application for either normal or psoriatic skin in spite of extensive enzymatic activity in the skin (3,5). Hence, psoriasis is a reasonable target for antisense ON therapy.

Mehta et al. (13) topically applied 20-nucleotide PS intercellular adhesion molecule-1 (ICAM-1) antisense ON (ISIS-2302) in a cream formulation. ISIS-2302 topical cream is being developed as a potential therapeutic agent for plaque

psoriasis. The vehicle contained glyceryl monostearate (10%), hydroxypropyl methylcellulose (0.5%), isopropyl myristate (10%), methylparaben (0.5%), propylparaben (0.5%), polyoxy-40-stearate (15%), and water. Antisense ON effects were concentration dependent, sequence specific, and resulted from reduction of ICAM-1 mRNA levels in the skin. Compared with intravenous ON administration that had no pharmacological effects, topical delivery produced a rapid and a significantly higher accumulation of ON in the epidermis and dermis. ISIS-2302 (ALICAFORSEN^{TM}) is in phase IIa human clinical trials. In preclinical studies, topical ISIS-2302 formulation showed suppression of upregulated ICAM-1 by the epidermal and dermal skin layers implicated in the pathogenesis of psoriasis. Topical formulations were well tolerated with more than 4000-fold greater accumulation of the intact drug observed in the epidermis and 150-fold more in dermal layers of the skin than with the intravenous injection (13). From these results, topically applied antisense ON in a cream type formulation can be delivered to target sites in the skin and may be of value in the treatment of psoriasis and other inflammatory skin disorders.

VIII. LIPOSOMAL FORMULATIONS

Although the SC is considered a major barrier to percutaneous absorption, it is also regard as the main pathway for penetration. Compounds and vehicle systems that loosen or fluidize the lipid matrix of the SC may enhance permeation. Among these delivery systems, liposome formulations offer several advantages over more conventional formulations (43). Liposomes are of great interest for the delivery of ONs and their application in medicine have been extensively studied.

Topical delivery of ON and/or DNA using liposomes formulation included conventional liposomes, stealth liposomes coating with polyethylene glycol, targeted liposomes containing antibodies, ligands, and polysaccharides, cationic and nonionic liposomes. Raghavachari and Fahl (22) reported that nonionic liposomes were their most efficient vehicles for transdermal systems. Rat pups treated with nonionic liposomes formulations showed the highest reporter gene expression 24 hour following liposomes application, followed by nonionic/cationic liposomes and phospholipid formulations (Table 3). Surprisingly, the traditional phospholipid-based liposome carriers were not effective as delivery vehicles for luciferase or galactosidase DNA when compared to nonionic liposomes. Jayaraman et al. (44) explained the high efficiency of nonionic liposomes as a facilitator of drug delivery to the unique lipid composition. They suggest that polyoxyethylene and glyceryl dilaurate act as penetration enhancers. Raghavachari and Fahl (22) also showed kinetic studies to assess the longevity of expression of the delivered luciferase and galactosidase genes. The maximum expression was 24 hours postdelivery and expression level returned to near basal levels at 72 hours. This indicated that the process of topical delivery of DNA facilitates a transient, high-level expression of the exogenous gene delivered into the skin cells. This result is important in treating skin diseases and immunization.

Liposomes are widely used in the topical ocular delivery of ON. Among these applications, the treatment of viral diseases has been approached using liposomes encapsulated ONs. Bochot et al.(45) reported on ophthalmic delivery system for ON based on a liposomal dispersion within a thermosensitive gel. Ocular distribution and clearance from the vitreous humor of a model antisense ON were investigated after intravitreal injection to rabbits of the ON free or encapsulated into liposomes.

Table 3 Luciferase and Galactosidase Activity in Rat Pup Skin Following Treatment with Liposomes-DNA Formulations

Liposome composition	Relative luciferase activity (RLU/mg protein)[d]	Relative galactosidase activity (m units/mg protein)[e]
Nonionic[a]	57,000	6.0
Nonionic/cationic[b]	32,000	5.4
Phospholipid[c]	8900	3.3

[a]Composition: glyceryldilaurate (GDL)/cholesterol (CHOH)/polyoxyethylene-10 stearyl ether (POE-10) (58:15:27, w/w ratio)
[b]Composition: GDL:CHOH:POE-10:DOTAP (50:15:23:12 w/w ratio)
[c]Composition: dioleoylphosphatidylethanolamine-2000 (PEGylated):CHOH:distearylphosphatidylcholine (1:5:0.1, molar ratio)
[d]Treated skin was dissected out and homogenized. To 100 μL of the tissue homogenate was added 100 μL of the luciferase assay buffer containing substrate, and the emitted light was measured in a Monolight 2010 luminometer.
[e]Galactosidase activity was measured by adding 100 μL of the tissue homogenate to an equal volume of assay buffer. The reaction mixture was incubated for 30 minutes at 37°C and terminated by the addition of 100 μL 1 M sodium carbonate, and the absorbance at 420 nm was measured.

Liposomes provided higher drug levels than the control solution one day postinjection. After 14 days, the residual concentration of ON using liposomal suspension was 9.3-fold higher than that obtained with ON control solution. The intravitreal injection ON containing of liposomes led to a controlled release, thus offering interesting prospective in the ocular delivery of ONs effective for the treatment of some retinal infections.

Enhancers can be also used with liposome formulations. Dimethylsulfoxide increased ON skin delivery with liposome formulation (46). Brand and Iversen (16) reported the combined effect of skin enhancers: a mixture of polyethylene glycol and linoleic acid reduced the SC barrier function. The ON flux was near 20 times greater than iontophoretic delivery of the same sequence containing a PS backbone. Recently, we have tested the percutaneous delivery of NF-kB decoy with various formulation systems. Among these formulation systems, liposomes containing 10% urea were an efficient composition to transfer into skin (personal communication). Hence, liposomal creams containing these enhancers may be suited to use in the delivery of therapeutic ON.

IX. FIRST OLIGONUCLEOTIDE DRUG: ISIS 2922

The ONs have potential for the treatment of ocular severe viral infections due to herpes simplex virus or to the cytomegalovirus (CMV). The use of ONs to inhibit CMV was evaluated by two groups. A series of ONs complementary to the translation start sites, coding regions, intron/exon region and 5′ caps in RNAs including the DNA polymerase, and immediate early genes IE 1 and IE 2 was evaluated by Azad et al. (47,48). The most potent was a 21-mer (ISIS 2922) against the coding regions of IE 2, with an IC_{50} of about 0.1 μM. Recently, the first ON drug was marketed: Vitravene® (ISIS 2922) is delivered to the eye by intravitreal administration for the treatment of CMV infections in patients having AIDS.

Marketed ONs require repeated administrations. In order to target more effectively these ONs and to obtain a slow release pattern of the compounds, the use of liposomes would be a good alternative. The use of liposomes for intravitreal administration can be promising since these lipid vehicles are stable and protect ONs against degradation by nuclease, they allow increased retention time in the vitreous.

X. CONCLUSIONS

The technology of ON antisense for the manipulation of specific gene expression has therapeutic potential. Topical delivery of ONs is highly feasible and offers the advantages for local treatment of skin diseases. ISIS-2922 as an antisense ON drug for viral therapy is commercially available and many other ON drugs are in clinical trial. Liposomal creams containing enhancers are well suited to use in the delivery of therapeutic ON in terms of cost, efficacy, compliance, and comfort. These systems provide a likely direction for future studies.

REFERENCES

1. Zon G. Oligonucleotide analogues as potential chemotherapeutic agents. Pharm Res 1988; 5:539–549.
2. Stein CA, Cheng YC. Antisense oligonucleotides as therapeutic agents-Is the bullet really magical? Science 1993; 261:1004–1012.
3. Regnier V, Tahiri A, Andre N, Lemaitre M, Le Doan T, Preat V. Electroporation-mediated delivery of 3′-protected phosphodiester oligonucleotides to the skin. J Control Rel 2000; 67:337–346.
4. Rojanasakul Y. Antisense oligonucleotide therapeutics: drug delivery and targeting. Adv Drug Deliv Rev 1996; 18:115–131.
5. White PJ, Gray AC, Fogarty RD, Sinclair RD, Thuminger SP, Werther GA, Wraight CJ. C-5 propyne-modified oligonucleotides penetrate the epidermis in psoriatic and not normal human skin after topical application. J Invest Dermatol 2002; 118:1003–1007.
6. Choi MJ, Zhai H, Maibach HI. Effect of tape stripping on percutaneous penetration and topical vaccination. Exogenous Dermatol 2003; 2:262–269.
7. Regnier V, Preat V. Localization of a FITC-labeled phosphorothioate oligonucleotide in the skin after topical delivery by iontophoresis and electroporation. Pharm Res 1998; 15: 1596–1602.
8. White PJ, Fogarty RD, Liepe IJ, Delaney PM, Werther GA, Wraight CJ. Live confocal microscopy of oligonucleotide uptake by keratinocytes in human skin grafts on nude mice. J Invest Dermatol 1999; 112:887–892.
9. Wraight CJ, White PJ, Mckean SC, Fogarty RD, Venables DJ, Liepe IJ, Edmondson SR, Werther GA. Reversal of epidermal hyperproliferation in psoriasis by insulin-like growth factor I receptor antisense oligonucleotides. Nat Biotechnol 2000; 18:521–526.
10. Oldenburg KR, Vo KT, Smith GA, Selick HE. Iontophoretic delivery of oligonucleotides across full thickness hairless mouse skin. J Pharm Sci 1995; 84:915–921.
11. Regnier V, De Morre N, Jadoul A, Preat V. Mechanism of a phosphorothioate oligonucleotide delivery by skin electroporation. Int J Pharm 1999; 184:147–156.
12. Weaver J. Electroporation theory. Concepts and mechanism. Methods Mol Biol 1995; 47:1–26.
13. Mehta RC, Stecker KK, Cooper SR, Templin MV, Tsai YJ, Condon TP, Bennett CK, Hardee GE. Intercellular adhesion molecule-1 suppression in skin by topical delivery of anti-sense oligonucleotides. J Invest Dermatol 2000; 115:805–812.

14. Vlassov VV, Karamyshev VN, Yakubov LA. Penetration of oligonucleotides into mouse organism through mucosa and skin. FEBS Lett 1993; 327:271–274.
15. Raychaudhuri SP, Sanyal M, Raychaudhuri SK, Duff S, Farber EM. Severe combined immunodeficiency mouse-human skin chimeras: a unique animal model for the study of psoriasis and cutaneous inflammation. Br J Dermatol 2001; 144:931–939.
16. Brand RM, Iversen PL. Transdermal delivery of antisense compounds. Adv Drug Deliv Rev 2000; 40:51–57.
17. Wertz PW. Lipids and barrier function of the skin. Acta Derm Venereol 2000; 208:7–11.
18. Weerheim A, Ponec M. Determination of stratum corneum lipid profile by tape stripping in combination with high-performance thin-layer chromatography. Arch Dermatol Res 2001; 293:191–199.
19. Hollern WM, Ginns EI, Menon GK, Ginndmann J-U, Fartasch M, Mckinney CE, Elias PM, Sidransky E. Consequences of beta-glucocerebrosidase in epidermis. J Clin Invest 1994; 93:1756–1764.
20. Butler M, Stecker K, Bennett CF. Cellular distribution of phosphorothioate oligodeoxynucleotides in normal rodent tissues. Lab Invest 1997; 77:379–388.
21. Fan H, Lin Q, Morrissey GM, Khavari PA. Immunization via hair follicles by topical application of naked DNA to normal skin. Nat Biotechnol 1999; 17:870–872.
22. Raghavachari N, Fahl WE. Targeted gene delivery to skin cells in vivo: a comparative study of liposomes and polymers as delivery vehicles. J Pharm Sci 2002; 91:615–622.
23. Bochot A, Couvreur P, Fattal E. Intravitreal administration of antisense oligonucleotides: potential of liposomes delivery. Prog Retin Eye Res 2000; 19:131–147.
24. Hanvey JC, Peffer NJ, Bisi JE, Thomson SA, Cadilla R, Josey JA, Ricca DJ, Hassman CF, Bonham MA, Au KG, Carter SG, Bruckenstein DA, Boyd AL, Noble SA, Babiss LE. Antisense antigene properties of peptide nucleic acids. Science 1992; 258:1481–1485.
25. Castier Y, Chemla E, Nierat J, Heudes D, Vasseur MA, Rajnoch C, Bruneval P, Carpentier A, Fabbiani JN. The activity of c-myb antisense oligonucleotide to prevent intimal hyperplasia is non-specific. J Cardiovasc Surg 1998; 38:1–7.
26. Ellington AD, Szostak JW. Selection in vitro of single strand DNA molecules that fold into specific ligand-binding structures. Nature 1992; 355:850–852.
27. Galbraith WM, Hobson WC, Giclas PC, Schechter PJ, Agrawal S. Complement activiation and homodynamic changes following intraveneous administration of phosphorothioate oligonucleotides in the monkey. Antisense Res Dev 1994; 4:201–206.
28. Krieg AM. CpG DNA: a novel immunomodulator. Trends Microbiol 1999; 7:64–65.
29. Seo N, Tokura Y, Nishijima T, Hashizume H, Furukawa F, Takigawa M. Percutaneous peptide immunization via corneum barrier-disrupted murine for experimental tumor immunoprophylaxis. Proc Natl Acad Sci USA 2000; 97:371–376.
30. Takigawa M, Tokura Y, Hashizume H, Yagi H, Seo N. Percutaneous peptide immunization via corneum barrier-disrupted murine for experimental tumor immunoprophylaxis. Ann NY Acad Sci 2001; 941:139–146.
31. Watabe S, Xin K-Q, Ihata A, Liu L-J, Honsho A, Aoki I, Hamajima K, Wahren B, Okuda K. Protection against influenza virus challenge by topical application of influenza DNA vaccine. Vaccine 2001; 19:4434–4444.
32. Zhang L, Li L, Hoffmann GA, Hoffmann RM. Depth-targeted efficient gene delivery and expression in the skin by pulsed electric fields: an approach to gene therapy of skin aging and other diseases. Biochem Biophys Res Commun 1996; 220:633–636.
33. Prausnitz MR, Edelman ER, Gimm JA, Langer R, Weaver JC. Transdermal delivery of heparin by skin electroporation. Biotechnol 1995; 13:1205–1209.
34. Vanbever R, LeBoulange E, Preat V. Transdermal drug delivery of fentanyl by electroporation. I. Influence of electrical factors. Pharm Res 1996; 13:557–563.
35. Zewert TE, Pilquett UF, Langer R, Weaver JC. Transdermal transport of DNA antisense oligonucleotide by electroporation. Biochim Biophys Res Commun 1995; 212: 286–292.

36. Brand RM, Iversen PL. Iontophoretic delivery of a telomeric oligonucleotides. Pharm Res 1996; 13:851–854.
37. Brand RM, Wahl A, Iversen PL. Effects of size and sequence on the iontophoretic delivery of oligonucleotides. J Pharm Sci 1998; 87:49–52.
38. Banga AK, Bose S, Ghosh TK. Iontophoresis and electroporation: comparisons and contrasts. Int J Pharm 1999; 179:1–19.
39. Ledger PW. Skin biological issues in electrically enhanced transdermal delivery. Adv Drug Deliv Rev 1992; 9:289–307.
40. Branda RM, Singh P, Aspe-Carranza E, Maibach HI, Guy RH. Acute effects of iontophoresis on human skin in vivo: cutaneous blood flow and transepidermal water loss measurements. Eur J Pharm Biopharm 1997; 43:133–138.
41. McAllister DV, Allen MG, Prauznitz MR. Microfabricated microneedles for gene and drug delivery. Ann Rev Biomed Eng 2000; 2:289–313.
42. Mikszta JA, Alarcon JB, Brittingham JM, Dutter DE, Pettis RJ, Harvey NG. Improved genetic immunization via micromechanical disruption of skin-barrier function and targeted epidermal delivery. Nat Med 2002; 8:415–419.
43. Egbaria K, Weiner N. Liposomes as a topical drug delivery system. Adv Drug Deliv Rev 1990; 5:287–300.
44. Jayaraman SC, Ramachandran C, Weiner N. Topical delivery of erythromycin from various formulation: an in vivo hairless mouse study. J Pharm Sci 1996; 85:1082–1084.
45. Bochot A, Fattal E, Couvreur P. Design of a new eye delivery system for oligonucleotide based on a liposomal dispersion within a thermosensitive gel. In: Proceeding of the 2nd World APGI/APV Meeting on Pharmaceutics, Biopharmaceutics and Pharmaceutical Technology, Paris, 1998:1089–1090.
46. Heckert RA, Elankumaran S, Oshop GL, Vakharia VN. A novel transcutaneous plasmid-dimethylsulfoxide delivery technique for avian nucleic acid immunization. Vet Immunol Immunopathol 2002; 89:67–81.
47. Azad RF, Driver VB, Tanaka K. Antiviral activity of a phosphorothioate oligonucleotide complementary to RNA of the human cytomegalovirus major immediate-early region. Antimicrob Agents Chemother 1993; 37:1945–1954.
48. Azad RF, Brown-Driver VB, Buckheit RW, Anderson KP. Antiviral activity of a phosphorothioate oligonucleotide complementary to human cytomegalovirus RNA when used in combination with antiviral nucleoside analogs. Antiviral Res 1995; 28:101–111.

56

Transcutaneous Immunization: Antigen and Adjuvant Delivery to the Skin

Gregory M. Glenn, Sarah A. Frech, Richard T. Kenney, and Larry R. Ellingsworth
IOMAI Corporation, Gaithersburg, Maryland, U.S.A.

I. INTRODUCTION

The outermost layer of the living skin has a large component of immune cells committed to host defense against pathogens. The outer layer of the skin is in direct contact with the hostile microbial world and is well equipped to detect invasion by pathogens and orchestrate effective immune responses. The skin immune system is highly sensitive to the danger signals presented by microbes that trigger effective immune responses. Vaccinologists seek to replicate effective immune response to infections by presenting all or some portions of a microbe in a form that leads to protective immune responses without creating the symptoms of disease. The recent advances in characterization of the skin immune system, and the demonstration that new delivery technologies and adjuvants can target the dendritic cells in the skin to stimulate immune responses, together suggest that skin immunization techniques will become established immunization regimens.

Recent work in our labs and others has focused on vaccine delivery into the skin using a patch or similar means for vaccine delivery. The skin, as a non-invasive route for vaccine delivery, has great potential for safe use of potent immune stimulating compounds that can target the dense population of immune cells found in the skin. The use of such compounds to stimulate the skin immune system leads to strong and effective immune responses, and this immune responsiveness, in combination with a high safety margin, has fostered a great deal of interest in targeting the skin with vaccines. The basic insights gained through initial studies have led to several efforts to formulate and test human use vaccines. This chapter attempts to summarize preclinical and clinical experience with delivery of proteins to the skin, and while a great deal of data has been generated to date, there is much to be learned regarding the transit pathways and mechanism of delivery, and room to improve the efficacy and effectiveness of this new route of delivery.

II. BACKGROUND

Mammalian skin is composed of three primary layers (Fig. 1). The stratum corneum (SC), the outermost layer of the skin, is composed of 10–20 layers of quiescent, cornified epidermal skin cells called keratinocytes that are continuously shed. During the formation of the SC, the keratinocytes secrete lipids that form a type of lipid mortar that encases the dead and dying keratinocytes. The human SC is 10–20 μm thick in a "bricks and mortar" format, and represents an effective but fragile barrier to microbes, fluids, and foreign material. The epidermis underlies the SC and is composed of epidermal keratinocytes and other skin elements in a continuous growing layer of epithelium. The epidermis is also a dynamic immune environment, with active traffic of immune cells in and out of the epidermis. The primary antigen-presenting cell (APC) found in the epidermis is the Langerhans cell (LC), a bone-marrow-derived dendritic cell that migrates from the bone marrow into the skin and plays the dual role of immune surveillance and antigen presentation (1). Confocal microscopy in human skin demonstrated that LCs cover 25% of the total skin surface area, although they account for approximately only 1–3% of the epidermal cells (2). Their density, accessibility and antigen presentation function create an ideal target for vaccine delivery. The final layer of the skin, the dermis, supports the epidermis with connective tissue, contains the blood vessels (generally the target for transdermal drug delivery) and lymphatics, and provides a foundation for the epidermal appendages such as hair and sweat glands. The dermis contains dendritic cells (DC) and LCs in transit, but the density of APCs in the dermis does not match that of the epidermis (3). Hair follicles, which extend into the dermis, have their own unique microenvironment of immune cells (4). The normal practice of vaccine delivery by needle perforates the skin to deliver antigens to other tissues, bypassing the highly attractive skin immune system. In transcutaneous immunization, antigen and immune-activating adjuvants are applied to the skin. The activated LCs take up antigen, and migrate to the draining lymph node, where they orchestrate potent

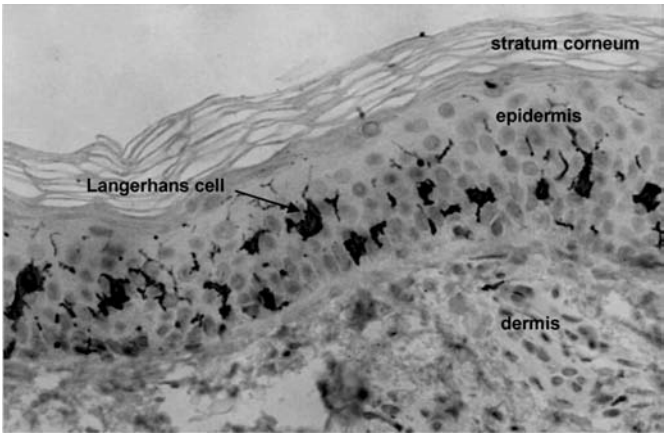


Figure 1 The skin is composed of 3 principal layers: the dermis, epidermis, and stratum corneum. Existing vaccine delivery involves perforation through the skin, bypassing the immune-rich layers of the skin. New technologies targeting the skin take advantage of the skin immune system elements, such as epidermal Langerhans cells, shown above. Nat Med 2000;6: 1403–1406, with permission.

systemic immune responses. This is in contrast to transdermal drug delivery, where drugs and delivery systems typically target blood vessels in the dermis, requiring a breach of the formidable layers of the skin. It is also worth noting that immunization requires delivery of only small quantities of material, possibly picograms into the epidermis, to provide effective immune responses. Thus, we and others use the term "transcutaneous immunization" to describe antigen/adjuvant delivery into the skin and to differentiate the mechanisms and concepts from transdermal drug delivery.

III. ADJUVANTS AND THE SKIN

Transcutaneous immunization (TCI), the delivery of antigens and adjuvants to the skin for the purpose of immunization, is consistently dependent on the presence of an adjuvant in the formulation for induction of robust immune responses (5–10). In general, adjuvants greatly augment the immune responses to co-administered antigens and there are a wide variety of adjuvants that may be used (11). The bacterial ADP-ribosylating exotoxins (bAREs) are potent adjuvants in the context of the skin and include cholera toxin (CT), heat-labile enterotoxin of *Escherichia coli* (LT), and their mutants and subunits. bAREs have had extensive use as adjuvants via intranasal and oral routes, and are causative agents in self-limiting diarrheal diseases, the latter suggesting that their topical use would not be accompanied by long-term side effects (9,11–18). Their safety profile is reviewed elsewhere (19).

The adjuvanticity of the bAREs on the skin appears to correlate with the level of ribosyl-transferase activity as it does in oral and most nasal immunization studies (9). Purified cholera toxin B-subunit (pCTB) and mutant toxins that retain ribosyl-transferase activity act as adjuvants on the skin, in contrast to recombinant CTB (rCTB) that is devoid of ribosyl-transferase activity and is subsequently far less potent as an adjuvant (9). Other adjuvants, including bacterial DNA, cytokines, LPS, and LPS analogues, have been shown to have activity in the context of the skin, but their comparative potency on the skin needs to be further evaluated (9).

IV. OPTIMIZATION OF DELIVERY

The SC is an effective barrier to penetration of fluids, large molecules, particles and microbes. Disruption of the SC leads to greater immune responses, which are the most relevant surrogates for measuring antigen delivery. There are a variety of simple techniques to overcome this barrier function, including chemical and physical penetration techniques developed for transdermal drug delivery. Long-held maxims of skin penetration have stated that even with use of skin penetration techniques, delivery of drugs and bioactive molecules greater than 500 Da was not possible. However, it has become clear that these maxims were based on transdermal delivery of drugs to the blood vessels in the dermis or due to the failure to deliver larger moieties such as insulin through the combined barrier created by the SC, epidermis, and dermis, whereas TCI merely requires delivery to the epidermis.

The superficial nature of anatomical targets for antigen delivery suggests that few restrictions for antigen size apply to TCI. In human skin, which is the most relevant setting for testing vaccine delivery concepts, we have shown that very large recombinant antigens on the order of 1,500,000 Da can be delivered to elicit strong systemic immune responses using crude patches and minimal SC disruption (8). This study followed initial observations that LT (86,000 Da) was effectively delivered

through human skin by simply applying LT in solution to gauze onto the skin without any other manipulation (20). Most currently licensed vaccine antigens fall within this size range, (e.g., tetanus toxoid $\sim$ 160,000 Da). These striking findings have largely been overlooked by investigators in the field of transdermal drug delivery but are well known and accepted by vaccinologists. Extensive animal data has shown that whole viruses (21), recombinants (22), and even whole bacterial cells (L.R. Ellingsworth, unpublished observations) can be effectively delivered to the skin immune system. These observations suggest that the delivery of a variety of antigens and adjuvants is feasible, and that the maxims for transdermal drug delivery can be refined based on the findings.

Disruption of the SC may be important for efficient delivery and lends itself to relatively simple techniques. Occlusion, wetting of the skin, and other methods lead to hydration of the SC. Hydration of the SC results in swelling of the keratinocytes and pooling of fluid in the intercellular spaces, leading to dramatic microscopic changes in the SC structure (23) that have no lasting effect once the skin is allowed to dry. Hydrated SC clearly allows a variety of antigens to pass through the skin (20). The transit pathways utilized by antigens (as well as transdermal drugs) to traverse the SC are not well characterized. Transdermal drug delivery of polar small molecule drugs is thought to occur through aqueous intercellular channels formed between the keratinocytes in hydrated skin, and it is possible that similar pathways are engaged for antigen delivery by TCI (23).

Physical and chemical penetration enhancement techniques that disrupt the integrity of the SC have also been described (5,24–27). We have tested concepts with clinical relevance to patch delivery in model systems and subsequently applied them to human skin where penetration enhancement appears to represent an improvement over simple hydration of the skin. For product development, we have focused on the use of simple, inexpensive materials with clinical utility in other settings, and simple methods of use/application that lead to consistent, heightened immune responses. Device-based techniques also disrupt the SC and use various means for delivery of antigens and adjuvants into the epidermis. With the exception of gas-powered gun delivery, these techniques have not to date been proven to work in the clinic, and only limited animal immunization data exists.

Modeling skin delivery of vaccines is not straightforward, unlike some transdermal drug systems. Investigators in our field are cognizant of the interspecies differences in the skin, but have also encountered the limitations on the relevance of animal modeling for vaccine delivery to the skin. Hairless guinea pigs can be used to examine the effect of mild abrasives or devices to disrupt the SC, as they have an epidermis and SC that is similar in thickness to humans and have been widely used for studying penetration enhancement techniques. Biopsy of skin treated to disrupt the SC suggested that this method might aid in efficiency of antigen delivery and allow optimization and testing of agents to disrupt the SC (25). However, the hairless guinea pig may not be suitable for topical immunization studies due to the high lipid content of its skin, and thus should be carefully compared with other pretreatment techniques such as the use of microneedles (27). It has been suggested that hair follicles play an important role in topical administration, but this hypothesis would not explain the enhancement seen with SC disruption (discussed below). The likelihood that follicles are not significant antigen transit pathways is supported by the observation that outbred CD1 mice with normal hair follicle development, and hairless SKH mice (same genetic background) with sparse, vestigial follicles, respond equally well to topical immunization and disruption of the SC (25).

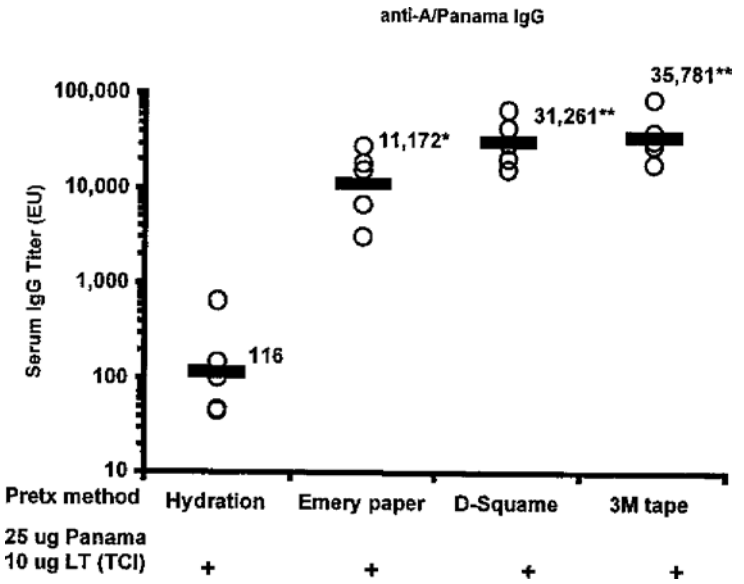


Figure 2 *Improved topical delivery of influenza split-virus vaccine by disruption of the stratum corneum.* C57BL/6 mice were shaved on the dorsal caudal surface two days prior to topical immunization. Exposed skin was hydrated by gently rubbing (20 strokes) with a saline saturated gauze sponge. The SC was disrupted by mild abrasion with emery paper (10 strokes) or tape stripping with D-Squame (10x) or 3M^{TM} tape (10x). A solution consisting of 25 μg A/Panama and 10 μg Lt was applied to the pretreated skin for 1 hr and then washed off with warm water. Groups were immunized three times (day 0, 14 and 28) and serum collected two weeks after the third immunization on day 42. Serum antibody titers to A/Panama were determined by ELISA, and titers were reported as ELISA Units (EU). The geometric mean titer for each group is indicated. Serum antibody elicited by hydration pretreatment was compared to antibody titers elicited by skin pretreatment with emery paper or by tape stripping. *$p = 0.012$; **$p \leq 0.006$. Expert Rev Vaccines 2003;2:253–267, with permission.

Although the human SC is the most significant barrier to topical immunization, it is a fragile barrier that can be easily disrupted, possibly allowing antigens to more readily diffuse into the superficial epidermis. Despite the differences in the thickness of human and mouse SC and epidermis, murine studies have been useful for screening pretreatment methods for human immune responses and, in conjunction with guinea pig models using histology to guide SC disruption techniques, clinically acceptable and simple SC disruption techniques have been optimized and taken into the clinic (8,9,20,22,25). Disruption of the SC using mild abrasive materials is a technique used clinically for enhancing conductivity of electrical fields through the skin to record EKGs. The same materials used in conjunction with hydrating solution improve antigen delivery, creating a single, simple treatment swab for use prior to patch placement. Studies in our lab have explored this concept and demonstrated its feasibility and effect on the delivery of both an antigen and adjuvant. In preclinical studies, the optimized application of a simple, wet patch compares well with the efficiency of adjuvanted, injected antigen. The effect of pretreatment in mouse models can be seen using split virus influenza vaccine (A/Panama) combined with LT and applied to intact skin that has been pretreated to disrupt the SC. As illustrated in Figure 2, shaved but untreated mouse skin was wetted with saline, or pretreated with emery paper (EKG prep, 10 gentle strokes on wet skin) or stripped

with D-Squame tape (10 applications) or 3M™ tape (10 applications). Two weeks after three topical applications, the serum antibody response to the influenza antigens was increased 100- to 300-fold when compared with hydration alone. The pretreatment techniques for SC disruption, skillfully done, are well tolerated and can be accompanied by mild, local and self-limiting rashes, but are likely to have an improved safety profile compared to the acceptable level of reactions that occur with parenteral immunization. When pretreatment is used, the delivery of antigen is sufficient to elicit immune responses similar to that seen with the same dose delivered by the parenteral route. As shown in Figure 3, mice given trivalent split virus vaccine by TCI respond equally to vaccine delivered by the im route. Note also the importance of the addition of adjuvant to achieve robust responses on the skin.

Although transdermal drug delivery developers use guinea pig or other mammalian human skin equivalent models to track or quantitate the amount of drug delivered after a topical application, this may be difficult to emulate with skin immunization due to the fact that standard transdermal delivery quantitative models require drug transit *through* the skin into a reservoir. By contrast, transcutaneous techniques deliver antigens *into* the skin that are likely to be extremely small amounts of material, but sufficient to elicit robust immune responses. In general, vaccine antigens delivered by any route must encounter APCs to prime the immune response. Thus, quantitation of an antibody response might be the most relevant measurement of antigen delivery.

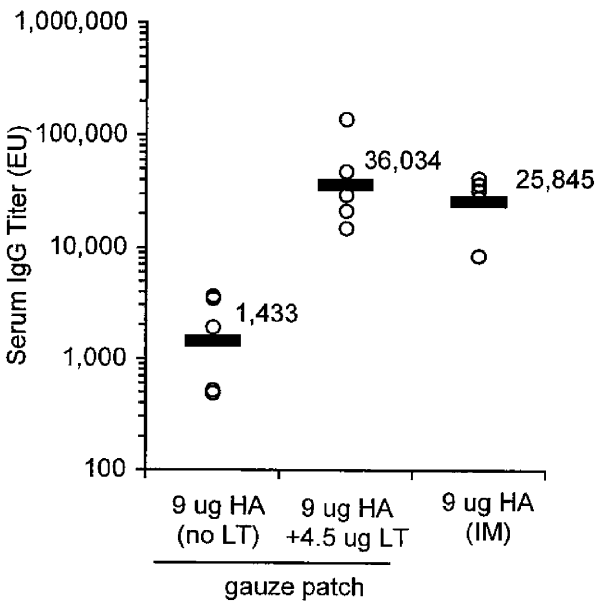


Figure 3 C57BL/6 mice were immunized using commercially obtained trivalent split virus influenza vaccine (Flushield) at day 0, 14 and 28. Intramuscular injection was done in the lateral thigh. Patch groups were immunized as previously described using the trivalent vaccine with or without LT applied to a gauze patch. Data shown using sera collected 2 weeks after the 3rd immunization. Sera assayed against a single representative strain, New Caledonia, as previously described. Vaccines: Frontiers in Design and Development, Moingeon P, Ed., Horizon Biosciences, 2005, pp. 81–104, with permission.

Bio-distribution of DNA vaccine delivered by gene gun into the skin lends itself to PCR analysis, which is a sensitive, amplified signal for detecting delivery in pigs' skin, a relevant model for gun delivery of DNA (28). At day *2,* the plasmid was detected only at the treatment site and the inguinal nodes; by day 57 it was detected only at the treatment site, and by day 141, it appeared to have cleared. These data suggest that skin delivery results in antigen localized only in the skin or draining lymph nodes (DLN). This is consistent with our findings that labeled adjuvant and antigen can only be detected in the DLN after topical application and not in distal nodes (25,29). However, more recent data suggests that some DCs loaded with adjuvant may also migrate to the mucosa in mice (30,31). Nasal immunization leads to more broadly distributed plasmid (32), but the relevance of this model for human bio-distribution of skin vaccination is doubtful (33).

Some early attempts to track antigen after TCI with radio-labeled CT suggested that the majority of CT remained in the skin (34). More recently, tracking studies with fluorescently-tagged antigen and adjuvant suggested that antigen delivered by simple wetting of the skin with antigen (no pretreatment) in solution in a gauze patch is somewhat less efficient at loading antigen APCs in the skin, compared to direct injection. In mice injected with labeled ovalbumin (OVA) by the intradermal route (id) or exposed to 6X the dose in a simple topical application, the total number of labeled cells in the TCI application approximated the number seen after id injection, which is, in essence, "complete delivery" of antigen. With the addition of adjuvant, the number of antigen-laden APCs increases significantly both with admixture of antigen and adjuvant on the skin and with application of adjuvant in a patch over the id injection. Thus, the adjuvant makes up some of the difference in efficiency due to the limitations of passive delivery, where no physical or chemical disruption of the SC is used. It is also of interest that human tracking studies using radio-labeled antigen delivered by intradermal injection have shown that ~5% of the injected dose reaches the DLN (35). This suggests that despite the premise that injection represents efficient delivery of antigen, in fact, only a small portion is taken into the immune environment even after intradermal injection, which is thought to be the most efficient method for targeting APCs and has been posited to represent "complete delivery" of antigen. Taken together, these studies suggest that the efficiency of antigen loading of APCs for TCI without optimization, and id injection, "complete antigen delivery," are not too dissimilar. As the addition of adjuvant by the safe and acceptable means of SC disruption leads to several log increases in the immune response compared to antigen alone, one could surmise that immune responses to injected antigens might be lower compared to TCI. An optimized system using pharmaceutically formulated patches, optimized for efficient delivery, may achieve the goal of providing a more efficient use of antigen and thereby lower the antigen dose in a particular vaccine compared to needle-based delivery. Clearly, a goal of the development program will be to optimize delivery in certain products and overall use of smaller amounts of antigen than by needle-based routes.

V. IMMUNE RESPONSES TO TCI—ADJUVANT AND ANTIGEN IN A PATCH

The early observation that CT could be used as an adjuvant for topical immunization with toxoid antigens (7) led to numerous studies showing that a wide variety of adjuvants and antigens can be used to induce systemic and mucosal immunity

(9,20,21,34,36–39). The mechanisms by which adjuvants exert their effects at the level of the skin are becoming increasingly clear and the enhancing effects are well documented. LT and its derivatives appear to be unmatched in their potency and can be safely used in the context of the skin (8,14). Given the availability of LT in commercial GMP supply, LT has been the focus of our development programs. However, it is clear that many adjuvants have a similar biological effect, and given sufficient commercial and biological rationale, could conceivably be developed in a product targeting the skin.

TCI represents a departure from other routes of immunization, yet results in "classic" immune responses similar to those induced by other routes of immunization. TCI is similar to intranasal or oral immunization, as the simple admixture of LT with a co-administered antigen such as tetanus toxoid (TTx) or influenza hemagglutinin results in markedly higher antibody levels compared to the administration of antigens alone, which can themselves elicit immune responses (7–9). Similarly, use of bAREs by TCI induces cell-mediated immunity to the co-administered antigens such as $CD4^+$ or $CD8^+$ T cells with a balanced T helper profile (40–43).

The use of adjuvant on the skin results in both primary and secondary serum antibody responses to co-administered antigens when boosting is conducted using adjuvants (34). Serial, repeated immunization with the same adjuvant but different antigens may readily be achieved despite the preexisting high titer antibodies to the adjuvant (12,34). Additionally, TCI appears to induce boostable, long-lasting, stable immune responses (44). The magnitude of the adjuvanticity correlates with the ribosyl-transferase activity and this is evident using a variety of adjuvants. Mice immunized with the model antigen TTx along with the adjuvants CT, rCTB, pCTB (which contains trace holotoxin activity), LT, LTR192G, LTK63, or LTR72 (13,45,46) show similarly boostable antibody responses to TTx, with the exception of rCTB, which lacks the ribosyl-transferase activity associated with the A subunit (9). Tetanus-specific T-cell proliferative responses in spleen and lymph nodes suggest that boosting is related to the T-cell responses (40). Priming by the intramuscular (im) route with TTx and alum, which induces T-cell memory, can be followed by a booster immunization on the skin to induce secondary responses (40). These and many other studies demonstrate that TCI induces T-cell responses and boostable antibody responses, and confirm that immunization via the skin can be expected to induce immune responses with characteristics similar to other routes of immunization.

It was clear in early studies that the use of an adjuvant can be important to the induction of high levels of antibodies to a co-administered antigen (7) and can result in the generation of functional immune responses. This has been confirmed in several other settings, such as gene-gun immunization (5,47). In an early TCI study, TTx delivered with increasing doses of LT as adjuvant produced robust levels of anti-TTx antibodies that are clearly dependent on the presence of adjuvant (9). The same animals were fully protected by systemic tetanus toxin challenge, and only animals receiving adjuvant with the antigen were fully protected (9,45). Many studies support the importance of the adjuvant. In live RSV (37) and chlamydia (48) challenges, the adjuvant was shown to play a crucial role in the protective responses (37). Other investigators have shown that antidiphtheria toxin antibodies generated by TCI in the presence of adjuvant neutralize the highly potent diphtheria toxin (49). More recent studies have shown that TCI with a helper peptide derived for HIV IIIB and the immunodominant CTL epitope from the V_3 loop of the HIV IIIB strain of HIV induced CTLs located in the intestinal Peyers patches (30). The CTL response correlated with protection against intrarectal challenge with gp 160

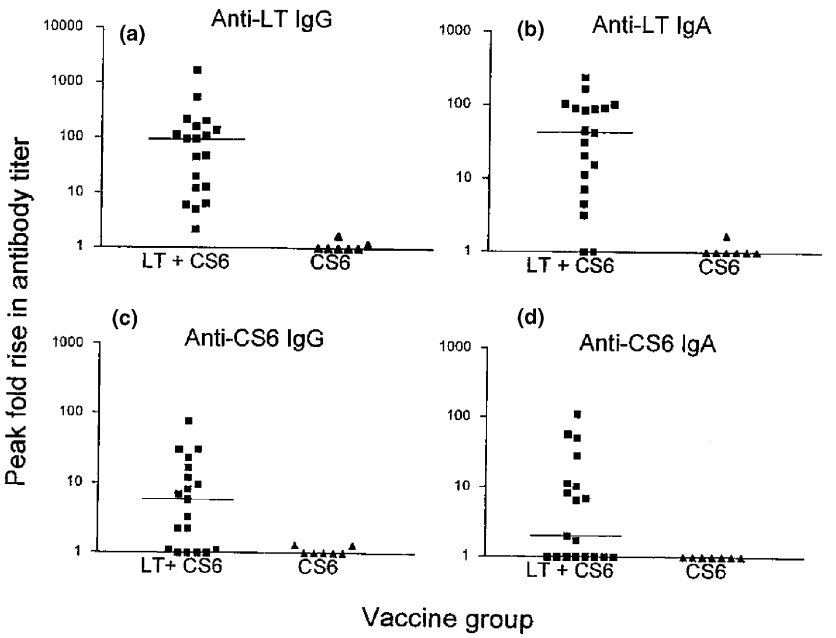


Figure 4 *Human serum IgG and IgA responses to co-administered CS6 and LT.* Normal adult volunteers were enrolled in a dose-escalating study of 250, 500, 1000 or 2000 μg CS6 alone or with 500 μg LT dosed at 0, 1, and 3 months. The peak fold-rise in antibody for each individual is shown (reported as fold rise over baseline), combining the dose groups as the responses were not significantly different, and the geometric mean for each group is shown as a bar. Infect Immun 2002; 70:1874–1880, with permission.

expressing vaccinia virus. Interestingly, whereas the majority of DCs clearly migrated to the draining lymph nodes, some DCs containing fluorescently-labeled LT appeared in the Peyers patches and DCs isolated after immunization could present antigen, suggesting that a population of DCs can present antigen directly to the mucosal immune system. Conversely, skin immunization with recombinant Protective Antigen (rPA) was protective in a live *B. anthracis* challenge both with and without adjuvant, despite log higher titers in the presence of adjuvant (50), suggesting that, in this model, even modest levels of antibodies are protective. These data have confirmed the assertion that skin-delivered antigen and adjuvants can result in robust, functional, and protective immune responses.

The critical role of the adjuvant for human immunogenicity has been shown using a recombinant *E. coli*/ETEC antigen, CS6 (8). This large antigen (>1.5 million Da) was delivered with and without LT using a simple patch. As shown in Figure 4, only subjects receiving both antigen and adjuvant produced anti-CS6 antibodies (Fig. 4C and D). This very clear and seminal study (discussed in detail below) confirmed the universal preclinical observation that adjuvants play an important role in inducing robust immune responses to antigens delivered to the skin.

VI. HUMAN STUDIES

The safety and immunogenicity of TCI and related approaches was shown by early-stage clinical investigations. The challenges in these early studies were to show

delivery of LT (86 kDa) in the context of human skin and to demonstrate the role of LT as an adjuvant, extending our preclinical observations. These points are now firmly established (20) and have been confirmed in subsequent studies (8). The next level of development will require further extension of safety observations, demonstration of the clinical utility of TCI with various antigens, optimization of their delivery by studying skin pretreatment and patch types, and assessment of the immune responses induced.

The initial proof of concept clinical study used a liquid application of LT alone in a simple patch on untreated skin in a dose escalation format to assess the safety and immune response (20). Volunteers received an LT solution in a gauze pad under an adhesive patch, and were immunized at 0, 1, and 9 months. No serious vaccine-related adverse reactions were observed, and histological sections of biopsies taken at the dosing sites were normal, consistent with the absence of DTH clinically. In vaccine studies, delivery is routinely assessed by measuring immune responses. Direct measurement of delivery, as manifested by pharmokinetics or pharmacodynamics data collected in drug studies, is never measured in vaccine studies. Using serum anti-LT IgG as a marker of delivery, subjects in the high dose group produced a greater than fourfold rise in serum antibodies against LT, along with IgG or IgA antibodies against LT in either the urine or stool. Antibodies against LT were durable and persisted long after the second immunization, with a clear booster response after the second and third dose. This was the first demonstration that a passively delivered vaccine antigen via hydration alone could elicit a systemic immune response in humans.

The importance of the role of an adjuvant in the induction of human immune responses to a co-administered antigen was initially tested in the context of *E. coli*-related traveler's diarrhea using the colonization factor CS6, a multisubunit intestinal epithelial cell-binding protein (51). Volunteers were given CS6 in a dose escalating fashion at 0,1, and 3 months (8). A total of 74% of volunteers in the combined groups had mild DTH skin reactions with the second or third dose, possibly to the colonization factor CS6 or LPS in the CS6 buffer. No other adverse events correlated with vaccine administration. As shown in Figure 4, only volunteers receiving LT as adjuvant produced serum anti-CS6 IgG and IgA. The anti-CS6 response compared favorably to responses seen after challenge infection using the live B7A ETEC strain, which results in full protection on rechallenge (52,53). Note also the robust anti-LT responses, which are important for protection against ETEC disease. Antibody secreting cells (ASCs) to CS6 were also detected in the peripheral blood. The lack of response to CS6 without LT and clear responses in the presence of LT confirmed the general observation in animal studies that the adjuvant plays a critical role in TCI. This study also confirmed that large antigens such as CS6 ($>$ 1,500,000 Da) can be readily delivered to the human skin immune system (22).

As noted above, preclinical studies suggested the dose of LT could be reduced with retention of immunogenicity by disruption of the SC. The effect of mild disruption of the SC on the delivery of LT was explored with commercially available medical products, including abrasive pads used to enhance EKG signal conductivity, or adhesive tape used to evaluate skin hydration. These strategies are in clinical practice to enhance the flux of drugs for topical application or electrical conductivity to improve the quality of electrocardiograms. To evaluate the penetration enhancement of various skin pretreatment methods in humans, we conducted a Phase I study in healthy adults. Subjects were pretreated prior to vaccination with one of the following techniques: (a) hydration alone with a glycerol/isopropyl alcohol (IPA) solution

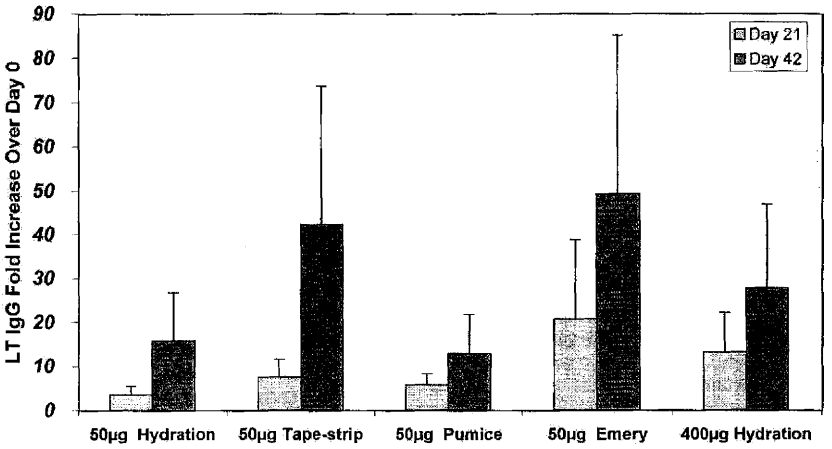


Figure 5 *Human LT IgG response after one and two doses in NLT105.* Eight subjects per group were pretreated with the indicated methods as described, then vaccinated with 50 μg or 400 μg LT on Day 0 and Day 21. LT IgG ELISA was run on sera from Day 0, 21, and 42, reported as fold increase of relative ELISA units. Expert Rev Vaccines 2003;2:253–267, with permission.

(Groups 1 and 5); (b) tape stripping followed by glycerol/IPA hydrating solution (Group 2); (c) glycerol/IPA hydrating solution followed by 10 strokes of pumice-impregnated IPA pad (Group 3); or (d) glycerol/IPA hydrating solution followed by 10 strokes of emery paper (Group 4). Following pretreatment, all groups were vaccinated twice, 21 days apart, with a patch composed of gauze containing 50 μg LT (Groups 1–4) or 400 μg LT (Group 5), covered by Tegaderm™. No significant adverse events were observed after either LT vaccination, apart from a mild, self-limited maculopapular rash that occasionally developed with or without associated pruritus at the site of vaccination (25).

Results from this study suggest that pretreatment with either emery paper or tape stripping delivered LT more efficiently than with glycerol/IPA hydration alone (Fig. 5). The number responding in these groups, defined as a twofold rise in LT IgG, was greatest in these groups. Following each vaccination, LT IgG geometric mean titers (GMT) showed greater response following pretreatment with glycerol/IPA hydration and emery paper (Group 4) and tape stripping (Group 2) when compared to glycerol/IPA hydration alone (Group 1). The improvements in LT IgG GMT seen in the emery and tape stripping treatment groups, with respect to hydration alone, suggest improved LT delivery with SC disruption using emery pretreatment. Subjects pretreated with tape stripping (Group 2) or emery paper (Group 4) and vaccinated with 50 μg showed no significant difference in GMT for LT IgG when compared to those receiving hydration alone and 400 μg LT (Group 5). These data indicate that an eightfold reduction in LT from 400 to 50 μg is possible when mild abrasive pretreatment, or its equivalent, is used. This study established the general tolerability of various penetration enhancement techniques, as well as the potential dose sparing such pretreatment can yield. Current trials using patch applications use 45 μg doses and have demonstrated similar immunogenicity with as little as 15 μg of LT based on these and other studies. In general, 45 μg LT dosed twice by TCI yields geometric mean IgG titers of 5000–10,000 and results in seroconversion in over 90% of the subjects (G.M. Glenn, unpublished observations).

The measurement of transepidermal water loss (TEWL) is widely used as an assessment of the effectiveness of chemical and physical SC disruption techniques for drug delivery. Its value as a surrogate for skin pretreatment enhancement prior to vaccination of human skin has not been previously described. We tested the applicability of TEWL assessments in the evaluation of pretreatment methods and materials and then utilized those conclusions to provide guidance for an antigen delivery trial in which the SC was disrupted to enhance delivery.

As noted in the trial described above, we found that delivery of the LT protein via a patch to human skin was augmented using tape stripping or emery paper pretreatment. The clear benefit provided by SC disruption of enhancing the immune responses to antigens delivered by a patch stimulated a broadened effort to evaluate commonly available materials in a screening system that would provide guidance for a vaccine study itself. Different pretreatment methods, including cotton swabs, emery paper, D-squame adhesive tape (a more aggressive adhesive tape), Buf-Puf™ dermabrasion pads, and non-woven abrasive pads (NWAP) used for EKG preparation were evaluated randomly in duplicate on the skin of the back for TEWL, erythema, excoriations, and tolerability in 20 subjects over 60 years of age.

After a 30-minute acclimation period, baseline TEWL measurements (described in detail below) were taken. Each material was then rubbed on or applied to the skin as per manufacturer's instructions with mild, firm pressure for a defined number of strokes. The skin was gently hydrated with 70% isopropanol rubbed over the designated area for 30 sec with a saturated cotton gauze pad after (for tape stripping) or before (for all others) each treatment. TEWL measurements were repeated 1 hr after each pretreatment was completed. The net change in TEWL measurements provided a way to rank each treatment for its effectiveness. The findings of the repeated measures ANOVA, followed by a Fisher's protected t-test, are summarized in Table 1. Groups with no statistical differences between one another are noted with the same Roman numeral. The treatments are listed in the order of maximum effect, from least to greatest. The mean TEWL prior to pretreatment for all sites was 5.89 g/m^2hr.

When this study was conducted, emery paper had been used in a vaccine patch delivery trial using 10 swipes (see Fig. 5). As shown here, the TEWL enhancements

Table 1 Transepidermal Water Loss (TEWL) Measurements: Values Are Given as the Difference Between the Pre- and Post-treatment Water Loss (g/m^2hr)

Treatment	Mean	±	SD	Statistical group
Net TEWL change at 60 min after treatment				
Cotton gauze	1.04	±	0.85	I
Buf-Puf × 20 strokes	1.42	±	0.90	I
Aggressive adhesive tape × 3 applications	1.55	±	0.87	I
Buf-Puf × 10 strokes	1.59	±	0.91	I
NWAP × 10 strokes	2.30	±	1.39	II
Emery paper × 10 strokes	2.67	±	1.79	II, III
D-squame × 20 applications	2.99	±	1.25	III
NWAP × 20 strokes	3.71	±	2.06	IV

Abbreviations: NWAP, non-woven abrasive pads.

Table 2 Expert Grader Safety Assessments: Values Are Given as the Mean Injury Scale (Range 0–8) Assessed by an Investigator Who Was Blinded to the Treatments

Treatment	Mean	±	SD	Statistical group
Clinical score at 30 min after treatment				
Cotton gauze	0.13	±	0.33	I
D-squame × 20 applications	0.42	±	0.51	I, II
Aggressive adhesive tape × 3 applications	0.55	±	0.72	I, II, III
Emery paper × 10 strokes	0.71	±	0.89	II, III
Buf-Puf × 10 strokes	0.84	±	0.87	III
Buf-Puf × 20 strokes	1.13	±	0.97	III, IV
NWAP × 10 strokes	1.24	±	1.05	III, IV
NWAP × 20 strokes	1.53	±	1.18	IV

Abbreviations: NWAP, non-woven abrasive pads.

seen with either emery paper or the NWAP using 10 strokes were not significantly different, which suggested that they might behave similarly in terms of disruption of the SC and protein delivery. Further enhancement of TEWL with a NWAP was achieved with more strokes, which was comparatively better than the tape stripping procedure that was designed to provide a benchmark for evaluating SC disruption.

A nine-point scale (0 = no redness to 8 = intense redness, flare, marked edema, or possible erosion) was used to evaluate skin reactions at 30 min after treatment. Subjects must have had a pretreatment erythema score of "0" with no excoriations present to qualify for the study. To maintain the expert grader's blindness to treatments, other clinical procedures and assessments were not conducted while the expert grader was present. The tolerability of the different materials and protocols are shown in Table 2. All procedures were seen to have mild effects with the NWAP scoring the highest (slight and diffuse redness). Interestingly, tape stripping resulted in little residual erythema while achieving similar TEWL enhancement.

Water loss measurements were obtained from the skin test sites following a 30-minute acclimation period in a controlled environment with the relative humidity maintained at less than 50% and temperature maintained at 70 + 2°F. TEWL measurements were taken using a calibrated DermaLab® Modular Systems with TEWL Probes, which are manufactured by Cortex Technology (Hadsund, Denmark) and are available in the US through cyberDERM, Inc. (Media, PA) (54,55). Measurements with this instrument are based on the vapor pressure gradient estimation method as designed by Nilsson and initially utilized by the Servo Med Evaporimeter. Probes contain two sensors that measure the temperature and relative humidity at two fixed points along the axis normal to the skin surface. This arrangement allows the device to electronically derive a value that corresponds to evaporative water loss expressed in g/m^2hr. The guidelines established for using the Servo Med Evaporimeter as described by Pinnagoda (56) are quite appropriate for the DermaLab TEWL Probe as well.

The next study was designed to further compare SC disruption on the back and arm as measured by TEWL using three materials commonly used clinically to enhance EKG signals. Test products evaluated in this study included microreplicated abrader pads, NWAP and emery paper, with a D-Squame control. The study design

Table 3 Transepidermal Water Loss (TEWL) Measurements in the First Session: Values Are Given as the Post-treatment Water Loss (g/m^2hr)

Treatment	Mean	±	SD	Statistical group
TEWL at 60 min after treatment				
Micro-abrasive pad × 10 strokes	9.47	±	4.90	I
NWAP × 20 strokes (2 directions)	9.93	±	4.06	I, II
Emery paper × 10 strokes	10.42	±	6.26	I, II
Micro Abrasive Pad × 20	10.84	±	4.91	I, II
NWAP × 15 strokes	11.02	±	5.24	I, II
NWAP × 10 strokes	11.31	±	7.50	I, II
NWAP × 20 strokes	12.75	±	6.38	II, III
D-Squame × 20 strokes	14.33	±	8.27	III

All abrasive treatments were done in one direction except as noted. The mean baseline TEWL was $5.44 \pm 1.76\, g/m^2hr$.
Abbreviations: NWAP, non-woven abrasive pad.

allowed for comparisons to be made between eight different pretreatment conditions using the materials and variable numbers of applications. The subjects were 10 male and 10 female volunteers who were ≥ 60 years of age with a median age of 69. As in the prior study, the study protocol, the informed consent form, and the product information were approved prior to study initiation by a qualified Investigational Review Board. The study was conducted in accordance with Good Clinical Practice guidelines.

This study was divided into two sessions. During the first session, eight different pretreatment methods were evaluated in duplicate on each subject's back for TEWL, erythema, excoriations, and tolerability. The back was used initially as it has more available surface area for testing. During the second session, subjects received three pretreatment methods (selected after review of the TEWL and safety data determined during first session) in duplicate on the upper arms (three on the right arm and three on the left arm), where vaccine patches would be placed in future studies. As shown in Table 3, tape stripping 20 times and the NWAP, swabbed 20 times in a single direction, gave a significantly greatest overall effect with a 2.3- and 2.7-fold increase, respectively, over baseline. Interestingly, the use of the NWAP in a single direction was more effective than the use in both directions, given the same number of strokes. The expert grader's assessment of the local erythema was generated by use of the same pretreatment methods and materials. The degree of erythema induced by stripping the skin surface 20 times with D-Squame (mean score of 1.00) was significantly less than most of the other pretreatments (mean scores of 1.53–1.88), although all mean values were within the slight to moderate range.

One week later, the two best abrasive treatments were compared on the deltoid surface of the arm where the vaccinations were planned for the active product trial. Emery paper was used as the control, given its use in our prior trials. Ten strokes with the NWAP caused a comparable post-treatment TEWL, while 20 strokes increased the response significantly (Table 4).

The data generated in these TEWL evaluations was used to design an antigen delivery study in elderly subjects ($\geq$60 years old) to test the effect of dose and time of patch wear on the immune response to LT using the optimal NWAP pretreatment protocol based on a balance of tolerability and increase in TEWL. A dry, formulated

Table 4 Transepidermal Water Loss (TEWL) Measurements and Erythema Grading After Treatment of Deltoid Skin

Treatment	Mean	±	SD	Statistical group
TEWL at 60 min after treatment				
Emery paper × 10 strokes	10.20	±	5.02	I
NWAP × 10 strokes	10.67	±	5.14	I
NWAP × 20 strokes	16.49	±	9.23	II
Clinical score at 30 min after treatment				
Emery paper × 10 strokes	1.45	±	0.99	I
NWAP × 10 strokes	1.60	±	0.79	I
NWAP × 20 strokes	2.08	±	1.21	II

Abbreviations: NWAP, non-woven abrasive pads.

adhesive patch system, which is manufacturable in large scale, was used for this trial, in contrast to simple wetted gauze pads placed on the skin and covered by overlays (see Fig. 5). The patch was prepared by compounding a solution containing the appropriate amount of LT in PBS with an adhesive blend that included a proprietary viscosity enhancing and protein stabilizing solution along with an adhesive base. This formulation was cast onto a polyester film backing and dried, then laminated to a release liner. This delivery/manufacture format is similar to that used for drug-in-adhesive products such as nicotine transdermal patches.

In the subsequent vaccine trial, the same emery paper pretreatment was used in the control group (C, $n = 40$) as in the previous studies, and the patch containing 45 μg of LT was left in place for 6 hr. The NWAP pretreatment was used (10 strokes) with two doses of LT: a 15 μg LT patch for Groups 1–3 and a 45 μg patch for Groups 4–6 ($n = 20$ per group). The patch was left in place for 15 minutes in Groups 1 and 4, 1 hour in Groups 2 and 5, and 6 hours in Groups 3 and 6, which creates a 3 × 2 factorial design for the study. Subjects were randomly assigned to groups that received two vaccinations on Days 0 and 21 with the same treatment. The safety profiles showed that dosing in all treatment groups was well tolerated, as there were no discontinuations due to adverse events and nearly all of the adverse events were mild or moderate in severity. The most frequently reported adverse events, after both the first and second vaccinations, were related to the patch site (i.e., local adverse events): mild rash, erythema, and pruritis. All reactions resolved spontaneously.

Figure 6 shows the immunogenicity results in terms of the LT IgG titer (geometric mean + 95% CI) before vaccination (Day 0), 3 weeks after the first dose (Day 21), and 3 weeks after the second dose (Day 42). The symbols represent the percent seroconversion (≥2-fold rise in LT IgG) on Day 21 (open diamonds) or Day 42 (filled circles). Baseline (Day 0) titers were comparable among the seven groups. In addition, a dose response can be seen comparing the 15 and 45 μg doses within each time of wear set of groups. On Days 21 and 42, the highest immune responses were observed in Groups 5, 6, and the control, with geometric mean fold-ratios of 3 or higher on Day 21 and 7 or higher after the second dose on Day 42, compared to 1.2–1.9 on Day 21 and 1.7–3.9 on Day 42 for other four groups ($p < 0.0001$). By Day 42, 90% or more of subjects from Groups C, 5, and 6 seroconverted compared to a rate of 39–75% for subjects from the other four groups

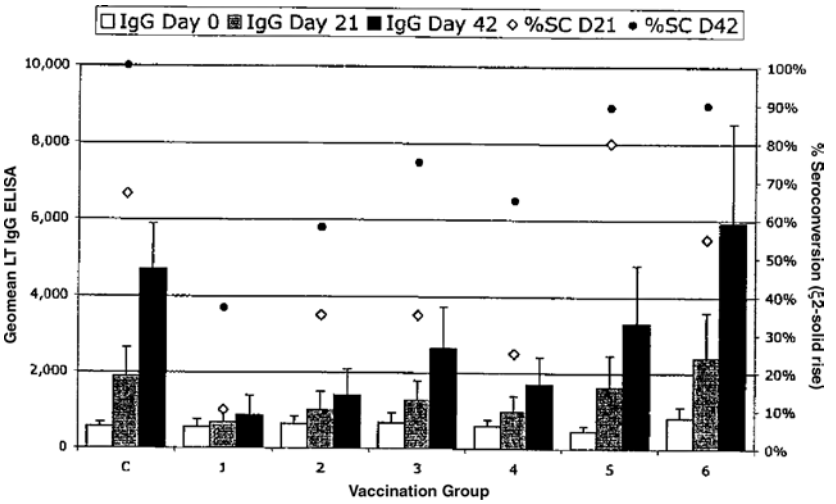


Figure 6 *Dose and time of wear effects on the LT IgG response*. Increasing the time of patch wear from 15 minutes (Groups 1 and 4) to 1 hour (Groups 2 and 5) to 6 hours (Groups 3 and 6) resulted in an improved serum immune response. A dose response relationship can be seen comparing the antibody response to 15 μg LT (Groups 1–3) vs. 45 μg (Groups 4–6) patches.

($p < 0.0001$). The comparison in the 3×2 factorial design for Groups 1–6 showed a strong impact on IgG outcomes as dry adhesive patch LT dose and time of wear increased. These findings were confirmed by covariate-adjusted regression models.

These LT patch delivery studies confirmed the conclusions reached in the assessments of pretreatment strategies using TEWL as an outcome, in that emery paper and the NWAP would cause similar delivery of LT as measured by antibody responses. The NWAP format provides a wetted pretreatment swab in a single step pre-application procedure. The LT dose response results and the dose response to time of wear matrix confirmed that this simple procedure could be performed in a highly consistent manner and provide reliable enhancement for antigen delivery. Overall, this study demonstrated that the dry adhesive patch could effectively deliver antigen and that pretreatment in a simple, product-based format could be performed to enhance delivery.

VII. SUMMARY

The skin provides both an attractive immune environment for vaccine antigen delivery and a safe and confined anatomical space for the use of potent adjuvants. It has been our presumption that LC as a class of DC should stimulate potent immune responses when presented with antigens and adjuvants, and this continues to be validated. Progress on SC disruption and simple pretreatment of the skin has led to well developed, simple use protocols not dissimilar from current protocols used to cleanse the skin prior to injection. In addition, antigen and adjuvant formulation optimization has progressed, leading to Phase II testing of the patch technologies using formulated, manufacturable patches. While delivery optimization and product testing is inevitably challenging, the major biological observations underlying TCI have been clearly established, in that large protein antigens have been delivered

clinically, resulting in immune responses with good safety profiles. At the time of publication, over 16 clinical trials with LT patches, including several Phase II trials have been conducted, representing the bias of the authors that the most critical lessons on skin delivery technologies will be learned in the clinic. Over the next 5 years, the challenge will be to conduct a development program that leads to safe and effective vaccination in the context of specific applications.

ACKNOWLEDGMENT

Supported in part by grants (1R43-AI 060071-01 and 2R44-AI 45264-02A2) from the National Institutes of Health to Iomai for research in skin immunization. The authors wish to thank Wanda Hardy for her help in the preparation of this manuscript.

REFERENCES

1. Jakob T, Udey MC. Epidermal Langerhans cells: from neurons to nature's adjuvants. Adv Dermatol 1999; 14:209–258.
2. Yu RC, Abrams DC, Alaibac M, Chu AC. Morphological and quantitative analyses of normal epidermal Langerhans cells using confocal scanning laser microscopy. Br J Dermatol 1994; 131(6):843–848.
3. Udey MC. Cadherins and Langerhans cell immunobiology. Clin Exp Immunol 1997; 107(suppl 1):6–8.
4. Christoph T, Muller-Rover S, Audring H, Tobin DJ, Hermes B, Cotsarelis G, Ruckert R, Paus R. The human hair follicle immune system; cellular composition and immune privilege. Br J Dermatol 2000; 142(5):862–873.
5. Chen D, Erickson CA, Endres RL, Periwal SB, Chu Q, Shu C, Maa YF, Payne LG. Adjuvantation of epidermal powder immunization. Vaccine 2001; 19(20–22):2908–2917.
6. Baca-Estrada ME, Foldvari M, Ewen C, Badea I, Babiuk LA. Effects of IL-12 on immune responses induced by transcutaneous immunization with antigens formulated in a novel lipid-based biphasic delivery system. Vaccine 2000; 18(17):1847–1854.
7. Glenn GM, Rao M, Matyas GR, Alving CR. Skin immunization made possible by cholera toxin. Nature 1998; 391(6670):851.
8. Güereña-Burgueño F, Hall ER, Taylor DN, Cassels FJ, Scott DA, Wolf MK, Roberts ZJ, Nesterova GV, Alving CR, Glenn GM. Safety and immunogenicity of a prototype enterotoxigenic *Escherichia coli* vaccine administered transcutaneously. Infect Immun 2002; 70(5):1874–1880.
9. Scharton-Kersten T, Yu J, Vassell R, O'Hagan D, Alving CR, Glenn GM. Transcutaneous immunization with bacterial ADP-ribosylating exotoxins, subunits, and unrelated adjuvants. Infect Immun 2000; 68(9):5306–5313.
10. Glenn GM, Alving CR. Adjuvant for transcutaneous immunization. U.S. Patent No, 5,980,898, 1999.
11. Kenney RT, Edelman R. Survey of human-use adjuvants. Expert Rev Vaccines 2003; 2(2):167–188.
12. O'Hagan DT, ed. Methods in Molecular Medicine. Totowa, NJ: Humana Press Inc. 2000.
13. Dickinson BL, Clements JD. Dissociation of *Escherichia coli* heat-labile enterotoxin adjuvanticity from ADP-ribosyltransferase activity. Infect Immun 1995; 63(5): 1617–1623.
14. Freytag LC, Clements JD. Bacterial toxins as mucosal adjuvants. Curr Top Microbiol Immunol 1999; 236:215–236.

15. Gluck R, Mischler R, Durrer P, Furer E, Lang AB, Herzog C, Cryz SJ Jr. Safety and immunogenicity of intranasally administered inactivated trivalent virosome-formulated influenza vaccine containing Escherichia coli heat-labile toxin as a mucosal adjuvant. J Infect Dis 2000; 181(3): 1129–1132.
16. Michetti P, Kreiss C, Kotloff KL, Porta N, Blanco JL, Bachmann D, Herranz M, Saldinger PF, Corthesy-Theulaz I, Losonsky G, Nichols R. Oral immunization with urease and *Escherichia coli* heat-labile enterotoxin is safe and immunogenic in Helicobacter pylori-infected adults . Gastroenterology 1999; 116(4):804–812.
17. Snider DP. The mucosal adjuvant activities of ADP-ribosylating bacterial enterotoxins. Crit Rev Immunol 1995; 15(3,4):317–348.
18. Weltzin R, Guy B, Thomas WD, Jr, Giannasca PJ, Monath TP. Parenteral adjuvant activities of *Escherichia coli* heat-labile toxin and its B subunit for immunization of mice against gastric Helicobacter pylori infection. Infect Immun 2000; 68(5):2775–2782.
19. Glenn GM, Kenney RT, Hammond SA, Ellingsworth LR. Transcutaneous immunization and immunostimulant strategies. In: Barth SE, ed. Immunology and Allergy Clinics of North America: Vaccines in the 21st Century. Philadelphia, PA: W.B. Saunders Company, 2003:787–813.
20. Glenn GM, Taylor DN, Li X, Frankel S, Montemarano A, Alving CR. Transcutaneous immunization: a human vaccine delivery strategy using a patch. Nat Med 2000; 6(12):1403–1406.
21. Hammond SA, Tsonis C, Sellins K, Porta N, Blanco JL, Bachmann D, Herranz M, Saldinger PF, Corthesy-Theulaz I, Losonsky G, Nichols R. Transcutaneous immunization of domestic animals: opportunities and challenges. Adv Drug Delivery Rev 2000; 43:45–55.
22. Yu J, Cassels F, Scharton-Kersten T, Hammond SA, Hartman A, Angor E, Corthesy B, Alving C, Glenn G. Transcutaneous immunization using colonization factor and heat labile enterotoxin induces correlates of protective immunity for enterotoxigenic *Escherichia coli*. Infect Immun 2002; 70(3):1056–1068.
23. Roberts MS, Walker M. Water, the Most Natural Penetration Enhancer. New York: Marcel Dekker, 1993.
24. Glenn GM, Alving CR, (inventors); Use of penetration enhancers and barrier disruption agents to enhance the transcutaneous immune response induced by ADP-ribosylating exotoxin. 1999.
25. Glenn GM, Kenney RT, Ellingsworth LR, Frech SA, Hammond SA, Zoeteweij JP. Transcutaneous immunization and immunostimulant strategies: capitalizing on the immunocompetence of the skin. Expert Rev Vaccines 2003; 2(2):253–267.
26. Guebre-Xabier M, Hammond SA, Ellingsworth LR, Glenn GM. Immunostimulant patch enhances immune responses to influenza vaccine in aged mice. J Virol 2004; 78(14):7610–7618.
27. Mikszta JA, Alarcon JB, Brittingham JM, Sutter DE, Pettis RJ, Harvey NG. Improved genetic immunization via micromechanical disruption of skin-barrier function and targeted epidermal delivery. Nat Med 2002; 8(4):415–419.
28. Pilling AM, Harman RM, Jones SA, McCormack NA, Lavender D, Haworth R. The assessment of local tolerance, acute toxicity, and DNA biodistribution following particle-mediated delivery of a DNA vaccine to minipigs. Toxicol Pathol 2002; 30(3):298–305.
29. Guebre-Xabier M, Hammond SA, Epperson DE, Yu J, Ellingsworth L, Glenn GM. Immunostimulant patch containing heat labile enterotoxin from *E. coli* enhances immune responses to injected influenza vaccine through activation of skin dendritic cells. J Virol 2003; 77(9):5218–5225.
30. Belyakov IM, Hammond SA, Ahlers JD, Glenn GM, Berzofsky JA. Transcutaneous immunization induces mucosal CTLs and protective immunity by migration of primed skin dendritic cells. J Clin Invest 2004; 113(7):998–1007.
31. Enioutina EY, Visic D, Daynes RA. The induction of systemic and mucosal immune responses to antigen-adjuvant compositions administered into the skin: alterations in

the migratory properties of dendritic cells appears to be important for stimulating mucosal immunity. Vaccine 2000; 18(24):2753–2767.
32. Oh YK, Kim JP, Hwang TS, Ko JJ, Kim JM, Yang JS, Kim CK. Nasal absorption and biodistribution of plasmid DNA: an alternative route of DNA vaccine delivery. Vaccine 2001; 19(31):4519–4525.
33. Zurbriggen R, Metcalfe IC, Gluck R, Viret JF, Moser C. Nonclinical safety evaluation of Escherichia coli heat-labile toxin mucosal adjuvant as a component of a nasal influenza vaccine. Expert Rev Vaccines 2003; 2(2):295–304.
34. Glenn GM, Scharton-Kersten T, Vassell R, Matyas GR, Alving CR. Transcutaneous immunization with bacterial ADP-ribosylating exotoxins as antigens and adjuvants. Infect Immun l999; 67(3):1100–1106.
35. Uren RF, Howman-Giles R, Thompson JF. Patterns of lymphatic drainage from the skin in patients with melanoma. J Nucl Med 2003; 44(4):570–582.
36. El-Ghorr AA, Williams RM, Heap C, Norval M. Transcutaneous immunisation with herpes simplex virus stimulates immunity in mice. FEMS Immunol Med Microbiol 2000; 29(4):255–261.
37. Godefroy S, Goestch L, Plotnicky-Gilquin H, Nguyen TN, Schmitt D, Staquet MJ, Corvaia N. Immunization onto shaved skin with a bacterial enterotoxin adjuvant protects mice against Respiratory Syncytial Virus (RSV). Vaccine 2003; 21(15):1665–1671.
38. Gockel CM, Bao S, Beagley KW. Transcutaneous immunization induces mucosal and systemic immunity: a potent method for targeting immunity to the female reproductive tract. Mol Immunol 2000; 37(9):537–544.
39. Beignon AS, Briand JP, Rappuoli R, Muller S, Partidos CD. The LTR72 mutant of heat-labile enterotoxin of *Escherichia coli* enhances the ability of peptide antigens to elicit CD4(+) T cells and secrete gamma Interferon after coapplication onto bare skin. Infect Immun 2002; 70(6):3012–3019.
40. Hammond SA, Walwender D, Alving CR, Glenn GM. Transcutaneous immunization: T-cell responses and boosting of existing immunity. Vaccine 2001; 19:2701–2707.
41. Porgador A, Staats HF, Faiola B, Gilboa E, Palker TJ. Intranasal immunization with CTL epitope peptides from HIV-1 or ovalbumia and the mucosal adjuvant cholera toxin induces peptide-specific CTLs and protection against tumor development in vivo. J Immunol 1997; 158(2):834–841.
42. Neidleman JA, Ott G, O'Hagan D. Mutant heat-labile enterotoxins as adjuvants for CTL induction. In: O'Hagan D, ed. Vaccine Adjuvants: Preparation Methods and Research Protocols. Totowa, NJ: Humana Press, 2000:327–336.
43. Seo N, Tokura Y, Nishijima T, Hashizume H, Furukawa F, Takigawa M. Percutaneous peptide immunization via corneum barrier-disrupted murine skin for experimental tumor immunoprophylaxis. Proc Natl Acad Sci USA 2000; 97(1):371–376.
44. Glenn GM, Kenney RT. Transcutaneous immunization. In: Levine MM, Kaper JB, Rappuoli R, Liu M, Good M, eds. New Generation Vaccines. New York: Marcel Dekker, 2004.
45. Tierney R, Beignon AS, Rappuoli R, Muller S, Sesardic D, Partidos CD. Transcutaneous immunization with tetanus toxoid and mutants of *Escherichia coli* heat-labile enterotoxin as adjuvants elicits strong protective antibody responses. J Infect Dis 2003; 188(5): 753–758.
46. Kotloff KL, Sztein MB, Wasserman SS, Losonsky GA, DiLorenzo SC, Walker RI. Safety and immunogenicity of oral inactivated whole-cell Helicobacter pylori vaccine with adjuvant among volunteers with or without subclinical infection. Infect Immun 2001; 69(6):3581–3590.
47. Matriano JA, Cormier M, Johnson J, Young WA, Buttery M, Nyam K, Daddona PE. Macroflux microprojection array patch technology: a new and efficient approach for intracutaneous immunization. Pharm Res 2002; 19(1):63–70.
48. Berry LJ, Hickey DK, Skelding KA, Bao S, Rendina AM, Hansbro PM, Gockel CM, Beagley KW. Transcutaneous immunization with combined cholera toxin and CpG

adjuvant protects against Chlamydia muridarum genital tract infection. Infect Immun 2004; 72(2):1019–1028.
49. Hammond SA, Guebra-Xabier M, Yu J, Glenn GM. Transcutaneous immunization: an emerging route of immunization and potent immunostimulation strategy. Crit Rev Ther Drug Carrier Sys 2001; 18(5):503–526.
50. Matyas GR, Friedlander AM, Glenn GM, Little S, Yu J, Alving CR. Needle-free skin patch vaccination method for anthrax. Infect Immun 2004; 72(2):1181–1183.
51. Wolf M, deHann LA, Cassels FJ, Willshaw GA, Warren R, Boedeker EC, Gaastra W. The CS6 colonization factor of human enterotoxigenic *Escherichia coli* contains two heterologous major subunits. FEMS Microbiol Lett 1997; 148(1):35–42.
52. Levine MM, Ristaino P, Sack RB, Kaper JB, Orskov F, Orskov I. Colonization factor antigens I and II and type 1 somatic pili in enterotoxigenic *Escherichia coli*: relation to enterotoxin type. Infect Immun 1983; 39(2):889–897.
53. Wolf M, Hall E, Taylor D, Coster T, Trespalacios F, Cassels F, deLorimier A, McQueen C, Use of the human challenge model to characterize the immune response to the colonization factors of enterotoxigenic *Escherichia coli* (ETEC). In: The 35th US-Japan Cholera and Other Bacterial Enteric Infections Joint Panel Meeting, December 3–5,1999; Baltimore, MD.
54. Grove GL, Grove MJ, Zerweck C, Pierce E. Computerized evaporimetry using the DermaLab® TEWL probe. Skin Res Technol 1999; 5(1):9–13.
55. Grove GL, Grove MJ, Zerweck C, Pierce E. Comparative metrology of the evaporimeter and the DermaLab® TEWL probe. Skin Res Technol 1999; 5:1–8.
56. Pinnagoda J, Tupker RA, Agner T, Serup J. Guidelines for transepidermal water loss (TEWL) measurement. A report from the standardization group of the European society of contact dermatitis. Contact Dermatitis 1990; 22(3):164–178.

57

Topical Vaccination of DNA Antigens: Topical Delivery of DNA Antigens

Howard I. Maibach
Department of Dermatology, School of Medicine, University of California, San Francisco, California, U.S.A.

Myeong Jun Choi
Charmzone Research and Development Center, 1720-1 Taejang 2-dong, Wonju, Kangwon-do, Korea

I. INTRODUCTION

Genetic immunization using naked plasmid DNA (pDNA) has gained considerable interest since demonstration of humoral and cellular immune response (1,2). The potential advantages of DNA vaccines over conventional vaccines include: (1) high stability of pDNA, (2) low manufacturing costs, (3) lack of infection risk associated with attenuated viral vaccines, (4) capacity to target multiple antigens on one plasmid, and (5) ability to elicit both humoral and cellular immune responses. Furthermore, DNA immunization has been effective in eliciting an immune response with various administration routes such as intramuscular (IM), intradermal (ID), intraperitoneal, intravenous, oral, intranasal (IN), ocular, and transdermal/topical administrtation (3). Until recently, i.m. injection was the primary route of administration for DNA vaccines. However, this method may be traumatic, especially in infants and painful and requires trained staff. Hence, much attention has been focused on pDNA vaccines, especially for topical DNA vaccination. In addition to common advantages of DNA vaccines (4,5), topical DNA vaccines can elicit mucosal immune response in vivo. Furthermore, topical DNA vaccines have the advantages of simplicity, accessibility, painlessness, and economy. But the immune responses elicited are relatively low and weak.

Despite major research and development efforts in topical systems and the many advantages of the topical vaccination, low stratum corneum (SC) permeability remains a major problem that limits their usefulness. To improve permeability, chemical and physical approaches have been examined. Different methods have been evaluated to deliver genes: liposomes (6), direct injection of naked DNA (7), gene guns (8), microseeding or puncture (9), viral systems (10,11), electroporation after i.d. injection (12,13), and micromechanical disruption methods (14,15).

Efficient delivery methods play a major role in developing DNA vaccines and gene therapy against viral diseases and cancers.

This paper reviews these methods of DNA and summarizes recent topical DNA vaccine data.

II. SKIN BARRIER AND PLASMID DNA PENETRATION

Why is skin a major target for genetic vaccination? The skin, an active immune surveillance site, is rich in potent antigen presenting dendritic cells (DCs) such as Langerhan's cells (LCs) in the epidermis (16). The LCs cells play a key role in the immune response to antigenic materials. Skin accessibility makes it an easy target for vaccination.

Many researchers thought highly charged large molecules such as pDNA could not penetrate the intact SC layer and topical DNA delivery could not elicit the immune responses in vivo, as the intracellular lipid domain of SC acts as a major barrier system in the skin to penetrate charged and large macromolecules. Unexpected results were detected when pDNA was applied topically (1,17,18). Currently, many believe that hair follicles may provide a mechanism for pDNA to access viable skin or immune cells. Fan et al. (17) demonstrated using hairless mice that the presence of normal hair follicles was required to elicit immune responses to expressed antigen after topical application. Wu et al. (19), investigating the effect of follicular structure on the gene expression using mouse model, reported C57 BL/6 mice expressed a mean value of 57.0 ± 10.8 pg human interferon-$\alpha 2/cm^2$ while the hairless mice expressed a mean value of 15.4 ± 2.2 pg human interferon-$\alpha 2/cm^2$ of treated skin. This result indicated the level of gene expression that could be achieved with normal follicular structure was higher than that observed in the abnormal follicles. Raghavachari and Fahl (20) compared the ability of vehicles to deliver pDNA to skin cells composing both the epidermis as well as hair follicles or the pilosebaceous unit in the skin of neonate, six-day-old rat pups. From these results, hair follicles appear to play a major role for penetrated naked pDNA (20,21). However, others could not obtain high level of gene expression and immune response without stripping (15,22,23). Hence, the mechanism of DNA delivery into skin requires elaboration.

III. STRIPPING VS. IMMUNE RESPONSE

Tape stripping is a commonly used in order to disrupt the epidermal barrier and to enhance the delivery of macromolecules (24,25). This technique has been used to disrupt the skin barrier before topical peptide and DNA vaccination (23,26). Transfer gene activity depends on the number of strippings. Yu et al. (27) found that transfer gene expression was higher in the skin samples stripped five times prior to DNA application compared with those stripped three times prior to DNA application.

Fan et al. (17) reported that topical DNA vaccine twice (without stripping) on the skin induced antibody response to hepatitis B surface antigen and enhanced the lymphoproliferation response. However, others could not obtain high levels of immune response using the same method (15,22,23).

Comparing the immune response with and without stripping, topical application without stripping the skin induced weak antibody response or weak DTH response and this immune response is disappeared after three months. In contrast, topical application of DNA vaccine with stripping induced strong immune responses,

Table 1 Effect of Stripping and Liposomes on the Topical Genetic Immunization

Immune groups	DNA amounts (μg)	Antibody titers (mean reciprocal log 2 ± SD)[a] Plasma IgG after 20 days	After 3 months	Fecal IgA after 3 months
IM	20	9.6 ± 0.3	7.1 ± 0.5	2.3 ± 0.3
Intact skin	100	7.7 ± 1.9	5.6 ± 1.0	NT
Stripping[b]	20	11.8 ± 0.7	8.0 ± 1.0	6.8 ± 0.8
Stripping	100	12.5 ± 1.4	8.2 ± 0.8	7.3 ± 1.2
Liposomes	20	12.3 ± 1.4	NT	9.2 ± 1.4
Liposomes+-mannan	20	13.0 ± 2.4	NT	9.0 ± 1.9
No immunization	—	2.5 ± 0.2	1.7 ± 0.6	2.2 ± 0.7

[a]On days 0, 7, and 14, BALB/c mice were immunized intramuscularly and topically.
[b]Fast-acting adhesive glue (Alon Alfa®) was smeared on a glass slide to cover approximately 0.5 cm near the rump and the slide was struk to the back of the mouse. After an interval of 20 to 30 seconds, the slide was ripped off.
Abbreviations: IM, intramuscular; NT, not tested.

and remained detectable after three months with all immunization methods. There was a significant difference between the results of topical application with and without stripping. Table 1 shows the effect of stripping on the topical DNA vaccination. In case of stripping, the level of antibody production induced by topical vaccination was similar to that obtained by i.m. injection. In addition to serum IgG, fecal IgA (mucosal immunity) was also observed on topical application of DNA. This result was consistent with the finding of Glenn et al. (28,29) but in contrast to that of Liu et al. (22).

Topical DNA vaccine also induced a substantial level of antigen-specific cytotoxic T lymphocytes (CTL) response in stripped skin [37% at an effector/targetor (E/T) ratio of 80:1]. The DNA vaccination without stripping did not result in a sufficient CTL reponses [12.8% at an E/T ratio of 80:1]. Hence, stripping facilitated the transfer of DNA vaccine through skin and the uptake of plasmids by antigen-processing cells, such as DCs or LCs. Thus, topical application of DNA vaccine resulted in successful induction of humoral, cellular, and mucosal immune response in mice. This method is an efficient route of DNA administration and can be used immunization against viral and bacterial diseases.

Human skin has 7 to 10 keratinocytic layers on the epidermis, whereas mouse skin has only 2 to 4 layers. It would be more difficult for DNA plasmid to be taken up by DCs of LCs without stripping in man. Although stripping would not be the most efficient way to obtain the immune response in clinical use, it is of great importance to induce protective effect of topical DNA vaccination at stripped skin. Modification of this method of SC removal, such as combinations with skin enhancers and vehicles systems, may be more acceptable.

IV. ELECTROPORATION

Electroporarion is a phenonmenon in which lipid bilayers exposed to high intensity electric field pulses are temporarily destabilized and permeablized (30,31). The most common use of high voltage pulsing is the introducing of DNA into isolated cells

and use for introducing oligonucleotides (ONs) into cells. This technique enhances the transdermal transport of moderate-sized molecules and macromolecules (32,33).

In vivo gene delivery by electroporation has been demonstrated to be efficient for introducing DNA into mouse skin (13,31). Gene delivery into skin by electroporation is attractive for several reasons. First, electroporation enhances the delivery nucleic acid in the SC and the viable skin. Second, skin electroporation is well tolerated. Third, the skin is particularly accessible. Finally, gene therapy or DNA vaccination represents possible applications.

Dujardin et al. (12) reported the pathway of pDNA transport, tissue viability, and DNA stability in skin. To determine whether pDNA penetrates into the keratinocytes, fluorescence-labeled plasmid was applied on the stripped skin (20 times with Scotch Crystal®) for 10 minutes with or without skin electroporation. Fluorescence-labeled pDNA was mainly localized around the keratinocytes. The pDNA delivered across partially stripped skin penetrated into keratinocytes. But, nuclear penetration of pDNA was not observed and the plasmid did not penetrate dermis. These results were inconsistent with ONs delivery that reached the nucleus within minutes after skin electroporation. Similar to ONs, the structural integrity of the plasmid was unaffected by electroporation, before contact with the skin. But, plasmid was slightly degraded after 10 minutes of skin contact. This result was consistent with the phosphodiester ON but in contrast to with modified ONs. Compared to passive diffusion, electroporation strongly enhanced DNA transfer into viable cells and increased the expression duration and intensity.

In addition, sonophoration (sonophoresis) can be used for delivering both DNA and protein based vaccine antigens transdermally. This technique uses ultrasound waves to disorganize SC lipids allowing the permeability of the skin to be increased (34). Membrane destabilizing devices such as electroporation and sonophoration offer great potential for DNA immunization in future.

V. MICROMECHANICAL DISRUPTION METHOD

Physical and chemical properties of the SC provide an effective barrier, preventing uptake of highly charged large molecules topically applied. Several device-based approaches have been developed to disrupt this barrier, including iontophoresis, sonophoresis, and electroporation. In addtion, Henry et al. (35) demonstrated that microfabricated microneedles approximately 150-μm long increased permeability of human skin. These arrays of microneedles create conduits across the SC potentially allowing transport of DNA and protein into the epidermis. Furthermore, McAllister et al. (14) developed micro-scale projections that penetrate only the outermost layers of skin using microelectrical mechanical system (MEMS)-based fabrication. With this, Mikszta et al. (15) improved genetic immunization via microfabricated silicon projections, termed mictoenhancer arrays (MEAs), to mechanically disrupt the skin barrier and targeted epidermal delivery of genetic vaccines. In man, these devices effectively disrupted the skin barrier, allowing direct access to the epidermis with minimal associated discomfort and skin irritation. Also, MEA-based delivery enabled topical gene transfer resulting in reporter gene activity up to 2800-fold above topical controls in a mouse model and efficiency of gene expression was superior to these of i.m. and i.d. injection.

Antibody titers in the MEA-treated group were less variable and significantly greater after the second and third immunization than the corresponding titers

induced via i.m. and i.d. injection. Thus, MEA-based delivery enabled 100% seroconversion following two immunizations, compared to only 40% via i.m. and 50% by i.d. injection. In contrast, control topical delivery was not ineffective. The MEA-based delivery enabled topical gene transfer and immunization with naked pDNA, stimulating humoral and cellular immune response of comparable or greater magnitude than via i.m. and i.d. injection, and reduced the number of immunization required for full seroconversion.

The MEA devices have several advantages; they mechanically disrupt the skin barrier and enable topical delivery without need for compels and potentially unsafe formulations. The MEA-based delivery is minimally invasive in man is simple to use as a needle but is safe as micro-projections do not penetrate dermal vessels. This technology is likely to be applicable to targeted therapy of epidermal disorders and skin cancer.

VI. LIPOSOME AND LIPOSOMAL CREAM FORMULATION

Topical DNA administration can elicit immune response in vivo with or without stripped skin. The immune response induced by DNA itself was too weak to induce protective effect against the diseases. Therefore, efficient delivery vehicles are required to induce strong immune responses. Among delivery vehicles, liposomes systems have been widely used to induce immune response in vivo. Liposomes have been used to deliver various protein antigens for immunization studies (36–38). In addition to protein delivery for immunization, pDNA has also been delivered using liposomes.

As compared with DNA vaccine plus cationic liposomes, only topical DNA vaccine resulted in weaker antibody response. The DNA vaccine plus cationic liposome induced higher levels of antibody production than DNA vaccine alone. This immune response was increased by addition of mannan into liposomes (23,39). As shown in Table 1, DNA vaccination with liposomes can induce strong humoral immune responses.

In addition to humoral immune response, liposomes increased the cellular immune response when compared with pDNA vaccine alone. The DNA vaccine by the topical route induced a substantial level of the CTL response at the stripped skin with influenza and HIV DNA antigen (Table 2). The DNA vaccination without stripping skin did not result in a CTL response. The DNA vaccination with mannan-coated liposomes induced high levels of CTL responses. Thus, DNA vaccination with liposomes can induce strong humoral and cellular immune response in vivo.

Topical delivery of DNA using liposome formulations included conventional liposomes, stealth liposomes coating with polyethylene glycol, targeted liposomes containing antibodies, ligands, and polysaccharides, cationic and nonionic liposomes. Raghavachari and Fahl (20) reported that nonionic liposomes were the most efficient for transdermal system; rat pups treated with nonionic liposome formulations showed the highest reporter gene expression (57,000 relative luciferase activity (RLA)/mg protein) 24 hours following liposomes application, followed by nonionic/cationic liposomes (32,000 RLA/mg protein) and phospholipid formulations [8900 RLA/mg protein]. Suprisingly, the traditional phospholipid-based liposome carriers were not effective as delivery vehicles for luciferase or galactosidase DNA when compared to nonionic liposomes. Jayaraman et al. (40) explained the high efficiency of nonionic liposomes as a facilitator of drug delivery to the unique lipid composition. They suggest that polyoxyethylene and glyceryl dilaurate act as penetration enhancers.

Table 2 Effect of Liposome Formulation on the Cytotoxic T Lymphocyte (CTL) Response

Immunization	Specific lysis (%) at effect: target ratio of 80:1	
	Influenza[a]	HIV[b]
Intact skin	12.7	18.5
Stripped skin[c]	37	34
Liposomes[d]	57.4	NT

[a]The CTL response of BALB/c mice against influenza M peptide antigen. Lymphoid cells from each immunized group were restimulated for five days using influenza M peptide-pulsed syngeneic spleen cells. The peptide-pulsed p815 cells were used as targets.

[b]The CTL response of BALB/c mice to HIV-1 IIIB peptide antigen. Lymphoid cell from each immunized group were restimulated for five days using HIV-1 IIIB V3 peptide-pulsed syngeneic spleen cells. The peptide-pulsed p815 cells were used as targets.

[c]Fast-acting adhesive glue (Alon Alfa^R) was smeared on a glass slide to cover approximately 0.5 cm^2 near the rump and the slide was struk to the back of the mouse. After an interval of 20 to 30 seconds, the slide was ripped off.

[d]The composition was (dimethylaminoethane)-carbamoyl cholesterol (DC-chol), dioleoyl phosphatidylethanolamine (DOPE), and mannan-cholestrol.

Furthermore, liposomes system can be also used with skin enhancer chemicals such as dimethylsulfoxide (DMSO), oleic acid and Azone® for topical DNA vaccination. The DMSO increased the DNA skin delivery with liposome formulations (41). Hence, liposomal cream or lotion containing of skin enhancers is well suited for the use in the delivery of DNA vaccines.

VII. MICROEMULSION DELIVERY SYSTEM

Cui and Mumper (4) first reported chitosan-based nanoparticles for topical genetic immunization; IgG titer in plasma was up to 32-fold greater when mice were immunized with pDNA coated on chitosan oligomer/carboxyl methylcellulose (CMC) nanoparticles (3:1 w/w ratio) as compared to those mice immunized with naked pDNA alone. Also, IgG titers of mice immunized with chitosan oligomer/CMC nanoparticles tended to be less variable than those immunized with naked pDNA. They also reported the genetic immunization using nanoparticles engineered from microemulsion precursors technique (42,43). The effects of incorporation of dioleoyl phosphatidylethanolamine (DOPE) into the nanoparticles and the mannan coating on the nanoparticles on the overall immune responses are shown in Table 3. The pDNA-coated nanoparticles led to over a 6-fold enhancement in total antigen-specific IgG titer over naked pDNA. Mice immunized with pDNA-nanoparticles with both DOPE and the mannan ligand resulted in an approximately 16-fold increase in antigen-specific IgG titer over naked pDNA. In contrast, topical immunization using β-galactosidase protein adjuvanted with Alum resulted in relatively low levels of antigen-specific IgG titer.

Microemulsion precursor based nanoparticles have several advantages because (1) all ingredients are potentially biocompatible; (2) the natural engineering process can easily be adapted to include many excipients such as adjuvant and ligands; (3) well-defined and uniform solid nanoparticles may be reproducibly made without the use of expensive devices; (4) no organic solvents are used during manufacturing;

Table 3 Antigen-Specific IgG Titer in Serum 28 Days After Topical Application of Formulation to Mice

Groups	Number responsed/ number tested[a]	Total mean ± SD	Mean ± SD[b]
pDNA	3/5	196 ± 169	320
b-Gal+Alum	5/5	256 ± 87	
Nanoparticles (NPs)	3/5	1284 ± 1275	2133 ± 739
NPs-Man	3/5	2564 ± 2555	4266 ± 1478
NPs-Man+DOPE	5/5	3072 ± 1144	

[a]The number of mice that tested positive/total number of mice vaccinated are shown after 28 days post-vaccination.

[b]Mean value is calcuated from positive three samples. A total of 100 μL of each formulation (5 μg of pDNA or 10 μg of β-galactosidase) were applied to anesthetized Balb/C mice on days 0, 7, and 14 to shaved skin.

Abbreviations: pDNA, naked plasmis DNA; β-gal+Alum, 10 μg of β-galactosidase antigen adjuvanted with 15 μg Alum; NPs, pDNA-coated nanoparticles; NPs-Man mannan-coated pDNA-nanoparticles; NPs-Man+ DOPE, mannan-coated pDNA-nanoparticles with dioleoyl phosphtidylethanolamine (5% W/W).

(5) high entrapment efficiencies are achievable; (6) the formed solid nanoparticles may have superior in vivo stability. Thus, microemulsion nanoparticles offers great potential for topical DNA vaccination.

VIII. Th1 AND Th2 RESPONSE OF TOPICAL DNA VACCINE

The degree of immunogenicity of DNA vaccine depends on the route of administration in mice. The i.m. immunization induced a potent Th1-type immune response (44) whereas administration with a subcutaneous gene gun and intranasal immunization induced a strong Th2 response (45–48). The topical administration of DNA elicited the Th1 and Th2 cytokine responses, but predominantly the Th2 response (Table 4). The increase in production of IL-4 has been greater than that of INF-γ after topical administration when compared with i.m. immunization. When pDNA was complexed with liposomes and nanoparticles, the immune response was shifted. The immune responses using mannan-coated liposomes were shifted to Th1 responses as evidenced by the dominant production of IgG2a and INF-γ. In addition, mannan coated liposomes led to significantly greater CTL responses compared to uncoated liposomes (23,49). Like liposomes, mannan-coated nanoparticles were also similar to the immune response (Table 5). Cui and Mumper (42) reported that immunization with pDNA-coated nanoparticles resulted in a strong Th1-based cytokine release as demonstrated by the significant increase (up to 300%) of Th1-type cytokines IL-2 and INF-γ. Mannan-coated liposomes and nanoparticles activate Th1-type immune responses and induce strong immune responses. The adjuvant effect of mannan-coated vehicles may relate to human and mouse DCs in the skin has numerous mannose receptors, and this receptor has been exploited to deliver antigens resulting in more robust Th1 and CTL responses (23,49,50).

Table 4 Effect of Stripping and Liposomes on the Th1 and Th2 Cytokine Release

	Amount of cytokines (Influenza)[a]		Amount of cytokines (HIV)[b]	
Immunogens	INF-γ (pg/mL)	IL-4 (pg/mL)	INF-γ (ng/mL)	IL-4 (pg/mL)
IM	13.1 ± 1.9	8.3 ± 1.4	6.0 ± 1.7	15.0 ± 5.3
Intact skin	5.2 ± 2.3	8.7 ± 1.2	—	—
Stripping	6.9 ± 2.1	22.6 ± 2.3	4.7 ± 2.0	51.0 ± 7.0
Liposomes	11.9 ± 2.7	20.8 ± 2.4	—	—
Liposomes +mannan	19.7 ± 3.6	15.0 ± 0.3	—	—
No immunization	2.3 ± 1.0	4.2 ± 0.9	0.6 ± 0.3	10 ± 7

[a]Balb/c mice were inoculated three times with 30 μg of DNA vaccine alone or liposomes complex by topical and intramuscular application. The regional lymph node cells were harvested from the mice and cultured with M1 peptide (KAVKLYRKLKRE) for 24 hours. Cytokine levels were assayed using commercial ELISA kits. The cytokine levels of each group represented the mean ± SE from six to eight mice.

[b]Balb/c mice were inoculated IM once with 10 μg of DNA vaccine or by topical application three times with 30 μg of DNA vaccine. Seven days after the final immunization, spleen cells were harvested from the mice and cultured with HIV-1 IIIB peptide (RGPGRAFVTI). Cytokine levels in the culture supernatants were assayed using commercial ELISA kits. The levels of each group represented the mean ± SE from four to six mice.

IX. MECHANISM OF TOPICAL DNA VACCINES

The mechanism of topical application to the skin is not fully understood. Fan et al. (17) and others (20,21) reported that naked DNA (pDNA) enters the human body through the hair follicles.

To confirm the importance of LCs, Robinson et al. (51) reported that strong immune response induced by i.d. injection of DNA vaccine indicated the importance of LCs in the epidermis. In addition, Ishii et al. (39) investigated the effect of anti-CD11c antibody on skin-mediated immune responses. The immune response induced by topical DNA vaccination was significantly inhibited by the injection of anti-CD-11c monoclonal antibody or anti-I-Ad/I-Ed monoclonal antibody. Hence, this result indicates that immune response induced by topical vaccination to the skin

Table 5 In Vitro Cytokine Release from Isolated Splenocytes

	Th1 type		Th2 type
Immunized group	IL-2 (pg/mL)	INF-g (pg/mL)	IL-4 (pg/mL)
Naive	546 ± 54	570 ± 28	< 1
Naked pDNA	1761 ± 164	19,971 ±393	54.4 ± 4.5
β-Gal+Alum	171 ± 13	678 ± 80	164.4 ± 14.5
Nanoparticles (NPs)	2,300 ± 167	15,098 ± 360	8.6 ± 2.4
NPs-Mannan	4,540 ± 346	24,902 ± 1,619	25.4 ± 5.5

Note: In vitro cytokine release from isolated splenocytes (5×10^6 cells) exposed to β-galactosidase protein for 60 hours. Mice were immunized with 5 μg DNA or 10 μg β-Gal (with 15 μg Alum) on days 0, 7, and 14 by subcutaneous injection. On day 28, the spleen were removed and pooled for each group. Isolated splenocytes (5×10^6 cells) with three replicates were stimulated with β-galactosidase protein (3.3 μg/well) for 60 hours at 37°C. Cytokine release was assayed using commercial ELISA kit (Endogen).

cell is mediated by the I-A/I-E and/or CD11c positive cells, presumably LCs in the epidermis and dermis.

When the skin is damaged physically, chemically, and biologically, keratinocytes and LCs become activiated. Nishijima et al. (52) reported that disruption of the skin barrier result in epidermal LCs activation as vigorous antigen presenters for T-helper cells. Furthermore, Liu et al. (22) reported that the stripped skin sections showed more S-100 protein staining and neutrophil-like cell infiltration was greater and more frequently observed. The S-100 protein is characteristic of mature DCs (LCs) cells that are effective in antigen presentation. From these results, epidermal LCs play an important role in the activation of immune response on both hair follicles and stripped skin.

X. TOPICAL DNA VACCINE EFFICACY

Many researchers confirmed the protective effect of influenza DNA vaccine administered to mice i.m. and i.n. injection (53–56). Until recently, i.m. and i.n. injection were the primary route of administration for DNA vaccines.

Watabe et al. (23) investigated the efficacy of topical DNA vaccine expressed the marix (M) gene of the influenza virus using mouse model. They topically applied pDNA onto the stripped skin on days 0, 7, and 14. After the third immunization, mice were challenged with $5LD_{50}$ of influenza virus. Thirteen of 20 mice (65%) survived when they were topically immunized with pDNA expressed the M gene. In the case of i.m. injection as a positive control, 71% of mice were protected. When mice were immunized with inactivated virus topically, only 18% of mice were protected. As in antibody and CTL response, pDNA complexed with liposomes increased the protection (75%). From the results, the topical administration of DNA vaccine induces a protective immunity against influenza challenge. In the case of melanoma tumor model, B16 tumor cells were virtually completely rejected after topical peptide immunization via a disrupted barrier (stripping) (26,57).

In addition to topical skin delivery, Daheshia et al. (58) reported that local administration of eyedrops containing gB DNA developed herpes simplex virus (HSV)-specific humoral and cellular immune responses and protected immunized animals from a lethal HSV infection. Inoue et al. (59) reported a new pDNA delivery method that was delivered topically to the conjunctival sac. As in the eyedrop method, this also elicited both humoral and cellular immune response in vivo and totally inhibited corneal stromal keratitis. Hence, topical DNA vaccination method is effective and can be used to prevent or protect viral and bacterial diseases. Topical application method of vaccination may have a promising future in clinical medicine.

XI. CONCLUSIONS

Genetic immunization using naked pDNA with and without vehicles has gained considerable interest since the first demonstration of both broad humoral and cellular immune response in vivo. Topical delivery of formulated pDNA in the formulations of patch, cream, lotion or gel can provide many advantages in terms of cost and patient compliance. Topical DNA delivery with physical methods such as stripping and devices also offer great potential for DNA vaccination in future. Currently, many DNA vaccines are undergoing clinical trials. Liposomes and nanoparticles containing of skin enhancers are well suited to use in the delivery of DNA antigens in terms of cost, efficacy, compliance, and comfort. These systems appear to be likely direction for future development.

REFERENCES

1. Tang D, DeVit M, Johnston SA. Genetic immunization is a simple method for eliciting an immune response. Nature 1992; 356:152–154.
2. Ulmer JB, Sadoff JC, Liu MA. DNA vaccines. Curr Opin Immunol 1996; 8:531–536.
3. Babiuk S, Baca-Estrada M, Babiuk LA, Ewen C, Foldvari M. Cutaneous vaccination: the skin as an immunologically active tissue and the challenge of antigen delivery. J Control Release 2000; 66:199–214.
4. Cui Z, Mumper RJ. Chitosan-based nanoparticles for topical genetic immunization. J Control Release 2001; 75:409–419.
5. Liu MA. The immunologist's grail: vaccines that generate cellular immunity. Proc Natl Acad Sci USA 1997; 94:10496–10498.
6. Alexander MY, Akhurst RJ. Liposome-mediated gene transfer and expression via the skin. Hum Mol Genet 1995; 4:2279–2285.
7. Hengge UR, Chan EF, Foster RA, Walker PS, Vogel JC. Cytokine gene expression in epidermis with biological effects following injection of naked DNA. Nat Genet 1995; 10:161–166.
8. Yang NS, Burkholder J, Roberts B, Martinell B, McCabe D. In vivo and in vitro-gene transfer to mammalian somatic cells by particle bombardment. Proc Natl Acad Sci USA 1990; 87:9568–9572.
9. Ciernik IF, Krayenbuhl BH, Carbone DP. Puncture-mediated gene transfer to the skin. Hum Gene Ther 1996; 7:893–899.
10. Badiavas E, Mehta PP, Falanga V. Retrovirally mediated gene transfer in a skin equivalent model of chronic wounds. J Dermatol Sci 1996; 13:56–62.
11. Lu B, Federoff H, Wang Y, Goldsmith LA, Scott G. Topical application of viral vectors for epidermal gene transfer. J Invest Dermatol 1997; 108:803–808.
12. Dujardin N, Van Der Smissen P, Preat V. Topical gene transfer into skin using electroporation. Pharm Res 2001; 18:61–66.
13. Titomirov AV, Sukharev S, Kistanova E. In vivo electroporation and stable transformation of skin cells of newborn mice by plasmid DNA. Biochem Biophys Acta 1991; 1088:131–134.
14. McAllister DV, Allen MG, Prauznitz MR. Microfabricated microneedles for gene and drug delivery. Ann Rev Biomed Eng 2000; 2:289–313.
15. Mikszta JA, Alarcon JB, Brittingham JM, Sutter DE, Pettis RJ, Harvey NG. Improved genetic immunization via micromechanical disruption of skin-barrier function and targeted epidermal delivery. Nat Med 2002; 8:415–419.
16. Banchereau J, Steinman RM. Dendritic cells and the control of immunity. Nature 1998; 19:245–252.
17. Fan H, Lin Q, Morrisssey GM, Khavari PA. Immunization via hair follicles by topical application of naked DNA to normal skin. Nat Biotechnol 1999; 17:870–872.
18. Li L, Hoffman RM. The feasibility of targeted selective gene therapy of the hair follicle. Nat Med 1995; 1:705–706.
19. Wu H, Ramachandran C, Bielinska AU, Kingzett K, Sun R, Weiner ND, Roessler BJ. Topical transfection using plasmid DNA in water-in-oil nanoemulsion. Int J Pharm 2001; 221:23–34.
20. Raghavachari N, Fahl WE. Targeted gene delivery to skin cells in vivo: a comparative study of liposomes and polymers as delivery vehicles. J Pharm Sci 2002; 91:615–622.
21. Hofmann U, Tokura Y, Nishijima T, Takigawa M, Paus R. Hair cycle-dependent chamges in skin immune functions: antigen-associated depression of sensitization for contact hypersensitivity in mice. J Invest Dermatol 1996; 106:598–604.
22. Liu L-J, Watabe S, Yang J, Hamajima K, Ishii N, Hagiwara E, Onari K, Xin K-Q, Okuda K. Topical application of HIV DNA vaccine with cytokine-expression plasmids induces strong antigen-specific immune responses. Vaccine 2002; 20:42–48.

23. Watabe S, Xin K-Q, Ihata A, Liu L-J, Honsho A, Aoki I, Hamajima K, Wahren B, Okuda K. Protection against influenza virus challenge by topical application of influenza DNA vaccine. Vaccine 2001; 19:4434–4444.
24. Choi MJ, Zhai H, Maibach HI. Effect of tape stripping on percutaneous penetration and topical vaccination. Exogeneous Dermatol. 2003; 2:260–269.
25. Yang L, Mao-Qiang M, Taljebini M, Elias PM, Feingold KR. Topical stratum corneum lipids accelerate barrier repair after tape stripping, solvent treatment and some but not all types of detergent treatment. Br J Dermatol 1995; 133:679–685.
26. Seo N, Tokura Y, Nishijima T, Hashizume H, Furukawa F, Takigawa M. Percutaneous peptide immunization via corneum barrier-disrupted murine for experimental tumor immunoprophylaxis. Proc Natl Acad Sci USA 2000; 97:371–376.
27. Yu WH, Kashari-Sabet M, Liggit D, Moore D, Heath TD, Debs RJ. Topical gene delivery to murine skin. J Invest Dermatol 1999; 112:370–375.
28. Glenn GM, Scharton-Kersten T, Vassell R, Mallett CP, Hale TL, Alving CR. Cutting edge: transcutaneous immunization with cholera toxin protects mice against lethal mucosal toxin challenge. J Immunol 1998; 161:3211–3214.
29. Glenn GM, Taylor DN, Li X, Frankel S, Montemarano A, Alving CR. Transcutaneous immunization: a human vaccine delivery strategy using a patch. Nat Med 2000; 6: 1403–1406.
30. Weaver J. Electroporation theory. Concepts and mechanism. Methods Mol Biol 1995; 47:1–26.
31. Zhang L, Li L, Hoffmann GA, Hoffmann RM. Depth-targeted efficient gene delivery and expression in the skin by pulsed electric fields: an approach to gene therapy of skin aging and other diseases. Biochem Biophys Res Commun 1996; 220:633–636.
32. Prausnitz MR, Edelman ER, Gimm JA, Langer R, Weaver JC. Transdermal delivery of heparin by skin electroporation. Biotechnol 1995; 13:1205–1209.
33. Vanbever R, LeBoulange E, Preat V. Transdermal drug delivery of fentanyl by electroporation I. Influence of electrical factors.. Pharm Res 1996; 13:557–563.
34. Mitragotri S, Edwards DA, Blankschtein D, Langer R. A mechanistic study of ultrasonically enhanced transdrmal drug delivery. J Pharm Sci 1995; 84:697–706.
35. Henry S, McAllister DV, Allen MG, Prausnitz MR. Microfabricated microneedles: a novel approach to transdermal drug delivery. J Pharm Sci 1998; 87:922–925.
36. Chang JS, Choi MJ, Kim TY, Cho SY, Cheong HS. Immunogenicity of synthetic HIV-1 V3 loop peptides by MPL adjuvanted pH-sensitive liposomes. Vaccine 1999; 17:1540–1548.
37. Chang JS, Choi MJ, Cheong HS, Kim K. Development of Th1-mediated CD8+ effector T cells by vaccination with epitope peptides encapsulated in pH-sensitive lipoosmes. Vaccine 2001; 19:3608–3614.
38. Griffiths GD, Bailey SC, Hambrook JL, Keyte MP. Local and sytemic responses against ricin toxin promoted by toxoid or peptide vaccine alone or in liposomal formulations. Vaccine 1998; 16:530–535.
39. Ishii N, Sugita Y, Liu L-J, Watabe S, Toda S, Xin K-Q, Okuda K. Immunologic characterization of HIV-specific DNA vaccine. J Invest Dermatol 2001; 6:76–80.
40. Jayaraman SC, Ramachandran C, Weiner N. Topical delivery of erythromycin from various formulation: an in vivo hairless mouse study. J Pharm Sci 1996; 85:1082–1084.
41. Heckert RA, Elankumaran S, Oshop GL, Vakharia VN. A novel transcutaneous plasmid-dimethylsulfoxide delivery technique for avian nucleic acid immunization. Vet Immunol Immunopathol 2002; 89:67–81.
42. Cui Z, Mumper RJ. Genetic immunization using nanoparticles engineered from microemulsion precursors. Pharm Res 2002; 19:939–946.
43. Cui Z, Mumper RJ. Topical immunization using nanoengineered genetic vaccines. J Control Release 2002; 81:173–184.
44. Ulmer JB, Deck RR, Dewitt CM, Donnhly JI, Liu MA. Generation of MHC class I-restricted cytotoxic T lymphocytes by expression of a viral protein in muscle cell: antigen presentation by non-muscle cell. Immunology 1996; 89:59–67.

45. Donnelly JJ, Ulmer JB, Shiver JW, Liu MA. DNA vaccine. Ann Rev Immunol 1997; 15:617–648.
46. Okada E, Sasaki S, Ishii N, Aoki I, Yasuda T, Nishioka K, Fukushima J, Miyazaki J, Wabren B, Okuda K. Intranasal immunization of a DNA vaccine with IL-12 and granulocyte-macrophage-stimulating factor (GM-CSF) expressing plasmids in liposomes induces strong mucosal and cell-mediated immune response against HIV-1 antigens. J Immunol 1997; 159:3638–3647.
47. Sasaki S, Sumino K, Hamajima K, Fukushima J, Ishii N, Kamamoto S, Mohri H, Kensil CR, Okuda K. Induction of systemic and mucosal immune responses to human immunodeficiency virus type-1 by a DNA vaccine formulated with QS-21 saponin adjuvant via intramuscular and intranasal routes. J Virol 1998; 72:4931–4939.
48. Xin K-Q, Hamajima K, Sasaki S, Honsho A, Tsuji T, Ishii N, Cao XR, Lu Y, Fukushima J, Shapshak P, Kawamoto S, Okuda K. Intranasal administration of human immunodeficiency virus type-1 (HIV-1) DNA vaccine with interleukin-2 expression plasmid enhance cell-mediated immunity HIV-1. Immunology 1998; 94:438–444.
49. Toda S, Ishii N, Okada E, Kusakake K-I, Arai H, Hamajima K, Gorai I, Nishioka K, Okuda K. HIV-1-specific cell-mediated immune response induced by DNA vaccination were enhanced by mannan-coated liposomes and inhibited by anti-interferon-gamma antibody. Immunology 1997; 92:111–117.
50. Tan MC, Mommas AM, Drijfhout JW, Jordens R, Onderwater JJ, Derwoerd D, Mulder AA, van der Heiden AN, Scheidegger D, Oomen LC, Ottenhoff TH, Tulp A, Neefjes JJ, Koning F. Mannose receptor-mediated uptake of antigens strongly enhances HLA class II-restricted antigen presentation by cultured dendritic cells. Eur J Immunol 1997; 27:2426–2435.
51. Robinson HL, Montefiori DC, Johnson RP, Manson KH, Kalish ML, Lifson JD, Rizvi TA, Lu S, Hu SL, Mazzar GP, Panicali DL, Herndon JG, Glickman R, Candido MA, Lydy SL, Wyand MS, McClure HM. Neutralizing antibody-independent containment of immunodeficiency virus challengers by DNA priming and recombinant pox virus booster immunization. Nat Med 1999; 5:526–534.
52. Nishijima T, Tokura Y, Imokawa G, Seo N, Furukawa F, Takigawa M. Altered permeability and disordered cutaneous immunoregulatory function in mice with acute barrier disruption. J Invest Dermatol 1997; 109:175–182.
53. Deck RR, DeWitt CM, Donnelly JJ, Liu MA, Ulmer JB. Characterization of humoral immune responses induced by an influenza hemagglutinin DNA vaccine. Vaccine 1997; 15:71–78.
54. Donnelly JJ, Friedman A, Martinez D, Montgomery DL, Shiver JW, Motzel SL, Ulmer JB, Liu MA. Preclinical efficacy of a prototype DNA vaccine: enhanced protection against antigenic drift in influenza virus. Nat Med 1995; 1:583–587.
55. Okuda K, Ihata A, Watabe S, Yamakawa J, Hamajima K, Yang J, Ishii N, Nakazawa M, Okuda K, Nakajima K, Xin K-Q. Protective immunity against influenza a virus induced by immunization with DNA plasmid containing influenza M gene. Vaccine 2001; 19:3681–3691.
56. Ulmer JB, Deck RR, DeWitt CM, Friedman A, Donnelly JJ, Liu MA. Protective immunity by intramuscular injection of low doses of influenza virus DNA vaccines. Vaccine 1994; 12:1541–1544.
57. Takigawa M, Tokura Y, Hashizume H, Yagi H, Seo N. Percutaneous peptide immunization via corneum barrier-disrupted murine for experimental tumor immunoprophylaxis. Ann NY Acad Sci 2001; 941:139–146.
58. Daheshia M, Kuklin N, Manickan Chun S, Rouse BT. Immune induction and modulation of plasmid DNA encoding antigens and cytokines. Vaccine 1998; 16:1103–1110.
59. Inoue T, Inoue Y, Hayashi K, Yoshida A, Nishida K, Shimomura Y, Fujisawa Y, Aono A, Tano Y. Topical administration of HSV gD-IL-2 DNA is highly protective against murine herpetic stromal keratitis. Cornea 2002; 21:106–110.

58

Topical Dermatological Vehicles: Engineering the Delivery System

C. G. Azzi, J. Zhang, C. H. Purdon, and Eric W. Smith
College of Pharmacy, University of South Carolina, Columbia, South Carolina, U.S.A.

Christian Surber
Institut für Spital-Pharmazie, Universitätskliniken, Kantonsspital, Basel, Switzerland

Howard I. Maibach
Department of Dermatology, School of Medicine, University of California, San Francisco, California, U.S.A.

I. INTRODUCTION

The skin is the largest organ of the body and is a complex, layered structure that forms a formidable barrier to the outside environment. Many factors govern the delivery of drugs and cosmetics into the skin from topically applied formulations. These include the size of the molecule, the lipophilicity of the component, type of formulation, presence of penetration enhancers, and physical state of the stratum corneum (SC) (1). In dermatology, the drug is rarely applied to the skin in the form of a pure chemical but, instead, is normally incorporated into a suitable carrier system—the vehicle. The term "vehicle" in this context is relatively new and was developed only when it became possible to differentiate the specific (therapeutic) effect of a chemical substance from the ancillary effects of "inactive" ingredients in a formulation. In crude terms, the vehicle or base may be regarded as the sum of the ingredients in which the drug is presented to the skin. In more sophisticated terms, we are now beginning to understand how to design and engineer a topical vehicle to deliver the active ingredient in a specific, dynamic pattern of penetration enhancement or retardation.

The nature of the topical vehicle is known to play a major role in promoting drug absorption into and through the skin. Conventional topical vehicles, such as ointments, creams, or gels, predominately exert their effect by releasing the drug onto the skin surface and the drug molecules then diffuse through the skin layers. During resent years, studies have suggested that novel vehicles (microemulsions, liposomes, and nanoparticles, for example) have the potential to increase cutaneous drug delivery of both lipophilic and hydrophilic drugs. Topical vehicle design is not a facile process since as many of the desirable pharmaceutical, pharmacokinetic, clinical, and

Table 1 Simple Classification System for Topical Dermatological Vehicles

System	Monophasic	Diphasic	Multiphasic
Liquid	Nonpolar solution often designated as oil	Emulsion (o/w, w/o) often designated as milk, lotion, shake microemulsions, liposomes	Emulsion (o/w/o, w/o/w) often designated as milk, lotion, shake, etc.
	Polar solution often designated as paint, lotion, etc.	Suspension often designated as paint, shake, etc.	Suspension often designated as paint, shake, etc.
Semisolid	Anhydrous nonpolar ointment polar ointment	Emulsion (o/w, w/o) often designated as washable (o/w), nonwashable (w/o) or amphiphilic (o/w, w/o) creams	Emulsion (o/w, w/o) with powder often designated as cream pastes
	Hydrous nonpolar gel polar gel	Suspension often designated as paste	
Solid	Powder	Transdermal patch	Transdermal patch

cosmetic properties of the formulation as possible must be fulfilled in this process. In practical terms, the vehicle is not only the sum of the formulation ingredients but also creates the chemical, physical, and structured matrix of the vehicle constituents. This formulation matrix can be monophasic (e.g., a simple lipid), biphasic (e.g., a cream) or tri- or multiphasic systems (e.g., multiple emulsions, patch systems, and nanostructures) into which a drug is incorporated (Table 1) (2).

II. VEHICLE EFFECTS ON PERMEATION OF DRUGS THROUGH THE SKIN

The vehicle can affect the flux of diffusants after topical application in the following ways.

A. Vehicle–Drug Interactions

Vehicle–drug interactions include all physical and chemical interactions that may take place between the drug molecules and the combined molecules of all the other formulation constituents. Solubility is of primary importance here as this parameter will define the physical state of the drug molecule in the vehicle (solution, suspension, ionized, or nonionized) and will define the magnitude of the concentration gradient established as the driving force for passive diffusion.

The parameters of Fick's law broadly define the factors controlling solute permeation through the skin. Flux depends on the solubility of the drug in the vehicle and the membrane, concentration difference across the membrane, the thickness of the membrane, and the ability of the vehicle to disrupt the membrane barrier to facilitate the permeation. One of the most important chemical vehicle–drug interactions is the establishment of the thermodynamic activity of the drug in vehicle (3). Thermodynamic activity is defined as the tendency of the molecule to leave the delivery vehicle environment and enter the stratum corneum. As a drug molecule dissolves from the surface of a crystal and enters into the matrix of solvent molecules in the delivery vehicle, there are a number of weak bonding interactions that take place between substituent groups on the solute and solvent species. This attractive interaction stabilizes the dissolved molecule in solution and prevents its precipitation. In dilute solutions there are infinite number of solvent molecules available for transient bonding interaction with the solute in this manner. The global sum of the attractive forces of the vehicle molecules for the (relatively few) solute species in this situation is considerable and the solute molecule would have a relatively low tendency (from energetic view point) to leave the solution and enter into a second environment. As the concentration of the solution increases, so the total number of the solvent molecules that are theoretically available to interact with each solute species decreases. Since each solute molecule is interacting with fewer solvent molecules (per unit time and space), there is a proportionally greater tendency for the solute molecules to be lost by partitioning into the membrane. In the latter situation, the solute molecules have greater thermodynamic activity or leaving potential. Ideally one can consider that a saturated solution is optimal as the maximal concentration gradient and maximal thermodynamic activity are achieved in this system compared with more dilute solutions. Furthermore, theory would predict that the solute leaving tendency is equal between two saturated solutions of the same drug in different solvents. However, this does not necessarily produce equal flux rates because the vehicle constituents often affect both the partitioning into the membrane and diffusive resistance of the barrier (2).

Supersaturated solutions are physically unstable by their nature; the drug tends to spontaneously crystallize upon preparation of the solution. Supersaturation is the state where the drug concentration in a vehicle is greater than the saturated solution under those ambient conditions. Therefore, a supersaturated solution increases the thermodynamic activity of the dissolved drug, generating greater leaving tendency, and an increase in the flux. Transient conditions of supersaturation can be achieved by employing the rapid evaporation of volatile solvents like ethanol or *n*-propanol, which can achieve appreciable increase in the permeant concentration beyond saturation (3). However, supersaturated vehicles continuously changes in composition (metamorphosis of the vehicle). In clinical and experimental situations, most dermatological vehicles (structural matrix and ingredients) undergo considerable physical and chemical changes after their application to the skin. Subsequently, the initial structural matrix of the vehicle will most likely change during and after the mechanical inunction associated with application of the product (shear effects and/or evaporation of the ingredients). As a consequence this could affect the thermodynamic activity of the drug within the formulation, as is clearly evident with the erratic flux over time achieved from supersaturated systems. Fang et al. (4) reported the use of antinucleant polymers like methyl cellulose (MC) and hydroxypropyl methylcellulose (HPMC) as a way to increase the stability of supersaturated drug vehicles and sustain the increased delivery potential. Therefore, from a maximal diffusion point of view, the solubility of drug in the vehicle should be maintained as close to saturation as possible. However, since these parameters do not operate in isolation, it is undesirable to have a base in which the drug is highly soluble as the partitioning of the permeant from this favorable solution to the skin will be retarded. Theoretically, a saturated solution of permeant in a hostile solvent should provide the best delivery system for molecules partitioning into the less hostile environment of the SC.

B. Vehicle–Skin Interactions

Vehicle–skin interactions include the broad spectrum of physical and chemical events that may take place once the vehicle comes into contact with the stratum corneum. The formulation constituents all have potential to partition from the applied vehicle and enter the stratum corneum. If one considers the holistic, classical approach to dermatological therapy, then the partitioning of the ancillary formulation substances into the skin have an important function in fulfilling the emollient and tactile functions of the formulation. Modern topical delivery theory may suggest that the partitioning of the ancillary formulation chemicals is unimportant in the therapeutic goal unless this partitioning modulates the delivery or diffusion of the active drugs. Recent technology has made use of this phenomenon in the form of penetration enhancer chemicals that are specifically designed to penetrate the stratum corneum from the applied vehicle and facilitate transport of the active drug principal through the barrier layer. Generally, penetration enhancers are vehicle components which interact with the stratum corneum to bring about changes in drug solubility, drug diffusion, or both (5). Penetration enhancers could improve flux via the transcellular route by swelling of the intracellular protein matrix, or alteration of the protein structure within the corneocytes. Enhanced passage of drug molecules by the intercellular route could be achieved by altering the crystallinity of the intercellular lipid bilayer through an increase in hydration of the lipid polar head groups. Alternatively, the lipid hydrophobic tails could be disordered to achieve the same effect.

Increased drug partitioning could also be facilitated into the aqueous spaces between the lipid bilayers. Therefore, the vehicle–skin interactions may have profound effects on the flux achieved through the skin.

C. Drug–Skin Interactions

Drug–skin interactions relate to the reactions between permeating drug molecules and the biochemicals of the SC. Initially believed to be a dead layer of cells, we are now only beginning to understand the complex metabolic activity that is possible in this tissue and the potential for using this phenomenon in terms of prodrug delivery. Table 2 summarizes some cutaneous metabolic reactions that have been reported in the literature. Riviere et al. (6) showed that 14% of the parent drug issorbide dinitrate is metabolized to the active form during transdermal delivery; indicating that substantial metabolic biotransformation does occur in the skin and may be used as a tool for enhanced delivery. Similarly, it has been demonstrated that a depot of topically delivered drug is rapidly established in the SC and that the active agent may be delivered from this binding site for days or weeks after initial application of the vehicle to the skin (6).

D. Vehicle–Drug–Skin Interactions

It is usually impossible to isolate separate effects of the vehicle, drug, and skin permutations. Significant, interrelated effects are common. Many pharmaceutical solvents, propylene glycol, for example, are known to have modest effects on reducing the skin barrier function (thereby altering the diffusivity of the drug through the skin) as well as influencing the solubility of the drug in the delivery vehicle (increasing the concentration gradient across the barrier layer), and changing the partitioning of the drug from the vehicle into the stratum corneum. In this example, one chemical is simultaneously and dynamically affecting three different parameters of the flux process.

Table 2 Localization and Type of Enzymes in the Skin (6)

Enzymes	Substrates	Species	Localization of enzymes
Oxidation reactions, aryl hydrocarbon, hydroxytase	Benzo(a) pyrene	Mouse	Superficial dermis containing sebaceous gland > epidermis > dermis
7- Ethoxycoumarin O-deethylase	7-Ethoxycoumarin	Hairless mouse	Sebaceous cells > basal cells
Cytochrome P- 450 dependent monooxygenase	2-amino anthracene	Rat	Epidermis > dermis
Esterases	6α-Methylprednisolone-17-propionate-21-acetate	Human	Epidermis=dermis
Aminopeptidases	Leucyl-β-naphthylamide	Human	Detection in full-thickness skin

Topical vehicle formulators are beginning to understand the complexities of this process and to make use of the interactions to engineer formulations that will perform in a specific manner. It is clear that skin delivery systems of the future will have greater complexity and will make use of novel and innovative technologies, like nano-sized molecular structures, to initiate, modulate and terminate delivery of active moieties to the skin in a time- or need-dependent fashion.

III. NOVEL TRANSDERMAL DELIVERY VEHICLES

Conventional topical drug formulations, such as ointments or creams, are reasonably safe but fail to efficiently overcome the skin barrier and therefore are not useful for transdermal drug delivery of a broad range of drugs. During the last two decades, several novel carrier systems have been evaluated in transdermal delivery for improving the efficiency of drug permeation to and through the skin.

A. Microemulsions

Microemulsions are colloidal systems composed of an aqueous phase, oil phase, and surfactants. Unlike macroemulsions, this novel vehicle has an ultra-low interfacial tension and a small droplet diameter of 10 to 140 nm. Microemulsions are transparent, optically isotropic, and thermodynamically stable. Many studies have indicated that microemulsion formulations possess improved transdermal and dermal delivery potential. Peltola et al. (7) showed that estradiol delivery across human abdominal skin in vitro could be increased 200- to 700-fold over controls using various o/w microemulsions. Multiple factors may influence the drug delivery rate from a microemulsion formulation. The ultra-low interfacial tension and small droplet size ensure an excellent surface contact between the skin and the vehicle at the application site. The potential enhancer effect of microemulsions is typically attributable to the individual components rather than the specific microemulsion structure. The high content of both aqueous and lipophilic phases facilitates delivery of both lipophilic and hydrophilic drugs from the relatively hydrophilic vehicle to the very lipophilic stratum corneum (8). Surfactants in the microemulsions can diffuse into the skin and facilitate diffusion through the barrier phase, either by disruption of the lipid structure of the stratum corneum, or by increasing the solubility of the drug in the skin (9).

B. Phospholipid Vesicular Carriers

1. Liposomes

Liposomes are biphasic vesicles, typically consisting of phospholipids and cholesterol. The lipid composition is similar to that of the SC, which enables them to penetrate the barrier to a greater extent than conventional vehicles. Liposomes, act not only as "drug transporters," but also show localizing effects whereby vesicles can accumulate drugs in the SC and reduce systemic effects (10). An extensive freeze–fracture electron microscopic study was carried out by Foldvari (1) to evaluate the interaction of phospholipid liposomes with the SC layer of excised abdominal skin. Significant ultrastructural changes were shown within the SC, with numerous intact vesicles accumulating in the intercellular lipid regions. Although other explanations are possible, it was suggested that the liposomal lipids might penetrate after disintegration (becoming "molecularly dispersed") and, by interacting with skin lipids,

form new vesicular structures. Some corneocyte swelling was also observed after liposome treatment in this study. Subsequent to the freeze–fracture studies, small-angle x-ray scattering measurements demonstrated definite changes in the diffraction pattern of liposome-treated skin, indicating mixing of liposomal and skin lipids. Liposome encapsulation forms of corticosteroids, retinoids, and local anesthetics have been studied, since these drugs may have severe side effects by conventional delivery or show insufficient clinical effects when applied topically.

2. Transfersomes

Transfersomes are lipid, elastic vesicles with ultradeformability that can efficiently penetrate intact through the skin—a situation that is usually impossible for other chemical structures of comparable size. It is advantageous that such carriers can be made entirely from pharmaceutically acceptable ingredients with standard methods established in the industry. To prepare these vesicles, surfactant molecules need to be incorporated into the vesicular membrane at specific concentrations (edge activators). Sodium cholate or sodium deoxycholate has been used for this purpose. Transfersomes require nonoccluded conditions with an osmotic gradient operating from the relatively dry skin surface towards fully hydrated viable tissues, thereby driving transfersomes through the horny layer. Traditional liposomes in this situation are expected to confine themselves to the surface or upper layers of stratum corneum, where they dehydrate and fuse with skin lipids. EI Maghraby et al. (11), assessed the potential mechanisms of enhanced permeation achieved by transfersomes and suggested the following possibilities:

1. Drug molecules are released from the vesicle and independently permeate the skin.
2. Enhanced permeation due to the release of lipids from vesicles and interaction with skin lipids.
3. Different entrapment efficiencies of the liposomes control the drug delivery.
4. Penetration of the SC by intact liposomes.

To date, transfersomes have been used to deliver numerous small chemical entities, (12) relatively large therapeutics (13), and proteins (14) across the skin in many preclinical and phases I and II clinical experiments.

3. Ethosomes

Ethosomes are composed of phospholipid, ethanol and water. The vehicle can penetrate the skin and improve drug delivery both to deep skin strata and systemically. Compared to liposome, ethosomes contain relatively high concentrations of ethanol (20–50%), which acts as an effective penetration enhancer. The ethanol and phospholipid vesicles appear to act synergistically on the stratum corneum. Delivery by ethosomes is significantly enhanced relative to classic liposomes or any of the system components alone (15). This is thought to be because the ethanol fluidizes both ethosomal lipids and bilayers of the stratum corneum intercellular lipid; the soft, malleable vesicles then penetrate the disorganized lipid bilayers.

C. Polymeric Microspheres

In recent years, microsphere drug delivery systems have emerged as one of the most promising strategies to achieve site-specific drug delivery for oral and parenteral

administration. De Jalo'n et al. (16) reported that the Poly DL-lactic-co-glycolic acid (PLGA) microparticles could effectively penetrate the stratum corneum and reach the epidermis in a relatively high number, although the largest structures remained in the skin surface. Consequently these carriers seem to be promising for topical drug administration, although they have not been studied extensively.

Microsponge delivery systems (MDS) are based on microscopic, polymer-based microspheres that can bind, suspend or entrap a wide variety of substances, and then be incorporated into a formulated product such as a gel, cream, liquid, or powder. A single MDS structure consists of numerous crosslinking voids within a noncollapsible structure that can stabilize a variety of drugs. The outer surface is typically porous, allowing the sustained flow of substances out of the sphere. Microsponge systems are primarily used as reservoirs for releasing active ingredients over a prolonged period of time, and as receptacles for absorbing undesirable substances, such as excess skin oil. The safety of the MDS has been well documented and they are used in many OTC drug and skin care cosmetics.

D. Solid Lipid Nanoparticles (SLN)

Solid lipid nanoparticles (SLN) are an alternative particulate drug carrier system made from solid lipids with a particle size between approximately 50 and 1000 nm. Similar to liposomes, they are composed of biocompatible lipids which seem to be well suited for use on damaged or inflamed skin. The very small particle size may lead to adhesive properties causing film formation on the skin. This may be useful as a protective lipid film on the skin or the film can have an occlusive effect that reduces transepidermal water loss and enhances the penetration of drugs through the SC by increased hydration. Additionally, a SLN carrier could affect penetration by facilitating contact of lipophilic drugs with the stratum corneum because of their large surface area, thereby increasing the amount of penetration into the skin. Advantageously, incorporation of active compounds into the SLN matrix can protect the active against chemical degradation. Stability enhancement was reported for coenzyme Q10 and also for retinol. In terms of pharmacodynamics, biphasic SLN often deliver active via an initial burst release, followed by prolonged delivery phase as observed in many studies (17). This pattern could be useful in transdermal applications as the burst release can rapidly saturate binding sites within the SC (reducing the lag time), while the sustained release period becomes more important for continuous delivery over a long period, or for ingredients with irritating effects at chronic high concentrations.

IV. CONCLUSIONS

The vehicle may be described as a drug carrier with specific pharmaceutical, technological, and biopharmaceutical usage. There is no "universal vehicle" for use in topical drug administration due to the multifaceted complexity of this type of dosage forms, and the need to individualize the delivery matrix for each active moiety. Whether using a conventional topical delivery vehicle or a novel engineered system, a multitude of interacting factors must be considered. The potential of the vehicle to release the drug is dependent on the physicochemical properties of the diffusant and the matrix of chemicals that have been combined together to form the drug vehicle. The thermodynamic leaving potential is greater as the concentration in solution

increases and is maximal for a saturated solution. The potential for the diffusant to partition across the vehicle–membrane interface will depend on its solubility in, and affinity for, the chemical environment of each system.

Additionally, the penetration of the formulation chemicals into the SC can, and usually do, affect the barrier properties of this structure appreciably. Clearly as knowledge in this field advances, formulators will gain a more complete understanding of the complex interactions between vehicle, drug, and skin. Moreover, formulators will continue to use this knowledge to improve the engineering of new delivery vehicles that more efficiently and more safely achieve specific therapeutic roles.

REFERENCES

1. Foldvari M. Non-invasive administration of drugs through the skin: challenges in delivery system design. Res Focus 2000; 3:417–423.
2. Smith EW, Surber C, Maibach HI. Topical dermatological vehicles, a holistic approach. In: Bronaugh RL, Maibach HI, eds. Percutaneous Absorption. 1997:779–787.
3. Surber C, Smith EW. The vehicle: the pharmaceutical carrier of dermatological agents. In: Garbard B, Elsner P, Surber C, Treffel P, eds. Dermatopharmacology of Topical Preparations. A Product-Development Oriented Approach. Berlin: Springer-Verlag, 1999:5–21.
4. Fang JY, Kuo CT, Huang YB, Wu PC, Tsai YH. Transdermal Delivery of sodium nonivamide acetate from volatile vehicles: effects of polymers. Int J Pharm 1999; 176:257–167.
5. Barry BW. Mode of action of penetration enhancers in humans skin. J Control Release 1987; 6:85–97.
6. Riviere JE, Brooks JD, William PL, McGown E, Michael B, Francoeur B. Cutaneous metabolism of isosorbide dinitrate after transdermal administration in isolated perfused porcine skin. Int J Pharm 1996; 127:213–217.
7. Peltola S, Savolainen PS, Kiesvaara J, Suhonen TM, Urtti A. Microemulsions for topical delivery of estradiol. Int J Pharm 2003; 254:99–107.
8. Kreilgaard M. Influence of microemulsions on cutaneous drug delivery. Adv Drug Deliver Rev 2002; 54(suppl 1):S77–S98.
9. Lam AC, Schechter RS. The theory of diffusion in microemulsions. J Colloid Interface Sci 1987; 120:56–63.
10. Fresta M, Puglisi G. Application of liposomes as potential cutaneous drug delivery systems: in vitro and in vivo investigation with radioactivity labelled vesicles. J Drug Target 1996; 4:95–101.
11. EIMaghraby G, Williams AC, Barry BW. Skin delivery of estradiol from deformable and traditional liposomes: mechanistic studies. J Pharm Pharmacol 1999; 51:1123–1134.
12. Cevc G, Blume G, Schätzlein A. Transfersomes-mediated transepidermal delivery improves the regio-specificity and biological activity of corticosteroids in vivo. J Control Release 1997; 45:211–226.
13. Cevc G, Schätzlein A, Richardsen H. Ultradeformable lipid vesicles can penetrate the skin and other semi-permeable barriers unfragmented. Evidence from double label CLSM experiments and direct size measurements. Biochim Biophys Acta 2002; 1564:21–30.
14. Cevc G, Bachhawat BK. Transdermal immunization with large proteins by means of ultradeformable drug carriers. Eur J Immunol 1995; 25:3521–3524.
15. Touitou E, Dayan N, Bergelson L, Godin B, Eliaz M. Ethosomes novel vesicular carriers for enhanced delivery: characterization and skin penetration properties. J Control Release 2000; 65:403–418.

16. Dejalo'n EG, Bianco-Prý′eto MJ, Ygartua P, Santoyo S. PLGA microparticles: possible vehicles for topical drug delivery. Int J Pharm 2001; 226:181–184.
17. Hu FQ, Yuan H, Zhang HH, Fang M. Preparation of lipid nanoparticles with clobetasol propionate by a novel solvent diffusion method in aqueous system and physicochemical characterization. Int J Pharm 2002; 239:121–128.

59

Effect of Tape Stripping on Percutaneous Penetration and Topical Vaccination

Hongbo Zhai, Frank Dreher, and Howard I. Maibach
Department of Dermatology, School of Medicine, University of California, San Francisco, California, U.S.A.

Myeong Jun Choi
Charmzone Research and Development Center, 1720-1 Taejang 2-dong, Wonju, Kongwon-do, Korea

Harald Löffler
Philipp University of Marburg, Marburg, Germany

I. INTRODUCTION

The skin protects the body from unwanted environmental effects. The stratum corneum (SC), only 10 to 30-μm thick, provides a barrier to the percutaneous penetration of drugs and macromolecules (1). Despite major research and development efforts in topical/transdermal systems and the advantages of these routes, low SC permeability remains a major limit for the usefulness of the topical approach (2,3). To increase permeability, chemical and physical approaches have been examined to decrease barrier properties. Physical approaches for skin penetration enhancement such as stripping (4–12), iontophoresis (13), and electroporation (13,14) have been evaluated. In addition, penetration enhancers and vesicle systems had been used to enhance permeability (15–17). Tape stripping is commonly used to disrupt the epidermal barrier to enhance the delivery of applied drug and biological macromolecules.

Tape stripping is putatively simple, inexpensive, and minimally invasive. The number of tape strips needed to remove the SC varies with age, gender, anatomical site, skin condition, and possibly ethnicity (18). Tape stripping has been used in dermatological and pharmaceutical fields: to measure SC mass and thickness (4–6), to investigate percutaneous penetration of topically applied drug in vivo (7–9), and to disrupt skin barrier function (19). Also, this technique has been used to collect SC lipids and protein samples (4,20), detect proteolytic activity associated with the SC (21), quantitatively estimate enzyme levels and activities in the SC (22), and allows detection of metal in the SC (23,24). Tape stripping has been used to disrupt the skin barrier before percutaneous peptide and DNA immunization (25–28). In addition, tape stripping is of sufficient utility to have been proposed by the Food

and Drug Administration (FDA) as part of a standard method to evaluate bioequivalence of topical dermatological dosage forms (29).

This paper reviews the stripping method and its application on the penetration enhancement into SC and topical vaccination and defines restrictions and drawbacks.

II. SKIN BARRIER FUNCTION

The SC is a permeability barrier that depends upon the presence of a unique mixture of lipids in the SC's intercellular domains. The SC consists of keratin-filled cells, the corneocytes, entirely surrounded by crystalline lamellar lipid regions. The composition and thickness of the SC lipids strongly differs depending on animal species (30). The major lipid classes in the SC are ceramides (CERs), cholesterol (CHOL), and free fatty acids (FFAs). Both qualitative and quantitative compositions of the barrier lipids are important in maintain on efficient skin barrier.

These lipids exist as a continuous lipid phase; occupying about 20% of the SC volume, arranged in multiple lamellar structures. All CERs and fatty acids found in SC are rod and cylindrical in shape; this physical attribute makes them suitable for the formation of highly ordered gel phase membrane domains. The CHOL is capable of either fluidizing membrane domains or of enhancing rigidity, depending on the physical properties of the other lipids and the proportion of CHOL relative to the other component (31). Intracellular lipids that form the only continuous domain in the SC are required for a competent barrier.

Efforts have been undertaken to characterize the lipid lamellar regions. Based on freeze–fracture electron microscopy, differential scanning calorimetry and X-ray diffraction studies, the lipids appear arranged as lamellar structures, whose organization is strongly dependent on lipid composition (1). Human lipids are organized in two lamellar phases with periodicity of approximately 13 and 6 nm, respectively. SC lipids, CERs, CHOL, and FFAs form the orthorhombic lateral packing, a densely packed structure. However, in equimolar mixtures prepared for CHOL and CERs the major lipid fraction forms a lamellar phase (hexagonal lateral packing) with periodicity of 12.8 nm. Addition of FFAs to CER/CHOL mixtures induced a transition from a hexagonal to orthorhombic lateral packing (32).

Diseases such as atopic dermatitis, psoriasis, and contact dermatitis, are associated with barrier dysfunction. Most skin disorders that have a diminished barrier function present a decrease in total CER content with some differences in their pattern (33–35). Pilgram et al. (36) reported that in case of diseased skin, an impaired barrier function is related to an altered lipid composition and organization. In atopic dermatitis SC, they found that, in comparison with healthy SC, the presence of the hexagonal lattice (gel phase) is increased with respect to the orthorhombic packing (crystalline phase). From lipid composition studies of atopic skin, intercellular lipids, especially CERs, play an important role in the barrier function and lipid organization. The lipid differences may be partially due to secondary (increased cell turnover)—rather than a primary cause and effect relationship.

III. STRIPPING FACTORS

When tape stripping is employed, several factors are important for standardization, (a) number of strips, (b) types and size of tapes, (c) the pressure applied to the strip

Table 1 Comparison of Tape Stripping Methods

Type of tape (brand name)	Number of strippings	Size	Applied pressure	Applied time (sec)	References
D-Squame (CuDerm)	40	25 mm	10 kPa	2	(6)
Transpore (3M)	40		10 kPa	2	(6)
Micropore (3M)	40		10 kPa	2	(6)
D-Squame (CuDerm)	16	25 mm	80 g/cm^3	5	(9)
Leukoflex (Beiersdorf)	18–20	1.5 × 5 cm	Soft pressure		(20)
3M invisible (3M)	7		Controlled condition	10	(59)
Adhesif 6204 (3M)	10	2 × 10 cm		2	(22)
Scotch Book tape 845 (3M)	20		By rubbing six times		(60)
Scotch (3M)	7		1 kg rubber weight was rolled over it 10 times		(61)
Scotch 600 (3M)	2–5	4 cm	By rubbing with finger three movements		(62)
Blenderm (3M)	6	4 cm^2			(63)
Transpore (3M)	20	2.5 × 5 cm	Firm pressure		(8)
Transpore (3M)	10	5 × 5 cm			(7)
Teasfilm (Beiersdorf)	20	4 cm^2			(19)
D-Squame (CuDerm)	16	25 mm	0.365 N/cm^2		(64)
D-Squame (CuDerm)	25	25 mm	Uniform pressure	5	(65)
Tesa (Beiersdorf)	20	1.5 × 2.0 cm	2 Kg pressure	10	(15)
D-Squame (CuDerm)	20	3.8 cm^2	Uniform pressure	5	(4)

Tape stripping is employed with different adhesive tape, size, number of strips, and the pressure applied to the strip prior to stripping and the peeling force applied for removal.

prior to stripping and the peeling force applied for removal, and (d) anatomic sites. Some parameters are summarized in Table 1. We compared the experimental method, i.e. the type and size of tape, pressure and time applied on the skin, and number of strips on the stripping. Stripping data vary according to experimental conditions.

Dreher et al. (4) improved the method by quantifying the mass of human SC removed by each strip utilizing a colorimetric protein assay. With this method, Bashir et al. (6) determined the physical and physiological effect of SC tape stripping, utilizing tapes with different physicochemical properties: D-Squame® (CuDerm, Dallas, TX), Transpore® (3M, St. Paul, Minnesota, U.S.A), and Micropore® (3M, St. Paul, Minnesota, U.S.A). They demonstrated differences in the mean TEWL

values between the tapes. Mean TEWL increased significantly as the deeper layers of the SC were reached by tape stripping for D-Squame and Transpore, but not for Micropore. Therefore, D-Squame and Transpore tapes induce a significant increase in the TEWL, while Micropore tape did not. The TEWL value differed depending on the tapes and the amount of SC removed.

The number of tape strips to remove SC differs by according to experimental conditions (Table 1). As the number of tape strips increased, TEWL value also increased. Proposed FDA bioequivalence guideline recommends 10 tape strips after drug application. Weerheim and Ponec (20) reported that the average numbers of tapes in vivo could be 18 to 20 strips to remove SC completely. However, this number is not universal; some individuals, 40 adhesive tape strips, regardless of the type of tape does not disrupt the SC barrier to water (6).

IV. TAPE STRIPPING VS. PERCUTANEOUS ABSORPTION AND PENETRATION

Percutaneous absorption and penetration is a complex physical and physiological process. This process initiates a series of absorption, distribution, and excretion that are influenced by numerous factors. Percutaneous absorption of drug depends mainly on the permeability coefficient of the drug, which is affected by drug polarity, molecular size, the vehicle in which the drug is applied, and the skin barrier. Other important factors are application conditions (non-occlusion or occlusion), and skin integrity, which is affected by disease and trauma, body site, and age (3,12,32,37–40).

The intercellular lipid domain is a major pathway for permeation of most drugs through the SC and also acts as a major barrier for penetration. As a consequence of its hydrophobic nature, the SC barrier allows the penetration of lipid soluble molecules more readily than water-soluble. Generally, small, non-polar, lipophilic molecules are the most readily absorbed, while high water solubility confers less percutaneous absorptive capacity through normal skin (41).

Tape stripping is mainly used to measure drug concentration and its concentration profile across the SC. The SC is progressively removed by serial adhesive tape stripping and consequently, percutaneous absorption and penetration is significantly increased in stripped skin (Table 2). Benfeldt et al. (7,8) reported that in microdialysis experiment salicylic acid was increased in tape stripped skin in humans and hairless rats at 157- and 170-fold, respectively. Morgan et al. (41) reported that in microdialysis experiment tape stripping increased penciclovir absorption by 1300-fold and aciclovir absorption by 440-fold. Although tape stripping increased the penetration of some drugs (42–46), this is not universal (47,48). Physiological and pathological factors affect drug transport across the living human skin. Bos and Meinardi (49) suggested the 500-Da rule for the skin penetration of chemical compounds and drugs. This size limit may be changed by the skin abnormalities such as atopic dermatitis and disrupted skin.

In addition to organic drugs, tape striping increased the penetration of biological macromolecules such as peptide and DNA into viable skin (25–28). Topically applied oligonucleotides (ONs) and DNA do not penetrate normal human SC. But, removal of SC by tape stripping lead to extensive penetration of ONs and DNA throughout the epidermis. Regnier et al. (14) compared ONs penetration through intact and stripped hairless rat skin. Stripping increased ONs concentration by one or two orders of magnitude (24 to 166-fold increase) (Table 2). In case of

Table 2 In Vivo Drug Penetration Studies in Barrier-Perturbed Skin

Barrier perturbation	Species	Drug	Penetration ratio[a]	Reference
None			1	
Tape stripping	Human	Hydrocortisone	2	(37)
	Human (occlusion)	Hydrocortisone	32.7	(37)
	Human	Low molecular weight Heparin	1	(48)
	Human	Methylpredniso-lone aceponate	91.5	(45)
	Human	Salicylic acid	157	(8)
	Human	Penciclovir	1,300	(41)
	Human	Aciclovir	440	(41)
	Hairless guinea pig	Benzoic acid	2.1	(47)
	Hairless guinea pig	Hydrocortisone	3	(47)
	Rat	Nicotinic acid	10.8	(43)
	Rat	Cortisone	2.5	(43)
	Rat	Salicylic acid	0.8–46	(44)
	Hairless rat	Oligonucleotide	24–166	(14)
	Hairless rat	Salicylic acid	170	(7)
	Hairless mouse	Nitroglycerin	9.0	(46)
	Hairless mouse	Enoxacin	7.5	(42)

[a]Penetration ratio varies among drugs and species investigated. Most studies used traditional radiolabeling techniques, where the penetration is measures as total drug absorption over 4 to 10 days. In the case of salicylic acid, the study defined the cutaneous penetration and systemic absorption during 20-minutes intervals over a period of four hours after drug administration.

plasmid DNA, Yu et al. (50) reported that transfer gene activity depends on the number of stripping. They applied a CMV-CAT expression plasmid to stripped area and found that the transfer gene expression was higher in the murine skin samples stripped five times prior to DNA application compared with those stripped three times prior to DAN application. This result indicated that abrasion of the skin prior to DNA application could improve cutaneous gene transfer and expression. Taken together, tape stripping is a commonly used to enhance the delivery of chemical drugs and biological macromolecules.

V. TAPE STRIPPING AND TOPICAL VACCINATION

Why is the skin a major target for topical vaccination? The skin, an active immune surveillance site, is rich in potent antigen-presenting dendritic cells (DCs) such as Langerhan's cells (LCs) in the epidermis. The LCs play a key role in the immune response to antigenic materials. Skin accessibility makes it an easy target for vaccination. Thus, skin is an attractive target site for topical vaccination and has become the focus of intense study for the induction of antigen-specific immune responses (51,52). Wang et al. (53) observed that protein penetrates SC barrier following occlusion by patch application, but immune responses generated in this way are Th2 predominant. This immune response does not elicit cytotoxic T lymphocytes (CTL) response that is important in preventing and therapy against viral infections and tumors.

In addition to disruption of the epidermal barrier, stripping enhances in vitro T cell mediated immune response (54). Tape stripping is immunostimulatory and results in the production and release of IL-1α, IL-1β, TNF-α, IL-8, IL-10, and INF-γ (26,54,55). Skin barrier disruption by tape stripping also increases co-stimulatory molecule expression (CD86, CD54, CD40, and MHC class II) and the antigen-presenting capacity of epidermal DCs (26,56). In addition, tape stripping facilitates the generation of Th1 immune responses and stimulates LCs migration to cutaneous lymph nodes (56).

Seo et al. (25) reported that topical application of tumor-associated peptide onto the SC barrier disrupted by tape stripping in mice induces protective anti tumor response in vivo and in vitro. They investigated induction of CTL response on tape stripped earlobes of C57/BL6 mice by application of CTL epitope peptide onto the SC. The optimal condition of CTL response was observed 12 and 24 hours after tape stripping at peptide doses of 48 and 96 μg per mouse. On the other hand, CTL induction was virtually absent when peptide was applied to intact skin (Table 3). Kahlon et al. (56) reported optimization of topical vaccination for the induction of CTL with peptide and protein antigens. They found that tape stripping significantly enhanced antigen-specific antibody (protein) and CTL responses (peptide and protein) measured at three and two weeks following immunization, respectively (Table 3). Stripping resulted in prolonged CTL responses at least two months after single

Table 3 Comparison to Cytotoxic T lymphocyte (CTL) Activity of Peptide, Protein, and DNA Immunization With and Without Stripping

Antigen	Immunization	Specific lysis (%)
Peptide	Intact skin	11.0
	Stripped skin[a]	80.0
	Stripped skin + cholera toxin[b]	70.0
Protein[c]	Intact skin	8.0
	Stripped skin	46.0
DNA[d]	Intact skin	12.7
	Stripped skin	37.0

[a]Cervical lymph node cells (effectors) obtained from mice immunized 10 days earlier with tyrosinase-related protein 2 peptide (VYDFFVWL, 96 μg per mouse) either through intact earlobes or earlobes tape stripped 12 hours earlier were subjected to CTL assay using L^{kb} target cells pulsed with tyrosinase peptide. The CTL assays were performed at effector-to-target ratio of 10.

[b]C57BL/6 mice were immunized on the ear with 25 μg ovalbumin peptide (SIYRYYGL) and 25 μgcholera toxin following tape stripping. Mice were boosted in similar fashion at one week and sacrificed at two weeks. Ovalbumin expressing EG7 cells were used as target and CTL assays were performed at effector-to-target ratio of 50. The ear skin on the dorsal and ventral side was tape-stripped 10 times (using Scotch Brand 3710 adhesive tape).

[c]C57BL/6 mice were immunized on the ear with 250 μg ovalbumin protein and 25 μg cholera toxin following tape stripping. Mice were boosted in similar fashion at one week and sacrificed at two weeks. Ovalbumin expressing EG7 cells were used as target and CTL assays were performed at effector-to-target ratio of 50. The ear skin on the dorsal and ventral side was tape-stripped 10 times (using Scotch Brand 3710 adhesive tape).

[d]BALB/c mice were immunized with plasmid DNA coded influenza M protein. Lymphoid cells from each immunized group were restimulated for five days using influenza M peptide-pulsed syngenic spleen cells. The peptide pulsed p815 cells were used as targets. The CTL assays were performed at effector-to-target ratio of 80. Fast-acting adhesive glue (Alon Alfa®) was smeared on a glass slide to cover the mouse. After an interval 20 to 30 seconds, the slide was ripped off.

immunization. These results suggest that stripping can be widely used in inducing immune responses with topical vaccination in vivo.

In addition to peptide and protein antigen, tape stripping increased the humoral and cellular immune responses of topical DNA antigens (27,28). Comparing the immune response with and without stripping, topical application without stripping induced weak antibody response and did not elicit a sufficient CTL response. In contrast, topical application of this vaccine with stripping induced strong antibody responses and elicited substantial CTL responses. There was a significant difference between the results of topical application with and without stripping (27,52).

To confirm the protective effect of topical vaccination, Watabe et al. (28) and Seo et al. (25) used an influenza and melanoma mouse model, respectively. Watabe et al. (28) investigated the efficacy of a topical DNA vaccine that expressed the matrix gene of the influenza virus using a mouse model. They topically applied plasmid DNA onto the stripped skin on days 0, 7, and 14. After the third immunization, the mice were challenged with $5LD_{50}$ of influenza virus. Thirteen of 20 mice (65%) survived when they were topically immunized with plasmid DNA that expressed the matrix gene. When the mice were immunized with inactivated virus topically, only 18% of mice were protected and all mice were dead at seven days after virus inoculation in case of unimmunized control group. These results suggest that the topical administration of DNA vaccine induce a protective immunity against influenza challenge. Seo et al. (25) investigated the efficacy of topical peptide vaccination for tumor immunotherapy. Mice were immunized twice with tumor-associated peptide at barrier-disrupted skin and were challenged with B16 melanoma tumor cells. The B16 tumor cells were virtually completely rejected after epitope peptide immunization via a disrupted barrier. Also when tumor bearing mice were treated with epitope peptide on tape stripped skin, tumor cells regressed with peptide application, and 100% of the mice survived for one month and 95% for over 60 days. However, mice treated with peptide application to intact skin died after 34 days. Thus, topical immunization provides a simple, non-adjuvant system, and non-invasive means of inducing potent anti tumor immunity that may be exploited for cancer immunotherapy in human.

VI. UNANSWERED QUESTIONS

Surber et al. (57) reviewed the standardized tape stripping technique; many factors remain to be investigated. As shown in Table 1, the types and sizes of tapes utilized equally affect the method and the pressure applied to the strip prior to stripping. A proposed FDA guideline describes serial tape stripping to determine the amount of drug within the skin. In this guideline, the first tape strip is discarded, the drug is extracted from the remaining pooled strips and the quantified amount is expressed as a mass per unit area. From the guidelines, it is impossible to express the amount of drug substance per unit mass of SC and to determine the proportion of the SC that has been sampled by the tape stripping method. Although tape stripping is relative simple to execute, there are many opportunities for experimental artifacts to develop. Tape stripping samples have high surface-to-volume ratio, and losses by evaporation can be significant even for chemicals with relatively low volatility. In addition, the tape stripping experiment is unsuitable for volatile chemical (58). Considering the current application of tape stripping method, topical vaccination, and clinical

trials for the determination of bioequivalence of topical dermatological products could be improved by stripping standardization.

VII. CONCLUSION

Tape stripping is commonly used to disrupt the epidermal barrier, to enhance the delivery of drugs, and to obtain information about SC function. In addition, this technique is of sufficient utility to have been proposed by the FDA as part of a standard method to evaluate bioequivalence of topical dermatological dosage forms. Application of this technique is greatly increasing in various dermatological and pharmaceutical fields. Considering the current application of tape stripping method, clinical trials for the determination of bioequivalence of topical dermatological products could be improved tape stripping standardization.

REFERENCES

1. Bouwstra JA, Honeywell-Nguyen PL, Gooris GS, Ponec M. Structure of the skin barrier and its modulation by vesicular formulations. Prog Lipid Res 2003; 42:1–36.
2. Rojanasakul Y. Antisense oligonucleotide therapeutics: drug delivery and targeting. Adv Drug Del Rev 1996; 18:115–131.
3. White PJ, Gray AC, Fogarty RD, Sinclair RD, Thuminger SP, Werther GA, Wraight CJ. C-5 propyne-modified oligonucleotides penetrate the epidermis in psoriatic and not normal human skin after topical application. J Invest Dermatol 2002; 118:1003–1007.
4. Dreher F, Arens A, Hostynek JJ, Mudumba S, Ademola J, Maibach, HI. Colorimetric method for quantifying human stratum corneum removed by adhesive tape stripping. Acta Derm Venereol 1998; 78:186–189.
5. Kalia YN, Albert I, Naik A, Guy RH. Assessment of topical bioavailability in vivo: the importance of stratum corneum thickness. Skin Pharmacol Appl Skin Physiol 2001; 14:82–86.
6. Bashir SJ, Chew AL, Anigbogu A, Dreher F, Maibach HI. Physical and physiological effects of stratum corneum tape stripping. Skin Res Technol 2001; 7:40–48.
7. Benfeldt E, Serup J. Effect of barrier perturbation on cutaneous penetration of salicylic acid in hairless rats: in vivo pharmacokinetics using microdialysis and non-invasive quantification of barrier function. Arch Dermatol Res 1999; 291:517–526.
8. Benfeldt E, Serup J, Menne T. Effect of barrier perturbation on cutaneous salicylic acid penetration in human skin: in vivo pharmacokinetics using microdialysis and non-invasive quantification of barrier function. Br J Dermatol 1999; 140:739–748.
9. Potard G, Laugel C, Schaefer H, Marty JP. The stripping technique: in vitro absorption and penetration of five UV filter on excised fresh human skin. Skin Pharmacol Appl Skin Physiol 2000; 13:336–344.
10. Rougier A, Dupuis D, Lotte C, Maibach HI. Stripping method for measuring percutaneous absorption in vivo. In: Broncugh RL, Maibach HI, eds. Percutaneous Absorption. Drug-Cosmetics-Mechanism-Methodology. New York: Marcel Dekker, 1999:375–394.
11. Schwindt DA, Wilhelm KP, Maibach HI. Water diffusion characteristics of human stratum corneum at different anatomical sites in vivo. J Invest Dermatol 1998; 111:385–389.
12. Rougier A, Dupuis D, Lotte C, Roguet R, Wester RC, Maibach HI. Regional variation in percutaneous absorption in man: measurement by the stripping method. Arch Dermatol Res 1986; 278:465–469.
13. Regnier V, Preat V. Localization of a FITC-labeled phosphorothioate oligonucleotide in the skin after topical delivery by iontophoresis and electroporation. Pharm Res 1998; 15:1596–1602.

14. Regnier V, Tahiri A, Andre N, Lemaitre M, Le Doan T, Preat V. Electroporation-mediated delivery of 3′-protected phosphodiester oligonucleotides to the skin. J Control Release 2000; 67:337–346.
15. Verma DD, Verna S, Blume G, Fahr A. Particle size of liposomes influences dermal delivery of substances into skin. Int J Pharm 2003; 258:141–151.
16. Magnusson BM, Walters KA, Roberts MS. Veterinary drug delivery: potential for skin penetration enhancement. Adv Drug Deliv Rev 2001; 50:205–227.
17. Chattaraj SC, Walker RB. Penetration enhancer classification. In: Smith EW, Maibach HI, eds. Percutaneous Penetration Enhancers. Boca Raton, Florida: CRC press, 1995:5–20.
18. Palenske J, Morhenn VB. Changes in the skin's capacitance after damage to the stratum corneum in humans. J Cutan Med Surg 1999; 3:127–131.
19. Fluhr JW, Dickel H, Kuss O, Weyher I, Diepgen TL, Berardesca E. Impact of anatomical location on barrier recovery, surface pH and stratum corneum hydration after acute barrier disruption. Br J Dermatol 2002; 146:770–776.
20. Weerheim A, Ponec M. Determination of stratum corneum lipid profile by tape stripping in combination with high-performance thin-layer chromatography. Arch Dermatol Res 2001; 293:191–199.
21. Beisson F, Aoubala M, Marull S, Moustacas-Gardies AM, Voultoury R, Verger R, Arondel V. Use of the tape stripping technique for directly quantifying esterase activities in human stratum corneum. Anal Biochem 2001; 290:179–185.
22. Mazereeuw-Hautier J, Redoules D, Tarroux R, Charveron M, Salles JP, Simon MF, Cerutti I, Assalit MF, Gall Y, Bonafe JL, Chap H. Identification of pancreatic type I secreted phospholipase A2 in human epidermis and its determination by tape stripping. Br J Dermatol 2000; 142:424–431.
23. Cullander C, Jeske S, Imbert D, Grant PG, Bench G. A quantitative minimally invasive assay for the detection of metals in the stratum corneum. J Pharm Biomed Anal 2000; 22:265–279.
24. Hostynek JJ, Dreher F, Nakada T, Schwindt D, Anigbogu A, Maibach HI. Human stratum corneum absorption of nickel salts. Investigation of depth profiles by tape stripping in vivo. Acta Derm Venereol 2001; 212:11–18.
25. Seo N, Tokura Y, Nishijima T, Hashizume H, Furukawa F, Takigawa M. Percutaneous peptide immunization via corneum barrier-disrupted murine for experimental tumor immunoprophylaxis. Proc Natl Acad Sci USA 2000; 97:371–376.
26. Takigawa M, Tokura Y, Hashizume H, Yagi H, Seo N. Percutaneous peptide immunization via corneum barrier-disrupted murine for experimental tumor immunoprophylaxis. Ann NY Acad Sci 2001; 941:139–146.
27. Liu LJ, Watabe S, Yang J, Hamagima K, Ishii N, Hagiwara E, Onari K, Xin KQ, Okuda K. Topical application of HIV DNA vaccine with cytokine-expression plasmids induces strong antigen-specific immune responses. Vaccine 2001; 20:42–48.
28. Watabe S, Xin KQ, Ihata A, Liu LJ, Honsho A, Aoki I, Hamajima K, Wahren B, Okuda K. Protection against influenza virus challenge by topical application of influenza DNA vaccine. Vaccine 2001; 19:4434–4444.
29. Shah VP, Flynn GL, Yacobi A, Maibach HI, Bon C, Fleischer NM, Franz TJ, Kaplan LJ, Kawamoto J, Lesko LJ, Marty JP, Pershing LK, Schaefer H, Sequeira JA, Shrivastara SP, Wilkin J, Williams RL. Bioequivalence of topical dermatological dosage forms—methods of evaluation of bioequivalence. Pharm Res 1999; 15:167–171.
30. Hammond SA, Tsonis C, Sellins K, Rushlow K, Scharton-Kersten T, Colditz I, Glenn GM. Transcutaneous immunization of domestic animals: opportunities and challenges. Adv Drug Deliv Rev 2000; 43:45–55.
31. Wertz PW. Lipids and barrier function of the skin. Acta Derm Venereol 2000; 208:7–11.
32. Bouwsta JA, Honeywell-Nguyen PL. Skin structure and mode of action vesicles. Adv Drug Deliv Rev 2002; 54:s41–s55.

33. Matsumoto M, Umemoto N, Sugiura H, Uehara M. Difference in ceramide composition between ''dry'' and ''normal'' skin in patients with atopic dermatitis. Acta Derm Venereol 1999; 79:246–247.
34. Okamoto R, Arikawa J, Ishibashi M, Kawashima M, Takagi Y, Imokawa G. Sphingosylphosphorylcholine is upregulated in the stratum corneum of patients with atopic dermatitis. J Lipid Res 2003; 44:93–102.
35. Macheleidt O, Kaiser HW, Sandhoff K. Deficiency of epidermal protein-bound omega-hydroxyceramides in atopic dermatitis. J Invest Dermatol 2002; 119:166–173.
36. Pilgram GS, Vissers DC, van der Meulen H, Pavel S, Lavrijsen SP, Bouwstra JA, Koerten HK. Aberrant lipid organization in stratum corneum of patients with atopic dermatitis and lamellar ichthyosis. J Invest Dermatol 2001; 117:710–717.
37. Feldmann RJ, Maibach HI. Penetration of ^{14}C hydrocortisone through normal skin. Arch Dermatol 1965; 91:661–666.
38. Feldmann RJ, Maibach HI. Regional variations in percutaneous penetration of ^{14}C cortisol in man. J Invest Dermatol 1967; 48:181–183.
39. Wester RC, Maibach HI. Cutaneous pharmacokinetics: 10 steps to percutaneous absorption. Drug Metab Rev 1983; 14:169–205.
40. Rougier A, Lotte C, Maibach HI. In vivo percutaneous penetration of some organic compounds related to anatomic site in man: predictive assessment by the stripped method. J Pharm Sci 1987; 76:451–454.
41. Morgan CJ, Renwick AG, Friedmann PS. The role of stratum corneum and dermal vascular perfusion in penetration and tissue levels of water-soluble drugs investigated by microdialysis. Br J Dermatol 2003; 148:434–443.
42. Fang JY, Hong CT, Chiu WT, Wang YY. Effect of liposomes and niosomes on skin permeation of enoxacin. Int J Pharm 2001; 219:61–72.
43. Bronaugh RL, Stewart RF. Methods for in vitro percutaneous rat absorption studies V: penetration through damaged skin. J Pharm Sci 1985; 74:1062–1066.
44. Murakami T, Yoshioka M, Okamoto I, Yumoto R, Higashi Y, Okahara K, Yata N. Effect of ointment bases on topical and transdermal delivery of salicylic acid in rats: evaluation by skin microdialysis. J Pharm Pharmacol 1998; 50:55–61.
45. Günther C, Kecskes A, Staks T, Täuber U. Percutaneous absorption of methyprednisolone aceponate following topical application of Advantan lotion on intact, inflamed and stripped skin of male volunteers. Skin Pharmacol Appl Skin Physiol 1998; 11:35–42.
46. Higo N, Hinz RS, Lau DTW, Benet LZ, Guy RH. Cutaneous metabolism of nitroglycerin in vitro. II. Effect of skin condition and penetration enhancement. Pharm Res 1992; 9:303–306.
47. Moon KC, Wester RC, Maibach HI. Diseased skin models in the hairless guinea pig: in vivo percutaneous absorption. Dermatologica 1990; 180:8–12.
48. Xiong GL, Quan D, Maibach HI. Effect of penetration enhancers on in vitro percutaneous absorption of low molecular weight heparin through human skin. J Control Release 1996; 42:289–296.
49. Bos JD, Meinardi MMHM. The 500-Dalton rules for the skin penetration of chemical compounds and drugs. Exp Dermatol 2000; 9:165–169.
50. Yu WH, Kashari-Sabet M, Liggit D, Moore D, Heath TD, Debs RJ. Topical gene delivery to murine skin. J Invest Dermatol 1999; 112:390–375.
51. Babiuk S, Baca-Estrada M, Babiuk LA, Ewen C, Foldvari M. Cutaneous vaccination: the skin as an immunologically active tissue and the challenge of antigen delivery. J Control Release 2000; 66:199–214.
52. Choi MJ, Maibach HI. Topical vaccination of DNA antigens: topical delivery of DNA antigens. Skin Pharmacol Appl Skin Physiol 2003; 116:271–282.
53. Wang L, Lin JY, Hsieh KH, Lin PW. Epicutaneous exposure of protein antigen induces a predominant Th-2 like response with high IgE production in mice. J Immunol 1996; 156:670–678.

54. Nishijima T, Tokura Y, Imokawa G, Seo N, Furukawa F, Takigawa M. Altered permeability and disordered cutaneous immunoregulatory function in mice with acute barrier disruption. J Invest Dermatol 1997; 109:175–182.
55. Nickoloff BJ, Naidu Y. Perturbation of epidermal barrier function correlates with initiation of cytokine cascade in human skin. J Am Acad Dermatol 1994; 30:535–546.
56. Kahlon R, Hu Y, Orteu CH, Kifayet A, Trudeau JD, Tan R, Dutz JP. Optimization of epicutaneous immunization for the induction of CTL. Vaccine 2003; 21:2890–2899.
57. Surber C, Schwarb FP, Smith EW. Tape-stripping technique. In: Broncugh RL, Maibach HI, eds. Percutaneous Absorption. Drug-Cosmetics-Mechanism-Methodology. New York: Marcel Dekker, 1999:395–409.
58. Reddy MB, Stinchcomb AL, Guy RH, Bunge AL. Determining dermal absorption parameters in vivo from tape strip data. Pharm Res 2002; 19:292–298.
59. Fernandez C, Nielloud F, Fortune R, Vian L, Marti-Mestres G. Benzophenone-3: rapid prediction and evaluation using non-invasive methods of in vivo human penetration. J Pharm Biomed Anal 2002; 28:57–63.
60. Alberti I, Kalia YN, Naik A, Bonny JD, Guy RH. In vivo assessment of enhanced topical delivery of terbinafine to human stratum corneum. J Control Release 2001; 71: 319–327.
61. Wissing SA, Muller RH. Solid lipid nanoparticles as carrier for sunscreens: in vitro release and in vivo skin penetration. J Control Release 2002; 81:225–233.
62. Betz G, Nowbakht P, Imboden R, Imanidis G. Heparin penetration into and permeation through human skin from aqueous and liposomal formulations in vitro. Int J Pharm 2001; 228:147–159.
63. Couteau C, Perez-Cullel N, Connan AE, Coiffard LJM. Stripping method to quantify absorption of two sunscreens in human. Int J Pharm 2001; 222:153–157.
64. Chatelain E, Gabard B, Surber C. Skin penetration and sun protection factor of five UV filters: effect of the vehicle. Skin Pharmacol Appl Skin Physiol 2003; 16:28–35.
65. Simonsen L, Petersen MB, Benfeldt E, Serup J. Development of an animal model for skin penetration in hairless rats assessed by mass balance. Skin Pharmacol Appl Skin Physiol 2002; 15:414–424.

60

Percutaneous Absorption of Arsenic from Environmental Media

Yvette W. Lowney and Michael V. Ruby
Exponent, Boulder, Colorado, U.S.A.

Ronald C. Wester, Xiao-Ying Hui, Sherry Barbadillo, and Howard I. Maibach
Department of Dermatology, School of Medicine, University of California, San Francisco, California, U.S.A.

Rosalind A. Schoof
Integral Consulting, Mercer Island, Washington, U.S.A.

Stewart E. Holm
Georgia-Pacific Corporation, Atlanta, Georgia, U.S.A.

I. INTRODUCTION

In the Middle Ages, arsenic was well known as a poison to the nobility, who employed (presumably expendable) food tasters to ensure that their wine, tea, or soup contained no dissolved arsenical threat to the noblemen's health. Arsenic's reputation as a poison persisted through the centuries and was again popularized in the 1940s play "Arsenic and Old Lace."

Today we face a different situation. Although arsenic is still available as a poison (e.g., pesticides), many other beneficial uses for the chemical have emerged, and it is used extensively in various industries and in specific products. As a result, arsenic has become distributed in the environment, and much study has been devoted to assessing the effects of environmental arsenic exposure on human health. Much of this research addresses the potential routes of exposure to arsenic; this chapter focuses on percutaneous absorption.

Applied research on percutaneous exposure of humans to arsenic spans the past decade, although some of the earlier research is not applicable to arsenic in solid environmental media, for reasons discussed below. Also presented are factors to consider in evaluating percutaneous absorption, essential features of effective study design, and appropriate application of results from in vivo testing of environmentally relevant media.

New interest has focused on the issue of percutaneous arsenic exposure because of the controversy surrounding lumber that is treated with chromated copper arsenate (CCA). CCA-treated wood has been used extensively to build playground

equipment, decks, and other structures, owing to the extended lifetime of CCA-treated wood as compared to its untreated counterparts. Because of the inherent toxicity of the arsenic and chromium used in CCA treatment, regulatory and public attention has become focused on the potential risks from this exposure source. In particular, exposure of children to arsenic from CCA-treated wood used in decks and play sets has received considerable attention. At this writing, a sizeable quantity of CCA-treated wood is in use in the United States. In Florida alone, there is approximately 540 million cubic feet of CCA-treated wood. This amounts to 24,308,390 kg of arsenic (1).

Recent research is summarized in this chapter, and implications for this field of inquiry are discussed. Finally, because arsenic occurs naturally in the environment and canbe detected in both drinking water and food, unique research needs include knowledge of pre-study levels of arsenic being absorbed through the diet. Such a baseline will facilitate correct interpretation of the data and provide appropriate risk communication.

II. TOXICITY OF ARSENIC FROM PERCUTANEOUS ABSORPTION

Current knowledge of the systemic toxicity of inorganic arsenic is derived primarily from studies in which humans have ingested arsenic, often as a medicine (e.g., Fowler's solution) or via contaminated drinking-water supplies, and from studies in which arsenic was administered orally or parenterally to laboratory animals. Human and animal studies indicate that, following oral administration, arsenic is distributed throughout the body (2). However, limited information exists concerning the distribution and toxic effects following percutaneous exposure (3). Currently, default assumptions are used in estimating percutaneously absorbed arsenic. Basically, an assumption is made that the systemic dose of arsenic achieved from percutaneous administration is the same as from oral administration. Assessment of risk from percutaneous exposure to arsenic currently relies on the use of oral toxicity data to assess risks for percutaneously absorbed doses. In the United States risk assessments for arsenic, the oral toxicity dose–response of arsenic is described by a reference dose and a cancer potency factor, which are derived from epidemiological studies of people exposed to soluble, inorganic arsenic in drinking water.

Other critical assumptions are also important features in the risk assessment. Reference doses and cancer potency factors are typically based on intake (administered doses) rather than on absorbed dose (delivered dose). Consequently, application of oral toxicity values to another exposure route requires several steps. First, an estimate of oral absorption must be used to convert the toxicity values to an absorbed dose (e.g., by multiplying the reference dose by the orally absorbed fraction of administered dose). Second, the percutaneously absorbed dose must be estimated and compared to the oral toxicity value. The critical underlying assumption for this procedure is that absorbed arsenic will elicit similar toxic effects, regardless of the exposure route. This assumption, in turn, is based on the assumption that the pharmacokinetic profile of arsenic will be the same regardless of exposure route. However, because orally absorbed inorganic arsenic is subject to a first-pass effect in the liver, where much of it is metabolized to monomethylarsenic and dimethylarsenic, differences in the pharmacokinetic profile of oral vs. percutaneous arsenic exposures are likely. An additional complication arises from the possibility that arsenic is

retained in the skin after percutaneous exposure, a factor that introduces uncertainty in estimating the percutaneously absorbed dose.

A. Percutaneous Absorption

For arsenic, the research that forms the basis for the standardized approach (4) to estimating the magnitude of percutaneous absorption was conducted in the early 1990s (5). This research used Rhesus monkeys to evaluate the percutaneous absorption of arsenic in two matrices: (1) soluble arsenic in aqueous solution and (2) soluble arsenic freshly mixed with soil (which may not be representative of arsenic in environmental samples), at two dose levels for each matrix. Radiolabeled arsenic (As^{73}) was applied to the abdomens of rhesus monkey's, and excretion of the radiolabel in the monkey's urine was measured. Because of the negligible background concentrations of As^{73} in monkey urine, and the low analytical detection limits for the radiolabel, absorbed arsenic from small applied doses could be detected. The results indicated in vivo percutaneous absorption values of 2.0% to 6.4% for arsenic in solution and 3.2% to 4.5% for arsenic mixed with soil (5).

However, the binding kinetics of arsenic in environmental samples, such as soil or sediment, can vary greatly from the samples used by Wester et al. Nonetheless, regulatory agencies have relied on the arsenic absorption data developed by Wester et al. (5) as the technical basis for specific absorption values (6,7a,7b). Consequently, evaluations indicate that percutaneous absorption may contribute significantly to overall risk (4). As discussed in section 2.2, data from biomonitoring studies of human populations exposed to arsenic from environmental sources suggest that percutaneous absorption of arsenic does not contribute significantly relative to other pathways of exposure (i.e., ingestion or inhalation). The apparent disconnect between the results that can be calculated based on Wester et al. (5) and the results of the biomonitoring Studies has suggested the need for new research using more relevant substrates.

B. Relative Contribution of the Percutaneous Pathway to Arsenic Exposure

Evidence from biomonitoring studies indicates that the standard exposure assessment assumptions for soil ingestion conservatively account for measured soil arsenic exposure, and that any additional exposure via percutaneous absorption is negligible. Two EPA studies (8,9) compared arsenic dose estimates via soil ingestion to measured urinary arsenic levels in human populations. In both studies, the calculated exposures either matched or overestimated the actual levels compared to the biomonitoring data. In summary, these studies found no contribution of arsenic dose due to percutaneous absorption. In other words, this indicates that the relative contribution of arsenic from the percutaneous pathway is negligible in comparison to the amount of exposure via oral intake. This likely is part of the rationale used in some risk assessments conducted by EPA in determining that percutaneous absorption of arsenic is unlikely to contribute significantly to overall exposures (e.g., Ref. 10).

C. Geochemical Controls on the Percutaneous Absorption of Arsenic

The geochemical factors that control the oral absorption of arsenic from environmental matrices have received considerable attention (11–13). These studies also

provide information on the geochemical factors that likely control percutaneous absorption of arsenic. In the case of oral absorption, primary factors that control bioavailability include the forms of arsenic present in soil (e.g., forms originally deposited in soil and forms that result from soil alteration processes), particle size of the arsenic-bearing grains, and morphology of the arsenic-bearing grains (12). Because arsenic in soil must be dissolved in gastrointestinal fluids for oral absorption to occur, the form of arsenic, and hence its solubility, is a particularly important determinant of the extent to which it will be bioavailable. Forms of arsenic with low solubility (e.g., arsenic sulfides [FeAsS], arsenic in phosphate minerals [$Ca_5(PO_4)_2$ $(AsO_4)Cl$]), or ones that are stable in acidic fluids (e.g., scorodite [$FeAsO_4$]) will yield low bioavailability, whereas arsenic forms with greater solubility (e.g., arsenic trioxide [AS_2O_3]) will be more bioavailable. In addition, the particle size of the arsenic forms controls the extent of bioavailability, with smaller particles producing greater bioavailability, due to increased surface area compared to larger particles. Finally, the morphology of the arsenic-bearing grains, in relation to other soil minerals, plays a role in determining arsenic solubility and bioavailability. For example, arsenic-bearing particles that are cemented together with less soluble mineral phases (such as iron oxides or clay) will be less available for dissolution, and thus will be less bioavailable. A schematic of how different arsenic species, particle sizes, and morphologies affect oral arsenic bioavailability is presented in Figure 1.

The situation with percutaneous absorption of arsenic from environmental matrices (such as soil, sediment, or CCA-treated wood) is analogous to that of oral absorption with the exception that the processes controlling dissolution of arsenic are much less aggressive. Leaching of arsenic in sweat is limited by the high solid-to-fluid ratio and a lack of mixing, while leaching in the gastrointestinal tract is enhanced by the acidic stomach fluid and mixing due to peristalsis. Thus, arsenic forms in soil that have limited solubility will exhibit negligible percutaneous absorption. For example, arsenic in the New York test soil described later in this chapter is

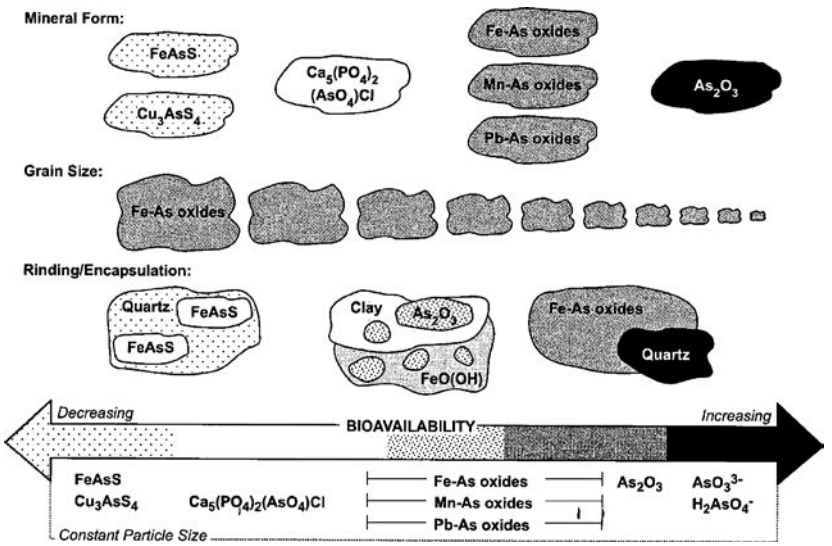


Figure 1 Schematic of how different arsenic species, particle sizes, and morphologies affect arsenic bioavailability.

present primarily in iron oxides and in iron silicate mineral forms. Because neither of these arsenic forms will liberate much arsenic in the presence of sweat (a near-neutral pH fluid with a salt content about equal to that of seawater), the percutaneous bioavailability of arsenic from this soil will be considerably less than that of soluble arsenic. These geochemical controls are the reason for the negligible percutaneous arsenic absorption from this soil.

D. Research on Environmentally Relevant Substrates

As described above, research on the percutaneous absorption of soluble arsenic administered to monkeys in water and freshly mixed with soil (5) produced mean percutaneous absorption rates in the range of 2.0 to 6.4% of the applied dose. Percent absorption did not vary across applied doses that ranged across five orders of magnitude (i.e., an applied dose range of 0.000024 to 2.1 $\mu g/cm^2$). Also, the absorption rates for arsenic from the test soil fell within the range of the rates for percutaneous absorption of the arsenic administered in water. Subsequently, questions arose as to whether the data on percutaneous absorption of soluble arsenic mixed with soil immediately prior to percutaneous application are representative of arsenic absorption from environmental media (4). Previously described factors such as arsenic form and the effects of weathering on environmental media all have the potential to affect the nature of arsenic, and its potential for percutaneous absorption. Therefore, additional research has been undertaken (discussed below) using methods similar to those used by Wester et al. (5) to assess percutaneous arsenic absorption from environmental media.

Models other than in vivo investigations using monkeys are available, including other animal models, in vitro models using human skin, and using synthetic substrates (14). Recent research into percutaneous absorption of arsenic from environmental substrates paralleled the Wester et al. (5) monkey study as closely as possible. In designing the new study, the researchers considered using in vitro techniques. However, for use in regulatory decision making, it is difficult to supplant current information from in vivo research with new results from in vitro testing. When conducted in parallel with in vivo studies using rhesus monkeys, research on the percutaneous absorption of arsenic, using in vitro methods with human cadaver skin, indicated somewhat lower absorption rates (i.e., <1 % from soil and $<2\%$ from water using the cadaver skin model, versus 4.5% and 6.4% from soil and water, respectively, from the in vivo methodology at similar dosing levels). It is not clear which of these models more closely mimics in vivo human percutaneous absorption, but the monkey model was selected because it is more conservative and has been shown to yield percutaneous absorption estimates only slightly greater than those of humans (15).

As described above, assessment of the risk associated with percutaneous exposure to arsenic requires estimation of a percutaneously absorbed dose. However, it is possible to estimate the variation in percutaneous absorption among exposure media without directly measuring the total dose absorbed. Such a comparison may yield an estimate of relative bioavailability. The default percutaneous absorption value used in risk assessment of arsenic in soil is 3% (4), based on the data reported in Wester et al. (5). Alternative assumptions may be supported by demonstrating a difference between the exposure matrix being assessed and the reference soil mixture. If the difference can be quantified, then the default bioavailability assumption can be revised.

Since recent studies of weathered soils could not rely on the use of an arsenic radioisotope to measure absorbed dose, it was particularly important to include a reference soil for purposes of comparison. Without reliance on a radioisotope, background exposures of the monkeys to naturally occurring arsenic from diet and drinking water were determined to be a significant limiting factor in the ability to detect percutaneously absorbed arsenic. Several approaches were attempted to increase study sensitivity: one was to provide a diet low in arsenic, in an attempt to attenuate baseline urinary arsenic concentrations, and another was to use a more sensitive analytical method that measured speciated arsenic (e.g., inorganic vs. methylated arsenic species) instead of total arsenic. The speciated arsenic analyses did not provide substantial benefits for quantifying absorbed arsenic, so the purified diet was used, despite palatability concerns, to reduce background urinary arsenic concentrations.

Note that measurement of relative bioavailability obviates the need for a mass balance determination. Mass balance evaluation, in which the total amount of a chemical that can be recovered in tissues and excreta is measured and compared to the administered dose, can be useful during bioavailability study method development. This can be especially important if there may be variations in pharmacokinetic behavior between different exposure routes. However, most absorbed arsenic is excreted rapidly in the urine, and this is true regardless of exposure route or exposure medium. Mass balance evaluation has been conducted previously for the monkey model used in these studies and demonstrated good recovery (5). Subsequent use of this model for estimates of relative bioavailability can reasonably rely on the prior mass balance determination, and focus on comparison of urinary arsenic excretion.

E. Key Considerations in Study Design

Along with the myriad issues that must be addressed in the design of research with biological systems, there are several issues that are unique to evaluation of percutaneous absorption from solid matrices. Among these are issues of particle size, appropriate application rates, and ensuring skin contact.

1. Particle Size Considerations

The chemical-bearing environmental media of interest for potential human exposures are limited to those media that an individual might contact. For soils, the soil depth horizon that is generally the focus of human health evaluations is 0 to 2 cm or 0 to 2 in of surface soil. For exposures that might occur from percutaneous absorption (or even for oral absorption of soil that might result from hand-to-mouth contact), the materials of appropriate focus are the subset of materials that adhere to the skin. Because larger particles fall off or are easily dislodged from the skin, the materials that are retained by the skin are the small particle size fraction (i.e., less than 150–250 μm in diameter, Ref. 16).

2. Application Rates

Existing literature and guidance from regulatory agencies provides a significant body of information regarding the rates at which soil adheres to skin, including loading during different activities and for different body parts (4,17–22). However, the amount of the matrix that may adhere to skin is not the appropriate target for dosing trials. As soil loading increases, the fraction absorbed will be constant until the sur-

face is uniformly covered by soil (4,17). From the "monolayer" present on the skin surface, percutaneous absorption is related to the direct interaction of the applied dose with the skin surface. As the loading onto the skin increases beyond monolayer coverage, the absorption is also affected by the ability of the chemical to migrate through the soil and to the surface of the skin. Therefore, once the monolayer of coverage is exceeded, then the fraction absorbed from the soil may decrease. Increasing the loading above the monolayer will bias the measured absorption low (when expressed as the fraction absorbed), for evaluating percutaneous absorption of arsenic from environmental samples. Estimates of soil adherence rates for a monolayer of different soil types (Soil Conservation Service soil classifications) are available (e.g., Ref. 4). For other matrices, it is important to understand the loading that is applied in order to ensure appropriate study design and interpretation of resulting data.

3. Ensuring Skin Contact

If the applied dose is not maintained in direct contact with the skin surface, resulting estimates of percutaneous absorption may be biased low. This is not a consideration in the application of aqueous doses, because direct contact of the skin with the material delivered in an aqueous dose is ensured after the material dries on the skin. However, for solid matrices applied to live animals, conscious effort must be directed at ensuring that the applied material is maintained in contact with the skin surface.

F. Statistical Evaluation

The statistical approach used to evaluate data must be targeted to the research study design. Because the number of animals that can be used in primate research is constrained, the crossover study design—wherein each individual animal is dosed in each dose group, and data from each individual monkey can be used as its own "comparison control"—was specifically selected for use in this research. This study design optimizes the potential to observe statistically significant results despite the small number of animals used. However, it does necessitate the use of specific statistical approaches that are consistent with the study design.

To determine whether the difference in the results for the two percutaneous exposure groups was statistically different from background or from each other, an ANOVA analysis followed by a Tukey's multiple comparison test should be conducted. In a study with a small number of animals, the variability among animals could be greater than the differences in absorption for different treatment groups; thus, statistical differences should be assessed after accounting for overall differences among monkeys. Because of the sequential nature of the data generated (i.e., at specified time points after dosing), analyses must also account for any time-dependent patterns present over the sampling period evaluated (e.g., comparing data within a given timepoint). The ANOVA model used to evaluate these data should include factors for monkey, time, and treatment group. The factor for monkey controls for inter-monkey differences in mass excreted, allowing each monkey to serve as its own control. Monkey number was included as a random factor, because the monkeys tested were not specifically of interest, but rather represented a random selection of monkeys. To incorporate the sampling order, time period was included in the ANOVA model as an ordered factor. After accounting for monkey and time period differences, the treatment factor (i.e., soluble or residue dose group) was assessed for significance and followed by Tukey's multiple comparison test to iden-

tify which treatments are different from one another, using an overall significance level of 0.05% or 95% confidence.

III. STUDY DESIGN

The rhesus monkey model was used to measure the percutaneous absorption of arsenic from water, from an environmental soil sample, and from residues collected from the surface of CCA-treated wood. An open crossover design was used, in which each animal is dosed with each of the test materials (soluble arsenic in solution applied to the skin, arsenic-bearing soil applied to the skin, CCA residue applied to the skin, and intravenous [IV] injection), with a washout period of at least 14 days between each dose. This crossover design allows for each animal to serve as its own internal control. Total concentrations of arsenic from the four dosing test materials (IV, soluble, soil, and CCA wood residue) are presented in Table 1. The intravenous dose (1060 μg arsenic/monkey) was administered as a solution of sodium arsenate heptahydrate in de-ionized (DI) water (2120 mg/L arsenic). For the intravenous dose, each monkey received 0.5 mL of the dosing solution injected into the saphenous vein. The intravenous dose was given while the monkeys were in their metabolic cages, so the monkeys did not spend any time in the metabolic restraint chairs, as they did with the topical doses.

For the soluble arsenic dose, arsenic was administered in water onto the monkey's skin at an application rate of 5 $\mu L/cm^2$ applied evenly across 100 cm^2 of skin, to achieve a total percutaneous dose of 1430 μg arsenic. The solution was prepared from sodium arsenate heptahydrate in DI water, which was acidified with 1% nitric acid (trace-metal grade).

The soil sample used in the percutaneous absorption study was a surficial soil (0–3 in) collected adjacent to a pesticide production facility that had historically produced arsenical pesticides. Arsenic in this soil most likely resulted from overland transport in storm water from the facility. Based on site activities, arsenic would have been resident in this soil for a minimum of 30 years and possibly as long as 60 years. Although calcium and lead arsenate compounds were produced at this facility, studies of arsenic mineralogy in surficial soils collected near where the test

Table 1 Arsenic Doses Given During Recent and Earlier Dermal Absorption Studies

Study		Arsenic concentration in dosing material	Volume of dosing material administered	Arsenic mass dosed (μg)	Arsenic mass per unit area ($\mu g/cm^2$)
Soluble dose		2,860 mg/L[a]	0.5 mL	1,430	14.3
Soil		1,400 μg/g (dry)	400 mg	560	5.6
CCA residue		3,555 μg/g (wet)[a]	400 mg	1,422	14.2
Intravenous dose		2,120 mg/L	0.5 mL	1,060	—
Soluble dose;	High dose	—	0.06 mL	76	2.1
Ref. 5	Low dose	—	0.06 mL	0.00086	0.000024

Note: —, not available or not applicable.
[a]Average of duplicate analyses.

soil was obtained indicated that arsenic now occurs primarily in iron oxide and iron silicate mineral phases. The particle size fraction used for the percutaneous absorption study was $<150\,\mu m$. For very fine soil (i.e., silty clay), a loading of $5.4\,mg/cm^2$ of skin results in a monolayer (7). In order not to exceed a monolayer of application, a percutaneous loading rate of $4\,mg/cm^2$ was selected for study of this soil. Application of $4\,mg/cm^2$ on $100\ cm^2$ of skin resulted in a total dose of $560\,\mu g$ arsenic. The soil was applied dry and spread evenly across the exposure area.

The CCA residue, in the form of a fine particulate, was supplied by the American Chemistry Council (23), and represents the material present on the surface of weathered CCA-treated wood, which an individual might contact during use of, or play on, structures made of treated wood. Because the residue appears similar in particle size distribution to silty clay, and a loading rate of $4\,mg/cm^2$ of the residue provides complete coverage on a flat surface, a loading rate of $4\,mg/cm^2$ was selected for this study. Application of $4\,mg/cm^2$ on $100\,cm^2$ of skin area resulted in a total dose of $1422\,\mu g$ arsenic. The residue was applied as a dry powder, and spread in an even layer across the exposure area.

A. Test Animals

Female Rhesus monkeys were selected because of their ability to duplicate the biodynamics of percutaneous absorption in humans (19,24), and because previous studies of percutaneous arsenic absorption have used this same model (5). Prior research indicates that percutaneous absorption in the Rhesus monkey is similar to absorption in humans across a variety of chemicals and a range of percutaneous penetration characteristics (15). This research indicates that measurements from the monkey are just slightly higher than their counterparts in the human. Results from other species (pig, rat, and rabbit) are not nearly as close to the values measured in man, and indicate that, of the species tested, absorption in the monkey is closest to that in the human.

The monkeys tested were approximately 20 years old, which is the same approximate age as the monkeys used in the previous percutaneous arsenic absorption research (5). The animals reside within the monkey colony maintained by the University of California, San Francisco, and had not been used for active research for 18 months. Prior to the beginning of the current series of studies, no topical doses had been applied to the skin of these animals for more than 4 years.

1. Background Exposures from Diet

Significant exposure to arsenic occurs from the normal diet of monkeys, as it does with humans (25–27). Urinary excretion of total arsenic for Rhesus monkeys on a standard diet of Purina Monkey Chow falls in the range of 5 to $15\,\mu g$/day—levels that would obscure accurate detection of the arsenic that might be absorbed following topical application of arsenic. Therefore, the monkeys were provided a low-arsenic diet (Primate Liquidiet from BioServe Inc.) for seven days prior to each dose. The powdered Liquidiet formulation was prepared into meal bars, which were provided ad libitum to the monkeys during the research period (seven days prior to dosing through seven days after dosing). The diet was supplemented with pieces of banana and apple, which are both known to be low in total arsenic (25). DI water was provided ad libitum. The liquid diet was provided as both liquid and solid forms. The monkeys demonstrated a preference for the solid form, and maintained their

body weight during the study. Full methodological details for this in vivo model have been presented elsewhere (28).

B. Results from Testing of Environmental Samples

Data for the mass of urinary arsenic excreted by the monkeys following percutaneous dosing are presented in Table 2 (soluble arsenic), Table 3 (soil), Table 4 (CCA residue), and Table 5 (intravenous dose). Data on the background arsenic excretion for each monkey for the days prior to the dosing period are included. The value reported for the 0 to 24-hour period is the combined arsenic mass from the urine collected during the eight hour dosing period, a wash of the urine collection pan, and the urine collected from 8 to 24 hours after the monkeys were returned to their cages. The right-most column in each of these tables presents the mass of arsenic excreted for each 24-hour period, corrected for background levels of arsenic in urine, on a monkey-specific basis. This correction was applied to the data to reduce the influence of dietary arsenic on the excreted arsenic mass. The mass of arsenic excreted that is associated with the percutaneously applied dose is calculated by adding the mass excreted from the time of dosing through 96 hours after dosing. After 96 hours, the arsenic excretion has returned to background levels.

Prior research indicates that, for female rhesus monkeys, urinary excretion of an intravenous dose of arsenic was $80 \pm 6.7\%$ of the administered dose (5). The intravenous dose given during this study resulted in $82.1 \pm 2.2\%$ of the administered arsenic dose excreted in urine (28).

For the soluble dose, absorption rates were 3.4%, 0.62%, and 4.4% for the three monkeys in the study (Table 2), resulting in an average value of 2.8% (Table 5). Despite the nearly sevenfold difference in the percutaneous loading rates of soluble arsenic between the this study and that of Wester et al. (Ref. 5; comparison to "high" dose), the extent of arsenic absorption was equivalent. These results are consistent with the Wester et al. (5) study, wherein absorption rates were relatively steady (range of 2–6.4%), despite a five-orders-of-magnitude change in the dose levels (i.e., an applied dose range of 0.000024–2.1 $\mu g/cm^2$). These data strongly support the suggestion that the difference in the measured absorption rates in Wester et al. (5) research reflects experimental variability rather than dose-related differences in absorption (7). This is compatible with our understanding of individual variability in percutaneous absorption in humans and animals (29,30).

Converse to the results for soluble arsenic, data from percutaneous application of soil or CCA residue indicate virtually no absorption. Absorption rates following percutaneous application of soil and residue are presented in Tables 3 and 4, respectively: urinary excretion of arsenic following percutaneous application of arsenic in these environmental media does not cause a detectable increase in urinary arsenic excretion.

The time profiles for urinary arsenic excretion by each monkey following percutaneous application of arsenic (soluble, soil, or CCA residue) are provided in Figure 2. These charts show a consistent time course for the three monkeys: peak excretion of absorbed arsenic occurs within 24 hours of the percutaneous application of the soluble dose, with a rapid return to near-background levels of excretion within 48 to 72 hours. Peak 24-hour urinary arsenic excretion following the soluble dose ranged up to a maximum value of 41.6 μg. The time profile for arsenic excretion following percutaneous application of the soil CCA residue is also consistent across all

Table 2 Urinary Arsenic Data Following Dermal Application of Arsenic in Soluble Dose

	24-hr mass excreted (μg)	24-hr mass excreted (corrected) (μg)
Animal 1		
Background (24–48 hr)	5.07	0.00
Background (0–24 hr)	1.56	0.00
0–24 hr	41.58[b]	35.50
24–48 hr	7.22	1.13
48–72 hr	8.08	1.99
72–96 hr	7.21	1.12
	Total arsenic mass excreted (0–96 hr):	39.74
Total arsenic mass excreted with urinary arsenic excretion fraction correction (0–96 hr):		48.41[c]
	Percent absorption (0–96 hr):	3.4%[d]
Animal 2		
Background (24–48 hr)	6.30	0.82
Background (0–24 hr)	7.08	1.61
0–24 hr	10.22[b]	4.75
24–48 hr	6.96	1.48
48–72 hr	5.32	0.00
72–96 hr	6.53	1.05
	Total arsenic mass excreted (0–96 hr):	7.28
Total arsenic mass excreted with urinary arsenic excretion fraction correction (0–96 hr):		8.87[c]
	Percent absorption (0–96 hr):	0.62%[d]

(*Continued*)

Table 2 Urinary Arsenic Data Following Dermal Application of Arsenic in Soluble Dose (*Continued*)

	24-hr mass excreted (μg)	24-hr mass excreted (corrected) (μg)
Animal 3		
Background (24–48 hr)	5.20	1.79
Background (0–24 hr)	3.07	0.00
0–24 hr	30.35[b]	26.94
24–48 hr	20.98	17.56
48–72 hr	4.52	1.10
72–96 hr	9.16	5.75
Total arsenic mass excreted (0–96 hr):		51.35
Total arsenic mass excreted with urinary arsenic excretion fraction correction (0–96 hr):		62.55[c]
Percent absorption (0–96 hr):		4.4%[d]

[a]Corrected mass calculated by subtracting median of the eight background arsenic masses for each monkey. If corrected mass is calculated less than zero, corrected mass is set to zero.
[b]Sum of (zero to eight hours), pan wash, and (8–24 hours). Pan wash concentration is calculated using pan wash concentration minus average of wash water concentrations.
[c]Calculated by correcting excreted mass for fractional excretion of arsenic from IV dose (i.e., 0.821% or 82.1 %).
[d]Percent absorption calculated using soluble applied dose mass of 1,430 μg.

Table 3 Urinary Arsenic Data Following Dermal Application of Arsenic in Soil

	24-hour mass excreted (corrected) (μg)	24-hour mass excreted (μg)
Animal 1		
Background (48–72 hr)	2.29	0.60
Background (24–48 hr)	1.70	0.01
Background (0–24 hr)	1.07	0.00
0–24 hr	2.22[a]	0.53
24–48 hr	0.80	0.00
48–72 hr	0.78[c]	0.00
72–96 hr	0.78[c]	0.00
Total arsenic mass excreted (0–96 hr):		0.53
Total arsenic mass excreted with urinary arsenic excretion fraction correction (0–96 hr):		0.65[d]
Percent absorption (0–96 hr):		0.12%[e]
Animal 2		
Background (48–72 hr)	1.53	0.25
Background (24–48 hr)	1.81	0.53
Background (0–24 hr)	0.50	0.00
0–24 hr	1.10[b]	0.00
24–48 hr	0.97	0.00
48–72 hr	1.30[c]	0.02
72–96 hr	1.30[c]	0.02
Total arsenic mass excreted (0–96 hr):		0.05
Total arsenic mass excreted with urinary arsenic excretion fraction correction (0–96 hr):		0.06[d]
Percent absorption (0–96 hr):		0.01%[e]

(*Continued*)

Table 3 Urinary Arsenic Data Following Dermal Application of Arsenic in Soil (*Continued*)

	24-hour mass excreted (corrected) (μg)	24-hour mass excreted (μg)
Animal 3		
Background (48–72 hr)	1.75	0.16
Background (24–48 hr)	1.80	0.20
Background (0–24 hr)	1.23	0.00
0–24 hr	2.42[b]	0.83
24–48 hr	1.88	0.29
48–72 hr	1.46[c]	0.00
72–96 hr	1.46[c]	0.00
Total arsenic mass excreted (0-96 hr):		1.12
Total arsenic mass excreted with urinary arsenic excretion fraction correction (0–96 hr):		1.37[d]
Percent absorption (0–96 hr):		0.24%[e]

[a]Corrected mass calculated by subtracting average of the background arsenic masses by monkey and by dose. If corrected mass is calculated less than zero, corrected mass is set to zero.
[b]Sum of (zero to eight hours), pan wash, (8–24 hours), and cage wash (8–24 hours).
[c]24-hour mass excreted is estimated as half of 48 to 96–hour sample mass.
[d]Calculated by correcting excreted mass for fractional excretion of arsenic from IV dose (i.e., 0.82% or 82%).
[e]Percent absorption calculated using applied dose mass of 560 μg for soil applied dermaily.

Table 4 Urinary Arsenic Data Following Dermal Application of Arsenic in Chromated Copper Arsenate (CCA) Residue

	24-hr mass excreted (μg)	24-hr mass excreted (corrected[a]) (μg)
Animal 1		
Background (96–120 hr)	7.88	1.79
Background (48–72 hr)	6.44	0.35
Background (0–24 hr)	5.73	0.00
0–24 hr	4.84[b]	0.00
24–48 hr	4.90	0.00
48–72 hr	4.86	0.00
72–96 hr	5.89[c]	0.00
	Total arsenic mass excreted (0–96 hr):	0.00
Total arsenic mass excreted with urinary arsenic excretion fraction correction (0-96 hr):		0.00[d]
	Percent absorption (0–96 hr):	0.00%[e,f]
Animal 2		
Background (96–120 hr)	5.79	0.32
Background (48–72 hr)	1.92	0.00
Background (0–24 hr)	4.59	0.00
0–24 hr	4.17[b]	0.00
24–48 hr	2.93	0.00
48–72 hr	3.77	0.00
72–96 hr	3.78[c]	0.00
	Total arsenic mass excreted (0–96 hr):	0.00
Total arsenic mass excreted with urinary arsenic excretion fraction correction (0–96 hr):		0.00[d]
	Percent absorption (0–96 hr):	0.00%[e,f]

(*Continued*)

Table 4 Urinary Arsenic Data Following Dermal Application of Arsenic in Chromated Copper Arsenate (CCA) Residue (*Continued*)

	24-hr mass excreted (μg)	24-hr mass excreted (corrected[a]) (μg)
Animal 3		
Background (96–120 hr)	4.40	0.99
Background (48–72 hr)	4.88	1.47
Background (0–24 hr)	3.44	0.03
0–24 hr	4.24[b]	0.83
24–48 hr	3.26	0.00
48–72 hr	3.94	0.53
72–96 hr	3.39[c]	0.00
Total arsenic mass excreted (0–96 hr):		1.37
Total arsenic mass excreted with urinary arsenic excretion fraction correction (0–96 hr):		1.66[d]
Percent absorption (0–96 hr):		0.12%[e,f]

[a]Corrected mass calculated by subtracting median of the eight background arsenic masses for each monkey. If corrected mass is calculated less than zero, corrected mass is set to zero.
[b]Sum of (zero to eight hours), pan wash, and (8–24 hours).
[c]24-hour mass excreted is estimated as one fourth 72 to 168–hour sample mass.
[d]Calculated by correcting excreted mass for fractional excretion of arsenic from IV dose (i.e., 0.821% or 82.1%).
[e]Percent absorption calculated using CCA residue applied dose mass of 1,422 μg.
[f]Not statistically different from background.

Table 5 Summary of Dermal Arsenic Absorption Values from Various Dosing Substrates

	Percent absorption	
Substrate	Average ± SD	Range
Soluble dose	2.8 ± 1.9	0.62 – 4.4
Soil	0.12 ± 0.12	0.01 – 0.24
CCA residue	0.04 ± 0.07	0.00 – 0.12
Ref. 5		
Soluble		
Low dose	6.4 ± 3.9	—
High dose	2.0 ± 1.2	—
Soluble mixed with soil		
Low dose	4.5 ± 3.2	—
High dose	3.2 ± 1.9	—

Note: —, not available or not applicable.
Not statistically different from background for any monkey.

three monkeys. Figure 2 depicts that, following application of soil or the CCA residue, there is no increase in urinary arsenic excretion, followed out through time.

Results indicate that the urinary arsenic excretion levels in the animals exposed to arsenic in the soil sample or the CCA residue are not statistically greater than background. The range of daily urinary excretion following exposure to CCA residue falls well within the range of background urinary arsenic excretion. Conversely, the urinary arsenic excretion in the animals exposed to soluble arsenic in solution is significantly greater than background, and significantly greater than the soil and residue exposure groups.

The in vivo results for percutaneous absorption of arsenic from CCA residue and arsenic-bearing soil are consistent with the physical limitations to arsenic dissolution from these test materials. Arsenic in the CCA residue is present primarily as a chromium/arsenic metal cluster consisting of a chromium dimer bridged by an arsenic (V) oxyanion, with the chromium molecules bound to carboxyl groups of the wood structure (31). As a result, arsenic in the CCA residue is not available for dissolution at the skin surface and thus cannot be absorbed by this route. In the case of the test soil, arsenic is present primarily in iron oxide and iron silicate mineral phases, with small amounts present as calcium arsenate and arsenic trioxide. In this case, arsenic could be slightly more bioavailable than from the CCA residue, due to the presence of some soluble arsenic phases (calcium arsenate and arsenic trioxide) and the potential for arsenic that is weakly adsorbed to soil surfaces to become available. However, the bulk of arsenic in the soil sample is still unavailable for percutaneous absorption due to its presence in sparingly soluble mineral phases. This premise is borne out by the absence of detectable percutaneous absorption of arsenic from the test soil, relative to soluble arsenic.

IV. CONCLUSIONS

Many factors may affect the percutaneous absorption of arsenic from environmental media, and arsenic in these substrates cannot be assumed to be absorbed to the same degree as soluble arsenic in solution. The development of an appropriate research

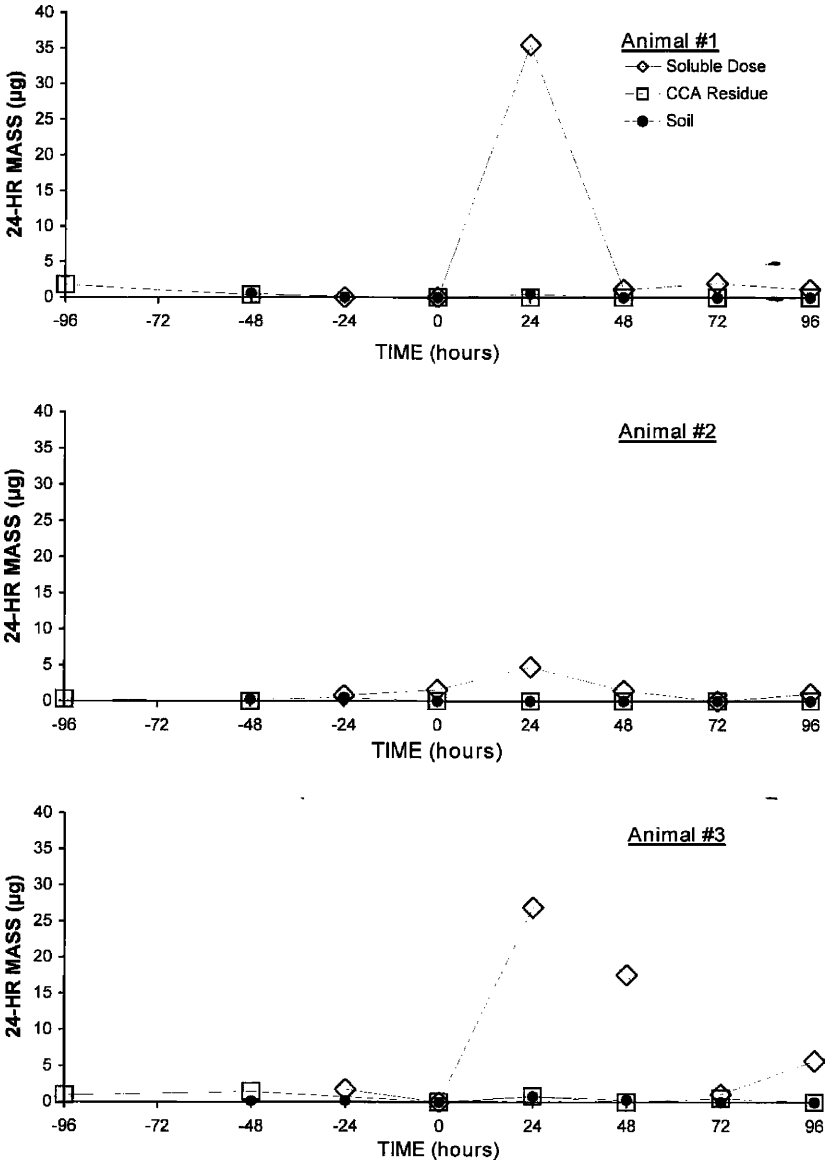


Figure 2 Time profile for arsenic excretion

method to test percutaneous absorption of arsenic from environmental media was challenging, due to analytical limitations and the need to accurately replicate expected exposure conditions. The magnitude of background arsenic exposure from the diet and the potential for that background exposure to obscure any signal from a percutaneously applied dose of arsenic were particularly problematic.

The results indicate that percutaneous absorption of arsenic from environmental media is negligible compared to soluble arsenic and soluble arsenic mixed with soil. The finding that the percutaneous absorption of arsenic from the environmental media evaluated is much lower than for arsenic in solution is consistent with our understanding of the chemistry of arsenic in the tested substrates. More generally,

there are likely to be many site- or sample-specific factors that will control the absorption of arsenic, and matrix-specific analyses may be required to understand the degree of percutaneous absorption. Studies conducted to date suggest that percutaneous arsenic absorption is not a risk factor for the media tested. This may be true for other metals that form similarly stable complexes in the environment. These results show that issues such as arsenic in children's playground equipment and in the soil can be studied effectively, and the results can be applied in estimating potential human health hazards.

REFERENCES

1. Townsend T, Stook K, Tolaymat T, Song J, Solo-Gabriele H, Hosein N, Khan B. New lines of CCA-treated wood research: in-service and disposal issues. Report submitted to the Florida Center for Solid and Hazardous Waste Management, 2001.
2. ATSDR. Toxicological profile for arsenic. U.S. Department of Health and Human Services, Agency for Toxic Substances and Disease Registry. September, 2000.
3. NRC. Arsenic in drinking water. Washington, DC: National Research Council, National Academies Press, 1999..
4. U.S. EPA. Risk Assessment Guidance for Superfund-Volume I: Human Health Evaluation Manual (Part E, Supplemental Guidance for Dermal Risk Assessment, Interim Review Draft. EPA/540/R/99/005. OSWER Directive 9285.7-02. Washington, DC: U.S. Environmental Protection Agency, Office of Emergency and Remedial Response, http://www.epa.gov/oerrpage/superfund/programs/risk/ragse/introduction.pdf. 2001a.
5. Wester RC, Maibach HI, Sedik L, Melendres J, Wade M. In vivo and in vitro percutaneous absorption and skin decontamination of arsenic from water and soil. Fund Appl Toxicol 1993; 20:336–340.
6. U.S. EPA. Risk Assessment Guidance for Superfund, Volume I: Human Health Evaluation Manual Supplemental Guidance; Dermal Risk Assessment Interim Guidance. Washington, DC: U.S. Environmental Protection Agency, 1998.

7a. U.S. EPA. Children's Exposure to CCA-Treated Wood Playground Equipment and CCA-Contaminated Soil. Washington, DC: U.S. Environmental Protection Agency, Office of Pesticide Programs, 2001b.

7b. U.S. EPA. 2004. Integrated Risk Information System. Entry for inorganic arsenic last updated December 3, 2002. Accessed July 2004 at http://www.epa.gov/iris/subst/0278.htm.

8. Glass GL, SAIC. Baseline risk assessment Ruston/North Tacoma Operable Unit, Commencement Bay Nearshore/Tideflats Superfund site, Tacoma, Washington. Prepared for U.S. EPA Region 10. Science Applications International Corporation, Bothell, WA. January, 1992.
9. Walker S, Griffin S. Site-specific data confirm arsenic exposure predicted by the U.S. Environmental Protection Agency. Environ Health Persp 1998; 106(3):133–139.
10. U.S. EPA Butte Priority Soils Operable Unit Baseline Human Health Risk Assessment for Arsenic. Silver Bow Creek/Butte area NPL Site. Prepared for U.S. Environmental Protection Agency, Region VIII, Montana Ofice. Golden, Colorado: CDM Federal Programs Corporation, 1996.
11. Davis A, Ruby MV, Bloom M, Schoof R, Freeman G, Bergstrom PD. Mineralogic constraints on the bioavailability of arsenic in smelter-impacted soils. Environ Sci Technol 1996; 30(2):392–399.
12. Ruby MV, Schoof R, Brattin W, Goldade M et al. Advances in evaluating the oral bioavailability of inorganics in soil for use in human health risk assessment. Environ Sci Technol 1999; 33(21):3697–3705..

13. Kelly ME, Brauning SE, Schoof RA, Ruby MV. Assessing Oral Bioavailability of Metals in Soil. Columbus, Ohio: Battelle Press, 2002.
14. U.S. EPA Dermal exposure assessment: Principles and applications. Office of Health and Environmental Assessment. EPA/600/8-91/011B. Washington, DC: U.S. Environmental Protection Agency, 1992.
15. Wester RC, Maibach HI. Percutaneous absorption in the rhesus monkey compared to man. Tox Appl Pharmacol 1975; 32:394–398.
16. Duggan MJ, Inskip MJ. Childhood exposure to lead in surface dust and soil: a community health problem. Public Health Rev 1985; 13:1–54.
17. Duff R, Kissel J. Effect of soil loading on dermal absorption efficiency from contaminated soils. J Toxicol Environ Health 1996; 48(1):93–106.
18. Holmes K, Shirai J, Richter K, Kissel J. Field measurement of dermal soil loadings in occupational and recreational activities. Environ Res 1999; 80:148–157.
19. Kissel J, Richter K, Fenske R. Investigation of factors affecting soil adherence to skin using a hand-press technique. Bull Environ Contam Toxicol 1996; 56(5):722–728.
20. Kissel J, Shirai J, Richter K, Fenske R. Investigation of dermal contact with soil in controlled trials. J Soil Contam 1998; 7(6):737–752.
21. Lepow ML, Bruckman L, Gillette M, Markowitz S, Robino R, Kapish J. Investigations into sources of lead in the environment of urban children. Environ Res 1975; 10:415–426.
22. Roels HA, Buchet JP, Lauwerys RR, Bruaux P, Claeys-Thoreau F, Lafontaine A, Verduyn G. Exposure to lead by the oral and pulmonary routes of children living in the vicinity of a primary lead smelter. Environ Res 1980; 22:81–94.
23. American Chemistry Council (ACC). Dislodgeable material collection procedure. CCA-Treated Wood Work Group. May 12, 2003.
24. Wester RC, Maibach HI. In vivo animal models for percutaneous absorption. In: Brouaugh R, Maibach H, eds. Percutaneous Absorption. 2nd ed. New York: Marcel Dekker, 1989:221–238.
25. Schoof RA, Yost LJ, Eickhoff J, et al. A market basket survey of inorganicarsenic in food. Food Chem Toxicol 1999a; 37(8):839–846.
26. Schoof RA, Eickhoff J, Yost LJ, Crecelius EA, Cragin DW, Meacher DM, Menzel DB. Dietary exposure to inorganic arsenic. Proceedings of the Third International Conference on Arsenic Exposure and Health Effects. Chappell WR, Abernathy CO, Calderon RL. eds. Elsevier Science Ltd. 1999.
27. Yost LJ, Tao SH, Egan SK, Barraj LM, Smith KM, Tsuji JS, Lowney YW, Schoof RA, Rachman NJ. Estimation of dietary intake of inorganic arsenic in U.S. children. Human Ecol Risk Assess 2004; 10:473–483.
28. Wester RC, Hui X, Barbadillo S, Maibach HI, Lowney YW, Schoof RA, Holm SE, Ruby MV. In vivo percutaneous absorption of arsenic from water and cca-treated wood residue. Toxicol Sci 2004; 79:287–295.
29. Wester RC, Maibach HI. Individual and regional variation with In vitropercutaneous absorption. In: Brouaugh R, Maibach H, eds. In Vitro Percutaneous Absorption. Boca Raton, FL: CRC Press, 1991:25–30.
30. Wester RC, Maibach HI. Toxicokinetics: dermal exposure and absorption of toxicants. In: Bond J, ed. Comprehensive Toxicology, Vol. 1. General Principles. Oxford, UK: Elsevier Science, Ltd,1997:99–114.
31. Nico P, Fendorf S, Lowney Y, Holm S, Ruby M. (in press). Chemical structure of arsenic and chromium in CCA-treated wood: implications of environmental weathering. Environ Sci Technol 2004.

61

Clinical Testing of Microneedles for Transdermal Drug Delivery*

Raja K. Sivamani and Gabriel C. Wu
UCSF/UC Berkeley Joint Department of Bioengineering, University of California, San Francisco, California, U.S.A.

Boris Stoeber and Dorian Liepmann
University of California, Berkeley, California, U.S.A.

Hongbo Zhai and Howard I. Maibach
Department of Dermatology, School of Medicine, University of California, San Francisco, California, U.S.A.

I. INTRODUCTION

Much research has been done in developing drug delivery methods different from traditional oral ingestion and hypodermic needle injections. Oral and subdermal delivery routes are successful methods of drug delivery but have drawbacks that can affect efficacy and patient comfort. Orally ingested drugs pass through the acidic environment of the stomach and then are absorbed in the intestines. The acid in the stomach can degrade or denature many drugs and serves as one barrier in oral ingestion. When the drug passes through the stomach, it must be small enough to be absorbed through the intestinal wall. Larger drugs, like insulin, are not absorbed through the intestinal wall and are ineffective when taken orally. Once the drug passes through the intestinal wall, it then passes through the hepatic circulation and the drug can be significantly cleared by the liver before passing onto the rest of the body. Only then, can the drug take effect. As a result, the bioavailability of orally ingested drugs can be low. Also, because the drug must pass through the liver, drugs that have significant liver toxicity would not be suitable as an oral drug agent.

A major barrier to transdermal drug delivery is the stratum corneum, the 10 to 15–μm thick outer layer of skin. Traditionally, hypodermic needles have been used to pierce through this barrier and deliver various types of drugs, vaccines, and treatments. Hypodermic needle injections allow for solubilized drugs to be delivered directly into or near the bloodstream. This method has an advantage over oral delivery in that it is

* Notified with permission from Skin Research and Technology.

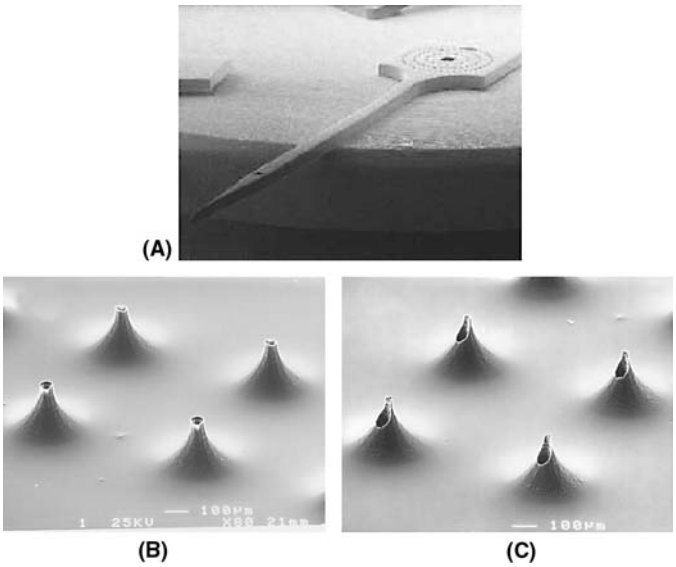


Figure 1 Silicon microneedles. (**A**) In-plane microneedle (5), (**B**) symmetric hollow microneedles, and (**C**) pointed hollow microneedles. The symmetric and pointed hollow microneedles are approximately 200-μm high with a lumen diameter of 40 μm.

effective for delivering drugs of larger sizes and the drugs do not have to pass through the liver and undergo metabolism before reaching systemic blood circulation. Although effective in drug delivery, a major drawback of hypodermic needles is that they cause pain and many patients have needle phobia (1,2). However, recent applications of semiconductor fabrication techniques led to the development of microneedles.

Microneedles are designed to pierce and successfully deliver injections past the stratum corneum, but are too short to stimulate the pain nerves (3,4). Microneedles exist in two basic designs: in-plane and out-of-plane (Fig. 1). In-plane microneedles have been integrated with circuitry, pumps, and sensors (5–7) and have been used in clinical tests to measure blood glucose levels (8). Reed and Lye (9) provide an extensive review of in-plane microneedle fabrication methods. In-plane microneedles are more easily integrated with electronic processes, but a disadvantage is that fabrication is restricted to one-dimensional arrays (9). Out-of-plane microneedles can be incorporated into two-dimensional arrays that allows for drug delivery over a greater area, similar in design to a ''patch.''

Out-of-plane microneedles have been fabricated in several designs. Solid microneedles have been shown to increase skin permeability (3). Hollow microneedles were subsequently developed so that fluid could be injected through them (10–13). Although most microneedles have been fabricated out of silicon, others have been fabricated from glass (11), metal (11), and polymers (11,14). Stoeber and Liepmann (10) fabricated a microsyringe backing along with the microneedle array and measured in vitro dye injection depths of 75 to 100 μm. Some in vivo injection studies have been performed with out-of-plane microneedles but few human studies have been done. Kaushik et al. (4) carried out the first human study to show that microneedles were painless upon insertion. Sivamani et al. (15) performed clinical injection studies and showed that microneedles helped compounds bypass the stratum corneum more quickly. Prausnitz (16) provides an overview of solid microneedle in vivo

studies that investigate insulin permeability and vaccine delivery. McAllister et al. (11) used a single glass microneedle to inject insulin into diabetic rats and reduce their blood glucose by 70%. Gardeniers et al. (12) infused insulin into diabetic rats through a microneedle array and showed that it was comparable to subcutaneous insulin injection. Matsuda and Mizutani (14) implanted polymer microneedles for a month in rats to study the polymer degradation characteristics.

Microneedles can serve as a painless drug delivery alternative because they are too short to stimulate pain nerve endings, but long enough to bypass the stratum corneum. One could imagine that an array of microneedles could be used to deliver painless vaccines to adults and children, and that microneedle ''patches'' could be worn for continual painless delivery of drugs, such as insulin for diabetics. Clinical tests with microneedles were carried out by Kaushik et al. (4) and Sivamani et al. (15), showing their potential utility in humans.

II. CLINICAL STUDIES

Kaushik et al. (4) performed a pain study that asked volunteers to rate their pain when microneedles were inserted into their skin. When compared against a flat piece of silicon and a hypodermic needle, human subjects rated the microneedles to be similar to a flat piece of silicon. Both the microneedles and the smooth piece of silicon were rated as zero on a 0 to 40 scale suggesting that the microneedles were painless upon insertion.

Sivamani et al. (15) performed a clinical injection study to investigate if microneedles enhanced percutaneous penetration of methyl nicotinate. In their study they used two types of microneedles as shown in Figures 1A, B and glued them onto a syringe as shown in Figure 2. Methyl nicotinate is a vasodilator that has been used in many studies of percutaneous penetration (17–22). Methyl nicotinate induced dilation of surface capillaries have been shown to follow circadian rhythms (23) with the maximum being at about noon and the minimum being at about midnight.

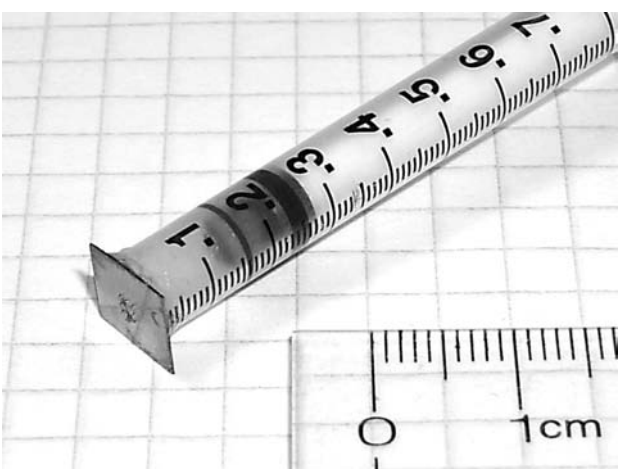


Figure 2 Microneedles on syringe. Eight-needle array of microneedles glued onto the tip of a syringe.

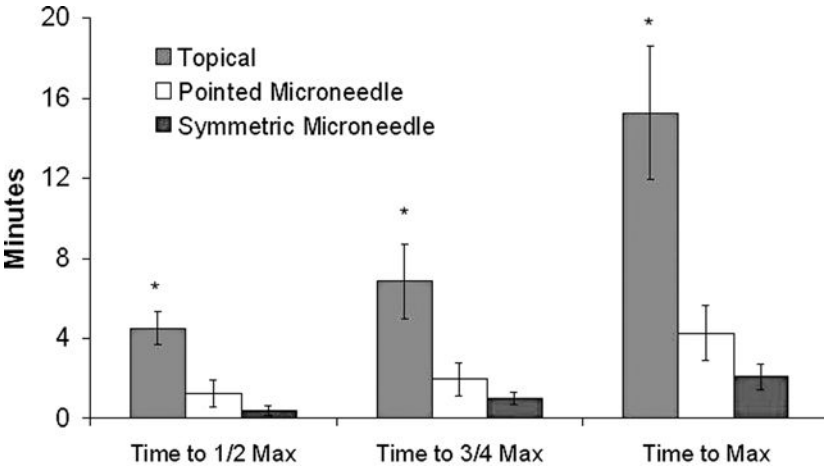


Figure 3 Time to reach maximum blood flux. Following 30 second treatments with methyl nicotinate, times to reach maximum flux were significantly longer for the topical treatment ($p < 0.05$). The pointed and the symmetric microneedle treatments were not statistically different in times to maximum blood flux.

Because of this, the experiments were carried out at the same times each day to make the results comparable to one another. Measurement of the blood flow through the skin capillaries was measured with a Laser Doppler Perfusion Monitor DRT-4 (Moor Instrument, Devon, England). Baseline blood flows of each volunteer were measured before application of the methyl nicotinate. In this way, each volunteers served as their own control.

Injections and topical applications of 0.1 M methyl nicotinate (Sigma, St. Louis, Missouri, U.S.A) were administered to the volar forearms. Four treatments were carried out with each patient: topical application (TA), pointed microneedle injection (PMn), symmetric microneedle (SMn), microneedle control (MnC). The microneedle control refers to pressing an empty syringe/microneedle device on the arm. Each treatment was applied for 30 seconds over 1 cm^2.

Maximum blood fluxes and the time to reach maximum flux were measured. Both pointed and symmetric hollow microneedles (Fig. 3) significantly decreased time to maximum blood flux compared to topical application of methyl nicotinate, but were statistically comparable to each other ($p = 0.09$). However, the pointed microneedle injections showed a higher maximum blood flux than symmetric microneedle injection or topical application (Fig. 4). The symmetric microneedle and topical application of methyl nicotinate had similar maximum blood fluxes ($p = 0.07$).

Pointed and symmetric microneedles differ in the placement of the needle lumen (Figs. 1A, B). The piercing and entry zone of the symmetric microneedle coincides with its lumen; in pointed microneedles, the lumen is offset from its piercing and entry zone. As a result, the symmetric microneedles may more susceptible to clogging and have an increased resistance to fluid flow. Also, the pointed microneedle has a larger area for delivery and thereby lower resistance to fluid flow due to the elipitical structure of its lumen. This may explain why the symmetric microneedle induced maximal blood flux was lower than the pointed microneedles (Fig. 4). Both are able to bypass the stratum corneum as reflected in the decreased time to maximum blood flux (Fig. 3), but the pointed needle may deliver more methyl

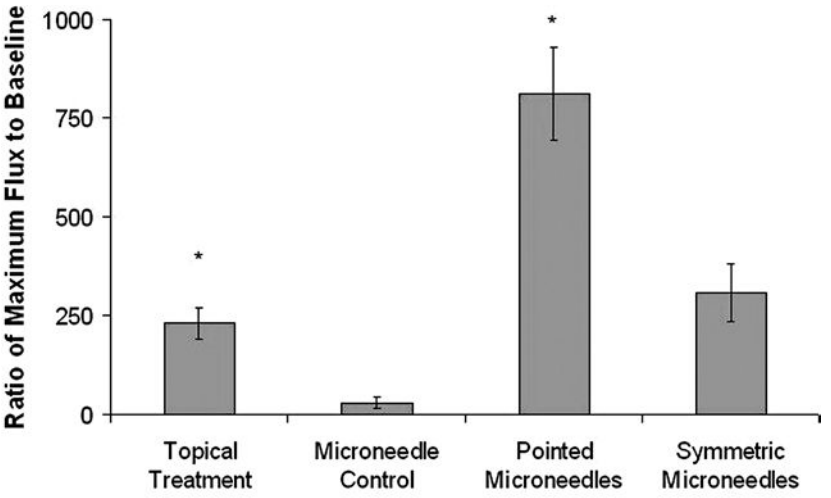


Figure 4 Percent increase over baseline at maximum blood flux. Following 30-seconds treatments with methyl nicotinate, maximum blood fluxes were compared to baseline blood fluxes and pointed microneedles significantly increased the maximum blood flux over topical and symmetric microneedle treatments ($p < 0.05$). The microneedle control consisted of an empty microneedle syringe that was pressed onto the skin.

nicotinate into the skin over the 30-seconds injection period. Hollow microneedles designed with a lumen different from the pierce and entry zone may increase drug injection efficacy.

All volunteers were asked to describe what they felt during the injection and all responded by saying that they felt pressure but no pain, in agreement with Kaushik et al. (4).

These results show that hollow microneedles can painlessly bypass the stratum corneum during injections and deliver drugs to the skin capillaries in humans. Traditional hypodermic needle injections will continue to be advantageous in treatments requiring deeper penetration past the epidermis, like subdermal, muscular, or intravenous injections. However, hollow microneedles offer distinct advantages: they are painless and can reduce needle phobia in patients, are simpler to use than traditional injections, and can be integrated into devices for controlled, continuous drug delivery. Another advantage for hollow microneedles among transdermal drug delivery systems is the potential to inject large-sized protein formulations, such as sustained-release insulin formulations that range from 2 to 30 μm (24). The lumens of the hollow microneedle are 35 to 300 μm (10–13) and could successfully inject these formulations. Microneedles will be beneficial from a public health perspective too, because more people may be willing to receive vaccinations due to increased convenience and comfort of microneedle injection.

The design of the microneedle can impact how quickly drugs can be introduced through the needles. Microneedles can serve as a painless alternative to hypodermic vaccine injection and to administer drugs that may normally be administer in a topical manner. Revolutionary continuous and controlled drug therapies can be possible when pumps and sensors are mounted onto microneedle arrays.

REFERENCES

1. Nir Y, Paz A, Sabo E, Potasman I. Fear of injections in young adults: prevalence and associations. Am J Trop Med Hyg 2003; 68(3):341–344.
2. Kleinknecht RA, Thorndike RM, Walls MM. Factorial dimensions and correlates of blood, injury, injection and related medical fears: cross validation of the medical fear survey. Behav Res Ther 1996; 34(4):323–331.
3. Henry S, McAllister DV, Allen MG, Prausnitz MR. Microfabricated microneedles: a novel approach to transdermal drug delivery. J Pharm Sci 1998; 8:922–925.
4. Kaushik S, Hord AH, Denson D, McAllister DV, Smitra S, Allen MG, Prausnitz MR. Lack of pain associated with microfabricated microneedles. Anesth Analg 2001; 92: 502–504.
5. Zahn JD. Microfabricated Microneedles for Minimally Invasive Drug Delivery, Sampling and Analysis. Thesis, UC Berkeley and San Francisco.
6. Zahn JD, Deshmukh AA, Pisano AP, Liepmann D. Continuous on-chip micropumping through a microneedle. In: MEMS 2001: Proceedings of the 14th IEEE International Conference on Micro Electro Mechanical Systems, Interlaken, Switzerland, 2001: 503–506.
7. Chen J, Wise KD, Hetke JF, Bledsoe SC Jr. A multichannel neural probe for selective chemical delivery at the cellular level. IEEE Trans Biomed Eng 1997; 44(8):760–769.
8. Smart WH, Subramanian K. The use of silicon microfabrication technology in painless blood glucose monitoring. Diab Tech Ther 2000; 2(4):549–559.
9. Reed ML, Lye W-K. Microsystems for drug and gene delivery. Proc IEEE 2004; 92(1): 56–75.
10. Stoeber B, Liepmann D. Fluid injection through out-of-plane microneedles. In: Proceedings of the International IEEE-EMBS Special Topic Conference on Microtechnologies in Medicine and Biology, 2000:34.
11. McAllister DV, Wang PM, Davis SP, Park J-H, Canatella PJ, Allen MG, Prausnitz MR. Microfabricated needles for transdermal delivery of macromolecules and nanoparticles: fabrication methods and transport studies. PNAS 2003; 100(24):13755–13760.
12. Gardeniers HJGE, Luttge R, Berenschot JW, de Boer MJ, Yeshurun SY, Hefetz M, van't Oever R, van den Berg A. Silicon micromachined hollow microneedles for transdermal liquid transport. J Microelectromech Syst 2003; 12(6):855–862.
13. Griss P, Stemme G. Side-opened out-of-plane miconeedles for microfludic transdermal liquid transfer. J Microelectromech Syst 2003; 12(3):296–301.
14. Matsuda T, Mizutani M. Liquid acrylate-endcapped biodegradable poly (ε-caprolactone-*co*-trimethylene carbonate). II. Computer-sided stereolithographic microarchitectural surface photoconstructs. J Biomed Mater Res 2002; 62(3):395–403.
15. Sivamani RK, Stoeber B, Wu GC, Zhai H, Liepmann D, Maibach H. Clinical microneedle injection of methyl nicorinate: stratum corneum penetration. Skin Res Technol 2005; 11(2):152–156.
16. Prausnitz MR. Microneedles for transdermal drug delivery. Adv Drug Del Rev 2004; 56:581–587.
17. Guy R, Wester RC, Tur E, Maibach HI. Noninvasive assessments of the percutaneous absorption of methyl nicotinate in humans. J Pharma Sci 1983; 72(9):1077–1079.
18. Guy RH, Tur E, Bjerke S, Maibach HI. Are there age and racial differences to methyl nicotinate-induced vasodilation in human skin? J Am Acad Derm 1985; 12(6): 1001–1006.
19. Guy RH, Carlstrom EM, Bucks DAW, Hinz RS, Maibach HI. Percutaneous penetration of nicotinates: in vivo and in vitro measurements. J Pharm Sci 1986; 75(10):968–672.
20. Müller B, Kasper M, Surber C, Imanidis G. Permeation, metabolism and site of action concentration of nicotinic acid derivatives in human skin: correlation with topical pharmacological effect. Eur J Pharm Sci 2003; 20:181–195.

21. Boelsma E, Anderson C, Karlsson AMJ, Pnec M. Microdialysis technique as a method to study the percutaneous penetration of methyl nicotinate through excised human skin, reconstructed epidermis, and human skin in vivo. Pharm Res 2000; 17(2):141–147.
22. Caselli A, Hanane T, Jane B, Carter S, Khaodhiar L, Veves A. Topical methyl nicotinate-induced skin vasodilation in diabetic neuropathy. J Diab Comp 2003; 17:205–210.
23. Reinberg AE, Soudant E, Koulbanis C, Bazin R, Nicolai A, Mechkouri M, Touitou Y. Circadian dosing time dependency in the forearm skin penetration of methyl and hexyl nicotinate. Life Sci 1995; 57:1507–1513.
24. Takenaga M, Yamaguchi Y, Kitagawa A, Ogawa Y, Kawai S, Mizushima Y, Igarashi R. Optimum formulation for sustained-release insulin. Int J Pharm 2004; 271:85–94.

62

Skin Impedance–Guided High Throughput Screening of Penetration Enhancers: Methods and Applications

Amit Jain, Pankaj Karande, and Samir Mitragotri
University of California, Santa Barbara, California, U.S.A.

I. INTRODUCTION

The idea of delivering drugs through the skin is as old as human civilization, but the excitement has increased in recent times after the introduction of the first transdermal patch in 1970s. Although transdermal route of drug administration offers several advantages such as reduced first-pass drug metabolism, no gastro-intestinal degradation, long-term delivery (>24 hours) and control over delivery and termination, only few drug molecules have been formulated into transdermal patches (1). The cause of this imbalance between the benefits of this route and the number of products in the market lies in the skin itself. Skin's topmost layer, Stratum Corneum (SC), forms a barrier against permeation of xenobiotics into the body and water evaporation out of the body. This barrier must be altered to maximize the advantages of transdermal route of drug administration. This has engaged pharmaceutical scientists, dermatologists, and engineers alike in research over the last couple of decades (2). High research activity in this field has led to the introduction of a variety of techniques including formulation-based approaches (3), iontophoresis (4), electroporation (5,6), acoustical methods (7), microneedles (8), jet injection (9), and thermal poration (10).

All of the above techniques have their own benefits and specific applications. Formulation-based approaches have a number of unique advantages such as design, simplicity and flexibility, and ease of application over a large area (11). The last 20 years have seen extensive research in the field of chemical enhancers, which form the core component of formulation-based strategies for transdermal drug delivery. More than 200 chemicals have been shown to enhance skin permeability to various drugs. These include molecules from a diverse group of chemicals including fatty acids (12–14), fatty esters (15), non-ionic surfactants (16), anionic surfactants (17), and terpenes (18,19). However, identification of potent yet safe permeation enhancers has proved challenging. To date, only few chemicals are to be found in currently

marketed transdermal products. These include oleic acid, sorbitan monooleate, and methyl laurate among others.

Even though individual Chemical Penetration Enhancers (CPEs) have found limited applications, combinations of CPEs represent a huge opportunity that has been sparsely tapped. Several reports have indicated that combinations of CPEs offer better enhancements of transdermal drug transport compared to their individual constituents (20,21). However, such combinations do not necessarily yield safer enhancers. It should be feasible, in principle, to use CPEs as building blocks to construct new microstructures and novel formulations that offer enhancement without irritation. However, the challenge now shifts to screening the potency of enhancer combinations. Random mixtures of CPEs are likely to exhibit additive properties, that is, their potency and irritancy are likely to be averages of corresponding properties of their individual constituents. Occurrence of truly synergistic combinations is likely to be rare. In the absence of capabilities to predict the occurrence of such rare mixtures, one has to rely on a brute force screening approach. Starting with a pool of >200 individual CPEs millions of binary and billions of higher-order formulations can be designed. Screening of these mixtures is a mammoth task.

Screening of chemical enhancers can be performed in vitro as well as in vivo. In vivo experiments are likely to yield better results; however, several issues including variability, cost, and practicality limit their applications for screening a large database of enhancers. Accordingly, in vitro screening based on excised tissue (human or animal) presents a more practical alternative (22). A number of models exist to predict in vivo pharmacokinetics based on in vitro data (23–27). The use of in vitro models for screening is also supported by the fact that SC, the principle site of enhancer action, shows similar behavior in vivo and in vitro except for the extent of metabolic activity (28). Majority of in vitro studies on transdermal drug transport have been performed using Franz Diffusion Cells (FDCs). The throughput of this traditional set up of diffusion chamber is very low; not more than 10–15 experiments at a time. These permeation studies are time-consuming and are resource-expensive as analytical methods such as high-pressure liquid chromatography (HPLC) or radio labeled drugs for liquid scintillation counting are expensive. Automated in-line flow through diffusion cells have been developed in the last few years to increase the throughput of skin permeation experiments (29,30). Although these methods have facilitated the experiments, the throughput of these methods has not been significantly improved. Furthermore, these methods are also cost prohibitive. Accordingly, standard FDCs still dominate the screening of CPEs.

The urgent need to increase experimental throughput has led to the development of high throughput screening methods. Although in early stages, these methods have already shown promise in discovering novel formulations for transdermal drug delivery. A high throughput assay to be used for screening of transdermal formulations should meet the following requirements:

i. *Ability to screen a large number of formulations*: increasing the throughput by at least two to three orders of magnitude would result in significant reduction in the effort and time spent in the very first stage of formulation development (31).
ii. *Use of a surrogate end point that is quick, easy and independent of the physicochemical properties of the model permeant*: permeation experiments using radio labeled (32), fluorescent (33), HPLC-detectable (27), or RIA/ELISA-detectable (34,35) markers necessitate the need of extensive

sample handling and sample analysis. This accentuates the cost of sample analysis and overall time spent in characterizing the efficacy of formulations. Furthermore, current state of the art fluidics systems put a fundamental limit on the number of samples handled in a given time. Permeation of a model solute across the skin in presence of an enhancer is dependent not only on the inherent capacity of the enhancer to permeabilize skin but also on the physicochemical interactions of the enhancer with the model solute (36–39). An end point, to characterize the effect of an enhancer on skin permeability, should be able to decouple these two effects to assure the generality of the results.

iii. *Low incubation times to further increase the throughput and hence time efficiency*: the FDC experiments typically use incubation times of 48 to 96 hours thereby reducing the throughput of permeation experiments. Low incubation times favor high turnover frequencies for assay utilization.

iv. *Minimal use of test chemicals and efficient utilization of model membrane such as animal skin*: the FDCs typically require application of 1 to 2 mL of enhancer formulations over about 3 to 4 cm^2 of skin per experiment. This makes it cost prohibitive to include candidates that are expensive in the test libraries as well as to screen a large number of formulations.

v. *Adaptability to automation to reduce human interference*: typical FDC setup requires manual sampling with little opportunities for process automation (30).

In addition to these requirements of the assay tool, the high throughput screening methodology should also satisfy, if possible, the following experimental constraints:

vi. *Use of a common model membrane to represent human skin*: it is common to find in transdermal literature the use of a variety of different models to represent human skin such as rat skin (40), pig skin (41), snake skin (42), excised human skin, etc. While human skin is difficult to procure on a large scale, animal models show deviations in permeability characteristics from human skin (38–40,43). Also, results on one model cannot be directly translated to a different model.

vii. *Use of consistent thermodynamic conditions for enhancer formulations*: permeation enhancement efficacy of a CPE is a function of its chemical potential (44,45), temperature (46,47), and co-solvent (48,49) amongst other thermodynamic parameters. These thermodynamic conditions need to be standardized for all the enhancers that are being tested to create direct comparison of their efficacies in increasing skin permeation.

This chapter focuses on a specific high throughput screening method called in vitro Skin Impedance Guided High Throughput (INSIGHT) screening that was recently introduced (50). This method is described in detail with respect to its fundamentals, validation, and outcomes.

II. OVERVIEW OF INSIGHT SCREENING

INSIGHT screening offers >100-fold improvement in screening rates of transdermal formulations (50). This improvement in efficiency comes from two factors. First, the INSIGHT, in its current version, can perform up to 50 tests/in^2 of skin compared to

about $>2\,cm^2$ of skin per test in the case of FDCs (Fig. 1). About 100 formulations can be screened per INSIGHT array. Second, INSIGHT screening uses skin impedance as a surrogate marker for skin permeability.

Skin impedance has been previously used: (i) to assess the skin integrity for in vitro dermal testing (51–53), (ii) to evaluate the irritation potential of chemicals in a test known as Skin Integrity Function Test (SIFT) (54), and (iii) to monitor skin barrier recovery in vivo following the application of current during iontophoresis (55,56). Since it is evident from the literature that skin impedance can be used to confirm skin integrity it is logical to hypothesize that alteration in skin barrier due to chemical enhancers can be used as an in vitro surrogate marker for permeability. Scattered literature data support this hypothesis. A study by Yamamoto and Yamamoto (57,58) showed that total skin impedance reduces gradually with tape stripping and after 15 stripping skin impedance approaches the impedance value of deep tissues (57,58). However, quantitative relationships between skin impedance and permeability in the presence of chemical enhancers and their validity for a wide range of markers have not been previously documented.

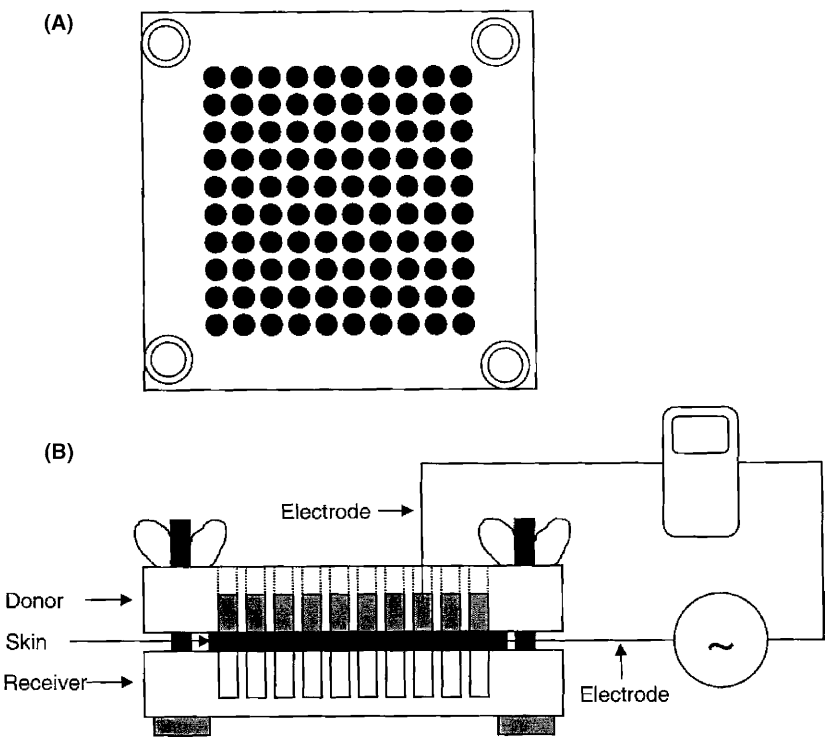


Figure 1 Schematic of the INSIGHT screening apparatus. The INSIGHT screen is made up of a donor array (*top*) and a symmetric receiver array (*bottom*). A single screen can screen 100 formulations at one time. The skin is sandwiched between the donor (Teflon) and receiver (Polycarbonate) and the formulations contact the stratum corneum from the donor array. Conductivity measurements are made with one electrode inserted in the dermis and a second electrode moved sequentially in the donor wells. (**A**) is top and (**B**) is side view of the INSIGHT apparatus.

III. SKIN IMPEDANCE–SKIN PERMEABILITY CORRELATION

The SC is a composite of proteins and lipids in which protein-rich corneocytes are surrounded by lipid bilayers (59). Approximately 70 to 100 bilayers are stacked between two corneocytes (60,61). Because of its architecture the SC is relatively non-conductive and possesses high electrical impedance (62). Skin impedance (AC) can be measured either by applying a constant current and measuring the potential across the skin or by measuring transepidermal current following the application of a constant AC potential. Data reported in this chapter is based on measurement of transepidermal current following the application of a constant potential (100 mV rms). Frequency of the applied potential is also an important parameter. Due to the capacitive components of the skin, the measured electrical impedance of the skin decreases with increasing frequency (57,58). While the use of higher frequencies facilitates measurements due to decreased impedance, the correlation between electrical impedance and solute permeability is stronger at lower frequencies. Thus, an optimal frequency must be chosen. All experiments reported in chapter were performed at a frequency of 100 Hz.

The INSIGHT screening is founded on the relationship between skin's electrical impedance (reciprocal of skin conductance) and solute permeability. There is a dearth of literature on skin impedance (conductivity) and permeability relationship and moreover in most of the studies this relationship was used to elucidate the mechanism of transport of hydrophilic molecules across the skin under the influence of temperature (63), hydration (64), electric current (65,66) or ultrasonic waves (67,68). Therefore, existing data cannot be used to generalize the relationship between skin impedance and permeability. Accordingly, a large dataset was first generated to assess the correlation between skin impedance and permeability to small (mannitol) and macromolecule (inulin) hydrophilic solutes in the presence of different chemical enhancer formulations. A set of 22 enhancer formulations, chosen from the candidate pool was used to validate the relationship between skin conductivity and skin permeability. The candidate pool comprised of 15 single enhancer formulations and seven binary enhancer formulations. In order to establish the correlation between skin impedance and permeability for wide range of chemical enhancers, formulations were made from different classes of chemicals including cationic surfactants (CTAB, Cetyl trimethyl ammonium bromide; BDAC, Benzyl Dodecyl ammonium chloride), anionic surfactants (NLS, *N*-lauorylsarcosine sodium; SLA, Sodium laureth sulfate; SLS, Sodium lauryl sulfate), zwitterionic surfactant (HPS, *N*-Hexadecyl-*N*,*N*-Dimethyl-3-ammonio-1-propanesulfonate), non-ionic surfactant (PEGE, Polyethylene dodecyl glycol ether; S20, Sorbitan monolaurate; T20, Polyoxyethylene sorbitan monolaurate), fatty acid and their sodium salts (LA, Lauric acid; OL, Oeic acid; SOS, Sodium octyl sulfate; SO, Sodium oleate), fatty acid ester (TET, Tetracaine HCI; IPM, Isopropyl myristate), and others (DMP, *N*-dodecyl 2-pyrrolidone; MEN, Menthol). Skin impedance and permeability to two model solutes, mannitol, and inulin were measured. Inulin (MW 5 kDa) was selected as a model solute as it satisfactorily represents a macromolecular hydrophilic drug. Mannitol (MW 182.2 Da, log $K_{o/w}$ −3.1) was used as a representative of small hydrophilic drugs.

A strong correlation was observed between skin impedance and permeability of mannitol and inulin for different enhancer formulations (Figs. 2–4). The measurements reported in Figure 2A and B were performed in FDCs. There is a reasonable scatter in these data, which is inherent to biological systems such as skin that exhibit

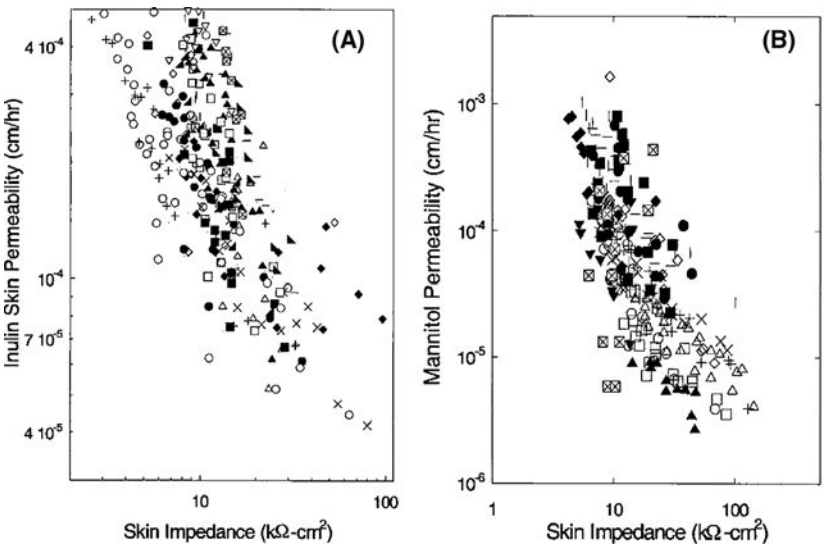


Figure 2 Skin impedance–permeability correlation for (**A**) inulin and (**B**) mannitol. Test formulations used in this study (in parentheses total concentration of chemical enhancer w/v, weight fraction used): (**A**) •, MEN (1.5%w/v); ■, SO (1.5%w/V); ▲, PEGE (1.5%w/v); △, OL (1.5%w/v); □, S20 (1.0%w/v); O, DMP (1.5%w/v); ▽ OL:MEN (1.5%w/v, 0.4:0.6); ◇, IPM (1.5%w/v); ×, TET (2.0%w/v); +, LA (1.5%w/v); ♦, NLS (1.0%w/v); ⊙, SOS (2.0%w/v); ⊠, NLS:S20 (1.0%w/v, 0.6:0.4); ⊡, TET:SLS (1.0%w/v, 0.6:0.4); ◣, TET:HPS (2.0%w/v, 0.1:0.9); ◢, MEN:T20 (2.0%w/v, 0.5:0.5); ∗, DMP:TET (2.0%w/v, 0.4:0.6); Γ, CTAB (1.0%w/v). (**B**) Γ, OL (1.5%w/v); ▲, DMP (2.0%w/v); ▼, DMP-TET (2.0%w/v, 0.4:0.6); △, PEGE (1.5%w/v); ⊠, TET (2.0%w/v); ×, LA (1.5%w/v); +, S20 (1.0%w/v); ■, HPS (1.5%w/v); O, NLS (1.0%w/v); □, BDAC (1.5%w/v); ■ MEN

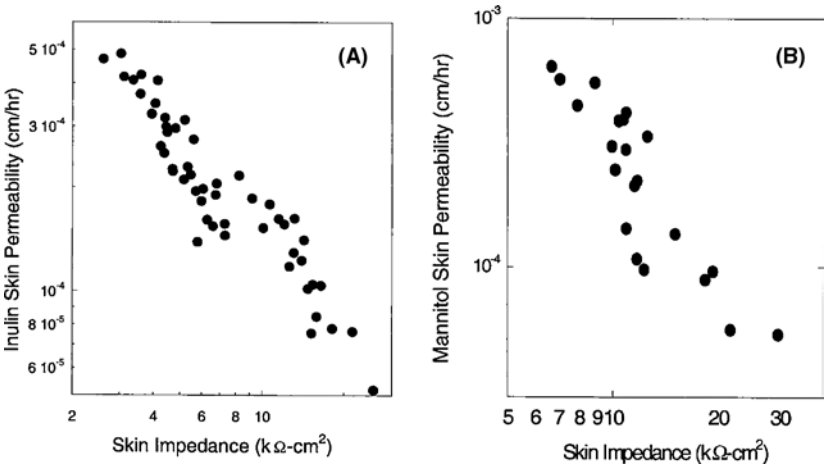


Figure 3 Skin impedance–permeability correlation for single enhancer: (**A**) Plot of skin permeability to inulin versus skin impedance in presence of DMP (1.5%w/v in 1:1EtOH:PBS); (**B**) Plot of skin permeability to mannitol versus skin impedance in presence of NLS (1.5%w/v in 1:1EtOH:PBS). A much tighter correlation can be observed compared to Figure 2.

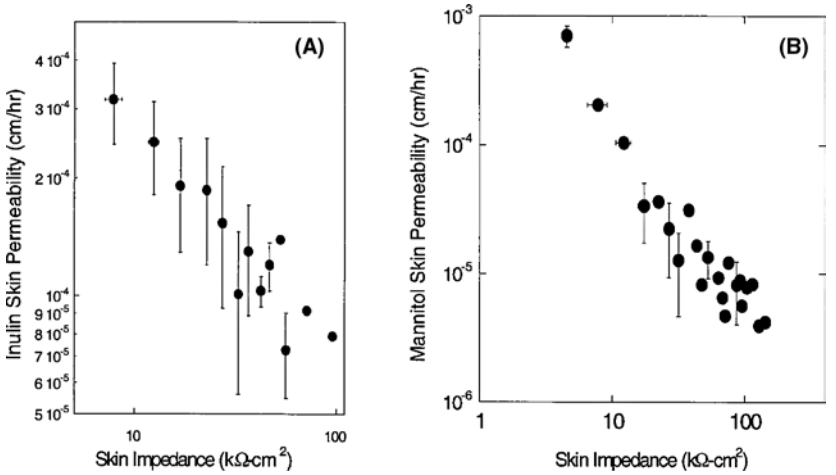


Figure 4 Skin impedance–permeability correlation for (**A**) inulin and (**B**) mannitol. Modified plot of permeability–impedance data shown in Figure 2. Permeability data for different enhancers is grouped in the bins of 5 kΩ cm^2 along the *x*-axis representing skin impedance. The correlation is much tighter as compared to the one in Figure 2.

high variability. Also, measurements reported in Figure 2A and B represent an aggregate of experiments performed over several different animals and anatomical regions. The correlation between skin permeability and impedance was improved when data for individual enhancers were plotted separately; example for inulin (with DMP enhancer $r^2 = 0.85$) and mannitol (with NLS enhancer $r^2 = 0.86$) is given in (Fig. 3A and B). The correlation between skin permeability and impedance can be clearly seen in Figure 4A and B where data in Figure 2A and B are replotted after averaging over ~5-kΩ-cm^2 intervals (inulin $r^2 = 0.86$ and for mannitol $r^2 = 0.90$). Permeability data of mannitol and inulin with a variety of chemical enhancer formulations showed that skin impedance is inversely related to permeability of hydrophilic solutes, which is in agreement with existing data in literature. Correlation coefficient (inulin $r^2 = 0.86$ and mannitol $r^2 = 0.90$) of average data for all enhancer formulations indicates that a remarkable correlation exists between skin permeability and impedance for single and binary enhancers formulations irrespective of the nature of the formulation. These results indicate that skin impedance can be used a parameter to measure the extent of barrier alteration by chemicals irrespective of their mode of action (which, in most cases, is not precisely known). Specifically, good correlations were observed between permeability and skin impedance for enhancers, which act by lipid extraction (NLS, MEN, and BDAC) or by lipid bilayer fluidization (OL, LA, and IPM). Note however, that the nature of these correlations is an integral function of the physico-chemical properties of the drug or permeant. Educated discretion must therefore be exercised when selecting a delivery formulation for a particular model permeant or drug of interest.

IV. VALIDATION OF INSIGHT WITH FDCs

Conductivity enhancement ratio (ER), that is, the ratio of skin impedances at time zero and 24 hours following the application of enhancer formulation, measurements

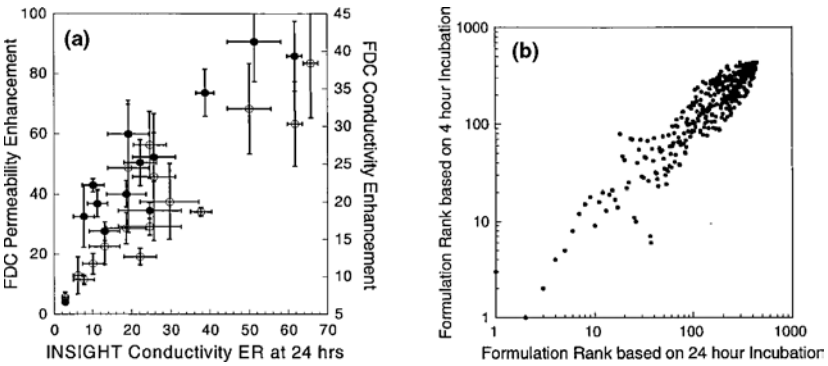

(a)
FDC Permeability Enhancement
FDC Conductivity Enhancement
INSIGHT Conductivity ER at 24 hrs
(b)
Formulation Rank based on 4 hour Incubation
Formulation Rank based on 24 hour Incubation

Figure 5 Validation of INSIGHT predictions with FDC. (**A**) Plot of conductivity enhancement ratios in INSIGHT at 24 hours versus conductivity and permeability enhancement ratios in FDC at 96 hours for 19 enhancer formulations. A strong linear correlation indicates the validity of observations in INSIGHT when compared with those from traditional tools like FDC. The closed circles indicate conductivity enhancement numbers and the filled circles indicate permeability enhancement numbers in FDC. (**B**) Plot of 24-hours predictions in INSIGHT versus four hours predictions in INSIGHT on the potency of enhancer formulations. A strong correlation indicates that predictions on potency of formulations can be obtained at significantly lower incubation periods of four hours.

in INSIGHT were plotted against conductivity enhancement and permeability enhancements in FDCs (Fig. 5A). Inulin was used as a model permeant in these studies. Results shown in Figure 5A reflect that the predictions obtained from INSIGHT on the potency of enhancer formulations are essentially the same as those obtained from FDCs. However, INSIGHT allows collection of information at a much greater speed ($\sim$1000 per day) and less skin utilization (about 0.07 cm^2 per experiment as compared to 2 cm^2 in a 16 mm diameter FDC, >25-fold reduction in skin utilization).

Further improvements in INSIGHT screening speed can be obtained by reducing the formulation incubation period. Capabilities of INSIGHT in assessing formulation potency after a foue-hour incubation are demonstrated in Figure 5B, where potency rankings of 438 single and binary formulations randomly prepared from the enhancer library based on four-hour screening are compared to those based on 24-hour screening. Rank 1 corresponds to most potent formulation in the library and rank 438 to the weakest formulation. The predictions of the potency made in 4 hr were consistent with those made after a contact time of 24 hours, thus indicating that the efficiency of INSIGHT screening can be further improved.

V. APPLICATIONS OF INSIGHT SCREENING

A. Discovery of Rare Formulations

The INSIGHT screening can be used to screen huge libraries of chemicals within a short span of time and without the fear of failure that exists with traditional tools. Many current single enhancers are also potent irritants to the skin at concentrations necessary to induce meaningful penetration enhancement. Attempts have been made to synthesize novel chemical enhancers such as Azone, however achieving sufficient potency without irritancy has proved challenging, especially for macromolecules.

A number of studies have shown that formulations made up of combination of chemical enhancers are more potent than its individual components (20,50,69). The addition of components increases the number of formulations exponentially. However, the use of INSIGHT screening allows one to tackle this challenge in a more cost-effective way compared to FDCs. In addition, synergies between CPEs not only lead to new transdermal formulations but also potentially offer insight into mechanisms by which CPEs enhance skin permeability. Prediction of synergies from the first principles is challenging. The INSIGHT screening offers an effective tool for identifying synergies (positive or negative) between the CPEs.

To identify synergistic combinations of penetration enhancers (SCOPE) formulations, a library of chemical enhancers was first generated from 32 chemicals chosen from a list of >250 chemical enhancers belonging to various categories. Random pairing of CPEs from various categories led to 496 binary chemical enhancers pairs. For each pair, 44 distinct chemical compositions were created with the concentration of each chemical enhancer ranging from 0% to 2% w/v, yielding a library of 25,000 candidate SCOPE formulations. About 20% of this library (5040 formulations) was screened using INSIGHT the largest ever-cohesive screening study reported in the transdermal literature. Each formulation was tested at least four times in over 20,000 experiments (50). Using the traditional tools for formulation screening, it would have taken over seven years to do these many experiments. With INSIGHT screening, the same task was accomplished in about two months with screening rate of 500 to 1000 experiments per day.

Binary formulations exhibited a wide range of enhancements. The percent of randomly generated enhancer combinations that exhibit ER above a certain threshold decreases rapidly with increasing threshold (Fig. 6A). The inset shows a section of the main figure corresponding to high ER values. Less than 0.1% of formulations exhibited more than 60-fold enhancement of skin conductivity. Discovery of such rare formulations by brute force experimentation is contingent on the throughput of the experimental tool. The INSIGHT screening opens up the possibility of discovering such rare formulations.

One of the formulations discovered by INSIGHT, Sodium Laureth Sulfate: Phenyl Piperazine (SLA:PP) was shown to increase the permeability of macromolecules such as inulin across porcine skin by 80- to 100-fold compared to passive skin permeability of inulin (50). The SLA:PP also increased the skin permeability of molecules such as methotrexate, low molecular weight heparin, leutenizing hormone releasing hormone (LHRH) and oligonucleotides by 50- to 100-fold. Animal experiments in hairless rats also confirmed delivery of a synthetic analog of LHRH, leuprolide acetate in vivo. The amount of leuprolide acetate delivered using a SCOPE formulation (SLA:PP) is significantly more than that delivered from a control solution and lies in the therapeutic window.

B. Generation of Database for Quantitative Understanding

Looking beyond searching for potent combinations of enhancers, the sheer volume of information generated via INSIGHT screening on the behavior of a wide variety of penetration enhancers will provide, for the first time, a platform to build further investigations of the fundamental aspects of enhancer–skin interactions. Quantitative descriptions of structure-activity relations (QSARs) for CPEs, which have had limited success in the past (70,71), may lead to better outcomes in light of the availability of large volumes of data collected in a consistent manner. As exemplified in

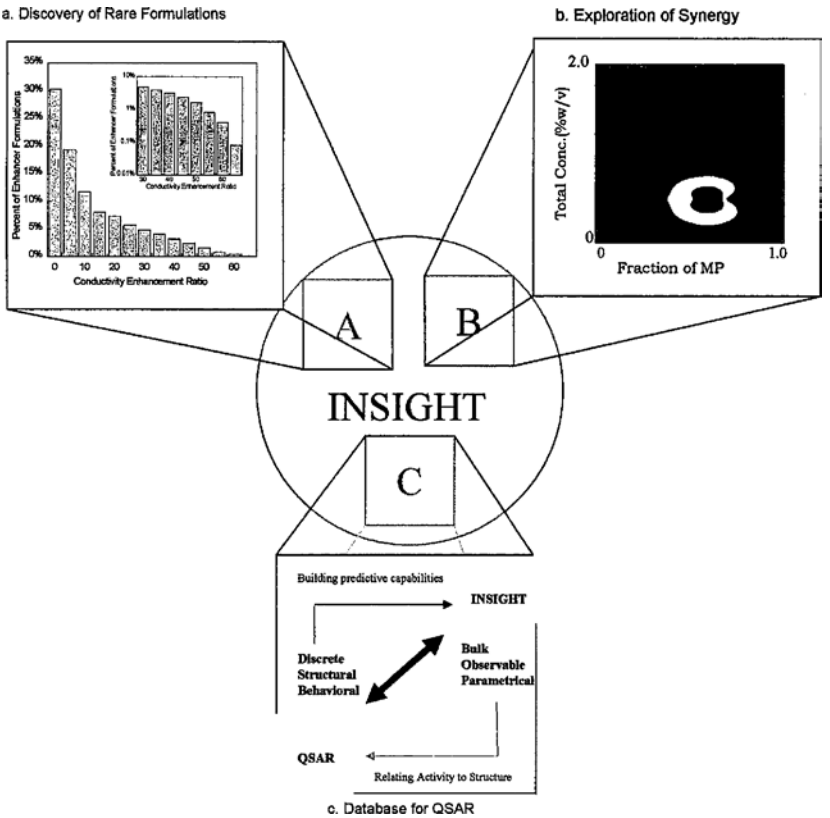


Figure 6 Applications of INSIGHT screening. (**A**) Discovery of rare enhancer formulations that are significantly potent in increasing skin permeability. Such formulations are difficult to discover using the traditional tools like FDC due to their low experimental throughput. The success rate of discovering these potent formulations is very small (~0.1%) requiring a tool with high experimental throughput. (**B**) INSIGHT screening is used to quantify the extent of interactions between the components of CPE mixtures in terms of Synergy. Regions of high synergy almost always overlap with the regions of high potency. (**C**) INSIGHT screening can be used to generate large volumes of data on the interaction of CPEs with skin. The information is used to relate chemistry of the enhancer to its potency using QSAR.

Figure 6, this information should help in generating hypotheses relating the chemistry of CPEs to their potencies. For working hypotheses, this knowledge can then help refine our selection rules for designing next generation transdermal formulations. Repeating the experiment-hypothesis loop over a vast but limited number of candidate penetration enhancers will provide the missing pieces in solving a vast multivariate problem. Also, this knowledge should significantly reduce the cost and effort of designing therapeutics for use on skin in the future.

REFERENCES

1. Barry BW. Novel mechanisms and devices to enable successful transdermal drug delivery. Eur J Pharm Sci 2001; 14(2):101–114.
2. Mitragotri S. Breaking the skin barrier. Adv Drug Deliv Rev 2004; 56(5):555–556.

3. Williams AC, Barry BW. Penetration enhancers. Adv Drug Deliv Rev 2004; 56(5): 603–618.
4. Kalia YN, Naik A, Garrison J, Guy RH. Iontophoretic drug delivery. Adv Drug Deliv Rev 2004; 56(5):619–658.
5. Weaver JC, Vaughan TE, Chizmadzhev Y. Theory of electrical creation of aqueous pathways across skin transport barriers. Adv Drug Deliv Rev 1999; 35(1):21–39.
6. Prausnitz MR. A practical assessment of transdermal drug delivery by skin electroporation. Adv Drug Deliv Rev 1999; 35(1):61–76.
7. Mitragotri S, Kost J. Low-frequency sonophoresis: a review. Adv Drug Deliv Rev 2004; 56(5):589–601.
8. Prausnitz MR. Microneedles for transdermal drug delivery. Adv Drug Deliv Rev 2004; 56(5):581–587.
9. Hlngson RA, Figge FH. A survey of the development of jet injection in parenteral therapy. Curr Res Anesth Analg 1952; 31(6):361–366.
10. Sintov AC, Krymberk I, Daniel D, Hannan T, Sohn Z, Levin G. Radiofrequency-driven skin microchanneling as a new way for electrically assisted transdermal delivery of hydrophilic drugs. J Control Release 2003; 89(2):311–320.
11. Prausnitz MR, Mitragotri S, Langer R. Current status and future potential of transdermal drug delivery. Nat Rev Drug Discov 2004; 3(2):115–124.
12. Jain AK, Panchagnula R. Transdermal drug delivery of tricyclic antidepressants: effect of fatty acids. Methods Find Exp Clin Pharmacol 2003; 25(6):413–421.
13. Golden GM, McKie JE, Potts RO. Role of stratum corneum lipid fluidity in transdermal drug flux. J Pharm Sci 1987; 76(1):25–28.
14. Aungst BJ, Blake JA, Hussain MA. Contributions of drug solubilization, partitioning, barrier disruption, and solvent permeation to the enhancement of skin permeation of various compounds with fatty acids and amines. Pharm Res 1990; 7(7):712–718.
15. Chukwumerije O, Nash RA, Matias JR, Orentreich N. Studies on the efficacy of methyl esters of n-alkyl fatty acids as penetration enhancers. J Invest Dermatol 1989; 93(3): 349–352.
16. Lopez A, Llinares F, Cortell C, Herraez M. Comparative enhancer effects of Span20 with Tween20 and Azone on the in vitro percutaneous penetration of compounds with different lipophilicities. Int J Pharm 2000; 202(1–2):133–140.
17. Nokhodchi A, Shokri J, Dashbolaghi A, Hassan-Zadeh D, Ghafourian T, Barzegar-Jalali M. The enhancement effect of surfactants on the pertetration of lorazepam through rat skin. Int J Pharm 2003; 250(2):359–369.
18. Williams AC, Barry BW. Terpenes and the lipid-protein-partitioning theory of skin penetration enhancement. Pharm Res 1991; 8(1):17–24.
19. Jain AK, Thomas NS, Panchagnula R. Transdermal drug delivery of imipramine hydrochloride. I. Effect of terpenes. J Control Release 2002; 79(1–3):93–101.
20. Mitragotri S. Synergistic effect of enhancers for transdermal drug delivery. Pharm Res 2000; 17(11):1354–1359.
21. Thomas NS, Panchagnula R. Combination strategies to enhance transdermal permeation of zidovudine (AZT). Pharmazie 2003; 58(12):895–898.
22. Priborsky J, Muhlbachova E. Evaluation of in-vitro percutaneous absorption across human skin and in animal models. J Pharm Pharmacol 1990; 42(7):468–472.
23. Wu PC, Huang YB, Chang JJ, Tsai YS. Evalution of pharmacokinetics and pharmacodynamics of captopril from transdermal hydrophilic gels in normotensive rabbits and spontaneously hypertensive rats. Int J Pharm 2000; 209(1–2):87–94.
24. Naito SI, Tsai YH. Percutaneous absorption of indomethacin from ointment bases in rabbits. Int J Pharm 1981; 8:263–276.
25. Guy RH, Hadgraft J, Maibach HI. A pharmacokinetic model for percutaneous bsorption. Int J Pharm 1982; 11:119–129.

26. Ogiso T, Ito Y, Iwaki M, Atago H. A pharmacokinetic model for the percutaneous absorption of indomethacin and the predication of drug disposition kinetics. J Pharm Sci 1989; 74:319–323.
27. Takayama K, Nagai T. Simultaneous optimization for several characteristics concerning percutaneous absorption and skin damage of ketoprofen hydrogels containing Dlinomene. Int J Pharm 1991; 74:115–126.
28. Chang P, Rosenquist MD, Lewis RWn GPK. A study of functional viability and metabolic degeneration of human skin stored at 4 degrees C. J Burn Care Rehabil 2000; 19(1 pt 1):25–28.
29. Cordoba-Diaz M, Nova M, Elorza B, Cordoba-Diaz D, Chantres JR, Cordoba-Borrego M. Validation protocol of an automated in-law flow-through diffusion equipment for in vitro permeation studies. J Control Release 2000; 63(3):357–367.
30. Bosman IJ, Lawant AL, Avegaart SR, Ensing K, De Zeeuw RA. Novel diffusion cell for in vitro transdermal permeation, compatible with automated dynamic sampling. J Pharm Biomed Anal 1996; 14(8–10):1015–1023.
31. Karande P, Mitragotri S. High throughput screening of transdermal formulations. Pharm Res 2002; 19(5):655–660.
32. Rosado C, Cross SE, Pugh WJ, Roberts MS, Hadgraft J. Effect of vehicle pretreatment on the flux, retention, and diffusion of topically applied penetrants in vitro. Pharm Res 2003; 20(9):1502–1507.
33. Ogiso T, Niinaka N, Iwaki M. Mechanism for enhancement effect of lipid disperse system on percutaneous absorption. J Pharm Sci 1996; 85(1):57–64.
34. Magnusson BM, Runn P. Effect of penetration enhancers on the permeation of the thyrotropin releasing hormone analogue pGlu-3-methyl-His-Pro amide through human epidermis. Int J Pharm 1999; 178(2):149–159.
35. Xing QF, Lin S, Chien YW. Transdermal testosterone delivery in castrated Yucatan minipigs: pharmacokinetics and metabolism. J Control Release 1996; 52(1–2):89–98.
36. Auner BG, Valenta C, Hadgraft J. Influence of lipophilic counter-ions in combination with phloretin and 6-ketocholestanol on the skin permeation of 5-aminolevulinic acid. Int J Pharm 2003; 255(1–2):109–116.
37. Lee SJ, Kim SW. Hydrophobization of ionic drugs for transport through membranes. J Control Release 1987; 6:3–13.
38. Takács-Novak K, Szász G. Ion-pair partition of quaternary ammonium drugs: the influence of counter ions of different lipophilicity, size, and flexibility. Pharm Res 1999; 16:1633–1638.
39. Schmook FP, Meingassner JG, Billich A. Comparison of human skin or epidermis models with human and animal skin in in-vitro percutaneous absorption. Int J Pharm 2001; 215(1–2):51–56.
40. Sekkat N, Kalia YN, Guy RH. Biophysical study of porcine ear skin in vitro and its comparison to human skin in vivo. J Pharm Sci 2002; 91(11):2376–2381.
41. Itoh T, Xia J, Magavi R, Nishihata T, Rytting JH. Use of shed snake skin as a model membrane for in vitro percutaneous penetration studies: comparison with human skin. Pharm Res 1990; 7(10):1042–1047.
42. Auner BG, Valenta C, Hadgraft J. Influence of phloretin and 6-ketocholestanol on the skin permeation of sodium-fluorescein. J control Release 2003; 89(2):321–328.
43. Panchagnula R, Stemmer K, Ritschel WA. Animal models for transdermal drug delivery. Methods Find Exp Clin Pharmacol 1997; 19(5):335–341.
44. Shokri J, Nokhodchi A, Dashbolaghi A, Hassan-Zadeh D, Ghafourian T, Barzegar Jalai M. The effect of surfactants on the skin penetration of diazepam. Int J Pharm 2001; 228(1–2):99–107.
45. Francoeur ML, Golden GM, Potts RO. Oleic acid: its effects on stratum corneum in relation to (trans)dermal drug delivery. Pharm Res 1990; 7(6):621–627.
46. Ongpipattanakul B, Burnette RP, Pottos RO, Francoeur ML. Evidence that oleic acid exists in a separate phase swithin stratum corneum lipids. Pharm Res 1991; 8(3):350–354.

47. Narishetty ST, Panchagnula R. Transdermal delivery of zidovudine: effect of terpenes and their mechanism of action. J Control Release 2004; 95(3):367–379.
48. Yamane MA, Williams AC, Barry BW. Terpene penetration enhancers in propylene glycol/water co-solvent systems: effectiveness and mechanism of action. J Pharm Pharmacol 1995; 47(12A):978–989.
49. Larrucea E, Arellano A, Santoyo A, Ygartua P. Combined effect of oleic acid and propylene glycol on the percutaneous penetration of tenoxicam and its retention in the skin. Eur J Pharm Biopharm 2001; 52(2):113–119.
50. Karande P, Jain A, Mitragotri S. Discovery of transdermal penetration enhancers by high-throughput screening. Nat Biotechnol 2004; 22(2):192–197.
51. Davies DJ, RJ W, Heylings JR. Multi-species assessment of electrical resistance as a skin integrity marker for in vitro percutaneous absorption studies. Toxicol In Vitro 2004; 18(3):351–358.
52. Fasano WJ, Manning LA, Green JW. Rapid integrity assessment of rat and human epidermal membranes for in vitro dermal regulatory testing: correlation of electrical resistance with tritiated water permeability. Toxicol In Vitro 2002; 16(6):731–40.
53. Lawrence JN. Electrical resistance and tritiated water permeability as indicators of barrier integrity of in vitro human skin. Toxicol In Vitro 1997; 11:241–249.
54. Heylings JR, Clowes HM, Hughes L. Comparison of tissue sources for the skin integrity function test (SIFT). Toxicol In Vitro 2001; 15(4–5):597–600.
55. Turner NG, Kalia YN, Guy RH. The effect of current on skin barrier function in vivo: recovery kinetics post-iontophoresis. Pharm Res 1997; 14(9):1252–1257.
56. Curdy C, Kalia YN, Guy RH. Post-iontophoresis recovery of human skin impedance in vivo. Eur J Pharm Biopharm 2002; 53(1):15–21.
57. Yamamoto T, Yamamoto Y. Electrical properties of the epidermal stratum corneum. Med Biol Eng 1976; 14(2):494–500.
58. Yamamoto T, Yamamoto Y. Dielectric constant and resistivity of epidermal stratum corneum. Med Biol Eng 1976; 14(2):151–158.
59. Madison KC, Swartzendruber DC, Wertz PW, Downing DT. Presence of intact intercellular lipid lamellae in the upper layers of the stratum corneum. J Invest Dermato 1987; 88:714–718.
60. Elias PM, MCNutt NS, Friend DS. Membrane alterations during cornification of mammalian squamous epithelia: a freeze-fracture, tracer, and thin-section study. Anat Rec 1977; 189(4):577–594.
61. Elias PM. Epidermal lipids, barrier function, and desquamation. J Invest Dermatol 1983; 80(suppl):44s–49s.
62. Lakermeier AH, McAdams ET, Moss GP, Woolfson AD. In vivo ac impedance spectroscopy of human skin. Theory and problems in monitoring of passive percutaneous drug delivery. Ann N Y Acad Sci 1999; 873:197–213.
63. Peck KD, Ghanem AH, Higuchi WI. The effect of temperature upon the permeation of polar and ionic solutes through human epidermal membrane. J Pharm Sci 1995; 84(8):975–982.
64. Tang H, Blankshtein D, Langer R. Prediction of steady-state skin permeabilities of polar and nonpolar permeants across excised pig skin based on measurements of transient diffusion: characterization of hydration effects on the skin porous pathway. J Pharm Sci 2002; 91(8):1891–1907.
65. Li SK, Ghanem AH, Peck KD, Higuchi WI. Characterization of the transport pathways induced during low to moderate voltage iontophoresis in human epidermai membrane. J Pharm Sci 1998; 87(1)::40–48.
66. Sims SM, Higuchi WI, Srinivasan V. Skin alteration and convective solvent flow effects during iontophoresis: I. Neutral solute transport across human skin. Int J Pharm 1991; 69(2):109–121.

67. Tang H, Mitragotri S, Blankschtein D, Langer R. Theoretical description of transdermal transport of hydrophilic permeants: application to low-frequency sonophoresis. J Pharm Sci 2001; 90(5):545–568.
68. Tezel A, Sens A, Mitragotri S. Description of transdermal transport of hydrophilic solutes during low-frequency sonophoresis based on a modified porous pathway model. J Pharm Sci 2003; 92(2):381–393.
69. Tezel A, Sens A, Tuchscherer J, Mitragotri S. Synergistic effect of low-frequency ultrasound and surfactants on skin permeability. J Pharm Sci 2002; 91(1):91–100.
70. Moss GP, Dearken JC, Patel H, Cronin MT. Quantitative structure-permeability relationships (QSPRs) for percutaneous absorption. Toxicol In Vitro 2002; 16(3):299–317.
71. Walker JD, Rodford R, Patlewicz G. Quantitative structure-activity relationships for predicting percutaneous absorption rates. Environ Toxicol Chem 2003; 22(8):1870–1884.

Index

β-adrenoceptor antagonists, 56
β-Cyclodextrin, 713
γ-Radiation, 524
β-Rays, 364
[methylene-^{14}C]-benzyl acetate, 236
l-Dodecylazacycloheptan-2-one. *See* Azone®
1,4,5,8-Tetraaminoanthraquinone (DB1). *See* Disperse blue 1
^{133}Xe washout technique, 332
^{14}C-DEA. *See* Diethanolamine.
^{14}C-labeled octyl salicylate, 687
2,4-Dichlorophenoxyacetic acid, 696
24 hr in vitro study, 147, 267–268, 272
2-Butoxyethanol, 308, 568
2-Ethylhexyl salicylate (octyl salicylate), 682
2-Ethylhexyl-4-methoxycinnamate, 682
2-Nitro-*p*-phenylenediamine (2NPPD), 47, 605
  dosing solutions, 607
  liquid chromatography method, 607
  metabolism, 606
    in rat, 47
  skin absorption of, 606
    in animals, 607
    in humans, 607
  skin metabolism, 608
    in humans, 610
    in rats, 608
  skin penetration, 608
2-Phenoxyethanol, 236
2T GE CSI nuclear magnetic resonance (NMR), 364
3,4,4$_0$-trichlorocarbanilide, 220
3-[4,5-dimethylthiazol-2yl]-2,5-diphenyltetrazolium bromide (MTT) assay, 46
4-Cyanophenol, 167
4-Nitrobenzo-2-oxa-1,3 diazol, 374
5-Fluorouracil cream (Effudex), 371
7-(2Hnaphtho[1,2-d]triazol-2-yl)-3-phenylcoumarin (7NTPC), 45
7-Ethoxycoumarin, 46
8-Methoxsalen (8-MOP), 712
8-Methoxypsoralen (8-MOP), 362

Abbreviated new drug application (ANDA), 478
Absorption, 156
  dermal, 157
    of topical permethrin, 157
  half-life, 28
  physical chemical parameters, 156
  values, 47
Accelerator mass spectrometry, 257
Acceptable daily intake (ADI), 598
Accountability, 319
Acetylcholine, 342
Acetylethyl tetramethyl tetralin (AETT), 46
Acyclovir concentration, 29, 375
Adjuvanticity, 771
Alachlor, 277
Allure (perfume), 733
Alpha hydroxy acids (AHAs), 272
Alzheimer's disease, 349
American Academy of Dermatology, 681
Analysis of variance (ANOVA), 514
Anatomical site, 392
Animal models, 413, 456
  hairless, 413
Antisense oligonucleotides (ONs) technology, 759
Apha-2-adenoreceptor, 339
Application time, 387
  effects, 387
Aqueous phase model
  effect of, compounds, 443
Area under the curve (AUC), 239
  effect (AUEC), 35
Arginine vasopressin, 341
Aroclor, 114

Arsenic, 824
  exposure, 825
    percutaneous pathway, 825
  geochemical controls, 825
  leaching of, in sweat, 826
  and Old Lace, 823
  toxicity, 824
Arsenic (V) oxyanion, 840
Atmospheric sampling glow discharge ionization (ASGDI), 317, 431
Atopic dermatitis, 140, 337
Atopy patch test, 141
[^{35}S]-dATP-labeled DNA, 425
Atrazine, 172, 257
Attenuated total reflectance infrared spectroscopy (ATR-IR), 403, 664
Aum Shinrikyo attacks, 556
Autoradiography, 371
Autosomal dominant ichthyosis vulgaris (ADI), 585
Avestin, 723
Avidin–biotin–peroxidase complex (ABC), 420
Axon reflex vasodilator response, 335
Azinphos-methyl, 172
Azone®, 449, 193, 858

B16 melanoma tumor cells, 817
Bacterial ADP-ribosylating exotoxins (bAREs), 771
Barrier disruptions, 61
Barrier function, 160
Basket-weave appearance, 197
Battelle Memorial Institutional Review Board (IRB), 429
Beach sunscreens. *See* sunscreens
Benzo(a)pyrene, 45–47, 171, 266, 273, 282
  benzo[a]pyrene 7,8,9,10-tetrahydrotetrol, 47
  metabolism in mouse, 45
  metabolites, 47
Benzocaine, 46
  ester hydrolysis, 46
  N-acetylation, 46
Benzoic acid (BA), 46, 96, 388, 585
  penetration, 585
Benzophenone-3, 682
  in breast milk, 682
Beraprost sodium treatment, 346
Bioconversion, 24
  in skin, 24
Biotransformation, 160
Biowaivers, 478
[Biowaivers]
  for gel preparations, 479
Blood flow, 331
  calcium, 342
    channel blockers, 347
  facial palor, 341
  hyperoxia, 340
  hypertension, 3.43
    gestational, 342
  measurement, 333
    in LDF. *See* Laser Doppler flowmetry (LDF).
  in percutaneous absorption, 331
  physical activity, 341
  pregnancy, 342
  in psoriatic plaques, 337
  smoking, 342
  vasoconstrictive tests, 334
  vasodilative tests, 334
Borates, 258
Butylated hydroxytoluene (BHT), 46

Cadaver ski, 266, 295, 312, 552
  VX, 482
Calcitonin gene-related peptide (CGRP), 337
Cantharidin blister technique, 363
Cantharidin–acetone solution, 363
Carnauba wax, 721
Cavitation, 749
  outside the skin, 750
  within skin, 751
  in transdermal transport, 750
Cellulose dialysis fiber, 371
Ceramics, 148
Characterization, 702
Chemical interactions, 157
  with adnexial structures, 158
  classification, 157
  dermis, 158
  enhancers, 159
  enzymes, 160
  epidermis, 158
  mechanisms, 157
  stratum corneum, 158
  surface of skin, 157
Chemical warfare agent (CWA), 91, 487, 529
  decontamination procedure, 487
  in Japan's subway gas attack, 555
  structure
    and percutaneous absorption, 532
    and toxicity, 532
Chemically labile actives, 726
Chemical "cocktails", 556

Chemicals, 165, 157, 440
fraction of, in skin (FA), 167
organic, 165
volatile, 172
Cholera toxin (CT), 771
Cholinesterase inhibition assay, 554
Chorioallantoic membrane (HET-CAM), 711
Chromated copper arsenate (CCA), 823
Circardian differences, 336
CMV-CAT expression plasmid, 815
Cnidaria nano injectors, 521
application, 524
cnidocyst, 521
basic structure, 522
drug delivery, 525
operation principle, 522
structure, 526
topical formulation, 524
Coat and poke approach, 499
Coefficients, 167
effective diffusion, 167
octanol–water partition coefficient, 171
partition, 167
permeability, 167, 170
ratio of permeability, 167
Coenzyme Q10, 808
Cognitive test, 334
Colorimetric assay, 553, 813
Compartmental pharmacokinetic models, 22, 27
steady state conditions, 29
Comprise ceramides (CER), 760
Compritol 888 ATO, 727
Concanavalin A, 149
Concentration gradient, 167
Concentration, 319
and water temperature, 324
duration of contact, 325
surface area, 325
Concentration–distance profiles, 20–21
Confocal laser scanning microscopy (CLSM), 419
Contact dermatitis, 336
Contact urticaria, 140
Convective blood flow, 33
Corneocytes, 195
in SC barrier, 195
Corneometer CM 825, 728
Cornified cell envelopes (CEs), 196
Correlation, 230, 515, 619, 855
hair dye absorption, 619
with partition coefficients, 619
in vitro–in vivo, 230
percutaneous absorption, 515
[Correlation]
and TEWL, 515
skin impedance–skin permeability, 855
Cortex Technology, 780
Corticosteroids, 65, 476
in vitro release, 476
Cosmetic chemicals, 595–604
dermal exposure, 595–596
exposure estimate, 596
acute and chronic exposure, 598
percutaneous absorption, 597
risk management, 599
safety assessments, 597, 598
of carcinogenic, 599
Cosmetic ingredient review expert panel, 606
Cosmetics, 362
tanning products, 362
Coumarin absorption, 566
Covariate-adjusted regression models, 783
Creams, 720–730
lightening effect,
Critical micelle concentration (CMC), 492
Crystacide, 338
Cutaneous blood blow (CBF), 584
Cutaneous microcirculation, 331
laser Doppler, 331
limitations, 332
methodology, 332
photoplethysmograph, 331
Cutaneous postischemic reactive hyperemia test, 334
Cutaneous xenometabolism, 61
Cyanoacrylate, 248
Cytochrome P-450 monooxygenases
isoenzymes, 53–54
mechanism of action, 53
Cytochrome P450, 48
Cytomegalovirus (CMV), 765
Cytotoxic T lymphocytes (CTL), 791
response, 815

Data analysis sanity, 318
Data, 444, 608
analysis, 608
2NPPD, 608
relations, 444
Debye layer thickness, 36
Declaration of Helsinki principles, 248
Defibrotide, 346
Delivery systems, 801
microsponge (MDS), 808
novel transdermal, 806
Dendritic cells, 789, 815

Dermal
delivery, 182
flux, 436
irritation, 524
reservoir, 228
washing efficiency, 283
DermaLab® Modular Systems, 780
Dermatomed skin, 312
Dermatopharmacokinetic, 404
Dermatopharmacology, 399
tape stripping technique, 399
methodology, 400
Dermovac cap, 362
Desert Storm, 303
Desquamation, 165, 224
effect of, on dermal absorption, 166
herbicide .uazifop-butyl, 166
rate of, 165
role of, on SC reservoir effect, 224
Determination, 267
in vitro cell diffusion study, 267
Di(2-ethylhexyl) phthalate, 47
Diabetes mellitus, 344
insulin, 345
nociceptive C fibers, 345
Diclofenac, 454
Diethanolamine (DEA), 273
absorption, 274
Diethyl malonate, 45
degradation, 45
Diethylene glycol monoethyl ether (Transcutol), 371
Diethyltoluamide (DEET), 89
Diffusion
cell assembly, 475
coefficient, 694
controlled release, 21
pharmacokinetic models, 30
SC–vehicle partition coefficient, 30
Diffusive Transport Processes, 23
concentration dependent, 23
Diffusivity (D), 157
Dimethylsufoxide (DMSO), 720
Dioleoyl phosphatidylethanolamine (DOPE), 794
Dip and scrape approach, 499
Diphenylhydramine hydrochloride (DPH), 709
Discovery II ion trap tandem mass spectrometer (MS/MS), 431
Disodium octaborate tetrahydrate (DOT), 111, 259
Disperse Blue 1 (DB1), 275, 615
dermal penetration, 617
Divisions of Biotechnology and GRAS Notice Review (DBGNR), 602
Divisions of Petition Review, 602
DNA, 774, 814, 789–800
biodistribution, 774
immunization, 811
mechanism, 814
topical, vaccines, 795–796
plasmid DNA (pDNA), 789
genetic immunization, 789
tape stripping, 814
Th1 and Th2 response, 795
vaccine, 774, 791
Dose accountability, 327
Dose, 389, 449
dependent response, 501
response, 317
curves, 155
interrelationships, 319
in real time, 317
on SC concentration and percutaneous absorption, 389
single vs. many, 449
triple daily dose, 452
Dosing and Surface Washing Procedures, 646
Draining lymph nodes (DLN), 774
Drug delivery, 643, 663
nails, 643–653
non-invasively one-line monitoring, 663
Drugs, 361, 473
analytical techniques, 371
C^* concept, 376
concentration, 361
continuous transcutaneous drug collection (CTDC), 364
controlled clinical trials, 473
effects, 361
fluorescence, 373
acridinorange, 374
free drug concentration, 375
release characteristics, 476
sample collection, 374
parameters, 374–375
sampling techniques, 362
related techniques, 364
surface recovery, 364
serum concentration vs. time curve, 361
D-Squame tape, 773
D-Squame®, 813
Dust fraction, 112
Dyeing procedure, 624
human volunteers, 624
rhesus monkeys, 624
Dyes, 612

[Dyes]
HC Yellow No. 4 (10), 612
Dynamic light scattering (DLS), 704
Dyskeratosis follicularis (DD), 585

Eagles minimum essential media (MEM), 312
Earle's balanced salt solution (BSS), 312
EcoNail, 645
Edema, 371
EDETOX, 567
Electropermeabilization. *See* Electroporation
Electroporation, 461, 762, 791
EMF, 461
fluorescence-labeled plasmid, 792
oligonucleotides, 762
and ultradeformable liposomes, 465
Emergent properties, 160
Emla, 526
Emulsion, 683
oil-in-water, 683
water-in-silicone, 686
Endoplasmic reticulum, everted, 57
End-organ effect, 62
Enhancers, 851
chemical, 498
chemical penetration (CPEs), 852
screening, 851
skin impedance, 851
Enzyme induction, 60
Enzymes, 25, 51, 142
homogenous distribution, 25
metabolizing, 25
skin conditions, 142
xenobiotic-metabolizing, 51
Epicutaneous sensitization, 145
Epidermal, 165
permeation rate, 694
sterologenesis, 65
viable (ve), 165
Epoxide hydrolase activity (EPOH), 61
effects, 61
Erythema, 34, 334, 782
grading after treatment, 782
methyl nicotinate, 334
UVB-induced, 336
Erythrokeratoderma variabilis (EKV), 585
Esterase activity, 46
[^{3}H] Estradiol-17β, 372
Estradiol, 45
Ethyl aminobenzoate (benzocaine), 46. *See* Benzocaine
Ethylene glycol
and Triton X-100, 389
[Ethylene glycol]
water and Triton X-100 mixtures, 393
Ethylene oxide, 307
Ethylene-vinyl acetate (EVA), 676
Eudragit®, 727
Eutanol®, 706
Exhaled breath analysis, 429
in humans, 429
exposure conditions, 429
Experimental, 623
hair dyes, 623
Exposure
system (Kloss), 434
time, 166
periods, 549
on FA, 167
Extended focal image (EFI), 249

FA. *See* Chemicals: fraction in skin.
Facilitated transdermal delivery, 35
in modeling, 35
Faraday's constant, 36
Fast inverse Laplace transforms (FILT), 6
FDA bioequivalence guideline, 814, 475
on tape stripping, 814
Fick's first law of diffusion, 157, 160, 803
Fick's second law, 671
Fischer 344 rats, 236
Fisher's protected t-test, 780
Flip–flop kinetics, 27
Flow-through diffusion cell, 45
Fluazifop butyl (FB), 565
in rats, 565
Fluocinolone acetonide, 65
Fluoroscent microscopy, 419
Flux, 5, 161, 167, 218, 460, 628
on donor phase removal, 8
electroosmotic flux, 461
iontophoretic, 36
and permeability coefficient, 259
SC reservoir, 218
at steady-state, 5, 168
in sunscreens, 684
time profiles, 8
Flynn database, 119
Follicle, 417
free guinea pig skin, 417
Follicular
analysis, 183
biopsies, 420
delivery, 182–183
density, 238
deposition

[Follicular]
[^{14}C]pyridostigmine bromine formulation effects on, 422
permeation, 412
assessment methods, 418
effect of drug, 420
experimental design, 412
quantification, 184
real time diffusion, 185
visualization, 184
fixed skin, 184
nonfixed skin, 184
Food and Drug Administration (FDA), 596, 605
Forearm (ventral-elbow), 97
Fourier Transform Infrared Spectroscopy, 663–680
Fowler's solution, 824
Franz Diffusion Cells (FDCs), 194, 201, 422, 476, 673, 710, 852
Franz flow-through diffusion cells, 731
Freeze fracture electron microscopy (FFEM), 702, 812
Frequency, 319
FT-IR spectrum, 664
penetration of drugs, 669

Gaulin 5.5, 723
Geiger–Müller counter, 364
Gene expression, 421
in follicular permeation, 421
lacZ reporter gene, 421
Gentamicin, 482
Glyphosate (water soluble herbicide), 303
Gore-Tex film, 112
Gulf War Syndrome, 157, 309, 485, 576. *See* Chemical warfare agents.

Hair dye
coal-tar, 605
penetration, 623
in man, 623
in monkey, 624
Hair Follicle, 177
anatomy, 412
density, 254
distribution, 247
growth cycle, 181
in vitro histocultures, 418
structure, 180
Hair, 366
permeation, 252
Hanks balanced Salt solution (HBSS), 565
HC Blue No. 1, 633
Henderson–Hasselbach equation, 444
Henle's layer, 181
Heparin, 740
HEPES isotonic buffer, 422
HEPES-buffered Hanks' balanced salt solution (HBHBSS), 45
Herbicide triclopyr butoxyethyl ester (triclopyr BEE), 236
Herpes simplex virus (HSV), 375, 376, 765
responses, 797
Hexyl nicotinate (HN), 239, 584
High-performance liquid chromatography (HPLC) analysis, 257, 366, 420, 476, 852
Human epidermal membranes (HEM), 201
Huxley's layer, 181
Hydrocortisone (HC), 239, 452
dosing sequence, 452
Hydrogen bonding acceptor ability, 26
Hyperproliferation, 170
Hypertension, 343
gestational, 342
Hypotonic water (sweat), 179

IgE antibodies, 140
Immunohistochemistry, 420
Imwitor®, 721
[^{125}I]-d-interferon, 423
In vitro diffusion models, 1, 3
In vitro flow-through diffusion cell methodology, 597
In vitro human studies, 685–686
In vitro percutaneous absorption, 23
processes affecting, 23
In vitro release, 473
applications, 478
automation, 475
corticosteroids. *See* Corticosteroids.
methodology, 474
rate, 475, 479
receptor medium, 476
sample applications, 474. *See also* Sample
semisolid dosage forms, 473
dissolution methodology, 473
quality control tests, 474
solid oral dosage formulation, 473
studies, 479
SUPAC-related changes, 476
testing, 474
In vitro skin permeability studies, 740
constant donor concentration, 3, 9

[In vitro skin permeability studies]
defined input flux, 12
finite receptor volume, 9
sink receptor conditions, 3
diffusion limited finite donor, 17
sink receptor condition, 17
finite donor volume, 14
finite clearance from the epidermis into the receptor, 16
receptor sink conditions, 4
two layer diffusion limitations, 19
desorption, 20
SC heterogeneity, 20
in transport, 19
In vivo decontamination model, 277
in rhesus monkey, 277
In vivo dermal studies
in vitro studies in human skin, compared, design, 570
skin reservoir, 569
variability, 567
In vivo drug penetration, 815
In vivo relationship, 95–106, 384
TEWL and percutaneous absorption, 95–106
In vivo skin irritation study, 491
Inflammation, 336
Insert and infuse approach, 499
INSIGHT screening, 853
applications, 858
validation with FDC, 857
Inspiratory gasp, 334
Insulin dependent diabetes mellitus (IDDM), 346
Insulin, 500
Interaction, 23, 196, 657, 803, 859
concentration-dependent, 23
keratin–water binding, 196
solute–skin, 26
drug–skin, 658, 805
enhancer–skin, 859
multiple, 160
vehicle–drug, 657, 803
vehicle–drug–skin, 659, 805
vehicle–skin, 26, 658, 804
Interface, 12
membrane–vehicle, 12
skin–system, 12
Intracellular lipid domain, 790
Intracutaenous needle stimulation, 335
Investigational Review Board, 781
Iododeoxyuridine, 402
Iontophoresis, 35, 341, 460, 762
electrorepulsion, 461
[Iontophoresis]
endothelium dependent vasodilation, 341
flux, 36
oligonucleotides, 762
and ultradeformable liposomes, 462–463
Ion-trap mass spectrometer, 260
IR Microspectroscopy, 668
lateral drug diffusion, 676
Iraqis attack on Halabja, 556
ISIS 2922, 765
Isolated perfused porcine skin flap (IPPSF), 236
Isometric test, 334
Isopropyl myristate (IPM), 703
Isotonic test, 335

Jet fuel, 161
topical absorption, 31
performance additives, 160

Kaposi's sarcoma, 349
Keratinization, 181
Keratinocytes, 160, 770
layers, 791
Ketanserin, 348
Kiistala's method, 362

Labrasol®/Cremophor® RH 40
Lactate curves, 312
Lag times, 5, 167
Langerhan's cells, 789, 815
Langmuir adsorption, 24
Laplace, 2
domain, 2, 220
transform, 14
variable, 6
Laser Doppler flowmetry (LDF), 331, 421, 584
advantages, 332
burns, 338
concepts, 333
diabetes mellitus, 344. *See* Diabetes mellitus
flushing, 341
measurement, 333
mechanism of pain relief, 339
peripheral vascular disease, 343
pigmentary lesions, 338
pregnancy, 342
gestational hypertension, 342
principles, 332

[Laser Doppler flowmetry (LDF)]
study design, 333
follicular permeation, 412
Laser Doppler velocimetry (LDV), 239, 319, 328
Lasso formulation, 282
Latex, 142
allergy, 142
proteins, 145
LDV response-time curve, 239
Leutenizing hormone releasing hormone (LHRH), 859
Lewis triple response, 335
Light and Neutron Scattering, 704
Lipid soluble pesticides, 305
Lipids, 459, 719, 752, 812
in barrier function of skin, 812
definitions, 721
hexagonal lateral packing, 812
matrix, 459
nanoparticle cream preparation, 725
nanoparticle gel preparation, 724
nanostructured lipid carriers (NLC), 720
penetration of actives, 730
scents and perfumes, 733
production, 721
homogenization, 722
removal, 752
solid lipid nanoparticles (SLN), 720
types of, 729
Lipophilicity, 167
on FA, 168
Liposome, 422, 459, 764, 793
cream formulation, 793
electrical potential, 460
formulation, 764
physical methods, 467
ultradeformable, 459
Liquid scintillating counting, 440
Living skin equivalent (LSE) model, 56
Local anesthesia, 525
Local lymph node assay (LLNA), 144
Local transport regions (LTRs), 465
Lowest observed adverse effect level (LOAEL), 599

Macaque monkey, 418
Macromolecules
lectins, 146
skin penetration, 146
Magnetic resonance spectroscopy (MRS), 364
Malathion, 239, 305, 456, 529
multidose, 456
Mann and Whitney's U-test, 250
Marker, 159
Mathematical modeling, 1–44, 681
application, 36
percutaneous processes, 2
perspectives, 1
from physicochemical data, 681
McDougal model, 31
Measurements, 257
[^{14}C] atrazine, 257–258
borates, 258
Mecamylamine, 494
Melanoma, 338
Metabolism, 52, 572
aromatic hydrocarbon hydroxylase (AHH), 58
benzoic acid, 55
cutaneous, 59
glycine conjugation, 54
phase I, 52
phase II, 54
polycyclic aromatic hydrocarbons (PAHs), 58
Methotrexate (MTX), 713
Methyl nicotinate (MN), 570, 845
Methyl salicylate, 47
Methylene bisphenyl isocyanate (MDI), 286
Mexoryl SX®, 685
Michaelis–Menten kinetics, 25
Michelson interferometer, 664
Miconazole, 477
Microdialysis, 370, 570
in vitro, 570
in volunteers, 570
Micro-electrical mechanical system (MEMS), 499, 763, 792
Microemulsion (ME), 701
advantages, 701
delivery
dermal, 708
transdermal, 708
droplets, 704
light scattering, 704
neutron scattering, 706
properties, 701
Microemulsion, 806
delivery system, 794
Micro-enhancer arrays (MEAs), 763, 792
Micromechanical disruption method, 792
Micron LAB40, 723
Micron pathways, 498
Microneedles, 498, 792, 843

[Microneedles]
convenience, 505
delivery scenarios, 498–499
drug delivery, 499
hollow, 500
solid, 499
in electroporation, 792
fabrication, 499. *See* Micro-electro-mechanical systems.
impact of design, 847
multi needle arrays, 498
out-of-plane, 844
pain, 502–503
avoidance, 503
safety, 504
testing, 843
Micropore®, 813
Microscopy, 702
Miglyol 812, 721, 727
Minicollagen, 522
MINIM 3.09, 3
Minimal inhibition concentration (MIC), 402, 651
MINITAB, 441
Minolta chromameter, 403
Minoxidil, 319
Mobile protons, 196
Model, 166, 587
animal skin for human skin, 588
dermal absorption, 166
design, 529
desquamation, 166
in vitro methods for in vivo experiments, 587
mathematical model, 166
Monoclonal antibody to doxorubicin (MAD11), 420
Monte carlo simulation, 602
dermal exposure, 602
MULTI FILT, 2
Multi-compartment "dermatatoxicokinetic" model, 31
Multiple dose application, 325
Musk xylol, 267, 599
case study, 599–604
human skin, 272
in hairless guinea pig, 272
Mycosis infections, 406

N,*N*-diethyl-*m*-toluamide, 323
Nail, 366, 643
bed, 646
incubation, 646
[Nail]
penetration, 643
methods, 645
properties affecting, 644
plates, 646
sampling procedure, 646
Nano injectors, 521
natural, 521
topical drug delivery, 521
Nanometer Pathways, 497
skin permeability, 497
Napthalene, 160
National toxicology program (NTP), 596
Needle-free injection, 754
Neurotoxic agents, 579
Neutrol®, 724
Newtonian flow, 703
in MEs, 703
Nicotine, 676
Nicotinic acid, 388
Nitro-Dur, 676
Nitroglycerin buccal tablets, 511
n-Methyl pyrrolidone (NMP), 712
No-interaction hypothesis, 155, 156
Non-insulin dependent diabetes mellitus (NIDDM), 346
Non-woven abrasive pads (NWAP),779
No-observed-effects levels (NOEL), 578
Northern California Transplant Bank, 312
NRC subcommittee, 579
Nubral® 4HC, 710

Occlusion, 65, 282, 366, 719, 727
dressing, 235, 366
early washing, 282
effects of, 282
effects of, 74
glass-chamber, 68
and hydration, 79
in vivo penetration, 65
effects of, 241–242
in percutaneous absorption, 235
Octanol/water partition coefficient, 532, 629, 694
Ocular distribution, 764
Office of Pesticide Programs, 172
Oligonucleotides, 760
modification, 760
skin interaction, 760
One-dimensional model, 17
Onychomycosis, 643
Organisation for Economic Co-operation and Development (OECD) guidelines, 561

Organization for Economic and Cultural Development guidelines, 267
in vitro skin absorption studies, 267
Organophosphorus compounds, 529
skin absorption data, 540–546
Ovalbumin (OVA), 143, 775
o-Xylene, 429

p-Aminobenzoic acid (PABA), 46, 415, 683
acetyl-PABA, 46
Paniculate delivery systems, 422
Parafilm®, 236
Parameters
property of absorbed chemical, 167
Paraquat, 87
in humans, 87
[^{14}C]Paration, 482
Parathion, 239, 605, 529
structures, 306
Partition coefficient (PC), 156
Partitioning studies, 441
PCP. *See* Pentachlorophenol: PC of
Pennsaid. *See* Diclofenac
Pentachlorophenol (PCP), 159, 238
PC of (PCP), 159
Percent dose absorption, 580
Percus–Yevick approximation, 707
Percutaneous absorption, 45, 95,123, 235, 265, 295, 384, 509, 583, 814
determination, 267. *See also* determination.
diffusion cell, 265
formation of retinol, 47
in vitro techniques, 265
in vivo, 237
in animals, 237
individual variation, 512
measurement methods, 95, 123, 590
recovery in, 267
regional variation, 510
in humans, 510
and SC concentration, 384
studies, 45
vs. tape stripping, 814
trinitrobenzene, 47
types of compound, 591
Perfused porcine ear (PPE) model, 567
Permeability coefficient, 3, 259, 429, 561
Permeability constant, 157, 268, 547
Permethrin, 575
bioavailability, 576
body burden calculations, 577
characteristics, 576
[Permethrin]
leaching, 576
Pesticides, 59, 172
Petroleum jelly, 682
Peyers patches, 776
Pharmacodynamic modeling, 34
Pharmacokinetic and pharmacodynamic models, 31
physiologically based (PBPK/PD), 31
Pharmacokinetic model, 12, 33
deconvolution analysis, 33
Pharmacokinetics, 576
permethrin, 576
Phenanthrene, 47
metabolites, 47
Phenols, 71
in humans, 71
Phonophoresis, 739–758
electroporation, 739
heating, 748
skin surface, 748
within skin, 749
low frequency, 747
mechanism, 747
pharmacokinetic data, 740
stratum corneum, 739
studies in, 740
transdermal transport, 739–758
ultrasound, 740
Phospholipid vesicular carriers, 806
ethosomes, 807
liposomes, 806
transferosomes, 807
Physiologically based pharmacokinetic (PBPK) model, 317, 429, 431
Pilocarpin electrophoresis, 338
Pilosebaceous unit, 179, 411
Piroxicam-β-cyclodextrin, 710
Plastic Hill Top chamber, 68
p-Nitrophenol, 31
Poke and patch approach, 498
Poly DL-lactic-co-glycolic acid (PLGA), 808
Poly-γ-glutamate matrix, 522
Polychlorinated biphenyls (PCBs), 564
Polycyclic aromatic hydrocarbons (PAH), 510
Polyethylene glycol oleyl ether, 271
Polymeric microsphere, 425, 807
Potential Systemic Exposure Estimate, 603
Potential toxicity, 156
Potts–Guy equation, 484, 555
Potts-Guy model, 193
Powdered human stratum corneum (PHSC), 291

[Powdered human stratum corneum (PHSC)]
chemical decontamination, 297
chemical partitioning, 293
diseased skin, 296
enhanced topical formulation, 297
environmentally hazardous chemicals, 296
percutaneous absorption, 294
QSAR predictive modeling, 298
skin barrier function, 295
p-Phenylenediamine (PPDA), 66
in guinea pigs, 66
Precutaneous absorption, 531
in clothing, 531
moisture, 531
Protein allergens, 139
skin, 139
studies, 143
Protein contact dermatitis, 140
Psoriasis, 337
Purified cholera toxin B-subunit (pCTB), 771

Quantitative descriptions of structure-activity relations (QSARs), 859
Quantitative understanding, 859
Quenching, 364

Radioactivity scintillation counting, 645
Radioactivity-excretion curve, 449
Radioisotopes, 440
Radiolabel deposition, 418
Raman spectroscopy, 185
Raynaud's phenomenon, 332, 347–349
Real-time breath analysis, 260
and PBPK modeling, 260
Receptor fluid, 266, 271
accumulations, 453
bovine serum albumin, 266
modification, 271
solubilizing agents, 267, 268
Receptor medium, 474
Recombinant CTB (rCTB), 771
Reference listed drug (RLD), 478
Regional variation, 85, 530
applications in Risk assessment, 91
in animals, 89
in human, 85, 530
index for parathion, 549
principles, 85
Release profiles, 21
suspended drug by diffusion, 21
R-enantiomer, 57
Reservoir, 213
effect, 27
function, 213
stratum corneum corticosteroid, 215
Retinol, 47
Retinyl palmitate, 47
Rhesus monkey, 321, 823
RIFM Dermal Exposure Estimate, 600
Risk assessment, 116, 155, 257, 481, 529, 578
chemical warfare, 529–559
limitations, 261
rate-determining step, 257
bioavailability, 257
US regulatory agencies, 155
VX, 481
Rubbing alcohol, 285
Rule of 9, 547

S-100 protein staining, 797
Salmonella typhimurium, 606
in DB1, 615
Sample, 474–475
in drug release testing, 475
analysis, 475
applications, 474
sampling time, 474
Saran film, 214
Saran Wrap, 69
Sarin (GB), 529
Scar–tissue formation, 371
Schultz size distribution function, 707
Schwefellost (gelbes Kreuz cross), 547
SCIENTIST 2.01, 3
Scopolamine transdermal drug delivery, 394
Scotch Crystal®, 792
Scrotum, 510, 530
Sea anemone, 524
Sebaceous gland, 412
anatomy, 412
Sebum, 366
collection, 366
Sensitization test, 525
serotonin-2-(5-HT-2)-receptor, 348
Servo Med Evaporimeter, 781
Showering, 555
Shunt Transport, 27
Skin, 26, 45, 54, 65, 155, 177, 193, 262, 335, 367, 439, 494, 519, 554, 566, 592, 595, 681, 728, 772, 801, 815
absorbed material, 272
acetone treatment, 592
acetylation
primary amines, 46

[Skin]
age, 338
appendages, 178
barrier function, 584, 789
barrier properties, 262, 511, 519
barrier requirements, 65
binding sites, 441
biopsy, 367, 772
blok, 184
chronic venous insufficiency, 338
contact time, 115
contamination, 107
cosmetics, 595
cutaneous ulcers, 338
decontamination, 486
with soap, 555
methylene bisphenyl isocyamate (MDI), 487
dermatome section, 266
determination of, 440
effects of surface loss, 26
elasticity, 728
environmental temperature, 340
fate, 273
formation, 272
function, 177
glabrous, 342
glucose utilization, 45
hairless guinea pig, 47
hydration, 728
integrity Function Test (SIFT), 854
irritation, 494
layer separation, 440
membrane water partition coefficient, 440
metabolism, 46
effect of, on biological response, 48
studies in, 46
nervous system, 339
partitioning of chemicals, 439
varying lipophilicity, 439
pathology, 335
percutaneous penetration, 335
kinetics, 336
pharmacology, 335
physiology, 335
plasmid DNA
preparation of, 266
receptor conditions, 3
reservoir, 272
role of appendages, 193
morphology, 592
sectioning techniques, 368–369
manual, 369
[Skin]
semiautomated, 368
source, 266, 440
split thickness, 566
structure, 177
sunscreens, *See* sunscreens.
surface biopsy technique, 406
target site, 375
TEWL vs percutaneous absorption, 584
topical vaccination, 815
toxic chemicals, 155
transferase activity, 54
viability of, 45, 266
MTT assay, 46
Sodium lauryl sulfate (SLS), 158, 490
and parathion, 158
Soil and risk assessment, 116
Soil matrix, 31
Soil, 112
load, 115
study design, 112
Solid lipid nanoparticles (SLN), 808
Soluene 350, 384, 440
Solvents, 260
Soman (GD), 529
Sonophoresis, 36, 752, 792
imaging pathway, 752
inverse, 754
Spanish fly, 363
Sprague Dawley rats, 124, 384, 744
SS-flux, 585
Staphylococcus aureus superantigen, 336
Static light scattering (SLS), 704
Statistical evaluation, 829
Steady state
absorption rate, 268
approximation, 3
value, 128
Steroid
absorption, 241
in humans, 69
Stokes–Einstein equation, 706
Stratum corneum (SC), 165, 148, 159, 193, 217, 235, 265, 292, 411, 497, 521, 583, 752, 770, 801, 811, 851
asymmetry on, transport, 197
barrier disruption, 148
dysfunction and diseases, 812
guinea-pig footpad, 293
heterogeneity, 193
hydration, 235, 772
integrity, 126
lipid-enriched, 265
lipids, 161, 752

[Stratum corneum (SC)]
penetrating, 521
parameters, 521
percutaneous penetration, 811
properties, 292
removal, 267
skin barrier function, 812
skin-water barrier integrity
substantivity, 218
sunscreen agents, 688
thickness measurement, 124
Stripping method, 123, 387
Structural matrix, 656
characteristics, 656
Studies in,
rats, 579
rhesus monkey, 579
Study design, 828
particle size, 828
Substantivity, 268
defined, 268
Substrates, 827
environmentally relevant, 827
Suction blister technique, 362
Sulfur mustard (HD), 518, 529, 547, 587
lipophilic, 587
and TEWL, 518
toxicity, 548
Sun protection factor (SPF), 733
Suncreens, 681, 732
animal models, 689–690
application, 682
common, 682
risks, 695
release of, 732
skin permeation, 681, 691–692
in vivo human studies, 682
ultraviolet radiation, 681
US FDA definition, 681
use, 695
SUPAC-SS, 478
Surface area, 319
Sweat gland, 179
Synthetic membrane, 474
Syrian hamster ear, 417
sebaceous glands, 423
Systemic absorption, 272
methods, 272
Systemic metabolism. 265

Tape stripping, 403, 685, 761, 790, 811
comparison of methods, 813
factors, 812
[Tape stripping]
vs. immune response, 790
oligonucleotides, 761
potential, 403
and topical vaccination, 815
Teflon®, 236, 266
Teledyne 3DQ Discovery ion trap mass spectrometer (MS/MS), 317
Tesa®-stripping test, 731
Test animals, 831
Testosterone, 45
metabolism, 45
Tetanus toxoid (TTx), 775
Tetracycline, 365
Tetrahydrocannabinol, 372
TEWL values, 814
Theophyline, 57, 388
in partitioning, 441
Theoretical constructs, 547
in percutaneous absorption and toxicity, 547
Thermal test, 335
Time of exposure, 319
Topical
application site, 33
penetration in tissues, 33
in creams and gels, 723
DNA, 793
delivery, 793
vaccines, 795
efficacy, 797
formulations, 723
mechanism, 795–796
nitrates, 57
Toxicity, 532, 597
percutaneous absorption, 547
and structure, 532
threshold, 597
Transcutaneous immunization (TCI), 769
antigen-presenting cell (APC), 770
delivery optimization, 771
needle-based delivery, 775
immune responses to, 775
mechanisms, 775
toxoid antigens, 775
mammalian skin, 770
studies, 777
clinical, 777
vaccine delivery, 769
modeling, 772
Transcutol® CG, 694
Transdermal
clinical studies, 844
electrical enhancement, 459

[Transdermal]
drug delivery, 182, 459, 497, 843,
systems, 235
formulations, 852
requirements, 852
Transepidermal water loss (TEWL), 509, 514, 583, 712, 779, 789
correlation studies, 584
measurements, 7, 583
plasma cortisol levels, 586
in skin barrier function, 489
measurement, 489
variables, 518
Transferases, 54
Transfersomes, 148, 460
formulation, 460
Transfollicular absorption, 253
Transmission electron microscope (TEM), 702
Transpore®, 813
Trinitrobenzene, 47
metabolites, 47
Tristan®, 724
Triton X-100, 96
Tukey's multiple comparison test, 829

U.S. Environmental Protection Agency, 172
U.S. Food and Drug Administration (FDA), 35
Ultrasound, 740
biological consequences, 751
drug stability, 753
frequency, 740
high and medium, 752
low, 752
intensity, 740
mode, 740
skin tolerance, 753
Urine, 625
4-amino-2-nitrophenol, 628
application, 626
collection, 625
Human volunteers, 625
Rhesus monkeys, 625
radioactivity determination, 625
dyed hair, 626
stratum corneum, 626
UV blockers, 733
UV-radiation, 524

Vasoconstrictor effect, 220
Vasoreactivity, 591
Vehicle, 123, 390, 655, 790, 801

[Vehicle]
choice, 659
conditions, 659
classification of topical, 655, 802
commercially used, 682
conventional topical, 801
effects on permeation, 803
ideal, 656
mannan-coated, 795
membrane interface, 809
metamorphosis of, 804
partitioning, 123
pDNA, 790
vehicle–drug interactions. *See* Interactions
Velocity of diffusion, 133
Venoartriolar response, 334
Venoruton, 338
Viability of skin, 272, 312
systemic absorption, 272
dermatomed, 312
Viscosimetry, 703
Vitravene®. *See* ISIS 2922
Volatile compounds, 66
Volatility, 237
VX, 306, 481, 529, 553
absorption methodology, 481–483
decontamination, 486–487
risk potential for, 484
surrogate model, 482
toxicity, 306, 307

Washing-in effect, 284
Water solubility, 265
Water, 111
doses, 111
Wet-on-wet principle, 659

Xenobiotic metabolism, 56
corticosteroids, 56
Xenobiotics
in hair, 366
in nails, 366
Xeroderma pigmentation, 759
X-gal, 421
X-linked recessive ichthyosis (XRI), 585
X-ray analysis, 721

Y estimate, 300
Yalkowsky's solubility, 26
Yperite, 547

Zeta potentials, 463

about the book . . .

Updating and expanding the scope of topics covered in the previous edition, this Fourth Edition supplies new chapters on topics currently impacting the field including cutaneous metabolism, skin contamination, exposure to protein allergens, in vitro absorption methodology, the percutaneous absorption of chemical mixtures, the penetration of chemicals through the hair follicles, dermal drug delivery, mechanisms of absorption, nanoparticles and dermal absorption, the absorption of drugs and cosmetic ingredients, nail penetration, and other current research.

With contributions from 90 leading experts at the forefront of the discipline, this reference contains recent studies on the role of the skin as a key portal of entry for chemicals into the body…serves as a detailed reference source for recent advances in the field, as well as an experimental guide for laboratory personnel…details in vivo and in vitro methods for measuring absorption, dermal decontamination, mechanisms of transdermal delivery, and the relationship of transepidermal water loss to percutaneous absorption…considers a range of mathematical models, the safety evaluation of cosmetic ingredients, the absorption of hair dyes, nanoparticles for drug delivery, and other novel methods of drug delivery…and discusses topics including skin metabolism, the skin reservoir, and the effects of desquamation on absorption.

about the editors . . .

ROBERT L. BRONAUGH is the Lead Scientist for Dermal Toxicology, Office of Cosmetics and Colors, Food and Drug Administration, Laurel, Maryland. Since joining the FDA in 1978, Dr. Bronaugh has been involved in many different studies related to the percutaneous absorption and metabolism of topically applied chemicals. He is a member of the Society of Toxicology and the Society of Cosmetic Chemists and is a Fellow of the Academy of Toxicological Sciences. He serves on the editorial boards of *Toxicology and Applied Pharmacology* and the *Journal of Toxicology/Cutaneous & Ocular Toxicology*. Dr. Bronaugh has presented nearly 70 guest lectures and has authored over 200 articles in scientific publications. He received the Ph.D. degree (1972) in pharmacology from the University of Colorado, Boulder.

HOWARD I. MAIBACH is Professor of Dermatology at the University of California at San Francisco School of Medicine. The author of over 1700 papers in dermatology, toxicology, pharmacology, physiology, and related fields, he is the coeditor of *Cosmeceuticals; Cutaneous Infection and Therapy*; *Cutaneous Infestations and Insect Bites*; *Neonatal Skin*; *Percutaneous Absorption, Third Edition*; and *Psoriasis, Third Edition* (all titles, Marcel Dekker). Dr. Maibach serves on the editorial boards of the *International Journal of Dermatology* and *Excerpta Medica*, among others, and is a Fellow of the American College of Physicians, as well as a member of the American Academy of Dermatology, the Society for Investigative Dermatology, the American Federation for Clinical Research, and the American Dermatological Association. Dr. Maibach received the M.D. degree (1955) from Tulane University, New Orleans, Louisiana.

Printed in the United States of America

DK5703

ISBN 1-57444-869-2

90000

9 781574 448696

Taylor & Francis

Taylor & Francis Group

www.taylorandfrancisgroup.com